IAEA-TECDOC-335

NUCLEAR STANDARD REFERENCE DATA

PROCEEDINGS OF AN ADVISORY GROUP MEETING
ON NUCLEAR STANDARD REFERENCE DATA
ORGANIZED BY THE
INTERNATIONAL ATOMIC ENERGY AGENCY
IN CO-OPERATION WITH THE
OECD NUCLEAR ENERGY AGENCY
NUCLEAR DATA COMMITTEE (NEANDC)
AND HELD AT THE
CENTRAL BUREAU FOR NUCLEAR MEASUREMENTS,
JOINT RESEARCH CENTRE,
COMMISSION OF THE EUROPEAN COMMUNITIES,
GEEL
12–16 NOVEMBER 1984

A TECHNICAL DOCUMENT ISSUED BY THE
INTERNATIONAL ATOMIC ENERGY AGENCY, VIENNA, 1985

The IAEA does not maintain stocks of reports in this series However, microfiche copies of these reports can be obtained from

INIS Clearinghouse
International Atomic Energy Agency
Wagramerstrasse 5
P O Box 100
A 1400 Vienna, Austria

Orders should be accompanied by prepayment of Austrian Schillings 80 00 in the form of a cheque or in the form of IAEA microfiche service coupons which may be ordered separately from the INIS Clearinghouse

EDITORIAL NOTE

In preparing this material for the press, staff of the International Atomic Energy Agency have mounted and paginated the original manuscripts as submitted by the authors and given some attention to the presentation.

The views expressed in the papers, the statements made and the general style adopted are the responsibility of the named authors. The views do not necessarily reflect those of the governments of the Member States or organizations under whose auspices the manuscripts were produced.

The use in this book of particular designations of countries or territories does not imply any judgement by the publisher, the IAEA, as to the legal status of such countries or territories, of their authorities and institutions or of the delimitation of their boundaries.

The mention of specific companies or of their products or brand names does not imply any endorsement or recommendation on the part of the IAEA.

Authors are themselves responsible for obtaining the necessary permission to reproduce copyright material from other sources.

CONTENTS

SESSION IV

SESSION V

SESSION VI

SESSION VII

SESSION VIII

SESSION IX

WORKING GROUP SESSION I

WORKING GROUP SESSION II

WORKING GROUP SESSION III

SUMMARY OF SESSION I

Chairman: A.J. Deryutter

Summary

In this Session three papers were presented:

(1) 'Requirements for nuclear standard reference data from the users' point of view' by myself;

(2) 'The neutron cross-section standard evaluations for ENDF/B VI' by A.D.Carlson;

(3) 'INDC/NEANDC Standards File, Status Report' by H. Condé,

and a fourth paper was submitted to the session by M.V. Blinov containing information with respect to the IAEA Standards File entitled: 'IAEA Standards File: Some comments and recommendations'.

In the first paper the general requirements for the standards reference data from the measurers' point of view were discussed. Requirements concerning accuracy of the data, traceability, representation, availability of materials in suitable form and applicability in real life detectors, internal consistency of standards as well as requirements for additional basic information required for making corrections with confidence or to impose constraints on the data were discussed.

In the discussion that followed the presentation it was recognized that the difference between primary standards and secondary standards is not very meaningful because of the large number of requirements introduced by the use of the standards in applicatiions. However, in view of the amount of work involved, it was argued that no further standards should be added to the set unless good arguments are given and applications are specified. It was mentioned that also standards for neutron production were needed.

In the second paper a 'first pass' at determining the standards for ENDF/B-VI was reported by A. Carlson.

The CSEWG (Cross Section Evaluation Working Group) decided that the hydrogen scattering cross-section would be fixed in ENDF B-VI and the new evaluation by Dodder and Hale has been accepted as the new hydrogen standard for ENDF/B-VI.

A simultaneous evaluation is being performed with a generalized least squares program and the cross-sections being evaluated are $^{6}Li(n,\alpha)$, $^{6}Li(n,n)$, $^{10}B(n,\alpha_o)$, $^{10}B(n,\alpha_1)$, $^{10}B(n,n)$, $^{197}Au(n,\gamma)$, $^{235}U(n,f)$, $^{238}U(n,f)$, $^{238}U(n,\gamma)$ and $^{239}Pu(n,f)$. This evaluation uses a large data base file, and a full covariance analysis is being performed.

The R matrix is being applied for the ^{6}Li and ^{10}B cross-section standards.

A procedure for combining the simultaneous and R-matrix evaluations has been defined but is not yet implemented.

The output will be adjusted R-matrix parameters for the $^{6}Li+n$ and $^{10}B+n$ systems and final point cross-sections for the remaining reactions.

Preliminary results were presented for the ^{6}Li and ^{10}B standard cross-sections from the simultaneous and R-matrix evaluations and compared to the EDNF/B-V results. Some trends for the $^{197}Au(n,\gamma)$ and $^{235}U(n,f)$ cross-sections compared with EDNF/B-V were discussed.

In the discussion that followed clarification on the data base used and the combination of the simultaneous and R-matrix evaluations were given. Especially the acceptance of the new H(n,n) cross-section and the procedure to obtain the accuracy of differential cross-sections was discussed. The envisaged data for finalizing the standard evaluations for ENDF/B-VI was given as middle 1985.

In the third paper the 1982 version of the INDC/NEANDC Standard File published as an IAEA Technical Report (N° 227, Vienna 1983) was discussed. All items contained in the file were briefly commented and additional information given when available. The procedure of updating the file and the responsibilities of NEANDC and INDC in this respect were mentioned.

In the discussion that followed the presentation concern was expressed about the conformity of the updated document when published by OECD with the IAEA Technical Report N° 227.

In the paper submitted to this section by M.V. Blinov et al comments related to several of the evaluated standards in the INDC/NEANDC Standards File are made and these should be carefully considered by the responsible reviewers in view of the coming NEANDC updating.

Conclusions from the Session:

(1) Ways and means to speed up the iterative process of approaching accurate values for standard reference data should be found.

(2) A more rigorous approach to systematic problems both in design and execution of experiments is required. Especially long-standing sources of systematic errors need to be thoroughly investigated.

(3) A thorough investigation of the limitations in the use and the resulting systematic errors in the execution of the measurements should be made before a standard is classified as such. (Also before a new measurement on a standard is made the impact on the accuracy of that standard should be evaluated).

(4) Additional basic information obtained by theory or experiment should be used to improve accuracy and reliability of standard data by allowing better funded corrections or by imposing constraints on the data.

(5) Only one set of standards data should be used by the user community. In this standards set numerical values should be given for all standards and a more rigorous scheme of updatings would improve traceability. The standard data measurements on which the evaluations and updatings are based should be fully documented and traceable in the literature.

(6) This standards set should be the INDC/NEANDC Standards File. A few suggested improvements with respect to the present file are: For the use of differential cross-sections for H(n,n), additional information on the coefficients of the Legendre polynomials in the relative centre-of-mass neutron angular distributions is required. For each standard a unique set of values and uncertainties (with correlation matrix) should be given. Numerical values of standard reference data in the file should be consistent when related.

(7) The results of the neutron cross-section standards evaluations for ENDF/B-VI performed by the U.S. Cross-Section Evaluation Group should be carefully considered in the next version of the INDC/NEANDC Standards File. Any updating of the present file should wait until these evaluations are finalized.

(8) The permanent reviewers of the standards cross-sections in the framework of the INDC/NEANDC should take into account all technical information presented at this meeting.

RECOMMENDATIONS TO THE I.A.E.A.

(1) The IAEA/NDS through the INDC should convene at regular intervals Advisory Group Meetings on Standards Reference Data. These meetings should preferably be linked with updatings of the INDC/NEANDC Standards File.

(2) The IAEA/NDS through INDC should convene small expert meetings on topics of special interest in the standards field.

(3) The IAEA/NDS should give continuity to the publication of the INDC/NEANDC Standards File.

SUMMARY OF SESSION II

Chairman: G.M. Hale

SUMMARY

- Hale: Discussed ^{7}Li system data and calculations, with implications for $^{6}Li(n,t)$ reaction mechanism. Present R-matrix analysis agrees well with low-energy data, gives cross sections close to ENDF-V values. Some problems representing $^{6}Li(n,t)$ angular distributions and some other data for E_n in the MeV range. Doublet-doublet amplitudes appear consistent with d-exchange mechanism. Particle exchange arises naturally in R-matrix theory through channel overlap terms - still needs to be included in ^{7}Li analysis.

- Poenitz: Reviewed the status of n-^{6}Li and n-^{10}B data. New data for the n+^{6}Li reactions appear to be reasonably consistent with each other, and do not indicate large changes from the ENDF-V evaluation. New data for n-^{10}B (and a closer look at earlier data) show many internal discrepancies except at thermal and indicate some differences with the $^{10}B(n,\alpha)$ ENDF-V cross sections in the standards range, and possible large differences above. Recommends that $^{6}Li(n,t)$ be used as the standard below 100-150 keV until problems with $^{10}B(n,\alpha)$ data base resolved.

- Bastian: Described relative measurement of $^{6}Li(n,\alpha)$ ratio, using rotating samples to remove inhomogeneities and angular distribution effects. Within the errors of the present experiment, no significant deviation outside the errors of the evaluations from the ratio of the ENDF-V cross sections was observed in the range 2 eV - 300 keV. Above 400 keV large deviations were seen, but background corrections were also large there. Peak position in ratio at slightly higher energy in measurement than in calculation. Plans to repeat measurement with smaller errors.

- Lajtai: Measured efficiency of thick (9.55 mm) NE-912 ^{6}Li glass detector relative to thin (.835 mm) NE-908 ^{6}Li glass, then determined absolute efficiency of the thick glass by a Monte Carlo calculation of the thick glass efficiency. The measured thick-glass efficiencies were then compared with MC calculations and found to be 2-20% higher for $.02 \leqslant E_n \leqslant 2$ MeV. Correction factors for resonances other than ^{6}Li(n,α) [primarily those from O, Si, and ^{7}Li], attained values as high as 1.7 for the thick glass. Feels that this is a well-characterized, relatively efficient detector for measurements on U, Pu, and Ca at energies up to 2 MeV.

- Drosg: Proposed measuring ratios of the inverses of some of the standards cross sections by the quasi absolute method, using a common target for the two reactions. For instance, if ^{4}He(t,n)^{6}Li and ^{4}He(^{7}Li,n)^{10}B were measured with the same system (identical gas target) such that the outgoing neutron energies are the same, only statistical errors (and background subtraction) would, in principle, be present. Method requires bunched ^{7}Li and t beam facilities. Possibly could be done at Los Alamos.

CONCLUSIONS

1. Standards cross sections need to be studied over a far wider energy range than the recommended one in order to understand them, and possibly to extend the recommended range.

2. Data base, evaluations for n-^{6}Li cross sections appear to be converging on results not very different from ENDF-V cross sections for $E_n \leq 1$ MeV.

3. Data base for n-^{10}B reactions in a state of confusion due to large disagreements between new measurements and earlier ones [esp. for ^{10}B(n,α_1)]. Response of the simultaneous and R-matrix evaluations to the new n-^{10}B information tends to be in the same direction, but large differences (~6%) presently remain.

SUGGESTED RECOMMENDATIONS

- Evaluations: Continue work on combined simultaneous/R-matrix evaluations of standard cross sections. Try to resolve problems in existing n-^{10}B data base as much as possible, but recognize that final errors in the evaluated ^{10}B(n,α) cross sections may hinder its use as a standard below ~100 keV.

- Measurements: Re-measurement of Bastian ^{6}Li/^{10}B ratio with smaller errors is encouraged, as is Drosg's proposal to measure ratios of inverse reactions with beams or targets in common. A direct measurement of ^{4}He(^{7}Li,n)^{10}B would also be a useful check of the recent ^{7}Li(α,n) cross sections that disagree so much with previous data. Urgently need <u>absolute</u> ^{10}B(n,α_1) measurements at a few energies in the 50 keV - 1 MeV range, or a detailed shape measurement that goes down to low enough energies to be strongly tied to the thermal numbers.

SUMMARY OF SESSION III

Chairman: A.D. Carlson

The session began with Dr. Kornilov describing the PADE approximation parameterization as applied to the $^{6}Li(n,t)$ and $^{10}B(n,\alpha)$ cross sections from 0.1 keV to ~ 2 MeV. Only 11 parameters were required to fit each of these cross-sections to an accuracy of ~ 0.5%.

Dr. Kornilov then reported on his evaluation of the $^{27}Al(n,\alpha)$ cross-section from 5.5-20 MeV which also employed the PADE approximation parameterization. With the available experimental data, the fitting was possible with 8 parameters. A correlation matrix was deduced for the experimental data and bounds were obtained for the accuracy of the $^{27}Al(n,\alpha)$ evaluation. This evaluation is in agreement with ENDF/B-V. The agreement with the Vonach evaluation on the INDC/NEANDC standards file is within the errors of the evaluation, i.e. $\pm$ 2%, only near 14 MeV. The Vonach evaluation is generally lower than this evaluation. The apparent presence of structure in this cross section from 6.- 8.5 MeV must be taken into account in the use of this cross section. It was emphasized that an improvement in the accuracy of this cross-section is only possible if experiments with 1-2% uncertainty are performed with high neutron energy resolution. Recommendation: The reason(s) for the differences in the Vonach and Kornilov evaluations should be investigated.

Dr. Condé reported on the investigation of Andersson et al. concerning the influence of background neutrons on activation measurements in the neutron energy region for 2 - 7.7 MeV. An extensive effort has been made to identify sources of background neutrons and reduce their effect on activation measurements. The main sources of these background neutrons were found to be charged particle reactions in the target materials and secondary neutrons from non-elastic reactions of neutrons in the sample and surrounding materials. The $^{115}In(n,\gamma)$ cross section was selected for this investigation. This cross section falls off rather sharply with increasing neutron energy so low energy background neutrons can be a significant problem. The measurements were made relative to the $^{115}In(n,n')$ cross section which allowed the reaction rate and flux determination to be made with the same sample. In addition to the results of the background investigation the cross section was also determined. The uncertainties obtained were typically 10-20%. At the higher neutron energies, the cross sections obtained are lower than previous measurements. Preliminary results on the $Au(n,\gamma)$ cross section were also obtained in this investigation.

These measurements fall systematically below the ENDF/B-V evaluation for $E_n \geq$ 3 MeV. Some comments were made by participants of the AGM concerning the usefulness of the gold capture standard for neutron energies above ~ 1 MeV where the cross section is small and background can be a significant problem.

Dr. Cosack then presented a paper on the influence of target scattered neutrons in cross section measurements. The work was motivated by a recent international intercomparison of fluence measurements for monoenergetic fast neutrons. The scattered neutron problem caused considerable difficulty in this intercomparison. A Monte-Carlo program was written which simulates the experimental situation for neutron scattering in the target materials. The program calculates the fluence, spectral distribution and time-of-flight distribution for neutrons which interact with the target materials. Comparisons of measured and calculated time-of-flight spectra at 570 keV obtained with a lithium glass detector are in reasonable agreement. The differences in these spectra are believed to be due mainly to measurement problems. The total fluence of scattered neutrons was determined to be 1.3% of the fluence at this energy.

Recommendation: Further work on this technique is recommended in an effort to understand the international intercomparison results.

In addition to the work reported on at this session, a paper titled "Comments to the Evaluation of Fast Neutron Capture by ^{197}Au Given in the Book of Standard Nuclear Data" by V.A. Tolstikov was distributed to the particpants at the AGM. In this paper the author points out that the gold capture standard does not have a good data base for high neutron energies. He advocates the use of the cross section as a standard from neutron energies below 200 keV by properly handling the structure in the cross section. The author notes that significant new data have been obtained since the ENDF/B-V evaluation and suggests that a new evauation be performed.

SUMMARY OF SESSION IV

Chairman: M.G. Sowerby

This session considered the fission cross-sections of U-235 and U-238, six papers dealing with U-235 and 3 papers with U-238. In addition a short presentation of the U-235 fission cross-section evaluation of Konshin (USSR) was made. Throughout the session comparisons were made with the ENDF/B-V data though we had heard in the first session of the meeting that the preliminary U-235 ENDF/B-VI evaluation was approximately the same as version V above 4 MeV but 1-2% lower from 1 to 4 MeV and ~2% lower from 0.1 to 1 MeV. The papers considered are listed below.

(1) "Review of recent measurements of the U-235 fission cross-section and fission fragment angular distribution between 0.1 and 20 MeV"
M. G. Sowerby and B. H. Patrick

(2) "New results on the U-235(n,f) fission integrals"
C. Wagemans and A. J. Deruytter

(3) "Absolute measurements of the U-235(n,f) cross-section for neutron energies from 0.3 to 3 MeV"
A. D. Carlson, J. W. Behrens, R. G. Johnson and G. E. Cooper

(4) "AEP measurements of U-235(n,f) and U-238(n,f) cross-section"
Yuan Hanrong

(5) "Absolute measurement of the U-235 fission cross-section at 4.45 MeV neutron energy using the time correlated associated particle method (TCAPM)"
R. Arlt, C. M. Herbach, M. Josch, G. Musiol, H. G. Ortlepp, G. Pausch, W. Wagner, L. V. Drapchinsky, E. A. Ganza, O. I. Kostochkin, S. S. Kovalenko and V. I. Shpakov.

(6) "Fission fragment mass, kinetic energy and angular distribution for U-235(n,f) in the neutron energy range from thermal to 6 MeV"
Ch. Straede, C. Budtz-Jørgensen and H.-H. Knitter

(7) "The U-238 fission cross-section, threshold to 20 MeV"
Y. Kanda

(8) "Neutron induced fission cross-section of U-238 in the second plateau region"
A. A. Goverdovsky

In addition the following paper was presented in Working Group Session 11 but will be considered in this summary.

"Fission ratios involving U-238, Np-237, Pu-239 and U-235 fission cross-sections"
Y. Kanda and Y. Uenohara

In the first paper Sowerby and Patrick reviewed the U-235 data between 0.1 and 20 MeV. They found that

(1) there had been few new data since 1978
(2) the new data tend to be lower than B-V from 0.1-1 and 2.5-5 MeV
(3) time correlated associated particle type measurements tend to be lower than measurements by other techniques
(4) revisions to B-V are constrained by accurate fission spectrum averages
(5) there were too many reviews of the data and too few new measurements
(6) the recommendations of the Smolenice meeting (IAEA(NDS)-146) were endorsed and in particular it was noted that
    (i) the ±1% accuracy needed has not been achieved, except perhaps at 14 MeV
    (ii) the best way to achieve this accuracy seems to be the measurement of accurate spot points which can be used to normalise good shape determinations
(7) the required accuracy of ±1% is unlikely to be achieved unless
    (i) there are improvements in the measurement of neutron flux and in the accuracy of the H(n,n) cross-section (as given in ENDF/B-V)*
    (ii) tests are performed to confirm that the TCAP method is free from serious systematic error (Dr. Poenitz in the discussion showed how random coincidences between the correlated particles and background fission events might produce errors)

---

*The accuracy of the H(n,n) cross-section and its angular distribution were discussed by the meeting. The new evaluation of Dodder and Hale accepted for ENDF/B-VI has a lower uncertainty than ENDF/B-V and Poenitz felt that the cross-section is well known below 3 MeV (±0.3%). At higher energies uncertainties in the angular distribution become more important and it was believed that the data will not always be accurate enough over the whole energy range to 20 MeV to permit flux measurements to be made to an accuracy of ±0.7%.

In the second paper Wagemans and Deruytter reported new results on the U-235 fission integrals from 7.8 to 11 eV (I_1) and 0.1 to 1 keV (I_2) made with an improved experimental arrangement. Considering their new data together with the previous measurements they find that I_1 is 246±2 b.eV if the thermal cross-section is assumed to be 587.6 b. However, there are problems with I_2; the ratio I_2/I_1 seems to depend on whether the incident neutron flux was measured using the B-10(n,α) or the Li-6(n,α) cross-section. All values of I_2/I_1 based on Li-6 are lower than any ratio based on B-10 with the average ratio being 4% lower. Further work is requested to resolve this problem (Corvi in Session 7, however, showed data indicating that I_2/I_1 will be the same whether B or Li is used). It is unlikely therefore that there are errors in the assumed energy dependence of the boron and lithium cross-sections; errors are more likely in their use in practical detectors. However, as Knitter pointed out, the angular distributions of the (n,α) reactions may produce problems.

Carlson et al reported on the absolute measurements made between 0.3 and 3 MeV with the NBS Linac. These excellent data are the first absolute measurements made with a Linac and have a total uncertainty of ~±2%. The measurements use the same fission chamber and black detector as Wasson et al employed on the Van de Graaff between 0.2 and 1.2 MeV. The data agree with other recent measurements though they tend to be lower than the other data below ~1 MeV. They also suggest that ENDF/B-V should be revised downwards between 0.3 and 3 MeV.

Yuan discussed the many AEP measurements of the U-235 fission cross-section made since ~1964 and also gave some recent absolute U-238 data (some of the U-235 measurements are relative to the fission cross-sections of U-233 and Pu-239). The measurements were made using the AEP Van de Graaff, Cockcroft-Walton and heavy water moderator reactor. Five measurements concern the thermal and resonance energy range, the remainder are in the energy ranges 0.03 - 5.6 MeV and/or 14-18 MeV. On the whole the U-235 data agree with the other available data. However, in view of the discrepacies in the present data base around 2.5 MeV an absolute measurement is to be made at this energy using the TCAP methods. The new U-238 absolute data between 4 and 5.5 MeV are greater than the ENDF/B-V evaluation and agree with JENDL-2. In view of the ~10% spread in data for the U-238/U-235 fission ratio above ~10 MeV a measurement of the U-238 fission cross-section is to be made in the 14 MeV energy range.

Blinov presented the paper of Arlt et al on the U-235 fission cross-section at 4.45 MeV neutron energy measured using the time correlated associated particle technique. The accurate and careful measurement, which was made following the recommendation of the IAEA Consultants' Meeting at Smolenice, gives a value which is lower than ENDF/B-V. The error of 2.1% is dominated by errors in areal density, homogeneity and statistics. Further efforts will be directed to more precise measurements of the areal density.

Blinov then briefly discussed the evaluation of the U-235 fission cross-section by Konshin where special attention was given to the evaluation of the error. The evaluation, which was carried out in two energy regions 100 eV to 100 keV and 100 keV to 20 MeV, agrees with the ENDF/B-V evaluation to within 1% and has similar errors. It was found that the existing data base is not consistent and that the quoted errors in some measurements are too small. It was proposed that there should be an exchange of programmes for the calculation of the corrections applied to the measurements.

Straede et al presented some very elegant measurements of the fission fragment mass, kinetic energy and angular distribution of fission fragments for U-235 in the neutron energy range thermal to 6 MeV. These impressive data were obtained using a double Frisch gridded ion chamber which provides information on the energy and angle of both fission fragments. The angular anisotrophy obtained agrees well with the evaluation of Kapoor.

Kanda reviewed the U-238 fission cross-section data produced since the 1976 Specialists' Meeting at the Argonne. Ten new measurements have been reported in this period and almost all of these agree well with the previous data and evaluations. The cross-sections in the 14 MeV energy range are well known though there are still some shape differences between measurements at higher energies. The available data appear to meet the users' requests over the energy range 1.5 to 15 MeV, but it is still desirable to improve the data base. There is structure in the cross-section around 2 MeV and this may be a possible limitation in U-238(n,f) as a standard.

Kornilov presented the comments of Goverdovsky on the evaluation of U-238 in the region of the second plateau (5-10 MeV). The data in this energy range appear to be higher from monoenergetic measurements made with electrostatic accelerators than measurements made with white sources. Goverdovsky felt that more weight should be given to the monoenergetic data in future evaluations.

Kanda and Uenohara surveyed the fission cross-sections of the actinides to see which would be the best to use as standards. They selected U-235, U-238, Np-237 and Pu-239 as the most suitable candidates and then investigated the available data base for the four cross-sections. They suggested that the four should be evaluated together and that the user should select from them the most appropriate standard for his application. In order to improve the data base they recommended that the ratios between the four cross-sections should be precisely determined and that absolute fission cross-section measurements should also be made.

Conclusions

(1) The fission cross-section of U-235 is not known to the required ±1% accuracy and additional work which emphasises either different techniques and/or aims for accuracies of ~±1% is needed.

(2) The U-238 fission cross-section data meet the required accuracy though as it is a standard further improvements are necessary.

(3) The ±1% accuracy required for U-235 will not be achieved unless there are improvements in the accuracy of flux measurements.

(4) There is a continuing need for inter-comparisons of neutron flux measurement techniques.

(5) Corrections applied to fission and neutron flux measurements are very important and it is desirable to compare the methods of calculation and their results.

(6) The recommendations made by the IAEA Consultants' Meeting on the U-235 Fast Neutron Fission Cross-section at Smolenice are endorsed.

SUMMARY OF SESSION V

Chairman: E.J. Axton

Two papers were presented on the simultaneous evaluation of the thermal parameters of the fissile nuclides and $\bar{\nu}_T$ for ^{252}Cf by Axton and by Divadeenam and Stehn, the latter presented by Dr. Carlson.

Conclusions which may be drawn from these two papers are:

1. Apart from the relatively unimportant scattering cross sections (which were treated differently), there are no significant differences in the fitted parameters.

2. In general, but not in all cases, Axton's uncertainties in the fitted parameters are slightly larger than those of Divadeenam due to the inclusion of more correlations.

3. The correlations in the uncertainties of the fitted values are significantly greater in the case of Axton's results. For example, for each nuclide the average correlation between σ_a, σ_f, and eta, is 86%, and between σ_c, and α, is 95%.

4. The authors agree that the inclusion of the input covariance matrix places the estimates of the output uncertainties on a more realistic basis.

5. More of the measurements would benefit from reinterpretation along the lines of Axton's third appendix, and as recommended by W. Poenitz in his working group session on Wednesday morning.

6. There still seem to be some differences occurring when the parameters are fitted with a data set which exludes the Maxwellian data. See for example Axton's table six. These are principally the ~9% difference in σ_c and α for ^{233}U, about 2% difference in σ_c and α for ^{235}U, and 2.5b difference in σ_f for ^{235}U.
   However, these differences must not be confused with discrepancies. The distribution of residuals obtained with the complete data set reveals a reasonably normal distribution, but with less than the

expected number of measurements which differ by more than one or more than two standard deviations from the fitted values. The above differences are therefore not regarded as discrepancies.

Likewise the difference between the Spencer et al. and Axton et al. measurements of $\bar{\nu}_T$ for ^{252}Cf cannot be regarded as discrepant. It follows naturally from the assumption of a normal distribution of input uncertainties.

7. Even in 1984 authors are still not presenting sufficient information on their various contributions to overall uncertainty. In particular information on correlations is missing. Further efforts are needed to persuade authors to provide sufficient information such as that listed by W. Poenitz in his working group session.

8. Divadeenam suggested remeasurements of some key cross sections, and eta and alpha values, and also Monte Carlo evaluations of more of the Maxwellian spectrum-based measurements.

9. Axton suggests that further work on this subject should be preceded by a simultaneous evaluation of the standard reference thermal neutron cross section involved in the study.

10. If the fitted parameters are propagated into reactor calculations, they should <u>always</u> be accompanied by the appropriate correlation matrix.

    However, before any further effort is expanded on this subject the potential users of the data should be canvassed to determine whether or not their requirements have already been met.

The third contribution to this session was by C. Wagemans and A.J. Deruytter who described some preliminary measurements on the sub thermal ^{235}U fission cross section.

The fission cross section below 20 meV contributed about 25% to the Westcott g_f factor at 20.44°C and it thus introduces a significant uncertainty to g_f which is correlated with the values at other temperatures.

These values are very relevant to the thermal constants evaluations discussed earlier.

It is hoped that when the data become final they will be used to produce a new table of temperature-dependent g_f factors.

SPECIFIC RECOMMENDATIONS

1* It is again necessary to stress to authors the importance of providing full information on the various contributions to the uncertainty of their measurements and the correlations between them.

2. A simultaneous evaluation standard thermal neutron cross sections such as hydrogen, boron, gold, cobalt, manganese and sodium is required. This would improve not only the status of the standards but also that of other thermal cross sections measured relative to the standards, and of many fast neutron cross sections as well.

[Specific to Session V]

3. Before recommending any further work on the evaluation of the thermal constants of the fissile nuclides and $\bar{\nu}_T$ for ^{252}Cf, potential users of the fitted data should be convinced to determine whether or not their requirements have already been met.

4. When the fitted values re propagated into reactor calculations they should <u>always</u> be accompanied by the associated correlation matrix.

---

* There should be a reference to a comprehensive list of required information such as that produced by Dr. Poenitz in his Working Group Session.

SUMMARY OF SESSION VI

Chairman: J.W. Boldeman

In Session VI, two aspects of neutron standard reference data were discussed:

1. The absolute value of $\bar{\nu}$ for ^{252}Cf, the $\bar{\nu}$ ratios and the P_ν distributions.

2. The prompt neutron spectrum from the spontaneous fission of ^{252}Cf.

In all two papers were devoted to the first item while the second item was the most thoroughly discussed aspect of standard data with 11 papers devoted to the subject.

1. Nubar Data

The first paper in the session from Holden and Zucker dealt with a recent evaluation of the $\bar{\nu}$ ratios and the P_ν probability distributions. This work responded to the requirements of the safeguards community for accurate nuclear data for neutron coincidence counting systems.

It was concluded that excellent agreement exists between the different measurements of the $\bar{\nu}$ ratios and that no further experimental data of this kind is required at the moment. It was noted that the agreement between the different measurements of the neutron probability distributions were in reasonable agreement. However, some improvement in the data may become necessary as more sophisticated neutron coincidence counting systems are developed.

The second paper on this topic presented by Boldeman, outlined the status of the absolute value of $\bar{\nu}$ for the spontaneous fission of ^{252}Cf.

It was concluded that from the viewpoint of nuclear power applications the data were adequate and any further measurements were

unlikely to have any impact upon the evaluated figure. However, it was noted that there is probability a small discrepancy within the liquid scintillator measurements. This matter could be relevant within the context of neutron coincidence counting methods for safeguards applications and therefore some experimental effort to investigate this problem was justified.

2. The Prompt Neutron Spectrum from the Spontaneous Fission of ^{252}Cf

This part of the session was introduced by Seeliger who presented a status report of the data and some recent theoretical calculations with which he had been associated. In his review an exhaustive analysis was presented of the important experimental considerations that should be taken into account in accurate measurements. The theoretical descriptions of the data discussed, included various versions of the Madland-Nix Model, the generalized Madland-Nix Model, the Complex Evaporation Model of Seeliger and Hauser-Feshbach calculations. Finally a comparison of the experimental data was presented.

The next paper in the session was delivered by Madland. The parameters for two representations of the Poenitz data, namely Maxwellian and Madland-Nix, were derived. From a comparison of the integrated cross sections for a number of threshold reactions calculated using these two representations and the NBS spectrum with actual integral data, it was clear that a Maxwellian description was inadequate. On the other hand, the NBS and Madland-Nix representations produced data that were in accord with the various integral experiments, but the NBS spectrum is in clear disagreement with the spectrum of Poenitz.

Following this theoretical paper, Blinov reviewed recent experimental determinations at his laboratory and at other institutes in the Soviet Union. The presentation also included a discussion of the recent statistical model calculations of Gerasimenko. The experimental data presented were consistent with a Maxwellian description with T = 1.42 MeV at energies below 1 MeV. In the region 1 MeV to 6 MeV the data were consistent with the same Maxwellian determination but they were also consistent with the data from ANL

which showed a small positive deviation from the Maxwellian in the vicinity of 2.3 MeV. Above 6 MeV, the data were in accord with the almost general trend of other recent experimental data in showing a clear negative deviation from the Maxwellian shape based on a T = 1.42 MeV.

A paper dealing with the first results fom an evaluation of the spectrum was then presented by Mannhart. This presentation began with a plea to all experimentalists to document completely the experimental data and all aspects of the experimental method so that a full assessment could be made of their experiment. The preliminary results from this evaluation parallel the conclusions of Madland that a single Maxwellian description was inadequate. The spectrum was represented by a Maxwellian shape with T = 1.42 MeV from 0 to 6 MeV and above that energy by the NBS evaluation.

Based on integral data alone, no substantial deviation from this shape was identified in the evaluation. In addition, a preliminary covariance matrix with reduced uncertainties in the high energy range has been obtained.

The next paper in the session was presented by Boldeman. This presentation described a number of measurements of the ^{252}Cf fission neutron spectrum in the range from 0.124 MeV to 15 MeV. These data disagreed with other recent experiments in that the departure of the spectrum from the Maxwellian shape above 6 MeV was not seen. In this experiment provision was made for sources of experimental errors that have recently been identified as important in fission spectrum measurements. It was suggested that the efficiency curve of the neutron detection at energies above 6 MeV be reinvestigated.

This presentation was followed by one from Seeliger who presented recent measurements of the spectrum in the very high energy range that were made at Dresden by Märten and in collaboration with PTB. These experimental data supported recent experiments in showing the negative departure from the Maxwellian distribution above 6 MeV.

However, the most important aspect of this experimental work was the confirmation of a large excess of neutrons, above 20 MeV. This departure is now considered to be a real effect.

The recent measurements of the prompt neutron spectra for the energy range 30 keV - 4 MeV from the thermal neutron fission of ^{233}U, ^{235}U and ^{239}Pu were then described by Lajtai. The presentation included a complete description of the experimental system. The data were analysed using a Maxwellian distribution. For thermal neutron fission of ^{233}U, ^{235}U and ^{239}Pu, the data could be reproduced using Maxwellian descriptions with temperatures of T = 1.32, 1.315 and 1.38 MeV respectively.

The following paper by Budtz-Jörgensen described the experimental program at the CBNM laboratory which aims to measure the complete neutron emission data, $N(E_n, O, M, E_T)$, for the spontaneous fission of ^{252}Cf. Preliminary data were presented which showed the fission neutron spectrum at various angles with respect to the fragment deviations. The data were compared with those from the measurement of Bowman et al.

Finally, Carlson presented a summary of the status of the research program of Schröder et al. at NBS which aims to measure with high precision the integral cross section of ^{235}U in a ^{252}Cf spontaneous fission neutron spectrum.

Conclusions and Recommendations

In deriving the recommendations presented below the recommendations and presentations from the IAEA Specialists Meeting on the Prompt Fission Neutron Spectrum from the Spontaneous Fission of ^{252}Cf held in Smolenice 1983, were added to the deliberations of this meeting.

1. It is important that a complete evaluation of the differential pointwise data from all adequately described experiments be completed in order to obtain the optimum representation of the experimental evidence of the prompt fission neutron spectrum from the spontaneous fission of ^{252}Cf. In this context it is strongly recommended that

all experimental teams provide complete documentation of all aspects of their experiments. The data must be presented in tabular form with uncertainty components for all data points. For a visual presentation of the shape of the data, a ratio plot of the data relative to a Maxwellian distribution with T = 1.42 MeV would be valuable.

2. When a final recommended set of data becomes available an analytical description of the evaluated data using the Madland-Nix Model, the improvements made on this model (generalized Madland-Nix Model) from Seeliger at TUD or the Complex Evaporation Model (also TUD) should be pursued. However, it is considered that in the long term a complete description by a full Hauser-Feshbach calculation would be desirable. Continued work by Browne and Dietrich, Rubchenaya, Gerasimenko and Madland-Nix is supported.

3. To assist the development of the various theoretical models better basic data of the mechanism involved in the neutron emission process in spontaneous fission of ^{252}Cf are needed. The experimental program at the CBNM, RIL and at other laboratories on the study of these processes is commended. The experimental data will also allow improved corrections to be made in the spectrum measurements.

4. As a temporary measure until the completion of the evaluation of the differential data, a recommended shape for the prompt neutron spectrum from spontaneous fission of ^{252}Cf is required. This problem was also addressed at the Smolenice meeting. At that meeting a renormalized two component shape for the spectrum was adopted. The energy range from 0.01 to 6 MeV was represented by a Maxwellian with T = 1.42 MeV and the NBS evaluation used for higher energies. Since that time there has been real development in the theoretical description of the spectrum, so that a physically more realistic shape can be derived. In the energy range 0.5 to 10 MeV, the Madland-Nix, generalized Madland-Nix, Complex Evaporation Model and the Statistical calculation all reproduce reasonably well the shape of the spectrum and are therefore in agreement with each other. Therefore for this energy range these theoretical shapes can be recommended. The numerical data for all four representations should

be transmitted to the IAEA immediately. For the representation of the spectrum outside this energy range the Complex Evaporation Model can be used.

5. When the evaluation of the differential data has been completed, it is proposed that the IAEA convene a meeting in Vienna to consider the outcome and consequences of the evaluation.

6. The status of $\bar{\nu}$ data was considered to be adequate for reactor calculations. The experimental data for the $\bar{\nu}$ ratios were in excellent agreement while the agreement in the P_ν values was regarded as acceptable. For the absolute value of $\bar{\nu}$ for ^{252}Cf, the agreement of the data was such that any future measurement would be unlikely to have any effect on an evaluated value. However, it was noted that a small discrepancy probably existed between liquid scintillator determinations and some research to resolve this problem could be justified for safeguards applications.

SUMMARY OF SESSION VII

Chairman: H. Condé

The possibility to determine neutron fluences is in many cases the limiting factor on the accuracy of a cross section measurement. If a cross section shall be measured with e.g. 1 percent uncertainty, the neutron fluence must be measured with an accuracy of 0.7 - 0.8 percent or better.

The choice of detector and experimental technique for the fluence measurement is depending on the characteristics of the neutron source, background conditions, etc.

The international fluence rate intercomparison under the auspices of BIPM for 0.14, 0.565, 2.5, 5.0 and 14 MeV neutrons reviewed by Liskien and Ryves gives an indication of the state of art of fluence measurements for monoenergetic neutron ources. The results up to now give a fairly good overall consistency within $\pm$ (2 - 3)% but larger deviations are observed between individual measurements.

A thorough evaluation of the intercomparison activity should be done before any further steps are proposed.

In the efforts to improve the accuracy of fluence measurements many corrections have to be carefully investigated.

Two papers were presented on the subject, one dealing with the associated particle method by Michikawa and one with proton recoil detectors by Cosack et al.

Michikawa reported about a correction due to the ingrowth of ^{3}He in old tritium targets. Above 300 - 400 keV neutron energy the ^{3}He(d,p)α reaction gave a considerable contribution to the alpha production rate for a 2 year old target ($\sim$10 percent). The work underlines the importance of using the time correlated associated particle method above 15.5 MeV neutron energy if high accuracy is requested.

The uncertainties connected with different effects in proton recoil detector mesurements at 6 and 14 MeV were estimated in the work by Cosack et al. The total uncertainty was more than 2 percent, mainly due to uncertainties of the H(n,n) cross section, the number of protons in the radiator and background pulses. The work points to the fact that without a substantial improvement of the accuracies in the H(n,n) total and differential cross sections, a 1-procent accuracy in flux determination is not within reach using proton recoil detectors

at higher energies above about 10 MeV. The problems with estimating the number of protons in the radiator were further discussed in the Working Group Session III.

A good agreement was reported by A. Carlson between the calculated and the experimentally determined efficiency of 2.3 MeV of the NBS black neutron detector. The efficiency was measured with an accuracy of 1.2% using the TPAC method. The biggest systematic error with the associated particle counting was estimated to be 0.6 percent. This underlines the high potential of the TCAP method for measurements of monoenergetic neutron fluences.

Aside of a report about the neutron fluence rate measurement using the associated particle method at BIPM, V.D. Huynh gave information of radioactive neutron source strength measurement using a Mn-bath. The accuracy obtained was 1 percent and 0.4 percent for the (α,n)- and (γ,n)-type sources, respectively.

Three papers were devoted to flux detectors and measurement techniques with white neutron source.

Gayther reviewed the status and dealt with both "flat response" detectors and "standard cross-section detectors". No single detector meets the request to cover the full energy range of commonly used white sources with good accuracy (1-2%).

Among the "flat response detectors" the black detectors (ORNL, NBS and ANL) give a higher accuracy (~ 1 percent) than other alternatives as e.g. boron-vaseline sphere (~2%).

Among the detectors based on standard cross sections the "2π-ionization chamber" utilizing the $^{10}B(n,\alpha)$-reaction gives the best accuracy (~ 2 percent) below 100 keV and the recently developed "double scintillator" at NBS (~ 2 percent) above 1 MeV.

Two papers were presented from CBNM by S. Wartena and F. Corvi about low and high efficiency detectors used at GELINA. Spectral ratio measurement using ^{6}LiF-, ^{10}B- and ^{235}U-ionization chambers between 8 eV and 100 keV was reported. The ratio between the ^{6}LiF and ^{10}B-ionization chambers was constant within 1.1 and 3.4 percent in the incident energy range from 8 eV to 10 keV and from 8 eV to 30 keV, respectively. At energies above 30 keV a larger change in the ratio was observed which had to do with problems concerning the gamma-ray background in ^{6}Li-detector.

For the high efficiency detectors results were reported by Corvi of intercomparisons of flux measurements using a ^{6}Li glass scintillator against a

^{10}B double gridded ionization chamber and a ^{235}U fission chamber. The ^{6}Li glass to ^{10}B ionization chamber intercomparison was in agreement within $\pm$ 2% from 5 eV up to about 10 keV. Above 10 keV the measurements disagree by as much as 10 percent at 30 keV.

The fission cross section of ^{235}U measured relative to $^{6}Li(n,\alpha)$ cross section was within the estimated uncertainty of 2.5 percent in agreement with the same value calculated from ENDF/B-V.

As a summary white neutron source fluence rate can be measured with an accuracy of about 2 percent over most of the energy range and over certain restricted regions covered by the block detection to the order of 1%.

CONCLUSIONS

1. Await outcome of the BIPM intercomparison before deciding further work of that type.
2. Improvement is needed of the total and differential H(n,n) cross section before the fluence rate can be measured to 1 percent accuracy using proton recoil detectors.
3. Investigations should be encouraged to check the uncertainties of the TCAP method.
4. Further developments of detectors like the NBS dual thin scintillation and the Geel gridded chamber are encouraged.
5. Information about neutron fluence detectors should be included in relevant cross-section status reports of the updated version of the standard file.

SUMMARY OF SESSION VIII

Chairman: D. Seeliger

At the Session on Neutron Energy Standards there have been presented only three talks by Sowerby (James), Wiedling and Cosack.

From the review presented by Sowerby have been derived the following conclusions:

(1) Resulting from new experiments at Karlsruhe and Geel, energies of 3 Standards should be revised. New values are

C-12 2078.43 $\pm$ 0.48 keV

C-12 6296.80 $\pm$ 0.39 keV

C-12 12.1 MeV (Exact value awaited)

(2) Following the suggestion by Priesmeyer, the oscillator level at 0.12 eV for protons in ZrH should be adopted as a standard. (Further work required to define energy more precisely).

(3) Discrepancy between Geel data and recommended values for 5 resonances in ^{56}Fe, ^{32}S, ^{16}O and ^{12}C should be resolved.

(4) All data used to produce recommended values should be reanalyzed taking account of covariances in the averaging.

(5) Additional standards below 0.1 eV are required for measurements of cross sections as well as solid state structures at white neutron sources. Suitable candidates could be the edges of C, Be, Fe and MgO.

By Wiedling some proposals for the energy calibration of neutron TOF spectrometers were presented. The energy calibration of a neutron time-of-flight spectrometer can be made with good accuracy by use of neutron lines produced by the $T(p,n)^3He$, $T(d,n)^4He$, and $^9Be(d,n)^{10}B$ reactions with a well energy calibrated accelerator facility.

Beryllium would be one possible choice of target material and would also be advantageous to use since several neutron groups of wellknown

energies are emitted at each used deuteron energy in the $^{9}Be(d,n)^{10}B$ reaction.

By Cosack an information was given on the neutron energies selected by the ISO for calibration of radiation protection instruments.

The International Organization of Standardization (ISO/TC85/SC2/WG2) is concerned with standardizing reference radiations for calibrations of radiation protection instruments. It selected radionuclide neutron sources: ^{252}Cf, ^{252}Cf in D_2O moderator (diam.: 30 cm), ^{241}Am Be(α,n) and ^{241}Am B(α,n). A list of monoenergetic neutron energies was put up for the purpose of determining the response as a function of neutron energy.

The reason was, to make the results of type tests of instruments and the legal requirements in different states easily exchangeable. The advantage of intercomparisons of calibration at the same fixed energies is obvious.

There may exist the problem to make fluence measurements or cross section determinations directly comparable without inter- or extrapolation. For this reason it is advisable to put up a list of preferable energies which should be taken in cross section measurements. This can be a guide, at which energies experiments should be carried out if there are no other reasons for a different choice. It could help to improve the normalization of data from different investigations.

Recommendations to the IAEA:

- By the INDC Standards S.C. the choice of a definite new standard below 0.1 eV should be recommended. The status of the mentioned above neutron energy standards to be reviewed at the next INDC meeting.

- By the INDC S.C. "B" should be considered the proposal on having a list of preferable energies for cross section measurements.

- The status of neutron energy standards should be presented in a review at the IAEA AGM on Neutron Sources in Leningrad, 1986.

SUMMARY OF SESSION IX

Chairman: C.W. Reich

The following invited papers were presented at this session:

"Actinide Half-Lives as Standards for Nuclear Data Measurements: Current Status", by C.W. Reich;

"Emission Probabilities of Selected Gamma Rays for Radionuclides used as Detector-Calibration Standards", by R. Vaninbroukx; and

"Emission Probabilities of Selected X Rays for Radionuclides used as Detector-Calibration Standards", by W. Bambynek.

Two papers submitted to this Advisory Group Meeting by N.E. Holden were appropriate for this session. Their titles are

"Total and Spontaneous Fission Half-Lives of the Uranium and Plutonium Nuclides" and

"Total and Spontaneous Fission Half-Lives of the Americium and Curium Nuclides."

Since Holden was not present at this meeting, selected portions of his papers, giving the results of his half-life evaluations, were included as a portion of the oral presentation of C.W. Reich. Copies of the full text of these two papers were distributed to the conference participants.

The material in the paper of C.W. Reich was marked as "Preliminary Version Only." This was done because it was felt desirable that the half-life values given there be in agreement with those to be recommended by the IAEA Coordinated Research Programme (CRP) on the Measurement and Evaluation of Transactinium Isotope Nuclear Decay Data. The final research coordination meeting of this CRP was held in Vienna during the week 5-9 November, 1984, immediately preceding this Standards Advisory Group Meeting. Consequently, final "recommended" values for these half-lives were not available at the time of the preparation of this paper. The CRP-recommended values, however, are incorporated in the revised version of this paper, which is the one that will appear in the proceedings of this Advisory Group Meeting.

M.V. Blinov made a presentation giving the results of the evaluation of actinide-nuclide half-life values done within the Soviet Union by V.P. Chechev.

In his presentation, Blinov also gave a list of additional actinide nuclides and their half-life values that might be useful calibration standards. This information is included as Section VI of the paper

"IAEA Standards File: Some Comments and Recommendations", by M.V. Blinov et al.,

which is published in the proceedings of this AGM.

E.J. Axton pointed out that a new measurement of the ^{252}Cf half-life exists. This new value,

$$2.6509 \pm 0.0031 \text{ years},$$

is given in the paper

"Neutron Yield from the Spontaneous Fission of ^{252}Cf ($\bar{\nu}$), by E.J. Axton and A.G. Bardell,

which has been submitted for publication in the journal Metrologia.

J. Blachot asked about calibration standards in the region of 2.7 MeV, which would be useful in, e.g., short-lived fission-product studies. R. Vaninbroukx indicated that it was possible to do this, but he had not done it as a part of his work reported to this AGM.

No questions were raised regarding the paper on X-ray emission probabilities.

The following two points need to be brought to the attention of the participants in this AGM:

a) The "recommended" half-life values of ^{233}U, ^{234}U, ^{239}Pu and ^{241}Pu, based on direct measurement, are in excellent agreement with values deduced for them in the recent works of Divadeenam and Stehn and of Axton from an evaluation of the thermal-neutron constants of these nuclides. This former work has been published in the Journal of Nuclear Energy 11, 375 (1984), and this latter work, entitled "Evaluation of Thermal Neutron Constants of ^{233}U, ^{235}U, ^{239}Pu and ^{241}Pu and the Fission Neutron Yield of ^{252}Cf", will be published in the proceedings of this AGM.

b) While the overall status of the half-life values for the actinide nuclide considered here as standards has improved considerably in recent years, two cases warrant further study. The ^{237}Np half-life is based on the

results of only one measurement, and additional high-precision measurements to check the reliabilty of this value are called for. Additional work is needed to clarify the present situation regarding the ^{252}Cf half-life.

SUMMARY OF WORKING GROUP SESSION I

Chairman: W.P. Poenitz

The intend of this working group session was to consider the procedures presently used for the evaluation of reference cross section data, the requirements for the documentation of the experiments and for the reporting of the data.

There has been an increasing utilization of simultaneous evaluations in recent years. In contributions to this meeting the simultaneous evaluations of the thermal parameters by Axton and by Divadeenam and Steen were described, as well as a simultaneous evaluation of the fission neutron spectrum of ^{252}Cf by Mannhart. A presentation of a simultaneous evaluation of 14.7 MeV cross sections was made in this working group session by Ryves. The simultaneous evaluation of the experimental data of the reference cross sections and other principal cross sections for ENDF/B-VI was described by Poenitz. Generalized least-squares fits which include the variance-covariance information of the experimental data were used in the evaluations by Axton, by Mannhart and by Poenitz.

It was emphasized in the discussions that such combinations of multiple experimental observations are only a first step of the evaluation process. The least-squares fit of the experimental data retains the statistical scatter of the input data. It also does not yet include all knowledge achieved. Improvements will be obtained from the utilization of auxiliary parameters obtained from other experimental evidence in the unitary framework of nuclear models and other theoretical constraints. For ENDF/B-VI much of these benefits will come from the direct involvement of the R-matrix theory for the light elements.

The evaluation of the experimental data requires that originally measured values are available with information on uncertainty components and correlation information. Bastian explained in a short presentation a scheme utilized at CBNM to preserve uncertainty and correlation information for spectral data. An example of a data file used for the evaluation of ENDF/B-VI was discussed. It was emphasized that mainly the uncertainty components are required by the evaluation instead of a correlation matrix constructed by the experimentor. The correlation matrix is constructed

from the uncertainty components and cross-experiment correlation information given in the data file.

Requirements for experimental procedures were discussed as well, specifically in a part of the working group session devoted to the ^{252}Cf prompt-neutron emission spectrum. In a contribution on the experimental aspects of the Cf fission spectrum measurements, Klein stressed again the importance of several major effects which may not have been considered in measurements made prior to ~1979. It will be important to compare older as well as the new experiments against a checklist of effects which might be an influence on the measurement results. The question is not a specific effect in itself but whether it has been recognized and corrected for. It was discussed that it is important to have cross-checks on the uncertainties of detector efficiency determinations. The possibility of measuring a neutron source reaction cross section with the various detectors involved in the experiments was mentioned.

The improvements of the theoretical models were commented on, specificially the generally good agreement between them over the energy range from ~0.5 - 10 MeV which includes the major fraction of the neutron spectrum.

It is recommended that measurements of reference data should be reported in such way that reanalysis and updating of various components is possible.

Originally measured data, their uncertainty components and correlation information should be contained on data files.

Evaluations of standard data should utilize simultaneous evaluation techniques if such data are interrelated.

SUMMARY OF WORKING GROUP SESSION II

Chairman: H. Klein

Conclusions and Recommendations

The discussion of various topics can be summarized in three subsections:

(1) New Standards?

The working group did not reach agreement on definitely recommending a further cross section to be added to the current standard file.

(a) The activation reaction $^{56}Fe(n,p)^{56}Mn$

In particular, the proposal of K. Kudo (ETL, Japan) and T.B. Ryves (NPL, UK) that the evaluated $^{56}Fe(n,p)^{56}Mn$ activation cross section should become a reference standard was not accepted because the reaction $^{27}Al(n,\alpha)^{24}Na$ is already available as a standard in the same energy region. Nevertheless, the activation of natural Fe samples may be used as a reference taking advantage of the higher specific activity. For this purpose an evaluation is highly recommended.

(b) The reaction $^{3}He(n,p)T$

The total cross section of the reaction $^{3}He(n,p)T$ may again become a standard when the practical application in precise neutron fluence measurement has been successfully demonstrated in a wide energy range (NBS).

(c) The fission yields of ^{235}U

In the conclusion of his review of fission yield evaluations J. Blachot recommended to use selected isotopes of the recently evaluated fission yields of ^{235}U induced by thermal neutrons as a reference. The fission yields of ^{235}U must be evaluated for the

entire neutron region up to 20 MeV before this data set can be added to the standards file.

(2) Reference Data?

Reliable reference data were requested for experimental fields where the existing standards cannot be easily applied.

(a) Continuous neutron emission spectroscopy

In the 14 MeV region double differential neutron emission spectra $N(E_n, \vartheta_n)$ are requested for fission reactor design purposes (WRENDA 84). Suitable reference data are required in order to confirm the energy and efficiency calibration of the spectrometer as well as the analysis method. Due to the large variety of parameters (energy, sample size, angle, material) the evaluation should be performed for carefully selected examples only. As proposed by D. Seeliger, multiline and continuous spectra emitted at 90° from natural C, Nb, Fe and Pb samples should be available for certain experimental set-ups (typical energy, sample size and target-sample distance). Both the original as well as the corrected spectra should be passed on to the users.

(b) Neutron producing reactions as neutron flux standard

In his comprehensive review, M. Drosg showed that the differential cross section of various neutron-producing reactions is well known within uncertainties of less than ± 2 %. For practical reasons (projectile energies available, specifications of targets) it is recommended that absolute differential cross sections (complete angular distributions) of the $^{2}H(d,n)^{3}He$ reaction for projectile energies around 5 MeV and the zero degrees cross section for projectile energies above 3 MeV be applied as a neutron flux standard using a gas target. For relative calibration purposes the reactions $T(d,n)^{4}He$ and $T(p,n)^{3}He$ can also be considered. Regarding the data base, accuracies of ± 2 % can be obtained.

Uncertainties and the correlation matrix of the evaluated Legendre expansion coefficients are still not available, but are necessary

to make a reliable estimate of the uncertainties to be expected. An extended evaluation is therefore highly recommended.

(3) Request for a precise measurement

For the activation reaction $^{27}Al(n,\alpha)^{24}Na$ and the induced fission reaction $^{235}U(n,f)$, uncertainties of less than 1 % are achieved in the 14 MeV region. The performance of precise ratio measurements is encouraged in order to test these uncertainties obtained in independent evaluations.

In summary, we conclude that at the moment, new standards are not needed, but reliable reference data are required for various types of experiments and should therefore be evaluated.

SUMMARY OF WORKING GROUP SESSION III

Chairman: H. Liskien

In applying Neutron Standard Reference Data the overall uncertainty is not only determined by the uncertainty of the reference cross section. These other uncertainties depend on the detector system and should determine the requested accuracy for the reference cross section. The discussion was limited to the application of the standard reactions.

a) H(n,p) and
b) ^{235}U(n,f).

a) Concerning the application of the n-p scattering cross section, two new systems were presented: (1) The 'Dual Thin Scintillator Configuration' from NBS[1] which avoids multiscattering corrections, eliminates spectrum distortion by recoil escape, and yet has an efficiency of ~1% at ~10 MeV. At present its accuracy is verified by comparing with the AP-technique and repeating and extending an ^{235}U(n,f) experiment, where it replaces a black detector. (2) The use of a "Frisch-gridded ionization chamber" is presently under investigation at CBNM[2]. This system combines an advantageous 2π-geometry with good background rejection, because both proton recoil energy and recoil angle are determined. The presently used hydrogeneous radiator foils have proven to be insufficiently homogenous.

The discussion concentrated on the reliability of the hydrogen content for the used samples/detectors. While there had been difficulties with the long-term stability of thin plastic layers in the past, there seems to be no such problems with polyethylene and tristearine. A quantitative investigation at PTB, ETL and CBNM shows that such changes are not bigger than ± 0.1%. However, warnings were uttered concerning the homogeneity of bigger samples and concerning changes in the composition during sample processing. A general concern exists in obtaining reliable uncertainties for the chemical analysis of the hydrogen content of scintillators and thin radiator layers. At present such information is very often only

deduced from repetitive measurements with the same equipment. It is suggested that this problem is studied by sample producers and chemical analysists. Meanwhile, chemical analysis should be asked from more than one analytical laboratory, should cover all potential elements and the hydrogen reference material (benzoic acid, acetalinid etc.) should be known.

b) Concerning the application of the ^{235}U-fission cross section, progress has been made by employing a Frisch-gridded ionization chamber with plate distance greater than FF-range. This detector can also be used successfully for sample assay with obtainable accuracies of ~±0.3%[3]. It is desirable that this device replaces the usual 2π-α-particle counting. Low geometry α-particle counting is regarded as an independent method and should be applied additionally, if applicable.
Mass-intercomparison of 15 samples from 6 differently enriched materials has been finalized at ANL[4]. The analysis takes into account

- masses, as quoted by producers
- masses, derived from absolute α-counting
- 2πα-ratio measurements
- 28 FF-ratio measurements

Using these data in a least-squares adjustment results in best masses never deviating by more than 0.35% from the originally quoted masses. It is therefore concluded that - with the presently known ^{235}U(n,f) reference cross sections - the assay of U-235 layers is not essentially contributing to the overall uncertainties. A comparison of two foils from Dresden/Leningrad is presently performed at NBS.

Prompted by a request of INDC the working group discussed the future storage and distribution mechanism of internationally available U-235 foils. There was agreement that - if such a mechanism is introduced - such foils should be stored at one of the foil-producing laboratories and that IAEA should act as coordinator and mail-box.
Due to the absence (except CBNM) of experts from foil-producing laboratories no suggestion was made with respect to the storage laboratory.

However, many of the participants questioned the necessity and even the usefulness of such a storage and distribution mechanism. Arguments are

- foils are available by sale, without any restriction.
- characteristics of internationally available foils may not ideally suit the envisaged intercomparison.
- destructive analysis for internationally available foils is excluded.

1) "Application of the Dual Thin Scintillator neutron flux monitor in a $^{235}U(n,f)$ cross section measurement".
M.S. Dias et al.

2) "Investigation for a precise and efficient neutron fluence detector based on the n-p scattering process".
H.-H. Knitter et al.

3) Assaying of ^{235}U fission layers for nuclear measurements with a gridded ionization chamber".
C. Budtz-Jörgensen, H.-H. Knitter.

4) "Final Results of the International ^{235}U Sample Intercomparison and the Half-life of ^{234}U".
W.P. Poenitz, J.W. Meadows.

SUMMARY REPORT

Chairman: A.J. Deruytter

1. Introduction:

This Advisory Group Meeting organized at CBNM-Geel by INDC (IAEA) and NEANDC (OECD) Standard Subcommittee had a worldwide participation of experts and dealt with the selected set of standard cross-sections in their respective energy ranges that are used as references to measure partial cross-sections in order to avoid making absolute flux determinations. These cross-sections are H(n,n)H (1 keV to 20 MeV), $^{6}Li(n,t)^{4}He$ (thermal to 0.1 MeV), $^{10}B(n,\alpha)^{7}Li^{*}$ and $^{10}B(n, \alpha_{o} + \alpha_{1})^{7}Li$ (thermal to 0.2 MeV), C(n,n) (1 keV to 2.0 MeV), $^{197}Au(n,\gamma)^{198}Au$ (0.2 MeV to 3.5MeV), $^{235}U(n,f)$ FF (0.1 MeV to 20 MeV) and the ^{235}U FF anisotropies, $^{238}U(n,f)$ FF (threshold to 20 MeV), $^{27}Al(n,\alpha)^{24}Na$ (threshold to 20 MeV). This is the restricted set of standard reactions on which effort of real absolute work as well as evaluation effort are concentrated. They are the cross-sections and energy-regions selected in the INDC/NEANDC Standards File.

Other important standard data considered are: neutron energy standards; actinide half-lives; thermal parameters for ^{233}U, ^{235}U, ^{231}Pu, ^{241}Pu; nubar of ^{252}Cf and the prompt fission neutron spectrum of ^{252}Cf; decay data for radionuclides used as calibration standards.

Also neutron fluence intercomparisons were discussed.

Working group sessions dealt with (1) evaluation, documentation and presentation of reference data; (2) the question whether new standards are required; (3) improvements in detectors and measuring techniques leading to more accurate determinations and use of standards.

2. Reference cross-sections:

A first pass at determining the standards for ENDF/B-VI was reported by A. Carlson.

For the new ENDF standards evaluation it was felt that a simultaneous evaluation should be performed to assure consistent use of the available information. Thus ratio measurements of standard cross-sections will have an impact on the evaluation of each of the standard cross-sections in the ratio.

Correlations in the experimental data will also be taken into account in the simultaneous evaluation. This simultaneous evaluation is being performed with a generalized least squares programme and the cross-sections being evaluated are $^{6}Li(n,\alpha)$, $^{6}Li(n,n)$, $^{10}B(n,\alpha_o)$, $^{10}B(n,\alpha_1)$, $^{10}B(n,n)$, $^{197}Au(n,\gamma)$, $^{235}U(n,f)$, $^{238}U(n,\gamma)$ and $^{239}Pu(n,f)$. This evaluation uses a large data base file and a full covariance analysis is being performed. In this simultaneous evaluation the H(n,n) cross-section will be 'frozen' since it is quite well-known and the evaluation of Dodder and Haler is accepted as the hydrogen standard for ENDFB-VI. The simultaneous evaluation will yield pointwise cross-section data for the standards, $^{6}Li(n,t)$, $^{10}B(n,\alpha)$, $^{10}B(n,\alpha_1\gamma)$, $^{197}Au(n,\gamma)$ and $^{235}U(n,f)$.

The R-matrix method is being applied to the ^{6}Li and ^{10}B cross-section standards because such analysis provides coupling to reaction theory and gives a smooth meaningful analytical expression for the energy-dependence of the cross-section, and this method can take into account the charged particle reactions leading to the same compound nuclei (^{7}Li and ^{11}B) and utilize angular distribution data.

A procedure for combining the simultaneous and R-matrix evaluations has been defined but is not yet implemented.

The reviewed status of the n-^{6}Li reactions appear to be reasonably consistent with each other and do not indicate large changes from the ENDF/BV evaluation. New data for n-^{10}B (and a closer look at earlier data) show many internal discrepancies except at thermal and indicate some differences with the ENDF B-V cross-sections in the standards energy range, and possibly large differences above. It is recommended that $^{6}Li(n,t)$ be used as the standard below 100-150 keV until problems with the $^{10}B(n,\alpha)$ data base are resolved. Urgently needed are absolute $^{10}B(n,\alpha_1)$ measurements at a few energies in the 50 keV to 1 MeV range, or a detailed shape measurement that goes down to low enough energies to be strongly tied to the thermal values.

An evaluation of Kornilov of the $^{27}Al(n,\alpha)$ cross-section from 5.5 to 20MeV with an 8 parameter PADE approximation parameterization proved to be in agreement with ENDF/B-V. With the Vonach evaluation in the INDC/NEANDC Standards file it is only in agreement (2%) near 14 MeV. The Vonach evaluation is generally lower.

For $^{197}Au(n,\gamma)$ the evaluation in ENDF/B-VI is very similar to that of ENDF/B-V but there are changes of 5-6% in the range from 200 to 270 keV as a result of new data (Macklin and Kononov et al.) which show structure due to competition with inelastic scattering. The use of the cross-section as a standard

from neutron energies below 200 keV was advocated by properly handling the structure in the cross-section.

For ^{235}U(n,f) the preliminary ENDF/B-VI evaluation is approximately the same as version V above 4 MeV but 1-2% lower from 1 to 4 MeV and about 2% lower from 0.1 to 1 MeV. Sowerby and Patrick from their review concluded that the $\pm$ 1% accuracy has not been achieved, except perhaps at 14 MeV and that the way to achieve this accuracy seems to be measurements of accurate spot points which can be used to normalise good shape determinations. They also suggest as time correlated associated particle type measurements tend to be lower than other techniques that serious tests are performed to confirm that the TCAP method is free of serious systematic error (Measurement of Arlt at 4.45 MeV).

The thermal normalisation via the fission integral from 7.8 to 11 eV seems to be well settled as reported by Wagemans (246 $\pm$ 2 b.eV, 587.6b).

Carlson reported the first absolute data measured with a Linac with a total uncertainty of about 2%. The measurements use a fission chamber at 69 m and the black detector at 200 m. The data agree with other recent measurements though they tend to be lower than the other data below about 1MeV. They also suggest that ENDF B/V should be revised downwards between 0.3 and 3 MeV.

In view of the goal of 1% accuracy on σ_f ^{235}U corrections applied to fission and neutron flux measurements are very important. An elegant way of measuring fission fragment mass, kinetic energy and angular distribution was reported by Straede in the neutron energy range from thermal to 6 MeV.

The ^{238}U(n,f) data base meets the required accuracy, though as a standard further improvement is required, e.g. with respect to the structure in the cross-section around 2 MeV.

3. Other standard quantities:

The evaluations of the thermal neutron constants of ^{233}U, ^{235}U, ^{239}Pu and ^{241}Pu and the fission neutron yield of ^{252}Cf by Axton and Divadeenam and Stehn agree among each other and these data form by now a consistent set. The evaluation of Axton includes the input covariance matrix and places the estimates of the output uncertainties on a more realistic basis. First results of ^{235}U fission cross-section measurements in the meV region at GELINA with a liquid nitrogen cooled methane moderator were shown which should yield a new better based g_f-factor.

It was concluded that agreement exists between the different measurements of $\bar{\nu}$ and $\bar{\nu}$-ratios, although Boldeman stated that there is still a discrepancy between the most accurate liquid scintillator determination and the average of the $MnSO_4$ bath measurements.

The most thoroughly discussed aspect of standard data with 11 papers discussing the subject was the prompt neutron spectrum from the spontaneous fission of ^{252}Cf.

Theoretical models for the calculation of fission neutron spectra are based on the predominant emission mechanism, i.e. the evaporation from fully accelerated fission fragments. However, because of the complexity, practical calculations require several approximations. An exhaustive analysis of recent developments was presented by Seeliger including various versions of the Madland-Nix Model, the Generalized Madland-Nix Model, the Complex Evaporation Model of Seeliger and Hauser-Feshbach calculations all compared to recent experimental data and all of them relative to a Maxwellian distribution with T = 1.42 MeV, with the following conclusions:

1) recent experimental data are close to the Maxwellian for E < 1 MeV.

2) recent experimental data are in very good agreement between 1 and 5 MeV. They exceed the Maxwellian by about 3%.

3) in the 5 to 20 MeV region the data tend to be lower than the Maxwellian by -20% at 10 MeV and -25% at 16 MeV.

4) Recent theoretical calculations of the Cf neutron spectrum agree very well with measured data. The complex cascade evaporation model permits a description of recent experimental data in the whole energy range (1 keV - 20 MeV) when introducing the CMS anisotropy of emission.

Excess neutrons have been found above 20 MeV. They should be attributed to non-equilibrium emission.

In view of clarification of the fraction of so-called scission neutrons, first attempts to do multiple-differential measurements $N(E_n, \theta_n, A, TKE)$ with a gridded ionization chamber were reported at the meeting by Budtz-Jørgensen et al.

From a comparison of the integrated cross-sections for a number of threshold reactions calculated using three representations of Poenitz data with actual measured integral data, Madland clearly demonstrated that a Maxwellian

description was inadequate, but the other two, the NBS-spectrum and the Madland-Nix representations, were in accord.

Also Mannhart showed from measurements of integral cross-sections in a ^{252}Cf spectrum for a large number of reactions that a single Maxwellian description of the spectrum was inadequate. However, agreement was reached for a Maxwellian shape with T = 1.42 MeV from 0 to 6 MeV and above that energy the NBS evaluation.

The possibility to determine neutron fluences is in many cases the limiting factor on the accuracy of a cross-section measurement. If a cross-section shall be measured with e.g. 1% uncertainty, the neutron fluence must be measured with an accuracy of 0.7% or better. The BIPM fluence intercomparisons (0.14, 0.565, 2.5, 5.0 and 14.0 MeV neutrons) give the state of the art for monoenergetic sources: 2 to 3%.

Work at PTB (Cosack et al.) showed that without substantial improvement of the accuracies in the H(n,n) total and differential cross-sections a 1% accuracy in flux determination is not within reach using proton recoil detectors at E_n larger than about 10 MeV.

The efficiency of the NBS black neutron detector was measured at 2.3 MeV with an accuracy of 1.2% using the TCAP method which underlines the TCAP potential for measurements with monoenergetic sources.

In his review Gayther dealt with both 'flat response' detectors and 'standard cross-section detectors' and concluded that no single detector meets the request to cover the full energy range of commonly used white sources with good accuracy (1-2%). Among the 'flat response detectors' the black detectors (ORNL, NBS and ANL) give a higher accuracy (~1%). Among the detectors based on standard cross-sections the '2)(-ionization chamber' utilizing the $^{10}B(n,\alpha)$-reaction gives the best accuracy (~2%) below 100 keV and the recently developed 'double scintillator' at NBS (~2%) above 1 MeV. So white neutron source fluence rate can be measured with an accuracy of about 2% over most of the energy range and over certain restricted regions covered by the black detectors to the order of 1%.

In a session dealing with neutron energy standards several energies were updated and a new standard adopted, i.e. the oscillator level at 0.12 eV for protons in ZrH. Also additional standards below 0.1 eV are required, possibly the edges of C, Be, Fe and MgO.

The actinide-nuclide decay data were also considered in this meeting, especially the actinide half-lives used as standards for nuclear data standards.

It was also recognized that the existence of an internationally produced and accepted file of carefully evaluated decay data suitable for detector-efficiency caibration would be an extremely valuable contribution to the field of quantitative γ-ray spectrometry.

4. Working Group Sessions:

The first working group dealt with evaluation, documentation and presentation of reference data. There has been an increased utilization of simultaneous evaluations in recent years. At this meeting several such evaluations were presented. The generalized least-squares fits which include the variance-covariance information of the experimental data were used in the evaluations of Axton (thermal parameters), Mannhart (Cf neutron spectrum) and by Poenitz (ENDF/B-VI cross-sections). The least-squares fit of the experimental data retains the statistical scatter of the input data. It does not yet include all knowledge achieved. Improvements will be obtained from the utilization of auxiliary parameters obtained from other experimental evidence in the unitary framework of nuclear models and other theoretical constraints. (For ENDF/B-VI the direct involvement of R-matrix theory for the light elements). It was emphasized that mainly the uncertainty components are required by the evaluator instead of a correlation matrix constructed by the experimentor. The example of a data file used for the evaluation of ENDF/B-VI was discussed.

In the second working group no agreement was reached to recommend a further cross-section to be added to the current standards file. However, an evaluation of $^{56}Fe(n,p)^{56}Mn$ was recommended because of its advantage over $^{27}Al(n,\alpha)^{24}Na$ with respect to the higher specific activity. A set of several fission products from the ^{235}U fission were suggested as standards for fission yields measurements by the γ-spectrometry method. The data base: 'fission yields of these products as a function of neutron energy relative to the thermal values' is not complete.

Multiline and continuous spectra emitted under 90°, induced by 14 MeV neutrons should be available to confirm the calibration of the spectrometers as well as the analysis method. Suggested materials were natural C, Nb, Fe and Pb.

As a neutron producing reaction suitable as a neutron flux reference, for practical reasons (projectile energies available, specification of targets) it was recommended to apply the 0°-yield of the D(d,n) reaction as a neutron flux standard using a gas target in the energy region $E_d > 3$ MeV.

In applying neutron standard reference data, the overall uncertainty is not only determined by the uncertainty of the reference cross-section. These other uncertainties depend on the detector system and should determine the requested accuracy for the reference cross-section. In the third working group session the discussion was limited to the application of the standard reactions: H(n,p) and ^{235}U(n,f).

For H(n,p) two new systems were presented : (1) the dual thin scintillator configuration from NBS and (2) the use of a Frisch-gridded ionization chamber at CBNM. The discussion concentrated on the reliability of the hydrogen content for the used samples and detectors. Especially warnings were given concerning the homogeneity of larger samples and concerning changes in the composition during sample processing.

For ^{235}U(n,f) it was concluded that with the presently known ^{235}U(n,f) reference cross-sections the assay of ^{235}U-layers is not contributing essentally to the overall uncertainties.

SPECIFIC RECOMMENDATIONS TO THE IAEA (NUCLEAR DATA SECTION)

Chairman: A.J. Deruytter

I. General:

(1) The IAEA/NDS through the INDC should convene at regular intervals Advisory Group Meetings on Standards Reference Data. These meetings should preferably be linked with updatings of the INDC/NEANDC Standards File. (Session I).

(2) The IAEA/NDS through the INDC Standards Subcommittee should review the status of the standards discussed at this meeting and especially the neutron energy standards. In this respect a definite choice of an energy standard below 0.1 eV should be made (Session VIII).

(3) The IAEA/NDS through the INDC Subcommittee B should consider the proposal of having a list of preferable neutron energies where cross-sections are to be measured. (Session VIII).

(4) Prompted by a request of INDC the AGM discussed the future storage and distribution mechanism of internationally available U-235 foils. There was agreement that - if such a mechanism is introduced - such foils should be stored at one of the foil-producing laboratories and that IAEA should act as coordinator and mail-box.

Due to the absence (except CBNM) of experts from foil-producing laboratories no suggestion was made with respect to the storage laboratory (WG III).

II. The future of the INDC/NEANDC Standards File (Technical Report Series No. 227).

(1) The IAEA/NDS should give continuity by scheduled updatings to the publication of the INDC/NEANDC Standards File, in a format similar to the present Technical Report No. 227 (1983) (Session I.)

(2) The IAEA/NDS through INDC should care that under the item 'Thermal parameters for ^{233}U, ^{235}U, ^{239}Pu' in the Standards File advice is given on the use of the set, i.e. when the fitted values are propagated in reactor calculations they should always be accompanied by the associated correlation matrix. (Session V).

(3) The IAEA/NDS through INDC should care that information about neutron fluence detectors is included in relevant cross-section status reports of the updated version of the standards file. (Session VII).

III. The IAEA/NDS through INDC should convene (small) expert meetings on topics of special interest in the standards field. The following were recommended by this Advisory Group:

(1) There has been a real development in the theoretical description of the Cf 252 prompt neutron spectrum, so that a physically more realistic shape can be derived. In the energy range 0.5 to 10 MeV the Madland-Nix, Generalized Madland-Nix, Complex Evaporation Model and the Statistical Calculation all reproduce reasonably well the shape of the spectrum and are therefore in agreement with each other. Therefore for this energy range these theoretical shapes can be recommended. The numerical data for all four representations should be transmitted to the IAEA immediately. For the representation of the spectrum outside this energy range the Complex Evaporation Model can be used. When the evaluation of the differential data has been completed, it is proposed that the IAEA convene a meeting in Vienna to consider the outcome and consequences of the evaluation. (Session VI).

2. The need for a common base of radionuclide decay data to serve as standards for the efficiency calibration of gamma-ray detectors has become increasingly apparent over the past few years. A number of nuclides are presently being employed in various measurement laboratories for this purpose. The existence of an internationally produced and accepted file of carefully evaluated decay data suitable for detector-efficiency calibration would be an extremely valuable contribution to the field of quantitative gamma-ray spectrometry.

Accordingly, the participants in the Advisory Group Meeting on Nuclear Standard Reference Data agree that a meeting, convened by the IAEA of a small number of experts in precision gamma-ray spectrometry could make a major contribution. Those involved in such a meeting should examine the present status of the radionuclide decay data currently used for detector-efficiency calibration, address the adequacy of this information, identify additional nuclides appropriate as either primary or secondary calibration standards and implement appropriate actions to produce a file of decay data to serve as a standard set for gamma-ray detector-efficiency calibration (Session IX).

PROGRAMME OF THE MEETING

Monday, 12 November 09h00

General Opening

Welcome speech R. Batchelor, Director of CBNM

Announcements

Session I Chairman: A.J. Deruytter

P-1 Requirements for nuclear standard reference data from the users' point of view
A.J. Deruytter (CBNM, Geel)

P-2 The neutron cross section standards evaluations for ENDF/B-VI
A.D. Carlson (NBS), W.P. Poenitz (ANL)
G.M. Hale (LANL), R.W. Peele (ORNL)

P-3 INDC/NEANDC Standard File, Status Report
H. Condé (Gustaf Werner Inst. Uppsala)

P-4 IAEA Standards File: some comments and recommendations *1)
M.V. Blinov, S.K. Vasil'ev, V.D. Dmitriev, Yu.A. Nemilov, V.P. Chechev, E.A. Shlyamin, V.I. Shpakov, A.V. Sorokina (V.G. Khlopin Radium Inst. Leningrad), A.A. Goverdovskii, V.N. Kornilov, V.A. Tolstikov (FEI, Obninsk), V.A. Konshin, E.Sh. Sukhovitskii (Inst. Nuclear Power, Minsk)

Session II Chairman: G.M. Hale

P-5 Theoretical calculations of the $^{6}Li(n,t)$ cross-section
G.M. Hale (LANL)

P-6 The data for the neutron interactions with ^{6}Li and ^{10}B
W.P. Poenitz (ANL)

P-7 Measurement of the $^{6}Li(n,\alpha)/^{10}B(n,\alpha)$ ratio with a xenon gas scintillator
C. Bastian, H. Riemenschneider (CBNM)

---

*1) The paper was not introduced at this session but it covered the comments in the several sessions

Those paper numbers underlined are invited

P-8 Determination of the neutron detection efficiency of a thick ^{6}Li glass detector by measurement and by Monte Carlo calculation

A. Lajtai, J. Kecskeméti (Central Research Inst. for Physics, Budapest), V.N. Kononov, E.D. Poletaev, M.V. Bohovko, L.E. Kazakov, V.M. Timohov, P.P. Dyachenko L.S. Kutsaeva, E.A. Seregina (FEI, Obninsk)

P-9 Proposal for measuring the ratio of the neutron standards $^{6}Li(n,\alpha)^{3}H$ and $^{10}B(n,\alpha)^{7}Li$ by the quasi-absolute method using the time-reversed reactions, and the ratios of these standards to the $^{3}He(n,p)^{3}H$ reaction in the 0.25 to 9 MeV neutron energy range

M. Drosg (University of Vienna)

Session III Chairman: A.D. Carlson

P-10 Evaluation of the $^{27}Al(n,\alpha)$ reaction cross-section in energy range 5.5 MeV - 20 MeV

N.V. Kornilov, N.S. Rabotnov, S.A. Badikov, E.V. Gay, A.B. Kagalenko, V.I. Trykova (FEI, Obninsk)

P-11 Neutron-capture cross section measurements for ^{197}Au and ^{115}In in the energy region 2.0-7.7 MeV using the activation technique

P. Andersson, R. Zorro, I. Bergqvist (University Lund) presented by H. Condé

P-12 Influence of target-scattered neutrons on cross-section measurements

H. Lesiecki, M. Cosack, B.R.L. Siebert (PTB, Braunschweig)

P-13 Comments to the evaluation of fast neutron radiation capture by ^{197}Au given in the book of Standard Nuclear Data

V.A. Tolstikov (FEI, Obninsk) presented by V.N. Kornilov

Session IV Chairman: M. Sowerby

P-14 Review of recent measurements of the U-235 fission cross-section and fission fragment angular distribution between 0.1 and 20 MeV

M.G. Sowerby, B.H. Patrick (AERE Harwell)

P-15 New results on the $^{235}U(n,f)$ fission integrals

C. Wagemans (SCK-CEN Mol), A.J. Deruytter (CBNM)

P-16 Absolute measurements of the $^{235}U(n,f)$ cross section for neutron energies from 0.3 to 3 MeV

A.D. Carlson, J.W. Behrens, R.G. Johnson, G.E. Cooper (NBS)

P-17 AEP measurements of $^{235}U(n,f)$ and $^{238}U(n,f)$ cross-section
Yuan Han-Rong (AEP, Beijing)

P-18 Absolute measurement of the ^{235}U fission cross-section at 4.45 MeV neutron energy using the time-correlated associated particle method (TCAPM)
R. Arlt, C.M. Herbach, M. Josch, G. Musiol, H.G. Ortlepp, G. Pausch, W. Wagner (TU Dresden), L.V. Drapchinsky. E.A. Ganza, O.I. Kostochkin, S.S. Kovalenko, V.I. Shpakov (V.G. Khlopin Radium Inst. Leningrad) presented by M.V. Blinov

... Konshin's evaluation on $^{235}U(n,f)$
introduced by M.V. Blinov (see paper P-4)

P-19 Fission fragment mass, kinetic energy and angular distribution for $^{235}U(n,f)$ in the neutron energy range from thermal to 6 MeV
Ch. Straede, C. Budtz-Jörgensen, H.-H. Knitter (CBNM)

P-20 The ^{238}U fission cross section, threshold to 20 MeV
Y. Kanda (Kyushu University, Fukuoka)

P-21 Neutron-induced fission cross-section of ^{238}U in the second plate region *2)
A.A. Goverdovsky (FEI, Obninsk)

P-22 Fission ratios involving ^{238}U, ^{237}Np, ^{239}Pu, and ^{235}U fission cross-sections *3)
Y. Kanda, Y. Uenohara (Kyushu University, Fukuoka)

Tuesday, 13 November 09h00

Session V Chairman: E.J. Axton

P-23 Evaluation of the thermal neutron constants of ^{233}U, ^{235}U, ^{239}Pu and ^{241}Pu and the fission neutron yield of ^{252}Cf
E.J. Axton (CBNM)

P-24 Sub-thermal fission cross-section measurements
C. Wagemans (SCK-CEN Mol), A.J. Deruytter (CBNM)

P-25 A least-square fit of thermal data for fissile nuclei
M. Divadeenam, J.R. Stehn (BNL)
presented by A.D. Carlson

---

*2) Contribution only
*3) Presented on Wednesday at Working Group Session II

Session VI Chairman J.W. Boldeman

P-26 Nubar for the spontaneous fission of ^{252}Cf
J.W. Boldeman, M.G. Hines (AAEC, Lucas Heights)

P-27 A re-evaluation of the average prompt neutron emission multiplicity (nubar) values from fission of Uranium and Transuranium nuclides
N.E. Holden, M.S. Zucker (BNL)
introduced by J.W. Boldeman

P-28 Measurement and theoretical calculation of the ^{252}Cf spontaneous fission neutron spectrum
H. Märten, D. Seeliger (TU, Dresden)

P-29 Differential and integral comparison of three representations of the prompt neutron spectrum for the spontaneous fission of ^{252}Cf
D.G. Madland, R.J. LaBauve, J.R. Nix (LANL)

P-30 Calculation of the $^{252}Cf(SF)$ neutron spectrum in the frame work of a complex cascade evaporation model (CEM)
H. Märten, D. Seeliger (TU, Dresden)

P-31 Statistical calculation of the ^{252}Cf spontaneous fission prompt neutron spectrum
B.F. Gerasimenko, V.A. Rubchenya (V.G. Khlopin Radium Inst. Leningrad) presented by M.V. Blinov

P-32 Recent developments in the investigation of ^{252}Cf spontaneous fission prompt neutron spectrum
M.V. Blinov (V.G. Khlopin Radium Inst. Leningrad)

P-33 State and first results of the evaluation of the ^{252}Cf fission neutron spectrum
M. Mannhart (PTB, Braunschweig)

P-34 Measurements of the prompt neutron fission spectrum from the spontaneous fission of ^{252}Cf
J.W. Boldeman, B.E. Clancy, D. Culley
(AAEC, Lucas Heights)

P-35 New measurement of the $^{252}Cf(SF)$ neutron spectrum in the high-energy range
H. Märten, D. Richter, D. Seeliger (TU, Dresden)
R. Böttger (PTB, Braunschweig), W.D. Fromm (Zentral Inst. Rossendorf)

P-36 Prompt neutron spectra for the energy range 30 keV to 4 MeV from fission of ^{233}U, ^{235}U and ^{239}Pu induced by thermal neutrons
A. Lajtai, J. Kecskeméti, J. Safar
(Central Research Inst. for Physics, Budapest)

P-37 Neutron emission from the spontaneous fission of ^{252}Cf
C. Budtz-Jörgensen, H.-H. Knitter, R. Vogt (CBNM)

P-38 Measurement of the ^{235}U fission cross-section for ^{252}Cf spontaneous fission neutrons
I.G. Schröder, Li Linpei, D.M. Gilliam, C.E. Eisenbauer (NBS) presented by A.D. Carlson

Session VII Chairman: H. Condé

P-39 International fluence rate intercomparison for 2.5, 5.0 and 14 MeV neutrons
H. Liskien (CBNM), V.E. Lewis (NPL, Teddington)

... Comment for situation of ongoing intercomparison by T.B. Ryves (NPL, Teddington) - oral presentation

P-40 Some practical problems in the standardization of monoenergetic fast neutron fluences
T. Michikawa, K. Kudo, T. Kinoshita (ETL, Tskuba)

P-41 Measurement of the NBS black neutron detector efficiency at 2.3 MeV
K.C. Duvall, A.D. Carlson, O.A. Wasson (NBS)

P-42 Neutron measurements at Bureau International des Poids et Mesures (BIPM)
V.D. Huynh (BIPM, Sèvres)

P-43 Neutron fluence measurements with a proton recoil telescope
H.J. Brede, M. Cosack, H. Lesiecki, B.R.L. Siebert (PTB, Braunschweig)

P-44 Flux measurement techniques for white neutron sources
D.B. Gayther (AERE, Harwell)

P-45 A neutron detector comparison in the GELINA spectrum
J.A. Wartena, H.-H. Knitter, C. Budtz-Jörgensen, H. Bax, Cl.-D. Bürkholz, R. Pijpstra, R. Vogt (CBNM)

P-46 Flux detector intercomparisons: High efficiency detectors - Part II
F. Corvi, H. Riemenschneider, T. Van der Veen (CBNM)

Session VIII Chairman: D. Seeliger

P-47 Neutron energy standards
G.D. James (AERE, Harwell) presented by M. Sowerby

P-48 The energy calibration procedure of TOF spectrometers for fission neutron spectrum measurements
T. Wiedling (Studsvik Science Res. Lab., Nyköping)

P-49 Neutron energies selected by ISO for the calibration of radiation protection instruments
M. Cosack (PTB, Braunschweig)

Wedenesday, 14 November 08h50

Session IX Chairman: C.W. Reich

P-50 Actinide half-lives as standards for nuclear data measurements: Current status
C.W. Reich (EG & G, Idaho Falls)

P-51 Total and spontaneous fission half-lives of the Uranium and Plutonium nuclides *4)
N.E. Holden (BNL)

P-52 Total and spontaneous fission half-lives of the Americium and Curium nuclides *4)
N.E. Holden (BNL)

P-53 Emission probabilities of selected gamma rays for radionuclides used as detector-calibration standards
R. Vaninbroukx (CBNM)

P-54 Emission probabilities of selected X-rays for radionuclides used as detector-calibration standards
W. Bambynek (CBNM)

Working Group Session I

DOCUMENTATION AND PRESENTATION OF STANDARD MEASUREMENTS AND ERRORS

Chairman: W.P. Poenitz

Simultaneous evaluations;

Covariances;

Documentary information needed by an evaluator from a measurer of standard data.

Contributions:

W-1: The simultaneous evaluation of interrelated cross-sections by generalized least-squares and related data file requirements
W.P. Poenitz (ANL)

W-2: A simultaneous evaluation of some important cross-sections at 14.70 Mev
T.B. Ryves (NPL, Teddington)

W-3: Properties of Cf fission fragment detection systems used for neutron time-of-flight measurements
H. Klein, R. Böttger (PTB, Braunschweig)
A. Chalupka, B. Strohmaier (IRK, Vienna)

---

*4) Not presented at the meeting, but included in the Chairman's summary

Working Group Session II

NEW STANDARDS

Chairman: H. Klein

Should $^{3}He(n,p)T$ be reconsidered as a standard?;

Continuous neutron emission spectra as standards (^{56}Fe and ^{93}Nb);

Standards in fission yields (^{99}Mo, ^{140}Ba and the Nd isotopes);

Others.

Contributions: *5)

... $^{3}He(n,p)$ detector (oral presentation)
A.D. Carlson (NBS)

... Continuous neutron emission spectra as standards ^{56}Fe and ^{93}Nb (oral presentation)
D. Seeliger (TU, Dresden)

W-4: Standards for the fission yields measurements
J. Blachot (CEN, Grenoble)

W-5: Cross-section measurements of $^{56}Fe(n,p)^{56}Mn$ and $^{27}Al(n,\alpha)^{24}Na$ between 14.0 and 19.9 MeV
K. Kudo, T. Michikawa, T. Kinoshita, Y. Hino
Y. Kawada (ETL, Tsukuba)

W-6: Neutron production using gas targets
H. Klein (PTB, Braunschweig)

W-7: Candidates for fast neutron standards among neutron producing reactions
M. Drosg (University of Vienna)

W-8: About ^{237}Np fission cross-section standardization
A.A. Goverdovsky (FEI, Obninsk)
presented by N.V. Kornilov

---

*5) Kanda's paper on cross section ratio is transfered to Session IV.

Thursday, 15 November 09h00

Working Group Session III

IMRPOVEMENTS IN DETECTORS AND MEASURING TECHNIQUES LEADING TO MORE ACCURATE DETERMINATION AND USE OF STANDARDS

Chairman: H. Liskien

Contributions:

W-9: Application of the dual thin scintillator neutron flux monitor in a $^{235}U(n,f)$ cross-section measurement
M.S. Dias, A.D. Carlson, R.G. Johnson, O.A. Wasson (NBS)

W-10: Investigation for a precise and efficient neutron fluence detector based on the n-p scattering process
H.-H. Knitter, C. Budtz-Jörgensen, H. Bax (CBNM)

... Comment: Assaying on hydrogen content in stearin foil (oral presentation)
J. Pauwels (CBNM)

W-11: Assaying of ^{235}U fission layers for nuclear measurements with a gridded ionization chamber
C. Budtz-Jörgensen, H.-H. Knitter (CBNM)

... ^{235}U foil mass determination
I.G. Schröder, D.N. Gilliman (NBS)
oral presentation by A.D. Carlson

W-12: Final results of the international ^{235}U sample intercomparison and the half-life of ^{234}U
W.P. Poenitz, J.W. Meadows

Visits to CBNM 14h00 - 17h30

Friday, 16 November 09h00 - 16h30

Conclusions

Chairman: A.J. Deruytter

REPORTS BY CHAIRMEN ON MONDAY AND TUESDAY SESSIONS

DISCUSSION

REPORTS BY CHAIRMEN OF THE WORKING GROUP SESSIONS

DISCUSSION

RECOMMENDATIONS TO THE IAEA CONCERNING

- Task forces for special problems
- The future of the INDC/NEANDC Standards File

SESSION I

REQUIREMENTS FOR NUCLEAR STANDARD REFERENCE DATA FROM THE USERS' POINT OF VIEW

A.J. DERUYTTER
Central Bureau for Nuclear Measurements,
Joint Research Centre,
Commission of the European Communities,
Geel

Abstract

The requirements from the users' point of view for nuclear standards reference data with respect to accuracy of the data, traceability (documentation), representation (i.e. numerical values with uncertainties and correlation matrices, parametrization), availability of materials in suitable form (well-defined layers, gases) and applicability in real life detectors (Q-values of reactions, type of particles or photons produced, smoothness and magnitude of cross-section) will be discussed.

From these primary requirements additional requirements follow for internal consistency (via ratio measurements), for verification of physical constraints (total cross-section, inverse reaction), for additional basic information (angular distributions of reaction products, fragment energy distributions, description and understanding of the basic processes).

The user is seen as the measurer who determines values of partial cross-sections or other quantities relative to one or more of the selected standard reference data.

1. Introduction

In this paper the requirements with respect to nuclear standards reference data will be scrutinized from the viewpoint of a measurer who determines values of partial cross-sections or other quantities relative to one or more of the selected standard reference data.

This delimitation means that I do not deal with requirements resulting from the processing of data via group cross-sections to be used as data input to the actual reactor calculations. Of course some standard reactions coincide

with neutron reactions of importance in a reactor, e.g. the ^{235}U fission cross-section as fissile material or the (n,α) reaction of ^{10}B as absorber material and enter in this capacity directly into the evaluated-data library for reactor calculations. Another important standard quantity which enters indirectly is nubar for Cf 252 via the energy dependent nubar ratio measurements for the fissile and fertile materials in view of their evident relationship with k_{eff}. But these requirements are expected to be reflected in the requests for those standards by the national nuclear data committees channeled through and critically examined by NEACRP (NEANDC and INDC).

So in fact we deal with requirements for neutron metrology that suffers from the difficulty to determine on an absolute basis neutron fluxes and consequently partial cross-sections. And obviously a measurer wants to avoid this problem of absolute flux determination and bypasses it by making cross-section determinations relative to other cross-sections, i.e. standards. This restricted set of standard reactions on which effort of real absolute work as well as evaluation effort are concentrated, is listed in Table 1, and illustrated in Fig. 1. They are the cross-sections and energy regions selected in the INDC/NEANDC Nuclear Standards File.[1]

TABLE 1

NUCLEAR DATA STANDARDS FOR NUCLEAR MEASUREMENTS

REACTION	ENERGY RANGE
H(n,n)H	1 keV TO 20 MeV
$^{6}Li(n,t)^{4}He$	THERMAL TO 0.1 MeV
$^{10}B(n,\alpha_1)^{7}Li$ *	THERMAL TO 0.2 MeV
$^{10}B(n,\alpha_0+\alpha_1)^{7}Li$	THERMAL TO 0.2 MeV
C(n,n)C	1 keV TO 2.0 MeV
$^{197}Au(n,\gamma)^{198}Au$	0.2 MeV TO 3.5 MeV
$^{235}U(n,f)$	0.1 MeV TO 20 MeV
$^{238}U(n,f)$	THRESHOLD TO 20 MeV
$^{27}Al(n,\alpha)$	THRESHOLD TO 20 MeV

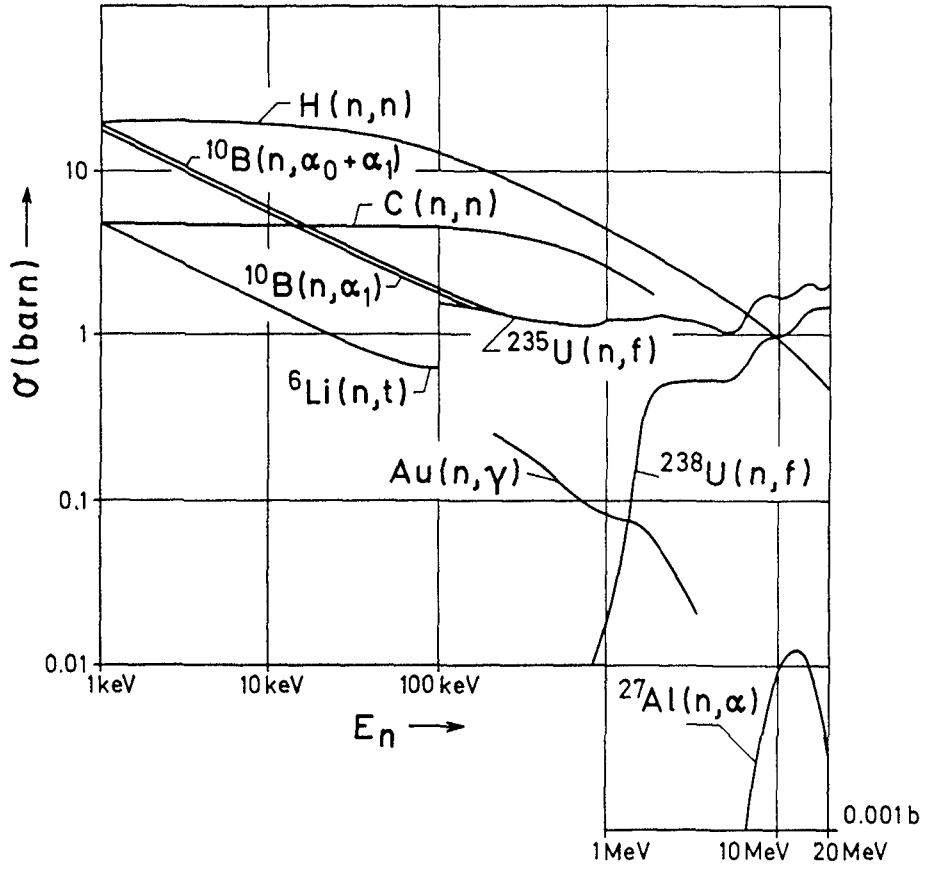

FIG. 1 : THE ANGLE-INTEGRATED CROSS-SECTIONS FOR THE ACCEPTED NEUTRON STANDARD REACTIONS IN THEIR ACCEPTED ENERGY RANGE. BELOW 1 keV THE ACCEPTED REACTIONS $^{6}Li(n,t)$, $^{10}B(n,\alpha_1)$ and $^{10}B(n,\alpha_0+\alpha_1)$ FOLLOW ESSENTIALLY THE 1/v-LAW.

TABLE 2

NUCLEAR DATA STANDARDS

NEUTRON ENERGY STANDARDS
ACTINIDE HALF-LIVES
THERMAL PARAMETERS FOR ^{233}U, ^{235}U, ^{239}Pu, ^{241}Pu
NUBAR OF ^{252}Cf
PROMPT FISSION NEUTRON SPECTRUM OF ^{252}Cf
^{235}U FISSION FRAGMENT ANISOTROPIES
DECAY DATA FOR RADIONUCLIDES USED AS CALIBRATION STANDARDS

In Table 2 the non cross-section standard data which were incorporated in the INDC/NEANDC Standard File are given. The importance of these different items is not equally distributed but the relevance of some is direct (nubar of ^{252}Cf and fission neutron spectrum, thermal parameters of the fissile isotopes), for others indirect (half-lives, fission fragment anisotropies) and requirements are considered accordingly.

Before discussing the general requirements for these nuclear data standards, it is useful to consider the presently outstanding high priority nuclear data measurement requirements for the reactor programme in the area of standards as tabulated in NEACRP-A-568[2] and reproduced in Table 3. There we find as expected $^{235}U(n,f)$ and ^{252}Cf nubar (and neutron energy spectrum) requested to high accuracy. We note that requests for ^{235}U reach down to 1 keV and for $^{10}B(n,\alpha)$ and α_0/α_1 reach to 1 MeV, i.e. outside the range where these cross-sections are considered as standards.

Also recently additional precise absolute measurements of the $^{10}B(n,\alpha_0)$ and (n,α_1) cross-sections at a few energies between 50 and 800 keV are requested to help to resolve a He-production discrepancy for ^{10}B that

TABLE 3

HIGH PRIORITY REQUEST LIST : STANDARDS

REACTION	ENERGY RANGE	TYPICAL ACCURACY REQUEST (PERCENT)	REQUESTER	STATUS REMARKS
$^{10}B(n,\alpha)$ AND α_0/α_1 (n,γ)	100K-1M THERMAL-200K	2 20	E UK	ALTHOUGH THE ENDF/B-V EVALUATION CLAIMS ACCURACIES CLOSE TO THIS REQUEST, AN INDEPENDENT EVALUATION BY LISKIEN AND WATTECAMPS SUGGESTS THAT LARGER UNCERTAINTIES MAY BE WARRANTED
$^{235}U(n,f)$	1K - 14M	1	US	(RATIO TO H(n,p) AND $^{10}B(n,\alpha)$ AND POSSIBLY OTHER STANDARDS). THE ENDF/B-V EVALUATION IS SAID TO HAVE AN ACCURACY OF APPROXIMATELY 3% IN THE RANGE 150K TO 10M.
$^{252}Cf\ \nu_s$		0.25	US	QUOTED ACCURACIES 0.2% BUT DIFFERENCES IN EVALUATED VALUES OF 0.5%. FURTHER ANALYSIS NEEDED.
$^{252}Cf,X(E)$	$\bar{E}$ $\phi(E)$ (E >5M) (E<250K)	1-2 5-10	E, US	ESTIMATED ACCURACY OF $\bar{E}$ IS 2% BUT THE SHAPE REQUIREMENTS ARE NOT MET.

was recently detected.[3] In fact comparisons of careful He-measurements in several assemblies with values calculated from ENDFB/V suggest that the ENDF/B-V results are from 9 to 15% too low. The neutron spectra from these assemblies sample the He-production cross-section from the low keV-region to several MeV neutron energy. The covariance files for the evaluation on the other hand indicate that the (n,α) data are accurate to better than 2%, and the combined cross-section and spectrum uncertainty for the calculations is less than 4%. This results in an additional request for ^{10}B.

But let me now turn to the general requirements for the standard reference data from the users' point of view. Requirements concerning accuracy of the data, traceability, representation, availability of materials in suitable form and applicability in real life detectors will be discussed. From these requirements follow additional requirements for internal consistency, verification of physical constraints, additional basic information on angular distribution and kinetic energy spectra of reaction products and in general a better description and understanding of the basic processes.

2. General requirements for standard reference data

First a remark on the common use of the word standards in this paper and at many other occasions. It is obviously used here and in the neutron community in a broader sense as a reference set of data than the definitions used in classical legal metrology would permit. If you look at the definitions of the term 'standard' in legal metrology, two distinct meanings emerge.[4]

Firstly, a 'SPECIFICATION STANDARD' which is 'a widely adopted specification, technical recommendation or similar document'. (norme), and secondly a 'MEASUREMENT STANDARD, OR ETALON' which is 'a material measure, measuring instrument or system intended to define, realize, conserve or reproduce a unit or one or more known values of a quantity in order to transmit them to other measuring instruments by comparison.'

However, although some additional terms such as primary and secondary are also defined in relation with measurement standards, these specifications may be used more generally. In fact the definition of 'PRIMARY STANDARD' is 'a standard, which has the highest metrological qualities in a specified field.' So the concept of primary standard is equally valid for base units and for derived units. Such a standard is ABSOLUTE if the values provided have been established in terms of the relevent base units without recourse to another standard of the same quantity. Furthermore a 'SECONDARY STANDARD' is 'a standard whose value is fixed by comparison with a primary standard'. The definitions of primary, secondary and absolute may be transferred to our 'standard reference data.'

How should we formulate the requirements for a primary standard for neutron flux measurements? AN ATTEMPT: A good primary flux standard should respond to the following specifications: its cross section should be accurately known, smooth and as large as possible, over a broad energy interval. The basic neutron reaction should have a large positive Q-value. Corresponding standard samples used for detection should be relatively easy to prepare and to assay accurately for chemical and isotopic composition, quantity, uniformity and homogeneity. They should remain unaltered under normal conditions of use. Substances used for sample preparation should be easy to obtain in a chemically pure form and suitable for precise mass-spectrometric analysis. A detector of reasonable size should be available, which, if combined with a precise sample is capable of fast response ($\leq$ 10 ns), has good efficiency and good discrimination against unwanted particles or photons (e.g. low γ sensitivity).

In fact of course, all preceding requirements have played a rôle of some sort in the selection of the reference data that will be discussed during this meeting. To my feeling the distinction between primary and secondary standards has become less clear-cut than it was some fifteen years ago when propositions were made, such as 'to adopt as primary flux standards $^{10}B(n,\alpha)$ up to 100 keV and $^{1}H(n,n)$ above 100 keV.'[5] This attitude change is a consequence of the experience gained in the painstaking experiments and evaluations that have followed and with the conclusion that there are no primary standards, that have proven outstanding quality in all the above mentioned requirements.

For example, it is a true statement that the hydrogen cross-section is the best known in a wide energy region, but it is equally true that this does not mean that the measurement using the hydrogen cross-section is always preferable over any other because so many other quantities are involved such as the efficiency of the detectors. An absolute measurement of the ^{235}U fission cross-section may bring us indeed a better usable reference cross-section than the use of the hydrogen would allow us to do because of the high efficiency of the fission detector. In such a situation different answers are possible; one answer being: let us use $^{235}U(n,f)$ and associated detector; another attitude is: let us investigate whether an efficient neutron fluence detector based on the n-p scattering process can be constructed, e.g. an ionisation chamber with Frisch-grid to detect the recoil protons induced by fast neutrons in an advantageous 2π-geometry, of course with all problems associated with the determination of the number of hydrogen atoms in a thin foil. So much

TABLE 4

APPLICATIONS OF STANDARD REACTIONS IN DETECTION SYSTEMS

REACTION	ENERGY RANGE	WAY OF DETECTION	APPLICATION AREA	OBSERVATIONS
H(n,n)H	1 keV - 20 MeV	DETECTION OF ALL RECOIL PROTONS IN HYDROGEN OR METHANE FILLED PROPORTIONAL COUNTERS. DETECTION OF RECOIL PROTONS EMITTED IN A CERTAIN SOLID ANGLE (IN TELESCOPE ARRANGEMENTS, IF NECESSARY). AS STANDARD IN NEUTRON SCATTERING EXPERIMENTS VIA DETECTION OF SCATTERED NEUTRONS.	NEUTRON FLUX MEASUREMENTS (ABOVE ABOUT 0.5 MeV). MEASUREMENT OF THE RELATIVE RESPONSE FROM HYDROGENOUS RADIATORS. MEASUREMENT OF OTHER ELASTIC CROSS-SECTIONS. DIFFERENTIAL SCATTERING CROSS-SECTIONS FOR CALCULATION OF NEUTRON DETECTION EFFICIENCY OF ORGANIC SCINTILLATORS VIA COMPUTER CODES.	USE REQUIRES KNOWLEDGE OF ANGULAR DISTRIBUTIONS IN BOTH HEMISPHERES.
$^{6}Li(n,t)^{4}He$	THERMAL-0.1 MeV	VIA DETECTION OF TRITON + α-PARTICLE BY SCINTILLATION (GLASS, LiI(Eu), PLASTIC FOILS, GAS) OR BY SURFACE BARRIER DETECTORS AND IONIZATION CHAMBERS.	STANDARD CROSS-SECTION BELOW 100 KeV (FLUX).	USE REQUIRES KNOWLEDGE OF TRITON ANGULAR DISTRIBUTION.
$^{10}B(n,\alpha_1)^{7}Li^{*}$	THERMAL-0.2 MeV	VIA DETECTION OF THE ISOTROPIC 478 keV γ-EMISSION OF $^{7}Li^{*}$ IN BORON SLAB DETECTORS.	STANDARD CROSS-SECTION BELOW 200 keV (FLUX).	
$^{10}B(n,\alpha_0+\alpha_1)^{7}Li$	THERMAL-0.2 MeV	VIA DETECTION OF α-PARTICLES IN IONIZATION CHAMBERS, WITH SURFACE BARRIER DETECTORS OR SCINTILLATORS.		
C(n,n)C	1 keV - 1.8 MeV	ONLY AS STANDARD IN NEUTRON SCATTERING EXPERIMENTS VIA DETECTION OF ELASTICALLY SCATTERED NEUTRONS.	SCATTERING STANDARD.	
$^{197}Au(n,\gamma)^{198}Au$	0.2 MeV-3.5 MeV	ONLY AS STANDARD IN FAST NEUTRON CAPTURE EXPERIMENT VIA PROMPT γ-DETECTION OR ACTIVATION.	CAPTURE STANDARD.	
$^{235}U(n,f)F.F.$	0.1 MeV-20 MeV	DETECTION OF FISSION FRAGMENTS IN IONIZATION CHAMBERS, WITH SURFACE BARRIER DETECTORS OR SCINTILLATORS.	REACTOR CALCULATIONS. FISSION AND CAPTURE STANDARD ABOVE 100 keV.	REQUIRES FISSION FRAGMENT EMISSION ANISOTROPIES. KINETIC ENERGY DISTRIBUTION OF FISSION FRAGMENTS.
$^{238}U(n,f)F.F.$	THRESHOLD-20 MeV	DETECTION OF FISSION FRAGMENTS IN IONIZATION CHAMBERS, WITH SURFACE BARRIER DETECTORS OR SCINTILLATORS.	FAST NEUTRON FLUX, FISSION CROSS-SECTION STANDARD DOSIMETRY APPLICATIONS.	I D E M
$^{27}Al(n,\alpha)^{24}Na$	THRESHOLD-20 MeV	BY ACTIVATION.	CATEGORY I DOSIMETRY REFERENCE. DOSIMETRY AND ACTIVATION MEASUREMENTS.	

differences between primary and secondary are academic and all standards which are enlisted for this meeting should be dealt with on nearly the same footing. This attitude is also reflected into the simultaneous evaluation efforts on standard cross-sections that are going on at present and will be amply discussed at this meeting. However, in view of the amount of work involved one should not add further standards unless good reasons are given and applications are specified.

At this point it is appropriate to look to the ways in which the most important standard reactions are applied in actual measurements, because of the complex set of requirements for the use of a standard cross-section. The way of detection of these standard reactions is indicated briefly in Table 4, and also the main application areas are summarized, as well as some additional requirements resulting from detector peculiarities. Also for the other standard quantities tabulated in the 1982 INDC/NEANDC Standards File briefly application area and special requirements are given in Table 5.

In the following we will deal with the specific requirements without search for completeness but with hopefully illustrative examples.

3. Requirements for accuracy of standards data

In the measurement community two distinct attitudes seem to prevail as to the accuracy requirements for standard data (and even measurements in general). On the one hand 'standard reference data should be measured as accurately as possible' irrespective of whether this kind of accuracy is required and on the other hand 'standard reference data should be measured as accurately not to have a sizeable influence on other data measured relative to them.' This distinction is not always academic, because an enormous effort is often required to further improve the accuracy.

As an example we can take the evaluation of the thermal neutron constants of ^{233}U, ^{235}U, ^{239}Pu and the fission yield of ^{252}Cf which was recently performed at CBNM by Axton[6] and at BNL by Divadeenam and Stehn[7]. The conclusion of these recent studies is that the recommended fissile thermal parameters constitute a self-consistent set. Problems encountered in earlier evaluations have been found not to be significant any longer in casting doubts on the consistency of certain types of input data (such as nubar measurements and

TABLE 5

NON CROSS-SECTION STANDARD QUANTITIES IN STANDARDS FILE

QUANTITY	APPLICATION AREA	OBSERVATIONS
NEUTRON ENERGY STANDARDS	• NORMALIZATION OF ENERGY SCALES FOR EVALUATIONS AND OTHER USERS OF DATA	RESOLUTION OF SPECTROMETERS
ACTINIDE HALF-LIVES	• SAMPLE ASSAY FOR FISSION CROSS-SECTIONS, MASS DETERMINATION OF SAMPLES	
THERMAL PARAMETERS FOR ^{233}U, ^{235}U, ^{239}Pu, ^{241}Pu	• NORMALISATION OF CROSS-SECTION CURVES AT THERMAL AND AT HIGHER ENERGIES BY SUCCESSIVE NORMALISATION VIA RESONANCE INTEGRALS • REACTOR CALCULATIONS	REQUIRE ACTINIDE HALF-LIVES AND $\bar{\nu}$ OF Cf 252
NUBAR OF ^{252}Cf	• $\bar{\nu}$-MEASUREMENTS • NEUTRON EMISSION RATE IS AN EXPERIMENTAL CALIBRATION REFERENCE • REACTOR CALCULATIONS (INDIRECT)	REQUIRES ASSOCIATED NEUTRON EMISSION SPECTRUM
PROMPT FISSION NEUTRON SPECTRUM OF ^{252}Cf	• REFERENCE FOR MICROSCOPIC AND MACROSCOPIC MEASUREMENTS • NUBAR Cf 252 • RELATIVE FLUX STANDARD IN INSTRUMENT CALIBRATIONS	
DECAY DATA FOR RADIONUCLIDES USED AS CALIBRATION STANDARDS	CALIBRATION OF GAMMA DETECTORS OF IMPORTANCE FOR ACCURATE MEASUREMENT OF ENERGIES AND INTENSITIES OF γ-RAYS	
NEUTRON FLUX COMPARISONS	IMPROVEMENT OF FLUENCE RATE DETERMINATIONS AT DIFFERENT LOCATIONS	

observations made in pile and Maxwellian neutron spectra) with the main body of input data. This statement does not mean that small differences between e.g. the Maxwellian and 2200 m/s data sets are fully resolved as illustrated in Table 6 where the output of Axton's evaluations are shown for the nubar-values and the fission cross-sections with and without the incorporation of Maxwellian data in the fit. From the Table we learn that all fission cross-sections are reduced and all nubar values increased by the introduction of the Maxwellian data, but the global set of measurements is consistent with the output. In fact only one measurement falls outside two standard deviations with respect to the output value where we expect eight for a normal distribution.
We could say that the agreement between important subsets of the data is at the 0.5% level, whereas internal consistency of the subsets would be 0.2%. The history how this consistency came about is a long story of resolving systematic discrepancies by an iterative process which is essentially the fundamental way for making any accurate determination of a physical quantity. In this process different types of measurements and techniques, simultaneous evaluations (IAEA panels) making use of physical constraints and taking correlated errors into account in different ways played an important rôle.

The question now is: should we go further in trying to improve the accuracy of such a data set knowing that in the normal iterative process the costs of the efforts increase exponentially with the increase of the required accuracy and that for present reactor applications the present consistency is adequate? We recognize that in such a situation any individual effort (measurement) is only likely to create an additional value with no sizeable influence on the available accuracy unless a new revolutionary highly accurate technique is introduced in measurement or analysis.

To avoid a discussion on the ultimate accuracy we can achieve due to technological factors such as intensity of neutron sources (present and future) or the analytical power of computer codes (present and future), I would at this stage rephrase the accuracy requirement to 'STANDARD REFERENCE DATA SHOULD BE MEASURED AS ACCURATELY AS POSSIBLE WITH THE PRESENTLY AVAILABLE TECHNIQUES', that is to say, we adapt the accuracy requirement to 'the presently achievable' where this term means using all available means: different types of measurements and techniques, evaluation and including physical

TABLE 6

2200 m/s FISSION CROSS-SECTIONS AND NUBAR VALUES FOR FISSILE NUCLIDES

		AXTON (1982) 2200 m/s EVALUATION	AXTON (1984) 2200 m/s AND MAXWELLIAN DATA	DIFFERENCE
σ_f^o	^{233}U	532.4 ± 2.4 b	529.7 b ± 1.3 b	+ 2.7 b
	^{235}U	585.5 1.7	582.9 1.3	+ 2.6
	^{239}Pu	748.2 2.6	747.2 2.1	+ 1.0
	^{241}Pu	1020.9 11.5	1011.9 6.6	+ 9.0
NUBAR	^{233}U	2.485 ± 0.005	2.492 ± 0.004	- 0.007
	^{235}U	2.425 0.005	2.432 0.004	- 0.007
	^{239}Pu	2.878 0.006	2.880 0.005	- 0.002
	^{241}Pu	2.940 0.007	2.944 0.006	- 0.004
	^{252}Cf	3.7631 0.0050	3.7655 0.0048	- 0.0024

constraints. It means that we have to stay with our iterative process of approaching accurate values but look for ways and means for speeding up the process. How to reach that may be more appropriate to discuss in the recommendations for future work in the standards area.

An important question to ask at this time is: Do we reach the 'presently achievable' at any given moment? At this point I have to refer to a paper by Coates et al. presented at the Antwerp Conference[8] that analysed in detail the history of two discrepancies in standard data: (1) the $^6Li(n,\alpha)t$ cross-section in the vicinity of the 247 keV resonance and (2) the ^{235}U fission cross-section measurements near 14 MeV. One of the conclusions concerning the first study was that there were no technical reasons why the $^6Li(n,\alpha)$ cross-section should not have been measured at least in 1970 to its presently known accuracy, and that still to-day discrepancies of a few percent exist between the most recent direct measurements with no obvious reasons.

But even more disturbing is that quoted accuracies on standard data were in error mainly because of two reasons: unidentified systematic errors which cannot be ruled out but mainly the inadequate treatment of known error sources. In fact our practices in general do not meet the normal scientific standards expected for measurements which are intended to be accurate. And in full accordance with Coates et al. I plead again for reliability of error statements and this means also a more rigorous approach in which experimenters show a more critical awareness of systematic problems both in the design and execution of experiments. In particular some of the long-standing sources of systematic error need to be more thoroughly investigated, and more detailed treatment needs to be given to those which are already understood. In Table 7, recognized sources of systematic error as taken from ref. 8 are tabulated.

TABLE 7
RECOGNISED SOURCES OF SYSTEMATIC ERROR (8)

EXPERIMENTAL	ANALYTIC
1. BACKGROUND	1. INADEQUATELY VALIDATED COMPUTER PROGRAMS
2. INADEQUATE UNDERSTANDING OF DETECTOR RESPONSE	2. INADEQUATELY SOPHISTICATED DATA ANALYSIS
3. SAMPLE CHARACTERISATION	3. INADEQUATE APPLICATION OF SIGNIFICANT CORRECTIONS
4. FAULTY APPARATUS (e.g. ELECTRONIC FAULTS)	4. INADEQUATE USE OF AVAILABLE STATISTICAL INFORMATION IN ASSIGNING ERRORS
5. FAULTY DATA ACQUISITION (e.g. DEAD TIME EFFECTS)	
6. INACCURATE ENERGY CALIBRATION	
7. INACCURATELY KNOWN RESOLUTION FUNCTION	

Returning to my introduction: Wouldn't it be a blame for this Community if the He-production discrepancy for ^{10}B measured in several assemblies were due to the (inaccurate) $^{10}B(n,\alpha)$ cross-section?

4. Traceability (documentation)

Since 1983 we have the Technical Series Report 227[1] published by the IAEA on 'Nuclear Data Standards for Nuclear Measurements' which is in fact the 1982 INDC/NEANDC Nuclear Standards File, for which the large majority of the recommended numerical data for the standard cross-sections is taken from ENDF/B-V, produced by the United States Cross Section Evaluation Working Group. The remainder of the numerical data is from evaluations by individuals or groups closely connected with INDC and NEANDC.

It is clear that in order to improve the accuracy and consistency of experimental results the standard data from that report should be adopted for all measurements and that when converting relative measured values to cross-section values the numerical values given herein should be employed. This practice will certainly facilitate further evaluation work and ease later renormalizations when improved standard reference information becomes available, because they will all be traceable to that report.

However the statement that 'certain important standard values are omitted from this tabulation because the present situation is judged to be in a state of flux' is not acceptable from the users' point of view, because it is in contradiction with the above and prevents later easy renormalization. We should strive towards a complete set of numerical values.

Another often heard comment of users with respect to the set of standard reference data is the speed with which numerical values change, be it small changes. Although constant revision and updating is required, a good practice would be to publish numerical values only every two years.

Confidence in the tabulated values will also largely depend on the care with which the evaluations and updatings are performed. Arguments for selection and adaptation of data have to be presented and documented. Standard data measurements used in the evaluation should be thoroughly documented and traceable in the literature. In connection also with paragraph 3 on accuracy, I would like to stress here the remarkable shortage of well-documented

evidence on systematic errors, which receive very often only cursory and peripheral treatment in published papers. This has made it generally difficult and sometimes impossible to trace in a reasonably precise way how consistency improvements have occurred in measurements. The argument that editors of journals are unlikely to accept such detail can be overcome by preparing comprehensive laboratory reports which are then to be made generally available. In Table 8 from own experience on the basis of the 2200 m/s fission cross-section value of ^{235}U I show you what changes occur in published values and why traceability is important. This table illustrates partly how consistency was finally reached for the 2200 m/s fission cross-sections. See Axton (1982) and Table 6 of this paper.

TABLE 8

CBNM 2200 m/s FISSION CROSS-SECTION VALUE FOR ^{235}U (ONLY MAJOR CHANGES)

	1968 [9]	1973 [10]	1984 [11]
VALUE σ_f^o	577 ± 5 b	587.6 ± 2.6 b	586.1 ± 2.6 b *
$T_{1/2}$ ^{234}U	(2.488 ± 0.016)x10^5 yr	(2.446 ± 0.007)x10^5 yr	(2.454 ± 0.006)x10^5 yr
σ_B^o	3835 ± 5 b	3835 ± 5 b	3838 ± 6 b

* WHEN ACCEPTING THE NEW VALUE OF POENITZ AND MEADOWS [18] FOR $T_{1/2}$ ^{234}U OF (2.4566 ± 0.0044)x10^5 yr, our σ_f^o-VALUE BECOMES 585.5 ± 2.6 b.

5. Representation

The representation of standard reference data in the INDC/NEANDC Standards File, by giving numerical values and percentage uncertainties to energy ranges and associated correlation matrices gives us all the information required for the angle-integrated cross-sections. However, when differential cross-sections are needed, e.g. for H(n,p), the information given on the Legendre polynomial coefficients of the relative centre-of-mass neutron angular distributions is insufficient to deduce uncertainties for the differential cross-sections. Also uncertainties as a function of neutron energy and a correlation matrix are required for the Legendre coefficients.

As will be discussed at this meeting by A. Carlson[12] the R-matrix method is being applied to the ^6Li and ^{10}B cross-section standards in the ENDF/B-VI evaluation. These evaluations are particularly important because they can take into account charged particle reactions leading to the same compound nuclei (^7Li and ^{11}B) and use angular distribution data. The results of these analyses are R-matrix parameters which can be used to calculate the ^6Li and ^{10}B cross-sections at the desired energy. For the user it will be difficult to choose whether the resonance parameters or the numerical values are to be used. It is recommendable that only a unique final result is offered to the user as is planned.

6. Internal consistency of standards

A further request to the set of standard data has to be consistency. As an example the 2200 m/s fission cross-section of ^{235}U in the thermal parameter set should be consistent with the ^{234}U half-life value and the 2200 m/s $^{10}B(n,\alpha)$ cross-section, given in the same file.

The user of standard data expects the standard data to be consistent in such a way that he finds the same answer within the associated uncertainties when he measures e.g. a fission cross-section relative to $^{10}B(n,\alpha)$ (α particle detection or 478 keV gamma-ray detection) or $^6Li(n,t)$ in the low energy range, at least when he uses the standards correctly and takes them from the INDC/NEANDC standards file. This was not always true in the past.
As a consequence more simultaneous evaluations of standard cross-sections are being made at present in which all available information is used on a larger set of data with the use of physical constraints. These evaluations will certainly improve the consistency of the standards and point to weaknesses in the use of the standard cross-sections by several experimenters. Papers on this topic will be presented at this meeting by W. Poenitz[13], T. Ryves[14] and E.J. Axton[6]. Also accurate ratio measurements between standards are in progress (Bastian[15], this meeting) which should contribute to the same objective.

This effort reflects the attitude of the measurements community which considers that there are no real primary standards because of the complexity of using a standard in actual measurement conditions.

7. Availability of materials in suitable form and applicability in real life detectors

For the user it is obvious that a standard should be easy to use in the experimental environment of his measurement.

It means e.g. that well-defined layers with accurately known numbers of atoms of the standard material can be produced which allow the detection of the reaction products in a 'good' geometry (e.g. a 2π solid angle). Thicknesses of the layers that can be used will depend on the energies of the particles produced (Q-values of the reactions) and on the stopping powers of the reaction products in the target material. Fission fragments (^{235}U and ^{238}U) have very large energies, but also high stopping powers. Tritons and alpha-particles from $^{6}Li(n,\alpha)$ have much smaller energies but lower stopping powers.

Another criterium is the selectivity of the detection system to isolate the wanted particles by energy selection (i.e. α particles from fission fragments) or pulse-shape discrimination (neutrons from photons in an organic scintillator detector).

A large cross-section will allow the use of thin samples (hence high resolving power for the reaction products). The smooth behaviour of the cross-section (e.g. the 1/v low energy part of the $^{10}B(n,\alpha)$ and $^{6}Li(n,\alpha)$ cross-sections) makes them less sensitive to the energy resolution of the neutron spectrometers used.

Such an enumeration is not exhaustive. The final aim is of course to be able to determine accurately a (sizeable) fraction of the reactions taking place in an accurately known number of target atoms at a specific neutron energy. Preferably that fraction should be large (high-efficiency) to assure small statistical errors and to avoid elaborate calculations to determine the efficiency of the detector, even when proven that the calculations can be performed accurately.

All these characteristics that are required for the accurate use of standards will be discussed at this meeting. Significant examples are (1) the study of an ionization chamber with Frisch-grid to detect recoil protons induced by fast neutrons in a hydrogeneous material in an advantageous 2π-geometry, (Knitter and Budtz-Jørgensen[16], this meeting). (2) the important improvement in the assaying of ^{235}U fission layers with a gridded ionization chamber in 2π geometry[17]. (3) the results of ^{235}U fission foil intercomparisons that increase our confidence in their assay, and lead to better agreement in the cross-section as well (W. Poenitz[18], this meeting).

8. Requirements for additional basic information

Angular distribution information for the reaction fragments as function of the neutron energy is required when a non-4π geometry is used in order to be able to correct for the effect as a function of energy. For H(n,n), $^{6}Li(n,t)$ and $^{235}U(n,f)$ the required information is given in the INDC/NEANDC Standards File. Although for H(n,n) the information given is not sufficient to determine the uncertainty for a differential cross-section as mentioned above.

For the light elements only few interactions are involved and the total cross-sections, which can be determined by transmission, become useful as a physical constraint.
For the light elements and particularly for (^{6}Li + n) the work of Hale[19] using the R-matrix method has shown the importance of being able to take into account the charged particle reactions leading to the same compound nucleus ^{7}Li, and to be able to use the angular distribution data. This analysis led to a consensus for the modern measurements for the neutron interaction with ^{6}Li including total, scattering and absolute and relative (n,α) measurements.

For nubar of ^{252}Cf the average neutron energy and preferably the fission neutron spectrum has to be known. For this reason and other applications as a reference spectrum, it is introduced in the standards file (cfr Table 5).

For a theoretical description of this standard neutron spectrum which will be discussed thoroughly at this meeting (Session VI, this meeting), it is important to have a good knowledge of the mechanism of neutron emission, i.e. to know the fraction of scission neutrons and the emission of neutrons during fragment acceleration, etc. Therefore not only measurements of the neutron spectrum $N(E_n)$ are required, but also multiple differential measurements $N(E_n,\theta_n: A, TKE)$ are helpful to clarify the nature of the fission neutrons.

The gridded ionisation chambers developed at CBNM provide a powerful tool for such measurements, since fission fragment angle (with respect to neutron emission direction), kinetic energy and mass distribution can be determined simultaneously with an angular efficiency close to 4π.

Also the knowledge of the energy spectrum of the reaction products is important, e.g. for fission fragments. Variations of kinetic energy distributions of the fission fragments with neutron energy may result in small variations of the fission chamber efficiency as a function of E_n. Also here a well-funded and quantitative theoretical description of these variations would be welcomed.

These few examples illustrate that additional basic information (experimental and theoretical) is required to make corrections with confidence or to impose physical conditions on standard data, with as a result improved accuracy and reliability.

9. Conclusions

A good primary neutron flux standard should fulfil as well as possible the following specifications: its cross-section should be accurately known, smooth and large over a broad energy region. The reaction should have a large Q-value. Standard samples for detection should be easy to prepare and to assay accurately and remain unchanged in normal use. Substances should be easy to obtain in chemically pure form and suitable for mass-spectrometric analysis. A detector of reasonable size should be available, which if combined with a precise sample is capable of fast response, has good efficiency and good discrimination against unwanted particles or photons.

Standard reference data should be measured as accurately as possible with presently available techniques and ways and means to speed up the iterative process of approaching accurate values should be looked for. Error statements should be reliable. A more rigorous approach to systematic problems both in design and execution of experiments is required. Long-standing sources of systematic errors need to be thoroughly investigated.

Only one set of standards data should be used by the user community to improve the consistency of experimental results. In this standards set numerical values should be given for all standards and a fixed period between updatings would improve traceability. The standard data measurements on which the evaluations and updatings are based should be fully documented and traceable in the literature with well-documented evidence on systematic errors, be it in laboratory reports.

For the use of differential cross-sections, especially for H(n,n), additional information on the coefficients of the Legendre polynomials in the relative centre-of-mass neutron angular distributions is required. For each standard a unique set of values and uncertainties (with correlation matrix) should be given. Numerical values of standard reference data in the file should be consistent when related. Standards for the same energy range should be compatible within uncertainties.

A thorough investigation of the limitations in the use and the resulting systematic errors in the execution of the measurements should be made before a standard is classified as such. Also before a new measurement on a standard is made the impact on the accuracy of that standard should be evaluated.

Additional basic information obtained by theory or experiment should be used to improve accuracy and reliability of standard data by allowing better funded corrections or by imposing physical constraints on the data.

References

(1) Nuclear Data Standards for Nuclear Measurements, 1982 INDC/NEANDC Nuclear Standards File, Technical Reports Series No. 227, International Atomic Energy Agency, Vienna 1983.

(2) High Priority nuclear data measurement requirements for the reactor programme, NEACRP-A-568, NEANDC-A-180, September 1983.

(3) P.G. Young, The $^{10}B(n,\alpha)^{7}Li$ reaction, submitted to INDC for publication in the 1984 'Nuclear Data Discrepancies' informal report under 'Data of special importance' (published by the OECD Nuclear Energy Agency, Paris, France) LA-UR 84-2083.

(4) W.A. Jennings, 'Why Metrology?', Chapter AI, p. 3-14, Ionizing Radiation Metrology, Edited by E. Casnati, Editrice Compositori Bologna, 1977.
International Vocabulary of Basic and General Terms in Metrology, published by ISO on behalf of a Joint Working Group of BIPM, IEC,

ISO and OIML, International Standards Organisation, 1 Rue de Varembe, 1211, Geneva 20, Switzerland, 1984.

(5) J. Spaepen, Primary Standard Data and Standard Samples, Nuclear Data for Reactors, Vol. I, p. 241, IAEA Vienna 1967.

(6) E.J. Axton, European Applied Research Reports, Vol. 5, No. 4, 609-676 (1984), E.J. Axton, 'Evaluation of the thermal neutron constants of ^{233}U, ^{235}U, ^{239}Pu and ^{241}Pu and the fission neutron yield of ^{252}Cf', This meeting.

(7) M. Divadeenam and J.R. Stehn, 'A least-square fit of thermal data for fissile nuclei', BNL-34211, submitted to Annals of Nuclear Energy and this meeting.

(8) M.S. Coates, D.B. Gayther, G.D. James, M.C. Moxon, B.H. Patrick, M.G. Sowerby and D.B. Syme, Nuclear Data for Science and Technology, pp. 977-986, 1982.

(9) A.J. Deruytter, J. Spaepen and P. Pelfer, Neutron Cross-Sections and Technology, Proceedings of a Conference, Washington DC, 1968, D.T. Goldman (Ed.) NBS-Special Publications 299, Vol. 1, p. 491, US Government Printing Office, Washington D.C., 1968

(10) A.J. Deruytter, J. Spaepen and P. Pelfer, Journal of Nuclear Energy, 27, 645, 1973

(11) Input value to Axton evaluation, this meeting.

(12) A.D.Carlson, W.P. Poenitz, G.M. Hale, and R.W. Peelle, 'The neutron cross-section standards evaluations for ENDF/B-VI', this meeting.

(13) W.P. Poenitz, 'The simultaneous evaluation of interrelated cross-sections by generalized least-squares and related data file requirements', this meeting.

(14) T.B.Ryves, 'A simultaneous evaluation of some important cross-sections at 14.70 MeV', this meeting.

(15) C. Bastian and H. Riemenschneider, 'Measurement of $^{6}Li/^{10}B(n,\alpha)$ cross-section ratio', this meeting.

(16) H.-H. Knitter and C. Budtz-Jørgensen, 'Investigation for a precise and efficient neutron fluence detector based on the n-p scattering process', this meeting

(17) C. Budtz-Jørgensen and H.-H. Knitter, 'Assaying of ^{235}U fission layers for nuclear measurements with a gridded ionisation chamber', this meeting.

(18) W.P. Poenitz and J.W. Meadows, 'Final results of the international ^{235}U sample intercomparison and the half-life of ^{234}U', this meeting.

(19) G.M. Hale, 'Theoretical calculations of the $^{6}Li(n,t)$ cross-section', this meeting.

THE NEUTRON CROSS-SECTION STANDARDS EVALUATIONS FOR ENDF/B-VI

A.D. CARLSON
National Bureau of Standards,
Gaithersburg, Maryland

W.P. POENITZ
Argonne-West,
Argonne National Laboratory,
Idaho Falls, Idaho

G.M. HALE
Los Alamos National Laboratory,
Los Alamos, New Mexico

R.W. PEELLE
Oak Ridge National Laboratory,
Oak Ridge, Tennessee,

United States of America

Abstract

As a first step in the development of the new ENDF/B-VI file, the neutron cross section standards are being evaluated. These standards evaluations are following a different process compared with that used for earlier versions of ENDF. The primary effort is concentrated on a simultaneous evaluation using a generalized least squares program, R-matrix evaluations, and a procedure for combining the results of the evaluations. The ENDF/B-VI standards evaluation procedure is outlined, and preliminary simultaneous evaluation and R-matrix results are presented.

INTRODUCTION

A primary function of the Cross Section Evaluation Working Group (CSEWG) is the evaluation of cross sections for the Evaluated Nuclear Data File, ENDF/B. This group is now focusing its efforts on the development of a new version of the file, ENDF/B-VI. As a first step in this process, the neutron cross section standards are being evaluated by the Standards Subcommittee of CSEWG. It was recognized that many evaluations have suffered from the procedure of qualitatively or semi-quantitatively combining complicated data sets by drawing a smooth curve through the existing data. Such evaluations are difficult to document and it is not clear how to determine uncertainties and covariance information.

In previous standards evaluations for ENDF/B, a hierarchical approach was followed. The order is generally the following: H(n,n) was considered the best known standard and was evaluated first and independently of the other standards. This standard is considered to be so well-known that measurements relative to the hydrogen standard are often called absolute measurements. The $^{6}Li(n,\alpha)$ cross section evaluation was then performed. The only $^{6}Li(n,\alpha)$ data which were used were absolute measurements or those measured relative to the H(n,n) which were converted to cross sections using the adopted hydrogen evaluation. Then the ^{10}B+n standard cross sections were evaluated. The only $^{10}B(n,\alpha_1)$ and $^{10}B(n,\alpha)$ data used were absolute measurements and those relative to H(n,n) or $^{6}Li(n,\alpha)$ which were converted using the new hydrogen and lithium evaluations. This process was continued for all the standards. This method for using ratio measurements does not properly use all the information available. For example, a ratio of the $^{10}B(n,\alpha)$ to $^{6}Li(n,\alpha)$ cross sections would be used in the $^{10}B(n,\alpha)$ cross section evaluation but not in the $^{6}Li(n,\alpha)$ evaluation. For the new ENDF standards evaluation it was felt that a simultaneous evaluation should be performed to assure consistent use of the available information. Thus ratio measurements of standard cross sections will have an impact on the evaluation of each of the standard cross sections in the ratio. Correlations in the experimental data should also be taken into account in the simultaneous evaluation.

To the extent that good quality absolute data on a given cross section are available in addition to measurements of that cross section relative to standards, the evaluation of that cross section (though it is not recognized as a "standard") should be performed simultaneously with the standards evaluation since it in principle will affect the values of the evaluated standard cross sections and their uncertainties. As a practical matter this combination of data from many nuclides can become a very immense problem

though it can be handled with enough time and money. Very few cross sections would have any appreciable impact on the determination of a standard cross section other than other standards. Including data on $^{238}U(n,\gamma)$, $^{238}U(n,f)$, and $^{239}Pu(n,f)$ could improve the quality of the standards evaluations since precise absolute measurements exist and many ratio measurements to the standards are available. There is, of course, the side benefit that evaluations of these important fuel cross sections will be obtained.

On the other hand, the Standards Subcommittee felt that it is important to include R-matrix analyses in the evaluation of the light element standards. Such analyses provide coupling to reaction theory and give a smooth meaningful analytical expression for the energy dependence of the cross section. The accurate determination of the R-matrix level parameters does require a large data base. This method had been used successfully in earlier versions of ENDF/B in the evaluation[1-4] of the ^{6}Li and ^{10}B standard neutron cross sections. Data in addition to angle integrated neutron cross sections such as differential cross sections, polarizations, and charged particle measurements involving the same compound nucleus were shown[5] in these analyses to have a significant impact on the standard cross sections. In the R-matrix analysis different reactions leading to the same compound nucleus are linked by unitarity to the standard cross section. This condition imposes constraints on the standard cross section which are particularly strong near resonances. The R-matrix method also should be less sensitive to systematic uncertainties assuming these uncertainties are uncorrelated among data for different reactions.

The ENDF/B-VI standards evaluation will, therefore, involve a simultaneous evaluation and R-matrix analyses. This approach will take advantage of the strengths of the two different analysis modes which make use of different classes of experimental information to impact on the evaluation of the standard cross sections. In the final versions of this work independent data bases will be used for the two methods of evaluation. It will then be necessary to combine the information obtained from these analyses in a proper way to form the final evaluation and its variance-covariance matrix.

EVALUATION PROCEDURE

The evaluation as outlined above will require a simultaneous evaluation using generalized least squares, R-matrix evaluations for the $^{6}Li+n$ and $^{10}B+n$ systems and a procedure for combining the results of these evaluations.

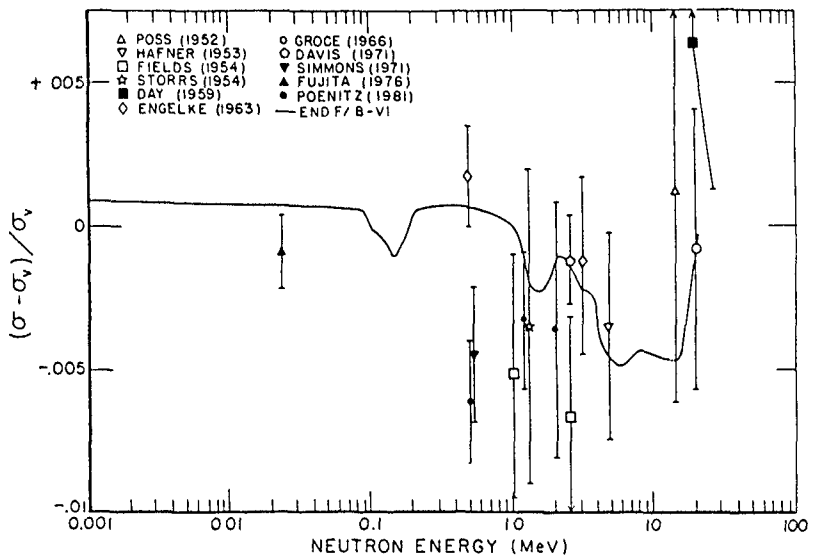

1. Comparison of high accuracy measurements of the hydrogen total neutron cross section and the ENDF/B-VI evaluation with the ENDF/B-V evaluation. References for the experimental data are given in Ref. 16.

It was decided that the hydrogen scattering cross section used in this evaluation would be fixed since it is known quite well. The new evaluation[6] by Dodder and Hale has been accepted as the new hydrogen standard for ENDF/B-VI. This evaluation is a result of the analysis of n-p and p-p data using the R-matrix formalism. In Fig. 1 the ENDF/B-VI evaluation and high accuracy total neutron cross section measurements are compared with ENDF/B-V. The ENDF/B-VI evaluation is in somewhat better agreement with measurements than the ENDF/B-V (Hopkins-Breit)[7] results. There is also a reduction in the reported uncertainty of the hydrogen cross section for the new evaluation, compared with that of ENDF/B-V.

The thermal cross sections recommended by Holden[8] for $^{6}Li(n,\alpha)$, $^{10}B(n,\alpha)$, and $Au(n,\gamma)$ and by Divadeenam[9] for $^{235}U(n,f)$, and $^{239}Pu(n,f)$ have been used as input data for the evaluations, though they have not yet been officially accepted as ENDF/B-VI data.

Measurements of the fission cross sections of ^{235}U and ^{239}Pu averaged over the ^{252}Cf spontaneous fission neutron spectrum are also to be included in the data base. These data can be obtained with high accuracy and are only weakly dependent on the uncertainties in the ^{252}Cf spontaneous fission neutron spectrum.

The simultaneous evaluation[10] is being performed with the generalized least squares program GMA. The cross sections being evaluated are $^{6}Li(n,\alpha)$, $^{6}Li(n,n)$, $^{10}B(n,\alpha_0)$, $^{10}B(n,\alpha_1)$, $^{10}B(n,n)$, $^{197}Au(n,\gamma)$, $^{235}U(n,f)$, $^{238}U(n,f)$, $^{238}U(n,\gamma)$, and $^{239}Pu(n,f)$. This evaluation uses a large data base file being assembled at Argonne National Laboratory. The data base includes both shape and absolute measurements of these cross sections and their ratios. In addition, total cross section measurements for ^{6}Li and ^{10}B are contained in the data base since the scattering and (n,α) data are interrelated to these measurements. Considerable effort has been expended in examining the various experiments looking for corrections, etc. which have not been fully documented in the published papers. Ratio measurements other than those to the hydrogen standard which have been converted to cross section values are reinstated to the originally measured quantities. Measurements relative to hydrogen have been converted using the new ENDF/B-VI evaluation. Perhaps the most difficult part of this work has been the determination for each experiment of the correlations in that experiment and with other experiments. This information is used to form covariance matrices for the measurements so that a full covariance analysis can be performed for the evaluation. An energy grid is defined for the evaluation which is the same for all cross sections involved in the evaluation and the fitting parameters are the values of the cross section at these grid points.

The R-matrix fits[11] are being done at Los Alamos National Laboratory with the program EDA. In these analyses the experimental data are used as measured with weighting normally based on the quoted uncertainties. It is assumed that no correlations other than overall normalizations are present among the measurements. The code uses automated search routines to minimize X^2 of the fits to the input data. In addition to the R-matrix parameters, derivatives with respect to these parameters and the covariance matrix are available as output. Following the fitting process, the cross sections will be calculated for the same energy grid as is used for the simultaneous evaluation to permit the combination of the results. The $^{6}Li+n$ and $^{10}B+n$ analyses are each being done separately with this code. For the ^{7}Li system the data base includes ^{6}Li total, $^{6}Li(n,n)$ integrated, $^{6}Li(n,n)$ differential, $^{6}Li(n,n)$ polarization, $^{6}Li(n,\alpha)$ integral, $^{6}Li(n,\alpha)$ differential, $^{4}He(t,t)$ differential, and $^{4}He(t,t)$ polarization data. For the ^{11}B system the data base includes ^{10}B total, $^{10}B(n,n)$ integrated, $^{10}B(n,n)$ differential, $^{10}B(n,n)$ polarization, $^{10}B(n,\alpha_0)$ integrated, $^{10}B(n,\alpha_0)$ differential, $^{10}B(n,\alpha_1)$ integrated, $^{10}B(n,\alpha_1)$ differential, $^{7}Li(\alpha,\alpha_0)$ differential, $^{7}Li(\alpha,\alpha_1)$ differential, and $^{7}Li(\alpha,n)$ differential data.

A procedure[12] for combining the simultaneous and R-matrix evaluations has been defined but not yet implemented. It is based on the observation that the individual fitting processes described above include computation of sums that can be combined to produce the same overall output parameters as would have been obtained from a global least squares fit of all the input data in terms of R-matrix parameters for the $^{6}Li+n$ and $^{10}B+n$ systems and pointwise values for the other cross sections. A program for performing the combination is being written at Oak Ridge National Laboratory. This procedure requires that the boron and lithium experimental data be separated into two uncorrelated groups, one to be used in the simultaneous evaluation and the other in the R-matrix analyses.* All ratio measurements other than those to the hydrogen standard are used in the simultaneous evaluation. The combining procedure makes use of the variance-covariance matrices from the separate fits as well as the derivatives with respect to the evaluation parameters of the fitted values corresponding to the input data elements. The output would be adjusted R-matrix parameters for the $^{6}Li+n$ and $^{10}B+n$ systems and final point cross sections for the remaining reactions, by taking into account in a consistent manner all the input data sets. If the procedure succeeds, the adjusted R-matrix parameters will be used to calculate the $^{6}Li+n$ and $^{10}B+n$ cross sections for ENDF/B-VI. It is expected that the procedure will work if the results of the simultaneous and R-matrix evaluations are not discrepant.

*A version of the method has been identified for handling a limited number of common data sets. This technique would allow evaluated data for thermal neutrons to be used in both analyses.

PRELIMINARY RESULTS OF THE EVALUATION

As a first step in the evaluation process, the R-matrix and simultaneous analyses have been performed without separating the lithium and boron experimental data into uncorrelated groups. Data base differences are thus reduced for these analyses and better consistency should be obtained. This also represents a baseline to be compared with the results obtained with the separate data bases. The degree of change in the cross sections for the different data bases will provide information about the sensitivity to data base changes.

The results to be presented are very preliminary. Output for the ^{6}Li and ^{10}B standard cross sections from the simultaneous and R-matrix evaluations will be shown compared to the ENDF/B-V results. For $^{197}Au(n,\gamma)$ and $^{235}U(n,f)$ the results of the simultaneous evaluation will not be shown but trends from the evaluation will be highlighted. It must be emphasized that any conclusions made here are based on the assumption that the results will not change significantly with the final grouping of the data and the use of the combination procedure.

In Fig. 2 the $^{6}Li(n,\alpha)$ results are compared with ENDF/B-V for the energy region from 1-100 keV. This cross section is identified as a standard for ENDF/B-V for neutron energies below 100 keV. There is no smoothing of the output from the simultaneous evaluation. Smoothing of these data will not be required in the final evaluation since the information from the simultaneous evaluation will be used to help create the adjusted R-matrix parameters. There is general agreement between the simultaneous and R-matrix results but the simultaneous evaluation results are systematically somewhat higher than those of the R-matrix calculations. The ENDF/B-V evaluation agrees well with the present results. From 10-100 keV the version V evaluation is generally between the results of the simultaneous and R-matrix evaluations. In Fig. 3 the $^{6}Li(n,\alpha)$ results near the ~ 240 keV resonance are compared. The agreement is good for all three sets of data, especially for the cross section at the peak of the resonance. The small differences between the present R-matrix results and those of ENDF/B-V indicate that the present data base is consistent with that used in the R-matrix analysis for ENDF/B-V. The systematically higher cross sections from the simultaneous evaluation persist, except very near the peak of the resonance. From these data alone one would

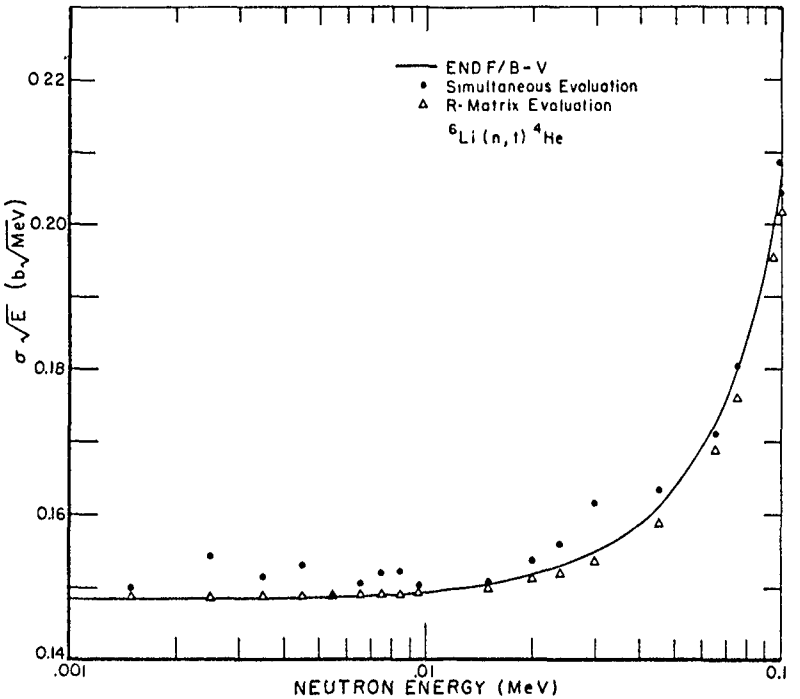

2. Preliminary results of the simultaneous and R-matrix evaluations for the $^{6}Li(n,\alpha)$ cross section for neutron energies from 1-100 keV compared with the ENDF/B-V evaluation.

conclude that the resonance is somewhat wider with larger cross sections in the wings than indicated by the R-matrix results.

The $^{10}B(n,\alpha_1)$ and $^{10}B(n,\alpha)$ results are shown in Fig. 4 for neutron energies from 1-100 keV. Note the highly expanded scale and suppressed zero. There is agreement among the evaluations except at the higher neutron energies where the simultaneous evaluation results are higher. This difference is to some extent due to the choice of data base used in the R-matrix analysis. In Figs. 5-6 the $^{10}B(n,\alpha_1)$ and $^{10}B(n,\alpha)$ results from 0.1-1 MeV are shown. Clear differences are evident in this energy range. The difference in the new R-matrix data base compared with that used for the ENDF/B-V evaluation is apparent. An important change in the data base is new $^{10}B(n,\alpha_0)$ data. For

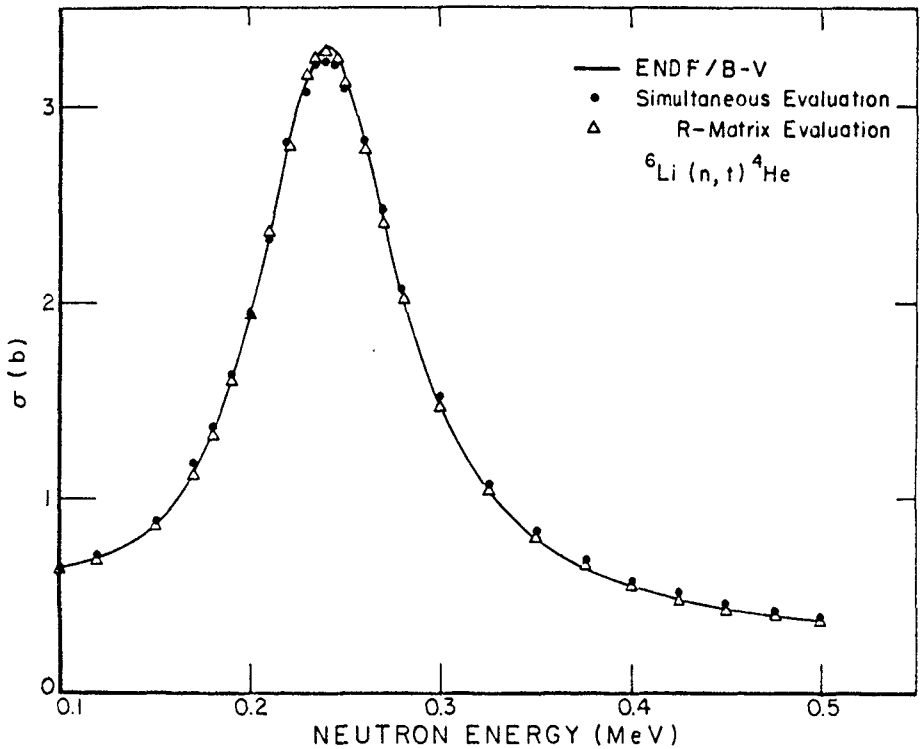

3. Preliminary results of the simultaneous and R-matrix evaluations for the $^{6}Li(n,\alpha)$ cross section for neutron energies from 100-500 keV compared with the ENDF/B-V evaluation.

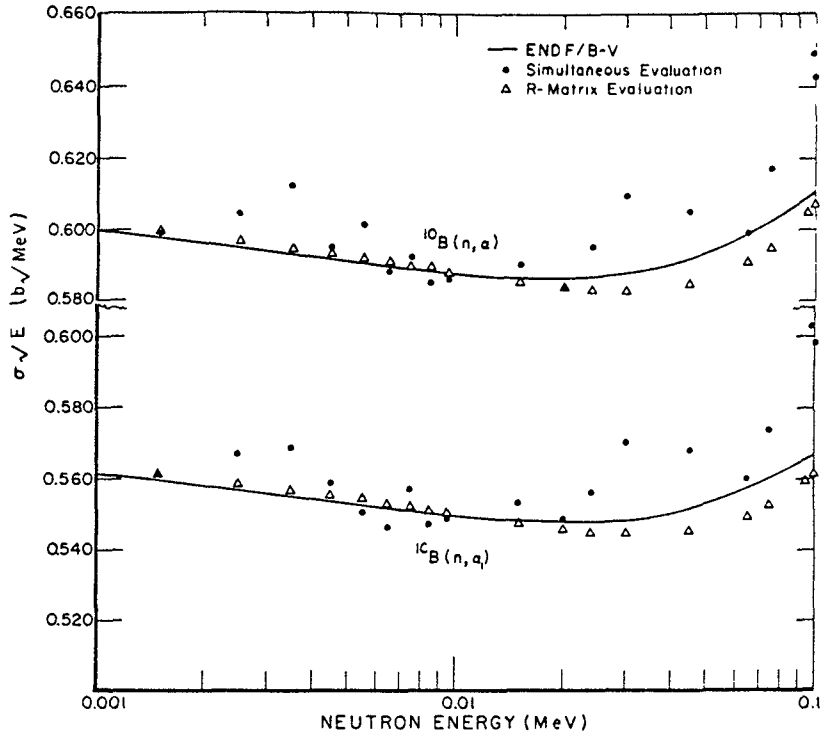

4. Preliminary results of the simultaneous and R-matrix evaluations for the $^{10}B(n,\alpha)$ cross sections for neutron energies from 1-100 keV compared with the ENDF/B-V evaluation.

the new R-matrix evaluation the resonances at ~ 0.3 and ~ 0.5 MeV are more pronounced, particularly for the $^{10}B(n,\alpha)$ cross section, and the cross sections are clearly higher at the higher neutron energies. The simultaneous evaluation results are distinctly larger than those of the R-matrix from 0.1-0.2 MeV, from 0.3-0.5 MeV and near 1 MeV. These differences are largely a result of the relatively poor data base for the neutron data.

The $^{197}Au(n,\gamma)$ evaluation is very similar to that of ENDF/B-V. There are changes of 5-6% in the energy range from 200-270 keV compared to ENDF/B-V as a result of the inclusion of data[13,14] which show structure due to competition with inelastic scattering. Otherwise, there are no obvious trends compared with ENDF/B-V at the present stage of this evaluation.

For the $^{235}U(n,f)$ preliminary evaluation a number of trends can be pointed out. Near 14 MeV the cross section is very well defined as a result of the number of very accurate measurements which have been made since the ENDF/B-V evaluation. In Fig. 7 the time correlated associated particle data measured near 14 MeV are shown. The simultaneous evaluation yields a cross section of 2.072 barns at 14 MeV which is in excellent agreement with the measurements and ENDF/B-V. The new evaluation is approximately the same

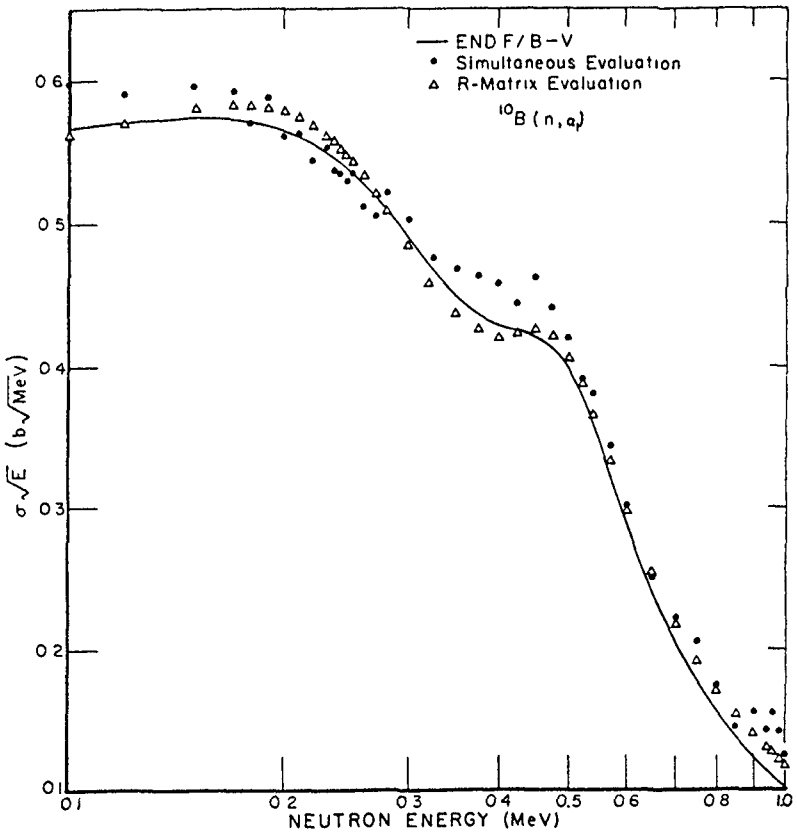

5. Preliminary results of the simultaneous and R-matrix evaluations for the $^{10}B(n,\alpha_1)$ cross section for neutron energies from 0.1-1. MeV compared with the ENDF/B-V evaluation.

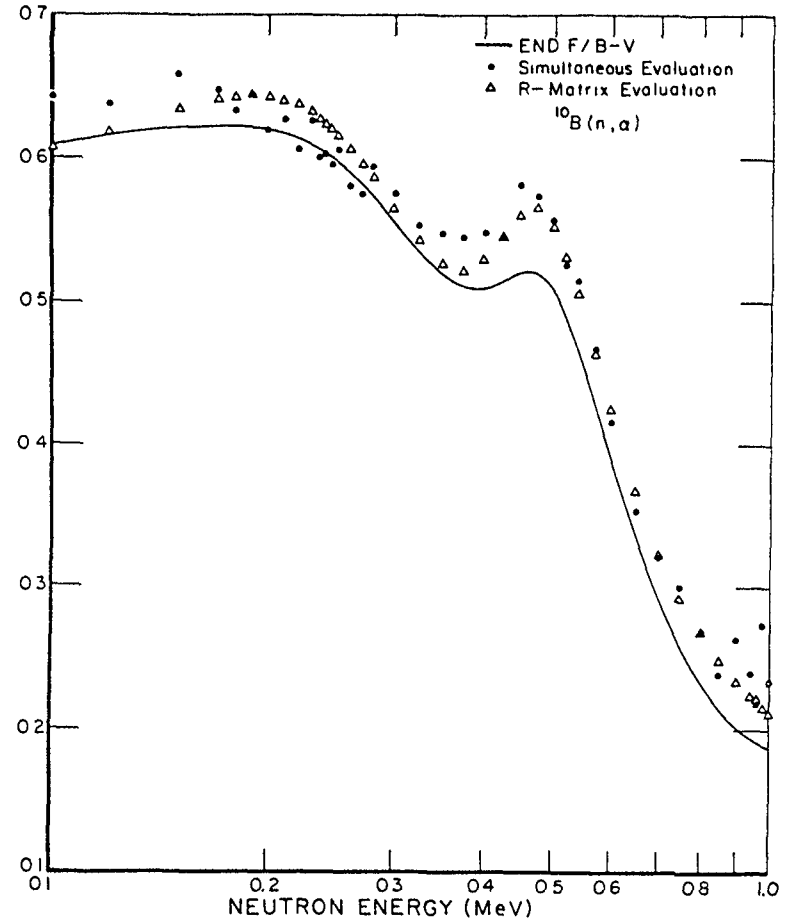

6. Preliminary results of the simultaneous and R-matrix evaluations for the $^{10}B(n,\alpha)$ cross section for neutron energies from 0.1-1. MeV compared with the ENDF/B-V evaluation.

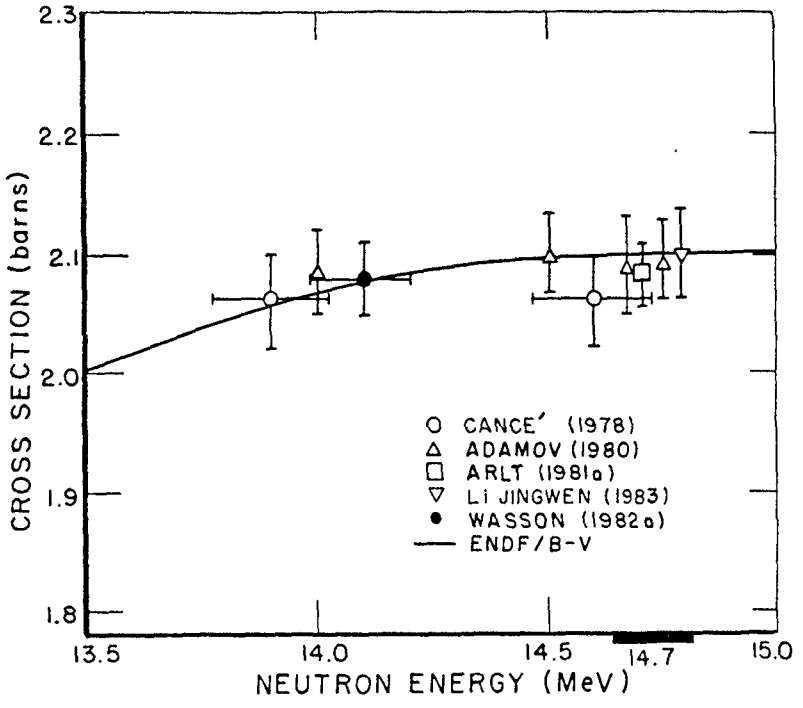

7. Measurements of the $^{235}U(n,f)$ cross section near 14 MeV compared with the ENDF/B-V evaluation. The preliminary value for the ENDF/B-VI evaluation at 14 MeV is 2.072 b. References for the experimental data are given in Ref. 16.

above 4 MeV, ~ 1-2% lower from 1-4 MeV and ~2% lower from 0.1-1 MeV compared with ENDF/B-V. An indication of the reduction in the evaluated cross section is given by the calculated average $^{235}U(n,f)$ cross section in a ^{252}Cf spontaneous fission neutron spectrum. This quantity is ~1.5% lower with the new evaluation compared with ENDF/B-V. Somewhat larger values of the thermal cross section and the integral from 7.8-11 eV are noted from this evaluation compared with the values recommended by Divadeenam[9] and Poenitz.[15]

CONCLUSIONS

The results reported here represent a "first pass" at determining the standards for ENDF/B-VI. The comparisons of the simultaneous and R-matrix evaluations are generally encouraging for both the boron and lithium standards when the quality of the neutron cross section data base is taken into account. For $^{197}Au(n,\gamma)$ and $^{235}U(n,f)$ noteworthy trends have been observed compared with ENDF/B-V. A significant amount of work remains to be done in determining sensitivity to various experiments, the grouping of the lithium and boron data, performing the combining procedure and resolving any inconsistencies.

REFERENCES

1. G.M. Hale, D. Dodder and P. Young, "ENDF/B-IV Summary Documentation for ^{6}Li," in ENDF-201 (BNL-17541) "ENDF/B Summary Documentation," compiled by D. Garber (1975).

2. G.M. Hale, R.A. Nisley and P.G. Young, "ENDF/B-IV Summary Documentation for ^{10}B," in ENDF-201 (BNL-17541) "ENDF/B Summary Documentation, compiled by D. Garber (1975).

3. G.M. Hale, L. Stewart and P.G. Young "ENDF/B-V Summary Documentation for ^{6}Li," in ENDF-201 (BNL-17541) "ENDF/B Summary Documentation," compiled by R. Kinsey (1979).

4. G.M. Hale, L. Stewart and P.G. Young "ENDF/B-V Summary Documentation for ^{10}B," in ENDF-201 (BNL-17541) "ENDF/B Summary Documentation," compiled by R. Kinsey (1979).

5. G.M. Hale, "R-matrix Analysis of the Light Element Standards" in Proc. of a Conf. on Nuclear Cross Sections and Technology, Washington, D.C. (Eds. R.A. Schrack and C.D. Bowman) NBS Spec. Publ. 425, p. 302 (1975).

6. D.C. Dodder and G.M. Hale, private communication (1983).

7. J.C. Hopkins and G. Breit, Nucl. Data A9, 137 (1971).

8. N.E. Holden, "Neutron Capture Cross Section Standards for BNL-325 Fourth Edition," USDOE(BNL) Report BNL-NCS-51388 (1981).

9. M. Divadeenam and J.R. Stehn, Ann. Nucl. Energy 8, 375 (1984).

10. W.P. Poenitz, "Data Interpretation, Objective Evaluation Procedures and Mathematical Techniques for the Evaluation of Energy-Dependent Ratio, Shape and Cross Section Data," Proc. of the Conf. on Nuclear Data Evaluation methods and Procedures, Brookhaven National Laboratory (Eds. B.A. Magurno and S. Pearlstein) BNL-NCS-51363 Vol. I, p. 249 (1981).

11. G.M. Hale, "R-Matrix Analysis of the ^{7}Li System," Proc. of the International Specialists Symposium on Neutron Standards and Applications, National Bureau of Standards (Eds. C.D. Bowman, A.D. Carlson, H.O. Liskien, and L. Stewart) NBS Spec. Publ. 493, p. 30 (1977).

12. R.W. Peelle (1983), private communication.

13. R.L. Macklin, private communication (1981).

14. V.N. Kononov, B.D. Yurlov, E.D. Poletoev and V.M. Timokhov, Sov. J. Nucl. Phys. 26, 500 (1977).

15. W.P. Poenitz, "Evaluation of ^{235}U(n,f) Between 100 keV and 20 MeV," USDOE (ANL) Report ANL/NDM-45 (1979).

16. A.D. Carlson, Prog. in Nucl. Energy 13, 79 (1984).

INDC/NEANDC STANDARDS FILE, STATUS REPORT

H. CONDÉ
Gustaf Werner Institute,
Uppsala, Sweden

Abstract

The technical cooperation between the IAEA International Nuclear Data Committee (INDC) and OECD/NEA Nuclear Data Committee (NEANDC) in producing a Nuclear Standards File is described. The objective of the file is to provide concise and readily usable reference guidelines to essential nuclear standard quantities for a variety of basic and applied endeavors.

The file consists of status summaries for sixteen nuclear data standards and include references to recent relevant work and areas of continuing uncertainties.

The 1982 version of the INDC/NEANDC Nuclear Standards File was published as an IAEA Technical Report (IAEA No. 227, 1983). The status of the individual nuclear standards in the 1982 version are summarized and the plans of updating the file are presented.

1 Introduction

Already at its first meeting in 1960 the European-American Nuclear Data Committee (EANDC), the precursor to the OECD/NEA Nuclear Data Committee (NEANDC), pointed out the importance of nuclear standard cross sections.

As a result of a proposal by R Bachelor a first standard meeting was held in Oxford in 1963 which was charged to point out suitable standard cross sections and flux monitors. At this meeting the cross sections for the ^{3}He(n,p), ^{6}Li(n,α), ^{10}B(n,α), ^{197}Au(n,γ) and ^{235}U(n,f)-reactions were discussed. A mayor problem at this time was the availability of detectors and samples.

The EANDC decided to send the report of this first standard meeting to the International Nuclear Data Scientific Working Group (INDSWG) within IAEA, the precursor to the International Nuclear Data Committee (INDC), which had met for the first time in May 1963. In this way a cooperation on nuclear standards was initiated between the two international data committees, which since then has become well established.

Since the first standard meeting in Oxford several standard cross section meetings have been arranged by INDC and NEANDC.

1 IAEA Panel on Standards, Brussels, 1967

2 EANDC Symposium on Neutron Standards and Flux Normalizations, ANL, 1970

3 Second IAEA Panel on Standard Reference Data, Vienna, 1972

4 Specialists' Meeting on Neutron Standards and Applications, Gaithersburg, 1977 (in cooperation with US/NBS)

Furthermore, special sessions have been devoted to nuclear standards at the occasion of the large regional nuclear data conferences e.g. in Knoxville 1979 and Antwerp 1982.

Several expert meeetings highlighting selected standard items of particular interest have also been arranged by INDC and NEANDC. As examples can be mentioned the IAEA consultants' Meeting on the U-235 Fast Fission Cross Section and the Cf-252 Fission Neutron Spectrum, Smolenice, Czechoslovakia, 1983.

In 1965 the EANDC decided to set up a standing sub-committee on standards. The counterpart within INDC was set up in 1970. A procedure was agreed upon in 1974 to exchange information on those standard items which were common to the Standard Files of both Committees.

The standards files of INDC and NEANDC consists of tabulated reference values and a status summary. The narrative summaries consists of concise statements on nuclear reference standards judge of importance by the Committees. These statements prepared by selected specialists outline the justification for each standard, provide guidelines for use, outline the contemporary status, including shortcomings, and suggest possible avenues toward improvements.

In 1981 the INDC, whith agreement of NEANDC, decided to publish and widely distribute the INDC/NEANDC Standard File. The objective to publish the file was to provide concise and readily usable reference guidelines to essential nuclear standard quantities for variety of basic and applied endeavors.

The NEANDC also agreed to take on the next publication of the file which is foreseen in a few years time.

2 The 1982 version of the INDC/NEANDC Standard File

The 1982 version of the INDC/NEANDC Standard File was published as an IAEA Technical Report (IAEA Techn Report Series No. 227, Vienna, 1983).

It consists of status summaries for sixteen nuclear data standards and data tabulations (table 1).

The large majority of the recommended numerical data is taken from ENDF/B-V, produed by the United States Cross Section Evaluation Working Group (CSEWG). The remainder of the numerical data is from evaluations undertaken by individuals or groups closely connected with nuclear data activities promoted by INDC and NEANDC.

Table 1. INDC Reference-Data-Type and Review Responsibilities 1981/1982

Standard	Responsibility National	Personnel
H(n,n)H	UK	CA Uttley
$^{6}Li(n,t)^{4}He$	USA	AB Smith/JM Hale
$^{10}B(n,\alpha)^{7}Li$	BCNM	E Wattecamps
C(n,n)C	USA	AB Smith
$^{197}Au(n,\gamma)^{198}Au$	BCNM	F Corvi
$^{235}U(n,f)$	USSR	GB Yankov
^{235}U Fiss Fragm Anisotropy	India	SS Kapoor
$^{238}U(n,f)$	USA	AB Smith
$^{27}Al(n,\alpha)$	Austria	H Vonach
Neutron Energy Standards	UK	GD James
Actinide Half-lives	IAEA/BCNM	A Lorenz/R Vaninbroukx
Thermal Parameters	IAEA/USA	HD Lemmel/N Holden
^{252}Cf Fission Spectrum	IAEA/USSR	HD Lemmel/GB Yankov
^{252}Cf Nu-bar	USA	AB Smith
Neutron Flux Comparisons	France	A Michaudon/G Grenier
Gamma-ray Standards	France/IAEA	J Legrand/A Lorenz

The **H(n,n)** cross section was reviewd by CA Uttley, Harwell. The ENDF/B-V numerical data were adopted between 1 keV and 20 MeV. The main concern was about the accuracy of the differential scattering cross section. This cross section was not known well enough from measurements and can not be calculated with high accuracy because the uncertainties in P-wave phases, particularly in $\sigma(^{1}P_{1})$. More analytical work which should include the accurate n-p analysing power data of Tornow et al (1) and all nucleon-nucleon scattering observables was recommended in the energy range 14 to 35 MeV.

The ENDF/B-V **$^{6}Li(n,t)$** cross sections was recommended as a standard between thermal and 100 keV neutron energy. It was concluded in the review by G Hale, LANL that a restriction on the usefulness of the $^{6}Li(n,t)$ cross section has been the lack of reliably determined cross sections for ^{6}Li over the 240 keV resonance but also above that energy. Problems, which were pointed out, were the differences in recent measurements over the resonance (2, 3, 4, 5, 6, 7), need for more measurements in the energy region 0.8-3 MeV and uncertainties of the reaction mechanism in the $n+^{6}Li$ process.

The status of the **$^{10}B(n,\alpha)$** cross section was summarized by E Wattecamps, CBNM. The applicable energy region for this standard

cross section was from thermal to 200 keV neutron energy and the numerical data were taken from ENDF/B-V. From thermal energy up to 40 keV the uncertainty on the recommended $^{10}B(n,\alpha_1)$ value in ENDF/B-V is claimed to be 0.3 %. The uncertainty rises with increasing energy and amounts to 1.2 % at 200 keV. On the other hand fairly large uncertainties are obtained between calculated (using ENDF/B-V data) and measured reaction rate ratios of commonly accepted standards e.g. the $^{10}B(n,\alpha)$ and $^{6}Li(n,\alpha)$ (8) and the $^{10}B(n,\alpha)$ and $^{3}He(n,p)$ (9) reaction ratios. Improving the accuracy of the underlying experimental data base for ^{10}B is a very demanding task.

The **$^{12}C(n,n)$** cross section is adopted as a neutron scattering standard up to 2 MeV or below the sharp resonance at 2.087 MeV. In the status report AB Smith, ANL points out that the ENDF/B-V data are reasonable accurate below 5 MeV (1 %). He also claims that this scattering standard could be very useful to 10 MeV if the elastic scattering cross sections were well known at selected energies in the range 5-10 MeV. Measurements towards defining the elastic scattering cross section away from prominent resonances to accuracies of about 1 % are encouraged.

The **$^{197}Au(n,\gamma)$** cross section is recommended as a standard in the energy region 0.2-3.5 MeV. F Corvi, BCNM concludes in his status report that the most recent measurements (10, 11, 12) have cross section values lower (5-20 %) than the ENDF/B-V data for neutron energies above 1 MeV. This trend contineous also at lower energies based on the data by Macklin (12). Below 200 keV the cross section shows fluctuations. It is therefore suggested that in this energy region (from 5 to 200 keV) experimentalists give, whenever possible, in parallel with a pointwise representation, also averages in determined energy intervals.

The recommended neutron energy range of application for the **$^{235}U(n,f)$** cross section is from 0.1 to 20 MeV. In this energy range GB Yankov, KUR compares recent measurements with the ENDF/B-V file. At 100 keV the measurements by Mostovaya et al (13) and Corvi (14) are 3-4 % lower than the corresponding ENDF/B-V value and at 2.6 MeV the measurement by Arlt et al (15) gives about 3 % lower value than that of Cancé et al (16) which in turn agrees with the ENDF/B-V value. Good agreement (~1 %) were observed between recent measurements and ENDF/B-V at 14 MeV. It was concluded that the energy range from 3.0 to 6.0 MeV is likely to be the major one where uncertainties remain.

A knowledge of the **^{235}U fission fragment anisotropies** is of importance in the evaluation of experimental fission cross section measurements. For that reason the status of this item was reviewed for the INDC/NEANDC Standard File by SS Kapoor, BARC. The scattering of experimentally determined anisotropies ($W(0^o)/W(90^o)$) are very large, in praticular above 5 MeV. This means, in turn, that the present knowledge of K_0^2 (the variance of the assumed Gaussian distribution of K) is inadequate in particular above 5 MeV and more measurements are requested.

The **$^{238}U(n,f)$** cross section is included in the Standard File as being a useful reference standard from threshold to 20 MeV in fast neutron flux determinations. However, the cross section shows fluctuations of several percent, as remarked by AB Smith, ANL, well into the few-MeV range with a periodicity of a few tens of keV. Systamatic discrepancies also remain in certain energy regions and with respect to some data sets.

The **$^{27}Al(n,\alpha)$** cross section is widely employed as a standard in dosimetry and activation measurements. A recent evaluation between threshold and 20 MeV by Tagesen and Vonach (17) was adopted for the Standard File. Except for the low threshold region and about 8-9 MeV the accuracy of the evaluated data was claimed to be better than 5 %. In particular, an accuracy of about 0.5 % was estimated for the $^{27}Al(n,\alpha)$ cross section at 14 MeV. A measurement of the ratio $^{235}U(n,f)/^{27}Al(n,\alpha)$ was suggested in order to verify that the desired accuracies (~1 %) of these two cross sections at 14 MeV have been achieved.

Neutron resonances to be used as **energy standards** were compiled and reviewed by GD James, AERE in consultation with members of an INDC Sub-Group on Neutron Energy Calibration. Forty neutron resonances between 0.6528 eV and 12.1 MeV were recommended as energy standards. For some of the resonances, measurements are sparse and not of high accuracy. Experiments should be encouraged to provide energy measurements of the highest attainable accuracy and precision for these poorly measured resonances. The ratio of the resonance width to the resonance energy should also be given so that the suitability of a given resonance for accurate standardization can be quickly judged.

The **actinide half-lives** enter as major parameters in the correction for sample decay in the precision measurement of fission cross sections of fissile isotopes, as well as in the mass determination of samples. Thus, the half-lives for the alpha- and spontaneous fission decay modes of $^{233,234,235,238}U$, ^{237}Np, $^{239,240,241,242,244}Pu$ and ^{252}Cf are given in the file. The list has been produced and updated within a co-ordinated research programme on the measurement and evaluation of transactinium isotope decay data pursued under IAEA auspicies for several years. The data have been drawn from the Evaluated Nuclear Structure and Decay Data File (ENSDF), the actinide file of the Idaho National Engineering Laboratory and UK Chemical Nuclear Data Committee Heavy Element Decay Data File.

The status of evaluations for the **thermal parameters** was reviewed by HD Lemmel, IAEA. Data from three different evaluations of the 2 200 m/s cross sections for $^{233,235}U$, ^{239}Pu and ^{241}Pu are given, namely the ENDF/B-V, NNDC (18) and Axton evaluations (19). It is remarked that the discrepancy in the fission and capture cross section of ^{235}U between σ_o, measured with monoenergetic neutrons of 0.0253 eV and $\langle\sigma\rangle$ measured in a thermal Maxwellian neutron spectrum is resolved by the new evaluations of NNDC and Axton owing to revised values of half-lives, ν and g-factors.

The review of the **prompt fission neutron spectrum** of ^{252}Cf was written by HD Lemmel, IAEA, GB Yankov, IAE and H Condé, FOA at a time when several new measurements and calculations were in progress. Up to that time a wealth of older information was available but neither the shape nor average energy was known to a good acuracy. Pending a new evaluation it was recommended that a Maxwellian form of the ^{252}Cf spectrum with a temperature T=1.42 MeV would be used as a contemporary reference.

For a long period of time there has been a serious discrepancy (~2 %) between measurements of **nu-bar for ^{252}Cf** using liquid scintillators and manganese bath. The status report by AB Smith, ANL gives information about recent accurate measurements where the old discrepancy is not seen. A final recommended value is not given but it is noted that the two recent evaluations by AJ Axton (19) and Stehn et al (18) both give a value of total nu-bar=3.766 with estimated errors of ±0,005.

A review by G Grenier, BRC is also given in the INDC/NEANDC standard report about ongoing **neutron flux comparisons** under the sponsorship of the "Comité Consultatif pour les Etalons de Mesure des Rayonnements Ionisants" (BIPM). The methods, the neutron energies, the participating and co-ordinating laboratories are given. The neutron flux determined by the in-house equipment was compared with a flux monitor which was transferred between the laboratories and could be either a fission chamber, $^{115}In(n,\gamma)^{116}In$, $^{115}In(n,n')^{115}In$ or $^{93}Nb(n,2n)$ depending on the neutron energy.

The calibration of gamma detectors is of fundamental importance for the accurate measurement of energies and intensities of gamma rays. Thus, a list of **decay data for radionuclides used as calibration standards** has been incorporated into the Standard File.

The radionuclides chosen to be included in the list were selected on the basis of their inclusion in the following compilations:

- The 1980 version of the INDC/NEANDC Standard File
- The 1979 list of standards for gamma ray energy calibration recommended by the International Union of Pure and Applied Chemistry (IUPAC)
- The 1980 report by the AECL Radioisotope Standardization Group to the Spectrometry Working Group of the International Committee for Radionuclide Meteorology (ICRM).

The most recent values of the half-lives, gamma-ray energies and emission probabilities were selected from several different publications and compilations of evaluated data. Most of the data are available in the ENSDF library. The intention is to update these gamma-ray standards as new evaluation are performed and in co-operation with the efforts of the International Committee for Radionuclide Meteorology (ICRM) Working Group on alpha-, beta- and gamma-ray spectroscopy.

3 Updating of the INDC/NEANDC Standard File

A procedure was agreed upon to update the 1982 version of the INDC/NEANDC Standard File. The responsibility for the updating will be with the NEANDC and in particular with the NEANDC Standard Subcommittee.

The present NEANDC reviewers of the different items in the file are listed in table 2. For most of the standards the reviewers are the same for two Committees.

Table 2. INDC/NEANDC Review Responsibilities 1984

Item	INDC	NEANDC
H(n,n)H	USA P Young	
$^{6}Li(n,t)^{4}He$	USA AB Smith/G Hale	
$^{10}B(n,\alpha)^{7}Li$	CBNM E Wattecamps	
C(n,n)C	USA AB Smith	
$^{197}Au(n,\gamma)^{198}Au$	CBNM F Corvi	
$^{235}U(n,f)$	USSR V Konshin	UK M Sowerby
^{235}U Fiss Fragm Anisotropy	INDIA S Kapoor	- -
$^{238}U(n,f)$	JAPAN K Harada/S Igarasi/Y Kanda	
$^{27}Al(n,\alpha)$	AUSTRIA H Vonach	
Neutron Energy Standards	ITALY C Coceva	
Actinide Half-lives	IAEA/CBNM A Lorenz/R Vaninbroukx	
Thermal Parameters	IAEA HD Lemmel	
Low Energy Cross Section Dependence	BELGIUM C Wagemans	
^{252}Cf Fission Spectrum	IAEA H Lemmel USSR H Blinov	USA AB Smith D Olsen
^{252}Cf Nu-bar	AUSTRALIA JW Boldeman	
Neutron Flux Comparison	FRANCE A Michaudon/G Grenier	
Gamma-ray Standards	FRANCE J Legrand IAEA A Lorenz	

The preparation of the next version of the INDC/NEANDC Standard File will to a large extent benefit of the discussions which will take place at this meeting. This concerns both the status of the present nuclear standards in the file and proposals on new standards.

References

1 W Tornow, PW Lisowski, RC Byrd and RL Walter. Nuclear Physics A340 (1980) 34

2 C Renner, JA Harvey, NW Hill, GL Morgan and K Pusk. Bull Am Phys Soc 23 (1978) 526

3 RL Macklin, RW Ingle and J Halperin. Nucl Sci Eng 71 (1979 205

4 GP Lamaze, RA Schrack and OA Wasson. Nucl Sci Eng 68 (1978) 183

5 HH Knitter, C Budtz-Jørgensen, M Mailly and R Vogt. CBNM Report EUR 572e (1977)

6 AB Smith, P Guenther, D Havel and JF Whale. ANL Report ANL/NDM 29 (1977)

7 JA Harvey and NW Hill. Proc Conf on Neutron Cross Sections and Tech, March 3-7, 1975, Washington DC, NBS Special Publication 425

8 JB Czirr and AD Carlsson. Proc Int Conf on Nuclear Cross Sections for Technology, Knoxville 1979 p 84

9 CD Bowman, JW Behrens, R Gwin and JH Todd. Proc Int Conf on Nuclear Cross Sections for Technology, Knoxville 1979 p 97

10 S Joly, J Voignier, G Grenier, DM Drake and L Nilsson. Nucl Sci Eng 70 (1979) 53

11 AN Davletshin, SV Tikhonov, AO Tipankov and VA Tolstikov. At Energ 48, 2 (1980) 87

12 RL Macklin. Nucl Sci Eng 79 (1981) 265

13 TA Mostovaya, VI Mostovoj, SA Biryukov, AA Ossochinikov and AV Shvetsov. Proc 5th All-Union Conf of Neutr Phys, Kiev 1980, Part 3, (1980) 30

14 F Corvi, private communication (1981)

15 R Arlt et al. INDC(GDR)-16/6 (1981)

16 M Cancé, G Grenier, D Gimat and D Parisot. NEANDC(E) 211/L (1981) 14

17 S Tageson and H Vonach. Physics Data 13-1, Fachinformationzentrum, Karlsruhe (1981)

18 JR Stehn, M Divadeenam and NE Holden. Proc of Conf on Nucl Data for Science and Tech, Antwerp 1982 p 685

19 EJ Axton. CBNM Report CBNM/Ph/1/83 (1983)

IAEA STANDARDS FILE: SOME COMMENTS AND RECOMMENDATIONS

M.V. BLINOV, S.K. VASIL'EV, V.D. DMITRIEV,
Yu.A. NEMILOV, V.P. CHECHEV, E.A. SHLYAMIN,
V.I. SHPAKOV, A.V. SOROKINA
Khlopin Radium Institute,
Leningrad

A.A. GOVERDOVSKIJ, V.N. KORNILOV, V.A. TOLSTIKOV
Institute of Physics and Power Engineering,
Obninsk

Union of Soviet Socialist Republics

V.A. KON'SHIN, E.Sh. SUKHOVITSKIJ
Institute of Nuclear Power,
Minsk,
Byelorussian Soviet Socialist Republic

Abstract

The paper contains comments and recommendations on: radioactive fast neutron capture cross-section of ^{197}Au; ^{235}U fission cross-section; ^{238}U fission cross-section; the possibility of using the ^{237}Np fission cross-section as a standard; $^{27}Al(n,\alpha)$ reaction cross-section; actinide half-lives; ^{252}Cf spontaneous fission prompt neutron spectrum; the average number of neutrons per ^{252}Cf spontaneous fission event; and on the data on radionuclide decay used as calibration standards.

Introduction

This report is prepared by competent specialists of the USSR Institutes and it shows their standpoint on the current state of a number of nuclear data approved by the IAEA as standards. Separate sections of this report are prepared by the specialists concerned with the measurements and evaluations in these specific fields and present critical remarks and recommendations on improvement of the available data. The report is redacted by V.D. Dmitriev and V.I. Shpakov.

The editors accentuated debatable questions, for the discussion of vexed points can help to solve the problem of increasing the reliability and accuracy of evaluated nuclear constant values.

1. Radiative fast neutron capture cross-section of ^{197}Au

The values of $^{197}Au(n,\gamma)$ reaction cross-section are used as a standard in the energy range E_n = 0,195-4 MeV. The absence of reliable data in the region E_n > 4 MeV prevents us at present from raising the question of cross-section standardization in this energy range. Under specified conditions the capture cross-section of gold in the energy region E_n < 200 keV, in spite of its resonance structure, can be quite a good standard for the measurements on a well-known neutron spectrum, when small shifts of neutron energy do not cause a significant variation of averaged cross-section.

For the neutron energy range, where the $^{197}Au(n,\gamma)$ cross-section is used as a standard, the results of many works /1-9/ have been published in recent years. In the energy region E_n < 2 MeV the new data, in the main, agree well with the ENDF/B-V evaluation, but in the range of 100-200 keV the results of /5/ are almost 10% lower than evaluated ones. In the range of energies E_n > 2 MeV the results of new measurements agree well with each other and with preliminary results of Bergkwist /9/, which are almost 30% lower than the evaluation.

The results available at present make it possible to draw a conclusion about the necessity of a new evaluation for ^{197}Au fast neutron capture cross-section. It should be useful to perform new measurements for E_n > 1,5 MeV and to develop well-grounded correct approaches to the evaluation of cross-section in the range from 3 to 14 MeV.

II. ^{235}U fission cross-section

^{235}U fission cross-section at neutron energies from 100 keV to 20 MeV is one of the basic standards responsible for accurace

of a great number of nuclear data and a number of other neutron standards such as prompt neutron spectrum of ^{252}Cf spontaneous fission and ^{238}U fission cross-section. Therefore high requirements for its accuracy are justified.

The evaluation of ENDF/B-V library presently used as a standard was performed in 1979 and did not include the results of subsequent works on $\sigma_f(^{235}U)$ cross-section measurement /1-7/, which differ from those obtained earlier by modern organization of experiment and lower experimental errors. On the whole, the new data show lower values of $\sigma_f(^{235}U)$. In this connection V.A. Kon'shin, E.Sh. Sukhovitskii et al. performed a new evaluation of $\sigma_f(^{235}U)$ including simultaneously old and new data. Together with the σ_f evaluation, a special attention was given to the evaluation of error, since the errors of many experimental. Works are strongly correlated because of similar techniques and identical standard cross-sections used for normalization. The evaluation technique giving the possibility to analyse the correlations between errors is described in /8/. The evaluation has been carried out in two energy regions: 100 eV - 100 keV and 100 keV - 20 MeV.

The comparison of the evaluated data with those of ENDF/B-V shows their agreement within 1%. The analysis of experimental technique errors and of experimental data agreement allowed us to conclude that in the range of neutron energies 30÷150 keV the error is within ±4%, in the range 150 keV - 4 MeV it is ±3%, in the range 4-10 MeV 3,5%, in the range 10-15 MeV ±4% and in the range 15-20 MeV ±6%.

Thus for the existing system of experimental data the evaluation of ENDF/B-V is adequate.

At the same time, the analysis of the existing system used as a basis for evaluations shows that this system is not self-consistent. Any evaluation procedure based on the analysis of declared errors and other measurement characteristics cannot provide the values evaluated with required accuracy (1-1,5%).

In the range of neutron energies 100-200 keV the disagreement in time-of-flight data and measurement results at some points reaches 6%. The data available for the energy region 200 keV - 1 MeV (except for those of F. Kappeler /9/) agree within 3%; however the last results of O.A. Wasson obtained with different techniques /5, 6/, being in agreement with each other and with preliminary results of A.D. Carlson /10/, are systematically lower than earlier data.

In the 1-7 MeV region the scatter of results reaches 10%, and these data are distinguished by the value and the shape of energy dependence, therefore their agreement connot be provided by means of re-normalization. Basic data in this region are devided into two groups: the data with higher σ_f values characterized by a convex curve and those with lower σ_f values characterized by a concave curve.

In the 7-20 MeV region the data present the results of four measurements of shape /11-14/. Moreover, if in the range of 7-13 MeV their discrepancy does not exceed 5-7%, in the range of 15-20 MeV the difference reaches 10-15%. An exception is a narrow energy interval from 14 to 15 MeV, where there is a very good agreement between two measurements of shape /13-14/ and five monoenergetic measurements carried out using time-correlated associated particle technique /TCAPT/ /1, 2, 7, 15, 16/ and monitoring neutron flux by reaction on iron /17/.

In most cases the disagreement of experimental data is much greater than declared errors of measurements (1,5-3%), which points to the existence of unidentified systematic errors in some or many measurements. Thus, the acquisition of reliable cross-section values is determined by critical analysis of the data base system with the purpose of detecting these errors, correcting appropriate data and, perhaps, reducing the weight of the least reliable data of eliminating them from the evaluation.

Some characteristic features of measurements can be noted. A.D. Carlson's measurement results /14/ have a shape substan-

tially different from that of other authors and involve a number of structures whose existence seems doubtful. The results of J.B. Czirr /13/ and A.D. Carlson /14/ obtained with an analogous technique disagree substantially. The results of B. Leugers /11/ and K. Kari /12/ obtained practically with the same technique are systematically higher than the bulk of data. This may be connected with underestimation of the neutron flux value because of the loss of cases with small energies of recoil protons due to the discrimination threshold in the gas scintillation counter used in measurements. This particularly relates to the neutron energy range 1-6 MeV. At any rate it is clear even now that in the neutron energy range from 14 to 15 MeV the results of these works are obviously overestimated.

It should be noted that in a number of cases the results of measurements obtained by the same outhors substantially diverge /18, 19/. It is evident that systematic errors responsible for these differences can be determined best of all by the authors of these works. In such cases the authors should be recommended to analyze carefully the results and to present fitted reliable values.

One of the ways of discovering unidentified systematic errors can be absolute monoenergetic measurements. Such measurements give good results at neutron energies 14-15 MeV. The most part of these measurements /1, 2, 7, 15, 16/ is carried out with the same technique (TCAPT), and their results are strongly correlated by the nature of main sources of systematic errors. Howeven these results agree well with those of three other measurements performed with other methods /13, 14, 17/. At the same time the TCAPT makes it possible to reduce appreciably systematic errors of measurements (the effect of scattered neutrons is eliminated, there is no need for determination of associated particle integral and for inclusion of geometry effects).

At present in the most divergent region (1-6 MeV), in addition to early data of White, there are five results of monoenergetic measurements: three results of M. Cancé obtained with reference to a standard - neutron scattering cross-sections on hydrogen at neutron energies 2,5 MeV (two) and 4,5 MeV, the result of measurement with TCAPT at 2,6 MeV performed within the frames of collaboration between Technical University of Dresden (TUD) and V.G. Khlopin Radium Institute of Leningrad (RIL) /3/ and recent result obtained by the same investigators with the same method at neutron energy 4,5 MeV ($\sigma_f(^{235}U)$ = = (1,057 ± 0,022)). Two values of $\sigma_f(^{235}U)$ measured by M. Cancé are somewhat higher than the ENDF/B-V evaluation and they are in the middle of two above-mentioned groups of data. Both the third result of M. Cancé for neutron energy 2,5 MeV, and the results of joint measurement by TUD and RIL agree well with lower group of data, particularly with the results of W.P. Poenitz /18/. It is evident that to solve the question of reliability of one or another group of data, supplementary monoenergetic measurements are necessary. Withir the frames of collaboration between TUD and RIL the measurement at neutron energies 1,7 and 19 MeV are under way. At the same time the realization of experiments with worse accuracy but uncorrelated with available experimental data may be justified.

The intercomparison of targets used in the USA and the USSR taking place now is of great importance for determination of unidentified systematic errors sources and for improvement of data reliability. It weems important to determine not only common characteristics, e.g. nuclei number, surface density and layer homogencity, but also such characteristics as fragment flight in the layer and efficiency of fragment registration versus neutron energy using, for example, C. Budtz-Jörgensen technique /20/. It seems also promissing to organize the exchange of programs for calculation of different corrections and of detailed documentation on experiments between interested specialists for combined examination and for development of recommendations on new evaluations.

III. ^{238}U fission cross-section

The ^{238}U fission cross-section is used as a standard for measurements of neutron fluxes, threshold neutron cross-sections and for dosimetry. The requirements on accuracy of $\sigma_f(^{238}U)$ value determination are very high ($\delta \approx 1$-2%); they are determined by the demands of reactor technology /1/.

The data on $\sigma_f(^{238}U)$ available at present can be conditionally devided into two groups. The first group includes the works performed with the use of monoenergetic neutrons /2-6/; hte second one includes the data obtained using neutron sources with continuous energy spectrum /7-10/. Absolute measurements of ^{238}U fission cross-section have been carried out only for neutron energies E_n = 14,2 MeV /6/ and W4,7 MeV /11/, but the main part of results has been obtained by measurement of ^{235}U and ^{238}U cross-section ratios. Thus, the scatter of $\sigma_f(^{238}U)$ absolute values is connected to a large extent with determination of ratio of fission fragment registration efficiences and of that of both nuclide nuclei numbers in samples.

In most works /2-6, 10/ absolutisation of cross-section ratios has been carried out using "isotopic admixture" or "threshold cross-section" method /10/, which eliminates the need for determination of absolute efficiencies of fission fragment registration. Moreover, in the works /3, 4/ comparative α-spectrometry of samples has been performed, which considerably increases the reliability of ratio normalization in the range of E_n from 2 to 3 MeV. The avaluation ENDF/B-V adopted at present as a standard of $\sigma_f(^{238}U)$ is essentially based on the second group data characterized by a number of shortcomings: a low efficiency of fission fragment registration /7/, the absence of data normalization /9/ and great statistical and total errors as compared with the first group data. Fig. 1 presents for comparison the deviations from the ENDF/B-V evaluation of the first group results (including new measurements /2, 4/ (a) and of the second one (b). The values of ^{235}U fission cross-section for determination of $\sigma_f(^{238}U)$ and $\sigma_f(^{235}U)$ evaluation ratios are taken from /12/. The figure shows that the first group results are systematically higher that the evaluated values of $\sigma_f(^{238}U)$ by 1,5-2% in the energy region 5-8 MeV and by 0,5-1% in the energy region $E_n > 8$ MeV, At the same time the second group data (for example /7/) are on the average 5% lower than the evaluated ones.

Taking into consideration the above-mentioned, it seems advisable to perform a new evaluation of $\sigma_f(^{238}U)$ in which it is suggested to take into account new results and to decrease the weight of the data from /7/. It should be noted that the accuracy of $\sigma_f(^{238}U)$ evaluated values does not satisfy the requirements of a standard, therefore it is important to carry out new measurements, especially absolute and monoenergetic ones in the entire energy range.

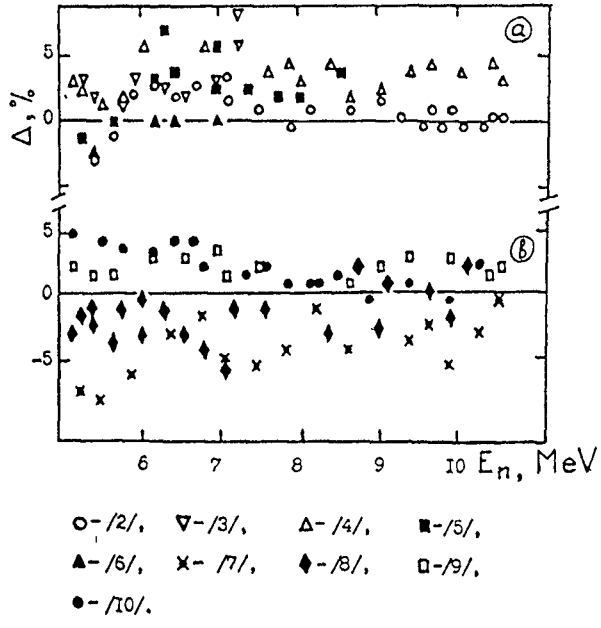

Fig. 1. The deviations of experimental data on ^{238}U fission cross-section from ENDF/B-V evaluation.

IV. On the possibility of using the ^{237}Np fission cross-section as a standard

On recent years the problem of using $\sigma_f(^{237}Np)$ together with $\sigma_f(^{238}U)$ as standards for threshold neutron cross-section measurements and for dosimetry has been discussed. At present there is no general opinion about this problem, since this method has both great advantages and serious difficulties.

The advantages:

- ^{237}Np fission cross-section is almost two times larger than that of ^{238}U;
- high α-activity of Np facilitates the conditions of target certification (determination of nuclei number, monogencity of layer etc.);
- a lower, as compared with ^{238}U, threshold which offers a means of enlarging the energy range of the standard use.

The shortcomings:

- high α-, β- and γ-activities complicate the measurements (as compared with ^{238}U);
- a comparatively high fissionability below the observed threshold can exert an adverse effect when using high-background neutron sources;
- a great scatter of experimental data available at present,

The most serious objection against using ^{237}Np as a standard raises the third point, since the experience of working with radioactive samples shows that other difficulties are surmountable.

The most of the data on $\sigma_f(^{237}Np)$ are obtained by the measurements with reference to ^{235}U fission cross-section. Absolute measurements have been carried out for neutron energies 0,15-1,5 MeV /1/, 0,770 and 0,964 MeV /2/, 2,5 MeV /3/, 8,5 and 14,7 MeV /4-6/. In the work /7/, where ^{237}Np neutron cross-sections are evaluated in a wide neutron energy range, the results of fission cross-section measurement published up to 1980 are also discussed.

In the neutron energy range from the threshold up to the first plateau ($E_n \sim 1$ MeV) the most of experimental data agree satisfactory with each other except for the range $E_n > 0,8$ MeV, where the results of rather old measurements /1/ and /8/ show a significant discrepancy with other data: the results of /1/ are lower and those of /8/ higher than the evaluation of /7/. At neutron energies 1-6 MeV (the region of the first plateau) the results of different authors are grouped in deviation interval 5-6%. The most significant discrepancy exists in the energy range $E_n > 6$ MeV. Except for the results of the work /9/, which in the range of 6-8 MeV agree with the data of /10/, other new measurements /11, 12/ show lower values of $\sigma_f(^{237}Np)$ and are in a fair agreement with each other and also with the results of absolute measurements /1-6/ and with those of the work /13/.

The foregoing shows that the scatter of $\sigma_f(^{237}Np)$ values, especially in the range of $E_n > 8$ MeV, is rather significant and may be connected with the errors of absolutisation of cross-section energy dependences, although the situation is not a dramatic one.

Thus at present there is no common opinion about the necessity of introducing a new standard - ^{237}Np cross-section. However it is undoubtful that for standardization of this cross-section, along with thorough examination of available data, new measurements, in particular absolute ones, are needed.

V. $^{27}Al(n,\alpha)$ reaction cross-section

The $^{27}Al(n,\alpha)$ reaction is widely used both in reactor dosimetry and as a reference cross-section for monoenergetic neutron flux measurements in the energy range from 5 to 20 MeV. The evaluation of H. Vonach and S. Tagesen /1/ which agrees well with ENDF/B-V evaluation /2/ is recommended as a standard.

The accuracy of evaluated curve is unlikely to be satisfactory, as its errors are 3-5%, and in the energy ranges 5-6 and 8-9 MeV they reach 9-10%. Only at neutron energies 13,5-14,5 MeV the reaction cross-section can be thought to be known with accuracy of 0,5%.

A great error of evaluated curve is connected with the fact that the data used for evaluation have a considerable scatter. The measurements have been carried out under different experimental conditions, at different level of experimental technique, at great uncertainties of neutron energy (> 100 keV) and with the use of different means for neutron flux evaluation. The discrepancy of experimental data, particularly in the energy range 7,5-8,5 MeV, is likely to be connected with the errors in determination of neutron mean energy for the experiments with a poor resolution. The variation of energy by 20 keV can cause a 3%-variation of cross-section value in this region.

An important problem, which is insufficiently discussed, is the possibility of describing the reaction excitation function by a smooth dependence. So, in the work /3/ performed with resolution berrer than 100 keV significant fluctuations of cross-section in the range of 6-8,5 MeV have been found. In many experimental data for the neutron energy region near 12 MeV a possible structure is seen.

It should be noted that the cross-section calculated by evaluated curve and averaged by ^{252}Cf spontaneous fission neutron spectrum agrees well with the results of integral measurements /4/.

In using the $^{27}Al(n,\alpha)$ reaction cross-section as a standard it is necessary to take into account nonmonotonic character of cross-section in the range 6-8,5 MeV and, perhaps, at higher energies. Attention should be drawn to the fact that the fluctuations of cross-section slightly decrease the validity of this reactnon as a standard.

For further refinement of cross-section values it is necessary to conduct the experiments with the accuracy of 1-2% and with a sufficiently high energy resolution (better than 100 keV) in the whole energy range. The measurements at several reference points with a higher monoenergeticity of neutrons and the comparison of results obtained with different reference cross-sections and with different neutron flux measurement techniques are desirable.

VI. Actinide half-lives

The half-life values of 11 most important transactinium radionuclides /1/ adopted as standards are based on the compilation of α -decay and spontaneous fission data /2/. The list of recommended data /3/ after revision of /2/ includes the following changes in $T_{1/2}$ values of actinides:

1. According to the recommendation of /4/ ^{238}U spontaneous fission half-life is taken to be $(8,08 \pm 0,26)\cdot10^{15}$ years instead of $(8,19 \pm 0,09)\cdot10^{15}$ years.

2. For ^{240}Pu α-decay in accordance with the results of calorimetric measurements /5/ the value of $T_{1/2}$ is taken to be $(6,537 \pm 0,10)\cdot10^{3}$ years instead of $(6,55 \pm 0,02)\cdot10^{3}$ years.

3. For ^{244}Pu the value of $T_{1/2(\alpha)}$ measured with the least declared error - $(8,026 \pm 0,09)\cdot10^{7}$ is recommended instead of the evaluated value $(8,2 \pm 0,1)\cdot10^{7}$ years.

4. The value of ^{252}Cf total half-life - $(2,64 \pm 0,01)$ years is revised taking into account recent alaytical review /6/ and is assumed to be $T_{1/2} = (2,645 \pm 0,007)$ years.

The compilations /1- 3/are based on the existing data files ENSDF, ENDF/B, UKNDC. Independently of these works an evaluation of transactinium radionuclides half-lives is performed on the basis of analysis and examination of the data obtained in 1950-1983. The main features of evaluation technique are described in /7, 8/. The evaluation results are given in Table 1, where for comparison the data adopted at present as standards

are also presented. On the basis of analysis of experimental results the following remarks can be made on $T_{1/2}$ values of transactinium nuclides:

1. The results of $T_{1/2(\alpha)}$ measurements for ^{233}U, ^{239}Pu and ^{242}Pu show a good agreement within the limits of errors declared by authors. Evaluated values obtained with our technique taking into account the degree of data agreement /7, 8/ have no significant discrepancy with recommended values /1/. However, taking into consideration the scatter of available experimental data, it is advisable to decrease the error of $T_{1/2}(\alpha)$ for ^{239}Pu and to increase the error of $T_{1/2}(\alpha)$ for ^{242}Pu.

2. The value $T_{1/2}(\alpha)$ = (6537 ± 10) years recommended for ^{240}Pu /3/ does not agree with the result of the most accurate measurement - (6569 ± 6) years /9/. Therefore this change of recommended earlier value /1/ seems to be weak-grounded.

3. The results of $T_{1/2}(\alpha)$ measurements for ^{234}U performed in 1965-1975 are grouped around $2{,}454 \cdot 10^5$ years with mean-square deviation ~ 0,1%, whereas the recent data /10/ point to a higher value. Taking into account this discrepancy, it is not recommended to show the third digit after the comma in the standard of ^{234}U $T_{1/2}(\alpha)$.

4. New mass-spectrometric and radiometric measurements of ^{241}Pu half-life lead to weighted mean value of $T_{1/2}(\alpha)$ = (14,36 ± 0,02) years which agrees with the results of calorimetric measurements /11/, but substantially differs from the results of earlier mass-spectrometric measurements /12/.

5. Evaluated value of ^{252}Cf total half-life given in Table 1 is obtained accounting for recent measurement result $T_{1/2}$ = (2,639 ± 0,007) years /13/. The change /3/ of the recommended in /1/ standard seems to be weak-grounded, since unweighted mean value of measurement results obtained in 1965-1983 is, as before, close to 2,638 years, and the scatter of data does not permet the weighted mean value tob be used as a recommended one. Errors reported by the authors of experimental works seem to include undetected components of systematic errors.

Table 1

Nuclide	Decay type	Half-life			
		Unit of measurement (years)	Recommended value	Evaluated value	Proposed standard
1	2	3	4	5	6
^{233}U	α	10^5	1,592 (2)	1,593 (2)	1,593 (2)
	SF	10^{17}	1,2 (3)	-	-
^{234}U	α	10^5	2,454 (6)	2,448 (5)	2,45 (1)
	SF	10^{16}	1,42 (8)	-	1,42 (8)
^{235}U	α	10^8	7,037 (11)	7,038 (5)	7,04 (1)
	SF	10^{18}	9,8 (28)	-	9,8 (28)
^{236}U	α	10^7	-	2,342 (2)	2,342 (2)
	SF	10^{16}	-	2,43 (13)	2,43 (13)
^{238}U	α	10^9	4,468 (5)	4,468 (3)	4,468 (5)
	SF	10^{15}	8,19 (9)	8,1 (3)	8,1 (3)
^{237}Np	α	10^6	2,14 (1)	2,14 (1)	2,14 (1)
	SF	10^{18}	1	-	1
^{238}Pu	α	10^1	-	8,774 (3)	8,774 (3)
	SF	10^{10}	-	4,77 (14)	4,77 (14)
^{239}Pu	α	10^4	2,411 (3)	2,411 (2)	2,411 (2)
	SF	10^{15}	5,5	-	5,5
^{240}Pu	α	10^3	6,55 (2)	6,56 (1)	6,55 (2)
	SF	10^{11}	1,15 (4)	-	1,15 (4)
^{241}Pu	α	10^5	6,00 (5)	-	6,00 (5)
	β	10^1	1,44 (2)	1,436 (2)	1,44 (1)
^{242}Pu	α	10^5	3,76 (2)	3,75 (3)	3,75 (3)
	SF	10^{10}	6,84 (8)	-	6,84 (8)
^{244}Pu	α	10^7	8,2 (1)	-	8,26 (9)
	SF	10^{10}	6,56 (32)	-	6,56 (32)
^{241}Am	α	10^2	-	432,1 (3)	432,1 (3)
	SF	10^{14}	-	1,1 (2)	1,1 (2)
^{243}Am	α	10^3	-	7,37 (2)	7,37 (2)
	SF	10^{13}	-	-	3,4 (3)
^{244}Cm	α	10^1	-	18,11 (3)	18,11 (3)
	SF	10^7	-	1,344 (4)	1,344 (4)
^{245}Cm	α	10^3	-	8,51 (6)	8,51 (6)
^{246}Cm	α	10^3	-	4,76 (5)	4,76 (5)
	SF	10^7	-	1,81 (4)	1,81 (4)
^{252}Cf	α,SF	10^0	2,64 (1)	2,638 (5)	2,64 (1)
	α	10^0	2,72 (1)	-	2,72 (1)
	SF	10	8,538 (39)	8,53 (3)	8,54 (4)

6. It is advisable to supplement the list of standards with half-life values of ^{236}U, ^{238}Pu, ^{241}Am, ^{243}Am, ^{244}Cm, ^{245}Cm and ^{246}Cm for which sufficiently reliable results of $T_{1/2}(\alpha)$ and $T_{1/2}(SF)$ measurement exist.

The values of proposed new half-lives are given in the last column of Table 1. In brackets the errors are expressed as the last significant digit units.

VII. ^{252}Cf spontaneous fission prompt neutron spectrum

This spectrum is recommended as a standard neutron spectrum and used both in microscopic and in macroscopic measurements. The spectrum is used as a standard of flux for calibration of facilities.

INDC/NEANDC Nuclear Standards File of 1982 is based on the works performed till 1982. The file recommends to use Maxwellian distribution with T = 1,42 MeV as a ^{252}Cf fission neutron spectrum standard. This representation has been chosen as a first approximation before performing new precision measurements and new evaluation.

After 1981 a series of measurements has been made in a wide interval of energies (0,001 - 30 MeV) using differential and integral methods /1-3/. These works show a good agreements with Maxwellian spectrum (T = 1,42 MeV) below 6 MeV, but above 6 MeV a gradual deviation from this spectrum to lower neutron intensities is observed. The measurements performed with integral method (activation foils) /11-13/ confirm differential data. Theoretical calculations carried out using the evaporation model and the statistical Hauser-Feschbach model are indicative of an analogous type of spectrum /14-16/. Only the work /10/ shows a substantially different result: the agreement with Maxwellian spectrum is obtained up to 15 MeV. Unfortunately this work is outlined very briefly. In the range of low energies (0,01 - 1 MeV) the works /3, 5, 7/ show an agreement with Maxwellian spectrum.

At present the maximum discrepancies are observed in the energy region above 8 MeV (especially in the interval from 10 to 15 MeV) where the discrepancies reach 20%. In the region of mean energies (1-7 MeV) more accurate measurements are desirable to determine whether small deviations from Maxwellian distribution exist. Some measurements indicate a possible exceeding ($<$ 5%) in the range of 2-4 MeV. In the region of low energies ($<$ 1 MeV) the works /3, 5, 7/ confirm that there is no significant exceeding of spectrum compared with the Maxwellian one, as it has been shown in some earlier works. However, it is desirable that the accuracy of data should be improved and the spectrum shape refined.

Considering all the experimental and theoretical information, the IAEA Consultants Meeting in Smolenice, 1983 recommended on the base of recent works (1981-1983) to use the Maxwellian distribution in the range of energies from 1 keV to 6 MeV and the evaluation of National Bureau of Standards, USA (NBS) in the region above 6 MeV. It is advisable to use the recommendation of Meeting in Smolenice untill a new evaluation based on precision works with files of errors is published.

VIII. Average number of neutrons per ^{252}Cf spontaneous fission event

The data on $\bar{\nu}$ (^{252}Cf) measurements up to the end of 1982 are summarized in Table 2.

By the end of 1982 new works on $\bar{\nu}$ (^{252}Cf) measurements with new precision techniques have been published. Special attention should be paid to the work of J.R. Smith /10/ where the 2π-technique developed at NBS was used for fission fragment measurements. Absolute n-f and f-f techniques for fission fragment counting have also been analyzed and simulated in this work. The method of neutron-fragment coincidence has been recognized as the most preferable. The authors have got the highest value of $\bar{\nu}$ (^{252}Cf) (3,767 $\pm$ 0,013) of all interesting works perfermed with the use of manganese bath method.

Table 2

Authors	Method	$\bar{\nu}$ (^{252}Cf)
I. Asplund-Nilsson et al. /1/		3,792 ± 0,040
J.C. Hopkins, B.C. Diven /2/	Large liquid	3,777 ± 0,031
J.W. Boldeman /3/	scintillation	3,755 ± 0,016
R.R. Spencer et al. /4/		3,782 ± 0,008
H. Zang, Z. Liu /5/		3,752 ± 0,18
Weighted mean value		= 3,774 ± 0,006
P.H. White, E.J. Axton /6/		3,815 ± 0,040
E.J. Axton et al. /7/	Manganese	3,744 ± 0,023
Dc Volpi, K.G. Porges /8/	bath	3,747 ± 0,019
B.M. Alexandrov et al. /9/		3,758 ± 0,015
J.R. Smith, S.D. Reider /10/		3,767 ± 0,013
V. Spiegel et al./11/		3,789 ± 0,037
H. Bozorgmanesh /12/		3,744 ± 0,023
Weighted mean value		= 3,760 ± 0,006
D.W. Colwin et al. /13/	Boron boiler	3,739 ± 0,021
G. Edwards et al. /14/	Boron counter in oil moderator	3,752 ± 0,029
Weighted mean value of all the data		= 3,766 ± 0,005

The discrepancy of $\bar{\nu}$ (^{252}Cf) values measured with large liquid scintillator (LLS) and manganese bath methods observed over alomost 20 years remains practically invariable and is equal to 0,85%. The attempts to reveal the sources of systematic errors in manganese bath method, which could cause the increase of $\bar{\nu}$ (^{252}Cf) without any change of $\bar{\nu}$ value obtained from multiparametric fits of nuclear constants for v = 2200 m/s through the η value, have failed. Thermal neutron capture cross-section of sulphur σ_s = (0,52 ± 0,03)b used during the last 30 years has been the only possibility for fitting the results of measurements with manganese bath and LLS. Of the cross-section σ_s had been equal to 0,57 b as it follows from the analysis of an old works /13/ and from measurements on beam passage with crystal spectrometer MTR /16/, all values of $\bar{\nu}$ measured with manganese bath method would have grown by 0,5%. However the works /17, 18/, in which the values of σ_s equal to 0,53 ± 0,01 b and 0,543 ± 0,005 b have been obtained, leave insolved the problem of fitting the results.

In 1983 E.J. Axton published the results of a new evaluation of thermal constants for reactor isotopes of uranium and plutonium and of $\bar{\nu}$ (^{252}Cf) /19/. Unlike the last evaluation of 1975 made by IAEA, where all input data were considered as independent variable, Axton took into account all correlated errors introducing a full covariant matrix. For $\bar{\nu}$ (^{252}Cf) evaluation he used J.R. Smith's evaluation /20/ and new $\bar{\nu}$ (^{252}Cf) measurements carried out with different techniques /5, 10, 11, 14/. The ratios of $\bar{\nu}$ values were taken only from J.W. Boldeman's work /21/, and the input data were used without corrections for difference of average fission energy, for delayed γ-quanta und neutrons, for californium source backing thickness etc. The introduction of corrections was performed by evalaution program in itself and by plotting a covariation matrix. Thus all the measurements with liquid scintillator proved to be correlated through the cited errors.

All measurement with manganese bath have been correlated through the uncertainty of sulphur thermal cross-section or through total uncertainty of NPL bath in the case of using neutron sources measured in NPL as reference ones. Correlations of measurement results of V. Spiegel /11/ and K. Bozorgmanesh /12/ have been based on the use of reference sources NBS-I and NBS-II for bath calibration. E.J. Axton results are compared with those of earlier evaluations in Fig. 2, where 1 - J.R. Stehn et al. /22/, 2 - H.D. Lemmel (only the data for neutrons with v = 2200 m/s), 3 - H.D. Lemmel (all the data), 4 - ENDF/B-V, 5 - N.M. Steen /24/.

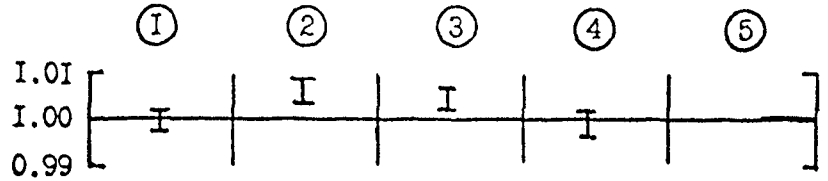

Fig. 2. The ratio of different $\bar{\nu}$ (^{252}Cf) evaluations to that of E.J. Axton /19/. (See the text).

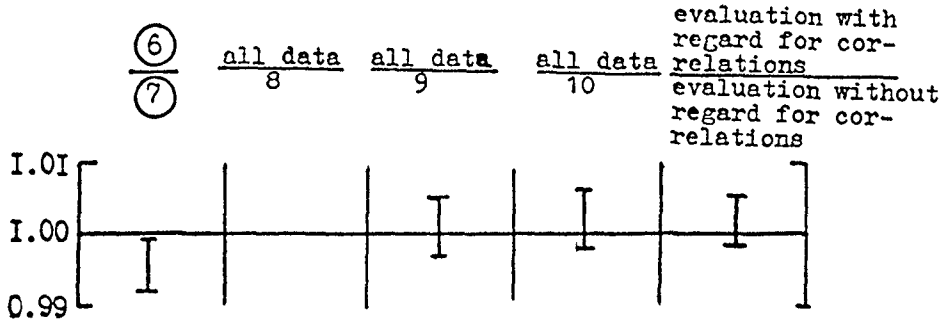

Fig. 3. The ratios of different variations of $\bar{\nu}$ (^{252}Cf) evaluations (See the text).

For verification of data compatibility several cycles of calculations have been carried out (see Fig. 3). In these calcalations the absolute values of fitted quatities are based on: 6 - the data of measurements with manganese bath, 7 - the data of measurements with LLS, 8 - the η -data, 9 - the data of all the measurements without η -data, 10 - the data without σ_f. In the last column of Fig. 3 the ratio of all the data obtained with covariation matrix to those without this matrix is presented. For example, the value of $\bar{\nu}$ (^{252}Cf) obtained ignoring the covariation decreases from 3,7661 ± 0,0054 to 3,7630 ± 0,0044. The first column illustrates historical discrepancy of results obtained with LLS and with manganese bath. The difference is (0,475 ± 0,3)%. This situation becomes complicated with publication of R.R. Spencer's work /4/, where the highest value of $\bar{\nu}$ is obtained with the highest declared accuracy. In spite of a very detailed description of procedure for introduction of corrections, the LLS techni que does not eliminate the possibility of small unaccounted effects leading to overestimation of final results.

The analysis of $\bar{\nu}$ (^{252}Cf) evaluations carried out during the period from 1979 to 1982 practically does not change the value $\bar{\nu}$ = 3,766 ± 0,005 adopted by IAEA as a standard in 1982. Thus the evaluation of $\bar{\nu}$ (^{252}Cf) approved by IAEA can be considered as the most reliable, and without elucidating the causes of discrepancy of data obtained with LLS and with manganese bath there is no grounds for revision of the existing evaluation.

IX. The data on radionuclide decay used as calibration standards

In this section of IAEA Standards File the most accurate of available data on radioactive isotope decay used for graduation of gamma-spectrometers are presended. The prpposed set of standards shows well the modern status of norms used in gamma-

spectrometer graduation procedure for measurement of γ-quanta energies and intensities. These data (~ 250 values of γ-quanta energies and intensities) permit the range 30-3500 keV to be covered at graduation satisfying the requirements of the most of measurements performed.

It should also be noted the following:

1. Due to the increase of accuracy and reliability of nuclear-spectroscopic standards connected with the development and the use of a new optic X-ray method of γ-quanta wavelength measurements, the relative errors in wavelengths obtained with this method are several times (~7) lower than that of the conversion factor "wavelength-energy". Since this fact has not allowed the accuracy of measurement to be conserved in this set of standards, there are indications /1/ of the possibility of revising this conversion factor, which can lead to a change of calibration standards.

2. In the work /2/ it has been noted that because of the discrepancy of experimental values the deuteron bind energies of /3/ and /4/ should not be recommended as energy standards for γ-quanta emitted in (n,γ)-reactions; their energies can be obtained by using correctly measured mass doublet differences (see, for example, /4/). Later this discrepancy has been eliminated /5/. Moreover in the works /6, 7/ close values of deuteron bind energy have been also obtained. To our mind the available results allow us to consider the question of including in the rank of standards the energies of gamma-quanta emitted in the following reactions:

$^{1}H(n,\gamma)^{2}H$	E_γ = 2223,3 keV
$^{2}H(n,\gamma)^{3}H$	E_γ = 6250,3 keV
$^{12}C(n,\gamma)^{13}C$	E_γ = 4945,3 keV
$^{13}C(n,\gamma)^{14}C$	E_γ = 8173,9 keV
$^{14}N(n,\gamma)^{15}N$	E_γ = 10829,1 keV

which enlarges substantially the energy region of recomended standards.

3. It is wise to supplement the set of recommended values of γ-quanta energies and intensities with the data on ^{160}Tb and ^{144}Ce + ^{144}Pr decay taking for the basis the results of /8, 9, 10, 11/.

4. There are inexactitudes (misprints) in the list of recommended values. For example, γ-quanta energies of ^{56}Co must be 2113,107 and 2212,921 keV, and the intensity of $K_{\alpha 1}$ X-ray line of ^{203}Hg with the energy of 72,8715 keV is equal to 0,064 $\pm$ 0,002.

References

I

1. V.N. Kononov et al. Proc. of the 5-th All-Union Conf. on Neutron Physics, Kiev, 1980, vol. 2, p. 282.
2. N. Yamamura et al., Journ. of Nucl. Sci. and Technology, 80, 797 (1983).
3. A.N. Davletshin et al. Proc. of the 6-th All-Union Conf. on Neutr. Physics, Kiev, 1983, To be published.
4. A.N. Davletshin et al. Atomnaya Energiya, 48, 87 (1980).
5. R.Z. Macklin. Nucl. Sci. and Engng., 79, 265 (1979).
6. S.K. Gupta et al. Nucl. Instrum. and Methods, 148, 77 (1978).
7. S. Joly et al. Nucl. Sci. and Engng., 70, 53 (1979).
8. Chen Ying et al. Proc. of the 1982 Antwerp Conf. on Nuclear Data for Sci. and Technology, Antwerp, Belgium, 1982, p. 462.
9. Nucl. Data Standards for Nuclear Measurements. Technical Report Ser., No 227, 1982, IAEA, Vienna, p. 53.

II

1. R. Arlt et al. Proc. of the Internat. Conf. on Nucl. Cross. Sect. for Technology, Knoxwille, 1979, NBS Spec. Publ. 594, p. 990.
2. V.M. Adamov et al. Ibid p. 995.

3. R. Arlt et al. Kernenergie, 24, 48 (1981), Kernenergie, 25, 199 (1982).
4. M. Cancé, G. Grenier. Proc. of the Internat. Conf. on Neutr. Physics and Nucl. Data, Harwell, 1978, p. 864.
5. O.A. Wasson. Proc. of the NEANDC/NEACRP Spec. Meeting on Fast Fission Cross Sect., Argonne, 1976, ANL-76-90, p. 183.
6. O.A. Wasson et al. Nucl. Sci. and Engng., 81, 196 (1982).
7. O.A. Wasson et al. Nucl. Sci. and Engng., 80, 282 (1982).
8. V.A. Kon'shin et al. Determination of errors in evaluated data with regard for correlations and $\sigma_f(^{235}U)$ evaluation. Preprint, HMTI, Minsk, 1978.
9. F. Kappeler. Proc. of a Panel on Neutr. Stand. Ref. Data, Vienna, IAEA-PL-246-2/27, 1974, p. 213.
10. A.D. Carson, J.W. Behrens, See Ref. /18/, p. 456.
11. B. Leugers et al. See Ref. /115/, p. 246.
12. K. Kari. Report KFK-2673, Karlsruhe, 1978.
13. J.B. Czirr, G.S. Sidhu. Nucl. Sci. and Engng., 57, 18 (1975).
14. A.D. Carlson, B.N. Patrick, See Ref. /115/, p. 880.
15. M. Cancé, G. Grenier. Nucl. Sci. and Engng., 68, 197 (1978).
16. Li Jingwen et al. See Ref. /18/, p. 55.
17. M. Mahdavi et al. Ibid p. 58.
18. W.P. Poenitz. Nucl. Sci. and Engng., 64, 894 (1977).
19. W.P. Poenitz. Nucl. Sci. and Engng., 53, 370 (1974).
20. C. Budtz-Jörgensen, H.-H. Knitter. Proc. of the IAEA Consultants Meeting on the U-235 Fast Neutr. Fission Cross Section. Smolenice, 1983, INDC(NDS)-146, p. 131.

III

1. World Request List for Nucl. Data Section, WRENDA 83/84, IAEA, 1983.
2. A.A. Goverdovsky et al. Atomnaya Energiya, 56, 162 (1984).
3. B.I. Fursov et al. Atomnaya Energiya, 43, 181 (1977).
4. J.W. Meadows. ANL/NDM-83, 1983, Argonne Nat. Laboratory.
5. C. Nordborg et al. See Ref. /115/, p. 128.
6. M. Cancé, G. Grenier, Ibid p. 237.
7. S. Cierjacks et al., Ibid p. 94.
8. M. Coates et al. Proc. of the 4-th Conf. on Nucl. Cross. Sect. and Technology, Washington, 1975, vol. 2, p. 568.
9. F.S. Difilippo et al. Nucl. Sci. and Engng., 68, 43 (1978).
10. J.M. Behrens, G.W. Carlson. Nucl. Sci. Engng., 63, 250 (1977).
11. Ref. /117/.
12. Nuclear Standards File, 1980, Version, INDC-36/LM, IAEA, Vienna, 1981.

1V

1. B.M. Gohberg et al. Preprint 6398 of Atomic Energy Institute, Moscov, 1961.
2. G. Grenier. Private Communication in Ref. /IV-7/.
3. D.J. Grady, G.T. Baldwin, G.F. Knoll, See Ref. /II-1/, p. 946
4. Ref. /II-1/.
5. Ref. /II-2/.
6. R. Arlt et al. See Ref. /II-20/ p. 53.
7. H. Derrien, J.P. Doat, E. Fort, D. Lafond. INDC(Er)-42/L, 1980.
8. H.X Schmitt, R.B. Murray. Phys. Rev., 116, 1575 (1959).
9. J.W. Meadows. Nucl. Sci. and Engng., 85, 271 (1983).
10. V.M. Pankratov. Atomnaya Energiya, 14, 177 (1963).
11. J.W. Behrens et al. Nucl. Sci. and Engng., 80, 393 (1982).
12. A.A. Goverdovsky et al. Preprint 1552 of Physioal Energetical Institute, Obninsk, 1984.
13. A.D. Carlson, B.H. Patrick. See Ref. /II 1/ p. 971.

V

1. H. Vonach, S. Tagresen. Nuclear Standards File INDC-36/LN, 1981.
2. ENDF/B-V Mat. 6313.
3. H.W. Smith, J. Halperin. Phys. Rev., 12, 827 (1981).
4. W. Manhart, See Ref. /1-8/ p. 492.

VI

1. R. Vaninbroux, A. Lorenz. Actinide Half-Lives. Ref /I-9).
2. A. Lorenz. INDC(NDS)-139/NE (December 1982).
3. A. Lorenz. Proposed Recommended List of Heavy Element Radionuclide Decay Data. INDC(NDS)-149/NE (December 1983).
4. N.E. Holden. The Uranium Half-Lives. A critical review. Report BNL-NCS-51320, January 1981.
5. F.L. Oetting. Proc. Symp. Thermodyn. Nucl. Mater. with Emphasis on Solution System., Vienna, Austria, 1968.
6. J.R. Smith, Nowit's the Californium-252 Half-Life Discrepancy. INDC(NDS)-147/GE, 1983.
7. Yu.V. Kholnov., V.P. Chechev. Evaluation of Characteristics of Radionuclides Widely Used, Proc. of SEV Symp. Marianske Lasne, 1979, ML 3/7, Prague, 1979, p. 236.
8. Yu.V. Kholnov et al. Irradiation Characteristics of Radioactive Nuclides Used in National Economy. Evaluated Data. Moscov, Atomizdat, 1980.
9. A.H. Jaffey et al. Phys. Rev., C18, 969 (1978).
10. A.M. Geidelman. Izvestiya AN SSSR, Phys. Ser., 44, 929 (1980).
11. W.W. Strohm, K.C. Jordan. Trans. Amer. Nucl. Society, 18, 185 (1974).
12. R.K. Zeiger., Y.J. Ferris. Journ. of Inorg. Nucl. Chemistry, 35, 3417 (1973).
13. F. Lagoutine, J. Legrand. Int. J. Appl. Rad. Isotopes, 33, 711 (1982).

VII

1. R. Bötger, H. Klein et al., See Ref. /I-8/ p. 484.
2. W. Poenitz et al., Ibid p. 465.
3. H. Märten et al., Ibid p. 486.
4. L.V. Blinov et al., Ibid p. 498.
5. A. Laitai et al., See Ref. /II-20/ p. 191.
6. W. Poenitz, T. Tamura, Ibid p. 175.
7. O.I. Batenkov et al., Ibid p. 161.
8. H. Märten et al., Ibid p. 195.
9. H. Klein et al., Ibid p. 191.
10. J. Boldeman et al., INDC/P(83)-59.
11. W. Manhart, See Ref. /I-8/ p. 429.
12. W. Manhart, INC/NDC-146 IAEA, Vienna, 1983, p. 213.
13. Z. Dezso, J. Csikai, Ibid p. 225.
14. D. Madland, J. Nix, Preprint LA-UR-83-3034 (1983).
15. D. Maldand, J. Nix. Preprint LA-UR-84-129 (1984).
16. V.A. Rubchenya, B.F. Gerasimenko. Preprint 187 of the Khlopin Radium Institute.

VIII

1. I. Asplund-Nilsson et al. Nucl. Sci. and Engng., 16, 124 (1963).
2. J.C. Hopkins, B.C. Diven. Nucl. Phys., 48, 433 (1963).
3. J.W. Boldeman. Nucl. Sci. and Engng., 55, 188 (1974).
4. R.R. Spencer et al. Nucl. Sci. and Engng., 80, 603 (1982).
5. H. Zang, Z. Lui. Chinese Nucl. Phys., 2, 29 (1980).
6. P.H. White, E.J. Axton. J. Nucl. Energy, 22, 73 (1968).
7. E.J. Axton, A.G. Bardell. Metrologia, 18, 97 (1982).
8. De Volpi, K.G. Porges. Phys. Rev., C1, 683 (1970).
9. B.M. Alexandrov et al. See Ref. /I 1/ vol. 4, p. 119.
10. J.R. Smith, S.D. Reeder. Trans. Amer. Nucl. Soc., 35, 549 (1980).
11. V. Spiegel et al. Proc of the Nu-Workshop, Sheraton- Washington Hotel, Nov. 1980, ed. A.D. Carlson (NBS, 1981).
12. H. Bozorgmanesh. Thesis, Univ. of Michigan, 1977.
13. D.W. Colvin et al. Proc. of the IAEA Conf. on Nucl. Data for Reactors, Vienna, 1, 307 (1967).
14. G. Edwards et al. Ann. Nucl. Energy, 9, 127 (1982).
15. H. Pomerance. Phys. Rev., 83, 64 (1951).
16. J.R. Smith, See Ref. /II-1/ p.
17. L. Koester et al. Z. für Phys., A289, 399 (1979).
18. V.P. Vertebnyi. Yadernye Konstanty, 1(45) (1982).
19. E.J. Axton. UK NDC(83)P 109, p. 8.
20. J.R. Smith. EPRI NP-1098 (1979).

21. J.W. Boldeman, J. Frehaut. Nucl. Sci. and Engng., 76, 49 (1980).
22. J.R. Stehn et al., See Ref /I-8/ p.
23. H.D. Lemmel. Proc. of the Conf. on Neutr. Cross-Sections and Technology, Washington, 1975, NBS Spec. Publ. 425, vol. 1, p. 826.
24. N.M. Steen. Westinghouse Atomic Power Division Report WARD-RM-1052.

IX

1. E.R. Cohen, A.H. Wapstra. Nucl. Instr. and Meth., 211, 153 (1983).
2. R.J. Helmer et al. At. Data Nucl. Data Tables, 24, 39 (1979),
3. Z. Vylov et al. Yadernaya Fizika, 28, 1137 (1978).
4. R.C. Greenwood, R.E. Chrien. Phys. Rev., C21, 498 (1980).
5. Z. Vylov. Preprint 6-82-108 of the Joint Inst. on Nucl. Research Dubna, USSR.
6. C. van der Leun, C. Alderliesten. Nucl. Phys., A380, 261 (1982).
7. I. Adam et al. Chesh. J. Phys., 1333, 465 (1983),
8. R.J. Helmer et al. Nucl. Instrum. and Meth., 155, 289 (1978).
9. J. Jin et al. Nucl. Instrum. and Meth., 212, 259 (1983).
10. R.C. Greenwodd et al. Nucl. Instrum. and Meth., 159, 465(1979).
11. R.J. Gehrke et al. Nucl. Instrum. and Meth., 146, 405 (1977).

SESSION II

THEORETICAL CALCULATIONS OF THE ^{6}Li(n, t) CROSS-SECTION

G.M. HALE
Los Alamos National Laboratory,
Los Alamos, New Mexico,
United States of America

Abstract

The origin of the 1/v cross section for the ^{6}Li(n,t) reaction and the behavior of its angular distribution are discussed in the context of (1) conventional R-matrix analyses, (2) PWBA calculations of deuteron exchange, and (3) consistent R-matrix analyses. Results of a comprehensive, conventional R-matrix analysis of reactions in the ^{7}Li system are presented, and the possible interpretation of some of its parameters in terms of the deuteron exchange mechanism is discussed. An extension of the usual PWBA calculation to include internal bound-state effects in a simple model is shown to introduce additional poles into the T matrix and broaden the energy range over which particle exchange may be important. A consistent R-matrix treatment of the scattering equations in the internal and external regions leads to channel overlap terms that appear to include particle-exchange effects automatically with the resonances in an unitary fashion.

I. INTRODUCTION

The ^{6}Li(n,t) cross section has been an interesting and sometimes controversial subject for the past several years. Although measurements and theoretical descriptions of the reaction have been converging in recent years, questions of interpreting the theoretical results in terms of reaction mechanisms have remained open. The major questions to be answered are (a) What is the origin of 1/v behavior of the cross section at low energies? and (b) How does one account for the rather complicated behavior of the angular distribution at higher energies? These questions will be discussed in the context of three different descriptions: (1) conventional R-matrix approach; (2) deuteron exchange in plane-wave Born approximation; and (3) consistent R-matrix approach.

II. CONVENTIONAL R-MATRIX APPROACH

In conventional R-matrix analyses, the 1/v cross section comes from poles in the R matrix located either above or below the n-^{6}Li threshold. At low energies, about 80% of the cross section comes from the J = ½ S-wave transition.[1] Early attempts[2,3] to explain the n-^{6}Li reactions put a pole in the J = ½ S-wave just below the n-^{6}Li threshold. Our comprehensive study[4] of reactions in the ^{7}Li system, including t-α scattering, from which the ENDF-V cross sections for ^{6}Li were obtained, found that such a pole was inconsistent with t-α scattering data, a result that was later reinforced by a study[5] of low-energy n-^{6}Li elastic scattering done in the Soviet Union. Distant levels both above and below the n-^{6}Li threshold were tentatively ascribed in Ref. 4 to a direct-reaction mechanism for the ½$^+$ transition. Knox and Lane[6] recently reported an R-matrix analysis of the n-^{6}Li reactions in which the 1/v cross section in the J = ½ state is attributed to a level above the n-^{6}Li threshold that they associate with a compound nuclear state.

All of these R-matrix analyses appear to agree, however, that the J = 3/2 component that accounts for the remaining 20% of the low-energy 1/v cross section comes from a 3/2$^+$ level in ^{7}Li that occurs at $E_x \sim 9.5$ MeV. Therefore, the pole positions and associated reaction mechanisms seem to be least clear for the J = ½ transition, which accounts for most of the 1/v cross section at low energies.

Recently we extended the analysis that was used for ENDF-V ^{6}Li cross sections to include more data and higher energies so that it is the most comprehensive R-matrix study of reactions in the ^{7}Li system that has been done. This analysis will provide Li(n,t) cross sections for the combined ENDF-VI standards file, as described by Carlson[7] at this conference, as well as the other neutron cross sections at energies below 4 MeV for the ENDF-VI ^{6}Li evaluation. The table below lists the channel configuration and the types of data for the various reactions that were included in the analysis.

TABLE I

CHANNELS AND DATA TYPES INCLUDED IN ^{7}Li R-MATRIX ANALYSIS

Arrangement	Channel Radius (fm)	ℓ_{max}
t-^{4}He	4.02	5
n-^{6}Li	4.50	2
n-^{6}Li*	4 50	1

Reaction	Energy Range (MeV)	Integrated Cross Section	Differential Cross Section	Polarization	Number Data Points
^{4}He(t,t)^{4}He	3.1-14.2	σ_R	x	x	2063
^{4}He(t,n)^{6}Li	8.7-14.4		x		39
^{4}He(t,n)^{6}Li*	12.9		x		4
^{6}Li(n,n)^{6}Li	0-4	σ_T, σ_{Elas}	x	x	761
^{6}Li(n,t)^{4}He	0-3.5	x	x	x	734

Figure 1 shows the types of fits obtained to the t-α elastic scattering cross-section and analyzing-power measurements of Jarmie et al.[8] One sees considerable structure in these observables as functions of both energy and angle, corresponding to relatively narrow resonances in ^{7}Li. Fits to n-^{6}Li elastic scattering cross sections[9,10] and polarizations[11,12] are shown in Fig. 2. Figures 3 and 4 show calculated neutron total and elastic scattering cross sections compared to some of the measurements.[13-16] Calculated ^{6}Li(n,t) cross sections, plotted at low energies as $\sigma_{n,t}E_n^{½}$ to show deviations from 1/v behavior, are shown compared with some of the measurements[17-19] in Fig 5. These figures, together with the comparisons of thermal cross sections given in Table II, illustrate that the analysis gives generally very good representations of the integrated cross sections in the standards region

TABLE II

THERMAL n-^{6}Li CROSS SECTIONS

		Recommended[a]	Calculated from R-Matrix Analysis
$\sigma_{n,t}$	(b)	940 ± 4	939.46
$\sigma_{n,n}$	(b)	.75 ± .02	0.74

[a] Taken from Neutron Cross Sections, Vol. 1, Part A, by S. F. Mughabghab, M. Divadenam, and N. E. Holden, Academic Press (1981)

The ^{6}Li(n,t) angular distribution changes markedly in the region $E_n \leq 4$ MeV, but there does not yet seem to be an experimental concensus on the details of the changes. Calculations from the R-matrix analysis of the zero-degree and 180-degree differential cross sections are compared in Fig. 6 with recent measurements[20,21] at neutron energies below 400 keV. The relative Legendre coefficients of Knitter et al.[20], which were derived from rather complete angular distributions at energies between 0.035 and 325 keV, have been converted to zero- and 180-degree cross sections whose normalizations are determined by the fitting process. Also shown are absolute measurements at zero and 180 degrees by Brown et al.,[21] which appear to be energy-shifted with respect to the Knitter data.

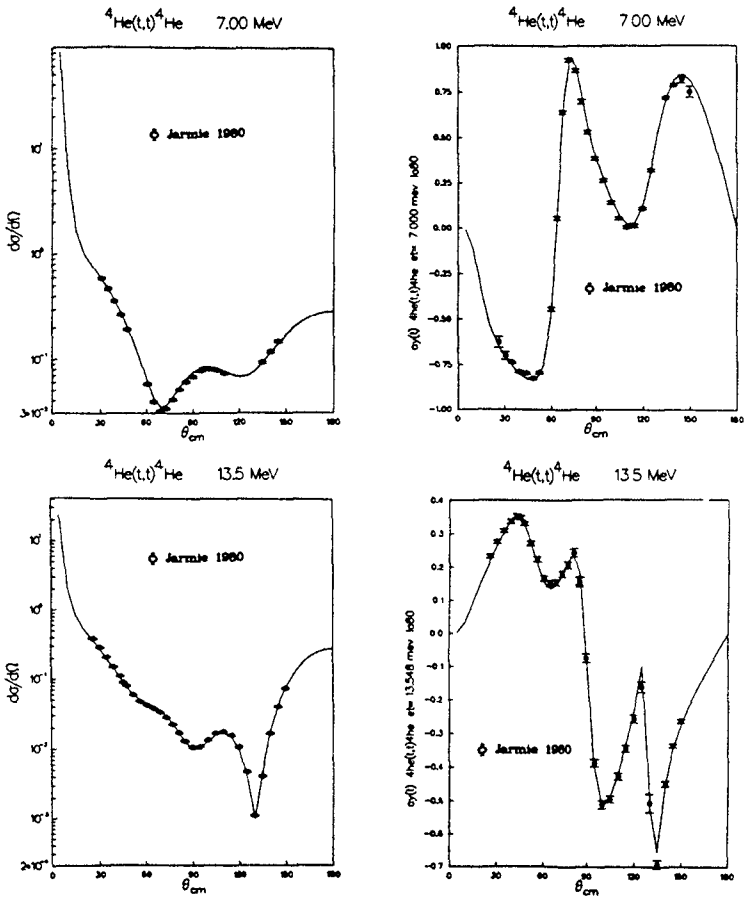

Fig. 1. Differential cross sections (left) and analyzing powers (right) for t-α elastic scattering at E_t = 7 and 13.5 MeV. The solid curves are the R-matrix calculations and the data are those of Jarmie et al.[8]

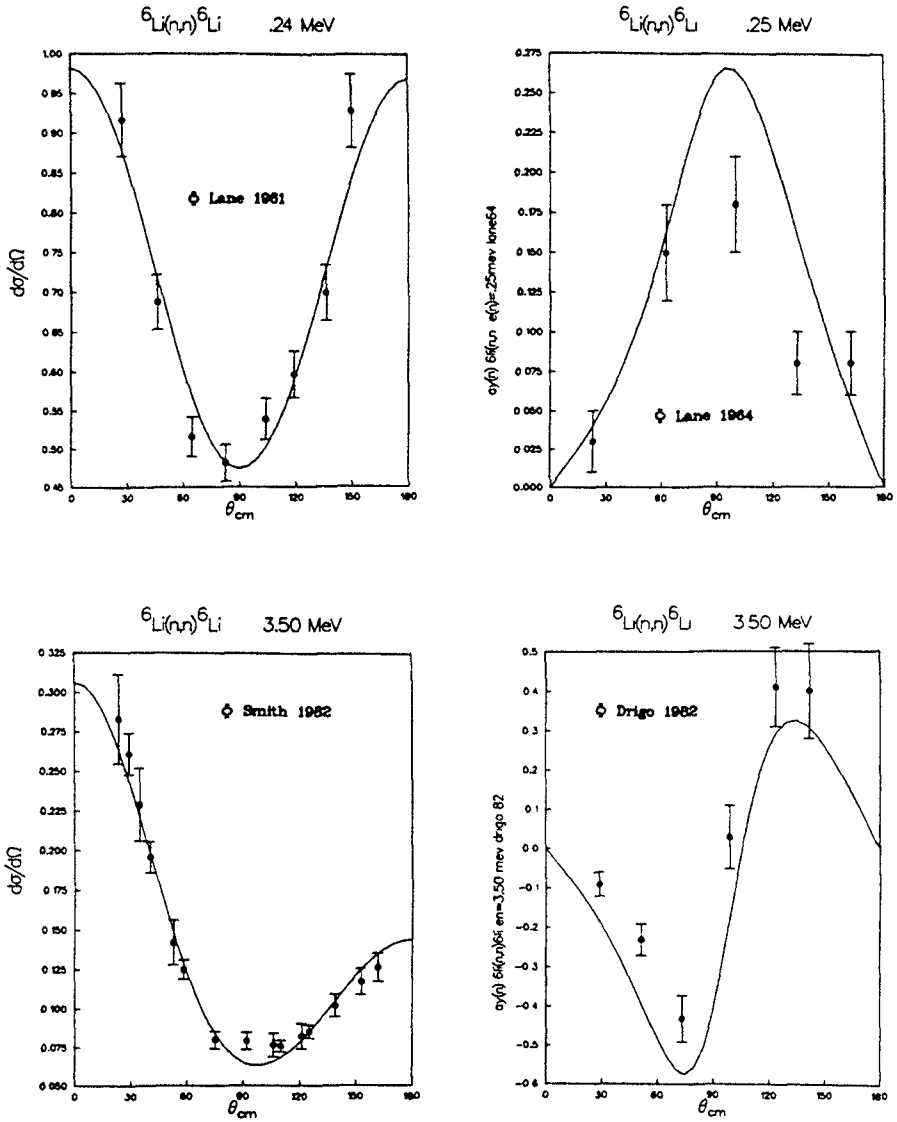

Fig. 2. Differential cross sections (left) and polarizations (right) for n-^{6}Li elastic scattering at E_n = 0.25 and 3.5 MeV. The solid curves are the R-matrix calculations and the data are those of Lane,[9,10] Smith,[11] and Drigo.[12]

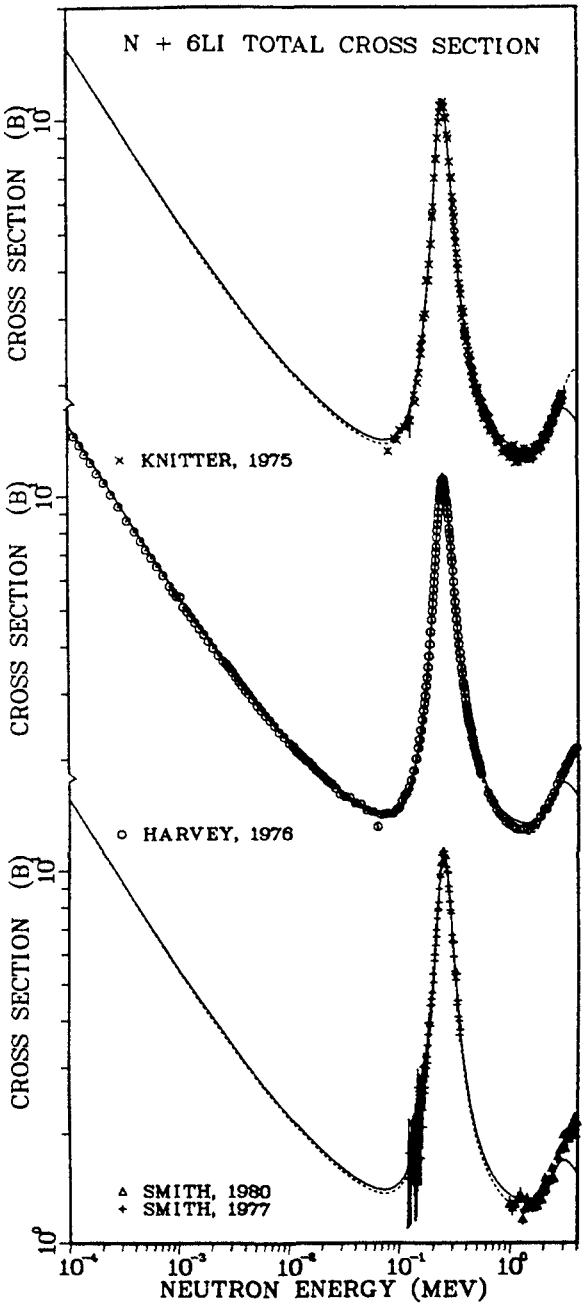

Fig. 3. Comparison of the R-matrix calculation (solid line) to the n+^{6}Li total cross-section measurements of Knitter,[14] Harvey,[15] Guenther,[16] and to the ENDF-V cross section (dashed line). The scales for the three parts of the figure are offset by a factor of 10.

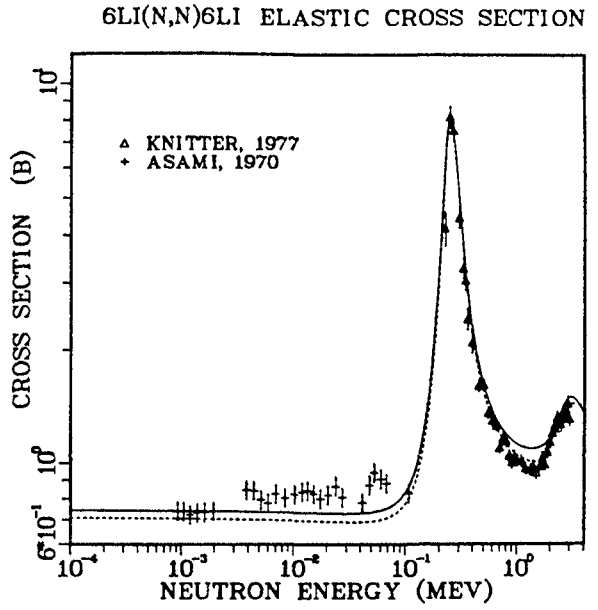

Fig. 4. Comparison of the R-matrix calculation (solid curve) of the n-^{6}Li integrated cross section with data of Asami[13] and of Knitter,[14] and with the ENDF-V cross section (dashed curve).

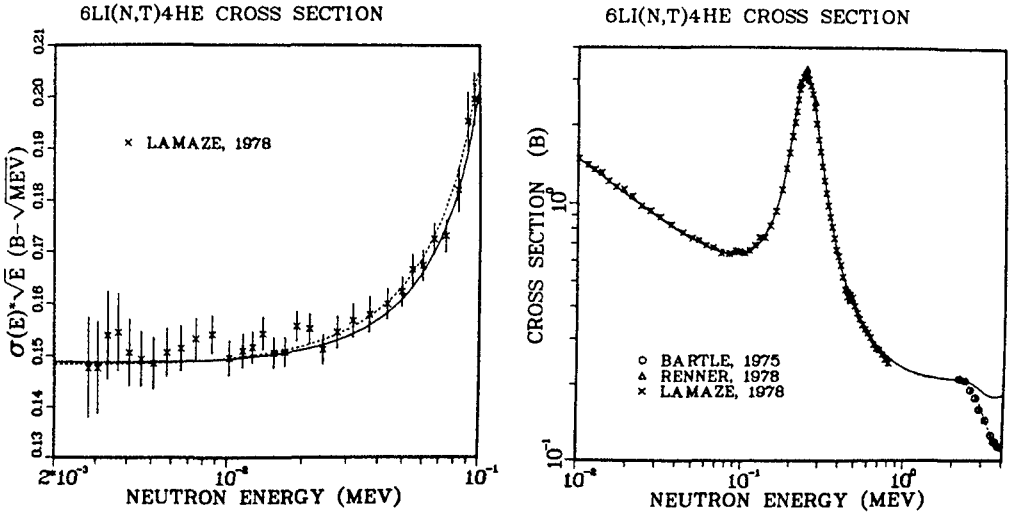

Fig. 5. Comparison of the R-matrix calculation of the ^{6}Li(n,t)^{4}He integrated cross section (solid curve) with the data of Lamaze,[17] Renner,[18] and Bartle,[19] and with ENDF-V (dashed curve). In the righthand figure, $\sigma\sqrt{E}$ is plotted to show deviations from 1/v behavior at energies below 100 keV.

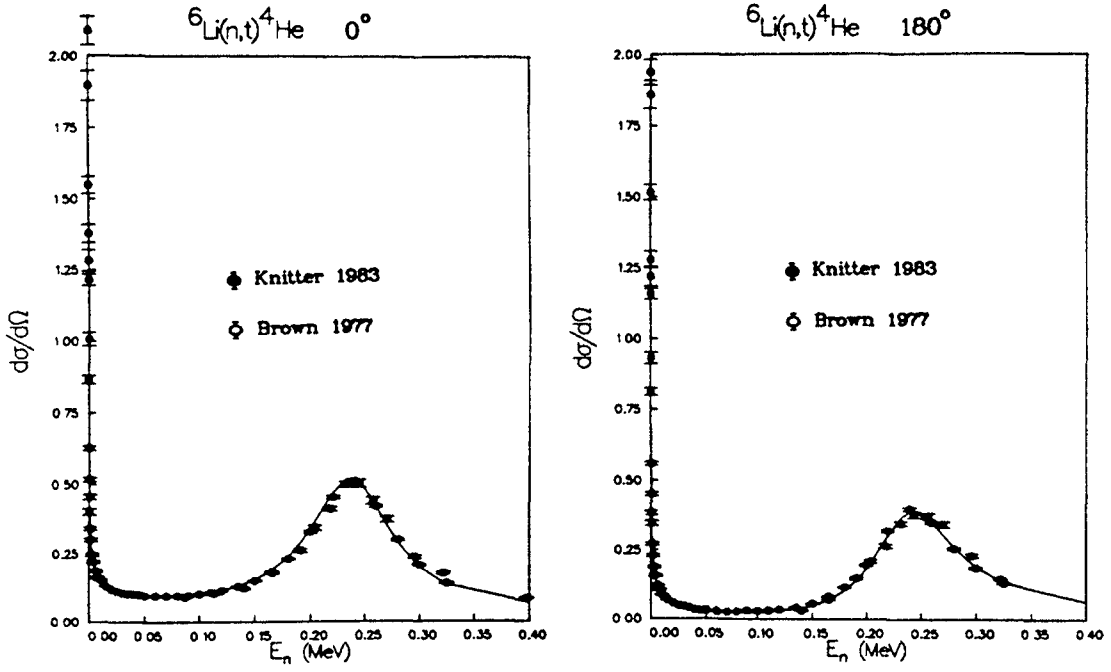

Fig. 6. R-matrix calculations (solid curves) compared to the measurements of Knitter[20] and Brown[21] of the ^{6}Li(n,t)^{4}He differential cross section at 0° (left) and 180° (right).

Absolute ^{4}He(t,n)^{6}Li zero-degree differential cross-section measurements by Drosg[22] are compared with the calculations in Fig. 7. The calculation lies ~ 16% below the data in the region $9 \leq E_t \leq 13.5$ MeV. In a comparison with Overley's[23] ^{6}Li(n,t) differential cross-section measurement in Fig. 8, one sees again the tendency of the calculation to be low at forward angles in the range $0.4 \leq E_n \leq 1$ MeV, although the overall shape agreement is fairly good.

The problems with shape disagreements among recent measurements in regions where the angular distribution is changing rapidly are illustrated in Figs. 9 and 10. The top panel of Fig. 9 shows relative measurements of Condé[24] compared with Overley's[23] absolute measurements (bottom panel) at nearly the same energies, and with the calculations. One sees that, with the exception of a few isolated Condé points, the measurements are generally consistent with each other and with the calculations at these energies. The situation is not so clear in Fig. 10 where the Condé data (top) are compared with ^{4}He(t,n)^{6}Li differential cross-section measurements by Drosg[22] (bottom) at nearly equivalent energies. In this case, the fit has assumed a shape intermediate between the two measurements, but clearly more data are required to better define the angular distributions in the 2-4 MeV region.

Of particular interest in this analysis is the level structure affecting the spin-½ transitions (of which the $\frac{1}{2}^+$ is one). In the S- and P-waves, there are levels a few MeV below the t-α threshold (in the P-waves, they are bound states), positive-energy levels at $E_x \sim 12.0$ MeV, and higher-lying background states. The reduced-width products, $\gamma_n\gamma_t$, in the negative-energy (relative to t-α) levels have the opposite sign from those in the ~ 12 MeV positive-energy levels. A possible interpretation of such structure comes from considering the deuteron exchange contribution to the ^{6}Li(n,t) reaction in plane-wave Born approximation (PWBA).

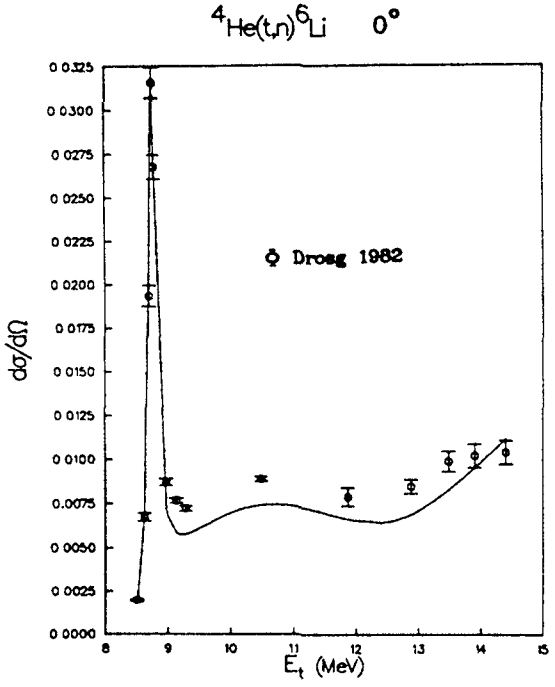

Fig. 7. R-matrix calculation of the ^{4}He(t,n)^{6}Li differential cross section at zero degrees compared with the measurement of Drosg.[22]

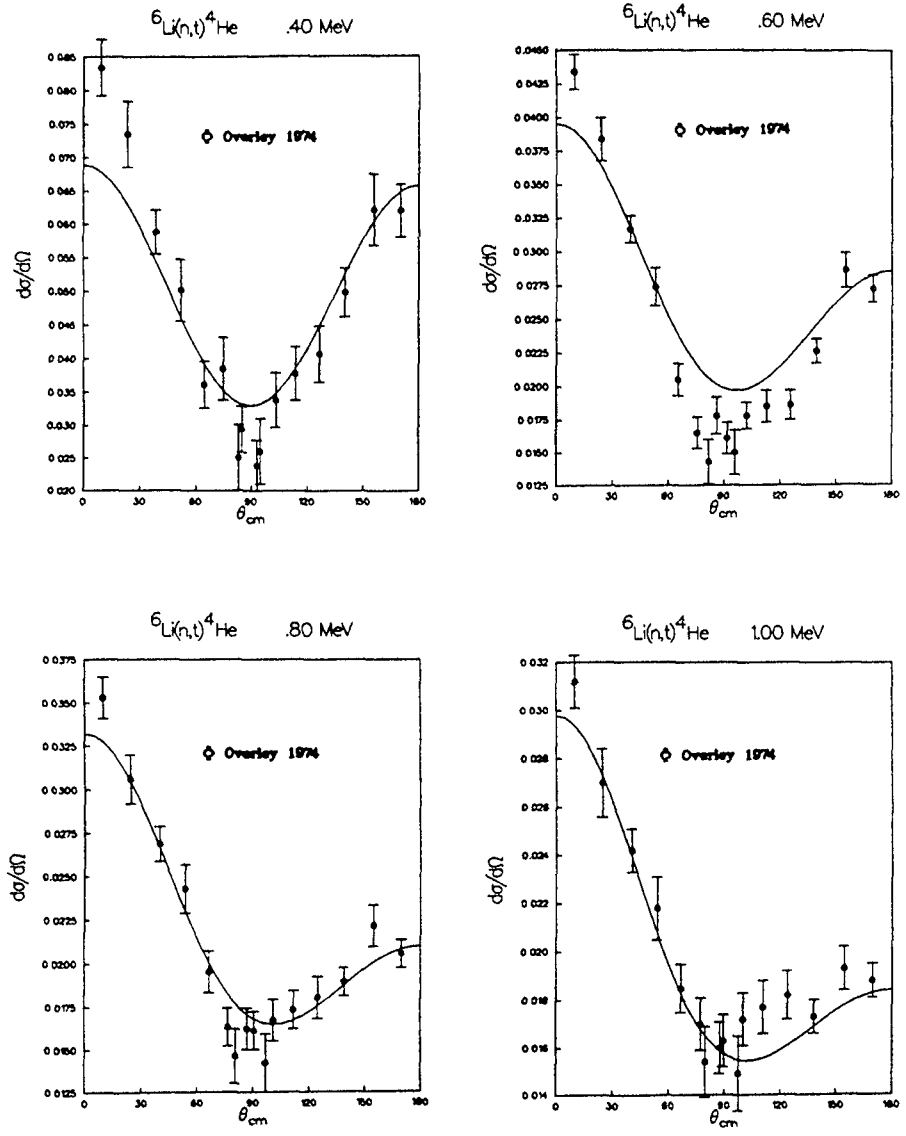

Fig. 8. Calculated ^{6}Li(n,t)^{4}He differential cross sections compared with the measurements of Overley[23] at neutron energies between 0.4 and 1 MeV.

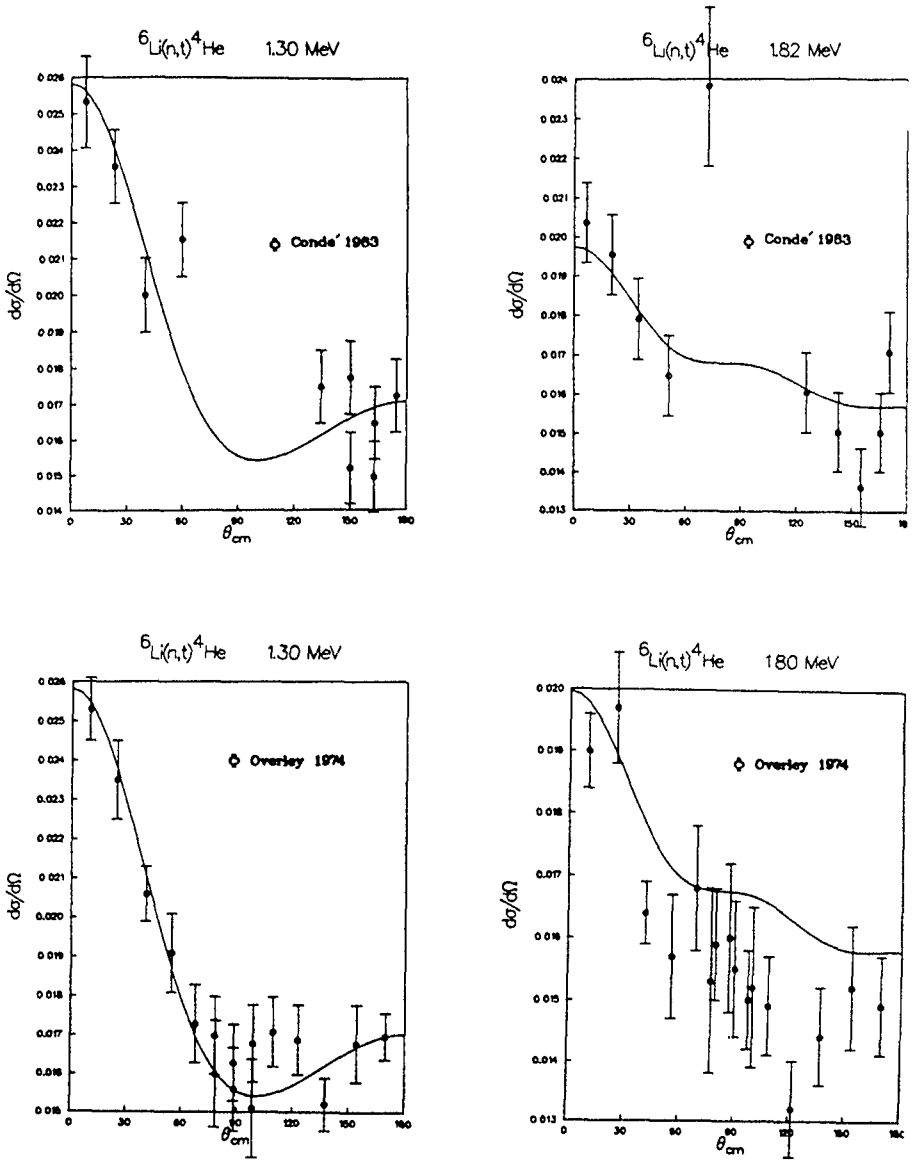

Fig. 9. R-matrix calculations (solid curves) of ^{6}Li(n,t) differential cross sections compared with measurements of Condé[24] (top) and of Overley[23] (bottom) at energies near E_n = 1.3 and 1.8 MeV.

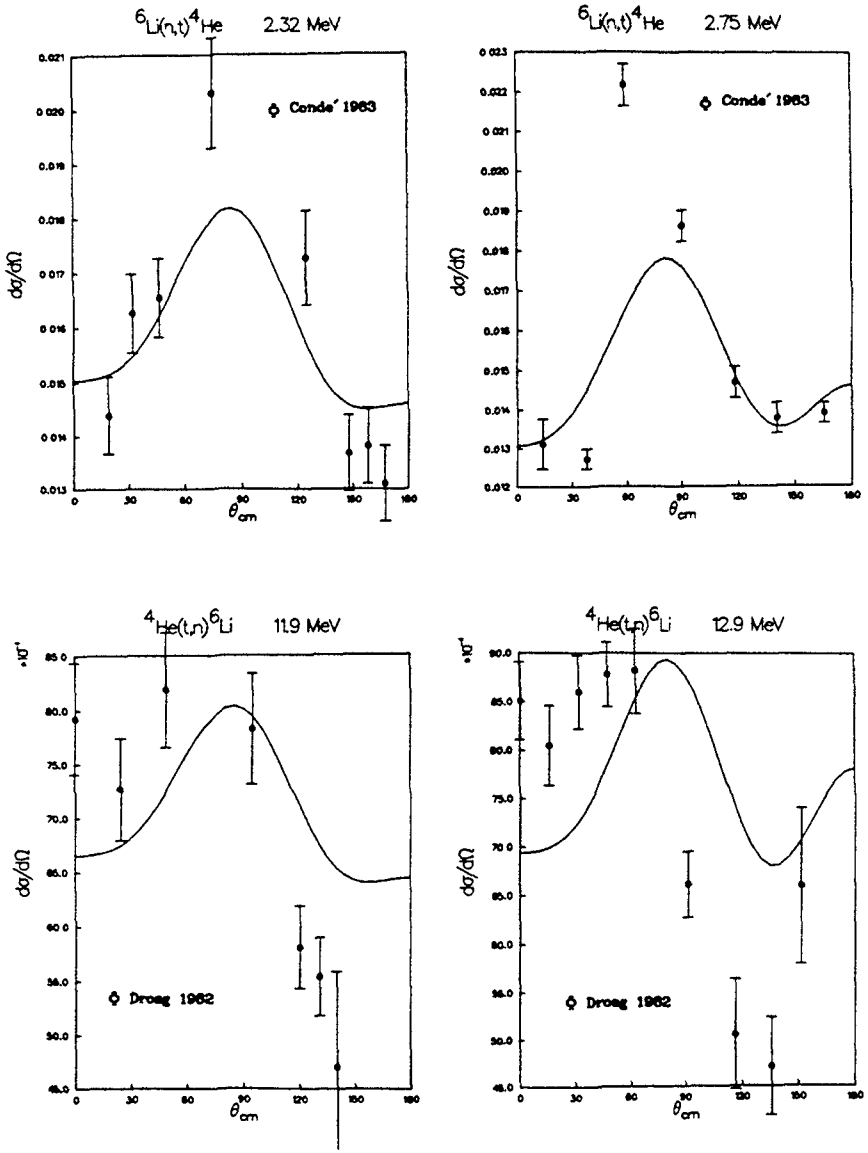

Fig. 10. Calculations of ^{6}Li(n,t)^{4}He differential cross sections compared with data of Condé[24] (top) at E_n = 2.32 and 2.75 MeV, and of ^{4}He(t,n)^{6}Li differential cross sections at approximately corresponding values of E_t (bottom) compared with measurements of Drosg.[22]

III. DEUTERON EXCHANGE IN PWBA

Weigmann and Manakos[25] have suggested that deuteron exchange may account for the $\frac{1}{2}^+$ component of the Li(n,t) 1/v cross section at low energies, and serve as a "background" mechanism at low energies for the resonant behavior of the angular distributions. Their PWBA calculation (which appears to have inherited errors in numerical factors from earlier work) makes the standard assumption that the bound-state wavefunctions for ^{6}Li and ^{3}H have their exponentially decaying asymptotic forms all the way in to zero radius, with the result that the Born-approximate T matrix has only negative-energy poles. A more realistic calculation would take into account the internal behavior of the bound-state wavefunctions, properly matched to the exponentially decaying asymptotic forms. This calulation cannot be done in a model-independent fashion, but even a simple model of the internal behavior of the bound-state wavefunctions gives qualitatively different effects.

We have assumed S-wave, square-well eigenfunctions (sine functions) for the internal bound-state wavefunctions. The depths (V_i^0) and ranges (c) of the square wells were determined by matching the binding energies and asymptotic normalization constants ($\tilde{C}^2$) for d-α binding in ^{6}Li and for n-d binding in ^{3}H. These values are given in Table III.

TABLE III

SQUARE-WELL POTENTIAL PARAMETERS FOR ^{6}Li AND ^{3}H BOUND STATES

	V_i^0 (MeV)	c_i (fm)	B_i (MeV)	$\tilde{C}_i^2$	Recommended $\tilde{C}_i^{2(a)}$
^{6}Li(d-α)	5.08	4.45	1.474	4.62	4.60
^{3}H(n-d)	38.51	1.95	6.258	2.57	2.59

(a) Taken from M. P. Locher and T. Mizutani, Phys. Rep. 46, 43 (1978).

The Born-approximate T matrix in this model is given by

$$T_{31}^{BA}(\theta) = \frac{1}{4\pi^2} V_1^0 V_3^0 (1-\alpha)^3 \frac{\hbar^4}{\mu_1\mu_3}(\beta_1\beta_3)^{\frac{1}{2}} \frac{K_1K_3}{D(\varepsilon,\theta)[D(\varepsilon,\theta)-(1-\alpha)V_1^0][D(\varepsilon,\theta)-(1-\alpha)V_3^0]} \quad (1)$$

in which the label 1 refers to n-^{6}Li, 3 refers to α-t, μ_1 is the d-α reduced mass, μ_3 is the n-d reduced mass, B_1 is the binding energy of α and d in ^{6}Li, B_3 is the binding energy of n and d in ^{3}H, and $\beta_i^2 = \frac{2\mu_i}{\hbar^2} B_i$. The energy denominator is

$$D(\varepsilon,\theta) = B_1 + B_3 + (1+\alpha)\varepsilon - 2\sqrt{\alpha(\varepsilon+B_1)(\varepsilon+B_3)}\cos\theta \quad , \tag{2}$$

in terms of the total center-of-mass energy ε (relative to the n+d+α mass), and scattering angle θ between the incident neutron and outgoing triton. We also have the residue factors

$$K_1 = \tilde{C}_1 \left(\cos q_1 c_1 + \frac{\beta_1}{q_1} \sin q_1 c_1\right) e^{-\beta_1 c_1} \quad , \tag{3}$$

which are functions of momentum transfer

$$q_1 = \left[\frac{2\mu_1}{(1-\alpha)\hbar^2} D(\varepsilon,\theta) - \beta_1^2\right]^{1/2} \quad , \tag{4}$$

and the mass factor $\alpha = \frac{m_n m_\alpha}{m_t m_{^6Li}} = \frac{2}{9}$

Using the identity

$$\frac{(1-\alpha)^2 V_1^0 V_3^0}{D[D-(1-\alpha)V_1^0][D-(1-\alpha)V_3^0]} = \frac{1}{D} - \frac{V_3^0}{V_3^0-V_1^0}\frac{1}{D-(1-\alpha)V_1^0} + \frac{V_1^0}{V_3^0-V_1^0}\frac{1}{D-(1-\alpha)V_3^0} \quad , \tag{5}$$

Eq. (1) can be reduced to a sum of pole terms, in which D gives the negative-energy pole in the squared momentum transfer ($q_1^2 = -\beta_1^2$), and the other terms give positive-energy poles, the lowest of which has a residue with opposite sign from that of the D^{-1} term since $V_3^0 > V_1^0$. This is qualitatively the same as the pole structure seen in our R-matrix analysis for the spin-½ transitions although the comparison is quite approximate. The point is, however, that including the internal behavior of the bound-state wavefunctions appears to broaden the energy range over which particle exchange contributes to a reaction, so that its effects need not be concentrated just at low energies in negative-energy poles, but may be manifest in positive-energy poles as well.

IV CONSISTENT R-MATRIX APPROACH

The similarities between our R-matrix amplitudes for the spin-½ transitions and a PWBA calulation including internal behavior of the bound-state wavefunctions lead one to seek a more definitive correspondence within the unitary framework of R-matrix theory The deuteron exchange mechanism in the ^{6}Li(n,t) reaction belongs to a larger class of effects that come from non-orthogonal channels that are neglected in conventional R-matrix theory. This is because the equations used to relate the R matrix to the T (or S) matrix come from matching to an asymptotic scattering solution that is valid only at infinity, where the channel overlap effects vanish

When a consistent R-matrix formulation of the scattering equations in the external (asymptotic) region is matched to the R-matrix solutions in the internal region, additional terms due to channel overlap appear in the relation between the T matrix and R matrix, which can be considered as off-diagonal contributions to the "hard-sphere" amplitude. These terms are mathematically similar to the PWBA T-matrix contributions from particle exchange, except that they are properly unitary. We are presently reducing the integrals for the partial-wave amplitudes of these terms to computational form so that they can be included in our R-matrix calculations. The expectation is that these terms will account for most of the spin-½ transition strength presently coming from poles in our conventional R-matrix analysis.

V. SUMMARY AND CONCLUSIONS

A comprehensive, conventional R-matrix fit to reactions in the ^{7}Li system gives a good representation of almost all the data included. In this analysis, the 1/v cross section for the ^{6}Li(n,t) reaction at low energies comes primarily from the constructive interference of J = ½ S-wave levels below the t-α threshold and above the n-^{6}Li threshold. Similar levels for the s = ½ P-wave transitions provide the forward-peaked background underlying the behavior of the ^{6}Li(n,t) angular distributions, although this contribution appears to be somewhat too small in the region $0.4 \lesssim E_n \lesssim 1$ MeV.

A PWBA calculation of the deuteron exchange contribution to the reaction that takes into account the behavior of the internal bound-state wavefunctions

gives, in addition to the pole normally encountered at negative squared momentum-transfer ($q^2 = -\beta^2$), poles at positive q^2 that interfere constructively (residues with opposite sign) with it. This is qualitatively the pole structure we see for the $s = \frac{1}{2}$ transitions in the R-matrix analysis, and suggests, along with the similarity of the shapes of the angular distributions calculated for those transitions with the PWBA results, that the dominant mechanism for the $s = \frac{1}{2}$ transitions in the Li(n,t) reaction is deuteron exchange.

Channel overlap terms that correspond to deuteron exchange in a simple model of the bound states for this reaction arise naturally in R-matrix theory with a properly consistent treatment of the scattering equations in both the internal and external regions. These terms, which are similar to the PWBA results except that they are unitary, may account for most of the $s = \frac{1}{2}$ transition strength observed in the ^{6}Li(n,t) reaction. The final results of the Los Alamos ^{7}Li R-matrix analysis, including these channel overlap effects, will be used in the combined ENDF/B-VI standards evaluation and in the Version VI general-purpose cross-section evaluation for ^{6}Li.

ACKNOWLEDGEMENTS

The author is indebted to Dr. M. Drosg for providing on rather short notice numerical values of some of his ^{4}He(t,n)^{6}Li differential cross sections prior to publication. He also wishes to thank Dr. P. G. Young for making some of the figures, and A. Mutschlecner for preparing the manuscript.

REFERENCES

1. H. Glättli, A. Abragam, G. L. Bacchella, M. Fourmond, P. Méreil, J. Piesvaux, and M. Pinot, Phys. Rev. Lett. 40, 748 (1978).

2. R. J. Holt, F. W. K. Firk, G. T. Hickey, and R. Nath, Nucl. Phys. A237, 111 (1975).

3. Y. H. Chiu and F. W. K. Firk, Nucl. Phys. A364, 43 (1981).

4. G. M. Hale, Proc. Int. Specialists Symp. on Neutron Standards and Applications, Gaithersburg, 1977, NBS Special Publication 493, p. 30 (1978).

5. V. P. Alfimenkov, S. B. Borzakov, Vo Van Thuan, L. B. Pikelner, and L. I. Sharapov, Proc. Int. Conf. on Nuclear Data for Science and Technology, Antwerp, 1982, K. Böckhoff, Ed., D. Reidel, Pub., p. 353 (1983).

6. H. D. Knox and R. O. Lane, Nucl. Phys. A403, 205 (1983).

7. A. Carlson, W. Poenitz, G. Hale, and R. Peelle, Proc. of the Advisory Group Meet. on Nuclear Standard Reference Data, Geel, November 1984.

8. N. Jarmie, F. D. Correll, R. E. Brown, R. A. Hardekopf, and G. G. Ohlsen, Los Alamos National Laboratory report LA-8492 (1980).

9. R. O. Lane, Ann. Phys. 12, 135 (1961).

10. R. O. Lane, A. J. Elwyn, and A. Langsdorf, Jr., Phys. Rev 136, B1710 (1964).

11. A. B. Smith, P. T. Guenther, and J. F. Whalen, Nucl. Phys. A273, 305 (1982).

12. L. Drigo and G. Torniellı, Nuovo Cimento 70A, 402 (1982).

13. A. Asami and M. C. Moxon, Proc. Conf. on Nuclear Data for Reactors, Vol. 1, Helsinki, 1970, I.A.E.A, Vienna, p. 153 (1970).

14. H.-H. Knitter, C. Budtz-Jørgensen, M. Mailly, and R. Vogt, Commission of the European Communities report EUR 5726 e (1977).

15. J. A. Harvey and N. W. Hill, Proc. Conf. on Nuclear Cross Sections and Technology, Washington, D.C., 1975, NBS Special Publication 425, p. 244 (1975).

16. P. Guenther, A. B. Smith, and J. Whalen, Argonne National Laboratory report ANL/NDM-52 (1980).

17. G. P. Lamaze, R. A. Schrack, and O. A. Wasson, Nucl. Sci. Eng. 68, 183 (1978).

18. C. Renner, J. A. Harvey, N. W. Hill, G. L. Morgan, and K. Pusk, Bull. Am. Phys. Soc. 23, 526 (1978).

19. C. M. Bartle, Nucl. Phys. A330, 1 (1979).

20. H.-H. Knitter, C. Budtz-Jørgensen, D. L. Smith, and D. Marletta, Nucl. Sci. Eng. 83, 229 (1983).

21. R. E. Brown, G. G. Ohlsen, R. F. Haglund, Jr., and N. Jarmie, Phys. Rev. C16, 513 (1977).

22. M. Drosg, D. M. Drake, R. A. Hardekopf, and G. M. Hale, Los Alamos National Laboratory report LA-9129-MS (1982) and private communication with M. Drosg (1984).

23. J. C. Overley, R. M. Sealock, and D. H. Ehlers, Nucl. Phys. A221, 573 (1974).

24. H. Condé, T. Andersson, L. Nilsson, and C. Nordborg, Proc. Int. Conf. on Nucl. Data for Science and Technology, Antwerp, 1982, K. Böckhoff, Ed., D. Reidel, Pub., p. 447 (1983).

25. H. Weigmann and P. Manakos, Z. Phys. A289, 383 (1979).

THE DATA FOR THE NEUTRON INTERACTIONS WITH ^{6}Li AND ^{10}B

W.P. POENITZ
Argonne-West,
Argonne National Laboratory,
Idaho Falls, Idaho,
United States of America

Abstract

The $^{10}B(n,\alpha)$, $^{10}B(n,\alpha_1)$ and, increasingly in more recent measurement, the $^{6}Li(n,\alpha)$ cross sections are the major references used in low energy experiments. Many data from modern measurements are available for the neutron interaction with ^{6}Li, including total, scattering, and absolute and relative (n,α) cross sections. A consensus has been reached with these new ^{6}Li + n data. In contrast, the data base for the ^{10}B neutron interaction cross sections is unfortunately poor. This is even the case for the total cross section which is supposed to be the easiest quantity to be measured. The most serious deficiency is the absence of data from absolute measurements of the $^{10}B(n,\alpha)$ and $^{10}B(n,\alpha_1)$ cross sections in the last 10-15 years. The available cross section data which were used for the ENDF/B-VI evaluation will be discussed.

I. INTRODUCTION

The $^{10}B(n,\alpha_1)$ and the $^{10}B(n,\alpha)$ reactions have been used as the major reference cross sections in most low-energy (e.g. < 100 Kev) cross section measurements in the past. The ^{6}Li (n,α) cross section has been increasingly utilized in the last 10 years. Consequently, the available data base for these cross sections has to be of major concern. However, because the ^{7}Li and ^{11}B compound nuclei can be very well described with R-matrix theory, data for other reaction channels, angular distributions and total cross sections are of interest as well.

The ^{6}Li + n and ^{10}B + n data were extensively discussed at the 1975 Standards Symposium in Gaithersburg.[1,2] Recent reviews of the "Standard Cross Sections"[3] and of the "Control Materials and Light Coolant Cross Section Data"[4] also addressed the ^{6}Li and ^{10}B data bases.Thus the present discussions will be restricted to the data base in view of its use for the ENDF/B-VI evaluation of the standards and other principal cross sections. This evaluation extends from thermal energy to 20 MeV for some cross sections. For ^{6}Li and ^{10}B the upper energy limits of 3.0 and 1.5 MeV, respectively, are determined by the usefulness of higher energy data to affect the low-energy "standard" range, as well as the opening of additional reaction channels besides the (n,n) and (n,α) reactions.

A short discussion of the thermal cross sections will be given in Section II. The ^{6}Li + n data base will be discussed in Section III and the ^{10}B + n data base in Section IV. A general discussion about the usefulness of these standards and some conclusions are contained in Section V.

II. THE THERMAL CROSS SECTIONS

There are three experimental values of the $^{6}Li(n,\alpha)$ cross section available. The weighted average of 941 ± 3b[5] is consistent with the value of ~ 940b inferred by $1/\sqrt{E}$ extrapolation from the total cross section measurement by Utley[6] but somewhat higher than the corresponding value measured by Harvey[7]. The ENDF/B-VI value is 935.9b[8] and in close agreement with the measurement by Harvey.

The thermal $^{10}B(n,\alpha)$ cross section which was measured very accurately in several experiments some 15-20 years ago is a bright point in the dismal data base for ^{10}B + n. A recent evaluation yields a value of 3838 ± 6b which should be accurate enough for any application. The ENDF/B-V value of 3836.6b[9] is in good agreement with this value.

The available data for the α_0/α_1 ratio show large discrepancies (see Fig. 1). The earlier proportional counter and ionization chamber measurements resulted in substantial differences which are multiples of the

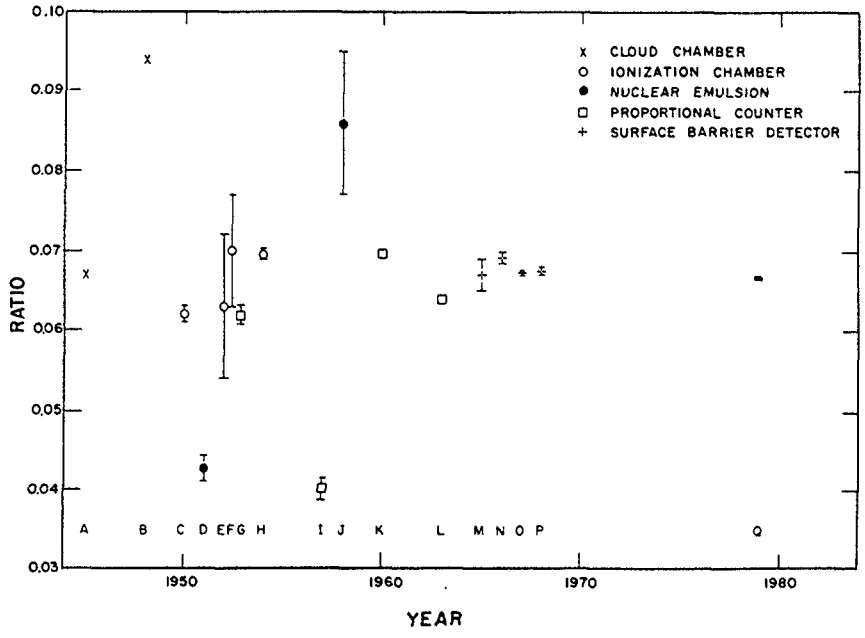

Fig. 1. Comparison of the Available $^{10}B(n,\alpha_0)/^{10}B(n,\alpha_1)$ Data Base[44].

claimed uncertainties. The later surface-barrier detector measurements resulted in substantially smaller difference but are also discrepant by nearly twice the combined uncertainties. The probability that a data base with a corresponding χ^2 occurs is $<10^{-17}$. An evaluated average of 6.723 ± 0.039% has been obtained for α_0/α_1 by increasing the quoted uncertainties of those values which deviate from the average by more than two standard deviations, and by increasing the evaluation uncertainty by $\sqrt{\chi^2}$. The evaluated average is in good agreement with the average from the surface-barrier detector measurements (6.722 ± 0.018)% as well as with the weighted average of all data (6.715 ± 0.006)%. This is the consequence of the two most accurate measurements [10,11] having substantially higher weights than all other data. The "preevaluated" value will be used for the ENDF/B-VI evaluation of the standards.

III. THE ^{6}LI + N DATA BASE

Several new ^{6}Li neutron total cross section data sets have become available since the evaluation of ENDF/B-V [12,13]. These measurements rely on samples from CBNM, thus they are correlated by the sample mass uncertainties. A common feature of the new measurements is a higher peak cross section (e.g. 11.26[13]) for the 240 KeV p-wave resonance than obtained in previous measurements (e.g. 11.0b[7]). This may be in part the result of uncertainties of the areal density of the samples used in the different experiments which might be expected from the procedure used to make some of the samples. The areal density of the CBNM sample was investigated as part of an additional total cross section measurement which has not yet been fully analyzed[14]. It was found that the maximum contribution to the uncertainty due to areal density variations of this particular sample is 0.3%. The new measurements are in good agreement except for an energy scale shift of ~ 2.5 KeV.

The major importance of the total cross section is its effect on the (n,α) cross section in an R-matrix fit. The relatively high value of the (n,α) peak cross section of ENDF/B-IV was the result of the low total cross section data by Uttley and Diment[6].

New scattering cross section data have also become available [12,13,14]. Of specific interest is the measurement by Alfimenkov et al.[15] at lower energies which appears to be much more consistent with R-matrix prediction than the previously available two data sets[16,17]. The latter were discrepant by ~ 50%. The data by Alfimemkov et al., are unfortunately not available in tabulated form so far. Only one of the new measurements extends over part of the 240 KeV p-wave resonance[12] with uncertainties of 6-10% for the experimental values.

Several absolute measurements of the ^{6}Li(n,α) cross section were made since 1970 [16-23]. The status of the data by Fort et al.,[16,18] is presently unclear: a renormalization of the data has been suggested based upon additional measurements of the amount of ^{6}Li in the Li-glass used in these experiments[24]. However, with this renormalization the cross section in the ~$1/\sqrt{E}$ region comes in substantial conflict with the extrapolation of the thermal cross section. The data are not being used for the evaluation. Only the data from the first measurement by Poenitz and Meadows[20] will be used for the evaluation because the later additions[21] were most likely affected by poor resolution caused by high humidity during neutron target production. This explains why the integral over the resonance is in reasonable good agreement with other data[1]. The data by McPherson and Gabbard[17] are uncorrected rough data and thus unuseable for any evaluation. The remaining three data sets which provide absolute data below 1 MeV are compared in Fig. 2. After adjustment of the energy scale in order to obtain the resonance peak at 240 KeV the three data sets are in good agreement with exception of the peak cross section value by Overley *et al.*[19]

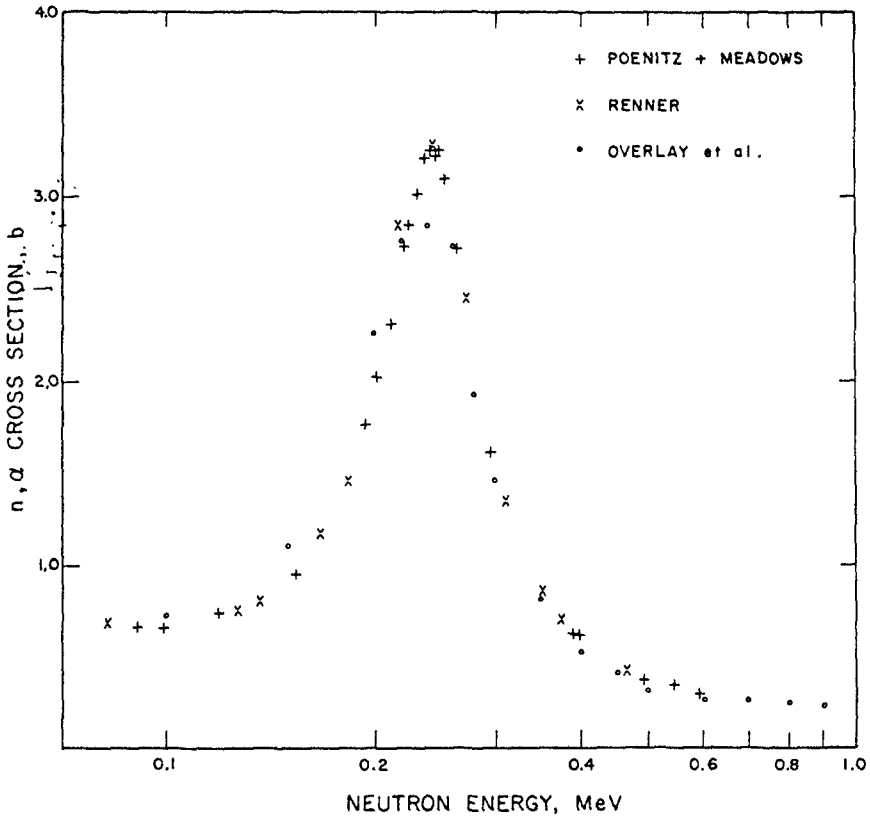

Fig. 2. Comparison of Absolute Measurements of the ^{6}Li(n,α) Cross Section[20,22,19].

There is an additional new measurement in which an absolute value was obtained at ~ 23 KeV with a quoted uncertainty of ~ 2.4%[23]. It is ~ 4.4% lower than the $1/\sqrt{E}$ extrapolation from a thermal value of 941b and ~ 6% lower than ENDF/B-V. It might be difficult to explain this value with the known resonances of the ^{7}Li compound nucleus.

An increasing number of the measurements of the ^{235}U(n,f) cross section in recent years has been carried out relative to the ^{6}Li(n,α) cross section[25-29].

More recently it has been recognized that the $^{235}U(n,f)$ cross section is probably better known than the $^{6}Li(n,\alpha)$ cross section and measurements were carried out extending over the higher KeV energy range[30-34]. All the $^{6}Li(n,\alpha)/^{235}U(n,f)$ and $^{235}U(n,f)/^{6}Li(n,\alpha)$ measurements are shape measurements with some extending to thermal energies[25,27,30,32] or to the 7.8-11.0 eV integral of the $^{235}U(n,f)$ cross section[26,28]. These data are shown in Fig. 3 as $^{6}Li(n,\alpha)/^{235}U(n,f)$ values. These data are in remarkably good agreement (~ 1-2%), Aside from a energy shift of ~ 5 KeV of the Van de Graaff data[32] and with exception of the 80-90 KeV region where there is a larger spread of the values. There seems to be a polarization at the peak of the Li resoance where the values of Czirr et al.[27] and Gaythe[33] are in good agreement but ~ 4% higher than the values by Poenitz and Meadows[32] and by Macklin[34] which in turn are also in good agreement.

It should be emphasized that all data in Fig. 3 have been renormalized with the normalization factors obtained from the evaluation of the standards and other principal cross sections for ENDF/B-VI. The normalization factors obtained from GMA are based on all absolute data. However, because of their low uncertainties, the thermal values have most likely the highest weight.

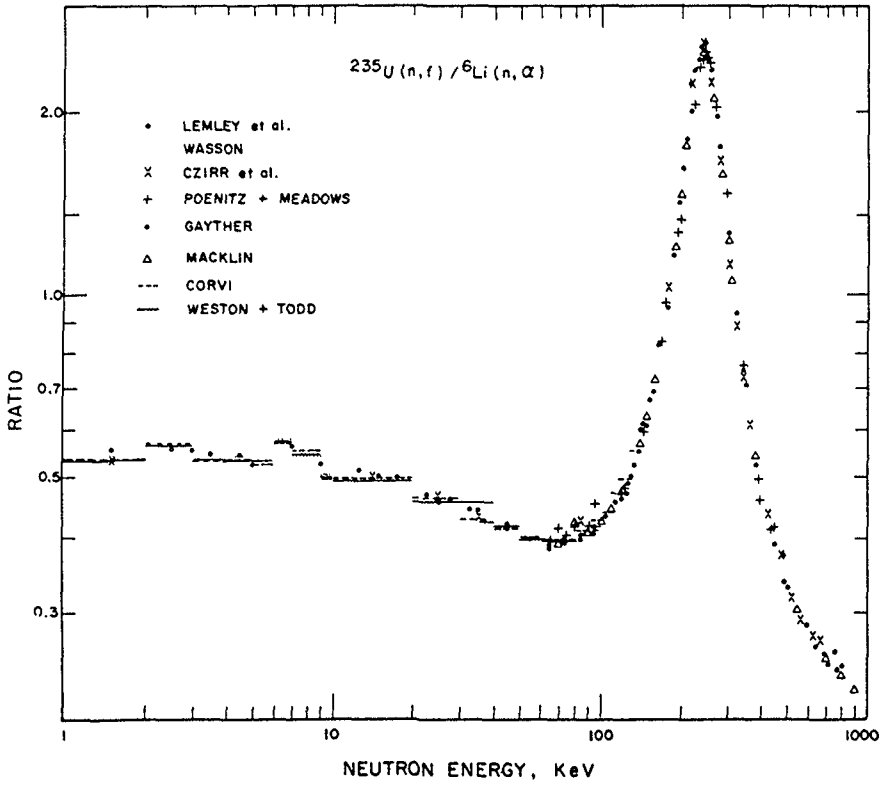

Fig. 3. Comparison of Shape Measurements of the $^{6}Li(n,\alpha)/^{235}U(n,f)$ Ratio[25-34].

It appears that the $^{6}Li(n,\alpha)/^{235}U(n,f)$ ratio is one of the best known quantities between thermal and 1 MeV neutron energy. This means that below 10 KeV the $^{235}U(n,f)$ cross section will be strongly influenced by the $^{6}Li(n,\alpha)$ cross section, and above 200-300 KeV the $^{6}Li(n,\alpha)$ cross section will be mainly determined by the $^{235}U(n,f)$ cross section.

IV. THE ^{10}B + N DATA BASE

Whereas the ^{6}Li + n data base has substantially improved in recent years, few new measurements have been made for the ^{10}B + n interaction. The data base for ^{10}B + n is not as extensive as it might appear because much double counting has been made in tables and figures shown in reviews and used in evaluations.

A new measurement of the total neutron cross section of ^{10}B has been reported by Auchampaugh et al.[35]. The original intent was to provide data above 1.5 MeV. However, values between 1.0 and 1.5 MeV were later also extracted form this experiment. Though the data are outside the range of interest for

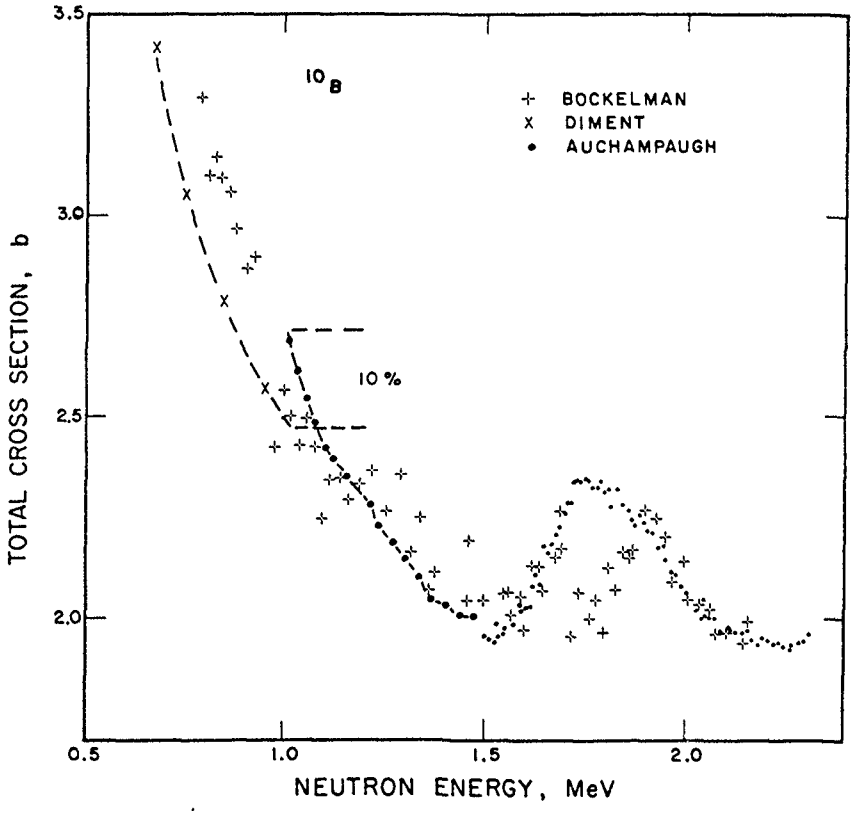

Fig. 4. Comparison of Total Cross Section Measurements of ^{10}B+n[35,36,45].

the application of the ^{10}B + n reference cross sections, they indicate an alarming 10% discrepancy with the total cross section data by Diment[36] around 1 MeV. This problem is shown in Fig. 4. Other available data are not useful for defining the total cross section with the required accuracy, as can be concluded from Fig. 4.

The data by Diment[36] have been the major basis for evaluations in the past. The measured cross section spans a large energy range but the data were obtained in segments. Though Diment stressed the importance of overlap regions between these segments, data for the overlap regions are not available. Some confidence in our knowledge of the total cross section has come from the good agreement between the data by Diment[36] and by Mooring et al.[37]. A comparison of the two data sets is shown in Fig. 5. Though the agreement is good over most of th energy range, it is apparent that the sample used by Mooring et al. had some oxygen in it. The more recent measurement by Beer and Spencer[38] is also shown in Fig. 5. Different results for the analysis of the sample used in this experiment resulted in a 5% systematic difference for the calculated

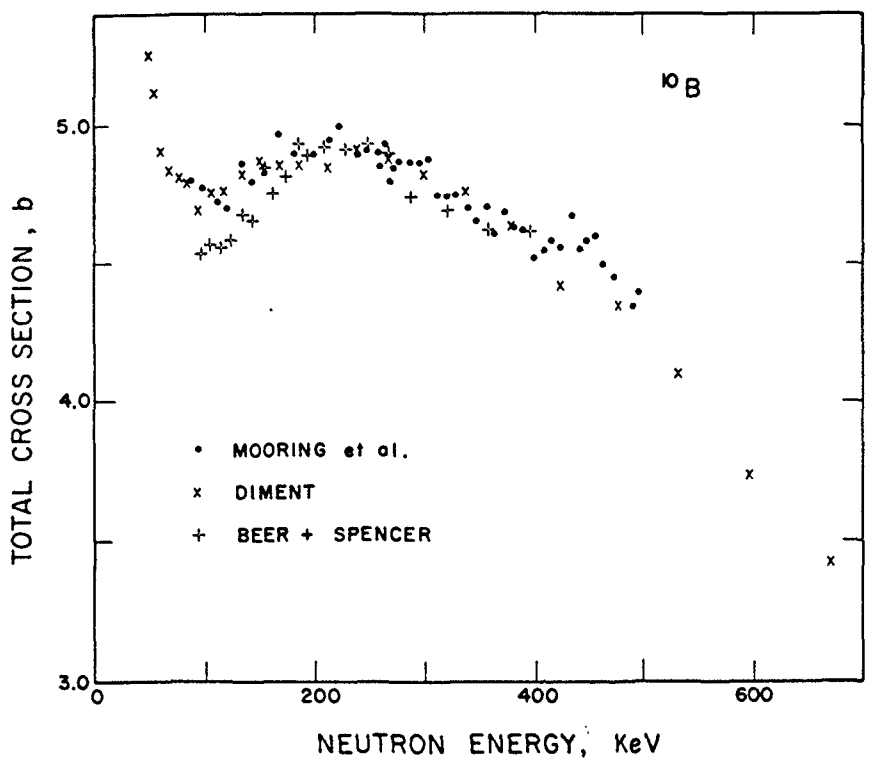

Fig. 5. Comparison of Total Cross Section Measurements of $^{10}B+n$[36,38].

cross sections. The result of one sample analysis was selected because it gave the best agreement with the prior data[36,37]. This, of course, means that these new data are biased and uncertain by at least 5%. One might note in addition that the agreement with the prior measurement appears not to be as good as suggested (see Fig. 5).

New measurements of the scattering cross section in the energy range of interest (e.g. < 2 MeV) have not been made. Though there is good agreement between the data by Mooring et al.[37] and Lane et al.[39], a substantial difference remains at lower energies with the data by Asami and Moxon[40].

The only important new contributions have been made for the $^{10}B(n,\alpha_0)$ cross section. Two new data sets are available which were obtained from measurements of the inverse reaction cross section[41,42]. These new measurements deviate from ENDF/B-V by up to 40% around 500 KeV, but also differ among themselves by ~ 10% at this energy (see Fig. 6). It is interesting that an average from the past α_0/α_1 ratio data and the evaluated α_1 of ENDF/B-V supports the higher α_0 data.

A new measurement of the (n,α_1) cross section has been carried out above 100 KeV[43]. However, this is only a shape measurement and therefore does not help to resolve the substantial discrepancies which exist for the (n,α_1) and (n,α) data base.

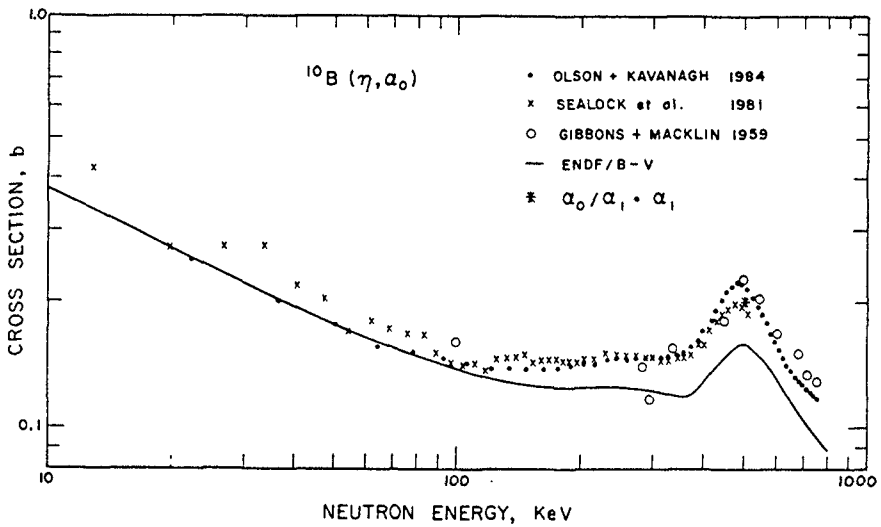

Fig. 6. Comparison of Absolute Measurements of the $^{10}B(n,\alpha_0)$ Cross Section[41,42,46].

V. DISCUSSIONS

Consideration of the ^{6}Li + n and the ^{10}B + n data bases shows that substantial progress has been made for the $^{6}Li(n,\alpha)$ cross section but the $^{10}B(n,\alpha)$ and the $^{10}B(n,\alpha_1)$ cross sections remain poorly defined. There are few absolute measurements of these cross sections and those available have large uncertainties and/or are flawed by various shortcommings. In most of the applications of these cross sections the experimenters have relied upon a "close to $1/\sqrt{E}$ behaviour of the ^{10}B + n cross sections at low energies. However, the degree of the deviations from $1/\sqrt{E}$ will have to be defined by the data in regions of resonances which cause these deviations. The ^{11}B compound nucleus has the disadvantage of higher level density than ^{7}Li. Both display very broad resonances (with exception of the 240 KeV p-wave resonance of 7Li) which are therefore difficult to define experimentally.

For ^{6}Li + n we have two total cross section measurements which extend to very low energies and several which cover the 240 KeV p-wave resonance. We have absolute data for the $^{6}Li(n,\alpha)$ cross section over the resonance which have acceptably low uncertainties ($\sim$ 2.3% and $\sim$ 3.5%). We also have a large number of $^{6}Li(n,\alpha)/^{235}U(n,f)$ measurement which help to define the cross section at higher energies via the absolute $^{235}U(n,f)$ data base. Undeniably there are some shortcommings as well. Scattering data over the 50-240 KeV range, which is the low energy side of the p-wave resonance, are sparce. The two measurements of the shape of the $^{6}Li(n,\alpha)$ cross section which extend to the low energy range differ systematically by 3-4% between 20-120 KeV and by 7% in the peak of the p-wave resonance though they agree well above 300 KeV and below 20 KeV.

In contrast, for ^{10}B + n we have only one total cross section measurement which extends to very low energies but which unfortunately has a segment end just at the energy where repeatedly a resonance has been suggested. We do not have sufficient total cross section data over the non- $1/\sqrt{E}$ range. In addition, we have discrepancies between the available data.

We do not have any valid absolute measurement of the $^{10}B(n,\alpha)$ cross section in the KeV-MeV range made in the last 20 years. The shape measurements which are available and extend to low energies are discrepant by 20-40%.

The situation is similar for the $^{10}B(n,\alpha_1)$ cross section. Though an absolute measurement has been reported $\sim$ 15 years ago, substantial corrections are required for this measurement. The available information is insufficient to calculate these corrections to any acceptable accuracy. There are similar discrepancies for the shape measurements, which extend to low energies, as for the $^{10}B(n,\alpha)$ cross section.

Absolute cross section measurements have been made for the $^{10}B(n,\alpha_0)$ cross section. However, this reaction is not used as a reference cross section. The uncertainties of these measurements are large (e.g. >5%) and their utility is limited because the α_0/α_1 data are also discprepant and/or very uncertain.

In spite of the dismal data situation, the least squares fit of all the available data will probably give a resonable answer. However, it is clear that the true uncertainty of such result is large.

It is therefore recommended that the $^{6}Li(n,\alpha)$ cross section should be used as a reference cross section below 100-150 KeV until a reasonable data base for the ^{10}B + n interactions becomes available.

ACKNOWLEDGEMENT

This work was performed under the auspices of the U.S. Department of Energy.

REFERENCES

1. H. Derrien and L. Edvardson, Proc. Conf. on Neutron Standards and Applications, NBS Spec. Pub. 493, 14 (1977).

2. E. Wattecamps, Proc. Conf. on Neutron Standards and Applications, 493, 67 (1977).

3. A.D. Carlson, Prog. Nucl. Energy, 13, 79 (1984).

4. P.G. Young and L. Stewart, Prog. Nucl. Energy, 13, 193 (1984).

5. N.E. Holden, Brookhaven National Laboratory Report BNL-NCS-52388 (1981).

6. C.A. Uttley and K.M. Diment, British Reports AERE-PR/NP-14, -15, -16 (1969).

7. J.A. Harvey and N.W. Hill, Proc. Conf. on Nuclear Cross Sections and Technology, NBS Spec. Publ. 425, 244 (1975), and private communication (1981).

8. G.M. Hale, et al., ENDF/B-V Summary Documentation for ^{6}Li, ENDF-201 (1979).

9. G.M. Hale, et al., ENDF/B-V Summary Documentation for ^{10}Li, ENDF-201 (1979).

10. A.J. Deruytter and P. Pelfer, ANE21, 833 (1967).

11. M.L. Stelts, et al., PR C19, 1159 (1979).

12. H.H. Knitter, et al., Euratom Report EUR 5726e (1977).

13. A.B. Smith, et al., NP A373, 305 (1982).

14. W.P. Poenitz, unpublished (1982 and 1984).

15. V.P. Alfimenkov, et al., Proc. Conf. on Nuclear Data for Science and Technology, p. 353, Antwerp (1982).

16. E. Fort, Proc. Conf. on Nuclear Data for Reactors, Vol. 1, 253 Helsinki (1970).

17. M.R. McPherson and F. Gelbard, Proc. Conf. on Neutron Cross Sections and Technology, CONF-710301, Vol. 2, 611 (1971).

18. E. Fort and J.P. Marquette, Cadarache Report, EMNDC(eE) 148 "U" (1972).

19. J.C. Overley, et al., NP A221, 573 (1974).

20. W.P. Poenitz and J.W. Meadows, Proc. Conf. on Neutron Standard Reference Data, p. 95, Vienna (1972).

21. W.P. Poenitz, Z.F. Physik 268, 359 (1974).

22. C. Renner, Thesis, Univ. Sao Paulo (1978).

23. J.C. Engdahl, et al., NSE 78, 44 (1981).

24. E. Fort, Cadarache, private communication (1974).

25. J.R. Lemley, et al., NSE 43 281 (1971).

26. O.A. Wasson, et al., NSE 81, 196 (1982).

27. J.B. Czirr and G.W. Carlson, NSE 64, 892 (1977).

28. F. Corvi, Central Bureau of Nuclear Measurements, private communication (1983).

29. L.W. Weston and J.H. Todd, subm. NSE (1983).

30. J.F. Barry, Proc. Conf. on Nuclear Cross Sections and Technology 763, Washington (1966).

31. W.P. Poenitz, NSE 53, 370 (1974).

32. W.P. Poenitz and J.W. Meadows, private communication to CSEWG (1976).

33. D.B. Gayther, ANE 4, 515 (1977).

34. R.L. Macklin, et al., NSE 71, 205 (1979).

35. G.F. Auchampaugh, et al., NSE 69, 30 (1979).

36. K.M. Diment, UKAEA Research Group Report, EANDC (UK) 85 'S' (1967).

37. F.P. Mooring, et al., NP 82, 16 (1966).

38. H. Beer and R.R. Spencer, NSE 70, 98 (1979).

39. R.O. Lane, et al., PR c, 380 (1971).

40. A. Asami and MC. Moxon, Harwell Report AERE-R-5980 (1969).

41. R.M. Sealock, et al., NP A357, 279 (1981).

42. M.D. Olson and R.W. Kavanagh, Subm. PR (1984).

43. G. Viesti and H. Liskin, ANE 6, 13 (1979).

44. A: J.K. Boggild, Mat-fys. Skr. 23, 4 (1975), B: C.W. Gilbert, Proc. Camb. Phil. Soc. Math Phys. Sci., 44, 447 (1948), C: G.C. Hanna, Phys. Rev. 80, 530 (1950), D: P. Cuer and J.P. Longchamp, C.R. Hebd. Seanc. Acad, Sci., Paris 232, 1824 (1951), E: J. Rodes, et al., Phys. Rev. 87, 141 (1952), F: H. Bichsel, et al., Helv. Phys. Acta 25, 119 (1952), G: U.H. Hauser, Z. Naturf, 7a, 781 (1952), H: J.A. DeJuren and H. Rosenwasser, Phys. Rev. 93, 831 (1954), I: L.M. Segal, Indian J. Phys. 31, 329 (1957), J: E. Bujdoso, Nucl. Phys 6, 107 (1958), K: H.F. Brinkman and D. Gerber, Kernenergie 3, 309 (1960), L: S. Malskog, Physica 29, 987 (1963), M: R.L. Macklin and J.H. Gibbons, Phys. Rev. 140B, 325 (1965), N: W.M. Toney and A.W. Waltner, Nucl. Phys. 80, 237 (1966), O: Ref. 10, P: R.L. Macklin and J.H. Gibbons, Phys. Rev. 165, 1147 (1968), Q: Ref. 11.

45. C.K. Bockelman, et al., Phys. Rev. 84, 69 (1951).

46. J.H. Gibbons and R.L. Macklin, Phys. Rev. 114, 571 (1959).

118 MEASUREMENT OF THE $^{6}Li(n,\alpha)/^{10}B(n,\alpha)$ RATIO WITH A XENON GAS SCINTILLATOR

C. BASTIAN, H. RIEMENSCHNEIDER
Central Bureau for Nuclear Measurements,
Joint Research Centre,
Commission of the European Communities,
Geel

Abstract

The charged particle emission of ^{6}LiF and ^{10}B sample layers placed alternatively in the neutron beam of GELINA was detected by scintillation in Xenon gas. In order to compensate for the anisotropy of the emission, each sample was deposited on the inside of a hollow cylindrical quarz support. Recording of a dummy sample support was also included in the measurement sequence. The ratio of $^{6}Li(n,\alpha)$ to $^{10}B(n,\alpha)$ cross-sections, thus measured under the same conditions, agrees up to 400 keV with point data deduced from ENDFB/V, within the estimated uncertainty.

1. INTRODUCTION

The (n,α) cross-sections of ^{6}Li and ^{10}B are both widely used in the determination of neutron fluences, often outside of their domain of definition as standards. Few direct determinations of their ratio are published, and they may be divided into:

- detection of a well defined, small angular domain of the charged particle yield (typically with surface barrier detectors wiewing the emission 90 degrees with respect to the incident neutron beam),
- or 2π charged particle detection (typically with parallel plate ion chambers detecting as well the front- as the backwards emission).

In either case, the results are not to be trusted above a few keV of neutron energy, due to the anisotropy of the charged particle emission.

On the other hand, 4π detectors such as the BF3 counter and the ^{6}Li glass scintillator are by definition insensitive to emission anisotropies, so they may be used up to the MeV range of neutron energy. However, they rely on different detection mechanisms, so that they cannot be used to determine the ratio of cross-sections directly out of the ratio of detector responses.

We present here a method of alternate recording of the charged particle yield of two thin samples of ^{6}Li and ^{10}B observed under the same conditions, whereby the anisotropy effects are compensated by a cylindrical sample geometry.

2. EXPERIMENTAL SETUP

2.1. Detector geometry

We consider a sample layer deposited on the inside surface of a thin walled cylindrical support. The sample is irradiated with its axis perpendicualr to the neutron beam. The reaction products emitted to the sample inside volume are detected by a gas scintillator.

It can be shown that (1) that this geometry integrates the angular distribution of the emission independently of its anisotropies. One thereby assumes that the sample geometry is truly rotation symmetric, i.e. that the sample density does not depend on the angle, and that the neutron beam fluence is uniform over the whole sample.

Absorption of the beam in the sample support and of the reaction products in the sample introduce only small corrections, which are proportional to the ratio A2 / A0 of the two first even terms in the Legendre expansion of the angular distribution (1).

The geometry behaves exactly like the half of a 4π detector, selecting the reaction products which are emitted to the inside volume.

2.2. Detector construction (Fig. 1)

Each sample support is a barrel-like assembly of thin (5 mm) quarz plates on the inside of which the sample layers are evaporated.

Three such supports are placed on a revolver sample changer. Here we report on measurements on 2 sample layers of 200 cm^2 of ^{10}B or ^{6}LiF (4 and 19 mg respectively) and one "dummy" sample, i.e. without any neutron sensitive deposit.

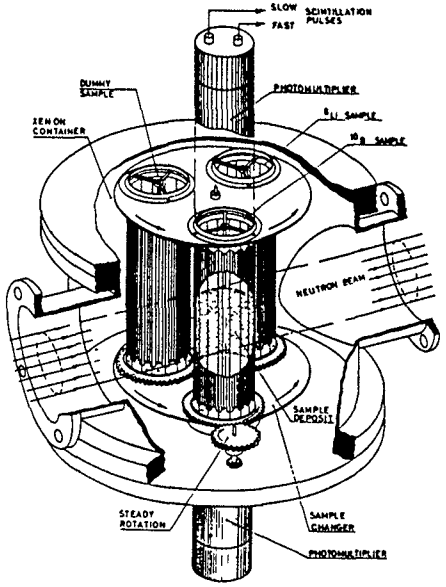

Fig. 1 Xenon scintillation detector

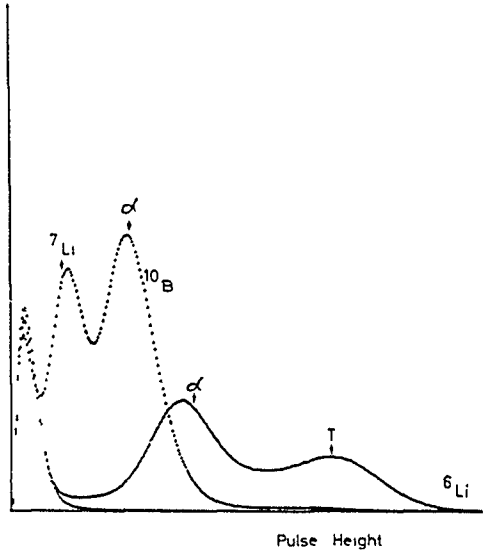

Fig. 2 Scintillation p.h. distribution

Once in irradiation position, the sample is rotated slowly around its axis to fulfil the rotation invariance condition mentioned before.

The sample changer is operated in a Xenon container at atmospheric pressure. The scintillator properties of the gas are highly dependent on its purity, so it is continuously circulated in a Titanium oven in order to absorb the outgassing of the detector container and parts.

2.3. Detection and acquisition system

Scintillations inside of the sample volume are detected by two photomultipliers viewing it from both ends and operated in coincidence. Fast pulses at the anodes are used for coincident timing, thus determining the neutron energy by its time of flight. Slow pulses from the dynodes are added to determine the energy of the reaction products out of the scintillation amplitude.

Neutron TOF and/or product energy information is digitised and passed to a ND 6600 acquisition computer, which also cares for a cyclic operation of the CAMAC driven sample changer.

3. DISCUSSION OF RESULTS

3.1. Scintillation pulse height distributions

Scintillations due to low energy products - e.g. ^{7}Li recoils from the $^{10}B(n,\alpha)$ reaction - give pulses comparable to the noise of the photomultipliers. This is the reason for working in coincidence, with a very low level of pulse discrimination. One thus finds a low amplitude peak in the pulse height spectrum, even with the dummy sample. This implies that a background component has to be compensated out of the spectra (Fig. 2).

3.2. Analysis of TOF spectra

We report here on a measurement at a flight distance of 11.45 m from the GELINA neutron source (repetition rate 800 Hz). To reduce the gamma flash and the out-of-time neutrons, the beam was filtered with 10 mm of ^{238}U and 2 mm Cd.

Scintillation events were sorted by their TOF and/or pulse height content and accumulated in 3 multichannel spectra of 8192 channels each (1 per sample).

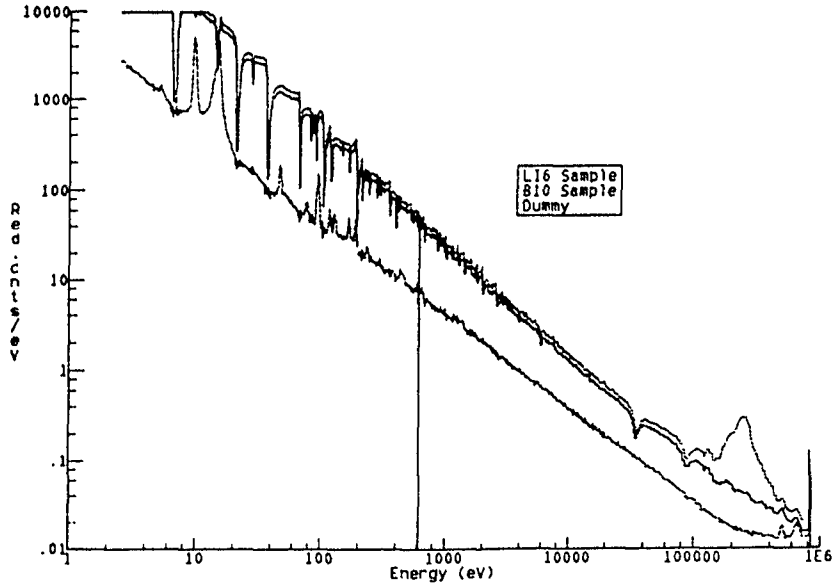

Fig. 3 Direct Spectra

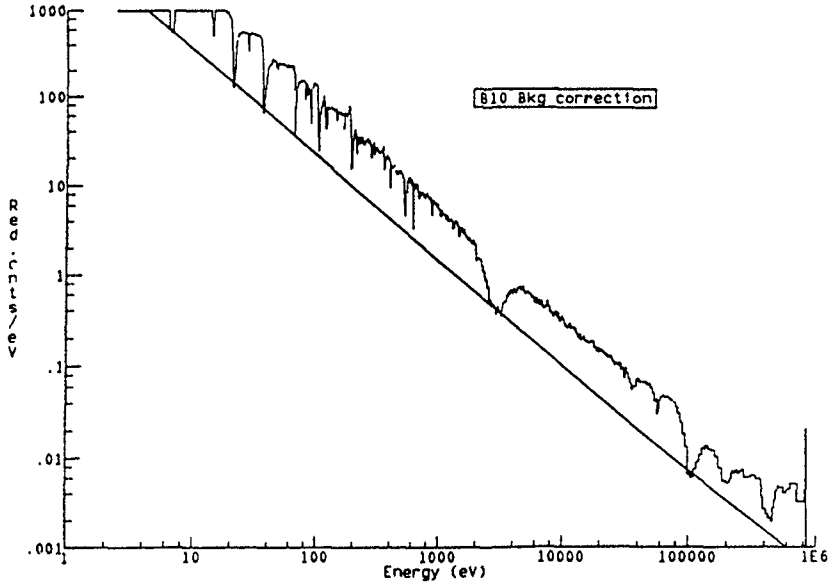

Fig. 4 Spectra with black resonance filters

These spectra were first condensed dynamically to reduce the counting fluctuations, then the TOF was converted to neutron energy and the count rate normalised to a channel width of 1 eV and an irradiation of 10^6 counts of the GELINA central monitor.

The results of this first step of analysis is plotted on Fig. 3. One notes a non negligible recording with the dummy sample. A part of it may be attributed to (n,X) reactions in Xenon, as to be seen from the low-energy resonance.

The background was compensated by a separate irradiation with Na and S black resonance filters. An example of background fit is given on Fig. 4. Obviously, this background estimate is not te be trusted too much beyond the last black resonance at 100 keV.

After substraction of the background estimates from the direct spectra of the ^6Li and ^{10}B samples, those were divided channel by channel. The quotient was normalised to .244 (from ENDFB/V) in the 2-5 eV range, yielding a series of point values of the requested ratio.

The plots of Fig. 5 and 6 are comparisons of the measured ratio and its overall uncertainties with point values deduced from ENDFB/V.

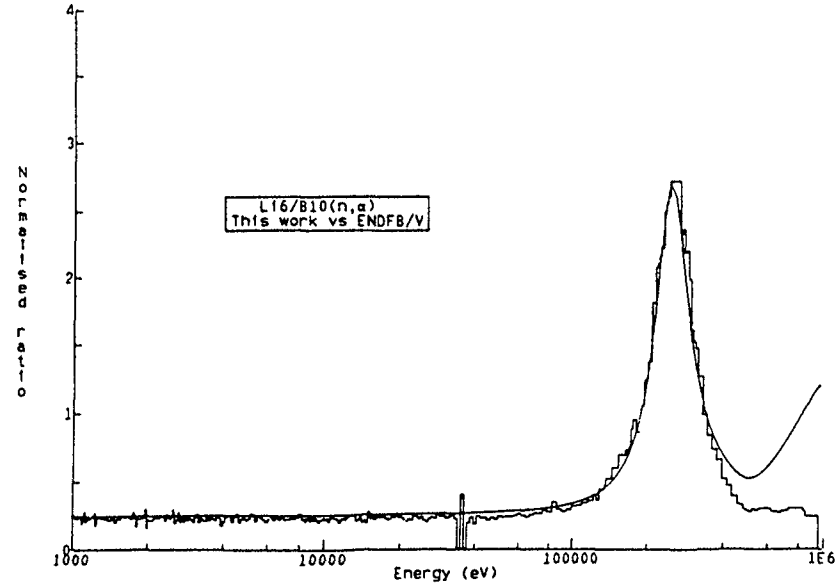

Fig. 5 Normalised results

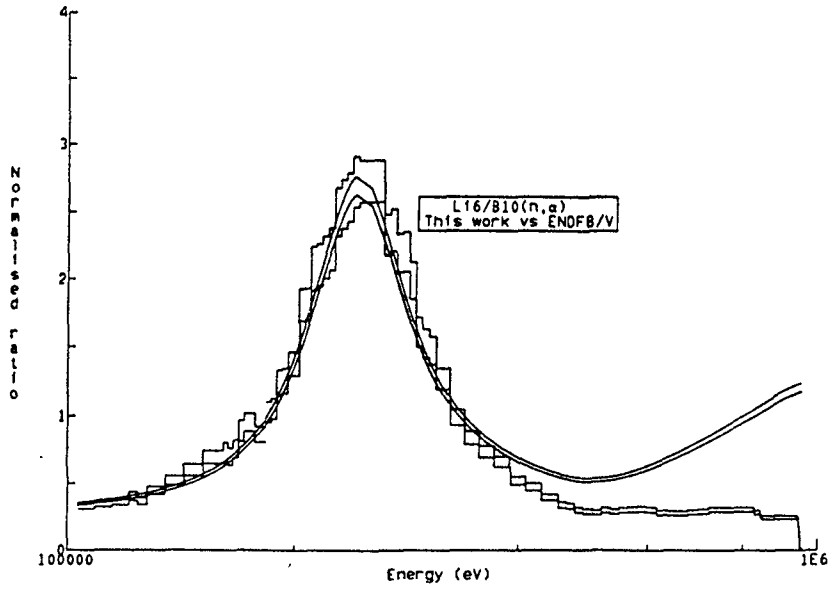

Fig. 6 Normalised results (high energy)

The correlated and uncorrelated uncertainty estimates of the measurement are summarised in the following table, together with the corresponding precision of ENDFB/V.

Neutron Energy	Correl.Err. %	Uncorr. Err. %	Total Err. %	ENDFB/V %
10 eV	1.6	2.0	2.56	2.26
100 eV	2.3	4.0	4.61	2.26
1 keV	3.8	5.0	6.28	2.28
10 keV	5.04	7.0	8.63	2.35
100 keV	5.20	6.0	7.94	2.48

3.3. Conclusions

Although an overall agreement with the ratio values deduced from ENDFB/V was reached within the estimated uncertainty from 2 eV to 400 keV the precision of the results has to be increased significantly before they become of real use for evaluation. A special effort has to be put on the reduction of the scintillator background level, mainly in the high energy part of the TOF spectra, just after the gamma flash.

REFERENCE

(1) C. Bastian, European Applied Research Report, .. in preparation.

122 DETERMINATION OF THE NEUTRON DETECTION EFFICIENCY OF A THICK ^{6}Li GLASS DETECTOR BY MEASUREMENT AND BY MONTE CARLO CALCULATION

A. LAJTAI, J. KECSKEMÉTI
Central Research Institute for Physics,
The Hungarian Academy of Sciences,
Budapest, Hungary

V.N. KONONOV, E.D. POLETAEV, M.V. BOHOVKO,
L.E. KAZAKOV, V.M. TIMOHOV, P.P. DYACHENKO,
L.S. KUTSAEVA, E.A. SEREGINA
Institute of Physics and Power Engineering,
Obninsk,
Union of Soviet Socialist Republics

Abstract

The neutron detection efficiency of a 9.55 mm thick NE-912 lithium glass scintillator has been determined for the energy range from 25 keV to 2 MeV. It was measured relative to a thin, 0.835 mm thick NE-908 glass, which was determined by Monte Carlo calculation. The measured efficiency curve shows the marked effect of the ^{16}O resonance at 442 keV, and a strong increase with energy E_n>1.2 MeV, due to (n,n'γ) reactions.

Simultaneously we calculated the efficiency for the thick glass detector by Monte Carlo method and it was compared to the experimental results.

The Monte Carlo calculation served also the response function for the detector, which has to be used at the evaluation of the neutron time-of-flight spectra.

Introduction

Neutron spectroscopy at low energies, E_n<1.5 MeV, makes considerable use of ^{6}Li glass scintillators. These have well known characteristics, i.e. zero energy threshold, short light flash and the ^{6}Li(n,α) cross section, which essentially determines the efficiency of this detector |1,2,3|. Their detection efficiency can be calculated with good accuracy, however, only for thin (up to about 1 mm thick) glasses. For thicker ones the multiscattering and attenuation effects due to the complex chemical abundance strongly limit the accuracy of the calculations. However, to have sufficiently high efficiency in low energy neutron detection one has to use thick lithium glasses. It would thus seem that the solution lies in a combined method of efficiency determination, i.e. to measure the relative efficiency of the thick glasses relative to that of a thin one, the absolute efficiency values of which can be determined by Monte Carlo calculation.

In this paper the determination of the neutron detection efficiency of a 9.55 mm thick NE-912 ^{6}Li glass is described and is related to an efficiency measurement for a 0.835 mm thin NE-908 ^{6}Li glass and a Monte Carlo calculation for this latter at energies from 25 keV to 2 MeV.

Recent work has been motivated by the fact that this thick ^{6}Li glass was used in a measurement |4| to determine the energy distribution of neutrons from the spontaneous fission of ^{252}Cf. At the analysis of this measurement it was also necessary to know the response function of the thick detector. For this purpose Monte Carlo calculations have been performed for the thick glass detector. These calculations served the absolute efficiency, too.

Experimental method

The efficiency measurements were carried out at the Van de Graaff accelerator in the Institute of Physics and Power Engineering, Obninsk. The experimental arrangement is shown in Fig. 1. The neutron beam was produced in ^{7}Li(p,n)^{7}Be and ^{3}H(p,n)^{3}He reactions by a pulsed proton beam, the pulse width frequency and mean current on the target being 16 ns, 300 kHz and 2μA, respectively. The glass

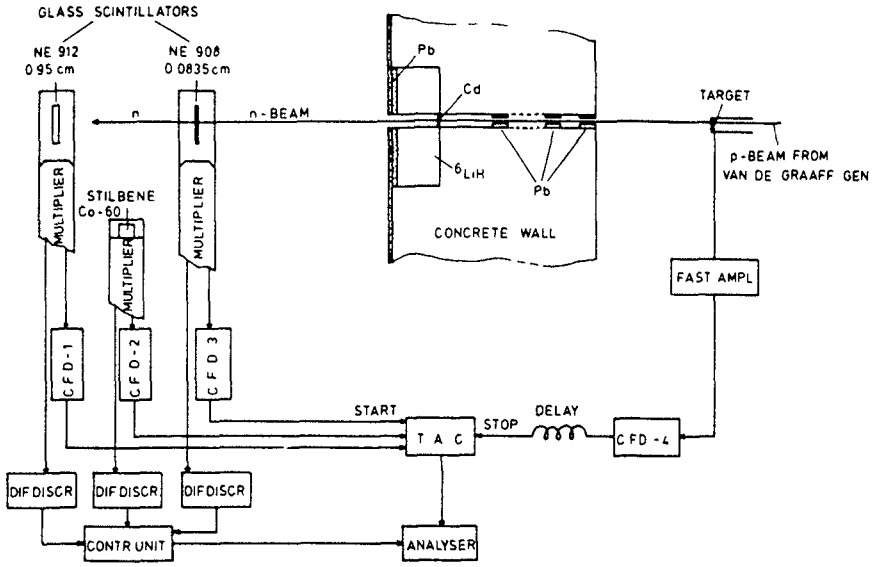

Fig. 1 Experimental arrangement.

detectors were separated from the accelerator room by a 2 m thick concrete wall. The neutron beam, lead through this wall by a collimator system, had a diameter of 28 mm with an angular divergence of 6.7 mrad. The two neutron detectors with NE-912 and NE-908 scintillators were placed at 2.8 m and 2.2 m from the target, respectively. A third detector with a stilbene crystal, placed out of the beam and looking at a ^{60}Co γ-source, was used to check the integral and differential linearity of the system during the experiment.

Two measurements were carried out, one for the continuous energy distribution of neutrons from a thick metallic Li target in the 25 keV < E_n < 1.2 MeV energy range and one for neutrons of fixed energies E_n=0.08, 0.22, 0.5, 1.0, 1.2, 1.4, 1.6, 1.8 and 2.0 MeV, using thin LiF (0.1 mg cm^{-2}) and T-Sc (0.35 mg cm^{-2}) targets.

The thin NE-908 glass was suspended in the centre of thin-walled aluminium chamber placed on a FEU-30 photomultiplier. The entrance and exit windows of the chamber were made of 80 μm Al foil. The contruction and characteristics of such a detector are described in [5] in more detail. The relative detection efficiency of the thick NE-912 glass scintillator was measured in two different positions: in the first (position I) its position was similar to that of the thin glass (Figs. 1 and 5); in the second (position II) it was mounted directly on the multiplier (Fig. 6). The diameters of the NE-908 and NE-912 glasses were 35 mm and 45 mm, respectively.

The energy of the detected neutrons was determined by the time-of-flight (TOF) method. The start signals were given by pulses of the three detectors, formed by the constant fraction discriminators CFD_1, CFD_2 and CFD_3. The stop signal was given by the pulse at the target after being formed in CFD_4 and delayed by 2 μs. All three start signals were fed into the same time-to-amplitude converter (TAC). The analyser was gated by the signals of three differential discriminators, fed through a special control unit. The lower and upper thresholds corresponded to 1.2 MeV and 7.0 MeV γ-ray energies for the neutron detectors and to 0.2 MeV and 1.3 MeV for the detector with the stilbene crystal, respectively. The identification of events from different detectors was ensured by the control unit.

The time scale of the TOF system was calibrated by the positions of the prompt γ-ray peak and of the peak due to the E_n=242 keV resonance in the ^{6}Li(n,α) cross section. Additional calibration measurements after each run were performed with a fluorene plastic filter placed in the neutron beam at 10 cm from the target. A typical transmission spectrum with the NE-912 detector is shown in Fig. 2. The three ^{19}F resonances at E_n=27.02, 49.1 and 97 keV were also used in the time calibration.

The beam attenuation due to the thin glass detector was also determined experimentally. Its value was between 0.5 % and 3.5 % in the energy range 25 keV-1.2 MeV.

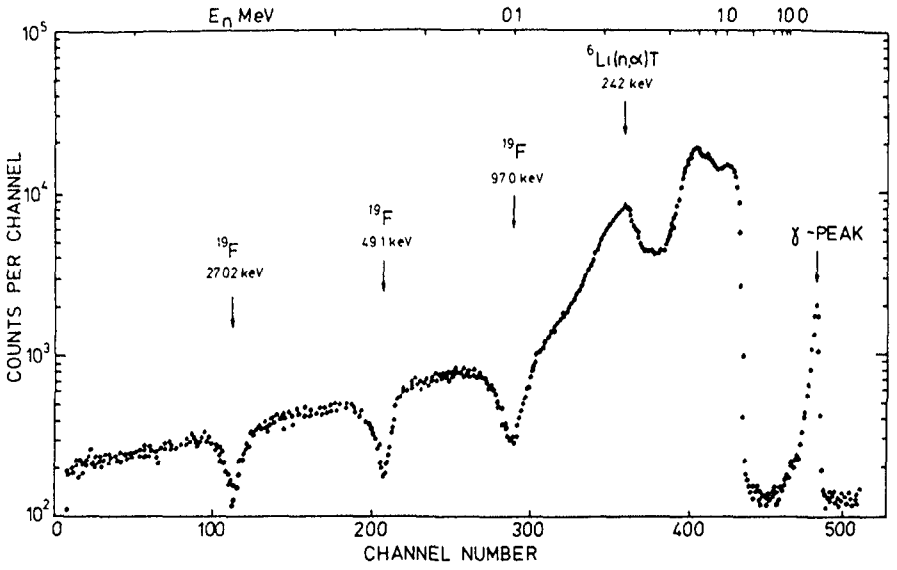

Fig. 2 Calibration spectrum measured with fluorene plastic filter.

For the relative efficiency determination of NE-912 we obtained the following spectra: TOF spectra of the thin and thick glass detectors in position I using the continuous neutron beam in the energy range from 25 keV to 1.2 MeV; TOF spectra as above but with the thick glass detector in position II; TOF spectra as above but with monoenergetic neutrons in the range 80 keV < 2.0 MeV.

For the absolute efficiency calculation of the thin NE-908 glass it was necessary to determine its ^{6}Li content $n_o x$. This was accomplished by a transmission measurement in the eV range, when the accelerator worked in the microsecond regime with a frequency f=7.14 kHz, and the metallic Li target was surrounded by a 2.5 cm thick polyethylene moderator. The applied method was the same as in Ref. |6|. The background was determined by using the "black" ^{115}In resonances at 3.68 and 9.12 eV. The time calibration was done by nine known resonances of In and Cd. The slope of the $^{6}Li(n,\alpha)$ reaction cross section in the $1/\sqrt{E_n}$ scale had the value of 148.87 barn/eV$^{1/2}$, in accordance with ENDF/B-V |7,8|. As a result we obtained $n_o x = 1.44 \cdot 10^{21}$ cm^{-2} for the number of ^{6}Li nuclei in the thin glass.

In order to see the background contribution of the correlated γ-rays a separate experiment was carried out by substituting the NE-912 glass for a ^{7}Li containing NE-913 one. It was found that this background was negligibly small for neutron energies below 1.2 MeV.

Results and discussions

The measured TOF spectra were corrected for the random coincidence background and, in the case of the NE-912 glass, for the thin glass transmission. After transforming into energy scale we formed the efficiency ratios of the two glass scintillators in position I

$$R_1 = \frac{N^{912}_{1,I}(E)}{N^{908}_{1,I}(E)} \quad \text{and} \quad R_3 = \frac{N^{912}_{3,I}(E)}{N^{908}_{3,I}(E)}$$

Here $N^{912}_{1,I}(E)$, $N^{908}_{1,I}(E)$, $N^{912}_{3,I}(E)$ and $N^{908}_{3,I}(E)$ are the neutron energy spectra for the NE-912 and NE-908 detectors in position I and for continuous and discrete neutron spectrum measurements.

It can be seen in Fig. 3 that the results with continuous and discrete neutron energy (R_1 and R_3, respectively) agree well with each other in the energy range below 1.2 MeV. As expected the relative efficiencies show a definite energy dependence: they are characterized by a pronounced peak centred at $E_n \sim 450$ keV, and by a strong increase for energies $E_n > 1.2$ MeV. The peak shows that the multiscattering effects connected with the 442 keV ^{16}O resonance become more dominant for larger glass thickness. The increase of R_3 in the high energy region can be attributed to the contribution from

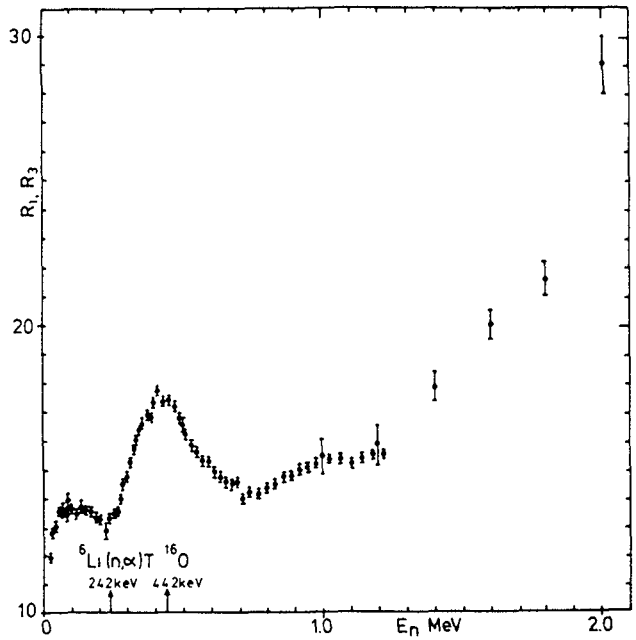

Fig. 3 Ratio of efficiencies of the thick NE-912 glass detector to the thin NE-908 one in Position I
• measurements with continuous neutron spectrum
o measurements with monoenergetic neutrons.

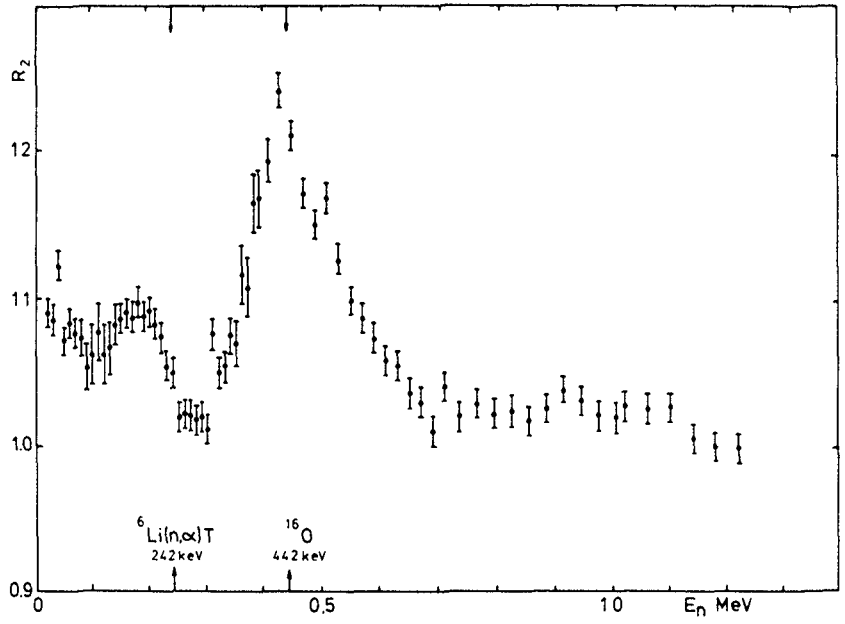

Fig. 4 Ratio of efficiencies of the thick NE-912 glass in position II to that in position I.

(n,n'γ) reactions; the thick glass is more sensitive to γ -rays than the thin one. This effect does not appear at lower energies since the detection threshold of γ-rays was set to 1.2 MeV.

Comparison of the neutron detection efficiencies of NE-912 glass in positions I and II

$$R_2 = \frac{N^{912}_{2,II}(E) \,/\, N^{908}_{2,I}(E)}{N^{912}_{1,I}(E) \,/\, N^{908}_{1,I}(E)}$$

is shown in Fig. 4. Here $N^{912}_{2,II}(E)$ is the neutron energy spectrum measured with the NE-912 in position II for continuous neutron distribution. The efficiency of the thick neutron detector in position II is greater than that in position I (the maximum difference being 20 % at 450 keV) in the whole energy range. Such behaviour can be explained by the influence of the detector material in position II. In particular the enchancement of the peak at E_n~450 keV can be interpreted as an increase in the detector efficiency in position II due to back-scattering of neutrons at the 442 keV resonance of ^{16}O contained in the PM-photochathode glass.

Table 1. Neutron detection efficiency ε(E) (%) in position I. (ε(E_n) I) and in position II. (ε(E_n) II)

E_n, keV	ε(E)I	ε(E)II	E_n, keV	ε(E)I	ε(E)II
25	1.89±0.04	2.06±0.04	35	1.70±0.04	1.84±0.04
45	1.53±0.03	1.69±0.04	55	1.39±0.03	1.49±0.04
65	1.35±0.03	1.46±0.04	75	1.29±0.03	1.39±0.04
85	1.29±0.03	1.38±0.04	95	1.32±0.03	1.39±0.04
105	1.34±0.03	1.42±0.04	115	1.38±0.04	1.49±0.05
125	1.40±0.04	1.49±0.05	135	1.48±0.07	1.58±0.08
145	1.58±0.08	1.71±0.09	155	1.74±0.09	1.89±0.1
165	1.94±0.10	1.12±0.12	175	2.65±0.14	2.87±0.15
185	2.62±0.14	2.88±0.15	195	3.78±0.20	4.11±0.2
205	4.58±0.24	5.0 ±0.25	215	5.38±0.28	5.83±0.3
225	5.40±0.28	5.81±0.3	235	6.52±0.34	6.87±0.35
245	6.54±0.34	6.58±0.35	255	5.72±0.30	8.84±0.32
265	5.00±0.26	5.27±0.28	275	5.16±0.27	5.26±0.28
285	4.54±0.23	4.62±0.25	295	3.35±0.17	3.42±0.2
305	2.97±0.15	3.01±0.18	315	2.70±0.14	2.9 ±0.15
325	2.69±0.14	2.83±0.15	335	2.19±0.11	2.31±0.14
345	2.04±0.11	2.19±0.12	355	1.88±0.10	2.01±0.12
365	1.89±0.10	2.11±0.12	375	1.79±0.09	1.98±0.10
385	1.62±0.08	1.88±0.1	395	1.59±0.08	1.86±0.1
410	1.48±0.08	1.76±0.1	430	1.36±0.07	1.68±0.08
450	1.28±0.07	1.55±0.08	470	1.11±0.06	1.3 ±0.07
490	1.00±0.05	1.15±0.06	519	0.89±0.05	1.04±0.06
530	0.82±0.04	0.92±0.05	550	0.76±0.04	0.83±0.05
570	0.74±0.04	0.81±0.05	590	0.71±0.04	0.76±0.05
610	0.68±0.04	0.72±0.05	630	0.65±0.03	0.68±0.05
650	0.63±0.03	0.65±0.04	670	0.62±0.03	0.64±0.04
690	0.60±0.03	0.61±0.04	710	0.56±0.03	0.58±0.04
735	0.54±0.03	0.55±0.04	765	0.52±0.03	0.53±0.04
795	0.53±0.03	0.54±0.04	825	0.54±0.03	0.55±0.04
855	0.54±0.03	0.55±0.04	885	0.53±0.03	0.54±0.04
915	0.53±0.03	0.55±0.04	945	0.53±0.03	0.54±0.04
975	0.54±0.03	0.55±0.04	1005	0.54±0.03	0.55±0.04
1020	0.53±0.03	0.54±0.04	1060	0.52±0.03	0.53±0.04
1100	0.50±0.03	0.51±0.04	1140	0.51±0.03	0.51±0.04
1180	0.50±0.03	0.5 ±0.04	1220	0.50±0.03	0.51±0.04
1400	0.57±0.3	-	1600	0.64±0.3	-
1800	0.68±0.3	-	2000	0.91±0.3	-

The absolute neutron detection efficiency data of the NE-912 lithium glass in positions I and II for different neutron energies were obtained on the basis of the relation

$$\varepsilon(E)^{912} = \varepsilon(E)^{908} \quad \frac{N(E)^{912}}{N(E)^{908}}$$

and are presented in Table 1. The efficiency of NE-908 glass $\varepsilon(E)^{908}$ was calculated by Monte Carlo method using the BRAND program |9|. For this calculation the ^6Li concentration was determined from the experimental data, as described above. For the ^7Li, O and Si concentrations we used the data from |1|. The neutron cross-section data for ^6Li and for ^7Li, O, Si were taken from the ENDF/B-V and ENDF/B-IV files, respectively. In the calculations it was assumed that the neutrons are detected by the $^6Li(n,\alpha)^3T$ reaction only.

Errors presented in Table 1 include the statistical errors of R and $n_o x$ measurements, the statistical accuracy of the calculation of $\varepsilon(E)^{908}$ and the accuracy of the $^6Li(n,\alpha)^3T$ cross sections. The accuracy of the cross sections was taken to be ± 2 % for the energy range E_n<100 keV and ± 5 % for higher energies.

The ratios of the experimentally determined neutron detection efficiencies to the values $\varepsilon_o = n_o x \sigma(n,\alpha)$ in positions I and II are shown in Figs 5 and 6. One can see that the corrections factors correspond generally to 20-40 % of the primary detection process, i.e. the $^6Li(n,\alpha)$ reaction, but in the region of the ^{16}O resonance they can reach even 80-100 % of that.

The effect of the multiplier glass on the neutron detection efficiency can be seen even more clearly in the ratio ε(II)/ε(I) in Fig. 7. This ratio reflects the result of the backward scattering of neutron in the multiplier glass, showing especially well the resonances of the main consituents Si(187 keV) and O (445 keV and 1 MeV).

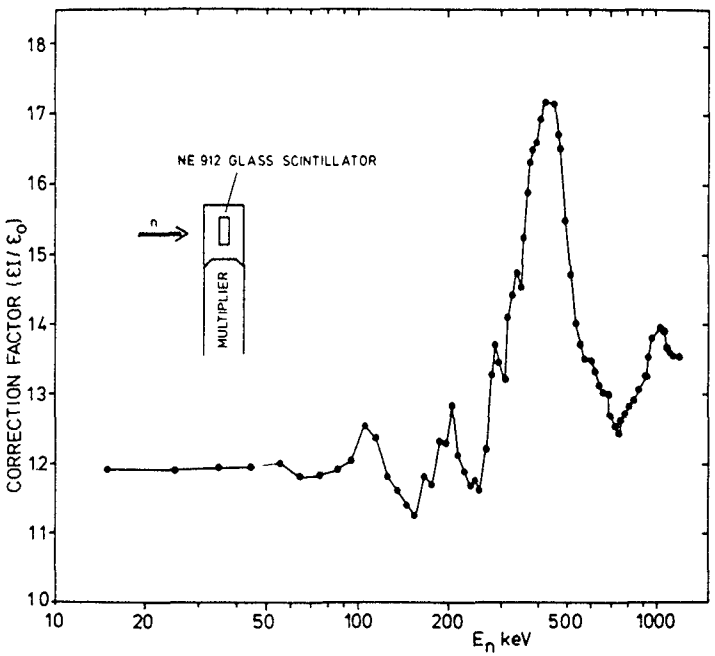

Correction factor $\varepsilon(E)I/\varepsilon_o$ for position I.

Fig. 5

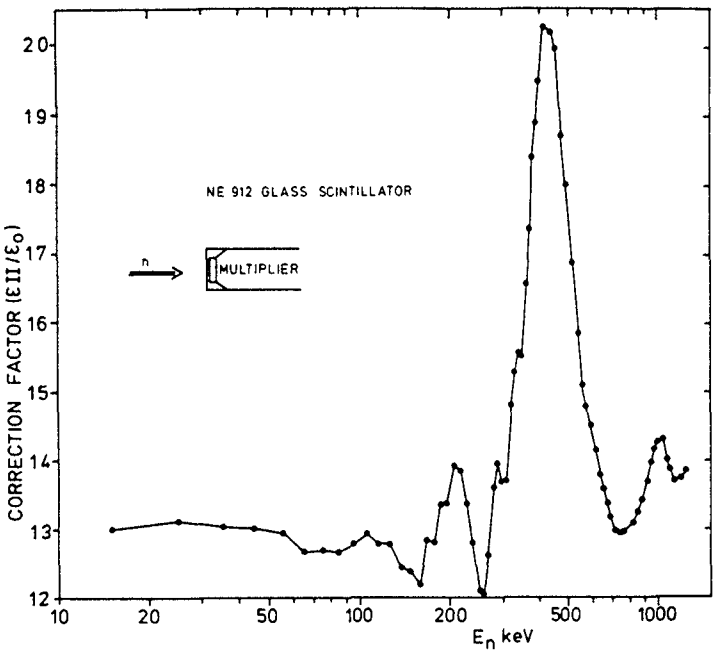

Correction factor $\varepsilon(E)II/\varepsilon_o$ for position II.

Fig. 6

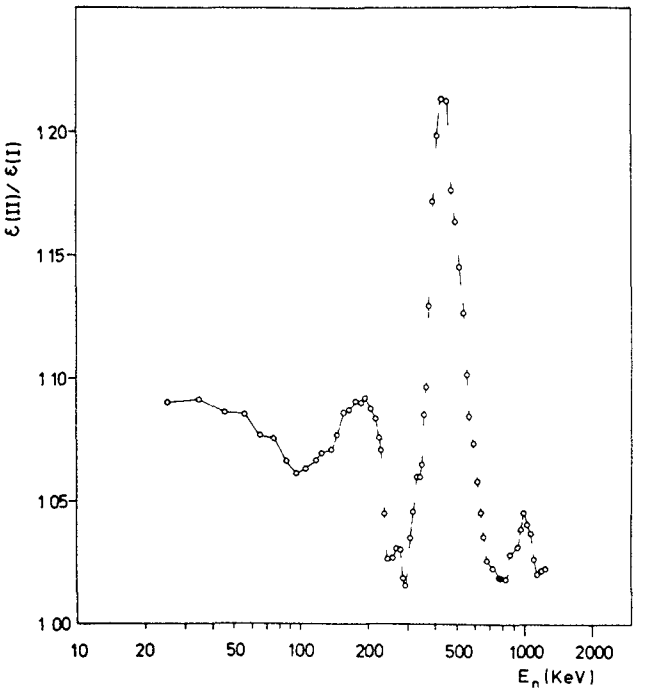

Ratio of $\varepsilon(II)/\varepsilon(I)$, the effect of the 56 AVP multiplier glass.

Fig. 7

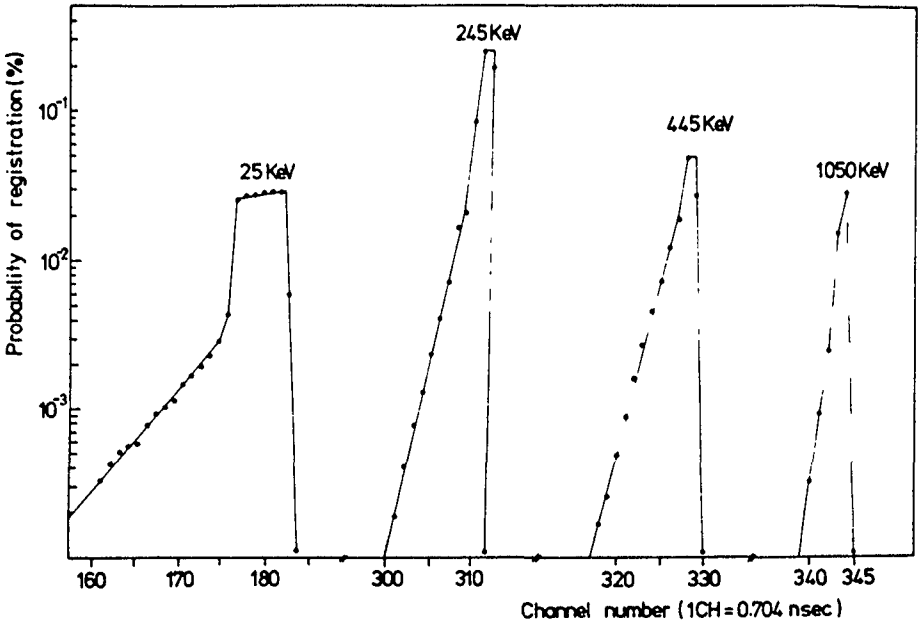

Fig. 8 Response function of the thick Li glass detector.

It was also necessary to know the time distribution of the detection process for the actual experimental conditions, i.e. the response function of the neutron detector. This was calculated also with the Monte Carlo code for the energy range below 2 MeV. The results are shown in Fig. 8 for four projectile energies (25 keV, 245 keV, 445 keV and 1005 keV). It can be seen, that at E_n=445 keV the respons function has an enhanced broadening.

As a result of these calculations we got also the calculated absolute efficiency for the ^{6}Li glass detector. Fig. 9 shows the correction factors $\varepsilon/\varepsilon_o$ for the thin (0.835 mm) NE-908 and thick (9.55 mm) NE-912 detectors, got from the Monte Carlo calculations. Similar but less detailed calculations have been performed earlier too [2,10,11]. It can be seen that for the thick glass the calculated correction factors are less than the measured ones. Fig. 10 shows the $\varepsilon(I)/\varepsilon(MC)$ ratio. The value of the ^{6}Li content for this calculation was taken from the Nucl. Ent. catalogue, however, it does not correspond to the actual concentration exactly. Therefore in the analysis of experiments one should use the measured absolute efficiency.

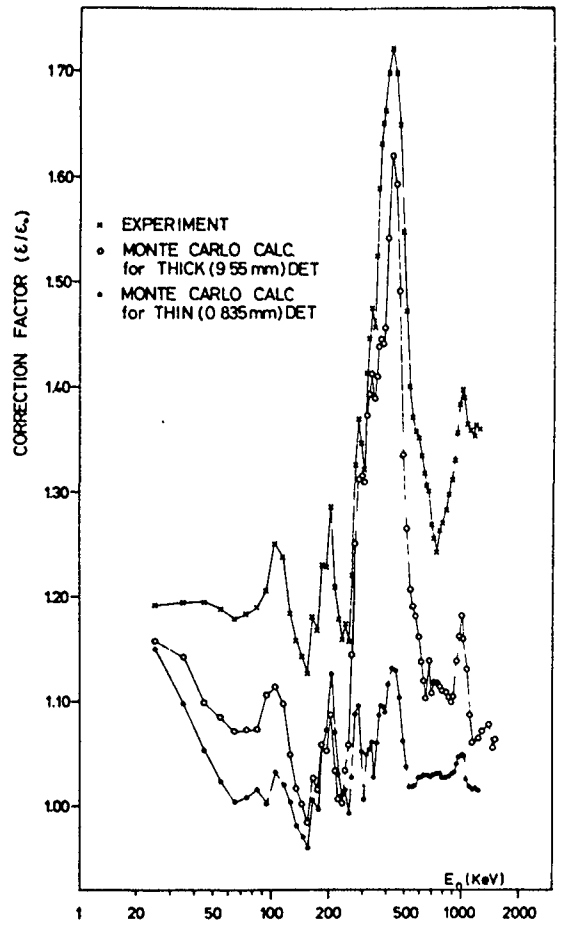

Fig. 9 Correction factors $\varepsilon/\varepsilon_o$ for the thin detector (M.C. calc.) and for the thick detector (M.C. calc. and exp.)

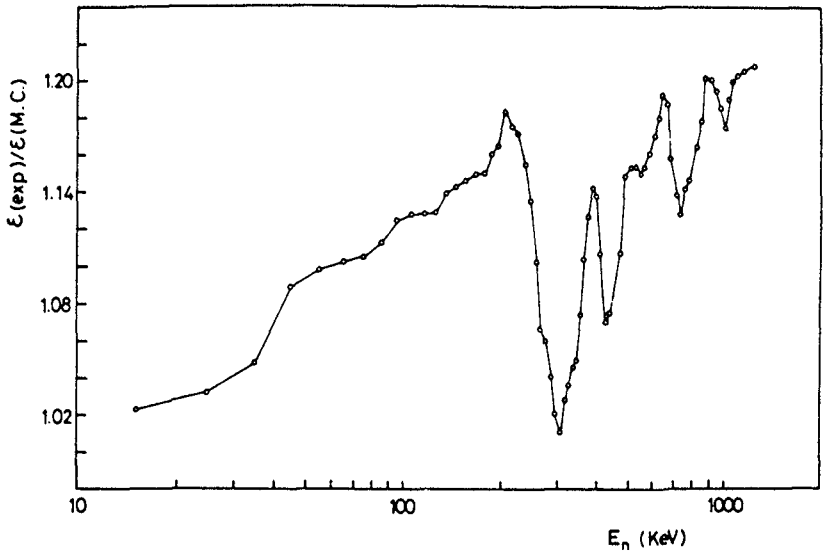

Fig.10 Ratio ε(I)/ε (M.C.)

References

|1| J.M. Neill, D. Huffman, C.A. Preskitt and J.C. Yung, Nucl. Instr. and Meth. 82 (1970) 162.

|2| G.P. Lamaze, Symp. on Neutron Standards and Applications, NBS,SP 493 (1977) 37

|3| J.A. Harvey and N.W. Hill, Nucl. Instr. and Meth. 162 (1979) 507.

|4| A. Lajtai et al., INDC (NDS)-146/L (1983) 177

|5| V.N. Kononov, E.D. Poletaev, M.V. Bohovko and L.E. Kazakov, PTE. N3 (1979) 77.

|6| M.C. Moxon, J.D. Dawnes and D.A.J. Endacott, UDAEC Report AERE-R 8409, Harwell (1976)

|7| G.P. Lamaze, R.A. Schrack and O.A. Wasson, Nucl. Sci. and Eng. 68 (1978) 183.

|8| G.M. Hale, Symp. on Neutron Standards and Applications, NBS-SP 493 (1977) 30

|9| P.A. Androsenko and A.A. Androsenko, Preprint FEI-1300 (1982)

|10| W.P. Poenitz, Z. Physik 268 (1974) 359

|11| E. Fort, Nucl. Instr. and Meth. 87 (1970) 115

130 PROPOSAL FOR MEASURING THE RATIO OF THE NEUTRON STANDARDS $^{6}Li(n,\alpha)^{3}H$ AND $^{10}B(n,\alpha)^{7}Li$ BY THE QUASI-ABSOLUTE METHOD USING THE TIME-REVERSED REACTIONS, AND THE RATIOS OF THESE STANDARDS TO THE $^{3}He(n,p)^{3}H$ REACTION IN THE 0.25 TO 9 MeV NEUTRON ENERGY RANGE

M. DROSG
Institut für Experimentalphysik,
University of Vienna,
Vienna, Austria

Abstract

The quasiabsolute method in monoenergetic neutron production work allows to measure cross sections: for identical targets to better than 1 % because many error contributions cancel. The time reversed reactions of $^{3}He(n,p)^{3}H$, $^{6}Li(n,t)^{4}He$ and $^{10}B(n,\alpha)^{7}Li$ are such neutron producing reactions. There are two avenues for the ratio measurements. The straight comparison of $^{4}He(^{7}Li,n)^{10}B$ with $^{4}He(t,n)^{6}Li$ and the comparison of $^{7}Li(\alpha,n)^{10}B$ with $^{3}H(\alpha,n)^{6}Li$ through 4 intermediate steps, namely $^{7}Li(p,n)^{7}Be$, $^{1}H(^{7}Li,n)^{7}Be$, $^{1}H(t,n)^{3}He$ and ^{3}He and $^{3}H(p,n)^{3}He$. The latter avenue, at the same time, yields ratios to the $^{3}He(n,p)^{3}H$ reaction as well. Combining both approaches does not only give complete angular distributions (and, therefore, integrated cross sections, too) but allows to check the consistency of the uncertainties.
The experimental limitations using time-of-flight technique will be discussed. The ultimate accuracy of the ratios will be limited by the signal-to-background ratio which is difficult to predict.

Introduction

The quasiabsolute or ratio method has been successful in establishing one common scale for the neutron production cross sections involving the hydrogen isotopes (1). In this paper it is shown that also the scale of the two neutron standards $^{6}Li(n,t)^{4}He$ (2) and $^{10}B(n,\alpha)^{7}Li$ (3) can be compared by the quasiabsolute method taking advantage of time reversal.

I. Background

The ratio method has the advantage that most experimental uncertainties are correlated (even identical) so that a rather high accuracy of the ratio can be obtained. By measuring neutron production cross section ratios from identical targets, the determining error is the uncertainty of the relative efficiency curve. Exactly speaking, it is the uncertainty in the efficiency ratio at the neutron energies. If the neutron energies coincide, even this error vanishes and the statistical or background error will dominate. The important part of an efficiency determination in a stable and reproducible time-of-flight arrangement is (aside from the structure showing up at lower biases) the correct slope of the curve. Uncertainties of $\pm$ 1% per 10 MeV have been reported (4) and can be achieved with little pain using the accurate cross sections for neutron production by the hydrogen isotopes (1,5,6). So very favorable conditions are present for applying the ratio method to neutron producing reactions. And the two standards n-^{6}Li and n-^{10}B become, after time reversal the neutron producing reactions $^{4}He(t,n)^{6}Li$ and $^{4}He(^{7}Li,n)^{10}B$, having even identical targets. The energy conversion for the time reversed case can be done by

$$E_{pr} = A + B \cdot E_n \qquad /1/$$

with the projectile energy after conversion E_{pr}, the unconverted neutron energy E_n and the factors A and B from Table 1.

Table 1. Kinematics Data (All energies in MeV.)

	Threshold		Threshold for single valued neutron emission			B
	A:Particle energy	Max.neutron energy	Time rev. neutr.en.	Particle energy	Max.neutr. energy	
$^{6}Li(n,t)^{4}He, Q = 4.784$						
$^{4}He(t,n)^{6}Li$	8.392	0.518	0.809	9.608	2.374	1.5028
$^{3}H\ (\alpha,n)^{6}Li$	11.136	0.912	1.601	14.329	4.699	1.9942
$^{10}B(n,\alpha)^{7}Li, Q = 2.790$						
$^{7}Li(\alpha,n)^{10}B$	4.382	0.146	0.187	4.650	0.619	1.4271
$^{4}He(^{7}Li,n)^{10}B$	7.682	0.448	0.659	9.330	2.176	2.5015
$^{3}He(n,p)^{3}H,\ Q = 0.764$						
$^{3}H(p,n)^{3}He$	1.019	0.064	0.128	1.147	0.288	0.9998
$^{1}H(t,n)^{3}He$	3.051	0.573	7.337	25.011 a)	17.640	2.9932
$Q = 1.644$						
$^{7}Li(p,n)^{7}Be$	1.881	0.030		1.920	0.121	-
$^{1}H(^{7}Li,n)^{7}Be$	13.095	1.439		16.514 a)	3.843	-

a) break-up threshold

II. Procedure

In Table 2 it is shown that the two standards (after time reversal) can be combined directly or indirectly. Having a second route has the advantage of an independent check. In addition it allows to tie the standards to the well known neutron production cross sections of the hydrogen isotopes and to the may-be standard n-^{3}He (7).

Table 2. The Two Reaction Chains for Measuring the Cross Section Ratio of n-^{6}Li and n-^{10}B by the Inverse Reactions Using the Quasiabsolute Method

Direct Ratio	Indirect Ratio
$^{4}He(^{7}Li,n)^{10}B$	$^{7}Li(\alpha,n)^{10}B$
	$^{7}Li(p,n)^{7}Be$
	$^{1}H(^{7}Li,n)^{7}Be$
	$^{1}H(t,n)^{3}He$
$^{4}He(t,n)^{6}Li$	$^{3}H(p,n)^{3}He$
	$^{3}H(\alpha,n)^{6}Li$
	$^{3}H(d,n)^{4}He$
	$^{2}H(t,n)^{4}He$
	$^{2}H(d,n)^{3}He$

The direct ratio measurement has the advantage that the targets are identical and the errors consequently small. The indirect method is a chain of three reaction pairs with identical targets and of two pairs with identical cross sections (inverse reactions). If the angular overlap of the inverse reactions is big enough a reliable combination of the data is possible.

Table 3 summarizes some important aspects of the proposed experiment. The energy range that can be covered by the time reversed reactions depends on several kinematics and experimental factors. Under the conditions

a) that only differential cross sections over the complete angular range are of value,

Table 3. Factors Determining the Range or Limiting the Accuracy of the Proposed Cross Section Ratio Measurement

ACCURACY :

1) Gain stability (detector + analyzer): usual bias at 40 keV or 300 keV proton energy
2) Effective target thickness: reproducibility of gas fillings; ^{7}Li-target
3) Yield accuracy: statistics, background substraction
4) Knowledge of relative efficiency curve
5) Energy determination
6) 0^{o} determination
7) Angle determination
8) Geometric corrections: nonlinearity of cross sections, of center-of-mass conversion
9) Energy resolution: (dependent on energy spread of projectiles, kinematics spread, time resolution): affects SNR, important when structures in cross section

RANGE :

1) Energy range of accelerator
2) Energy range of efficiency curve where the relative efficiency is accurately known and the detector operation is stable
3) Angular range of angular distribution set-up
4) Angular range limited by kinematics (neutron cone)

Table 4. Energy Ranges for Complete Angular Distributions (For a discussion, see text)

Reaction	E_n (MeV)	E_p (MeV)	E_t (MeV)	E_α (MeV)	E_{Li} (MeV)
n - ^{3}He	0.06	1.079	3.230	-	-
	3.951	4.969	14.875	-	-
n - ^{6}Li	0.20	-	8.692	11.534	-
	4.731	-	15.502	20.571	-
n - ^{10}B	0.06	-	-	4.468	7.832
	5.167	-	-	11.756	20.607
p - ^{7}Li	-	2.000	-	-	13.927
	-	4.272	-	-	29.752
Projectile	-	1.079	3.230	4.468	7.832
Range	-	4.969	15.502	20.571	29.752

b) that for neutrons below 0.08 MeV a measurement with fast neutron time-of-flight technique is not accurate enough,
c) that (arbitrarily) lab angles in excess of 140^{o} are not accessible,
d) that only angles are measured where the change of the lab to c.m conversion factor inside 1^{o} stays below 10%(chosen arbitrarily) and
e) that (again arbitrarily) the efficiency has only be measured accurately up to 10 MeV

then Table 4 summarizes the energy ranges involved. The 10 MeV cutoff condition is presently no real limitation, because there seems to be little interest in extending the range of the standards beyond a few MeV. In Table 4 the projectile energies corresponding to the 10 MeV neutron energy limit are underlined.

Fig.1 through 3 show the connection between the original incoming neutron energy and the neutron energies to be measured in the time reversed reaction at 0°, 90°_{CM}, 140°_{Lab} and at Θ_m. Θ_m is the maximum lab emission angle which occurs when the center-of-mass energy is bigger than the neutron energy in the center-of-mass system. For endothermic reactions this maximum angle of the neutron cone is given (nonrelativistically) by

$$\sin^2\Theta_m = \frac{M_2 M_4}{M_1 M_3}\left(1 - \frac{E_{th}}{E_{pr}}\right) \qquad /2/$$

with the threshold energy E_{th}, the projectile energy E_{pr} and the masses M_i those of the projectile, of the target, of the neutron and of the residual nucleus, resp.

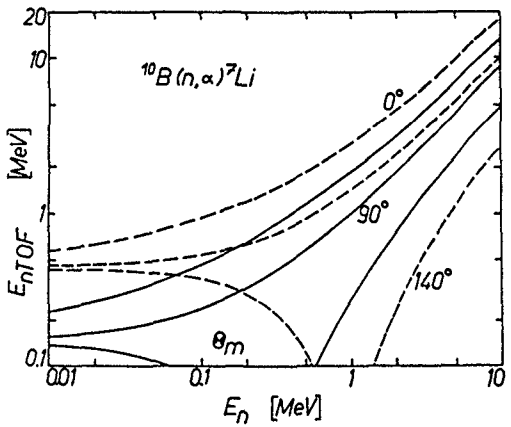

Fig.1. Relation between E_n, the neutron energy of the n-^{10}B standard and the experimental neutron energy for measurements of the time reversed reaction at 0°, 90°, Θ_m and 140°. The solid curve is for α-^{7}Li, the dashed curve for ^{7}Li-^{4}He.

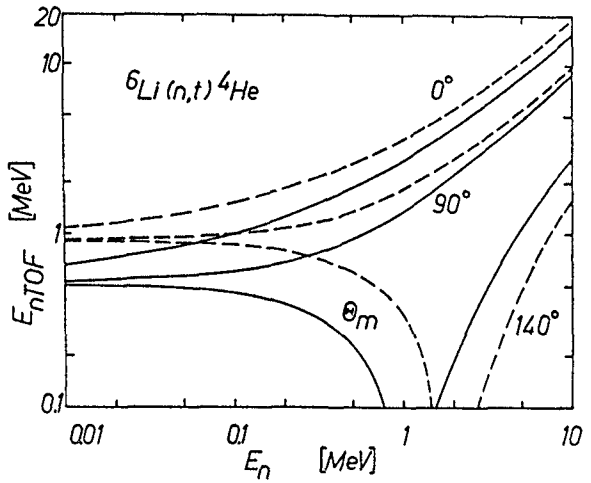

Fig.2. Relation between E_n, the neutron energy of n-^{6}Li standard and the experimental neutron energy for measurements of the time reversed reaction at 0°, 90°, Θ_m and 140°. The solid curve is for t-^{4}He, the dashed curve for α-^{3}H.

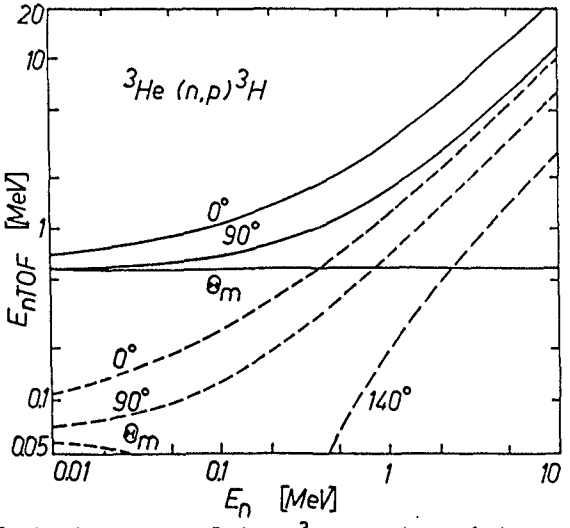

Fig.3. Relation between E_n of the n-^{3}He reaction and the experimental neutron energy for the measurements of the time reversed reaction at 0°, 90°_{CM}, Θ_m and 140°. The solid curve is for t-H, the dashed curve for p-T.

III. Realization

The proposed ratio measurement is feasible with present day technique. Bunched Li-beams have been used for neutron production (8), and also bunched triton beams (9). Also alphas on ^{7}Li (10) have been used before. However, this was not done at the same installation. Unfortunately, each measurement chain must be performed with one TOF set-up and, therefore, it cannot be split up.
The obvious installation where such an experiment could be set up is the Van de Graaff at LANL, where triton beams have been used for years.
In the experiment the actual low energy limit will be higher than given in Table 4 because gas targets will have to be used which introduce energy and angular straggling so that together with the target thickness, several tens of keV-energy spread will result. On the other hand the target thickness must be big enough to enhance the signal over the background. In cases of narrow neutron cones (at lower energies) the angular straggling (which is more serious at low energies) will be difficult to correct for, so this effect, too, will raise the lower limit of the useful range.
In the indirect ratio chain of Table 2 the ^{7}Li target is the weak link. The evenness of this target averaged over the beam spot size will be essential. Therefore the usefulness of such a target will have to be checked by using different beam positions.

IV. Conclusion

The proposed experiment allows to measure cross sections of the two standards n-^{6}Li and n-^{10}B relative to each other in two different ways. The second way also combines these two standards with the n-^{3}He cross section, the p-^{7}Li cross sections and the cross sections for neutron production by the hydrogen isotopes.

If complete angular distributions are aimed at the kinematics and experimental restraints will not allow measurements below 0.1 MeV. To obtain a sufficient counting rate, the target thickness which limits the resolution, must be chosen carefully. Information on the seriousness of the background is sparse(e.g.(9)),so that the final accuracy is difficult to predict. Under favorable conditions an error in the ratio close to 1% can be expected.
A restriction to a measurement of the direct ratio makes the experiment much simpler. Then, however, the angular distributions would not be complete and the connection to the other cross sections would not be established.

Acknowledgment

Thanks are due to W.Penits and H.Wurz for competent technical assistance in preparing this paper.

REFERENCES:

(1) M. DROSG, Nucl.Sci.Eng.67, 190 (1978)
(2) G.M. HALE, IAEA Techn.Rep.Ser.No.227, 11 (1983)
(3) E. WATTECAMPS, IAEA Techn.Rep.Ser.No.227, 19 (1983)
(4) M. DROSG, Nucl.Instr.Meth. 105, 573 (1972)
(5) M. DROSG, Z.Phys.A300, 315(1981) and Report LA-8532, Los Alamos Scient.Lab. (1980)
(6) M. DROSG, O. SCHWERER, to be published
(7) H. KLEIN, chairman: discussion during this Meeting
(8) J.H. DAVE, C.R. GOULD, S.A. WENDER, S.M. SHAFROTH, Nucl. Instr.Meth.Phys.Res.200, 285 (1982)
(9) M. DROSG, D.M. DRAKE, R.A. HARDEKOPF, G.M. HALE, Report LA-9129-MS, Los Alamos Nat.Lab. (1982)
(10) R.M. SEALOCK, H.-Y. WU, J.C.OVERLEY, Nucl.Phys. A357, 279 (1981)

SESSION III

EVALUATION OF THE $^{27}Al(n,\alpha)$ REACTION CROSS-SECTION IN ENERGY RANGE 5,5 MeV – 20 MeV

N.V. KORNILOV, N.S. RABOTNOV, S.A. BADIKOV,
E.V. GAY, A.B. KAGALENKO, V.I. TRYKOVA
Institute of Physics and Power Engineering,
Obninsk,
Union of Soviet Socialist Republics

Abstract

The energy dependence of the $^{27}Al(n,\alpha)$ reaction cross-section was evaluated and expressed in terms of the rational function of energy, (Pade-approximation). The error of the evaluation was also calculated and analyzed. The results are compared with experimental data and earlier evaluations.

Introduction.

The $^{27}Al(n,\alpha)$ reaction is widly used both in reactor dosimetry and for measuring of the monoenergetic neutron flux, as a reference cross-section. The experimental date cover a wide energy range from 5 to 20 Mev. The results agree within the experimental errors as a rule. Accordingly the recomended curres [1,2] agree within the errors evaluated. In [2] practically for the whole energy range an error ~ 5% was assigned. The use of the new data in the vicinity of E ~ 14 Mev in evaluation [1] enabled the authors to conclude, that for energy range 13.5 - 14.7 MeV the $^{27}Al(n,\alpha)$ reaction cross-section is known with accuraly ~ 0.5%. At the same time at E ~ 9 MeV the uncertainty of the evaluated curve reaches ~ 9%. The $^{27}Al(n,\alpha)$ reaction was used together with $^{56}Fe(n,p)$, $^{238}U(n,f)$ reactions etc. on our experimental works [3] to determine neutron flux in the energy range 6 - 11 MeV. The results due to various reference reactions were in better agreement, well inside the errors evaluated in work [1] . Thus we regard the evaluation of the $^{27}Al(n,\alpha)$ reaction cross-section still as an open problem.

Another major question insufficiently discussed is a possibility to describe the reaction excitation function by a smooth curve. Only work [7] performed with resolution $\lesssim$ 100 kev reveals considerable cross-section fluctuations in the energy range 6÷ 8.5 Mev. The deviatons from the smoth dependence may well exist for higher energies also, but there are no experimental data substantiating this assumption.

Work [4] suggests a method of the analytical approximation of experimental dependences by rational functions (Pade-approximation) and of obtaining errors of evaluated curves. The method was used in evaluating cross-section of number of reactions, it was effectively employed for converting the evaluated data file BOSPOR [5] to a more compact form convenient for storing and computational use. The Pade-approximation has certain theoretical advantages over the polynominal approximation. Besides, a comparison of the results obtained on the basis of the Pade-approximation with other methods of evaluation is expected to produce new reasonings when substantiating the approximant's errors selection.

The above factors did stimulate the present work. Its objectives may be formulated in the following way. On the basis of the analytical approximation of the experimental data the $^{27}Al(n, \alpha)$ reaction cross-section should be obtained and approximant's errors should be analyzed to understand existing situation and to determine the needed accuracy of the future studies.

2. Experimental data used for evaluation.

All the experimental data are summarized in [6] . The data contradicting to the majority of others were omitted and the data of the recent studies were added. The renormalisation was not needed for the majority of the experimental data , or the way of the data renormalization does not follow from the experiment's discription.

In [8] the $^{27}Al(n,\alpha)$ reaction cross-section was measured relative to the $^{32}S(n,p)$ reference reaction. Utilization of the evaluated $^{32}S(n,p)$ reaction cross-section from ENDF/B-V results in an essential disagreement of the results from work [8] with the data of works [13,14] . That is why the original values of the work [8] were considered for the evaluation. The data of work [7] were renormalized taking into account new information on ^{238}U half-life ($4.468 \cdot 10^9$ years instead of $4.51 \cdot 10^9$ years) and ^{238}U fission cross-section [16] . Besides, due to the ^{238}U fission cross-section being currently known with a higher accuracy (2 - 3%) an error of the data was reduced to 5%. The error of the work [9] , which we consider unreasonably low was increased to the values given in [11] . The common feature of the studies mentioned (except [7]) is a rather poor energy resolution. The overall energy spread is 200 - 300 keV.

The experimental data utilized for evaluation are given in fig. 1.

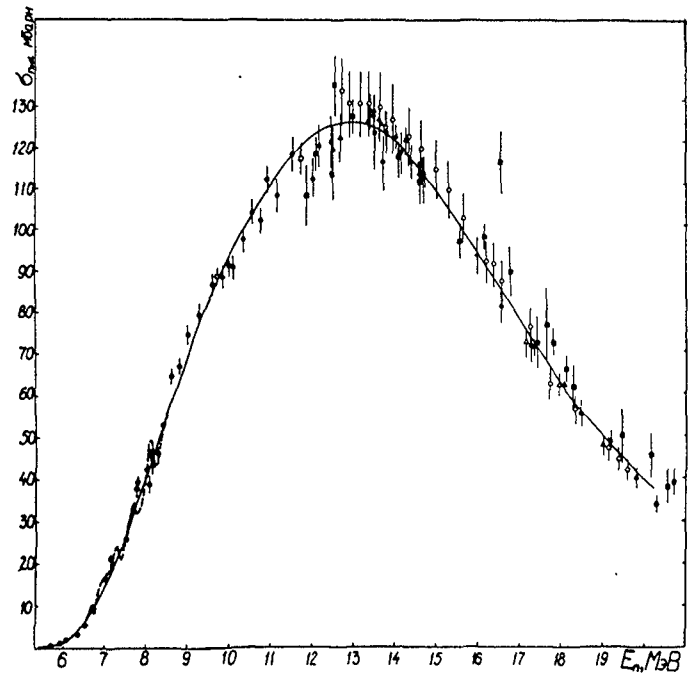

Fig.1. Experimental Data used in Evaluation
- - - - [7], ● - [8], ■ - [9],
◒ - [10], ○ - [11], ▲ - [12],
△ - [13], □ - [14], ▲ - 15 .
The solid line represents approximant (1) with the parameters from Table 1.

3. A method of Analytical Approximation.

Without going into details of the method (see work [4]) we shall outline it briefly.

The solution is sought in the form of a ratio of polynomials of N_1 and N_2 powers (Pade-approximation):

$$f(E) = \frac{P_{N_1}(E)}{Q_{N_2}(E)} = \sum_{i=1}^{n} \frac{\alpha_i (E-\varepsilon_i) + \beta_i}{(E-\varepsilon_i)^2 + \gamma_i^2} + \sum_{i=1}^{m} \frac{a_i}{E-\rho_i} + C \qquad (1)$$

The total number of parameters is $L = N_1+N_2+1 = 4n + 2m + 1$. The parameters of expression (1) are obtained by minimizing the functional:

$$M = \sum_{i=1}^{K} (y_i - f(E_i))^2 / \Delta y_i^2 \quad , \qquad (2)$$

where K - is the number of experimental points.

y_i and Δy_i - are the experimental values and their uncertainties, correspondently.

Non-linearity of the problem restrained the practical use of the Pade-approximation in the last-squares method. In [4] a convenient linearization technique was proposed.

Some L - experimental points out of K are selected so that the polinominals determined by the set of equations:

$$P_{N_1}(E_i) = y_i \cdot Q_{N_2}(E_i)$$

minimize the functional M. This solution is close the conventional solution of the least-squares method if the number of experimental points is large enough. After the f(E) function is found in the explicit form, the ordinates of the any L points of this curve may be used as parameters. Among those points there are such ones f_i, that Fisher's information matrix A_{ik}(i,k = 1 ...L) becomes diagonal:

$$A_{ik} = \sum_{i,k}^{L} \overline{\frac{\partial M}{\partial f_i} \cdot \frac{\partial M}{\partial f_k}} = \lambda_i \cdot \delta_{ik} \qquad (3)$$

In this case the approximant dispersion $\Delta(E)$ and the correlation coefficients $\rho(E_1,E_2)$ are defined as follows:

$$\Delta^2(E) = \sum_{i=1}^{L} \left(\frac{\partial f(E)}{\partial f_i}\right)^2 \Delta f_i^2$$
$$\rho(E_1,E_2) = \sum_{i,k=1}^{L} \frac{\partial f(E_1)}{\partial f_i} \frac{\partial f(E_2)}{\partial f_k} \Delta f_k \cdot \Delta f_i / \Delta(E_1) \cdot \Delta(E_2), \qquad (4)$$

where $(\Delta f_i)^2 = 1/\lambda_i$.

The above method of constructing the analytical dependence has certain advanteges over a common polynominal description:

1. the decision is sought over a broder class of functions,
2. the equal accuracy of experimental data description requires less parameters, as a rule,
3. the desision is more stable at the edges of interval permitting a more substantiated extropolation,
4. the uncertainties of curve can be found without the inversion of the information matrix.

4. Approximation Results and lower estimate of the reaction cross-section error:

The parameters of the approximant represented in the form of "polar expansion" (1) are given in the table 1 and the

Table 1.

Parameters for Reaction Cross-Section Calculation in the Energy Range 8.5 - 20 MeV.

parameters i	α_i	β_i	ε_i	γ_i
1	$-2.2281\ 10^2$	$4.0302\ 10^3$	$1.3673\ 10^1$	5.7475
2	$8.8603\ 10^1$	$-4.9556\ 10^2$	6.9145	2.9359

Table 2.

$^{27}Al(n,\alpha)$ Reaction Cross-Sections. Intermediate Cross-Section Values in the 6.0 - 8.5 Range are Determined by Linear Extrapolation.

E_n, MeV	$\sigma_{n\alpha}$, mb	E_n, MeV	$\sigma_{n\alpha}$ mb	E_n, MeV	$\sigma_{n\alpha}$ mb
5.5	0.15	7.40	21.1	12.0	121.6
6.0	1.47	7.50	25.5	12.5	124.7
6.1	1.9	7.60	31.0	13.0	125.8
6.2	2.6	7.70	34.3	13.5	124.8
6.3	3.7	7.80	31.5	14.0	121.7
6.40	4.4	7.90	34.0	14.5	116.7
6.50	5.9	8.00	41.5	15.0	110.3
6.60	8.2	8.10	48.9	15.5	102.8
6.66	9.4	8.20	43.9	16.0	94.7
6.70	8.3	8.24	42.1	16.5	86.4
6.73	7.9	8.30	45.0	17.0	78.2
6.60	10.7	8.40	50.6	17.5	70.3
6.9	14.9	8.50	54.8	18.0	62.9
7.00	16.7	9.0	68.5	18.5	56.2
7.10	18.2	9.5	80.9	19.0	50.0
7.20	21.4	10.0	92.0	19.5	44.5
7.27	23.7	10.5	101.6	20.0	39.6
7.30	22.8	11.0	109.9		
7.37	20.7	11.5	116.5		

corresponding curve is protted in figure 1. The optimal number of parameters is L = 8, χ_ν^2 =119, for ν = 106 and E > 8.5 MeV. The resulting dependence can be an estimate of the $^{27}Al(n,\alpha)$ reaction cross-section in the energy range E > 8.5 MeV. For the energy interval 6.0 - 8.5 Mev we propose to keep the renormalized data from [7] with the error 5% (see section 2). The results work [7] were taken into account when constructing the approximant which enable us to associate the average trend of the cross-section from work [7] with the results obtained with the worst resolution and with the cross-section behaviour at higher energies.

The statistical error of the approximant as a function of energy calculated by formula (4) is given in figure 2. Note that the error $\Delta(E)$ is evaluated an the assumption that the total set of the experimental point deviations from "real" curve is not correlated and in particular there is not systematic errors. Thus, the value $\Delta(E)$ is the lower boundary of the reaction cross-section error.

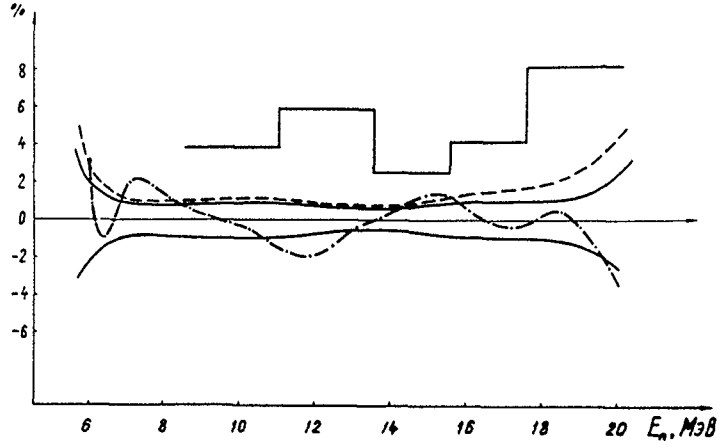

Fig. 2. Accuracy of Reaction Cross-Section Evaluation for Different Neutron Energies.

——— a region limited by values ± Δ (E)
– – – – polynominal estimate error
—·—·— a ratio of the 9th-power polynom and approximant (1). Histogram shows D_k values.

To verify the dependence of the approximant and error of the evaluation on the approximating function class selection, the polynominal approximation was carried out for the same set of the initial data. The 9th power polynominal appeared optimal (I=10). The polynominal description error evaluated in all case somewhat exceeds the Pade-approximation errors, but they are in fair agreement (Fig.2). As it was expected the disagreements increase at the edges of the interval.

The experimental errors given by the authors are usually determined worse than the values themselves. The model calculation was done to test the approximant's stability to input values of errors. The $\tilde{f}(E)$ function which is similar to (1) was constructed for the case when all data have the equal statistical weight. The average ratio $\tilde{f}(E)/f(E)$ was 1.003, and its dispersion ~1.6%.

5. Correlation Matrix of Experimental Data and the Upper Estimation of Cross-Section Error.

A priori, information experimental correlation being ambiguous or totally lacking, we shall attempt to establish correlations of different studies on the basis of their comparison with approximant.

Consider the values $\xi_{ki} = y_{ki}/f(E_i) - 1$, where k- is the experiment number, i - is the number of the experimental value beloning to the k's experiment . For each experiment the following ratios can be written:

$$\xi_{ki} = S_k + r_{ki}$$

where S_k - is a systematic error, constant for each experiment, r_{ki} - is a random uncertainty.

$$\sum_{i=1}^{n_k} r_{ki} = 0, \qquad S_k = \sum_{i=1}^{n_k} \xi_{ki} / n_k$$

$$D_k^2 = \sum_{i=1}^{n_k} \xi_k^2 / n_k = S_k^2 + R_k^2 , \qquad (5)$$

$$R_k^2 = \sum_{i=1}^{n_k} r_{ki}^2 / nk ,$$

n_k - is the number of points in each experiment. If n_k is sufficiently large then the energy range for each experiment can be divided into smaller intervals where S_k - is constant. The covariance matrix of the studies (or intervals) k,l is :

$$V_{kl} = \begin{cases} D_k^2 , & k = l \\ S_k S_l , & k \neq l. \end{cases}$$

The correlation matrix C_{kl} is :

$$C_{kl} = S_k S_l / D_k D_l .$$

Using the above ratios the experimental data of [8, 9, 11, 12, 13] for three energy intervals 8.5 - 12 MeV, 12 - 15 MeV, 15 - 20 MeV were analyzed. The results are given in table 3.

Values (5) can be calculated for various energy intervals without singling out separate experiments.

Hence, apparently, D_k is the upper boundary of the approximant's uncertainty. The resulting values D_k for different energy intervals are shown in figure 2 and table 4.

Thus, on the basis of the data from sections 4,5, the real curve error is expected to lie between the values $\Delta(E)$ and D_k defined by the approximant's accuracy on the assumption of normality and non-correlation of the data and dispresions of the initial experimental values.

Table 3.

Correlation Matrix of Experimental Data.
The horisontal rows of numbers in the top part of the table indicate: a serial number, an energy interval 1 - (8.5 - 12) MeV; 2 - (12 - 15) MeV; 3 - (15 - 20) Mev, the number of the work in References.
The bottom. diagonally figures indicate the correlation of points inside the interval.

	1	2	3	4	5	6	7	8	9	10
	1	2	3	2	3	2	3	2	2	3
		[8]		[11]		[9]		[12]		[13]
1	100 5									
2	-13	100 33								
3	-16	39	100 47							
4	21	-55	-65	100 92						
5	-3	9	11	-15	100 2					
6	-9	23	28	-39	6	100 16				
7	20	-51	-61	85	-14	-36	100 79			
8	8	-22	-26	36	-6	-15	34	100 14		
9	3	-9	-10	14	-2	- 6	13	6	100 2	
10	-9	23	27	-38	6	16	-35	-15	-6	100 5

Table 4.

The upper D_k and lower $\Delta(E)$ boundaries of the $^{27}Al(n,\alpha)$ reaction cross-section uncertainty. For the energy intervals (5.5 - 6.0) MeV and (6.0 - 8.5) MeV the uncertainties are 15% and 5% respeetively.

$E_1 + E_2$ MeV	$\Delta(E)$ %	D_k %
8.5 - 11	0.8	3.8
11 -- 13.50	0.7	5.8
13.5 - 15.50	0.6	2.5
15.5 - 17.50	0.9	4.1
17.5 - 20.0	1.4	7.6

6. Comparison with the Results of Other Studies.

On the basis of the data given in [3] the ratios of the $^{27}Al(n,\alpha)$ and $^{238}U(n,f)$ reactions cross-srctions were calculated (Table 5). The ratio $\sigma n\alpha / \sigma nf$ uncertainty is defined by the uncertainties of measuring aluminum foils activity 2.5%, the number of nuclei ^{238}U - 2% and calculation of various corrections $\lesssim$ 1%. The total error is 3.4%. These data were not taken into account when calculating the approximant parameters and are utilized to control the results. In the energy range 8.5 - 10.5 MeV the experimental data confirm both the (n,α) cross-section value and the uncertainty evaluated (Fig. 3). The cross-section trend is confirmed in the energy range 6.5 - 7.5 MeV, also (Fig. 1, 3). The situation is more vague for the erergis 7.5 - 8.5 MeV, where the cross-section essentially fluctuates. The disagreement of the experimental values with the recomended dapendence as well as substantial spread of the data of different works are most likly associated with the error of average energy detarmination in

Table 5.

The Ratio of $^{27}Al(n,\alpha)$ and $^{238}U(n,f)$ Reaction Cross-Sections.

E_n, MeV	$\sigma_{n\alpha}/\sigma_{nf}$	E_n, MeV	$\sigma_{n\alpha}/\sigma_{nf}$
6.45	$(8.71\pm 0.29)\ 10^{-3}$	7.70	$(3.42\pm0.11)\ 10^{-2}$
6.75	$(1.12\pm 0.04)\ 10^{-2}$	7.95	$(4.13\pm 0.14)\ 10^{-2}$
6.94	$(1.76\pm 0.06)\ 10^{-2}$	8.50	$(5.42\pm 0.18)\ 10^{-2}$
7.07	$(1.90\pm 0.06)\ 10^{-2}$	9.00	$(6.79\pm 0.23)\ 10^{-2}$
7.19	$(2.29\pm 0.07)\ 10^{-2}$	9.50	$(8.32\pm 0.28)\ 10^{-2}$
7.45	$(2.58\pm 0.09)\ 10^{-2}$	10.00	$(9.23\pm 0.31)\ 10^{-2}$

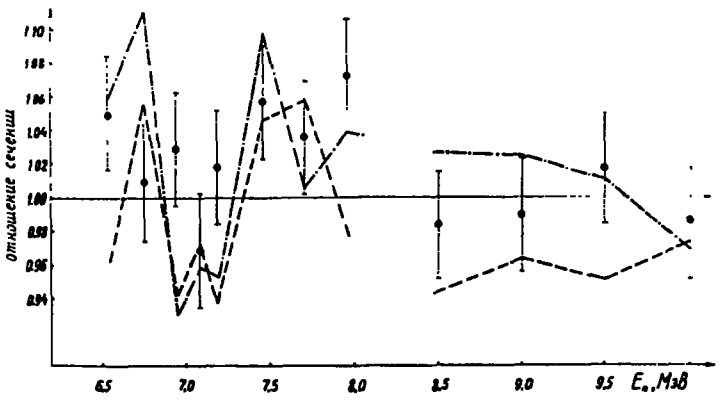

Fig. 3. Comparison of the cross-section recommended in the present work with experimental data and estimetas of other studies. A ratio of cross-sections from work - - - - [1] and —·—·— [2] to the present work results. ● — a ratio of the experimental data and the present work estimate. The $^{27}Al(n,\alpha)$ reaction cross-section was obtained from the data of Table 5 and the $^{238}U(n,f)$ cross-section of work [16]. In the energy range E < 8.5 MeV The present work cross-section was averaged by the enargy spread of neutrons.

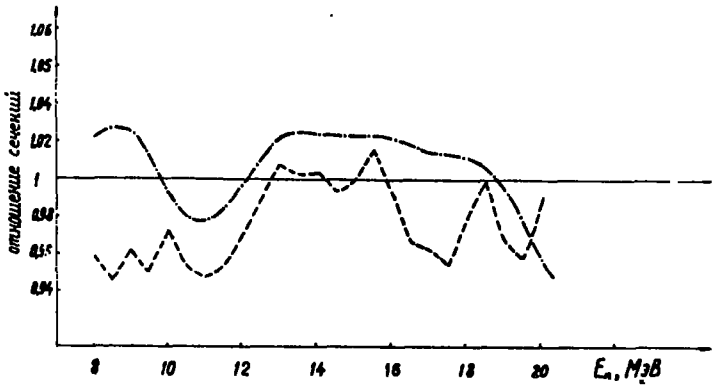

Fig. 4. A Ratio of Cross-Sections Recommended in [1] - - - - - and [2] —·—·— to the cross-section recommended present work.

experiments with poor resolution. The variation of energy about 20 keV can results in 3% variation of the $^{27}Al(n,\alpha)$ cross-section in this energy range. In figure 4 the present work evaluation is compared with the results of [1,2]. A good agreement of the present work results and ENDF/B-V is observed. The agreement with the results of work [1] within the errors determined in this work is observed only in the vicinity of energy 14 MeV. The low values of the cross-section in the energy range 8 - 12 MeV in work [1] are not confirmed by the experimental data mentioned.

The $^{27}Al(n,\alpha)$ reaction cross-section was averaged with ^{252}Cf neutrons spectrum [17]. The response function was integrated in the energy range 5.5 - 20 MeV. The correction to the average cross-section accounted for an energy interval from the threshold to 5.5 MeV was determined from the ratio of integrals for ranges (5.5 - 6) MeV and (6 - 6.5) MeV. The data shown in the table 6, illustrate essential disagriments between calculated and experimental values. A low cross-section on the basis of the results of work [1] may well be due to the integral

Table 6.

$^{27}Al(n,\alpha)$ Reaction Cross-Section Averaged by ^{252}Cf Spectrum. When calculating the errors in present work the values D_k were used.

$\langle\sigma\rangle$ mb	The sourse of information on $\sigma_{n\alpha}(E)$
1.043 ± 0.034	present work, calculation
1.059 ± 0.058	[2], calculation from [18]
1.012 ± 0.029	[1], calculation from [18]
1.006 ± 0.022	[18], experiment

experiments being taken into account by the authors of [1] when evaluating. This resulted in the reduction of the cross-section in the energy range 8 - 11 MeV.

Conclusions and recomendations.

1. The analytical dependence of the $^{27}Al(n,\alpha)$ reaction cross-section has been constructed using rational expression (Pade-approximation. The lower and upper boundaries of the approximant's error have been determined.
2. When utilizing the $^{27}Al(n,\alpha)$ reaction cross-section as standard one a non monotonous character of the cross-section in the energy range 6 - 8.5 MeV and as high energies as possible must be taken into account. Note, that cross-section fluctuations somewhat reduce the $^{27}Al(n,\alpha)$ reaction worth as a standard.
3. An improvment of the accuracy of the evaluated cross-section is possible only on the basis of the experiments with an accuracy 1 - 2% and energy resolution high enough (the total energy spread $\leq$ 100 KeV).

References.

1. Vonach H., Tagesen S. Nuclear Standarts fila. INDC-36/LN, 1981.
2. ENDF/B-V, Mat. 6313.
3. Kornilov N.V., Baryba V.Ya., Salnikov O.A. et al. Atomnaya Energia, 1980, 49, 283.

   Kornilov N.V., Darotsy Sh. et al. "Measurement of the $^{58}Ni(n,p)$, $^{93}Nb(n,2n)$, $^{197}Au(n,2n)$ Reactions Cross-Sections of Neutron Energies 8.92, 9.39 and 9.90 MeV". Presentetion of the All-Union Conference of Neutronics, Kiev, 1983.

   P. Raics, S. Darotsy et al. "Measurement of the cross-sections for the Th(n,2n) reaction in the 6.8 to 10.5 Mev energy range". I bit. Presentation of the All-Union Conference of Neutronics, Kiev, 1983.
4. Badikov S.A., Gay E.V., Rabotnov N.S., et al. Atomnaya Energia.

   Vinogradov V.N., Gay E.V., Rabotnov N.S. Preprint, FEI-434, Obninsk, 1974.
5. Badikov S.A. Gay E.V., Rabotnov N.S., et al. Voprosy Atomnoy Nauki i Tekhniki. Seria "Yadernye Konstanty".
6. Bychkov V.M., Manokhin V.N. et al. "Cross-Section of Neutron-Induced Thkeshold Reactions", Moscow, Energoizdat, 1982. (BOSPOR).
7. Scmitt H.W., Halperin J. Phys. Rev., 1961, 12, 3, p.827.
8. Buttler J.P., Santry D. Can. J. Phys., 1962, 41, p. 372.
9. Mani G.S., Mc Callum G,J, et al. Nucl. Phys, 1960, 19, p.535.
10. Liskien H., Paulsen A. Nucleonic, 1966, 8, p. 315.
11. Paulsen A., Liskien H. J. of Nucl. Ener. A/B, 1965, 19, p.907.
12. Csikai J. et al. Nuclear Data for Scien. and Tech., Antwerpen, 1982, p. 639.
13. Lu Hanlin et al. Data EXFOR 30523, 003.
14. Swinhoe M. AERE-PR/Np26, 1979, Data EXFOR 20986, 003.

15. Ryves et al. J. of Phys. G., 1978, 4, 11, p. 1783, EXFOR 20867. 006.

16. ENDF/B-V , Mat - 6398.

17. Grundl J. Eisenhaner C.M. Tech. Doc., IAEA-205, 1978, 1, p. 53.

18. Manahart W., Nucl. Data for Scienc. and Tech., Antwerpen, 1982, p. 429.

NEUTRON-CAPTURE CROSS-SECTION MEASUREMENTS FOR ^{197}Au AND ^{115}In IN THE ENERGY REGION 2.0–7.7 MeV USING THE ACTIVATION TECHNIQUE

P. ANDERSSON, R. ZORRO, I. BERGQVIST
Department of Physics,
University of Lund,
Lund, Sweden

The cross sections for the reactions $^{197}Au(n,\gamma)^{198}Au$ and $^{115}In(n,\gamma)^{116m}In$ have been measured with the activation method in the energy range 2.0 - 7.7 MeV. The influence of background neutrons on the results has been studied in considerable detail. The main problems are caused by low-energy neutrons produced by charge-particle reactions (e.g. (p,n) and (d,n) reactions) in the target material and secondary neutrons from nonelastic reactions (e.g.(n,n') and (n,np) reactions) in the sample and surrounding materials. Low-mass target-sample assemblies have been constructed to reduce the influence of secondary neutrons. Methods to correct for the background neutrons have been developed and applied to the cross section results.

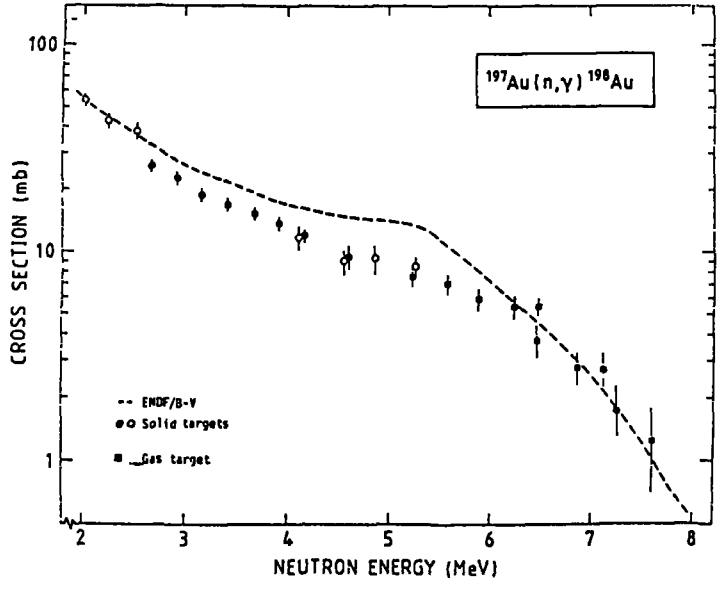

The measured capture cross sections are generally lower than previous results. The deviation increases with increasing neutron energy for both ^{197}Au and ^{115}In.

The present capture cross section results and data for the reference reaction

	$^{115}In(n,\gamma)^{116m}In$		$^{197}Au(n,\gamma)^{198}Au$		$^{115}In(n,n')^{115m}In$
E (MeV)	σ (mb)	Δσ	σ (mb)	Δσ	σ [a] (mb)
2.03	133	13	54	5	269
2.26	109	11	43	4	287
2.54	89	9	38	4	337
2.68	60	4	25.8	1.7	343
2.93	47	3	22.6	1.6	348
3.17	39	3	18.7	1.5	"
3.42	33	3	16.8	1.4	341
3.68	26.3	2.0	-	-	336
3.69	-	-	15.2	1.1	"
3.86	22.4	1.7	-	-	328
3.93	-	-	13.6	1.0	329
4.06	20.4	1.6	-	-	327
4.13	16	3	11.8	1.6	320
4.18	-	-	12.0	1.0	325
4.21	17.3	1.4	-	-	"
4.36	15.5	1.2	-	-	321
4.46	13.2	2.0	-	-	"
4.50	10.3	1.0	-	-	320
4.56	9.8	1.7	9.0	1.3	322
4.61	10.5	1.6	9.5	1.3	318
4.73	9.7	1.4	-	-	320
4.87	10.1	1.7	9.3	1.5	348
4.90	10.2	1.9	-	-	"
5.03	6.9	1.4	-	-	340
5.24	7.3	1.0	7.5	0.8	351
5.27	8.5	1.0	8.4	1.0	355
5.35	7.0	0.9	-	-	"
5.42	6.6	1.4	-	-	350
5.58	7.3	1.1	7.0	0.8	354
5.85	5.9	0.8	-	-	361
5.90	5.6	0.9	5.9	0.8	363
6.25	5.0	0.9	5.4	0.8	358
6.43	3.7	0.5	-	-	348
"	4.3	0.6	-	-	"
6.47	4.2	0.5	3.7	0.7	"
6.49	-	-	5.4	0.6	"
6.82	4.7	0.7	-	-	323
6.84	3.6	0.7	-	-	"
6.86	3.5	0.5	2.8	0.5	317
"	3.4	0.7	-	-	"
7.03	3.3	0.5	-	-	311
7.13	2.6	0.4	2.7	0.6	"
"	2.2	0.5	-	-	"
"	2.4	0.7	-	-	"
7.26	2.6	0.5	1.8	0.5	310
7.60	2.5	0.4	1.3	0.5	308
"	2.9	0.8	-	-	310
7.66	2.0	0.5	-	-	"
"	2.3	0.4	-	-	"

a) Uncertainty 6-7%.

INFLUENCE OF TARGET-SCATTERED NEUTRONS ON CROSS-SECTION MEASUREMENTS

H. LESIECKI, M. COSACK, B.R.L. SIEBERT
Physikalisch-Technische Bundesanstalt,
Braunschweig, Federal Republic of Germany

Abstract

Monoenergetic neutrons produced with accelerators are usually accompanied by degraded and secondary neutrons which arise from reactions of source neutrons in the material of the target construction. A Monte Carlo code was written which takes into account the kinematics and the angular source strength of the neutron producing reaction and the interactions of the neutrons with the material in the immediate vicinity of their production. The calculation of the spectral distribution of the neutron fluence is compared with the result of a time-of-flight measurement.

1. Introduction

Monoenergetic neutrons are frequently produced via nuclear reactions using particle beams from accelerators. The target nuclei are either confined in a gas cell or in solid layers which are necessarily surrounded by some other material, i.e. the target backing, the beam stop and the vacuum chamber. These materials, in particular, give rise to neutron scattering[1),2)] or reactions which often deteriorate fluence or cross section determinations[3)] (see also ref. 4 at this meeting). Recent international intercomparisons of fluence measurements for monoenergetic fast neutrons revealed this effect as the reason for considerable errors[5)]. An investigation of neutron reactions from material close to the target was therefore considered to be necessary.

2. Monte Carlo Program

For the determination of the neutron fluence from perturbing interactions in the immediate vicinity of the target, a Monte Carlo code was written. The situation is similar to that met with a gas target[6]. Nevertheless, a different program had to be developed in order to allow for the special geometry and the extended data sets for the relevant materials.

The geometry calculated is a disc serving as the target backing which is surrounded by a ring. The ring represents either the screw cap for the target backing or the tube of the vacuum chamber. The beam spot can be displaced from the centre of the disc and runs on a circle to simulate the case of a wobbling target, fig. 1.

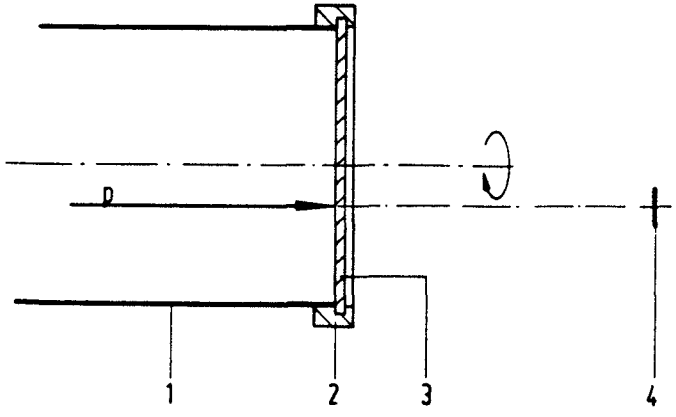

Fig. 1 Target assembly
1. Tube of vacuum chamber
2. Mounting ring for the target backing
3. Target backing
4. Detector

Different data sets are necessary for the neutron-producing and the neutron-induced reactions including the energy and angular dependence of the cross sections. Data arrays for the most frequently occurring materials were prepared as an input for the program using the information from ENDF. The kinematics of the neutron production and neutron reactions are calculated in suitable subroutines.

The Monte Carlo code determines the spectral distribution of the fluence at a particular point and the time-of-flight distribution for the neutrons which were subject to an interaction. The correspondence of the time-of-flight distribution and the spectral distribution is generally not trivial, as the neutrons have different path lengths before and after the interaction. The time-of-flight distribution was therefore calculated for the evaluation of the experiment.

Several test calculations were performed with different geometries. In the cases where simple analytical calculations were possible the results were in good agreement. This makes us confident that the Monte Carlo code works correctly and gives an adequate description of the situation.

3. Time-of-Flight Measurements

A time-of-flight experiment was carried out with a lithium glass scintillation detector measuring neutrons of an energy of 570 keV from the $^{7}Li(p,n)^{7}Be$ reaction. The flight path was 1.2 m and the overall time resolution approximately 4 ns (FWHM). The target was metallic lithium (mass per area 0.14 mg/cm^2) on a tantalum backing (thickness: 1 mm; diameter: 38 mm). The iron ring had a length of 0.7 cm and a thickness of 0.4 cm. The spectral distributions of the neutrons obtained by calculation and measurement are given in fig. 2. The calculated spectrum was multiplied by the energy-dependent cross section of the reaction of $^{6}Li(n,\alpha)T$ and provided with an appropriate energy resolution.

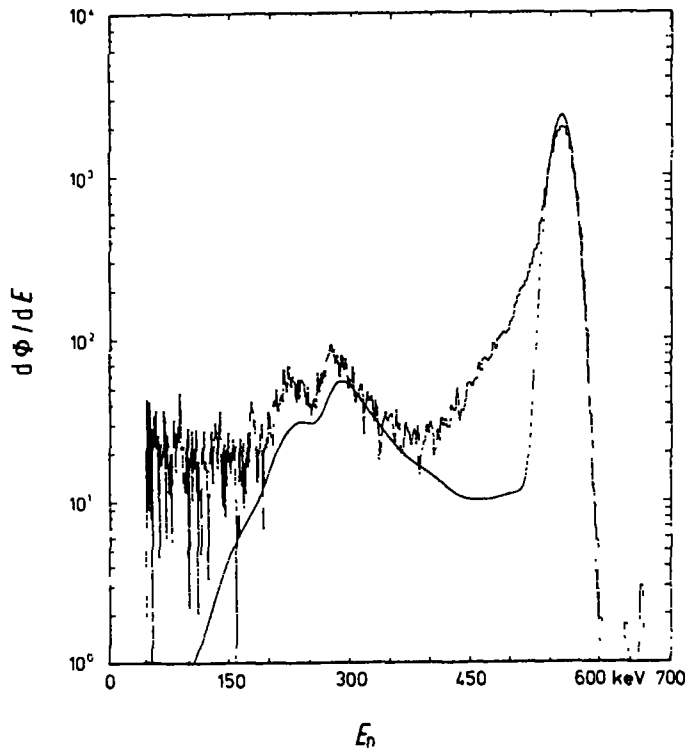

Fig. 2 Spectral distributions of the neutron fluence Φ as determined by
a) Time-of-flight measurement
b) Monte Carlo calculation folded with an appropriate energy resolution

Part of the difference of the curves near the main peak results from an unsatisfactory time structure of the particle pulses from the accelerator. In this region of the distribution an enhanced background of room-scattered neutrons is usually observed. In addition, the response of the lithium glass detector has a maximum in this energy region because of a resonance of the neutron scattering cross section in oxygen which is a constituent of the glass of the scintillator and the photomultiplier. There is qualitative agreement of the two curves at lower energies. For the determination of the fluence of neutrons scattered from the target material into the detector the dependence of the detector response on the neutron energy was assumed to follow the cross section of $^{6}Li(n,\alpha)T$. The fluence of scattered neutrons with energies from 200 keV to 400 keV yields 1.3 % of the fluence at 570 keV. The target-scattered neutrons are mainly to be expected in this energy range.

The energy and the fluence of the scattered neutrons depend of course on the peculiarity of the neutron-producing reaction. At higher energies, not only the elastic but increasingly the inelastic scattering and (n,2n) reactions have to be considered. As the cross sections and detector responses generally increase with decreasing neutron energy even small contributions of secondary neutrons may cause considerable errors.

The influence of target-scattered neutrons may be determind experimentally without their spectral distribution being known. However, the reliability of measurements is improved or tedious experimental investigations can be avoided if the spectral distribution of the 'monoenergetic' neutron fluence is calculated.

Monte Carlo calculations will therefore be performed for other sources of monoenergetic neutrons for the limited set of ISO[7] energies.

In addition, we volunteered to calculate correction factors for an earlier international intercomparison of fluences[5].

References

1. H. Schölermann: Berechnung des Anteils von Streuneutronen an verschiedenen Meßplätzen. PTB Report: PTB-ND-1 (1970)

2. H. Klein, H.J. Brede, B.R.L. Siebert: Energy and Angle Straggling Effects in a $D(d,n)^{3}He$ Neutron Source Using a Gas Target. Nucl. Instr. and Meth. 193 (1982) 635 - 644

3. T.B. Ryves: Calculations on the Scattering of keV Neutrons from the $^{7}Li(p,n)^{7}Be$ Reaction in a Typical Target Assembly. Journ. of Nucl. Energy 27 (1973) 365

4. P. Andersson, R. Zorro, I. Bergqvist: The Influence of Background Neutrons on (n,γ) Activation Measurements in the Neutron Energy Region 2.0 - 7.7 MeV. Contrib. to this meeting

5. H. Liskien: International Fluence-Rate Intercomparisons for 2.5 MeV and 5.0 MeV Neutrons. Metrologia 20 (1984) 55 - 59

6. H. Klein: Neutron Production Using Gas Targets. Contrib. to this meeting

7. M. Cosack: Neutron Energies Selected by ISO for the Calibration of Radiation Protection Instruments. Contrib. to this meeting

COMMENTS TO THE EVALUATION OF FAST NEUTRON RADIATION CAPTURE BY ^{197}Au GIVEN IN THE BOOK OF STANDARD NUCLEAR DATA

V.A. TOLSTIKOV
Institute of Physics and Power Engineering,
Obninsk,
Union of Soviet Socialist Republics

Abstract

The experimental results obtained since 1975 with a use of various methods of measurements are compared with each other and with the evaluation of ENDF/B-Y. To check in the range 0.2 MeV $\leq E_n \leq$ 4 MeV we have used a curve plotted through point data for $\sigma_{n,\gamma}$ ^{197}Au on the basis of the IAEA nuclear standard file. For $E_n < 0.2$ MeV the evaraged data on the "Grucon" programme have been used. A conclusion on the necessity of a new evaluation is made.

The book adopts the evaluation ENDF/B-Y as a standard. In figure I the solid line shows the data in the neutron energy range 0.195 - 4 MeV recommended by the authors of the work /1/. The curve is plotted through the values tabulated in /1/.

Insufficiency and low reliability of accessible experimental data for $E_n > 4$ MeV would hardly enable us to consider the ^{197}Au (n,γ) reaction cross-section in this energy range as a fairly satisfactory standard.

In an energy range < 200 keV $\sigma_{n\gamma}$ ^{197}Au data in ENDF/B-Y file are represented in the following way. For an energy range below 4.827 KeV they can be calculated by the resonance parameters recommended in the evaluation. In an interval 4.827 - 200 keV the data by Macklin et al /2/ are assumed as the evaluated ones renormalized to the $^{6}Li(n,\alpha)$ reaction cross-section value of the same system of evaluated ENDF/B-Y data. To compare the data by different authors the point-by point (obtained by averaging

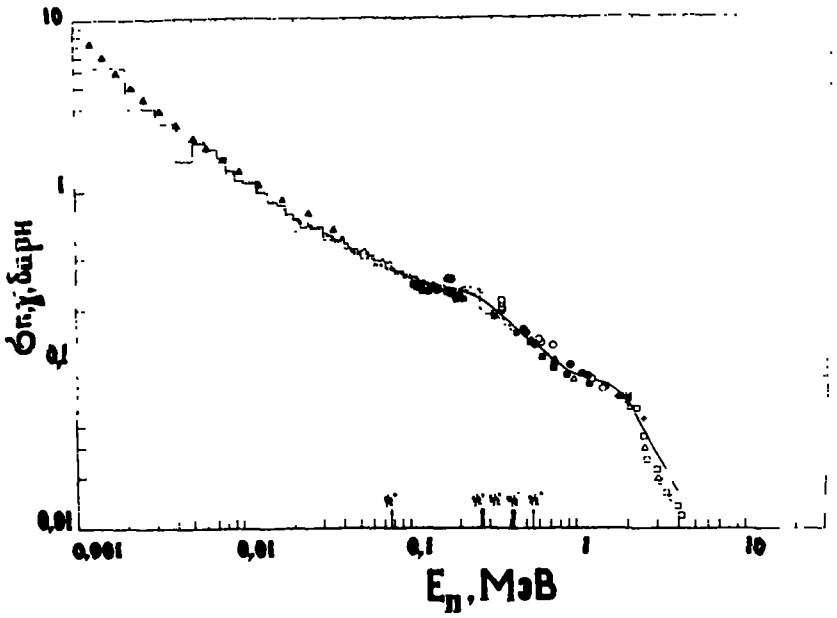

Fig. 1. ^{197}Au Radiative Capture Cross-Sections in the Energy range 0.001 - 4 MeV.
● - IPPE /5, 1983/ ; ○ - IPPE /6, 1980/; ⌐ - ENDF/B-Y evaluation, Grucon;
— - ENDF/B-Y for $E_n > 0.2$ MeV; ⌐ - Kononov /3/; ▲ - Chelnokov /11, 12/;
□ - Bergqvist /1/; △ - Joly /9/; + - Gupta /8/; ■ - Macklin /7/;
⌐ - Yamamuro /4/; $\frac{i(-)}{}$ - position, spin, parity of excited levels of ^{197}Au.

as well) representation of the data by Macklin et al being a bulky data file, is considered unreasonable. To simplify the comparison J. Korchagina and V. Sinitsa (IPPE) have averaged the ENDF/B-Y data in the range < 200 keV by the special "Grukon" programme. The results of this averaging are shown in figure I in the form of a stepped curve fitted to a smooth one. Averaging has been carried out through intervals 100 eV in the range 0 - 1 keV; I keV - in the range 1 - 10 keV; 2 keV - in the range 10 - 100 keV; 10 keV - in the range 100 - 200 KeV. The averaged cross-section has been determined by the formula:

$$\bar{\sigma} = \frac{\int_{En}^{Ek} \sigma(E)\, dE}{\int_{En}^{Ek} dE}$$

, where En and Ek - are the begining and the end. of the interval of averaging.

Here we should point out, that we consider in the energy range below 200 KeV an Au - capture cross-section can also be a good standard though under certain conditions regardless of its unsmoothness i.e. its resonance structure. We mean measurements with a well-known, rather broad spectrum of neutrons, with insignificant neutron energy shifts not resulting in essential changes in an averaged cross-section. For these measurements a spectrum-averaged cross-section of Au may be a good standard, with an error insiguificantly worse than in the interval 0.1 - 1 MeV. This viewpoint may well be confirmed by a good agreement of the data by Kononov (TOF) /3/ and Yamamuro (TOF) /4/ with the ENDF/B-Y evaluation for E_n < 200 KeV (i.e. finally, with the data by Macklin /2/ forming its basis).

We would rather suggest for the experimentors measuring capture cross-sections by the TOF method in a great amount of energy points, to present their own data and averaged data through the 28-group of BNAB nuclear data both with and without correction for the effects associated with resonance shielding especially for E_n < 200 KeV. It is of great practical value for the analysis and comparisones of the data.

The data from /3/ and /4/ together with the data of other recent studies not used in the ENDF/B-Y evaluation are plotted in figure 1 for the purpose of comparison. Here is a brief account of these studies in a chronological order.

The studies by Chelnokov, Tolstikov, Stavissky et al /11, 12, 1976/. A method of moderation in lead. A resent discovery of a certain shift in averaged neutron energy values and renormalization at $\sigma_{n,\alpha}$ ^{10}B in /I/, is likely to impreve the agreement of these data with ENDF/B-Y (with /2/, /3/, /4/, respectively).

The data by Macklin et al /2/, 1975 and a private communication, see /1/ and /7, 1979/ . A time-of-flight method. The studies lask numerical data, they are given (in the averaged form) in work /1/ with a short comments for $E_n > 0.2$ MeV. Though the data of work /2/ are the basis of the ENDF/B-Y evaluation for $E_n > 0.2$ MeV, in the region of "fitting" (0.1 - 0.2 MeV) the evaluation (i.e. actually the data from work /2/) and the data from work /7/ are in a poor agreement.

The Gupta's results/TOF, 8, 1978/ for 1.68 MeV agree with Macklin's /7/, for 1.98 MeV are closer to ENDF/B-Y and for 2.44 MeV ~10% over estimate ENDF/B-Y.

Cross-sections from the work by Joly et al /9,1979, TOF/ with the exception of a point for E_n= 0.94 MeV are in a perfect agreement with ENDF/B-Y for $E_n \leq$ 2 MeV. Two values for $E_n >$ 2 MeV being in agreement with the tentative data of the unpublished work by Bergqvist given in /1/ considerably underestimate ENDF/B-Y ($\gtrsim$ 30%).

The studies performed in IPPE /5, 1983/ and /6, 1980/ being close to methodical features should be considered together. Let's note, that the tentative data on the measurements /6, 1980/ were presented at the 5th Kiev conference on neutronics in 1979. The both studies have been carried out by an activation method in regard to the n-p scattering cross-section and by proportional hydrogeneous counters of different designs. The results of 1983 with the exception of two points in the area of ~170 keV within the uncertainties of measurements are very close to the ENDF/B-Y evaluation. The latter are close to the time-of-flight experimental data by Kononov /3, 1980/ and Yamamuro /4, 1983/, almost overlapped within one root-mean-square error. A ~ 15% overstimation of the earlier measurements /6,1980/ from the ENDF/B-Y evaluation at 700 KeV and 350 KeV are under investigation.

At the 1982 conference in Antwerp a work by a group of authors - Chen Jang et al /10, 1982/ from INE. AS of China was presented. The study was carried out by the activation method for E_n in the range 0.1 - 1.5 MeV, methodically it was very close to the report /5, 1983/. Unfortunately, it lacked numerical data, they were given in the form of a diagrams in the double logarithmic scale and compared to the ENDF/B-Y evaluation to which they seemed to be very close.

And, finally, about the tentative data by Kononov /3, 1980/ and the work by Yamamuro /4,1983/. Both studies were carried out by the TOF method, a neutron source in work /3/ was a Li-target at the Pulsed Van-de-Graaff accelerator, and in work /4/ - the linear electron accelerator with a photoneutron target. In the energy range 0.03 - 0.2 MeV the data of both studies are in a good agreement. Certain disagreements are observed at the methodical "edges" of the energy interval covered in work /3/.

Without going into more details we shall only note, that the degree of correlation of the above-mentioned studies and their agreement with the ENDF/B-Y evaluation (which in fact represents the data of "earlier" studies - before 1976) may be a criterion of the degree of $\sigma_{n,\gamma}{}^{197}Au$ confidence level in the corresponding energy intervals. For example, the agreement between work /9/ by Joly and /1/ by Begqvist for $E_n >$ 2 MeV may well be the illustration of our early assumption that the data of the studies being taken as a basis of the ENDF/B-Y evaluation for $E_n >$ 2 MeV to be slightly overestimated. This may be due to the inadequate consideration of the scattered neutron background in this energy region - the studies are carried out basically by the activation method.

This facts demand a new evaluation of the ^{197}Au capture cross-section to bring it into line with the new experimental data, some new measurement for $E_n >$ 1.5 MeV, a use of the most correct and verified theoretical representations and approaches for the evaluation in the region 3 MeV $\leq E_n \leq$ 14 MeV.

REFERENCES

1. Nuclear Data Standards for Nuclear Measurement. Technical Reports Series N 227, 1982. INDC/NEANDC Nuclear Standards File. IAEA, Vienna, October 1983, p. 33-38.
2. R.L. Macklin, S. Halperin, R.R. Winrers. Gold neutron capture cross-section from 3 to 550 keV. Phys. Rev. C., vol.11, 4, p. 1270-1279, April 1975, and private communication, cm /1/.

3. V.N. Kononov, E.D. Poletaev, M.B. Bokhovko, L.E. Kazakov, V.M. Timokhov.
"An Absolute Method of Measuring Fast Neutron Radiation Capture Cross-Section in ^{238}U". Neutron's, Proceedings of the 5th All-Union Conference on Neutronics, Kiev, 15-19 September 1980, part 2, p. 282-284, M., 1980.

4. N. Yamamuro, M. Igashira, T. Sekiya and H. Shicayanagi.
Kev-Neutron Capture in Cesium-133, Gold-197 and Tantalum-181. Jorn. of Nucl. Sci. and Technology, vol.20, N 1, p. 797-811, October 1983.

5. A.N. Davletshin, A.O. Tipunkov, S.V. Tikhonov, V.A. Tolstikov, V.V. Tuzhilov, S.N. Baykalov, V.S. Korolev.
The Results of $_{n,}{}^{197}Au$ Measurements with Reference to $_{n,p}$ in the Neutron Energy Range 0.16 - 1.15 MeV.
Presentation at the 6th Conference on Neutronics in Kiev, October 1983.

6. A.N. Davletshin, S.V. Tikhonov, A.O. Tipunkov, V.A. Tolstikov.
The Measurement of Neutron Radiative Capture Cross-Sections for ^{238}U and ^{197}Au with Reference to Elastic Scattering Cross-Section on Protons. Atomnaya Energiya, v. 48, N 2, p. 87-91, 1980.

7. R.Z. Macklin.
Gold Neutron Capture Cross-Section from 100 to 2000 keV.
Nucl Sci. and Eng., v. 79, N 3, p. 265-268, 1979.

8. S.K. Gupta, J. Prehaut and R. Bois.
Radiactive capture cross section measurements for fast neutrons using a large loaded liquid scintillator.
Nucl. Instr. Methods, v. 148, N 1, p. 77-84, 1978.

9. S. Joly, J. Voignier, G. Grenier, D.M. Drake and Z. Nilson.
Neutron Capture Cross Sections of Rhodium, Thulium, Indium and Gold between 0.5 and 3.0 meV. Nucl. Sci. Eng. 70, 1979, p. 53-59 and J. Voignier private communication, cm /1/.

10. Chen Ying, Ziang Saugshen, Zuo Dexing, Shu Shengyun, Zhon Zuying.
Measurements of neutron capture cross sections for ^{197}Au and ^{169}Tm between 0.1 - 1.5 meV. Nucl. Data for Science and Technology. Proc. of the Instr. Conf. Antwerpen, 6-10 September, 1982, p. 462-464, Gell, Belgium.

11. V.B. Chelnokov, V.A. Tolstikov.
Calculation of Resonance Self-Shielding Effect at a Spectrometer by Neutron Moderation Time in Lead, Preprint FEI-294, Obninsk, 1971.

12. V.V. Chelnokov, V.A. Tolstikov, Yu. Ya. Stavissky, A.A. Bergman, A.E. Samsonov.
A Measurement of Neutron Cross-Sections of Radiative Capture and Fission for Some Heavy Nuclei in the Moderation Time Method in Lead. Preprint FEI-292, Obninsk, 1971.

SESSION IV

REVIEW OF RECENT MEASUREMENTS OF THE U-235 FISSION CROSS-SECTION AND FISSION FRAGMENT ANGULAR DISTRIBUTION BETWEEN 0.1 AND 20 MeV

M.G. SOWERBY, B.H. PATRICK
Atomic Energy Research Establishment,
United Kingdom Atomic Energy Authority,
Harwell, Didcot, Oxfordshire,
United Kingdom

Abstract

The data on the U-235 fission cross-section in the energy range 0.1 - 20 MeV published since the ENDF/B-V evaluation was performed are reviewed and conclusions drawn on the present status and future work required. The data on the fission fragment angular distribution over the same energy range obtained in the past two years are also considered.

1. Introduction

The U-235 fission cross-section is a recommended standard over the energy range 0.1 to 20 MeV. In WRENDA 83/84 there are requests for measurements to an accuracy of ±1% over the whole energy range. The main purpose of this review is to consider the recent (i.e. post 1978 Harwell Conference on Neutron Physics and Nuclear Data for Reactors and Other Applied Purposes) measurements of the cross-section. Only limited attention will be paid to the fission fragment angular distribution as it has recently been reviewed by Kapoor[1] and uncertainties in the distribution only lead to small ($\lesssim$0.3%) errors in measured cross-sections. Data below 100 keV will not be considered even though it is recognised that the normalisation integrals of the cross-section between 7.8 and 11 eV and 100 eV and 1 keV are important for the normalisation of data above 100 keV. These integrals were surveyed by Wagemans and Deruytter at the IAEA Consultants' Meeting at Smolenice[2] and will be discussed by them at this meeting.

2. Recent measurements of the fission cross-section

Table 1 lists measurements reported in detail since the Harwell Conference. The results are plotted in Fig. 1 along with the ENDF/B-V evaluation which is the recommended standard cross-section at this time. The most striking aspect of the results is that below 5 MeV virtually all the new data lie below the ENDF/B-V values. The scarcity of new data between 1.2 and 14 MeV is also noticable although this situation will be rectified to some degree by presentations to be made at this meeting. A third feature is that many new measurements have used the time correlated associated particle (TCAP) technique.

Table 1

Recent U-235(n,f) measurements

Reference	Comments
Zhagrov + Proc. 1980 Kiev Conf., Vol. 3, p.45	Fission fragment detection, solid state detector, manganese bath, Van de Graaff, absolute 120 keV.
Cancé and Grenier CEA-N-2194 (1981)	Fission chamber back to back with polyethylene foil for counter telescope, flux at 2.5 MeV also measured with long counter, absolute, Van de Graaff 2.5 and 4.45 MeV.
Wasson + NSE 80, 282 (1982)	Fission chamber, time correlated associated particle technique, absolute, Van de Graaff, 14.1 MeV.
Wasson + NSE 81, 196 (1982)	Fission chamber, black neutron detector, absolute, Van de Graaff, 0.2 - 1.2 MeV. Also reports revised data from Wasson ANL-76-90, p.183 (1976). Fission chamber, hydrogen proportional counter, shape, linac, 5 to 700 keV, normalised through another experiment to 7.8 - 11 eV.
Li Jing-wen + Antwerp Conf. EUR 8355, p.55 (1983)	Fission chamber, time correlated particle technique, absolute measurement, Cockcroft-Walton, 14.7 MeV.
Carlson + Behrens Antwerp Conf. EUR 8355, p.456 (1983)	Fission chamber, black neutron detector 0.3 - 3 MeV, linac, not completed at this time (see below), absolute.
Mahdavi + Antwerp Conf. EUR 8355, p.58 (1983)	Counted fission fragments in track etch films, flux from Fe-56(n,p) and Al-27(n,α) reactions. Cockcroft-Walton accelerator, 14.63 MeV, measured fission fragment angular distribution. Only recent 14 MeV measurement not directly using TCAP method, absolute.
Dushin + Sov. At. En. 55, 656 (1983)	Gathers together and analyses results of measurements made by V. G. Khlopin Radium Institute, Leningrad and Technical University, Dresden which were done jointly. This reference updates the results given by: Adamov et al 79 Knoxville p.995 (1980) Arlt et al 79 Knoxville p.990 (1980) Arlt et al Kernenergie 2, 48 (1981) Arlt et al Kernenergie 25, 199 (1981) Data measured at 2.6, 8.5, 14.0, 14.5 and 14.7 MeV using time correlated associated particle technique, Cockcroft-Walton, tandem, fission chamber, absolute.

Table 1 (continued)

Recent U-235(n,f) measurements

Reference	Comments
Arlt + this meeting	Fission chamber, D(d,n)He-3 reaction, time correlated associated particle technique, tandem, 4.45 MeV, absolute.
Dias + this meeting	Fission chamber, dual thin scintillator, linac, absolute, 1-6 MeV, preliminary data only.
Carlson + this meeting	Fission chamber, black neutron detector, 0.3 - 3 MeV, linac, absolute.
Ye Zhongyuan et al (1984) private communication (original publication Yan Wuguang et al, Atom. En. Sci. Techn., 2 (1975) 133)	Fission chamber, proton recoil proportional counter, absolute, Van de Graaff, 0.5 and 1 MeV.

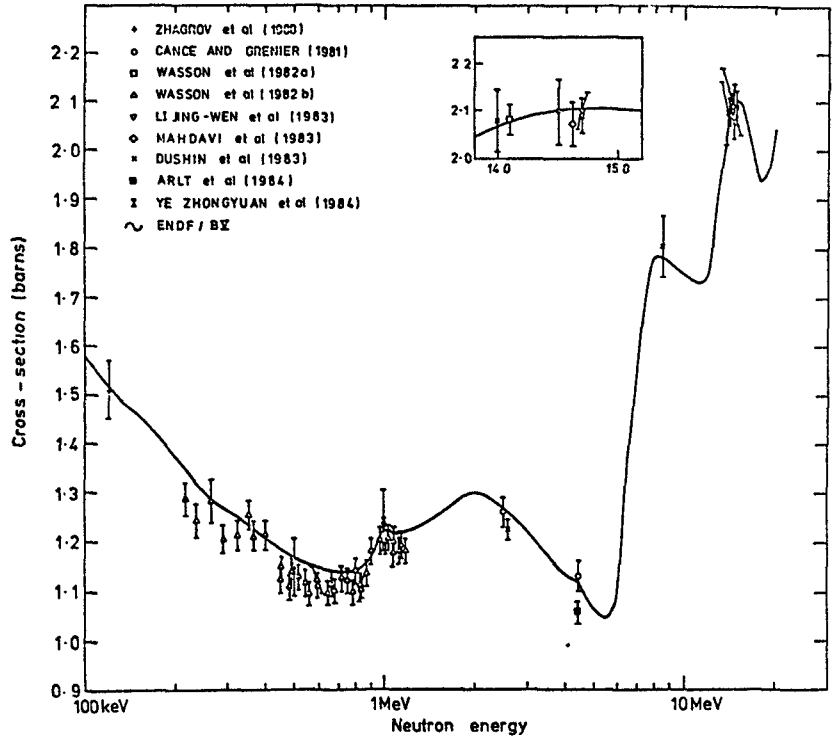

FIG. 1. POST 1978 MEASUREMENTS OF THE U-235 FISSION CROSS-SECTION

It can also be seen that results with this technique tend to give lower values than obtained with other techniques. On the basis of the new results it would appear to be reasonable that an evaluation of the cross-section might now reduce the values below those of ENDF/B-V around the minimum in the hundreds of keV energy range and between ~2.5 and 3 MeV.

However, the U-235 fission cross-section, averaged over the Cf-252 fission neutron spectrum, has been measured to high accuracy, the most recent data[3,4,5] being shown in Table 2. The importance of this quantity lies in its insensitivity to the knowledge of the Cf-252 fission neutron spectrum. The cross-section average therefore provides a useful constraint on the U-235 fission cross-section as a function of energy, particularly in the energy range 100 keV to 5 MeV which contains ~92% of the spectrum. The ENDF/B-V spectrum averaged value is 1231 mb, which is in good agreement with the measurements and therefore any changes to the ENDF/B-V values will necessarily be small in the energy region which contributes most to the Cf-252 spectrum averaged value.

Table 2

Measurements of the U-235 fission cross-section averaged over the Cf-252 fission neutron spectrum

Authors	Cf-252 fission spectrum averaged cross-section (mb)
Davis and Knoll[3]	1215±22
Adamov et al[4]	1241±18
Heaton et al[5]	1216±19

3. Some comments on the present data base

We have seen that since the Harwell Conference there have been ~14 new measurements. In the same period there have been at least 11 papers reviewing the problem or discussing evaluations. It seems that there is no shortage of people willing to advise how measurements should be improved but a shortage of people and funding to enable no more than a handful of good new measurements to be performed.

In April 1983 the IAEA held a Consultants' Meeting on the U-235 Fast Neutron Fission Cross-section at Smolenice[2] and the conclusions and recommendations reached there still stand. It was concluded at the meeting that the accuracies in Table 3 applied. It can be seen that, except at 14 MeV, the ±1% accuracy requested in WRENDA 83/84[6] was not achieved except perhaps at 14 MeV. (The ±1% accuracy at 14 MeV assumes that there are no serious systematic errors in the TCAP method - this will be considered again later.) Between April 1983 and this meeting there have been no new measurements and therefore these errors still apply today (unless the ENDF/B-VI evaluation has significantly changed them by making a simultaneous evaluation of the standard cross-section data).

Table 3

Uncertainties in U-235(n,f) cross-section suggested by the IAEA Consultants' Meeting at Smolenice* in April 1983 (see IAEA(NDS)-146)

E_n (MeV)	$\frac{\Delta\sigma_{nf}}{\sigma_{nf}}$ (%)
0.1	2-3
1.0	2-3
3.0	2-3
5.0	3-4
8.0	3-4
13	4
14	1.0
15	2
20	6

*One participant felt that the cross-section is known to 1-2% over much of the energy range below 13 MeV.

It is now apparent that the funding available for nuclear data measurements, particularly those related to fast reactors, is being or has been significantly reduced. It is therefore appropriate to ask if the presently achieved accuracy is sufficient or is there still a need for data accurate to ±1%? U-235 is primarily a standard for fission cross-section measurements and there are requests for U-238 and Pu-239 fission cross-sections to ±2%. It follows therefore that the U-235 fission cross-section still needs to be known more accurately and ±1% is a reasonable goal.

Can such an accuracy be achieved? A measurement of the cross-section basically requires

(1) the measurement of the number of fissions
(2) the assay of the amount of fissile material
and (3) the measurement of the incident neutron flux.

The assay of fissile material should not be a problem as Poenitz and Meadows[7] have shown, by intercomparing the masses of fifteen U-235 fission foils obtained from seven laboratories, that the masses determined by the laboratories agree to within ±~0.3%. When the time correlated associated particle technique is used, however, the areal density and non-uniformity of the fission foil have to be determined as the cone of neutrons correlated with the associated charged particles does not have uniform intensity and does not illuminate the whole fission foil. The errors due to these effects can be made small (Wasson et al[8] give the errors in the fission cross-section as ±0.5% (areal density) and ±0.3% (deposit non-uniformity and neutron beam shape)) but it can be greater (Arlt et al[9] for example give the errors as ±0.93% and ±0.72% respectively).

The measurement of the number of fissions can in principle be made accurately though there can be significant errors due to the background, the loss of fission fragments and the extrapolation of fission fragment pulse height spectrum to zero bias. Further work requires to be done to understand the science underlying these (see report of Smolenice meeting[2] and the work of Budtz-Jørgensen and Knitter[10]). However these errors - except that due to background - can be reduced by having thin fissile deposits but this leads to other problems such as low count rate. The background is not a problem if a monoenergetic pulsed source or the time correlated associated particle method are employed. When a white spectrum source is used the background error can also be made small though background determinations at high neutron energies tend to be indirect and of a "hand waving" variety. There can also be problems because the energy resolution functions of the fission detector and flux measuring equipment are probably different and not well known. However, with care all these errors can be made small enough so that the errors in fission counting lead to cross-section errors that are significantly less than ~±1% (say ±0.7%).

It follows therefore that the accuracy of the measurement of neutron flux is crucial and must be ~±0.7% for a fission cross-section measurement to be made to the required ±1% accuracy. The primary standard cross-section for neutron flux measurements in the 100 keV to 20 MeV energy range is H(n,n) and this is known (ENDF/B-V) to ±0.7, ±0.9 and ±1% between 0.1 and 1, 1 and 14 and 14 and 20 MeV respectively. There are additional errors of up to ±0.5% to allow for the uncertainties in the angular distribution. It follows, therefore, that it is not possible to measure flux accurately enough using hydrogen as the standard. (Below 1 MeV, where the cross-section is better known and angular distribution effects are small, the reaction is more difficult to use). There are many other methods of measuring neutron flux* but in general these also do not have the accuracy needed. Two methods which appear to be more suitable are the "Black Detector" and the time correlated associated particle (TCAP) technique. (The black detector can be used for spot point measurements and with white spectrum sources while the TCAP method can only be used at spot points).

*For a full discussion of neutron flux measurements for white spectrum sources see paper by Gayther at this meeting.

However, at the present time we doubt if either can be used to make flux measurements accurate to ±0.7% (we will return to the TCAP accuracy later). It can therefore be concluded that if measurements of the U-235 fission cross-section are required to ±1% improvements to the accuracy of flux measurements are needed and in particular the accuracy of the H(n,n) cross-section needs to be improved.

In principle 1% accuracy can be obtained by performing a number of independent lower accuracy measurements (4 at ±2% for instance). However, because of correlations there is little value in producing more measurements of the fast fission cross-section of U-235 with accuracies in the range 2-3% or worse using established techniques. However, this should not be interpreted as an attempt to stifle new and innovative techniques. On the contrary, new methods, which may provide independent determinations, are to be encouraged even if they produce accuracies in the 2-3% range.

There is a general belief that the TCAP method provides the most accurate data and, indeed, there are a number of measurements in the 14 MeV region of the U-235 fission cross-section, each done to about 2% accuracy, which are in good agreement. The Smolenice meeting in 1983 recommended the use of the TCAP method at as many energies as possible to establish accurate spot point values to which good shape measurements can be normalised. While strongly endorsing this conclusion, we feel that there is also a need to demonstrate conclusively that the TCAP method is capable of producing the accuracies claimed and that there are no unknown systematic errors. The question then arises as to what tests have been, or need to be, carried out to demonstrate the reliability of the method.

Two separate groups are known to have performed black neutron detector calibrations with the TCAP method and compared the results against calculations of the black detector efficiency. An NBS group[11] carried out measurements at 500, 700 and 880 keV, finding agreement between measurement and calculation at the 1.5% level. A similar measurement by Grenier[12] gave good agreement (~2% accuracy) with calculation at energies near 5 and 14 MeV. However, these comparisons raise the question as to what is actually being tested - the TCAP method or the black detector efficiency calculations. It seems reasonable to believe that for "black detectors" which are nearly 100% efficient (say, > 95%), the calculations of the efficiency are likely to be accurate as they are essentially independent of the nuclear data involved. In this case, the comparisons should be a good test of the TCAP method. But where the efficiency is significantly less than 100%, the calculations must be more suspect and the comparison should be viewed as a test of the calculations.

An alternative test of the TCAP method would be to use it to measure a known cross-section and the only one with anything like sufficient accuracy is the differential n-p scattering cross-section. Such a comparison was carred out by Grenier[12] but to an accuracy of only 3%. It is suggested that measurements of this type should be used to test the TCAP technique, although it has to be recognised that the accuracy achievable cannot be better than the knowledge of the differential n-p cross-section (~1%), and will probably be more like 2% at best. Additionally, it may not be sufficient for a test to be carried out at one laboratory; it should be performed at each TCAP facility as there are bound to be differences in the experimental arrangements. Not only is

there a need to assess such corrections as background and scattering effects, count loss corrections due to dead-time effects must also be thoroughly investigated and shown to be accurate. Only in this way will highly accurate, dependable data be achieved.

In recent years, much emphasis has been placed on the full documentation of experiments and the provision of covariance data, particularly for the most accurate, and therefore, most important, data sets. One such set of data resulted from a series of measurements by White[13] in which the U-235 fission cross-section was measured at spot points in the range 40 keV to 14.1 MeV. Although these measurements were performed in the 1960's, they are still of considerable importance in determining the evaluated cross-section. In an effort to make the data even more valuable, White has recently provided a breakdown of the errors and their correlations for the individual measurements. This has enabled a full covariance matrix to be assembled, the result being shown in Table 4. Many of the error components are totally correlated over all, or almost all, of the measurements so that the correlation between the result at one energy and that at another is generally fairly large, being ~0.5 for all energies below 5.4 MeV.

Table 4

The variance-covariance matrix for the measurements of the U-235 fission cross-section by White[13] at energies from 40 keV to 14.1 MeV

(In units of $(\%)^2$)

En (keV)	40	67	127	160	207	312	404	505	1000	2250	5400	14100
40	8.46	4.04	3.81	3.81	3.81	3.81	3.81	3.81	3.81	3.81	2.12	2.12
67		8.46	3.81	3.81	3.81	3.81	3.81	3.81	3.81	3.81	2.12	2.12
127			6.46	3.63	3.63	3.63	3.63	3.63	3.63	3.63	2.12	2.12
160				6.46	3.63	3.63	3.63	3.63	3.63	3.63	2.12	2.12
207					6.46	3.63	3.63	3.63	3.63	3.63	2.12	2.12
312						6.46	3.63	3.63	3.63	3.63	2.12	2.12
404							6.46	3.63	3.63	3.63	2.12	2.12
505								6.46	3.63	3.63	2.12	2.12
1000									6.46	3.63	2.12	2.12
2250										7.60	4.00	2.12
5400											14.98	2.12
14100												5.16

4. Fission fragment angular distributions

The U-235 fission fragment angular distribution data have recently been reviewed by Kapoor[1]. Since then the only new measurement is that of Mahdavi et al[14] at 14.63 MeV though new data are to be presented at this meeting by Straede et al. Mahdavi et al obtained a value of W(0°)/W(90°) of 1.426±0.024 which is higher than earlier measurements in the 14 MeV energy range where the values were typically 1.3. However, this difference makes only small changes ($\lesssim$0.3%) to the measured fission cross-sections because virtually all experiments collect fission fragments over a 2π solid angle. The principal exception is Mahdavi et al - if their measured anisotropy is incorrect and the earlier value of 1.3 is used then their measured cross-section would have to increase by roughly 2.5%. It is obviously desirable from a physics point of view to confirm the angular distribution data of Mahdavi et al at ~14 MeV and to improve the data at other energies. However, such improvements will do very little to improve the accuracy of the vast majority of fission cross-section measurements.

5. Conclusions

The U-235 fission cross-section measurements in the energy range 0.1 to 20 MeV have been reviewed by considering the new data reported since the 1978 Harwell Conference on Neutron Physics and Nuclear Data for Reactors and Other Applied Purposes. The following main points arose from the review.

There are few new data and these tend to give lower values in the energy regions around a few hundred keV and from 2.5 to 5 MeV. The measurements made using the time correlated associated particle (TCAP) technique usually seem to be lower than the values obtained by other methods. The revision of evaluations downwards is however constrained by the accurate measurements of the fission spectrum average cross-section. Though there have been few measurements there are nearly an equal number of papers reviewing or evaluating the data. There are too many people considering and advising what should be done but too few doing measurements and improving techniques.

There was an IAEA Consultants' Meeting in Smolenice in April 1983 on the U-235 Fast Neutron Fission Cross-section and the conclusions and recommendations from that meeting still stand. The main ones were:

(1) Full documentation of measurements is always required.

(2) There is little value in repeating measurements with accuracies of 2-3% or worse using established techniques.

(3) One must pay particular attention to understanding the properties of detectors and the corrections applied to them (the recent work of Poenitz and Meadows on foil assay and Budtz-Jørgensen and Knitter on the investigation of fission layers using the gridded ionization chamber must be particularly commended).

(4) The best way to get more accurate values seems to be accurate monoenergetic measurements combined with accurate shape measurements.

(5) The needed accuracy of ±1% has only been achieved near 14 MeV subject to tests on the TCAP method (see Table 3).

Some consideration was given in this paper as to whether or not the ±1% accuracy is still needed. It was concluded that it was but that it is unlikely to be achieved unless there are improvements in the accuracy of measurement of neutron flux and of the H(n,n) cross-section. Much reliance is being put on the accuracy of the TCAP method but very few accurate tests of the method have been performed. More are required and each system used for such measurements needs to be tested.

The data on fission fragment angular distributions have changed little since the review of Kapoor (1982). Uncertainties in the angular distribution have little effect on the accuracy of fission cross-section measurements so there is little incentive to make improved measurements.

6. Acknowledgements

We would like to acknowledge the assistance of Dr. P. H. White, who provided the data to enable the covariance matrix for his measurements to be derived, and of Dr. D. B. Gayther for numerous discussions.

References

(1) Kapoor S. S., Nuclear Data Standards for Nuclear Measurements, IAEA Tech. Report Series No. 227, page 47 (1983).
(2) IAEA Consultants' Meeting on U-235 Fast Neutron Fission Cross-section and the Cf-252 Fission Neutron Spectrum, Smolenice, Czechoslovakia, INDC(NDS)-146 (1983).
(3) Davis M. C. and Knoll G. F., Ann. Nucl. En., 5 (1978) 583.
(4) Adamov V. M., Alkhazov I. D., Gusev S. E., Drapchinsky L. V., Dushin V. N., Fomichev A. V., Kovalenko S. S., Kostochkin O. I., Malkin L. Z., Petrzhak K. A., Pleskachevsky L. A., Shpakov V. I., Arlt R. and Musiol G., Proc. of Int. Conf. on Nuclear Cross-sections for Technology, NBS Spec. Publication 594, p.995 (1980).
(5) Heaton H. T., Gilliam D. M., Spiegel V., Eisenhauer C. and Grundl J. A., ANL-76-90, p.333 (1976); also Grundl J. A. and Gilliam D. M., Trans. Am. Nucl. Soc. 44 (1983) 533.
(6) WRENDA 83/84, INDC(SEC)-88/URSF (1983).
(7) Poenitz W. P. and Meadows J. W., ANL/NDM-84 (1983).
(8) Wasson O. A., Carlson A. D. and Duvall K. C., Nucl. Sci. and Eng. 80 (1982) 282.
(9) Arlt R., Herbach C. M., Josch M., Musiol G., Ortlepp H. G., Pausch G., Wagner W., Drapchinsky L. V., Ganza E. A., Kostochkin O. I., Kovalenko S. S. and Shpakov V. I., paper presented to this meeting.
(10) Budtz-Jørgensen C. and Knitter H. -H., Nucl. Sci. and Eng. 86 (1984) 10.
(11) Lamaze G. P., Meier M. M. and Wasson O. A., Nuclear Cross-sections and Technology Vol. 1 (1975) p.73; see also Meier M. M., NBS Spec. Publication 493 (1977) p.221 and Wasson O. A., Meier M. M. and Duvall K. C., Nucl. Sci. and Eng. 81 (1982) 196.
(12) Grenier G., Third Symposium on Neutron Dosimetry in Biology and Medicine, EUR 5848 (1972).
(13) White P. H., J. Nucl. En. part A/B 19 (1965) 325.
(14) Mahdavi M., Knoll G. F. and Robertson J. C., Nuclear Data for Science and Technology EUR 8355 (1983) p.58.

NEW RESULTS ON THE $^{235}U(n,f)$ FISSION INTEGRALS

C. WAGEMANS
Centre d'étude de l'énergie nucléaire,
Mol
and
Nuclear Physics Laboratory,
Gent,
Belgium

A.J. DERUYTTER
Central Bureau for Nuclear Measurements,
Joint Research Centre,
Commission of the European Communities,
Geel

Abstract

New measurements of the $^{235}U(n,f)$ cross-section relative to $^{10}B(n,\alpha)^{7}Li$ have been performed in the neutron energy region from 0.02 eV up to 30 keV. From these data, the fission integrals $I_1 = \int_{7.8\ eV}^{11\ eV} \sigma_f(E)dE$ and $I_2 = \int_{0.1\ keV}^{1.0\ keV} \sigma_f(E)dE$ have been calculated.

These results are compared with the literature, and the present status of the integrals I_1 and I_2 is reviewed.

1. Introduction

At the IAEA Consultants Meeting on the ^{235}U Fast-Neutron Fission Cross-Secti (Smolenice, 1983), we reviewed some fission cross-section normalization problems [1]. Especially, the ^{235}U fission integrals $I_1 = \int_{7.8\ eV}^{11\ eV} \sigma_f(E)dE$ and $I_2 = \int_{100\ eV}^{1000\ eV} \sigma_f(E)dE$ were discussed. In the mean time, we performed a new series of measurements at GELINA, superseding the preliminary data reported at Smolenice. At ORNL an important new set of σ_f-data were released [2].

In the present paper, the status of the integrals I_1 and I_2 is reconsidered, taking into account these new informations.

2. Experimental conditions

The aim of the ongoing $^{235}U(n,f)$ cross-section measurements at GELINA is two-fold: (1) determine I_1 and I_2 in one single experiment, directly normalized in the thermal region (2) cover the neutron energy region from 0.02 eV up to 30 keV in that same experiment, thus realizing a link between the absolute measurements at thermal and in the keV-energy region.

To cover the large dynamic range needed for such an experiment, a 4 ns time-coder with two million channels was used. Via an "accordeon" system, this coder was linked to an Intertechnique Tridac multichannel analyser. In this way, the $^{235}U(n,f)$ and the neutron flux time-of-flight spectra were both recorded in 8192 channels with variable t.o.f. channel width taking into account the varying resolution. GELINA was operated at a repetition frequency of 100 Hz and with a 14 ns pulse width.

A large cylindrical vacuum chamber(Ø 50 cm) was installed at a 8.2 m flight path. A ^{10}B layer was mounted back-to-back with a ^{235}U layer in the center of this chamber. The $^{10}B(n,\alpha_0+\alpha_1)$ and the $^{235}U(n,f)$ fragments were detected by two collinear 20 cm^2 gold-silicon surface barrier detectors placed outside the neutron beam. The corresponding pulse-height spectra are shown in fig. 1a and b. The background was determined using the black resonance technique.

This low detection geometry with the detectors outside the neutron beam was one of the differences compared to the measurements reported at Smolenice [1], in which an almost 2π-geometry was used. In the present experiments, also the neutron beam collimation was improved, and the permanent Al-background filter was positioned about mid-way between the neutron source and the detectors.

For the measurements reported at Smolenice, the Al-filter was mounted much closer to the detection chamber.

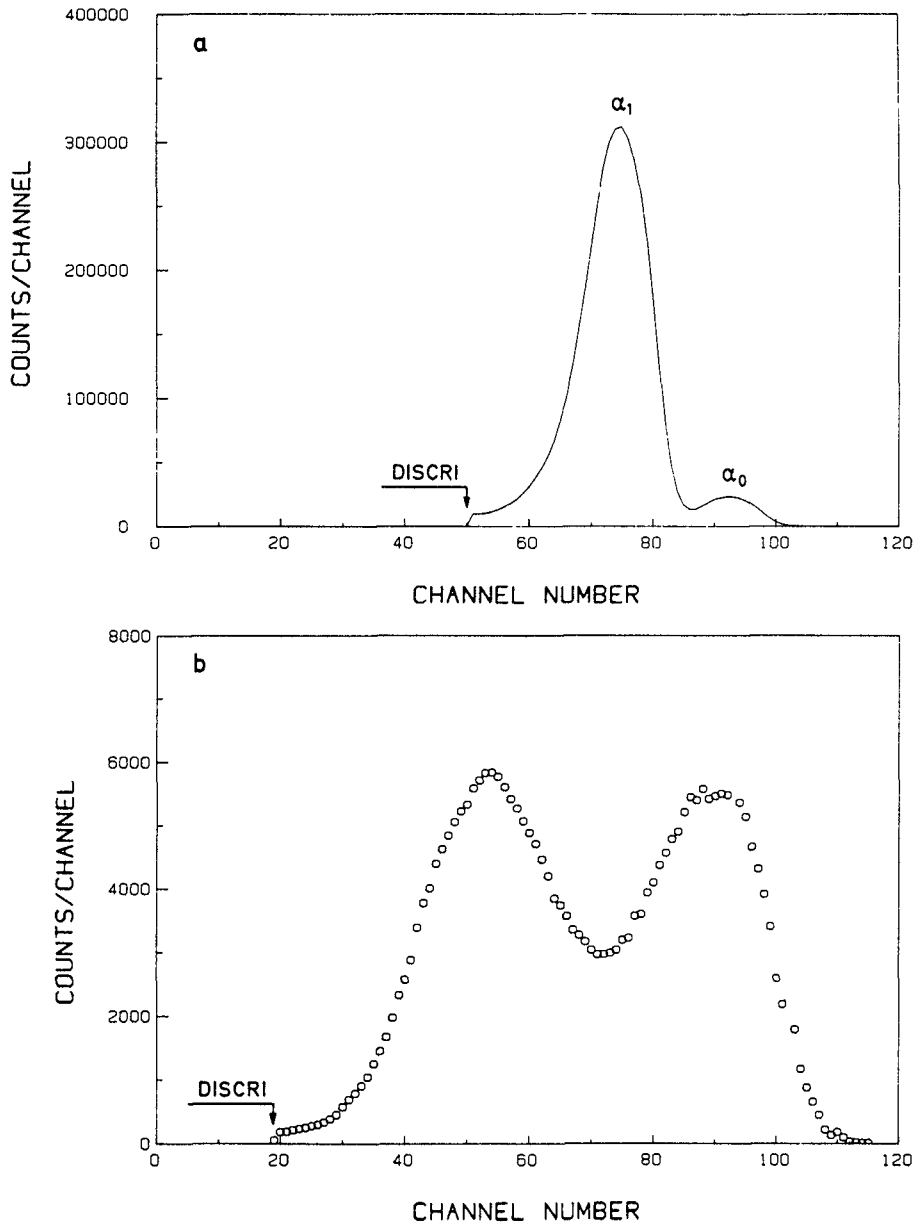

Fig. 1 : (a) The $^{10}B(n,\alpha_0+\alpha_1)$ pulse height spectrum
(b) The $^{235}U(n,f)$-fragments pulse height spectrum.

The targets were both prepared by vacuum evaporation upon a 0.2 mm thick Al disk. The thickness of the ^{10}B-layer was 50 $\mu g/cm^2$ and that of the $^{235}UF_4$-layer was 494 $\mu g/cm^2$.

3. Results

The raw data were analysed in the same way as described previously [3]. In the present work however, the data were analysed once under the assumption of a 1/v-shape for the $^{10}B(n,\alpha_0+\alpha_1)$ cross-section, and a second time using the ENDF-B V values for this cross-section. In both cases, the data were normalized in the thermal region to the fission integral

$$\int_{0.0206\ eV}^{0.06239\ eV} \sigma_f(E)dE = (19.26 \pm 0.08)\ barn.eV$$

as determined by Deruytter et al.[4] and corresponding to a thermal σ_f-value of 587.6 ± 2.6 barn. The $\sigma_f(E)\sqrt{E}$-data obtained in this way are shown in the energy region below 1 eV, together with the absolute $\sigma_f(E)\sqrt{E}$-values as determined by Deruytter et al.[4] (fig.2). Obviously, both data sets are in good agreement. The $\sigma_f(E)$-curves covering the energy region of the integrals I_1 and I_2 are shown in fig. 3.

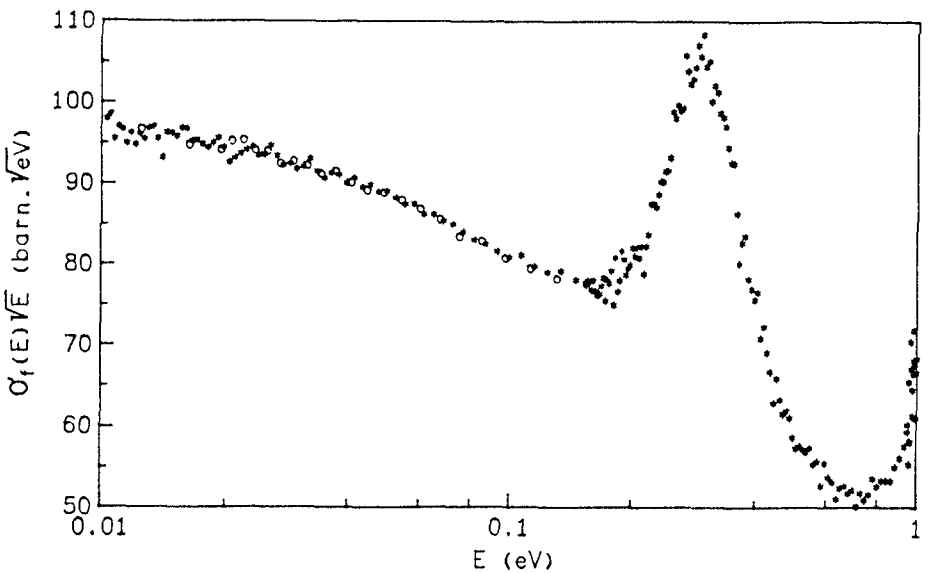

Fig. 2 : The $\sigma_f(E)\sqrt{E}$-data below 1 eV obtained during these measurements (*) compared with the corresponding results of Deruytter et al.(4) (o).

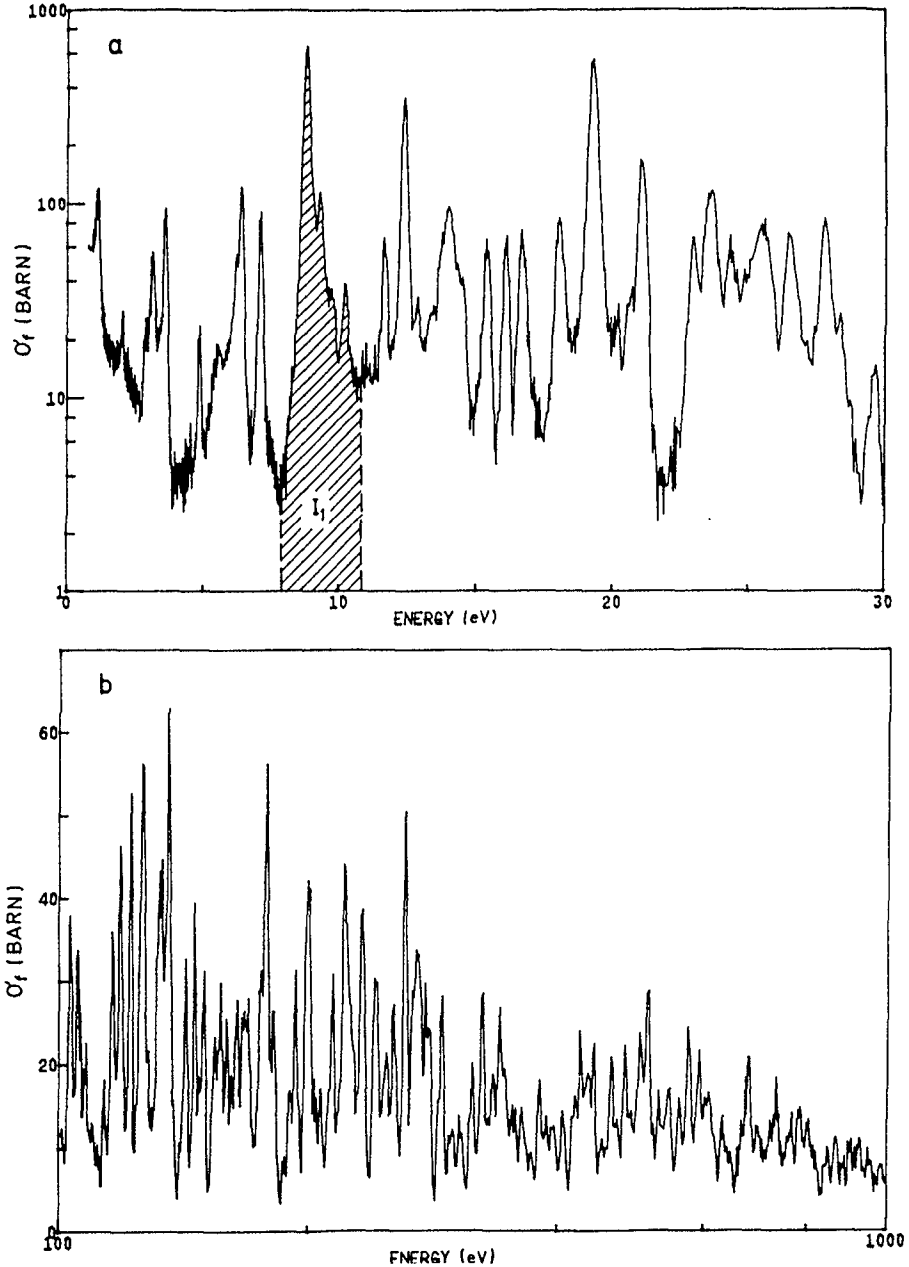

Fig. 3 : Present $\sigma_f(E)$-values from 0.5 to 30 eV (a) and from 100 to 1000 eV (b)

From the present data, values I_1 = 246.1 barn.eV and I_2 = 12.37 barn.keV were calculated under the assumption of a 1/v-shape for the $^{10}B(n,a_0+a_1)$ cross-section. With the ENDF-B V values for this cross-section, I_2 = 12.22 barn.keV was obtained. These values supersede the preliminary results reported at Smolenice (1), which probably suffered from neutron inscattering effects.

4. Discussion

In Table 1 a comparison is made of the fission integrals I_1 and I_2 relative to their thermal normalization values. Only measurements directly normalized in the thermal region were considered. For the I_1/σ_f°-ratio, the situation is rather encouraging. If we consider all the data reported in this table, an

Table 1 : Comparison of the original values of the secondary normalization integrals I_1(7.8 eV, 11 eV) and I_2(0.1 keV, 1 keV) relative to their thermal normalization values. Only measurements which were directly normalized in the thermal region are considered.

Reference	σ_f° (barn)	I_1(barn.eV)	I_1/σ_f° (eV)	I_2(barn.keV)	I_2/σ_f° (eV)	I_2/I_1
Bowman et al.(5)	577.1	246.7	0.427			
Deruytter & Wagemans (6)	587.9	240.2 [a]	0.409			
Gwin et al.(7) [b]	580.2	234.6	0.404	11.79	20.32	50.26
Czirr et al.(8)	585.4	244.7	0.418	11.54	19.71	47.16
Wagemans & Deruytter (3)	587.6	246.2	0.419			
Gwin et al.(2)	587.6	248	0.422	12.44 [c]	21.17 [c]	50.16
				12.30 [d]	20.93 [d]	49.60
This work	587.6	246.1	0.419	12.37 [c]	21.05 [c]	50.26
				12.22 [d]	20.80 [d]	49.66
Average			0.417		20.44	

(a) a recalculation by Leonard (9) yields I_1 = 245 after renormalization to σ_f° = 587.6 barn

(b) superseded by ref. 2; the ENDF-B III $^{10}B(n,a)$-values were used here

(c) data analysed under the assumption of a 1/v-shape for the $^{10}B(n,a_0+a_1)$ cross section

(d) data analysed using the ENDF-B V values for the $^{10}B(n,a_0+a_1)$ cross section; these data were used for the calculation of the average I_2/σ_f°-value.

average I_1/σ_f°-value of 0.417 is obtained, corresponding to I_1 = 245 barn.eV with σ_f° = 587.6 barn. If we cancel the earlier results of Gwin et al. (7), an average I_1/σ_f°-value of 0.419 is obtained, corresponding to I_1 = 246.2 with σ_f° = 587.6 barn.

In 1980, Bath (15) evaluated a I_1-value of 241.2 barn.eV relative to σ_f° = 583.5 barn (i.e. I_1/σ_f° = 0.413). The inclusion of the more recent data indicates that this I_1/σ_f°-ratio is probably about 1% too low.

As far as the ratio I_2/σ_f° is concerned, only four measurements directly normalized in the thermal region are available. Our present data are in perfect agreement with the new results of Gwin et al. (2); both values are however more than 5% higher than that reported by Czirr et al. (8).

To investigate this problem, five additional I_2-measurements are considered in Table 2. These measurements were not normalized in the thermal region, but they cover the energy region of the integral I_1. So the I_2/I_1-ratios can be calculated. All this information is summarized in Table 2, together with the reaction used for the neutron flux determination. Obviously, the I_2/I_1-ratio obtained by Czirr et al. (8) is significantly lower than all other values reported in this table. Moreover, all I_2/I_1-ratios obtained relative to the $^6Li(n,\alpha)$-reaction are lower than any ratio obtained relative to $^{10}B(n,\alpha)$. So the average I_2/I_1-value for the measurements done relative to $^6Li(n,\alpha)$ is more than 4% lower than the corresponding average for the measurements relative to $^{10}B(n,\alpha)$. This apparent correlation between the I_2/I_1-values and the neutron flux monitor used needs to be further investigated, before the integral I_2 can be safely used for normalization purposes.

5. Conclusions

For the integral I_1, the experimental data converge to a value of 246 barn.eV (estimated uncertainty : 2 barn.eV) with σ_f° = 587.6 barn. For the integral I_2, the situation is not quite clear. Considering all data reported in Table 2, an average value I_2 = 12.20 barn.keV is obtained (also relative to σ_f° = 587.6 barn). Here however further efforts are required to investigate the influence of the neutron flux monitor used. In this respect, additional measurements are planned at CBNM.

Table 2 : Comparison of the original values of the secondary normalization integrals I_1(7.8 eV, 11 eV) and I_2(0.1 keV, 1 keV), including measurements not directly normalized in the thermal region (marked with an asterisk).

Reference	I_1(barn.eV)	I_2(barn.keV)	I_2/I_1	Φ
De Saussure et al.(10)*	236.7	12.30	51.97	B
Wagemans & Deruytter (11)*	240.0 a)	12.29 c)	51.20	B
		12.14 d)	50.60	
Wasson (12)*	238.4 a)	(11.68)	(48.99)	Li
Moore et al.(13)*	241.2 a)	11.59	48.05	Li
Corvi (14)*	241.2 a)	11.88	49.25	Li
Gwin et al.(7) b)	234.6	11.79	50.26	B
Czirr et al.(8)	244.7	11.54	47.16	Li
Wagemans & Deruytter (3)	246.2	12.51 c)	50.81	B
		12.36 d)	50.20	
Gwin et al.(2)	248	12.44 c)	50.16	B
		12.30 d)	49.60	
This work	246.1	12.37 c)	50.26	B
		12.22 d)	49.66	
Average			49.57	B, I
			50.38	B
			48.36	Li

(a) normalization value
(b) superseded by ref.2
(c) data analysed under the assumption of a 1/v-shape for the $^{10}B(n,\alpha)$ cross sectio
(d) data analysed using ENDF-B III (refs. 3, 11) and ENDF-B V (ref. 2 and this work values for the $^{10}B(n,\alpha)$ cross section; these data were used for the calculation of the average.

Acknowledgements

Mr. R. Barthélémy and Mr. J. Van Gils are acknowledged for their help during the experiments and their analysis.

REFERENCES

(1) C. WAGEMANS and A.J. DERUYTTER, Proc. IAEA Consultants Meeting on the ^{235}U Fast Fission Cross-Section (Smolenice), IAEA Vienna, INDC (NDS) 146, (1983) 79

(2) R. GWIN, R. SPENCER, R. INGLE, J. TODD, S. SCOLES, Nucl. Sci. Eng. 88 (1984) 37

(3) C. WAGEMANS, G. CODDENS, A.J. DERUYTTER, Proc. Int. Conf. on Nuclear Cross-Sections for Technology (Knoxville), NBS-SP-594 (1979) 261 (revised values)

(4) A.J. DERUYTTER, J. SPAEPEN, P. PELFER, J. Nucl. En. 27 (1973) 645

(5) C. BOWMAN, G. AUCHAMPAUGH, S. FULTZ, M. MOORE, Proc. Conf. on Neutron Cross-Section Techn. (Washington) II (1966) 1004

(6) A.J. DERUYTTER and C. WAGEMANS, J. Nucl. En. 25 (1971) 263

(7) R. GWIN, E. SILVER, R. INGLE, Nucl. Sci. Eng. 59 (1976) 79

(8) J. CZIRR and W. CARLSON, Nucl. Sci. Eng. 64 (1977) 892

(9) B. LEONARD, ANL-76-90 (1976) 281

(10) G. DE SAUSSURE, L. WESTON, R. GWIN, R. INGLE, J. TODD, R. HOCKENBURY, R. FULLWOOD, A. LOTTIN, Proc. Conf. on Nuclear Data for Reactors (Paris) II (1967) 233

(11) C. WAGEMANS and A.J. DERUYTTER, Ann. Nucl. En. 3 (1976) 437

(12) O. WASSON, ANL-76-90 (1976) 183

(13) M. MOORE, J. MOSES, G. KEYWORTH, J. DABBS, N. HILL, Phys. Rev. C 18 (1978) 1328

(14) F. CORVI, private communication (1982)

(15) M. BATH, BNL-NCS-51184 (1980)

162 ABSOLUTE MEASUREMENTS OF THE $^{235}U(n,f)$ CROSS-SECTION FOR NEUTRON ENERGIES FROM 0.3 TO 3 MeV

A.D. CARLSON, J.W. BEHRENS, R.G. JOHNSON, G.E. COOPER
National Bureau of Standards,
Gaithersburg, Maryland,
United States of America

Abstract

Measurements of the ^{235}U neutron fission cross section have been made at the NBS linac neutron time-of-flight facility. The neutron flux was measured with a Black Neutron Detector located at the 200 m experimental station of this facility. The efficiency of this detector has been calculated with a Monte Carlo program. Experimental measurements of the efficiency using the associated particle technique have verified the calculated values. The fission events were detected with a well-characterized ^{235}U fission ionization chamber located 69 m from the neutron producing target on the same beam line as the Black Detector. The data were accumulated in a two-parameter (pulse height vs time-of-flight) format on a million word disk. With this data acquisition system biases could be chosen after the experiment was completed. Extensive investigations of backgrounds and systematic errors were made. The data have been grouped to statistical precisions of ~ 1%. Total uncertainties are about 2%.

INTRODUCTION

The neutron standards program at the National Bureau of Standards has focused much of its effort on measurements of the ^{235}U neutron fission cross section. The present work makes use of well-characterized fission and neutron flux detectors to make absolute measurements of this cross section using a linac neutron source. The objective of this work is to improve the accuracy of this cross section and understand the systematic errors which so often plague neutron cross section measurements.

EXPERIMENTAL DETAILS

Many of the experimental details for the present measurements have been discussed at a recent conference[1] so only a general outline of the experiment with appropriate updates will be presented here.

The neutron flux was measured at the 200 m experimental station of the NBS Neutron Time-of-Flight Facility with the NBS Black Neutron Detector. The fission reaction rate was determined with a parallel plate ionization fission chamber located 69 m from the target on the same beam line as the Black Detector. The data for both detectors was obtained with a computer based two parameter (pulse height and time-of-flight) data acquisition system.

The ^{235}U mass in the fission chamber was determined[2] relative to a well-characterized NBS reference deposit by using fission counting in a thermalized neutron beam. By measuring the mass in this manner, problems due to surface conditions of the foils and uncertainty in the range of the fission fragments are simplified. Corrections to the present measurements are made for fission fragment absorption, but due to the mass determination method, only the change in the absorption between the energy of interest and thermal is important. For these measurements this change is very small. The uncertainty in the absorption correction is contained within the ^{235}U mass uncertainty. Additional corrections for the fission chamber include the extrapolation to zero pulse height of the fission chamber pulse height distribution, and neutron scattering from the materials in the fission chamber.

The neutron beam was collimated so that the deposits in the fission chamber could view the entire neutron target. The Black Detector was used with a collimator (~ 1.2 cm diameter) which defined the beam size to appreciably less than the size of the Black Detector reentrant hole. It was found that conventional optical techniques for collimator alignment over the great distance involved are not reliable even when the alignment is done at night (with the beam tube windows removed) when apparent thermal equilibrium has been obtained. The collimator was made by a company which produces gun barrels which are "straight" to 0.002 cm in 60 cm. It was determined that the collimator did not meet these specifications. The effective area of the collimator as it was positioned for the neutron flux measurements was

accurately determined by taking x-ray radiographs with the film carefully positioned near the collimator. The x-ray source for these exposures was the bremsstrahlung obtained by using the same target and electron beam from the linac as was used for the cross section measurements. By making the radiographs in this manner, the measured effective area includes small penumbra corrections which must be used for the neutron flux determination. Radiographs were made with no filters and with 1/8 inch of uranium in the beam. The results from these two types of measurements are in agreement. For each film the optical density (which was converted to intensity) was determined as a function of position with analog and digitizing scanning microdensitometers. Both the length and optical density scales were calibrated for each of the systems used. Good agreement was obtained for each of the densitometers. The overall accuracy of the effective area determination is ~ 0.2%.

The small size of the collimator was necessary in order to reduce the counting rate in the Black Detector so that the dead-time correction factor was less than 1.3. In order to maintain a near constant counting rate during the data taking and thus reduce uncertainties in the dead-time correction, a computer control system was employed which only allowed data accumulation when the electron beam current was within a narrow range.

For both detectors the neutron energy scales were determined realistically from the measured flight paths and gamma flash channels. For the fission chamber, the gamma flash channel was obtained from $^{235}U(\gamma,f)$ events from the high energy bremsstrahlung gamma rays. A small difference between the energy scales of the two detectors was observed which was attributed to a time difference in the fission chamber. The fission chamber gamma flash channel was shifted to produce agreement between the energy scales of the detectors, based on observed resonances in aluminum, oxygen, and nitrogen.

Time dependent backgrounds for both detectors were reduced to negligible levels. To eliminate background from neutrons that scatter from the Black Detctor, data was accumulated in a one count per linac pulse mode, with a time window for data acquisition which included the highest energy neutrons from the target. With these conditions, neutrons which would have caused background, produce a pulse in the Black Detector and stop the accumulation of data for the remainder of that linac pulse. Thus the backgound event is not recorded.

DATA ANALYSIS

The large amount of data obtained in this experiment was separated into 11 groups taken under the same experimental conditions. For each of these groups consistency checks were made of the fission chamber and Black Detector pulse height distributions as a function of neutron energy. The measured Black Detector pulse height distributions were compared with Monte Carlo calculations with a program originally developed by Poenitz[3] and modified by Meier and Wasson[4] to include the Poisson statistics for the limited numbers of photoelectrons as was suggested by Lamaze.[5] This program has also been recently improved by updating the cross section libraries used in the calculations and making a few modifications. In addition to providing information on the consistency of the various groups, which was excellent, the comparison leads to determinations of the efficiency of the detector as a function of neutron energy and pulse height bias channel. The measured shapes of the pulse height distributions agree very well with the Monte-Carlo calculations for neutron energies up to ~ 2 MeV. Above this energy, shape differences between measurements and calculation appear which worsen with higher neutron energies. The differences are not a result of saturation or non-linearities in the electronics employed for the measurements. They may be due to modelling problems in the calculations, and this raises questions about the uncertainty in the efficiency at these higher neutron energies. A measurement[6] of the efficiency of the detector was therefore made at 2.3 MeV using the time-correlated associated particle technique. The agreement between the calculated and measured efficiencies is excellent. Based on this agreement and the earlier efficiency measurements[7] below 900 keV, it is estimated that the uncertainty in the Black Detector efficiency is 1% or less throughout the energy range of this experiment. The efficiency of the detector at a bias of 0.3 times the peak pulse height channel was parameterized and used in the analysis procedure.

Each of the groups of data was analyzed with comprehensive programs which

1. Dead-time correct the fission chamber and Black Detector data.
2. Make transmission corrections for the materials in the neutron beam between the center of the fission chamber and the Black Detector using ENDF/B-V cross sections.

3. Apply Gaussian smearing to the Black Detector data to make it have the same time resolution as the fission chamber data.
4. Sort the fission chamber data with a constant bias channel. Then corrects the data for extrapolation to zero pulse height channel, fission fragment absorption and neutron scattering in the materials in the fission chamber.
5. Sort the Black Detector data with a bias of 0.3 times the peak pulse height channel. Then correct the data for efficiency.
6. Correct for ambient background for both the fission chamber and Black Detector.
7. Form an equivalent energy mesh for the fission chamber and Black Detector data.
8. Calculate the cross section for each energy channel from

$$\sigma = \frac{FC}{BD} \quad \frac{A}{N} \quad \left(\frac{FPBD}{FPFC}\right)^2$$

where FC = the corrected fission chamber counts
BD = the corrected Black Detector counts
A = the area of the Black Detector collimator
N = the number of ^{235}U atoms in the fission chamber
FPBD = the distance from the target to the end of the Black Detector collimator
FPFC = the distance from the target to the center of the fission chamber

The cross sections from each group were then combined to form the final cross section results. The data have been grouped to a statistical precision of 1%. The total uncertainty is about 2%. The components of the cross section uncertainty include Black Detector efficiency (~ 1%), timing (~ 0.5%), transmission correction (~ 0.3%), background (~ 0.1%), collimator area (~ 0.2%), ^{235}U mass which includes the fragment absorption uncertainty (~ 1.2%), extrapolation to zero pulse height for the fission chamber (~ 0.4%), statistical (1%), Black Detector bias (~ 0.5%), flight path (0.02%), dead-time correction (0.2%) and neutron scattering for the fission chamber (0.1%).

RESULTS AND COMPARISONS

In Fig. 1 the present measurements from 0.3 to 1.2 MeV are compared with previous NBS measurements in this energy range. The Wasson (1976) data[8] are linac measurements made using a hydrogen gas proportional counter for the neutron flux determination and are essentially uncorrelated with the present data. The Wasson et al. (1982) measurements[9] are the Van de Graaff data which were obtained with the same fission chamber and Black Detector as was used for the present measurements. Thus there are appreciable correlations between these sets of measurements. There is generally good agreement among the measurements throughout the entire energy range; however, the present data are systematically somewhat lower than the previous measurements, particularly in the central part of the energy range. All three data sets are lower than the ENDF/B-V evaluation.

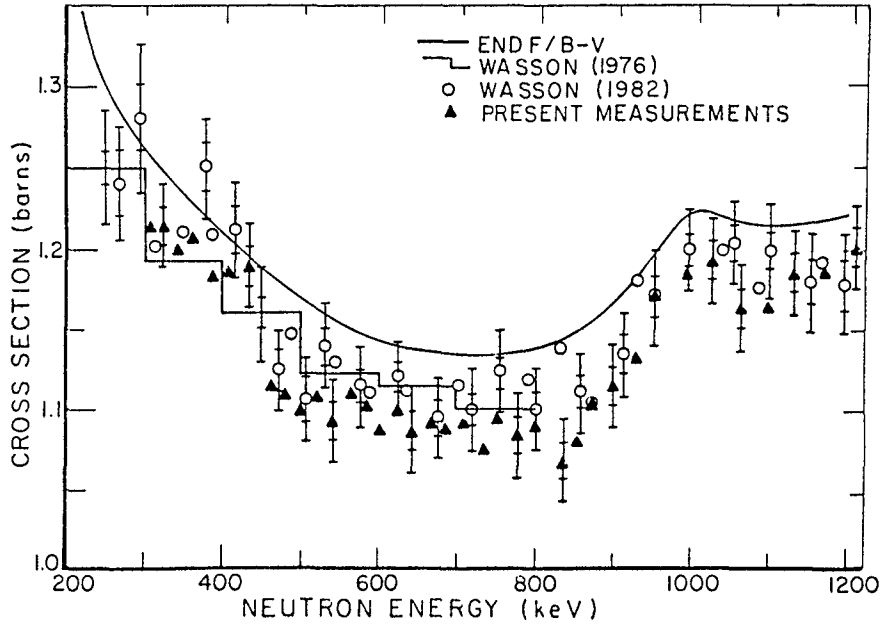

1. The present measurements of the $^{235}U(n,f)$ cross section from 0.3-1.2 MeV compared with the data of Wasson[8] (1976) and Wasson et al.[9](1982). The solid curve is the ENDF/B-V evaluation. The statistical and total uncertainties are indicated for each result by the small and large error bars, respectively.

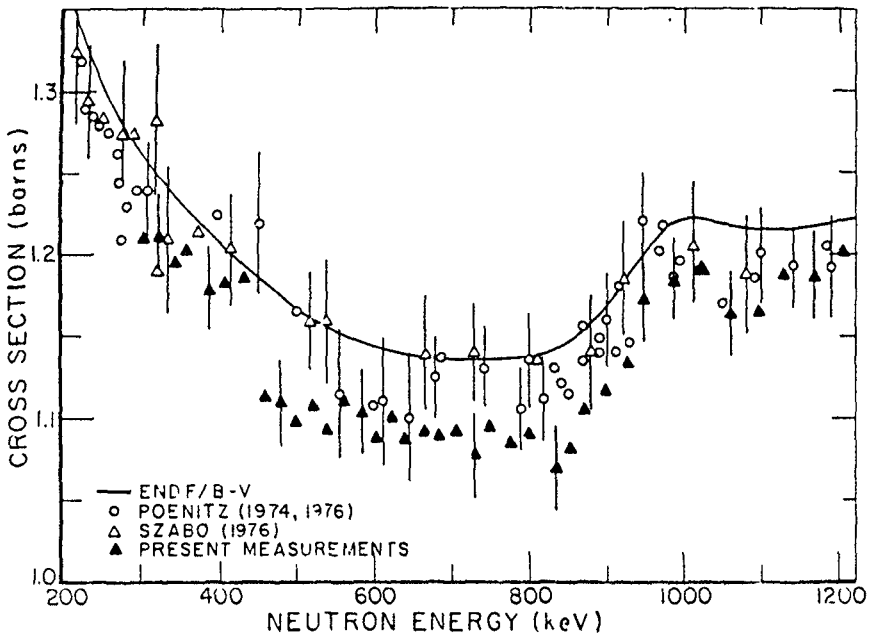

2. The present measurements of the $^{235}U(n,f)$ cross section from 0.3-1.2 MeV compared with the data of Poenitz[10,11] and Szabo and Marquette.[12] The solid curve is the ENDF/B-V evaluation.

In Fig. 2 the present measurements are compared with the Van de Graaff data of Poenitz,[10,11] and Szabo and Marquette[12] for the energy interval from 0.3 to 1.2 MeV. The present results are lower than these earlier data except in a few isolated regions, e.g., near 600 keV.

In Fig. 3 the present data are compared with those of Poenitz[11] and Szabo and Marquette[12] for neutron energies from 1.2-3 MeV. Also shown is the shape data of Carlson and Patrick[13] which have been normalized to the present absolute data over the interval from 1.5-2.5 MeV. The present measurements agree well with the data sets shown. The shape data, as normalized here, agree well with the Poenitz and Szabo data. The data sets shown here are generally lower than the ENDF/B-V evaluation.

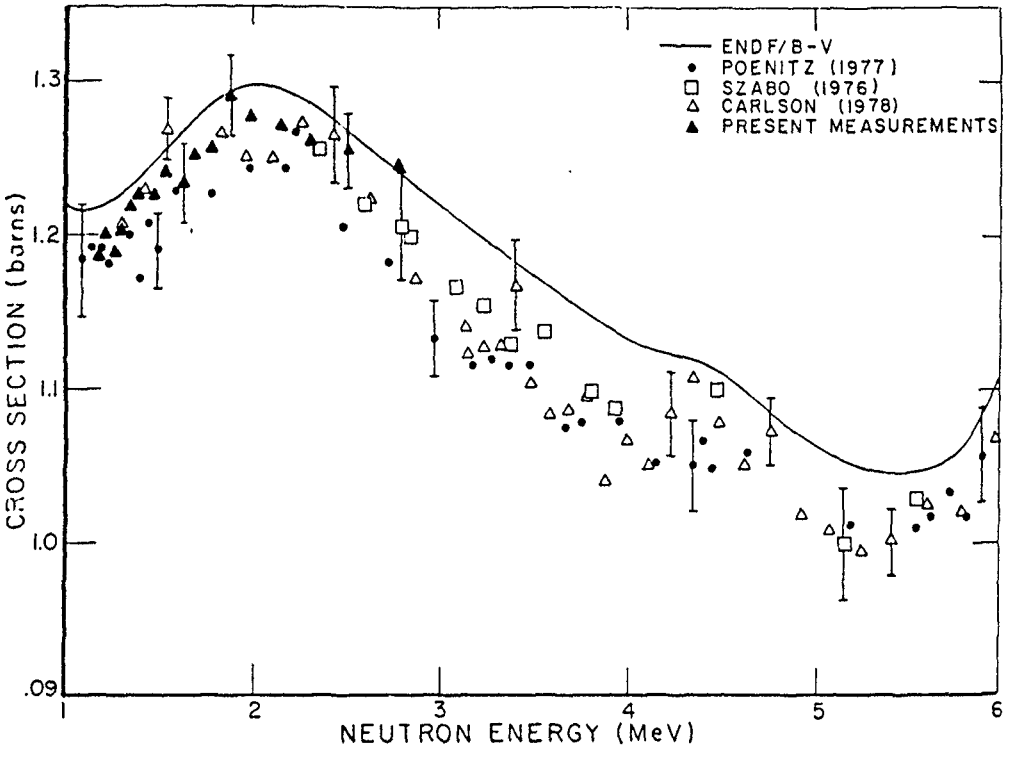

3. The present measurements of the $^{235}U(n,f)$ cross section from 1.2-3 MeV compared with the data of Poenitz[11] and Szabo and Marquette.[12] Also shown in the shape data of Carlson and Patrick[13] normalized to the present measurements over the interval from 1.5-2.5 MeV. The solid curve is the ENDF/B-V evaluation.

SUMMARY

Absolute measurements have been made of the ^{235}U neutron fission cross section for neutron energies from 0.3-3 MeV with statistical uncertainties of 1% and total uncertainties of about 2%. These data agree with some recent measurements, and suggest that the $^{235}U(n,f)$ ENDF/B-V cross section is too large from 0.3-3 MeV.

REFERENCES

1. A.D. Carlson and J.W. Behrens, Measurement of the $^{235}U(n,f)$ Cross Section From 0.3 to 3.0 MeV Using the NBS Electron Linac," in Proc. of the Int. Conf. on Nuclear Data for Science and Technology, Antwerp, (Editor, K.H. Böckhoff) Reidel Pub. Co. p. 456 (1983).

2. O.A. Wasson and M. Meier, Nucl. Instr. Meth. 190, 571 (1981).

3. W.P. Poenitz, Nucl. Instr. Meth. 109, 413 (1973).

4. M.M. Meier and O.A. Wasson, Bull. Am. Phys. Soc., 23, 72 (1978).

5. G.P. Lamaze, M.M. Meier, and O.A. Wasson, "A Black Detector for 250 keV-1000 keV Neutrons," in Proc. of a Conf. on Nuclear Cross Sections and Technology, Washington, D.C., (Eds. R.A. Schrack and C.D. Bowman), NBS Spec. Publ. 425, p. 73 (1975).

6. K.C. Duvall, A.D. Carlson, and O.A. Wasson, "Measurement of the NBS Black Neutron Detector Efficiency at 2.3 MeV," this meeting.

7. M.M. Meier, "Associated Particle Methods," in Proc. of the Int. Specialists Symposium on Neutron Standards and Applications, National Bureau of Standards, (Eds. C.D. Bowman, A.D. Carlson, H.O. Liskien, and L. Stewart), NBS Spec. Publ. 493, p. 221 (1977).

8. O.A. Wasson, "The ^{235}U Neutron Fission Cross Section Measurement at the NBS Linac" in Proc. of the NEANDC/NEACRP Specialists Meeting on Fast Neutron Fission Cross Sections of U-233, U-235, U-238, and Pu-239, Argonne National Laboratory (Eds. W.P. Poenitz and A.B. Smith) ANL-76-90, 183 (1976), see also Ref. 9.

9. O.A. Wasson, M.M. Meier, and K.C. Duvall, Nucl. Sci. Engng., 81, 196 (1982).

10. W.P. Poenitz, Nucl. Sci. Engng. 53, 370 (1974).

11. W.P. Poenitz, Nucl. Sci. Engng. 64, 894 (1977).

12. I. Szabo and J.P. Marquette, "Measurement of the Neutron Induced Fission Cross Sections of Uranium-235 and Plutonium-239 in the MeV Energy Range" in Proc. of the NEANDC/NEACRP Specialists Meeting on Fast Neutron Cross Sections of U-233, U-235, U-238, and Pu-239, Argonne National Laboratory (Eds. W.P. Poenitz and A.B. Smith) ANL-76-90, p. 208 (1976).

13. A.D. Carlson and B. H. Patrick, "Measurement of the ^{235}U Fission Cross Section in the MeV Energy Region," in Proc. of an Int. Conf. on Neutron Physics and Nuclear Data for Reactors and Other Applied Purposes, Harwell, p. 880 (1978).

AEP MEASUREMENTS OF $^{235}U(n,f)$ AND $^{238}U(n,f)$ CROSS-SECTION

HANRONG YUAN
Institute of Atomic Energy,
Beijing, China

Abstract

A series of AEP measurements of ^{235}U fission cross section made since~1964 and some recent absolute ^{238}U fission cross section are discussed. The measurements were made using the AEP Van de Graaff, Cockcroft-Walton and heavy water moderator reactor. Five measurements concern the thermal and resonance energy range, the remainder are in the energy ranges 0.03-5.6 MeV and/or 14-18 MeV. On the whole the ^{235}U data agree with the other available data and the new ^{238}U absolute data between 4 and 5.5 MeV are greater than the ENDF/B-V evaluation and agree with JENDL-2.

As is known to all, the neutron-induced fission cross section of ^{235}U is one of the most frequentely used nuclear standard reference data. The ^{238}U fission cross section is frequentely used as a reference standard too. They are also of significant importance in reactor calculation. In consideration of the importance of these two fission cross sections in nuclear applications, a series of measurements of these two fission cross sections have been made at the Institute of Atomic Energy, Beijing (AEP). In this paper the results of the various experiments performed at the AEP Van de Graaff, Cockcroft-Walton and the heavy water moderated reactor will be presented.

The first absolute measurement of ^{235}U fission cross section for thermal neutrons was made at the AEP heavy water moderated reactor[1]. The ^{235}U fission cross section ratio relative to the natural boron absorption cross section was measured using the nuclear emulsions loaded ^{235}U and natural boron separately. They were irradiated simultaneously in the mono-energetic neutron beam provided by the single crystal spectrometer. The absolute value of the ^{235}U thermal neutron fission cross section (582±9 barns) was obtained by making use of the known value of thermal neutron absorption cross section of natural boron which was just measured at the same laboratory[2]. The experimental result is slightly lower than that of the new evaluations (584.7±1.7 barns[3] and 585.4±1.7 barns[4]), but it is in accordance with them within the scope of experimental error.

A relative measurement of ^{235}U fission cross section in the thermal neutron energy region was also made at the AEP heavy water moderated reactor[5]. The measurement covered the energy region from 0.01 to 1.6 eV neutron energy, and the mono-energetic neutrons were provided by the single crystal spectrometer as well. A gaseous scintillation fission chamber which was a cylinder 10 cm in diameter and 10 cm in height and was filled with helium gas of 1.5 atmosphere was used for detecting fission fragments. A BF_3 proportional counter was used for detecting neutrons. This experiment relies on the thermal value[1] for the cross section normalization. On the basis of experimental data the resonance parameters were analyzed by means of the multiple level formula given by Feshbach et al[6]. The results obtained are as follows: E_o~-1.38 eV, $\sigma_{f_o}\Gamma^2$~473 barn.eV^2; E_o=0.290±0.006 eV, Γ=124±12 meV, $\sigma_{f_o}\Gamma$=10.3±1.2 barn.eV; E_o=1.14±0.04 eV, Γ=154±8 meV, $\sigma_{f_o}\Gamma$=12.9±0.9 barn.eV. These data are in agreement with that given in BNL-325 (1973)[7].

A shape measurement of ^{235}U fission cross section in the neutron energy range from 0.04 to 100 eV was carried out also[8]. A mechanical selector installed beside the horizontal channel of the heavy water moderated reactor was employed for this measurement.

The fission chamber used in this experiment employed 10 fission foils arranged in parallel with each other and alternated with the anodes. A BF_3 proportional counter was used as a neutron detector. The measurement was carried out in three neutron energy regions, i.e. 0.04-1 eV, 0.6-10 eV and 4.5-100 eV. The results of the ^{235}U fission cross section were roughly in accordance with that of the other laboratories and the resonance parameters obtained were in agreement with that given by Ref.5.

The ratio of the ^{233}U, ^{235}U thermal fission cross sections was also measured using the single crystal spectrometer[9]. The fission chamber employed two fission foils in back to back geometry. The ^{233}U deposit mass determination was carried out by measuring the alpha decay rate in a low solid angle equipment. The half life of the ^{233}U used in this determination was (159300±1600) years. Besides the alpha decay rate measurement in a low solid angle equipment, the ^{235}U deposit mass was determined by weigh as well. Two samples of ^{235}U and one sample of ^{233}U were used in this experiment. A result of 0.916±0.018 was obtained for the fission cross section ratio.

In order to investigate the fission cross section shapes of the fissile nuclei, a relative energy dependance of ^{239}Pu, ^{233}U, ^{235}U fission cross sections and the ratio of these cross sections in 0.02-0.30 eV neutron energy region were measured as well[10]. The shapes of these cross sections were measured relative to the $^{6}Li(n,t)^{4}He$ reaction cross section simultaneously. In this experiment a non-pedestal Au(Si) surface barrier type detector was used for detecting the tritium particles. It was placed in the ionization chamber behind the ^{233}U, ^{235}U, ^{239}Pu and ^{6}Li samples. The results obtained were normalized to 585±2 barns[9] for thermal neutron fission cross section of ^{235}U. The results of ^{235}U fission cross section in the neutron energy region from 0.02 to 0.1 eV were in accordance with Langner[11] and slight higher than Langner in 0.1-0.3 eV region.

In the fast neutron energy region, a measurement of ^{235}U fission cross section and the ratio of ^{233}U, ^{235}U fission cross sections were made at the AEP Van de Graaff and Cockcroft-Walton accelerators[12]. This measurement covered the neutron energy region from 0.03 to 5.6 MeV and from 14 to 18 MeV. The fission chamber employed two fission foils in back to back geometry. It was filled with argon and 5-10% methane gases. The isotopic components were given by three independent mass spectrographic analyses. The neutron flux measurements at 0.5 and 1.0 MeV neutron energy were made by means of the proton recoil proportional counter, and then the absolute values of the ^{233}U and ^{235}U fission cross sections at these two points were obtained. They were 1.962±0.098 barns and 1.964±0.098 barns for ^{233}U, 1.148±0.058 barns and 1.243±0.063 barns for ^{235}U at the 0.5 and 1.0 MeV neutron energy respectively. The results of ^{235}U fission cross section at 0.5 and 1.0 MeV are in agreement with the ENDF/B-V evaluation within the scopes of experimental uncertainty.

A measurement of the ratio of ^{239}Pu, ^{235}U fission cross sections in the neutron energy regions from 0.3 to 5.6 MeV and from 14 to 18 MeV was also made at the AEP[13]. The fission chamber used in this experiment was similar to that of Ref.12. In order to shorten the rising time and reduce the width of the ionization impulse, the fission chamber was filled with methane gas of one atmosphere. At the same time the fast electronic circuits was used. The results of measurement are quite good in accordance with the CNDC evaluations[14].

The absolute measurement of ^{235}U fission cross section induced by 14.7 MeV neutrons[15] was begun at the time when 5% differences existed in determination of this cross section in the 14 MeV neutron energy region[16-18]. This experiment was carried out simultaneously with the measurement of ^{239}Pu fission cross section using the time correlated associated particle technique. Neutrons with energy 14.7 MeV were produced by $T(d,n)^{4}He$ reaction on the 600 kV Cockcroft-Walton accelerator at the AEP. The fission ionization chamber was a cylindrical one 10 cm in diameter and 5 cm

in length, which was composed of two identical halves. It was also filled with methane gas of one atmosphere. The samples of uranium and plutonium were electrodeposited on platinum backing. Three methods were used to determine the quantity of uranium contained in the samples: by direct weighing, by alpha counting in a low solid angle equipment and by titration. For plutonium the alpha counting technique and the constant current Coulomb method were used. The nonuniformity of the deposited layers was tested by alpha counting. From this experiment it was obtained that the ^{235}U and ^{239}Pu fission cross sections induced by 14.7 MeV neutrons were 2.098±0.040 barns and 2.532±0.050 barns respectively. The result of the ^{235}U fission cross section measurement is shown in Fig.1 compared with other time correlated associated particle measurements and ENDF/B-V. The agreement among these measurements is excellent and they confirm the ENDF/B-V evaluation.

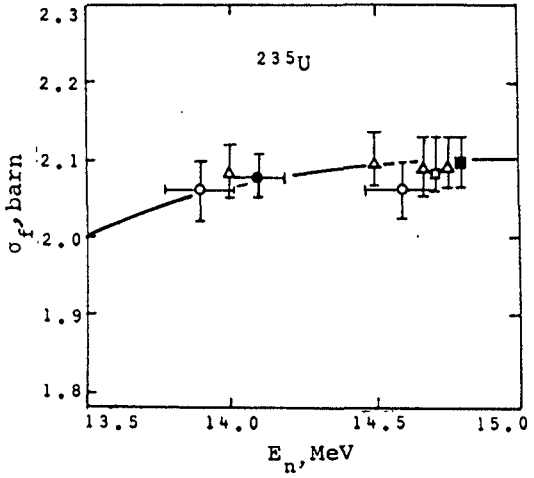

Fig.1 Comparison of the AEP value of ^{235}U fission cross section with ENDF/B-V and some reported values obtained by TCAP method in the 14 MeV range

- ■ Li jingwen (1983)
- ▲ Adamov (1979)
- ● Wasson (1981)
- ○ Cancé (1978)
- ▫ Arlt (1981)
- — ENDF/B-V

In addition, a measurement of ^{235}U fission cross section for 14.2 MeV neutrons is now being investigated using TCAP method at the AEP. The experimental condition is similar to that of Ref.15, only some new samples of ^{235}U are used besides the older one. The experimental data has been taken and analysis is nearly complete. At the present state of the analysis the preliminary result indicates value in good agreement with that of the ENDF/B-V evaluation.

As for the ^{238}U fission cross section, a determination of the ^{238}U fission cross section in the 4.0-5.5 MeV neutron energy region has been made at the AEP Van de Graaff[22]. For this experiment a proton recoil semiconductor detector telescope and fission ionization chamber placed back-to-back system were employed (as shown in Fig.2). A piece of copper 0.15 mm in thickness mounted between the fission foil and the hydrogen radiator isolated the proton recoil telescope from the fission ionization chamber. The fission ionization chamber was filled with 1 atm methane gas, while the

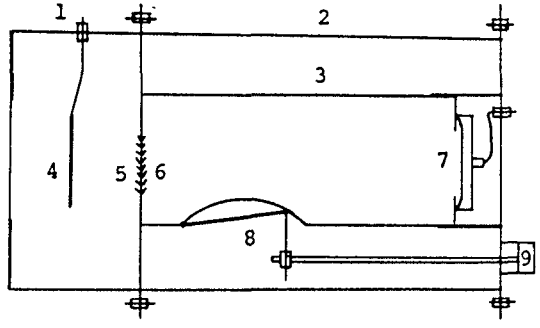

Fig. 2 Schematic diagram of the back-to-back detection system

1 fission ionization chamber, 2 proton recoil telescope
3 diaphragm cylinder, 4 collecting electrode
5 ^{238}U fission foil, 6 polyethylene
7 semiconductor detector, 8 stainless steel disc
9 micro-motor

proton recoil telescope was kept at 10^{-2}mm Hg vacuum. The semiconductor detector was a Au(Si) surface barrier detector with 700 mm^2 sensitive area. To measure the background produced by neutrons in the semiconductor detector a movable stainless steel disc was mounted between the radiator and the semiconductor detector. By a micro-motor the disc could be moved in or out of the viewing field of the proton recoil telescope. The whole detector system was 10 cm in diameter and 17 cm long.

U_3O_8 (with 99.9% ^{238}U abundance) was deposited onto platinum backing 3.2 cm in diameter by electrodeposition. The amount of the deposit was determined by residue weighing with an accuracy better than 1%. The hydrogen radiator was made of thin polyethylene foil 2.9 cm in diameter. The impurity of the polyethylene foil was less than 0.2%. To measure the areal density of the polyethylene foil a 10^{-5} balance was used to measure the weight and an optical microscope was used to measure the size of the foil to 0.003 cm accuracy. The error in the measured areal density of the polyethylene foil was less than 1%. Three pieces of fission foil and two pieces of polyethylene foil were used to obtain four different combinations. Corrections for fission detection efficiency, fission layer self-absorption, neutron flux attenuation, neutron scattering, effective diaphragms, n,p differential cross section and the geometry factor were made for this experiment.

The fission cross sections of ^{238}U obtained in this experiment for neutron energies 4.0 MeV, 4.5 MeV, 5.0 MeV, 5.5 MeV are 0.566±0.011 barns, 0.565±0.011 barns, 0.562±0.011 barns and 0.553±0.014 barns respectively.

Fig.3 shows a typical fission fragment pulse height spectrum measured in this experiment.

Fig.4 shows a recoil proton pulse height spectrum obtained with 5.0 MeV neutrons.

Fig.5 shows a comparison of the ^{238}U fission cross sections measured in this experiment with that of ENDF/B-V and JENDL-2 evaluations[23].

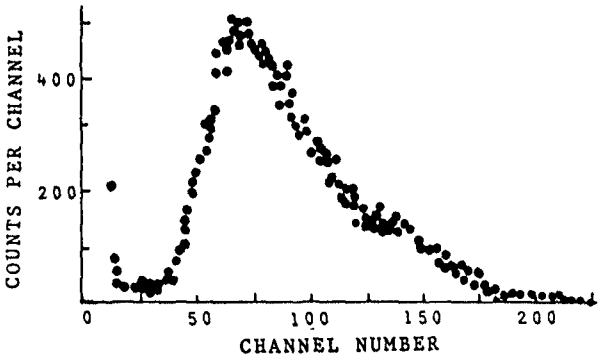

Fig.3 ^{238}U fission fragment pulse height spectrum

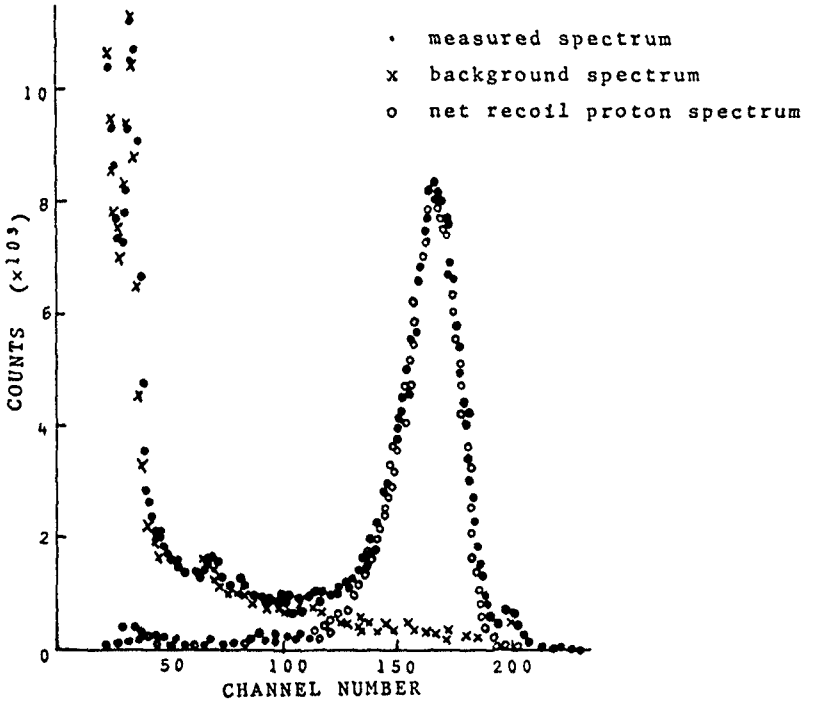

Fig.4 Recoil proton pulse height spectrum

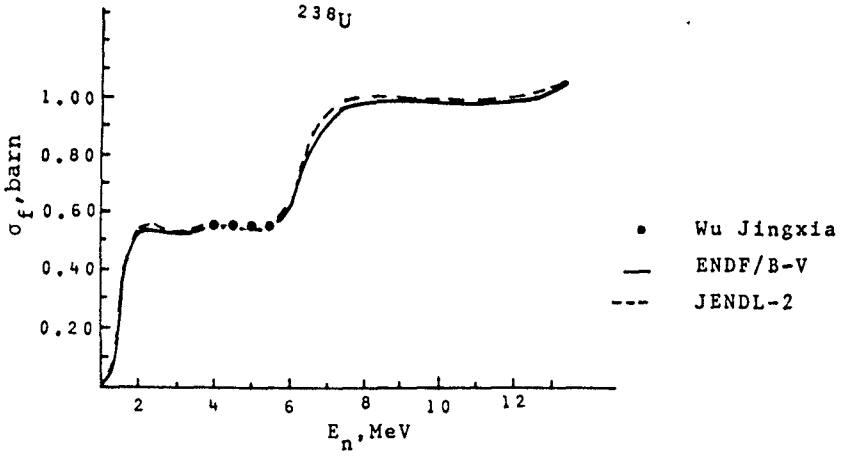

Fig.5 Comparison of the AEP values of ^{238}U fission cross section with ENDF/B-V and JENDL-2

As it can be seen in Fig.5 the AEP results show good agreement with the JENDL-2 evaluation.

The gists of the AEP measurements of ^{235}U and ^{238}U fission cross section are listed in Table 1.

Taking a view of the present status of experimental data of fast neutron-induced fission cross section of ^{235}U, it appears to be very good agreement among the modern measurements near the 14 MeV energy region. It seems that the ^{235}U fission cross section value for 14 MeV neutron energy is well known (1%) and could be used for normalization of shape measurements. But except the data around the 14 MeV point the experimental data in various energy regions couldn't be achieved the accuracy requirements (1%). In some neutron energy regions especially in a few MeV neutron energy region, the results of many measurements differ from each other by more than the experimental uncertainties. Some of them differ by up to 10% (see, for example, figures given in Ref.24, 25) while the measurements claim accuracies in some cases of 2%. It is worth to

Table 1 Gists of the AEP Measurements of $^{235}U(n,f)$ and $^{238}U(n,f)$ cross section

Nuclei	Quantity	Neutron energy	Comments	Accuracy	Ref.
^{235}U	σ_f	0.0253eV	nucl. emulsion rel. to σ_a(P)	1.5%	1
^{235}U	σ_f	0.016-1.6eV	scint. chamber norm.to σ_f^o=582±9b	2.0%	5
^{235}U	σ_f	0.04-100eV	fiss. chamber Ar, 5% CO_2	2-6%	8
^{235}U	$3\sigma_f/5\sigma_f$	0.0253eV	fiss. chamber Ar, 5% CH_4 back-to-back		9
^{235}U	σ_f	0.02-0.3eV	fiss. chamber semic. detector rel. to $\sigma_a(^6Li)$ norm.to $^5\sigma_f^o$=585±2b	1.2-3%	10
^{235}U	σ_f $3\sigma_f/5\sigma_f$	0.03-5.6MeV; 14-18MeV	fiss. chamber Ar, 5% CH_4 hydr.prop.counter back-to-back	2.4-2.9%	12
^{235}U	$9\sigma_f/5\sigma_f$	0.03-5.6MeV; 14-18MeV	fiss. chamber, CH_4 back-to-back	2.0-2.6%	13
^{235}U	σ_f	14.7MeV	fiss. chamber, CH_4 TCAP, TOF	1.9%	15
^{238}U	σ_f	4.5-5.5MeV	fiss. chamber, CH_4 proton rec. tel. back-to-back	2.6%	22

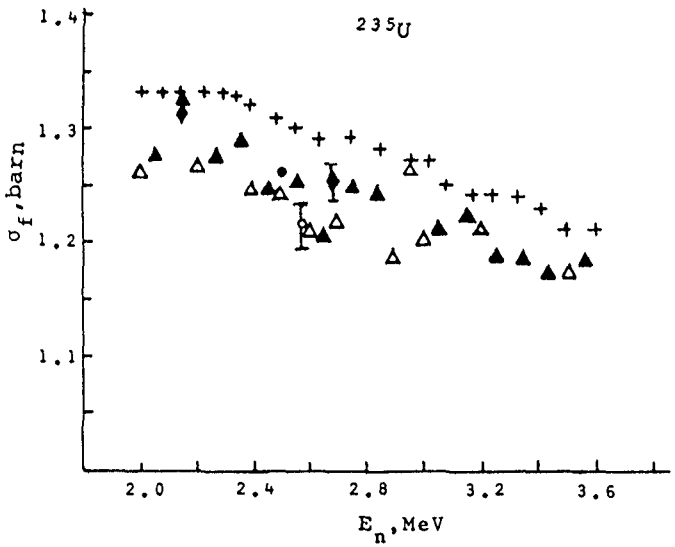

Fig.6 Some experimental results of ^{235}U fission cross section near 2.5 MeV

△ Barton (1976)
▲ Leugers (1976)
† Kari (1978)
• Cancé (1981)
♦ Karlson (1982)
o Arlt (1980)

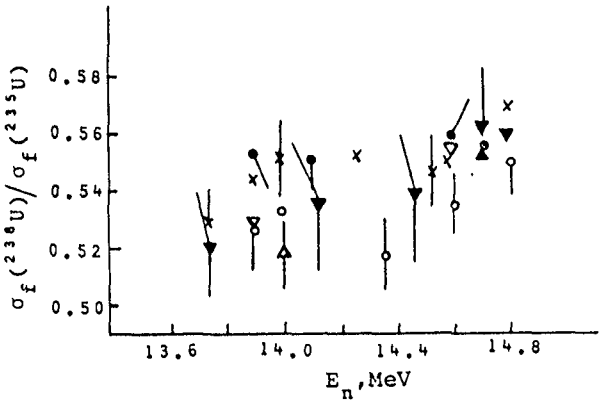

Fig. 7 Some experimental results of $\sigma_f(^{238}U)/\sigma_f(^{235}U)$ near 14 MeV

▲ Arlt (1981)
o Coates (1976)
▼ Varnagy (1980)
⊛ White (1976)
• Cance' (1978)
▽ Adams (1961)
× Cierjacks (1976)
△ Uttley (1956)
⊕ Adamov (1979)

point out especially that the latest absolute cross section measurements near 2.5 MeV carried out by different authors give rather conflicting results and differ obviously from each other (see Fig.6). In other words, it is significant to make some precision measurements in this energy region. As for the experimental method, although one cannot rule out the possibility of existing systematic error in use of time correlated associated particle method, it might be the most desirable method at the present time after all. In the light of specific conditions at the AEP, a measurement of ^{235}U fission cross section in the 2.5 MeV neutron energy region with the TCAP technique is being taken into consideration.

As for the ^{238}U fission cross section, the conspicuous problem is that of existing the scattered experimental data in the important neutron energy region, the 14 MeV neutron energy region (see Fig.7). It cause some confusions in the normalization of shape measurements of this cross section. So it is of great value to measure the ^{238}U fission cross section in the 14 MeV neutron energy region. This measurement is being taken into consideration at the AEP as well.

References

1. Ye Chuntang et al., Atomic Energy Sci. Techn., 4, 349(1964).
2. Yuan Hanrong et al., Atomic Energy Sci. Techn., 2, 127(1964).
3. E.J.Axton, European Appl. Rept.-Nucl. Sci. Techn., 5, 609(1984).
4. Yuan Hanrong, On Evaluation of Thermal Neutron Standard Cross Section, 1983, to be published.
5. Yuan Hanrong et al., Chinese Atomic Energy, 11, 1038(1964).
6. H.Feshbach et al., Phys. Rev., 96, 448(1954).
7. S.F.Mughabghab et al., BNL-325, 3rd adition, Vol.1, 1973.
8. Yu Ansun et al., Atomic Energy Sci. Techn., 10, 1114(1964).
9. Jia Wenhai et al., Atomic Energy Sci. Techn., 1, 19(1975).
10. Zhou Huimin et al., Atomic Energy Sci. Techn., 2, 193(1977).
11. I.Langner et al., KFK-750 (1968).
12. Yan Wuguang et al., Atomic Energy Sci. Techn., 2, 133(1975).
13. Deng Xinlu et al., Atomic Energy Sci. Techn., 1, 12(1981).
14. Liu Jichai, hsj-75005(bp), 1976; hsj-77061(bp), 1978.
15. Li Jingwen et al., Chinese Nucl. Phys., 5, 45(1983).
16. P.H.White, J.Nucl. Energy, A/B 19, 325(1965).
17. J.B.Czirr et al., Nucl. Sci. Eng., 57, 18(1975).
18. M.Cancé et al., Nucl. Sci. Eng., 68, 197(1978)
19. V.M.Adamov et al., Proc. of the Int. Conf. on Nuclear Cross Sections for Technology, Knoxville, 1979, NBS Spec. Publ. 594, p.995, 1980.
20. R.Arlt et al., Kernenergie, 24, 48(1981).
21. O.A.Wasson et al., Nucl. Sci. Eng., 80, 282(1982).
22. Wu Jingxia et al., Chinese Nucl. Phys., 5, 158(1983).
23. Y.Kanda, Private communication, 1984.
24. V.G.Pronyaev et al., INDC (NDS)-146, 107, 1983.
25. M.R.Bhat, INDC(NDS)-146, 119, 1983.
26. M.Varnagy et al., Proc. of the 5th all Union Conf. on Neutron Physics, Kiev, 15-19 Sept. 1980, Vol.3. p.13.
27. S.Cierjacks et al., ANL-76-90, 94(1976).
28. M.S.Coates et al., NEANDC(UK)116 AL (1976).
29. P.H.White et al., J.Nucl. Energy, 21, 671(1967).
30. B.Adams et al., J.Nucl. Energy, 14, 85(1961).
31. C.A.Uttley et at., AERE NP/R 1996(1956).
32. D.M.Barton et al., Nucl. Sci. Eng., 60, 369(1976).
33. K.Kari, KFK-2673 (1978).
34. A.D.Carlson, Proc. of the Int. Conf. on Nuclear Data for Science and Technology, Antwerp, Sept. 1982, p.456.
35. B.Leugers et al., ANL-76-90, p.246 (1976).
36. M.Cance', CEA-N-2194 (1981).
37. R.Arlt et al., Proc. of the Int. Conf. on Nuclear Cross Sections for Technology, Knoxville, 1979, NBS Spec. Publ. 594, p.990, 1980.

174

ABSOLUTE MEASUREMENT OF THE ^{235}U FISSION CROSS-SECTION AT 4.45 MeV NEUTRON ENERGY USING THE TIME-CORRELATED ASSOCIATED PARTICLE METHOD (TCAPM)

R. ARLT, C.M. HERBACH, M. JOSCH, G. MUSIOL,
H.G. ORTLEPP, G. PAUSCH, W. WAGNER
Technical University of Dresden,
Dresden, German Democratic Republic

L.V. DRAPCHINSKY, E.A. GANZA, O.I. KOSTOCHKIN,
S.S. KOVALENKO, V.I. SHPAKOV
Khlopin Radium Institute,
Leningrad,
Union of Soviet Socialist Republics

Abstract

Following the recommendations of the IAEA Consultant's Meeting on the ^{235}U Fast Neutron Fission Cross Section at Smolenice 1983 the ^{235}U fission cross-section was measured absolutely at a neutron energy of (4.45 ± 0.20) MeV using the time correlated associated particle method. Neutrons were produced in the D(d,n) ^{3}He reaction. Fission events were counted by a multi plate fission chamber in coincidence with the ^{3}He particles identified by a silicon detector telescope.

The measurements resulted in a value of (1.057 ± 0.022) b for the ^{235}U fission cross-section at a neutron energy of (4.45 ± 0.20) MeV.

Following the recommendations of the IAEA Consultant's Meeting in Smolenice, 1983 [1], the ^{235}U fission cross-section was measured absolutely at (4.45 ± 0.2) MeV neutron energy by means of the TCAP method. Employing an experimental arrangement similar to our 8.4 MeV measurements [2-4] an accuracy of 2.1 % was obtained. The measured value σ_f = (1.057 ± 0.022) b is about 5% lower than the ENDF/B-V evaluation and supports the result of POENITZ [5].

Experimental Method

The principle of our TCAPM measurements is shown in fig. 1. An AP detector registers the associated charged particles (AP) of the neutron producing reaction within a fixed cone $\Delta\Omega_{AP}$. the neutrons belonging to the registered AP form a cone $\Delta\Omega_n$ which has to be intercapted completely by the homogeneous fission foils placed inside an ionization fission chamber. Under this condition the fission cross-section is given by the number N_f of fission events registered in coincidence with an AP, divided by the number N_{AP} of counted associated particles and the number n of fissionable nuclei per unit of area. The experimental set-up (fig. 2) is placed inside a 40 cm in diameter vacuum chamber coupled to the ion guide of the 5 MV tandem Van de

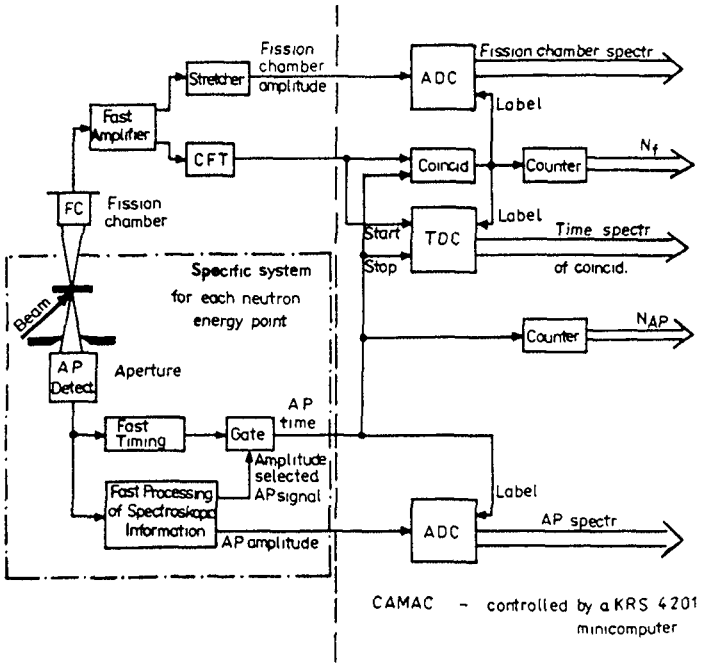

Fig. 1: Principle scheme of the TUC/RIL fission cross-section measurements

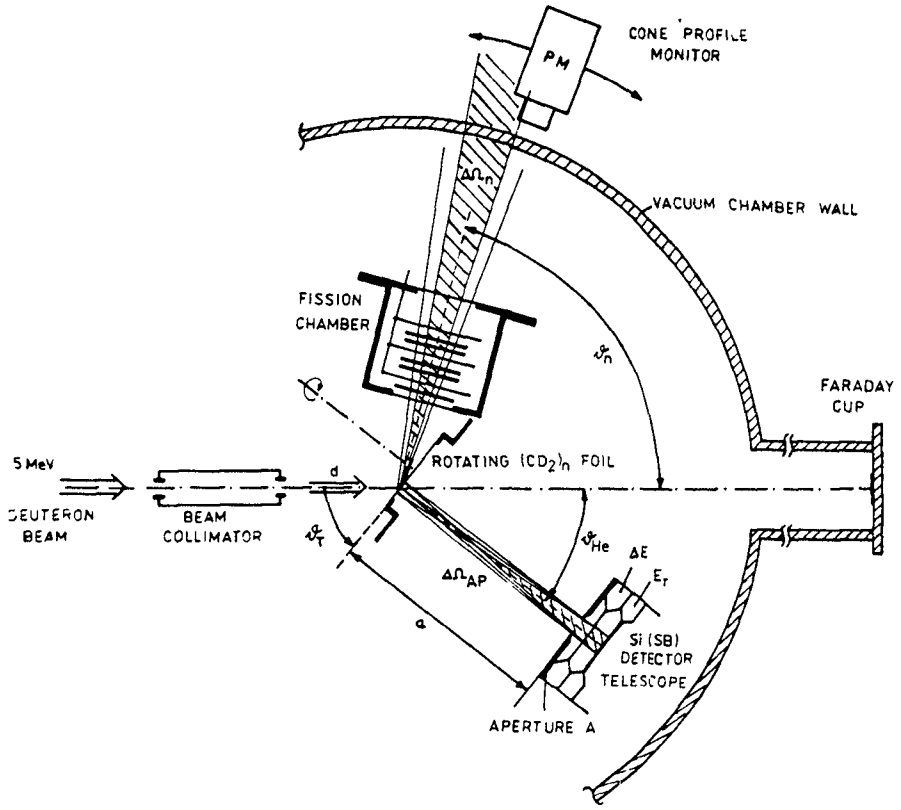

Fig. 2: Experimental set-up of the 4.45 MeV measurement

Graaff accelerator of the CINR Rossendorf (GDR). A 5 MeV deuteron beam is focussed on a rotating deuterated polyethylene foil of about 1 mg/cm^2 thickness and generates neutrons by the D(d,n)^{3}He reaction. The beam collimator determines the spot of neutron production and limits possible drifts of the beam focus. The cone of registered associated ^{3}He particles is fixed by an aperture A.

Because of the relative broad energy distribution of the associated helions due to the target foil thickness and the effect of the cone aperture on the reaction kinematics, the identification of the AP by single pulse hight spectrometry would cause a high portion of background events due to background reaction products (especially alpha particles from the ^{12}C (d,α) reaction) and pile-up pulses of scattered deuterons [6,7]. Therefore a telescope of two completely depleted Si (SB) detectors was used together with a fast particle identification system [8,9] based on a linear approximation of the BETHE-BLOCH equation in small dynamic ranges. The basic ideas of the used electronic system are described as follows:

i) A fast timing signal (STROBE) with ns resolution is obtained as a fast coincidence of the pulses formed by constant fraction timing (CFT) of the ΔE and E_r detector current pulses.

ii) Amplitude information of the ΔE and E_r channels is obtained by integrating the clipped charge pulses using fast gated integrators [10]. The STROBE signal starts the integration. Deuteron pulses are suppressed by setting the CFT threshold in the ΔE channel high enough . This leads to a strong reduction of the rate of events which have to be processed.

iii) The total energy (E_g) and particle amplitude (A_p) signals representing linear sums of the ΔE and E_r amplitude signals with different coefficients are formed by a fast particle identification circuit (PI) which is a modified version of the circuit described in [11]. Associated particles are selected by means of discriminator thresholds in the E_g and A_p spectra. The A_p spectrum only contains events with a total energy lying within the E_g window.

iv) The PI circuit represents a gate for the delayed STROBE signal. If all threshold conditions are fulfilled and no pile-up is detected by the fast integrators, the STROBE is allowed to pass the gate and then represents the AP timing signal t_{AP} containing the complete AP information.

The minimum timing interval between t_{AP} signals is given by the fixed (~1μs) dead-time of the PI circuit. Counting losses due to this dead-time influence only the total AP rate, but not the measured cross-section. Therefore, no dead-time correction is necessary. AP counting rates up to

3000/s were obtained with the described system, using a ΔE detector of 9μm thickness. The portion of background events was determined by replacing the deuterated by a non-deuterated target foil of a comparable thickness [12]. The construction of the target support allows an exchange without opening the vacuum chamber. Fig. 3 shows a typical A_p spectrum, the amount of alphas registered within the ^{3}He window is illustrated by hatching. Because of the thinner ΔE detector the separation between ^{3}He and ^{4}He particles is not as good as in the 8.4 MeV experiment [3]. Using a 13μm thick ΔE detector, alpha particles from the ^{12}C(d,α) reaction are stopped and do not reach the E_r detector. Therefore, the background is much lower (fig. 4), but the effective target foil thickness and consequently the AP counting rate are reduced because of the minimum ^{3}He energy which is necessary to pass the detector.

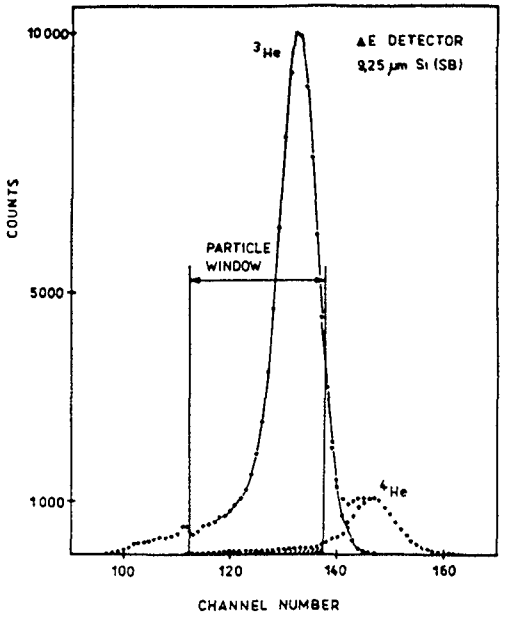

Fig.3: Particle amplitude spectrum obtained with a 9μm ΔE detector. The measured background spectrum is normalized to the corrected alpha peak.

Tab. 1 summarizes the main features of the neutron production and AP detection system. Neutron cone profile and energy distribution of the in-cone neutrons were calculated from the reaction kinematics considering

i) the deuteron energy loss within the target foil,
ii) the finite beam focus including drifts within the limits given by the beam collimator,
iii) diameter and distance of the AP aperture,
iv) the energy- and angular dependence of the D(d,n) reaction cross-section.

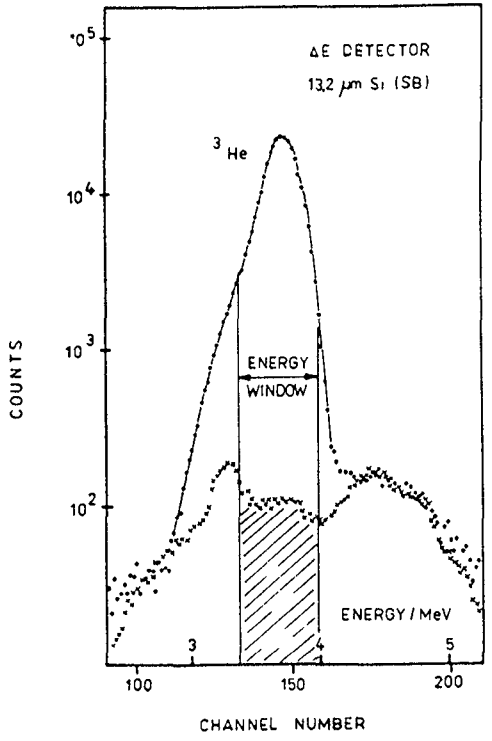

Fig.4: Total energy spectrum obtained with a 13μm ΔE detector. The measured background spectrum is normalized.

The uncertainty of E_n (tab.1) includes a maximum possible deviation of the telescope angle δ_{He} relative to the beam axis ($\pm 1^o$) as well as the effect of the varying foil thickness. A five plate ionization fission chamber filled with methane at a pressure of ~110 kPa was used to detect fission events. Fission fragment energy loss spectrum and fission chamber timing signal are obtained by stretching the fast current pulses to a length of ~1μs [13] and by constant fraction timing (CFT), respectively (fig. 1).

Deuteron beam	
Deuteron energy	5 MeV
Beam current	(400-600) nA
Beam collimator	2 apertures with diameters of 3mm
Target foil	deuterated polyethylene
thickness	(0.5-1.8) mg/cm^2
Angle relative to the beam axis	$\delta_T = 52^o$
Rotation frequency	(2-4) Hz
Detector telescope	
Angle relative to the beam axis	$\delta_{He} = 38^o$
Detector ΔE	9μm / 13 μm Si(SB)
Detector E_r	37 μm Si(SB)
Calculated neutron energy distribution	
Averaged energy E_n	(4.45 ± 0.20) MeV
Half width	0.23 MeV
Total width of the calculated neutron cone profile	8^o

Tab.1: Main features of the experimental set-up

The CAMAC data acquisition system [14,15] is designed to collect all data which are necessary to perform the corrections of the measured cross-section. Coincident fission events are identified by a fast coincidence circuit and labeled in both the coincidence timing and fission chamber spectra. The particle amplitude spectrum A_p is monitored during the whole experiment and labeled with the t_{AP} signal. This allows a correct determination of the ^{4}He background within the ^{3}He window taking into account the effect of target foil waste.

Measurements

Three independent measurements were carried out using the same experimental set-up and the same set of fission foils, prepared at the Khlopin Radium Institute (KRI) Leningrad by HF sputtering. The areal densities (tab.2) were determined at the KRI by low geometry alpha counting and refer to half-lives listed in tab.3. During the measurements, the neutron cone profile was checked continuously by means of a scintillation detector operated in coincidence with the AP detector, and the fission chamber was adjusted to the maximum of the measured distribution. An experimental determination of the

Isotope	Isotopic composition %	Half-live
^{234}U	0.00111 ± 0.00001	(2.446 ± 0.007) 10^5 Y [21]
^{235}U	99.9972 ± 0.0003	(7.0381 ± 0.0048) 10^8 Y [22]
^{236}U	0.0017 ± 0.0003	(2.391 ± 0.018) 10^7 Y [23]

Tab.2: Isotopic composition of the fission foils obtained by mass spectrometry (^{236}U) and alpha spectroscopy (^{234}U)

Position	Angular extent	Areal density	Inhomogenity
1/F	20.5^o	445.0 ± 1.0 %	1.0 %
2/B	18.6^o	267.2 ± 0.75%	0.8 %
3/F	17.6^o	401.0 ± 1.0 %	0.2 %
4/B	16.2^o	256.7 ± 0.75%	1.0 %
5/F	15.3^o	403.8 ± 1.0 %	0.7 %

Tab.3: Properties of the used fission foils. The angular extent results from the diameter of the fissile layer ant it's distance from the neutron source.
F - forward, B - backward geometry

cone "tail" down to 0.01% of the maximum value became possible using a stilben scintillator and a n/γ discrimination circuit [16] (fig.5). The coincidence rate was corrected for random coincidences, and the effect of neutron scattering at the vacuum chamber wall (0.3 cm stainless steel) could be taken into account by performing a further cone profile measurement where a chamber wall of the double thickness was simulated by an additional scatterer.

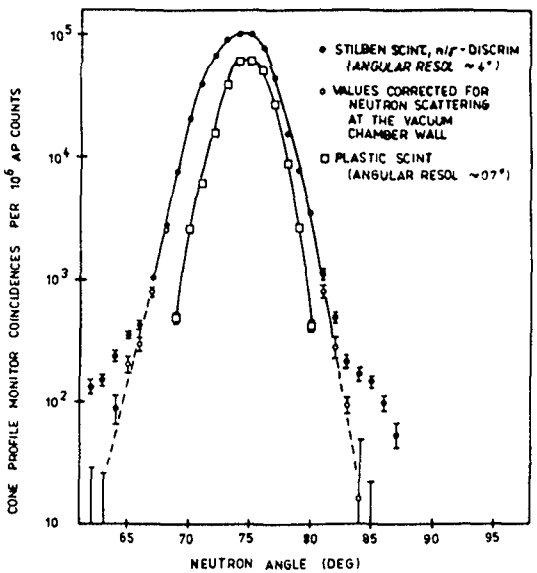

Fig. 5 Measured neutron cone prolile

During the first and the second measurement a 13μm thick ΔE detector was applied. Because of the low alpha background no particle amplitude spectrum was generated in the second measurement, and the background correction was determined using the total energy spectrum (fig. 4). The energy scale was calibrated by means of thin ^{239}Pu - ^{241}Am - ^{244}Cm alpha sources.

By applying a thinner ΔE detector in the third measurement, the AP counting rate was increased (tab.4). To determine the shape of the ^{3}He peak, particle spectra were recorded in coincidence with the neutrons registered by the cone profile monitor.

	Measurements		
	I Aug. 83	II Febr. 84	III March 84
ΔE detector thickness	13.2 μm	13.2 μm	9.25 μm
Average AP counting rate	1300/s	1500/s	2100/s
AP background correction	0.10 % ± 0.20 %	0.57 % ± 0.25 %	3.89 % ± 1.00 %
AP/fission coincidence time resolution	3.5 ns	3 ns	6 ns

Tab. 4: Experimental conditions averaged over the whole measuring time

This is important in the case of a 9 μm ΔE detector, where the normalization factor for the background spectrum has to be determined from the undisturbed alpha peak of the particle amplitude spectrum.

Fission chamber and coincidence timing spectra of the second measurement are shown as examples in fig. 6-7.

Result

For each measurement the ratio

$$r^{i}_{exp} = \frac{(N^{i}_{f} - N^{i}_{rc})\,(1 + \varepsilon_{ext})}{N^{i}_{AP}\,(1 - \varepsilon^{i}_{b})}$$

was determined. This value represents the number of coincident fissions, corrected for random coincidences (N^{i}_{rc}) and the amount ε_{ext} of fission chamber pulses lower than the CFT threshold, related to the number of counted "true" associated helions. Thereby the numbers N_{rc} were obtained from the coincidence timing spectra. The corrections ε_{ext} were calculated by linear extrapolation of the plateau region of the measured coincident fission chamber spectra to pulse hight zero (fig.6). The portions ε_{b} of

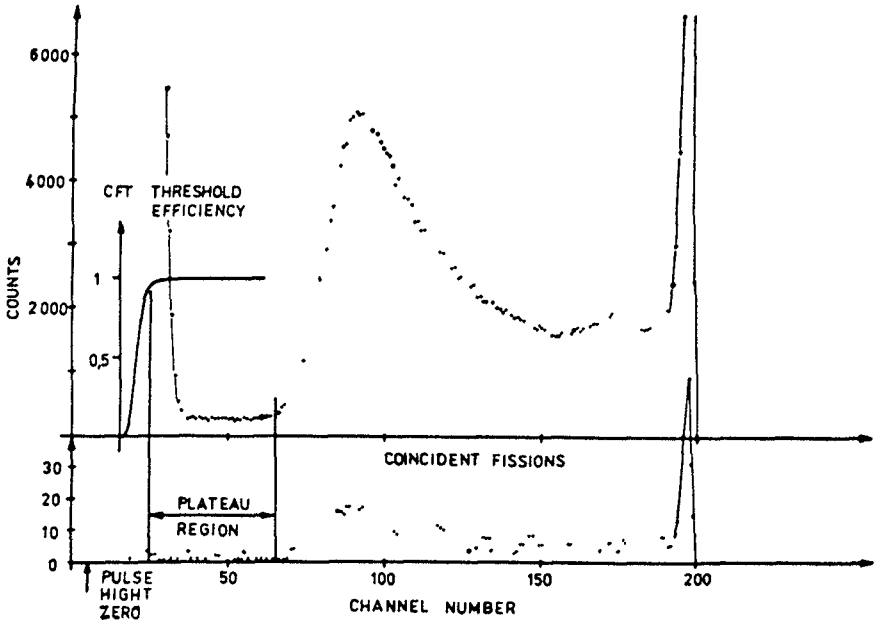

Fig.6. Fission chamber spectrum of the second measurement

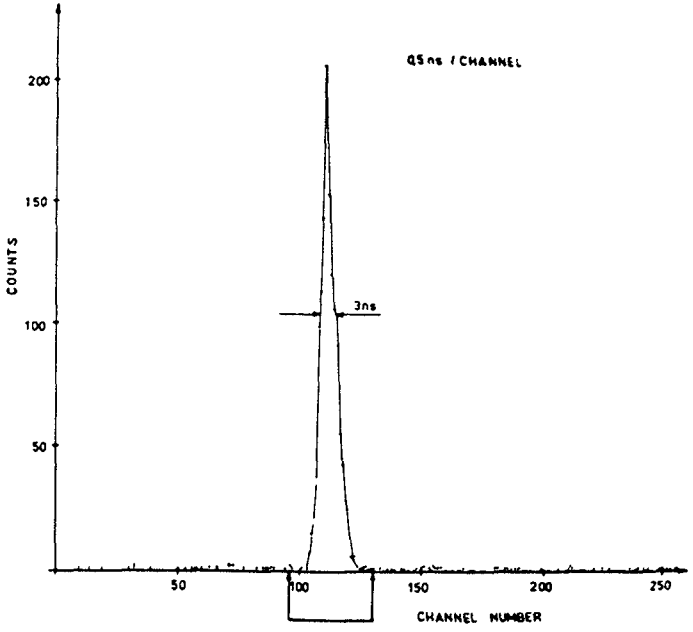

Fig 7. Coincidence timing spectrum of the second measurement

	Correction	Error contribution
Fissile layers		
- Areal density		0 93 %
- Inhomogenity		0 72 %
Fission chamber efficiency		
- Extrapolation to pulse hight zero	1 18%	0 26%
- Fragment absorption	2 00 %	0.85 %
Counting coincidences		
- Statistics		1 26 %
- Random coincidences	1 40 %	0 17 %
AP counting		
- Background	2 32 %	0 67 %
Neutron cone		
- Neutron scattering	0 25 %	0 40 %
- Effective fission foil thickness due to the cone aperture	0 05 %	0 05 %
Result σ_f = (1 057 $\pm$ 0 022) b		2 10 %

Tab 5 Summary of the error contributions and final result of the fission cross-section measurement

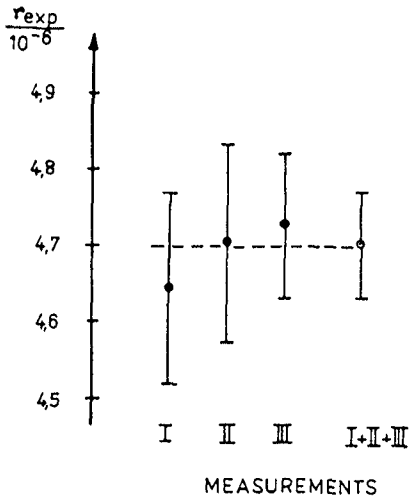

Fig.8: Measured ratios r_{exp} of the three independent measurement

background events within the AP window were determined from the background spectra, which were normalized to the background peaks of the AP spectra recorded during the runs. In this way the ratio r_{exp} includes all corrections, which are obtained from the recorded spectra and may have changing values due to the actual threshold settings and detector properties. Fig. 8 shows the excellent agreement of the three independent measurements within the error limits, given by the statistics of N_f and N_{rc} and the uncertainties of the corrections. After summarizing the three measurements, the final result (tab.5) was calculated from the equation

$$\sigma_f = \frac{r_{exp}}{(1 - \varepsilon_{abs})} \cdot \frac{1 + \varepsilon_{sc}}{n(1 + \varepsilon_T)}$$

The correction ε_{abs} for fission fragment absorption within the fissile layers is based on a R = 7.5 mg/cm^2 range [17], but a $\pm$ 2 mg/cm^2 uncertainty due to the insufficient knowledge of an effective range considering the realistic properties of the used fissile layers [18]. The neutron scattering correction ε_{sc} was determined by means of a Monte-Carlo simulation, taking into account the real experimental geometry [19]. The correction ε_T considers the enlarged effective fission foil thickness due to the cone aperture. It was obtained from the calculated two-dimensional cone profile.

Further efforts will be directed to more precise measurements of the areal densities of the fission foils.

Acknowledgements

The authors thank Prof. K.A. Petrshak for his stimulating interest and discussions throughout this program; I.D. Alkhazov, H. Bohne, A.V. Fomichev, V. Kusmin, H. Müller, K. Merla, and A. Schnalke for their assistance during the runs; V.N. Dushin for calculating the scattering correction; W.D. Fromm for his valuable support and advice in programming the on-line experiment; H.Maerten for placing at our disposal the computer-coupled two-parameter unit [20] which simplified the adjustment of the telescope electronics; and S.Woitek for preparing the target polyethylene foils. Especially we thank the operating staff of the tandem accelerator for their engagement and support in technical details.

References

[1] Conclusions and Recommendations of the IAEA Consultant's Meeting on the U-235 Fast-Neutron Fission Cross-Section, Smolenice, Czechoslovakia, 1983, INDC(NDS)-146, p.13

[2] R.Arlt et al., Proc. Conf. Nucl. Cross-Sections and Techn., Knoxville, USA, 1979, NBS Spec. Publ., Vol.594, p.990

[3] R.Arlt et al., Zfk-459 (1981), p.35

[4] R.Arlt et al., Zfk-491(1982), p.135

[5] W.P. Poenitz, Nucl. Sci. Eng. 64(1977), p.894

[6] D.G.Schuster, Nucl. Instr. Meth. 76(1969), p.35

[7] C.M.Bartle and P.A.Quin, Nucl. Instr. Meth. 121(1974), p.119

[8] H.G.Ortlepp, Zfk-491(1982), p.141

[9] R.Arlt et al., to be published as a TU Dresden report

[10] K.Andert et al., report JINR Dubna P13-10110, 1976

[11] R.Arlt et al., ZfK-350(1978), p.209
[12] C.M.Bartle et al., Nucl. Instr. Meth. 144(1977), p.437
[13] R.Arlt et al., ZfK-350(1978), p.211
[14] H.G.Ortlepp, G.Pausch, to be published in the ZfK Annual Report 1983 (in print)
[15] G.Pausch, W.D.Fromm, to be published in the ZfK Annual Report 1983 (in print)
[16] R.Arlt et al., ZfK-408(1980), p.154
[17] P.H.White, Nucl. Instr. Meth. 79(1970), p.1
[18] W.P.Poenitz, J.W.Meadows, INDC(NDS)-146, 1983, p.27
[19] V.N.Dushin, ZfK-382(1979), p.153
[20] H.Maerten, W.D.Fromm, to be published in the ZfK Annual Report 1983 (in print)
[21] Prop. Rec. List of Transact. Isot. Decay Data, Part I: Half-Lives, Dec. 1980 ed., INDC(NDS)-121/ne
[22] A.H.Jaffey et al., Phys. Rev. C4(1971), p.1889
[23] E.H.Fleming et al., Phys. Rev. 88(1952), p.642

FISSION FRAGMENT MASS, KINETIC ENERGY AND ANGULAR DISTRIBUTION FOR $^{235}U(n,f)$ IN THE NEUTRON ENERGY RANGE FROM THERMAL TO 6 MeV

Ch. STRAEDE, C. BUDTZ-JØRGENSEN, H.-H. KNITTER
Central Bureau for Nuclear Measurements,
Joint Research Centre,
Commission of the European Communities,
Geel

Abstract

A double Frisch gridded ionization chamber has been used for the measurements. For both fission fragments the mass, kinetic energy and emission angle is found. Data have been measured at different neutron energies, E_n, ranging from thermal to 6.0 MeV in steps of 0.5 MeV. The measured angular anisotropies will be shown. A fit, based on statistical theory, to earlier measurements of negative anisotropies for $E_n \leq 0.2$ MeV will be discussed.
The measured total kinetic energy averaged over all fragment masses, $\overline{TKE}$ (E_n), shows a sudden decrease at $E_n \approx 4.5$ MeV in agreement with earlier measurements. This sudden decrease can not be explained by the measured change in the mass distribution. The present data of $\overline{TKE}$ (E_n) as function of mass-split reveal that $\overline{TKE}$ (E_n) decreases with E_n for mass splits around the 104/132 split as predicted by calculations of B.D. Wilkins et al. It is also seen that $\overline{TKE}$ (E_n) increases with E_n for the symmetric and the extreme asymmetric fissions. The very structured mass distribution from approximately cold fragmentation will be presented.

INTRODUCTION

Lately Frisch gridded ionization chambers have become widely used for measurements of angular distributions and of kinetic energies of fission fragments. A version of the Frisch gridded parallel plate ionization chamber has been developed at CBNM, Geel, ref. 1. In the present experiment a double chamber

has been used, Fig. 1. With this setup the detector has a large angular efficiency (~ 4π), and the detection efficiency is ~ 100 %. With the chamber simultaneous values of fission fragment masses, kinetic energies and angular distributions are found for neutron induced fission of ^{235}U. The neutron energy ranges from thermal to 6 MeV, and measurements are made in steps of 0.5 MeV.

The angular distributions are important for the application of the $^{235}U(n,f)$ standard cross section and have been investigated in several previous measurements, refs. 2, 6 - 13. Mostly the angular distributions are averaged over all fission fragment masses. In the present experiment the angular distributions are found as function of both neutron energy and mass. This experiment also gives data on the kinetic energy of the fragments as function of mass and neutron energy. These data contain information about the so-called cold fragmentation. When the total kinetic energy of a fragment pair is close to the Q-value for the specific split, the fragments are very close to their ground state and no prompt neutrons can be emitted. The cold fragmentations occur only for 1 out of ~ 10^4 - 10^5 fissions. Therefore the high efficiency of the detector is important, since it makes a rather high countrate possible even with a thin U-sample where energy losses of the fragments are kept small. For the thermal neutrons a countrate of 60 fiss/sec was reached and for the higher neutron energies ~ 2 fiss/sec were measured.

The kinetic energy versus mass and neutron energy also give new information about the sudden drop in TKE averaged over all masses that was found in ref.2. This measurement is mainly aimed at the determination of the mass distributions and the kinetic energies of the fission fragments as function of incident neutron energy. Because of the nature of this meeting the present paper concentrates more on the angular distribution data. The other data will only be presented briefly here, and discussed in more detail elsewhere.

EXPERIMENTAL APPARATUS

Neutrons with energies $\leq$ 0.5 MeV were produced by the $^{7}Li(p,n)^{7}Be$ reaction, using a LiF target. Thermal neutrons were produced by thermalization in a hydrogeneous moderator. For 1.0 MeV $\leq E_n \leq$ 3.5 MeV the neutrons were produced by the $T(p,n)^{3}He$ reaction, using an occluded TiT target. For 4.0 MeV $\leq E_n \leq$ 6.0 MeV the $D(d,n)^{3}He$ reaction was used. For 4.0 MeV $\leq E_n \leq$ 5.5 MeV the target was an occluded TiD target, and finally a deuterium gas target was used at 6 MeV. The protons and deuterons were accelerated by the 7 MV Van de Graaff accelerator at CBNM. The energy spreads of the neutrons were between 40 keV and 100 keV for $E_n \leq$ 3.5 MeV and for E_n = 6 MeV. For 4.0 MeV $\leq E_n \leq$ 5.5 MeV the energy spreads were between 150 keV and 250 keV.

The uranium sample is positioned at the center of the common cathode for the two chamber-sides. The backing for the uranium sample constitutes the center of the cathode. Therefore the backing must be conducting, and still so thin that the fission fragments can penetrate it without serious straggling. The backing was made of a gold layer of ~ 25 $\mu g/cm^2$ on a non-conducting poliimide layer of ~ 33 $\mu g/cm^2$. The uranium sample was prepared by vacuum deposition of UF_4. The deposit was 2.8 cm in diameter and 45 $\mu g/cm^2$ thick. The abundances of different uranium isotopes in the UF_4 sample were ^{235}U : 97.66 %, ^{234}U : 1.67 %, ^{238}U : 0.52 % and ^{236}U : 0.15 %.

Fission fragments emitted in a direction perpendicular to the sample surface would on average loose ~ 1.5 MeV in the UF_4 and ~ 2.5 MeV in the backing. The chamber was constructed of 0.5 mm thick stainless steel with teflon insulators. It was operated as a flow chamber (0.1 l/min) at 1 bar absolute pressure. The dimensions of the ionization chamber are chosen so that the fission fragments are stopped between the cathode and the grids.

SIGNALS, PULSE HEIGHT DEFECT AND ELECTRONICS

The chamber and the electronic setup are shown in Fig. 1. The fission fragments are stopped by the detector gas. In this process a number, N, of electron-ion pairs are created along the track. The energy of a fragment and N are related in the following way :

$$E = N \cdot W + PHD$$

where W is the energy lost per electron-ion pair created. PHD is the so-called pulse height defect. This defect is mainly caused by non-ionizing collisions between the fragment and the nuclei in the gas. A measurement of the PHD for an ionization chamber with 90 % Ar + 10 % CH_4 gas has been made at the University of Aarhus, Denmark in collaboration with CBNM, Geel, ref. 4.

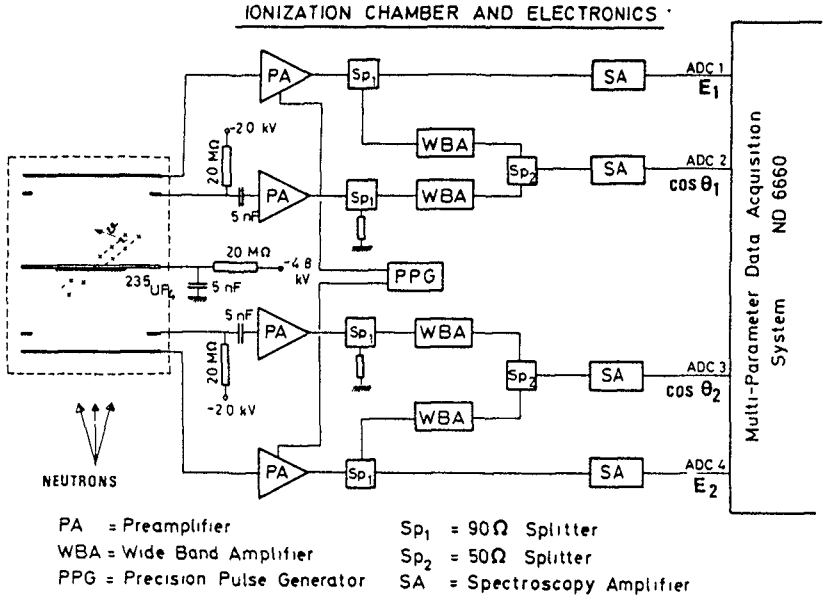

Fig. 1.
Ionization chamber and electronics setup.
PA : preamplifier, SP_1 : splitter 93 Ω, SP_2 : splitter 50 Ω,
WBA : wide band amplifier, SA : spectroscopy amplifier, PPG : precision pulse generator.

These values have been used in the evaluation of the present data. The PHD is ~ 2.5 - 3.5 MeV for light fission fragments and ~ 5 - 6 MeV for heavy fission fragments in a 90 % Ar + 10 % CH_4 gas. This PHD is between 30 % and 40 % smaller than the PHD for a Si detector. The anode and grid signals have been discussed in ref. 1. The positive ions created along the ionization track move with a velocity which is about 1000 times smaller than the electron drift velocities. With appropriate timing filters in the electronic chains it is therefore possible to get only the fast signals induced by the electrons created along the track. As the electrons move from the grid to the anode a charge, -Ne, is induced on the anode and picked up by the charge sensitive preamplifier. The grid signal has a complicated asymmetrical bipolar shape

since a negative charge is induced as the electrons move towards the grid, and a positive charge, + Ne, is induced as the electrons move from the grid to the anode. It is therefore very difficult to obtain the wanted pulse height information with sufficient accuracy from this signal. However, by adding the grid and anode signal, see Fig. 1, an unipolar simple shaped signal, created as the electrons move towards the grid, is left. This signal is easy to treat further. Let D be the grid-anode distance, $\overline{X}$ the position of the center of electron charges along the ionized track measured from the start at the cathode and Θ the emission angle of the fragment measured relative to the normal of the chamber plates. Then it is easily seen, that the summed signal is proportional to $-Ne(1 - \overline{X}/D \cos \Theta)$, and is, apart from the sign, equal to the cathode signal described in ref. 3.

Apart from the PHD the anode signal is proportional to the fragment kinetic energy, and cos Θ for the fragments can be found as shown in ref. 3. A description of corrections for grid inefficiency and of appropriate potentials for the detector plates are given in refs.3, 5.
Stability of the setup was checked by a precision pulse generator on all four electronic chains throughout the experiments. Furthermore all measurements with $E_n > 0.5$ MeV were regularly interrupted for measurements with thermal neutrons. In this way the thermal values could be used as reference values with respect to an absolute calibration, and stability of the chamber itself would also be checked.
An absolute energy calibration was made using the α-particles from the uranium target and assuming the energies of these α-particles to be well known. It was further assumed that PHD for α-particles is zero.

RESULTS AND DISCUSSION

Only data for fragments with $\cos \Theta \geq 1/2$ are used since straggling effects become more important as the stopping in the uranium sample and backing increases. In the evaluation of the angular distributions all data from the whole cos Θ range are used.

Angular distributions

In ref. 3 it has been shown how cos Θ values for fission fragments can be found from the cathode signal in a single chamber. The same procedure is

used in the present experiment for the summed anode-grid signal. The resolution in cos Θ is ~ 0.05. The cos Θ data are only corrected for the center of mass motion by averaging the two cos Θ values for a fragment pair. For the neutron energies used in this experiment this is sufficient. In order to correct for distortions induced by target and backing and other detector effects the final angular distributions were obtained by dividing the distributions for $E_n \geq 0.5$ MeV by the thermal data. The normalized data were fitted with even legendre polynomials. Good fits (based on chi squared tests) were obtained using only P_0 and P_2, and only in some cases small improvements were obtained by including legendre polynomials of higher order. Therefore all data were fitted with

$$W(\Theta) = A + B \cos^2\Theta$$

The results for the anisotropies, $\frac{W(0)}{W(90)} - 1$, averaged over all masses are shown in Fig. 2. Data of refs. 2, 6 are also shown. Furthermore a fit, ref. 7, to all existing data up to 1982 is shown. Overall good agreement is found.

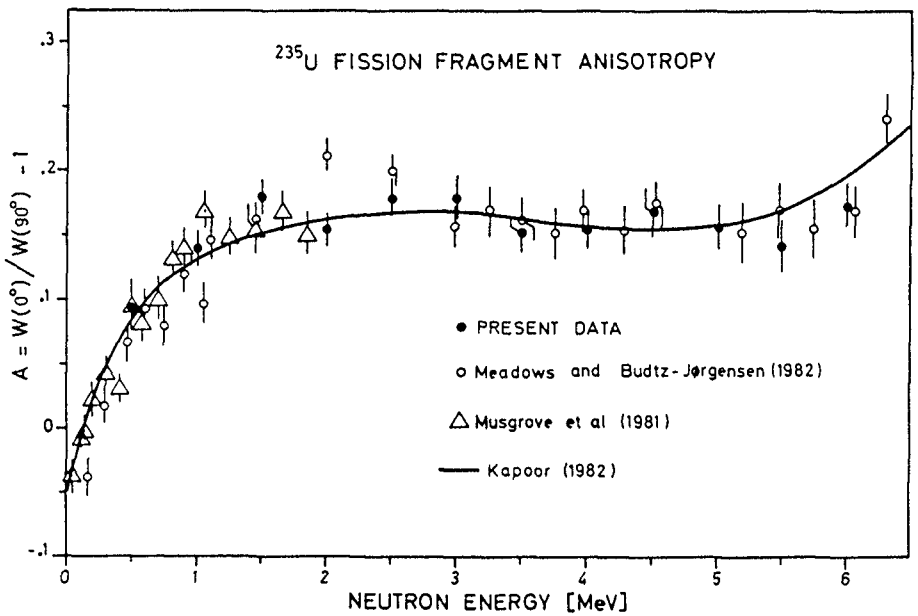

Fig. 2.
The ^{235}U(n,f) fragment angular anisotropy averaged over all mass splits. o ref. 2, △ ref. 6, — ref. 7, ● present data.

The present experiment also gives the angular distributions as function of mass split. For most masses the anisotropies seem to deviate very little from the average values, as far as the statistical uncertainties allow to it to be seen. In Fig. 3 the anisotropies calculated for the average angular distributions for the mass splits 98/138, 97/139, 96/140 and 97/141 are shown as an example. Only for the anisotropies found for the mass splits 110/126, 109/127, 108/128 and 107/129 a systematic deviation from the overall average is seen, Fig. 4. An explanation for this deviation for 2.5 MeV $\leq E_n \leq$ 5 MeV has not yet been found.
The data of refs. 2, 6, 8 - 13 show negative anisotropies at low neutron energies, E_n = 0.1 - 0.2 MeV. In the present work theoretical calculations based on statistical theory, refs. 14, 15, were made to investigate if it was possible to reproduce the negative anisotropies. In the calculations

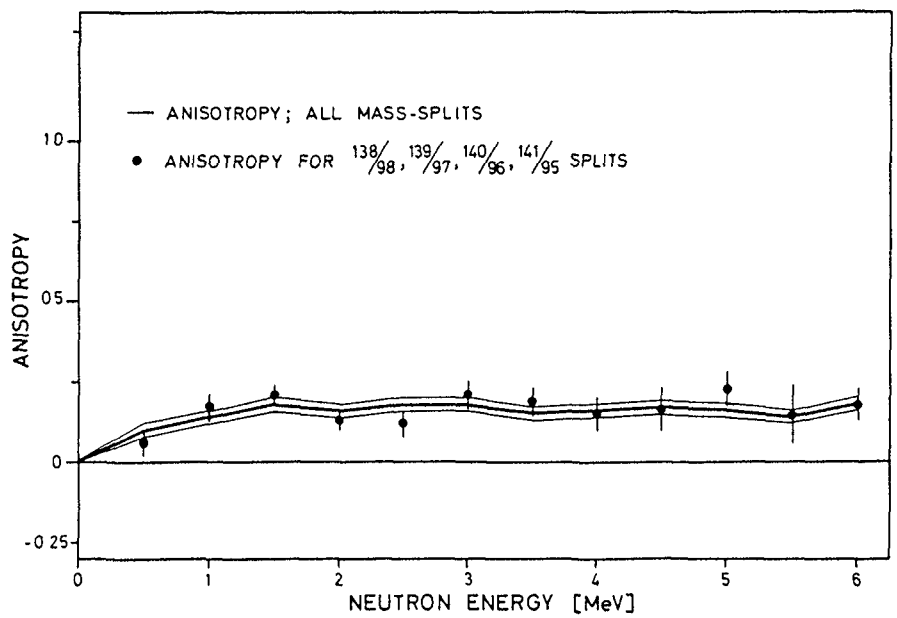

Fig. 3.
The ^{235}U(n,f) fragment anisotropy of the angular distributions averaged over the 138/98, 139/97, 140/96, 141/95 mass splits, ● . These data are compared to the average over all mass splits. ═

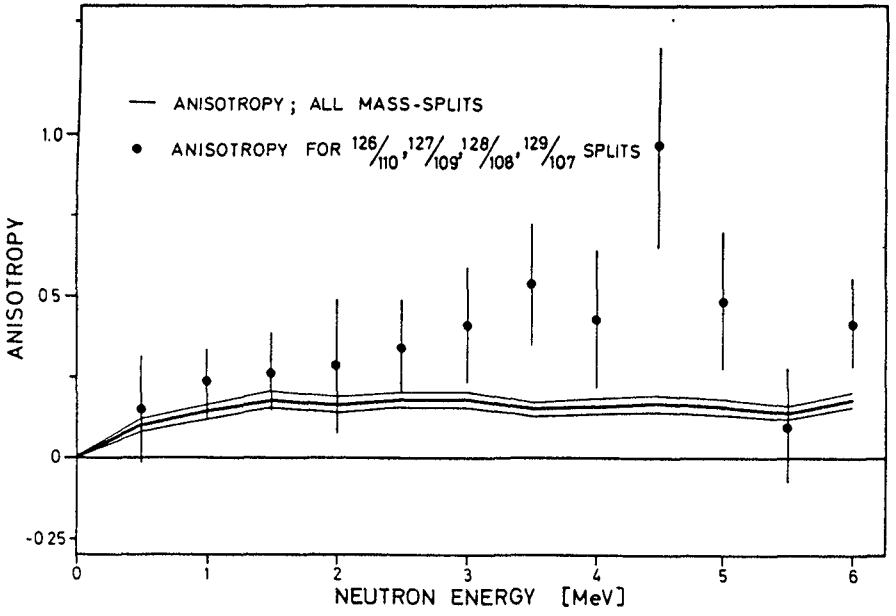

Fig. 4.
The $^{235}U(n,f)$ fragment anisotropy of the angulat distributions averaged over the 126/110, 127/109, 128/108, 129/107 mass splits, ● . The data are compared to the average over all mass splits, ═.

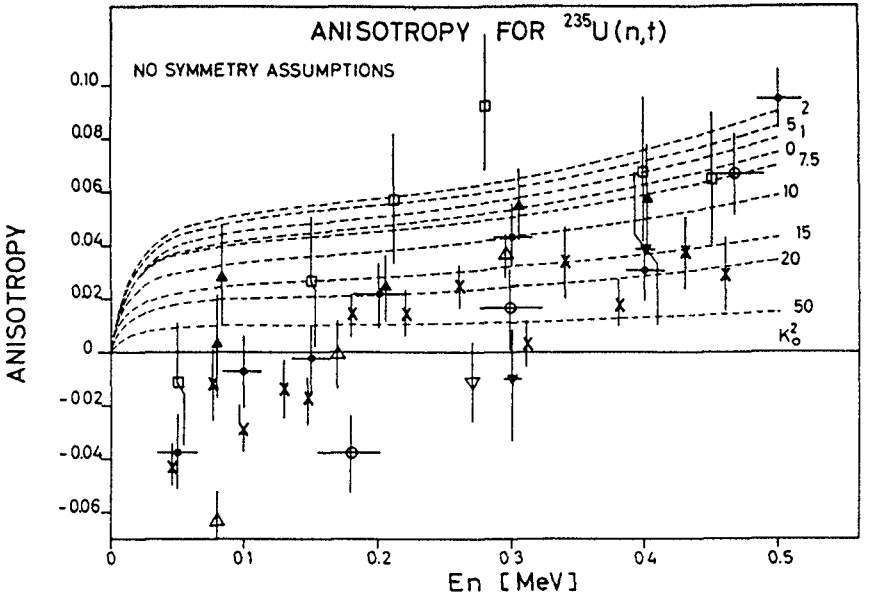

Fig. 5.
The anisotropy for $^{235}U(n,f)$, $E_n \leq 0.5$ MeV.
Experimental data : ○ Ref. 2, ● ref. 6, ▼ ref. 8, ▲ ref. 9, △ ref. 10, □ ref. 11, ▽ ref. 12, X ref. 13.
Theoretical calculations, , based on refs. 14, 15. No assumptions about symmetries are made.

it is assumed that the distribution of K is a gaussian centered around K = 0. K is the projection of the total angular momentum, J, of the compound nucleus on the symmetry axis. If the only selection rules are the ones imposed by the Clebsch-Gordon coefficients used in the calculations, it is found that the negative anisotropies can not be reproduced, see Fig. 5. The K_o^2 values indicated on the figure are the variances of the K-distributions.

The negative anisotropies can be reproduced either by assuming invariance to the R operator with eigenvalue, r = + 1 or invariance to the S operator with eigenvalue s = + 1, see ref. 16 . The R operation is a rotation of 180 degrees around an axis perpendicular to the symmetry axis. R invariance with eigenvalue r = + 1 would mean that for K = 0, J^π can have the values $J^\pi = 0^\pm, 2^\pm, 4^\pm \ldots$, and for K > 0 there would be no restrictions on J^π. The S operator is equal to R·P, where P is the parity operator. The S operation is therefore a reflection in a plane containing the symmetry axis. S invariance would mean that for K = 0, J^π could only have the values $J^\pi = 0^+, 1^-, 2^+, 3^- \ldots$, and for K > 0 there would be no restrictions on J^π. For $E_n \leq 0.2$ MeV only neutrons with angular momentum, ℓ, equal to 0 or 1 relative to the target nucleus, ^{235}U, are of importance. The ground state in ^{235}U is a $7/2^-$ state. Therefore R invariance with eigenvalue r = + 1

would mean $J^\pi = 2^+$, $4^\pm$ for K = 0, and S invariance with eigenvalue s = + 1 would mean $J^\pi = 2^+$, 3^-, 4^+, for K = 0. For K > 0 the same states would be possible in both cases. So for $E_n \leq 0.2$ MeV the only difference between the two invariances is that in case of R invariance and K = 0 a $J^\pi = 4^-$ state is possible, where in case of S invariance and K = 0 a $J^\pi = 3^-$ state is possible instead. The anisotropies of fragments from fission through the $JK\pi = 30^-$ state and the $JK\pi = 40^-$ state are almost the same. Furthermore the probability for the $JK\pi = 30^-$ state in case of S invariance is almost the same as for the $JK\pi = 40^-$ state in case of R invariance. Therefore the two invariances can not be distinguished for $E_n < 0.2$ MeV by a fit to the experimental anisotropy data, but it seems necessary to assume one of the two invariances to be able to fit the data.

S invariance would be in agreement with the suggestion of ref. 17, that the nucleus at the saddle point would be pearshaped. In a review article ref. 18, it is also mentioned that S invariance and lack of R invariance might be expected for the nuclear shape at the outer barrier deformations. In Fig. 6 the calculated anisotropies as function of neutron energy and variance, K_o^2, of the gaussian K distribution is shown for S invariance with eigenvalue s = + 1. It is seen that the negative anisotropies, refs. 2, 6, 8 - 13, can be reproduced.

Mass distribution

In Fig. 7 the preneutron emission mass distribution from $^{235}U(n,f)$ is shown for E_n = thermal and Fig. 8 shows the mass distribution for E_n = 6 MeV. For the evaluation of the preneutron masses, $\nu(m)$ values from ref. 19 were used for thermal incident neutrons. For E_n = 0.5 MeV and 5.5 MeV $\nu(m)$ values from ref. 20 were used. For the other neutron energies the $\nu(m)$ values were found by linear interpolation between the two data sets from ref. 20. Typical fine structures in the mass distributions due to shell and pairing effects are seen in Figs. 7 and 8. It is also clearly seen by comparison of Figs. 7 and 8 that the asymmetric mass yield peaks become broader with increasing neutron energy. A clear change in the yield of the symmetric fissions is also seen. It is found that the peak to valley ratio of the mass distributions changes exponentially with E_n and follows $P/V = 535 \exp(-0.46 \cdot E_n\ [\text{MeV}])$. Furthermore the variance of the asymmetric mass distributions follows $\sigma^2 \approx 30 + \exp(0.45 \cdot E_n\ [\text{MeV}])$.

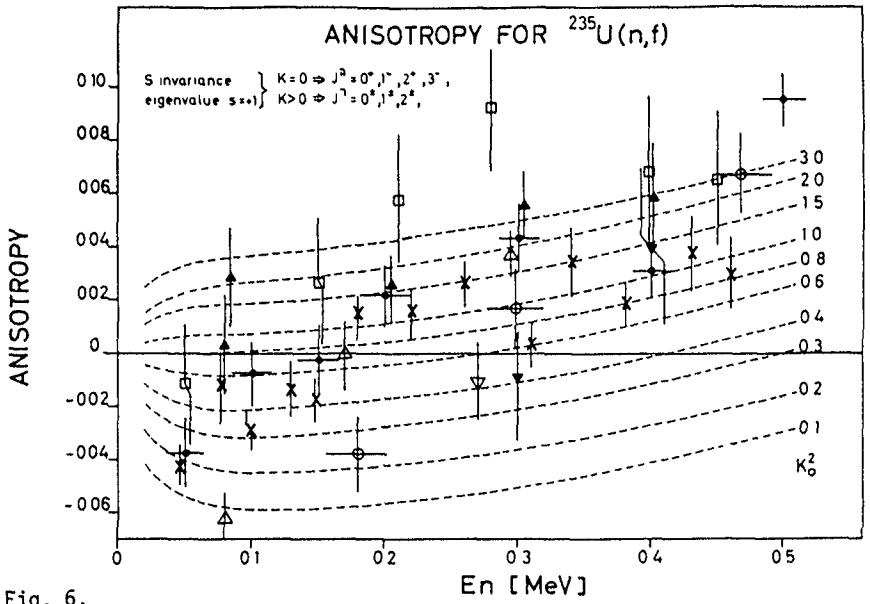

Fig. 6.

Experimental data, as in Fig. 5.

Theoretical data, – – –, as in Fig. 5, but S-variance is also assumed (see text).

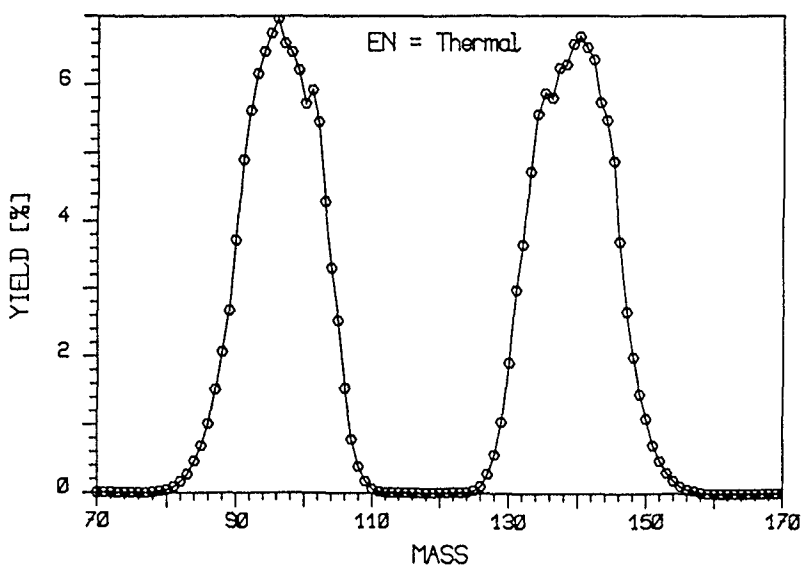

Fig. 7.

Preneutron emission mass distribution for $^{235}U(n,f)$, E_n = thermal.

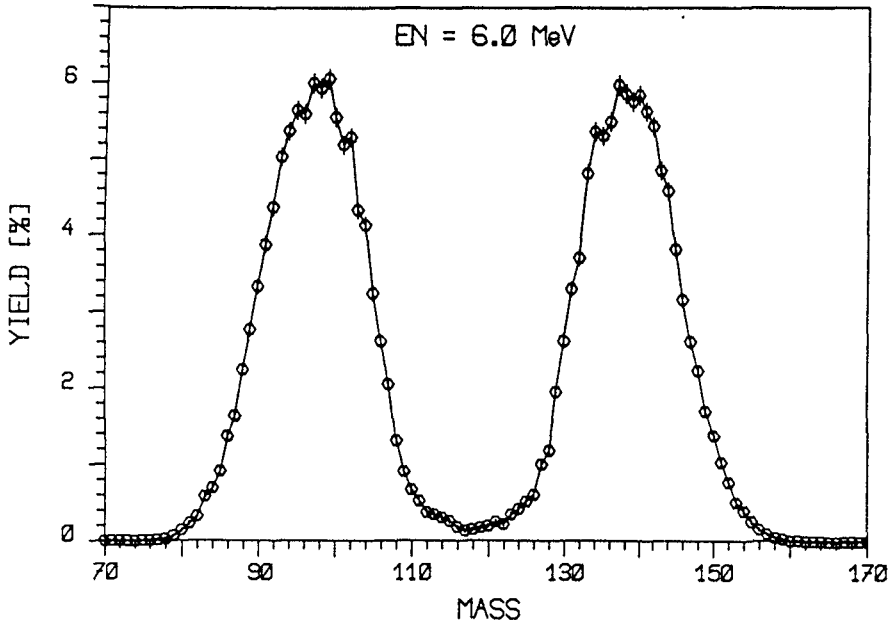

Fig. 8.
Preneutron emission mass distribution for $^{235}U(n,f)$, E_n = 6.0 MeV.

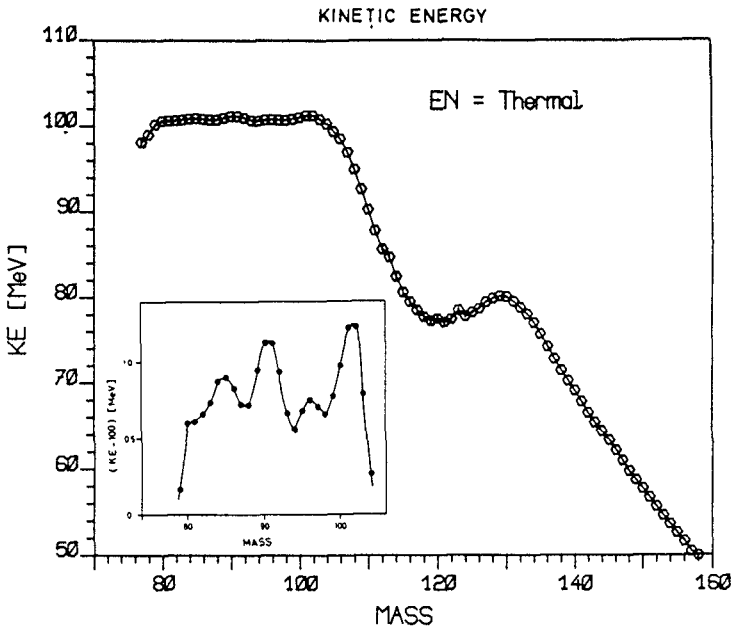

Fig. 9.
Kinetic energy as function of mass split for $^{235}U(n,f)$, E_n = thermal. Inset shows blowup of structure in KE for the light fragments.

Kinetic energy and cold fragmentation

In Fig. 9 the preneutron emission average kinetic energy, KE, as function of fragment mass is shown for thermal neutrons. A blow up of the structure in KE for the light fragments is also shown in the inset. There are clear peaks around mass 86, mass 90 - 92, mass 96 and mass 102. These peaks are well understood as results of shell and pairing effects.
In Figs. 10 and 11 is shown how the mass distribution for the light fragments changes with selected kinetic energies. The data are from thermal neutron induced fission. The energies are indicated on the figures. Each window covers KE $\pm$ 0.5 MeV. As the window is raised the available energy for excitation of the fragments decreases and the cold fragmentation situation is approached. As expected the peaks in the mass yield occur for the same masses as the peaks in KE on Fig. 9 . The mass distribution changes significantly with shifts of the KE window. The solid lines in Fig. 10 show data from measurements at the mass-spectrometer LOHENGRIN, ref. 21. Since the mass resolution of LOHENGRIN is ~ 0.2 amu, it is believed from this comparison that the resolution of the relatively simple ionization chamber is not worse than ~ 3 amu.

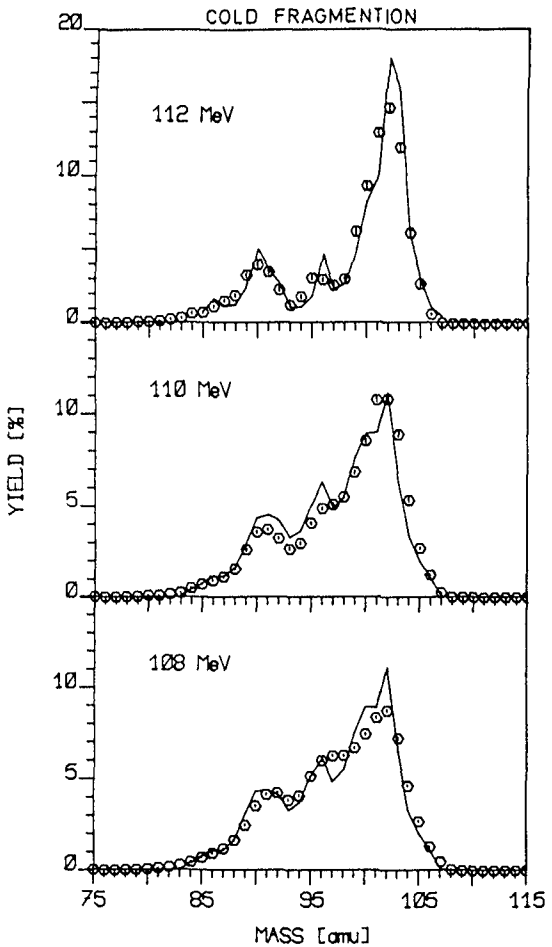

Fig. 10.
Mass distribution of light fragments from $^{235}U(n,f)$, E_n = thermal, at approximately cold fragmentation.
— ref. 21, ○ present data.
The kinetic energies of the fragments are indicated. For the data of ref. 21 the energy window is only a few keV. For the present data the energy window is KE ± 0.5 MeV.

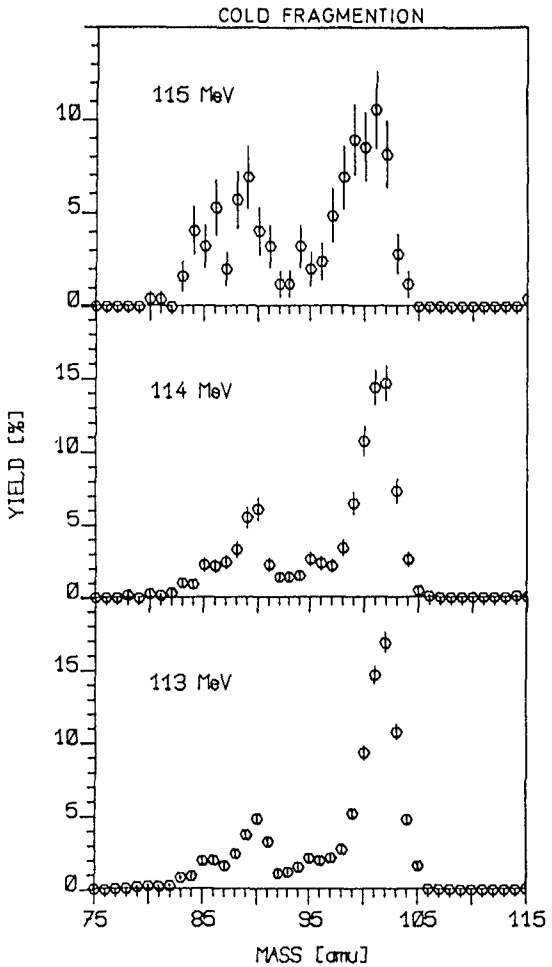

Fig. 11.
See Fig. 10.

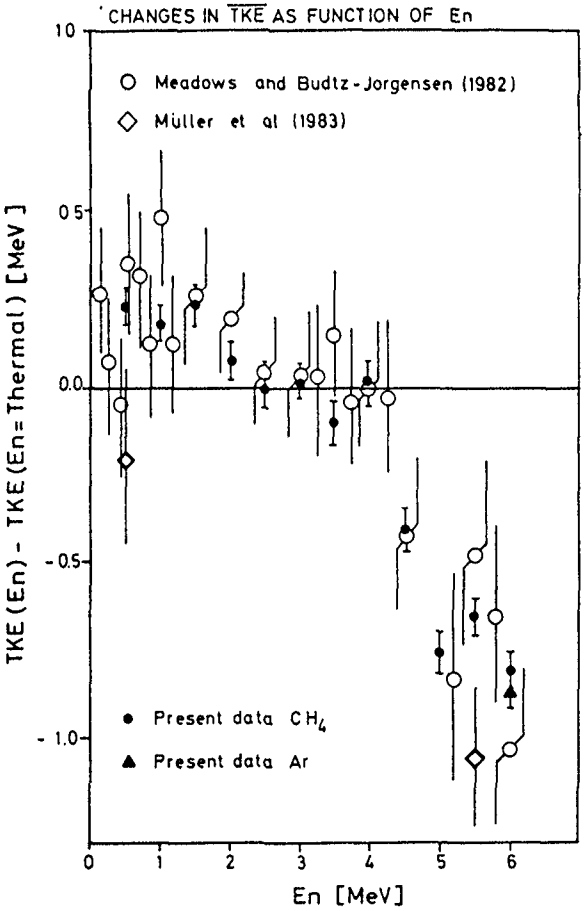

Fig. 12.
Changes in $\overline{TKE}$ as function of E_n.
○ ref. 2, ◇ ref. 20, ● present data.

Total kinetic energy as function of E_n and mass-split

The changes in the average TKE values as function of E_n are shown in Fig. 12. The present data are compared to data of refs. 2, 20. The data of ref. 20 were given as absolute values, and in Fig. 12 they are plotted relative to the absolute $\overline{TKE}$ value for thermal neutrons found in this experiment, 170.6 ± 1.0 MeV. A general shift between the data of ref. 20 and the present data is probably caused by differences in the absolute calibration.
The sudden decrease in $\overline{TKE}$ for $E_n \approx 4.5$ MeV, that was reported in ref. 2, is confirmed. These two data sets also indicate $\overline{TKE}$ values ~ 0.2 MeV higher than the thermal values for $E_n \leq 2$ MeV. In Fig.13 it is seen that the changes in the mass distribution with E_n have very little effect on $\overline{TKE}$, and that the changes mainly come from changes in TKE for the different mass splits. In Fig.14 it is shown how the TKE changes as function of neutron energy and mass split for E_n = 2.5 MeV, 4.5 MeV and 5.5 MeV. It is seen how the kinetic energy increases for the symmetric and extreme asymmetric fissions, and how a drastic decrease in TKE occurs around the 102/134 mass split. Smaller decreases are also found around the 96/140 and the 91/145 split. Structure is also seen around the 86/150 split. These changes in TKE with neutron energy might be explained within the scission point model of ref. 22. In this model the changes in TKE are explained by changes in the deformation of the fragments at the scission point - larger deformations give smaller coulomb repulsion and thereby smaller total kinetic energy. The model predicts changes in the deformations that qualitatively would explain the measured shift in kinetic energy for the symmetric, the 96/140 and the 102/134 mass splits.
Furthermore it seems that the structure in the TKE changes are coupled to mass splits close to the 86/150, 90/146 - 92/144, 96/140 and 102/134 splits. The same masses give structure in the mass distribution, the cold fragmentation and the kinetic energy.

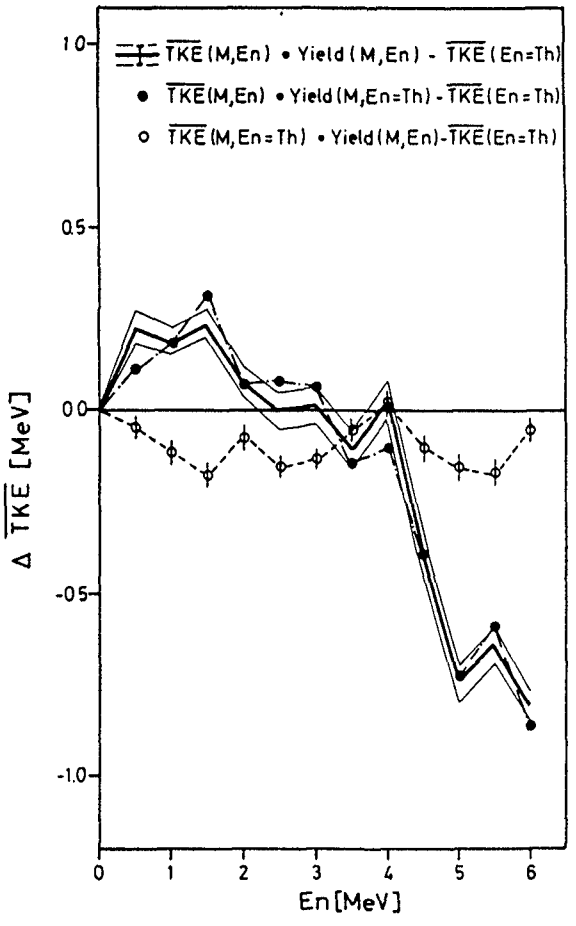

Fig. 13.
Changes in $\overline{TKE}$ as function of E_n for $^{235}U(n,f)$. The changes in $\overline{TKE}$ caused by changes in the mass distribution and in the kinetic energy for the different mass splits are separated.
≡ present data with statistical uncertainty band, the measured data.
○ changes in $\overline{TKE}$ caused by changes in the mass distribution.
● changes in $\overline{TKE}$ caused by changes in the kinetic energy for the different mass splits.

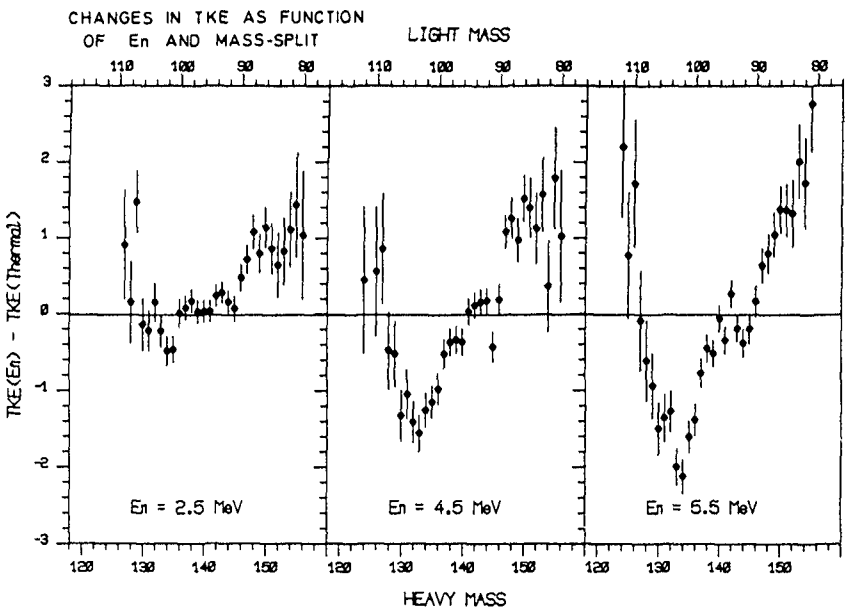

Fig. 14.
Changes in the total kinetic energy as function of neutron energy and mass split for $^{235}U(n,f)$.

REFERENCES

1. H.-H. Knitter and C. Budtz-Jørgensen, Proc. Knoxville Conference, NBS Special Publication 594, 947 (1980).

2. J.W. Meadows and C. Budtz-Jørgensen, Argonne National Laboratory, Nuclear Data and Measurement Series ANL/NDM - 64 (1982).

3. C. Budtz-Jørgensen and H.-H. Knitter, Nucl. Sci. Eng. 86, 10 (1984).

4. N. Rud and P. Nielsen, Physics Institute, University of Aarhus, Denmark, Private Communication.

5. O. Bunemann, T.E. Craushaw and J.A. Harvey, Can. J. Res. A27, 191 (1949)

6. A.R. de L. Musgrove et al., J. Phys. G. (London) Nucl. Phys. 7, 549 (1981).

7. S.S. Kapoor, Nuclear Data Standards for Nuclear Measurements. Technical Reports Series N° 227, pg. 47, I.A.E.A., Vienna, 1983.

8. S. Ahmed et al., Nucl. Sci. Eng. 71, 208 (1979).

9. I. Caruana et al., Proc. Symp. Indian Nuclear Physics Solid State Physics, Trombay, (Dec. 1974).

10. V.G. Nesterov et al., Sovj. J. Nucl. Phys. 4, 713 (1967).

11. D.M. Nadkarni et al., Nucl. Phys. Solid State Physics (Bombay) 2, 133 (1968).

12. S.T. Hsue et al., Nucl. Sci. Eng. 66, 24 (1978).

13. G. Smirenkin et al., JETP Lett. 11, 333 (1970).

14. R. Vandenbosch and J.R. Huizenga, "Nuclear Fission", Academic Press, 1973.

15. A. Sicré, Ph. D. Thesis, University of Bordeau, 1976.

16. A. Bohr and B.R. Mottelson, "Nuclear Structure", Vol. 2, 1975.

17. A. Bohr, Proc. First International Conf. on the Peaceful Uses of Atomic Energy, P/911, Vol. 2, p. 151 (1956), United Nations, New York.

18. S. Bjørnholm and J.E. Lyn, Rev. Mod. Phys. 52, 725 (1980).

19. V.F. Apalin et al., Nuclear Physics 71, 553 (1965).

20. R. Müller et al., Kernforschungszentrum Karlsruhe, KFK 3220, 1981.

21. W.L. Lang et al., Nucl. Phys. A345, 34 (1980).

22. B.D. Wilkins et al., Phys. Rev. C14, 1832 (1976).

THE ^{238}U FISSION CROSS-SECTION, THRESHOLD TO 20 MeV

Y. KANDA
Department of Energy Conversion Engineering,
Kyushu University,
Kasuga, Fukuoka,
Japan

Abstract

It has been discussed what accuracies are achieved in the recommended reference data for the ^{238}U fission cross section. The new experimental data reported since 1977 as well as the discussion at the Argonne meeting in 1976 have been taken into account However, it is not necessary to revise largerly the early conclusion In the region from threshold to 10 MeV the recommended cross sections are as accurate as a few percent, and above 10 MeV the difference of the experimental data is as large as 10 % of the values It should be emphasized to users that the recommended data and their uncertainties are not directly measured but estimated as the most probable values from existing experimental data

1 Introduction

In the course of developments in nuclear reactors, neutron cross sections have always been one of the most basic quantity At a stage where development of thermal reactors was main task, the cross sections in the neutron energy region in eV and low keV were interested in Necessity of the cross sections in the keV and MeV regions has arisen in accordance with the development in fast reactor design and fusion reactor technology Naturally, the standard reference cross sections in these energy regions are in demand The fission cross section of ^{238}U is recommended as a nuclear data standards for nuclear measurements.[1]

An important meeting on the fission cross section of ^{238}U as well as those of ^{233}U, ^{235}U and ^{239}Pu was held at Argonne National Laboratory in 1976[2] . Majority of the experiments which should be referred to in discussion on the ^{238}U fission cross section was presented there. Since the Argonne meeting, review papers on the ^{238}U fission cross section were reported by Cierjacks[3] at National Bureau of Standard in 1977, by Patrick[4] at Harwell in 1968, and by de Saussure and Smith[5] at Antwerp in 1982 Cierjacks discussed the aspects of using the fission cross section of ^{237}Np and ^{238}U as possible standards in the MeV region and suggested the experiments to achieve an ultimate accuracy of 2 % with measurements employing ^{237}Np or ^{238}U as secondary standards Patrick reviewed the fission cross sections of five transactinide isotopes including ^{238}U between 100 keV and 20 MeV De Saussure and Smith discussed the interaction of 1 eV to 20 MeV neutron with ^{238}U with emphasis on recently resolved and remaining issue relevant to both application and physical understanding

In this report, the experimental data published since the Argonne meeting are compared with the recommended reference data for the ^{238}U fission cross section There are not so many as the number of the data presented in the Argonne meeting The uncertainty achieved in the measurement is compared with that of the demand in application. The meaning of the recommended data and their uncertainties are discussed on application in reactor simulation measurements

2 Status of Experimental Data

A greater number of the experimental data to be referred in the discussion of the ^{238}U fission cross section had been published until the Argonne meeting They are studied in detail and discussed on the uncertainty achieved in the experimental data Since the meeting a few measurements are reported and they do not materially affect the conclusion at that time Figs 1, 2 and 3 show the data of the ^{238}U fission cross section and ratio measurements reported since 1977. The experiments reported in the

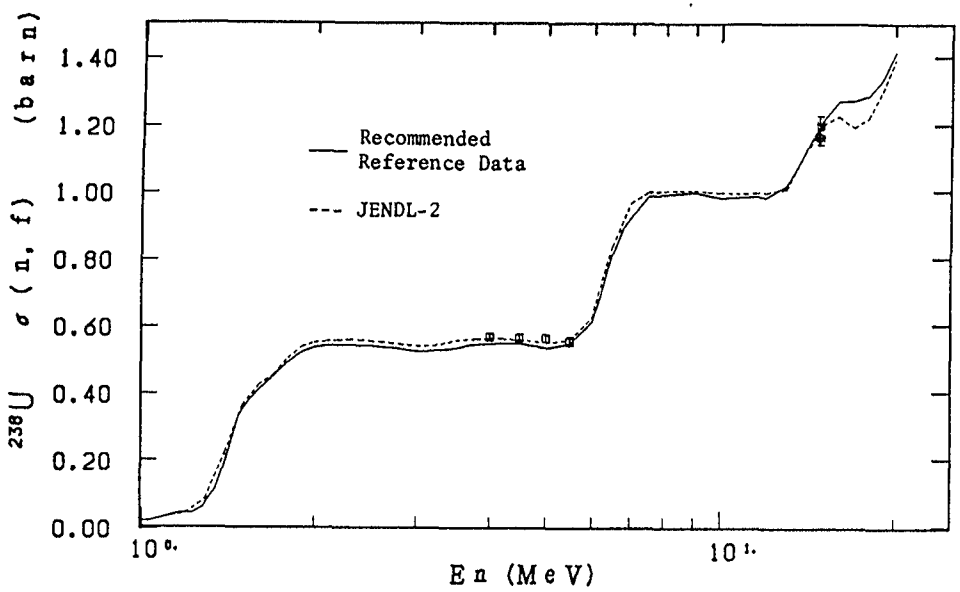

Fig. 1 Fission cross section of ^{238}U. Experimental data reported since 1977. See text. □ : Wu et al. ,○ : Arlt et al. ,+ : Adamov et al.

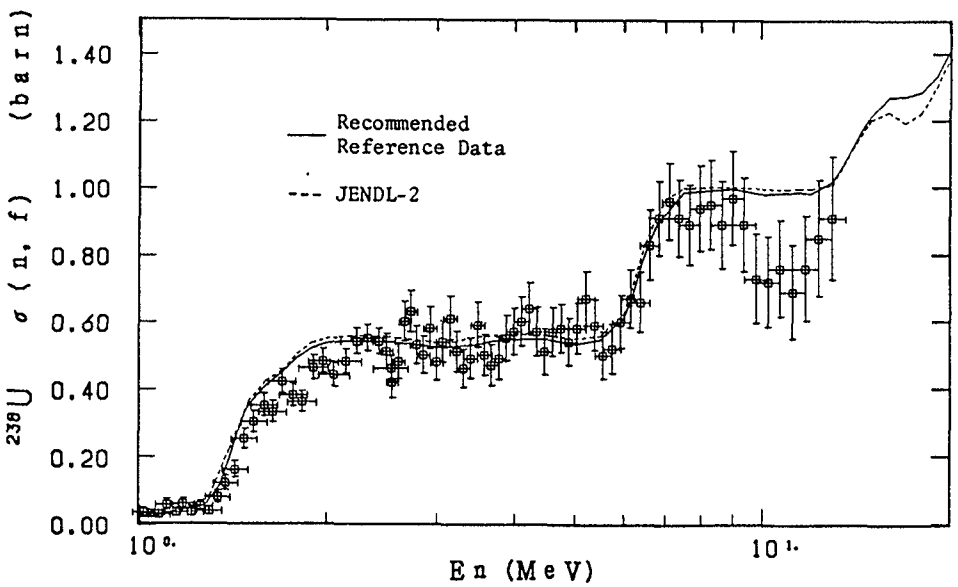

Fig. 2 Fission cross section of ^{238}U. Experimental data reported since 1977. See text. □ : Osterhage et al.

Argonne meeting are not shown here, even if they appear as the reports in jounals since 1977.

Osterhage et al.[6] The main aim of the experiment was to observe the shape of the ^{238}U fission cross sections in the energy range from 0.3 to 12.5 MeV. They used a gas scintillation counter to detect fission events. The ^{238}U/^{235}U fission ratio were measured and normalized using the ^{235}U fission data evaluated by Sowerby et al.[7]

Fursov et al.[8] The ^{238}U/^{235}U fission ratio was measured using two back-to-back ionization chamber in the range between 1 and 7 MeV. The shape measurement was normalized to the absolute ratio obtained in this experiment.

Blons et al.[9] The report has not been available. It was described by Cierjacks[3] that the experiment was carried out by the Saclay LINAC.

Arlt et al.[10] They measured an absolute cross section by an associated particle method at 14.7 MeV.

Adamov et al.[11] They measured an absolute cross section by an associated particle method at 14.7 MeV.

Varnagy et al.[12] The ^{238}U/^{235}U fission ratio was measured using two solid-state nuclear track detecters and a fission chamber. The neutron energies were between 13.5 and 14.8 MeV using a Cockcroft-Walton accelerator.

Wu et al.[13] The ^{238}U fission cross section was measured as ratios to the H scattering cross sections in the energy range from 4.0 to 5.5 MeV. The fission events were detected with a fission chamber and the recoiled protons were measured with a semiconducter detector. Both ^{238}U sample and H sample were set back-to-back. The neutron source was D(d,n) reaction using an electrostatic accelerator.

K. Kanda et al.[14] The ^{238}U/^{235}U fission ratio was measured using a back-to-back fission chamber in the energy range between 1.52 MeV and 15.01 MeV. The neutrons were produced by ^{3}H(p,n) reaction using a Dynamitron and by ^{3}H(d,n) reaction using a Cockcroft-Walton accelerator.

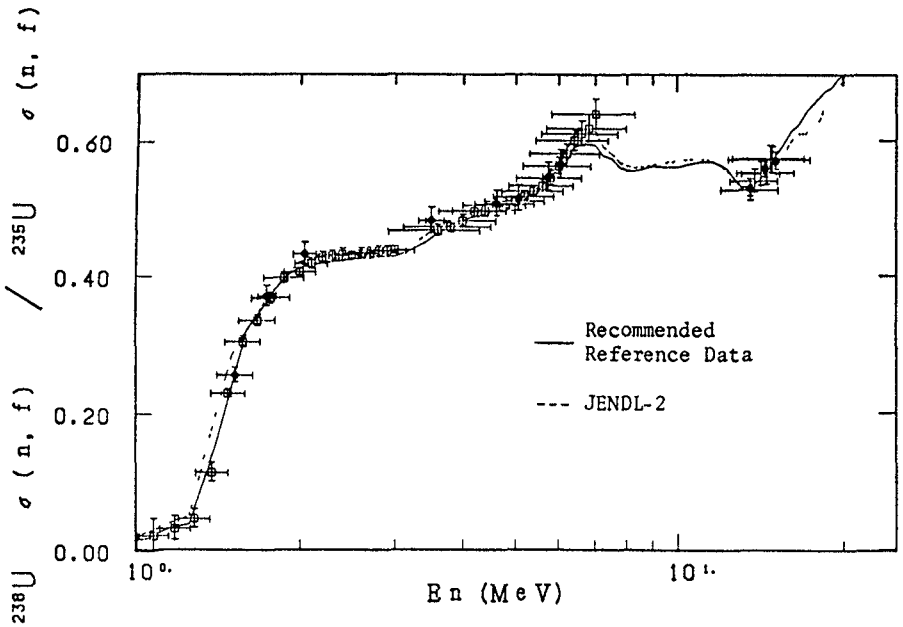

Fig. 3 Fission cross section ratio : ^{238}U / ^{235}U. Experimental data reported since 1977 See text. □ : Furusov et al. , ● : K. Kanda et al. + : Varnagy et al.

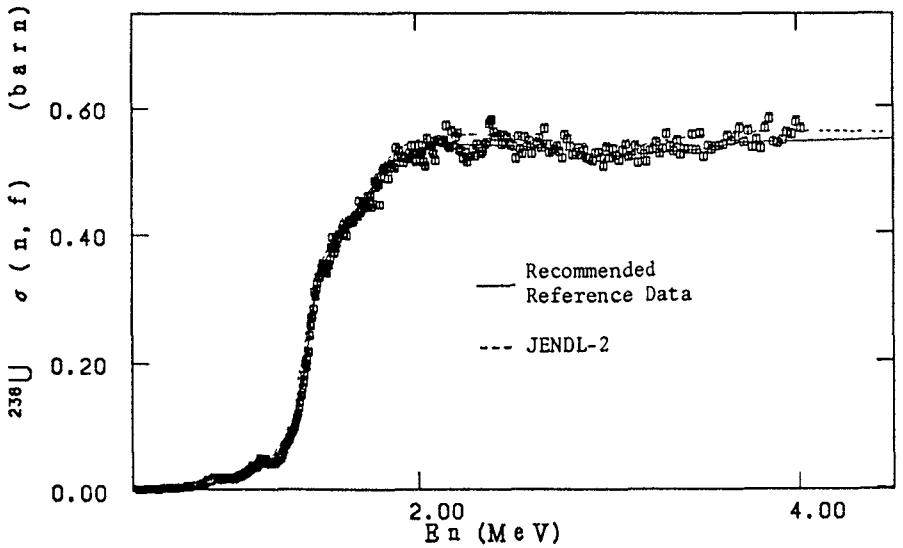

Fig. 4 Fission cross section of ^{238}U. Experimental data reported since 1977. See text. □ : Blons et al.

Two experiments on the ^{238}U fission cross section in MeV region reported in the Kiev Conference[15] in 1983 are found in the list of CINDA 84.[16] Information on them is not available yet.

In these data, Osterhage et al's result disagree significantly with the prior data. This is excluded in the present discussion, because they have large errors Blons et al's data are also excluded in the quantitative discussion, because their aim is a measurement of the fluctuation in the excitation curve.

3. Comparison of the Reference Data with Experimental Data

The experimental results reported since 1977 agree well with the previous data and evaluations Therefore, it is not necessary at the present time to revise the conclusion at the Argonne meeting[2] It was described that a large number of experiments on $^{238}U/^{235}U$ fission ratio can be brought into what some would consider excellent agreement in the energy region from threshold to 10 MeV after energy scale changes and after adjustments for possible mass changes, and an evaluation could achieve better than ±2 % accuracy. For the ^{235}U fission cross section, it was generally agreed that between 1 and 8 MeV there is no measure controversy regarding the evaluated curve with a ±3 % uncertainty The experimental data for the ^{235}U fission reported since 1977 are shown in Fig.5 Although there are new data which are not, strictly speaking, in the band of ±3 % uncertainty, the agreement reached at the Argonne meeting can be regarded to be available A simple estimation based on both uncertainties of the $^{238}U/^{235}U$ fission ratio and of the ^{235}U fission cross section bears that the uncertainty of the ^{238}U fission cross section is expected in an evaluation to be below 4 % between 1 and 10 MeV This approximately agree with the uncertainties given for the recommended reference data in the IAEA publication[1] , those values are ploted in Fig 9 . The uncertainties for the reference data locally are better than 4%

The total errors given in the cross section measurement of Wu et al [13] and in the ratio measurement of Fursov et al [8] in

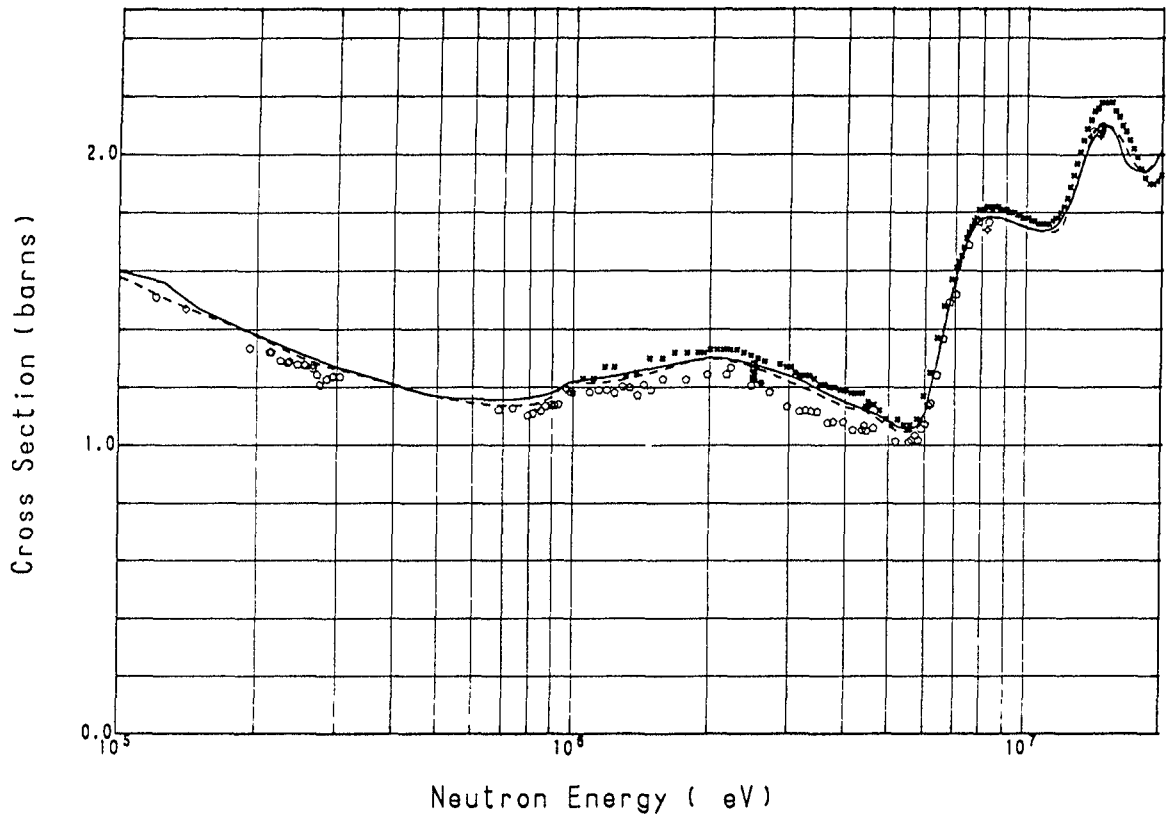

Experimental Data Reference

———	JENDL-2	MAT NO. 2923	MF NO. 3	MT NO. 18	
------	ENDF/B-V	MAT NO. 1395	MF NO. 3	MT NO. 18	
○	W.P.POENITZ	'77	ANL .*.	NSE,64,894	10711002
▽	W.MEILING+	'78	TUD . .	KE,21	30461002
*	K.KARI+	'78	KFK . .	78BNL,	20786006
◆	M.CANCE+	'78	BRC .*.	NSE,68	20779002
□	B M.ALEKSANDROV+	'79	RI . .	AE,46	40546003
●	R.ARLT+	'80	TUD . .	TU-05-43-80	30559002
✳	M.CANCE+	'80	BRC . .	CEA-N-2194	21620002
○	E.A.ZHAGROV+	'80	RI . .	80KIEV,3,45	40610003
◇	R.ARLT+	'80	TUD . .	ZFK-410,122	30558002
○	M.CANCE+	'80	BRC . .	CEA-N-2194	21620002
○	R.ARLT+	'81	TUD . .	KE,24,48	30475002
◎	O.A.WASSON+	'82	NBS .*.	NSE,80,282	10971002
◎	LI JINGWEN+	'82	AEP . .	82ANTWER,	30634002

Fig. 5 Fission cross section of ^{235}U. Experimental data reported since 1977.

the energy range from 2 to 6 MeV are less than 2.6 % and approximately 2%, respectively. The two data sets agree well with the JENDL-2[17] data rather than the recommended reference data[1] . In this energy range, the differences between the two data are 2 % for the ^{238}U fission cross section and 3 % for the $^{238}U/^{235}U$ fission ratio in each magnitude. Since the number of data points and data sets are sparse, it can not be determined in the present which evaluation is correct. However, such comparison should be made in order to obtain the reference data having the uncertainty less than 2%.

The ^{238}U fission cross section curve has two plateaus between 2 and 12 MeV, and is expected as the most possible cross section standard in this region which is important in fusion technology. In the second plateau from 7 to 12 MeV, new measurements have not reported since 1977. The status of the experimental and evaluated data in this region is as same as or slightly wronger than that in the energy range between 2 and 6 MeV.

As the cross section measured by the associated particle method is independent of the other cross section, it is an excellent absolute measurement method. Available experimental

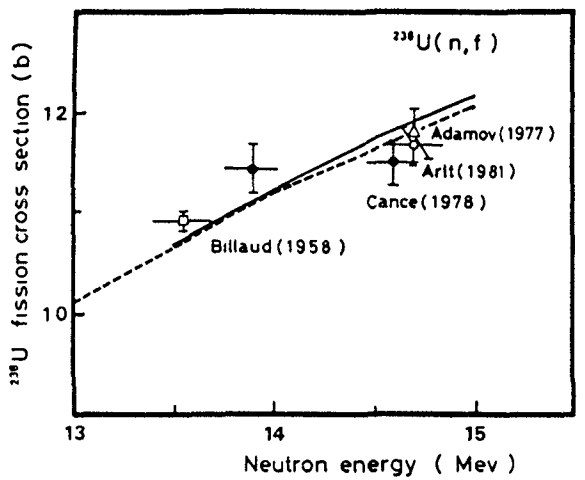

Fig. 6 Fission cross section of ^{238}U measured at 14 MeV by the associated particle method.

data measured by this method are shown in Fig 6 The weighted mean at 14 0 MeV to which every value are reduced along the recommended reference data is 1 126 ±0 008 b (0 7 %) The error of the weighted mean is much smaller than the uncertainty of the recommended reference data at 14 0 MeV Both cross section values agree very well, the recommended one is 1 120 b Since in this region of the neutron energy the cross section curve has a gradient of 0 1 b/MeV, the error in determination of the neutron energy in the associated particle method contribute greatly to the uncertainty of the cross section value The recommendation on the energy measurements in the Argonne meeting [2] is not applied in this method It was that measurement in the MeV range should include are check on the energy of the 2 07 MeV carbon resonance to confirm the accuracy of MeV energy scales In order to obtain 1 % accuracy for the cross section at the 14 MeV, the uncertainty for the energy should be less than 50 keV which is one third of the available experiments

Above 10 MeV the new data have not become available except two 14 MeV data since 1977 Therefore, the discrepancy in this energy region indicated at the Argonne meeting[2] and in the report of Cierjacks[3] remains to be a question There are two groups in the ^{238}U/^{235}U fission ratio data in this energy region The one group having larger values is cyclotron measurements using gas scintillators and the another of lower values is linac measurement using ion chambers The difference between both groups increase to 10 % at 20 MeV It is difficult to assess this problem on the basis of the data at 14 MeV because the difference is too small to discriminate them at this energy

Fluctuations in the ^{238}U fission excitation function were discussed in Cierjacks report[3] referring to Blons et al s measurement[9] between 0 5 and 2 9 MeV shown in Fig 4 Although the data can be obtained from the NEA data bank, the detailed documentation of their experiment is not published In this energy region, Fursov et al s measurement[8] was reported in 1978 As seen in Fig 3, the fluctuations are not found in their experiment Since the energy resolution of both data are very different, it is difficult to discuss strictly on this problem The data of Fursov et al agree well with those of Behrens and Carlson [18] in this region, shown in Fig 7 If the observed fluctuation are real, it remain to be an important problem concerning about the use of the ^{238}U fission cross section as the reference data

In the review of de Saussure and Smith [5] , it is described that the in the energy region just above 2 MeV the recommended reference data[19], are 4-5 % smaller than Difilippo et al s data[20] The feature that the reference data are smaller than the recent experimental data can be seen in Figs 3 7 and 8 comparing the reference data with the experiment of Fursov et al [8] , Difilippo et al [20] and Behrens and Carlson[18], respectively Therefore, it is better to increase the recommended value of the ^{238}U/^{235}U ratio by 2-3% If this is done with fixed ^{235}U fission data, the value of the ^{238}U fission are increased and resulted in rather better agreement with the experiments The

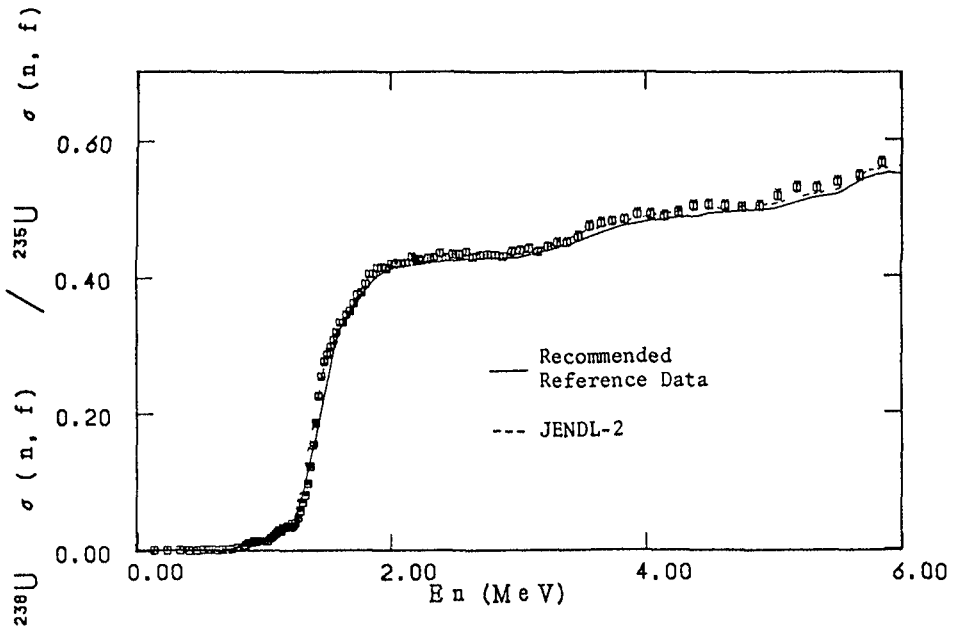

Fig. 7 Fission cross section ratio : ^{238}U / ^{235}U. Data of Behrens and Carlson below 6 MeV.

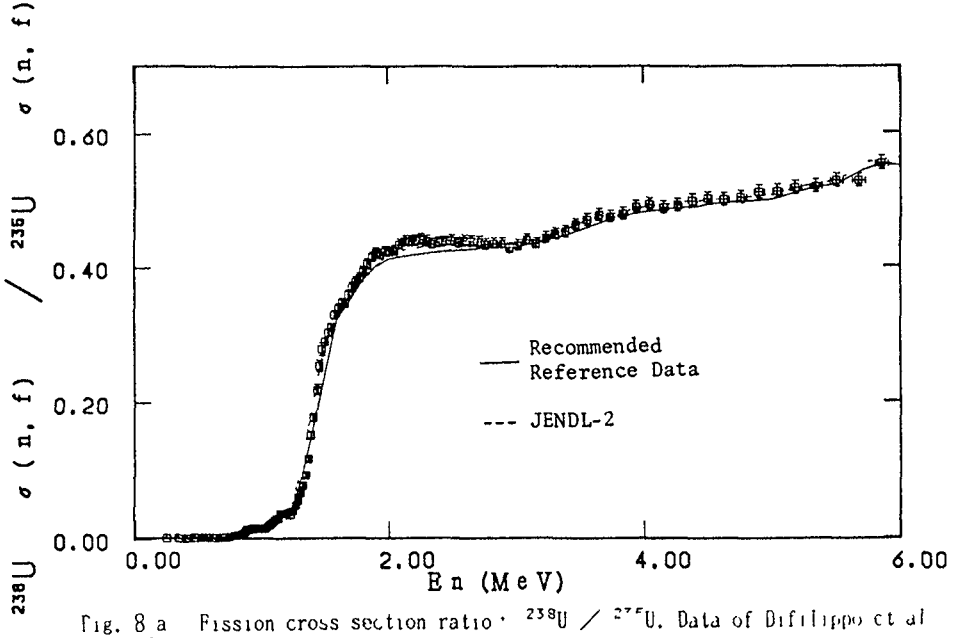

Fig. 8 a Fission cross section ratio : ^{238}U / ^{235}U. Data of Difilippo et al below 6 MeV.

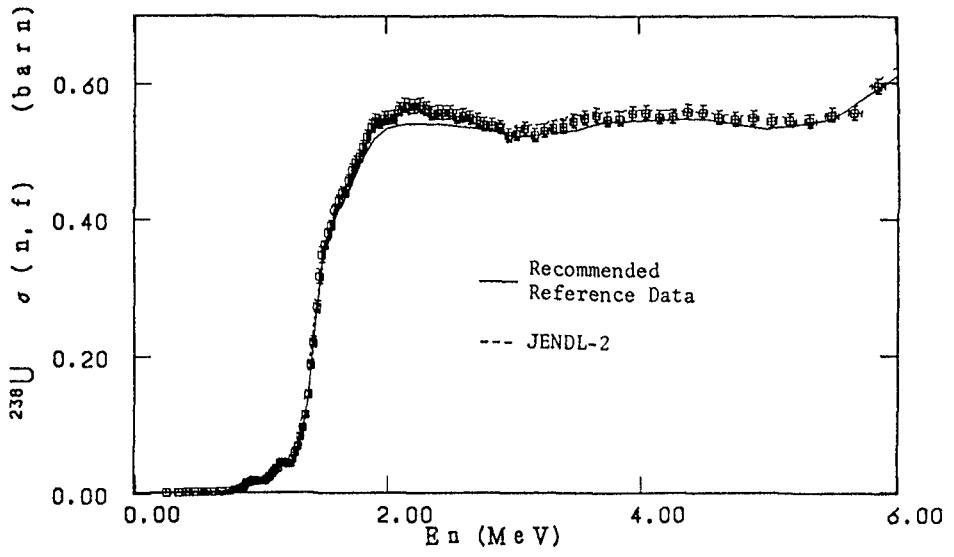

Fig. 8-b Fission cross section of ^{238}U. Difilippo et al's data normalized by the recommended reference data for the ^{235}U fission sections

revise including this problem should be left to the reevaluation programs working in few places

4 Confirmation of Achievement on Uncertainty

Availability of the recommended reference data and their uncertainties has been discussed in detail comparing with the recent experimental data Although the parts of them should be slightly revised, they are sufficiently valid in the present time The next problem is whether the uncertainty given for the data fully meet the demands in application This can be simply and plainly shown by comparing the uncertainties given to the reference data with those demanding in WRENDA 83/84[21] It is presented in Fig 9 The demands in WRENDA 83/84 are listed with comments describing their basis However, in the present discussion, the reasons of the demand are not taken into account

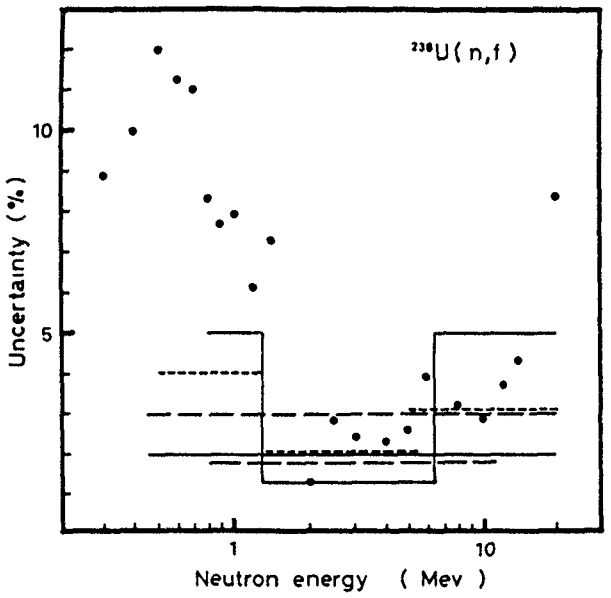

Fig. 9 Comparisons of the uncertainty of the recommended reference data for the ^{238}U fission section with the uncertainty requested in WRENDA

In the energy region between 1.5 and 15 MeV, the demands are roughly filled, particularly near 2 MeV the severest demand is satisfied Since improvement of the uncertainties in reevaluations are expected as described in the last section, achievement enough to practical users is probably reached in those works However, it is natural that the uncertainty of the reference data must be as small as possible and endeavor to improve the uncertainty of the ^{238}U fission cross section must be continued

In addition to supplying the accurate reference data it should be suggested what experimental conditions have to be satisfied in the measurement using the ^{238}U fission as the standard. The reliable measurements are conducted applying the highly developed experimental technique and the carefully computed corrections. The high accuracy oriented evaluation is performed adjusting the experimental data under the attentive consideration and studying the experimental condition. The nuclear data standards for nuclear measurements are recommended through these process. Such an ideal experimental condition and data processing is not always satisfied in the measurement of neutron flux using the ^{238}U fission cross section as a monitor. Especially, when they are used in the experiments not of the nuclear data measurements but of the reactor simulation measurements, systematic errors in the latter are probably larger than those in the former because of limited conditions in their proper experiment. The recommendation given in the report of the working group of the Argonne meeting[2] is useful for the nuclear data experimenters. A counterpart to it should be prepared for the user except the nuclear data experimenter

References

1) Nuclear Data Standards for Nuclear Measurements, 1982 INDC/ NEANDC Nuclear Standards File, Technical Report Series No. 227 (IAEA, Vieena, 1983)
2) Proc NEANDC/NEACRP Specialists Meeting on Fast Neutron Fission Cross Sections of U-233, U-235, U-238 and Pu-239, Argonne National Laboratory Report ANL-76-90 (1976)
3) S. Cierjacks, Symp. on Neutron Standards and Applications, Nat'l. Bureau of Standards, Gaithersburg, 28-31 Mar 1977, p. 278
4) B H Patrick, Proc. Int. Conf on Neutron Physics and Nuclear Data for Reactors and Other Applied Purposes, AERE Harwell, 25-29 Sep 1978, (OECD/NEA, 1978) p 76.
5) De Saussure and A. B. Smith, Proc Int Conf on Neuclear Data for Science and Technology, Antwerp, 6-10 Sept 1982, Ed K H Boeckhoff (Dr Reidel Publishing Co 1983) p. 9
6) W. W Osterhage et al., J. Phys G, 4, 587 (1978)
7) M. G Sowerby, Ann Nucl. Sci. and Energ 1, 409 (1974)
8) B I. Fursov et al., Sov, J, At, Ener , 43 808 (1978)
9) J. Blons et al., Private communication to the NEA Data Bank (1977)

10) R. Arlt et al., Proc. Conf. on Nuclear Cross Sections for Technology, Knoxville, 22-26 Oct. 1979. NBS Spec. Publ. 597,2, 3, Ed. J. L. Fowler and J. H. Johnson (1980) p.990.
11) V. M. Adamov et al., ibid. p. 995.
12) M. Varnagy et al., Nucl. Instr. Meth., 196 465 (1982)
13) Wu Jing-Xia et al., Chi. J. Nucl. Phys. 5, 158 (1983) (In Chinese)
14) K. Kanda et al., NETU-43, Research Report, Dept. Nucl. Eng. Tohoku Univ. P. 1 (1984) (In Japanese)
15) 6 th All Union conf. on Neutron Physics, Kiev, 2-6 Oct. 1983
16) CINDA 84, The Index to Literature and Computer Files on Microscopic Neutron Data, IAEA, Vieena, May 1984
17) JENDL-2, The Japanese Evaluated Nuclear Data Library Version 2, JAERI-M 84-103 (NEANDC(J) 99/AU, INDC(JPN) 86/GL) (June, 1984)
18) J. W. Behrens and G. W. Carlson, Nucl. Sci. Eng. 63, 250 (1977)
19) In ref. 5, the authors refer the data of ENDF/B-V. The recommended reference data in ref. 1 are the data of ENDF/B-V.
20) F. C. Difilippo et al., Nucl. Sci. Eng. 68, 43 (1978)
21) WRENDA 83/84, World Request List for Nuclear Data, Ed. V. Piksaikin, IAEA, INDC(SEC)-88/URSF (Vieena, 1983)

NEUTRON-INDUCED FISSION CROSS-SECTION OF ^{238}U IN THE SECOND PLATE REGION

A.A. GOVERDOVSKIJ
Institute of Physics and Power Engineering,
Obninsk,
Union of Soviet Socialist Republics

Fission cross-section of ^{238}U (σ_f^8) is used often in the capacity of the standard in the threshold neutron-induced cross-section measurements ((n,a);(n,2n)) from 4 to 10 MeV. Therefore the precision requirements of σ_f^8 are highly hard- 1-2%[1]. There are two groups of the nuclear data about σ_f^8 : 1) data of the workes, which were performed at the electrostatic generators[2-6]; 2) data of the TOF-experiments at the pulse opirated LINAC orCyclotrons[7-10]. The majority of the experimental information is available in the form of fission-cross-section ratios relative to the ^{235}U fission cross-section, therefore the most part of the total uncertainty of σ_f^8 is consist in the two values determination: a) fission fragments detection efficiency; b) nuclear ratio of the samples. To determine the relation of nuclei numbers ^{235}U and ^{238}U in the samples a method of isotope impurities or " threshold method " was emploed in the works[2-6,10]. In addition to that, the alfa-spectrometry analysis of the samples was emploed (the first group[3,4]) with the purpose of the normalizing procedure reliability rising.

Second group works have a deficiency row- low fission fragments detection efficiency[7]; lack of independent normalizing procedure[9]. Statistical and total uncertaities of the second group data are greater than the first. However, there is a few-percent (1.5-2.5%) tendency for the ENDF-B/5[11] deduced values to be systematically lower than the observatious of much of the energy range from 5 to 10 MeV for the first group data (fig.a) and to be in

good agreement with the second group data (fig.b).
Recomendation- the evaluation[11] should be redone from 4 to 10 MeV, including all first group experimental information more attentively.

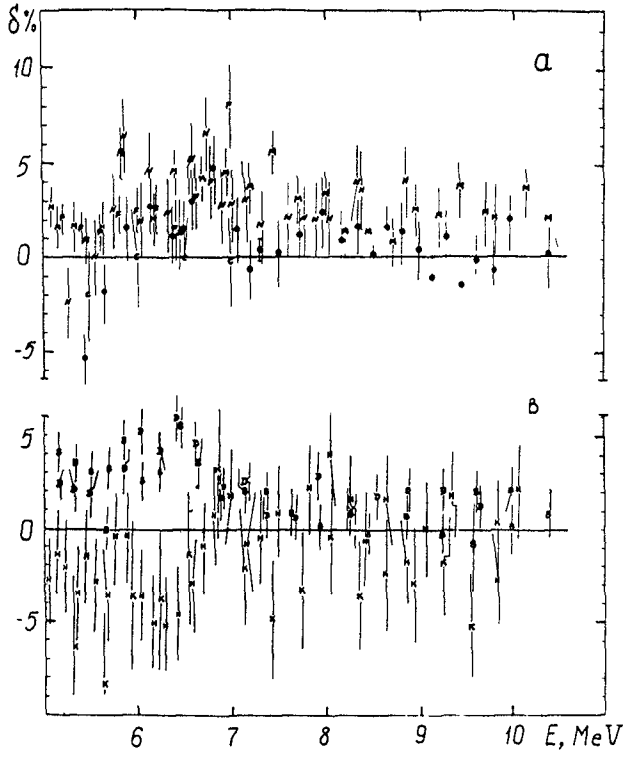

$$\delta = R_5^8{}_i - R_5^8{}_{ENDF-B/5}$$

● - 2 , F- 3 , M- 4 , N- 5 , C- 6 ,
K - 7 , H- 8 , D- 9 , B- 10.

REFERENCES

1. World Req. List for Nuclear Data Section,WRENDA 83/84,IAEA.
2. Goverdovsky A.A. et.al.-At.Energy,1984,v.56,p.162.
3. Fursov B.I. et.al.- At.energy,1977,v.43,p.181.
4. Meadows J.W.-ANL/NDM-83, 1983.
5. Nordborg C.,et.al.-In: Proc. of the NEANDC/NEACRP Special Meeting on fast neutron fission cross-sections of U-233 , U-235,U-238,Pu-239,1976, ANL-76/90, p.128.
6. Cance M.,Granier G.- ibid,p.90.
7. Cierjaks S.,et.al. - ibid,p.94.
8. Coates M.,et.al.- In: Proc.4th Conf.Tchn.,Washington,1975, v.2,p.568.
9. Difilippo F.S.,et.al.-Nucl.Sci.Engng.,1978,v.68,p.43.
10. Behrens J.W.,Carlson G.W.-Nucl.Sci.Engng.,1977,v.43,p.250.
11. INDC/NEANDC, Nucl.st.File,1980 Version, IAEA,1981,p.B-73.

FISSION RATIOS INVOLVING ^{238}U, ^{237}Np, ^{239}Pu AND ^{235}U FISSION CROSS-SECTIONS

Y. KANDA, Y. UENOHARA
Department of Energy Conversion Engineering,
Kyushu University,
Kasuga, Fukuoka,
Japan

Abstract

The fission cross sections of ^{235}U, ^{238}U, ^{237}Np and ^{239}Pu are large in MeV region The two of the formers have already been recommended as the reference data and extensively used as the nuclear data standards and the neutron spectrum monitors The accuracy of the evaluated fission cross sections of these nuclides has been studied comparing the cross sections and cross section ratios of available evaluation files The ratios of the fission cross sections of the three nuclides to that of the ^{235}U agree well in the evaluation files but the agreement of the ratios to the fission cross section of ^{238}U is insufficient It is because the number of the experiments for the former ratios is much larger than that of the latter The measurements for the fission cross section ratios of the pairs in the three nuclides expect ^{235}U are desired

1 Introduction

Requirements for an ideal standard reaction for nuclear data measurement in MeV region to be supplied in general are adequately described in ref 1 Briefly summarizing, the cross sections of the reactions should be large, be accurately known, and smoothly vary, a good sample and a suitable detector should be preparable, they should be threshold reactions Besides, recent development in fast reactor design and fusion reactor technology demands precise standards for neutron spectrum monitors as well as such standards for nuclear data measurement The requirements for both standards are similar In the present time, there are not any reactions meeting completely these requirements Therefore, possible reactions used as the standard in the MeV region should be searched for in extensive kinds of reactions On this point of view, fission cross sections of actinides have been investigated because their values in MeV region are much larger than those of any kinds of reaction cross sections and development of fission detectors have been enough to measure fission events with high efficiency

Available experimental data of the fission for the isotopes of the actinides have generally surveyed Those of ^{235}U, ^{238}U, ^{237}Np and ^{239}Pu are selected as the possible candidates for the standards Main reasons rejecting the other isotopes are that their cross section curves have a noticeable structure, for example ^{233}Th, and that experimental data are scarce, scatter in wide band or distribute apart in few groups the fission cross sections of ^{235}U and ^{238}U have been already registered in a list of the standard [2] Cierjacks[1] demonstrated the availability of ^{237}Np as the standard for the MeV range as well as ^{238}U but suggested additional measurements proposing in detail experimental conditions In view of the standard cross section in MeV region and the neutron spectrum monitor, a threshold characteristic of excitaion function of the ^{238}U and ^{237}Np is greatly important, since large fission cross sections of the ^{235}U and ^{239}Pu in ev and keV region can result in an undesirable contribution from even small admixture of slow neutrons Therefore, the ^{239}Pu fission cross section which has neither the threshold characteristic nor highly accurate data has not been considered a possible standard However, in order to utilize effectively the large cross sections as the standard references, the four fission cross sections determined consistently should be used Therefore, in the present work, it is proposed that the four fission cross sections must be discussed taking account of their correlation in the experimental data

2 Experimental Data

Major data for the ^{235}U fission cross sections have been measured intending to obtain absolute values The H(n,n) cross section is used predominantly in the ^{238}U measurements The former is recognized as the most reliable standard reference The three residual fission cross sections have been usually measured as the relative values to that of the ^{235}U Of course, if these ratio data are inverted, they are the relative value of the ^{235}U fission cross section to the others Experimenters and evaluators have been, however, understood that they are the ratio data to the ^{235}U fission cross section This inclination has come from some reasons The fission cross section of the ^{235}U as a fuel in reactors is predominantly important in nuclear technology They are very large in energy ranges of fission neutrons and slowing-down neutrons of them As a great number of available measurements scatter contrary to our expectation, experimenters wish to challenge for precise measurement On the other hand, recent developments in fast breeding reactor design have turned the interest in accurate neutron data to substantial extent towards the neutron cross sections for the ^{238}U as a fissile, the ^{239}Pu as a fuel, and the ^{237}Np as a neutron dosimeter To meet the demands, many measurements on them has recently performed On experimental technique, an application of neutron sources using high energy accelerators made it possible in the MeV region to measure precisely the magnitude and shape of the fission cross sections

An important meeting[3] on the fission cross sections of ^{233}U, ^{235}U, ^{238}U and ^{239}Pu was held at Argonne in 1976 The ^{237}Np fission cross section was not included the experimental data newly presented in this meeting and old data were studied in detail to summarize what accuracy was achieved for every fission cross section For example, it was shown for ^{235}U that between 1 and 8 MeV there was no major controversy regarding the evaluated curve with a ±3 % uncertainty

As an object of the present work is not a review of the experiments, the measured data are not systematically shown but selectively presented They are shown in Fig 1-5

3 Evaluated Data

Evaluated data can be regarded as the most probable values estimated and recommended from the experimental data available at the time They may not coincide with the others, even if every evaluator has the rightly same data set in his hand The evaluated values depend on the experiments and the estimation method adopted by the evaluator Features of the experimental data naturally affect the evaluated results It belongs to the evaluator which experimental data sets are selected from disagreeing groups It is expected, however, that they should converge to the definite values within the uncertainties given to the evaluated results Therefore, a comparison of the available evaluated data forms a good judgment on accomplishing a current object In Figs 1-5, the comparisons of the four fission data in the five evaluation data, JENDL-2[5] , ENDF/B-V[6] , ENDL 82[7] , KEDAK-4[8] , and UKNDL-1981[9] are shown In the present work, correlations between the experimental data and the evaluated data in the individual evaluations are not discussed, since our object are not in a critical review of the evaluations but in the comparison of their values

3 1 ^{235}U fission cross section

Figs 6 and 7 show the comparisons of the five evaluation data and the ratios of the four data to the ENDF/B-V data for the ^{235}U fission cross section, respectively The differences in the five data are approximately ±7 % including the UKNDL If it is rejected, the remains agree with each other in below, ±4 % over the MeV regions The agreement in the ^{235}U data is the best in four sets

3 2 ^{238}U fission cross section

Discussions on the ^{238}U data are in detail presented in another report in this meeting The differences of the data sets are below ±6 % including the UKNDL and below ±4 % not including it between 2 and 15 MeV These are comparable with the values in the ^{235}U data They are found in Figs 8 and 9 The similar comparisons in the ratio data to the ^{235}U fission cross section are shown in Figs 10 and 11 The disagreement of these data are ±3 %

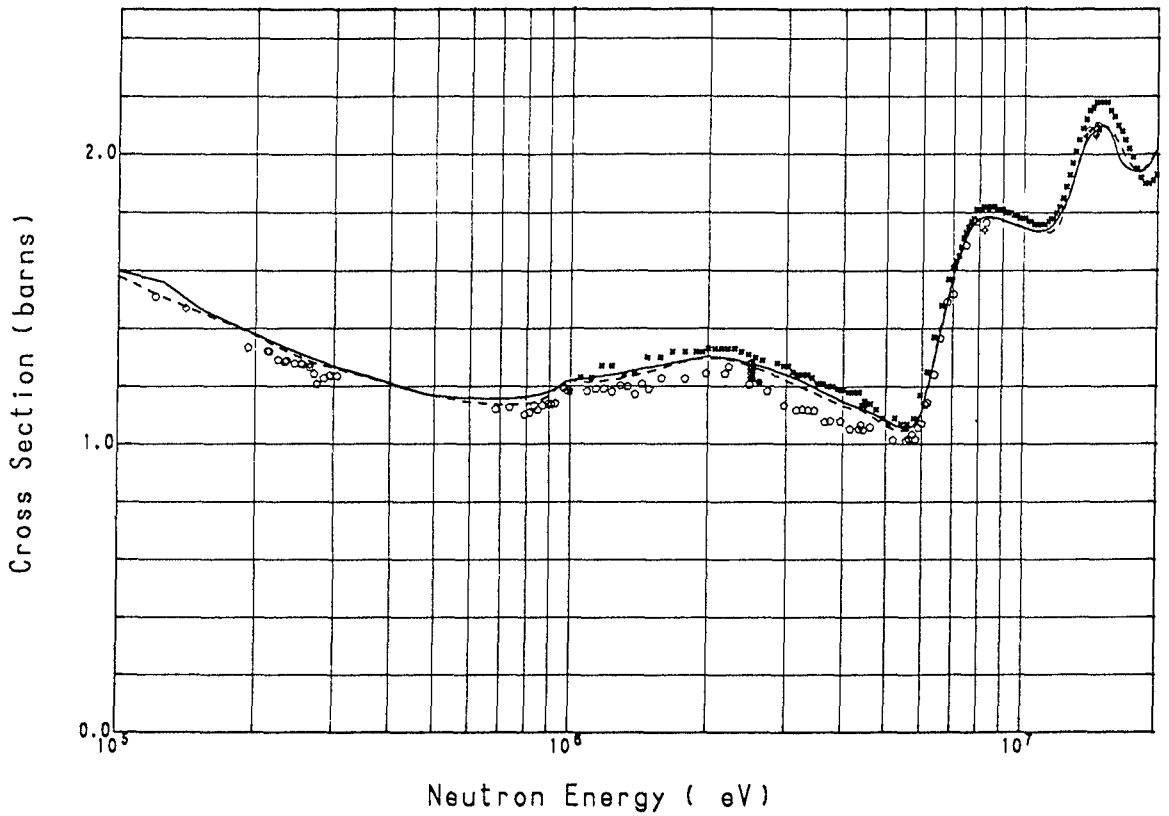

——	JENDL-2	MAT NO	2923	MF NO	3	MT NO	18
-----	ENDF/B-V	MAT NO	1395	MF NO	3	MT NO	18
○	W P POENITZ	'77	ANL	•	NSE,64,894		10711002
▽	W WEIL NG+	78	TUD		KE,21		3046 002
■	K KARI+	78	KFK		788NL,		20786006
◆	M CANCE+	'78	BRC	•	NSE,68		20779002
□	B M ALEKSANDROV+	'79	RI		AE,46		40546003
●	R ARLT+	'80	TUD	. .	TU-05-43-80		30559002
✱	M CANCE+	'80	BRC		CEA-N-2194		21620002
○	E A ZHAGROV+	'80	RI	.	80KIEV,3,45		40610003
◇	R ARLT+	'80	TUD	. .	ZFK-410,122		30558002
○	M CANCE+	'80	BRC	.	CEA-N-2194		21620002
○	R ARLT+	'81	TUD		KE,24,48		30475002
●	O A WASSON+	82	NBS	•	NSE,80,282		10971002
●	LI JINGWEN+	'82	AEP	.	82ANTWER,		30634002

Fig. 1 Fission cross section of ^{235}U. See references at the end of text.

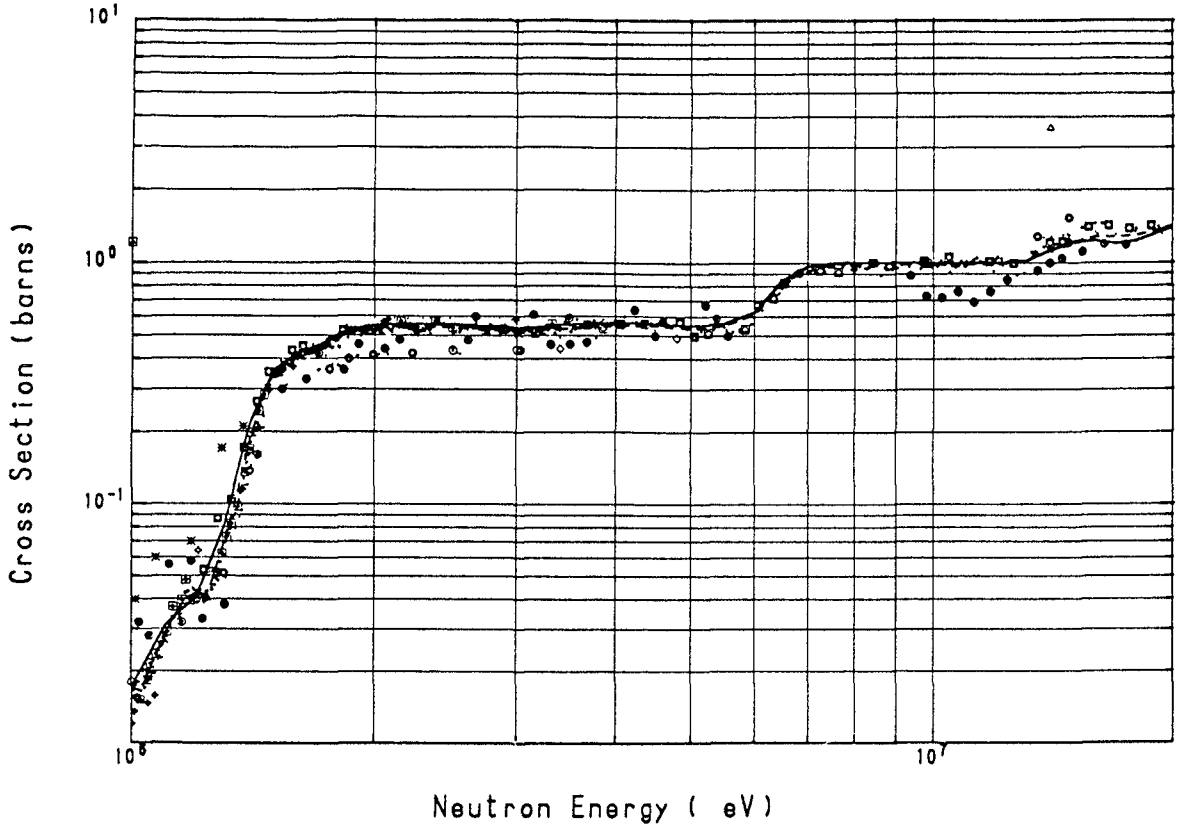

Fig 2 Fission cross section of ^{238}U See references at the end of text

——	JENDL 2	MAT NO	2925	MF NO	3	MT NO	18
-----	ENDF/B V	MAT NO	6398	MF NO	3	MT NO	18
◇	J H W LLIAMS	46	LAS		LA 520		12312004
▽	W NYER	48	LAS		LA 719		12514002
△	A PHILLIPS+	48	LAS		LAMS 774		12495002
◆	R W LAMPHERE	56	ORL		PR 104 1654		12338008
✱	F NETTER	56	SAC		NETTER		21093003
□	C A UTTLEY+	56	HAR		AERE NP/R 1996		2 468002
◆	R K SMITH+	57	LAS	•	BAP 2		12316011
○	W D ALLEN+	57	HAR		PPS/A 70 573		21075004
●	P BILLAUD+	58	SAC		58GENEVA 16 106		21452002
⊕	A KATASE	61	KYU		KATASE		20299003
⊙	B ADAMS+	61	ALD	•	JNE 14 85		21209002
●	M MANGIALAJO+	63	CIS		NP 43 124		21127002
●	R BATCHELOR+	65	ALD		NP 65 236		21019024
●	V EMMA+	65	CAT		NP 63 641		21134002
⊕	J A GRUNDL	67	LAS	•	NSE 30 39		104 7004
○	R C BARRALL+	69	STF		AFWL R 58 134		10022025
○	R C BARRALL+	69	STF		AFWL TR 68 134		10022025
○	P E VOROTN KOV+	71	KUR		YFI 12 22		40110002
●	I M KUKS+	71	CCP		AE 30		40081002
○	W P POENITZ+	72	ANL		JNE 26 483		10232006
○	W P POENITZ+	72	ANL		JNE 26 483		10232005
○	W P POENITZ+	72	ANL		JNE 26 483		10232003
○	W P POENITZ+	72	ANL		JNE 26 483		10232002
○	W P POENITZ+	72	ANL		JNE 26 483		10232004
●	I D ALKHAZOV+	74	RI		73KIEV 4 13		40256002
●	P E VOROTN KOV+	75	KUR		YFI 20 9		40325002
○	J W MEADOWS	75	ANL		M ACOWS		10504002
◘	I D ALKHAZOV+	76	RI		YFI 22 12		4 408003
●	W W OS ERHAGE	76	GLS	•	OSTERHAGE		20715003
◘	B LFUGERS+	76	KFK		76ANL 246		20943003
⊠	V M A AMOV+	77	RI		YFI 23 17		40547007
⊞	J+	77	SAC		B ONS		20796003
•	M CANCE+	78	BRC	•	NSE 68		20779003
⊠	B M ALEKSANDROV+	79	RI		AE 46		40546004
■	R ARLT+	81	TUD		KE 24 48		30475003

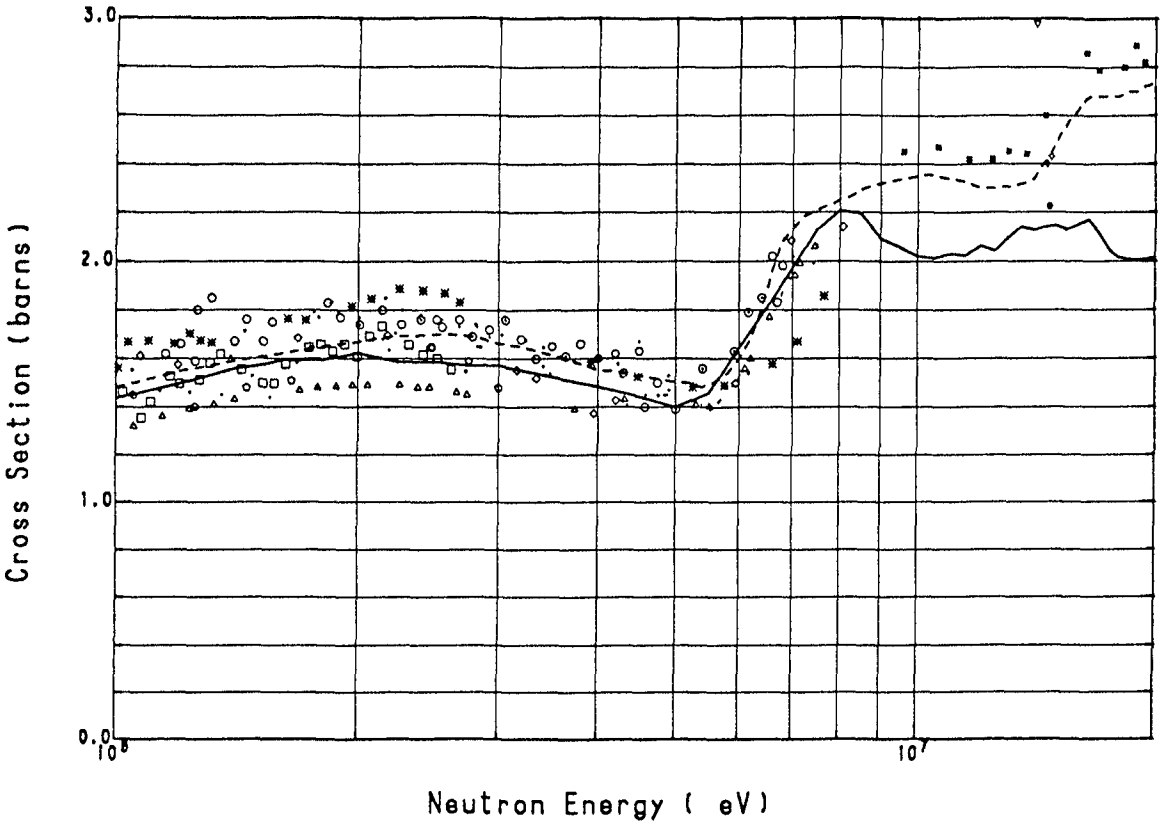

——	JENDL-2	MAT NO	2931	MF NO	3	MT NO	18	
-----	ENDF/B-V	MAT NO	1337	MF NO	3	MT NO	18	
○	E D KLEMA	'47	LAS		PR,72,88			12492002
△	R L HENKEL	'57	LAS		LA-2114			12321006
◆	A N PROTOPOPOV+	58	CCP		AE,4,(2),190			40390003
○	H W SCHMITT+	59	ORL		PR,116,1575			12488003
○	H W SCHMITT+	'59	ORL		PR,116,1575			12488002
*	*V M PANKRATOV+*	*60*	CCP	•	AE,9,399			40638003
◇	J A GRUNDL	'67	LAS	•	NSE,30,39			10417003
▽	R H IYER+	'69	TRM	•	69ROORKEE 2,289			30035005
□	W K BROWN+	'70	LAS		NP/A,156,609			10060002
✱	R J JIACOLETTI+	'72	LAS		NSE,48,412			10182002
○	K KOBAYASHI+	'73	KTO		,KOBAYASHI			20300002
◆	I D ALKHAZOV+	'77	RI	•	77KIEV,3,155			40552003
●	R ARLT+	81	TUD		KE,24,48			30475004
○	M CANCE+	82	BRC	•	82ANTWER,51			21821006

Fig. 3 Fission cross section of ^{237}Np. See references at the end of text.

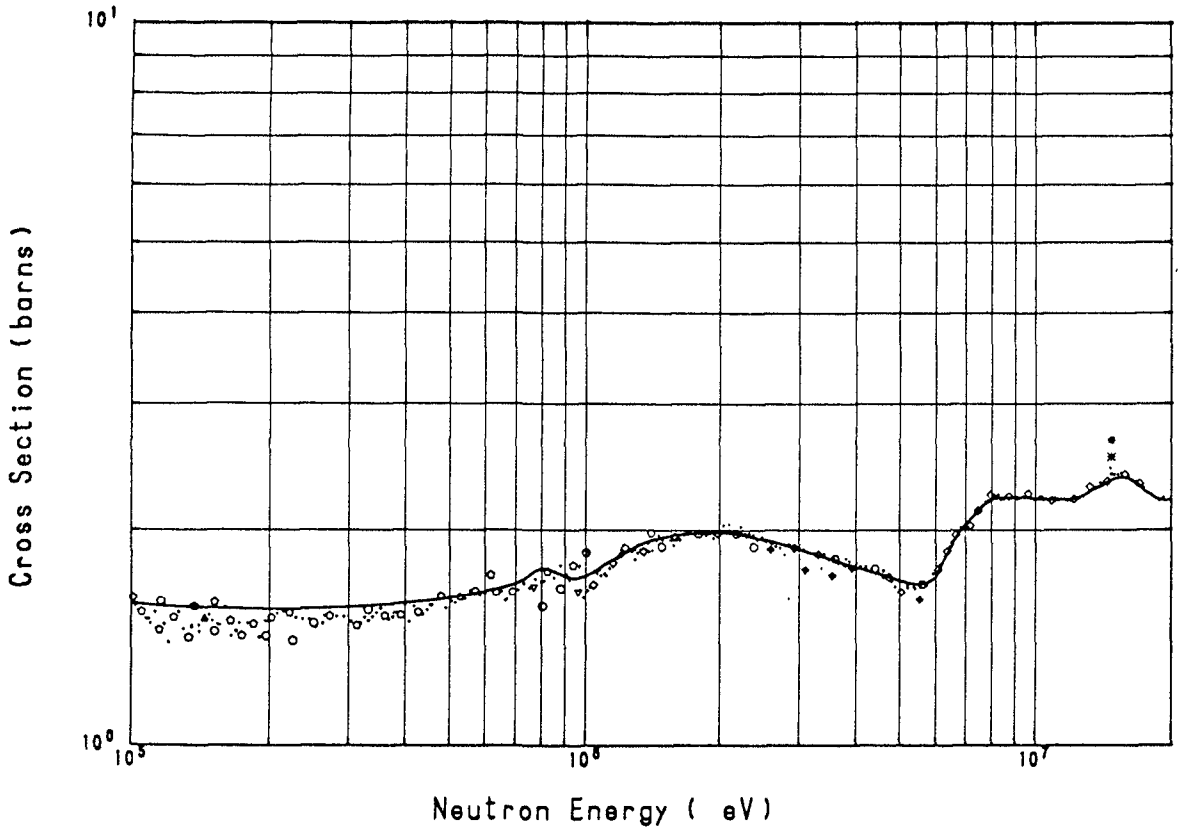

——	JENDL-2	MAT NO. 2943	MF NO. 3	MT NO. 18	
△	K.D.ZHURAVLJOV+	'75	NIR . .	75KIEV,6,67	40476003
○	D.B.GAYTHER	'75	HAR . .	75WASH,GB-6	20428002
◆	I.SZABO+	'76	CAD . .	76ANL,,	20618003
○	I.SZABO+	'76	CAD . .	76ANL,208	20567003
○	I.SZABO+	'76	CAD . .	76ANL,208	20570003
○	I.SZABO+	'78	CAD . .	76ANL,208	20569003
▽	M.C.DAVIS+	'78	MHG . .	ANE,5,569	10545002
◇	K.KARI+	'78	KFK . .	78BNL,	20786004
■	M.CANCE+	'78	BRC . .	NSE,68,(2),197	20779005
□	R.ARLT+	'81	TUD . .	KE,24,48	30475005
✱	LI JING-WEN+	'82	AEP . .	82ANTWER,,55	30634003
◆	M.MAHDAVI+	'82	MHG . .	82ANTWER,,58	12826003
○	ZHOU XIAN-JIAN+	'82	AEP . .	CHP,4,(2),131	30670002
●	I.GARLEA+	'83	PIT . .	GARLEA	30647007

Fig. 4 Fission cross section of ^{239}Pu. See references at the end of text.

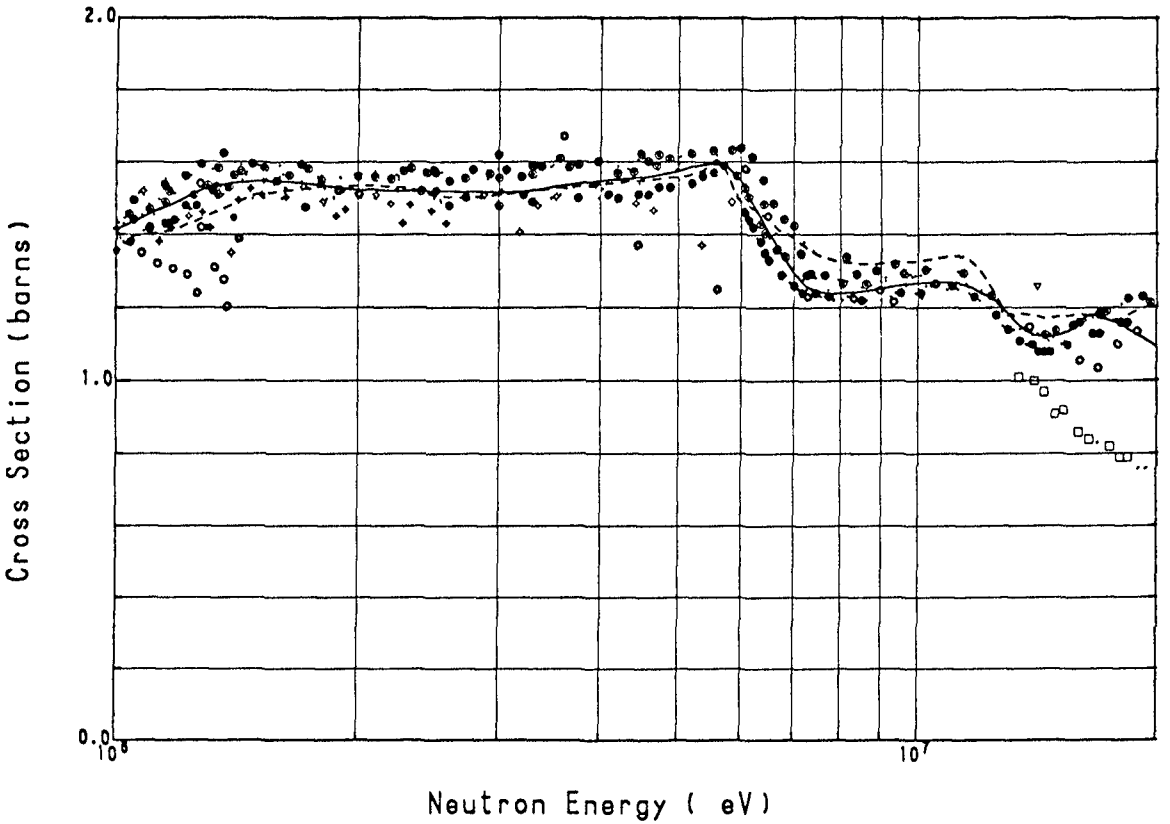

Fig. 5 Fission cross section ratio: $^{239}Pu/\ ^{235}U$. See references at the end of text.

——	JENDL-2	MAT NO	2943	MF NO 3	MT NO	8
-----	ENDF/B-IV	MAT NO	1264	MF NO 3	MT NO	8
◇	J H W LLIAMS	46	LAS	LA-S20		12312005
▽	J S WAHL+	54	LAS	• LA-1681		12437004
□	B ADAMS+	61	ALD	• JNE,14 85		21209004
✱	P H WHITE+	67	ALD	• JNE,21 671		21195007
◆	G N SM RENKIN+	67	FEI	ICD-4		40027005
◆	G N SMIRENKIN+	'67	FEI	ICD-4		40027003
○	V G NESTEROV+	68	FEI	AE,24,(2) 185		40309002
◆	M V SAVIN+	69	KUR	YFI-8,12		40020002
●	W P POENITZ	70	ANL	NSE,40,383		10086004
○	M SOLEILHAC+	'70	BRC	70HELSINKI,2		14520568003
⊙	E PFLETSCHINGER+	70	KFK	• NSE,40,375		20363003
●	W P POENITZ	'72	ANL	• NSE 47,228		10253002
●	B I FURSOV V M KUPRI	75	FEI	75KIEV 6 3		40501002
●	S CIERJACKS+	76	KFK	76ANL 94		20409003
⊙	E F FOMUSHKIN+	77	KUR	YFI-24,10		40543002
●	K KARI+	78	KFK	78NL		20786005
●	J W MEADOWS	78	ANL	NSE,68 360		10734002
○	G W CARLSON+	78	LRL	• NSE 66,205		10562002
○	M CANCE+	78	BRC	• NSE,68 (2),197		20779006
●	M VARNAGY+	82	KOS	NIM,196,465		30588005

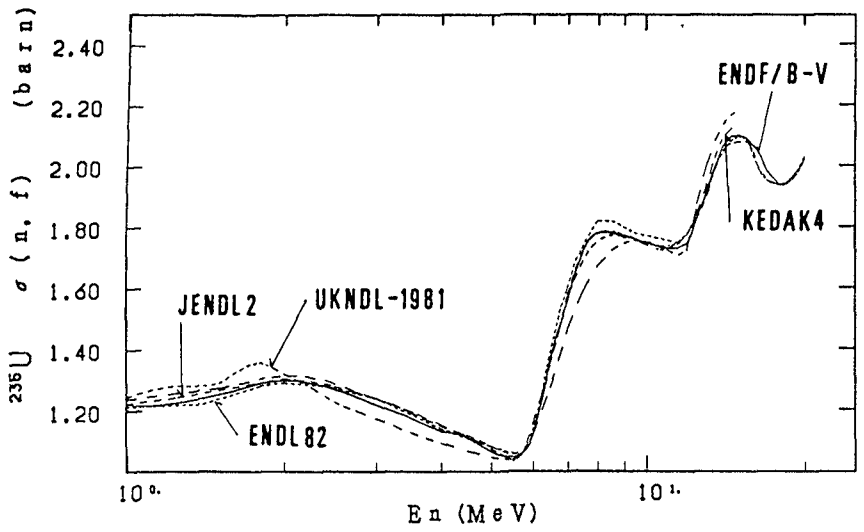

Fig. 6 Comparison of the five evaluated data for the ^{235}U fission cross section

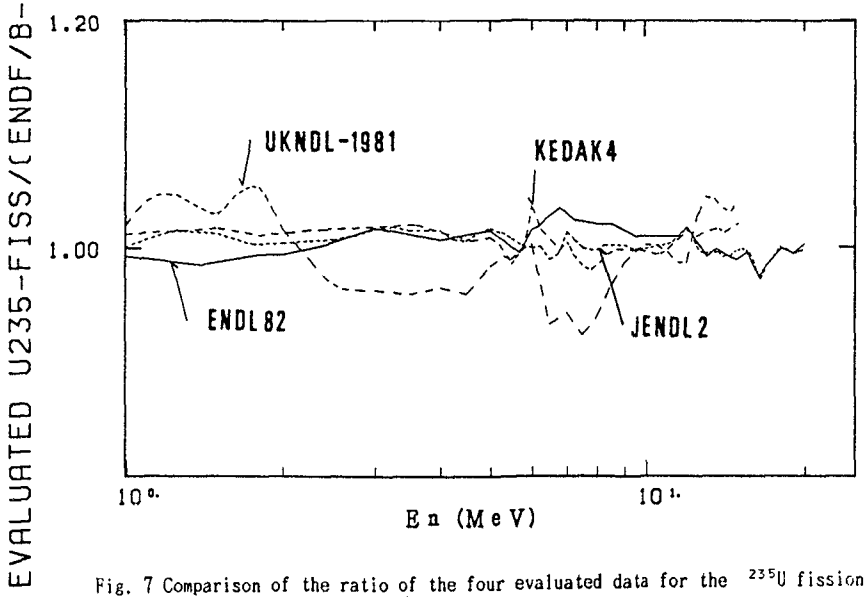

Fig. 7 Comparison of the ratio of the four evaluated data for the ^{235}U fission cross section to that of ENDF /B-V.

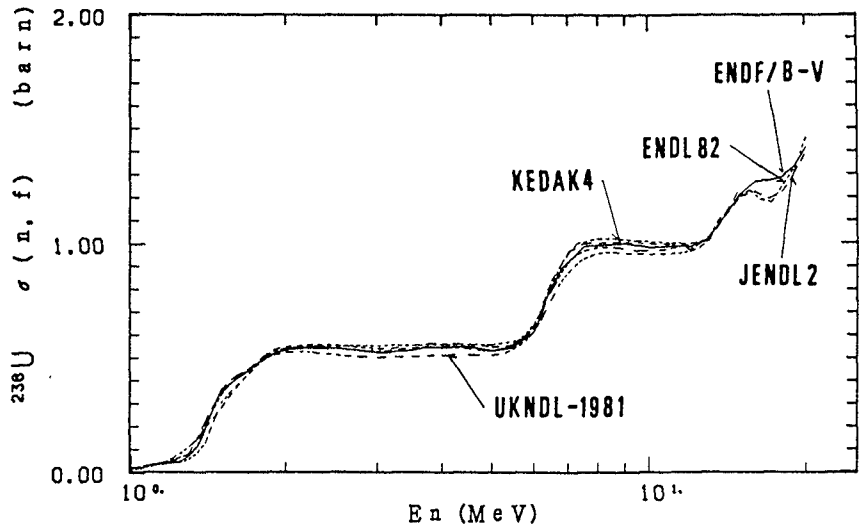

Fig. 8 Comparison of the five evaluated data for the ^{238}U fission cross section.

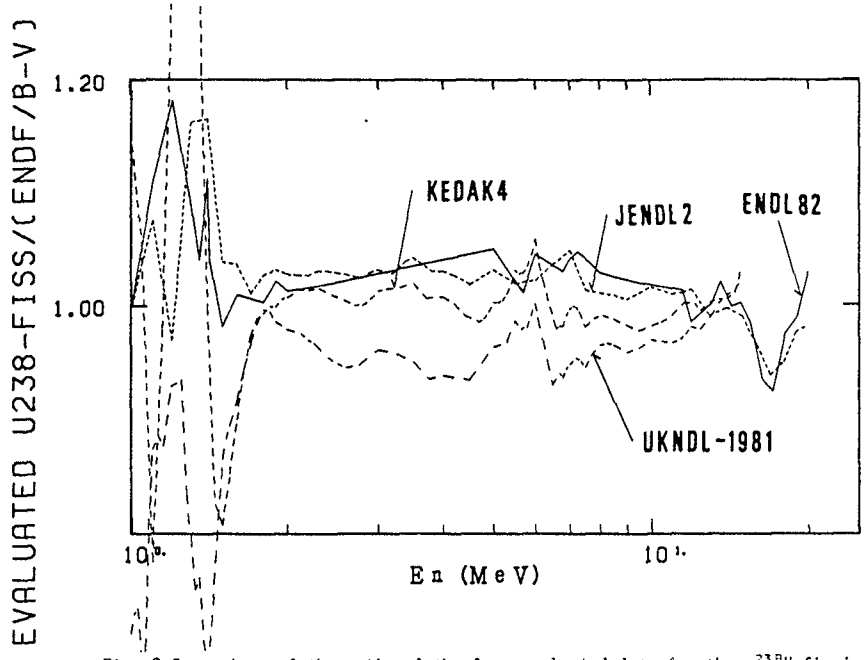

Fig. 9 Comparison of the ratio of the four evaluated data for the ^{238}U fission cross section to that of ENDF /B-V.

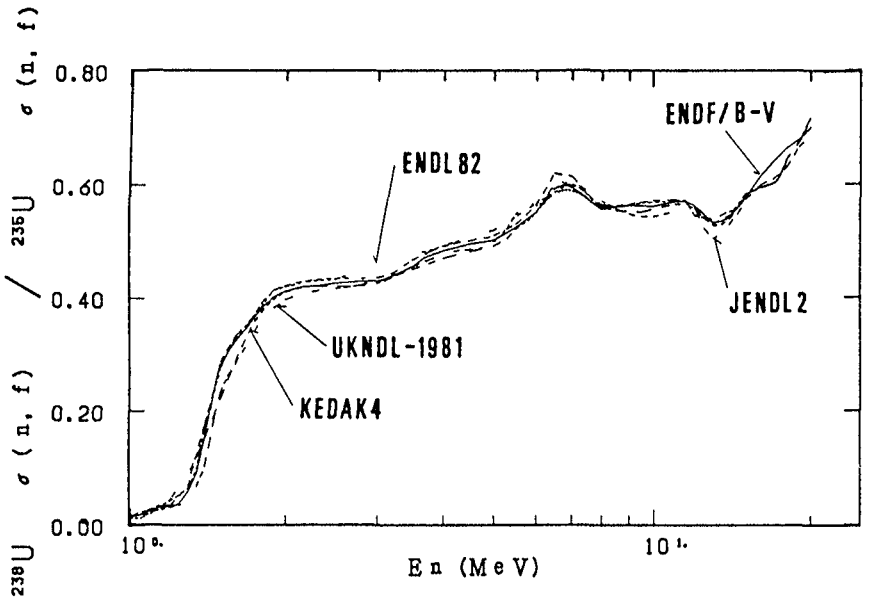

Fig 10 Comparison of the five ^{238}U / ^{235}U fission ratio in the five evaluated data

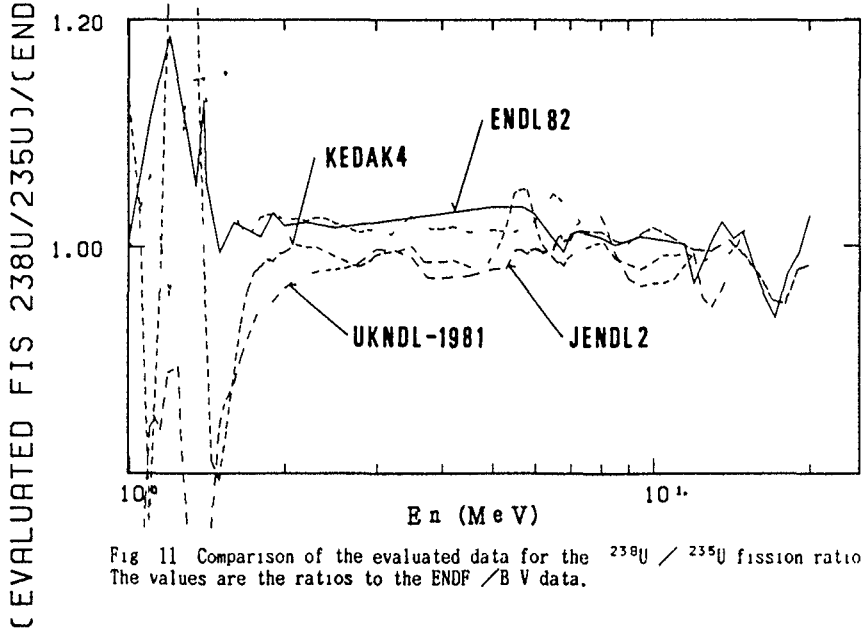

Fig 11 Comparison of the evaluated data for the ^{238}U / ^{235}U fission ratio The values are the ratios to the ENDF /B V data.

3 3 ^{237}Np fission cross section

In Fig 12, the five evaluated data for the ^{237}Np fission cross section are compared Between 0 8 and 10 MeV, they agree well Below 0 8 MeV near the threshold and above 10 MeV, disagreement among the five data are recognized The latter come from the two experimental groups The difference of the evaluated data is ±6 % between 0 6 and 10 MeV This is shown in Fig 13 as the ratios of the data to the ENDF/B-V data In Figs 14 and 15, the ratios to the ^{235}U data are presented In these figures, the differences of about ±10 % including UKNDL and ±3 % not including it between 0 6 and 10 MeV are seen

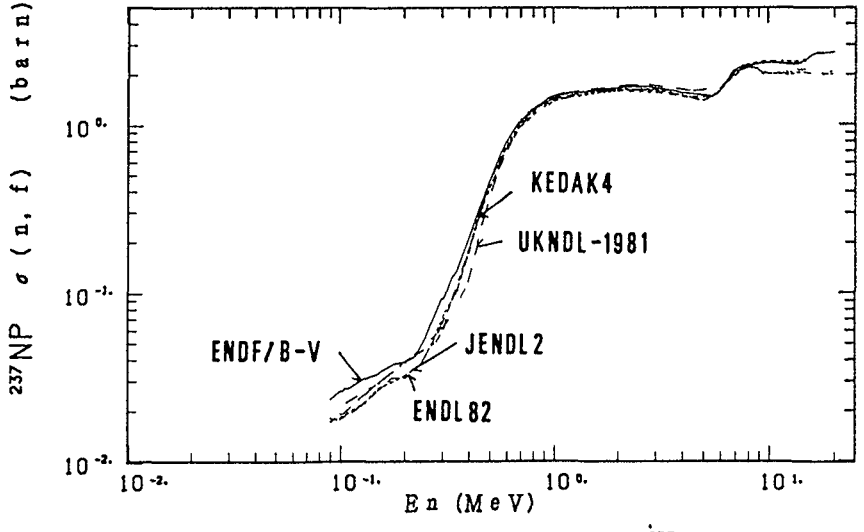

Fig. 12 Comparison of the five evaluated data for the ^{237}Np fission cross section.

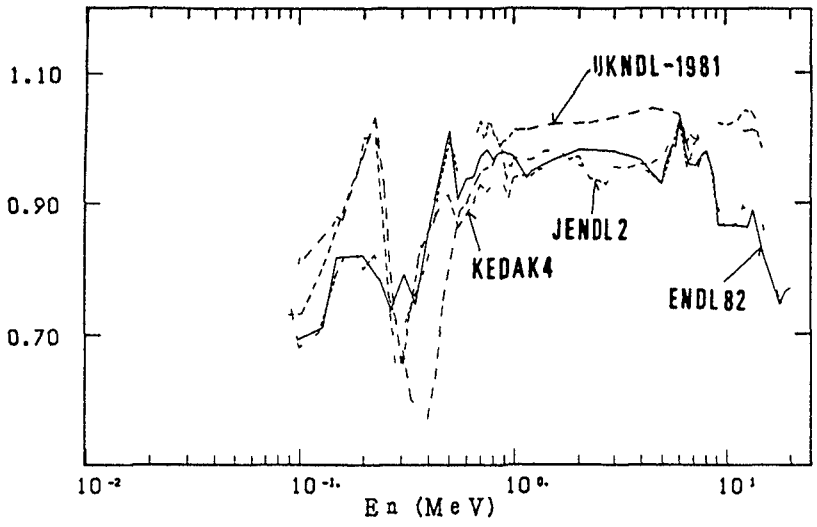

Fig 13 Comparison of the ratio of the four evaluated data for the ^{237}Np fission cross section to that of ENDF /B V.

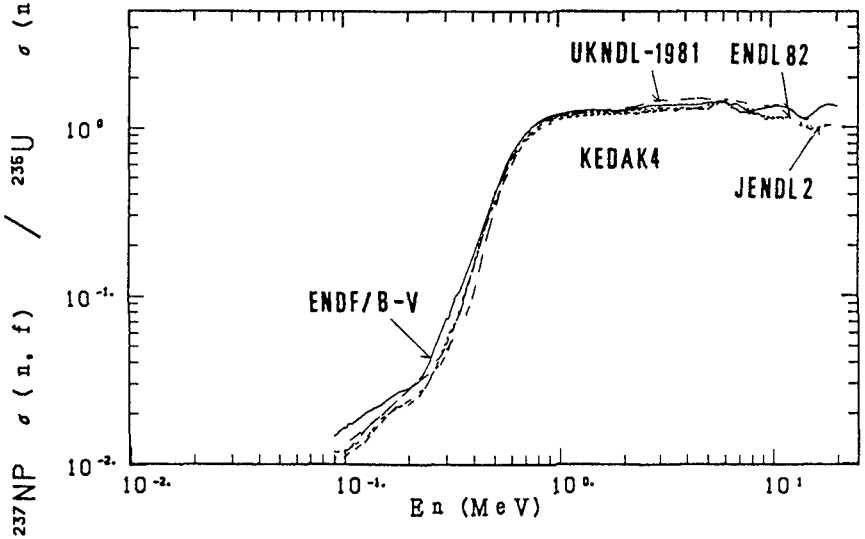

Fig 14 Comparison of the five ^{237}Np/ ^{235}U fission ratio in the five evaluated data

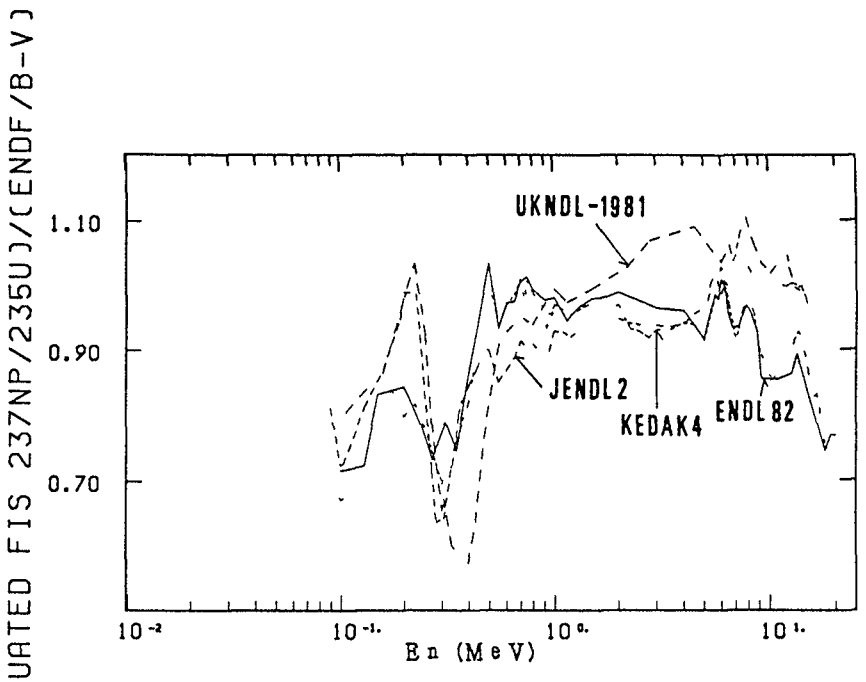

Fig 15 Comparison of the evaluated data for the ^{237}Np/ ^{235}U fission ratio The values are the ratios to the ENDF /B V data

3 4 ^{239}Pu fission cross section

As seen in Fig 16, the five evaluated data extended reflecting a wide distribution in the experiments above 10 MeV Fig 17 shows the ratio of the evaluated cross sections to those of the ENDF/B-V data Below 10 MeV the five data agree with each other in ±15 % and the four data without the UKNDL-1981 do in ±3 % The ratio of the ^{239}Pu fission cross sections to the ^{235}U data are presented in Figs 18 and 19 showing their values and their fractions to the ENDF/B-V data, respectively The differences of the five ratio data are about ±5 % below 10 MeV

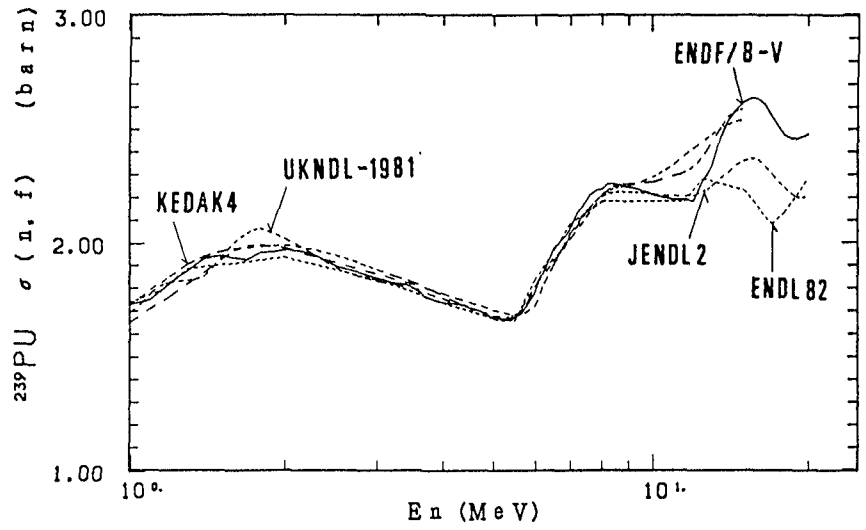

Fig. 16 Comparison of the five evaluated data for the ^{239}Pu fission cross section.

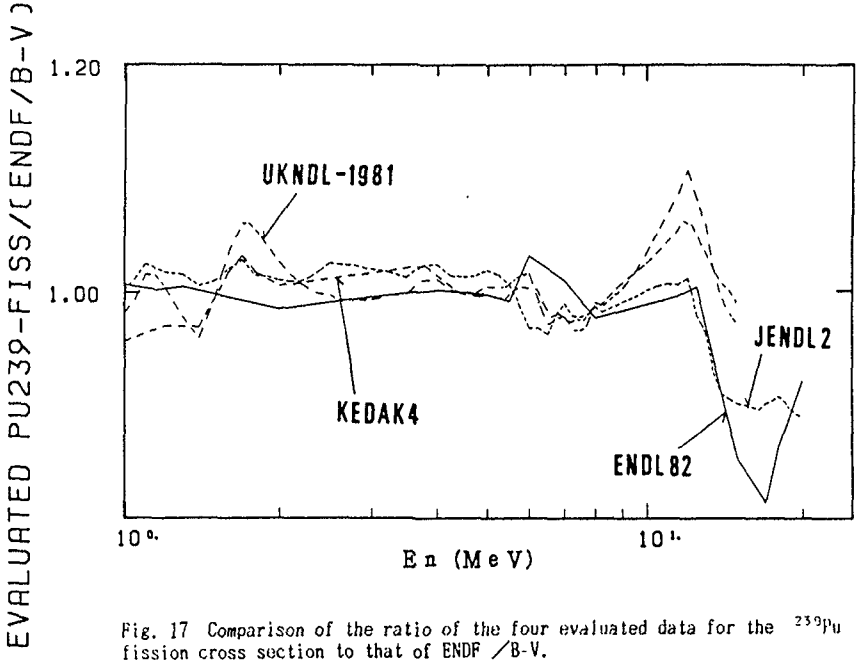

Fig. 17 Comparison of the ratio of the four evaluated data for the ^{239}Pu fission cross section to that of ENDF /B-V.

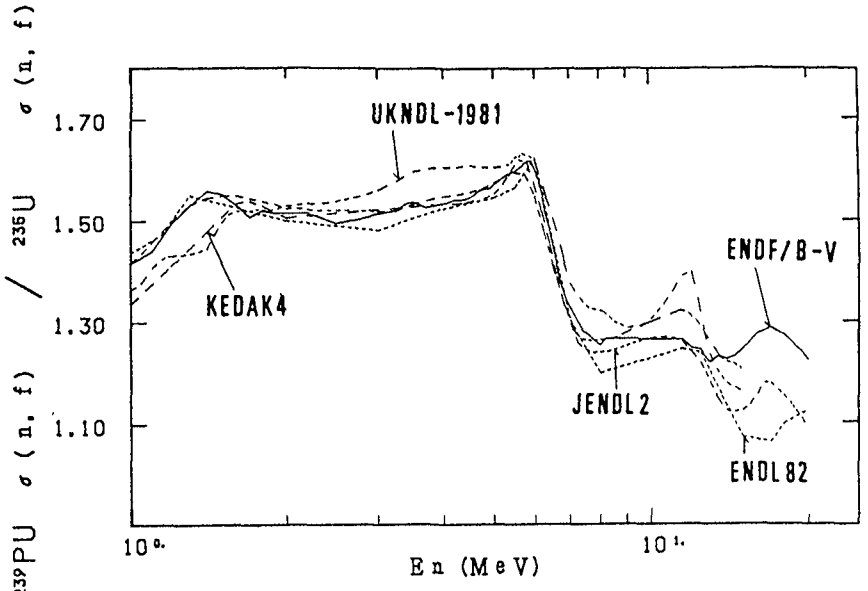

Fig. 18 Comparison of the five $^{239}Pu/^{235}U$ fission ratio in the five evaluated data.

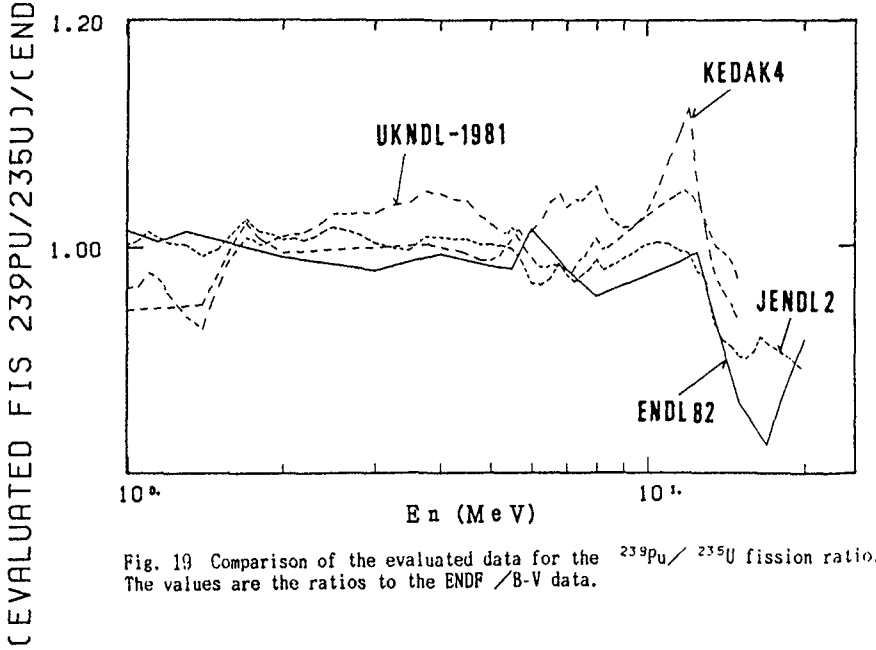

Fig. 19 Comparison of the evaluated data for the $^{239}Pu/^{235}U$ fission ratio. The values are the ratios to the ENDF /B-V data.

3 5 Comparison of ^{237}Np and ^{239}Pu fission cross section with ^{238}U fission cross section

The ^{237}Np and ^{239}Pu fission cross section are compared with ^{238}U fission cross section in Figs 20 and 21, respectively The ratio for ^{239}Pu is larger than that for ^{237}Np The comparison of the ratio of the ^{237}Np and ^{239}Pu fission cross section to the ^{238}U fission cross section with ENDF/B-V were seen in Figs 22 and 23, respectively The difference of the ratios is 20 %

3 6 Summary on comparisons in the evaluated data

Comparisons of the evaluated data in the valid energy region clarify the following status

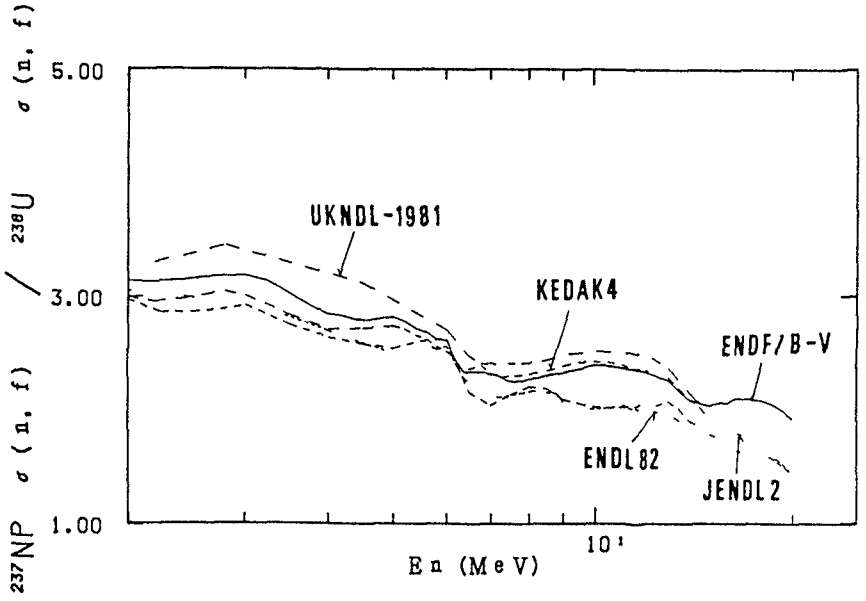

Fig 20 Comparison of the five $^{237}Np/\ ^{238}U$ fission ratio in the five evaluated data

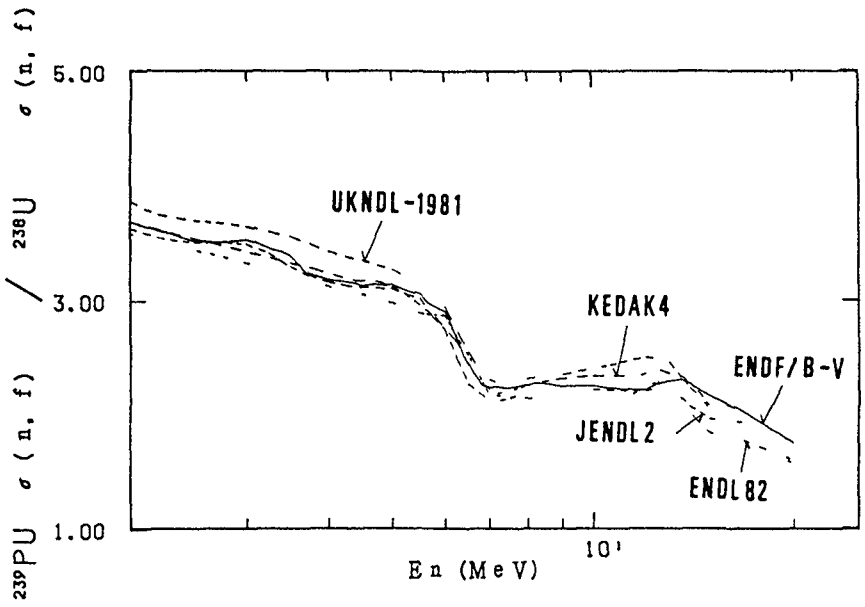

Fig. 21 Comparison of the five $^{239}Pu/\ ^{238}U$ fission ratio in the five evaluated data

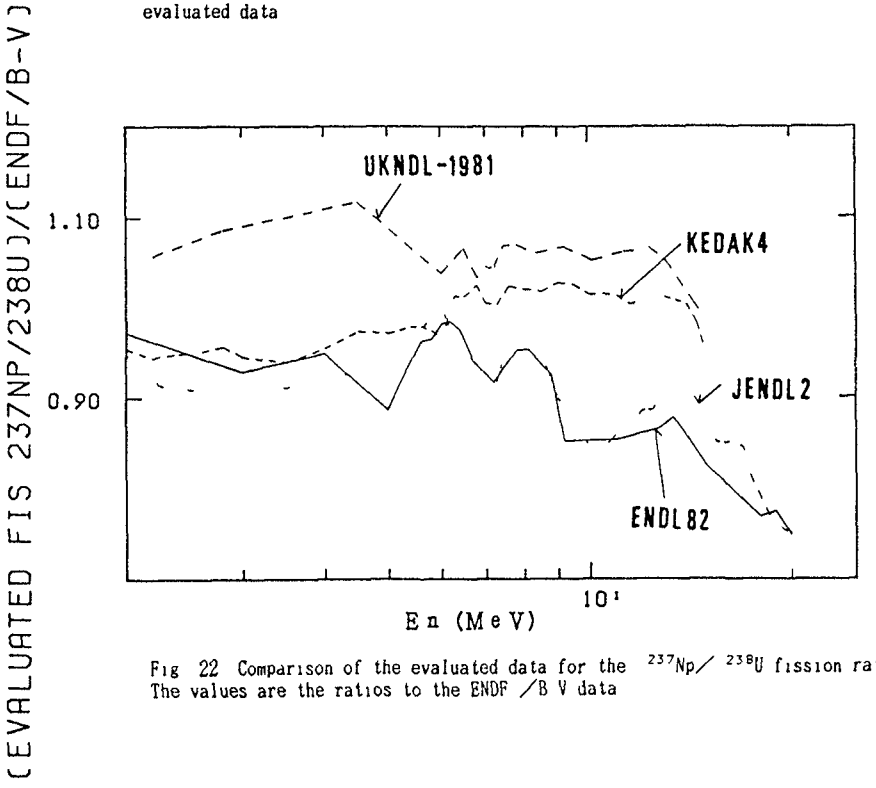

Fig 22 Comparison of the evaluated data for the $^{237}Np/\ ^{238}U$ fission ratio The values are the ratios to the ENDF /B V data

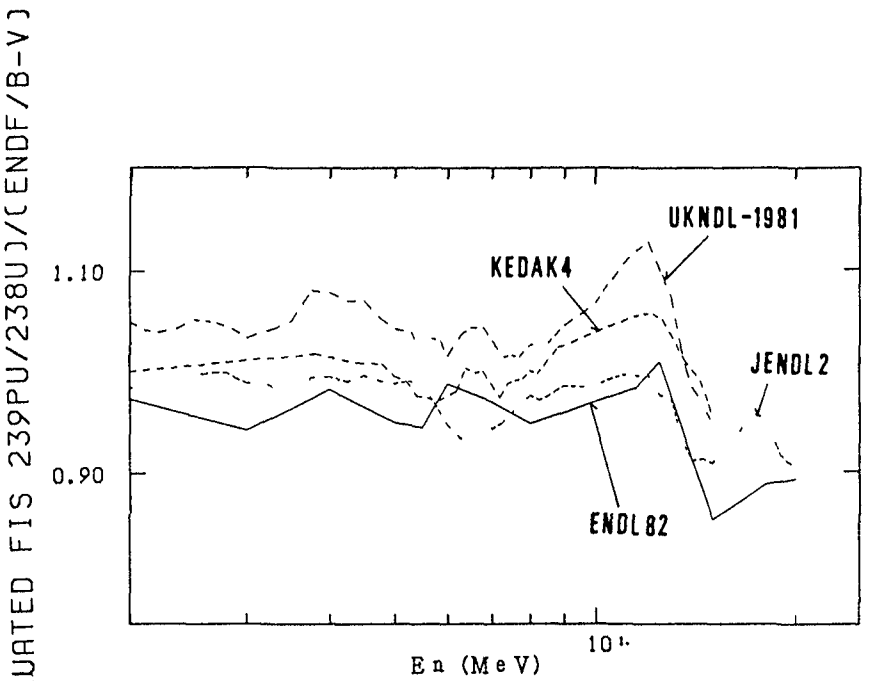

Fig. 23 Comparison of the evaluated data for the $^{239}Pu/^{238}U$ fission ratio. The values are the ratios to the ENDF /B V data.

(i) The five evaluated data of the fission cross section for the four nuclides disagree with each other in the range from 5 to 7 % If the UKNDL-1981 is not included the differences are decreased to about 4 %

(ii) The ratios of the evaluated values for the ^{238}U, ^{237}Np and ^{239}Pu fission cross sections to that for the ^{235}U are from 3 to 10 % for the five evaluations If the UKNDL-1981 is not included, the disagreement is about 3 %

(iii) The differences in the ratios of the ^{237}Np and ^{239}Pu fission cross section to the ^{238}U fission cross section are larger than the case of the ^{235}U standard.

The reason that the UKNDL dose not agree with the others in all cases come from the difference of the evaluated values for the ^{235}U fission cross section This can be seen in Fig 6

4 Concluding Comments

The fission cross section of ^{235}U used extensively as the standard reference in neutron cross section measurements is not always pre-eminent above those of ^{238}U, ^{237}Np and ^{239}Pu for the standard cross section Especially, the status of the ^{235}U fission data in the MeV region is similar to that of the three nuclides regarding with both the experimental data and evaluated data Although the number of absolute measurements for ^{235}U are overwhelmingly more than for the others, their agreements have not been achieved enough to obtain the recommended value having much smaller uncertainties given for the recommended reference data of the ^{235}U are comparable with those of ^{238}U And the former is larger than the latter in the specific region where the curve of the ^{238}U fission cross section is plateaulike The plateau-shaped excitation function is very valuable for the standard cross section because of insensitivity to neutron energy fluctuation during the measurement The fission cross section curve of the ^{237}Np has a similar feature although the curve of the ^{238}U apparently looks better than one of the ^{237}Np Both fission cross sections have threshold This characteristic is profitable for the standard reference in the MeV region are pointed out in section 1

The fission cross section of the ^{239}Pu is the largest in the four However, it has never been used and even considered as the standard cross section owing to the scarcity of the experimental data and the difficulties of a sample handling and mass assay The reasons that it is adopted as one of the possible standard are that the experimental data have been considerably accumulated and have an accuracy comparable with the others as shown in the preceding sections In addition, since the shape of the ^{239}Pu fission cross section is similar to that of the ^{235}U, it is advantage for the counterpart of the ^{235}U in contrast with a pair of the ^{238}U and ^{237}Np when the ratios of the fission cross section are regarded

Major data of the fission cross sections for the actinides have been usually measured as the ratios to the ^{235}U fission cross section Available ratio data for the other kinds of pairs are very scarce in the fission experiments Therefore, the fission cross section of every nuclide has particularly strong correlation with those of the ^{235}U A typical example of this relation has been indicated on UKNDL-1981 in the last section The deviation of the evaluated ^{235}U fission curve of this file from the curves in the other files propagate to the evaluations for the other nuclides through the ratio data to ^{235}U fission If the other ratio data, e g ^{238}U to ^{237}Np, ^{239}Pu to ^{238}U, are numerously present the correlation of the other pairs become so strong that biased evaluated data in one fission cross section do not directly affect to the other evaluated results In this way, many kinds of ratio data possibly produce the most probable results for the four fission cross sections

The absolute cross sections of the individual nuclides should be also measured although the ratio data have been intensively discussed It is not expected in the near future that the data for a specific nuclide among those are most accurately measured The recommended fission cross sections of the four nuclides should be simultaneously considered and decided taking account of their absolute and ratio measurement The standard reference data can be selected the most appropriate data from application In this context, since the available ratio data in the present are predominantly ones to ^{235}U, the experiments of the other pairs are ardently desired

Acknowledgement

The authors are very greatful, to Dr S Igarashi(JAERI) for his valuable discussion and Mrs T Asami and Y Nakagawa (JAERI) for their kind help to the preparation of the manuscript

References

1) S Cierjacks, Symp on Neutron Standards and Applications, Nat'l Bureau of Standards, Gaithersburg, 28-31 Mar 1977, p 278
2) Nuclear Data Standards for Nuclear Measurements, 1982 INDC/NEANDC Nuclear Standards File, Technical Report Series No 227 (IAEA, Vieena, 1983)
3) Proc NEANDC/NEACRP Specialists Meeting on Fast Neutron Fission Cross Sections of U-233, U-235, U-238 and Pu-239, Argonne National Laboratory Report ANL-76-90 (1976)
4) The NEA Data Bank at Saclay, France
5) JENDL-2, The Japanese Evaluated Nuclear Data Library Version 2 compiled by the Japanese Nuclear Data Committee, JAERI-M 84-103 (NEANDC(J) 99/AU, INDC(JPN) 86/GL) (June, 1984)
6) ENDF/B-V, The Evaluated Nuclear Data File, B-Format, version V (U S A), Data are obtained from the NEA Data Bank
7) ENDL-82, Evaluated Nuclear Data Library, UCRL-50400 vol 4, Data are obtained from NEA Data Bank
8) KEDAK-4, The German Nuclear Data Library (1983 edition), Data are obtained from NEA Data Bank
9) UKNDL-1981, The UK Nuclear Data Library, UKNDL-1981 edition, Data are obtained from NEA Data Bank

References for the experimental data shown in Figs 1, 2, 3, 4 and 5

SESSION V

EVALUATION OF THE THERMAL NEUTRON CONSTANTS OF ^{233}U, ^{235}U, ^{239}Pu AND ^{241}Pu AND THE FISSION NEUTRON YIELD OF ^{252}Cf

E.J. AXTON
Central Bureau for Nuclear Measurements,
Joint Research Centre,
Commission of the European Communities,
Geel

Abstract

In 1982 a simultaneous least-squares evaluation of the thermal neutron constants of ^{233}U, ^{235}U, ^{239}Pu, and ^{241}Pu together with the fission neutron yield from the spontaneous fission of ^{252}Cf was performed with, for the first time, a full covariance matrix for the input data. The input data set was limited in that measurements in Maxwellian reactor spectra were excluded.(A) Concurrently, a similar evaluation was performed at Brookhaven which included the Maxwellian data set but which did not have an input covariance matrix, although the more important correlations were handled by other methods. (B).

In the present work the Maxwellian data from B has been added to A, and the differences between the input and output data for the various evaluations are discussed.

1. Introduction.

The importance of these data stems from the role they play in the prediction of the neutron economy in nuclear power reactors. The continued appearance of new data, and the improvement in standard reference data has prompted a continuous re-evaluation over the years since the late 1950's. Previous evaluations which are relevant to the present study are those of Sjostrand and Story (1961), Westcott, Ekburg, Hanna, Pattenden, Sanatini, and Attree (1965), Hanna, Westcott, Lemmel, Leonard, Story, and Attree (1969), Lemmel (1982), Axton (1984), and Divadeenam and Stehn (1984). Of these, that of Axton (1984), which describes work carried out in 1982, is the only one in which the input data is accompanied by a full covariance matrix.

The input data, however, were limited in that measurements made in Maxwellian reactor spectra was excluded for various reasons.

The purpose of the present study is to update the 1982 data set in various stages as follows:

1. To update the 1982 data set in the light of new measurements and new interpretations of old measurements.
2. To add the Maxwellian component of the data set of Divadeenam et al.(1984).
3. To update the Maxwellian component of this data set.

Although some of the more important correlations in the uncertainties in Divadeenam et al. (1982) were accommodated by other techniques, it is important to identify all of the correlations. Also some of the measurements have been re-calculated with new standard reference data.

In order to avoid too much repetition, this paper should be regarded as a supplement to Axton (1984) and read in conjunction with it. Thus, measurements will not be discussed or referenced in this paper unless there have been changes in them, but, for convenience the earlier reference list is reproduced as Append.x 5.

2. Comments on the fitting procedures.

The fitting procedure used here was described in Axton (1984). The problem is non-linear, and it is therefore necessary to introduce starter values (guess-parameters) for each of the floating variables to be fitted. The observation vector consists of the fractional difference between the measured values and the values calculated from the guess-parameters using the functions which describe the measurements. The covariance matrix consists of fractional variances and covariances, and the solution consist of fractional corrections to the guess parameters. It is preferable, but not essential, for the guess-parameters to be close to the anticipated fitted values. The process is iterated by using the corrected guess values as input to the next fit, and it is continued until the output corrections become zero or negligible. The functions describing the measurements are known as 'APL executable functions'. They consist of 'base' functions which represent the independent variables which float in the fit, and 'derived' functions which are functions of the base functions. For example ABS and FIS which represent 2200 ms^{-1} absorption and fission cross sections respectively and NUB which represents $\bar{\nu}_T$, are base functions, whereas CA, which is ABS-FIS, and ETA, which is NUB x FIS - ABS, are derived functions. There is no limit to the number of derived functions which can be written.

A list of the functions used in this evaluation appears in appendix 1 together with the identifiers used to identify the nuclides involved. As an example 33 FFH 35 represents the 20° Maxwellian fission cross section of ^{235}U multiplied by the half-life (neglecting powers of 10) of ^{233}U.

The principles of the fitting procedure were described in Axton (1984) where the solution of the normal equations $A^TZ^{-1}A = A^TZ^{-1}y$ by inversion of the n by n covariance matrix Z is given by

$$b = (A^TZ^{-1}A)^{-1}A^TZ^{-1}y,$$

where A is the n by p design matrix containing the differentials of each measurement with respect to each of the p parameters to be fitted, and y is the n element observation vector. However, inversion of Z is not the best way to obtain the solution. If the matrix is singular it cannot be inverted, and if it is near singular the solution could be in error. It is safer to use the method of Choleski decomposition which also has the advantage that it uses less computer time at space.

The covariance matrix is factorised by calculation of a vector R such that $R^T.R = Z^{-1}$ and the solution is given by

$$b = R\ .\ A.y.\ (R.A)^{-1}$$

The APL program used in 1982 has been re-written by Bastian (1984) in a much more sophisticated and easy-to-use manner which simplifies the input of data and the construction of the specification and covariance matrices, and also provides a choice of the two methods of solution. With the present data set the two methods give almost identical results but the Choleski method gives a marginally better χ^2.

In the other evaluations listed in the introduction, the covariance matrices contain no non-zero off-diagonal elements, and the data are

simply weighted according to the inverse variance. All evaluators make the assumption that the uncertainties are both normally distributed and evaluated at the level of one standard deviation.

3. Changes to the 1982 data set.

3.1. The provisional NPL value for $\bar{\nu}_T$ for ^{252}Cf (3.744 ± .006) is replaced by the final value (3.7509 ± .0107) (Axton and Bardell (A 1984)).

3.2. Recent improvements in the knowledge of σ_{Mn} and σ_S (Axton, (A) 1984) and Mughabgab, Divadeenam, and Holden (1981)) enable a reduction in the common uncertainty in NPL Manganese bath measurements from 0.239% to 0.211%. Similarly the common uncertainty in all manganese bath measurements due to the uncertainty in the factor $(1 + \alpha_S / \sigma_{Nn})$ is reduced from 0.122% to 0.073%, and the common uncertainty between the $\bar{\nu}_T$ ^{252}Cf measurements of Smith and Aleksandrov is reduced to 0.111%.

3.3. Half-life dependent fission cross section measurements are now entered as σ_f x half-life products in conformity with other recent evaluations, and the half-lives are allowed to float.

3.4. The four new $\bar{\nu}_p$ ratios of Gwin, Spencer and Ingle (1984) replace the two ratios previously released. As with the older values there still seems to be some uncertainty in the response of the ^{252}Chamber which requires normalization of the ratio. The normalization factors are not listed in the publication. For this and other reasons there is some guesswork involved in quantifying the correlations in this experiment, subject to further advice from the authors.

3.5. The revised σ_T for ^{241}Pu (Smith 1984) replaces the previous value.

3.6. A recent measurement of ^{239}Pu η is added (Lloyd et al (1981).

4. Changes to the Maxwellian Data Set of Divadeenam et al.(1984).

In this section it is not proposed to describe in detail every change which has been made to the data. This information is readily available from a scrutiny of the tables and the explanatory notes in appendix 4. However, it is informative to consider some examples of the type of changes which have been made.

4.1. The measurements of Gwin (1962) are measurements of the $^{233}U/^{235}U$ and $^{239}U/^{235}U$ ratios of $\eta\sigma_a$. These ratios are based on ratios of reactivities determined from oscillator measurements in a Maxwellian reactor neutron spectrum. The quoted results as revised by Magnuson (1971) are 0.953 ± .014 and 1.631 ± .0245 respectively. The ^{235}U reactivity in the denominator is common to both ratios. The authors do not quote uncertainties on the reactivities, but the uncertainties of the ratios are both $2^{1/2}$% which implies an uncertainty of 1% for each of the three reactivities involved. The ratios are therefore 50% correlated.

4.2. In some measurements an uncertainty in the Maxwellian Temperature (ΔT) is quoted by the author or assumed by a previous evaluator. The values are then calculated for two different temperatures T and $T+\Delta T$, the difference in the result is regarded as an additional uncertainty which is correlated between all measurements made in that spectrum. For example Lisman (1967) and Conway (1967).

4.3. Measurements relative to a reference standard, such as cobalt or sodium, are correlated by the uncertainty in that standard.

4.4. In some cases the correlations could be determined only by recalculating the results from the equations provided by the author, for example the measuremens $(\eta-1)\hat{\alpha}_a$ by Muelhause (1959) which are described in appendix 2.
Another example is provided by the $\hat{\sigma}_c$ and $\hat{\alpha}$ measurement of Cabell (1968) which are described in appendix 3. In order to obtain the correlations due to the uncertainty in the assumed temperature and in the fluence measurements it was necessary to write five new derived functions to describe the measurements. They provide a striking example of the flexibility of the method of programming.

5. Input data.

The input data are listed in table 1 where each line represents a single measurement. It contains the name of the first author, the function describing the measurement, the measured value, the fitted value, the total uncertainty of the measurement expressed as a percentage of the value, and the residual resulting from the fit. The residual, in this case is defined as the difference between the measured

Table 1

Author	Ref	Measured Function	Note	Y	YF	%ERRF	Res	Num
LAPONCHE	1972	(FA 39)-FA 35	7	1.6491E00	1.646E00	.583	.32	1
CORNISH	1956	CAF 39	8	3.1200E02	3.092E02	4.490	.20	2
HALPERIN	1963	CAP 33	10	4.9530E01	4.751E01	6.400	.64	3
CABELL	1971	FLEM	11	9.8270E-02	9.922E-02	3.348	-.29	4
LEMMEL	1982	CAP 34	3	9.5900E01	9.583E01	2.086	.04	5
POPOVIC	1953	FF 35	13	5.7110E02	5.691E02	2.211	.16	6
POPOVIC	1955	33 FFH 33	13	8.4472E02	8.385E02	3.145	.23	7
KEITH	1968	33 FFH 33	14	8.2848E02	8.385E02	1.589	-.76	8
KEITH	1968	33 FFH 35	14	8.8019E02	9.052E02	1.659	-1.71	9
KEITH	1968	39 FFH 39	14	1.8843E03	1.903E03	1.534	-.64	10
BIGHAM	1975	33 FFH 33	15	8.3520E02	8.385E02	.647	-.61	11
JAFFEY	1955	(FF 41)-FF 39	17	1.3552E00	1.340E00	1.424	.78	12
WHITE	1967	(FF 39)-FF 35	18	1.3583E00	1.386E00	2.139	-.94	13
WHITE	1967	(FF 41)-FF 35	18	1.8806E00	1.857E00	2.802	.45	14
VIDAL	1970	(FF 33)-FF 35	2	9.3200E-01	9.263E-01	.966	.63	15
BIGHAM	1975	(FF 33)-FF 35	15	9.3230E-01	9.263E-01	.450	1.43	16
SWEET	1973	(39 FFH 39)-34 FFH 35	2	1.3544E00	1.359E00	1.403	-.27	17
BIGHAM	1975	(39 FFH 39)-33 FFH 33	15	2.2796E00	2.269E00	.645	.70	18
BIGHAM	1975	(39 FFH 39)-33 FFH 35	15	2.1239E00	2.102E00	.687	1.50	19
BIGHAM	1975	F1BIG	15	5.5270E-01	5.553E-01	.561	-.82	20
LOUNSBURY	1970	(CA 33)-FIS 33	19	8.6100E-02	8.550E-02	2.239	.31	21
LOUNSBURY	1970	(CA 35)-FIS 35	19	1.6970E-01	1.693E-01	1.709	.13	22
LOUNSBURY	1970	(CA 39)-FIS 39	19	3.5550E-01	3.624E-01	1.603	-1.22	23
INGHRAM	1956	(CAP 33)-FF 33	2	9.4030E-02	9.012E-02	3.190	1.30	24
CORNISH	19c	(CAP 35)-FF 35	2	1.8800E-01	1.720E-01	7.447	1.15	25
OKAZAKI	1964	(CAP 33)-FF 33	20	9.0200E-02	9.012E-02	1.731	.05	26
OKAZAKI	A1964	(CAP 35)-FF 35	20	1.7050E-01	1.720E-01	1.056	-.81	27
LISMAN	1967	(CAP 33)-FF 33	21	9.3000E-02	9.012E-02	2.128	1.45	28
LISMAN	1967	(CAP 35)-FF 35	21	1.7120E-01	1.720E-01	.886	-.51	29
CONWAY	1967	(CAP 33)-FF 33	21	8.5100E-02	9.012E-02	4.935	-1.20	30
CONWAY	1967	(CAF 35)-FF 35	21	1.7050E-01	1.720E-01	4.223	-.20	31
DURHAM	1967	(CAP 35)-FF 35	22	1.7460E-01	1.720E-01	1.145	1.32	32
DURHAM	1967	(CAP 39)-FF 39	22	3.8820E-01	3.922E-01	1.520	-.67	33
CAPELL	1971	(CAP 33)-FF 33	23	8.5700E-02	9.012E-02	3.048	-1.69	34
CABELL	1971	(CAP 35)-FF 35	23	1.6960E-01	1.720E-01	1.759	-.79	35
CABELL	1971	(CAP 39)-FF 39	23	3.8120E-01	3.922E-01	4.808	-.60	36
DEBOISBLANC	1961	(F1ETA 33)-F1ETA 35	24	1.1150E00	1.102E00	.717	1.63	37
FAST	1967	(F1ETA 39)-F1ETA 35	25	9.9700E-01	9.970E-01	1.625	.00	38
FAST	1967	(F1ETA 41)-F1ETA 35	25	1.0520E00	1.046E00	1.653	.39	39
CABELL D	1965	(F3ETA 33)-F3ETA 35	26	1.0461E00	1.031E00	2.357	.61	40
CABELL D	1965	(F3ETA 39)-F3ETA 35	26	1.6079E00	1.636E00	2.403	-.74	41
CABELL G	1965	(F3ETA 33)-F3ETA 35	26	1.0309E00	1.031E00	3.919	-.01	42
CABELL G	1965	(F3ETA 39)-F3ETA 35	26	1.6223E00	1.636E00	4.161	-.21	43
GWIN	1962	(F2ETA 33)-F2ETA 35	27	9.5300E-01	9.494E-01	1.414	.27	44
GWIN	1962	(F2ETA 39)-F2ETA 35	27	1.6310E00	1.641E00	1.414	-.44	45
GWIN	A1962	F3ETA 33	28	7.4035E02	7.392E02	1.186	.13	46
GWIN	A1962	F3ETA 35	28	7.2410E02	7.169E02	1.050	.95	47
LAPONCHE	1972	(F3ETA 39)-F3ETA 35	7	1.6058E00	1.636E00	1.107	-1.73	48
LAPONCHE	1972	(F3ETA 41)-F3ETA 39	7	1.4687E00	1.430E00	3.580	.73	49
ALIKHANOV	1956	(F3ETA 33)-F3ETA 35	29	1.0390E00	1.031E00	3.561	.21	50
ALIKHANOV	1956	(F3ETA 39)-F3ETA 35	29	1.5650E00	1.636E00	6.709	-.68	51
MUELHAUS	1959	(F3ETA 33)-F3ETA 35	30	1.0221E00	1.031E00	1.811	-.49	52
MUELHAUS	1959	(F3ETA 39)-F3ETA 35	30	1.6043E00	1.636E00	2.271	-.88	53
DIVADEENAM	1984	WGA 33	4	9.9884E-01	9.995E-01	.120	-.54	54
DIVADEENAM	1984	WGA 35	4	9.7870E-01	9.787E-01	.092	-.03	55
DIVADEENAM	1984	WGA 39	4	1.0767E00	1.078E00	.269	-.54	56
DIVADEENAM	1984	WGA 41	4	1.0444E00	1.044E00	.191	.08	57
DIVADEENAM	1984	WGF 33	4	9.9640E-01	9.952E-01	.201	.58	58
DIVADEENAM	1984	WGF 35	4	9.7740E-01	9.765E-01	.164	.55	59
DIVADEENAM	1984	WGF 39	4	1.0562E00	1.056E00	.275	.34	60
DIVADEENAM	1984	WGF 41	4	1.0452E00	1.044E00	.670	.12	61
EGELSTAFF	1954	(ABS 35)+SCR 35	5	7.2433E02	6.960E02	3.590	1.09	62
MELKONIAN	1953	(ABS 35)+SCR 35	5	6.9432E02	6.960E02	2.016	-.12	63
PALEVSKY	1954	(ABS 35)+SCR 35	5	7.0032E02	6.960E02	1.428	.43	64
NITIKIN	1955	(ABS 35)+SCA 35	5	7.1032E02	6.977E02	2.956	.60	65
SIMPSON	1960	(ABS 35)+SCR 35	5	6.9032E02	6.960E02	1.391	-.60	66
SAFFORD	1959	(ABS 35)+SCA 35	5	6.963?E02	6.977E02	.759	-.56	67
SAFFORD	1959	(ABS 35)+SCR 35	5	6.983?E02	6.960E02	.730	.45	68
BLOCK	1960	(ABS 35)+SCR 35	5	6.933?E02	6.960E02	.421	-.5	69
SAPLAKOGLU	1961	(ABS 35)+SCR 35	5	6.9632E02	6.960E02	.359	.11	70
GERASIMOV	1962	ABS 35	5	6.7031E02	6.815E02	2.089	-.80	71
ZIMMERMAN	1955	(ABS 39)+SCR 39	5	1.0225E03	1.025E03	1.271	-.17	72
NITIKIN	1955	(ABS 39)+SCA 39	5	1.0405E03	1.026E03	2.979	.47	73
BOLLINGER	1958	(ABS 39)+SCR 39	5	1.0225E03	1.025E03	1.369	-.16	74
PATTENDEN	A1956	(ABS 39)+SCR 39	5	1.0125E03	1.025E03	3.003	-.40	75
SAFFORD	1961	(ABS 39)+SCR 39	5	1.0185E03	1.025E03	.727	-.85	76
MUETHER	1954	(ABS 33)+SCR 33	5	5.9727E02	5.871E02	2.344	.72	77
NITIKIN	1955	(ABS 33)+SCR 33	5	5.7726E02	5.871E02	3.638	-.47	78
PATTENDEN	1956	(ABS 33)+SCR 33	5	5.9627E02	5.871E02	3.019	.51	79
GREEN	1957	ABS 33	5	5.7426E02	5.749E02	3.483	-.03	80
SIMPSON	1960	(ABS 33)+SCR 33	5	5.8727E02	5.871E02	.800	.03	81
SAFFORD	1960	(ABS 33)+SCA 33	5	5.8577E02	5.883E02	.990	-.44	82
SAFFORD	1960	(ABS 33)+SCR 33	5	5.8567E02	5.871E02	.410	-.61	83
BLOCK	1960	(ABS 33)+SCR 33	5	5.8727E02	5.871E02	.511	.04	84

Table 1 (Continued)

Author	Ref	Measured Function	Note	Y	YF	%ERRF	Res	Num
SIMPSON	1961	(ABS 41)+SCA 41	5	1.3866E03	1.385E03	3.606	.03	85
CRAIG	1964	(ABS 41)+SCA 41	5	1.3806E03	1.385E03	2.897	-.11	86
SMITH	1968	(ABS 41)+SCR 41	31	1.3956E03	1.384E03	1.433	.58	87
LEMMEL	1982	SCR 33	3	1.2306E01	1.219E01	5.688	.17	88
LEMMEL	1982	(SCA 33)-SCR 33	3	1.2006E00	1.175E00	49.977	.04	89
LEMMEL	1982	SCA 35	3	1.6508E01	1.626E01	7.875	.19	90
LEMMEL	1982	(SCA 35)-SCR 35	3	1.7008E00	1.677E00	44.097	.03	91
LEMMEL	1982	SCA 39	3	8.0037E00	7.873E00	12.494	.13	92
LEMMEL	1982	(SCA 39)-SCR 39	3	8.0037E-01	1.268E00	137.437	-.43	93
LEMMEL	1982	SCA 41	3	1.2006E01	1.220E01	21.657	-.07	94
LEMMEL	1982	(SCA 41)-SCR 41	3	1.2006E00	1.014E00	249.886	.06	95
DERUYTTER	1974	39 FH1 39	5	1.8121E03	1.803E03	.437	1.13	96
DERUYTTER	1973	34 FH1 35	5	1.4391E03	1.433E03	.428	.93	97
DERUYTTER	1961	FIS 35	5	5.8937E02	5.828E02	1.325	.84	98
WHITE	1967	(FIS 39)-FIS 35	18	1.2530E00	1.282E00	1.800	-1.30	99
WHITE	1967	(FIS 41)-FIS 35	18	1.7630E00	1.736E00	2.751	.55	100
BERCEANO	1977	34 FH1 35	5	1.4430E03	1.433E03	.782	.86	101
RAFFLE	1959	33 FH1 33	5	8.3426E02	8.425E02	3.300	-.30	102
RAFFLE	1959	FIS 35	5	5.8197E02	5.828E02	3.092	-.05	103
RAFFLE	1959	39 FH1 39	5	1.7148E03	1.803E03	2.840	-1.81	104
RAFFLE	1956	(FIS 41)-FIS 39	5	1.3319E00	1.354E00	6.000	-.28	105
MASLIN	1965	FIS 35	5	5.8371E02	5.828E02	1.449	.11	106
SAPLAKOGLU	1959	FIS 35	5	5.9317E02	5.828E02	2.232	.78	107
WATANABE	1964	FIS 41	5	9.8545E02	1.012E03	4.569	-.59	108
FRAYSSE	1965	(39 FH1 39)-34 FH1 35	5	1.2425E00	1.258E00	1.547	-.81	109
BORCEA	1970	(39 FH1 39)-34 FH1 35	5	1.2578E00	1.258E00	1.615	-.01	110
BOLDEMAN	1977	NUB 52	5	3.7549E00	3.766E00	.431	-.65	111
BOLDEMAN	1980	(NUB 33)-NUB 52	5	6.6049E-01	6.619E-01	.255	-.83	112
BOLDEMAN	1980	(NUB 35)-NUB 52	5	6.4318E-01	6.458E-01	.255	-1.57	113
BOLDEMAN	1980	(NUB 39)-NUB 52	5	7.6614E-01	7.648E-01	.243	.72	114
BOLDEMAN	1980	(NUB 41)-NUB 52	5	7.8028E-01	7.818E-01	.231	-.86	115
SPENCER	1982	NUB 52	5	3.7831E00	3.766E00	.221	2.10	116
GWIN	1984	(NUB 33)-NUB 52	32	6.5996E-01	6.619E-01	.340	-.86	117
GWIN	1984	(NUB 35)-NUB 52	32	6.4701E-01	6.458E-01	.265	.73	118
GWIN	1984	(NUB 39)-NUB 52	32	7.6530E-01	7.648E-01	.257	.26	119
GWIN	1984	(NUB 41)-NUB 52	32	7.8423E-01	7.818E-01	.290	1.06	120
HOPKINS	1963	NUB 52	5	3.7767E00	3.766E00	.838	.35	121
HOPKINS	1963	(NUB 33)-NUB 52	5	6.5483E-01	6.619E-01	.895	-1.20	122
HOPKINS	1963	(NUB 35)-NUB 52	5	6.4587E-01	6.458E-01	.838	.02	123
HOPKINS	1963	(NUB 39)-NUB 52	5	7.5047E-01	7.648E-01	.996	-1.92	124
ASPLUND	1963	NUB 52	5	3.7910E00	3.766E00	1.066	.63	125
CONDE	1965	(NUB 35)-NUB 52	5	6.4222E-01	6.458E-01	.847	-.65	126
WHITE/AX	1968	NUB 52	33	3.8156E00	3.766E00	1.033	1.27	127
AXTON	A1984	NUB 52	33	3.7509E00	3.766E00	.300	-1.30	128
COLV/AXT	1966	NUB 52	33	3.7262E00	3.766E00	.806	-1.31	129
COLV/ULL	1965	NUB 52	5	3.7405E00	3.766E00	.438	-1.52	130
COLVIN	1965	(NUB 33)-NUB 35	5	1.0204E00	1.025E00	.587	-.76	131
COLVIN	1965	(NUB 39)-NUB 35	5	1.1835E00	1.184E00	.675	-.10	132
COLVIN	1965	(NUB 41)-NUB 35	5	1.2102E00	1.211E00	.905	-.04	133
COLVIN	1965	(NUB 35)-NUB 52	5	6.4334E-01	6.458E-01	.472	-.80	134
MATHER	1964	(NUB 33)-NUB 52	5	6.7093E-01	6.619E-01	1.235	1.09	135
MATHER	1964	(NUB 35)-NUB 52	5	6.4145E-01	6.458E-01	.537	-1.25	136
MATHER	1964	(NUB 39)-NUB 52	5	7.7307E-01	7.648E-01	1.122	.95	137
ALEK-ROV	1981	NUB 52	33	3.7580E00	3.766E00	.483	-.41	138
SMITH	1984	NUB 52	33	3.7678E00	3.766E00	.303	.21	139
EDWARDS	1982	NUB 52	33	3.7603E00	3.766E00	.711	-.19	140
BOZ-NESH	1977	NUB 52	33	3.7438E00	3.766E00	.580	-1.00	141
DEVOLPI	1972	NUB 52	33	3.7470E00	3.766E00	.463	-1.07	142
ZHANG	1981	NUB 52	5	3.7534E00	3.766E00	.490	-.66	143
SPIEGEL	1981	NUB 52	33	3.7828E00	3.766E00	.759	.60	144
SMITH	1984	ETA 33	5	2.2972E00	2.296E00	.350	.14	145
SMITH	1984	ETA 35	5	2.0842E00	2.080E00	.386	.58	146
SMITH	1984	ETA 39	5	2.1120E00	2.114E00	.380	-.22	147
SMITH	1984	ETA 41	5	2.1690E00	2.170E00	.419	-.11	148
MACKLIN	1960	ETA 33	5	2.3121E00	2.296E00	.375	1.85	149
MACKLIN	1960	ETA 35	5	2.0757E00	2.080E00	.382	-.48	150
MACKLIN	1962	ETA 39	5	2.1163E00	2.114E00	.851	.14	151
REICH	1982	HLF 33	34	1.5920E00	1.591E00	.126	.69	152
REICH	1982	HLF 34	34	2.4570E00	2.459E00	.204	-.48	153
REICH	1982	HLF 39	34	2.4110E00	2.413E00	.124	-.66	154
REICH	1982	HLF 41	34	1.4400E01	1.439E01	.700	.13	155
CAPELL	1968	F1CAB	35	2.7384E02	2.901E02	4.960	-1.19	156
CAPELL	1968	F2CAB	35	1.1719E03	1.183E03	3.176	-.31	157
CAPELL	1968	F3CAB	35	3.2690E00	3.283E00	2.776	-.16	158
CAPELL	1968	F4CAB	35	3.0339E02	3.047E02	5.835	-.07	159
CAPELL	1968	F5CAB	35	3.8710E00	3.840E00	1.602	.49	160
BNL 325	1973	CA 40	36	2.8950E02	2.893E02	.484	.12	161
BNL 325	1973	CA 42	36	1.8500E01	1.851E01	2.162	-.04	162
BNL325 +	1973	GC116 39	37	1.3265E00	1.354E00	6.056	-.35	163
WESTCOTT	1960	GC116 40	37	1.0860E00	1.075E00	2.000	.50	164
BNL325 +	1973	GC116 41	37	1.1085E00	1.090E00	2.457	.68	165
WESTCOTT	1960	GC116 42	37	1.1335E00	1.135E00	2.670	-.04	166
BNL325 +	1973	GA116 39	37	1.1846E00	1.183E00	1.521	.10	167
WESTCOTT	1960	GA116 41	37	1.1073E00	1.109E00	.819	-.17	168
LLOYD	1982	(ETA 39)-FIS 39	4	2.7820E-03	2.829E-03	2.072	-.81	169

and fitted values divided by the uncertainty thus providing a ready check on the goodness of fit. The final column contains a serial number which facilitates cross referencing to other tables. Information about correlated uncertainties is provided in tables 2 and 3. Table 2 gives a list of all sources of correlated uncertainty, each of which is associated with an identification code which is either a letter of the alphabet, an underlined letter, or an APL symbol. The first column of table 3 lists the serial numbers of each measurement which has one or more correlated uncertainties, and the second column the identification code from table 2. Then the individual uncertainties, expressed as a percentage of the measured value, are listed in the same order as the codes.

6. Output from the least squares fit.

The output data are shown in Table 4, which shows in the first column, the identities both of the fitted variables and also of parameters such as eta and alpha which are derived from the fitted variables. Columns 2, 3, and 4 give the fitted values, their uncertainties, and the uncertainties expressed as a percentage. To facilitate comparison with the results of Divadeenam et al. (1984) their results are presented in column 5. A zero in this column signifies that the parameter was not fitted by them. The fifth column is the ratio of column 5 to column 2, and the final column is the ratio of the uncertainties from the two evaluations. In table 4(a) the same comparison is made with the results of Divadeenam et al. (A1984). The correlation matrix for the uncertainties of the fitted parameters is presented in table 5. Table 6 shows the results of a fit to the updated 1982 data set excluding the Maxwellian data.

Standard reference data used in this work appears in table 7.

Table 2

Codes	Causes Of Error
A	DERUYTTER COMMON ERROR
B	DERUYTTER TIMING
C	DERUYTTER-BERCEANO ASSAY
D	WHITE U235 ASSAY
E	MASLIN-SAPLAKOGLU LEM/DER CORRECTION
F	NPLCOMMON BATH ERROR
G	ERROR IN (1+SS-SMN) IN MANGANESE BATHS
H	MEAN ENERGY ERROR U233
I	MEAN ENERGY ERROR U235
J	MEAN ENERGY ERROR PU239
K	MEAN ENERGY ERROR PU241
L	MEAN ENERGY ERROR CF252
M	SLOPE CORRELATION (DIFFERENT AUTHORS)
N	BOLDEMAN SLOPE
O	GWIN SLOPE
P	HOPKINS SLOPE
Q	ASPLUND SLOPE
R	COLVIN SLOPE
S	MATHER SLOPE
U	U233 DELAYED NEUTRONS
V	U235 DELAYED NEUTRONS
W	PU239 DELAYED NEUTRONS
X	PU241 DELAYED NEUTRONS
Y	CF252 DELAYED NEUTRONS
Z	DELAYED GAMMAS
Δ	BOLDEMANS FOIL THICKNESS CORRECTIONS
A	GWIN COMMON ERROR
B	SPIEGEL BOZORGMANESH COMMON ERROR
C	BOLDEMAN COMMON ERROR
D	DIVEN COMMON ERROR
E	BORON PILE COMMON ERROR
F	SMITH COMMON ERRORWITH ALEKSANDROV
G	SMITH ETA NUBAR
H	ETA MONTECARLO CORRECTIONS
I	MATHER COMMON ERROR
J	WHITE PU239 ASSAY
K	WHITE PU 241 ASSAY
M	CABELL FLUX
N	CABELL TEMPERATURE
O	DIDO REFLECTOR q+rs FOR CAP, ABS PU239
P	DIDO REFLECTOR q+rs FOR CAP,ABS PU241
Q	CABELL 86° SPECTRUM ERROR
R	CABELL ERROR FROM SJOSTRAND AND STORY
S	CABELL ERROR FROM SJOSTRAND AND STORY
T	GWIN ERROR EVALUATED BY STORY
U	MUELHAUS ERROR EVALUATED BY AXTON
V	FAST SPECTRAL ERRORS FROM IN1060
W	MTR 70° SPECTRUM UNCERTAINTY
X	NRU 40° TEMPERATURE UNCERTAINTY
Y	NRU WESTCOTT r UNCERTAINTY
Z	LOUNSBURY TEMPERATURE
Δ	POPOVIC ERROR DUE TO Na CROSS SECTION
ρ	KEITH ERROR EVALUATED BY DIVADEENAM
↑	UNCERTAINTY IN Co CROSS SECTION
↓	+-20° UNCERTAINTY IN T
⍋	COMMON UNCERTAINTY IN U235 REACTIVITY
⍒	COMMON UNCERTAINTY IN U235 REACTIVITY

Num	Codes	Individual Uncertainties (Percent)								
2	↑	.161								
3	↑	.161								
6	▲	.943								
7	▲	.943								
8	ρ	.560								
9	ρ	.560								
10	ρ	.560								
13	DJ	1.225	.940							
14	DK	1.225	2.140							
21	Z	.226								
22	Z	.247								
23	Z	.818								
26	XY	-.660	.697							
27	XY	.237	.533							
28	W	1.280								
29	W	-.531								
30	W	.433								
31	W	-.562								
34	Q	1.802								
35	Q	.862								
36	Q	3.102								
38	V	.479								
39	V	.479								
40	R	1.701								
41	R	1.701								
42	S	2.830								
43	S	2.830								
44	↓	1.000								
45	↓	1.000								
46	I	.991								
47	I	.991								
50	♦	1.500								
51	♦	1.500								
52	U↓	1.233	.691							
53	U↓	1.233	1.614							
96	AB	.207	.232							
97	ABC	.207	.232	.185						
98	B	.232								
99	DJ	1.225	.940							
100	DK	1.225	2.140							
101	C	.300								
106	E	1.000								
107	E	-2.000								
111	LYZC	.056	.106	.070	.010					
112	HLMNUYZ▲C	.074	-.056	-.033	-.104	.009	-.106	.040	.024	.041
113	ILMNVYZ▲C	.069	-.057	-.047	-.149	.021	-.106	.040	.047	.060
114	JLMNWYZ▲C	.061	-.056	-.018	-.056	.011	-.106	.110	.005	.010
115	KLMNXYZ▲C	.074	-.056	-.017	-.052	.055	-.106	.110	.028	.020
116	LMOYZ	.019	.007	.022	.106	.051				
117	UYZ▲	.009	-.106	.120	.139					
118	VYZ▲	.021	-.106	.040	.117					
119	WYZ▲	.011	-.106	.096	.125					
120	XYZ▲	.055	-.106	.120	.078					
121	LMPYZ	.030	.018	.058	.106	.100				
122	HLMPUYZ▲D	.039	-.030	-.018	-.056	.009	-.106	.025	.006	.341
123	ILMPVYZ▲D	.036	-.030	-.025	-.079	.021	-.106	.025	.056	.383
124	JLMPWYZ▲D	.033	-.030	-.009	-.029	.011	-.106	.050	.051	.550
125	LMQYZ	.077	-.003	-.010	.106	.201				
126	ILMQVYZ	.094	-.077	-.083	-.263	.021	-.106	.125		
127	FGL	.211	.073	.057						
128	FGL	.211	.073	.057						
129	FGLYE	.211	.073	.057	.106	.231				
130	LYE	.013	.106	.231						
131	HIMRUV	.017	-.016	.003	.009	.009	-.021			
132	IJMRVW	-.016	.014	.007	.021	-.021	.011			
133	IKMRVX	-.016	.017	.007	.022	-.021	.055			
134	ILMRVY▲	.016	-.013	-.011	-.034	.021	-.106	.056		
135	HLMSUYZ▲I	.074	-.056	-.033	-.104	.009	-.106	.050	.067	1.000
136	ILMSVYZ▲I	.069	-.057	-.047	-.149	.021	-.106	.050	.084	.300
137	JLMSWYZ▲I	.061	-.056	-.018	-.056	.011	-.106	.136	.060	.500
138	GLE	.073	.028	.111						
139	GLMEG	.073	.034	.003	.111	.150				
140	FGLMY	.211	.073	.028	-.001	.106				
141	GLMB	.073	.028	-.001	.441					
142	G	.073								
143	LMYZ	.077	.010	.106	.070					
144	GLB	.073	.055	.508						
145	HMGH	.036	.008	.150	.167					
146	IMGH	.034	.009	.150	.167					
147	JGH	.030	.150	.167						
148	KGH	.036	.150	.167						
149	HMH	.036	.008	.167						
150	IMH	.034	.009	.167						
151	JMH	.030	.002	.167						
156	MN↑	2.230	.310	.161						
157	MN↑	2.230	1.210	.161						
158	N	-.540								
159	MN↑	2.230	-1.310	.161						
163	O	2.700								
165	P	1.100								
167	O	.680								
168	P	.370								

Table 4

Comparison Of Fitted Values With Divadeenam 1984

Par	Fitted	Error	%Error	Div	Div-YF	EDIV-ER
SCA 33	13.3619	.8859	6.6303	12.6000	.9430	.3386
SCA 35	16.2603	1.1323	6.9638	14.0000	.8610	.4416
SCA 39	7.8726	.9737	12.3683	7.3000	.9273	.4108
SCA 41	12.1957	2.6185	21.4704	9.1000	.7462	.3819
SCR 33	12.1871	.6688	5.4876	.0000	.0000	.0000
SCR 35	14.5830	1.2830	8.7981	.0000	.0000	.0000
SCR 39	6.6134	1.9190	29.0167	.0000	.0000	.0000
SCR 41	11.1839	3.6108	32.2854	.0000	.0000	.0000
ABS 33	574.9489	1.3131	.2284	574.7000	.9996	.7616
ABS 35	681.4590	1.3625	.1999	680.9000	.9992	.8073
ABS 39	1018.1312	3.0295	.2976	1017.3000	.9992	.9573
ABS 41	1372.8870	9.0940	.6624	1369.4000	.9975	.8467
FIS 33	529.6631	1.3456	.2541	529.1000	.9989	.8918
FIS 35	582.7848	1.2418	.2131	582.6000	.9997	.8858
FIS 39	747.2874	2.0787	.2782	748.1000	1.0011	.9621
FIS 41	1011.9575	6.6011	.6523	1011.1000	.9992	.9392
CA 33	45.2858	.6983	1.5421	45.5000	1.0047	1.0024
CA 35	98.6741	.8418	.8531	98.3000	.9962	.9504
CA 39	270.8437	2.1869	.8074	269.3000	.9943	1.0060
CA 40	289.3289	1.3933	.4816	.0000	.0000	.0000
CA 42	18.5145	.4001	2.1611	.0000	.0000	.0000
CA 41	360.9295	4.9410	1.3690	358.2000	.9924	1.0322
CAP 34	95.8290	1.9847	2.0711	.0000	.0000	.0000
NUB 33	2.4923	.0044	.1763	2.4933	1.0004	.8875
NUB 35	2.4316	.0039	.1597	2.4251	.9973	.8758
NUB 39	2.8798	.0053	.1842	2.8768	.9989	1.0745
NUB 41	2.9440	.0060	.2025	2.9369	.9976	1.2248
NUB 52	3.7655	.0048	.1282	3.7675	1.0005	.8288
ETA 33	2.2960	.0044	.1907	2.2957	.9999	.9133
ETA 35	2.0795	.0039	.1864	2.0751	.9979	.8515
ETA 39	2.1137	.0053	.2487	2.1153	1.0007	.9890
ETA 41	2.1700	.0077	.3561	2.1686	.9994	1.0354
ALPHA 33	.0855	.0014	1.6377	.0861	1.0070	1.0713
ALPHA 35	.1693	.0016	.9175	.1687	.9964	.9656
ALFHA 39	.3624	.0031	.8518	.3600	.9933	1.0365
ALPHA 41	.3567	.0049	1.3772	.3543	.9934	1.1604
HLF 33	1.5906	.0019	.1209	1.5913	1.0004	.8475
HLF 34	2.4594	.0045	.1821	2.4575	.9992	1.1253
HLF 39	2.4130	.0029	.1193	2.4101	.9988	.4063
HLF 41	14.3870	.0995	.6914	.0000	.0000	.0000
WGA 33	.9995	.0011	.1069	.9996	1.0001	1.0015
WGA 35	.9787	.0008	.0855	.9788	1.0000	.9918
WGA 39	1.0783	.0025	.2277	1.0784	1.0001	.9938
WGA 41	1.0442	.0020	.1898	1.0442	.9999	.9840
WGF 33	.9952	.0014	.1434	.9955	1.0003	1.0158
WGF 35	.9765	.0012	.1263	.9761	.9996	.9971
WGF 39	1.0552	.0023	.2146	1.0558	1.0005	1.0291
WGF 41	1.0443	.0055	.5273	1.0440	.9997	.8825
GC116 39	1.3543	.0385	2.8435	.0000	.0000	.0000
GC116 40	1.0751	.0196	1.8195	.0000	.0000	.0000
GC116 41	1.0900	.0181	1.6589	.0000	.0000	.0000
GC116 42	1.1348	.0303	2.6683	.0000	.0000	.0000
GA116 39	1.1829	.0131	1.1074	.0000	.0000	.0000
GA116 41	1.1089	.0082	.7427	.0000	.0000	.0000

Table 4(a)

Comparison Of Fitted Values With Divadeenam A1984

Par	Fitted	Error	%Error	Div	Div-YF	EDIV-ER
SCA 33	13.3619	.8859	6.6303	12.6000	.9430	.3386
SCA 35	16.2603	1.1323	6.9638	13.9000	.8548	.4416
SCA 39	7.8726	.9737	12.3683	7.3000	.9273	.4108
SCA 41	12.1957	2.6185	21.4704	9.1000	.7462	.3819
SCR 33	12.1871	.6688	5.4876	.0000	.0000	.0000
SCR 35	14.5830	1.2830	8.7981	.0000	.0000	.0000
SCR 39	6.6134	1.9190	29.0167	.0000	.0000	.0000
SCR 41	11.1839	3.6108	32.2854	.0000	.0000	.0000
ABS 33	574.9489	1.3131	.2284	575.1000	1.0003	.7616
ABS 35	681.4590	1.3625	.1999	681.4000	.9999	.8073
ABS 39	1018.1312	3.0295	.2976	1018.0000	.9999	.9573
ABS 41	1372.8870	9.0940	.6624	1371.0000	.9986	.8467
FIS 33	529.6631	1.3456	.2541	529.6000	.9999	.8918
FIS 35	582.7848	1.2418	.2131	582.9000	1.0002	.8858
FIS 39	747.2874	2.0787	.2782	748.2000	1.0012	.9621
FIS 41	1011.9575	6.6011	.6523	1009.7000	.9978	.9392
CA 33	45.2858	.6983	1.5421	45.4000	1.0025	1.0024
CA 35	98.6741	.8418	.8531	98.6000	.9992	.9504
CA 39	270.8437	2.1869	.8074	269.9000	.9965	1.0060
CA 40	289.3289	1.3933	.4816	.0000	.0000	.0000
CA 42	18.5145	.4001	2.1611	.0000	.0000	.0000
CA 41	360.9295	4.9410	1.3690	361.1000	1.0005	1.0322
CAP 34	95.8290	1.9847	2.0711	.0000	.0000	.0000
NUB 33	2.4923	.0044	.1763	2.4931	1.0003	.8875
NUB 35	2.4316	.0039	.1597	2.4287	.9988	.8758
NUB 39	2.8798	.0053	.1842	2.8807	1.0003	1.0745
NUB 41	2.9440	.0060	.2025	2.9461	1.0007	1.2248
NUB 52	3.7655	.0048	.1282	3.7682	1.0007	.8288
ETA 33	2.2960	.0044	.1907	2.2959	.9999	.9133
ETA 35	2.0795	.0039	.1864	2.0775	.9990	.8515
ETA 39	2.1137	.0053	.2487	2.1170	1.0015	.9890
ETA 41	2.1700	.0077	.3561	2.1700	1.0000	1.0354
ALPHA 33	.0855	.0014	1.6377	.0859	1.0047	1.0713
ALPHA 35	.1693	.0016	.9175	.1723	1.0176	.9656
ALPHA 39	.3624	.0031	.8518	.3639	1.0040	1.0365
ALPHA 41	.3567	.0049	1.3772	.3635	1.0192	1.1604
HLF 33	1.5906	.0019	.1209	1.5913	1.0004	.8475
HLF 34	2.4594	.0045	.1821	2.4575	.9992	1.1253
HLF 39	2.4130	.0029	.1193	2.4101	.9988	.4063
HLF 41	14.3870	.0995	.6914	.0000	.0000	.0000
WGA 33	.9995	.0011	.1069	.9998	1.0003	1.0015
WGA 35	.9787	.0008	.0855	.9788	1.0000	.9918
WGA 39	1.0783	.0025	.2277	1.0783	1.0000	.9938
WGA 41	1.0442	.0020	.1898	1.0441	.9998	.9840
WGF 33	.9952	.0014	.1434	.9957	1.0005	1.0158
WGF 35	.9765	.0012	.1263	.9766	1.0001	.9971
WGF 39	1.0552	.0023	.2146	1.0561	1.0008	1.0291
WGF 41	1.0443	.0055	.5273	1.0455	1.0011	.8825
GC116 39	1.3543	.0385	2.8435	.0000	.0000	.0000
GC116 40	1.0751	.0196	1.8195	.0000	.0000	.0000
GC116 41	1.0900	.0181	1.6589	.0000	.0000	.0000
GC116 42	1.1348	.0303	2.6683	.0000	.0000	.0000
GA116 39	1.1829	.0131	1.1074	.0000	.0000	.0000
GA116 41	1.1089	.0082	.7427	.0000	.0000	.0000

Table 5

Correlation Matrix Of Fitted Parameters

	1	2	3	4	5	6	7	8	9	10	11	12
1	1.000	.031	.003	.001	.752	.033	.006	.001	-.236	-.066	-.036	-.015
2	.031	1.000	.011	.004	.039	.833	.024	.005	-.132	-.472	-.137	-.050
3	.003	.011	1.000	.001	.004	.012	.472	.002	-.013	-.024	-.084	-.015
4	.001	.004	.001	1.000	.002	.004	.003	.719	-.005	-.009	-.015	-.083
5	.752	.039	.004	.002	1.000	.041	.008	.002	-.296	-.083	-.045	-.019
6	.033	.833	.012	.004	.041	1.000	.025	.005	-.140	-.498	-.145	-.053
7	.006	.024	.472	.003	.008	.025	1.000	.003	-.026	-.050	-.172	-.032
8	.001	.005	.002	.719	.002	.005	.003	1.000	-.006	-.011	-.018	-.100
9	-.236	-.132	-.013	-.005	-.296	-.140	-.026	-.006	1.000	.281	.154	.064
10	-.066	-.472	-.024	-.009	-.083	-.498	-.050	-.011	.281	1.000	.291	.107
11	-.036	-.137	-.084	-.015	-.045	-.145	-.172	-.018	.154	.291	1.000	.184
12	-.015	-.050	-.015	-.083	-.019	-.053	-.032	-.100	.064	.107	.184	1.000
13	-.203	-.121	-.010	-.004	-.255	-.128	-.021	-.005	.862	.257	.120	.045
14	-.061	-.375	-.022	-.008	-.077	-.396	-.045	-.009	.260	.795	.261	.092
15	-.039	-.146	-.058	-.014	-.049	-.155	-.119	-.016	.167	.310	.692	.164
16	-.016	-.051	-.014	-.071	-.020	-.054	-.028	-.085	.066	.108	.164	.848
17	-.052	-.016	-.005	-.003	-.065	-.016	-.010	-.003	.219	.033	.058	.032
18	-.017	-.210	-.007	-.003	-.021	-.222	-.015	-.004	.071	.446	.086	.037
19	-.013	-.051	-.061	-.008	-.016	-.054	-.125	-.010	.054	.109	.728	.098
20	.000	.000	.000	.000	.000	.000	.000	-.001	.000	.001	.002	.006
21	.000	.000	.000	.000	.000	.000	.000	.000	.000	.000	.000	-.001
22	-.007	-.024	-.010	-.059	-.008	-.026	-.021	-.071	.029	.052	.119	.707
23	.001	-.001	.000	.000	.001	-.001	.000	.000	-.003	.002	.001	.000
24	.009	-.003	-.002	-.001	.011	-.003	-.005	-.001	-.039	.006	.029	.014
25	-.003	.011	-.002	-.001	-.004	.011	-.004	-.001	.013	-.023	.023	.013
26	.000	.000	-.008	-.001	.000	.000	-.017	-.002	.002	-.001	.097	.016
27	.001	.004	-.003	-.008	.002	.005	-.007	-.010	-.006	-.009	.039	.097
28	.001	.003	-.002	-.001	.001	.003	-.003	-.001	-.003	-.006	.020	.014
29	.020	-.005	.000	.000	.025	-.006	.000	.000	-.085	.011	.002	-.002
30	-.002	.087	.000	.000	-.002	.091	-.001	.000	.007	-.184	.006	.002
31	-.001	.001	.029	.002	-.001	.001	.060	.002	.004	-.002	-.351	-.024
32	.000	.002	.002	.021	.000	.003	.003	.025	-.001	-.005	-.019	-.251
33	-.017	.004	-.003	-.002	-.021	.004	-.006	-.002	.072	-.009	.036	.023
34	-.001	-.108	-.002	-.001	-.002	-.115	-.003	-.001	.006	.230	.019	.013
35	.001	-.001	-.039	-.003	.001	-.001	-.080	-.004	-.003	.002	.464	.039
36	.001	.000	-.003	-.025	.001	.000	-.007	-.030	-.003	.000	.041	.301
37	.025	.020	-.003	-.002	.031	.022	-.006	-.002	-.107	-.043	.034	.020
38	.011	.089	-.004	-.001	.014	.094	-.008	-.001	-.046	-.189	.047	.010
39	-.001	.004	.017	-.001	-.001	.004	.036	-.002	.005	-.007	-.208	.017
40	.000	-.001	.000	-.002	.000	-.001	.001	-.002	.002	.002	-.006	.022
41	.045	-.028	-.002	-.001	.056	-.029	-.004	-.001	-.191	.059	.022	.006
42	-.013	.080	-.003	-.001	-.017	.085	-.007	-.001	.056	-.170	.038	.009
43	-.006	-.027	.024	-.001	-.007	-.029	.049	-.001	.025	.058	-.287	.012
44	.000	-.001	.000	.002	.000	-.001	.000	.003	.000	.002	.001	-.026
45	.038	-.032	-.005	-.002	.047	-.034	-.010	-.003	-.160	.068	.057	.030
46	-.020	-.020	-.003	-.001	-.025	-.021	-.006	-.002	.085	.042	.037	.015
47	-.020	-.028	.011	-.008	-.025	-.029	.022	-.009	.084	.059	-.129	.093
48	-.006	-.014	-.003	.043	-.007	-.015	-.007	.051	.025	.029	.040	-.511
49	.000	.002	.009	-.007	.000	.002	.019	-.008	.000	-.003	-.111	.084
50	-.001	-.002	-.001	-.002	-.001	-.002	-.001	-.003	.002	.004	.009	.025
51	.000	.001	.001	.016	.000	.001	.001	.019	.000	-.001	-.008	-.190
52	.000	.000	.000	.000	.000	.000	.000	.000	.000	.000	.000	-.001
53	.001	.005	.007	-.021	.001	.006	.015	-.025	-.004	-.011	-.085	.250
54	.001	.001	-.002	.013	.001	.002	-.004	.015	-.003	-.003	.022	-.152

Table 5 (Continued)

	13	14	15	16	17	18	19	20	21	22	23	24
1	-.203	-.061	-.039	-.016	-.052	-.017	-.013	.000	.000	-.007	.001	.009
2	-.121	-.375	-.146	-.051	-.016	-.210	-.051	.000	.000	-.024	-.001	-.003
3	-.010	-.022	-.058	-.014	-.005	-.007	-.061	.000	.000	-.010	.000	-.002
4	-.004	-.008	-.014	-.071	-.003	-.003	-.008	.000	.000	-.059	.000	-.001
5	-.255	-.077	-.049	-.020	-.065	-.021	-.016	.000	.000	-.008	.001	.011
6	-.128	-.396	-.155	-.054	-.016	-.222	-.054	.000	.000	-.026	-.001	-.003
7	-.021	-.045	-.119	-.028	-.010	-.015	-.125	.000	.000	-.021	.000	-.005
8	-.005	-.009	-.016	-.085	-.003	-.004	-.010	-.001	.000	-.071	.000	-.001
9	.862	.260	.167	.066	.219	.071	.054	.000	.000	.029	-.003	-.039
10	.257	.795	.310	.108	.033	.446	.109	.001	.000	.052	.002	.006
11	.120	.261	.692	.164	.058	.086	.728	.002	.000	.119	.001	.029
12	.045	.092	.164	.848	.032	.037	.098	.006	-.001	.707	.000	.014
13	1.000	.266	.177	.076	-.306	.024	-.003	.000	.000	-.017	.000	-.162
14	.266	1.000	.346	.128	-.024	-.189	.033	.001	.000	-.001	.002	-.034
15	.177	.346	1.000	.208	-.028	-.007	.008	.001	.000	.025	.002	-.018
16	.076	.128	.208	1.000	-.021	-.013	.030	.005	-.001	.225	.001	-.012
17	-.306	-.024	-.028	-.021	1.000	.088	.107	.000	.000	.087	-.006	.238
18	.024	-.189	-.007	-.013	.088	1.000	.126	.000	.000	.086	.001	.059
19	-.003	.033	.008	.030	.107	.126	1.000	.001	.000	.141	.000	.057
20	.000	.001	.001	.005	.000	.000	.001	1.000	.003	.004	.000	.000
21	.000	.000	.000	-.001	.000	.000	.000	.003	1.000	-.001	.000	.000
22	-.017	-.001	.025	.225	.087	.086	.141	.004	-.001	1.000	.000	.043
23	.000	.002	.002	.001	-.006	.001	.000	.000	.000	.000	1.000	-.003
24	-.162	-.034	-.018	-.012	.238	.059	.057	.000	.000	.043	-.003	1.000
25	-.036	-.145	-.040	-.024	.095	.177	.070	.000	.000	.056	.000	.621
26	-.047	-.058	-.125	-.050	.094	.085	.253	.000	.000	.096	-.001	.558
27	-.052	-.063	-.064	-.073	.089	.077	.115	.001	.000	.276	-.001	.510
28	-.032	-.041	-.032	-.019	.056	.051	.058	.000	.000	.051	.000	.359
29	.150	.012	.019	.010	-.449	.001	-.016	.000	.000	-.018	.001	.756
30	-.003	.166	.028	.009	.019	-.543	-.018	.000	.000	-.009	.000	.487
31	.020	.031	.198	-.001	-.032	-.049	-.674	.000	.000	-.043	.000	.358
32	.024	.027	.038	.212	-.048	-.049	-.063	-.002	.000	-.745	.000	.241
33	-.443	-.063	-.054	-.032	.989	.079	.102	.000	.000	.085	-.006	.249
34	-.039	-.408	-.087	-.042	.087	.974	.110	.000	.000	.080	.000	.063
35	-.060	-.081	-.319	-.040	.111	.122	.945	.001	.000	.126	-.001	.060
36	-.053	-.062	-.074	-.250	.097	.091	.126	.002	.000	.887	-.001	.048
37	-.103	-.038	.040	.023	-.002	-.014	.009	.000	.000	.007	-.001	.014
38	-.046	-.244	.077	.008	.002	.054	-.008	.000	.000	.008	.000	.006
39	.002	-.003	-.286	.014	.005	-.008	-.016	.000	.000	.012	.000	-.004
40	.002	.003	.001	.026	-.001	-.001	-.009	-.002	.000	.005	.000	-.001
41	-.036	.072	.050	.022	-.291	-.012	-.016	.000	.000	-.019	-.004	-.074
42	.069	.049	.064	.027	-.027	-.347	-.008	.000	.000	-.019	.001	-.026
43	.040	.064	-.064	.036	-.030	.000	-.337	.000	.000	-.027	.000	-.022
44	.001	.002	.003	-.017	-.002	-.001	-.001	.000	.000	-.025	.000	-.001
45	-.449	.026	.010	-.002	.565	.072	.070	.000	.000	.057	.009	.124
46	.047	-.377	-.034	-.020	.070	.624	.084	.000	.000	.054	.000	.048
47	.062	.013	-.367	.089	.037	.076	.170	.000	.000	.053	.001	.019
48	.014	.010	.035	-.628	.020	.033	.022	-.003	.000	-.102	.000	.009
49	.009	.011	.041	.081	-.019	-.022	-.192	.002	.001	.046	.000	-.010
50	.002	.003	.007	.021	.001	.001	.005	-.046	.012	.019	.000	.001
51	.021	.024	.033	.046	-.041	-.038	-.043	.002	.000	-.411	.000	-.020
52	.000	.000	.000	-.001	.000	.000	.000	.003	-.001	-.001	.000	.000
53	-.005	-.013	-.054	.203	.003	.000	-.067	.008	.003	.189	.000	.001
54	-.003	-.004	.005	-.146	.001	.001	.026	.006	-.001	-.085	.000	.001

Table 5 (Continued)

	25	26	27	28	29	30	31	32	33	34	35	36
1	-.003	.000	.001	.001	.020	-.002	-.001	.000	-.017	-.001	.001	.001
2	.011	.000	.004	.003	-.005	.087	.001	.002	.004	-.108	-.001	.000
3	-.002	-.008	-.003	-.002	.000	.000	.029	.002	-.003	-.002	-.039	-.003
4	-.001	-.001	-.008	-.001	.000	.000	.002	.021	-.002	-.001	-.003	-.025
5	-.004	.000	.002	.001	.025	-.002	-.001	.000	-.021	-.002	.001	.001
6	.011	.000	.005	.003	-.006	.091	.001	.003	.004	-.115	-.001	.000
7	-.004	-.017	-.007	-.003	.000	-.001	.060	.003	-.006	-.003	-.080	-.007
8	-.001	-.002	-.010	-.001	.000	.000	.002	.025	-.002	-.001	-.004	-.030
9	.013	.002	-.006	-.003	-.085	.007	.004	-.001	.072	.006	-.003	-.003
10	-.023	-.001	-.009	-.006	.011	-.184	-.002	-.005	-.009	.230	.002	.000
11	.023	.097	.039	.020	.002	.006	-.351	-.019	.036	.019	.464	.041
12	.013	.016	.097	.014	-.002	.002	-.024	-.251	.023	.013	.039	.301
13	-.036	-.047	-.052	-.032	.150	-.003	.020	.024	-.443	-.039	-.060	-.053
14	-.145	-.058	-.063	-.041	.012	.166	.031	.027	-.063	-.408	-.081	-.062
15	-.040	-.125	-.064	-.032	.019	.028	.198	.038	-.054	-.087	-.319	-.074
16	-.024	-.050	-.073	-.019	.010	.009	-.001	.212	-.032	-.042	-.040	-.250
17	.095	.094	.089	.056	-.449	.019	-.032	-.048	.989	.087	.111	.097
18	.177	.085	.077	.051	.001	-.543	-.049	-.049	.079	.974	.122	.091
19	.070	.253	.115	.058	-.016	-.018	-.674	-.063	.102	.110	.945	.126
20	.000	.000	.001	.000	.000	.000	.000	-.002	.000	.000	.001	.002
21	.000	.000	.000	.000	.000	.000	.000	.000	.000	.000	.000	.000
22	.056	.096	.276	.051	-.018	-.009	-.043	-.745	.085	.080	.126	.887
23	.000	-.001	-.001	.000	.001	.000	.000	.000	-.006	.000	-.001	-.001
24	.621	.558	.510	.359	.756	.487	.358	.241	.249	.063	.060	.048
25	1.000	.598	.547	.395	.510	.715	.370	.243	.095	.198	.079	.067
26	.598	1.000	.600	.399	.451	.446	.485	.220	.096	.092	.280	.119
27	.547	.600	1.000	.380	.409	.407	.326	.254	.092	.086	.130	.309
28	.395	.399	.380	1.000	.293	.298	.236	.156	.058	.057	.065	.059
29	.510	.451	.409	.293	1.000	.438	.354	.256	-.446	-.002	-.022	-.023
30	.715	.446	.407	.298	.438	1.000	.355	.245	.018	-.543	-.027	-.013
31	.370	.485	.326	.236	.354	.355	1.000	.229	-.033	-.052	-.703	-.043
32	.243	.220	.254	.156	.256	.245	.229	1.000	-.049	-.052	-.072	-.841
33	.095	.096	.092	.058	-.446	.018	-.033	-.049	1.000	.088	.114	.099
34	.198	.092	.086	.057	-.002	-.543	-.052	-.052	.088	1.000	.133	.099
35	.079	.280	.130	.065	-.022	-.027	-.703	-.072	.114	.133	1.000	.144
36	.067	.119	.309	.059	-.023	-.013	-.043	-.841	.099	.099	.144	1.000
37	.004	-.010	-.002	.000	.003	.006	-.004	.004	.014	-.004	-.004	-.005
38	.037	-.005	.007	.007	.000	-.044	.026	.000	.009	-.107	-.033	.004
39	-.006	.040	.009	.005	-.006	.000	-.042	.000	.004	-.007	.078	.005
40	-.001	-.004	-.002	-.001	.000	.000	.005	.006	-.002	-.002	-.009	-.007
41	-.028	-.027	-.027	-.017	.113	-.005	.009	.014	-.268	-.027	-.032	-.029
42	-.074	-.029	-.032	-.021	.001	.175	.004	.014	-.036	-.334	-.029	-.032
43	-.034	-.059	-.036	-.017	.003	-.018	.228	.024	-.035	-.015	-.298	-.044
44	-.004	-.002	.003	.000	.000	-.002	.000	.018	-.002	-.001	-.002	-.016
45	.068	.056	.052	.033	-.292	.015	-.016	-.029	.601	.061	.063	.058
46	.096	.060	.050	.031	.005	-.394	-.038	-.036	.059	.667	.090	.063
47	.042	.015	.011	.007	.000	-.012	-.245	-.005	.026	.067	.281	.011
48	.022	.013	.033	.007	-.003	-.001	.001	-.181	.017	.029	.009	.196
49	-.014	-.052	-.014	-.011	.003	.005	.140	-.015	-.019	-.023	-.196	.007
50	.000	.001	.003	.001	.000	.000	-.002	-.007	.001	.001	.003	.009
51	-.028	-.048	-.133	-.025	.009	.005	.011	.363	-.042	-.041	-.051	-.431
52	.000	.000	.000	.000	.000	.000	.000	.000	.000	.000	.000	.000
53	.002	-.006	.026	.002	-.001	-.001	.037	-.078	.003	.003	-.045	.092
54	.001	.006	-.004	.001	.000	.000	-.016	.013	.001	.002	.023	-.015

Table 5 (Continued)

	37	38	39	40	41	42	43	44	45	46	47	48
1	.025	.011	-.001	.000	.045	-.013	-.006	.000	.038	-.020	-.020	-.00
2	.020	.089	.004	-.001	-.028	.080	-.027	-.001	-.032	-.020	-.028	-.01
3	-.003	-.004	.017	.000	-.002	-.003	.024	.000	-.005	-.003	.011	-.00
4	-.002	-.001	-.001	-.002	-.001	-.001	-.001	.002	-.002	-.001	-.008	.04
5	.031	.014	-.001	.000	.056	-.017	-.007	.000	.047	-.025	-.025	-.00
6	.022	.094	.004	-.001	-.029	.085	-.029	-.001	-.034	-.021	-.029	-.01
7	-.006	-.008	.036	.001	-.004	-.007	.049	.000	-.010	-.006	.022	-.00
8	-.002	-.001	-.002	-.002	-.001	-.001	-.001	.003	-.003	-.002	-.009	.05
9	-.107	-.046	.005	.002	-.191	.056	.025	.000	-.160	.085	.084	.02
10	-.043	-.189	-.007	.002	.059	-.170	.058	.002	.068	.042	.059	.02
11	.034	.047	-.208	-.006	.022	.038	-.287	.001	.057	.037	-.129	.04
12	.020	.010	.017	.022	.006	.009	.012	-.026	.030	.015	.093	-.51
13	-.103	-.046	.002	.002	-.036	.069	.040	.001	-.449	.047	.062	.01
14	-.038	-.244	-.003	.003	.072	.049	.064	.002	.026	-.377	.013	.01
15	.040	.077	-.286	.001	.050	.064	-.064	.003	.010	-.034	-.367	.03
16	.023	.008	.014	.026	.022	.027	.036	-.017	-.002	-.020	.089	-.62
17	-.002	.002	.005	-.001	-.291	-.027	-.030	-.002	.565	.070	.037	.02
18	-.014	.054	-.008	-.001	-.012	-.347	.000	-.001	.072	.624	.076	.03
19	.009	-.008	-.016	-.009	-.016	-.008	-.337	-.001	.070	.084	.170	.02
20	.000	.000	.000	-.002	.000	.000	.000	.000	.000	.000	.000	-.00
21	.000	.000	.000	.000	.000	.000	.000	.000	.000	.000	.000	.00
22	.007	.008	.012	.005	-.019	-.019	-.027	-.025	.057	.054	.053	-.10
23	-.001	.000	.000	.000	-.004	.001	.000	.000	.009	.000	.001	.00
24	.014	.006	-.004	-.001	-.074	-.026	-.022	-.001	.124	.048	.019	.00
25	.004	.037	-.006	-.001	-.028	-.074	-.034	-.004	.068	.096	.042	.02
26	-.010	-.005	.040	-.004	-.027	-.029	-.059	-.002	.056	.060	.015	.01
27	-.002	.007	.009	-.002	-.027	-.032	-.036	.003	.052	.050	.011	.03
28	.000	.007	.005	-.001	-.017	-.021	-.017	.000	.033	.031	.007	.00
29	.003	.000	-.006	.000	.113	.001	.003	.000	-.292	.005	.000	-.00
30	.006	-.044	.000	.000	-.005	.175	-.018	-.002	.015	-.394	-.012	-.00
31	-.004	.026	-.042	.005	.009	.004	.228	.000	-.016	-.038	-.245	.00
32	.004	.000	.000	.006	.014	.014	.024	.018	-.029	-.036	-.005	-.18
33	.014	.009	.004	-.002	-.268	-.036	-.035	-.002	.601	.059	.026	.01
34	-.004	.107	-.007	-.002	-.027	-.334	-.015	-.001	.061	.667	.067	.02
35	-.004	-.033	.078	-.009	-.032	-.029	-.298	-.002	.063	.090	.281	.00
36	-.005	.004	.005	-.007	-.029	-.032	-.044	-.016	.058	.063	.011	.19
37	1.000	.025	.024	.001	-.026	-.012	.012	.000	-.014	-.020	.044	.00
38	.025	1.000	.033	.000	-.012	-.005	-.030	.000	-.006	.105	-.067	.00
39	.024	.033	1.000	.006	.001	-.007	.000	.002	.002	-.010	.023	.01
40	.001	.000	.006	1.000	.001	.001	.007	-.001	-.001	-.001	.008	-.03
41	-.026	-.012	.001	.001	1.000	.021	.017	.001	.411	.002	.008	.00
42	-.012	-.005	-.007	.001	.021	1.000	.035	.002	-.006	.257	.012	.00
43	.012	-.030	.000	.007	.017	.035	1.000	.003	-.019	-.003	.264	.00
44	.000	.000	.002	-.001	.001	.002	.003	1.000	-.001	-.001	.000	.03
45	-.014	-.006	.002	-.001	.411	-.006	-.019	-.001	1.000	.054	.040	.01
46	-.020	.105	-.010	-.001	.002	.257	-.003	-.001	.054	1.000	.096	.04
47	.044	-.067	.023	.008	.008	.012	.264	.000	.040	.096	1.000	.06
48	.008	.007	.015	-.037	.000	.003	.007	.038	.017	.040	.062	1.00
49	.001	.005	-.003	-.033	.005	.004	.067	-.002	-.011	-.016	-.035	-.05
50	.001	.000	.000	-.009	.000	.000	-.001	-.001	.001	.001	.002	-.01
51	.001	-.001	-.008	-.062	.012	.013	.011	.009	-.025	-.026	-.014	-.04
52	.000	.000	.000	.000	.000	.000	.000	.000	.000	.000	.000	.00
53	.001	-.004	.033	-.097	-.002	-.003	.040	-.007	.001	.000	.044	-.13
54	-.002	.001	-.013	.071	-.001	-.001	-.018	.004	.000	.002	-.022	.09

Table 5 (Continued)

	49	50	51	52	53	54
1	.000	-.001	.000	.000	.001	.001
2	.002	-.002	.001	.000	.005	.001
3	.009	-.001	.001	.000	.007	-.002
4	-.007	-.002	.016	.000	-.021	.013
5	.000	-.001	.000	.000	.001	.001
6	.002	-.002	.001	.000	.006	.002
7	.019	-.001	.001	.000	.015	-.004
8	-.008	-.003	.019	.000	-.025	.015
9	.000	.002	.000	.000	-.004	-.003
10	-.003	.004	-.001	.000	-.011	-.003
11	-.111	.009	-.008	.000	-.085	.022
12	.084	.025	-.190	-.001	.250	-.152
13	.009	.002	.021	.000	-.005	-.003
14	.011	.003	.024	.000	-.013	-.004
15	.041	.007	.033	.000	-.054	.005
16	.081	.021	.046	-.001	.203	-.146
17	-.019	.001	-.041	.000	.003	.001
18	-.022	.001	-.038	.000	.000	.001
19	-.192	.005	-.043	.000	-.067	.026
20	.002	-.046	.002	.003	.008	.006
21	.001	.012	.000	-.001	.003	-.001
22	.046	.019	-.411	-.001	.189	-.085
23	.000	.000	.000	.000	.000	.000
24	-.010	.001	-.020	.000	.001	.001
25	-.014	.000	-.028	.000	.002	.001
26	-.052	.001	-.048	.000	-.006	.006
27	-.014	.003	-.133	.000	.026	-.004
28	-.011	.001	-.025	.000	.002	.001
29	.003	.000	.009	.000	-.001	.000
30	.005	.000	.005	.000	-.001	.000
31	.140	-.002	.011	.000	.037	-.016
32	-.015	-.007	.363	.000	-.078	.013
33	-.019	.001	-.042	.000	.003	.001
34	-.023	.001	-.041	.000	.003	.002
35	-.196	.003	-.051	.000	-.045	.023
36	.007	.009	-.431	.000	.092	-.015
37	.001	.001	.001	.000	.001	-.002
38	.005	.000	-.001	.000	-.004	.001
39	-.003	.000	-.008	.000	.033	-.013
40	-.033	-.009	-.062	.000	-.097	.071
41	.005	.000	.012	.000	-.002	-.001
42	.004	.000	.013	.000	-.003	-.001
43	.067	-.001	.011	.000	.040	-.018
44	-.002	-.001	.009	.000	-.007	.004
45	-.011	.001	-.025	.000	.001	.000
46	-.016	.001	-.026	.000	.000	.002
47	-.035	.002	-.014	.000	.044	-.022
48	-.051	-.012	-.042	.000	-.139	.095
49	1.000	.010	.044	.001	.427	.110
50	.010	1.000	.008	.015	.034	.029
51	.044	.008	1.000	.000	.095	.396
52	.001	.015	.000	1.000	.004	-.001
53	.427	.034	.095	.004	1.000	.316
54	.110	.029	.396	-.001	.316	1.000

Table 6

Maxwellian Data Omitted

Comparison Of Fitted Values With Divadeenam 1984

PAR	FITTED	ERROR	%ERROR	DIV	DIV-YF	EDIV-ER
SCA 33	13.4994	.9138	6.7693	12.6000	.9334	.3283
SCA 35	16.3121	1.2069	7.3989	13.9000	.8521	.4143
SCA 39	7.8706	.9764	12.4052	7.3000	.9275	.4097
SCA 41	11.9756	2.5863	21.5960	9.1000	.7599	.3867
SCR 33	12.3176	.6997	5.6808	.0000	.0000	.0000
SCR 35	14.6450	1.3773	9.4046	.0000	.0000	.0000
SCR 39	6.6721	1.8370	27.5328	.0000	.0000	.0000
SCR 41	10.8304	3.8379	35.4362	.0000	.0000	.0000
ABS 33	574.0839	1.7728	.3088	575.1000	1.0018	.5641
ABS 35	681.3275	1.7304	.2540	681.4000	1.0001	.6357
ABS 39	1018.1303	3.9721	.3901	1018.0000	.9999	.7301
ABS 41	1382.1148	14.9107	1.0788	1371.0000	.9920	.5164
FIS 33	532.3129	2.3907	.4491	529.6000	.9949	.5019
FIS 35	585.2068	1.7010	.2907	582.9000	.9961	.6467
FIS 39	748.3183	2.6076	.3485	748.2000	.9998	.7670
FIS 41	1020.7414	11.4926	1.1259	1009.7000	.9892	.5395
CA 33	41.7710	1.7570	4.2063	45.4000	1.0869	.3984
CA 35	96.1208	1.7626	1.8337	98.6000	1.0258	.4539
CA 39	269.8121	3.3002	1.2231	269.9000	1.0003	.6666
CA 41	361.3734	6.1921	1.7135	361.1000	.9992	.8236
NUB 33	2.4849	.0054	.2182	2.4931	1.0033	.7191
NUB 35	2.4256	.0046	.1889	2.4287	1.0013	.7421
NUB 39	2.8785	.0060	.2080	2.8807	1.0008	.9522
NUB 41	2.9397	.0065	.2207	2.9461	1.0022	1.1253
NUB 52	3.7632	.0050	.1322	3.7682	1.0013	.8039
ETA 33	2.3041	.0063	.2716	2.2959	.9964	.6391
ETA 35	2.0834	.0054	.2575	2.0775	.9972	.6150
ETA 39	2.1156	.0067	.3156	2.1170	1.0006	.7788
ETA 41	2.1711	.0087	.3998	2.1700	.9995	.9217
ALPHA 33	.0785	.0035	4.5210	.0859	1.0947	.4228
ALPHA 35	.1643	.0033	1.9953	.1723	1.0490	.4577
ALPHA 39	.3606	.0047	1.3085	.3639	1.0093	.6782
ALPHA 41	.3540	.0059	1.6723	.3635	1.0267	.9628
HLF 33	1.5920	.0020	.1259	1.5913	.9996	.8132
HLF 34	2.4568	.0053	.2166	2.4575	1.0003	.9470
HLF 39	2.4116	.0029	.1222	2.4101	.9994	.3969

Table 7

Standard Reference Data

Capture Cross Sections	
197 Au	98.65 ± 0.009b
59 Co	37.18 ∓ 0.06b
55 Mn	13.41 ± 0.04b
Absorption	
10 B	3838 ± 6b
Sulphur	0.52 ± 0.01
Natural boron (Argonne)	757.3 ± 3.0
Half-lives	
233 U (Alpha)	(1.592 ± 0.002)E05y
234 U (Alpha)	(2.457 ± 0.005)E05y
239 Pu (Alpha)	(2.411 ± 0.003)E04y
241 Pu (Beta)	(14.4 ± 0.100)y

a Divadeenam and Stehn (1984)
b Axton (B1984)
c Mughabgab, Divadeenam, and Holden (1982
d Ljostrand and Story (1961)
e Reich(1984)

7. Discussion

A study of the residuals in table 1 reveals a reasonably normal distribution. ^{2} is 105 for 169 measurements and 126 degrees of freedom. Of the 169 residuals, 81 are positive and 88 are negative. 30 of the measurements differ from their fitted values by more than one standard deviation compared with an expected 54.

Only one measurement differs from its fitted value by more than 2 standard deviations compared with an expected 8. This may reflect some of the arbitrary down-weighting which has been carried out by previous evaluators. Evaluators tend to distrust 'measurements which do not agree within the error'. However, if all measurements were in agreement within this limit, the data set would be seriously abnormal.

Likewise, although measurers in general agree that thirty percent or so of the measurements are expected to be beyond one standard deviation, nobody wants his own measurement to fall into that category.

Two important measurements do fall into this category, namely the ^{252}Cf ϑ measurements of Spencer et al. (1982), and Axton et al. (1984), with residuals of + 2.1 and - 1.3 respectively. In view of the above discussion perhaps these measurements should not be considered to be discrepant after all, since the residuals are compatible with the assumptions regarding the uncertainties of the input data.

A disturbing feature of the new ϑ_p ratios of Gwin et al. (1984) is the unexplained disagreement between the responses of the various ^{252}Cf foils used in the measurements, which necessitates some renormalization of the ratios. Regarding the comparison with the results of Divadeenam et al (A 1984) in table 4, the main differences occur with the relatively unimportant scattering cross-sections and they are probably attributable to the fact that they chose to neglect the small differences between the bound-atom scattering cross sections used for liquid and powdered metal samples, and those used for rolled metal samples. These distinctions were introduced by Hanna et al.(1969) and retained by Lemmel (1982). The low uncertainty on the value of the ^{239}Pu half-life merely reflects the lower uncertainty in the input value.

There do not appear to be any significant differences in the more important of the fitted parameters, or in their uncertainties. The differences of up to 8% for $^{233}U\,\sigma_\gamma$ and α, and up to 2% for $^{235}U\sigma_\gamma$ and α, noted by Divadeenam in comparison with the earlier results of Axton (1984) are no longer evident. Neither is the 2 barn difference in σ_f for ^{235}U.

The agreement is perhaps to be expected since these two latest evaluations are based substantially on identical data apart from some revaluations of earlier experiments and the addition of some correlations. Many of the measurements have simply been transferred from one evaluation to the next with, perhaps, some changes in the uncertainties. Perhaps more experiments would benefit from re-interpretation along the lines of appendices 2 and 3 of this paper.

Some of the correlations between the output parameters are somewhat higher than those of Divadeenam. In each nuclide the correlation between σ_a, σ_f, and η averages 86%, and between σ_f and α 95%. $\bar{\nu}$ values for the fissile nuclides are correlated 34% with ^{252}Cf, and 54% with each other. The negative correlation between ^{233}U and ^{239}Pu for $\bar{\nu}$ seems rather strange in Divadeenams correlation matrix. (1984)

It should again be emphasized that if the fitted parameters are propagated into reactor calculations they should always be accompanied by the associated correlation matrix.

8. Conclusions.

The results of this evaluation shows satisfactory agreement with those of Divadeenam (A1984). Whilst this is encouraging, it would be disturbing indeed if it were not so since the evaluations are based on what is almost the same input data.

Although many of the uncertainties are greater than those of Divadeenam, some of them are lower. Divadeenam made some suggestions for further improvement of the data set, which included some remeasurements of various key cross sections, η , and α values, and Monte Carlo studies of some of the existing Maxwellian α and η experiments. His concluding statement was 'Finally a generalized least-squares analysis with the Covariance Matrix as a part of the input data would provide an estimate of the parameter errors on a more realistic basis.' This has now been done.

As discussed by Axton (B1984), very few thermal neutron cross sections are measured absolutely. They are nearly all measured relative to another cross section and most of them are eventually traceable to gold or boron which can be measured absolutely by transmission. However, when standard cross sections such as hydrogen, gold, boron, cobalt, sodium, and manganese etc., are evaluated for inclusion in a compilation of standard reference data they are always evaluated individually, and the correlation information is lost to the user of the compilation.

If the cross sections are evaluated simultaneously, the improvement in the knowledge of any single cross section would improve the values of all cross sections included in the evaluation as it would improve many fast neutron cross sections as well. It is hoped that any further work on the subject of this paper will be preceded by a simultaneous evaluation of all thermal cross sections which are regarded as standards.

9. Acknowledgements.

It is a pleasure to acknowledge the assistance of Dr.H.D. Lemmel in providing copies of the older references. Dr. C. Bastian gave valuable assistance with the APL programming.

APPENDIX 1

TABLE A1.1

Nuclide Identifiers

Nuclide Identifier	Nuclide
33	^{233}U
34	^{234}U
35	^{235}U
39	^{239}Pu
40	^{240}Pu
41	^{241}Pu
42	^{242}Pu

TABLE A1.2

Function Definitions

Function	Independent variable	Meaning
ABS	Yes	Monoenergetic absorption cross section (2200 ms^{-1})
FA		Maxwellian absorption cross section (20°C)
FIS	Yes	Monoenergetic fission cross section (2200 ms^{-1})
FF		Maxwellian fission cross section (20°C)
CA		Monoenergetic capture cross section (2200 ms^{-1})
CAP		Maxwellian capture cross section (20°C)
SCA	Yes	Scatter cross section
SCR	Yes	Scatter cross section (Rolled metal)
NUB	Yes	NUBAR
ETA		Monoenergetic ETA = NUB x FIS : ABS
F1ETA		Maxwellian ETA = NUB x FF : FA
F2ETA		Maxwellian FIETA x FA = NUB x FF
F3ETA		Maxwellian (FIETA - 1) x FA = NUB x FF - FA
FH1		Monoenergetic FIS x HLF
FFH		Maxwellian FF x HLF .eg (33 FFH 35) is FF 35 multiplied by HLF 33.
HLF	Yes	Relative half-life in years (omitting powers of 10). In the case of ^{241}Pu it is the B half-life in years.
WGA	Yes	Westcott parameter g for absorption (20°C)
WFA	Yes	Westcott parameter g for fission (20°C).
FLEM		(CAP 33) : ((FA 33) - (CAP 33))
F1CAB		((CA 40) x (GC116 40) - (CA 42) x (GC116 42))
F2CAB		((ABS 39) x (GA116 39)- (CA 42) x (GC116 42))
F3CAB		((ABS 39) x (GA116 39) : (GA 39) x (GC116 39))
F4CAB		((ABS 41) x (GA116 41) - (ABS 39) x (GA116 39)):F1HLF
F5CAB		((ABS 41) x (GA116 41) : (CA 41) x (GC116 41)): F2HLF
F1B1G		((FF 41) : (39 FFH 39)) : F3HLF. (Bighams half-life-dependent fission ratio).
GC116	Yes	Westcott's g + rs parameter for capture for T = 116°C and r = .00075 .(the Cabell functions F1CAB etc.)
GA116	Yes	Westcott's g + rs parameter for absorption for T = 116°C and r = .00075.
F1HLF		Dependence of F4CAB on HLF 41
F2HLF		Dependence of F5CAB on HLF 41
F3HLF		Dependence of F1BIG on HLF 41.

APPENDIX 2

Recalculation of the Results of Muelhause 1959.

Using the author's notation the measured quantity is

$$\sigma_p = f\,\sigma_a(1-g\eta)\cdot CRf(CR\ 1/v - 1) \div CR\ 1/v(CRf-1) \qquad (1)$$

where σ_p, which is negative, is the measured pile cross section
f is the Westcott parameter g(T)
g is the non-leakage factor for fission neutrons
CRi/v is the cadmium ratio of the (i/v) boron standard
CRf is the cadmium ratio for the fission spectrum.

The equation is rearranged to give

$$(\eta-1)f\sigma_a = [\,(-\sigma_p/g)\cdot CR\ 1/v\ (CRf-1) \div CRf\ (CR\ 1/v-1)\,] - f\sigma_a(1-1/g)$$

The σ_p are normalized to the boron cross section, and, because of the second term in equation it is necessary to assume values for the σ_a and the f. However, since the second term amounts only to about 10% the derived function is not very sensitive to the uncertainties in γ and σ_a. Nevertheless it is desirable to use the latest values for these and for the boron normalisation. The data appear in table A1.

TABLE A1

	Author's values				Revised values		
	σ_p	σ_a	f	CRf	σ_p	σ_a	f
^{233}U	-636±8	581±7	1	24±1	-638.27	574.7±1.0	.99664±.002
^{235}U	-597±8	694±8	.972	63±3	-599.13	680.9±1.1	.99740±.0016
^{239}PU	-954*±15	1026±13	1.079	69±4	-957.67	1017.3±2.9	1.05624±.0029

*The ^{239}Pu value in the author's table is provisional. The final value is given only for η_0. The input σ_p is therefore adjusted to give, using the author's data, the final value of η_0. The value of σ_B was 755±2. The σ_p are normalized to the Story (1961) value for Argonne boron which is 757.7±3.0b. The boron cadmium ratio is 110±5.
The uncertainties in the boron cross section, the boron cadmium ratio, and the leakage factor g are correlated, whereas those in the fissile nuclide σa, σp, cadmium ratios, and Westcott g factors are not. The statistical uncertainty is ± 0.1%. The new σ_a, and the g factors are taken from Divadeenam 1984.

The Maxwellian temperature T is not stated. It is assumed to be 20°C.

The results are shown in table 2 in comparison with the expectation value and the values used by previous evaluators.

TABLE 2

$(\bar{\eta} - 1)\bar{\sigma}_a$	This evaluation	correl. ± 20°C	uncert. other causes	Story 1961	Lemmel 1981 and Divadeenam 1984	Expect.
$^{233}U \div ^{235}U$	1.0221 ± 1.811	0.691	1.233	1.0014 ± 1.945	1.001 ± 3.90	1.031
$^{239}U \div ^{235}U$	1.6019 ± 2.273	1.614	1.233	1.5646 ± 3.365	1.513 ± 6.81	1.636

Uncertainties expressed as percent.

APPENDIX 3

Recalculation of the Measurements of Cabell 1968

These measurements were interpreted as measurements of $^{241}Pu\hat{\sigma}_a$, $^{239}Pu\hat{\sigma}_\gamma$, $^{241}Pu\hat{\sigma}_\gamma$, $^{239}Pu\ \hat{\alpha}$, and $^{241}Pu\ \hat{\alpha}$, and published by Cabell and Wilkins (1966). They were revised in Cabell (1968). For some of these measurements values of other data in the set were needed, and these were taken, not from the measurements in the set but from standard reference data. The ^{241}Pu measurements depend on the β half-life of ^{241}Pu which was very uncertain in 1968. Cabell calculated his values using two discrepant half life values of 14.05 ± .14 years and 14.98 ± 0.33 years and an additional uncertainty was added to cover the spread of the two sets of results. The measurements also depend on assumed values for $^{240}Pu\sigma\gamma$ and $^{242}Pu\sigma\gamma$.

It was decided to re-interpret these data in terms of five functions which describe the quantities actually measured. In this way they are easily updated with new ancillary data. It is also much simpler to keep track of the correlations. These are (see appendix I for function definitions):-

F1CAB = (CA 40) x (G116 40) - (CA 42) x (GC116 42)
F2CAB = (ABS 39) x (GA116 39) - (CA 42) x (GC116 42)
F3CAB = [(ABS 39) x (GA116 39)] ÷ [(CA 39) x (GC116 39)]
F4CAB = [(ABS 41) x (GA116 41) - (CA 41) x (GC116 41)] x F2HLF
F5CAB = [(ABS 41) x (GA116 41)] ÷ [(CA 41) x (GC116 41) x F2HLF]

From Cabell's two sets of calculations using different ^{241}Pu half lives, the half life dependence of these results can be expressed as

F1HLF = 1 + 0.12966 ((HLF 41) - 14.05) and
F2HLF = 1 + 0.02250 ((HLF 41) - 14.05).

The functions GA116 and GC116 are the Westcott g + rs factors for absorption and capture respectively for a temperature T = 116 and r = 0.00075.

The input data are shown in table A3. All the data in column 3 are input data to the least squares fit, except σ_a for boron, as floating variables to be fitted.

It would be tedious to introduce the 20°C g-factors but it could be done in order to preserve the correlation with other data.
The FCAB functions would become much more elaborate.
By allowing the 116° factors to change they cease to be part of a consistent set, but on the other hand they become more descriptive of the actual reactor spectrum.

TABLE A3

Parameter	Author value	Revised value	Percent correlated uncertainty Flux	± 9°C	Reference
F1CAB	276.2 ± 12.2	273.843	2.26	0.31	a
F2CAB	1182 ± 22.2	1171.914	2.26	1.21	a
F3CAB	3.269 ± 0.089	3.269 ± 0.089		- 0.54	
F4CAB	306 ± 10.3	303.389	2.26	- 1.31	a
F5CAB	3.871 ± 0.062	3.871 ± 0.062			
HLF 41	14.05 ± 0.14	14.4 ± 0. 1			c
(CA 40) x (GC116 40)	305.1 ± 7.6	-			
(CA 42) x (GC116 42)	21.0 ± 1.2	-			
GC116 39	1.3249	1.3265 ± .0803			b
GC116 40	1.0858 ± .0034	1.1097 ± .0037			b
GC116 41	1.0460	1.1085 ± .0274			b
GC116 42	-	1.1335 ± .0303			b
GA116 39	1.1869 ± .0136	1.1846 ± .0180			b
GA116 41	1.0841 ± .0073	1.1073 ± .0091			b
$^{59}Co\ \sigma_c$	37.5 ± .13	37.18 ± 0.6			d
CA 40	-	289.5 ± 1.4			e
CA 42	-	18.5 ± 0.3			e

a corrected to new σ_c for ^{59}Co
b The 116°C g-factors were taken from Westcott (1960) and the resonance integrals from BNL 325 3rd edition.
c Reich (1984)
d Divadeenam et al (1981)
e BNL 325 3rd edition.

Westcotts 1960 g+rs factors were used because they were the only set available at the time, but the output values are not sensitive to the values chosen for input. It simply involved more iteration of the program if they are seriously wrong.

Table A4 shows the input data for the five functions in comparison with their fitted values, and table A5 shows the data as represented in previous evaluations.

The uncertainties in tables A4 and A5 are expressed as percent.

TABLE A4

	Value	Fitted value
F1CAB	273.843 ± 4.96	290.07
F2CAB	1171.91 ± 3.176	1183.8
F3CAB	3.269 ± 2.776	3.284
F4CAB	303.389 ± 5.835	305.25
F5CAB	3.871 ± 1.602	3.841

Uncertainties are percent

TABLE A5

	Lemmel 1981	Divadeenam 1984	Fitted value
$^{241}Pu\ \hat{\sigma}_a$	1443 ± 2.15	1442.7 ± 2.13	1443.51
$^{241}Pu\ \hat{\sigma}_c$	372.7 ± 2.58	372.5 ± 2.55	376.70
$^{239}Pu\ \hat{\alpha}$	0.4048 ± 4.55	0.4048 ± 4.55	0.3922
$^{239}Pu\ \hat{\sigma}_c$	312 ± 4.49	310.66 ± 3.70	309.24
$^{241}Pu\ \hat{\alpha}$	.3480 ± 4.89	.3488 ± 4.59	0.3564

Uncertainties are percent

Appendix 4

Notes to the input data

1. As Sjostrand and Story (1961), Lemmel (1982) and Divadeeman (1984).
2. As Lemmel (1982) and Divadeenam (1984).
3. As Lemmel (1982).
4. As Divadeenam (1984).
5. As Axton (1984).
6. As Sjostrand and Story (1960) and Lemmel (1982).
7. See note 6.
8. See notes 2 and 9.
9. Cobalt correlation added .
10. See notes 4 and 9.
11. See note 4. Reformulated by Hanna.
12. Sodium correlation added.
13. See notes 4 and 12.
14. See note 4. Omits added uncertainty for sample absorption introduced by Lemmel (1982
15. See note 4. The uncertainties have been previously and arbitrarily expanded on account of the high accuracy claimed for the 1958 spectrometry. See note 16.
16. Dependence on β half life of ^{241}Pu introduced
17. See note 2. The experiment was last recalculated by Hanna (1969)with new α and β half lives for ^{241}Pu. He assumed T = 20° whereas the author quotes 25°. The experiment should be recalculated with modern reference data.
18. Values as Divadeenam (1984) and Lemmel (1982) but correlations due to assay appear in the covariance matrix.
19. See note 4. Based on Monte Carlo evaluation (Beer et al (1975)). Correlated through temperature uncertainty.
20. As Divadeenam (1984) and Lemmel (1982). Correlated through spectrum uncertainties.
21. Correlated through MTR 70° C temperature uncertainty.
22. For ^{239}Pu the spectrum uncertainty is negligible. For ^{235}U the spectrum uncertainty may be correlated with other measurements in NRU reactor shield.
23. See note 2. The uncertainties have been successively increased by various evaluators. Here the authors estimates are accepted as uncorrelated but correlated spectral uncertainties have been added.
24. The measurement is boron dependent, but the value of σ_B used by the author is not stated. See note 3;
25. See note 4. Correlated by the spectral uncertainties (S and P in the authors paper).
26. See note 3. The correlated uncertainties are dealt with by the covariance matrix instead of by the "Hanna triangle". (Hanna et al., 1969)

27. See note 2. There are no spectral correlations. But the measurements are correlated by the common denominator of the ^{235}U reactivity. The authors give no uncertainties. If it is assumed that each reactivity is accurate to 1 % this reproduces the authors uncertainties on the ratios, and leads to 50 % correlation.
28. See note 1. Divadeenam (1984) neglects the correlations specified by Sjostrand and Story (1960). Lemmel deals with them by means of the Hanna triangle.
29. See note 2. It is not possible to recalculate the experiment (Sjostrand 1960). The authors suggest uncertainties of $\pm$ 1.5 % per reactivity which is 2.121 % for a ratio. Sjostrand quoted uncertainties of 1.775 % and 3.365 % for 233/235 and 239/235 respectively. These were doubled by Westcott (1965). Lemmel (1982) and Divadeenam (1984) copied Westcott. There must be a correlation of at least 1.5 % between the two ratios for the common denominator.
30. See appendix 2 for reformulation and recalculation.
31. Revalued by Smith (1984).
32. The two ratios of Gwin (1978) have been replaced by the four ratios of Gwin (1984) and an attempt has been made to estimate the correlations between them, and between them and their ^{252}Cf $\bar{\nu}$ value.
33. Recent improvements in the knowledge of σ_{Mn} and σ_s and/or their uncertainties (Axton (A 1984), Mughabgab (1981) enable a reduction of the common uncertainty in NPL manganese bath measurements from 0.239 % to 0.211 %, and of the common uncertainty in all manganese bath measurements due to the uncertainty in the factor $(1 + \sigma_s/\sigma_{Mn})$ from 0.122 % to 0.073 %. The common uncertainty between the ^{252}Cf measurements of Smith and Alexandrov is correspondingly reduced to 0.111 %.
34. As Reich (1984).
35. Reformulated and recalculated in appendix 3.
36. Data taken from BNL 325 Third edition.
37. The 116° Westcott 9-factors are taken from Westcott (1960), and the resonance integrals from BNL 325 Third edition. The results are not very sensitive to the input values chosen.

Appendix 5

List of References From Axton (1984)

1. Aleksandrov, B.M., L.M. Belov, L.V. Drapchinskij, Ya.M. Kramarovskij, G.E. Lozhkomoev, V.G. Matyukhanov, K.A. Petrzhak, A.G. Prusakov, A.V. Sorokina, Eh.A. Shlyamin, O.A. Migun'kov, G.M. Stukov, V.T. Shchebolev, and I.A. Yaritsyna, V.G. Khlopin Radium Institute and D.I. Mendeleev All-Union Scientific Research Institute of Metrology, Proceedings of the 1975 Kiev Conference 5 (1976) 166-169.
2. Aleksandrov, B.M., E.V. Korolev, Ya.M. Kramarovskij, G.E. Lozhkomoev, V.G. Matyukhanov, K.A. Petrzhak, A.G. Prusakov, A.V. Sorokina, and Eh.A. Shlyamin, V.G. Khlopin Radium Institute, Proceedings of the 1980 Kiev Conference 4 (1981) 119-123.
3. Asplund-Nilsson, I., H. Condé, and N. Starfelt, Nucl. Sci. Engng. 16 (1963) 124.
4. Axton, E.J., P. Cross, and J.C. Robertson, J. of Nucl. En. A/B 19 (1965) 409.
5. Axton, E.J., A.G. Bardell, and B.N. Audric, J. of Nucl. En. A/B 23 (1969) 457.
6. Axton, E.J., A.G. Bardell, and B.N. Audric, EANDC(UK) (1969)-110, 70.
7. Axton, E.J., Second IAEA Panel on Neutron Standard Reference Data, Vienna, Nov. 1972, Proc. Vienna (1974) p. 261 and 268.
8. Axton, E.J., Proc. Int. Symposium on Neutron Standards and Applications, NBS Special Publication (1977) 493, 237.
9. Axton, E.J., and A.G. Bardell, Metrologia 18, 97 (1982).
10. Axton, E.J. (1982A) To be published.
11. Beer, M., M.H. Kalos, H. Lichenstein, H.A. Steinberg, and E.S. Troubetskoy, (1975) EPRI-NP-163, Electric Power Research Institute.
12. Berceanu, I., C. Borcea, A. Buta, A. Constantinescu, F. Cirstoiu, A. Galeriu, K. Galawez, A. Isbăyescu, I. Lazăr, L. Marinescu, I.M. Mihailescu, P. Osiceanu, M. Petrascu, M. Petrovici, V. Simion, and G. Voiculescu, IFA - Nr. 60 (1977) (published later in Rev. Roum. Phys. (1978) 23, 867).
13. Becker, M., Trans. Am. Nucl. Soc. 24, 216 (1976).

14. Bigham, C.B., G.C. Hanna, P.R. Turnicliffe, P.J. Campion, M. Lounsbury, and D.R. Mackenzie,
Second Int. Conf. peaceful Uses Atom. Energy, Geneva 1958,
Proc. (New York 1959) 16, 125
Same authors, Int. Conf. on the Neutron Interactions with the Nucleus,
New York 1957, Proc. TID-7547, 112 and 113.

15. Block, R.C., G.G. Slaughter, and J.A. Harvey,
Nucl. Sci. Engng 8 (1960) 112.

16. Boldeman, J.W., and A.W. Dalton,
(1967) AAEC/E 172.

17. Boldeman, J.W. (1977),
NBS Special Publication 493, 182.

18. Boldeman, J.W., and J. Fréhaut,
Nucl. Sci. Eng. 76, 49 (1980).

19. Bollinger, L.M., R.E. Coté, and G.E. Thomas,
Second Int. Conf. on Peaceful Uses Atom. Energy (Proc. Conf. Geneva 1958)
15 UN New York (1959) 127.

20. Borcea, C., A. Borza, A. Buta, A. Isbasescu, L. Marinescu, I. Mihai,
T. Mascutiu, M. Petrascu, V. Savu, and V. Simion,
IFA-NR-33 (1970), Supplemented by private communication and Borcea et al.
(1973) IFA-NR-47.

21. Bozorgmanesh, H.,
Absolute Measurement of the number of neutrons per spontaneous fission
of Californium-252., Ph.D. Dissertation U. Michigan (1977).

22. Bozorgmanesh, H.,
Trans. Am. Nucl. Soc. 27, 864 (1977A).

23. Carlson, A.D.,
Proceedings of $\bar{\nu}$ workshop, Sheraton-Washington Hotel, 21-22 Nov. 1980,
NBS, 1981.

24. Colvin, D.W., and M.G. Sowerby,
in Physics & Chemistry of Fission (Proc. Symp. Salzburg, 1965), 2, IAEA,
Vienna (1965) 25.

25. Colvin, D.W., M.G. Sowerby, and R.I. MacDonald,
in Nucl. Data for Reactors (Proc. Conf. Paris, 1966) 1, IAEA, Vienna
(1967) 307.

26. Condé, H.,
Ark. Fys. 29 (1965) and H. Condé, and M. Holmberg,
in Physics and Chemistry of Fission (Proc. Symp. Salzburg, 1965) 2,
IAEA, Vienna (1965) 57.

27. Condé, H., J. Hansen, and L. Widén,
Symp. on Neutron Standards and Flux Normalization, Argonne (1970),
Proc. AEC Symp. Series 23, CONF-701002 (1971).

28. Cox, S., P. Fields, A. Friedman, R. Sjoblom, and A. Smith,
Phys. Rev. 112, 960 (1958).

29. Craig, D.S., and C.H. Westcott,
AECL-1948 (1964) and Can. J. Phys. 42 (1968) 2384.

30. Deruytter, A.J.,
J. Nucl. Energy A/B (Reactor Sci. Technol.) 15 (1961) 165.

31. Deruytter, A.J., J. Spaepen, and P. Pelfer,
Conf. Neutron Cross-Sections and Technology, Washington D.C. (1968),
NBS Spec. Publ. No. 299, 1, 491.

32. Deruytter, A.J., and W. Becker,
Second Int. Conf. on Nucl. Data for Reactors, Helsinki 1970,
Proc. (Vienna 1970) 1, 117.

33. Deruytter, A.J.,
Symposium on Neutron Standards and Flux Normalization, Argonne 1970,
Proc. AEC Symposium Series 23, CONF-701002 (1971) 221.

34. Deruytter, A.J., and C. Wagemans,
J. Nucl. Energy 25 (1971) 263.

35. Deruytter, A.J., and C. Wagemans,
J. Nucl. Energy 26 (1972) 293.

36. Deruytter, A.J., J. Spaepen, and P. Pelfer,
J. Nucl. Energy 27 (1973) 645.

37. Deruytter, A.J., and W. Becker,
Annals of Nucl. Sci. and Engng. 1 (1974) 311.

38. De Volpi, A., and K.G. Porges, (1967),
IAEA Conf. on Nuclear Data for Reactors, Paris 1966.

39. De Volpi, A., and K.G. Porges,
ANL 7642 (1969A).

40. De Volpi, A., and K.G. Porges,
Metrologia 5, 128 (1969B).

41. De Volpi, A., and K.G. Porges,
Phys. Rev. C1, 683 (1970)

42. De Volpi, A.,
J. Nucl Energy 26, 75 (1972).

43. Durham, R.W., G.C. Hanna, M. Lounsbury, C.B. Bigham, R.G. Hart, and R.W. Jones,
Nuclear Data for Reactors, Proc. Conf. Paris, 1966 2, 17, IAEA Vienna,
(1967).

44. Edwards, G., D.J.S. Findlay, and E.W. Lees,
Ann. Nucl. Energy 9, 127 (1982).

45. Egelstaff, P.A.,
J. Nucl. Energy 1 (1954) 92, and J.E. Lynn, and N.J. Pattenden,
First Int. Conf. peaceful Uses Atom. Energy (Proc. Conf. Geneva 1955)
Vol. 4 UN, New York (1956) 210, revised by P.A. Egelstaff,
AERE-NP/R-2104 (1957) p. 1.

46. Fieldhouse, P., E.R. Culliford, D.S. Mather, D.W. Colvin, R.I. MacDonald, M.G. Sowerby,
J. Nucl. Energy, Parts A/B, 20, 549 (1966).

47. Fraysse, G., and A. Prosdocimi,
CEA-2775 (1965); and in Physics and Chemistry of Fission (Proc. Symp.
Salzburg, 1965) 1, IAEA, Vienna (1965) 255.

48. Galanina, N.D.,
USSR Conf. peaceful Uses Atom. Energy, Moscow (1955), English
Translation AEC-TR-2435, p. 81.

49. Gerasimov, V.F., and V.S. Zenkevich,
Atomn. Energ. 13 (1962) 368, and Sov. Atom. Energy 13 (1963) 977.

50. Goldsmith, M., and J.J. Ullo,
Nucl. Sci. Eng. 60, 251 (1976).

51 Green, T.S., V.G. Small, and D.E. Glanville,
J. Nucl. Energy 4 (1957) 409.

52. Gwin, R., R.R. Spencer, R.W. Ingle, J.H. Tood, and H. Weaver,
ORNL/TM 6246 (1978).

53. Hanna, G.C., C.H. Westcott, H.D. Lemmel, B.R. Leonard Jr., J.S. Story, and P.M. Atree,
Atomic Energy Review 7 No. 4 (1969).

54. Holden, N.E.,
BNL-NCS-51388, (1981), Brookhaven Nat. Lab.

55. Holden, N.E.,
Report BNL-NCS-51320 (1981A), Brookhaven Nat. Lab. USA.

56. Hopkins J.C., and B.C. Diven
Nucl. Phys. 48, 433 (1963).

57. Jurney, E.T., S. Raman, and R.R. Spencer,
LA-UR-81-1755 (1981).

58. Koester, L., K. Knopf, and W. Waschkowski,
Z. Phys. A289, 399 (1979).

59. Lemmel, H.D.
Proceedings of the Conference on Neutron Cross-Sections and Technology, Washington D.C., 3-7 March 1975, NBS Special Publication 425 (Oct. 1975) 1, 286 (1975).

60. Lemmel, H.D.,
Proceedings of the Intern. Spec. Symp. on Neutron Stand. and Applications, Gaithersburg M.D., March 28-31, 1977, NBS Special Publication, 493, 170 (1977).

61. Lemmel, H.D.,
Private communication (1982), to be published as INDC(NDS)-132, IAEA Vienna.

62. Leonard, B.R. Jr.,
TNCC(US)-58 (1959).

63. Leonard, B.R. Jr., D.A. Kottwitz, and J.K. Thompson,
EPRI NP-157 (1976).

64. Leonard, B.R. Jr., and J.K. Thompson,
EPRI NP-1763 (1981).

65. Lorenz, A.,
INDC(NDS)-127/NE (1981).

66. Lounsbury, M., R.W. Durham, and G.C. Hanna,
Second Int. Conf. Nucl. Data for Reactors, Helsinki, 1, 287, IAEA Vienna, (1970).

67. Macklin, R.L., G. Desaussure, J.D. Kington, and W.S. Lyon,
USAEC Rep. ONRL-60-2-84 (1960) and Nucl. Sci. Engng. 8, 210 (1960).

68. Macklin, R.L., G. Desaussure, J.D. Kington, and W.S. Lyon,
Nucl. Sci. Engng. 14, 101 (1962).

69. Madland, D.G., and Nix, J.R.,
LA-UR-81-2968 (1981).

70. Maslin, E.E., J.A. Moore, J.M.A. Reichelt, and J.B. Crowden,
Phys. Rev. 139 (1965) 852.

71. Mather, D.S., P. Fieldhouse, and A. Moat,
Phys. Rev. 133 (1964), B1463 and Nucl. Phys. 66, 149 (1965).

72. Melkonian, E., W.W. Havens Jr., and M. Levin,
CU-115 (1953) Columbia University, New York, N.Y.

73. Moat, A., D.S. Mather, and M.H. McTaggart,
J. Nucl. Energy, Parts A/B 15, 102 (1961).

74. Muether, H., H. Palevsky,
unpublished. See Sjoestrand and Story (1961) and Goldberg, M.D., private communication (1968) quoting notes in the NNCSC archives. Data in EXFOR-50645.

75. Nefedov, V.N., A.K. Melkinov, and B.L. Starostov,
Prompt Fission Neutron Spectra (Proc. Consultants' Meeting, Vienna 1971). IAEA Vienna (1972), 89.

76. Nikitin, S.J., N.D. Galanina, K.G. Ignat'ev, V.V. Okorokov, and S.I. Sukhoruchkin,
First Int. Conf. peaceful Uses Atom. Energy (Proc. Conf. Geneva 1955) UN, New York (1956) 224, and Nikitin, S.J., S.I. Sukhoruchkin, K.G. Ignat'ev, and N.D. Galanina, USSR Conf. peaceful Uses Atom. Energy, Moscow (1955), English translation, AEC-TR-2435, p. 81.

77. Palevsky, H., R.S. Carter, R.M. Eisberg, and D.J. Hughes,
Phys. Rev. 94 (1954) 1088.

78. Pattenden, N.J.,
J. Nucl. Energy 3 (1956) 28.

79. Pattenden, N.J.,
J. Nucl. Energy 2 (1956A) 187 and Erratum same Vol. p. 300.

80. Petrascu, M.,
IFA-NR-22 (1965).

81. POPE, A.L., and J.S. Story,
AEEW Report WNDG-123, Winfrith Dorset (1973).

82. Raffle, J.F., and B.T. Price,
First Int. Conf. peaceful Uses Atom. Energy (Proc. Conf. Geneva 1955), Vol. 4 UN, New York (1956) 187.

83. Raffle, J.F.,
AERE/R-2998 (July 1959). Work done in 1954/55.

84. Robertson, J.C.,
Private communication (1982), University of New Mexico.

85. Safford, G.J., W.W. Havens Jr., and B.M. Rustad,
Nucl. Sci. Engng. 6 (1959) 433.

86. Safford, G.J., W.W. Havens Jr., and B.M. Rustad,
Phys. Rev. 118 (1960) 799.

87. Safford, G.J., and W.W. Havens, Jr.,
Nucl. Sci. Engng. 11 (1961) 65.

88. Saplakoglu, A.,
Second Int. Conf. peaceful Uses Atom. Energy (Proc. Conf. Geneva 1958),
16 UN, New York (1959) 103.

89. Saplakoglu, A.,
Nucl. Sci. Engng. 11 (1961) 312.

90. Simpson, O.D., M.S. Moore, and F.B. Simpson,
Nucl. Sci. Engng. 7 (1960) 187.

91. Simpson, O.D., and R.P. Schumann,
Nucl. Sci. Engng. 11 (1961) 111.

92. Simpson, O.D., and N.H. Marshall,
IDO-16679 (1961).

93. Sjostrand, N.G., and J.S. Story,
AERE-M-125, 17 (1961).

94. Smith, J.R.,
Private communication (1968) and WASH-1124 (1968) 64.

95. Smith, J.R., and S.D. Reeder,
Second Conf. on Nucl. Cross-Sections and Technology, Washington 1968,
Proc. NBS Spec. Publication 299 (1968) Vol. 1, p. 591.

96. Smith, J.R., S.D. Reeder, and R.C. Fluharty,
IDO-17083 (1966).

97. Smith, J.R., Proceedings of the ^{252}Cf Workshop, 6 Dec. 1977,
Brookhaven National Laboratory, N.Y. (1977).

98. Smith, J.R.,
EPRI NP-1258 (1979).

99. Smith, J.R.,
EPRI NP-1252 (1979A).

100. Smith, J.R.,
EPRI Report in preparation (1982).

101. Spencer, R.R., R. Gwin, and R. Ingle,
Nucl. Sci. Eng. 80, 603 (1982).

102. Spencer, R.R., R., Gwin, R. Ingle, and H. Weaver,
ORNL/TM/6805 (1979).

103. Spiegel, V., D.M. Gilliam, and W.E. Slater (1980), See Carlson, A.D.,
Proceedings of $\bar{\nu}$ Workshop, Sheraton-Washington Hotel 21-22 Nov. 1980,
NBS, 1981.

104. Steen, N.M.,
WAPD-TM-1052 (1972).

105. Stehn, J.R., M. Divadeenam, and N.E. Holden,
International Conference on Nuclear Data for Science and Technology,
Antwerp, Sept.6-10 (1982).

106. Story, J.S.,
Private communication (1982).

107. Ullo, J.J., and M. Goldsmith,
Nucl. Sci. Eng. 60, 239 (1976).

108. Ullo, J.J.,
Proceedings of ^{252}Cf $\bar{\nu}$ Workshop (1977), Brookhaven National Laboratory,
6 December 1977.

109. Watanabe, T., and O.D. Simpson,
Phys. Rev. 133B (1964) 390, and IDO-16995 (1964).

110. Wattecamps, E.,
Private communication 1974-5-13.

111. Wescott, C.H., W.H. Walker, and T.R. Alexander,
Proceedings of the Second International Conference on the Peaceful
Uses of Atomic Energy, Geneva, A/Conf. 15/P.202 (1958),
United Nations N.Y.

112. Westcott, C.H., K. Ekburg, G.C. Hanna, N.J. Pattenden, S. Sanatini,
and P.M. Attree,
Atomic Energy Review 3 No. 2 (1965).

113. White, P.H., J.M.A. Reichelt, and G.P. Garner,
in Nucl. Data for Reactors (Proc. Conf. Paris, 1966) 2, IAEA, Vienna
(1967) 29.

114. White, P.H., and E.J. Axton,
J. Nucl. Energy, 22, 73 (1968).

115. Young, T.B., and J.R. Smith,
WASH-1093 (1968) 60.

116. Zhang, H., and Z. Liu,
Chinese J. of Nucl. Phys. 2, 29 (1980), English translation available
from IAEA-NDS.

117. Zhang, H., and Z. Liu,
Private communication (1981), See Zhang and Liu (1980).

118. Zimmerman, R.L., and H. Palevsky, (1955) unpublished. See Ref.
Sjostrand and Story (1961), p. 17, and Leonard (1959) p. 10.
Data in EXFOR-52081. Sample apparently same as Palevsky H., D.J. Hughes,
R.L. Zimmerman, and R.M. Eisberg, J. Nucl. Energy 2 (1956) 177.

REFERENCES

Alikkanov, A.J., Vladimirsky, V.V. and Nitikin, S.J. (1956), 1st Geneva Conf. 4, 301, UN, New York

Axton, E.J. (1984), European Applied Research Reports (1984) 5 No. 4 (EUR 8805 EN)

Axton, E.J. and Bardell, A.G. (A 1984), Report EJA1/1984, submitted to Metrologia

Axton, E.J. (B 1984), Report EJA3/1984, submitted to Annals of Nuclear Energy

Bastian, C., (1984), CBNM Report GE/R/LI/142/84

Bigham, C.B., (1975), Nucl. Sci. Engng 59, 50
See also Bigham, Hanna, Tunicliffe, Lounsburg, Campion and Mckenzie (1959), 2nd Geneva Conf. 16, 125, UN New York

BNL 325 (Third Edition) (1973) 1

Cabell, M.J., Rose, H. and Tattersall, R.B., (1965), Report AERE-R/4946

Cabell, M.J. and Wilkins, M., (1966), J. Inorg. Nucl. Chem. 28, 2467

Cabell, M.J., (1968), Report AERE-R/5874

Cabell, M.J. and Wilkins, M., (1971), J. Inorg. Nucl. Chem. 33, 3972

Conway, D.E., (1967), Report WAPD-TM-613, and Private Communications

Cornish, F.W. and Lounsbury, M., (1956), Report AECL-510

Cornish, F.W., (1960), Report NRDC-129

Deboisblanc, D.R. and Fast, E. (1961), Trans. Am. Nucl. Soc. 4, 2

Divadeenam, M. and Stehn, J.R., (1984), Ann. Nucl. Energy 11, 375

Divadeenam, M. and Stehn, J.R. (A 1984), This Conference

Durham, R.W., Hanna, G.C., Lounsbury, M., Bigham, C.B., Hart, R.G. and Jones, R.W., (1967), Nuclear Data for Reactors (Paris) 2, 17, IAEA Vienna

Fast, E. and Aber, E.F., (1960), Report IN-1060 and Private Communication (1968)

Gwin, R. and Magnuson, D.W., (1962), Nucl. Sci. Engng 12, 359
Revised by Magnuson (1971)

Gwin, R. and Magnuson, D.W., (A 1962), Nucl. Sci. Engng 12, 364
Revised by Magnuson (1971)

Gwin, R., Spencer, R.R. and Ingle, R.W., (1984), Nucl. Sci. Engng 87, 381

Halperin, J., Johnston, F.J., Stoughton, R.W., Oliver, J.H., Blevins, E.L., Druschel, R.E., Harkness, A.L., Swarz, B.A., (1963), Nucl. Sci. Engng 16, 245

Inghram, M.G., Hess, D.C., Hayden, R.J., Stevens, C.M., (1956), 1st Geneva Conf. 4, 105, UN New York

Jaffey, A.H., Studier, M.H., Fields, P.R. and Bentley, W.C. (1955), Report ANL-5397

Keith, R.L.G., Mc Nair, A. and Rodgers, A.L., (1968), J. Nucl. Energy 22, 477

Laponche, B., Brunet, M. and Bouedo, Y., (1972), Nucl. Sci. Engng 48, 305

Lisman, F.L., Maeck, W.J., Fosters, R.E., Jr., Rein, J.E. (1967), Report IN-1064

See also Lisman, F.L. and Rider, B.F., (1967-68) Private Communications to Hanna
Maeck, W.J., Lisman, F.L. and Rein, J.E. (1967), Report IDO 14678
Lisman, F.L., Maeck, W.J. and Rein, J.E., (1968) Report IN-1178
Rider, B.F., Peterson, J.P., Ruiz, C.P. and Smith, F.R. Reports GEAP-5060(1965) and GEAP-5270(1966)

Lloyd, R.E., Libby, R.A. and Clayton, E.D., (1982), Nucl. Sci. Engng, 82, 325

Magnuson, D.W., (1971), Nucl. Sci. Engng 44, 266

Muelhause, C.O., (1959), Nucl. Sci. Engng 5, 225

Mughabgab, S.F., Divadeenam, M. and Holden, N.E., (1981), Neutron Cross Sections, 1, Academic Press

Okazaki, A. Lounsbury, M., Durham, R.W. and Crocker, I.H. (A 1964), Report AECL-1965

Okazaki, A., Lounsbury, M. and Durham (1964), Report AECL-2148

Popovic, D. and Grmeland, B., (1953), Jenner Report No. 19

Popovic, D. and Saeland, E.J., (1955), J. Nucl. Energy 1, 286

Reich, C.W., (1984) This Conference

Sjostrand, N.G. and Story, J.S. (1961), Report AEEW-M-125

Smith, J.R., (1984), Report EPRI NP-3436

Sweet, D.W., AEEW Unpublished Memo to J.S. Story, 26 July 1973

Vidal, R., Robin, M., da Silva, C.G. (1970), Nuclear Data for Reactors (Helsinki), 1, 295, IAEA Vienna

Westcott, C.H., (1960) Report AECL 1101

White, P.H., Reichelt, J.M.A. and Warner, G.P. (1967), Nuclear Data for Reactors (Paris) 2, 29, IAEA Vienna

SUB-THERMAL FISSION CROSS-SECTION MEASUREMENTS

C. WAGEMANS
Centre d'étude de l'énergie nucléaire,
Mol
and
Nuclear Physics Laboratory,
Gent,
Belgium

A.J. DERUYTTER
Central Bureau for Nuclear Measurements,
Joint Research Centre,
Commission of the European Communities,
Geel

Abstract

Accurate new neutron induced cross-section data in the sub-thermal energy region were requested recently by reactor physicists. To fulfill these requests, a liquid nitrogen cooled methane moderator was installed at GELINA, resulting in a five times increased neutron flux below 20 meV.

Preliminary measurements of the $^{235}U(n,f)$ cross-section in the meV-region and the influence of the cross-section shape on the Westcott g_f-factor are discussed.

1. Introduction

A need for new neutron induced cross-section data in the sub-thermal energy region became recently apparent, especially for ^{238}U and ^{235}U (1). This was due to the fact that the uncertainty in the shapes of σ_f and η of ^{235}U and σ_c of ^{238}U in the meV neutron energy region have a strong impact on the uncertainty of the temperature coefficient of thermal reactors. To fulfill these requests from the reactor physicists formulated in ref. 1, a liquid nitrogen cooled methane moderator has been installed at GELINA, in order to obtain for that group of projected experiments a strong increase of the neutron flux below 20 meV.

In the present paper, preliminary measurements of the $^{235}U(n,f)$ cross-section in the meV-region will be discussed. In view of the theme of this session of the meeting, special attention will be given to the influence of these data on the Westcott g_f-factor.

2. Experimental conditions and results

In 'normal' experimental conditions, the neutrons produced in the uranium target of GELINA are moderated in a water-beryllium or in a 4 cm thick polyethylene moderator. These moderators are optimized for measurements using resonance or keV-neutrons. In order to allow the planning for the σ_f-measurements with sub-thermal neutrons, a 'pilot experiment' was performed using a 12 cm thick polyethylene moderator. This resulted in a gain in neutron flux of 50% in the meV region compared to a 4 cm thick moderator. GELINA was operated at a 25 Hz repetition frequency with 2 μs burst widths. A 25 $\mu g/cm^2$ thick ^6LiF-layer was mounted back-to-back with a 100 $\mu g/cm^2$ thick $^{235}UF_4$ layer. For the final measurements, a thinner uranium layer will be used to avoid self-absorption effects. The $^6Li(n,\alpha)t$-particles and the fission fragments were detected with two 20 cm^2 large surface barrier detectors. After correction for background, the (n,f) and the α+t counting-rates were divided, which, under the assumption of a 1/v-shape for the $^6Li(n,\alpha)t$ cross-section, yielded the ^{235}U $\sigma_f(E)\sqrt{E}$ shape. This curve was normalized to the absolute σ_f-data of Deruytter et al. (2) via the integral $\int_{0.0206\ eV}^{0.06239\ eV} \sigma_f(E)dE = (19.26 \pm 0.08)$ barn.eV. These preliminary results are shown in fig. 1 (o), together with the data points of Deruytter et al. (2) (+). Obviously, both data sets agree in the neutron energy region from 10 to 200 meV. Below 10 meV they slightly diverge, which might be due to self-absorption effects in the layers.

Through this 'pilot experiment' it became clear that the requested accuracy of 1% on the σ_f-shape could only be realized after a substantial increase of the neutron flux in the meV-region. According to the formula for the Maxwell distribution, such an increase could be obtained by decreasing the temperature of the moderator. For various reasons, a liquid methane moderator (cooled with liquid nitrogen at 77 K) was preferred at GELINA. The technical characteristics of this moderator are given by J.M. Salomé (3). The neutron flux distribution obtained with this moderator is shown in fig. 2, in which also the corresponding

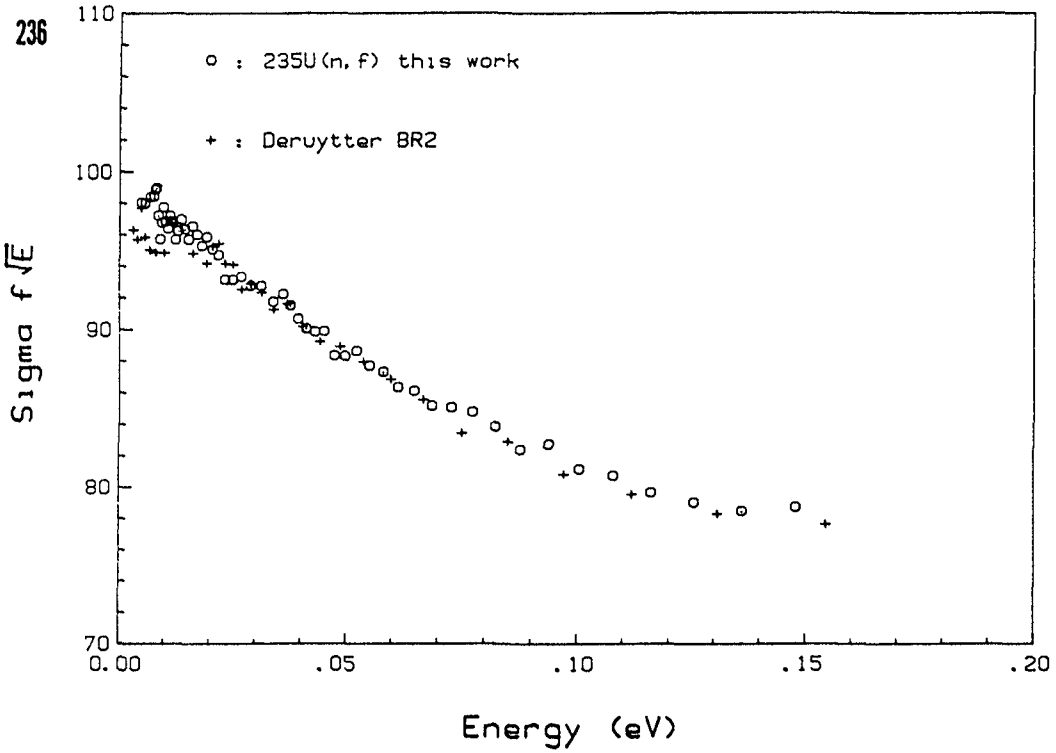

Fig. 1 : Preliminary results for $\sigma_f(E)\sqrt{E}$ from 5 to 200 meV(o) compared to the corresponding data of Deruytter et al. (2) (+).

distribution obtained with a water-beryllium moderator at room temperature is given. Obviously, the cold moderator yields about five times more neutrons below 20 meV than the moderator at room temperature.

Under these conditions, more accurate cross-section measurements with sub-thermal neutrons become feasable and will be started shortly.

3. Discussion

The fission cross-section data below 20 meV contribute with about 25% to the value of the Westcott g_f-factor (at 20.44°C). This strong influence of the

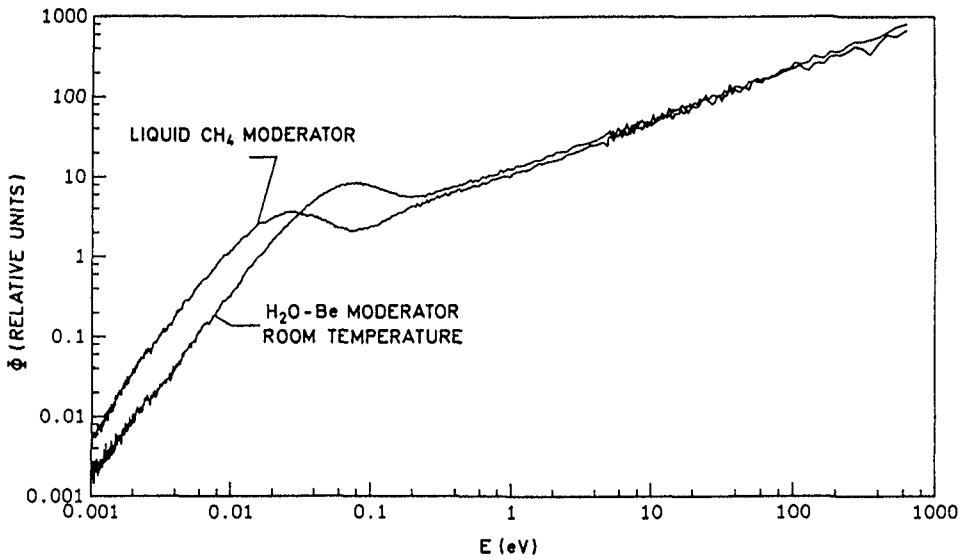

Fig. 2 : Neutron flux distributions obtained under identical experimental conditions with the nitrogen cooled liquid methane moderator and with the water-beryllium moderator at room temperature.

low-energy σ_f-data on g_f can easily be seen from the following relation, which gives the explicit temperature dependence of g_f :

$$g_f(T) = \frac{2}{\sigma_f^{\circ}\sqrt{\pi E_o}\,(kT)^{3/2}} \int_0^{\infty} \exp[-E/kT]\sqrt{E}\;\sigma_f(E)\sqrt{E}\,dE$$

Here k is the Boltzmann constant, T the absolute temperature and E_o = 0.025298 eV.

How well-known is σ_f in the neutron energy region below 20 meV ? If we scrutinize the literature, the number of experiments is rather limited and a substantial part of them were performed before 1960. Moreover, some of the data sets reveal structures due to crystalline effects (e.g. Bragg scattering).

The experimental situation up to 1969 is summarized in a report by Westcott (4), demonstrating a large scatter of data points in the $\sigma_f(E)\sqrt{E}$ versus E curves in the meV-region. Nevertheless, a g_f-factor with a (one standard deviation)

accuracy of 0.155% was calculated from these data. Later on, only few new experimental results became avaliable. Deruytter et al. (2) and Berceanu et al. (5) performed absolute σ_f-measurements at a thermal reactor beam with a slow chopper.

A few linac experiments (e.g. refs. 6-9) yielded σ_f-data points below 20 meV, without, however, being optimized for measurements at such low energies, Several other evaluation and status reports were made later on by Lemmel (10), Leonard et al. (11), Stehn et al. (12) and Divadeenam & Stehn (13). Their evaluated values for g_f are summarized in Table 1. This table is completed with two g_f-calculations performed by Deruytter et al. (2,6) and Gwin (14), based on σ_f-measurements made by these authors. Within the errors quoted, all these values are in agreement. Nevertheless, there are several reasons for not being completely satisfied: (1) the evaluated values are to a large extend based on the same data sets, treated in a more or less different way (2) in all cases analytical extrapolations of $\sigma_f(E)\sqrt{E}$ towards zero energy were performed based on fits to rather scattering $\sigma_f(E)\sqrt{E}$-data at very low energies. In this region however the cross-section shape is possibly influenced by one or more negative energy resonances near zero energy.

Table 1 Westcott g_f-factors at 20.44°C for ^{235}U

Reference	Year	g_f	Comment
Westcott (4)	1969	0.977 ± 0.00151	evaluation
Lemmel (10)	1975	0.9758 ± 0.002	"
Leonard et al. (11)	1976	0.9775 ± 0.0011	"
Stehn et al. (12)	1982	0.9771 ± 0.0010	"
Divadeenam & Stehn (13)	1984	0.9761 ± 0.0012	"
Deruytter et al. (2,6)	1971	0.978 ± 0.001	experimental*
Gwin (14)	1976	0.977 ± 0.002	"

* this means that g_f has been calculated by the authors mentioned based on their own σ_f-data.

In this respect, we want to investigate the suggestion of Erradi (15), who shifted the first strong negative ^{235}U neutron resonance to - 0.85 eV and who introduced a small (mainly capture) resonance at - 0.01 eV. These changes are compatible with the experimental data, although at the limits of the experimental uncertainties. This hypothesis results in a strong modification of the shape of η below 20 meV.

From a recent integral experiment performed at Chalk River, Jones et al. (16) conclude that the ENDF-B V data describe the $^{235}U(n,f)$ cross-section shape satisfactorily. We believe however that a differential cross-section measurement is the more unambiguous way to obtain information on this cross-section shape.

4. Conclusions

The uncertainty on the shape of the $^{235}U(n,f)$ cross-section below 10 meV has an influence on the shape of η and on the value of g_f. The installation of a nitrogen cooled liquid methane moderator at GELINA provides an excellent tool to improve our knowledge of the sub-thermal $^{235}U(n,f)$ cross-section shape.

Acknowledgements

Mr. R. Barthélémy and Mr. J. Van Gils are acknowledged for their help during the experiments and their analysis. Thanks are due to Mr. J.M. Salomé and his crew for their collaboration during the various test measurements preceding this paper.

REFERENCES

(1) J. BOUCHARD, C. GOLINELLI, H. TELLIER, Proc. Int. Conf. on Nuclear Data for Science and Techn., Antwerp (Belgium) 1982, 21

(2) A.J. DERUYTTER, J. SPAEPEN, P. PELFER, J. Nucl. En. 27 (1973) 645

(3) J.M. SALOME, internal report

(4) C. WESTCOTT, AECL-3255 (1969)

(5) I. BERCEANU et al., Rev. Roum. Phys. 23 (1978) 867

(6) A.J. DERUYTTER and C. WAGEMANS, J. Nucl. En. 25 (1971) 263

(7) C. WAGEMANS and A.J. DERUYTTER, this conference

(8) R. GWIN, E. SILVER, R. INGLE, H. WEAVER, Nucl. Sci. Eng. 59 (1976) 79

(9) R. GWIN, R. SPENCER, R. INGLE, J. TODD, S. SCOLES, Nucl. Sci. Eng. 88 (1984) 37

(10) H. LEMMEL, Proc. Conf. on Nuclear Cross-Sections and Techn., Washington DC, (U.S.A.) 1975, NBS-SP 425, 1, 286

(11) B. LEONARD, D. KOTTWITZ, J. THOMPSON, EPRI-NP-1763 (1976)

(12) J. STEHN, M. DIVADEENAM, N. HOLDEN, Proc. Int. Conf. on Nuclear Data for Science and Techn., Antwerp (Belgium) 1982, 685

(13) M. DIVADEENAM and J. STEHN, BNL 34211 (1984)

(14) R. GWIN, Nucl. Sci. Eng. 61 (1976) 1

(15) L. ERRADI, Dr. Sc. Thesis, Paris (Orsay) 1982

(16) R. JONES, G. DONCASTER, A. OKAZAKI, NEANDC (Can)-53 L (1984) 3

A LEAST SQUARES FIT OF THERMAL DATA FOR FISSILE NUCLEI

M. DIVADEENAM, J.R. STEHN
National Nuclear Data Center,
Brookhaven National Laboratory,
Upton, New York,
United States of America

Abstract

Recently we published a paper (Annals of Nuclear Energy, 11, 375, 1984) on the least-squares analysis of thermal constants for fissile nuclei U-233, U-235, Pu-239 and Pu-241. Since this work was completed some new information has become available. These are:

1. Recently published nu-prompt ratios of the four fissile nuclei by Gwin et al.
2. Hardy's analysis of Gwin-Magnuson critical assembly results.
3. Gwin's analysis of the same experimental results.
4. Axton and Bardell's finalized result for the Cf-252 nu-bar total value.

We have investigated the effect of including the new results in our least-squares study. The following observations result from the least-squares analysis:

- Gwin's nu-prompt ratios had an appreciable effect on the nu-bar for Pu-241, raising its value 0.3 percent and reducing its uncertainty.
- Hardy's new analysis of the critical assemblies had a lesser effect but did increase the U-233 capture cross section by 0.2 percent.
- The result of including the new input data produces a set of parameters each of which differs from what we published earlier this year by less than their uncertaintites assigned to them.

This work was supported by the U.S. Department of Energy.

Since the paper of the above title was written[1], we have learned of one new set of measurements that would have been included had we known of it: Gwin, Spencer and Ingle's measurement of the nu-prompt ratios of the four fissile materials with respect to ^{252}Cf. Their recently published paper[2] reports revised final results for ^{233}U, ^{235}U and ^{239}Pu and includes a measurement on $\bar{\nu}_p(241)/\bar{\nu}_p(252)$ that was not attempted previously. In some of the fitted results reported here, we have replaced their earlier 1978/1981 values by the final 1984 set[2]. The replacement has appreciable effect on some of the parameters.

	$\frac{\bar{\nu}_p(233)}{\bar{\nu}_p(252)}$	$\frac{\bar{\nu}_p(235)}{\bar{\nu}_p(252)}$	$\frac{\bar{\nu}_p(239)}{\bar{\nu}_p(252)}$	$\frac{\bar{\nu}_p(241)}{\bar{\nu}_p(252)}$
83 Fit	0.6615±0.0010	0.6407±0.0008	0.7636±0.0016	0.7771+0.0018
78/81	0.6630±0.0020	0.6441±0.0019	0.7650±0.0030	----
1984	0.6597±0.0018	0.6443±0.0014	0.7655±0.0014	0.7820±0.0018

Another revised value that we have used here is Axton's 1984 revision[4] (3.7509±0.0107) of his 1982 ^{252}Cf $\bar{\nu}_p$ value (3.744±0.021). The effect of including the revised result is not appreciable.

Ever since the 1962 critical experiments of Gwin and Magnuson[5] on spherical and cylindrical volumes of uranyl nitrate (both ^{233}U and ^{235}U), their interpretation has been a quandary. The approximations used by the authors have changed with time; each has separately proposed different approaches[6,7,8]. Reactor theorists Ullo and Hardy[9] have made a thorough study with a multigroup code and using the best set of cross-sections available at the time (ENDF/B-IV). Hardy[10] recently has further analyzed their calculation to bring out the best approximation to 2200 m/sec cross sections and he has used a more recently evaluated[11] hydrogen cross section value. We have made separate fits both with Gwin's and with Hardy's latest suggested parameters. Gwin's 1984 interpretation gives results slightly different from our previous paper, but Hardy's results cause appreciable changes (see below) in some of the parameters.

	Input			Output		
Parameter	1983 Fit[1]	Gwin[8]	Hardy[10]	1983 Fit	Gwin	Hardy
$(\eta_3-1)\sigma_a(3)$	740.4±8.6	741.4±5.0	744.7±4.0	738.4±2.4	739.1±2.3	741.0±2.1
$(\eta_5-1)\sigma_a(5)$	724.1±10.0	712.0±4.0	722.7±3.9	712.7±2.1	712.2±2.0	715.3±2.0

To show the greatest possible effect of the new data and the new interpretations, we used only Hardy's interpretation of the critical assembly results. The net result of using the three new inputs[2,4,10] is seen in Table 1, which is Table 36 of our Annals of Nuclear Energy paper with the changes Δ indicated for each quantity in an additional column for each nucleus.

Table 1

Least-Squares fit of 2200 m/sec Constants
A comparison of the 1983 Fit and the present fit

Quantity	^{233}U	Δ	^{235}U	Δ	^{239}Pu	Δ	^{241}Pu	Δ
σ_s(b)	12.6±0.3	-0.0	14.0±0.5	-0.1	7.3±0.4	-0.0	9.1±1.0	-0.0
σ_a(b)	574.7±1.0	+0.4	680.9±1.1	+0.5	1017.3±2.9	+0.7	1369.4±7.7	+1.6
σ_f(b)	529.1±1.2	+0.5	582.6±1.1	+0.3	748.1±2.0	+0.1	1011.1±6.2	-1.4
σ_γ(b)	45.5±0.7	-0.1	98.3±0.8	+0.3	269.3±2.2	+0.6	358.2±5.1	+2.9
g_a	0.9996±0.0011	+0.0002	0.9788±0.0008	+0.0000	1.0784±0.0024	-0.0001	1.0442±0.0020	-0.0001
g_f	0.9955±0.0015	+0.0002	0.9761±0.0012	+0.0005	1.0558±0.0023	+0.0003	1.0440±0.0049	+0.0015
η	2.2957±0.0040	+0.0002	2.0751±0.0033	+0.0024	2.1153±0.0052	+0.0017	2.1686±0.0080	+0.0014
α	0.0861±0.0015	-0.0002	0.1687±0.0015	+0.0004	0.3600±0.0032	+0.0007	0.3543±0.0057	+0.0034
$\bar{\nu}_t$	2.4933±0.0039	-0.0002	2.4251±0.0034	+0.0036	2.8768±0.0057	+0.0039	2.9369±0.0073	+0.0092

^{252}Cf $\bar{\nu}_t$ = 3.7675±0.0040 Δ=±0.0007

Of all the changes from the 1983 fit two of the changes Δ are greater than the corresponding uncertainty in the 1983 fit: $\bar{\nu}_t(235)$ and $\bar{\nu}_t(241)$. Gwin's higher value for $\bar{\nu}_p(241)/\bar{\nu}_p(252)$ when combined with the single other measured value resulted in a clear increase in $\bar{\nu}_t(241)$ to 2.9461±0.0056.

It is of interest that the statistical self-consistency of the fitting process was improved when the three new sets of values were included in the fit. As was stated on p. 395 of our paper, we had found the goodness-of-fit parameter, χ^2, to be only 85.8 for the 97 degrees of freedom available. We had observed that such a result might be taken to mean that the input errors had a tendency to be unduly large. With the present fit, however, χ^2=99.3 for the 98 degrees of freedom; and thus the input errors are just the right size. We had not sufficiently allowed for the breadth of the χ^2 distribution!

We are grateful to Dr. E. J. Axton for a table of his fitted values[12] that take into account both 2200 m/s and Maxwellian input data. His values are thus directly comparable with those of other evaluators, and we use them here in a repeat of the history of thermal constant evaluations. Tables 2-5 below are the same as Tables 30-34 of our paper except that Axton's newer values replace his 2200 m/s values.

The most striking aspect of the last columns of these tables, which show the range of variation among the various evaluations, is the 26%-34% range of scattering cross sections. This is in large part an artifact, despite considerable differences among the different evaluators. (We ourselves have produced the extrema in three of the four tables because we have chosen not to include data on the scattering of neutrons by atoms bound in crystalline structures). Nevertheless, σ_s appears in the fitting process only as a small subtractive quantity in the relation $\sigma_a=\sigma_t-\sigma_s$, which is the most direct way to calculate σ_a. Here it is the difference in barns, not in percent, that counts. These differences, not exceeding 4 barns, are less than 1% of σ_a. Ranges of up to 7% occur with σ_γ and with α, and those truly reflect the historic difficulties in measuring these two quantities. Other quantities appear to be agreed upon within about 1% by all evaluators. It is pleasing to see that the two most recent evaluations, Axton's and ours, agree very well.

The present work was supported by the U.S. Department of Energy.

Table 2

2200 m/s Thermal Constants for ^{233}U

Quantity	Westcott (1965)	Hanna (1965)	Steen (1972)	Lemmel (1975/82)	Axton (1984)	ENDF-V	Present (1983)	% Range (Max-Min)+ / Present
g_a	---	0.9965 ±0.0013	0.9990	1.0008 ±0.0018	0.9996 ±0.0011	0.9990	0.9996 ± 0.0011	0.4
g_f	---	0.9950 ±0.0021	0.9966	0.9967 ±0.0017	0.9952 ±0.0015	0.9966	0.9955 ± 0.0015	0.2
σ_s	---	10.7 ± 1.8	14.4 ± 4.3	13.3* ± 0.7	13.3* ± 0.9	12.6	12.6 ± 0.3	29.4
σ_a	576.3 ± 2.3	577.6 ± 1.8	571.0 ± 2.5	575.2 ± 1.3	575.1 ± 1.3	574.5	574.7 ± 1.0	1.1
σ_f	527.7 ± 2.1	530.6 ± 1.9	525.1 ± 2.4	529.9 ± 1.4	529.6 ± 1.4	528.7	529.1 ± 1.2	1.3
σ_γ	48.6 ± 1.5	47.0 ± 0.9	45.9 ± 0.2	45.3 ± 0.9	45.5 ± 0.7	45.8	45.5 ± 0.7	6.8
η	2.284 ±0.008	2.2844 ±0.0063	2.297 ±0.007	2.283 ±0.006	2.2979 ±0.0111	2.296	2.2957 ± 0.0040	0.6
α	0.0921 ±0.0029	0.0885 ±0.0018	0.0874 ±0.0005	0.086 ±0.002	0.0859 ±0.0015	0.0866	0.0866 ± 0.0015	7.1
$\bar{\nu}_t$	2.494 ±0.069	2.474 ±0.060	2.498 ±0.008	2.479 ±0.006	2.4952 ±0.0046	2.495	2.4933 ± 0.0039	0.8
$\bar{\nu}_t$ (252)	3.772 ±0.015	3.765 ±0.012	3.783 ±0.014	3.746 ±0.009	3.7656 ±0.0049	3.766	3.7675 ± 0.0040	1.0

+ - ENDF/B-V values were not considered in estimating the % range.

* - The σ_s corresponds to liquid sample values

Table 3

2200 m/s Thermal Constants for ^{235}U

Quantity	Westcott (1965)	Hanna (1969)	Leonard (1976)	Lemmel (1975/82)	Axton (1984)	ENDF-V	Present (1983)	% Range (Max-Min)+ / Present
g_a	---	0.9787 ±0.0010	0.9782	0.9797 ±0.0025	0.9787 ±0.0008	0.9781	0.9788 ±0.0008	0.2
g_f	---	0.9766 ±0.0016	0.9775 ±0.0011	0.9758 ±0.0014	0.9762 ±0.0012	0.9775	0.9761 ±0.0012	0.2
σ_s	---	17.6 ± 1.5	14.7	16.1* ± 1.1	16.4* ± 1.1	14.7	14.0 ± 0.5	25.7
σ_a	679.9 ± 2.3	678.5 ± 1.9	681.9	680.9 ± 1.7	681.2 ± 1.4	681.9	680.9 ± 1.1	0.5
σ_f	579.5 ± 2.0	580.2 ± 1.8	583.5 ± 1.7	583.5 ± 1.3	582.7 ± 1.2	583.5	582.6 ± 1.1	0.5
σ_γ	100.5 ± 1.4	98.3 ± 1.1	98.4 ± 0.8	97.4 ± 1.6	98.4 ± 0.8	98.4	98.3 ± 0.8	2.2
η	2.071 ±0.007	2.0719 ±0.0060	2.0713 ±0.0025	2.071 ±0.006	2.0794 ±0.0086	2.085	2.0751 ±0.0033	0.4
α	0.1734 ±0.0025	0.1694 ±0.0021	0.1686 ±0.0014	0.167 ±0.003	0.1689 ±0.0015	0.1686	0.1687 ±0.0015	2.8
$\bar{\nu}_t$	2.430 ±0.008	2.4229 ±0.0066	2.4205	2.416 ±0.005	2.4308 ±0.0040	2.437	2.4251 ±0.0034	0.6
$\bar{\nu}_t$ (252)	3.772 ±0.015	3.7653 ±0.0012	---	3.746 ±0.009	3.7656 ±0.0049	3.766	3.7675 ±0.0040	1.0

+ ENDF/B-V values were not considered in estimating the % range.

* The σ_s corresponds to liquid sample values

Table 4

2200 m/s Thermal Constants for ^{239}Pu

Quantity	Westcott (1965)	Hanna (1969)	Leonard (1981)	Lemmel (1975/82)	Axton (1984)	ENDF-V	Present (1983)	% Range (Max-Min)+ / Present
g_a	---	1.0752 ±0.0030	1.0762	1.0808 ±0.0039	1.0782 ±0.0024	1.0764	1.0784 ±0.0024	0.5
g_f	---	1.0548 ±0.0030	1.0535 ±0.0015	1.0555 ±0.0024	1.0562 ±0.0023	1.0582	1.0558 ±0.0023	0.3
σ_s	---	8.5 ±2.0	6.6 ±0.7	8.0* ±1.0	7.9* ±1.0	8.0	7.3 ±0.4	26.0
σ_a	1008.1 ± 4.9	1012.9 ± 4.1	1028.6 ± 5.1	1011.2 ± 4.1	1018.0 ± 3.0	1011.9	1017.3 ± 2.9	2.0
σ_f	742.4 ± 3.5	741.6 ± 3.1	754.8 ± 4.5	744.0 ± 2.5	747.8 ± 2.0	741.7	748.1 ± 2.0	1.8
σ_γ	265.7 ± 3.7	271.3 ± 2.6	273.8 ± 2.7	267.2 ± 3.3	270.2 ± 2.2	270.2	269.3 ± 2.2	3.0
η	2.114 ±0.010	2.1085 ±0.0066	2.1110 ±0.0081	2.106 ±0.007	2.1142 ±0.0118	2.119	2.1153 ±0.0052	0.4
α	0.3580 ±0.0054	0.3659 ±0.0039	0.3627 ±0.0043	0.359 ±0.005	0.3614 ±0.0031	0.3643	0.3600 ±0.0032	2.2
$\bar{\nu}_t$	2.871 ±0.0014	2.8799 ±0.0090	2.8766 ±0.0125	2.862 ±0.008	2.8781 ±0.0058	2.891	2.8768 ±0.0057	0.6
$\bar{\nu}_t$ (252)	3.772 ±0.015	3.765 ±0.012	---	3.746 ±0.009	3.7656 ±0.0049	3.766	3.7675 ±0.0040	0.7

+ ENDF/B-V values were not considered in estimating the % range.
* The σ_s corresponds to liquid sample values

Table 5

2200 m/s Thermal Constants for ^{241}Pu

Quantity	Westcott (1965)	Hanna (1969)	Leonard (1981)	Lemmel (1975/82)	Axton (1984)	ENDF-V	Present (1983)	% Range (Max-Min)+ / Present
g_a	---	1.0376 ±0.0014	---	1.0392 ±0.0028	1.0441 ±0.0019	1.043	1.0442 ±0.0020	0.6
g_f	---	1.0486 ±0.0053	---	1.0442 ±0.0048	1.0452 ±0.0049	1.0452	1.0440 ±0.0049	0.4
σ_s	---	12.0 ± 2.6	11.6	12.0* ± 2.6	12.2* ± 2.6	11.0	9.1 ±1.0	34.1
σ_a	1391 22	1375.4 ± 8.6	1368.5	1378 ±0.09	1371.8 ± 7.8	1376.4	1369.4 ± 7.7	1.6
σ_f	1009 9	1007.3 ± 7.2	1003.8	1015 ±0.07	1011.7 ± 6.2	1015.0	1011.1 ± 6.2	1.1
σ_γ	382 21	368.1 ± 7.8	364.7	267.2 ± 3.3	360.1 ± 4.6	361.4	358.2 ± 5.1	6.6
η	2.154 ±0.036	2.149 ±0.014	2.166	2.155 ±0.010	2.1684 ±0.0245	2.178	2.1686 ±0.0080	0.9
α	0.379 ±0.021	0.3654 ±0.0090	0.3633	0.357 ±0.007	0.3559 ±0.0051	0.3560	0.3543 ±0.0057	7.0
$\bar{\nu}_t$	2.969 ±0.023	2.934 ±0.012	2.9528	2.924 ±0.010	2.9402 ±0.0063	2.953	2.9369 ±0.0073	1.5
$\bar{\nu}_t$ (252)	3.772 ±0.015	3.765 ±0.012	---	3.746 ±0.009	3.7656 ±0.0049	3.766	3.7675 ±0.0040	1.0

+ ENDF/B-V values were not considered in estimating the % range.
* The σ_s corresponds to liquid sample values

References

1. Divadeenam, M., and Stehn, J. R. (1984), Ann. of Nucl. Energy, 11, 375.
2. Gwin, R., Spencer, R. R., and Ingle, R. W. (1984), Nucl. Sci. Engng. 87, 381.
3. Gwin, R. et al, (1978), ORNL/TM-6246; (1981), ORNL/TM-7988.
4. Axton, E. J. (1984), private communication, preprint submitted to Metrologia.
5. Gwin, R. and Magnuson, D. W. (1962), Nucl. Sci. Engng. 12, 364.
6. Magnuson, D.W. (1971), Nucl. Sci. and Engng. 44, 266.
7. Gwin, R., (1976), Nucl. Sci. and Engng. 61, 428.
8. Gwin, R., (1984), private communication.
9. Ullo, J.J. and Hardy, Jr., J. (1977), WAPD-TM-1299.
10. Hardy, Jr., J., (1984), private communication.
11. Muyhabyhab, S. F., Divadeenam, M. and Holden, N. E., (1981), Neutron Cross Sections: Vol. 1, Neutron Resonance Parameters and Thermal Cross Sections, Part A, Academic Press, N.Y.

SESSION VI

NUBAR FOR THE SPONTANEOUS FISSION OF ^{252}Cf*

J.W. BOLDEMAN, M.G. HINES
Lucas Heights Research Laboratories,
Australian Atomic Energy Commission Research Establishment,
Sutherland, New South Wales,
Australia

Abstract

A review is presented of all measurements of nubar ($\bar{\nu}$) for the spontaneous fission of ^{252}Cf. From this review it is clear that a definite discrepancy still exists between the most accurate liquid scintillator determination and the average of the $MnSO_4$ bath measurements. On the contrary, two other liquid scintillator measurements of $\bar{\nu}$ are consistent with the $MnSO_4$ bath average. One of these two is compared in detail with the most accurate liquid scintillator measurement in a search for a potential systematic erro. Any difference between them can only be attributed to the difference in the method of absolute calibration of the liquid scintillator tanks.

1. INTRODUCTION

The average number of neutrons emitted in the spontaneous fission of ^{252}Cf ($\bar{\nu}$ for total neutron emission, $\bar{\nu}_p$ for the prompt neutron emission) has been a standard for many years. Despite this status as a standard, there has been a long history of disagreement between the various experiments seeking to obtain values of high precision. The

* Research performed, in part, under contract with the Department of Foreign Affairs, Australia.

disagreement in the late sixties and early seventies was essentially a 2% discrepancy between the boron pile measurement[1] and the two liquid scintillator measurements of Hopkins and Diven[2] and Asplund-Nilsson et al.[3] The $MnSO_4$ bath measurements that had been completed at that time[4-6] tended to support the boron pile measurement. At the 1972 IAEA Panel on Neutron Standard Reference Data, a preliminary value from this laboratory[7], obtained using a large liquid scintillator tank, appeared to break the disagreement between the two types of measurements in that the value obtained lay between the two averages. Furthermore, it was apparent that some additional corrections which would reduce the measured values for the two earlier liquid scintillator measurements were required.

This apparent accord was purely ephemeral. All measurements that existed at that time have subsequently been revised. Two minor corrections were applied to our measurement[8,9] so that the final value was larger by 0.29%. From a re-analysis of the boron pile measurement, Ullo[10] recommended an increase in its value by 0.67%. In 1977, the two early liquid scintillator measurements were revised downwards slightly[10] and it was at about this time that Smith[11] began an extended investigation of the $MnSO_4$ bath technique which has led to a steady increase in the various values obtained using this technique.

Recently, Spencer et al.[12] have published a value of $\bar{\nu}$ for ^{252}Cf of very high precision - of the order of 0.2%. Their value, obtained using the liquid scintillator tank, was in reasonable agreement with a high precision $MnSO_4$ bath determination from Smith and Reeder[18] which was finalised at about the same time. Thus it was proposed in a recent review[13] that, since the most accurate of the liquid scintillator measurements was in reasonable agreement with the most accurate (at that time) $MnSO_4$ bath determination, the discrepancy had finally disappeared. The question to answer is, has the accord continued to the present day?

The definition of $\bar{\nu}$ for ^{252}Cf as a standard can be attributed to the distinct advantages this spontaneously fissioning source has over alternative isotopes. The use of ^{252}Cf as a standard source has been increasing in many physical applications in recent years. One application that is of considerable importance to our laboratory is in neutron coincidence counting which is a technique extensively used in safeguards non-destructive assay measurements. In a variation of this technique under development at this laboratory[14], a precision of at least 0.25% for $\bar{\nu}$ for ^{252}Cf is required.

2. STATUS OF $\bar{\nu}$ FOR ^{252}Cf

Table 1 lists all accurate measurements of $\bar{\nu}$ for the spontaneous fission of ^{252}Cf. Some recent modifications have been incorporated into the table. The two measurements from NPL, White and Axton (1968)[4] and Axton et al. (1969)[3] have been superseded by Axton and Bardell (1984)[15]. It has been assumed that the latest value from the group[16] at the V.G. Khlopin Radium Institute - Aleksandrov et al. (1980) - supersedes their earlier published value - Aleksandrov et al. (1975)[17]. The latest value from Smith and Reeder (1984)[18] is also listed.

The weighted mean of the $MnSO_4$ bath measurements is 3.7563±0.00062. This value is in agreement with the revised boron pile measurement and the recent measurement from Edwards et al.[21]. However, it is clearly

Table 1 $\bar{\nu}$ Values for Spontaneous Fission of ^{252}Cf

Experiment	Value	Weighted Mean of Group
Liquid Scintillator		
*Asplund-Nilsson et al. (1963)[3]	3.792±0.040	3.7754±0.0059 (with Spencer et al.)
*Hopkins and Diven (1963)[2]	3.777±0.031	
*Boldeman (1974)[8]	3.755±0.016	
Zhang and Liu (1980)[19]	3.754±0.018	3.7600±0.0107 (without Spencer et al.)
Spencer et al. (1982)[12]	3.782±0.007	
Manganese Bath		
White and Axton (1968)[4]	superseded	
Axton et al. (1969)[5]	superseded	
†De Volpi and Porges (1970)[6]	3.747±0.019	
Aleksandrov et al. (1975)[17]	superseded	3.7563±0.0062
Bozorgmanesh (1977)[20]	3.744±0.023	
Aleksandrov et al. (1980)[16]	3.758±0.015	
Smith and Reeder (1984)[18]	3.767±0.011	
Axton and Bardell (1984)[15]	3.7509±0.0107	
Boron Pile		
‡Colvin and Sowerby (1965)[1]	3.739±0.021	
Edwards et al. (1982)[21]	3.761±0.029	
Evaluation		
Axton (1984)[22]	3.7661∓0.0054	

*Revised by Boldeman (1977)[9]
†Revised by Smith (1977)[11]
‡Revised by Ullo (1977)[10]

in disagreement with the weighted average of all liquid scintillator measurements, namely, 3.7754±0.0059 even after provision is made within the two sets for common errors. The question that arises is whether this disagreement is one between the two techniques - liquid scintillator and $MnSO_4$ bath - or whether there is a more general disagreement. It should be noted that the two liquid scintillator measurements of Boldeman[8] and Zhang and Liu[19] are in agreement with the average of the $MnSO_4$ bath. In fact, there would appear to be a small discrepancy between Boldeman[8] and Spencer et al.[12] since the accuracy of the first measurement for comparison with the second reduces to 0.010. The difference between the two is almost three standard deviations.

3. COMPARISON OF TWO LIQUID SCINTILLATOR MEASUREMENTS

The principal details of the two liquid scintillator experiments of Spencer et al.[12] and Boldeman[8] are listed in Table 2. There is little in the difference between the two experiments to which a possible error could be attributed. The scintillator tank of Spencer et al. had several slight advantages over that used in our experiment - notably a higher efficiency for a higher bias setting. Furthermore, the geometry of the hole through the tank was slightly smaller. On the other hand, the calibration of the absolute efficiency of our scintillator had some advantages. The various corrections applied in each of the two measurements are listed in Table 3. As before, there is no obvious solution to the discrepancy in the list of corrections.

Table 2 Comparison of Experimental Details

	ORNL	LHRL
Tank volume	800 L	240 L
Photomultiplier tubes	12 x RCA 4522 1 bank	12 x EMI 9618A 3 banks (of 4 each)
Liquid scintillator	NE 224	NE 323
Per cent by weight Gd	0.22%	0.5%
Through tube	8.89 cm	7.5 cm
Neutron time constant	15 μs	11 μs
Gate length	80 μs	40 μs
Tank threshold	1 MeV and 3 MeV	0.48 MeV
Average efficiency for ^{252}Cf source neutrons	94.7% (3 MeV) 82.0% (1 MeV)	84.5%
Scintillator dead time	121 ns	78 ns
Delay to neutron scaler	750 ns	685 ns
Fission counter	|| plate ionisation chamber	|| plate ionisation chamber
Neutron calibration:		
Source neutrons	ORELA	3 MV Van de Graaff
Calibration detector	NE 213 plastic scintillator (pulse shape discriminator)	0-1 MeV surface barrier detector: hydrogen gas target 0.35-8.56 MeV surface barrier plus ΔE/Δx
Calculated response	Poitou and Signarbieux[23]	Clancy (unpublished) Ullo[24] Poitou & Signarbieux[23]

Table 3 Corrections to Liquid Scintillator Measurements and Uncertainties (%)

	Spencer et al. 1 MeV Threshold	Spencer et al. 3 MeV Threshold	Boldeman
Pileup correction	0.94±0.05	0.81±0.05	0.83±0.10
Reject correction	0.21±0.07	0.27±0.09	0.08±0.00
Off-centre correction	0.01±0.04	0.05±0.05	0.00±0.01
French effect	-0.04±0.02	-0.04±0.02	-0.10±0.10
Delayed γ-rays	-0.33±0.08	0.00	-0.28±0.07
Correction for ^{252}Cf	0.02±0.00	0.02±0.00	not considered
Uncertainty in $\bar{E}$ for fission spectrum	±0.04		±0.12
Accuracy of energy calibration	included elsewhere		±0.17
Estimated false zeros	+0.08 (maximum effect)		±0.02
Multiple scattering and proton escape in NE 213	-0.10		not applicable
Background error in proton recoil counter	not applicable		-0.33±0.10
Uncertainty in energies of calibrated neutrons	±0.02		included elsewhere
Tank asymmetry	±0.03		+0.05±0.05

Finally, the neutron emission probability distributions have been compared in Table 4. Here all the data have been renormalised to $\bar{\nu}_p$ = 3.757, the evaluated figure from Axton[22]. The exceptional agreement between the two sets of figures suggests that the neutron counting aspects of the two experiments are in agreement. In other words, this difference between the two experiments is probably related to the absolute calibration of the two scintillators. There is a need, therefore, for a new liquid scintillator measurement with a precision approaching that of Spencer et al. Since the precision of our systems could be improved to an accuracy of ±0.010 or better, a new absolute measurement has been started.

Table 4 Neutron Emission Parameters for Spontaneous Fission of ^{252}Cf

Experiment	Spencer et al.[12]	Spencer et al.[12]	Boldeman & Dalton[25]	Boldeman & Hines[26]		
No. of Fissions ($\times 10^6$)	21	13	20	8.7	8.4	6.8
Threshold	1 MeV	3 MeV	0.480 MeV	0.620 MeV	0.720 MeV	1.95 MeV
$\bar{\nu}_p$	3.757	3.757	3.757	3.757	3.757	3.757
P_0	0.00228±0.00007	0.00222±0.00019	0.00214±0.00008	0.00208±0.00012	0.00218±0.00012	0.00213±0.00014
P_1	0.02654±0.00129	0.02560±0.00090	0.02600±0.00025	0.02621±0.00037	0.02618±0.00038	0.02556±0.00043
P_2	0.12632±0.00138	0.12527±0.00125	0.1267 ±0.0005	0.1262 ±0.0008	0.1252 ±0.0008	0.1247 ±0.0009
P_3	0.27314±0.00107	0.27315±0.00106	0.2734 ±0.0008	0.2753 ±0.0012	0.2752 ±0.0012	0.2725 ±0.0014
P_4	0.30342±0.00048	0.30640±0.00065	0.3039 ±0.0010	0.3018 ±0.0015	0.3027 ±0.0015	0.3082 ±0.0017
P_5	0.18442±0.00055	0.18549±0.00087	0.1848 ±0.0007	0.1846 ±0.0010	0.1856 ±0.0010	0.1873 ±0.0012
P_6	0.06686±0.00035	0.06643±0.00053	0.0657 ±0.0006	0.0668 ±0.0009	0.0663 ±0.0009	0.0625 ±0.0011
P_7	0.01479±0.00012	0.01371±0.00018	0.0154 ±0.0003	0.0150 ±0.0005	0.0150 ±0.0005	0.0171 ±0.0010
P_8	0.00204±0.00003	0.00162±0.00005	0.0020 ±0.0002	0.0021 ±0.0003	0.0016 ±0.0003	0.0001 ±0.0001
P_9	0.00018±0.00001	0.00010±0.00002				
$\langle\nu^2\rangle_{av}$	15.73	15.70	15.724±0.007	15.727±0.010	15.711±0.010	15.685±0.011
$\sigma^2(\nu)$	1.6178	1.5840	1.608±0.003	1.611±0.005	1.599±0.005	1.569±0.005
R	0.8484 ±0.0001	0.8461 ±0.0002	0.8478 ±0.0005	0.8480 ±0.0008	0.8469 ±0.0008	0.8451 ±0.0009

$$\langle\nu^2\rangle_{av} = \sum \nu^2 P_\nu \qquad \sigma^2(\nu) = \sum P_\nu (\nu-\bar{\nu})^2 \qquad R = \frac{\langle\nu^2\rangle_{av} - \bar{\nu}}{(\bar{\nu})^2}$$

REFERENCES

1. D.M. Colvin and M.G. Sowerby (1965). Proc. IAEA Symp. Physics and Chemistry of Fission, Salzburg, Vol. 2, p. 25
2. J.C. Hopkins and B.C. Diven (1963). Nucl. Phys. 48, 433.
3. I. Asplund-Nilsson, H. Condé and N. Starfelt (1963). Nucl. Sci. Eng. 16, 124.
4. P.H. White and E.J. Axton (1968). J. Nucl. Energy 22, 73.
5. E.J. Axton, A.G. Bardell and B.N. Aubric (1969). J. Nucl. Energy 23, 457.
6. A. De Volpi and K.G. Porges (1970). Phys. Rev. C1, 683.
7. J.W. Boldeman (1972). Proc. IAEA Panel on Neutron Standard Reference Data, Vienna, p. 291.
8. J.W. Boldeman (1974). Nucl. Sci. Eng. 55, 188.
9. J.W. Boldeman (1977). NBS Special Publication 493, 182.
10. J.J. Ullo (1977). Proc. ^{252}Cf Workshop, Brookhaven National Laboratory, 6 Dec.
11. J.R. Smith (1977). Proc. ^{252}Cf Workshop, Brookhaven National Laboratory, 6 Dec.
12. R.R. Spencer, R. Gwin and R. Ingle (1982). Nucl. Sci. Eng. 80, 603.
13. W.P. Poenitz and G. de Saussure (1984). Prog. in Nucl. Energy 13, 129.
14. J.W. Boldeman, M.G. Hines, J.P. Fallon and I. Delaney (1984). Proc. 6th ESARDA Symp. Safeguards and Nuclear Materials Management, Venice, p. 285.
15. E.J. Axton and A.G. Bardell (1984). Paper submitted to Metrologia.
16. B.M. Aleksandrov, E.V. Korolev, Ya. M. Kramarovskij, G.E. Lozhkomoev, V.G. Matyukhanov, K.A. Petrzhak, A.G. Prusakov, A.V. Sorokina and Eh. A. Shlyamin (1980). Proc. 1980 Kiev Conf., Vol. 4, p. 119.
17. B.M. Aleksandrov, L.M. Belov, L.V. Drapchinskij, Ya. M. Kramarovskij, Gr. E. Lozhkomoev, V.G. Matyukhanov, K.A. Petrzhak, A.G. Prusakov, A.V. Sorokina, Eh. A. Shlyamin, O.A. Migun'kov, G.M. Stukov, V.T. Schchebolev and I.A. Yaritsyna (1975). Proc. 1975 Kiev Conference, Vol. 5, p. 166.
18. J.R. Smith and S.D. Reeder (1984). EPRI-NP-3436.
19. H.Q. Zhang and Z.H. Liu (1980). Chin. J. Nucl. Phys. 2, 29.
20. H. Bozorgmanesh (1977). Thesis, University of Michegan.
21. G. Edwards, D.J.S. Findlay and E.W. Lees (1982). Ann. Nucl. Energy 9, 127.
22. E.J. Axton (1984). European Appl. Res. Rept.-Nucl. Sci. Technol. 5, 609.
23. J. Poitou and C. Signarbieux (1974). Nucl. Instrum. and Meth. 114, 113.
24. J.J. Ullo (1976). WAPD-TM-1232.
25. J.W. Boldeman and A.W. Dalton (1967). Australian Atomic Energy Commission report E/172.
26. J.W. Boldeman and M.G. Hines (1984) - Paper submitted to Nucl. Sci. Eng.

248 A RE-EVALUATION OF THE AVERAGE PROMPT NEUTRON EMISSION MULTIPLICITY (NUBAR) VALUES FROM FISSION OF URANIUM AND TRANSURANIUM NUCLIDES

N.E. HOLDEN, M.S. ZUCKER
Brookhaven National Laboratory,
Upton, New York,
United States of America

Abstract

In response to a need of the safeguards community, we have begun an evaluation effort to upgrade the recommended values of the prompt neutron emission multiplicity distribution, P_ν and its average value, nubar. This paper will report on progress achieved thus far. The evaluation of the uranium, plutonium, americium and curium nuclide's nubar values will be presented. The recommended values will be given and discussed.

I. Introduction

The neutron emission multiplicity distribution, P_ν is the probability that a given fission will result in the emission of ν neutrons. The basic method used by all experimenters to generate P_ν data involves a way of detecting each fission as it occurs in a sample of the nuclide under study and correlates this fission with the detection of the emitted neutrons. Since the efficiency, ε, of the neutron detector for the detection of a single neutron is less than unity, allowance for those neutrons emitted but not detected must be made, with the resulting probability Q_n of actually observing n neutrons even if ν were emitted ($n < \nu$) being just:

$$Q_n = \Sigma\, P_\nu\, [\nu!/n!(\nu-n)!]\, \varepsilon^n\, (1-\varepsilon)^{\nu-n} \qquad (1)$$

The P_ν are constants of nature, whereas the Q_n depend on the efficiency of the particular detector used. From the above expression it follows directly that P_ν is given in terms of the observed relative frequencies of observation Q_n by the expression:

$$P_\nu = \Sigma\, Q_n\, [n!/\nu!(n-\nu)!]\, \varepsilon^{-n}\, (\varepsilon-1)^{n-\nu} \qquad (2)$$

Knowledge of the detector efficiency which is essential to relate the observed frequencies Q_n, to the multiplicities, P_ν, is usually determined from the count rate with a calibrating nuclide, whose nubar value is well known.

$$g = \varepsilon\, \langle\nu\rangle\, q \qquad (3)$$

where q is the fission rate of the sample of the calibrating nuclide and g is the gross count rate for the calibrating nuclide. (The efficiency is thus inversely related to the assumed value of $\langle\nu\rangle$.) This is possible because $\langle\nu\rangle$ can be determined independently of the determination of P_ν and with greater accuracy than if it were calculated from the P_ν distribution using

$$\langle\nu\rangle = \Sigma\, \nu\, P_\nu. \qquad (4)$$

In deriving the $\langle\nu\rangle$ values for the various nuclides, one standard value is assumed, for ^{252}Cf. From an earlier evaluation[1], a value of $\langle\nu\rangle = 3.757 \pm 0.010$ neut/fiss is derived.

In the following sections, we will review the direct determination of $\langle\nu\rangle$ values and then describe the method of comparing different sets of P_ν values.

II The Fissile Nuclides, ^{233}U, ^{235}U, ^{239}Pu and ^{241}Pu.

Of the various nubar values that have been determined, those for the fission via thermal neutrons of the four fissile elements have a special importance because of the thermal reactor program. They are important parameters in the least squares fit that determines the various neutron cross sections of these nuclides needed for reactor operation.

The most careful experiments on nubar have been those which compared the thermal neutron fission value for the fissile nuclide with the nubar value for spontaneous fission of ^{252}Cf. Table I lists the various experimental results for prompt nubar of ^{233}U to that of ^{252}Cf, while Tables II, III, and IV list similar results for ^{235}U, ^{239}Pu and ^{241}Pu, respectively. The reported values are listed along with the revised values based on an evaluation of each experiment.

Some general comments can be made about these Tables. Corrections were made for the effect of delayed gamma-rays, the effect of the different mean energies for the various fission neutron spectra involved, and for the loss of those events corresponding to fission fragments of low energy because of the thickness of the fission foil. Low kinetic energy fission fragments correspond to the release of higher numbers of neutrons and therefore thick foils depress the nubar value as a result.

The delayed gamma-ray effect was taken from Boldeman's 1977 review[2] without change. The mean energies of the fission spectrum were also taken from the same review except for ^{252}Cf, which came from the 1979 measurement of Boldeman[3]. However, the uncertainty included 50% for the shape of the efficiency curve and an additional uncertainty corresponding to the spread between the energy differences used in this calculation and the energy differences measured by Smith[4].

For some of the measurements, the ratios were determined for a neutron in the kev energy range and extrapolated back to a thermal value using a curve with a constant slope, which had been fit between the value at thermal energies and the value at 2 Mev. However, it is not clear that application of this constant slope is appropriate at 30-60 kev energy range. In fact, data from Gwin[5] and Prokhorova[6] would imply that the ratio ($\langle\nu\rangle$-^{235}U/$\langle\nu\rangle$-^{252}Cf) is slightly smaller in the 50-100 kev energy region than at thermal neutron energies. It is clear that in the region 0.5 - 1.0 Mev, the ratio is definitely larger. Until we can better evaluate this effect, we felt that our choice was either to discard these measurements or to assume that the 30 - 60 kev ratio was equivalent to the thermal value. We have chosen the latter assumption in this paper but have added the effect of the constant slope assumption as an uncertainty rather than as a correction.

For the foil thickness correction, we used three estimates: Gwin[7] - for Gwin's measurement, Malinovskii[8] - for the Obninsk measurements and Boldeman[9] - for all other measurements. Although we would agree with Gwin that the foil thickness corrections should preferably be determined for the exact geometrical arrangements of each experiment, when this is not yet available, we prefer to apply some correction rather than no correction at all for this effect. We have assumed a 50% uncertainty on this correction.

III Method of Comparing Different P_ν Sets.

The Q_n and P_ν can be considered vectors, whose components are probabilities, related by an operation and its inverse which converts one set of probabilities into the other, i.e. equation (1) and (2). Certain ratios composed of specific functions of the various moments of the distributions are independent of the efficiency, e.g. $\langle\nu(\nu-1)....(\nu-k)\rangle / \langle\nu\rangle^{k+1} = \langle n(n-1)..(n-k)\rangle / \langle n\rangle^{k+1}$. A particular case is Diven's parameter, for k = 1, $\langle\nu(\nu-1)\rangle / \langle\nu\rangle^2$, which can be considered as a measure of the shape of the P_ν distribution. However, another indicator of the distribution's shape, which is not conserved, (independent of ε) is the ratio of the mean square deviation to the square of the mean : $\langle(\nu-\langle\nu\rangle)^2\rangle / \langle\nu\rangle^2 = (\langle\nu^2\rangle - \langle\nu\rangle^2) / \langle\nu\rangle^2$.

For each given experiment, the equations (1) and (2) were used with the quoted distribution P_ν and the reported efficiency ε to derive the original Q_n set. The efficiency was then varied until the calculated $\langle\nu\rangle$ ($\Sigma\, \nu\, P_\nu$) value was obtained corresponding to the recommended value. In those few cases where the experimentalist did not report the efficiency, a reasonable value was assumed appropriate to the experimental conditions and then the above procedure was also followed.

After various sets of P_ν for the same nuclide are transformed so that each set yields the same $\langle\nu\rangle$, any remaining differences between the corresponding P_ν can be ascribed to systematic errors other than those in ε or $\langle\nu\rangle$, or to random errors (e g counting statistics) in the respective experiments. Evaluation of the standard deviation of corresponding values of P_ν gives a realistic estimate of the uncertainty involved in determining the P_ν Our earlier work[10] contains more details on the method

IV Recommendations and Discussion

The recommended values for $\langle\nu\rangle$ and P_ν for the various nuclides of uranium, plutonium, americium and curium are given in the Tables in section VII. The special importance of the $\langle\nu\rangle$ values for the fissile nuclides was mentioned earlier in this paper Additional work is planned to investigate the $d\nu/dE$ variation and the mean energy difference between the various fission neutron spectra and their effects on the reported results In this first study, it is not clear whether the recommended uncertainties in the $\langle\nu\rangle$ ratios, 0 16%-0 18%, are underestimated because of correlations This possibility will also be investigated later.

V Acknowledgements

The authors acknowledge helpful discussions with Mulki Bhat (BNL), Reg Gwin (ORNL), Joe Halperin (ORNL), Bob Howe (LRL) and Alan Smith (ANL) In addition, John Boldeman s release of a recent revision of his data prior to publication for our use is greatly appreciated

VI References

1 N E Holden and M S Zucker Proc ANS/INMM Topical Meeting on Safeguards and Technology Hilton Head S C , Nov 28-Dec 2 1983 Trans Amer Nucl Soc 45, suppl 1, 23 (1983)
2 J W Boldeman Proc Int Specialist s Symp on Neut Standards and Appl Gaithersberg, Md , Mar 28-31 1977 NBS Spec Pub 493, 182 (1977)
3 J W Boldeman D Culley and R J Crawley, Trans Amer Nucl Soc 32, 735 (1979)
4 A B Smith, P Guenther, G Winkler and R McKnight, Nucl Sci Eng 76, 357 (1980)
5 R Gwin et al , ORNL-TM-7148 (1980)
6 L I Prokhorova et al , Sov Atom Energy 30, 307 (1971)
7 R Gwin R R Spencer and R W Ingle, Nucl Sci Eng 87, 381 (1984)
8 V V Malinovskii et al , Sov Atom Energy 55, 501 (1984)
9 J W Boldeman and J Prehaut, Nucl Sci Eng 76, 49 (1980)
10 M S Zucker and N E Holden, Proc 6th ESARDA Symp on Safeguards and Nucl Material Management Venice, Italy, May 14-18 1984 p 341
11 B Nurpeisov et al , Sov Atom Energy 34 603 (1973)
12 J W Boldeman and A W Dalton AAEC/E-172 (1967)
13 S C Fultz et al Phys Rev 152 1046 (1966)
14 D W Colvin and M G Sowerby, Proc Symp on Phys Chem of Fission Salzburg Austria Mar 22-26 1965 Vol 2 25 (1965)
15 D S Mather, P Fieldhouse and A Moat, Nucl Phys 66, 149 (1965)
16 J C Hopkins and B C Diven Nucl Phys 48 433 (1963)
17 A DeVolpi and K G Porges Proc Int Conf on Nucl Data for Reactors Paris France Oct 17-21 1966 Vol 2 297 (1967)
18 H Conde, Ark Fys 29, 293 (1965)
19 D S Mather, P Fieldhouse and A Moat, Phys Rev 133, 1403 (1964)
20 J W Meadows and J F Whalen, Phys Rev 162, 197 (1962)
21 K E Bolodin et al , Sov Atom Energy 33, 1045 (1973).
22 M Divadeenam and J R Stehn, Ann Nucl Energy 11, 375 (1984)
23 E J Axton, Eur Appl Res Rep - Nucl Sci Technol Sect 5, 609 (1984)
24 J R Stehn, M Divadeenam and N E Holden, Int Conf on Nucl Data for Sci Technol Antwerp Belgium, Sept 6-10,1982
25 A H Jaffey and J L Lerner, Nucl Phys A145, 1 (1970)
26 S N Belenky, M D Skorokhvatov and A V Etenko, Sov Atom Energy 55, 528 (1983)
27 H Conde and M Holmberg, J Nucl Energy 25, 331 (1971)
28 A G Popeko et al , Sov J Nucl Phys 24, 245 (1976)
29 S N Hwang et al , Acta Phys Sinica 23, 46 (1974)
30 I Asplund-Nilsson et al , Nucl Sci Eng 15, 213 (1963)
31 R Sher and J Leroy, J Nucl Energy 12, 101 (1960)
32 B D Kuz minov et al , Sov Phys JETP 37, 290 (1960)
33 K W Geiger and D C Rose, Can J Phys 32, 498 (1954)
34 D A Hicks, J Ise,Jr and R V Pyle, Phys Rev 101, 1016 (1956)
35 C J Orth, Nucl Sci Eng 43, 54 (1971)
36 J W Boldeman, priv comm Oct 1984
37 H Zhang, Z Liu, S Ding and S Liu, Nucl Sci Eng 86, 315 (1984)
38 J Prehaut, G Mosinski, R Bois and M Soleilhac, CEA-R-4626 (1974)
39 H Zhang and Z H Liu, Chin J Nucl Phys 1, 9 (1972).
40 E Baron, J Prehaut, F Ouvry and M Soleilhac, Proc Int Conf Nucl Data for Reactors Paris, France, Oct 17-21,1966 Vol 2, 57 (1967)
41 B C Diven and J C Hopkins, Proc Sem Phys of Fast and Intermediate Reactors Vienna,Austria, Aug 3-11,1961 Vol 1, 111 (1962)
42 A Moat, D S Mather and M H McTaggert, J Nucl Energy 15, 102 (1961)
43 B C Diven, H C Martin, R F Taschek and J Terrell, Phys Rev 101, 1012 (1956)
44 G Edwards, D J S Findlay and E W Lees, Ann Nucl Energy 9, 127 (1982)
45 L Prokhorova, G N Smirenkin and Yu M Turchin, Sov Atom Energy 25, 1369 (1969)
46 V I Lebedev and V I Kalashnikova, Sov Atom Energy 5, 90 (1958)
47 J G Cuninghame, J Inorg Nucl Chem 4, 1 (1957)
48 R E Howe et al , Nucl Sci Eng 77, 454 (1981)
49 N I Kroshkin and Yu S Zamyatnin, Sov Atom Energy 29, 790 (1970)
50 J Halperin et al , Nucl Sci Eng 75, 56 (1980)
51 W W T Crane, G H Higgins and H R Bowman, Phys Rev 101, 1804 (1956)
52 K D Zhuraviev, Yu S Zamyatnin and N I Kroshkin, Nat Sov Conf on Neut Phys Kiev, USSR May 28-Jun 1,1973 Vol 4, 57 (1974)
53 R Schmidt and H Henschel, Nucl Phys A395, 29 (1983)
54 V V Golushko et al , Sov Atom Energy 34, 178 (1973)
55 L I Prokhorova et al , Sov Atom Energy 33, 875 (1973)
56 V I Bol shov L I Prokhorova, V N Okolovich and G N Smirenkin, Sov Atom Energy 17, 715 (1964)
57 R E Howe et al , Nucl Phys A407, 193 (1983)
58 R W Stoughton J Halperin, C E Bemis and H W Schmitt, Nucl Sci Eng 50, 169 (1973)
59 D M Dakovskii, Yu A Lazarev and Yu Ts Oganesyan, Sov J Nucl Phys 18, 371 (1974)
60 M C Thompson Phys Rev C2, 763 (1970)
61 J W Boldeman Nat Sov Conf on Neut Phys Kiev, USSR May 28-Jun 1 1973 Vol 4, 114 (1974)

VII Tabulated Results

Table 1 Measured Nubar ratios for $^{233}U/^{252}Cf$

Author (Year)	Ref No	Reported Ratio	Revised Ratio	Comment
Gwin(84)	7	0 6597 (0 0018)	0 6581 (0 0023)	
Nurpeisov(72)	11	0 6615 (0 0027)	0 6582 (0 0039)	
Boldeman(67)	12	0 6586 (0 0021)	0 6604 (0 0017)	
Fultz(66)	13	0 6720 (0 011)	0 6747 (0 0111)	Discarded-test value
Colvin(65)	14	0 6551 (0 0049)	0 6565 (0 0050)	
Mather(64)	15	0 6698 (0 0082)	0 6713 (0 0083)	
Hopkins(63)	16	0 6558 (0 0069)	0 6548 (0 0069)	

Table II Measured Nubar ratios for $^{235}U/^{252}Cf$

Author (Year)	Ref No	Reported Ratio	Revised Ratio	Comment
Gwin(84)	7	0 6443 (0 0014)	0 6438 (0 0015)	
Prokhorova(70)	6	0 6379 (0 0037)	0 6417 (0 0045)	
Boldeman(67)	12	0 6385 (0 0021)	0 6406 (0 0017)	
DeVolpi(66)	17	0 640 (0 011)	0 633 (0 027)	Discarded-discrepant data
Pultz(66)	*13*	*0 6429 (0 0212)*	*0 6451 (0 0213)*	*Discarded-test value*
Conde(65)	18	0 6400 (0 0053)	0 6433 (0 0055)	
Colvin(65)	14	0 6423 (0 0029)	0 6437 (0 0030)	
Mather(64)	19	0 6378 (0 0032)	0 6398 (0 0037)	
Hopkins(63)	16	0 6431 (0 0058)	0 6438 (0 0059)	
Meadows(61)	20	0 6449 (0 0104)	0 6412 (0 0092)	

Table III Measured Nubar ratios for $^{239}Pu/^{252}Cf$

Author (Year)	*Ref No*	*Reported Ratio*	*Revised Ratio*
Gwin(84)	7	0 7655 (0 0014)	0 7652 (0 0015)
Bolodin(73)	21	0 7679 (0 0040)	0 7666 (0 0076)
Boldeman(67)	12	0 7674 (0 0021)	0 7670 (0 0021)
Colvin(65)	14	0 7592 (0 0062)	0 7616 (0 0062)
Mather(64)	15	0 7750 (0 0090)	0 7735 (0 0091)
Hopkins(63)	16	0 7507 (0 0074)	0 7499 (0 0074)

Table IV Measured Nubar ratios for $^{241}Pu/^{252}Cf$

Author (Year)	Ref No	Reported Ratio	Revised Ratio
Gwin(84)	7	0 7820 (0 0018)	0 7820 (0 0018)
Boldeman(67)	*12*	*0 7788 (0 0018)*	0 7784 (0 0019)
Colvin(65)	14	0 7771 (0 0079)	0 7788 (0 0079)

Table V Comparison of Recent Recommended Nubar Ratios for the Fissile Nuclides

Author(Year)	Ref	$^{233}U/^{252}Cf$	$^{235}U/^{252}Cf$	$^{239}Pu/^{252}Cf$	$^{241}Pu/^{252}Cf$
This paper		0 6595 (0 0012)	0 6424 (0 0010)	0 7654 (0 0012)	0 7803 (0 0013)
Divadeenam(84)	22	0 6615 (0 0010)	0 6407 (0 0008)	0 7636 (0 0014)	0 7771 (0 0018)
Axton(84)	23	0 6603 (0 0015)	0 6416 (0 0012)	0 7638 (0 0016)	0 7800 (0 0017)
Stehn(82)	24	0 6610 (0 0015)	0 6421 (0 0011)	0 7648 (0 0015)	0 7784 (0 0018)
Boldeman(80)	9	0 6597 (0 0014)	0 6403 (0 0011)	0 7651 (0 0018)	0 7781 (0 0018)

Table VI Measured Nubar values for ^{232}U and ^{236}U

Nuclide	Author(Year)	Ref	Measured Value	Revised Value
232U	Jaffey(70)	25	3 13 (0 06)	3 14 (0 06)
236U	Belenky(83)	26	1 79 (0 18)	
236U	Conde(71)	27	1 90 (0 05)	

Table VII Measured Nubar values for ^{238}U

Author(Year)	Ref	Measured Value	Revised Value
Belenky(83)	26	1 97 (0 10)	
Popeko(76)	28	1 99 (0 03)	2 03 (0 03)
Hwang(74)	29	1 96 (0 05)	
Conde(71)	27	2 00 (0 05)	
Asplund-Nilsson(63)	30	1 97 (0 07)	1 95 (0 07)
Sher(60)	31	2 10 (0 08)	2 05 (0 08)
Kuz minov(59)	32	2 08 (0 08)	1 98 (0 08)
Geiger(54)	33	2 26 (0 16)	

Table VIII Measured Nubar values for ^{236}Pu, ^{238}Pu and ^{244}Pu

Nuclide	Author(Year)	Ref	Measured Value	Revised Value	Comment
236Pu	Hicks(56)	34	2 305 (0 19)	2 17 (0 19)	Spont Fiss
238Pu	Hicks(56)	34	2 33 (0 08)	2 21 (0 08)	Spont Fiss
238Pu	Jaffey(70)	25	2 90 (0 03)	2 89 (0 03)	Neut Fiss
238Pu	Kroshkin(70)	49	2 92 (0 12)	2 90 (0 12)	Neut Fiss
244Pu	Orth(71)	35	2 30 (0 19)	2 29 (0 19)	Spont Fiss

Table IX Measured Nubar values for ^{240}Pu

Author (Year)	Ref	Measured Value	Revised Value
Boldeman(84)	36	2 156 (0 010)	
Zhang(84)	37	2 141 (0 016)	2 149 (0 016)
Prehaut(74)	38	2 148 (0 015)	2 162 (0 015)
Prokhorova(71)	6	2 161 (0 016)	
Zhang(71)	39	2 138 (0 031)	
Baron(67)	40	2 153 (0 020)	2 139 (0 020)
Colvin(65)	14	2 118 (0 018)	2 144 (0 014)
Asplund-Nilsson(63)	29	2 154 (0 028)	2 130 (0 028)
Hopkins(63)	16	2 19 (0 03)	2 18 (0 03)
Diven(62)	41	2 167 (0 036)	
Moat(61)	42	2 13 (0 05)	2 169 (0 05)
Diven(56)	43	2 257 (0 045)	2 215 (0 045)

Table X Measured Nubar values for ^{242}Pu

Author (Year)	Ref	Measured Value	Revised Value
Edwards(82)	44	2 153 (0 014)	2 156 (0 014)
Boldeman(84)	36	2 145 no uncert	
Prokhorova(69)	45	2 13 (0 05)	2 14 (0 05)
Hicks(56)	34	2 18 (0 09)	2 07 (0 09)

Table XI Measured Nubar values for ^{241}Am

Author (Year)	Ref	Measured Value	Revised Value	Comment
Jaffey(70)	25	3 219 (0 021)		
Lebedev(58)	48	3 14 (0 05)	3 07 (0 05)	No efficiency correction
Cuninghame(57)	47	3 (0 5)		Calc from Fission Yields

Table XII Measured Nubar values for ^{242m}Am

Author (Year)	Ref	Measured Value	Revised Value
Howe(81)	48	3 269 (0 145)	
Jaffey(70)	25	3 264 (0 024)	3 285 (0 024)
Pultz(66)	13	3 24 (0 12)	3 22 (0 12)
Kroshkin(70)	49	3 28 (0 10)	3 26 (0 10)

Table XIII Measured Nubar Values for ^{242}Cm

Author (Year)	Ref	Measured Value	Revised Value
Zhang(84)	37	2 562 (0 020)	2 572 (0 020)
Halperin(80)	50	2 532 (0 013)	2 530 (0 013)
Hicks(56)	34	2 65 (0 09)	2 53 (0 09)
Crane(55)	51	2 33 (0 11)	2 48 (0 11)

Table XIV Measured nubar Values for ^{243}Cm, ^{247}Cm and ^{250}Cm

Nuclide	Author (Year)	Ref	Measured Value	Revised Value	Comment
243Cm	Zhuraviev(73)	52	3 39 (0 14)	3 40 (0 04)	Neut Fiss
243Cm	Jaffey(70)	25	3 430 (0 047)	3 432 (0 047)	Neut Fiss
247Cm	Zhuraviev(73)	52	3 79 (0 15)	3 80 (0 15)	Neut Fiss
250Cm	Orth(71)	35	3 31 (0 08)	3 30 (0 08)	Spont Fiss

Table XV Measured Nubar Values for ^{244}Cm

Author (Year)	Ref.	Measured Value	Revised Value
Zhang(84)	37	2.72 (0.02)	2.74 (0.02)
Schmidt(83)	53	2.73 (0.16)	2.74 (0.16)
Golushko(73)	54	2.68 (0.03)	
Prokhorova(73)	55	2.70 (0.014)	
Jaffey(70)	25	2.692 (0.024)	2.700 (0.024)
Kroshkin(70)	49	2.77 (0.08)	2.76 (0.08)
Bol'shov(64)	56	2.71 (0.04)	2.69 (0.04)
Diven(56)	43	2.81 (0.06)	2.68 (0.06)
Hicks(56)	34	2.84 (0.09)	2.71 (0.09)

Table XVI Measured Nubar Values for ^{245}Cm

Author (Year)	Ref.	Measured Value	Revised Value
Howe(83)	57	3.60 (0.06)	3.64 (0.06)
Kroshkin(70)	49	3.83 (0.16)	3.81 (0.16)
Jaffey(70)	25	3.832 (0.034)	3.84 (0.03)

Table XVII Measured Nubar Values for ^{246}Cm

Author (Year)	Ref.	Measured Value	Revised Value
Stoughton(73)	58	2.86 (0.06)	2.88 (0.06)
Dakovskii(73)	59	2.98 (0.03)	3.01 (0.03)
Golushko(73)	54	2.927 (0.027)	2.93 (0.03)
Prokhorova(72)	55	2.950 (0.015)	2.95 (0.015)
Thompson(70)	60	3.20 (0.22)	3.17 (0.22)

Table XVIII Measured Nubar Values for ^{248}Cm

Author (Year)	Ref.	Measured Value	Revised Value
Boldeman(73)	61	3.092 (0.007)	3.12 (0.007)
Stoughton(73)	58	3.14 (0.06)	3.16 (0.06)
Golushko(73)	54	3.173 (0.022)	3.17 (0.02)
Prokhorova(72)	55	3.157 (0.015)	3.16 (0.015)
Orth(71)	35	3.11 (0.09)	3.10 (0.09)

Table XIX Recommended Nubar Values for U, Pu, Am and Cm Nuclides

Nuclide	Value (Uncert.)	Nuclide	Value (Uncert.)
^{232}U	3.14 (0.06)	^{241}Am	3.22 (0.04)
^{233}U	2.485 (0.008)	^{242m}Am	3.26 (0.03)
^{235}U	2.414 (0.007)	^{242}Cm	2.54 (0.02)
^{236}U	1.89 (0.05)	^{243}Cm	3.43 (0.14)
^{238}U	1.98 (0.03)	^{244}Cm	2.72 (0.02)
^{236}Pu	2.17 (0.19)	^{245}Cm	3.75 (0.10)
^{238}Pu	2.21 (0.08)	^{246}Cm	2.93 (0.03)
^{239}Pu	2.876 (0.009)	^{247}Cm	3.80 (0.15)
^{240}Pu	2.154 (0.005)	^{248}Cm	3.13 (0.03)
^{241}Pu	2.932 (0.009)	^{250}Cm	3.30 (0.08)
^{242}Pu	2.149 (0.008)		
^{244}Pu	2.29 (0.19)		

Table XX

P_ν for $(^{233}U+n)$

	Gwin 84	Boldeman 84	Consensus	Std. Dev.
P_0	.0249152	.0266448	.0257800	.0012
P_1	.1517652	.1548291	.15329715	.0022
P_2	.3344314	.3289952	.3317133	.0038
P_3	.3225796	.3254248	.3240022	.0020
P_4	.1377542	.1296900	.13372210	.0057
P_5	.0259051	.0293501	.0276276	.0024
P_6	.0024540	.0050659	.00375995	.0018
P_7	.00019543	.0	.0000977	.0001
$\langle\nu\rangle$	2.48500000*	2.48500000*	2.48500000*	.008
$\langle\nu(\nu-1)\rangle$	4.8573	4.9058	4.8816	.0343
$\langle\nu(\nu-1)(\nu-2)\rangle$	7.1314	7.4340	7.2827	.2140
$\langle\nu(\nu-1)\rangle/\langle\nu\rangle^2$	.78658	.79443	.79051	.00555
$\langle\nu^2\rangle-\langle\nu\rangle^2$	1.1671	1.2156	1.1913	.0343
$\langle\nu^2\rangle$	7.3423	7.3908	7.3666	.0343

* data sets made to conform to this value

Table XXI

P_ν for $(^{235}U+n)$

	Gwinn 84	Boldeman 84	Consensus	Std. Dev.
P_0	.0306776	.0327670	.0317223	.0015
P_1	.1707282	.1726860	.1717071	.0014
P_2	.3384084	.3339897	.3361991	.0031
P_3	.3036614	.3042775	.3039695	.0004
P_4	.1295224	.1243698	.1269459	.0036
P_5	.0248181	.0285404	.0266793	.0026
P_6	.0019968	.0032675	.0026322	.0009
P_7	.0001872	.0001026	.0001449	.00006
$\langle\nu\rangle$	2.4140000*	2.4140000*	2.4140000*	.007
$\langle\nu(\nu-1)\rangle$	4.6172	4.6592	4.6382	.0297
$\langle\nu(\nu-1)(\nu-2)\rangle$	6.6985	6.9366	6.8176	.1683
$\langle\nu(\nu-1)\rangle/\langle\nu\rangle^2$	.79232	.79954	.79593	.00510
$\langle\nu^2\rangle-\langle\nu\rangle^2$	1.2038	1.2458	1.2248	.0297
$\langle\nu^2\rangle$	7.0312	7.0732	7.0522	.0297

* data sets made to conform to this value

Table XXII

P_ν for ^{238}U

	Hwang 74	Popeko 76	Consensus	Std. Dev.
P_0	.0443354	.0520000	.0481677	.0054
P_1	.2200429	.2770000	.2485215	.0403
P_2	.4846087	.3660000	.4253044	.0839
P_3	.2098187	.2470000	.2284094	.0263
P_4	.0346876	.0500000	.0423438	.0108
P_5	.0065066	.0080000	.0072533	.0011
$\langle\nu\rangle$	1.99000000*	1.9900000*	1.9900000*	.03
$\langle\nu(\nu-1)\rangle$	2.7745	2.9740	2.8743	.1411
$\langle\nu(\nu-1)(\nu-2)\rangle$	2.4818	3.1620	2.8219	.4810
$\langle\nu(\nu-1)\rangle/\langle\nu\rangle^2$	.70062	.75099	.72553	.03601
$\langle\nu^2\rangle-\langle\nu\rangle^2$	.8044	1.0039	.9022	.1411
$\langle\nu^2\rangle$	4.7645	4.9640	4.8643	.1411

* data sets made to conform to this value

Table XXIII

P_ν for ^{236}Pu P_ν for ^{238}Pu

	Hicks 56	** Std.Dev.	Hicks 56	** Std.Dev.
P_0	.0706805	.035	.0540647	.009
P_1	.1862416	.090	.2053880	.026
P_2	.3795474	.13	.3802279	.026
P_3	.2545524	.12	.2248483	.027
P_4	.0838837	.086	.1078646	.021
P_5	.0250943	.036	.0276366	.009
$\langle\nu\rangle$	2.17000000*	±.19	2.21000000*	±.08
$\langle\nu(\nu-1)\rangle$	3.7949		3.9567	
$\langle\nu(\nu-1)(\nu-2)\rangle$	5.0462		5.5960	
$\langle\nu(\nu-1)\rangle/\langle\nu\rangle^2$	.80590		.81011	
$\langle\nu^2\rangle-\langle\nu\rangle^2$	1.2560		1.2826	
$\langle\nu^2\rangle$	5.9649		6.1667	

* data sets made to conform to this values

** as assigned by author

Table XXIV

P_ν for (^{239}Pu+n)

	Diven** 56	Gwin 84	Boldeman 84	Consensus	Std. Dev.
P_0	.0059460-	.0108072	.0109130	.0108601	.00003
P_1	.1186641	.0973017	.1013071	.0993044	.0028
P_2	.1914874-	.2746513	.2750961	.2748737	.0003
P_3	.4899114+	.3299645	.3241354	.3270500	.0041
P_4	.1012346-	.2110361	.1984958	.2047660	.0087
P_5	.0568506	.0633398	.0822041	.0727720	.0133
P_6	.0359059+	.0116376	.0078484	.0097430	.0027
P_7	.0000000	.0012619	.0000000	.0006310	.0009
$\langle\nu\rangle$	2.8760000*	2.8760000*	2.8760000*	2.8760000*	.009*
$\langle\nu(\nu-1)\rangle$	6.7514	6.7304	6.7565	6.7435	.0184
$\langle\nu(\nu-1)(\nu-2)\rangle$	13.00888	12.5066	12.5828	12.5447	.0539
$\langle\nu(\nu-1)\rangle/\langle\nu\rangle^2$	.81624	.81370	.81685	.81528	.00223
$\langle\nu^2\rangle-\langle\nu\rangle^2$	1.3561	1.3351	1.3611	1.3481	.0184
$\langle\nu^2\rangle$	9.6274	9.6064	9.6325	9.6195	.0184

* data sets made to conform to this value

** set not used to arrive at consensus because of large divergences from more recent data

Table XXV

P_ν for ^{240}Pu

	Hammel** 55	Hicks** 56	Diven 56	Baron 66	Wang 74	Zhang 84	Boldeman 84	Consensus	Std. Dev.
P_0	.0674770	.0518555-	.0598767	.0672230	.0602461	.0628325	.0657477	.0631852	.0033
P_1	.2123022-	.2412679+	.2346677	.2296671	.2323636	.2307696	.2323544	.2319644	.0019
P_2	.3709042+	.3512038	.3290595	.3287954	.3417481	.3380100	.3290022	.3333230	.0061
P_3	.2208222-	.2298913-	.2625685+	.2535573	.2502577	.2466918	.2510283	.2528207	.0060
P_4	.1050492	.1090102	.0963776	.0996201	.0945106	.1015568	.1011654	.0986461	.0031
P_5	.0234452+	.0160176	.0167024	.0192328	.0159182	.0199289	.0183174	.0180199	.0017
P_6	.0000000	.0007536	.0007476	.0019044	.0049556	.0002106	.0023847	.0020406	.0018
$\langle\nu\rangle$	2.1540000*	2.1540000*	2.1540000*	2.1540000*	2.1540000*	2.1540000*	2.1540000*	2.1540000*	.005
$\langle\nu(\nu-1)\rangle$	3.7962	3.7328	3.7465	3.8162	3.7862	3.7797	3.8160	3.7889	.0290
$\langle\nu(\nu-1)(\nu-2)\rangle$	5.2528	5.0471	4.9803	5.2947	5.3196	5.1385	5.3193	5.2105	.1492
$\langle\nu(\nu-1)\rangle/\langle\nu\rangle^2$	.81820	.80454	.80749	.82250	.81604	.81465	.8224	.81663	.0063
$\langle\nu^2\rangle-\langle\nu\rangle^2$	1.3105	1.2471	1.2608	1.3304	1.3005	1.2940	1.3303	1.3032	.0290
$\langle\nu^2\rangle$	5.9502	5.8868	5.9005	5.9702	5.9402	5.9337	5.9700	5.9429	.0290

* data sets made to conform to this value

** data sets not used to form consensus because of several deviances beyond $\pm\sigma$

\+ means P_ν deviates by $> +\sigma$

\- means Pv deviates by $< -\sigma$

Table XXVI

P_ν for ^{241}Pu

	Gwin 84	Boldeman 84	Consensus	Std. Dev.
P_0	.0103533	.0110483	.0107008	.0005
P_1	.0880976	.0900637	.0890807	.0014
P_2	.2643341	.2667284	.2655313	.0017
P_3	.3343422	.3285560	.3314491	.0041
P_4	.2172018	.2117300	.2144659	.0039
P_5	.0716776	.0788167	.0752472	.0050
P_6	.0129416	.0095909	.0112663	.0024
P_7	.0010518	.0034661	.0006992	.0005
$\langle\nu\rangle$	2.9320000*	2.9320000*	2.9320000*	.008
$\langle\nu(\nu-1)\rangle$	7.0071	7.0552	7.0312	.0340
$\langle\nu(\nu-1)(\nu-2)\rangle$	13.2934	13.6606	13.4770	.2597
$\langle\nu(\nu-1)\rangle/\langle\nu\rangle^2$	.81510	.82069	.81790	.00395
$\langle\nu^2\rangle-\langle\nu\rangle^2$	1.3425	1.3906	1.3665	.0340
$\langle\nu^2\rangle$	9.9391	9.9872	9.9632	.0340

* data sets made to conform to this value

Table XXVII

P_ν for ^{242}Pu

	Hicks 56	Boldeman** 84	Std.Dev.
P_0	.0658845	.0679423	.0010
P_1	.1995462	.2293159	.0021
P_2	.3549338	.3341228	.0024
P_3	.3124876	.2475507	.0027
P_4	.0336161	.0996922	.0032
P_5	.0335318	.0182398	.0015
P_6	.0000000	.0031364	.0006
$\langle\nu\rangle$	2.1490000*	2.1490000*	.008
$\langle\nu(\nu-1)\rangle$	3.6588	3.8087	.036
$\langle\nu(\nu-1)(\nu-2)\rangle$	4.6936	5.3487	
$\langle\nu(\nu-1)\rangle/\langle\nu\rangle^2$	.79226	.82472	.002
$\langle\nu^2\rangle-\langle\nu\rangle^2$	1.1896	1.3395	.005
$\langle\nu^2\rangle$	5.8078	5.9577	.036

* data sets made to conform to this value

** because of the anomalous P_ν and P_5 in Hicks 56 it is recommended that Boldeman 84 be used alone; the Std.Dev. is as quoted in that paper, except for $\langle\nu\rangle$, where it is the evaluation of this paper

Table XXVIII

P_ν for ^{242}Cm

	Hicks 56	Halperin 80	Zhang 84	Consensus	Std. Dev.
P_0	.0166474-	.0228731	.0242445	.0212550	.0040
P_1	.1475553	.1340439	.1586229	.1467407	.0123
P_2	.3371507	.3291282	.3139804	.3267531	.0118
P_3	.3267925	.3389847+	.3147058-	.3268277	.0121
P_4	.1263383-	.1463070	.1398818	.1375090	.0102
P_5	.0414297	.0265274-	.0441874	.0373815	.010
P_6	.0033384+	.0020694	.0023659	.0025912	.0007
P_7	.0007477	.0000663	.0014512	.0007551	.0007
P_8	.000000	.000000	.0005602+	.0001867	.0003
$\langle\nu\rangle$	2.5400000*	2.5400000*	2.5400000*	2.5400000*	.02
$\langle\nu(\nu-1)\rangle$	5.1113	5.0433	5.2418	5.1321	.1009
$\langle\nu(\nu-1)(\nu-2)\rangle$	8.0363	7.3992	8.6735	8.0363	.6372
$\langle\nu(\nu-1)\rangle/\langle\nu\rangle^2$	.79225	.78171	.81248	.79548	.01564
$\langle\nu^2\rangle-\langle\nu\rangle^2$	1.1997	1.1317	1.3302	1.2205	.1009
$\langle\nu^2\rangle$	7.6513	7.5833	7.7818	7.6721	.1009

\+ means P_ν deviates by $> +\sigma$

\- means P_ν deviates by $< -\sigma$

* data sets made to conform to this value

Table XXIX

P_ν for ^{244}Cm

	Diven 56	Hicks 56	Dakovskii 74	Zhang 84	Consensus	Std. Dev.
P_0	.0128012	.0055032-	.0278773+	.0138381	.0150050	.0093
P_1	.1245815	.1186366	.0917423-	.1297295	.1161725	.0169
P_2	.3032554	.3013825	.3096042	.2851286-	.2998427	.0104
P_3	.3120112-	.3514536+	.3333684	.3358124	.3331614	.0162
P_4	.2011534+	.1763431	.1802425	.1773601	.1837748	.0117
P_5	.0299232-	.0412210	.0550183+	.0467494	.0429780	.0110
P_6	.0172741-	.0054600	.0021472-	.0102841	.0087914	.0066
P_7	.0000000	.0000000	.0000000	.0010977-	.0002744	.0005
$\langle\nu\rangle$	2.7200000*	2.7200000*	2.7200000*	2.7200000*	2.7200000*	.03
$\langle\nu(\nu-1)\rangle$	5.9891	5.8158	5.9471	6.0031	5.9388	.0853
$\langle\nu(\nu-1)(\nu-2)\rangle$	10.5080	9.4694	9.8848	10.5411	10.1008	.5180
$\langle\nu(\nu-1)\rangle/\langle\nu\rangle^2$	.80951	.78609	.80384	.81140	.80271	.01154
$\langle\nu^2\rangle-\langle\nu\rangle^2$	1.3107	1.1374	1.2687	1.3247	1.2604	.0853
$\langle\nu\rangle^2$	8.7091	8.5358	8.6671	8.7231	8.6588	.0853

\+ means P_ν deviates by $> +\sigma$

\- means P_ν deviates by $< -\sigma$

* data sets made to conform to this value

Table XXX

P_ν for ^{246}Cm

	Stoughton 73	Dakovskii 74	Consensus	Std. Dev.
P_0	.0130533	.0173831	.0152182	.0031
P_1	.0824850	.0700688	.0762769	.0088
P_2	.2512020	.2742057	.2627039	.0162
P_3	.3522395	.3376076	.3449236	.0103
P_4	.2258728	.2102577	.2180653	.0110
P_5	.0659829	.0851960	.0755895	.0139
P_6	.0091644	.0052810	.0072227	.0027
$\langle\nu\rangle$	2.9300000*	2.9300000*	2.9300000*	.03
$\langle\nu(\nu-1)\rangle$	6.9209	6.9595	6.9402	.0273
$\langle\nu(\nu-1)(\nu-2)\rangle$	12.5931	12.8173	12.7052	.1586
$\langle\nu(\nu-1)\rangle/\langle\nu\rangle^2$	.80617	.81067	.80842	.00318
$\langle\nu^2\rangle-\langle\nu\rangle^2$	1.2660	1.3046	1.2853	.0273
$\langle\nu^2\rangle$	9.8509	9.8900	9.8702	.0273

* data sets made to conform to this value

Table XXXI

P_ν for ^{248}Cm

	Boldeman 73	Stonghton 73	Consensus	Std. Dev.
P_0	.0063081	.0071623	.0067352	.0006
P_1	.0622386	.0570604	.0596495	.0037
P_2	.2272634	.2138438	.2205536	.0095
P_3	.3458147	.3559898	.3509030	.0072
P_4	.2435394	.2652139	.2543767	.0153
P_5	.0907591	.0879519	.0893555	.0020
P_6	.0206991	.0127780	.0167386	.0056
P_7	.0033775	.0000000	.0016888	.0024
$\langle\nu\rangle$	3.1300000*	3.1300000*	3.1300000*	.03
$\langle\nu(\nu-1)\rangle$	8.0299	7.8886	7.9592	.0999
$\langle\nu(\nu-1)(\nu-2)\rangle$	16.5585	15.3115	15.9350	.8818
$\langle\nu(\nu-1)\rangle/\langle\nu\rangle^2$	.81964	.80521	.81242	.0102
$\langle\nu^2\rangle-\langle\nu\rangle^2$	1.3630	1.2217	1.2923	.0999
$\langle\nu^2\rangle$	11.1539	11.0186	11.0892	.0999

* data sets made to conform to this value

MEASUREMENT AND THEORETICAL CALCULATION OF THE ^{252}Cf SPONTANEOUS-FISSION NEUTRON SPECTRUM

H. MÄRTEN, D. SEELIGER
Technical University of Dresden,
Dresden, German Democratic Republic

Abstract

Concerning the $^{252}Cf(sf)$ neutron spectrum remarkable progress in experiment and theory have been made during the last three years. Experimental techniques and analysis procedures have been improved. The precise measurement of the standard neutron spectrum from spontaneous fission of 252-Cf requires the optimum experimental arrangement corresponding to the energy range to be measured. Several typs of data corrections have to be considered with care. The most important requirements to be met in a 252-Cf(sf) neutron spectrum measurement are summarized briefly. We consider the high-energy range especially.

Theoretical models for the calculation of fission neutron spectra are based on the predominant emission mechanism, i.e. the evaporation from fully accelerated fragments. It is emphasized that an exact evaporation theory of fission neutron spectra should take into account the fragment distribution in nucleonic numbers, excitation energy, kinetic energy, and nuclear spin as well as the cascade neutron emission from highly excited, neutron-enriched fragments in competition to γ-ray emission. However, practical applications require several approximations. Some approaches which were studied in the framework of both the Weisskopf formalism and the Hauser-Feshbach theory are discussed. We point out some of the deviations in spectrum calculation if neglecting or approximating typical characteristics of fission neutron emission.

The results of new Cf spectrum calculations are compared with recent experimental data which confirm a Maxwellian spectrum at energies below ~ 1 MeV for T = 1.42 MeV. Between 1.5 and 4 MeV, measured data tend to exceed this Maxwellian by about 3 %. Significant deviations from a Maxwellian with T = 1.42 MeV appear between 6 and 20 MeV where a fit of experimental data yields a value of T close to 1.37 MeV.

Recent theoretical calculations of the Cf neutron spectrum agree very good with measured data. Especially, the complex cascade evaporation model permits a conformable description of recent experimental data in the whole energy range (1 keV - 20 MeV) if introducing the CMS anisotropy of emission.

1. Introduction

The ^{252}Cf(sf) neutron spectrum recommended as a standard by an IAEA Consultants' Meeting[1] is of high importance for practical applications as well as for theoretical studies of the fission process and the mechanism of fission neutron emission. It is employed as a reference in both microscopic and macroscopic measurements. Cf sources are widely used for instrument calibration.

The status of measurement, evaluation, and theoretical analysis of the ^{252}Cf spontaneous-fission neutron spectrum is viewed by the IAEA (INDC) resulting in regular summaries and recommendations[2,3]. Blinov presented a comprehensive review in 1980[4]. Therefore, the present review paper is focused on recent investigations of the Cf neutron spectrum.

As already outlined in the conclusions of the IAEA Consultants' Meeting[3], the accuracy of experiments as well as the theoretical description of the Cf spectrum have been improved substantially. Experimental data cover the energy range from 1 keV to 30 MeV at present and have been deduced from measurements with different types of both fission fragment (FF) detectors and neutron (n) detectors in overlapping energy ranges. Experimental arrangements have been developed to keep corrections as small as possible. The data analysis was refined; corrections are considered with more care.

The spontaneous fission of ^{252}Cf has been studied in many theoretical and experimental works concerning fragment distributions in kinetic energy, nucleon numbers, excitation energy, nuclear spin etc., concerning the diversity of particle emission processes in fission also. However, several fundamental problems are still open. In particular, the mechanism of fission neutron emission was/is a subject of the research in nuclear physics (see review in Ref. 5 and summary concerning scission neutron emission in Ref. 6). According to our present knowledge, at least 80 % of fission neutrons are evaporated from fully accelerated fission fragments. The nature of the remainder, i.e. scission neutrons or central component, has not yet been clarified in spite of many investigations. Therefore, hitherto published fission neutron spectrum calculations had been based on evaporation models considering the complexity of fission up to a certain degree. Nevertheless, recent activities give rise to an optimistic outlook and seem to terminate the stagnation appeared since the sixties. Here, the spontaneous fission of ^{252}Cf is the preferred subject.

2. On the experimental determination of the Cf neutron spectrum

2.1. Status of experiments. High effort concerning experimental technique as well as data analysis has been devoted to the precise determination of the ^{252}Cf(sf) neutron spectrum. However, the discrepancies between the data of various experiments are much higher than the estimated uncertainties.

The most frequently employed method was/is the neutron time-of-flight (TOF) technique based on neutron detection with[2,4]

i) organic scintillators ($E \gtrsim 0.2$ MeV),

ii) ^{6}Li-including materials (lithium glasses, ^{6}LiI crystals, $E \lesssim 2$ MeV),

iii) ^{235}U fission chambers (whole energy range),

iv) black neutron detectors[9] (organic scintillator, $E \gtrsim 0.2$ MeV).

Further techniques involve the registration of recoil protons as well as of reaction products from $^{3}He(n,p)$ and $^{6}Li(n,\alpha)$.

The improved measurements presented after 1980[7-15] have been carried out by employing TOF spectrometers.

The experiments dated before 1979 had been reviewed by Blinov[4]. He took note of large discrepancies concerning the deduced Maxwellian temperature T (spectrum hardness parameter) as well as the spectrum shape at very low and very high energies especially. The published T values cover the energy range

from 1.18 to 1.57 MeV. More recent measurements[7-10,14] confirm Blinov's conclusion that the $^{252}Cf(sf)$ neutron spectrum can approximately be described by a Maxwellian distribution with T = 1.42 MeV at low energies and in the intermediate-energy range. Remarkable deviations from a Maxwellian with T = 1.42 MeV appear in the energy range from 6 to 20 MeV[11-13] where a Maxwellian fit yields a value of T close to 1.37 MeV. Recent experimental data[7-9,11] exceed the Maxwellian with T = 1.42 MeV in the range from 1.5 to 4 MeV by about 3 % (see paragraph 4).

Blinov pointed out that the NBS evaluation[16] is not suited to reproduce the experimental data below 1 MeV especially. A new evaluation was strongly recommended at the IAEA Consultants' Meeting[3].

2.2. Requirements with regard to TOF measurements. Data correction. Fission neutron TOF spectroscopy involves the registration of both fission fragments and neutrons with a time resolution $\lesssim$ 1 ns. Chalupka et al.[17] discussed the requirements to be met by a FF detector. The preferred types are avalanche detectors, gas scintillators, and ionization chambers which provide a sufficient discrimination against the associated α-activity of Cf sources. To keep the corrections of spectrum contributions due to scattering effects and neutron producing reactions very small, a low-mass FF detector is necessary.

The measurable $^{252}Cf(sf)$ neutron spectrum is influenced by the anisotropic FF detection efficiency caused by absorption in the sample plane[6,9,11] due to the deposit thickness and backing roughness. The total fragment detector efficiency ε_{FF} should be close to 100 %. The ratio of the measurable neutron spectrum to the total (undisturbed) one was calculated in Ref. 6,13. A typical example is shown in Fig. 1. Similar studies have been performed by other groups[9,15]. Corrections with regard to ε_{FF} are nearly independent of E at about 60 deg (angle with regard to sample plane normal)[6,17]. The value ε_{FF} can be deduced from a FF-n-coincidence measurement as a function of β (angle of n detector position)[11] or from a $N(E,\beta=90\ deg)/N(E,\beta=0\ deg)$ measurement[9].

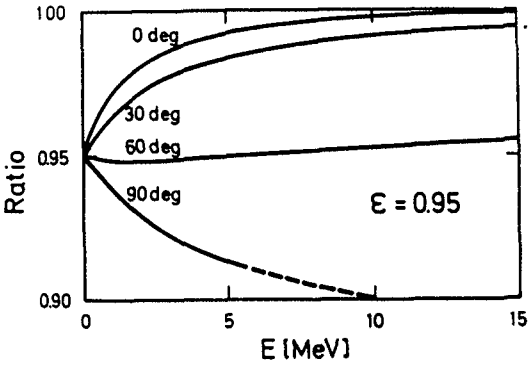

Fig. 1

Ratio of the measurable to the undisturbed Cf neutron spectrum represented for selected angles of neutron detector position with regard to the Cf sample plane normal. Calculation result for ε_{FF}=0.95. (Ref. 6,13).

In-/out-scattering effects concern the air column between source and n detector, the collimator and shielding system, and the construction materials of both the FF detector and the n detector. An improved version of a collimator and shielding system suited to keep scattering effects small was presented by Poenitz and Tamura[9]. The most simple correction is that one for neutron transmission on the base of total cross sections. The background caused by scattered neutrons, which cover the energy range below about (1-4) MeV predominantly (depending on geometrical conditions), should be studied by Monte Carlo calculations (MCC)[7,9,11]. A shadow cone experiment yields limited informations only.

The central task of a fission neutron spectrum measurement is the precise determination of the n detector efficiency ε_n. In the case of n detectors based on the $^6Li(n,\alpha)$ or the $^{235}U(n,f)$ reaction, ε_n is determined according to the standard cross sections[2]. For special corrections, we refer to original papers. The efficiency of a black neutron detector (BND) is close to 100 % due to its operation mode. Deviations from 100 % can be deduced from MCC. Therefore, uncertainties in ε_n are very low ($\approx$ (1-2) %)[9]. However, the energy resolution

of a BND has to be considered carefully. The uncertainties of the measured TOF spectrum become large at high energy especially due to the strongly increasing spectrum gradient. Organic scintillators with pulse shape discrimination properties are very often employed for fission neutron TOF spectroscopy at energies above 0.5 MeV (0.2 MeV). Such n detectors are characterized by an intermediate efficiency ($\sim$ (1-30) %) to be determined in separate experiments. A rather substantial effort is necessary to obtain $\varepsilon_n(E)$ with an uncertainty below 5 %. ε_n studies are commonly added by MCC to interpolate or extrapolate measured efficiency data. Here, the light output (LO) resolution has to be considered in a reliable way (for LO calibration purposes on the base of response functions especially). The γ background of organic scintillators can considerably be suppressed by pulse shape discrimination. The dynamic range of the used discriminator limits the measurable spectrum range at low neutron energy especially. The reliability of n/γ-discrimination can be enhanced if introducing the pulse shape amplitude as a further parameter in the measurement. For instance, the PTB group[11] carried out a four-dimensional measurement of neutron TOF, scintillator LO, pulse shape amplitude, and FF detector amplitude (ΔE signal from the fission chamber). An alternative method is at least the check-up of the n/γ-discriminator carried out simultaneously with the measurement (spectroscopy of the pulse shape amplitude for a selected LO window[13]). The flight paths in previous ^{252}Cf(sf) spectrum measurements are spread over the range from 20 cm (low-energy range) to 12 m (high-energy range). The flight path L is defined as the distance between the source and the average detection depth in the n detector. Consequently, it can be E-dependent in special cases. In general, the time resolution of the TOF spectrometer is also a function of E due to the detector depth[10,13]. The time resolution and, sometimes, the TOF bin width disturb the measured spectrum if the TOF distribution increases or decreases strongly, i.e. in the n detector bias region as well as at the high-energy spectrum end. This annoying effect depends on L mainly. Corrections can be carried out using unfolding methods. Nevertheless, L should be chosen sufficiently high to keep corrections in the % region. In the case of organic-scintillator n detectors, the determined γ-peak position should be checked by an additional measurement with and without n/γ-discrimination to avoid a possible annoying influence due to the amplitude-dependent timing, which occur in spite of developed timing methods in the case of large LO ranges to be analysed.
The time scale calibration should be checked and verified (for instance, C transmission measurement[9]).
The background due to non-correlated STOP signals (FF detector) was considered in recent experiments only. This partial (TOF-channel dependent) background can be avoided by a pile-up rejector[7] tolerating an extended dead time, or it can be deduced analytically[11,18] on the base of time scale characteristics and the Cf source strength.

2.3. Problems of the measurement of the ^{252}Cf(sf) neutron spectrum in the high-energy range. Large discrepancies of experimental data concerning the high-energy end of the Cf spectrum had been outlined by Blinov[4]. To obtain a rather good energy resolution at high E a sufficiently high flight path is required. Further, one should use a n detector with a high ε_n at a large solid angle $\Delta\Omega$. ^{235}U fission chambers are not suited because of their low efficiency. The use of a BND is questionable due to the high energy resolution effects on the TOF spectrum at high E. Consequently, an optimum arrangement seems to be

i) the use of an organic-scintillator n detector at a comparatively high flight path,

ii) the application of efficient background suppression methods (pulse shape discrimination, heavy shielding),

iii) the application of a rather strong Cf source,

iv) the two-dimensional (TOF,LO)-spectroscopy which permits the selection of the optimum LO bias depending on E generally, i.e. a maximum foreground/background ratio can be achieved.

These requirements have been met in Ref. 11-13 especially, but item (iv) was only considered in Ref. 12,13. In these two works, an efficient pulse shape discriminator was used to suppress both the γ-rays and the cosmic-myon background. The shape of the ^{252}Cf(sf) neutron spectrum at the high-energy end[12] is shown in Fig. 2. This result was confirmed in an experiment finished recently[13]. The data represented in Fig. 2 are in very good agreement with the PTB measurement[11] (concerning the energy range below 15 MeV).

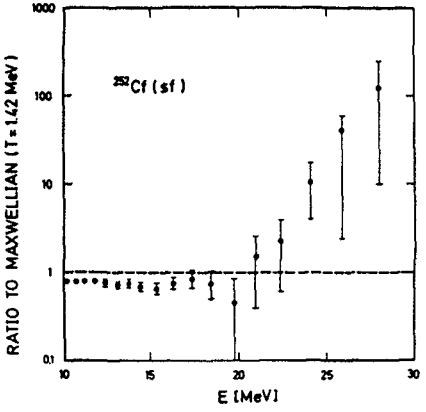

Fig. 2

The high-energy end of the Cf neutron spectrum represented with reference to a Maxwellian distribution with T = 1.42 MeV. The Fig. was taken from Ref. 12.

3. Theory of the ^{252}Cf(sf) neutron spectrum

3.1. The fission process and fission neutron emission. It was found early that the fission neutron emission probability is enhanced close to the fission axis[19]. Consequently, evaporation of fission neutrons from fully accelerated fragments was considered as the predominant emission mechanism. On the base of this assumption, fission neutron spectra have been described quite well (Ref. 20,21 and references therein). More precise experimental studies had shown that a ~10 % component of fission neutrons is emitted isotropically in the laboratory frame (LS). Further investigations have been summarized recently[6]. Published results are contrary. Therefore, the picture of scission neutron emission is not clear at present. The yield of scission neutrons as well as their differential emission probability are not known with sufficient accuracy. The partial spectra of the different eventual kinds of scission neutrons[23-26] have not yet been found theoretically. In particular, the rapid changes in nuclear potential as the fissioning nucleus moves from the saddle of the fission barrier to the scission point and at the transition of strongly deformed fragments into their equilibrium form may result in strong single-particle excitations and, hence, nucleon emission from non-equilibrium states. The reliability of hitherto existing analysis results is questionable due to the uncertainty in the model parameters concerning the time-dependent parametrisation of the nuclear potential as well as due to the restrictions of the models themselves.

The fission fragments become highly excited after dissipation of their deformation energy which they have at scission. Energy dissipation and fragment acceleration are two simultaneous processes which occur within about 10^{-20} s after scission[27]. Therefore, a possible emission mechanism of fission neutrons could be the evaporation (or emission from non-equilibrium states?) during fragment acceleration.

Fission is partly accompanied by charged-particle emission (ternary fission). Some of these light nuclei are instable. In particular, 11 % of the α-particles are originally emitted as ^{5}He nuclei which decay ($T_{1/2} \approx 8 \cdot 10^{-22}$ s) into an α-particle and a neutron[28].

3.2. Statistical-model approach of fission neutron spectra. Hitherto, calculations of the energy spectrum of fission neutrons which include all possible emission mechanisms have been infeasible. The bare main one, i.e. the evaporation from fully accelerated fission fragments, is a rather complex process. In this case, detailed calculations of emission spectra in the framework of statistical models have to account for many characteristics of fission and fission neutron emission:

i) nucleon (N, Z, A=N+Z), excitation energy (E^x), kinetic energy (E_k), and spin (I) distribution of the fission fragments (which depends on the features of the fissioning nucleus), i.e. $P(E^x,I,A,Z,TKE)$ (TKE - total kinetic energy of the fission fragments; E_k is defined by A and TKE according to moment conservation);

ii) cascade neutron emission from highly excited, neutron-enriched fragments in competition to γ-emission.

The fragment distribution of item (i) is not derivable from fission theory completely or/and with sufficient accuracy. Therefore, one has to consider experimental data and/or special assumptions.

Further, the emission of fission neutrons is not isotropic in the center-of-mass system (CMS) of the fragments due to the fragment spin ($\bar{I} \approx (6\text{-}8)\hbar$)[29,30]. This fact is often neglected.

Synopsis 1 represents the general scheme which has to be accounted for the calculation of fission neutron spectra on the base of a statistical model. The CMS probability of neutron emission $\varphi(\varepsilon)$ is calculated in the framework of either the Weisskopf formalism[31] (without P(I) consideration) or the Hauser-Feshbach theory[32]. In any case, the level density $\rho(U,I)$ of the residual nuclei (excitation energy U) and the transition probabilities (inverse cross section σ_c of compound-nucleus formation or transmission coefficients T_{lj} respectively) have to be taken into account. The dependence $\varphi(\vartheta)$ (CMS angular distribution) has been deduced by Gavron[30] by statistical calculations (integral in regard of ε !). He obtained a distribution which can be approximated by

$$\varphi(\vartheta) \sim (1 + B\cdot\cos^2\vartheta),\ B \approx 0.1. \qquad (1)$$

The sum over i (emission step index) in the first equation of synopsis 1 means consideration of cascade emission.

STATISTICAL-MODEL APPROACH TO THE $^{252}Cf(sf)$ NEUTRON SPECTRUM

CMS: $$\varphi(\varepsilon,\vartheta : A,Z,TKE) = \sum_i \sum_I \int dE^x \cdot P_i(E^x,I : A,Z,TKE)\cdot \varphi_i(\varepsilon,\vartheta : E^x,I,A,Z)$$

$\Downarrow$

TRANSFORMATION INTO LS USING $E_f = E_k/A = TKE\cdot(1/A - 1/252)$

$\Downarrow$

LS: $$N(E,\Theta : A,Z,TKE)$$

$\Downarrow$

$$N(E) = \sum_{A,Z} \int dTKE \int d\Omega \cdot P(A,Z,TKE)\cdot N(E,\Theta : A,Z,TKE)$$

SYNOPSIS 1

The transformation of the CMS distribution $\varphi(\varepsilon,\vartheta : A,Z,TKE)$ into the LS and the following weighted concentration taking into account the fragment occurrence probability P(A,Z,TKE) yields N(E). However, the whole scheme of synopsis 1 has not yet been observed. Hitherto published treatments take not into account the model dependence on Z. The calculations are carried out taking the average $\bar{Z}$ for a given A. The dependence $\varphi(\vartheta)$ was only considered roughly without correlation to ε, E^x, I, A, Z on the base of Eq. 1 [33,34]. The initial distribution in fragment spin[29] can only be introduced in Hauser-Feshbach calculations[35-37]. Using the Weisskopf ansatz one can approximately consider the influence of the spin distribution on spectrum shape if assuming $\rho(U,I) = \rho(U,I=0)$[38]. Most of the hitherto published theoretical studies of fission neutron spectra have been characterized in Ref. 6. Here, we focus on recent improved treatments.

3.3. Recent developments of models. The model proposed by Madland and Nix[39,40] was based on rough approximations concerning the description of level density and excitation energy distributions, but it is easily applicable to any fission reactions. It was successfully used to describe neutron spectra from induced fission reactions as well as from spontaneous fission of ^{252}Cf. A rather good agreement with experimental data can be achieved if adjusting the level density parameter

$$a = A/C. \qquad (2)$$

The neglection of the diversity of scission configurations is compensated by a higher value of C than physically reasonable. However, C is the only one free parameter of the model. Further input data are known well. Synopsis 2 includes the basic formulae of two versions of the Madland-Nix model (MNM). We know that the CMS spectra depend on A actually. This fact is neglected in the MNM but the consideration of $\bar{\epsilon}_C$ for the two fragment groups in version II.

Recent studies[42] have been carried out in the framework of a generalized Madland-Nix model (GMNM, synopsis 3).

Version III characterized in synopsis 3 considers the different maximum values T_m of the rest-temperature distribution as well as the different weights of the light and heavy fragment group (L, H). The full dependence of the input parameter on A is taken into account in version IV.[42]

The different model versions of MNM/GMNM have been compared for a fixed C = 8.0 MeV[42]. Fig. 3 shows how the spectrum is changed if using a more complex model for the calculation of the Cf neutron spectrum. The spectrum at high and low

---

MADLAND-NIX MODEL — MNM

(D.G. MADLAND AND J.R. NIX, LASL)

+++ WEISSKOPF FORMALISM

+++ DEPENDENCE OF CMS SPECTRA ON A, Z, AND TKE NEGLECTED

+++ CMS ANISOTROPY NEGLECTED

+++ CONSTANT-TEMPERATURE DESCRIPTION OF $\vartheta(U)$

+++ OPTICAL-MODEL CALCULATION OF $\bar{\epsilon}_C$

+++ TRIANGULAR-SHAPE DISTRIBUTION IN NUCLEAR TEMPERATURE OF RESIDUAL FRAGMENTS (MAXIMUM VALUE T_m), I.E. ROUGH IMPLICITE CONSIDERATION OF $P_0(E^x)$ AND CASCADE EMISSION

VERSION I

+++ $N(E) = N(E, \bar{E}_f, \bar{\epsilon}_C^A)$

VERSION II

+++ $N(E) = \frac{1}{2}\left[N(E, E_f^L, \bar{\epsilon}_C^L) + N(E, E_f^H, \bar{\epsilon}_C^H) \right]$

SYNOPSIS 2

energy increases and at intermediate energy decreases as the complexity of the model increases. The deviations are large at high energy especially. They can be compensated by adjusting C. However, the spectrum shape is changed if requiring an equal average LS emission energy (cf. paragraph 4).

GENERALIZED MADLAND-NIX MODEL — GMNM

(H. MÄRTEN AND D. SEELIGER, TUD)

+++ AS MNM, BUT CONSIDERATION OF

I) $T_m(A)$

II) $E_f(A)$

III) $\sigma_C(A)$

IV) WEIGHT $P(A)\cdot\bar{\nu}(A)$
(FRAGMENT YIELD AND NEUTRON YIELD RESPECTIVELY)

VERSION III

+++ $$N(E) = \frac{1}{\bar{\nu}_{tot}}\left[\bar{\nu}^L \cdot N(E,E_f^L,\sigma_C^L,T_m^L) + \bar{\nu}^H\, N(E,E_f^H,\sigma_C^H,T_m^H)\right]$$

VERSION IV

+++ $$N(E) = \frac{1}{\bar{\nu}_{tot}} \sum_A \bar{\nu}(A)\cdot P(A)\cdot N(E,E_f(A),\sigma_C(A),T_m(A))$$

SYNOPSIS 3

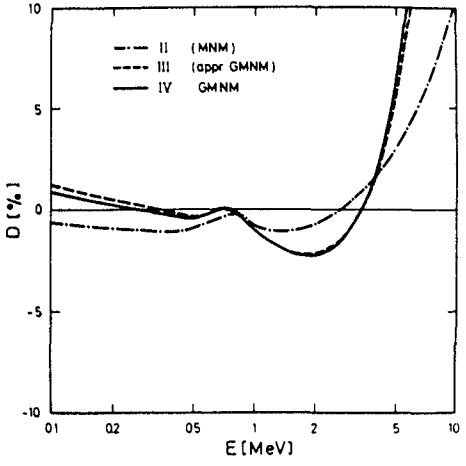

Fig. 3

The percentage deviation D of the Cf neutron spectra calculated in the framework of the versions II, III, and IV from the version-I distribution[42]. The calculations have been carried out for a fixed parameter C (8.0 MeV).

COMPLEX CASCADE EVAPORATION MODEL — CEM

(H. MÄRTEN AND D. SEELIGER, TUD)

+++ WEISSKOPF FORMALISM, CASCADE EMISSION

+++ DEPENDENCE OF CMS SPECTRA ON $\underline{Z}$ NEGLECTED

+++ ROUGH CONSIDERATION OF CMS ANISOTROPY

+++ SEMIEMPIRICAL DESCRIPTION OF $\Omega(U,I=0)$ BASED ON THE FERMI-GAS FORMULA WITH ENTROPY

$$S = 2\sqrt{\tilde{a}\cdot(U + \delta U'\cdot f(U) + \delta P'\cdot h(U))}$$

($\delta U'$, $\delta P'$ - SHELL AND PAIRING CORRECTION RESP.)

+++ OPTICAL MODEL CALCULATION OF σ_C

+++ $P_Q(E^*;A,TKE)$ GAUSSIAN SHAPE
(DEDUCED FROM EXPERIMENTAL $\bar{\nu}$, σ_ν^2, $\bar{E}_\gamma$ DATA)

+++ $$N(E) = \sum_A \int dTKE\;\; P(A,TKE)\cdot N(E;A,TKE)$$

+++ STUDY OF MULTIPLE-DIFFERENTIAL EMISSION PROBABILITIES $N(E,\Theta;A,TKE)$

SYNOPSIS 4

An improved version of the cascade evaporation model (CEM, synopsis 4) was used to calculate the ^{252}Cf(sf) neutron spectrum in the energy range from 1 keV to 40 MeV[34]. Previous studies[33] were concentrated on the high-energy range only. The new calculation is based on a complex consideration of scission configurations defined by A and TKE, i.e. asymmetry and elongation of the fissioning nucleus at scission respectively). Neglecting the TKE dependence one obtains a changed spectrum description at high energy especially (Fig. 4).

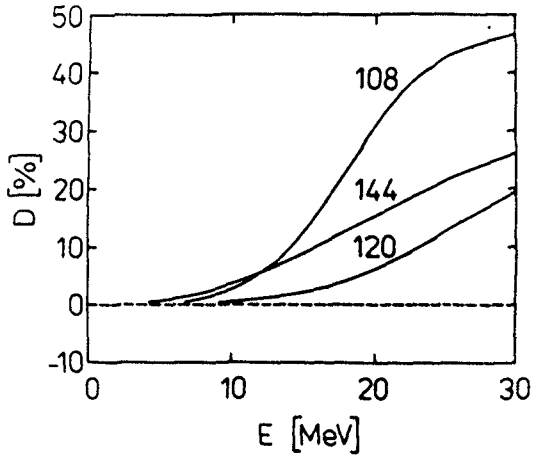

Fig. 4

The effect of the approximative spectrum calculation without consideration of the correlation between the CMS spectra and TKE (for fixed A) with reference to the "exact" one. Percentage deviations are represented in the case of typical fragment mass numbers (Ref. 6,33)

The consideration of the CMS anisotropy (Eq. 1) yields an enhancement of the low-energy spectrum part in particular (cp. paragraph 4). The CEM was also used to study the influence of the input data on the spectrum[6].

Applying the Hauser-Feshbach theory for fission neutron spectrum calculations one is able to consider the competition of neutron emission to γ-ray emission as well as the initial distribution in fragment spin which is known roughly[29]. The first study was presented by Browne and Dietrich[35]. Recent calculations have been carried out by Gerasimenko and Rubchenya[36,37] (Synopsis 5). They neglected the probability distribution in TKE for a given A as well as the CMS anisotropy.

HAUSER-FESHBACH CALCULATION — HFC

(B.F. GERASIMENKO AND V.A. RUBCHENYA, RIL)

+++ HAUSER-FESHBACH FORMALISM, CASCADE EMISSION

+++ DEPENDENCE OF CMS SPECTRA ON Z AND TKE NEGLECTED

+++ CMS ANISOTROPY NEGLECTED

+++ SEMIEMPIRICAL DESCRIPTION OF $\varrho(U,I)$ BASED ON THE FERMI-GAS FORMULA WITH THE ENTROPY

$$S = 2\sqrt{\tilde{a}\cdot(1 + f(U)\cdot\delta W/U)\cdot(U-\delta)}$$

(δW, δ - SHELL AND PAIRING CORRECTION RESP.)

+++ OPTICAL MODEL CALCULATION OF T_{lj}

+++ $P_0(E^x{:}A)$ GAUSSIAN SHAPE (DEDUCED FROM EXPERIMENTAL $\bar{\nu}$, σ^2_ν DATA)

+++ $P_0(I{:}A)$ CONSIDERED, $\bar{I} \approx (6\text{-}8)\hbar$

+++ $N(E) = \sum_A P(A)\cdot N(E{:}A)$

+++ STUDY OF MULTIPLE-DIFFERENTIAL EMISSION PROBABILITIES $N(E,\theta{:}A,TKE)$

SYNOPSIS 5

Synopsis 2-5 indicate that CEM and HFC involve the realistic consideration of the initial distributions in E^x shown in Fig. 5 for typical fragment mass numbers, i.e. $P_0(E^x{:}A)$ which is integral in regard of TKE. Both models are based on improved methods of level density description which take into account shell and pairing corrections (CEM - Ref. 43, HFC - Ref. 44).

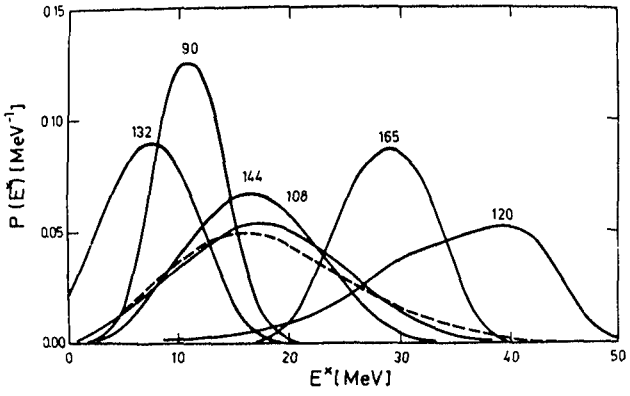

Fig. 5

Initial distributions in excitation energy for some typical mass numbers of fragments from spontaneous fission of Cf-252. The dashed line represents the weighted average. Fig. taken from Ref. 6.

4. Comparison between recent experimental data and theoretical calculations

Fig. 6 and 7 represent recent experimental data on the Cf neutron spectrum in comparison with the results of different calculations in the energy range between 1o keV and 20 MeV. Concerning the experimental results one can conclude:

i) Recent data are close to a Maxwellian distribution with T = 1.42 MeV for E < 1 MeV. The ANL data tend to lower emission probabilities (about -8 % deviation at 0.2 MeV).

ii) Recent experimental data are in very good agreement (with the exception of Ref. 11 (?)) in the energy range between 1 and 5 MeV. They exceed the Maxwellian with T = 1.42 MeV by about 3 %.

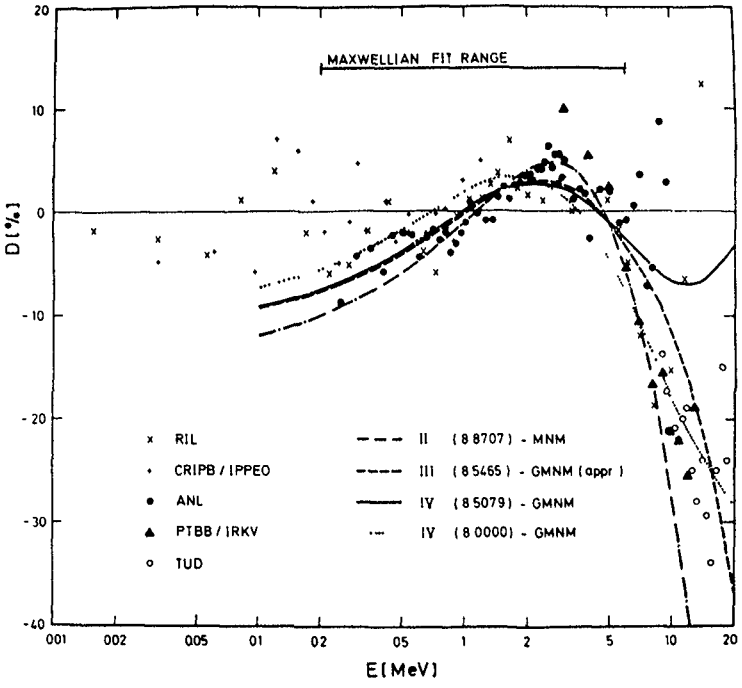

Fig. 6

Percentage deviations of recent experimental data (RIL - Ref. 7, CRIPB/IPPEO - Ref. 8, ANL - Ref. 9, PTBB/IRKV - Ref. 11 TUD - Ref. 12) on the Cf neutron spectrum from a Maxwellian distribution with T = 1.42 MeV. With the exception of calculation IV (8.0000), the C values (included in parenthesis) have been adjusted to obtain T = 1.42 MeV if fitting the calculated spectra to a Maxwellian in the shown energy range. The experimental errors are not represented for clearness. We refer to the original papers. Fig. taken from Ref. 42.

iii) In the (5-20) MeV region, the data tend to lower emission probabilities obviously with reference to the T = 1.42 MeV Maxwellian. Typical deviations are 0 % at 5 MeV, -20 % at 1o MeV, -25 % at 16 MeV.

iv) Excess neutrons have been found above 20 MeV[12,13].

Fig. 6 shows the results of different calculations in the framework of both the MNM (version II) and the GMNM (version III

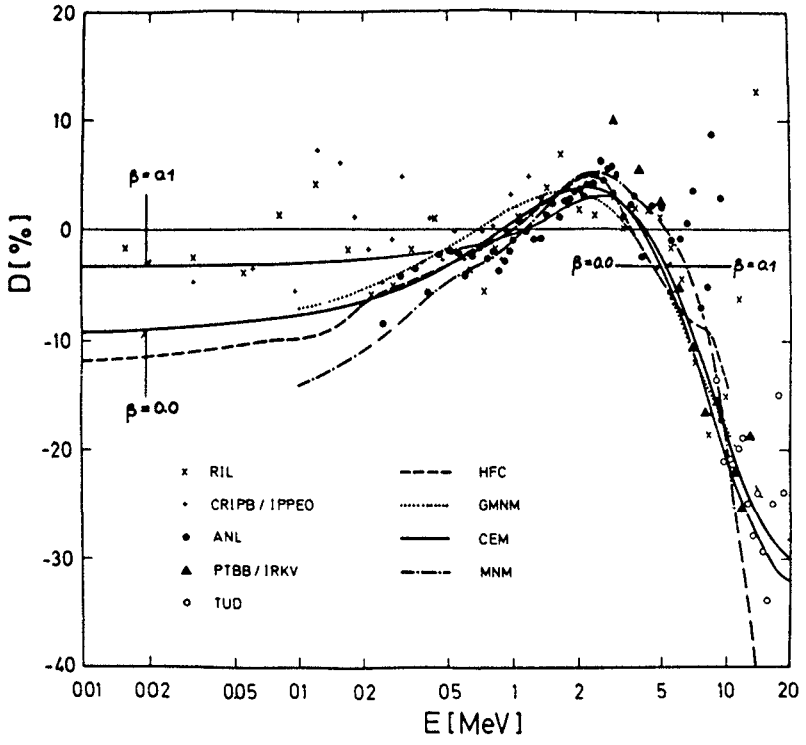

Fig. 7

As Fig. 6 concerning the experimental data. The results of the MNM and the HFC calculation were taken from Ref. 41 and Ref. 10 respectively. The shown GMNM spectrum was calculated for C = 8.0 MeV (Ref. 42, cp. Fig. 6). The Cf energy spectrum calculated in the framework of the CEM is represented for two CMS anisotropy parameter ß.

and version IV). Here, C of Eq. 2 was adjusted so that a fit of the calculated spectrum to a Maxwellian yields T = 1.42 MeV in each case[42]. Similar results are obtained in the (0.1 - 6) MeV energy region. Further, the result of a calculation using C = 8.0 MeV (the most probable value with reference to level density systematics) is represented. In this case, the high-energy data of recent experiments are reproduced.

Above 5 MeV, version II and version III yield a spectrum slope which is contrary to experimental data. This is a consequence of rough approximations (see synopsis 1-3).

In Fig. 6, we compare recent Cf spectrum calculations[34,37,41,42] with experimental data. Obviously, the MNM underestimates the experimental data at low energy ($E < 0.5$ MeV) as well as in the high-energy region ($E > 10$ MeV). The results of the GMNM, HFC, and CEM(ß=0.0) calculations are in very good agreement, but they tend to underestimate the low-energy data (-10 % deviation). Considering the CMS anisotropy roughly (ß = 0.1, Eq. 1), the spectrum is enhanced by about 5.5 % at 10 keV. The high-energy tail is also enhanced by about 2 %. Between 0.8 and 3 MeV, the calculation with ß=0.1 yields a somewhat lower emission probability (cf. study in Ref. 6, first consideration in Ref. 21). The CEM calculated spectrum with ß=0.1 agrees very good with experimental data in the whole energy range (1 keV - 20 MeV). However, this version takes into account the CMS anisotropy approximately, because Eq. 1 means that $\epsilon(\vartheta)$ is considered without correlation to $\mathcal{E}$. It is emphasized that the CEM calculation was not based on arbitrary normalizations or parameter adjustment. The measured spectrum above 20 MeV (Fig. 2) cannot be described by an evaporation model. The found neutron excess should be attributed to non-equilibrium emission[33].

5. Conclusions

The presented review paper refer to recent experimental data which have been deduced from improved measurements. Discrepancies between these recently measured Cf neutron spectra are much less than known from previous experiments (cf. Blinov's review).

The progress made concerning Cf spectrum calculations is emphasized. All statistical-model versions considered (MNM, GMNM, CEM, HFC) yield similar results in the energy range from 0.5 to 10 MeV. The MNM underestimates experimental data

at both spectrum ends (E < 0.5 MeV, E > 10 MeV). However, it can easily be applied for practical purposes. In particular, neutron spectra from induced fission reactions can be described with an sufficient accuracy in the most important energy region (0.5 - 10)MeV. The complexity of CEM and HFC calculations makes it necessary to consider a multitude of input data. According to our experience, precise consideration of nuclear structur is as important as the consideration of the fission process complexity including probability distributions, the exact CMS-LS transformation of the spectra (i.e. introduction of P(TKE) correlated with CMS spectrum) etc. However, such detailed studies are only applicable to well-investigated fission reactions (at present!).

The reviewed calculation methods don't take into account other possible emission mechanisms which might influence the total energy spectrum in certain energy ranges. Differential emission probabilities of neutrons which are evaporated during fragment acceleration as well as of neutrons originating from the ^{5}He decay have been estimated recently[45]. It was found that these processes are less important.

It was already pointed out[6,46] that further detailed investigations of multiple-differential emission probabilities of fission neutrons are necessary to clarify the open problems of fission neutron emission.

References

1) Prompt Fission Neutron Spectra, Proc. Cons. Meet., Vienna, 1971, (IAEA, Vienna)(1972)
2) Nucl. Data Standards for Nucl. Meas., Technical Reports Series No. 227 (IAEA, Vienna)(1983)
3) IAEA Cons. Meet. on the U-235 Fast-Neutron Fission Cross-Section, and the Cf-252 Fission Neutron Spectrum, Proc. INDC(NDS)-146/L(1983)
4) M.V. Blinov, Proc. IAEA Cons. Meet. on Neutron Source Properties, Debrecen, 1980, INDC(NDS)-114/GT(1980)
5) J. Terrell, Proc. IAEA Symp. on Physics and Chemistry of Fission, Salzburg, 1965, (IAEA, Vienna) Vol. II, 3
6) H. Märten et al., loc. cit. (3), p. 199
7) M. V. Blinov et al., Proc. Int. Conf. on Nucl. Data for Sci. and Techn., ed. by K.H. Böckhoff, D. Reichel Publ. Comp. Eindhoven (1983) 479 (Antwerp, 1983)
8) A. Lajtai et al., loc. cit. (3), p. 177
9) W.P. Poenitz and T. Tamura, loc. cit. (7), p. 465 and loc. cit. (3), p. 175
10) M.V. Blinov et al., preprint (1984)
11) R. Böttger et al., loc. cit. (7), p. 484
12) H. Märten et al., loc. cit. (7), p. 488
13) H. Märten et al., contributed paper to this AGM (Exp.)
14) J. Boldeman, Trans. Am. Nucl. Soc. 32(1979)733 and information about new measurements recieved via NDS (H.D. Lemmel, Note 84/5/11)
15) Mon Jiangshen et al., Chin. J. Nucl. Phys. 3(1981)163
16) J. Grundl and C. Eisenhauer, Natl. Bur. Stds. Pub., NBS-493(1977)
17) A. Chalupka et al., loc. cit. (3), p. 187
18) H. Klein et al., loc. cit. (3), p. 191
19) J. S. Fraser, Phys. Rev. 88(1952)536
20) B. E. Watt, Phys. Rev. 87(1952)1037
21) J. Terrell, Phys. Rev. 113(1959)527
22) H.R. Bowman et al., Phys. Rev. 126(1962)2120
23) V.S. Stavinski, Sov. Phys.-JETP 36(1959)629
24) R.W. Fuller, Phys. Rev. 126(1962)684
25) Y. Boneh and Z. Fraenkel, Phys. Rev. C10(1974)893
26) V.A. Rubtchenya, Leningrad report RI-28(1974)
27) B.C. Samanta et al., Phys. Lett. B108(1982)
28) E. Cheifetz et al., Phys. Rev. Lett. 29(1972)805
29) J.B. Wilhelmy et al., Phys. Rev. C5(1972)2041
30) A. Gavron, Phys. Rev. C13(1976)2561
31) V.F. Weisskopf, Phys. Rev. 52(1937)295 and J.M. Blatt, V.F. Weisskopf, Theoretical Nuclear Physics (New York, 1952)
32) W. Hauser and W. Feshbach, Phys. Rev. 87(1952)366
33) H. Märten and D. Seeliger, J. Phys. G 10(1984)349
34) H. Märten and D. Seeliger, contributed paper to this AGM (Theory, CEM)

35) I.C. Browne and F.S. Dietrich, Phys. Rev. C10(1974)2445
36) B.F. Gerasimenko et al., Neutron Physics (Proc. All-Union Conf., Kiev, 1980) Moscow, 1980, III, p. 137
37) B.F. Gerasimenko et al., Neutron Physics (Proc. All-Union Conf., Kiev, 1983) Moscow, 1984, I, p. 349
38) E. Nardi et al., Phys. Lett. 43B(1973)259
39) D. G. Madland and J.R. Nix, Nucl. Sci. Eng. 81(1982)213
40) D. G. Madland and J.R. Nix, loc. cit. (7), p. 473
41) D. G. Madland and R.J. LaBauve, preprint LA-UR-84-129 (1984)
42) H. Märten and D. Seeliger, INDC(GDR)-30/L
43) K.H. Schmidt et al., Z. Phys. A 308(1982)215
44) A.V. Ignatyuk et al., Yad. Fiz. 21(1975)485
45) H. Märten et al., loc. cit.(37), and INDC(GDR) in print (1984)
46) M.V. Blinov et al., loc. cit. (3), p. 161

DIFFERENTIAL AND INTEGRAL COMPARISONS OF THREE REPRESENTATIONS OF THE PROMPT NEUTRON SPECTRUM FOR THE SPONTANEOUS FISSION OF ^{252}Cf

D.G. MADLAND, R.J. LaBAUVE, J.R. NIX
Theoretical Division,
Los Alamos National Laboratory,
Los Alamos, New Mexico,
United States of America

Abstract

Because of their importance as neutron standards, we present comparisons of measured and calculated prompt fission neutron spectra N(E) and average prompt neutron multiplicities $\bar{\nu}_p$ for the spontaneous fission of ^{252}Cf. In particular, we test three representations of N(E) against recent experimental measurements of the differential spectrum and threshold integral cross sections. These representations are the Maxwellian spectrum, the NBS spectrum, and the Los Alamos spectrum of Madland and Nix. For the Maxwellian spectrum, we obtain the value of the Maxwellian temperature T_M by a least-squares adjustment to the experimental differential spectrum of Poenitz and Tamura. For the Los Alamos spectrum, a similar least-squares adjustment determines the nuclear level-density parameter a, which is the single unknown parameter that appears. The NBS spectrum has been previously constructed by adjustments to eight differential spectra measured during the period 1965 to 1974. Among these three representations, we find that the Los Alamos spectrum best reproduces both the differential and integral measurements, assuming ENDF/B-V cross sections in the calculation of the latter. Although the NBS spectrum reproduces the integral measurements fairly well, it fails to satisfactorily reproduce the new differential measurement, and the Maxwellian spectrum fails to satisfactorily reproduce the integral measurements. Additionally, we calculate a value of $\bar{\nu}_p$ from the Los Alamos theory that is within approximately 1% of experiment.

I. INTRODUCTION

The prompt fission neutron spectrum N(E) and average prompt neutron multiplicity $\bar{\nu}_p$ from the spontaneous fission of ^{252}Cf are used as reference standards in the experimental and applied neutron physics fields. Accordingly, demand for improvement in the accuracy of these standards is constantly driven by technical innovations and improvements that are occurring in these fields. For this reason we present detailed comparisons of recent measured and calculated prompt fission neutron spectra and average prompt neutron multiplicities for this standard reaction. In particular, we test three representations of N(E) against recent high-quality experimental measurements of the differential spectrum and threshold integral cross sections. These representations are the widely used Maxwellian spectrum, the National Bureau of Standards (NBS) spectrum,[1,2] and the Los Alamos spectrum based on the recent theory of Madland and Nix.[3-5]

For the Maxwellian spectrum, we obtain the value of the Maxwellian temperature T_M by a least-squares adjustment to the experimental differential spectrum of Poenitz and Tamura.[6,7] For the Los Alamos spectrum, a similar least-squares adjustment with respect to the same experimental spectrum determines the nuclear level-density parameter a, which is the single unknown parameter that appears. The NBS spectrum has been previously determined by empirical construction of line-segment corrections to a least-squares adjusted Maxwellian spectrum. Eight differential spectrum measurements from the period 1965 to 1974 were used in this determination.

Proceeding in three steps, we first present in Sec. II detailed descriptions of the physical content of the three spectrum representations to be tested. Second, in Sec. III we perform the least-squares adjustments of the Maxwellian and Los Alamos representations to the experimental differential spectrum of Poenitz and Tamura. We do not adjust the NBS representation since it has been previously determined. This is followed by a detailed comparison of the three spectra to the Poenitz and Tamura spectrum. We also compare in this section the value of $\bar{\nu}_p$ calculated with the Los Alamos theory to recent experimental values. Third, in Sec. IV we present fifteen integral cross-section calculations for each of the three spectrum representations and compare them with each other and with recent experimental integral cross sections as measured by Grundl et al.[8] and Kobayashi et al.[9,10] We present our conclusions from all comparisons in Sec. V.

II. THREE REPRESENTATIONS OF THE PROMPT FISSION NEUTRON SPECTRUM

In this section we describe the origin and physical content of the three representations of the prompt neutron spectrum for the spontaneous fission of ^{252}Cf that we are comparing in this work.

A. Maxwellian Spectrum.

The Maxwellian spectrum is given by

$$N(E) = \frac{2\sqrt{E}\,\exp(-E/T_M)}{\sqrt{\pi}\,T_M^{3/2}} , \tag{1}$$

where E is the energy of the emitted neutron and T_M, the single parameter of the spectrum, is the Maxwellian temperature expressed in units of energy by absorption of the Boltzmann constant. Like all spectra considered in this work, this spectrum has units of inverse energy and is normalized to unity when integrated from zero to infinity. The mean and mean-square energy are given, respectively, by

$$\langle E \rangle = \frac{3}{2} T_M , \text{ and} \tag{2}$$

$$\langle E^2 \rangle = \frac{15}{4} T_M^2 . \tag{3}$$

The Maxwellian spectrum neglects the center-of-mass motion of the fission fragments from which the neutrons are emitted, the distribution of fission-fragment excitation energy, and the energy dependence of the inverse process to neutron emission, namely, compound nucleus formation. Accordingly, it has little physical basis for describing fission neutron spectra other than the correct energy dependence at both low and high energies.

Nevertheless, it has been widely used for this purpose, partly because of the convenience of a single parameter representation and partly for the follow-

ing reason: In principle, the value of T_M must be rather large because T_M has to account not only for the average center-of-mass motion of the emitted neutrons, but also for the average center-of-mass motion of the fission fragments. In practice, however, the value of T_M is usually reduced in order that the spectrum reproduce the high-energy portion of the experimental spectrum. To preserve the normalization, this simultaneously increases the spectrum at lower energies, which then usually reproduces better the low-energy portion of the experimental spectrum. This spurious enhancement of energies below ~1 MeV simulates to some extent an effect that is due to the energy dependence of the cross section for the inverse process of compound nucleus formation, to be discussed later in this section. Thus, for the wrong physical reason, the Maxwellian spectrum reproduces a given experimental spectrum reasonably well, provided that the Maxwellian temperature T_M is suitably adjusted.

B. NBS Spectrum.

The NBS spectrum[1,2] is an empirically constructed spectrum that is based upon eight differential spectrum measurements performed during the period 1965 to 1974. The spectrum consists of a five-segment piecewise continuous representation containing twelve parameters and is given by

$$N(E) = \sum_{i=1}^{5} \mu_i(E)\, M(E) \quad , \tag{4}$$

where M(E) is the reference Maxwellian spectrum

$$M(E) = 0.6672 \sqrt{E} \exp(-E/1.42) \tag{5}$$

and $\mu_i(E)$ are five line-segment corrections given by

$$\begin{aligned}
\mu_1(E) &= 1 + 1.20E - 0.237, && 0 \leqq E \leqq 0.25 \text{ MeV}, \\
\mu_2(E) &= 1 - 0.14E + 0.098, && 0.25 \leqq E \leqq 0.8 \text{ MeV}, \\
\mu_3(E) &= 1 + 0.024E - 0.0332, && 0.8 \leqq E \leqq 1.5 \text{ MeV}, \\
\mu_4(E) &= 1 - 0.0006E + 0.0037, && 1.5 \leqq E \leqq 6.0 \text{ MeV, and} \\
\mu_5(E) &= \exp[-0.03(E - 6.0)], && 6.0 \leqq E < \infty \quad .
\end{aligned} \tag{6}$$

In these equations, E is in units of MeV and N(E) is in units of MeV^{-1}. The mean and mean-square energy of the NBS spectrum, obtained by numerical integration, are given, respectively, by

$$\langle E \rangle = 2.120 \text{ MeV, and} \tag{7}$$

$$\langle E^2 \rangle = 7.433 \text{ MeV}^2 \quad . \tag{8}$$

The NBS spectrum was constructed by first obtaining a reference Maxwellian spectrum M(E) from a weighted least-squares adjustment to eight measured differential spectra, and second, by obtaining five line-segment corrections in a final adjustment to the same measurements. The temperature parameter of the reference Maxwellian has the value T_M = 1.42 MeV, corresponding to a mean energy <E> = 2.130 MeV, which is 10 keV larger than the mean energy of the final spectrum. The difference is due largely to the influence of the exponential correction $\mu_5(E)$, which reduces slightly the high-energy portion of the reference Maxwellian M(E). In other words, the final adjustment in the NBS spectrum determined that the high-energy portion of the best-fit reference Maxwellian was still somewhat larger than experiment. At the low-energy end of the final adjusted spectrum, the linear corrections $\mu_1(E)$ and $\mu_2(E)$ indicate that the best-fit reference Maxwellian is, again, slightly larger than experiment for very low energies, but near 0.25 MeV is somewhat less than experiment. Thus, the NBS spectrum differs from a best-fit Maxwellian spectrum primarily by a reduction from that spectrum at very low and high energies and by an enhancement to that spectrum at energies near 0.25 MeV. The consequences of these differences will become evident in Secs. III and IV.

C. Los Alamos Spectrum.

The Los Alamos theory is directed at predicting N(E) and $\bar{\nu}_p$ as functions of both the fissioning nucleus and its excitation energy.[3] The formalism is based upon standard nuclear evaporation theory and accounts for the physical effects of (1) the center-of-mass motion of the fission fragments, (2) the distribution of fission-fragment excitation energy, and (3) the energy dependence of the cross section for the inverse process of compound nucleus formation. The expression for the Los Alamos spectrum is given by the average of the spectra

calculated for neutron emission from the light L and heavy H average fission fragments, namely

$$N(E) = \frac{1}{2}[N(E,E_f^L,\sigma_c^L) + N(E,E_f^H,\sigma_c^H)] \quad , \tag{9}$$

where E is the energy of the emitted neutron, E_f is the average kinetic energy per nucleon of a moving fission fragment, and σ_c is the compound nucleus formation cross section. The spectrum due to a moving fission fragment is given by

$$N(E,E_f,\sigma_c) = \frac{1}{2\sqrt{E_f}T_m^2} \int_{(\sqrt{E}-\sqrt{E_f})^2}^{(\sqrt{E}+\sqrt{E_f})^2} \sigma_c(\varepsilon)\sqrt{\varepsilon}\, d\varepsilon \times \int_0^{T_m} k(T)\, T \exp(-\varepsilon/T) dT \quad . \tag{10}$$

In this equation ε is the center-of-mass neutron energy, T is the fission-fragment residual nuclear temperature with a maximum value T_m, and k(T) is the temperature-dependent normalization constant for the corresponding center-of-mass spectrum.

The spectrum given by Eqs. (9) and (10) depends upon E_f^L, E_f^H, T_m, and the compound nucleus formation cross sections σ_c^L and σ_c^H, which are calculated by use of an optical-model potential. In this work we use the potential of Becchetti and Greenlees[11] to calculate these cross sections. The spectrum is evaluated numerically by Gaussian quadrature, as are its energy moments given by

$$\langle E^n \rangle = \int_0^\infty E^n N(E) dE \quad . \tag{11}$$

The values of E_f^L and E_f^H are obtained by use of momentum conservation, namely,

$$E_f^L = \frac{\langle A_H \rangle}{\langle A_L \rangle} \frac{\langle E_f^{tot} \rangle}{A} \quad , \text{ and} \tag{12}$$

$$E_f^H = \frac{\langle A_L \rangle}{\langle A_H \rangle} \frac{\langle E_f^{tot} \rangle}{A} \quad , \text{ where} \tag{13}$$

$\langle E_f^{tot} \rangle$ is the total average fission-fragment kinetic energy, A is the mass number of the compound nucleus undergoing fission, and $\langle A_L \rangle$ and $\langle A_H \rangle$ are the average mass numbers of the light and heavy fragments, respectively. For the spontaneous fission of ^{252}Cf, we use the values $\langle E_f^{tot} \rangle$ = 185.9 ± 0.5 MeV, $\langle A_L \rangle$ = 108, and $\langle A_H \rangle$ = 144 that are obtained from the measurements of Unik et al.[12]

The value of T_m is obtained from the initial total average fission-fragment excitation energy $\langle E^* \rangle$ by use of the relationship[13]

$$T_m = (\langle E^* \rangle / a)^{1/2} \quad , \tag{14}$$

where a is the nuclear level-density parameter. For spontaneous fission, $\langle E^* \rangle$ is given by

$$\langle E^* \rangle = \langle E_r \rangle - \langle E_f^{tot} \rangle \quad , \tag{15}$$

where $\langle E_r \rangle$ is the average energy release in fission. It is given exactly by

$$\langle E_r \rangle = \frac{\sum_{A_H} Y(A_H) E_r(A_H)}{\sum_{A_H} Y(A_H)} \quad , \tag{16}$$

where $Y(A_H)$ is the fission-fragment mass yield distribution, A_H is the heavy fragment mass number, and $E_r(A_H)$ is the average energy release for a given mass division. The latter quantity is obtained, in turn, by summing the contributions from all participating charge divisions, namely

$$E_r(A_H) = \frac{\sum_{Z_H} \rho(Z_H,A_H) E_r(Z_H,A_H)}{\sum_{Z_H} \rho(Z_H,A_H)} \quad , \tag{17}$$

where $\rho(Z_H,A_H)$ is the heavy fission-fragment charge distribution, Z_H is the heavy fragment atomic number, and $E_r(Z_H,A_H)$ is the energy release for a given mass and charge division. We assume the fission-fragment charge distribution to be of Gaussian form

$$\rho(Z_H,A_H) = \frac{1}{(2\pi\sigma_z^2)^{\frac{1}{2}}} \exp[-(Z_H - Z_H^P)^2/(2\sigma_z^2)] \quad , \tag{18}$$

with the most probable heavy fragment charge Z_H^P given by the relation

$$\frac{Z_H^P + c}{A_H} = \frac{Z}{A} = \frac{Z_L^P - c}{A_L} \quad , \tag{19}$$

where c is the charge division parameter.

For the spontaneous fission of ^{252}Cf we evaluate Eqs. (14)-(19) using experimental or derived systematic masses from the 1981 Wapstra-Bos evaluation[14] when they exist and otherwise the mass formula of Möller and Nix.[15] We use the fission-fragment mass-yield distribution $Y(A_H)$ measured by Weber et al.[16] and the value 0.5 charge units determined by Unik et al.[12] for the charge division parameter c, except for symmetric fission where c = 0. We also use a value of 0.5 charge units for the charge distribution width σ_z, which is approximately mid-range in the set of values determined by Wahl.[17] With these choices of mass sources, measured yields, and charge distribution parameters, we obtain a value for $\langle E_r \rangle$ of 218.886 MeV. This result was previously obtained in Ref. 4 and was used in Refs. 5 and 18. It is stable to within ± 55 keV for a change of ± 0.05 charge units in c and to within ± 220 keV for a change of ± 0.1 charge units in σ_z. These ranges are representative of the accuracy with which c and σ_z are known for the spontaneous fission of ^{252}Cf.

From Eqs. (14) and (15) we now obtain

$$T_m = (32.986/a)^{1/2} \text{ MeV}, \tag{20}$$

where the nuclear level-density parameter a is the single remaining parameter to be determined prior to calculating the spectrum. The determination of the level-density parameter and consequent calculation of the Los Alamos spectrum are presented in the next section. We will come back to Eq. (20) there.

Turning to the average prompt neutron mulitplicity, $\bar{\nu}_p$, the formalism for the Los Alamos spectrum gives[3]

$$\bar{\nu}_p = \frac{\langle E^* \rangle - \langle E_\gamma^{tot} \rangle}{\langle S_n \rangle + \langle \varepsilon \rangle} \quad , \tag{21}$$

where $\langle E_\gamma^{tot} \rangle$ is the measured total average prompt gamma energy, $\langle S_n \rangle$ is the average fission-fragment neutron separation energy calculated in the same way as $\langle E_r \rangle$, and $\langle \varepsilon \rangle$ is the average center-of-mass energy of the emitted neutrons calculated in an analogous way to the average laboratory energy $\langle E \rangle$ from Eq. (11). For ^{252}Cf(sf) we obtain $\langle S_n \rangle$ = 5.439 MeV, a result previously obtained in Ref. 4 and utilized in Ref. 5. We obtain the value $\langle E_\gamma^{tot} \rangle$ = 7.06 MeV from the experiment of Pleasonton et al.[19] Using these values in Eq. (21), we obtain

$$\bar{\nu}_p = \frac{25.926 \text{ MeV}}{5.439 \text{ MeV} + \langle \varepsilon \rangle} \quad , \tag{22}$$

where the evaluation of the average center-of-mass energy $\langle \varepsilon \rangle$ depends upon the evaluation of T_m, as given by Eq. (20). Accordingly, we return to Eq. (22) and the calculation of $\bar{\nu}_p$ in the next section.

III. DIFFERENTIAL COMPARISONS

In this section we compare the three representations of the prompt fission neutron spectrum that we are studying to each other and to a recent high-quality differential measurement of the spectrum. In fact, because of the use of the ^{252}Cf(sf) spectrum as a standard, we determine the Maxwellian temperature T_M by a least-squares adjustment to the experimental spectrum instead of by other means and, for the identical reason, we determine the nuclear level-density parameter a for the Los Alamos spectrum in the same way. The NBS spectrum, with twelve parameters, has been previously obtained by least-squares adjustments and therefore is already completely determined.

For our present purposes, we choose the recent differential spectrum measurement of Poenitz and Tamura[6,7] as our experimental reference spectrum. This experiment covers a secondary neutron energy range of 0.225 to 9 8 MeV with 51 points that represent approximately 95% of the total spectrum. The average experimental uncertainty in the set of 51 points is 3.6%.

A. Maxwellian Spectrum.

The least-squares adjustment of the Maxwellian spectrum to the experimental reference spectrum is performed with respect to the Maxwellian temperature parameter T_M. To obtain an absolute value of χ^2 per degree of freedom, the normalization of the experiment is recomputed for each iteration in the value of T_M. We find a minimum in χ^2, $\chi^2(\text{min}) = 1.201$, at a value of T_M = 1.429 MeV. This value yields mean and mean-square energies of the Maxwellian spectrum, from Eqs. (2) and (3), of 2.144 MeV and 7.658 MeV^2, respectively. These values are also given in Table I together with other properties of the Maxwellian spectrum.

The spectrum is computed using Eq. (1) and is compared to the experimental spectrum in Fig. 1 in absolute units, as well as in Figs. 2 and 3 where the ratio of the experimental spectrum to this spectrum is plotted. The highest energy experimental points on Fig. 1 indicate that perhaps the Maxwellian spectrum is slightly larger than experiment in this region. Inspection of Figs. 2 and 3 confirm this for energies greater than about 5 MeV, with departures from experiment that are perhaps as large as 10%. In addition, one sees that the Maxwellian spectrum is larger than experiment by 2-7% in the region below 0.4 MeV and that it is smaller by 2-5% in the region between 1.5 and 3.0 MeV. Thus, the spurious enhancement in the Maxwellian spectrum at low energies that we discussed in Sec. II.A is apparently too large at energies below 0.4 MeV. At high energy, despite the adjustment of T_M with respect to experiment, the Maxwellian spectrum is still somewhat greater than experiment, reflecting the fundamental difficulty that we discussed in Sec. II.A in accounting for two physical effects with a single parameter.

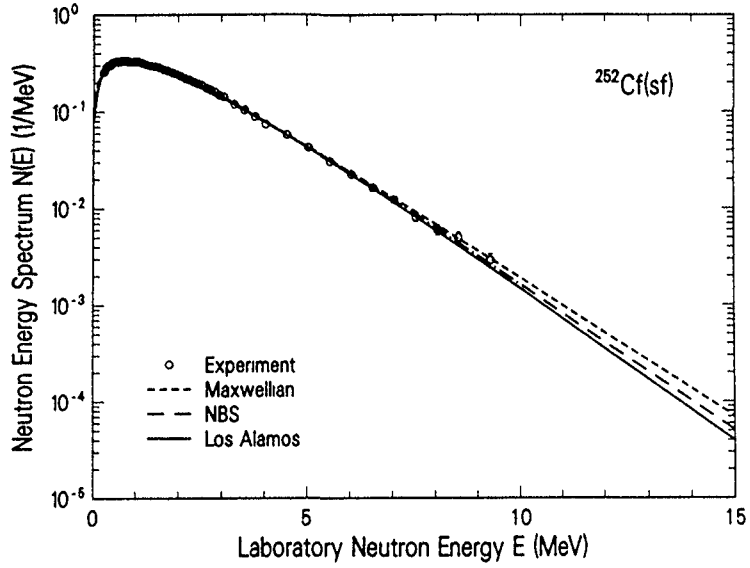

Fig. 1. Prompt fission neutron spectrum in the laboratory system for the spontaneous fission of ^{252}Cf. The dashed curve gives the least-squares adjusted Maxwellian spectrum calculated with Eq. (1), the dot-dashed curve gives the NBS spectrum calculated with Eq. (4), and the solid curve gives the least-squares adjusted Los Alamos spectrum calculated with Eq. (9). The experimental data are those of Poenitz and Tamura (Refs. 6 and 7).

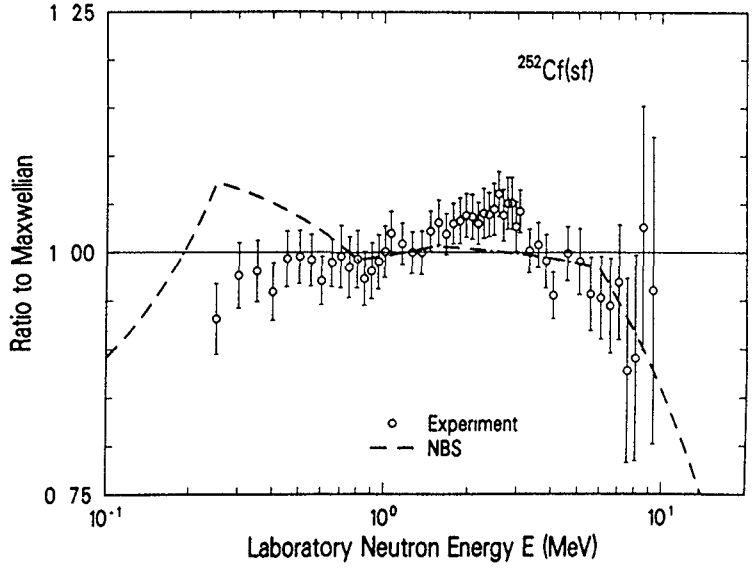

Fig. 2. Ratio of the NBS spectrum and the experimental spectrum to the least-squares adjusted Maxwellian spectrum, corresponding to the curves shown in Fig. 1.

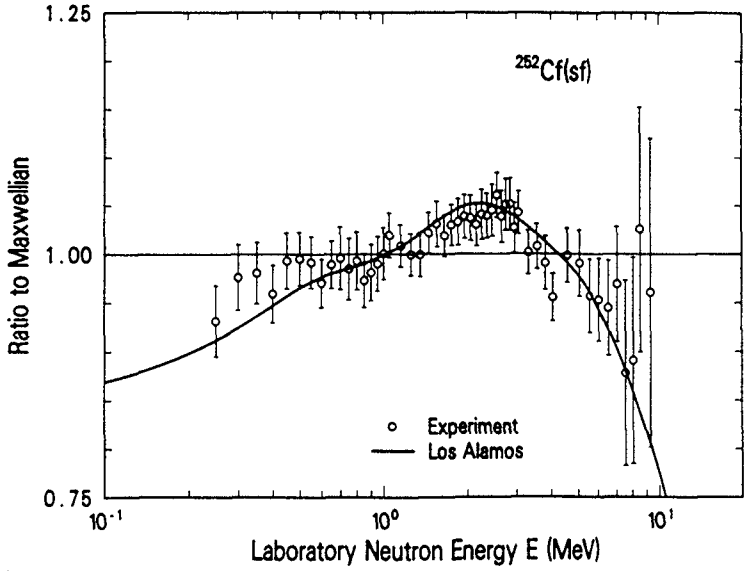

Fig. 3. Ratio of the least-squares adjusted Los Alamos spectrum and the experimental spectrum to the least-squres adjusted Maxwellian spectrum, corresponding to the curves shown in Fig. 1.

B. NBS Spectrum.

The NBS spectrum is calculated using Eqs. (4)-(6). The comparison of this spectrum to the experimental differential spectrum is shown in Fig. 1 in absolute units, and in Fig. 2, where the ratios of this spectrum and the experimental spectrum to the least-squares adjusted Maxwellian spectrum are shown. The computed value of χ^2 per degree of freedom for this previously determined spectrum is 1.922. The mean and mean-square energies are given by Eqs. (7) and (8), and are listed in Table I together with other properties of the NBS spectrum.

Figures 1 and 2 both indicate that the NBS spectrum agrees with the experimental reference spectrum in the high energy region better than the least-squares adjusted Maxwellian spectrum. On the other hand, the NBS spectrum lies about 5-15% above experiment at energies below 0.5 MeV, giving rise to the factor of 2 deterioration in the value of χ^2 per degree of freedom relative to that of the least-squares adjusted Maxwellian spectrum. In the region between 0.8 and 3.0 MeV, the NBS and adjusted Maxwellian spectra behave similarly, with departures from experiment ranging from 1 to 5%. Neither representation reproduces the structure in the experimental spectrum between 1.5 and 3.0 MeV.

C. Los Alamos Spectrum.

The least-squares adjustment of the Los Alamos spectrum to the experimental differential spectrum is performed with respect to the nuclear level-density parameter a. As before, to obtain an absolute value of χ^2 per degree of freedom, the normalization of the experiment is recomputed for each iteration in the value of a. We find a minimum in χ^2, $\chi^2(\text{min}) = 0.552$, at a value of a = A/9.15 (MeV). This result yields the value of T_m from Eq. (20). The values of the mean and mean-square energies are now obtained from Eq. (11) and are listed in Table I where they may be compared with the corresponding values from the

TABLE I

SOME PROPERTIES OF THREE REPRESENTATIONS OF THE PROMPT NEUTRON SPECTRUM FOR THE SPONTANEOUS FISSION OF ^{252}Cf

Quantity	Maxwellian	NBS	Los Alamos
Physical shape	smooth	five-segment piecewise continuous	smooth
Number of explicit parameters	1	12	3
Number of least-squares adjusted parameters in the present work	1	0	1
Adjusted Maxwellian temperature T_M (MeV)	1.429	—	—
Adjusted nuclear level-density parameter a (1/MeV)	—	—	A/9.15
<E> (MeV)	2.144	2.120	2.134
<E^2> (MeV^2)	7.658	7.433	7.364
$\bar{\nu}_p$	—	—	3.810
χ^2 (min)	1.201	1.922[a]	0.552

[a] In this case, χ^2 (min) is the only value of χ^2 and it is calculated assuming zero degrees of freedom.

Maxwellian and NBS spectra. The spectrum itself is evaluated using Eqs (9) and (10), and it is compared with the experimental differential spectrum in Figs 1 and 3

Figure 1 shows that the Los Alamos spectrum may be somewhat less than experiment at the two highest energy experimental points However, as shown by Fig 3, the uncertainties in these two data points are too large to draw any certain conclusion Figure 3 shows that the shape and magnitude of the Los Alamos spectrum agrees very well with experiment over the entire range, except for the region below 0 5 MeV where the experiment is under-predicted by amounts ranging from 1 to 5%.

The value of the nuclear level-density parameter a = A/9 15 (MeV) obtained in our least-squares adjustment also provides for the evaluation of Eq (22), which yields $\bar{\nu}_p$ = 3 810 This value is within 1.4% of the experimental value of 3 757 ± 0 009 obtained from the measurements of Amiel[20] and Smith,[21] and is within 1 0% of the experimental value of 3 773 ± 0 007 obtained by Spencer et al [22]

To conclude this section we combine Figs. 2 and 3 into Fig. 4, which then compares the experimental reference spectrum, the least-squares adjusted Maxwellian spectrum, the NBS spectrum, and the least-squres adjusted Los Alamos spectrum This figure clearly shows that the Los Alamos spectrum is the preferred representation for the present choice of the Poenitz and Tamura[6,7] experimental reference differential spectrum. This conclusion is reinforced by comparing the values of χ^2 per degree of freedom from Table I These show the Los Alamos spectrum to be the preferred representation by a factor ~ 3 over the NBS spectrum and by a factor ~ 2 over the Maxwellian spectrum. In addition to having the poorest agreement with the experimental differential spectrum, the NBS spectrum is somewhat unphysical in that it is only piecewise continuous.

IV. INTEGRAL COMPARISONS

In this section we calculate fifteen threshold integral cross sections for each of the three representations of the prompt fission neutron spectrum that we are studying and compare our results with recent high-quality experimental

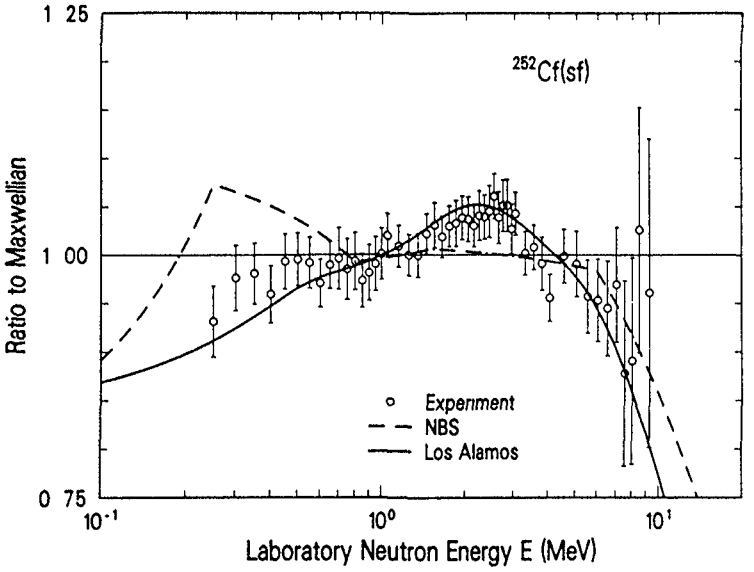

Fig. 4. Ratio of the NBS spectrum, the least-squares adjusted Los Alamos spectrum, and the experimental spectrum to the least-squares adjusted Maxwellian spectrum, corresponding to the curves shown in Fig. 1.

measurements carried out by Grundl et al.[8] and Kobayashi et al.[9,10] We also compare the trends of each of the three sets of calculated integral cross sections to assess the overall quality of the three spectrum representations being used. This latter comparison is, of course, only possible if identical pointwise cross sections are used in each set of calculations.

The integral cross section $\langle\sigma_r\rangle$ representing the net effect of the pointwise cross section $\sigma_r(E)$ in the presence of the neutron field N(E) is given by

$$\langle\sigma_r\rangle = \frac{\int_{E_1}^{E_2} \sigma_r(E)\, N(E)dE}{\int_{E_1}^{E_2} N(E)dE}, \qquad (23)$$

where E is the neutron energy, and E_1 and E_2 are the energy limits of the neutron field N(E). In this equation, $\sigma_r(E)$ is obtained from ENDF/B-V[23,24] with

one exception,[25] and N(E) is one of the three spectrum representations that we are comparing. By choosing ENDF/B-V cross sections, the values of E_1 and E_2 are set at 10^{-5} eV and 20 MeV, respectively. A trapezoidal integration of Eq. (23) is performed for each reaction studied.

For purposes of graphical presentation and discussion of our results, we define an effective threshold energy, E_{th}, for each reaction studied, as the energy that divides the pointwise cross section integral at 0.01% and 99.99%. We use the ratio C/E of calculated integral cross sections to experimental integral cross sections as a function of E_{th} in the graphical presentation of our results that we now discuss.

A. Maxwellian Spectrum

Our results for the least-squares adjusted Maxwellian spectrum are given in the fourth column of Table II where they can be compared directly with the experimental results in the third column, and in Fig. 5 where the C/E values are plotted as a function of the threshold energy E_{th}. There are three points to mention First, Table II shows that for a given set of pointwise cross sections and the Maxwellian spectrum, seven of the fifteen calculations are outside of the two-sigma measurement uncertainty. Second, Fig. 5 shows that nine of the fifteen calculations are outside of the one-sigma measurement uncertainty Third, the trend of the C/E ratios shown in Fig. 5 indicates that the accuracy of the Maxwellian spectrum is increasingly worse with increasing reaction threshold. That is, the Maxwellian spectrum is too large (hard) in the high energy portion of the spectrum This result is consistent with our conclusions for the differential spectrum comparisons of Sec. III As already discussed in Secs. II A and III.A, this illustrates a fundamental difficulty in accounting for two physical effects with a single parameter

B NBS Spectrum

Our results for the NBS spectrum are given in the fifth column of Table II and are illustrated in Fig. 6. Again, there are three points to be made. First, Table II shows for the identical set of pointwise cross sections and the NBS spectrum, only four of fifteen calculations are outside of the two-sigma

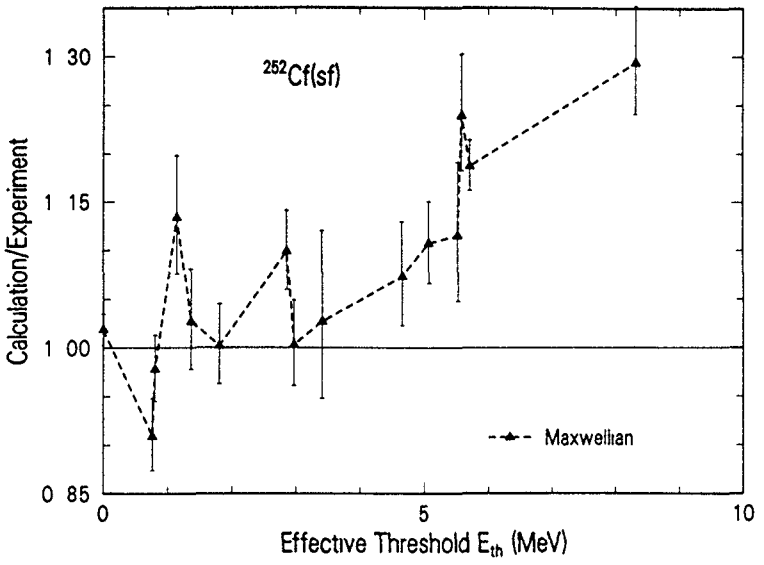

Fig. 5. Ratio of calculated to experimental integral cross sections for the prompt neutron spectrum from the spontaneous fission of ^{252}Cf as a function of the effective neutron threshold energy for the reaction. The calculated values are obtained using the least-squares adjusted Maxwellian spectrum from Eq. (1) in Eq. (23) together with ENDF/B-V pointwise cross sections. The experimental values are those of Grundl et al. (Ref. 8) and Kobayashi et al. (Refs. 9 and 10). The error bars shown are due only to the experimental uncertainties. The dashed line serves as a guide to the eye

measurement uncertainty. Second, Fig. 6 shows that only seven of the fifteen calculations are outside of the one-sigma measurement uncertainty. Third, the trend of the C/E ratios shown in Fig. 6 indicates that the NBS spectrum reproduces the experimental integral cross sections reasonably well for most values of the threshold energy.

C Los Alamos Spectrum.

Our results for the Los Alamos spectrum are given in the last column of Table II and are illustrated in Fig. 7. Once again, there are three points to address. First, Table II shows that for the identical set of pointwise cross sections and the Los Alamos spectrum, only two of the fifteen calculations are outside of the two-sigma measurement uncertainty. Second, Fig. 7 shows

TABLE II

COMPARISON OF MEASURED AND CALCULATED INTEGRAL CROSS SECTIONS FOR THREE REPRESENTATIONS OF THE PROMPT NEUTRON SPECTRUM FOR THE SPONTANEOUS FISSION OF ^{252}Cf†

Reaction	E_{th} (MeV)	Measurement[a]	Maxwellian Calc.	(C/E)	NBS Calc.	(C/E)	Los Alamos Calc.	(C/E)
$^{235}U(n,f)$	0.00	1216.0 ± 19.46	1238.657	(1.019)	1235.918	(1.016)	1235.720	(1.016)
$^{115}In(n,n')$	0.76	201.0 ± 8.2	182.804	(0.909)*	181.936	(0.905)*	186.009	(0.925)
$^{58}Ni(n,p)$	0.80	118.5 ± 4.1	115.888	(0.978)	113.891	(0.961)	114.039	(0.962)
$^{47}Ti(n,p)$	1.14	21.58 ± 1.16	24.463	(1.134)*	24.070	(1.115)*	24.209	(1.122)*
$^{54}Fe(n,p)$	1.36	87.63 ± 4.35	89.968	(1.027)	88.346	(1.008)	88.323	(1.008)
$^{32}S(n,p)$	1.80	72.52 ± 2.96	72.665	(1.002)	71.447	(0.985)	71.662	(0.988)
$^{27}Al(n,p)$	2.86	4.891 ± 0.179	5.375	(1.099)*	5.140	(1.051)	4.967	(1.016)
$^{46}Ti(n,p)$	2.97	14.04 ± 0.61	14.080	(1.003)	13.474	(0.960)	13.014	(0.927)
$^{51}V(n,p)$[b]	3.41	0.713 ± 0.059	0.732	(1.027)	0.688	(0.966)	0.657	(0.921)
$^{56}Fe(n,p)$	4.65	1.440 ± 0.070	1.546	(1.073)	1.416	(0.983)	1.322	(0.918)
$^{48}Ti(n,p)$	5.07	0.415 ± 0.016	0.460	(1.107)*	0.410	(0.986)	0.377	(0.907)*
$^{59}Co(n,\alpha)$	5.52	0.218 ± 0.014	0.243	(1.115)	0.217	(0.997)	0.200	(0.919)
$^{24}Mg(n,p)$	5.58	1.940 ± 0.093	2.404	(1.239)*	2.159	(1.113)*	1.995	(1.028)
$^{27}Al(n,\alpha)$	5.71	1.006 ± 0.022	1.195	(1.187)*	1.060	(1.053)*	0.973	(0.967)
$^{197}Au(n,2n)$	8.31	5.267 ± 0.226	6.817	(1.294)*	5.650	(1.073)	4.973	(0.944)

† Using ENDF/B-V pointwise cross sections, unless otherwise noted, and expressing the results in millibarns.

* Calculation outside two-sigma measurement uncertainty.

[a] The experimental measurements are those of Grundl et al. (Ref. 8) and Kobayashi et al. (Refs. 9 and 10).

[b] The pointwise cross section used in the calculation for this reaction is from Smith et al. (Ref. 25).

that nine of the fifteen calculations are outside of the one-sigma measurement uncertainty. Third, the trend of the C/E ratios shown in Fig. 7 indicates that the Los Alamos spectrum, like the NBS spectrum, reproduces the experimental integral cross sections reasonably well for most values of the threshold energy.

To conclude this section, we combine Figs. 5-7 into Fig. 8, to provide a comparison of the trends of the C/E values with E_{th} for the three spectrum representations compared. For visual clarity we delete the experimental uncertainties. This figure clearly shows that the least-squares adjusted Maxwellian spectrum is unsatisfactory when using the present choice of the Poenitz and Tamura experiment to determine the Maxwellian temperature T_M = 1.429 MeV. Although we do not show the results here, this same conclusion is obtained when

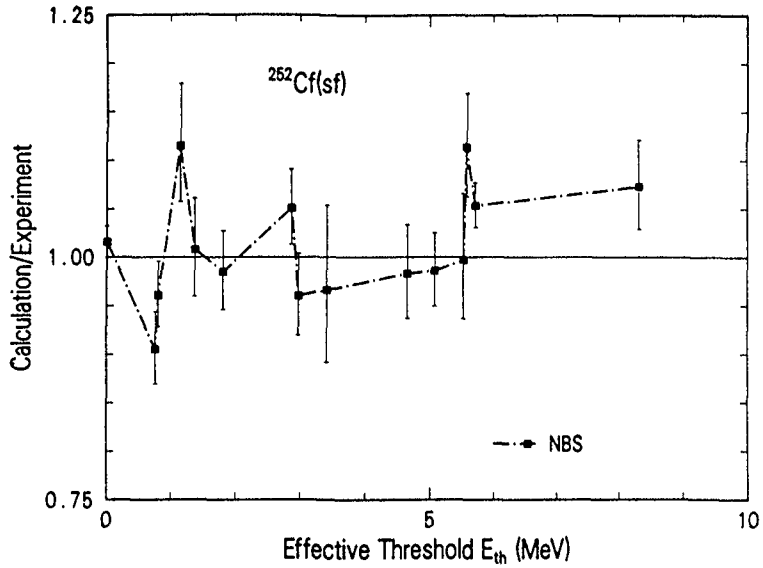

Fig. 6. Similar to Fig. 5 except that the calculated integral cross sections are obtained using the NBS spectrum from Eq. (4). The dot-dashed line serves as a guide to the eye.

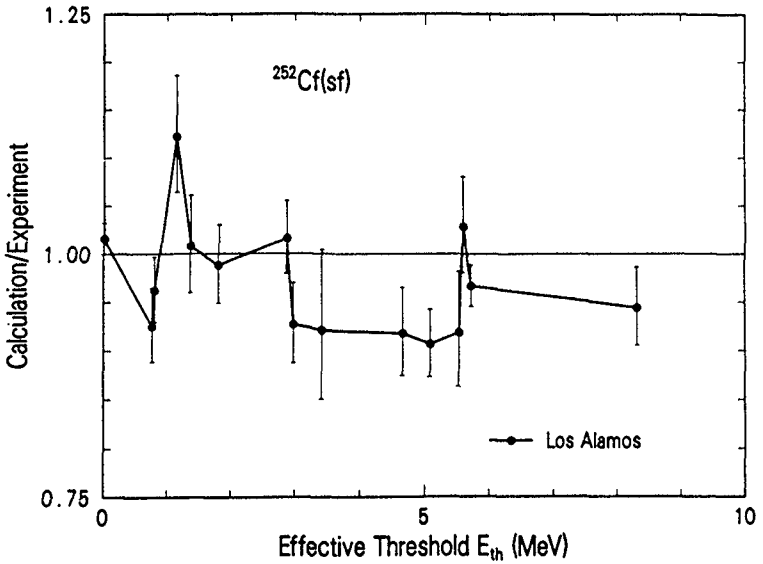

Fig. 7. Similar to Fig. 5 except that the calculated integral cross sections are obtained using the least-squares adjusted Los Alamos spectrum from Eq. (9). The solid line serves as a guide to the eye.

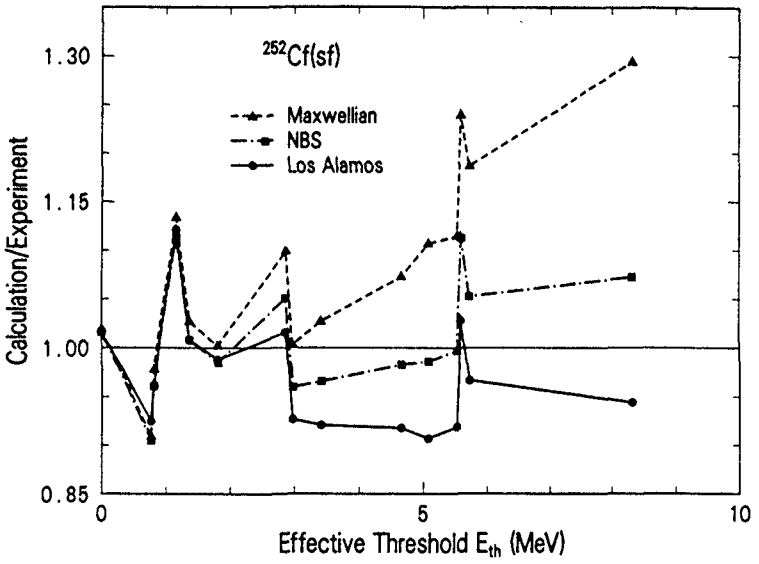

Fig. 8. Comparisons of ratios of calculated to experimental integral cross sections shown in Figs. 5-7 with error bars deleted for clarity. The dashed, dot-dashed, and solid lines serve as guides to the eye.

using the popular value T_M = 1.42 MeV. Finally, the figure also indicates, on the basis of the chosen set of experimental integral cross sections, that the NBS and Los Alamos spectra could each be adjusted somewhat, were it not for the constraints imposed by the experimental differential spectrum measurements.

V. CONCLUSIONS

On the basis of the comparisons presented here, we conclude that the Los Alamos spectrum is the perferred representation of N(E) because it best reproduces both the differential and integral measurements, assuming ENDF/B-V cross sections in the calculation of the latter. Although the NBS spectrum reproduces the integral measurements fairly well, it fails to satisfactorily reproduce the recent differential measurements, and the Maxwellian spectrum fails to satisfactorily reproduce the recent integral measurements. Additionally, we calculate a value of $\bar{\nu}_p$ from the Los Alamos theory that is within approximately 1% of experiment. In this study we have learned that well-measured high-threshold integral cross sections provide valuable constraints on the differential spectrum, assuming the pointwise cross sections are well known. Finally, we mention that the Los Alamos spectrum has been adopted as the preliminary standard spectrum for ENDF/B-VI. The spectrum is available in tabular form from the U.S. National Nuclear Data Center, Brookhaven National Laboratory.

ACKNOWLEDGMENTS

We are grateful to W. P. Poenitz and K. Kobayashi for the use of their experimental data and for several stimulating discussions and communications. This work was supported by the U.S. Department of Energy.

REFERENCES

1. J. A. Grundl and C. M. Eisenhauer, in Proc. Conf. on Nuclear Cross Sections and Technology, Washington, D.C., March 3-7, 1975, Vol. I, p. 250, National Bureau of Standards Special Publication 425, Washington, D.C. (1975).

2. J. Grundl and C. Eisenhauer, in Proc. First ASTM-EURATOM Symp. on Reactor Dosimetry, Petten, Holland, September 22-26, 1975, Part I, p. 425, Commission of the European Communities, EUR 5667 e/f (1977).

3. D. G. Madland and J. R. Nix, Nucl. Sci. Eng. 81, 213 (1982).

4. D. G. Madland and J. R. Nix, in Proc. Conf. on Nuclear Data for Science and Technology, Antwerp, Belgium, September 6-10, 1982, p. 473, D. Reidel, Dordrecht (1983).

5. D. G. Madland and J. R. Nix, in Proc. Specialists' Meeting on Yields and Decay Data of Fission Product Nuclides, Brookhaven National Laboratory, Upton, New York, October 24-27, 1983, p. 423, Brookhaven National Laboratory publication BNL-51778 (1984).

6. W. P. Poenitz and T. Tamura, in Proc. Conf. on Nuclear Data for Science and Technology, Antwerp, Belgium, September 6-10, 1982, p. 465, D. Reidel, Dordrecht (1983).

7. W. P. Poenitz, private communication (April 1983).

8. H. T. Heaton II, D. M. Gilliam, V. Spiegel, C. Eisenhauer, and J. A. Grundl, in Proc. NEANDC/NEACRP Specialist Meeting on Fast Neutron Cross Sections of U-233, U-235, U-238, and Pu-239, Argonne National Laboratory, Argonne, Illinois, June 28-30, 1976, p. 333, Argonne National Laboratory publication ANL-76-90 (1976); update by J. Grundl, D. Gilliam, D. McHarry, C. Eisenhauer, and P. Soran, in memorandum to CSEWG Subcommittee on Standards (May 1982).

9. K. Kobayashi, I. Kimura, and W. Mannhart, J. Nucl. Sci. Tech. 19, 341 (1982).

10. K. Kobayashi, I. Kimura, H. Gotoh, and H. Tominaga, submitted to Ann. Repts. of the Res. Reactor Inst., Kyoto Univ. (July 1984)

11. F. D. Becchetti, Jr., and G. W. Greenless, Phys. Rev. 182, 1190 (1969).

12. J. P. Unik, J. E. Gindler, L. E. Glendenin, K. F. Flynn, A. Gorski, and R. K. Sjoblom, in Proc. Third IAEA Symp. on Physics and Chemistry of Fission, Rochester, New York, August 13-17, 1973, Vol. II, p. 19, International Atomic Energy Agency, Vienna (1974).

13. J. Terrell, Phys. Rev. 113, 527 (1959).

14. A. H. Wapstra and K. Bos, private communication to the National Nuclear Data Center, Brookhaven National Laboratory (March 1982).

15. P. Möller and J. R. Nix, At. Data Nucl. Data Tables 26, 165 (1981).

16. J. Weber, H. C. Britt, and J. B. Wilhelmy, Phys. Rev. C 23, 2100 (1981).

17. A. C. Wahl, J. Radioanalytical Chem. 55, 111 (1980).

18. D. G. Madland and R. J. LaBauve, Trans. Am. Nucl. Soc. 46, 760 (1984).

19. F. Pleasonton, R. L. Ferguson, and H. W. Schmitt, private communication (April 1982).

20. S. Amiel, in Proc. Second IAEA Symp. on Physics and Chemistry of Fission, Vienna, Austria, July 28-August 1, 1969, p. 569, International Atomic Energy Agency, Vienna (1969).

21. J. R. Smith, in Proc Symp. on Nuclear Data Problems for Thermal Reactor Applications, Brookhaven National Laboratory, 1978, p. 5-1, Electric Power Research Institute publication EPRI-NP-1093 (1979).

22. R. R. Spencer, R. Gwin, and R. Ingle, Nucl. Sci. Eng. 80, 603 (1982).

23. B. A. Magurno, in Proc. Advisory Group Meeting on Nuclear Data for Reactor Dosimetry, Vienna, Austria, November 13-17, 1978, p. 1, International Atomic Energy Agency publication INDC(NDS)-103/M, Vienna (May 1979).

24. M. R. Bhat, in ENDF/B Summary Documentation, Brookhaven National Laboratory publication BNL-NCS-17541 (ENDF-201), Brookhaven National Laboratory (July 1979).

25. D. L. Smith, J. W. Meadows, and I. Kanno, Argonne National Laboratory report ANL/NDM-85, Argonne National Laboratory (June 1984).

CALCULATION OF THE ^{252}Cf(sf) NEUTRON SPECTRUM IN THE FRAMEWORK OF A COMPLEX CASCADE EVAPORATION MODEL (CEM)

H. MÄRTEN, D. SEELIGER
Technical University of Dresden,
Dresden, German Democratic Republic

Fission neutrons are predominantly emitted (evaporated) from fully accelerated fission fragments. The consideration of other eventual emission mechanisms[1,2] is practically impossible due to the poor knowledge of their characteristics.

The complex cascade evaporation model was successfully applied to calculate the Cf neutron spectrum in the high-energy range[1,2]. A comprehensive study of the model sensitivity in regard of input data variations was described in Ref. 2. The CEM is also used to describe multiple-differential probabilities of Cf fission neutron emission[2].

The previous version of the CEM[1] was improved regarding

i) the level density description[3,4] which takes into account shell correction as well as pairing condensation both depending on excitation energy,

ii) the full consideration of the model dependence on fragment mass number A and total kinetic energy TKE of complementary fission fragments, i.e. introduction of initial distributions in fragment excitation energy in dependence of both variables,

iii) the calculation of the inverse cross section for compound-nucleus formation on the base of the optical model,

iv) numerical procedures so as to have the possibility of spectrum calculations in the energy range from 1 keV to 40 MeV.

The CMS (center-of-mass system) anisotropy is taken into account roughly on the base of Gavron's study yielding a changed spectrum description (cf. Ref. 2 and Ref. 8)[5]: The calculated Cf spectrum is enhanced at low energy (+5.5 % at 10 keV) as well as in the high-energy range (+2 % for the (10-20) MeV region); the spectrum is reduced from 0.8 to 3 MeV. Results of the new calculation are compared with recent experimental data in Fig. 1. In the low-energy region, the deviations of the calculated spectrum from a Maxwellian with T=1.42 MeV are small (-3.5 % at 10 keV). The calculated average lab-frame emission energy amounts to 2.111 MeV. See Ref. 8 for further comparisons. The calculated spectrum is still preliminary pending check-up of input data (excitation energy distributions as a function of both A and TKE especially).

Fig. 1
The CEM spectrum of $^{252}Cf(sf)$ neutrons (continous line) in comparison with recent experimental data on the high-energy end of the energy distribution (crosses - Ref. 6, dots - Ref. 7). Data are represented as percentage deviations D from a Maxwellian spectrum with T=1.42 MeV. The NBS evaluation (Ref. 9) is shown, too (dashed line, above 6 MeV).

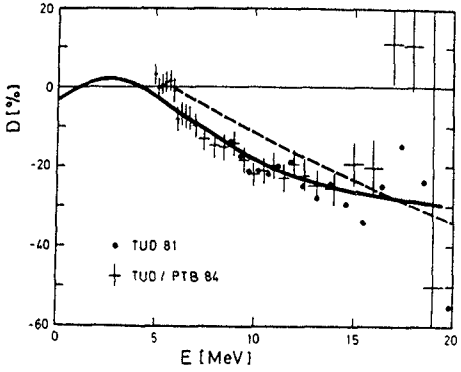

References

1 - H. Märten and D. Seeliger, J. Phys. G 10(1984)349

2 - H. Märten et al., Proc. IAEA Cons. Meet. on the U-235 Fast-Neutron Fission Cross-Section, and the Cf-252 Fission-Neutron Spectrum, Smolenice, 1983 INDC(NDS)-146/L (1983) 199

3 - K.H. Schmidt et al., Z. Phys. A 308 (1982)215

4 - J. Toke and W.J. Swiatecki, Nucl. Phys. A 372 (1981)

5 - A. Gavron, Phys. Rev. C 13 (1976) 2561

6 - H. Märten et al., INDC(GDR)-28/L (1984)

7 - H. Märten et al., contr. paper to this AGM

8 - H. Märten and D. Seeliger, review paper to this AGM

9 - J. Grundl and C. Eisenhauer, NBS-493 (1977)

STATISTICAL CALCULATION OF THE ^{252}Cf SPONTANEOUS FISSION PROMPT NEUTRON SPECTRUM

B.F. GERASIMENKO, V.A. RUBCHENYA
Khlopin Radium Institute,
Leningrad,
Union of Soviet Socialist Republics

The results of calculations of the prompt neutron spectrum and prompt neutron multiplicity for the ^{252}Cf spontaneous fission on the base of Hauser-Feshbach method are presented, similarly to /1/. The calculations were done on the assumption of the isotropic neutron emission in the center-of-mass system from heated fully accelerated fragments. The fragment excitation energy dispersion, the cascade character of neutron emission and the competition between the neutron emission and γ-emission were taken into account. The evolution of excitation energy distribution on each cascade stage was taken consistently into consideration. A different than in work /2/ relation between the average fragment excitation energy and the average number of the emitted neutrons was applied. The level density expression was used in the form accounting for shell effects. The transmission coefficients T_{lj} were calculated according to optical model with potential parameters suggested in work /3/. The calculations were done within the interval of neutron kinetic energies (in laboratory system) from 0.001 to 30.0 MeV.

In the figure the calculated integral spectrum of ^{252}Cf spontaneous fission prompt neutrons is shown in comparison with the experimental spectrum /1/. As seen from the figure, the calculated integral prompt neutron spectrum is in good agreement with experimental data in the region 0.001-15.0 MeV. The following theoretical values of the integral spectrum and of prompt neutron multiplicity parameters were obtained: $\bar{E}$ = 2.127 MeV, $\bar{\nu}$ = 4.087, σ_ν^2 = 1.46. The sensitivity of the calculations with regard to input data of the model is discussed.

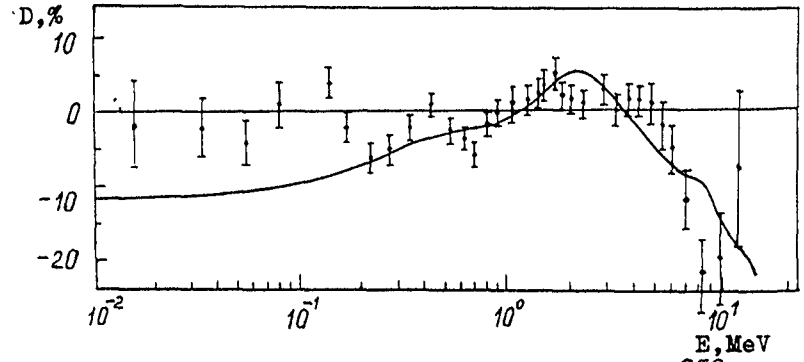

The calculated total prompt neutron spectrum of ^{252}Cf spontaneous fission and the experimental one. The spectra are given in the form of ratio to the Maxwellian distribution with T = 1.42 MeV. ——— - calculation (present paper), . - experiment /1/.

Table

The theoretical total prompt neutron spectrum ^{252}Cf spontaneous fission (E in units of MeV, N(E) in units of MeV^{-1})

E	0.20-02	0.40-02	0.60-02	0.80-02	0.10-01	0.12-01	0.14-01
N(E)	2.62-02	3.71-02	4.54-02	5.23-02	5.85-02	6.40-02	6.91-02
E	0.16-01	0.18-01	0.20-01	0.50-01	0.80-01	0.11+00	0.14+00
N(E)	7.38-02	7.82-02	8.24-02	1.29-01	1.61-01	1.86-01	2.07-01
E	0.17+00	0.20+00	0.35+00	0.50+00	0.65+00	0.80+00	0.95+00
N(E)	2.25-01	2.41-01	2.95-01	3.22-01	3.33-01	3.34-01	3.30-01
E	0.11+01	0.14+01	0.17+01	0.20+01	0.23+01	0.26+01	0.29+01
N(E)	3.22-01	3.00-01	2.74-01	2.42-01	2.10-01	1.80-01	1.52-01
E	0.32+01	0.35+01	0.44+01	0.53+01	0.62+01	0.71+01	0.80+01
N(E)	1.28-01	1.07-01	6.14-02	3.48-02	1.95-02	1.09-02	6.15-03
E	1.05+01	1.30+01	1.55+01	1.80+01	2.05+01	2.30+01	
N(E)	1.12-03	1.82-04	2.71-05	3.69-06	4.52-07	4.88-08	

REFERENCES

1. Batenkov O. I., Blinov M. V., Boykov G. S., Vitenko V. A., Rubchenya V. A. - Proc. of the IAEA Consultants'Meeting on the ^{235}U fission cross-sections and on the ^{252}Cf fission neutron spectrum. Vienna: IAEA, 1983, p. 161-173.
2. Browne J. C., Dietrich F. S. - Phys. Rev., 1974, vol.10C, N°6, p.2545-2549.
3. Becchetti F. D., Greenlees G. W. - Phys. Rev., 1969, vol. 182, N°4, p. 1190-1209.

RECENT DEVELOPMENTS IN THE INVESTIGATION OF ^{252}Cf SPONTANEOUS FISSION PROMPT NEUTRON SPECTRUM

M.V. BLINOV
Khlopin Radium Institute,
Leningrad,
Union of Soviet Socialist Republics

Abstract

The results of experimental and theoretical investigations carried out in the recent years for determination of the shape of the standard continuous neutron spectrum - energy distribution of ^{252}Cf spontaneous fission prompt neutrons are considered in the report.

1. INTRODUCTION

The review of experimental and theoretical investigations on the ^{252}Cf spontaneous fission neutron spectrum as an international standard of neutron spectrum was presented in a number of papers /1-5/. The files of INDC/NEANDC standards in 1980 and 1982 recommended to use this spectrum - - standard in the form of Maxwellian distribution with the parameter T = 1.42 MeV. The IAEA Consultant's meetings marked that this conception was a certain approximation and further measurements were necessary for specification of the spectrum.

After the last review /5/ in 1979 five years passed and a number of new experimental and theoretical works appeared during this period. Measurements were done in a broad energy interval from 0.001 to 30 MeV. The precision of those measurements was high as a rule. There were published several works carried out by the activation foils method (integral method), that is very useful, especially at high energies. Intensive theoretical calculations were done both by the evaporation model and by the statistical model. A number of investigations were fulfilled on studying the process of fission neutrons emission that is important both for correct calculations and for evaluations.

In the present report there is a brief consideration of the experimental and theoretical information on the spectrum of ^{252}Cf spontaneous fission prompt neutrons, obtained in the period 1980-1984.

2. SPECTRUM MEASUREMENTS (differential methods)

2.1. Methods of measurements and neutron detectors

Table 1 summarizes the data on the works done by differential methods /6-19/. The time of flight method was used in all the works except two /7, 9/. Böttger, Klein et al. in their works /11, 15/ used a liquid scintillation detector (NE-213) placed at a great flight distance (12 m) from the fission source. Good time resolution of the spectrometer (1.5 ns) in combination with a great flight base provided high energy resolution. In the work of Poenitz and Tamura /11, 17/ "black" neutron detectors with registration efficiency 77-98 % were applied. In works /12/ and /16/ fast ionization chambers with ^{235}U layers were used for neutron detection, providing time resolution ~ 1.5 ns. Such chambers are thresholdless detectors. Boldeman /18/ used a plastic scintillator NE-102 and lithium glasses. In the work of Lajtai et al. /14/ lithium glasses NE-912 were used in a special construction providing a sufficient distance of the glasses from the massive scatterer - the glass of the P. E. M. photocathode. Blinov, Vitenko et al. /6/ made use of thin (2 and 4 mm) crystals of ^{6}LiI (Eu) in a lightened packing. They applied different methods of decrease of the accidental coincidences background /20/

Table 1

Recent data (after 1979) on the ^{252}Cf Fission Neutron Spectrum (differential methods)

N	Year	Authors, ref.	Neutron energy range (MeV)	Method, neutron detector	T_{maxW}, $\bar{E}$ (MeV)
1	1980	Blinov et al. /6/	0.0003-1	TOF, crystal $^{6}LiI(Eu)$	Graphic presentation
2	1981	Jasicek, Bensch /7/	0.9-10	MRP*, proportional counter	1.409±0.015
3	1981	Mon Jiang-sken et al./8/	0.45-15	TOF, liquid scintillator	1.416±0.025 2.124±0.035
4	1981	Bolshov et al. /9/	1-11	MRP, stilben	1.413±0.017
5	1982	Poenitz et al. /10/	0.2-10	TOF, two "black" detectors	1.439±0.010 2.159
6	1982	Böttger et al. /11/	2-14	TOF, NE-213	1.355
7	1982	Blinov et al. /12/	0.01-7	TOF, chamber with U-235	1.418±0.024
8	1982	Märten et al. /13/	10-30	TOF, NE-213	Graphic presontation
9	1983	Lajtai et al. /14/	0.025-12	TOF, glass NE-912	Graphic and numerical presentation
10	1983	Batenkov et al. /16/	0.01-10	TOF, chamber with U-235	Graphic presentation
11	1983	Klein et al. /15/	2-14	TOF, NE-213	1.355
12	1983	Poenitz et al. /17/	0.2-10	TOF, "black" detectors	1.439±0.010 2.159
13	1983	Boldeman et al. /18/	1-14.6	TOF, plastic NE-102	1.424±0.013 2.136±0.020
			0.2-2	TOF, lithium glass	
14	1984	Boytsov et al. /19/	0.01-3	TOF, chamber with U-235, antracene	1.417±0.026

* MRP - Method of registration of the energy distribution of recoil protons

and managed to lower the measurement threshold to the energy 300 eV. Jasicek and Bensch /7/ measured the recoil proton spectrum with gas proportional counters filled with methane and krypton, and Bolshov et al. /9/ - with stilbene and antracene crystals.

2.2. Efficiency of neutron detectors

Much attention was payed to correct determination of efficiency in the works. As a rule, the efficiency was determined experimentally using definite neutron fluxes from different reactions on accelerators.

In the work of Boldeman /18/ the method of associated particles (precision ±2 %) was applied for determination of absolute efficiency. In work /8, 12/ the counter calibration was carried out in neutron fluxes of different energies, appearing in the reaction $D(d,n)^{3}He$. The determination of the flux was carried out by means of a telescope of recoil proton counters, that was used in the intercomparisons. For the type of the detector used in work /10, 17/ (black detector) the efficiency determination was done in other laboratories by the associated particles method. In the work the determination precision shown was 1 %.

It is worth mentioning that the necessity to measure the efficiency in exact geometrical conditions of the main experiment and using the same electronic system of the spectrometer is still an important problem. This is not always fulfilled that creates additional unaccounted uncertainties. In works /12, 16/ the efficiency of the detector-chamber with thin uranium layers was determined by the ^{235}U-standard cross-section with the corrections for the efficiency of fragments registration. The efficiency of thin lithium glasses (1 mm thick) /14/ and of $^{6}LiI(Eu)$ crystals (2 mm thick) /6/ was determined by the cross-section of the $^{6}Li(n,\alpha)$ reaction - standard and also by introducing the corrections, calculated by the Monte-Carlo method taking into account the development of the process in time (time function of the response). The efficiency of the thick (9.5 mm) glass in work /14/ was determined on Van-de-Graaf accelerator relative to the efficiency of a thin glass.

2.3. Californium layers and fragment detectors

In the work of Böttger, Klein et al. /11/ the quality of the layer was thoroughly investigated, though there was rather good discrimination of the pulses of fragments from alpha-particles. It was found that the fragments flying out at the angles 85° and 90° (to the perpendicular to the plane of the backing were not registered for the most part (fig. 1). The authors came to the conclusion that it is the influence of the quality of the backing - the roughness of its surface. In the work of Poenitz and Tamura /10/ there was not good discrimination of the pulses from fragments and alpha-particles, which could be connected with bad quality of the layer. On this account the authors considered their measurements to be preliminary and suggested to carry out new measurements with a good layer. The method of preparing and checking of the quality of the layer was

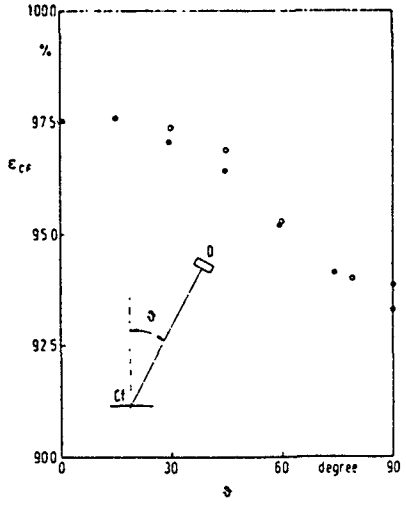

Fig. 1. Efficiency of fragments registration in dependence on the position of the neutron detector /11/. White dots-experiment, black - calculation.

discussed in detail in the works of Blinov and Batenkov /12, 16/. The authors measured the spectra of fragments from the californium layer with semiconductor detectors situated at the distance 100 cm from the layer at different angles (angular resolution 2°). The quality of the layer was shown to be very high (fig. 2) The backing was polished to high quality of the surface for this experiment. In works /8, 13, 14, 18/ the problem of the layer quality was not considered.

The analysis of the influence of other fissile nuclides in the layer under study was given in work /16/ only. It appeared to be equal $5 \cdot 10^{-4}$ in relation to ^{252}Cf. Neutrons from the reaction (α,n) do not influence the spectrum (except the increase of the accidental coincidences background) in case of fragment-neutron coincidences being realized in the set-up. In works /7/ and /9/ some distortion of the spectrum could take place due to the reaction (α,n).

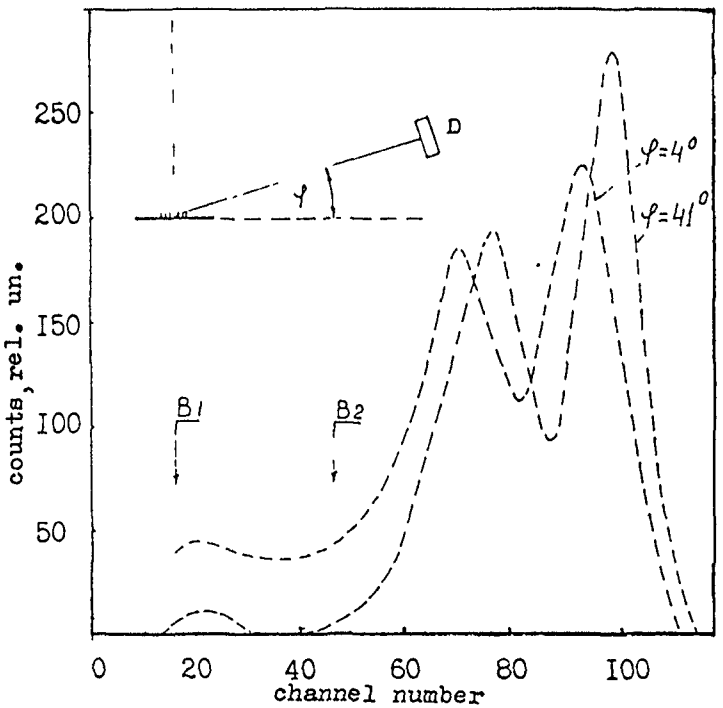

Fig. 2. Energy spectra of californium fission fragments in dependence on the angle of fragments detection (the angle-relative to the backing plane) /16/.

Recently miniature fast current ionization chambers have started to be widely used as fragment detectors, enabling to obtain time resolution ~ 1 ns, giving good discrimination of the pulses of fragments from alpha-particles and having low mass /11, 12/. Gas scintillation counters were used in the form of special constructions, in which the influence of neutron scattering from the photomultiplier was decreased /6, 10, 14/. Only in work /8/ a thin scintillation film was applied situated immediately on the photocathode of the P. E. M., that lead to considerable scattering of the neutrons.

2.4. Background conditions of the measurements

Much attention in works /10-17/ was payed to correct account of the accidental coincidences background component connected with the uncorrelated fission events. This component had not been taken into account in a number of works before, although its influence in some cases can be very considerable. For essential decrease of this background in works /6, 12, 14, 16/ the pile-up rejector was used - the device that did not allow to register the cases connected with the appearing of two fission pulses during the time interval of the measurements. This is especially important in the region of low energies of neutrons.

The influence of the scattered neutrons is discussed in the recent works thoroughly enough. As a rule, the authors try to reduce to minimum the masses of the detectors and construction elements of the set-ups /6, 14, 16, 18, 19/. Sometimes the influence of the air medium was taken into account /15, 16/. In works /10, 11, 15, 17/ big collimators were used that creates the sources of the scattered neutrons background. In work /11/ the study of the collimator's characteristics brought the authors to the conclusion that the cases with energy loss less than 10 % make a contribution less than 0.5 % to the main peak. In the work of Poenitz /10/ it is reported that the calculations show the summary scattering in the system of collimators to be less than 0.3 %. Though the effects are not great, still it seams that very thorough and convincing investigations of the scattering properties of the devices and detailed description of the results are necessary in all the works making use of collimating devices.

2.5. The results of the measurements

The results of four works in the low energy region: /6/ (energy region 0.0003-1 MeV), /14/ (0.025-1.2 MeV),

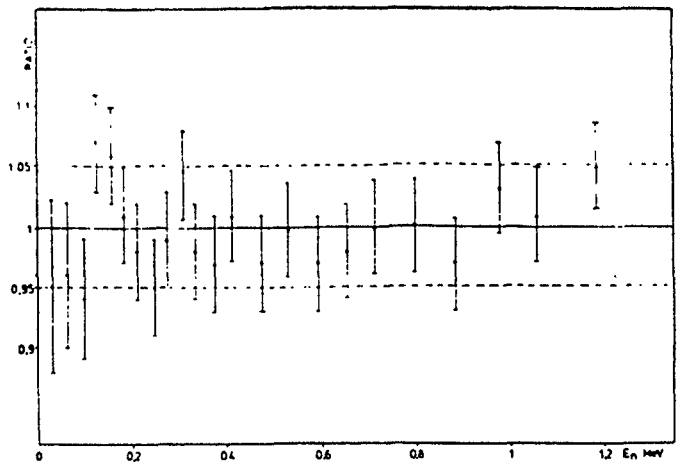

Fig. 3. Ratio of the experimental data of work /14/ to the Maxwellian distribution (T = 1.42 MeV).

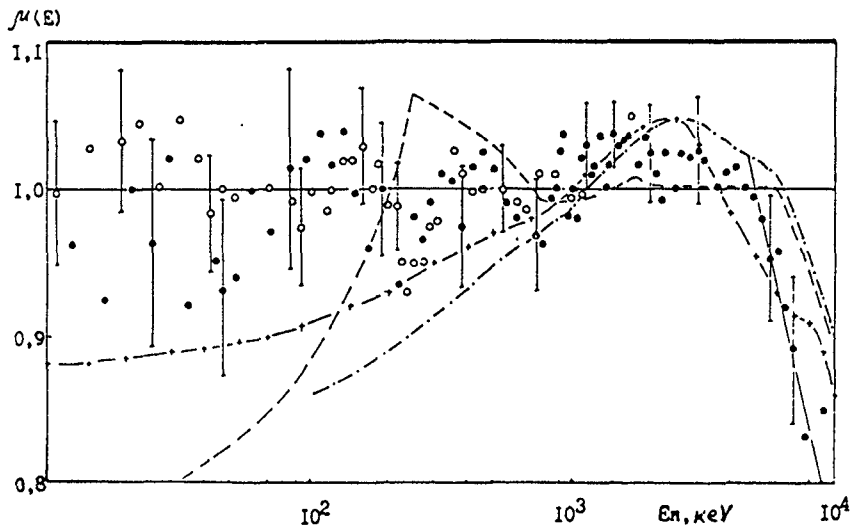

Fig. 4. Ratio of experimental data of works /16/ - • and /6/ - 0 to the Maxwellian distribution (T = 1.42 MeV). Dotted line-evaluation /38/. -+- calculation /32/, -•- calculation /30/.

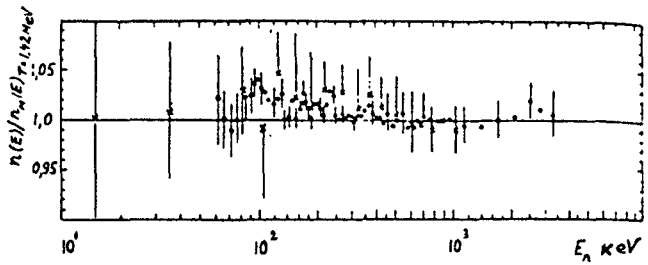

Fig. 5. Ratio of the experimental data of work /19/ to the Maxwellian distribution (T = 1.42 MeV).

/19/ (0.01-3 MeV) and /16/ (0.01-10 MeV) - are in good agreement with each other within the limits of experimental errors, and also with the Maxwellian distribution (T = 1.42 MeV) (fig. 3, 4, 5).

In the middle energy region (1-7 MeV) the shape of the spectrum is very close to the Maxwellian one, although a tendency appeares to exceed the Maxwellian by several per cent in the energy region 2-4 MeV.

For energies higher than 6-7 MeV the situation gets complicated; it is especially bad for energies 10-15 MeV, where the errors are high connected with the determination of the "zero" time, scale calibration and statistic uncertanties. The experimental data in this region (7-13 MeV) are between the Maxwellian distribution (T = 1.42 MeV) (Boldeman's results) /18/ and the negative deviation ~ 20 % at 10 MeV in the work of Böttger /11/ (fig. 6 and 7). The region of high energies (7-15 MeV) is the region of maximum discrepancies at present.

In the energy region more than 20 MeV there is yet only one work /13/ that has shown an interesting result - an essential excess of neutrons over the expected value (fig. 8).

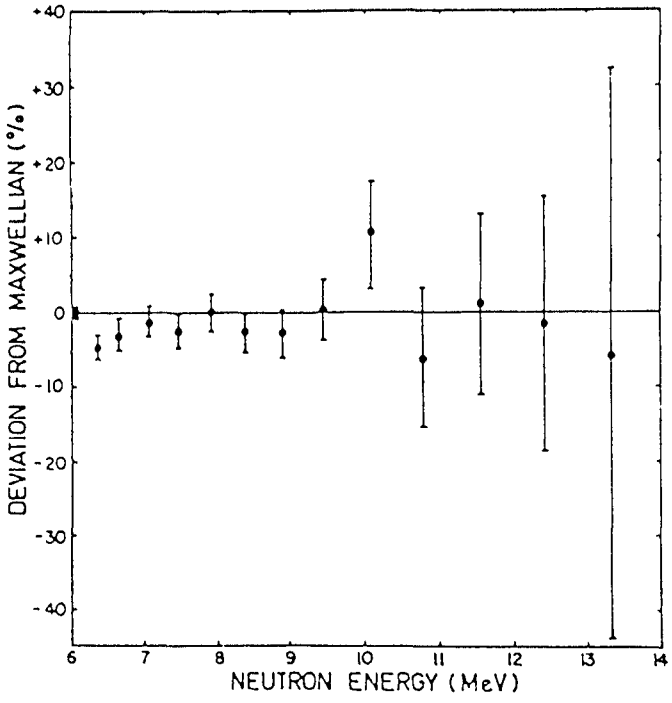

Fig. 6. Deviation of the experimental data of work /18/ from the Maxwellian.

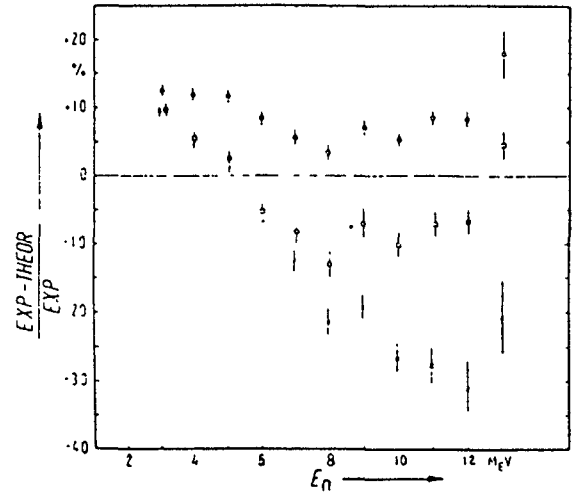

Fig. 7. Relative deviation of neutron yields in work /11/ from the NBS evaluation /38/ /□/, the Maxwellian distribution with the temperature parameter T = 1.355 MeV /o/ and T = 1.425 MeV /x/.

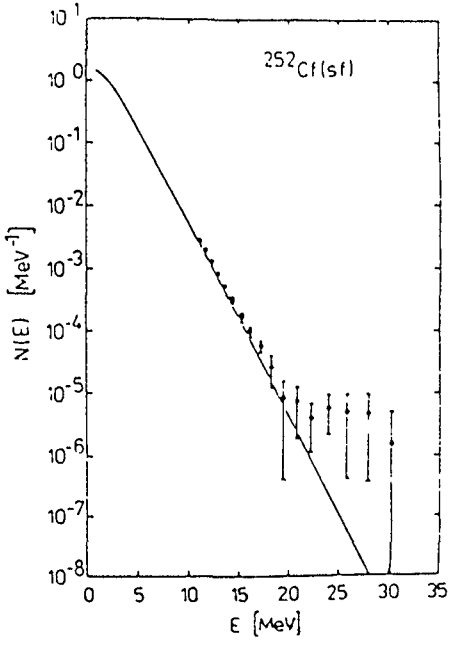

Fig. 8. Experimental data in the high energy range in comparison with calculation results by the cascade evaporation model /13/.

3. Spectrum measurements (integral methods)

In the period under consideration only one integral method was used - the method of activation of foils by different nuclear reactions (n, p), (n, α), (n, γ), (n, 2n) in the field of neutrons of ^{252}Cf spontaneous fission. If the dependence of the reaction cross-section on the energy of neutrons is well known, then, using a certain conception of the shape of neutron spectrum, it is possible to calculate the average cross-section and to compare it with the one obtained in the experiment. Such detectors were used on the base of almost 40 reactions.

In works /21-23/ the average cross-sections of a number of reactions were measured for different nuclides in the field of neutrons from a californium source. For most reactions sufficient agreement was observed between the results

of different works. In works /24/ and /25/ an analysis of several conceptions of the shape of ^{252}Cf fission neutrons spectrum was carried out for comparison of the data with average experimental cross-sections. In work /24/ three conceptions were used - the evaluation of the National Bureau of Standards (NBS) and two versions of the calculation of Madland and Nix (versions 1 and 2) /27/. The agreement with the calculations was comparatively satisfactory and good for the NBS evaluation. In the work of Mannhart /25/ an analysis was carried out of the spectra of the Maxwellian distribution of the NBS segment evaluation and of three versions of the Madland-Nix calculations. The author used in his work the results of his measurements of the average cross-sections of 22 threshold reactions /21, 26/ sensitive to the spectrum shape in the energy region 1-18 MeV. Mannhart came to the conclusion that versions 1 and 2 of the Madland-Nix calculations did not correspond to the experimental average cross-sections. The Maxwellian spectrum and the NBS segment evaluation equally well describe data lower than 6 MeV and over this value only the NBS evaluation gives good approximation. Version 3 of the Madland-Nix calculation is also in good agreement with the experimental data. Higher than 13 MeV this version shows a lowered value of the neutron intensity in comparison with the experimental data.

It is worth mentioning that, as a rule, the data from ENDF-B/V were used as the energy dependence of the cross-sections, and only for the reactions $^{27}Al(n,\alpha)$, $^{47}Ti(n, p)$, $^{58}Ni(n, 2n)$ and $^{63}Cu(n,\alpha)$ the data from some recent works were used.

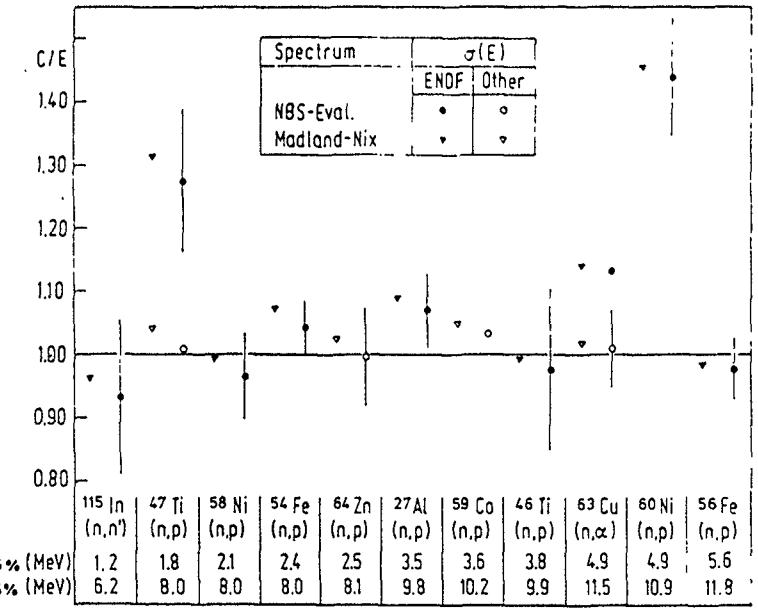

Fig. 9. Ratio of the calculated to the experiment data for average cross-sections of different reactions for the ^{252}Cf neutron spectrum /25/. Two kinds of the spectrum are used - the NBS evaluation and the spectrum of Madland-Nix /27/.

In fig. 9, 10, 11 the comparison is shown of Mannhart's experimental data on average cross-sections with the ones calculated by different kinds of spectra /25/.

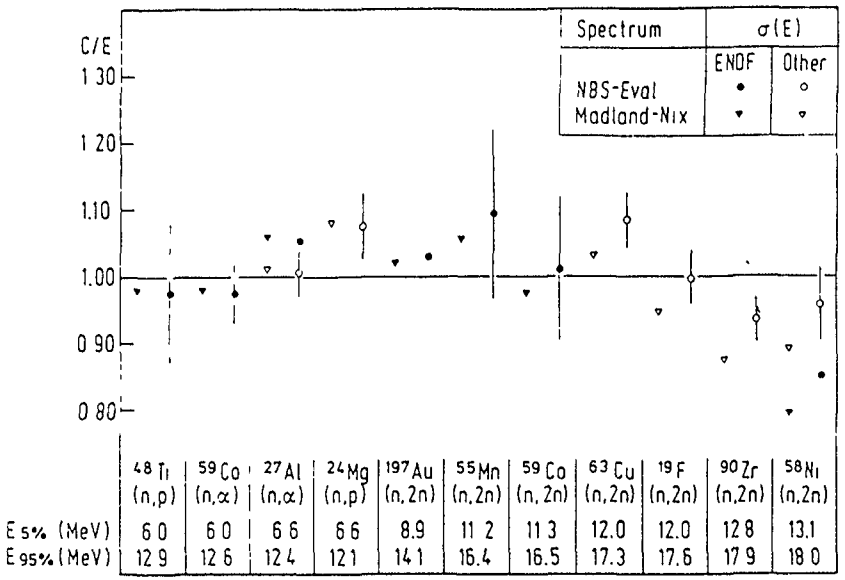

Fig. 10. Ratio of the calculated to the experimental data for reaction average cross-sections /25/. Two kinds of the spectrum are used-NBS evaluation and calculation of Madland-Nix.

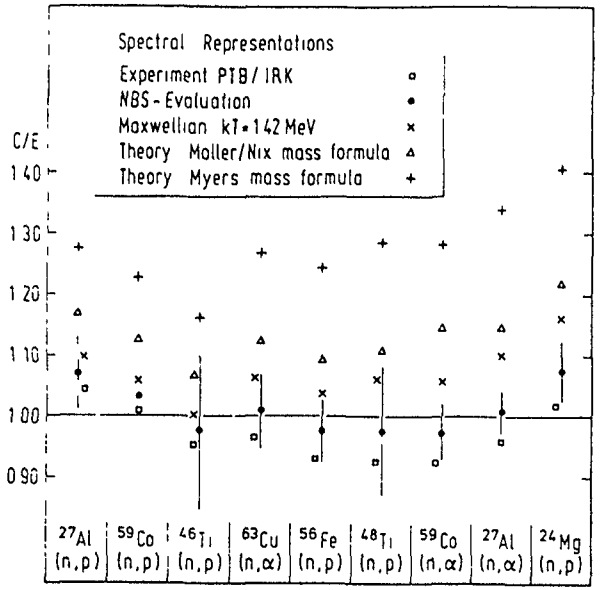

Fig. 11. Ratio of the calculated to the experimental data for reaction average cross-sections /25/. Five kinds of the spectrum are used: the NBS evaluation, the PTB experiment /11/, the Maxwellian with T = 1.42 MeV and two versions of the calculation of Madland-Nix.

4. Theoretical calculations of the spectrum

Madland and Nix /28-30/ carried out spectrum calculations on the base of the standard nuclear evaporation theory. The motion of the fragments, the distribution of the residual temperature of the fragments and the dependence of the cross-section of the inverse process on the energy (version 3) were taken into account in the work. Among the simplifications there is registration of only one average pair of fragments, neglect of the cascade, using of the triangle form of the residue nucleus temperature distribution. In the first two calculation versions the cross-section of the inverse process was considered constant. The calculated spectrum (version 3) (0.1-20 MeV) is close to the experimental data. Simplicity and possibility to calculate quickly neutron spectra for different nuclei and different excitation energies is a great advantage of the model. Yet it is desirable to show the influence of the used simplifications for a strict application in the case of calculation of a standard spectrum, where high precision is required.

In the work of Märten et al. /31/ the calculation was done by the cascade-evaporation model. The cascadeness of neutron evaporation from the fragments, the dispersion of the excitation energy were successively taken into account. The effect of neutron-gamma competition was neglected.

The authors present a calculated spectrum only in the region 5-25 MeV. The calculations fulfilled in this work seem to be very useful for the sensitivity of the final spectrum in respect to different input data. The results of the calculation show that the integral spectrum is sensitive in the region 0-2 MeV mainly to the neutrons of the heavy fragments group, in the region 2-12 MeV - to the light group and over 12 MeV - to the neutrons from the fragments with the masses close to 120.

Gerasimenko and Rubchenya /32/ carried out successive calculations on the base of the Hauser-Feschbach statistic method. An account was taken of the dispersion of the excitation energy and fragments spin, of the cascade character of neutron emission; the evolution of excitation distribution on each step of the cascade was successively accounted for. The competition between neutron and gamma-quanta emission was taken into consideretion. The calculations were done in the energy region 0.001-30 MeV. The advantage of the work is that the calculations of differential neutron spectra were carried out for *definite* masses and kinetic energies and the results were compared with the experimental data, which enables to control the input data.

It is worth mentioning that all the theoretical works are based on the model of equilibrium neutron evaporation from heated to the maximum temperatures fragments moving at full velocity. These fundamental statements must be yet checked in correlation experiments. Otherwise the theoretical calculations should take into consideration any deviation from this model. The results of the comparison of the calculations and experimental data are shown in fig. 14 and 15.

5. Study of the process of ^{252}Cf spontaneous fission neutron emission

The main problems in the study of the process mechanism are concerned first of all with the question if neutrons are emitted from fully accelerated fragments and what is the role of the so called "scission neutrons". Information is also needed on the energy spectra of the neutrons emitted by fragments of different masses and different excitation energies.

In work /33/ fulfilled at the Radium Institute the authors by a "direct" method managed to determine the fragments velocity at which neutrons were emitted. They found that in the spectra there is a clear minimum corresponding to the full fragments velocity. This minimum is observed

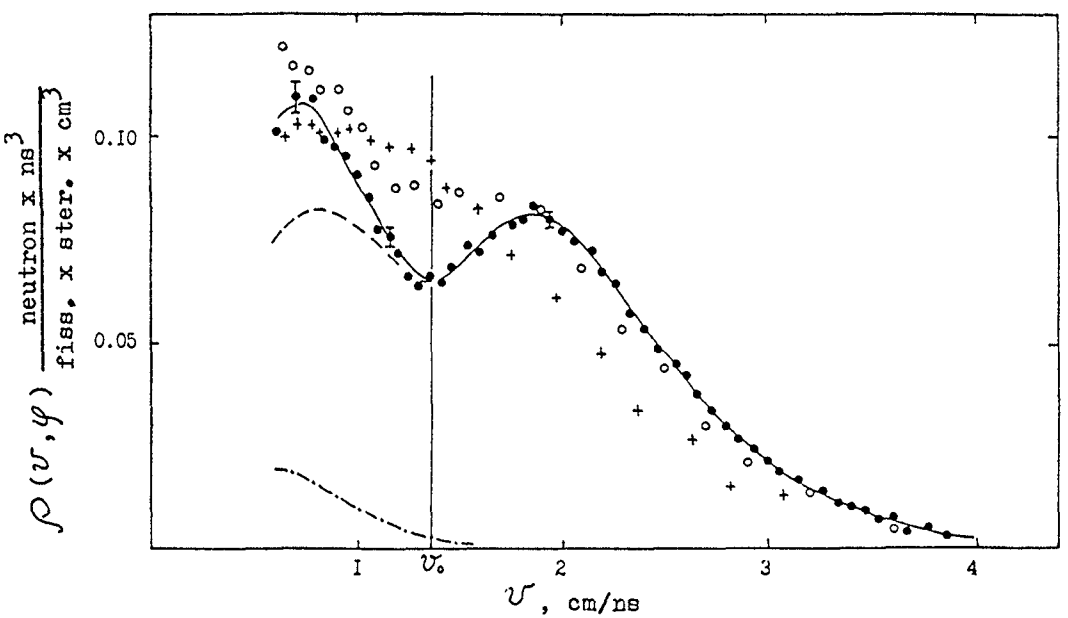

Fig. 12. Spectra of the neutrons emitted by a light fragment of ^{252}Cf spontaneous fission at the angles 5°, 15°, 30° in the l. s. /33/
- 5°, o- 15°, +- 30°.

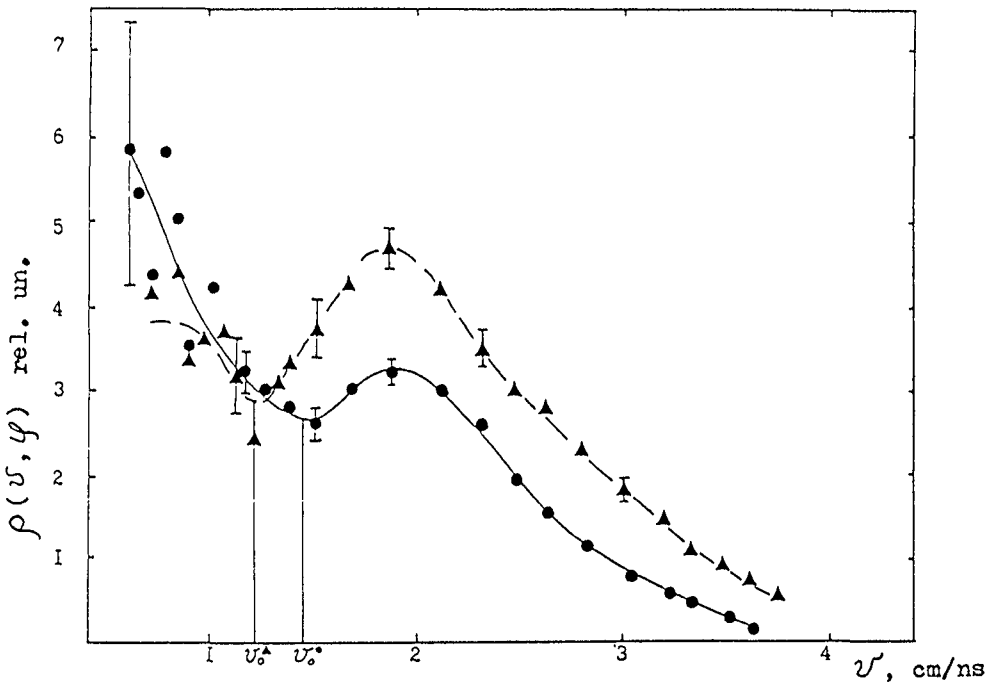

Fig. 13. Spectra of the neutrons emitted at the angle 5° /33/
• - M = 98±5 MU E_k = 175±5 MeV V_o = 1.44 cm/hs
▲ - M = 117±5 MU E_k = 175±5 MeV V_o = 1.22 cm/ns

at small (less than 10°) angles of neutron emission (in respect to the fission axis), and at angles > 10° it disappears (fig. 12). A correlation is observed between the position of the minimum and the kinetic energy of the fragments (fig. 13). Of course, from this one can not draw a conclusion that all the neutrons are emitted from fully accelerated fragments. In work /34/ by analysis of correlations between the energy and angular distributions of neutrons of different masses and the total kinetic energies of the fragments it was found that about 95 % of the emission of all the neutrons are within the limits of the ordinary model of evaporation from fully accelerated fragments. There is no interpretation of small deviations (5 %) in work /34/.

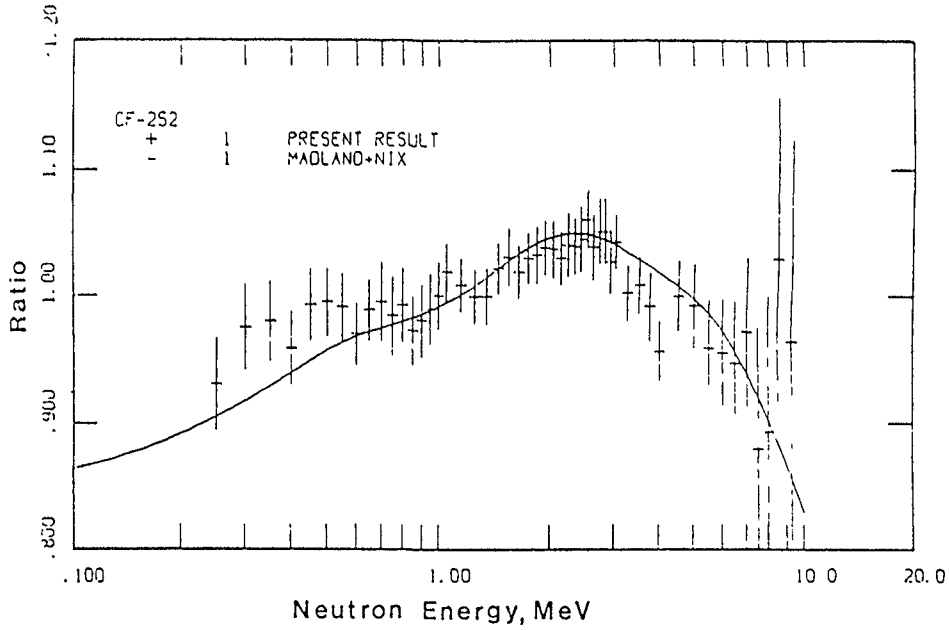

Fig. 14. Comparison of the calculated and experimental data. Calculation /30/, experiment /10/.

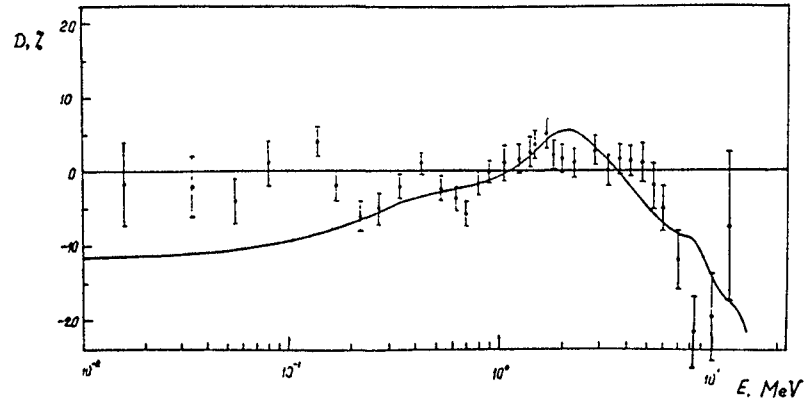

Fig. 15. Comparison of the calculated and experimental data. Calculation /32/, experiment /16/.

In work /35/ it was also found that a considerable part of the neutrons is within the framwork of the standard evaporation model. However, the authors of work /35/ also point out that they have found emission before full acceleration of the fragments ($0.7\ V_o < V < V_o$) for the fragments with high excitation energies. In work /36/ much higher deviations (~ 13 %) from the evaporation model were registred. The authors connect this part with the "scission" neutrons. Work /37/ considered the question about energy differential spectra for separeted masses of the fragments and in connection with this the correlation was discussed between the neutron emission time τ_H and the time of transition of the deformation energy into excitation energy τ_D. For several considered cases of the masses of fragments the experiment and the calculation /16/ are in good agreement, which points out that for these cases $\tau_H \gg \tau_D$.

The data of the double differential energy distributions are extremely important for correct calculations of the integral spectrum. Though in the works of the recent years the deviation of the experimental data from the predictions of the evaporation model have obviously reduced (especially in /34/), yet it is necessary to understand the nature of the remaining discrepancies.

6. Spectrum evaluations

In 1975 Grundl and Eisenhauer /38/ carried out a segment evaluation of the spectrum on the base of the results of a number of selected experimental works having been accomplished by that time. In 1980 Starostov et al. /39/ made a spectrum evaluation that was an averaging of a great number of works, including outdated ones. In 1983 Boytsov and Starostov /40/ renewed this evaluation, excluding some wrong and outdated results. But the approach to the evaluation was preserved - averaging of the results of the works with the errors indicated by the authors. The results of the evaluations are shown in fig. 16.

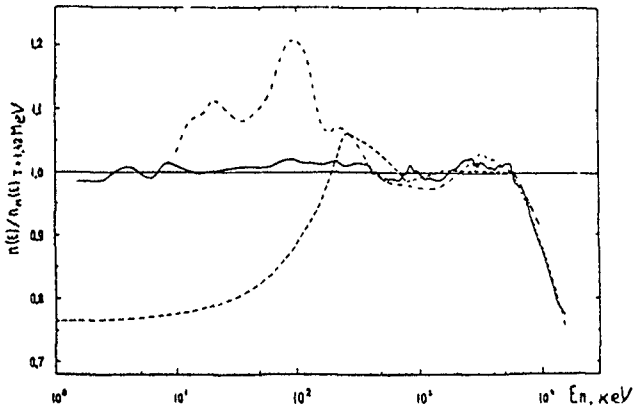

Fig. 16. Ratio of the data of three evaluations to the Maxwellian distribution with T = 1.42 MeV.
- - - /38/, -•- /39/, —— - /40/.

It's necessary to mention that all the fulfilled evaluations were based on brief publications where the full information on the measurement procedure, corrections and errors was absent. Numerical data were also seldom presented by the authors. All this reguires a new evaluation based on full information about the experiments and using a full file of errors.

7. Conclusion

Thus, a complex of experimental and theoretical works studying the shape of a standard spectrum and works studying the emission process were carried out in the last five years. New evaluation was realized.

The experimental works were done in the energy region 0.0003-30 MeV both by differential and integral methods. The precis ion of the measurements and error evaluation improved. Special attention was payed to the quality of

californium layers and to the efficiency of fragments registration. The efficiency of neutron counters was more precisely determined in the works.

The theoretical works were carried out in two directions: using of the evaporation model and of the statistic model of Hauser-Feschbach. The agreement of the calculated and the theoretical data was satisfactory.

In the low energy region four works /6, 14, 16, 19/ have proved that the spectrum has not any noticeable excess over the Maxwellian distribution (T = 1.42 MeV) and agrees with it within 5 % in the energy region 0.001-1 MeV. Theoretical spectra pass lower than the Maxwellian distribution by 10-20 % in this region. Probably, data compatibility may be provided by regulation of the input calculated parameters. Otherwise the difference can be connected with the existence of an "additional" source of low-energy neutrons, which is not accounted for in the calculations. Future measurements will clear the picture.

In the middle energy region, where the maximum intensity of the spectrum is (1-7 MeV), small deviations (<5 %) from the Maxwellian distribution are possible, which is shown both by experimental and theoretical data. It is desirable to increase the precision of the measurements in this region.

The energy region over 6-7 MeV and especially over 10 MeV is the region of maximum discrepancies. The difference of the results reaches 20 % at 10 MeV. Works /11, 15/ and /16/ are close to the theoretical calculations at E < 10 MeV, which increases their reliability. At E > 10 MeV one can expect some difference between the calculations and the experimental data, because at 20-25 MeV there is a great excess of neutrons /8/ over the expected intensity.

The high energy region is important for the purposes of reactor dosimetry and new efforts are necessary here for achieving higher precision.

8. Recommendations

Summing the experimental data of the recent years, obtained both by differential and integral methods, and taking into consideration the theoretical calculations, the IAEA Consultant's meeting in Smolenice in 1983//41/ recommended to use the Maxwellian distribution with T = 1.42 MeV in the energy region 0.001-6 MeV, and in the region 6-20 MeV - the data of the NBS evaluation /38/.

The evaluation carried out in 1983 /40/ shows a agreement with this recommendation.

Therefore, before making a new evaluation on the base of a full documented file of errors of all the recent experiments, it seems advisable to use the recommendations of the IAEA Consultant's meeting /41/.

It is desirable to secure and develop the progress of the recent years both in the experimental and the theoretical directions.

REFERENCES

1. T. Wiedling. EANDC Symp. Neutron Standards and Flux Normalisation (Proc. ANL), 1970, p. 437.
2. A. Smith. Prompt Fission Neutron Spectra (Proc. Consult. Meeting Vienna 1971), IAEA Vienna (1972), p. 3.
3. H. Knitter. IAEA-208 1 (1976) 183.
4. L. Stewart, J. Brown. Report BNL-NCS-51123 (1979) p. VI. 10.
5. M. V. Blinov. Proc. IAEA Consultants Meeting on Neutron Source Properties INDC (NDS)-114GT (1980).
6. M. V. Blinov, V. A. Vitenko, V. I. Jurevich. Nejtronnaya Physica (Proc. V All Union Conf. Kiev, 1980) Moskow 3 (1980) 109, ZFK-410, 1980, 104 (Rus.).
7. H. Jasicek, F. Bensch. Nucl. Sci. and Eng. 77, (1981), 51.
8. Mon Jiangshen et. al. Chenese Journal of Nucl. Phys. 1981, N 5.

9. V. I. Bolshov et al. "Vopr. At. Nauki i Techniki" Ser. Jad. Const. N 3 (42) (1981) 43 (Rus.).
10. W. Poenitz, T. Tamura. Nuclear Data for Science and Technology (Proc. Int. Conf. Antwerp, 1982), Brussels, 1983, p. 465.
11. R. Böttger, H. Klein et al., ibid, p. 484.
12. M. V. Blinov, G. S. Boykov, V. A. Vitenko, ibid, p. 479.
13. H. Märten, S. Seeliger, B. Stobinski, ibid, p. 488.
14. B. Lajtai, P. Dyachenko et al. INDC(NDS)-146, IAEA, Vienna, 1983, p. 177.
15. H. Klein, R. Böttger et al., ibid, p. 191.
16. O. I. Batenkov, M. V. Blinov et al., ibid, p. 161.
17. W. Poenitz, T. Tamura, ibid, p. 175.
18. J. Boldeman. INDC/P(83)-59, IAEA Vienna, 1983.
19. A. A. Boytsov, B. I. Starostov. Nejtronnaja Physica Moskow 2 (1984) 298 (Rus.).
20. M. V. Blinov, V. A. Vitenko, V. I. Jurevich. Nejtronnaya Physica. Moskow 4 (1980) 96 (Rus.).
21. W. Mannhart. Nucl. Sci. and Eng., 77 (1981) 40.
22. K. Kobayashi, J. Kimuro, W. Mannhart. J. of Nucl. Sci. 19(5) (1982) 341.
23. Z. Dezso, J. Csikai. INDC(NDS)-146, IAEA, Vienna, 1983, p. 225.
24. R. La Bauve, D. Madland et al. Applied Nuclear Data Research and Developments Report LA 9060 PR, 1981, p. 23.
25. W. Mannhart. INDC(NDS)-146, IAEA, Vienna, 1983, p. 213.
26. W. Mannhart. Nuclear Data for Science and Technology (Proc. Int. Conf. Antwerp, 1982), Brussels, 1983, p. 429.
27. D. Madland, J. Nix. Nucl. Sci. Ing. 81 (1982) 213.
28. D. Madland, J. Nix. Report LA-UR-79-2914 (1979).
29. D. Madland, J. Nix. Report LA-UR-82-2643 (1982).
30. D. Madland, J. Nix. Report LA-UR-83-3074 (1983).
31. H. Marten, D. Neumann, D. Seeliger. INDC(NDS)-146, IAEA, Vienna, 1983, p. 199.
32. B. F. Gerasimenko, V. A. Rubchenya. Nejtronnaya Physica Moscow 1 (1984) 349 (Rus.).
33. O. I. Batenkov et al. In ref. /32/ p. 334 (Rus.).
34. O. I. Batenkov et al. In ref. /32/ p. 339 (Rus.).
35. J. A. Vasiljev et al. In ref. /32/ p. 354 (Rus.).
36. P. Richs. Acta Physica Austriaca 53 (1981) 271.
37. O. I. Batenkov et al. In ref. /32/ p. 344 (Rus.).
38. J. Grundl, C. Eisenhauer. Proc. Intern. Conf. on Nucl. Cross Sections and Technology. Washington, 1 (1975) 250.
39. B. I. Starostov et al. "Vopr. At. Nauki i Techniki" Ser. Jad. Const. N 2 (37) (1980) 3 (Rus.).
40. A. A. Boytsov, B. M. Starostov. Nejtronnaya Physica Moskow, 2 (1984) 301 (Rus.).
41. INDC(NDS)-146, Vienna, IAEA, 1983.

STATE AND FIRST RESULTS OF THE EVALUATION OF THE Cf-252 FISSION NEUTRON SPECTRUM

W. MANNHART
Physikalisch-Technische Bundesanstalt,
Braunschweig,
Federal Republic of Germany

Abstract

The state of data to be used in the evaluation of the neutron spectrum of Cf-252 is reviewed. The demand for sufficiently detailed data and their uncertainties continues to be great. At present, only a limited set of data meets the requirements for use in an evaluation based on least-squares principles with a resulting complete covariance uncertainty matrix. Based on integral spectrum data (experimentally determined, spectrum-averaged neutron cross sections) a first evaluation has been made. The result is presented and discusssed. The present evaluation can be regarded as a first step towards future evaluations including further experiments, in particular time-of-flight spectrum measurements.

1. Introduction

For a long time the neutron spectrum of spontaneous fission of Cf-252 has been regarded as a standard for reactor dosimetry and neutron detector calibration purposes. Nevertheless, the shape of this neutron spectrum has not yet been unambiguously defined. The chief reason for this has been the contradictory experimental data of past experiments, reflected clearly by a review of data up to 1979 /1/. This unsatisfactory situation has resulted in a continuing interest /2,3/ in the determination of the neutron spectrum of Cf-252, both from the experimental /4-13/ and the theoretical /13-15/ side. Recent experiments performed with refined techniques have given more precise results and diminished the divergence of data. In parallel, recent experiments have shown the importance of a few corrections, the neglect of which may be the explanation of some of the problems with past experiments. Theoretical approaches to describing the Cf-252 neutron spectrum have given results which are in good agreement with the experimental data. The results of these calculations, based on nuclear evaporation models, have been further improved by adjustment of the parameters of the theory to experimental data.

All this has actuated the carrying out of a new evaluation of the Cf-252 neutron spectrum /2/ with regard to the recent data. The present review reflects the persistent problem of this evaluation in obtaining sufficiently documented data. With the deadline set at the 1st of September 1984, only a single set of data met the requirements for inclusion in the evaluation aimed at determining the Cf-252 neutron spectrum with a complete covariance uncertainty matrix. There is a great demand for this matrix to allow, for example, a correct propagation of the spectrum uncertainties to integral parameters determined in reactor dosimetry for pressure vessel surveillance purposes /16/.

2. State of data to be used in the evaluation

During the last five years much effort has been concentrated on recent experiments /4-13/ aimed at resolving the data discrepancies of the Cf-252 neutron spectrum at low (< 1 MeV) and high (> 6 MeV) neutron energies. The data available now cover the neutron energy range between 1 keV and 30 MeV. Most of the recent data have been of a preliminary nature, i.e. the final analysis has not been completed due to corrections requiring additional investigation.

In recent time-of-flight experiments, besides the problem of defining an accurate neutron energy scale and that of taking the time resolution properly into account, two corrections were identified which play an essential role in a correct analysis of the measured data. One is the correction for nonisotropic detection losses in the fission fragment detector /17/. Neglect of this correction with unfavorable experimental conditions can result in a remarkable hardening of the measured spectrum. Another correction

not regarded in most previously reported measurements, is for uncorrelated stop signals /18/. This correction essentially determines the time-dependent background in time-of-flight experiments and due to a renormalization of the measured distribution, changes the neutron spectrum at high energies. The influence of both these corrections strongly depends on the specific experimental conditions and has been taken into account in a few cases /9,10,19/.

In the present data overview only post 1979 measurements are dealt with. The taking into account of earlier experiments would almost require a complete re-analysis of these measurements, which would often seem to be hampered by a relatively poor documentation of most of the data.

This documentation problem also remains valid for the more recent experiments. In many cases the results are only given in the form of figures and detailed numerical data are not available. A detailed uncertainty analysis, the "sine qua non" for inclusion in an updated evaluation, is also missing. Very recently, such information became available for two experiments /19,20/. These data were outside the schedule of the present evaluation and will be included into the next step of the evaluation after examination of their comprehensiveness.

Besides the high resolution time-of-flight experiments, there is another group of experiments which must be regarded as "broad" resolution experiments. These experiments of spectrum-averaged cross-section measurements of threshold and non-threshold neutron reactions cover various energy ranges in the Cf-252 neutron spectrum between the limits of a few keV and about 18 MeV. The data can be determined at a high level of precision with relative uncertainties from 2 % to 3 %. Since 1979 the uncertainties resulting from the experiments have been consistently analyzed and covariances generated /21/. Based on this information, data from the various experiments have been combined by least-squares techniques /22,23/. This means that the results of spectrum-averaged neutron cross-section measurements are at present the only set of data with a complete covariance matrix containing the full uncertainty information required for evaluations based on the least-squares principle.

The above mentioned data form the basis of the present evaluation. It is planned to expand the evaluation in future steps and to include other experiments as soon as the covariances of these data are available.

3. Evaluation of the neutron spectrum by least-squares methods

The aim of an evaluation must be to obtain results which are based as far as possible on objective facts and to avoid subjectivity. This requires consistent attention to all data uncertainties involved in the evaluation process. The only method which meets this requirement is a generalized least-squares method. The urgent need of reactor technology to specify results with appropriate uncertainties /24/ has actuated such methods. A variety of computer codes for these purposes has recently become available, such as STAY'SL /25/, FERRET /26/ and others not mentioned here. All these evaluation methods are based on the least-squares principle and combine prior information and experimental data with full regard to their uncertainties with the objective of obtaining results with a maximum likelihood.

Application of this method to the present problem of evaluating the Cf-252 neutron spectrum has already been described in detail /27/. Only a few essential points of the procedure are repeated here, the main emphasis being placed on the data used in this evaluation.

3.1. Principles of the least-squares adjustment

Experimental reaction rates a_i^o of various neutron detectors i measured in the Cf-252 neutron field are compared with calculations

a_i based on energy-dependent cross-sections and the Cf-252 neutron spectrum. The minimization of the chi-squares gives a value of

$$\chi^2_{MIN} = \sum_i \sum_j (a_i^o - a_i)\, w_{ij}\, (a_j^o - a_j) \qquad (1)$$

The elements w_{ij} are the components of the weight matrix of the problem explained below. In the present case the experimental reaction rates are normalized by the neutron fluence rate, i.e. they are spectrum-averaged neutron cross-sections:

$$a_i^o \equiv \langle\sigma\rangle_i^{EXP} \qquad (2)$$

The corresponding calculated quantities are

$$a_i \equiv \langle\sigma\rangle_i^{CALC} = \int_0^\infty \sigma^i(E)\, \chi(E)\, dE \qquad (3)$$

The integral of eq. (3) contains the energy-dependent cross-section of the neutron reaction i and the normalized spectral flux density distribution of Cf-252 with

$$\int_0^\infty \chi(E)\, dE = 1 \qquad (4)$$

Both these quantities are parameters of the problem and can be formally written as a parameter vector P with an absolute covariance matrix $\underline{N}_p$, i.e.:

$$P = \begin{pmatrix} \chi \\ \Sigma \end{pmatrix} \quad \text{and} \quad \underline{N}_P = \begin{pmatrix} \underline{N}_\chi & 0 \\ 0 & \underline{N}_\Sigma \end{pmatrix} \qquad (5)$$

χ being the vector of the spectral distribution and Σ the vector of the full set of energy-dependent cross-sections involved in the problem.

The evaluation results in a new vector P' and a corresponding matrix $\underline{N}'_P$ which fulfils the minimum condition of eq. (1). P is often called the problems's "prior information". P' is then the most likely adjusted value with regard to the prior information and $\underline{N}'_P$ the resulting uncertainty covariance matrix with reduced uncertainties as a result of taking into account the experimental information in eq. (2). From eq. (5) it is clear that the spectral distribution as well as the energy-dependent cross-section data were adjusted. That is, the zero correlation of $\underline{N}_P$ in eq. (5) vanishes for $\underline{N}'_P$. From P' and $\underline{N}'_P$ the result of the adjusted neutron spectrum χ' and its covariance matrix $\underline{N}'_\chi$ is derived. The weight matrix of eq. (1) contains the uncertainties of the experimental data of eq. (2) as well as the uncertainties of the calculated data of eq. (3). The matrix is thus an inverse

$$[\underline{N}_A o + \underline{N}_A]^{-1} \qquad (6)$$

$\underline{N}_A o$ is the covariance matrix of the measured data of eq. (2) and $\underline{N}_A$ is the corresponding quantity of the calculated data of eq. (3). $\underline{N}_A$ comprises the covariance matrices $\underline{N}_\chi$ and $\underline{N}_\Sigma$ transformed to the calculated data (see eq. (7) and eq. (10) of /27/, for example).

3.2. Data on spectrum-averaged neutron cross-sections

These data, based on various experiments, have been pre-processed and were least-squares averages /22,23/. In all, the data from 25 different neutron reactions were used. The reactions and the numerical values of the spectrum-averaged cross-sections are listed in columns 1 and 2 of table 1. The covariance matrix is shown in the form of relative standard deviations in column 3 of table 1 and a correlation matrix given in table 2. It can be seen from table 1 that for 15 reactions the relative uncertainties were smaller than 2 %.

Table 1: Spectrum-averaged data used in the evaluation

Reaction	$\langle\sigma\rangle^{EXP}$ (barn)	Rel.Std. Dev.* %	$\langle\sigma\rangle^{CALC}$ (barn)	EXP/CALC	χ^2_{part}
F-19(n,2n)	1.628E-5	3.33	1.628E-5	1.000	0.00
Mg-24(n,p)	2.005E-3	2.39	2.160E-3	0.928	2.62
Al-27(n,p)	4.892E-3	2.16	5.140E-3	0.952	0.61
Al-27(n,α)	1.021E-3	1.42	1.013E-3	1.008	0.10
Ti-46(n,p)	1.420E-2	1.68	1.347E-2	1.054	0.16
Ti-48(n,p)	4.275E-4	1.81	4.096E-4	1.044	0.17
Mn-55(n,2n)	4.079E-4	2.26	4.462E-4	0.914	0.47
Fe-54(n,p)	8.729E-2	1.29	8.823E-2	0.989	0.17
Fe-56(n,p)	1.471E-3	1.73	1.415E-3	1.039	0.66
Ni-58(n,p)	1.176E-1	1.25	1.138E-1	1.034	0.19
Ni-58(n,2n)	8.965E-6	3.32	8.471E-6	1.058	0.72
Co-59(n,α)	2.221E-4	1.78	2.164E-4	1.027	0.32
Co-59(n,2n)	4.058E-4	2.49	4.107E-4	0.988	0.02
Cu-63(n,γ)	1.055E-2	3.08	9.772E-3	1.080	0.37
Cu-63(n,α)	6.897E-4	1.88	6.767E-4	1.019	0.08
Cu-63(n,2n)	1.866E-4	3.82	1.982E-4	0.941	2.96
Zn-64(n,p)	4.047E-2	1.85	3.922E-2	1.032	0.13
Zr-90(n,2n)	2.211E-4	2.78	2.058E-4	1.075	3.73
In-115(n,γ)	1.261E-1	2.19	1.222E-1	1.032	0.47
In-115(n,n')	1.981E-1	1.31	1.819E-1	1.089	0.52
Au-197(n,γ)	7.711E-2	1.54	7.720E-2	0.999	0.00
U-235(n,f)	1.210E+0	1.19	1.238E+0	0.978	1.89
Np-237(n,f)	1.356E+0	1.65	1.353E+0	1.003	0.00
U-238(n,f)	3.234E-1	1.72	3.134E-1	1.032	2.89
Pu-239(n,f)	1.811E+0	1.37	1.792E+0	1.010	0.05

*Correlation matrix on Table 2

Table 2: Correlation matrix of the experimental spectrum-averaged neutron cross-section

Correlation matrix (x 100)

F-19(n,2n)	100																								
Mg-24(n,p)	15	100																							
Al-27(n,p)	8	27	100																						
Al-27(n,α)	26	54	44	100																					
Ti-46(n,p)	23	33	33	57	100																				
Ti-48(n,p)	21	30	33	50	64	100																			
Mn-55(n,2n)	43	23	25	40	34	30	100																		
Fe-54(n,p)	31	39	40	65	55	50	46	100																	
Fe-56(n,p)	21	35	34	57	46	42	32	56	100																
Ni-58(n,p)	36	43	44	73	63	56	53	85	59	100															
Ni-58(n,2n)	28	15	13	26	22	20	40	30	21	35	100														
Co-59(n,α)	36	28	39	49	42	37	58	56	39	66	34	100													
Co-59(n,2n)	39	20	22	36	31	28	60	42	29	49	36	50	100												
Cu-63(n,γ)	17	18	49	29	23	23	21	28	23	30	11	23	19	100											
Cu-63(n,α)	24	25	29	42	35	32	36	50	34	57	29	50	32	16	100										
Cu-63(n,2n)	24	14	43	23	18	18	30	22	18	24	17	25	28	36	15	100									
Zn-64(n,p)	19	32	33	55	44	39	29	50	43	54	19	37	27	22	31	18	100								
Zr-90(n,2n)	35	19	19	32	27	25	50	37	26	43	38	41	45	16	30	25	24	100							
In-115(n,γ)	16	25	31	41	33	33	23	39	34	43	16	29	21	22	26	17	31	19	100						
In-115(n,n')	26	40	54	64	52	55	38	63	53	69	26	46	34	39	44	31	48	31	53	100					
Au-197(n,γ)	23	35	44	59	48	45	33	56	47	61	22	41	30	31	38	25	45	27	54	75	100				
U-235(n,f)	13	17	19	27	23	22	19	35	23	35	13	24	17	13	23	11	21	16	19	32	27	100			
Np-237(n,f)	9	12	14	20	16	16	14	25	17	25	9	17	13	10	17	8	15	11	13	23	19	67	100		
U-238(n,f)	8	10	12	17	14	13	12	22	14	22	8	15	11	8	15	7	13	10	12	20	17	78	67	100	
Pu-239(n,f)	11	14	16	23	19	18	16	30	20	30	11	20	15	11	20	9	18	13	16	28	23	79	66	67	100

3.3. Prior information on the neutron spectrum

As prior information the slightly modified data of an NBS evaluation /28/ of the Cf-252 neutron spectrum were used. The NBS evaluation covered spectrum measurements up to 1974 /29/ and parametrized the spectral distribution by a Maxwellian of kT = 1.42 MeV. The deviations of the data from the Maxwellian were taken into account by five energy-dependent segment correction functions fitted to the data. The result was:

$$\chi(E) = 0.6672 \sqrt{E} \exp(-E/1.42)\, f(E) \quad (E \text{ in MeV}) \tag{7}$$

The correction functions f(E) were linear below 6 MeV and exponential above this energy. The NBS evaluation shows some structure below 0.8 MeV which is not confirmed by recent measurements. The data of Lajtai et al. /12/ between 25 keV and 1.2 MeV show no deviations from Maxwellian with kT = 1.42 MeV. This is additionally confirmed by the data of Blinov et al. /6/ taken between 1 keV and 1 MeV. Further recent data of Blinov et al. /13/ show that between 10 keV and 5 MeV to 6 MeV, no essential deviations from the Maxwellian were identified. Above 6 MeV the NBS evaluation states a deficit of neutrons compared with the Maxwellian. This fact has been confirmed by spectrum-averaged cross-section measurements of high-threshold reactions /22/ and recently by direct spectrum measurements /11/. However, other data exist which contradict this /4/.

Taking all these facts as a basis, it was decided to represent the spectral distribution by a pure Maxwellian between 0 MeV and 6 MeV and to omit the segments of the NBS evaluation on this energy range, but include the segment of the NBS evaluation above 6 MeV. After a renormalization the following form was obtained:

$$\chi(E) = 0.6680 \sqrt{E} \exp(-E/1.42)\, g(E) \tag{8}$$

with

$$g(E) = \begin{cases} 1 & \text{for } 0 \le E \le 6 \text{ MeV} \\ \exp\,[-0.03(E-6)] & \text{for } 6 \le E \le 20 \text{ MeV} \end{cases} \tag{9}$$

Eq. (8) assumes that up to 6 MeV a Maxwellian of kT = 1.42 MeV with a scaling factor of 1.002 is valid and that the spectrum above 6 MeV is described by another Maxwellian of kT = 1.362 MeV with a scaling factor of 1.126. It is well kown that the Maxwellian is only a rough approach to describe the fission spectrum, but it is adequate and convenient for the present purposes.

In all, 30 group averages of eq. (8) were formed and used in the evaluation:

$$\bar{\chi}_i = \int_{E_i}^{E_{i+1}} \chi(E)\, dE \tag{10}$$

The energy bins $[E_i, E_{i+1}]$ were 0.5 MeV between 0 MeV and 10 MeV, and 1 MeV between 10 MeV and 20 MeV. With these group averages $\bar{\chi}_i$, eq. (4) must be rewritten as:

$$\sum_{i=1}^{30} \bar{\chi}_i = 1 \tag{11}$$

The NBS evaluation stated relative standard deviations (1σ-level) in various energy ranges determined from the scatter of the experimental data. These data are given in table 3 and were used in the generation of the covariance matrix of the neutron spectrum. The relative uncertainties of table 3 are very similar to those obtained by attributing a 2 % uncertainty to the kT = 1.42 MeV of a Maxwellian /30/. However, taking into account the Maxwellian shape of eq. (8) would result in full correlations between all the data of table 3 in the case of a non-normalized spectrum or in full

Table 3: Uncertainty of the NBS spectrum evaluation /28/ in different energy ranges

Energy range (in MeV)	Rel. Std. Dev.
0 - 0.25	13.0 %
0.25 - 0.8	1.1 %
0.8 - 1.5	1.8 %
1.5 - 2.3	1.0 %
2.3 - 3.7	2.0 %
3.7 - 6.0	2.1 %
6.0 - 8.0	2.1 %
8.0 - 12.0	8.5 %
12.0 - 20.0	15.0 %[a)]

[a)] This value bases on an estimate of the author.

correlations and anticorrelations for a normalized spectrum. These rigid conclusions hamper any adjustment procedure in obtaining sufficiently detailed results, as they indicate a pure shape adjustment (by a scale factor) of the spectrum over the whole energy range in the non-normalized case. (For a normalized spectrum the shape adjustment factor runs in opposit directions below and above the average energy of the Maxwellian). The implicit inclusion of the Maxwellian shape in the covariance matrix was therefore avoided.

After the generation of a union group structure /27/ containing the energy delimiters of table 3 as well as those of the groups of eq. (11), all diagonal elements of the union group matrix were filled with the corresponding uncertainties of table 3, which means that these uncertainties were regarded as belonging to a non-normalized spectrum. All data between one of the energy ranges of table 3 were assumed to be equally correlated by 75 %. No correlations between the different energy ranges were used. A correlation coefficient of 1.00 would mean that the whole range would be adjusted by the same factor, whereas a correlation coefficient of 0.50 surely underestimates the Maxwellian-like structure in the range. A correlation coefficient of 0.75 was therefore chosen. This procedure is a compromise which takes account of the lack of detailed information. It avoids fixing the adjustment procedure on a Maxwellian shape but it takes into account the fact that the data of a segment of the NBS evaluation must at least be correlated, due to the fitting functions.

The union group matrix was then collapsed to the final group structure of the evaluation. Up to this point, it had not been taken into account that the neutron spectrum is normalized according to eqs. (4) and (11). This was done by a transformation of the matrix from the non-normalized to the normalized case as shown in Ref. /27/ (eqs. (17) and (18)). The adjustment of the neutron spectrum in a certain energy group can now be compensated in other groups with a full conservation of the normalization. This is automatically taken into account due to the special structure of the absolute covariance matrix of the normalized spectral distribution with the sum over each row and over each column of the matrix being zero.

3.4. Energy-dependent cross-section data

Most of the cross-sections of the reactions listed in table 1 were taken from ENDF/B-V. For the reactions $^{24}Mg(n,p)$, $^{64}Zn(n,p)$, $^{90}Zr(n,2n)$ and $^{63}Cu(n,2n)$ the data were from /31/ and for $^{19}F(n,2n)$ from /32/. The ENDF/B-V data on the reactions $^{27}Al(n,\alpha)$, $^{63}Cu(n,\alpha)$ and $^{58}Ni(n,2n)$ were replaced by more recent data. For $^{27}Al(n,\alpha)$ the data were from /33/, for $^{63}Cu(n,\alpha)$ from /34/ and for $^{58}Ni(n,2n)$ from /35/.

The original point-wise data on the energy-dependent cross-sections were transformed to group cross-sections according to the structure of eq. (11). The data were weighted with the spectral distribution of eqs. (8) and (9). This resulted in an exact identity of the integral of eq. (3) with the sum over the group constants of the

cross-sections $\bar{\sigma}$ and of the spectral distribution $\bar{\chi}$ with:

$$\int_0^\infty \sigma^i(E)\ \chi(E)\ dE = \sum_{j=1}^{30} \bar{\sigma}^i_j\ \bar{\chi}_j \qquad (12)$$

Thus the usual problem of the group sums forming the integral only in a first approximation was avoided.

The covariance matrices of the energy-dependent cross-sections were taken from the literature (from ENDF/B-V and from the other references mentioned above). These matrices showing their own group structures were transformed to the group structure of the present problem according to the rules given in detail in /27/ and in /36/.

The ENDF/B-V covariance file shows a cross-correlation only between the reactions $^{235}U(n,f)$ and $^{239}Pu(n,f)$. For all other reactions no cross-correlations were stated. It is well known that this is far from experimental reality (see /37 - 39/, for example). But due to the lack of data, the covariance matrix of the whole set of energy-dependent cross-sections generated here shows no such cross-correlations. The $^{235}U(n,f)$ to $^{239}Pu(n,f)$ data were consequently neglected in the light of consistency with the other reactions, that is, the present covariance matrix contains only correlations between data belonging to the same reaction.

4. Result of the evaluation of the spectral distribution

Before the least-squares adjustment was performed, the minimum value of χ^2 of eq. (1) was calculated. This quantity is a measure of the consistency of the experimental data (section 3.2.) with the prior information of the spectral distribution and of the energy-dependent cross-section data used. This consistency test takes the uncertainties of all these data fully into account. An evaluation can only be justified when this consistency test is positive.

With the present data a minimum chi-square of 19.3 was obtained which should be considered at 25 degrees of freedom. The result indicated that an adequate consistency was given. The calculated spectrum-averaged cross-sections of eq. (3) are shown in column 4 of table 1. In addition, the ratio of experiment to calculation was formed, given in column 5 of the table. In the last column of table 1 the partial components χ^2_{part} of the minimum chi-square belonging to the various reactions are given. These values were obtained by performing only the second summation in eq. (1). The data should not be mistaken for individual chi-squares calculated without regard to the other reactions. The data of χ^2_{part} are of some use in identifying problems between experiment and calculation. Values exceeding unity indicate the probability of such problems. Here, this is true of the reactions $^{24}Mg(n,p)$, $^{63}Cu(n,2n)$, $^{90}Zr(n,2n)$, $^{235}U(n,f)$ and $^{238}U(n,f)$. Beyond their uncertainties, experiment and calculation disagree. These inconsistencies are not new and were already quoted for ^{235}U and ^{238}U in /16/ and for ^{24}Mg, ^{63}Cu and ^{90}Zr in fig. 5 of /40/. In all cases the inconsistency is not large enough to justify a rejection of the data. From the last two columns of table 1 it can also be seen that an EXP/CALC value strongly deviating from unity does not automatically result in a large contribution to the chi-square.

The input and the output of the evaluation are listed in table 4. In the first two columns of the table the energy delimiters of the group structure are listed. The averages of the spectral distribution of eqs. (8) and (9) and their uncertainties are listed in column 3 and 4. The relative standard deviations shown in column 4 are those obtained after the group collapsing and after the normalization of the input covariance matrix. This explains the deviations between 0 MeV and 4 MeV compared with the data of table 3. In the last two columns of table 4 the adjusted spectral distribution and its uncertainty are given. It can be seen that for the spectrum data above 8 MeV an essential uncertainty reduction was obtained.

The ratio of the output of the evaluation relative to the input is shown in fig. 1. The error bars quoted correspond to the

Table 4: Input and output of the evaluation

E_L (MeV)	E_U (MeV)	$\bar{X}_{IN}$	Rel.Std. Dev. %	$\bar{X}_{OUT}$	Rel.Std.* Dev. %
0.0	0.5	1.280E-1	4.51	1.253E-1	3.79
0.5	1.0	1.689E-1	1.03	1.691E-1	1.01
1.0	1.5	1.545E-1	1.65	1.544E-1	1.63
1.5	2.0	1.288E-1	1.21	1.294E-1	1.16
2.0	2.5	1.029E-1	1.05	1.034E-1	0.95
2.5	3.0	8.003E-2	1.86	8.056E-2	1.75
3.0	3.5	6.121E-2	1.87	6.160E-2	1.76
3.5	4.0	4.625E-2	1.40	4.650E-2	1.25
4.0	4.5	3.464E-2	2.09	3.480E-2	1.95
4.5	5.0	2.575E-2	2.09	2.587E-2	1.96
5.0	5.5	1.904E-2	2.10	1.913E-2	1.96
5.5	6.0	1.402E-2	2.10	1.408E-2	1.97
6.0	6.5	1.020E-2	2.24	1.025E-2	2.15
6.5	7.0	7.347E-3	2.25	7.376E-3	2.15
7.0	7.5	5.275E-3	2.25	5.296E-3	2.15
7.5	8.0	3.778E-3	2.25	3.793E-3	2.15
8.0	8.5	2.701E-3	8.49	2.675E-3	5.32
8.5	9.0	1.927E-3	8.49	1.912E-3	5.37
9.0	9.5	1.372E-3	8.49	1.363E-3	5.46
9.5	10.0	9.761E-4	8.49	9.695E-4	5.53
10.0	11.0	1.185E-3	8.49	1.177E-3	5.39
11.0	12.0	5.954E-4	8.49	5.863E-4	5.60
12.0	13.0	2.979E-4	15.02	2.839E-4	7.40
13.0	14.0	1.486E-4	15.02	1.502E-4	6.39
14.0	15.0	7.392E-5	15.02	7.663E-5	6.48
15.0	16.0	3.668E-5	15.02	3.790E-5	7.07
16.0	17.0	1.816E-5	15.02	1.860E-5	7.64
17.0	18.0	8.978E-6	15.02	9.150E-6	7.97
18.0	19.0	4.430E-6	15.02	4.503E-6	8.15
19.0	20.0	2.183E-6	15.02	2.215E-6	8.24

*Correlation matrix on Table 5

Table 5: Correlation matrix of the evaluated spectral distribution $\bar{X}_{OUT}$

Energy range (MeV)	Correlation matrix (x100)
0.0 - 0.5	100
0.5 - 1.0	-57 100
1.0 - 1.5	-48 44 100
1.5 - 2.0	-44 19 -3 100
2.0 - 2.5	-53 6 -15 57 100
2.5 - 3.0	-29 -17 -20 -11 40 100
3.0 - 3.5	-29 -16 -19 -10 41 68 100
3.5 - 4.0	-36 -10 -19 -4 18 27 27 100
4.0 - 4.5	-20 -3 -9 1 -11 -19 -18 53 100
4.5 - 5.0	-20 -2 -9 1 -10 -18 -18 54 72 100
5.0 - 5.5	-20 -2 -9 2 -9 -18 -17 54 72 72 100
5.5 - 6.0	-20 -2 -9 2 -9 -17 -17 54 72 72 72 100
6.0 - 6.5	-18 13 1 15 10 -4 -4 -2 -1 -0 -0 -0 100
6.5 - 7.0	-18 13 1 16 10 -4 -3 -2 -0 -0 -0 -0 76 100
7.0 - 7.5	-18 13 1 16 11 -4 -3 -1 -0 -0 0 0 76 76 100
7.5 - 8.0	-18 13 1 16 11 -4 -3 -1 -0 0 0 0 76 76 76 100
8.0 - 8.5	7 -6 -3 -6 -6 -2 -2 -4 -3 -3 -4 -4 -20 -20 -21 -21 100
8.5 - 9.0	6 -6 -3 -6 -6 -2 -2 -4 -3 -3 -3 -3 -19 -20 -20 -20 36 100
9.0 - 9.5	6 -5 -3 -5 -5 -1 -1 -4 -3 -3 -3 -3 -18 -19 -19 -19 37 37 100
9.5 - 10	6 -5 -3 -5 -5 -1 -1 -3 -3 -3 -3 -3 -18 -18 -19 -19 38 38 39 100
10 - 11	6 -5 -3 -5 -5 -1 -1 -3 -3 -3 -3 -3 -19 -19 -19 -20 36 37 38 39 100
11 - 12	6 -5 -3 -5 -5 -1 -1 -3 -3 -3 -3 -3 -17 -18 -18 -18 38 39 40 41 39 100
12 - 13	1 -1 -1 -0 -1 -0 -0 0 1 1 1 1 1 1 1 1 -5 -5 -5 -5 -5 -8 100
13 - 14	1 -1 -1 -0 -1 -1 -1 0 1 1 1 1 1 1 1 1 2 2 2 2 2 -0 -17 100
14 - 15	1 -1 -1 -0 -1 -1 -0 0 1 1 1 1 1 1 1 1 4 4 4 3 4 3 -6 -26 100
15 - 16	0 -1 -1 -0 -0 -0 -0 0 1 1 1 1 1 1 1 1 3 3 3 3 3 2 3 -15 -14 100
16 - 17	0 -0 -1 -0 -0 -0 -0 0 1 1 1 1 1 1 1 1 2 2 2 2 2 1 7 -6 -5 2 100
17 - 18	0 -0 -1 0 -0 -0 -0 0 1 1 1 1 1 1 1 1 2 2 2 2 2 1 10 -2 -0 6 12 100
18 - 19	0 -0 -1 0 -0 -0 -0 0 1 1 1 1 1 1 1 1 2 1 1 1 1 0 12 0 2 9 14 17 100
19 - 20	0 -0 -1 0 -0 -0 -0 .0 1 1 1 1 1 1 1 1 1 1 1 1 1 0 12 2 4 10 15 17 19 100

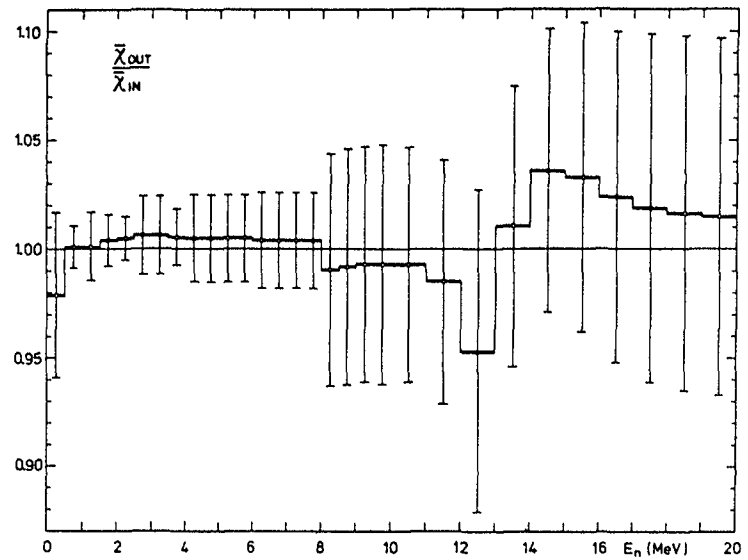

Fig. 1: Ratio of the output of the evaluation relative to the input for the spectral distribution of Cf-252

uncertainties of the output data. The figure shows that within the uncertainties the adjusted spectral distribution is fully consistent with the prior information. Between 0.5 MeV and 8 MeV the maximum deviation from eq. (8) is 0.6 %. Too high a value should not be placed on the remaining structures, especially at high neutron energies. Obviously a part of this structure is due to the missing cross-correlations between the various energy-dependent cross-section data sets. It must also be considered that not more than 0.93 % of the total spectrum intensity is above 8 MeV and only 0.06 % above 12 MeV neutron energy.

The absolute covariance matrix of the input spectrum $\underline{N}_\chi$ took into account the normalization of χ . As shown elsewhere /27/, this results automatically in an output covariance matrix $\underline{N}'_\chi$ which also fulfills the normalization condition. The correlation matrix of the adjusted spectral distribution, shown in table 5, therefore gives correlations as well as anti-correlations. The data in table 5 show that the ranges of maximum intensity of the spectral distribution are only weakly corrrelated with the low intensity ranges at high neutron energies. Between 4 MeV and 8 MeV the correlation pattern was only slightly modified due to the experimental data, whereas below 4 MeV and above 8 MeV the experimental data essentially changed the structure of corrrelations compared with the prior information.

5. Conclusions

The result of the present evaluation represents everything we know about the spectral distribution of Cf-252 with regard to a complete covariance uncertainty matrix, based on integral spectrum data (spectrum-averaged cross-sections measurements) also taking implicitly into account some recent direct spectrum measurements (in the prior information). This result must be updated and data from direct measurements in particular, should be explicitly included in the evaluation as soon as their covariances are available. Thus further steps in the evaluation are necessary in the future to yield an optimum result for the spectral distribution of Cf-252.

References:

/1/ M.V. Blinov: Proc. IAEA Consultants' Meeting on Neutron Source Properties, Debrecen (Hungary), 17-21 March 1980, INCD(NDS)-114/GT (1980) 79

/2/ Proc. IAEA Consultants' Meeting on the Cf-252 Neutron Spectrum, Smolenice (CSSR), 28 March - 1 April 1983, INDC(NDS)-146/L (1983)

/3/ "Nuclear Data for Science and Technology" (ed. K.H. Böckhoff), Proc. Int. Conf., Antwerp 6-10 September 1982, D. Reidel Publishing Company (1983)

/4/ J.W. Boldeman, D. Culley, R.W. Cawley: Trans. Am. Nucl. Soc. 32 (1979) 733

/5/ F. Bensch, H. Jasicek: INDC(AUS)-4 (1979)
/6/ M.V. Blinov, V.A. Vitenko, V.I. Yurevich: Proc. Int. Symp. Interaction of Fast Neutrons with Nuclei, Gaussig (GDR), 26-30 November 1979, ZfK-410 (1980) 104
/7/ Mon Jiangshen et al.: Chin. J. Nucl. Phys. 3 (1981) 163
/8/ M.V. Blinov, G.S. Boykov, V.A. Vitenko: Antwerp Conference /4/ (1983) 479
/9/ W.P. Poenitz, T. Tamura: Antwerp Conference /4/ (1983) 465
/10/ R. Böttger, H. Klein, A. Chalupka, B. Strohmaier: Antwerp Conference /4/ (1983) 484
/11/ H. Märten, D. Seeliger, B. Stobinski: Antwerp Conference /4/ (1983) 488
/12/ A. Lajtai, P.P Dyachenko, L.S. Kutzaeva, V.N. Kononov, P.A. Androsenko, A.A. Androsenko: Smolenice Meeting /3/ (1983) 177
/13/ O.I. Batenkov, M.V. Blinov, G.S. Boykov, V.N. Vitenko, V.A. Rubchenya: Smolenice Meeting /3/ (1983) 161
/14/ D.G. Madland, J.R. Nix: Antwerp Conference /4/ (1983) 473
D.G. Madland, J.R. Nix: Nucl. Sci. Eng. 81 (1982) 213
/15/ H. Märten, D. Neumann, D. Seeliger: Smolenice Meeting /3/ (1983) 199
/16/ J.J. Wagschal, R.E. Maerker, B.L. Broadhead: Antwerp Conference /4/ (1983) 436
/17/ A. Chalupka, B. Strohmaier, H. Klein, R. Böttger: Smolenice Meeting /3/ (1983) 187
/18/ A. Chalupka: Nucl. Instr. Meth. 165 (1979) 103
/19/ H. Märten, D. Richter, D. Seeliger: Report INDC(GDR)-28/L (September 1984)
/20/ M.V. Blinov, G.S. Boykov, V.A. Vitenko: (to be published)
/21/ W. Mannhart, F.G. Perey: Proc. 3rd ASTM-EURATOM Symp. on Reactor Dosimetry, Ispra (Italy), 1-5 October 1979, EUR 6813, Vol. II (1980) 1016
/22/ W. Mannhart: Antwerp Conference /4/ (1983) 429
/23/ W. Mannhart: (unpublished data)
/24/ R.W. Peelle: Adv. Nucl. Sci. Techn. 14 (1982) 11
/25/ F.G. Perey: ORNL/TM-6062 (1977)
F.G. Perey: ORNL/TM-6267 (1978)
/26/ F. Schmittroth: HEDL/TME 79-40 (1979)
/27/ W. Mannhart: Smolenice Meeting /3/ (1983) 229
/28/ H.T. Heaton II, D.M. Gilliam, V. Spiegel, C. Eisenhauer, J.A. Grundl: Proc. NEANDC/NEACRP Specialist Meeting, Argonne National Laboratory, 28-30 June 1976, ANL-76-90 (1976) 333
/29/ J. Grundl, C.M. Eisenhauer: NBS Spec. Publ. 425 (1975) 250
/30/ R.E. Maerker, J.J. Wagschal, B.L. Broadhead: Report EPRI NP-2188 (1981)
/31/ S. Tagesen, H. Vonach, B. Strohmaier: Physics Data 13-1 (1979)
/32/ B. Strohmaier, S. Tagesen. H. Vonach: Physics Data 13-2 (1980)
/33/ S. Tagesen, H. Vonach: Physics Data 13-3 (1981)
/34/ G. Winkler, D.L. Smith, J.W. Meadows: Nucl. Sci. Eng. 76 (1980) 30
/35/ G. Winkler, A. Pavlik, H. Vonach, A. Paulsen, H. Liskien: Antwerp Conference /4/ (1983) 400
A. Pavlik, G. Winkler: Report INDC(AUS)-9/L (1983)
/36/ D.W. Muir, R.E. MacFarlane, R.M. Boicourt: Proc. 4th ASTM-EURATOM Symp. Reactor Dosimetry, Washington D.C., 22-26 March 1982, NUREG/CP-0029, Vol. 2 (1982) 655
/37/ W. Mannhart: IAEA-TECDOC-263 (1982) 47
/38/ C.Y. Fu, D.M. Hetrick, F.G. Perey: NBS Spec. Publ. 594 (1980) 63
/39/ C.Y. Fu, D.M. Hetrick: Proc. 4th ASTM-EURATOM Symp. Reactor Dosimetry, Washington D.C., 22-26 March 1982, NUREG/CP-0029, Vol. 2 (1982) 877
/40/ W. Mannhart: Smolenice Meeting /3/ (1983) 213

MEASUREMENTS OF THE PROMPT NEUTRON FISSION SPECTRUM FROM THE SPONTANEOUS FISSION OF ^{252}Cf*

J.W. BOLDEMAN, B.E. CLANCY, D. CULLEY
Lucas Heights Research Laboratories,
Australian Atomic Energy Commission Research Establishment,
Sutherland, New South Wales,
Australia

Abstract

The prompt neutron emission spectrum from the spontaneous fission of ^{252}Cf has been measured for the energy range 0.124 to 15.0 MeV. In the measurement program, seven separate measurements were made of the spectrum between 1 and 15 MeV using a plastic scintillator as the neutron detector. For the energy range 0.124 to 2.66 MeV, a ^{6}Li glass scintillator was used as the neutron detector. The data are presented with respect to a Maxwellian distribution with T = 1.42 MeV. Some positive and negative deviations with respect to this distribution have been observed.

1. INTRODUCTION

The prompt neutron emission spectrum from the spontaneous fission of ^{252}Cf has been defined as a standard neutron spectrum[1,2], therefore, the detailed shape of the energy spectrum is required with high precision. We are especially interested in this spectrum because of the use of spontaneous fission sources of ^{252}Cf in the efficiency calibration of neutron coincidence counters[3-7] for use in nuclear safeguards applications.

Seven separate measurements of the spectrum between 1 and 15 MeV were made using an NE 102 plastic scintillator as the neutron detector. Preliminary data from the first five measurements were reported in ref. 8. Subsequently, these measurements were revised slightly using more accurate experimental data for the energy dependence of the absolute neutron detection efficiency of the plastic scintillator. The revised data were presented with a sixth measurement in ref. 9. More recently, a seventh measurement (referred to in Madland and Nix[10,11]) has been made with the plastic scintillator, together with a separate measurement of the spectrum in the lower energy range from 0.124 to 2.66 MeV, in which a ^{6}Li enriched glass scintillator was used as the neutron detector. In the present paper, aspects of the experimental program are highlighted, together with some recent work on the fission counter. The experimental program has been completed; however, some of the corrections are being reassessed before a final set of data points can be obtained.

2. EXPERIMENTAL DETAILS

All measurements were made using the time-of-flight method in which neutron detection in the appropriate detector initiated a count down to the time-delayed corresponding fission event. The program of measurements is summarised in Table 1. In Table 2, representative details of the experiments are listed, together with the important corrections. One interesting feature of the experiment was the use of a two-parameter recording system in which both the neutron flight time and the corresponding linear pulse height response in the particular

* Research performed, in part, under contract with the Department of Foreign Affairs, Australia.

TABLE 1

SUMMARY OF FISSION NEUTRON SPECTRUM MEASUREMENTS

Experiment No.	Detector	Energy Range (MeV)
1	NE 102	1.0-13.8
2	NE 102	1.0-14.2
3	NE 102	1.0-13.8
4	NE 102	1.0-14.6
5	NE 102	2.0-14.7
6	NE 102	2.0-13.7
7	NE 102	1.0-14.3
8	^{6}Li glass scintillator	0.124-2.660

neutron detector were recorded, event by event. The recording of the pulse height data was linear up to 3.5 MeV; however, all higher energy signals were pulse-height-limited because of the large dynamic range of such signals and the need to preserve sensitivity at the lower end of the energy spectrum. Typical experimental data (for experiment 1) are shown in Figure 1. The dual parameter data for the plastic scintillator measurements allow the use of a sliding linear bias in correcting the experimental data for the energy dependence of the neutron detection efficiency. The use of a sliding bias has two specific virtues. Firstly, it becomes possible to optimise the statistical accuracy of the experimental data, especially as the background decreased rapidly with increasing bias. Secondly, the

TABLE 2

SUMMARY OF EXPERIMENTAL CONDITIONS AND CORRECTIONS

Energy range	124-2660 keV	1.0-15.0 MeV
Flight path	40 cm	3.015 m
Detector	^{6}Li glass scintillator	NE 102 plastic scintillator
Detector dimensions:		
Diameter	50.8 m	50.8 m
Thickness	2.0 mm	25.4 cm
Fission rate	4.4×10^{4} fissions s^{-1}	$8\text{-}5 \times 10^{4}$ fission s^{-1}
Neutron detector calibration:		
Experimental	Relative 124-1349 keV	Absolute 2-11 MeV
Calculated	1349-2600 keV	1-2 MeV, 11-15 MeV
Recording	dual parameter- flight time, neutron detector response	dual parameter- flight time, neutron detector response
Corrections	1. Dead time (start and stop signal)	1. Dead time (start and stop signal)
	2. Air attenuation	2. Air attenuation
	3. Air scattered neutrons	3. Delayed γ-rays
	4. Delayed neutron response	4. Air scattered neutrons (90 mm shadow bar)
	5. Timing resolution	5. Timing resolution
	†6. Fission loss below bias	†6. Fission loss below bias

†No correction has yet been applied

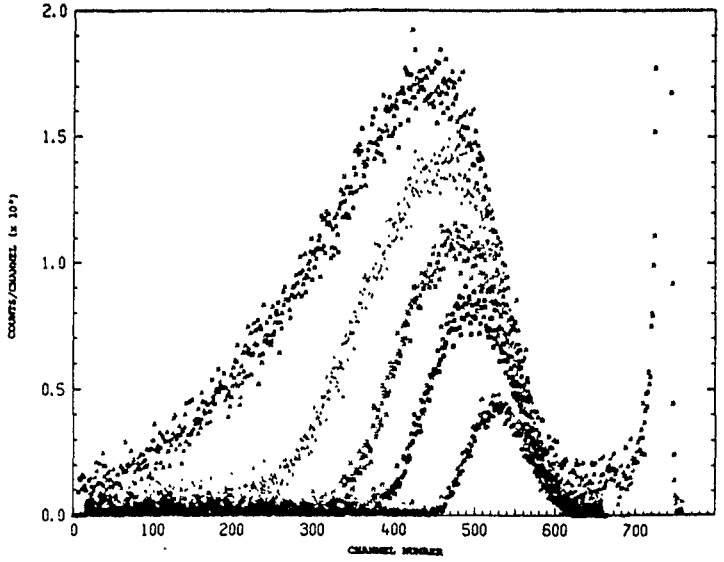

Figure 1 Typical experimental data - experiment 1 - for bias settings of 0.5, 1.0, 1.5, 2.0 and 3.0 MeV

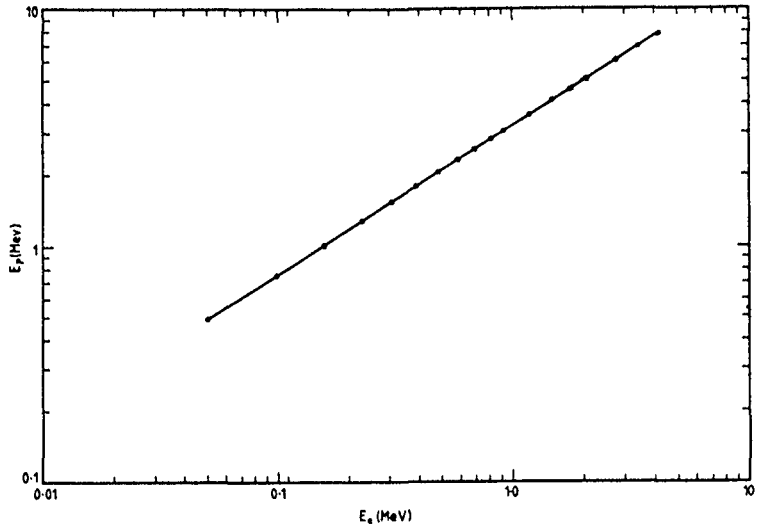

Figure 2 Relative response of the plastic scintillator for Compton scattered electrons and recoil protons

background corrected linear data for a particular segment of the time-of-flight spectrum can be compared with the linear response obtained in the calibration measurements. For the ^{6}Li enriched glass scintilator measurement, the dual parameter data confer only slightly increased value.

2.1 Calibration of the Neutron Detectors

The energy dependence of the absolute neutron detection efficiency of the NE 102 plastic scintillator was determined using the associated particle system that was installed on the EN tandem accelerator at the Australian National University[12,13]. In this system, neutrons were produced using the (D,D) reaction and the efficiency of the detector for neutrons of a particular energy was determined by placing the plastic scintillator at the appropriate angle with respect to the deuteron beam direction and by operating it in coincidence with a ^{3}He identification system at the recoil angle for the corresponding ^{3}He particles. The ^{3}He particle identification system fully discriminated against alpha particles from the ^{12}C(d,α) reaction. The relative response of the plastic scintillator for Compton scattered electrons and recoil protons is shown in Figure 2. The absolute efficiency curves for different values of the bias are shown in Figure 3. The efficiency data were extrapolated to lower and higher energies using a code written by Clayton[14].

The relative energy dependence of the 2 mm thick ^{6}Li enriched glass scintillator used for the lower energy measurements was measured

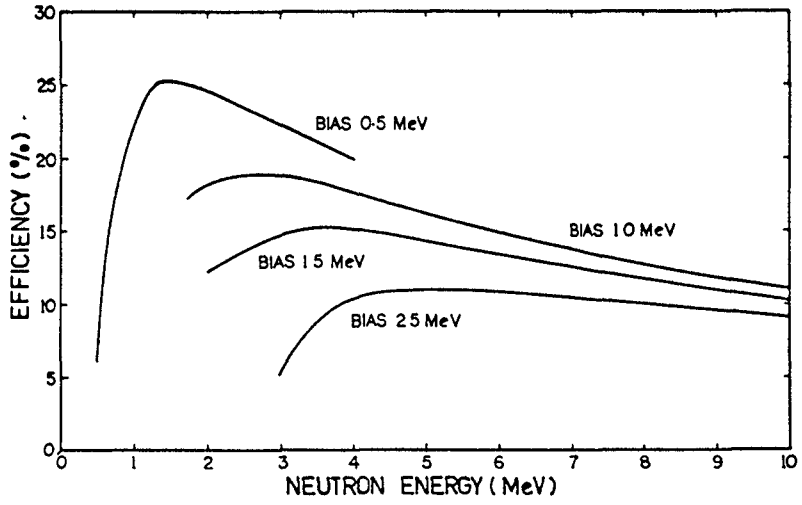

Figure 3 The neutron energy dependence of the absolute neutron detection efficiency of the plastic scintillator for different bias settings.

with respect to a calibrated long counter, using a 3 MV pulsed Van de Graaff accelerator to produce monoenergetic neutrons and with identical geometry and electronic conditions as those employed in the actual spectrum measurements. The efficiency data measured were the prompt-in-time neutron energy dependence. The full time-dependent response of the ^{6}Li glass scintillator in the geometry of the spectrum measurement was also obtained for the unfolding procedure of the analysis.

2.2 The Fission Counter

The fission counter used in these measurements was a parallel plate ionisation chamber with a plate spacing of 3 mm and pure methane as the filling gas. There is a correction in these measurements which depends on the proportion of the fission fragments which do not register above the discriminator bias. From the shape of the bias curves it was estimated that approximately 2% of the fission fragments were lost beneath the bias of the fission counter system.

An independent method has been developed recently to determine the fission rate of various spontaneously fissioning sources[7]. The method is based on the P_{ν} distributions for the spontaneous fission of these nuclei. This technique has been applied to the fission counter used in the spectrum measurement. The total fission rate so obtained is about 2 to 3% larger than that recorded under identical conditions in the fission spectrum measurement. However, there are some minor problems associated with the application of this technique that have still to be resolved, so this figure is preliminary.

3. ADDITIONAL CORRECTIONS

All corrections applied in the measurement program are listed in Table 2. Previous tabulations of the data from the present experiments did not include a correction for the effect of the time resolution of the time-of-flight system. This correction has been incorporated into the present results. Furthermore, the previous data had been corrected for the neutron attenuation effects of the aluminium wall thickness of an earlier version of the associated particle system. The chamber actually used had been specially modified to minimise neutron attenuation. A small correction is also required for the effect of the loss of the fission fragments. At this time, the magnitude of the effect has not been determined accurately so no correction for this effect has yet been applied.

4. RESULTS AND ANALYSES

The experimental data for each experiment were compared with a Maxwellian distribution N(E) = A.(exp-E/T) in which the average energy $\bar{E} = {}^{3}/_{2}\ T$, where T is the temperature of the distribution. In the analysis, the corrected experimental data for intervals of five channels in the time-of-flight spectrum were summed. This time-of-flight segment corresponded approximately to the energy resolution of the various experiments. The fitting procedure involved fitting the integral of the Maxwellian distribution between the lower and higher energy bounds for each five channel segment of the time-of-flight data.

In earlier descriptions of the preliminary data from the present measurements, a Maxwellian distribution with T = 1.424 MeV was consistent with the data. Following minor revision to the experimental data referred to in section 3, the pure Maxwellian description of the data is less appropriate. For the presentation of the totality of the experimental data, the following procedure was adopted. Each of the seven experiments with the plastic scintillator were fitted with a Maxwellian distribution in which the value of the temperature was fixed at T = 1.420 MeV. For the fit to the data from each experiment, a table of the deviations from the Maxwellian distribution $Y_{exp}/Y_{fit}(E_1)$ was obtained. For appropriate increments in the entire energy range of the experiments, the summed deviations, weighted according to the statistical significance of the specific points were obtained.

The lower energy data obtained with the ^{6}Li glass scintillator were treated in a slightly different way. As before, the data were fitted with a Maxwellian distribution with T = 1.42 MeV and the deviation from this distribution were obtained. The data from the ^{6}Li experiment were then normalised to the higher energy data by equating the deviations from this Maxwellian distribution in the energy region of the overlap of the two types of experiment, namely 1.00 to 1.65 MeV.

A comparison of the experimental data for the energy range 0.124 to 10.0 MeV with a Maxwellian distribution of T = 1.42 MeV is shown in Figure 4. In Figure 5, the combined experimental data for the plastic scintillator measurements from 1.0 to 14.25 MeV is shown. The accuracies given in the figures are statistical only and are less than 1% for the energy range 1.0 to 5.5 MeV. The data show a small negative deviation from 0.4 to 1.0 MeV, a positive deviation of about

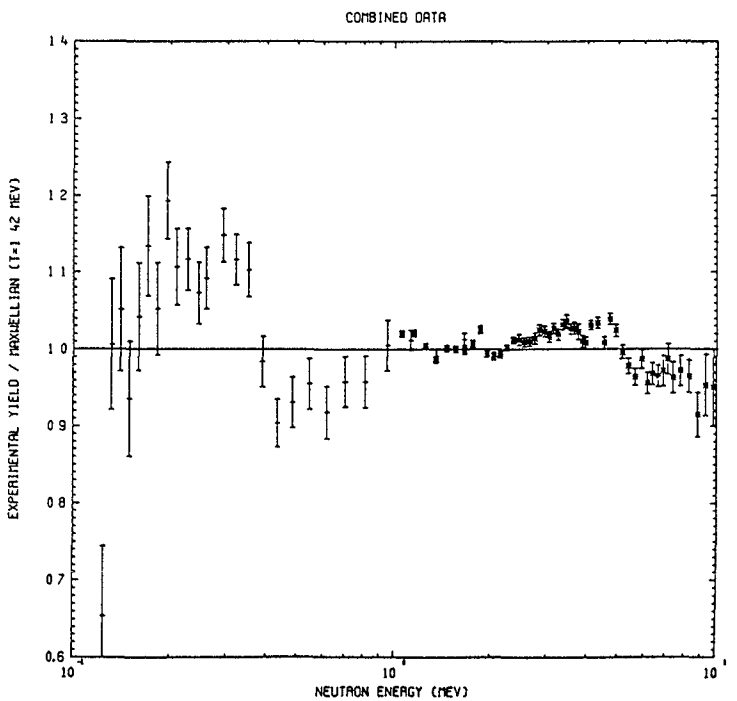

Figure 4 Comparison of combined experimental data and Maxwellian dependence with T = 1.42 MeV

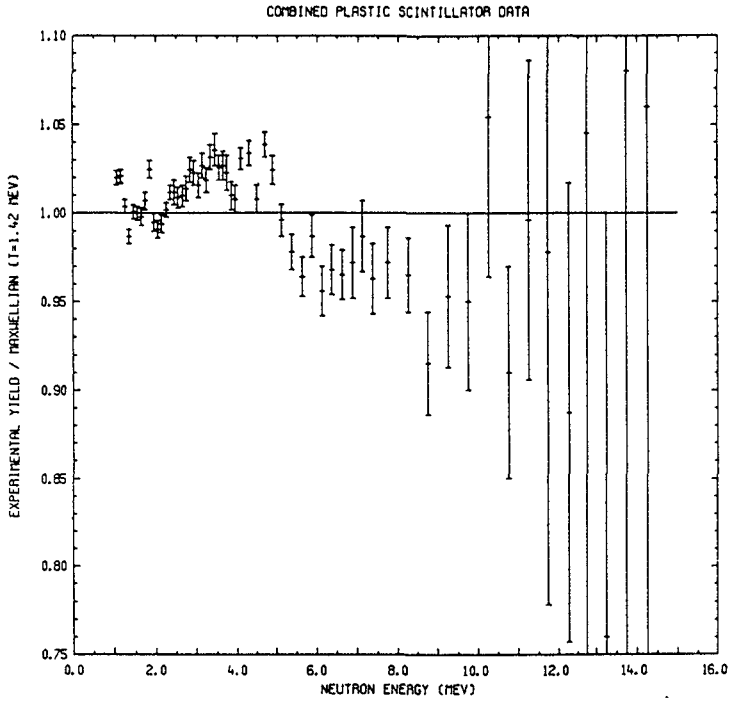

Figure 5 Comparison of combined plastic scintillator data and Maxwellian dependence with T = 1.42 MeV

2.5% between 2.5 and 5.0 MeV and a small negative deviation above 6.0 MeV. The data below 300 keV were subject to several significant corrections (for time-of-flight downscatter) and the statistical accuracies do not reflect the overall accuracy of the data. The positive deviation below 300 keV is therefore probably not genuine. The data above 10.0 MeV are not of sufficient precision to provide any definitive measure of a potential deviation. It should be emphasised that a small correction to these data is still required for the effect of the fission fragment loss.

5. ACKNOWLEDGEMENTS

We wish to acknowledge the technical assistance of J.P. Fallon, I.F. Senior, K.J. Thorpe, A. Croal and the late H.G. Broe. We would also like to thank R.J. Cawley for his assistance with the computer software, C.M. Bartle for the use of the associated particle system and E. Clayton for providing a computer code.

6. REFERENCES

1. Proc. IAEA Panel on Neutron Standard Reference Data, Nov. 1972, Vienna, p. 362.
2. Proc. IAEA Consultants' Meeting on Prompt Fission Neutron Spectra, Aug. 1971, Vienna, p. 169.
3. M.S. Krick, M.L. Evans, N. Ensslin, C. Hatcher, H.O. Menlove, J.L. Sapir, J.E. Swansen, M. de Carolis and A. Ramello, Proc. IAEA Symp. Nuclear Sageguards Technology, 1978, Vol. II p. 51.
4. R. Dierckx and W. Hage (1983). Nucl. Sci. Eng. 85, 325.
5. M.S. Zucker and E. Karpf (1984). Proc. 6th ESARDA Symp. Safeguards and Nuclear Materials Management, Venice, p. 279.
6. L. Bondar, K.P. Lambert, E.W. Lees, M. Poletti and F.J.G. Rogers (1984). Proc. 6th ESARDA Symp. Safeguards and Nuclear Materials Management, Venice, p. 297.
7. J.W. Boldeman, M.G. Hines, J.P. Fallon and I. Delaney (1984). Proc. 6th ESARDA Symp. Safeguards and Nuclear Materials Management, Venice, p. 285.
8. J.W. Boldeman, D. Culley and R.J. Cawley (1978). Proc. Int. Conf. Neutron Physics and Nuclear Data, Harwell, p. 916.
9. J.W. Boldeman, D. Culley and R.J. Cawley (1978). ANS Trans. 32, 733.

10. D.G. Madland and J.R. Nix (1982). Nucl. Sci. Eng. 81, 213.

11. D.G. Madland and J.R. Nix (1982). Proc. Int. Conf. Nuclear Data for Science and Technology, Antwerp, p. 473.

12. C.M. Bartle and P.A. Quin (1974). Nucl. Instrum. and Meth. 124, 119.

13. C.M. Bartle, D.W. Gebbie and C.L. Hollas (1977). Nucl. Instrum. and Meth. 144, 437.

14. E. Clayton, unpublished.

NEW MEASUREMENT OF THE ^{252}Cf(sf) NEUTRON SPECTRUM IN THE HIGH-ENERGY RANGE

H. MÄRTEN, D. RICHTER, D. SEELIGER
Technical University of Dresden,
Dresden, German Democratic Republic

R. BÖTTGER
Physikalisch-Technische Bundesanstalt,
Braunschweig, Federal Republic of Germany

W.D. FROMM
Zentralinstitut für Kernforschung Rossendorf,
Dresden, German Democratic Republic

The high-energy end of the ^{252}Cf spontaneous-fission neutron spectrum has been measured by employing a miniature ionization chamber with Cf sample (about 70 000 fissions per s). Two NE 213 neutron detectors (both 5" in diameter, thickness 1.5" and 5") with efficient pulse shape discrimination of γ-ray and cosmic-myon background were used at flight paths of 3.7 and 5.9 m and at angles (with reference to Cf sample plane normal) of 60 and 0 deg respectively. The neutron spectra have been measured by means of the two-dimensional (time-of-flight,scintillator response)-spectroscopy. Several additional spectra were recorded simultaneously to check up the stability of the spectrometer (time scale, scintillator response, particle discrimination, fragment detector amplitude). The time resolution with reference to FWHM of the γ-peak was 1.3 ns (1.5" detector) and 1.5 ns (5" detector). The total fragment detector efficiency was deduced from a measurement of fragment-neutron coincidences (0.9927 ± 0.0005).

Fig. 1

Preliminary experimental data on the Cf neutron spectrum (crosses - this work, dots - Ref. 1) represented as percentage deviations from a Maxwellian distribution with T = 1.42 MeV. The crosses indicate the full error and the energy bin width for which the data are stated as averages (grid scale). The NBS evaluation (Ref. 2) is shown above 6 MeV (dashed curve).

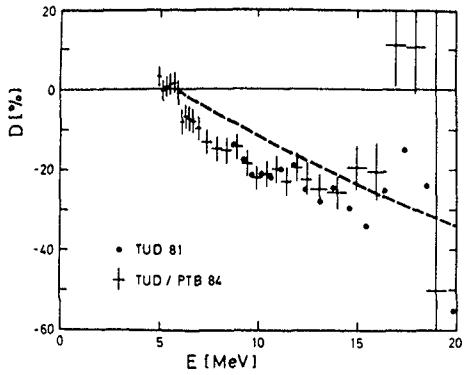

Fig. 2

The high-energy tail of the Cf neutron spectrum (histogram - this work, crosses - Ref. 1). The experimental errors of the data above 22 MeV amount to about 80-100 % (16).

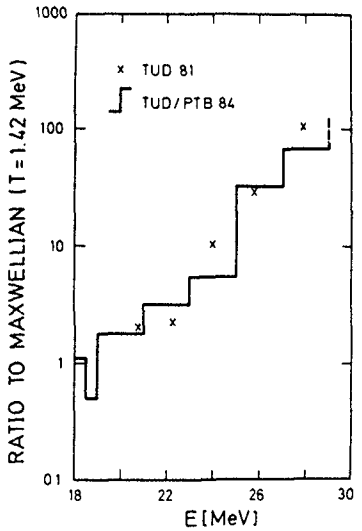

To obtain minimum experimental errors at high energy especially, the analysis procedure involves the selection of the optimum scintillator response bias depending on neutron energy. The measured spectra have been corrected for time resolution, time-of-flight bin width, fragment detector efficiency, transmission (air, detector walls) (cf. Ref. 1,3). The influence of non-correlated STOP signals as well as scattered neutrons was found to be neglegible at high energy. The deduced energy spectrum represented in the figures confirm the data of Ref. 1 and 3. The yield of highest-energy neutrons (above 20 MeV, Fig. 2) is comparable to the result of Ref. 1. Hence, the conclusions drawn in Ref. 1 are corroborated by the presented new measurement.

This work was supported by the Nuclear Data Section of the IAEA. The help of Dr. D. Hermsdorf (Monte Carlo calculations) and Dr. D. Schmidt (experimental arrangement) is greatfully acknowledged.

References

1 - H. Märten et al., Antwerp Conf. (1982), Proc. p. 488, H. Märten et al., INDC(GDR)-28/L (1984)

2 - J. Grundl and C. Eisenhauer, NBS-493 (1977)

3 - R. Böttger et al., loc. cit. (1a), p. 484

312 PROMPT NEUTRON SPECTRA FOR ENERGY RANGE 30 keV – 4 MeV FROM FISSION OF ^{233}U, ^{235}U AND ^{239}Pu INDUCED BY THERMAL NEUTRONS

A. LAJTAI, J. KECSKEMÉTI, J. SÁFÁR
Central Research Institute for Physics,
The Hungarian Academy of Sciences,
Budapest, Hungary

P.P. DYACHENKO, V.M. PIKSAIKIN
Institute of Physics and Power Engineering,
Obninsk,
Union of Soviet Socialist Republics

Abstract

The prompt neutron spectra for the energy range 30 keV - 4 MeV from fission of ^{233}U, ^{235}U and ^{239}Pu induced by thermal neutrons of VVRS-M type reactor tangentional channel have been measured by time-of-flight method with using of NE-912 and NE-913 lithium glass as neutron detector and gas scintillation counter for fission fragments. Prompt neutron spectrum from spontaneous fission of ^{252}Cf has been measured at the same experimental conditions as a standard.

The ^{233}U, ^{235}U and ^{239}Pu isotopes are the main component of nuclear fuel. Therefore, the study of the properties especially that of the fission neutron spectra of these nuclei is of great importance. A large amount of experimental data has been accumulated on the spectra in the E>1 MeV region, but there are very few data in the energy range below 1 MeV where approximately 25 % of the total number of fission neutrons is observed |1,2|.

The extrapolation of data from the high energy range to the low energy one on the basis of Maxwell's or Watt's distributions, as being done in nuclear reactor design calculation is not sufficiently verified and some measurements indicate significant deviations from these predictions at low energies.

We have studied the prompt neutron spectra from the thermal neutron induced fission of ^{233}U, ^{235}U and ^{239}Pu in the 0.03-4 MeV energy range. The measurements have been performed at a tangential beam of the Central Research Institute for Physics VVRM reactor using a special collimator with quartz, and bismuth polycrystal filters. The neutron detection was carried out with time-of-flight techniques, using Li glass detectors.

The fission fragments were detected by a scintillation counter filled with pure argon gas of 1 atm.

The construction of the fission chamber made is possible to change the different fissile samples without any distortion of the measuring conditions. To get an optimal pulse ratio for fission fragments and α-particles a 0.6 mm thick quartz plate of 65 mm diameter was placed at 9 mm and 41 mm from the fissile sample and from the photocathode, respectively. The experimental arrangement is shown in Fig. 1.

The diameter of all fissile samples was 45 mm, and their thickness was 1.0 mg/cm^2. The backings of the layers were stainless steel foils of 0.1 mm thickness. The values of the isotopic enrichment were 96 % for ^{235}U and 90 % for ^{233}U and ^{239}Pu. The fission fragment counting rates were $24.2 \cdot 10^3 s^{-1}$ for ^{252}Cf, $5.4 \cdot 10^3 s^{-1}$ for ^{233}U, $8.12 \cdot 10^3 s^{-1}$ for ^{235}U and $7 \cdot 10^3 s^{-1}$ for ^{239}Pu.

The lithium glasses NE912 and NE-913, 45 mm in diameter and 9.5 mm thick, were used as fission neutron and γ-ray detectors, respectively. In order to reduce the random coincidence background the neutron detector (or γ-ray detector) was surrounded by a shielding, consisting of paraffin, ^6Li hydride and lead.

In the present arrangement the neutron flight path, channel width and the over-all time resolution (FWHM of the γ-ray peak) were 30.5 cm, 0.487 ns and 2.5 ns, respectively.

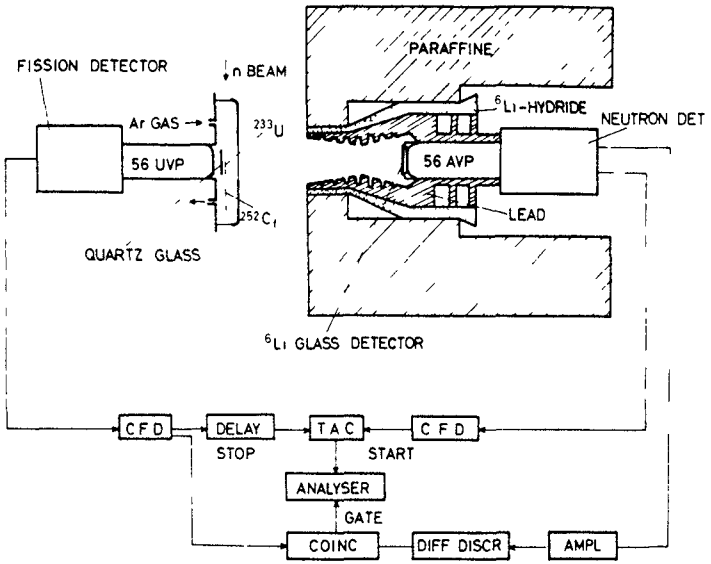

Fig. 1. Experimental arrangement.

Table 1.

Number of registrated fission fragments (10^9)

Sample / Detector configuration	^{252}Cf	^{235}U	^{233}U	^{239}Pu
NE 912	15532	15458	27011	16089
NE 913	20456	12713	22937	7.735
NE 912 with shedow cone	45101	12979	28487	15099
NE 913 with shedow cone	49.695	12287	15351	5953

The spectra of all three targets were measured with both NE-912 and NE-913 Li glass detectors, where the latter was used to determine the γ-ray contribution. For both detectors measurements were carried out without and with a 12 cm long Cu shadow cone, in order to determine the background due to scattering by the detector environment. All these measurements were carried out also for a ^{252}Cf sample having the same sizes as the fissile samples. Table 1 shows the registrated fission numbers for each sample in the above experimental configurations.

The experimental data for each sample were analysed in the same mauner. All measured spectra were corrected for the random coincidence background and after that normalized to the measured fission number. The relative contribution of the random coincidence background was about 130 % at 30 keV, 40 % at 60 keV and 20 % between 1 MeV and 2 MeV. Due to the low counting rates the channel dependent accidental coincidence background turned out to be negligible. In the next step we determined the γ-ray background measured with the NE-913 glass and that of the scattered neutrons. For the latter we have to note that the shadow cone method gives good result only in the case of a point like target. In the case of a finite target the cone inhibits a part of those neutrons, which give the scattered background. In order to determine this effect additional measurements were performed with a small, 7 mm diameter ^{252}Cf source. As a result we got that the measured scattered background in this case was about 15 % higher than in the case of the large ^{252}Cf source. This ratio was within $\pm$ 5 % energy independent in the range investigated. Therefore the measured scattered background contributions for each sample were corrected with this factor, and then subtracted together with the γ background from the primary spectra.

In the last step the corrected neutron time-of-flight spectra were transformed into energy scale. The evaluation

of the shape of the neutron energy spectra for ^{233}U, ^{235}U and ^{239}Pu was accomplished relative to that for ^{252}Cf. Assuming that the fission neutron spectrum of ^{252}Cf can be described by a Maxwellian distribution of T=1.42 MeV, an effective detector efficiency was extracted from the measured spectrum. Making use of this efficiency we determined the energy specta for the thermal neutron induced fission of ^{233}U, ^{235}U and ^{239}Pu. At this procedure we used the average prompt neutron multiplicities $\bar{\nu}$=3.757 for ^{252}Cf, $\bar{\nu}$=2.48 for ^{233}U, $\bar{\nu}$=2.42 for ^{235}U and $\bar{\nu}$=2.88 for ^{239}Pu. Fig. 2 shows the ratios of the so determined spectra to Maxwellian distributions with T=1.32 MeV for ^{233}U, T=1.315 MeV for ^{235}U and T=1.38 MeV for ^{239}Pu.

It can be seen that the prompt neutron spectra of these isotopes are satisfactorily described by these distributions in the energy range 30 keV<E_n<4 MeV within the error limits.

Since these spectra contain the ^{252}Cf neutron spectrum as a reference we felt it important to carry out an absolute determination for the latter. Therefore, the measured ^{252}Cf neutron spectrum was also evaluated using the measured absolute neutron detection efficiency, described in [3]. At this procedure we used the finite time resolution given by the γ-peak width and the response functions of the neutron detector, calculated by Monte Carlo method.

The ratio of the resulting absolute fission neutron spectrum, determined by using the measured fission number, neutron multiplicity $\bar{\nu}$=3.757 and ε(II) from Ref.[3]. to a Maxwellian distribution with T=1.42 MeV is shown in Fig. 3. The error bars contain statistical errors and the errors of the efficiency measurement. We note that the absolute efficiency was determined experimentally only up to the 1.2 MeV. For higher energies it was extrapolated making use of the $^{6}Li(n,\alpha)$ cross sections from the file ENDF/B-V. Therefore the data points in this region can be subject of possible systematic uncertainities.

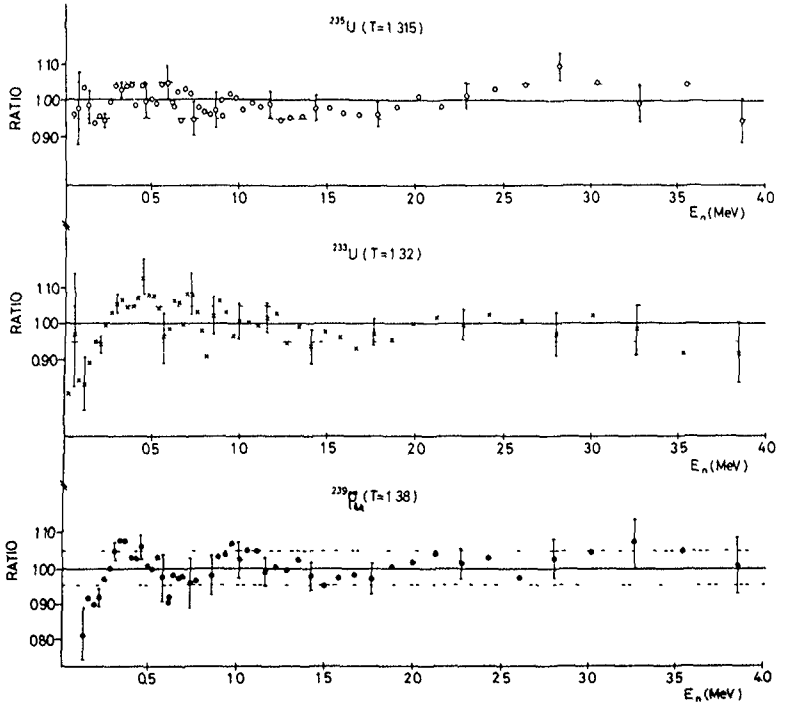

Fig. 2. The experimental data for ^{233}U, ^{235}U and ^{239}Pu divided by Maxwellian distributions.

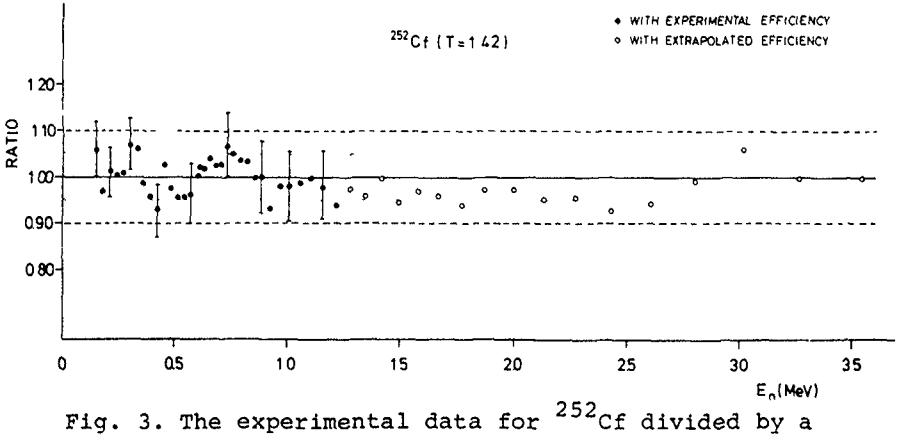

Fig. 3. The experimental data for ^{252}Cf divided by a Maxwellian distribution.

These results for the ^{252}Cf fission neutron spectrum are in agreement with those of Blinov et al |4|, and of an earlier measurement of us |5|, made at different experimental conditions.

References

|1| B.I. Starostov, A.F. Semenov, V.N. Nefedov, INDC (CCP)-164/L

|2| 6th All-Union Conf. on Neutron Physics, Kiev, USSR (1983)

|3| A. Lajtai et al., in this meeting

|4| M.V. Blinov et al., Proc. IAEA Consultants's Meeting Smolenice, INDC (NDS)-146/S (1983) 161

|5| A. Lajtai et al., ibid. p. 177.

NEUTRON EMISSION FROM THE SPONTANEOUS FISSION OF ^{252}Cf

C. BUDTZ-JØRGENSEN, H.-H. KNITTER, R. VOGT
Central Bureau for Nuclear Measurements,
Joint Research Centre,
Commission of the European Communities,
Geel

Abstract

The gridded ion chambers developed at CBNM provide a powerful tool for measurements of fission fragment angle, kinetic energy and mass distributions simultaneously with an angular efficiency close to 4π. They can also serve in measurements where fission neutron spectra are studied as function of these physical quantities. Preliminary tests have been made with a fission chamber loaded with a ^{252}Cf source of ~ $4 \times 10^3 . s^{-1}$. The fission neutrons were detected with a 4" x 1" plastic scintillator and conventional time-of-flight electronics. The coincidence resolution between the neutron detector and the fission chamber was < 2 ns. The neutron detector was placed 2.05 m from the ^{252}Cf source with a direction normal to the chamber electrodes. The cosines of the angles ϑ, between this direction and the path of the light fission fragments were determined using the chamber anode and cathode pulses. At higher neutron energies it can be seen, that the neutrons are emitted mainly in the direction of either the light or the heavy fragment, confirming that most of the neutrons are emitted from the fully accelerated fragments.

INTRODUCTION

Several attempts[1,2] have recently been made to give a theoretical description of the standard neutron spectrum of ^{252}Cf. These models are based on the assumption that the mechanism of neutron emission is the evaporation from fully accelerated fragments. However, experimental results[3] on the prompt neutron anisotropy have led to the conclusion that a fraction (~ 10 - 20 %) of the total number of fission neutrons is emitted isotropically in the laboratory frame. In spite of many further

investigations the knowledge about the so-called scission neutron emission is poor and partially contradictory. This is especially the case for scission neutron yield as function of fragment mass-split (A_L/A_H) and fragment total kinetic energy (TKE). There is therefore a strong need not only for precise neutron spectrum data, $N(E_n)$, but also for double- or multiple-differential measurements, $N(E_n,\vartheta_n,A,TKE)$ which can help to clarify the nature of the fission neutrons.

EXPERIMENTAL METHOD

At present a multiple parameter measurement of the ^{252}Cf prompt neutron spectrum, $N(E_n,\Theta_n,A,TKE)$ is being started at CBNM. The experimental set-up is shown in Fig. 1. Fission fragment detection is made using the gridded ion chambers developed at our lab with which fission fragment angle, kinetic energy and mass can be determined simultaneously with an angular efficiency

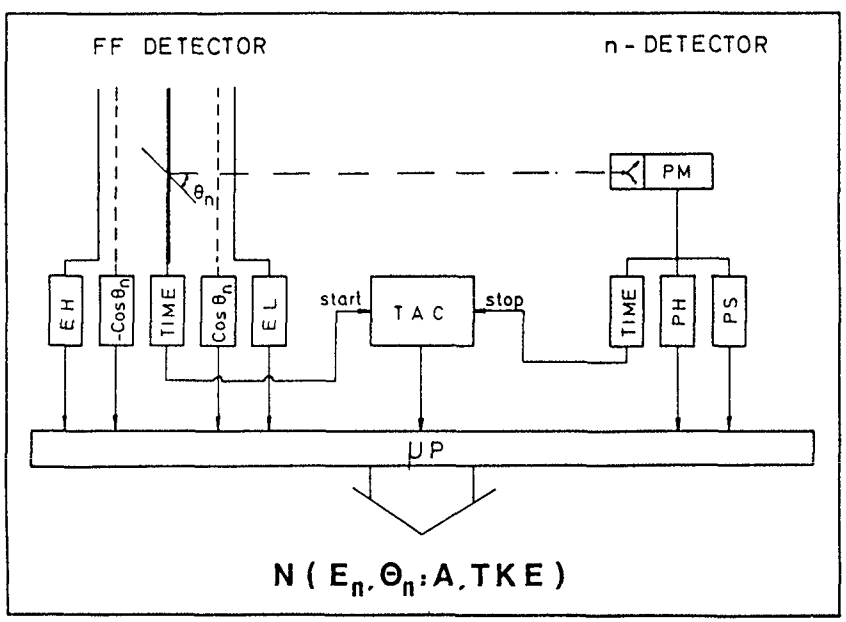

Fig. 1.
Experimental set-up.

close to 4π steradian. Such a detector has been used in a recent measurement of fission fragment mass, kinetic energy and angular distribution for $^{235}U(n,f)$ in the neutron energy range from thermal to 6 MeV on which a report[4] will be presented at the present meeting. The working principle and the data processing procedures used in connection with these chambers are described in ref. 5 - 10. The fission fragment kinetic energies (E_L,E_H) are determined using the anode pulses from the shown twin chamber. The fission fragment energy resolution is ~ 0.5 MeV and the detector pulse-height defect, which has been determined[11] in a cooperation with Institute of Physics, University of Aarhus, Denmark, is smaller than for conventional Si detectors. The double energy information is used to derive the fission masses. The angle information is determined as cosine of the angle ϑ between the normal of the electrodes and the path of the fission fragments. The cos ϑ resolution is typically ~ 0.05. Timing is made with the pulses from the common cathode.

The neutron detector is located on the centre axis of the ionization chamber. At present a 4" x 1" plastic scintillator is in use, but will be substituted by a NE 213 scintillator such that also pulse shape discrimination can be applied in order to suppress γ-rays. Neutron energies are determined using conventional time-of-flight technique.

All 7 parameters are digitized and stored sequentially on tape for off-line analysis.

TEST MEASUREMENTS

For the first test measurements a ^{252}Cf source on a 0.5 mm thick stainless steel backing was available. Since only one fragment could be detected per fission event only one chamber half was operational. The source having an activity of ~ $4 \cdot 10^3$ fiss.s^{-1} was prepared by electrolysis and the fragment spectrum, shown in Fig. 2, was rather distorted due to energy absorption in the source. This had as a consequence that only a rough distinction could be made between light and heavy fragments.

Fig. 3 displays the angle integrated neutron time-of-flight spectrum measured with the neutron detector placed at a distance of 2.05 m from the fission chamber. The time resolution as determined from the γ-peak is 2.2 ns and the velocity resolution of 1.1 ns/m is a factor of 4 better than the one employed in the fission neutron angular distribution measurement of ref. (3).

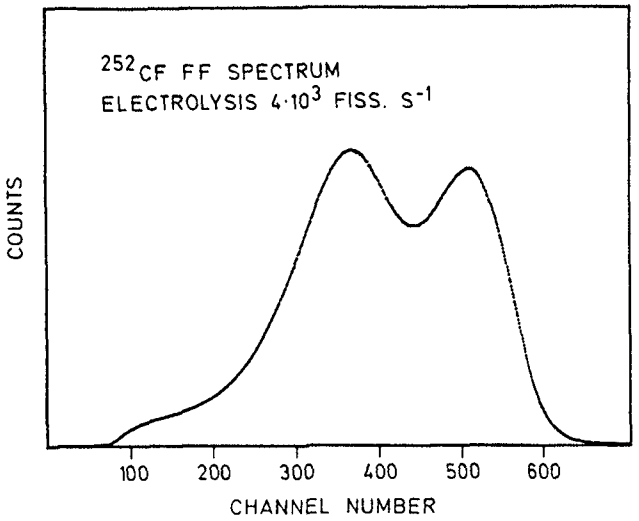

Fig. 2.
Pulseheight spectrum obtained with the ^{252}Cf source used in the test experiment.

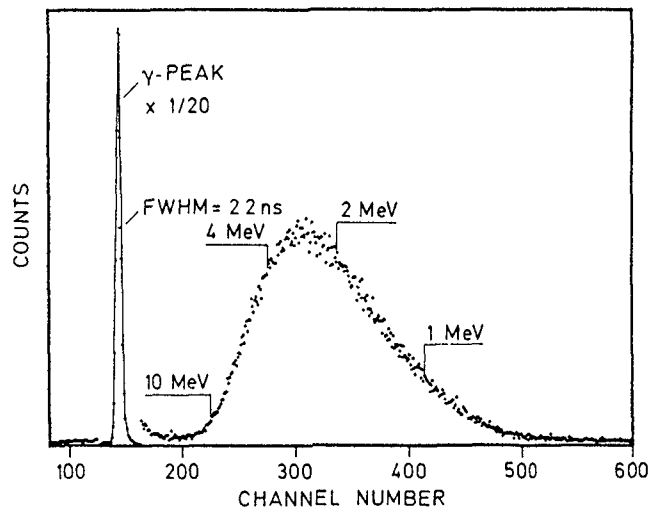

Fig. 3.
Neutron time-of-flight spectrum integrated over all fission fragments.

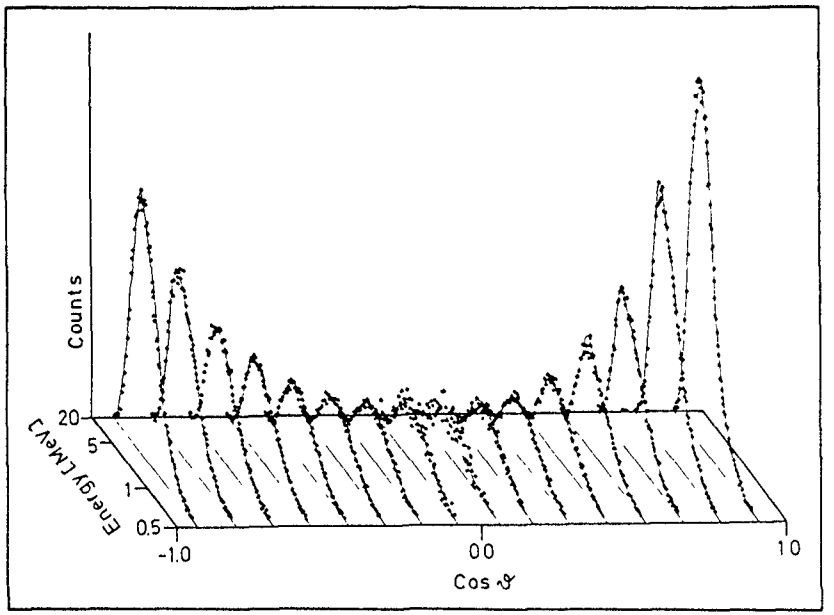

Fig. 4.
Biparametric plot of the number of neutrons versus cos ϑ and versus the neutron time-of-flight. On the time-of-flight axis some equivalent neutron energies are indicated.

The above spectrum was used to determine the relative efficiency of the neutron detector assuming that the ^{252}Cf fission neutron spectrum is a maxwellian distribution with a temperature of 1.42 MeV. However, since γ-rays suppression was not used in the present set-up, it was found that the spectrum was influenced by a background contribution of delayed γ-rays, relatively most pronounced above ~ 7 MeV neutron energy.
The cosine of the angles ϑ between the neutron directions and the path of the light fission fragment were determined using the recorded pulseheights of the fission chamber anode- and cathode pulses. Fig. 4 displays a biparametric plot of the number of neutrons versus cos ϑ and versus the neutron time-of-flight. At higher neutron energies it can be seen that the neutrons

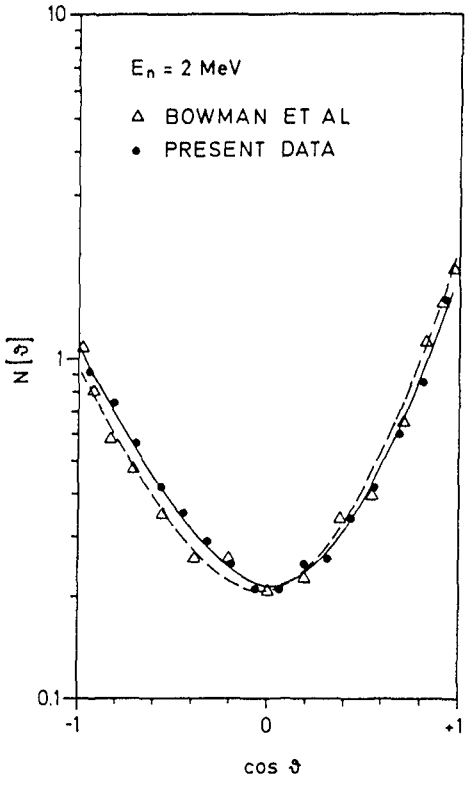

Fig. 5.
Fission neutron angular distribution at neutron energies of 2 MeV.

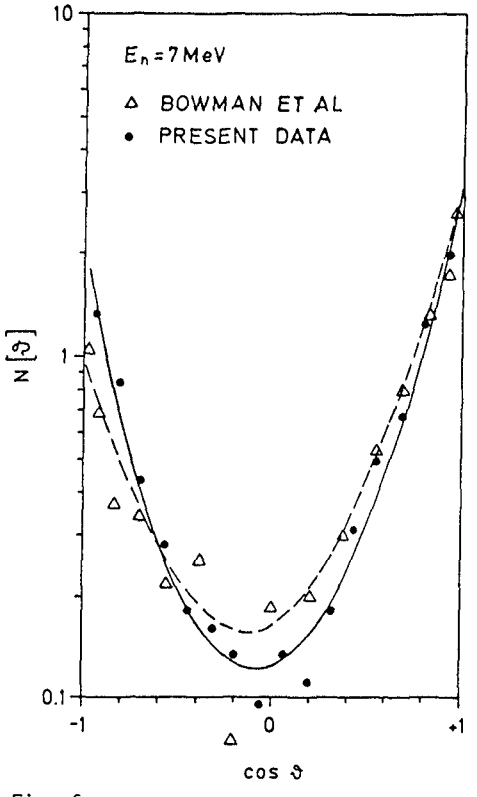

Fig. 6.
Fission neutron angular distribution at neutron energies of 7 MeV.

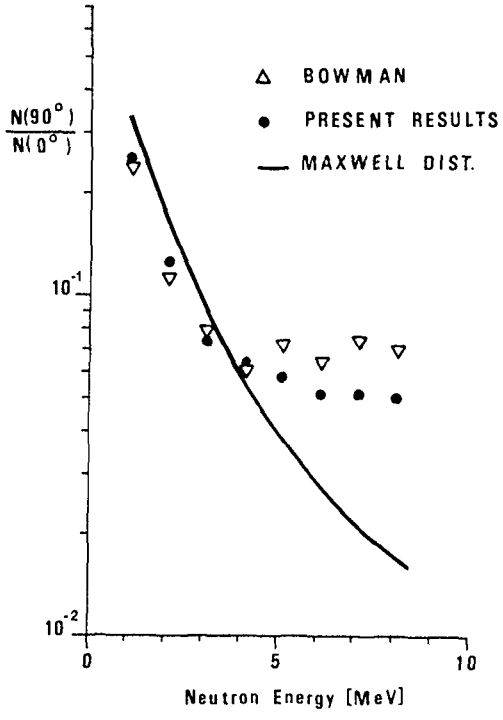

Fig. 7.
Intensity ratio N(90°)/N(0°) as function of neutron energy.

are emitted mainly in the direction of either the light or the heavy fragment, confirming that most of the neutrons are emitted from the fully accelerated fragments. It can also be seen that the energy spectrum for neutrons with cos $\vartheta \cong 0$ is softer than that at cos ϑ = 1 or -1. This is important for the use of the ^{252}Cf fission neutron spectrum as a standard spectrum since an inefficiency in fission fragment detection, e.g. due to absorption losses, can result in measured spectra deviating from the angle integrated ^{252}Cf spectrum.

Figs. 5 and 6 show the neutron angular distribution at 2 MeV and 7 MeV, respectively compared to the data of ref. (3). The agreement between the two measurements is fairly good. However, it can be seen that the present data show that more neutrons are emitted in the backward hemisphere (cos $\vartheta < 0$). The reason is, as mentioned above, that the distinction between heavy and light fragments is rough and the sign of cos ϑ is therefore in some cases not ambiguously determined.

The present angular distributions are at neutron energies above 5 MeV somewhat more anisotropic than the data of ref. (3). This is illustrated on Fig. 7 where the intensity ratios N(90°)/N(0°) are compared for the two measurements. Also shown here as a full curve is a calculation of the N(90°)/N(0°) intensity ratio based on the assumption that all neutrons are emitted from the fully accelerated fission fragments and that they have a maxwellian energy distribution in the fragment center of mass system, ref. (12).

$$\frac{N(E,90°)}{N(E,0°)} = \frac{1}{2} \exp\left[-2\cdot(E\cdot E_f)^{1/2}\cdot T^{-1}\right]$$

The average fragment kinetic energy per nucleon was assumed to be E_f = 0.75 MeV and the fragment nuclear temperature was T = 0.94 MeV. Below 4 MeV this simple model describes the trend of the measured anisotropies quite well, whereas there is a pronounced discrepancy at higher neutron energies. This behaviour confirms that a fraction of the fission neutrons are emitted before the nascent fragments are fully accelerated and therefore more or less isotropic in the compound nucleus (^{252}Cf) frame. However, part of this contribution could also have experimental origin. As explained earlier neither in the present nor in the measurement of ref. (3) γ-ray suppression was applied. An additional component of delayed γ-rays, which of course are emitted nearly isotropically in the laboratory frame, might explain why the N(90°)/N(0°) intensity ratio does not decrease with energy according to the evaporation model.

CONCLUSION

A multi differential measurement of the ^{252}Cf fission neutron spectrum as function of fragment mass, kinetic energy and angle has been investigated. A first test measurement showed that the proposed set-up yielded fission neutron angular distributions agreeing with those known from the literature. However, the experimental set-up has to include γ-ray suppression before the fraction of scission neutrons can be determined. The measurements will in the near future be continued using a ^{252}Cf source on a thin (120 $\mu g\cdot cm^{-2}$) Ni-foil backing, which will allow that both fragments can be detected, such that the ^{252}Cf fission neutron spectrum can be investigated also as function of fragment mass and kinetic energy.

REFERENCES

1. D.G. Madland and J.R. Nix,
Proc. Int. Conf. on Nuclear Data for Science and Technology, Antwerp,
Sept. 1982, page 473, D. Reidel Publ. Company, Dordrecht, NL.

2. H. Märten, D. Neumann and D. Seeliger,
Proc. IAEA Consultants' Meeting on the ^{235}U Fast Neutron Fission Cross-Section, and the ^{252}Cf Fission Neutron Spectrum, Smolenice, March 1983, page 199, INDC(NDS) - 146.

3. H.R. Bowman, S.G. Thompson, J.C.D. Milton, W.J. Swiatecki,
Phys. Rev. 126, 2120 (1962).

4. Ch. Straede, C. Budtz-Jørgensen and H.-H. Knitter,
Contribution to these proceedings.

5. C. Budtz-Jørgensen and H.-H. Knitter,
Nucl. Sci. Eng. 86, 10 (1984).

6. C. Budtz-Jørgensen and H.-H. Knitter,
Nucl. Instr. Meth. 223, 295 (1984).

7. H.-H. Knitter and C. Budtz-Jørgensen,
Proc. of the Int. Conf. on Nuclear Cross Scetions for Technology,
Knoxville, U.S.A., Oct. 1979, NBS Spec. Publ. 594, p. 947 (1980).

8. H.-H. Knitter, C. Budtz-Jørgensen, D.L. Smith and D. Marletta,
Nucl. Sci. Eng. 83, 229 (1983).

9. J.W. Meadows and C. Budtz-Jørgensen,
Proc. Int. Conf. on Nuclear Data for Science and Technology,
Antwerp, Sept. 1982, page 740, D. Reidel Publ. Company, Dordrecht, NL.

10. C. Budtz-Jørgensen and J.W. Meadows,
Lecture Notes in Physics, Vol. 158, 111 (1982).

11. P.T. Nielsen and N. Rud,
Institute of Physics, University of Aarhus,
Private Communication (1984).

12. J. Terrel, Phys. Rev. 127, 880 (1962).

320

MEASUREMENT OF THE ^{235}U FISSION CROSS-SECTION FOR ^{252}Cf SPONTANEOUS FISSION NEUTRONS

I.G. SCHRÖDER, L. LINPEI*, D.M. GILLIAM, C.M. EISENHAUER
National Bureau of Standards,
Gaithersburg, Maryland,
United States of America

Abstract

--The absolute ^{235}U fission cross section for ^{252}Cf spontaneous fission neutrons is a normalization datum for establishing the energy dependent cross section for ^{235}U fission. It is also a measurement standard for deriving integral cross sections from ratio determinations in benchmark neutron fields which serve reactor physics and neutron dosimetry. The measurements reported here were carried out with a small volume ^{252}Cf neutron source and two light-weight double fission chambers in compensated beam geometry. The important characteristics of the measurement are: 1) except for neutron scattering corrections, the cross section obtained depends only upon the source strength of a natural neutron source, a distance measurement, and the isotopic mass of four ^{235}U deposits, and 2) for any credible departure of the ^{252}Cf fission neutron spectrum from its experimentally determined shape, the cross section does not vary more than 0.4%.

The present measurement represents an extension of a previous measurement performed by Heaton et al. at the NBS a decade ago. Since then progress has been made in the characterization of fissionable deposit masses; in the determination of the source strength of ^{252}Cf sources relative to the internationally compared Ra-Be photoneutron standard neutron source NBS-I; and in the ability to accurately measure the distance between fission chambers in compensated beam geometry and to determine the position of the fissionable deposits inside the chambers. New calculational techniques have been developed to determine the residual scattering corrections for the fission chambers, deposit backings, and neutron source. Finally, new experiments have been performed to measure the effect of neutron return from the environment.

* Work performed while a Guest Worker from the National Institute of Metrology, Beijing, China.

I. Introduction

The absolute ^{235}U fission cross section for ^{252}Cf spontaneous fission neutrons is a normalization datum for establishing the energy dependent cross section for ^{235}U fission.[1] It is also a measurement standard for deriving integral cross sections from ratio determinations in benchmark neutron fields which serve reactor physics and neutron dosimetry.[2] The measurements reported here were carried out with a small volume ^{252}Cf fission neutron source and two light-weight double fission chambers in compensated beam geometry.[3,4,5] The important characteristics of the measurements are (1) except for neutron scattering corrections, the cross section obtained depends only upon the source strength of a natural neutron source, a distance measurement, and the isotopic mass of four ^{235}U deposits and (2) for any credible departure of the ^{252}Cf fission neutron spectrum from its experimentally determined shape , the cross section does not vary by more than 0.4%.

The present measurement represents an extension of a previous measurement performed by Heaton et al.[6] at NBS a decade ago. Since then progress has been made in the characterization of fissionable deposit masses; in the determination of the source strength of ^{252}Cf sources relative to the internationally compared Ra-Be photo-neutron standard neutron source NBS-1; and in the ability to accurately measure the distance between fission chambers in "compensated beam geometry" and to determine the position of the fissionable deposits inside the chambers. New calculational techniques have been developed to determine the residual scattering corrections for the fission chambers, deposit backings and neutron source. Finally, new experiments have been performed to measure the effect of neutron return from the environment.[7] This document describes the main features of the measurement, including error estimates. The final experimental value for the cross section will be reported when the results of an international Cf source strength intercomparison are available.

II. Experimental Procedure and Data Analysis

The present experiment was performed at the NBS ^{252}Cf Irradiation facility . Two double ^{235}U fission chambers[4] were symmetrically mounted, on a light frame, on opposite sides of a ^{252}Cf source. The "symmetric" placement of the two chambers with respect to the source, makes the present measurement independent of the exact position of the source and only dependent on the distance between chambers. The advantage of this experimental arrangement, (compensated geometry) is that it allows the distance between chambers to be measured accurately with the ^{252}Cf source absent.

The experimental data were taken with the front face of each chamber facing each other and also rotated by 180°. This rotation eliminates the need for fission fragment mementum corrections and creates geometric symmetry for neutron scattering in the fission chamber and in the fissionable deposit backings. Distance measurements were performed before and after each measurement.

The pulses from each of the four chambers, after proper amplification (charge-sensitive preamplifier and active filter shaping amplifier), were fed simultaneously to two integral discriminators and to a multiplexer which

allowed the pulse-height distribution from each chamber to be displayed on a multichannel pulse-height analyzer (PHA). The output of each discriminator was fed to a printing scaler. The eight printing scalers were controlled by a timer and recorded at preset intervals for analysis.

The raw data from each of the four fission chambers were computer analyzed. This analysis entailed determining the ratio between the counts of the lower and upper discriminators for each chamber and from this obtain an estimate of the number of fission events present under the low energy tail i.e. the extrapolation-to-zero. This allowed the calculation of the number of fission events in each chamber. The extrapolated fission events, after proper dead-time corrections, yielded a mean fission rate for each chamber. This is the raw experimenal data from which an absolute fission rate can be obtained.

III. The Deposit Masses and Mass Fission Ratios

The four deposits used in the present experiment were selected from a number of such deposits made at CBNM-Geel from $^{235}UF_4$ vacuum-evaporated by planetary rotation on to polished stainless steel backings. All these are labeled with the prefix 25A.

Table I. Thermal Fission Rate Ratios Corrected for ETZ, Dead-Time, Fission Rate in Other Isotopes, and Neutron Absorption and Scattering (not corrected for self-absorption of fragments within the deposit)

Mass Ratio	Fission Rate Ratio
25S-2-2 / 25A-3-2	0.6556 + 0.05%
25A-3-2 / 25A-3-4	1.0336 + 0.05%
25A-3-2 / 25A-3-6	1.0032 + 0.05%
25A-3-2 / 25A-5-2	0.6411 + 0.05%
25A-3-2 / 25A-5-6	0.6340 + 0.05%

Deposit 25A-3-2 previously alpha - and fission-compared with deposit 25A-3-1 was employed to determine the mass ratios of the four deposits used in the present experiment. This latter deposit was used in the re-evaluation of the NBS ^{235}U standard fissionable deposit mass (25S-2-2) and then destructively analyzed by IDMS. The standard deposit has been the subject of extensive intercomparisons [2] and has an assigned mass of:

$$M_s(25S\text{-}2\text{-}2) = 246.4 \pm 0.5\% \mu g$$

Furthermore, for the purpose of the present experiment the reference deposit 25A-3-2 was fission compared to 25S-2-2.

The fission ratios were obtained by placing pairs of deposits back-to-back in an NBS fission chamber [4] and fission counting them in a beam from the NBS Reactor thermal column. The fission counting was performed with essentially the same equipment as that used with the ^{252}Cf source. The analysis of the data follows along identical lines to those in the ^{252}Cf fission counting. The results of this analysis for the fission rate ratios are shown in Table I.

IV. Distance Measurements

The distance measurements consist of two separate determinations: a) the measurement of the distance between the two fission chambers, and b) the distance inside the fission chambers of the fissionable deposits with respect to the face of the fission chambers themselves. Once the fissionable deposits are mounted inside the chambers, a metallurgical microscope with an internal vernier scale allows one to measure the distance between the top fissionable deposit and the chamber face to better than 3×10^{-3} cm. Since the average distance between the two chamber faces is of the order of 10 cm, this represents a percentage error of 6×10^{-4} in the flux density.

After the deposit distances were measured the chamber was closed and mounted on a ring frame. A "dummy" source was then mounted in place of the ^{252}Cf source and the chambers aligned mechanically using both distance and height gauges. The ring frame containing the chambers was then rigidly mounted on an optical bench which formed the base of a computer controlled digital cathetometer. This optical instrument is capable of measuring the distance beween chambers to better than 1 part in 10^{-2} cm.

The distance measurements were performed before and after each run at the ^{252}Cf irradiation facility to insure that no misalignment had occurred during the course of the measurement. A typical measurement before and after an irradiation yields for the average 93.470 $\pm$ 0.079 mm and 93.461 $\pm$ 0.084 mm respectively.

As the irradiations were performed with both chambers facing each other and also rotated by 180°, after measuring the distances between chambers at the conclusion of a run, the chambers were rotated 180° (this rotation was mechanically designed into the ring holder) and the rotation verified by the optical cathetometer prior to making new distance measurements. Lastly, a

series of measurements were performed on the chambers to insure that the faces of the chambers were parallel to each other. This was accomplished by optically measuring at 3 mutually perpendicular positions (top and both sides of the chamber) the respective distance between them.

V. The Fission Cross Section

If R_o denotes the experimental fission rate obtained in the fission chamber from a given deposit, corrected for ETZ, dead-time, fission rate in other isotopes, neutron absorption and scattering, but not corrected for absorption and scattering of fission fragments in the deposit itself, then the fully corrected rate R is given by

$$R = R_o (1 + m\delta)$$

where m is the deposits mass thickness and δ is a correction factor which accounts for fission fragment absorption and scattering in the deposit. If one further denotes by R_{oi} the fission rate from the ith deposit obtained from measurements made at the thermal column and by $R(c)_{oi}$ the fission rate from the ith deposit in the californium field then the fully corrected fission rate, per unit mass, obtained for the ith deposit in the ^{252}Cf field is given by

$$\frac{R(c)_i}{M_i} = R(c)_{oi}\left(\frac{R_{or}}{R_{oi}}\right)\left(\frac{R_{os}}{R_{or}}\right)\frac{1+m_s\delta_s}{M_s}$$

where M_i denotes the mass of the ith deposit and the suffixes r and s denote the reference (or intermediate) deposit (25A-3-2) and the standard deposit (25S-2-2) respectively.

The absolute value of the ^{252}Cf fission-spectrum-averaged ^{235}U fission cross section obtained from the ith deposit is then given by

$$\sigma_i = \frac{4\pi A_i}{N_o}\frac{R(c)_i}{M_i}\frac{\langle D_i\rangle^2}{S}$$

where $\langle Di\rangle$ is the average distance between the ^{252}Cf source and the ith deposit, S is the ^{252}Cf source strength, N_o is Avogadro's number and A_i is the atomic number of the ith fissionable deposit.

Thus, in order to obtain the desired cross-section, one needs to know; a) The fission rate ratio between the reference deposit and each of the four deposits and the fission ratio between the standard and reference deposits, each of which are given in Table I, b) The mass of the standard deposit and the fission fragment absorption and scattering corrections for the standard deposit; c) The ^{252}Cf source strength and the distance between the deposits and the source.

VI. Fission Source Strength Calibration

The ^{252}Cf source (NS-100) used in the present experiment was calibrated in the NBS Manganous Sulfate Bath Facility against the internationally compared Ra-Be photoneutron source NBS-1. This source was last calibrated in 1961. The value obtained for this radium-beryllium (γ,n) natural neutron source agreed with source strength calibrations carried out earlier and was assigned an uncertainty of $\pm$ 1.1% based on a conservative propagation of systematic errors. Source strength intercomparisons undertaken with other laboratories agree to much better than $\pm$ 1%. If the propagation procedure for systematic errors recommended by PTB, the German Standards Laboratory at Braunschweig, is applied to the 1961 measurements, the total uncertainty for this determination would be $\pm$ 0.5%. More recently, experiments completed in 1980 checked the neutron emission rate of NBS-I against $\bar{\nu}$, the average number of neutrons emitted per fission for ^{252}Cf. Consistency with this quantity, which is known to $\pm$ 0.2%, is better than 0.5%. On the basis of this validation experiment, and the agreement of source strength measurement capabilities at various laboratories, the NBS continues to use the source strength value measured in 1961 but with an uncertainty reduced to $\pm$ 0.8% (one standard deviation).

VII. Scattering Corrections

In order to determine the cross-section, it is necessary to correct for the scattering of the neutrons in the source capsule and in the fission chamber, support structures, and deposit backings. Lastly, neutrons that scatter from the walls of the NBS ^{252}Cf Irradiation Facility must also be accounted for. Estimates of the five main scattering corrections and their corresponding uncertainties are given in Table II.

Table II. Scattering Corrections

Fission Chamber	1.013 $\pm$ 0.14%
Deposit Backing	1.008 $\pm$ 0.06%
Source Capsule	1.008 $\pm$ 0.4 %
Support Structures	1.003 $\pm$ 0.1 %
Room Return	1.001 $\pm$ 0.01%
Net Scattering Correction	1.033 $\pm$ 0.44%

A resume of the corrections and errors involved in the present measurement of the fission cross section is given in Table III.

Table III. Error Components in the Measurement of $\overline{\sigma_f}(U235, X_{Cf})$

	Correction	Percent Error in Cross Section
Fission Chamber Counts	--	± 0.15%
Fissionable Deposit Mass	--	± 0.5 %
Cf Neutron Source Strength	--	± 0.9 %
Fission in Other Isotopes	0.9973	± 0.1 %
Geometrical Measurements		
Fissionable Deposit Separation	--	± 0.3%
Deposit Diameter	1.0075	± 0.1%
Source Position	1.001	± 0.1%
Undetected Fission Fragments		
Extrapolation to Zero Pulse Height	1.009	± 0.3%
Absorption in Fissionable Deposit	1.0132	± 0.2%
Neutron Scattering		
Room Return	0.9990	± 0.01%
Source Capsule	0.9921	± 0.4 %
Fission Chamber	0.9872	± 0.14%
Support Structures	0.9970	± 0.1%
Deposit Backing	0.9921	± 0.06%
TOTAL ERROR		± 1.25%

References

1. W. P. Poenitz, J. W. Meadows, and R. J. Armani, "The Evaluation of ^{235}U(n,f) above 100 keV for ENDF/B-V and the Implications of a Unified ^{235}U Mass Scale", Proc. Int. Conf. on Nuclear Cross Sections for Technology, Knoxville, TN, October 22-26, 1979, p. 483, NBS SP 594, National Bureau of Standards (1980).

2. J. A. Grundl and D. M. Gilliam, Trans. Am. Nucl. Soc., 44, 533 (1983).

3. L. C. Williams, J. E. Bigelow and J. B. Knauer, Jr., Trans. Am. Nucl. Soc., 24, 493 (1976).

4. J. A. Grundl, D. M. Gilliam, N. D. Dudey and R. J. Popek, Nucl. Technol., 25, 237 (1975).

5. J. A. Grundl, V. Spiegel, C. M. Eisenhauer, H. T. Heaton II, D. M. Gilliam, and J. Bigelow, Nucl. Technol., 32, 315 (1977).

6. H. T. Heaton II, J. A. Grundl, V. Spiegel, D. M. Gilliam and C. Eisenhauer, "Absolute U Fission Cross Section for ^{252}Cf Spontaneous Fission Neutrons", Proc. Conf. on Nuclear Cross Sections and Technology, Washington, D. C., March 3-7, 1975, p. 266, NBS SP 425, National Bureau of Standards (1975).

7. Li Linpei, Rad. Prot. Dosimetry, 5, 227 (1984).

SESSION VII

INTERNATIONAL FLUENCE RATE INTERCOMPARISON FOR 2.5, 5.0 AND 14 MeV NEUTRONS

H. LISKIEN
Central Bureau for Nuclear Measurements,
Joint Research Centre,
Commission of the European Communities,
Geel

V.E. LEWIS
National Physical Laboratory,
Teddington, Middlesex,
United Kingdom

Abstract

Fluence determinations for 2.5, 5.0 and 14 MeV neutrons as performed in standard laboratories have been compared. Two methods of intercomparison were used : One is based on the determination of a γ-rate ratio between ^{115m}In as induced by fast neutrons in an indium sample on one hand and ^{51}Cr from a calibrated source on the other hand and is used at all energies. The second method is restricted to 14 - 15 MeV neutrons and is based on measuring the ^{92m}Nb γ-activity induced in a niobium sample.
Results show that the uncertainty contribution from the transfer methods does not essentially increase the overall uncertainty and that there is generally consistency.

1 INTRODUCTION

International fast neutron fluence rate intercomparisons between standardizing laboratories (or the equivalent) of many countries are organized under the auspices of CCEMRI/CIPM* Section III. A first intercomparison took place in the years 1973 - 1978[1]. A new series of intercomparisons consisting of four branches is now under way as summarized in Table I.

---

* Comité Consultatif pour les Etalons de Mesure des Rayonnements Ionisants/ Comité International des Poids et Mesures

TABLE I Summary of ongoing neutron fluence comparisons

transfer method	coordination	neutron energy (MeV) 0.144	0.565	2.5	5.0	14.8
$^{115}In(n,n')$ activ.	CBNM			X	X	X
$^{93}Nb(n,2n)$ activ.	NPL					X
$^{115}In(n,\gamma)$ activ.	NPL	X	X			
U(n,f) fiss.chamb.	AERE/NPL	X	X	X	X	X

In contrast to the earlier procedure the adopted four methods do not require a scientist to accompany the transfer instrument. The two last mentioned branches of the presently ongoing comparisons are performed sequentially and are therefore not yet ended. The present paper describes the procedure and the results for the two first mentioned branches which are performed in parallel. This speeds up the procedure and helps to keep the intercomparison blind.

2 TRANSFER METHODS

Both branches of fast neutron fluence rate intercomparisons presented here are based on activation. Each participating laboratory was asked to produce quasi-mono-energetic neutrons and to irradiate a provided sample. The neutron fluence rate $<\varphi>$ ($cm^{-2}s^{-1}$) averaged over the sample volume and over the irradiation time, and the resulting induced specific γ-activity extrapolated to saturation A/S ($s^{-1}g^{-1}$) had to be determined. Special care was taken to keep the uncertainty contribution of A/S small such that the consistency of the ratio

$$C = A / (S \cdot <\varphi>) \quad (g^{-1}cm^{2}) \qquad [1]$$

TABLE II Relevant sample and decay data

reaction	sample dimension (mm)	isotopic abundance (atom %)	half-life (h)	γ-energy (keV)	intensity (%)
$^{115}In(n,n')^{115}In$	10 Ø x 5	95.7	4.486	336	46
$^{93}Nb(n,2n)^{92m}Nb$	5 Ø x 25	100.0	243.6	935	99

as obtained by different laboratories reflects the consistency for the determination of $<\varphi>$. Evidently, γ-activity determination had not necessarily to occur on an absolute scale, equal base for all participants was sufficient. The saturation factor S is given by

$$S = k \cdot (1-\exp(-\lambda \cdot T)) \qquad [2]$$

T being the irradiation time. Small corrections (k) due to fluence-rate variations during irradiation had to be applied. The cross sections for the involved activation reactions $^{115}In(n,n')^{115m}In$ and $^{93}Nb(n,2n)^{92m}Nb$, are given in Fig. 1. Table II summarizes other relevant data. Due to the different half-lives involved, different ways to determine the specific γ-activity (A) were followed :

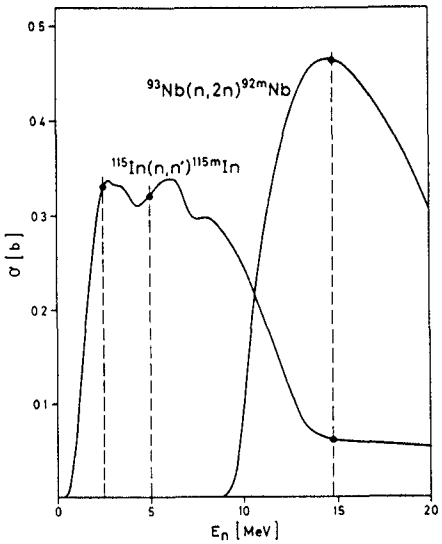

FIG 1 Cross sections of $^{115}In(n,n')$ and $^{93}Nb(n,2n)$

2.1 $^{115}In(n,n')^{115m}In$

The short half-life of ^{115m}In excluded γ-activity counting in the central laboratory. γ-activity determination with Ge(Li)-detectors had to be performed by each participating laboratory. However, to minimize uncertainties in the efficiency calibration of the used Ge(Li)-detectors, the central laboratory (CBNM) provided ^{51}Cr-sources. Their relative source strengths were known with $\pm$ 0.1 % accuracy. ^{51}Cr has a sufficiently long half-life (27.70 d) and emits a 320 keV γ-radiation, only 16 keV lower than that of ^{115m}In. Efficiency extrapolation to 336 keV was performed using a ^{133}Ba source which delivers several γ-lines in the region of interest (276, 303, 356, 384 keV) with known intensities. The metallic samples provided by CBNM were irradiated typically at distances between 10 and 20 cm from the neutron source. Participants used T(d,n) or D(d,n)-neutrons at 2.5 MeV, D(d,n)-neutrons at 5 MeV, and T(d,n)-neutrons at 14.8 MeV. The applied fluences varied between $1.1 \cdot 10^{8} cm^{-2}$ and $5.4 \cdot 10^{9} cm^{-2}$. Irradiation times were generally 5 hours. In

order to obtain the specific γ-activity at the end of irradiation the obtained γ-counting results had to be corrected for decay and divided by the sample mass. More details can be found in Ref. 2.

2.2 $^{93}Nb(n,2n)^{92m}Nb$

The relatively long half-life of ^{92m}Nb allowed γ-activity counting in a central laboratory (NPL). The use of one common detector avoids the need for each participating laboratory to set up its own calibrated detector and minimizes one possible source of random uncertainty. The samples provided by the central laboratory were held in small Teflon holders in which they were irradiated at distances of about 20 cm from the T(d,n)-neutron source. The fluences varied between $1.5 \cdot 10^{9} cm^{-2}$ and $1.4 \cdot 10^{10} cm^{-2}$. Irradiation times were generally between two and four hours, thus small compared to the ^{92m}Nb half-life. The samples were sent back to NPL, generally arriving about six days after activation, where the induced relative activity was measured in a well type Ge(Li) detector at least twice over a period of about four days. The detector efficiency was checked using a ^{137}Cs source and found to be constant within ± 0.4 %. More details can be found in Refs. 3,4.

3 PARTICIPATION AND FLUENCE DETERMINATION

In total 11 laboratories participated, although only three of them (CBNM Geel, NPL Teddington and PTB Braunschweig) were able to participate at all three energies. Details are given in Table III. If a laboratory was able to participate at a given neutron energy, then the method to determine the fluence rate is given by a two-letter-code :

PR Proton recoil counting. In all cases only proton recoils emitted inside a certain forward cone were counted. With the exception of SSRL, all laboratories used telescope counter devices. The standard n-p scattering cross section with an accuracy of ± 0.9 to 1.0 % stems from phase shift analysis work[5].

AP Associated particle (^{3}He or ^{4}He) counting.

LC Long counter[6]. The shape of the efficiency curve is based on the zero-degree yield and angular distributions of the neutron producing reaction T(p,n) and on calculation. The absolute efficiency scale is based on calibrations using radioactive neutron sources and was checked with a proton recoil telescope.

AL $^{27}Al(n,\alpha)$ activation. Absolute determination of the ^{24}Na activity of aluminium foils. The standard $^{27}Al(n,\alpha)$ cross section (accuracy ± 0.6 %) was taken from a recent evaluation[7].

FE $^{56}Fe(n,p)$ activation. Absolute determination of the ^{56}Mn activity of iron foils. In the NPL work the standard $^{56}Fe(n,p)$ cross section was taken from a recent evaluation[8] which quotes an accuracy of 0.6 %. BARC used a value determined previously there.

TABLE III Participation

Laboratory			2.5 MeV In(n,n')	5.0 MeV In(n,n')	14.8 MeV Nb(n,2n)	14.8 MeV In(n,n')
CBNM	Geel,	Belgium	PR (2)	PR (2)	PR (1)	PR (1)
BIPM	Sèvres,	France	AP (3)	-	AP (1)	AP (3)
NPL	Teddington,	U.K.	LC (3)	LC (3)	FE (2)	FE (2)
SSRL	Studsvik,	Sweden	PR (2)	PR (2)	-	-
PTB	Braunschweig,	FR Germany	PR (3)	PR (3)	PR (1)	PR (1)
ETL	Tsuhuba,	Japan	PR (11)	-	PR/AP(1)	PR/AP(11)
VNIIM	Leningrad,	USSR	AP (2)	-	-	AP (4)
IRK	Vienna,	Austria	-	-	AL (1)	-
NBS	Washington,	U.S.A.	-	-	AP (1)	AP (1)
IAE	Beijing,	PR China	-	-	AP (1)	AP (1)
BARC	Trombay,	India	-	-	FE (1)	FE (7)

(x) indicates that the measurement was performed x-times

4 RESULTS

Results based on $^{115}In(n,n')$-activation were adjusted for deviations from the nominal energies 2.5, 5.0 and 14.8 MeV. This effect was essential only for the results from VNIIM, which were obtained at 2.86 MeV instead of 2.50 MeV resulting in a (-2.1 ± 1.0) % correction. The excitation function of the $^{93}Nb(n,2n)$-reaction is unusually flat over the relevant energy region between 14.1 and 14.8 MeV. Therefore, the effect appears unlikely to exceed 1 % and results were not adjusted.

All involved uncertainties were interpreted as standard deviation and combined quadratically. The short half-life of ^{115m}In made it possible for the participants to repeat their measurements and to check the reproducibility of their results. Table III indicates the number of measurements made. Evidently, results from a given laboratory are correlated, not only for results at a given energy, but also - to a lesser extent - for results at different energies. When averaging, these correlations were taken into account. Fig. 2 depicts the averaged results. Only the variation of the results is relevant, not the absolute scale, because activity determinations were not performed on an absolute scale. The central shaded portion of the uncertainties indicates the contribution due to the fluence determination only. Overall uncertainties vary typically between ± 1 and ± 3 %, only two results exceed the ± 3 % uncertainty level. Numerical values can be found in Refs. 2,3. The reason for showing no 14 MeV results based on $^{115m}In(n,n')$ will be discussed in Section 5. The results of SSRL at 2.5 and 5.0 MeV were withdrawn. SSRL used a proton recoil device from another laboratory and,

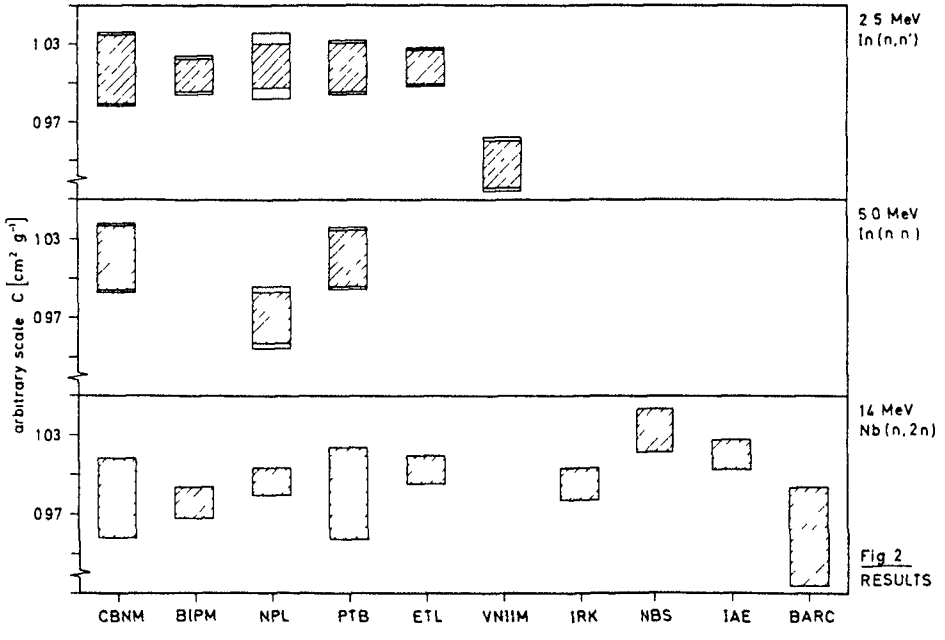

Fig 2 RESULTS

after the measurements were completed, they found a weakness in the construction of this instrument which was not straightforward to correct for.

In case of the 14 MeV branch based on $^{93}Nb(n,2n)^{92m}Nb$ it was also possible to obtain estimates of the neutron mean energy. The Teflon holder as mentioned in Section 2.2 contained also a Zr-sample which was simultaneously activated. Mean neutron energies were obtained by analyzing the $^{89}Zr/^{92m}Nb$ activity ratio, where the ^{89}Zr activity stems from the reaction $^{90}Zr(n,2n)$. More details may be found in Refs. 3,4.

5 DISCUSSION

Obviously, the above described neutron fluence rate intercomparison is at the same time a test of the transfer method. As may be seen from Fig. 2, the uncertainty due to the transfer has not essentially increased the overall uncertainty. For 14 MeV results based on Nb(n,2n) the difference can hardly be made visible.

At 2.5 MeV only the VNIIM value is inconsistent. This value, however, has been obtained under conditions deviating in several aspects. While all other results were obtained with neutrons of mean neutron energies very near to 2.50 MeV and source-sample distances of at least 10 cm, this measurement was performed with an extremely short source-sample distance of ≈ 3 cm and a mean neutron energy of 2.86 MeV. In addition, the γ-counting was not performed with a Ge(Li) detector but with a NaI(Tl) scintillator and these measurements were made at a time when the ^{51}Cr calibration source had decayed, such that an interim ^{65}Zn had to be used.

The results at 5.0 MeV are just consistent.

Concerning results at 14 MeV based on Nb(n,2n) six agree within their estimated standard deviations. The two relatively high results (NBS and IAE) are for γ-measurements made within a week of each other. No abnormal behaviour of the Ge(Li) detector was observed throughout the intercomparison and therefore this coincidence is probably fortuitous. It is thought that the IAE result was affected by adverse d-beam focusing conditions which resulted in alpha particles produced in a part of the TiT target not being "seen" by the surface-barrier detector. A second irradiation (not part of this intercomparison and without knowledge of the first result) made with tighter collimation of the beam, gave a value more consistent with those of the

majority of the other participants. The result for BARC is thought to have been significantly affected by lower-energy neutrons produced by scattering from and reactions within the relatively massive water-cooled target mount. The reported value is uncorrected for this effect.

Corrections for room-scattered and target-scattered neutrons of degraded energy are very important for results obtained at 14 MeV based on In(n,n'). In activation such neutrons have an over-proportional effect, as may be seen from the cross-section curve depicted in Fig. 2. Therefore, an intercomparison at this neutron energy is not only a test of the applied fluence determination method. It is, above all, a test of the cleanliness of the 14 MeV source and the corresponding corrections. This fact lead to withdrawals and remeasurements. Nevertheless, analysis of this effect on equal base for all participants (same set of nuclear input data, same method) is presently going on.

11 REFERENCES

1. V.D. Huynh, Metrologia, 16, 31 (1980).
2. H. Liskien, Metrologia, 20, 55 (1984).
3. V.E. Lewis, Metrologia, 20, 49 (1984).
4. V.E. Lewis and K.J. Zieba, Nucl. Instr. Meth., 174, 141 (1980).
5. J.C. Hopkins and G. Breit, Nucl. Data Tables, A9, 137 (1971).
6. J.P. Hunt, Report RS 5, NPL Teddington, 1976.
7. S. Tagesen and H. Vonach, Physics Data, 13, 3 (1981).
8. J.G. Hayes and T.B. Ryves, Ann. Nucl. Energy, 8, 469 (1981).

SOME PRACTICAL PROBLEMS IN THE STANDARDIZATION OF MONOENERGETIC FAST NEUTRON FLUENCES

T. MICHIKAWA, K. KUDO, T. KINOSHITA
Electrotechnical Laboratory,
Sakura-mura, Niihari-gun, Ibaraki,
Japan

Abstract

Among some important problems in the accurate determination of fluences of monoenergetic fast neutrons, the interference of the $^3He(d,p)\alpha$ reaction in the associated α particle counting for the d-T reaction is discussed in this paper, which cannot be negligible in the accurate measurements of fluences at neutron energies of 14 to 20 MeV.

There are some important problems in the accurate determination of fluences of monoenergetic fast neutrons, which include:

(1) Effect of non-parallel incident neutron beams on the estimation of the effective volume in the recoil proton proportional counter.[1)2)]

(2) Energy dependence of the $\bar{W}$ value for protons in CH_4 and/or H_2 gases below several hundred keV.

(3) Accuracy in the determination of hydrogen content in the polyethylene radiators used for the telescope.[3)]

(4) Contribution of the secondary neutrons produced in the target backing (Cu) and Ti to the d-T neutron field in the range of 14 to 20 MeV.[4)]

(5) Possible interference of the $^3He(d,p)\alpha$ reaction in the associated α particle counting for the d-T reaction.

Among these problems, present paper deals only with the last problem No.5.

The accumulation of ^3He in the TiT target occurs due to β-decay of ^3H with its half-life of 12.3y. The amount of ^3He increases by about 5% per year. The α particles from the d-^3He reaction occurring in the TiT target should be taken into account in the fluence determination by the associated α counting method. This is because the α particles from the d-^3He reaction have nearly the same energy as those from d-T reaction, and therefore it is difficult to distinguish between them.

The contribution of d-^3He reaction may be assessed by measuring directly the high energy protons emitted outside from the TiT target with either the CR-39 track detector or the CsI scintillation detector (used as the E-counter in our telescope). Our measurements were made at an angle of 0° to the incident deuteron beams in the energy range of 0.33- to 3.3- MeV of deuterons. The TiT target used was manufactured on January, 1983 by Amersham International and therefore from the half-life, about 10% of ^3H was estimated to be transformed to ^3He. The target backing is 0.3 mm thick copper plate.

Figure 1 shows the pulse height distributions of the d+^3He protons measured with the CsI scintillation detector. From such measurements we have obtained the ratio of fluences of protons to that of neutrons, designated by ϕ_p/ϕ_n, at the incident deuteron energies of 0.33 to 3.3 MeV. In this

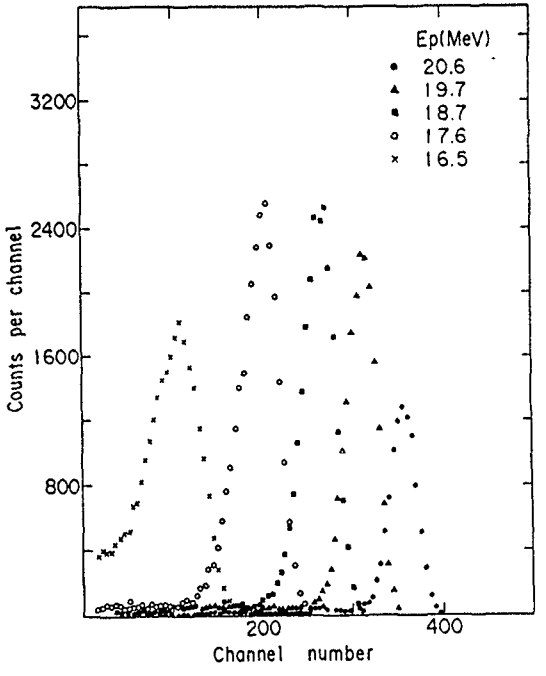

Fig. 1: Pulse height spectrum of d+^3He protons emitted outside from TiT target, as measured with the CsI scintillator at an angle of 0° to incident deuteron beams of energies from 0.59 to 3.25 MeV. Proton energy is the kinetic energy of protons produced by $^3He(d,p)\alpha$ reaction.

case we used the recoil proton telescope for the determination of neutron fluences ϕ_n. The table shows the result of the experiments.

Table: Results of measurements of d+^{3}He proton and d+T neutron fluences at angle of 0° to incident deuteron beam

Incident deuteron energy (MeV)	d+^{3}He proton fluence ϕ_p (p·sr^{-1}/PLC)*	d+T neutron fluence ϕ_n (n·sr^{-1}/PLC)*	Ratio ϕ_p/ϕ_n (%)
0.33	8.8×10^1**	2.91×10^4	0.3
0.59	2.60×10^3	2.99×10^4	9.0
1.18	2.55×10^3	2.92×10^4	8.7
1.87	2.28×10^3	2.65×10^4	8.6
2.56	1.81×10^3	1.87×10^4	9.6
3.25	9.5×10^2	9.65×10^3	9.8

* These units designate neutron or proton fluences per one count of the polyethylene long counter.

** This value was obtained with the CR-39 track detector.

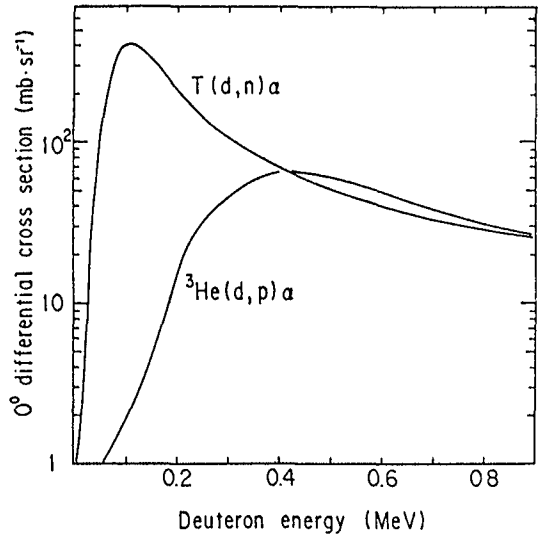

Fig. 2: 0° differential cross sections of T(d,n)α and ^{3}He(d,p)α reactions for deuteron energy in the laboratory system. The data of T(d,n)α and ^{3}He(d,p)α reaction cross sections are based on Ref.(5) and (6) respectively.

We obtained the following conclusions from the above experiments;

(1) Contribution of α particles from the ^{3}He(d,p)α reaction is about 0.3% at the neutron energy of 15.2 MeV for our TiT target which was 2 years old.

(2) The contribution increases at neutron energies higher than 15.8 MeV (neutron energy of 15.8 MeV corresponds to the deuteron energy of 0.5 MeV), and it was found to be 8 ~ 10% at these energies.

These conclusions seem to be consistent with the shape of the curves of the reaction cross section for deuteron energy. As shown in Fig. 2, the reaction cross section of the d-T reaction has its maximum at the deuteron energy of approximately 110 keV and is two orders of magnitude larger than that of the d-^{3}He reaction in the lower deuteron energy region. But, in the deuteron energy region above 400 keV, the both reactions have nearly the same values of the cross sections.

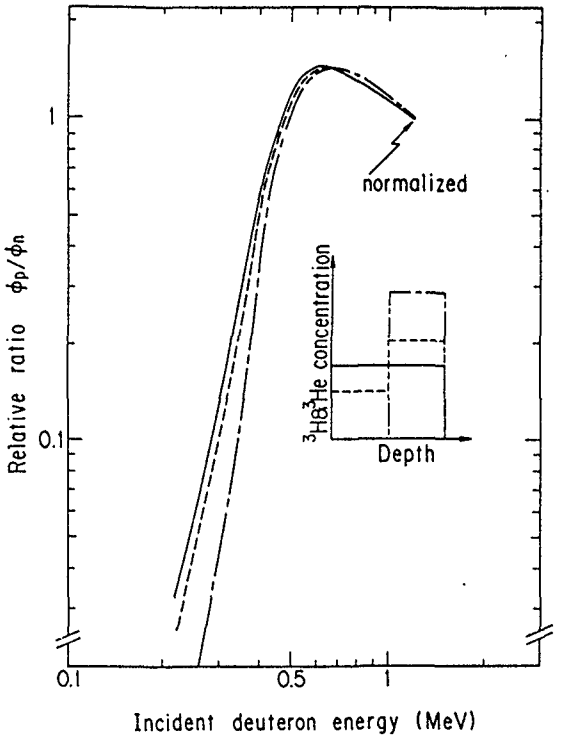

Fig. 3: Calculated result of the ratio ϕ_p/ϕ_n as a function of incident deuteron energy in three different cases of ^{3}H and ^{3}He depth-distributions in TiT layer having a thickness of 430 $\mu g \cdot cm^{-2}$. Solid curve is Case 1 where uniform depth-distribution in TiT is assumed, dotted curve is Case 2 where concentrations of ^{3}H and ^{3}He in first half layer are half of those in second half layer, and broken curve is Case 3 where ^{3}H and ^{3}He are present only in second half layer.

Finally, we'd like to point out the possibility of determining the ^{3}H depth-distribution in the TiT target from the measurements of the ratio of fluences of protons to that of neutrons (ϕ_p/ϕ_n). The ^{3}H depth-distribution in the TiT layer is important in the evaluation of the mean neutron energy around 14 ~ 15 MeV. Figure 3 shows that the dependency of this ratio upon the incident deuteron energy is sensitive to the ^{3}H- and ^{3}He- depth distributions in TiT layer in the deuteron energy range below 1 MeV.

Further measurements at lower deuteron energies are now in progress.

Acknowledgements: The authors wish to express their thanks to Mr. S. Yasubuchi, Nagase-Landauer Ltd. for measuring tracks of the CR-39, and to Dr. M. Yamashita to his kind criticism on this manuscript.

REFERENCES

1. K.W.Geiger: Nucl.Instrum.Methods, 166, 213 (1979).
2. N.Kobayashi, T.Kinoshita and T.Michikawa: Submitted to Nucl.Instrum.Methods.
3. H.Liskien: "Summary and Conclusions of Working Group III" in this AGM.
4. K.Kudo, T.Michikawa, T.Kinoshita, Y.Hino and Y.Kawada: "Cross Section Measurements of ^{56}Fe(n,p)^{56}Mn and ^{27}Al(n,α)^{24}Na between 14.0 and 19.9 MeV", cont. paper to this AGM.
5. H.Liskien and A.Paulsen: Nucl.Data Tables, 11, 569 (1973).
6. W.Möller and F.Besenbacher: Nucl.Instrum.Methods, 168, 111 (1980).

332 MEASUREMENT OF THE NBS BLACK NEUTRON DETECTOR EFFICIENCY AT 2.3 MeV

K.C. DUVALL, A.D. CARLSON, O.A. WASSON
National Bureau of Standards,
Gaithersburg, Maryland,
United States of America

Abstract

The absolute efficiency of the National Bureau of Standards (NBS) Black Neutron Detector at 2.3 MeV has been measured using the time-correlated associated particle method. Until recently, the NBS Black Neutron Detector had been utilized only in the limited energy range of 0.2 to 1.2 MeV, where the efficiency determination from Monte Carlo calculations has been verified by experiment. A result for the measured Black Neutron Detector efficiency at 2.3 MeV has been obtained with an experimental uncertainty of about ±1% and agrees well with the Monte Carlo calculated value. The measurement extends the usefulness of the Black Neutron Detector as an absolute neutron flux monitor to the higher energy region.

1. Introduction

A Black Neutron Detector (a large plastic scintillator described in section 3), originally developed by W. P. Poenitz [1] and further developed at the National Bureau of Standards (NBS) by G. P. Lamaze and M. M. Meier, [2] has been utilized rather extensively as an absolute neutron flux monitor in the energy range of 0.2 to 1.2 MeV [3-6]. The high efficiency, peaked pulse height and fast response make the Black Detector amenable to many different experimental conditions. The Black Detector efficiency is determined with a Monte Carlo calculation of neutron multiple scattering in the scintillator. The accuracy of the efficiency determination has been verified experimentally at several energies below 900 keV with the use of the $T(p,n)^3He$ source reaction and the time-correlated associated-particle method [7]. Recently, absolute neutron flux measurements with the Black Detector have been required in the neutron energy range up to 3.0 MeV. An efficiency measurement at 2.3 MeV has been carried out as a check on the Monte Carlo efficiency calculation at these higher neutron energies. The measurement utilizes the time-correlated coincidence method along with the $D(d,n)^3He$ source reaction. The details of the efficiency measurement at 2.3 MeV and the results are presented.

2. Experimental setup

The time-correlated associated-particle method is a recognized technique for measuring the absolute efficiency of active neutron detectors. The primary advantage of this method is its independence of factors involving the experimental geometry and the neutron background which usually contribute to the efficiency measurement. The only requirement is that the active portion of the neutron detector totally subtend the time-correlated neutron cone.

The experimental geometry used for the measurement of the Black Detector efficiency at 2.3 MeV is shown in Fig. 1. A continuous 500-keV molecular deuteron beam is incident on a thick titanium-

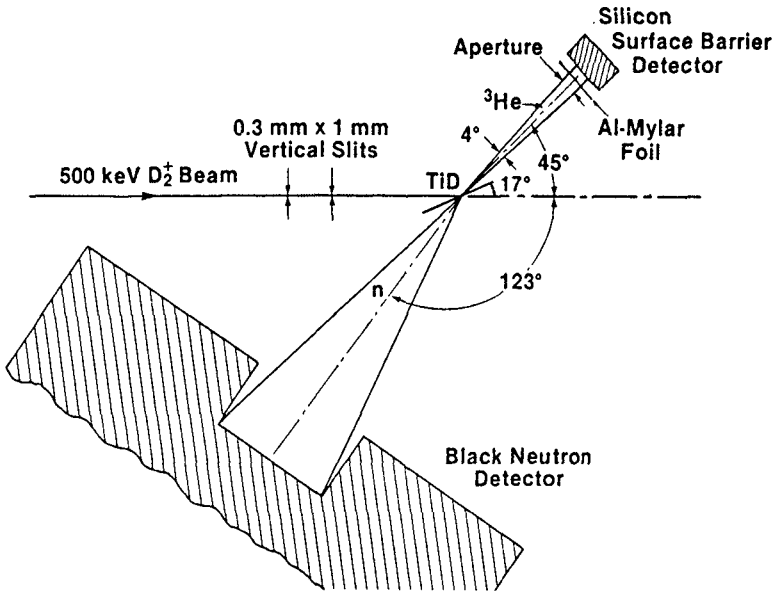

Fig. 1. The experimental geometry used for the measurement of the Black Neutron detector efficiency at 2.3 MeV.

deuteride (TiD) target. The deuteron beam is collimated to a 3-mm x 3-mm beam spot with an effective incident energy of 250 keV. The TiD target is oriented at 17° with respect to the beam axis and the associated particles from the D(d,n)^{3}He source reaction are detected at the forward angle of 45° with a silicon surface-barrier detector. The associated ^{3}He particles are collimated into a 4° cone with the resulting neutron cone located at an angle of 123° and having approximately a 20° full spread. The relatively large neutron cone is a result of the reaction kinematics and the range of deuteron energies obtained from stopping the 250-keV beam in the target. The neutron cone is also shown subtending the reentrant hole of the

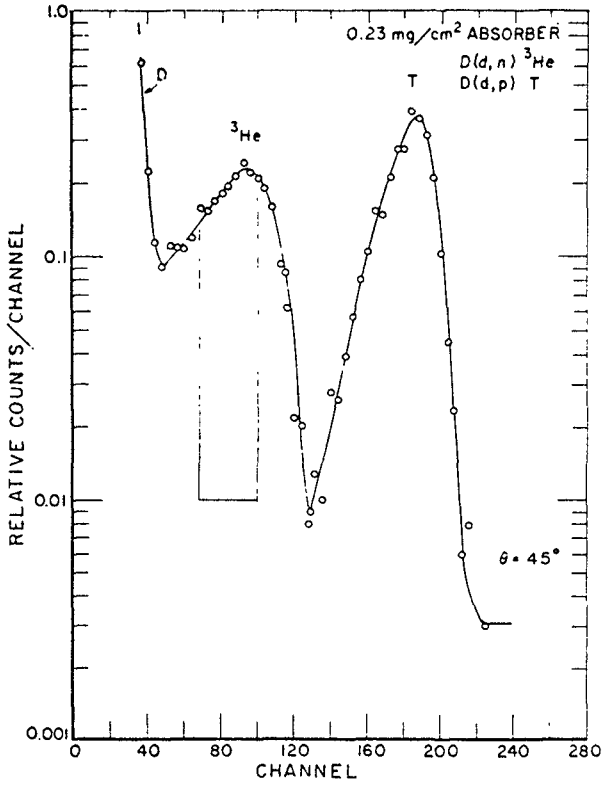

Fig. 2. The pulse-height spectrum obtained with a silicon surface-barrier detector behind a 0.23-mg/cm^2 aluminized-mylar foil. The window indicates the portion of the associated-particle spectrum used to measure the ^{3}He particle yield.

Black Detector. A thin 0.23-mg/cm^2 aluminized-mylar foil is positioned in front of the associated-particle detector to reduce the high scattered deuteron rate in the surface-barrier detector.

3. Associated particle measurement

A typical associated-particle spectrum obtained from the silicon surface barrier detector used in this setup is shown in Fig. 2.

The triton peak from the competing D(d,p)T reaction is also observed. The proton events resulting from this reaction are at a higher energy and are not shown. The low energy pileup edge of the scattered deuteron contribution overlaps a portion of the ^{3}He associated-particle events, however, a window can be easily selected above the pileup edge and sufficiently below the triton peak that will allow the ^{3}He events to be counted with a minimum background contribution. With approximately 1 μA of deuteron beam applied at the target along with ice water cooling, the target yield and associated-particle spectrum are stable for several hours.

The background contribution within the selected window of the associated particle spectrum is obtained from a separate measurement with an aluminized-mylar foil thick enough to eliminate the ^{3}He contribution without significantly altering the shape and position of the triton peak. The background contributions are from neutron interactions in the silicon surface-barrier detector and from the extended tail of the triton peak. This background correction is indicated in Table 1 as K_B.

4. Black Detector calibration at 2.3 MeV

The Black Detector is operated in coincidence with the associated-particle events falling within the selected pulse-height window. Since a one to one correspondence exists between the ^{3}He associated-particle events and the neutrons incident on the Black Detector, the efficiency is simply the ratio of coincidence events to associated-particle events. Corrections to the coincidence rate were applied for neutron attenuation due to outscattering in the

Table 1
Summary of quantities that contribute to the measured Black Detector efficiency at 2.3 MeV.

$$\varepsilon = \frac{^3He,n}{^3He}\left(\frac{K_w}{K_n K_B}\right)$$

Quantity	Value	Uncertainty (%)
Ratio of coincidence to associated particle events $\frac{^3He,n}{^3He}$	0.699	0.6
Correction for time-correlated neutrons extending beyond the uniformly sensitive region of the Black Detector K_w	1.005	0.5
Correction for time-correlated neutrons scattered from the beam K_n	0.933	0.6
Correction for background in associated particle singles K_B	0.991	0.6
Black Detector measured efficiency ε at a 30% bias	0.760	1.2
Neutron energy	2.29 MeV	0.015 MeV
Black Detector calculated efficiency ε' at a 30% bias	0.762	--

target backing and for neutron events extending beyond the uniformly sensitive region of the Black Detector (discussed in section 5). The incident neutron energy is determined from the kinematical relationships for the $D(d,n)^3He$ reaction.

The face of the Black Detector was positioned 6.9 cm from the neutron source and aligned with the centroid of the time-correlated neutron cone. This detector consists of a large Nell0 plastic scintillator, 12.7 cm in diameter and 17.78-cm long, mounted on a RCA 8854 photomultiplier tube. The front face of the detector contains a reentrant hole 5.08 cm in diameter and 2.54-cm deep. The reentrant hole was sufficiently large to subtend most of the time-correlated neutron cone.

The data was acquired for the Black Detector in a 2-parameter format by obtaining timing and pulse-height information simultaneously. The time distribution between the associated charged particle and neutron events in the Black Detector is shown in Fig. 3. The selected time windows for counting "coincidence" and "off-coincidence" (accidental) events are indicated. As a result of the low rates used, the number of lost time-correlated coincidence events due to uncorrelated stops in the time analyzer (TAC) was negligible. Shown in Fig. 4 is the Black Detector pulse height distribution obtained for events collected within the "coincidence" time window. The shape of the measured pulse-height distribution is in reasonable agreement with the distribution produced from the Monte Carlo calculation which is shown as the solid curve. The coincidence yield in the Black Detector is obtained from an integration of the counts above a bias that is 30%

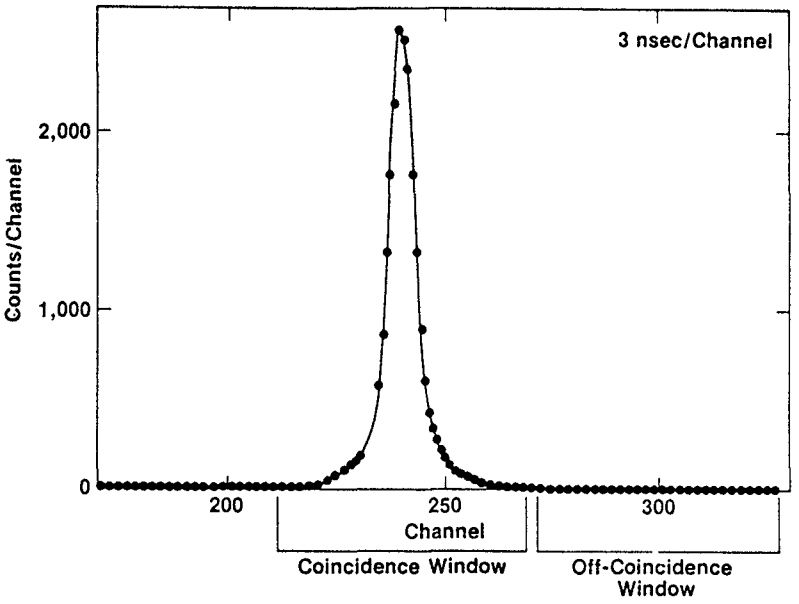

Fig. 3. The time distribution between the associated particles and the neutron events in the Black Detector taken for a 2-μsec range. The "coincidence" and "off-coincidence" windows are indicated

of the pulse-height peak position. Also recorded simultaneously is the scaler sum of associated particles detected within the designated pulse-height window. Typical detector rates are 1-3 counts per second in the associated-particle detector and 3,000 counts per second in the Black Detector.

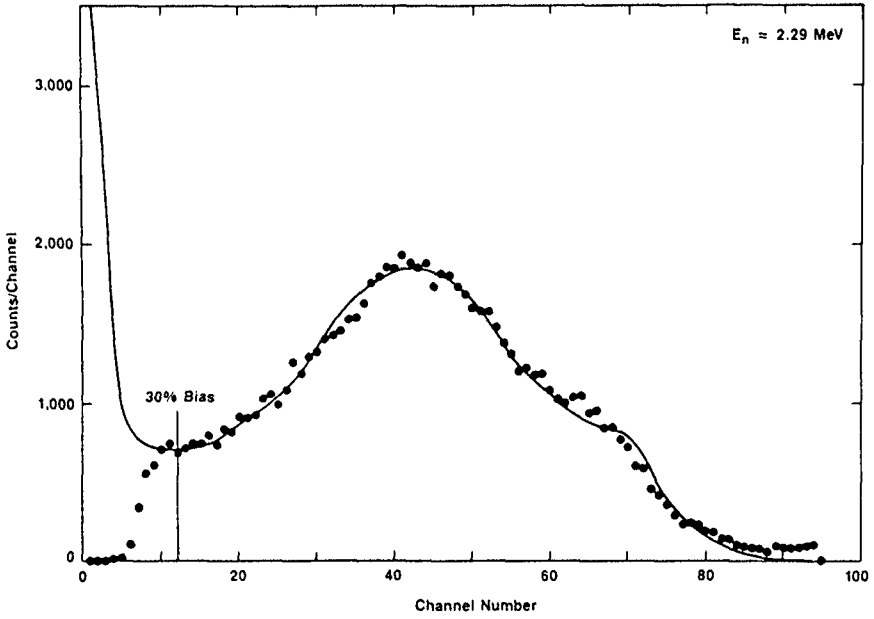

Fig. 4. The Black Neutron Detector pulse-height spectrum taken at a neutron energy of 2.3 MeV. The curve is a Monte Carlo calculated pulse-height distribution. The efficiency determination is based on the integrated sum of the counts taken above a bias of 30% of the peak position.

5. Results

A summary of the results of the Black Detector efficiency determination at 2.3 MeV is given in Table 1. Presented is the experimental result and a list of the corrections applied with the corresponding uncertainties. The correction for time-correlated neutrons removed from the neutron cone (K_n) was due to elastic and non-elastic scattering in the target backing material. Since the elastic scattering at 2.3 MeV is peaked in the forward direction, a significant fraction of the scattered events are detected by the Black Detector. These neutrons have energies near the primary energy and remain in coincidence with corresponding associated particles and therefore are included in the efficiency measurement. A correction is also applied for neutrons associated with the time-correlated neutron cone that are incident on the Black Detector and beyond the uniformly sensitive region of the detector (K_w). This correction includes the effect of the additional spreading of the neutron cone due to multiple scattering of the ^{3}He associated particles.

The Black Detector is designed to accept a collimated neutron beam incident within the 5.08 cm diameter reentrant channel. Neutrons incident on the detector beyond this region are not necessarily processed by the detector in a manner consistent with the multiple scattering model of the Monte Carlo calculation. This consideration is particularly important in determining the Black Detector response to the elastically scattered neutrons that may be incident anywhere on the detector face. The probability of detecting neutrons incident outside of the uniformly sensitive region of the Black Detector is based on the path length in the scintillator. This approach is illustrated in Fig. 5. Consideration of the angular distribution of the elastically scattered neutrons and the sensitivity of the Black Detector across the detector face allows the correction for neutrons removed from the neutron cone (K_n) to be determined.

The Black Detector efficiency at 2.3 MeV has been determined to be 0.760±1.2%. This value is in good agreement with the Monte Carlo

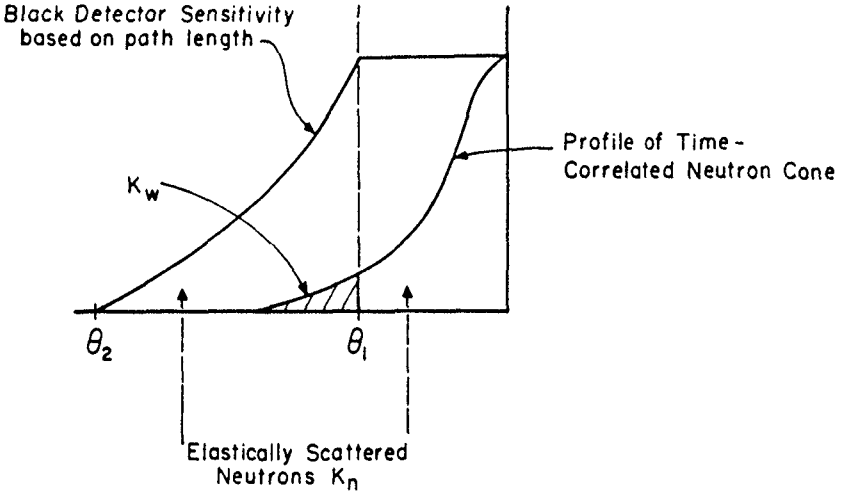

Fig. 5. An illustration of the Black Detector sensitivity across the face of the detector and particularly beyond the region of the reentrant channel. Also, shown in relation to the detector sensitivity is the profile of the time-correlated neutron cone. θ_1 and θ_2 are the angles subtended by the reentrant hole and the Black Detector, respectively.

calculated efficiency of 0.762. The measured and calculated efficiencies are determined for a bias that is 30% of the pulse-height peak position.

6. Summary

A measurement of the Black Neutron Detector efficiency at 2.3 MeV has been carried out using the time-correlated associated-particle method and the $D(d,n)^3He$ source reaction. The efficiency is determined from the measurement of the ratio of time-correlated coincidence events to associated-particle singles. The measured efficiency is in good agreement with the calculated value. The calculated efficiency curves can now be utilized in the higher energy range with confidence.

REFERENCES

[1] W. P. Poenitz, Proc. Panel Neutron Standard Reference Data, Vienna, Austria, November 20-24, 1972, p. 47, International Atomic Energy Agency (1974).

[2] G. P. Lamaze, M. M. Meier, and O. A. Wasson, Proc. Conf. Nuclear Cross Sections and Technology, Washington, DC, March 3-7, 1975, NBS Spec. Publ. 425, p. 73, U.S. National Bureau of Standards (1975).

[3] Oren A. Wasson, Michael M. Meier, and Kenneth C. Duvall, Absolute Measurement of the U-235 Fission Cross Section from 0.2 to 1.2 MeV, Nucl. Sci. Eng., Vol. 81, pp. 196-212 (1982).

[4] K. C. Duvall, O. A. Wasson, and M. M. Meier, NBS Neutron Monitor and Dosimeter Calibration Facility, Proceedings of the Int. Conf. on Nuclear Cross Sections for Technology, Univ. of Tennessee, Knoxville, TN., Oct. 22-26, 1979, NBS SP-594, pp. 747-751 (Sept. 1980).

[5] M. M. Meier, O. A. Wasson, and K. C. Duvall, Absolute Measurement of the U-235 Fission Cross Section from 0.2 to 1.2 MeV, Proceedings of the Int. Conf. on Nuclear Cross Sections for Technology, Univ. of Tennessee, Knoxville, TN. Oct. 22-26, 1979, NBS SP-594, pp. 966-970 (Sept. 1980).

[6] K. C. Duvall, M. M. Meier, O. A. Wasson, and V. D. Huynh, Neutron Flux Intercomparison at NBS, NBS Journal of Research, Vol. 83, No. 6, pp. 555-561 (Dec. 1978).

[7] M. M. Meier, Proc. Int. Specialists Symp. Neutron Standards and Applications, Gaithersburg, MD, March 28-31, 1977, NBS Spec. Publ. 493, p. 221, U.S. National Bureau of Standards (1977).

338 NEUTRON MEASUREMENTS AT THE BUREAU INTERNATIONAL DES POIDS ET MESURES

V.D. HUYNH
Bureau international des poids et mesures,
Sèvres, France

Abstract

The neutron measurements carried out at the Bureau International des Poids et Mesures can be summarized as follows: measurement of the emission rate of neutron sources with the manganese bath method, measurement of neutron fluence rate (2.5 MeV and 14.65 MeV) with the associated particle method, study of ionization chambers as reference and transfer instruments for international comparisons of kerma measurements, and calibration of the BIPM (d+T) neutron field in terms of tissue kerma in free air.

1. Introduction

The Bureau International des Poids et Mesures (BIPM) is a coordinating centre for national laboratories working in the field of metrology. One of its principal tasks is to organize periodically international comparisons in view of achieving uniformity on a world-wide scale and a long-term basis.

The research work carried out at BIPM by the neutron measurement group concerned firstly the measurement of the emission rate of neutron sources with the manganese bath method and the measurement of neutron fluence rate (2.50 MeV and 14.65 MeV) with the associated particle method. In recent years, the orientation of the neutron standards program has been shifting from neutron fluence measurements to include dosimetric quantities as well [1].

2. Measurement of the emission rate of neutron sources

The BIPM has installed a laboratory for measuring neutron sources and started by using the manganese sulphate bath method. A sphere of 1.0 m in diameter containing the $MnSO_4$ solution was used to determine the emission rate of the (α,n)-type neutron sources and a sphere of 0.50 m in diameter was used for the (γ,n)-type neutron sources.

Thanks to the development of a technique for measuring the (γ,n)-type sources by circulation of the $MnSO_4$ solution, the BIPM has been able to determine experimentally the ratio of thermal neutron absorption cross sections for hydrogen and manganese (σ_H/σ_{Mn}) from measurements made with various chemical concentrations of $MnSO_4$ solution. The ratio σ_H/σ_{Mn} is currently obtained with a standard deviation of 0.3 % [2], instead of the value of 1 % quoted previously in the literature by using the separated cross sections of σ_H and σ_{Mn}.

At present, the activity of the $MnSO_4$ solutions and the emission rates of the (α,n)-type and (γ,n)-type neutron sources are determined with an accuracy of 0.1 %, 1 % and 0.4 %, respectively.

3. Neutron fluence rate measurements

The BIPM has at its disposal two calibrated monoenergetic neutron beams: 2.5 MeV neutrons produced by the $^2H(d,n)^3He$ reaction and 14.65 MeV neutrons produced by the $^3H(d,n)^4He$ reaction. The deuterons are accelerated by a SAMES type electrostatic generator with a maximum energy of 150 keV. The absolute measurement of the neutron fluence rates is made using the associated particle method [3]. The present accuracy of measurements is 1.5 % (standard deviation).

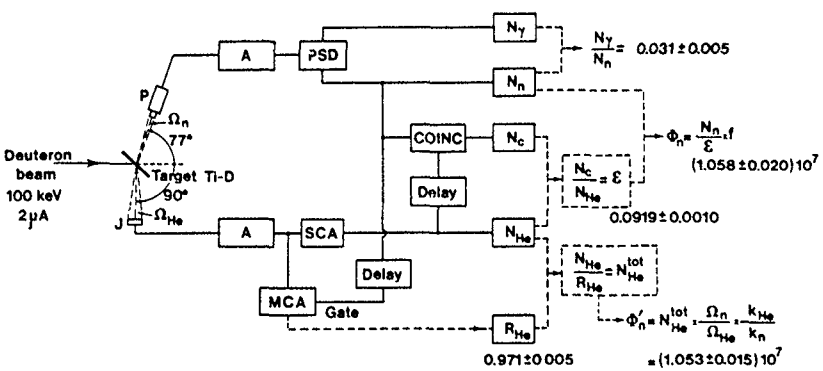

Fig. 1 - Measurement of neutron fluence. J = silicon surface barrier detector; P = stilbene scintillator; A = amplifier; PSD = pulse shape neutron-gamma discriminator; SCA = single channel analyser; MCA = multichannel analyser; COINC = neutron-^3He coincidence system; N_{He}, N_n, N_γ and N_c = numbers of counts for ^3He (single channel), neutrons, gamma rays and neutron-^3He coincidence, respectively; $R_{He} = N_{He}/N_{He}^{tot}$, the ratio of the partial ^3He counting (corresponding to that from single-channel analyser) to the total ^3He counting; ε = efficiency of the stilbene scintillator; f = correction factor taking into account neutron scattering, geometry effect, anisotropy and secondary neutron source, etc.; Ω_n, Ω_{He} = solid angles for stilbene scintillator and silicon detector, respectively; k_{He}, k_n = solid angle transformation factors from the centre-of-mass to laboratory system for ^3He and neutrons, respectively; Φ_n = fluence measured by the stilbene scintillator; Φ_n' = fluence measured by the silicon detector (with the solid angle subtended by the stilbene scintillator as a reference). The numerical values given in the figure are obtained for a measuring time of 12 000 s.

An example of research work carried out at BIPM in view of improving the accuracy of neutron fluence rate measurements is given below. It concerns the measurement of 2.5 MeV neutrons.

In addition to the associated particle method, a stilbene scintillator with a neutron-gamma discrimination system, based on pulse shape, is also used to measure the neutron fluence rate directly; the efficiency of this neutron detector is determined using the coincidences between the neutrons and the associated particles. The experimental set-up and the method of evaluation are indicated on figure 1.

The results of an intercomparison between these two methods show a very good agreement, so that increased confidence has been obtained for the absolute associated particle counting. Nevertheless, it should be pointed out that the measurement made with the stilbene scintillator is not a completely independent method and that the precision obtained is limited by the determination of the correction factor, f, specially due to the uncertainty in the evaluation of the scattered neutron and the gamma-ray contributions.

4. Neutron dosimetry measurements

In the area of neutron dosimetry, the principal activity consists, on the one hand, of the study of ionization chambers as reference and transfer instruments for the coming international comparison of kerma measurements and, on the other hand, of the calibration of the BIPM (d+T) neutron field in terms of tissue kerma in free air [4].

a) Study of ionization chambers

At the request of Section III (Mesures neutroniques) of the Comité Consultatif pour les Etalons de Mesure des Rayonnements Ionisants (CCEMRI), BIPM has carefully studied several types of ionization chamber and has identified a suitable tissue-equivalent (TE) ionization chamber (Exradin T2 type), and a suitable "neutron-insensitive" Mg/Ar ionization chamber (Exradin MG2 type) for separating out the gamma-ray component. The goal is for BIPM to provide an equipment capable of retaining a calibration over a long period of time and to organize the coming international comparison of kerma measurements by circulating some of these instruments.

b) Measurement of tissue kerma in free air at 14.65 MeV

For the BIPM (d+T) neutron field, the tissue kerma in free air, measured at 14.65 MeV with a TE ionization chamber (Exradin T2 type) and a GM counter (ZP1311 type), is compared to the kerma calculated from the measured fluence and using the Caswell-Coyne-Randolph kerma factors [5].

For the ionization chamber method [6,7], the neutron tissue kerma, K_N, and photon tissue kerma, K_G, in the mixed field, are measured at the reference point situated at a distance of 30 cm from the target and are normalized to a neutron fluence of 10^5 cm^{-2} which is chosen as one unit of monitor (u.m.). The results obtained are [4]

$$K_N = (6.670 \pm 0.370)\ 10^{-6}\ \text{Gy/u.m.}\ ,$$

$$K_G = (0.071 \pm 0.010)\ 10^{-6}\ \text{Gy/u.m.}\ ,$$

$$\frac{K_G}{K_N + K_G} = (1.05 \pm 0.15)\ 10^{-2}\ .$$

The fraction of photon component is only about 1 % of the total kerma in the BIPM (d+T) neutron field.

By applying a fluence-to-kerma conversion factor of $6.726 \cdot 10^{-11}$ Gy/cm^{-2} (with a relative uncertainty of 3 %) taken from Caswell et al. [5], the value of K_N corresponding to a measured fluence of 10^5 cm^{-2}, for 14.65 MeV neutrons, is calculated

$$K_N = (6.726 \pm 0.220)\ 10^{-6}\ \text{Gy/u.m.}\ ,$$

so that there is a good agreement between the two independent methods (ionization chamber and fluence). A difference of only 0.8 % has been observed.

References

[1] A. Allisy, Rapport BIPM-83/7, 1983; also in "Proceedings of the meeting on radiological protection and dosimetry", Centrecon, Itaipava, Rio de Janeiro, Brazil, March 1983.

[2] V.D. Huynh, L. Lafaye, C. Colas et C. Veyradier, Rapport BIPM-79/8, 1979

[3] V.D. Huynh, Metrologia 16 (1980) 31

[4] V.D. Huynh, "Proceedings of the Fifth Symposium on Neutron Dosimetry", Neuherberg, September 1984 (to be published)

[5] R.S. Caswell, J.J. Coynes and M.L. Randolph, Radiation Research 83 (1980) 217

[6] J.J. Broerse, B.J. Mijnheer and J.R. Williams, Brit. J. of Radiology 54 (1981) 882

[7] ICRU Report 26, 1977

340 NEUTRON FLUENCE MEASUREMENTS WITH A PROTON RECOIL TELESCOPE

H.J. BREDE, M. COSACK, H. LESIECKI, B.R.L. SIEBERT
Physikalisch-Technische Bundesanstalt,
Braunschweig, Federal Republic of Germany

Abstract

Correction factors and the associated uncertainties have been deduced for fluence determinations with a proton recoil telescope (PRT). A Monte Carlo code taking into account the properties of the deuteron beam, the deuterium gas target and the telescope was used. The results are given for two neutron energies of 6 MeV and 14 MeV. The main contributions of uncertainties come from the H(n,n)H cross section and the hydrogen content of the radiator. Other significant experimental uncertainties can be reduced. The analyses shows that an uncertainty of 2 % (standard deviation) can be obtained in fluence measurements.

1. Introduction

The proton recoil telescope (PRT) (Los Alamos type) has been a standard instrument for fluence measurements of fast neutrons since it was first conceived by Bame, Haddad et al.[1] in 1957. Cross section measurements were quite frequently based on fluence determination with a PRT. The significance of the instrument became especially apparent in recent international intercomparisons of fluence measurements for monoenergetic fast neutrons[2-4] as also discussed at this meeting. The response of a PRT has been compared to associated charged particle counting[5,6] several times to establish the reliability. Generally good agreement was found within the uncertainties for either method. But no reduction of the uncertainties of the PRT could be achieved in these measurements. It consequently appeared worthwhile to carry out a more careful study of the properties of a PRT including a detailed analysis of the uncertainties.

2. The Monte Carlo simulation

The PRT described here consists of a solid radiator of hydrogen-containing material (tristearate or polyethylene), two proportional counters and a surface barrier detector for the spectroscopy of the recoil protons (fig. 1). This instrument was used for neutron fluence measurements from 6 to 14 MeV in connection with a deuterium gas target. As the geometry of the experimental situation could not easily be analyzed with the

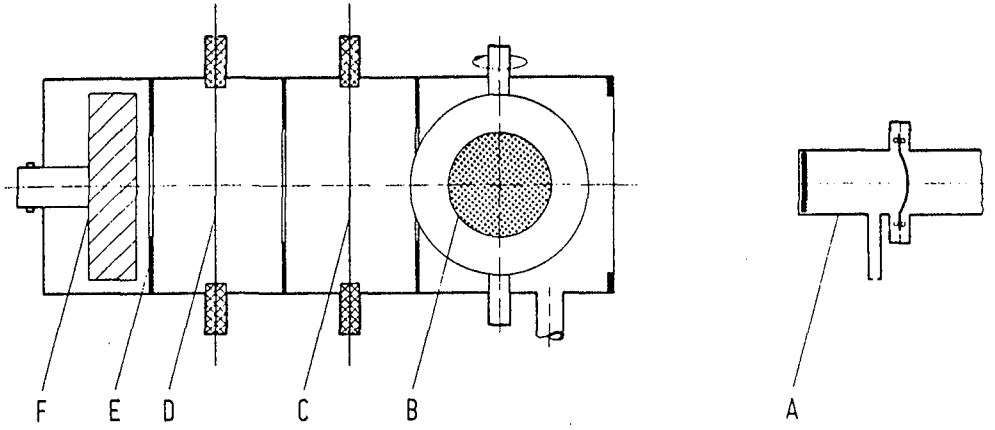

Fig. 1

Sketch of the proton recoil telescope. Background measurements are carried out by turning the radiator assembly (B) through 180°

A = Gas target
B = Radiator and radiator backing
C = Proportional counter
D =
E = Defining aperture
F = Silicon detector

application of existing efficiency tables, a detailed study became necessary. A Monte Carlo code (SINENA)[7] was written to give a full simulation of the experimental arrangement. It takes into account the following effects

- the spatial extension of the accelerated deuteron beam
- the energy distribution of the deuteron beam
- the mean energy loss and angular and energy straggling of the deuterons in the entrance foil of the gas target
- the energy loss of the individual deuteron in the deuterium gas before the reaction takes place
- the angular distribution of the neutrons from the target
- the attenuation of the neutrons in the walls of the gas cell, the walls of the PRT and the backing of the solid radiator
- the inscattering of neutrons from the material of the gas cell and the radiator backing
- the angular distribution of the recoil protons
- the energy loss and straggling of protons within the radiator of the PRT
- the energy loss of the protons in the counting gas of the proportional counters of the PRT
- the interaction (energy loss, in and outscattering) of the recoil protons with the wires of the proportional counters and the partial transparency of the defining apertures in the PRT.

3. Results

Several test calculations were performed to establish the reliability of the code. The values of the response given in the tables by Bame[1] were reproduced with appropriate simplifications in the input data. In addition, effects implemented in the Monte Carlo code were individually compared with analytical calculations. The results ascertain that the simulation of the experiment with the Monte Carlo method is adequate[8].
On the other hand, experimental confirmation was sought in different measurements. The influence of the neutron production including the construction of the gas cell and the properties of the reaction $D(d,n)^3He$ were investigated separately[9]. The results were in good agreement with the calculations and a sufficiently realistic and accurate description of the target can be assumed.
Fluence measurements were performed at neutron energies of 6.06 MeV and 13.76 MeV corresponding to a mean deuteron energy in the gas target of 2.79 MeV and 10.71 MeV. The experimental situation is characterized in table 1:

Table 1

Deuteron energy of the cyclotron beam:	3.31	MeV	11.06	MeV
σ of intensity distribution (X Plane):	1	mm	1	mm
σ of intensity distribution (Y Plane):	1	mm	1	mm
Beam divergence:	0.3°		0.3°	
Length of target cell:	30	mm	30	mm
Diameter of target cell:	11	mm	11	mm
Thickness of target housing:	0.2	mm	0.2	mm
Thickness of entrance foil (Mo):	5.5	µm	5.5	µm
Thickness of beam stop (Au):	0.5	mm	0.5	mm
Deuterium gas pressure at 20°C:	$1.10 \cdot 10^5$	Pa	$1.10 \cdot 10^5$	Pa
Mean deuteron energy inside the target:	2.790	MeV	10.714	MeV
Mean neutron energy at 0°:	6.055	MeV	13.759	MeV
σ of energy straggling distribution:	19.6	keV	19.6	keV
σ of angular straggling distribution:	2.36°		0.62°	
Distance target-radiator:	240.9	mm	140.9	mm
Thickness of PRT entrance window (Al):	0.5	mm	0.5	mm
Thickness of radiator backing (Ta):	0.5	mm	0.5	mm
Mass per area of radiator:	10.085	mg/cm²	10.085	mg/cm²
Radius of radiator:	13.99	mm	13.99	mm
Diameter of anode wires (W):	100	µm	100	µm
Distance radiator-defining aperture:	85.0	mm	85.0	mm
Radius of defining aperture:	10.48	mm	10.48	mm
Thickness of defining aperture disk(Ta):	1.0	mm	1.0	mm

Parameters of the deuteron beam the gas target and the PRT.
(σ is the variance of an assumed Gaussian distribution)

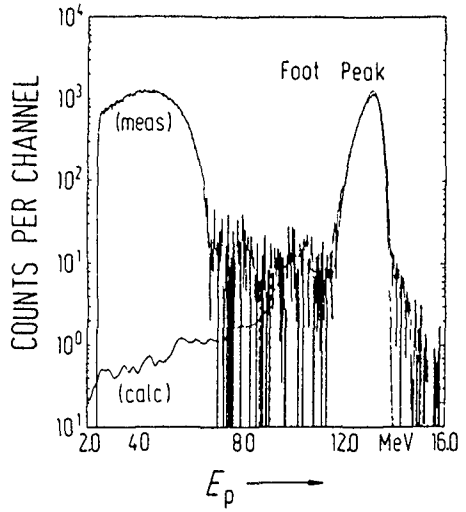

Fig. 2

Comparison between experimental PRT spectrum and Monte Carlo simulation using a deuterium gas target and a deuteron beam energy of 11.06 MeV.

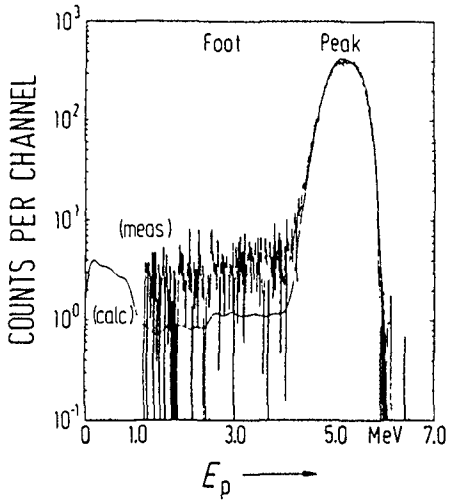

Fig. 3

Comparison between experimental PRT spectrum and Monte Carlo calculation using a deuterium gas target and a deuteron beam energy of 3.31 MeV.

The spectral recoil proton distributions as measured with a silicon surface barrier detector are given in fig. 2 for the neutron energy of 13.76 MeV and in fig. 3 for 6.06 MeV. The background resulting from the neutrons produced in the entrance foil of the gas target and in the beam stop and the recoil protons of the radiator backing was subtracted (the radiator including backing turned 180° and the gas removed from the gas cell). The spectral distributions as calculated with the Monte Carlo code are also shown. The considerable discrepancies in the spectral distributions at low energies are caused by the "break-up" reaction D(d,np)D which was not considered in the calculation. Above this energy the measurement is quite well described. The proton events above the monoenergetic peak come from pile-up effects, as could be verified experimentally. The region adiacent to the peak at lower energies shows a difference between the calculation and the experiment.It is not explained by the calculation and contributes to the overall uncertainty.

4. Correction factors and uncertainties

In the course of the Monte Carlo calculation different effects are treated separately, so that their influences can be given quantitatively. The resulting correction factors for the fluence determination at the positon of the radiator as given by the monoenergetic proton recoil peak are listed in table 2. These factors correspond to the data given in table 1, considering only the distance of 240.9 mm between gas target and radiator. Dead-time and pile-up corrections must also be applied.

Table 2	E_n = 6 MeV	E_n = 14 MeV
Neutron attenuation in the radiator backing and the outer skin of the telescope	1.016	1.013
Proton angular straggling in the radiator	1.004	1.002
Proton interaction with the defining aperture in front of the detector	0.999	0.999
Proton interaction with the anode wires of the proportional counters	1.010	1.013
Efficiency of the silicon detector	1.000	1.004
Undefined events in the "foot" region	0.995	0.992

A typical set of correction factors for neutron fluence determination at the position of the radiator

Many effects have small uncertainties. The main contributions come from the total cross section and the angular cross section of the reaction H(n,n)H, the hydrogen content of the radiator, differences in the experimental and simulated spectral recoil proton distributions adjacent to the peak and counting statistics. The attempt to treat the target and the telescope in separate calculations failed, as this led to a deviation of the response values of the PRT of about 1 % when taking the parameters of table 1. This problem could be avoided by taking large distances, but the resulting poor counting statistics would outweigh any improvement.

The uncertainties connected with the different effects are given in table 3.

Table 3	E_n = 6 MeV	E_n = 14 MeV
Properties of the neutron source $D(d,n)^3He$ (angular source strength)	0.1 %	0.1 %
Determination and reproducibility of the mean neutron energy at the position of the radiator	0.15 %	0.2 %
Systematic uncertainties of the length measurements	0.1 %	0.1 %
Distance radiator to neutron source	0.2 %	0.2 %
Neutron fluence attenuation by the radiator backing	0.1 %	0.1 %
The total H(n,p)n cross section*	0.9 %	0.9 %
Angular cross section of the reaction H(n,p)n*	0.2 %	0.6 %
Total number of protons in the radiator determined by mass**	0.8 %	0.8 %
Determination of the mass per area of protons (diameter of the radiator)	0.35 %	0.35 %
Angular straggling of protons inside the radiator	0.15 %	0.1 %
Internal geometry of the telescope including scattering by aperture and anode wires	0.25 %	0.25 %
Efficiency of the silicon detector	-	0.1 %
discrimination between the "peak" and the "foot" of proton recoil spectra	0.1 %	0.15 %
Difference between calculations and experimental results in respect to the "foot" region of the proton recoil spectra	0.5 %	0.8 %
Deadtime and pile-up effects	0.1 %	0.1 %
Statistical uncertainties of the experimental data	0.5 %	1.0 %

List of uncertainties (standard deviations) for neutron fluence determination

* According to IAEA Techn. Rep. Sev. No. 227 and ref. 8

** Chemical analysis commissioned by CBNM, Geel

5. Conclusion

In the reduction of uncertainties at PRT fluence measurements, a complete simulation of the experimental situation is necessary, including the particle beam, the target and the PRT. The Monte Carlo calculation gives correction factors and uncertainties which result in a typical overall uncertainty of 2 % (standard deviation). Although several effects and correlated uncertainties can be applied generally, individual calculations of the response of the PRT are necessary for each target, geometry and neutron energy. Examples have been given in this article. Further calculations will be carried out for solid targets and the neutron energy range from 1 MeV to 20 MeV. We intend to give lists of response values for the experimental situations most frequently met with.

References

1) S.J. Bame, E. Haddad, J.E. Perry, R.K. Smith: Absolute Determination of Monoenergetic Neutron Flux in the Energy Range 1 to 30 MeV. Rev. Sci. Instr. Vol. 28 (1957) 997, Rev. Sci. Instr. 31(1960) 911-913.

2) V.D. Huynh: International Comparison of Flux Density Measurements for Monoenergetic Fast Neutrons. Metrologia 16(1980) 31

3) V.E. Lewis: International Intercomparison of d+T Neutron Fluence and Energy Using Niobium and Zirconium Activation. Metrologia 20(1984) 49-55

4) H. Liskien: International Fluence Rate Intercomparison for 2.5 MeV and 5.0 MeV Neutrons. Metrologia 20(1984) 55-59

5) H. Liskien: Precise Flux-Measurement Methods and their Intercomparison between 0.5 and 15 MeV. Neutron Standards and Flux Normalization. Nat. Tech. Inf. Serv. Dept. of Commerce, Conf.-701002 (1971) 343-354

6) D.J. Thomas, V.E. Lewis, Nucl. Instr. and Meth. 179(1981) 397-404

7) B.R.L. Siebert, H.J. Brede, H. Lesiecki: A Monte Carlo Program for Transfering Proton Recoil Telescope Neutron Fluence Measurements to Detectors. PTB Report ND 23 (1982), Physikalisch-Technische Bundesanstalt, Braunschweig

8) B.R.L. Siebert, H.J. Brede, H. Lesiecki: Corrections and Uncertainties for Neutron Fluence Measurements with Proton Recoil Telescopes in Anisotropic Fields. Submitted to Nucl. Instr. and Meth., September 1984

9) H. Klein, H.J. Brede, B.R.L. Siebert: Energy and Angle Straggling Effects in a $D(d,n)^3He$ Neutron Source Using a Gas Target. Nucl. Instr. and Meth. 193 (1982) 635-644

FLUX MEASUREMENT TECHNIQUES FOR WHITE NEUTRON SOURCES

D.B. GAYTHER
Atomic Energy Research Establishment,
United Kingdom Atomic Energy Authority,
Harwell, Didcot, Oxfordshire,
United Kingdom

Abstract

Techniques for measuring the neutron spectra emitted by pulsed "white" neutron sources in the energy region from thermal to 20 MeV are reviewed. Developments since the 1977 Symposium on Neutron Standards and Applications are emphasized. Neutron detection systems are discussed under two classifications: detectors with a flat response to neutron energy, and detectors which rely for their operation on standard neutron cross-sections.

1. INTRODUCTION

White spectrum neutron sources are, by optical analogy, sources which emit neutrons with energies distributed continuously across a broad range. They can be provided by nuclear reactors or charged particle accelerators and are used extensively to measure microscopic neutron cross-sections from thermal energies to several tens of MeV.

In a cross-section measurement, a sample of material is placed in a beam of neutrons from the source and the rate of occurrence of a particular reaction is observed. In the idealized case of a thin sample and the detection of every reaction, the recorded count rate C(E) at neutron energy E will be given by,

$$C(E) = \emptyset(E) n \sigma_r(E),$$

$\emptyset(E)$ being the incident neutron flux, n the number of nuclei per unit area normal to the beam, and $\sigma_r(E)$ the neutron reaction cross-section. The determination of the neutron flux is clearly of central importance in a cross-section measurement and it is often the largest source of error when high accuracy is sought. The role of the standard cross-section in nuclear data measurements is that it eliminates the difficult task of measuring the flux directly. This is done by replacing the sample with one containing a nuclide whose cross-section is a reference standard for the reaction being studied and repeating the measurement.

The present paper discusses techniques which are available on white sources for determining neutron flux in the energy range thermal to 20 MeV. Apart from some comments on the measurement of background, the general problems of white source neutron spectrometry will not be considered, and the discussion will concentrate on neutron detection techniques. The review is not intended to be comprehensive; most consideration will be given to detectors which are capable of achieving the high accuracy required for measuring neutron standards, and there will be an emphasis on developments since the 1977 Symposium on Neutron Standards and Applications[1]. Progress in the past few years has been mainly confined to developing established techniques, and for detailed reviews of neutron detectors reference should be made to various papers in the Proceedings of the above Symposium, and to the articles by Harvey and Hill[2] and Grosshoeg[3] published in 1979.

In the following sections, after a brief discussion of the relevant properties of white neutron sources, the basic requirements of a neutron flux detector are considered. The relative merits of systems in use today are then discussed under two broad classifications: detectors with a flat response to neutron energy, and detectors which are based on standard neutron cross-sections.

2. DESIGN CRITERIA FOR WHITE SOURCE NEUTRON DETECTORS

The white spectrum sources which are used for nuclear data work are invariably pulsed, and the measurements are made by the Time-of-Flight method. The sample under investigation is placed at some distance from the source and the incident neutron energy is determined from the time it takes to traverse this distance. The features of white sources which have to be taken into account in designing the neutron detector are now discussed.

2.1 Properties of white neutron sources

The white sources can be classified into three types:

(i) High flux research reactors. These are either repetitively pulsed as in the Russian IBR[4], or steady-state with the neutron pulses provided by a mechanical "chopper". Pulse lengths range from a few microseconds to tens of microseconds and nowadays reactors are mainly used for specialized partial cross-section measurements at the low energy end of the neutron "slowing-down" spectrum.

(ii) Accelerator-based sources consisting of a heavy-mass target bombarded by pulsed beams of electrons, protons or deuterons with sufficient energy to produce an evaporation spectrum of neutrons. Pulse lengths range from one nanosecond to several microseconds. For very high energy resolution work it is possible to produce sub-nanosecond pulses with an electron linac. The primary spectrum of neutrons extends from a few keV to a few MeV. The neutron intensity is enhanced at low energies by placing a moderator near the target, and at high energies it is enhanced by raising the projectile energy. Sources of this type include the electron linacs ORELA[5], GELINA[6] and HELIOS[7], and the cyclotron at Karlsruhe[8].

(iii) Accelerator-based sources consisting of a low-mass thick target bombarded by monoenergetic protons or deuterons. The continuous neutron spectrum so produced covers a limited energy range and results from particle energy loss in the target. Pulse lengths can be about one nanosecond. Auchampaugh[9] has described an intense pulsed neutron source for use in the energy range 1 to 20 MeV which is produced by bombarding a thick beryllium target with 15 MeV deuterons from a tandem Van de Graaff.

The sources in the second of the above classifications cover the largest neutron energy range, and it is for this reason that they are the most widely used in nuclear data work. Most of the present considerations will be concerned therefore with this type of source.

A feature which is common to all sources is the accompaniment of the neutrons by a prompt burst of gamma-radiation, the total flux of which can be many times greater than the total neutron flux. For all but the electron linacs this does not impose too much constraint on the design of neutron detectors as the bulk of the radiation will be "soft" and its detection is automatically removed in the time-of-flight technique. Not so readily removed are the delayed 2.2 MeV gamma-rays produced by neutron capture when a hydrogenous moderator is present. This can be a significant source of background but it is easily identified. The prompt burst of bremsstrahlung which is produced in an electron linac target creates a severe problem in the design of detectors and their associated electronics. This "gamma-flash" from a powerful electron linac can easily deposit one GeV of energy in a detector, and the ability of the detector and electronics to recover rapidly from its effect determines the upper energy at which a measurement can be made.

It has to be remembered that the neutrons in a particular energy range of interest will be preceded by a burst of faster neutrons. These lattter neutrons can scatter out of the detector into the surrounding materials where after thermalization they can be captured and appear as background in the measurement. The background caused by shielding material which is placed around the detector must therefore be given careful consideration.

Figure 1 shows neutron spectra which are typical of electron linac targets.

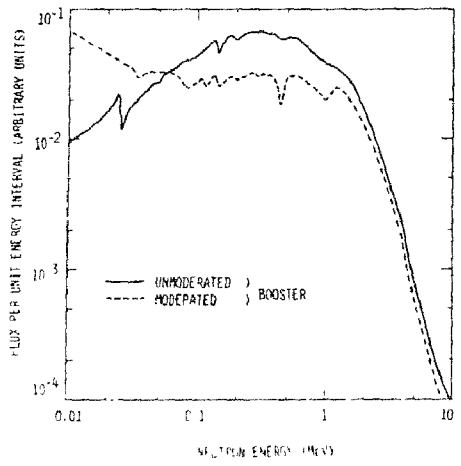

Fig. 1 The neutron spectrum emitted by the Harwell Neutron Booster Target, as measured by Coates et al[10]

The particular example is for the Harwell Booster target which is a sub-critical multiplying assembly of enriched uranium surrounded by a natural uranium reflector. This target is unique amongst electron linacs in that the gamma-flash is much reduced by self-shielding in the target assembly by comparison with a conventional non-multiplying assembly. The figure shows that both the moderated and the bare target spectra exhibit resonance structure caused by the constructional materials. The Harwell Booster target produces a pulse of about 100 nanoseconds duration as a result of its multiplying nature.

The resonance structure in the spectrum of a typical high resolution target (pulse length of a few nanoseconds) of tantalum or uranium can be very pronounced at low energies, and must be taken into account when comparing neutron spectra obtained with detectors of differing timing resolutions.

2.2 Detector requirements

Some aspects of the most important characteristics of a pulsed white source neutron detector are now considered.

(1) Neutron detection efficiency.

This should vary slowly with neutron energy and maintain its value over a wide energy range. In the past it has been common to determine only the relative energy-dependence of the efficiency and this may still be adequate if measurements can be made at energies such as thermal or 14 MeV where an absolute normalization can be made. If such a normalization is not possible it is preferable to know the absolute efficiency. A high efficiency is not necessarily desirable. Thus, a detector for measuring a partial cross-section can have an efficiency of say 10^{-5}, and the use of a very efficient flux detector can give rise to the type of geometrical problem which is discussed in section (6) below.

(2) Sensitivity to background.

Discrimination against the types of background mentioned in section 2.1 requires the rejection of events caused by gamma-rays. Detectors, such as the organic liquid scintillators, which allow discrimination between neutrons and gamma-rays on the basis of pulse shape can be used to advantage. Other types of background which have to be considered are caused by natural radioactivity and cosmic radiation, but unless the detector is very large these effects are not troublesome since they produce time-independent background.

(3) Timing resolution.

In the MeV region a timing resolution of one nanosecond or less is generally required, while in the eV region a resolution of several microseconds will be sufficient. In exploiting the sub-nanosecond timing capability of some accelerators, the timing resolution of the neutron detector may well be the limiting factor in a high resolution measurement.

(4) Sensitivity to gamma-flash from electron linac target.

The enormous amount of energy which can be deposited in the detector by the passage of the prompt gamma-radiation from an electron linac target poses severe problems if high neutron energies (and therefore short flight times) are to be studied. In an ionization detector the large amount of charge which is released will require restoring in as short a time as one microsecond before measurements can commence. Special circuits have been designed to enable rapid restoration of the charge[11]. In a scintillation detector, the gamma-flash can excite long-lived decay components which are otherwise unimportant. There may also be problems with "after-pulsing" in photomultipliers. Detectors with fast timing capability help, but on most targets it is found necessary to use either a filter of heavy material in the beam or mask the region of intense bremsstrahlung production with a shadow-bar. In a precision measurement at high neutron energy full recovery from the gamma-flash of the detector and its electronics needs to be demonstrated experimentally. The technique used by Carlson and Patrick[12] for this purpose is to be commended. They placed a strong radioactive source close to their detector and observed the detector pulses as a function of time after the gamma-flash.

(5) Geometrical effects.

It was noted above that the detector which is used to observe a reaction may have a very different efficiency from that used to measure the neutron flux. Counting rate considerations may dictate the use of different flight path lengths and this can have two effects. Firstly, each measurement will have a different energy resolution, and proper allowance must be made for this if there is structure in the incident spectrum. Secondly, the collimation must be designed so that each detector "sees" all regions of the neutron source with the same weight, otherwise it is possible that different neutron spectra will pertain to each measurement. In general, it is preferable to make the flux and reaction rate measurements at the same flight path position. The effects of collimation also need careful consideration if the area of neutron beam required by each detector is different.

(6) Pulse height resolution.

Although it is not essential to use a detector whose pulse height distribution is characteristic of the energy of the incident neutron, a peaked distribution with modest pulse height resolution (~10%) can be used to advantage. If, for example, the two parameters time-of-flight and pulse amplitude are recorded in the measurement, the amplitude spectra may yield information on the background which is present at a particular incident neutron energy. Another advantage of a peaked as opposed to a quasi-rectangular distribution, is a more accurate extrapolation below the detector bias to zero amplitude, with a corresponding improvement in the accuracy to which the detector efficiency is known.

The majority of detectors which are used for measuring neutron flux on white spectrum sources are conveniently classified into the following types:-

(i) Flat response detectors. These are detectors with an efficiency (normally $\gtrsim$90%) which varies slowly with incident neutron energy. The efficiency is relatively insensitive to the cross-sections of its constituents and so it can be calculated with some confidence. For convenience included under this heading are the small organic scintillators which are used in the MeV region and for accurate flux measurements require a calibration of efficiency.

(ii) Standard cross-section detectors. These are detectors which rely for their operation on the recording of one of the neutron cross-section standards: $H(n,n)H$, $^{3}He(n,p)T$, $^{6}Li(n,t)^{4}He$, $^{10}B(n,\alpha)^{7}Li$, $^{10}B(n,\alpha\gamma)^{7}Li$, $C(n,n)C$, $^{197}Au(n,\gamma)^{198}Au$, and $^{235}U(n,f)$. The $^{3}He(n,p)$ reaction has a large and smoothly varying cross-section over the whole energy region of interest. However, the present uncertainty in the value of the cross-section at the higher neutron energies, and difficulties in making practical detectors, preclude its use for accurate neutron flux measurements. The $C(n,n)$ reaction is suitable as a standard for scattering measurements but not as the basis for a flux detector. The $^{197}Au(n,\gamma)$ reaction is not known with sufficient accuracy to justify its use as a flux detector and like the $C(n,n)$ reaction will not be considered any further.

Detectors are discussed under the above headings in the following sections.

3. FLAT RESPONSE DETECTORS

These can be broadly divided into two categories: thick liquid or plastic scintillators which rely on proton recoil detection, and systems in which the capture gamma-rays are detected after the neutrons have been slowed down in a moderating medium. Because of their slow time response the latter are only suited to neutron energies below ~1 MeV on a white spectrum source.

3.1 Thick scintillator detectors

(1) The Argonne black detector.

The expression "black neutron detector" was coined by Poenitz[13] to describe a large hydrogenous scintillator for detecting MeV neutrons which was designed and built at the Argonne National Laboratory. By virtue of its size, incident neutrons lose most of their energy before escaping from the scintillator or falling below the detector bias, and the resulting pulse height distribution has the desirable peaked shape (section 2.2). This is illustrated in Fig. 2 in comparison with the response of a small conventional hydrogenous scintillator. The advantages of the large detector are two-fold:

(i) The extrapolation below the experimental bias level of the observed pulse height distribution to zero pulse height is small, and therefore the absolute total number of counts are determined accurately,

and (ii) Since the detection efficiency is high, its dependence on the differential neutron cross-sections of hydrogen and carbon is not large, and the efficiency can, accordingly, be calculated with some confidence.

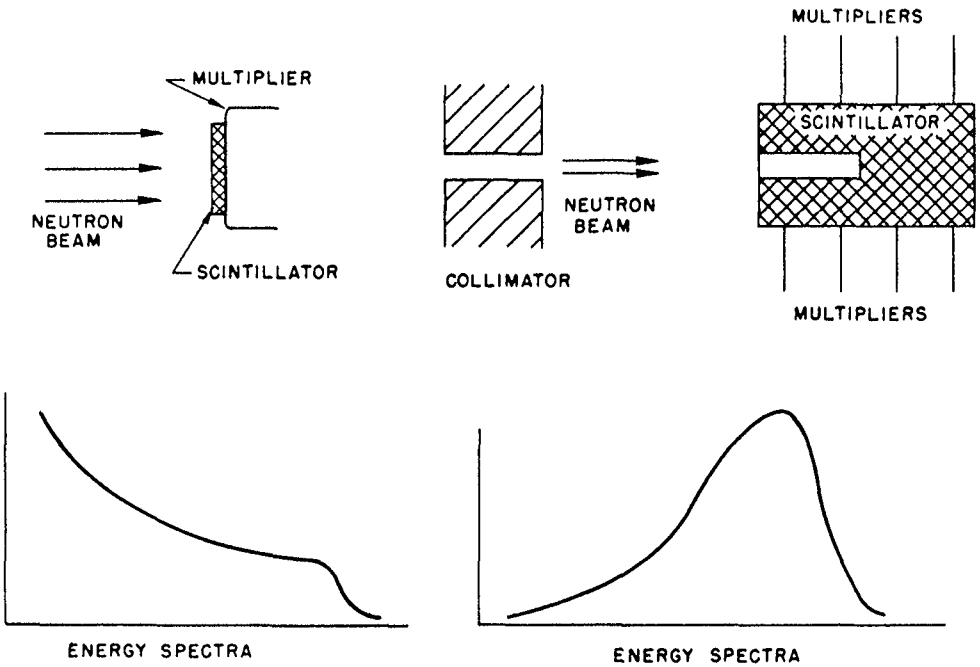

Fig. 2 Schematic comparison of a conventional scintillation detector (left) and the "black neutron detector", from Poenitz[13].

Detailed Monte Carlo calculations were made to optimize the design taking into account neutron efficiency, gamma-ray sensitivity, light attenuation, and timing resolution. The chosen dimensions were: a cylinder 40 cm long and 26 cm in diameter, with a 2.5 cm diameter channel 15 cm deep. The threshold neutron energy for this instrument is set at 0.3 MeV and its useful energy range is 1 to 10 MeV. The calculated neutron detection efficiency was estimated to be accurate to ~1%, and its value deviates by no more than 5% throughout the operating range from an average efficiency of 95%. The timing resolution of the system has a full width at half maximum of 4 nanoseconds but there is an appreciable tail extending to ~10 nanoseconds. A disadvantage of the large size of this detector is that its sensitivity to gamma-ray background requires it to be surrounded by a lead shield. The presence of the shield has to be considered in calculating the efficiency. The shield can also give rise to a time-dependent gamma-ray background from the capture of slow neutrons which escape from the scintillator.

(2) The NBS black detector.

The detector which has just been described was designed for use on a monoenergetic accelerator in the MeV region. With a white neutron source, the effective flight path length uncertainty introduced in the detection of incident neutrons of these energies with this system could appreciably affect the eutron energy resolution of a measurement. In the past few years the National Bureau of Standards have developed a smaller black detector which was designed to have an efficiency greater than 95% in the energy range 0.25 to 1 MeV[14]. The properties of this detector have been studied extensively and it has been used to measure cross-sections on both the NBS electron linac and Van de Graaff accelerators. Recently its use has been extended to 3 MeV[15]. The detector consists of a 12.5 cm diameter plastic scintillator 19 cm in length which is coupled directly to a 12.5 cm diameter photomultiplier tube. A re-entrant channel 5 cm in diameter and 2.5 cm in depth increases the efficiency of the device.

The efficiency of the NBS detector was calculated with a version of Poenitz's original Monte Carlo program[13] which was modified to include the Poisson statistics[16] for the small number of photoelectrons released from the photocathode at low neutron energy. Neutrons of 250 keV, for example, produce only about 9 photoelectrons. Figure 3 shows the excellent agreement which is obtained between measured and calculated pulse-height distributions for neutrons of energy 540 keV. Similar agreement is found at other energies. The

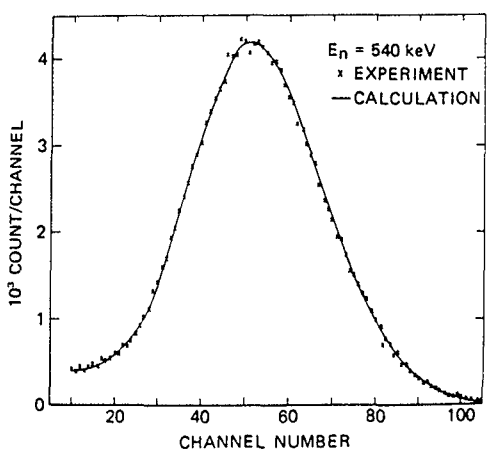

Fig. 3 Experimental and calculated response of the National Bureau of Standards black detector for 540 keV neutrons.

shape of the spectrum is determined mainly by the non-linearity in scintillator light output for proton and carbon recoils, and by the Poisson statistics. The calculated efficiency of the detector at a particular electronic bias is defined as the number of detected events divided by the number of neutrons incident on the re-entrant channel. The electronic bias, which has to be imposed to reject noise pulses, is typically 10% of the pulse height at the peak of the spectrum.

It is found that the number of incident neutrons determined from the calculated efficiency is very insensitive to the fraction of the spectrum which is recorded (i.e. to the bias). This indicates that both the light responses and the Poisson description of photoelectron production which are used are valid in a relative sense over the neutron energy range of interest. The uncertainty in the derived number of neutrons which is assigned to allow for error in fitting the observed pulse height spectrum is ~0.2%. For a bias of 10% of the peak position the calculated efficiency falls from 99% to 91% in the 0.2 to 1.2 MeV energy region.

Although the agreement between measured and calculated pulse height spectra is very good, it is important to confirm the calculated efficiency experimentally. This has been done by Meier[17] in the 0.5 to 0.9 MeV region who used the associated particle technique to determine the number of incident neutrons. The comparison is shown in Fig. 4 where it can be seen that there is reasonable agreement. On the basis of this comparison, and a consideration of the accuracy of the calculation, the calculated efficiency

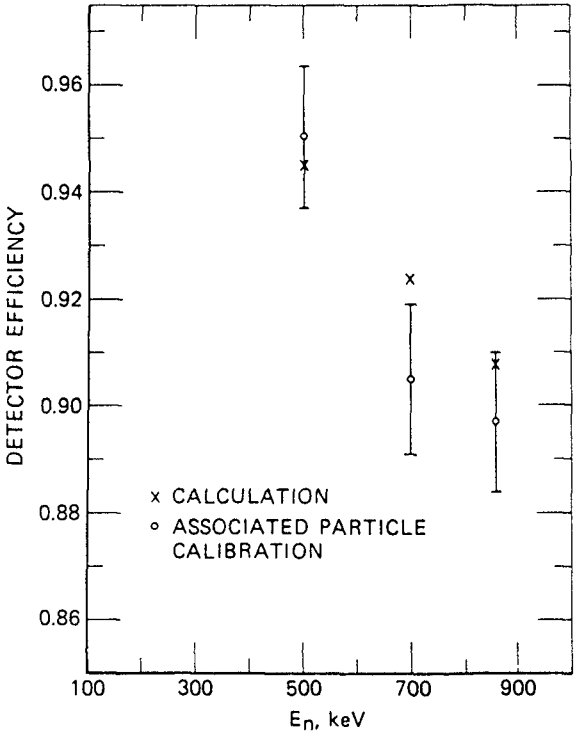

Fig. 4 Calculated and measured efficiency of the National Bureau of Standards black detector for three neutron energies. The error bars show the 1.4% systematic uncertainty in the associated particle method.

is conservatively assigned an uncertainty of 1.0%. The error in determining the number of neutrons incident on the detector consists of the 1.0% uncertainty in the efficiency calculation and the ~0.2% in the pulse height spectrum fitting procedure.

(3) The Oak Ridge black detector.

The NBS black detector is limited by the noise of the photomultiplier and the transparency of the scintillator to a lowest neutron energy of ~200 keV. At the Oak Ridge National Laboratory, a detector has been developed[18] which can be used in the energy region 80 keV to ~1 MeV. The detector consists of a cylinder of NE 110 plastic scintillator, 10.2 cm diameter and 7.6 cm deep coupled directly to the face of an RCA 8854 photomultiplier. The neutron beam is collimated to a diameter of ~2 cm and is incident on the plane face of the scintillator. A re-entrant channel for the incident beam was not used because it causes larger variations in light collection and also it restricts the diameter of the neutron beams which can be measured. Pulse height distributions were measured for 13 neutron energies provided by a thick iron filter placed in the white neutron beam from the Oak Ridge linac, ORELA. Comparisons were made with computed distributions using the Monte Carlo O5S code[19] modified to include Gaussian smearing arising from variations in light collection and photomultiplier gain as well as Poisson smearing for the number of photoelectrons produced, and excellent agreement was obtained. In the energy region 80 to 500 keV the efficiency is ~95% and is constant to ~0.5%. The absolute efficiency is accurate to ~1.0% in this energy region.

(4) Calibrated organic scintillators.

Although not strictly coming under the heading of "flat response detectors", mention should be made of the many medium sized detectors of efficiency ~15% which have been used to measure neutron flux in the MeV region. Neither "black" as the above detector, nor "thin" so that their efficiencies are simply related to the H(n,n) cross-section, accurate calculation of their efficiencies is difficult. Thus the number of events falling below the electronic bias will be inaccurately computed because the pulse height distributions are no longer peaked. Moreover, at energies above 2 MeV, where it is usual to use this type of detector, the efficiency will show structure due to the presence of carbon: apart from elastic scattering resonances, other reactions become possible such as $^{12}C(n,n')^{12}C^*$ above 4.8 MeV, $^{12}C(n,\alpha)^{9}Be$ above 6.2 MeV, $^{12}C(n,n')3\alpha$ above 8.3 MeV and $^{12}C(n,p)^{12}B$ above 13.6 MeV. The light yields for carbon recoils and alphas are poorly known and the pulse height distributions cannot be calculated with confidence. Nevertheless, for all but the highest precision measurements, this type of detector is worthy of consideration. They are capable of very fast timing resolution and because they can be made of modest sized liquid scintillators, pulse shape discrimination (PSD) can be used to reject events caused by gamma-rays. The technique of PSD cannot be applied to the black detectors not only because they are generally made of plastic scintillator, but also because of their size, light dispersion effects distort the scintillation pulse shape. Harvey and Hill[2] give a detailed discussion of small inorganic scintillators for neutron detection. More recently, Dietze and Klein[20] at PTB Braunschweig have made extensive studies of the response functions of small liquid scintillators for flux measurements in the MeV region. For the most accurate flux measurements, it is essential to calibrate the neutron detection efficiency of this type of detector experimentally, preferably by use of the associated particle method.

As an example of what can be achieved, Fig. 5 shows a comparison of the efficiency of a 5 cm diameter 3.8 cm thick NE 213 scintillator as measured by the associated particle technique[21] and calculated with two Monte Carlo codes[19,22]. Agreement is found to within ~3%. The uncertainty in the measured efficiency is about ±2%. This detector has been used by J. L. Fowler and co-workers to measure flux on the Harwell tandem Van de Graaff accelerator, but it is equally suited for measurements on a white neutron source in the energy region 1.5 to 25 MeV.

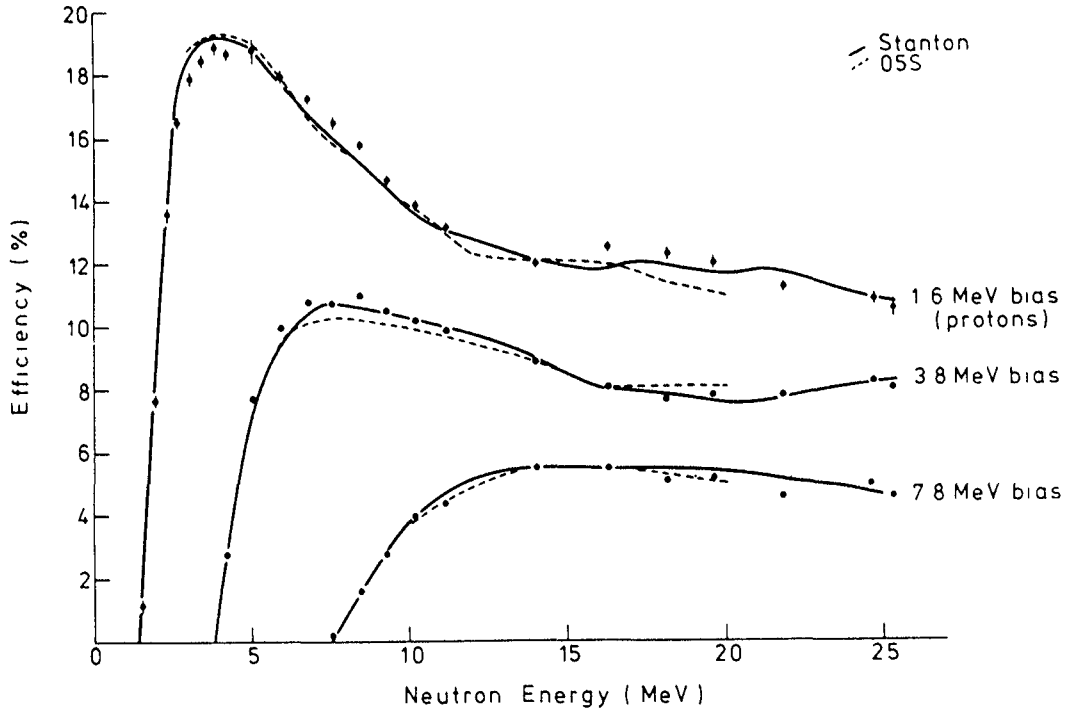

Fig. 5 Calculated and measured central efficiency of a 5 cm diameter, 3.8 cm thick NE213 liquid scintillator for three settings of the electronic bias.

3.2 Moderated neutron detectors

Poenitz[23] has described a "grey neutron detector" which is in effect a manganese bath[24] adapted to give semi-prompt timing. The detector consists of a moderator with an entrance channel for a collimated neutron beam. The neutrons are thermalized and captured in hydrogen and the subsequent 2.2 MeV capture gamma-rays are detected in a NaI detector as they leave the surface of the moderator. This system, however, has poor timing resolution and is really only suitable for use on a monoenergetic accelerator.

A similar system which is capable of being used up to a neutron energy of ~1 MeV on a white source has been described by Coates and Hart[25]. This is known as the Boron-Vaseline Sphere detector and it was developed for measuring flux on the 45 MeV electron linac at Harwell. The poor timing resolution of the Poenitz detector arises from the use of a large weakly capturing medium. The Coates detector uses a small strongly capturing medium to achieve faster time response. It consists of one kg of ^{10}B homogeneously mixed with vaseline (effectively $CH_{2.05}$) and contained in a thin spherical shell of aluminium 24 cm in diameter. A radial channel 8 cm deep and 2.5 cm in diameter allows a parallel neutron beam to fall on the inner end near the centre of the sphere.

Neutrons are moderated and captured in ^{10}B to produce 478 keV gamma-rays which are detected at the surface of the sphere in four NaI scintillation counters. Calculations with a Monte Carlo code showed that the efficiency varies by less than 4% over the energy range 10 eV to 0.7 MeV. At higher energies, neutrons are no longer totally absorbed in the sphere, and gamma-rays are produced in the NaI crystals by the inelastic scattering of leakage neutrons. These gamma-rays cannot be distinguished from the 478 keV ^{10}B gamma-rays and the efficiency can no longer be calculated with confidence. The neutron lifetime in the detector, defined as the time taken to capture 99% of the high energy incident neutrons, was calculated to be 0.7 microseconds.

It was demonstrated that the calculated efficiency in the region 10 eV to 0.7 MeV was insensitive to reasonable changes in the input nuclear data. The energy-dependence of the efficiency at low energies was confirmed on the 45 MeV linac by comparison with the $^{6}Li(n,\alpha)$ cross-section and in the energy region 68 keV to 700 keV by comparison with the Harwell long counter[26] using the Van de Graaff accelerator IBIS as the neutron source. In the region 0.7 to 2 MeV the IBIS measurements provide a calibration of the detector efficiency. As a result of these measurements it is considered that the relative efficiency has been established to ±2%.

Although the modest timing resolution of the Boron-Vaseline Sphere requires the use of a flight path length of at least 200 m if the highest neutron o have energies are to be measured, it is unique amongst flat-response detectors in he being able to cover the very wide energy range from thermal to 2 MeV. This ed avoids the problem, which occurs with detectors of more limited energy range, of normalization in the regions of energy overlap.

4. STANDARD CROSS-SECTION DETECTORS

For an up to date and comprehensive resumé of detector systems based on the neutron standard cross-sections reference should be made to the review by Carlson[27]. The accuracies to which the standard cross-sections are presently known are given in the reviews in reference 52.

4.1 H(n,n)H detectors

The scattering cross-section of hydrogen is the most accurately known of the neutron standards. At energies below 20 MeV the total cross-section is known to 0.5-1.0%. The angular distribution is isotropic up to a few MeV, but

at the higher energies it is known with less accuracy than the total cross-section. For example, even at 14 MeV the uncertainty in the angular distribution is about 2%. For the most accurate work up to the highest energies reliance must therefore be placed on detectors which record the proton recoils into the whole forward hemisphere. Above ~100 keV the total cross-section falls rapidly with increasing energy which makes an accurate measurement of the incident neutron energy and the energy resolution essential when using the cross-section to determine flux.

(1) 2π-detectors.

All detectors of this type will suffer from the problem of calculating the fraction of events which fall below the lowest observed pulse height, since the pulse height distribution will be quasi-rectangular. When carbon is present, as is usually the case, allowance will have to be made for the carbon recoils.

Gas proportional counters have been described by Friesenhahn et al[28] and Wasson et al[29]. Timing resolution restricts this type of detector to below 1 MeV, even with long flight paths (~200 m). The lowest energy at which they can be used is determined by gamma-ray background and the presence of carbon recoils if methane is used. The counter described by Wasson et al[29] uses hydrogen gas, and it can be used down to an energy of 5 keV. The accuracy with which relative neutron flux can be determined with this detector is ~2% at the higher energies.

A "thin" hydrogeneous scintillator backed by a photomultiplier is at first sight a convenient way of utilizing the hydrogen total cross-section. A neutron detection efficiency of a few per cent at 1 MeV would be achieved which is considerably higher than the efficiency of a proportional counter. Several effects have to be considered in calculating the response of a scintillator, however, and some of these have been mentioned in part (4) of section 3.1. Harvey and Hill[2] consider the problem in detail. When the scintillator is thin, the effect of multiple neutron scattering can be neglected, and the probability of an incident neutron producing a proton recoil will be accurately proportional to the product of the hydrogen density and the hydrogen total scattering cross-section. Unfortunately, in practice, many protons will escape from the surface without detection because the light they produce will fall below the imposed electronic bias. Czirr[30] has suggested a simple way of overcoming this effect. This is to back a thin plastic scintillator with enough ^{7}Li-glass scintillator to detect the most energetic recoil protons which escape from the plastic. A rather more elegant way of tackling the problem has recently been implemented at the National Bureau of Standards (Dias et al[31]). A dual thin scintillator configuration is used as shown in Fig. 6. The scintillators are NE110 2.54 mm in thickness; one is 47 mm in diameter and the other 49 mm in diameter. Each scintillator is coupled through perspex light guides to a pair of photomultipliers and is optically separated from its partner. Signals are processed to accept single events from scintillator 1 and coincident events between the two scintillators. Single events from scintillator 2 are rejected. Thus an accepted single event and no coincident event means the recoil proton was totally absorbed in scintillator 1, and a coincident event means the recoil proton originated in scintillator 1 but escaped from the surface. Very few recoils from scintillator 1 escape detection since the scintillator thickness is approximately the same as the range of a 15

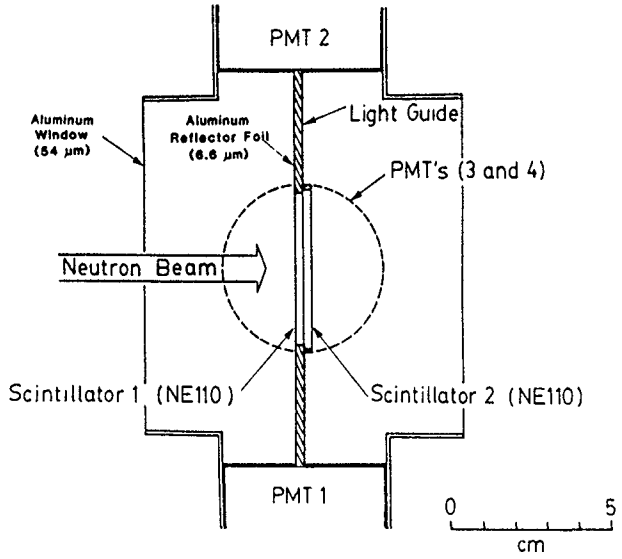

Fig. 6 The "dual thin scintillator" neutron flux monitor used at the National Bureau of Standards

MeV proton. The detector, in effect, behaves like a single 2.54 mm thick scintillator in which all proton recoils with energies above the bias are detected. The experimental bias has to be used to reject carbon recoils. This detector has been calibrated by the associated particle technique at 2.44 and 14.1 MeV. Theoretical Monte Carlo calculations have been made of the efficiency and pulse-height distributions to extend the region over which the efficiency is known to other energies between 1 and 15 MeV. It is considered that the accuracy of the detection efficiency is 1-2% in this range.

(2) Proton-recoil telescopes.

Proton-recoil telescopes have been used to measure neutron flux on white spectrum sources at Karlsruhe[32], Livermore[33], Oak Ridge[34] and the National Bureau of Standards[12]. For these detectors the probability of detecting a neutron is proportional to the product of the hydrogen density in the radiator foil and the cross-section for n-p scattering into the appropriate solid angle of the system. As mentioned earlier, because of the uncertainty in the differential cross-section, telescopes are not capable of giving as high an accuracy for flux determination as 2π-detectors. Figure 7 shows the arrangement used by Sidhu and Czirr[33]. Recoil protons from an annular polythene radiator foil are incident on a solid state detector which is protected from the incident neutron beam by a lead shadow bar. A similar arrangement has been used by Carlson and Patrick[12].

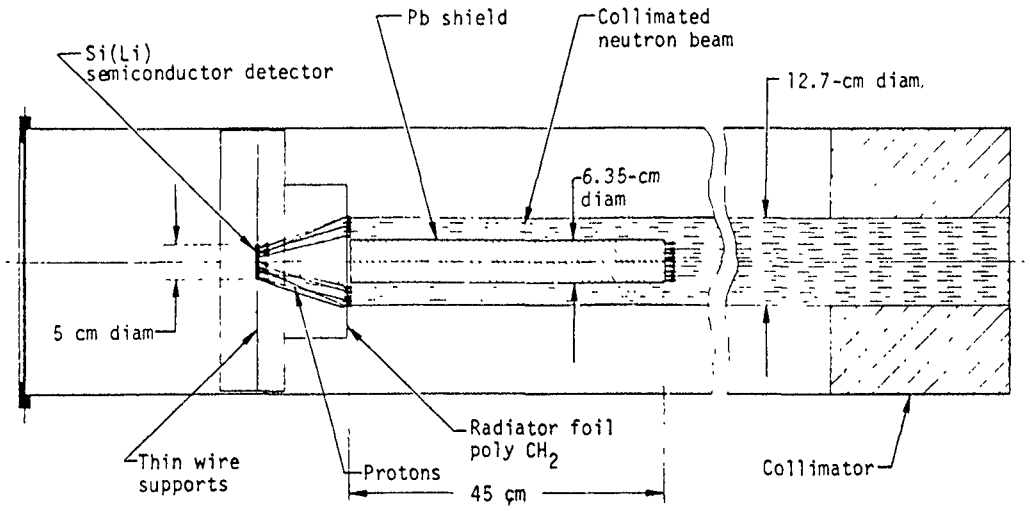

Fig. 7 The proton-recoil telescope used at the Lawrence Livermore Laboratory.

4.2 $^{6}Li(n,t)^{4}He$ detectors

The cross-section for the $^{6}Li(n,t)^{4}He$ reaction is known with an accuracy of between 0.5 and 2.0% below 100 keV. The large Q-value of 4.78 MeV which is available for neutron detection makes this one of the most widely used standards for flux measurement at low energies. At higher energies the presence of the resonance at ~240 keV and large uncertainties in the value of the cross-section, particularly above the resonance, make this reaction unsuitable as the basis for accurate neutron flux determination. At neutron energies above ~100 eV, the emitted tritons show a forward peaking in the laboratory system which increases with energy up to at least 100 keV. A neutron flux detector based on the $^{6}Li(n,t)^{4}He$ reaction must either account correctly for this energy dependent angular distribution or not be affected by it. Detector systems for using the $^{6}Li(n,t)^{4}He$ reaction have been reviewed by Weston[35], Lamaze[36] and Harvey and Hill[2].

(1) ^{6}Li scintillators.

Early applications used $^{6}LiI(Eu)$ detectors, but these are now rarely used because of resonance structure and neutron activation in the iodine. Cerium activated ^{6}Li loaded glass scintillators have been used in most laboratories since the early sixties. The reviews of Lamaze and Weston deal comprehensively with the special problems of ^{6}Li glass so only a brief description will be given.

The ^{6}Li glasses have high neutron detection efficiency and are capable of fast timing, although when thick glasses and light pipes are used neutron moderation can severely affect the timing resolution [2]. Multiple scattering effects can be kept small and calculable if a thickness of $\leq$1 mm is used. However, resonances in the materials of the glass can be troublesome, particularly if elements are being studied with resonances at the same energy. Again, to reduce multiple scattering to a minimum the photomultiplier should be kept out of the neutron beam. Figure 8 shows an arrangement designed by M. C. Moxon which has been used on the Harwell linac[37]. For absolute flux measurements the actual value of the ^{6}Li content, its distribution across the glass and its stability need to be checked. One of the chief drawbacks is the high sensitivity of the glasses to gamma-radiation. Pulse-shape discrimination to reject gamma-ray events has not been applied very successfully. With electron linacs the effect of the gamma-flash can be very serious as it excites long-term phosphorescence in the glass. Fortunately the main area of application is at the lower neutron energies and after ~10μs the slow component of light will generally have decayed sufficiently to fall below the electronic bias.

In spite of the above comments, the ^{6}Li-glasses provide one of the most convenient ways of measuring neutron flux below 100 keV. They are generally more suitable for relative rather than absolute measurements. The uncertainty in the neutron detection efficiency can be as low as 2-3% below 100 keV.

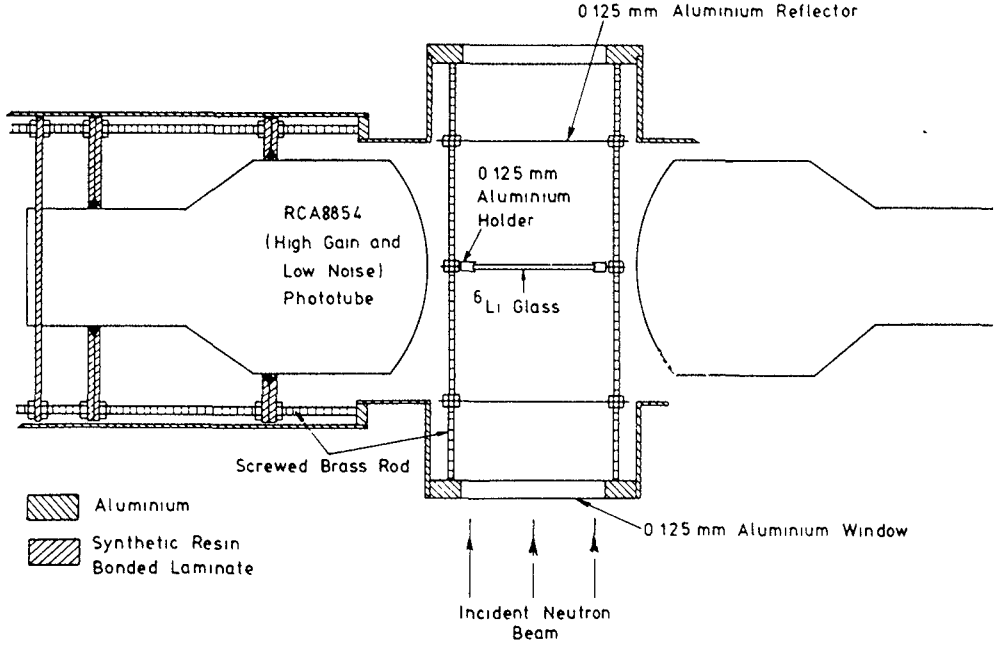

Fig. 8 A ^{6}Li-glass neutron flux monitor designed to minimise the effects of multiple neutron scattering.

(2) 2π-ionization chambers.

Gas ionization chambers employing electrodes coated with ^6Li compounds are very insensitive to gamma-radiation and they can have timing resolutions of ~10 nanoseconds. Their chief drawbacks are their low neutron detection efficiency and the complicated nature of their pulse height spectra.

The response of a chamber is affected by a number of factors, including loss of reaction products in the ^6Li layer and incomplete energy deposition in the chamber gas (for fast timing the electrode separation has to be made much smaller than the triton range). In the region above a few keV the response will also be affected by the dependence of the angular distribution of the ^6Li reaction on neutron energy. With a simple parallel plate chamber the pulse height is very dependent on the orientation of the particle and the observed distribution will be broad. The pulse height distribution is much improved by employing a chamber with a Frisch grid with a consequent improvement in the accuracy of determining the neutron detection efficiency. Such a detector has been described by Friesenhahn et al[38].

During the past few years, Knitter and Budtz-Jørgensen at the Geel laboratory have exploited the properties of a gridded ionization chamber very effectively[39]. This enables them to determine both the energy of a charged particle emitted from a source deposited on the cathode, and the angle of emission with respect to the normal of the cathode. It is thus possible to identify events which are unaffected by backscattering or self-absorption in the deposit. If the particles are produced by neutron-induced reactions in the source deposit, the number of interactions for particles within a given range of emission angle and energy can be determined precisely. Extrapolation to all angles and energies provides an accurate means of measuring neutron flux if a ^6Li deposit is used. Knitter et al[40] describe such a chamber for measuring the angular distributions of the $^6Li(n,t)^4He$ reaction in the energy region 10 eV to 325 keV.

(3) Solid-state detectors.

Solid state detectors can be used to detect the reaction products emerging from a thin ^6Li deposit placed close by. The arrangement in which the detector is positioned outside the neutron beam is sensitive to the angular distribution of the reaction. It can therefore only be used for accurate flux measurements below ~100 eV. The efficiency of this type of system is limited by the available solid angle for detecting the emergent particles. Wagemans[41] has described such a detector (see also Fig. 12 and section 4.3, (3)).

The detection efficiency can be increased by mounting the ^6Li layer in contact with the detector. Since the detector is now in the neutron beam, the arrangement suffers from the serious disadvantage that (n,charged particle) reactions will create background problems if neutrons with energy above ~5 MeV are present. This type of detector appears to have no advantage over a gaseous ionization chamber and will not be considered any further.

4.3 $^{10}B(n,\alpha)^7Li$ and $^{10}B(n,\alpha_1\gamma)^7Li$ detectors

The $^{10}B(n,\alpha)^7Li$ cross-section is defined here as the sum of the cross-sections for the reactions $^{10}B(n,\alpha_0)^7Li$ and $^{10}B(n,\alpha_1\gamma)^7Li$ which have Q-values respectively of 2.79 and 2.31 MeV. The gamma-ray emitted in the latter reaction has an energy of 478 keV. Both cross-sections are known with an uncertainty of less than 0.8% below 100 keV and therefore provide a more accurate basis for flux determination in this region than the $^6Li(n,t)^4He$ cross-section. With improved nuclear data, the ^{10}B standards would be useful up to at least 0.5 MeV. Above 0.5 MeV the cross-sections fall rapidly with increasing energy. Instruments for using ^{10}B as a standard have been reviewed by Carlson[42].

(1) Gamma-ray detectors.

More than thirty years ago Rae and Bowey[43] described a flux monitor in which the 478 keV gamma-rays from a ^{10}B sample mounted in the neutron beam were detected in NaI crystals placed outside the beam. Since that time several variants of this basic arrangement have been used to measure white neutron spectra. Figure 9 shows a typical detector. The gamma-rays have been detected with Ge(Li) diodes and with deuterated benzene (C_6D_6) scintillators. The application of C_6D_6 scintillators to this type of detector is mainly of specialized use when measuring capture cross-sections. In a typical capture measurement in which the prompt gamma-rays are detected in C_6D_6 scintillators[44] it is usual to measure the incident neutron spectrum by replacing the sample under study with a ^{10}B sample.

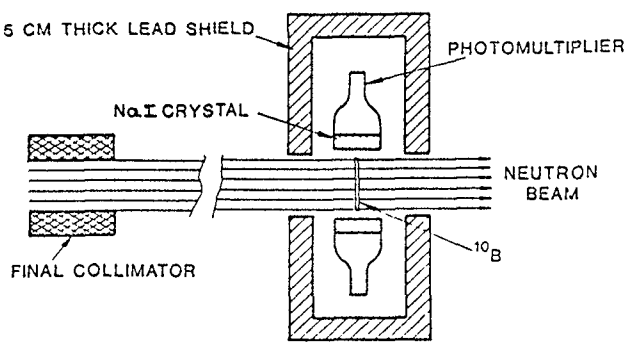

Fig. 9 Arrangement used at Harwell to detect the 478 keV gamma-rays from the $^{10}B(n,\alpha_1\gamma)$ reaction.

Deuterated benzene is very insensitive to scattered neutron background, but the pulse height resolution is poor and it is not suitable for general accurate flux measurements. With NaI crystals, on the other hand, high efficiency and modest resolution is obtained, but the sensitivity to neutrons scattered out of the ^{10}B sample is high. Not only do the scattered neutrons activate the iodine, but at higher energies gamma-rays which cannot be distinguished from the required 478 keV events are produced by inelastic scattering of the neutrons in the crystal. This is illustrated in Fig. 10 where it can be seen that at 510 keV incident neutron energy a broad peak in the pulse height spectrum is produced by inelastic neutron scattering. The scattered neutron background renders NaI crystals unsuitable for this type of flux measurement above about 300 keV. However, in the region below 100 keV where the $^{10}B(n\alpha_1\gamma)$ reaction is a good standard, the NaI-^{10}B combination provides a convenient and reasonably accurate means of determining flux. In general this arrangement has been used to measure the shapes, rather than the absolute values, of white source spectra. The detection efficiency can be calibrated absolutely by replacing the ^{10}B sample with a sample of equal area containing a known amount of ^{7}Be (which emits a 478 keV gamma-ray). The application of Ge(Li) diodes to this type of detector

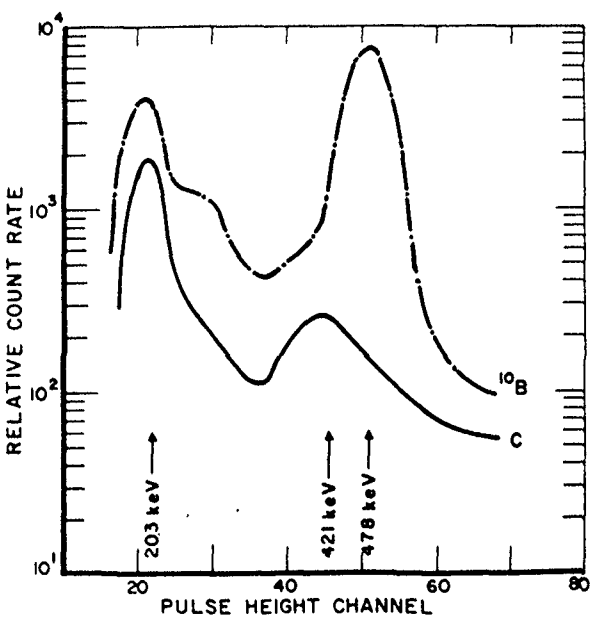

Fig. 10 Pulse height distributions obtained with a detector similar to that shown in Fig. 9 for incident 510 keV neutrons. The lower curve was obtained with a carbon sample replacing the ^{10}B. The arrows show the positions of gamma-rays from inelastic neutron scattering in Na and I. From reference 42.

allows good discrimination of sources of gamma-ray background at the expense of lower overall efficiency. A bismuth germanate crystal (BGO) can also be used as an alternative to NaI. The gamma-ray energy resolution of BGO is inferior to NaI, but it is somewhat less sensitive to scattered neutrons, nor does it suffer (as NaI) from the excitation of long-lived decay components in its light emission.

(2) 2π-ionization chambers.

Detection of the charged particle reaction products from the ^{10}B reactions in a 2π-gridded ionization chamber containing a ^{10}B-coated cathode provides one of the most accurate ways of measuring neutron flux below 100 keV.

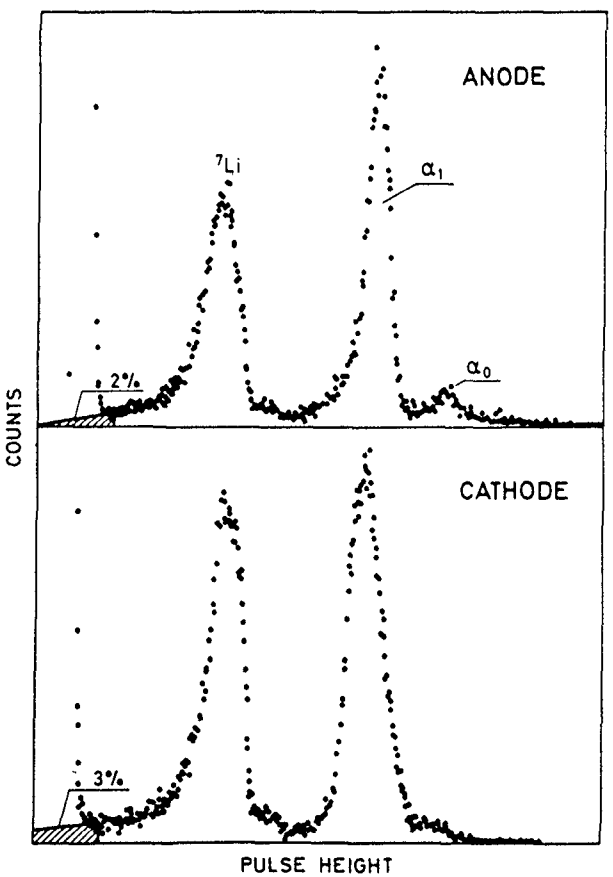

Fig. 11 The anode and cathode pulse height spectra obtained from a ^{10}B-gridded ionization chamber.

The considerations in section 4.2 with regard to detection of the $^{6}Li(n,t)^{4}He$ reaction products apply equally to the ^{10}B reactions. The lower Q-values in the latter, however, require the ^{10}B deposit to be thinner to avoid loss of particles at ~90° to the incident beam, with a consequent reduction in neutron detection efficiency. Friesenhahn[28] has described a chamber which employs eleven similar modules to obtain adequate efficiency.

Knitter et al[45] have reported a ^{10}B-chamber, similar to that mentioned in section 4.2, which is currently being used to measure the shape of the neutron spectrum from the Geel linac, GELINA. Two 30 $\mu g/cm^2$ layers of ^{10}B are mounted back-to-back on a common cathode of two chambers so that the reaction products in the whole 4π-solid angle are detected. Pulse height distributions obtained on the linac with this detector are shown in Fig. 11. It can be seen that the ^{7}Li and the two alpha groups are well separated from electronic noise and neutron-induced recoils in the counter gas. The timing resolution of this detector is ~20 nanoseconds.

(3) Solid-state detectors.

The detection of the $^{6}Li(n,t)^{4}He$ reaction products with solid state detectors was discussed in section 4.2. Figure 12 shows the arrangement of Wagemans and Deruytter to measure the ^{235}U fission cross-section relative to the $^{10}B(n,\alpha)^{7}Li$ cross-section in the region 5 eV to 30 keV[41]. The solid state detectors are protected from the neutron beam by collimators. Measurements were also made with a ^{6}Li deposit, but the final ^{235}U cross-section relied on the ^{10}B measurement because of its more isotropic angular distribution. The systematic errors in this measurement are ~1%.

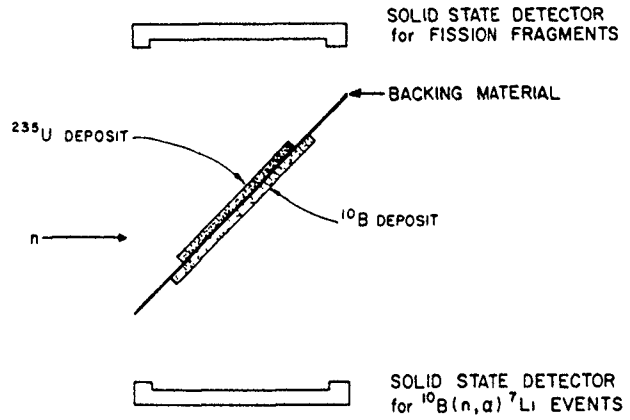

Fig. 12 The detector geometry employed on the Geel linac to measure the $^{235}U(n,f)$ cross-section relative to the $^{10}B(n,\alpha)$ cross-section.

For the reasons mentioned earlier, solid state detectors in 2π-geometry are not favoured for accurate measurements.

(4) Proportional counters.

Proportional counters filled with $^{10}BF_3$ gas have been used for many years to detect neutrons. Carlson[42] discusses their main features. For white source measurements the timing resolution which can be achieved limits their application to the lower neutron energies. The additional problems of "wall-" and "end-effects" introduce systematic uncertainties of 1 to 3% in determining the detection efficiency.

4.4 $^{235}U(n,f)$ detectors

The ^{235}U fission cross-section provides a standard in the energy range 100 keV to 20 MeV which is known to an accuracy of between 2 and 3%. In high resolution measurements below ~1 MeV it is important to take account of the structure which is present in the cross-section. The most direct way of using the standard is to detect the heavily-ionizing fission fragments but fission neutron detection provides an alternative. For fission cross-section measurements above 100 keV it is an obvious standard to use but the H(n,n)H cross-section is preferable because it is more accurately known.

(1) Fission fragment detectors.

As with the ^{6}Li and ^{10}B reactions, the inherently most accurate way of detecting the fragments is to use a gaseous ionization chamber. The energetic fragments give pulses which are well removed from pulses caused by alpha background and electronic noise, provided deposit thicknesses no greater than ~100$\mu g/cm^2$ are used. The actual mass of ^{235}U in the fissile deposit can be assayed with an accuracy of ~1/3%[46] and the systematic uncertainty in the absolute number of fission events in the chamber can be as low as ~1/2%. The neutron detection efficiencies of these chambers are essentially known as accurately as the ^{235}U cross-section itself. At the highest level of accuracy, problems still exist in calculating the loss of fragments in the deposit because of poorly known fragment ranges in the materials used. The gridded ionization chamber technique used by Knitter and co-workers[39], which was described in section 4.2, is capable of the highest precision.

For measurements below ~1 MeV the solid state detector arrangement shown in Fig. 12 is capable of the same accuracy as a gaseous ionization chamber, but at higher energies inadequate knowledge of the fragment angular distribution will lead to larger uncertainty in the detection efficiency. For absolute flux measurements it is also necessary to determine the solid angle of fragment detection.

Gas scintillation detectors for fission fragments have been described[47,48]. These are capable of very fast timing (~1 nanosecond) but generally have poorer pulse height resolutions and therefore less accurately known efficiencies than ionization chambers.

(2) Fission neutron detectors.

A problem with fragment detection is that the thin deposits which have to be used in accurate flux measurements mean inevitably that the neutron detection efficiency is low. On white sources, it is common to use multi-plate chambers, but the number of elements is limited, and a detection efficiency in the region of ~1 MeV of $\sim 10^{-5}$ is typical. Much higher efficiency can be achieved if fission neutrons rather than fragments are detected. There is no longer a need to use thin deposits and fissile samples of ~10 g can be used with only small corrections for self-shielding and multiple scattering. The fission neutrons are usually detected in organic liquid scintillators placed around a ^{235}U sample but out of the incident neutron beam. Gayther et al[49] describe such an arrangement with a detection efficiency of ~1%. Gamma-rays from neutron capture or inelastic scattering are rejected by pulse shape discrimination. The scintillators are biassed to reject neutrons below 1.5 MeV, and so neutrons below this energy which are incident on the sample cannot be detected after a scattering collision. The response of the detector is proportional to the product of the average number of neutrons per fission, $\bar{\nu}$, and the fission cross-section, and hence the energy-dependence of $\bar{\nu}$ must be taken into account when determining the efficiency. Neutron flux can be determined with this type of detector up to 1.5 MeV incident energy with a systematic uncertainty of ~3%, most of which is attributable to the uncertainty in the ^{235}U fission cross-section.

5. SOME COMMENTS ON BACKGROUND

The determination of the time-dependent component of background is one of the most difficult problems in a time-of-flight measurement on a white spectrum source. In the measurement of a neutron reaction cross-section, incident neutrons can be detected with an efficiency which is known to possibly better than 1%, and the uncertainty in determining the background can be the principal source of error.

The background in a time-of-flight measurement can be divided into three components:

(i) Time constant background produced by environmental effects such as cosmic radiation and inherent detector background such as alpha-particle events or electronic noise,

(ii) Time dependent background produced by radiation from the target which is emitted outside the collimated neutron beam,

and (iii) Time dependent background which accompanies the collimated neutron beam. This is produced by neutron interactions in the target structure and other nearby materials, in flight tube collimators and windows, and in the sample or detector itself.

If an adequate "overlap filter" is used, the neutron beam intensity at the sample is reduced to a negligible value at some time before the machine pulse occurs, at which time a background gate can be used to determine the first component. The second component can be measured by blocking off the beam close to the target. In most experiments the shielding will be sufficient to make this component small. The third component can be difficult to measure and it is this which will now be considered.

At the lower neutron energies it is usual to employ the "black resonance" or "notch filter" technique. Filters are placed in the beam which have negligible transmission at energies corresponding to isolated strong resonances. Measurements are made with several thicknesses and a suitable extrapolation is made to obtain the background with no filter present. The background is assumed to vary slowly and smoothly with time-of-flight to obtain the value between and beyond the energies of the black resonances. It can be shown that the method is only valid if the concept of an effective removal cross-section can be applied to the background radiation. If very different components make up the background, for example gamma- and neutron-radiation, then the derived background will be incorrect. Detectors, such as the ^{6}Li-glasses, which are highly sensitive to gamma-radiation can suffer from this problem. In applying the technique it is instructive to analyze the data to obtain cross-sections from runs with the filters in the beam. These cross-sections which can, of course, only be obtained for selected energy regions between the black resonances should be consistent with the open-beam results. Indeed the most reliable cross-sections are obtained at the lower energies with black filters permanently present. Syme[50] has proposed a new method of background determination which uses black resonance filter data both on and off resonance which is valid when more than one component is present in the background field. In applying the black resonance technique it is important to know the timing resolution function of the experiment, particularly at the higher energies to determine whether or not the resonance is "black". A full shape analysis of the resonance would give some insight into the background. The distinction between a tail on the timing resolution function and an actual background is not always clear.

The black resonance method cannot be applied above ~1 MeV because of the lack of suitable resonances. In the absence of any other information it will be necessary to extrapolate the background obtained at the lower energies. Fortunately, the ratio of the background to the open beam events generally falls with decreasing time-of-flight and if this ratio is already small its extrapolation should not introduce serious systematic error.

The above discussion shows that when the most accurate measurements are being undertaken, the black resonance method of measuring background is not entirely satisfactory. It is therefore necessary to either reduce the background to a negligible proportion by experimental design, or understand more clearly the nature of the components which go to make up the background.

A simple way of eliminating electronically the component of background in the NBS black detector which results from neutrons scattering from the detector and capturing in the surrounding shield is described by Carlson and Behrens[51]. In this method, data are accumulated in a one count per machine pulse mode and events produced by the most energetic neutrons from the target are included. Since a neutron which scatters from the detector has already been recorded its subsequent capture cannot also be recorded. This method can only be used on proton recoil detectors. In general, shielding materials should be placed as far away from the detector as possible to minimize scattered neutron background. In a totally absorbing detector like the

Boron-Vaseline Sphere, few neutrons leak out and localized background is small. If it is possible to transport the detector and its shield to a pulsed Van de Graaff accelerator then a time-of-flight measurement will reveal the extent of the background produced by neutron scattering from the sample.

The desirability of good pulse height resolution in a detector as a means of identifying background was mentioned in section 2.2. If the detector pulse height depends on neutron energy, as in a ^{6}Li-glass detector, then if pulse height as well as time-of-flight is recorded, background due to scattered neutrons will be seen as a tail in the distribution. Equally, a two-parameter data recording system will allow identification of background caused by particular gamma-rays, as for example the 2.2 MeV capture gamma-ray from hydrogen.

Neutron scattering in the flight path, collimators, and in materials near the target and the detector can be studied with Monte-Carlo methods. This technique is now sufficiently powerful to represent the experimental geometry in adequate detail to further help identify sources of background.

CONCLUSIONS

Figure 13 illustrates two of the main features of a selection of the neutron detectors discussed in this paper. Not shown in the figure is the uncertainty introduced in the actual measurement of the flux by other effects such as the determination of background. If these other effects are ignored, then it is clear that, at the present time, the highest accuracy which can be achieved in measuring neutron flux with a single detector is 1% (one standard deviation) in certain restricted energy ranges. For the highest accuracy to be attained over the complete energy range from thermal to 20 MeV, measurements with at least three different detectors are required. If only the shape of the neutron spectrum is being determined then inevitably the accuracy will suffer from the normalization procedure in the regions of energy in which the different measurements overlap. On the other hand, when absolute measurements are made, agreement in overlapping regions will increase confidence in the accuracy of the final spectrum.

The uncertainty in the neutron detection efficiency for the systems which rely for their operation on standard neutron cross-sections can be dominated by the uncertainty in the cross-section itself, as in the case of $^{235}U(n,f)$ detectors. As the fission cross-section of ^{235}U becomes better known, a ^{235}U fission chamber becomes an increasingly attractive way of measuring neutron flux above ~100 keV, provided due allowance is made for fine structure in the cross-section.

It is difficult to see how, with present techniques, the uncertainty in measuring a white source neutron spectrum over the whole energy range up to 20 MeV can be reduced much below 1%. Further improvement in accuracy is likely to come from a combination of developments, including:

(i) Greater understanding of, and therefore better allowance for, time-dependent background.

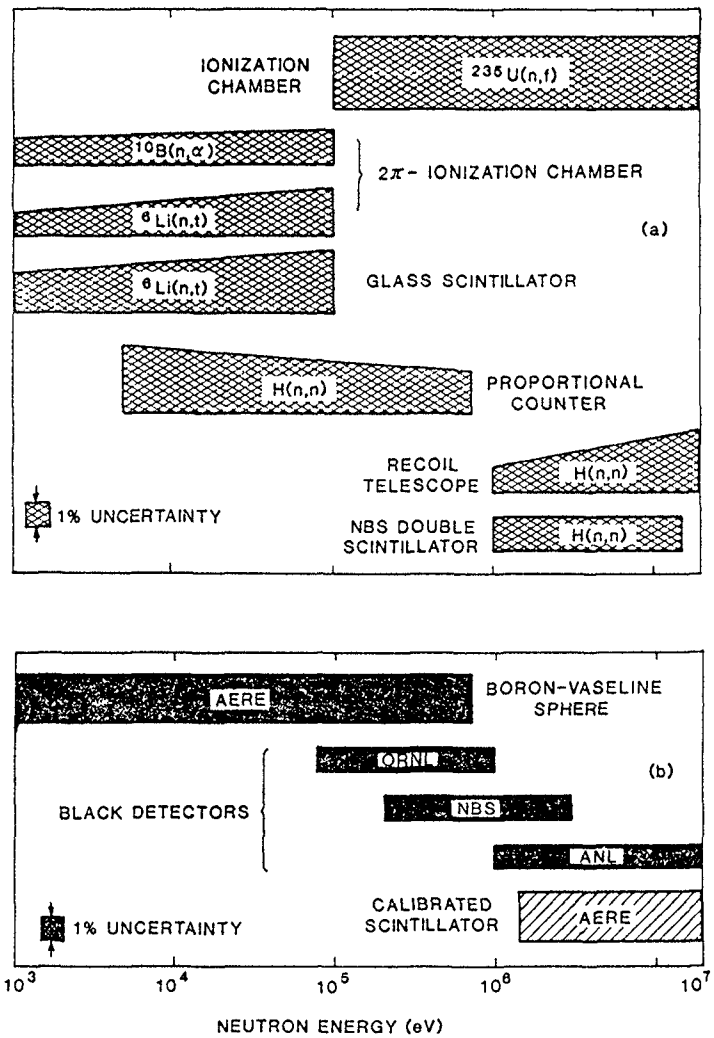

Fig. 13 Comparison of energy range and accuracy of neutron detection efficiency for a selection of (a) standard cross-section detectors and (b) flat response detectors. The vertical scale is only intended to give an approximate idea of the accuracy which can be achieved. The uncertainties shown for the Boron-Vaseline Sphere and the hydrogen proportional counter are for a relative (shape) measurement of flux; for the other detectors the uncertainty in the absolute efficiency is shown. The energy bounds for the application of the standard cross-sections are based on the reviews in reference 52.

(ii) More reliance on experimental confirmation of the calculated efficiencies of flat-response detectors, particularly using the time-correlated associated particle method. Also, extending the energy range of usefulness of this type of detector by experimental calibration.

(iii) Increased energy range of application and accuracy of the standard cross-section detectors as improved nuclear data become available. A single 2π-fission chamber containing ^{10}B and ^{235}U in a back-to-back configuration would be capable of covering the entire energy range of interest. The detection efficiency of such an arrangement would be low, but adequate timing resolution should be available to allow a short flight path to be used provided the effect of gamma-flash caused no problem.

(iv) Further development of new detectors such as the NBS dual thin scintillator and the gridded ionization chambers used at Geel.

REFERENCES

(1) Proceedings of the International Specialists' Symposium on Neutron Standards and Applications, Gaithersburg, National Bureau of Standards Special Publication 493, U.S. Dept. of Commerce (1977).

(2) J. A. Harvey and N. W. Hill, Nucl. Instrum. Meth. 162, 507 (1979).

(3) G. Grosshoeg, Nucl. Instr. Meth. 162, 125 (1979).

(4) I. M. Frank, Problemy Fiziki Elementarnykh Chastii i Atomnogo Yadra, 2, 4805 (1972).

(5) J. W. T. Dabbs, Proceedings of the International Conference on Nuclear Cross-sections for Technology, Knoxville, National Bureau of Standards Special Publication 594, p.929, U.S. Dept. of Commerce (1980).

(6) J. M. Salomé and K. H. Böckhoff, Proceedings of the International Conference on Nuclear Cross-sections for Technology, Knoxville, National Bureau of Standards Special Publication 594, p.534, U.S. Dept. of Commerce (1980).

(7) J. E. Lynn, Contemp. Phys. 21, 483 (1980).

(8) S. Cierjacks and K. H. Beckurts, Nuclear Structure Study with Neutrons, 562 (North-Holland 1966).

(9) G. F. Auchampaugh, S. Plattard and N. W. Hill, Nucl. Sci. Eng. 69, 30 (1979).

(10) M. S. Coates, D. A. J. Endacott, D. B. Gayther, G. D. James and A. Langsford, Harwell Report AERE-PR/NP 13, p.59 (1968).

(11) K. Kandiah and G. White, IEEE Trans. Nucl. Sci. NS28, No. 1, 613 (1981).

(12) A. D. Carlson and B. H. Patrick, Proceedings of an International Conference on Neutron Physics and Nuclear Data for Reactors and Other Applied Purposes, Harwell, 880, OECD Paris (1978).

(13) W. P. Poenitz, Nucl. Instr. and Meth. 109, 413 (1973).

(14) G. P. Lamaze, M. M. Meier and O. A. Wasson, Proceedings of a Conference on Nuclear Cross-sections and Technology, Washington, National Bureau of Standards Special Publication 425, p.73, U.S. Dept. of Commerce (1975).

(15) K. C. Duvall, A. D. Carlson and O. A. Wasson, "Measurement of the National Bureau of Standards Black Neutron Detector Efficiency at 2.3 MeV", this meeting.

(16) M. M. Meier and O. A. Wasson, Bull. Am. Phys. Soc. 23, 72 (1978).

(17) M. M. Meier, Proceedings of the International Specialists' Symposium on Neutron Standards and Applications, Gaithersburg, National Bureau of Standards Special Publication 493, p.221, U.S. Dept. of Commerce (1977).

(18) C. Renner, N. W. Hill, G. L. Morgan, K. Rush and J. A. Harvey, Nucl. Instr. and Meth. 154, 525 (1978).

(19) R. E. Textor and V. V. Verbinski, Oak Ridge National Laboratory Report ORNL-4160 (1968).

(20) G. Dietze and H. Klein, FRG Report PTB-Bericht ND-22 (1982).

(21) J. L. Fowler, J. A. Cookson, M. Hussain, R. B. Schwartz, M. T. Swinhoe, C. Wise and C. A. Uttley, Nucl. Instr. and Meth. 175, 449 (1980).

(22) N. R. Stanton, Ohio State Univ. Report COO-1545-92 (1971).

(23) W. P. Poenitz, Nucl. Instr. and Meth. 58, 39 (1968).

(24) J. E. Perry Jr., Fast Neutron Physics, Part 1 (J. B. Marion and J. L. Fowler eds.) p.623, Interscience Publishers Inc., New York (1960).

(25) M. S. Coates and W. Hart, UK Report EANDC(UK)109AL (1969).

(26) M. S. Coates, D. B. Gayther, G. J. Hunt and D. A. Boyce, Proceedings of a Panel on Neutron Standard Reference Data, p.41, International Atomic Energy Agency, Vienna (1974).

(27) A. D. Carlson, Progress in Nuclear Energy, 13, No. 2/3, p.79 (1984).

(28) S. J. Friesenhahn, A. D. Carlson, V. J. Orphan and M. P. Fricke, U.S. Report GULF-RT-A12210 (1972).

(29) O. A. Wasson, R. A. Schrack and G. P. Lamaze, Nucl. Sci. Eng. 68, 170 (1978).

(30) J. B. Czirr, Proceedings of the International Specialists' Symposium on Neutron Standards and Applications, Gaithersburg, National Bureau of Standards Special Publication 493, p.54, U.S. Dept. of Commerce (1977).

(31) M. S. Dias, R. G. Johnson and O. A. Wasson, Nucl. Instr. and Meth. 224, 532 (1984), also contribution of Dias et al to this meeting.

(32) I. Schouky, S. Cierjacks, P. Brotz, D.Gröschel and B. Leugers, Proceedings of a Conference on Nuclear Cross-sections and Technology, Washington, National Bureau of Standards Special Publication 425, p.277, U.S. Dept. of Commerce (1975).

(33) G. S. Sidhu and J. B. Czirr, Nucl. Instr. and Meth. 120, 251 (1974).

(34) R. J. Jaszczak and R. L. Macklin, Rev. Sci. Instr. 42, 240 (1971).

(35) L. W. Weston, Proceedings of the International Specialists' Symposium on Neutron Standards and Applications, Gaithersburg, National Bureau of Standards Special Publication 493, p.43, U.S. Dept. of Commerce (1977).

(36) G. P. Lamaze, Proceedings of the International Specialists' Symposium on Neutron Standards and Applications, Gaithersburg, National Bureau of Standards Special Publication 493, p.37, U.S. Dept. of Commerce (1977).

(37) D. B. Gayther, Annals Nucl. Energy 4, 515 (1977).

(38) S. J. Friesenhahn, V. J. Orphan, A. D. Carlson, M. P. Fricke and W. M. Lopez, U.S. Report AEC-INTEL-RT7011-001 (1974).

(39) H. -H. Knitter and C. Budtz-Jørgensen, Proceedings of the International Conference on Nuclear Cross-sections for Technology, Knoxville, National Bureau of Standards Special Publication 594, p.947, U.S. Dept. of Commerce (1980).

(40) H. -H. Knitter, C. Budtz-Jørgensen, D. L. Smith and D. Marletta, Nucl. Sci. Eng. 83, 229 (1983).

(41) C. Wagemans and A. J. Deruytter, Annals Nucl. Energy 3, 437 (1976).

(42) A. D. Carlson, Proceedings of the International Specialists' Symposium on Neutron Standards and Applications, Gaithersburg, National Bureau of Standards Special Publication 493, p.85, U.S. Dept. of Commerce (1977).

(43) E. R. Rae and E. M. Bowey, Proc. Phys. Soc. 66A, 1073 (1953).

(44) A. Brusegan, F. Corvi, G. Rohr, R. Shelley, T. Van der Veen, C. Van der Vorst and B. H. Allen, Proceedings of the International Conference on Nuclear Data for Science and Technology, Antwerp, p.127, D. Reidel Publishing Co. (1983).

(45) H. -H. Knitter, C. Budtz-Jørgensen, H. Bax and E. Vogt, CEC Report NEANDC(E)252'U' Vol. III Euratom, p.37 (1984) and also J. A. Wartena et al, "A Neutron Detector Comparison in the Gelina Spectrum", this meeting.

(46) W. P. Poenitz and J. W. Meadows, "Final Results of the International ^{235}U Sample Intercomparison and the Half-life of ^{234}U", this meeting.

(47) W. P. Poenitz, Nucl. Sci. Eng. 53, 370 (1974).

(48) K. Kari, FRG Report KFK-2673 (1978).

(49) D. B. Gayther, J. B. Brisland and D. A. Boyce, Proceedings of a Panel on Neutron Standard Reference Data, p.209, International Atomic Energy Agency, Vienna (1974).

(50) D. B. Syme, UKAEA Report AERE-R 10244 (1981).

(51) A. D. Carlson and J. W. Behrens, Proceedings of the International Conference on Nuclear Data for Science and Technology, Antwerp, p.456, D. Reidel Publishing Co. (1983).

(52) "Nuclear Data Standards for Nuclear Measurements", Technical Reports Series No. 227, International Atomic Energy Agency, Vienna (1983).

A NEUTRON DETECTOR COMPARISON IN THE GELINA SPECTRUM

J.A. WARTENA, H.-H. KNITTER, C. BUDTZ-JØRGENSEN,
H. BAX, Cl.-D. BÜRKHOLZ, R. PIJPSTRA, R. VOGT
Central Bureau for Nuclear Measurements,
Joint Research Centre,
Commission of the European Communities,
Geel

Abstract

Pulse ionization chambers loaded with ^{6}LiF-, ^{10}B- and ^{235}U-layers and a ^{10}B loaded parallel plate avalanche detector were simultaneously exposed to the same neutron beam of GELINA, successively at distances of about 8 m and 32 m from the neutron producing target. The neutron spectra and neutron spectral ratios, measured with these detectors by the time-of-flight method, were analyzed in order to determine the consistency of the detector responses. The studied neutron energy range extended from 0.7 eV to 200 keV.

I. INTRODUCTION

In neutron cross section measurements with a pulsed white neutron source it is necessary to determine :

a) the relative neutron flux as function of the neutron energy (shape measurement) and find the cross section normalization in any other way,
or to determine
b) the absolute neutron flux as function of neutron energy.

For the measurement of type a) one needs to ensure that the relative detection efficiencies of detectors are known as function of the neutron energy. This can be already in some cases a rather stringent demand. For the case b) the neutron detection efficiency is to be known in absolute terms as function of the neutron energy.

To check critically our abilities to perform at least a measurement of type a), four different detectors were positioned together in the same GELINA neutron beam and this successively at about 8 and 32 m distance from the neutron producing target. The spectrum measurements were performed simultaneously. If each of the measured spectra is divided by the relative neutron detection efficiency of the corresponding detector, then the ratio between two of these spectra must give a constant value in all the neutron energy range, since the detectors see the same neutron beam. This is however only true, if the three detectors which are nearest to the source have a high transparency for neutrons and do therefore not change the neutron spectrum.

II DESCRIPTION OF DETECTORS

The four neutron detectors which were compared with each other are ionization chambers loaded with ^{6}LiF- ^{10}B- and ^{235}U-layers, and a ^{10}B-loaded parallel plate avalanche detector.

1) Ionization chamber with ^{6}LiF deposits.

This ionization chamber is shown in the left part of fig. 1 and its working is based on the reaction ^{6}Li(n,t)^{4}He + 4.786 MeV. The detector consists of a cylindrical container which contains the electrodes and the two 4.5 cm diameter and 245 μg/cm^{2} thick ^{6}LiF deposits. A gas mixture of 95 % Ar and 5 % CO_2 was flowing with 0.1 l.min^{-1} through the chamber at a nominal pressure of 1 bar. The neutron entrance and exit windows have a diameter of 9 cm and consist of 0.06 mm aluminium foils. Also the electrodes and the supports of the ^{6}LiF-deposits are made with 0.06 mm thick aluminium foils which are spanned on stainless steel annuli with an inside and outside diameter of 9 and 12 cm respectively. The spacers between the electrodes are of teflon. The distance between the electrodes was chosen to 12 mm, so that the energy loss in the counter gas of the tritons emitted vertical with respect to the electrodes is about 300 keV. The threshold for the timing signals was put in the valley between the noise from the preamplifier plus detector and the pulses from the tritons and alphas. However, still a few percent of events are missed, because of loss of energy of alphas and tritons in the ^{6}LiF-layers. This is also reflected in the imperfect valley between noise and pulses from the emitted particles. In this

detector design it is not straight-forward possible to correct for lost events. Therefore this detector can serve only for neutron spectrum shape measurements, and even this with some reservation at higher neutron energy. The timing resolution of this detector is 46 ns when a slow branch with a timing single channel analyzer of type Canberra 2035 A is used to generate the timing signals.

2) Ionization chamber with ^{10}B and $^{235}UF_4$ deposits.

The set-up of this chamber is shown in the right part of fig. 1 and its working is based on the reactions $^{10}B(n,\alpha_0\alpha_1)^7Li^7Li^*$ + 2.793, 2.315 MeV and $^{235}U(n,f)$. The two ^{10}B-deposits of 4.5 cm diameter and 30 $\mu g/cm^2$ thickness are positioned back to back in the centre of the detector housing. In this design of the ^{10}B-chamber part, Frisch grids are inserted on each side of the two ^{10}B-layers at distances long enough to stop the reaction products in the gas volume. The insertion of Frisch grids allows to obtain energy proportional signals from the anodes, and one has therefore the possibility of a well determined positioning and control of the threshold for the timing signals obtained from the common cathode. The timing resolution of this detector is 32 ns when the same electronic setup is used as for the ^6LiF detector. Fig. 2 shows a pulse height spectrum measured with this detector at a neutron flight path length of 7.653 m. Gas mixture, flow and pressure were the same as for the ^6LiF-chamber. Also the electrodes, entrance and

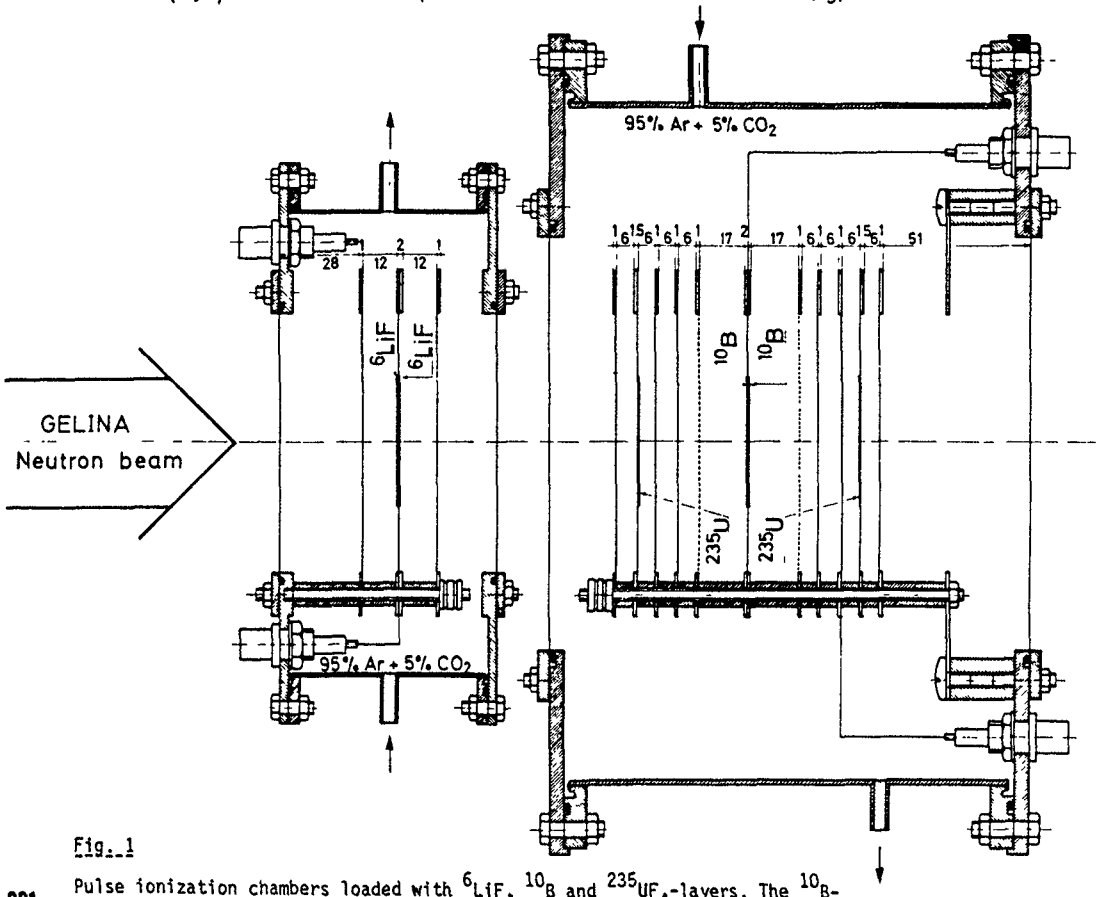

Fig. 1

Pulse ionization chambers loaded with ^6LiF, ^{10}B and $^{235}UF_4$-layers. The ^{10}B-chamber contains Frisch grids to obtain energy proportional signals from the anodes.

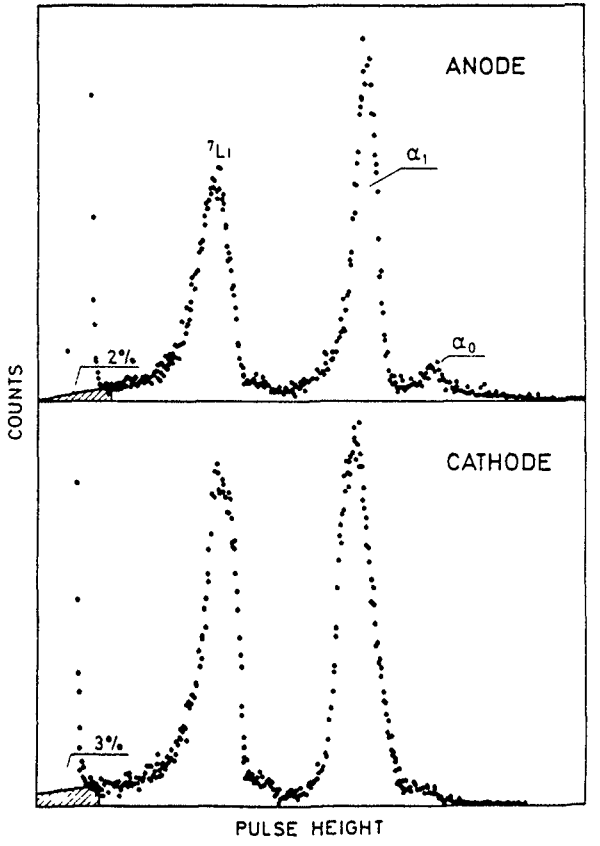

Fig. 2

Anode and cathode pulse height spectra obtained from the gridded ^{10}B-loaded ion chamber.

exit windows and ^{10}B- and $^{235}UF_4$-supports are constructed the same way as in the previous chamber. The ^{10}B-detector can certainly be used to measure the neutron fluence absolutely.

The detector housing contains also two evaporated $^{235}UF_4$ layers of 4.5 cm diameter and 193.5 $\mu g/cm^2$ ^{235}U thickness, which form together with another electrode two parallel plate ionization chambers. One detector is positioned before and the other behind the ^{10}B-detector. Due to the high energetic fission fragments, the timing signal can be well separated from the random alpha particle pulses. The timing resolution of this $^{235}UF_4$ detector is better than 4 ns using a timing filter amplifier and a constant fraction discriminator to generate the timing signals.

3) Avalanche detector with ^{10}B-deposit.

The parallel plate proportional counter shown in fig. 3 consists of 3 parallel electrodes. The outer electrodes are of 0.02 mm aluminium supporting each a ^{10}B deposit of 7.5 cm Ø and 1.28 mg/cm^2 thickness. They

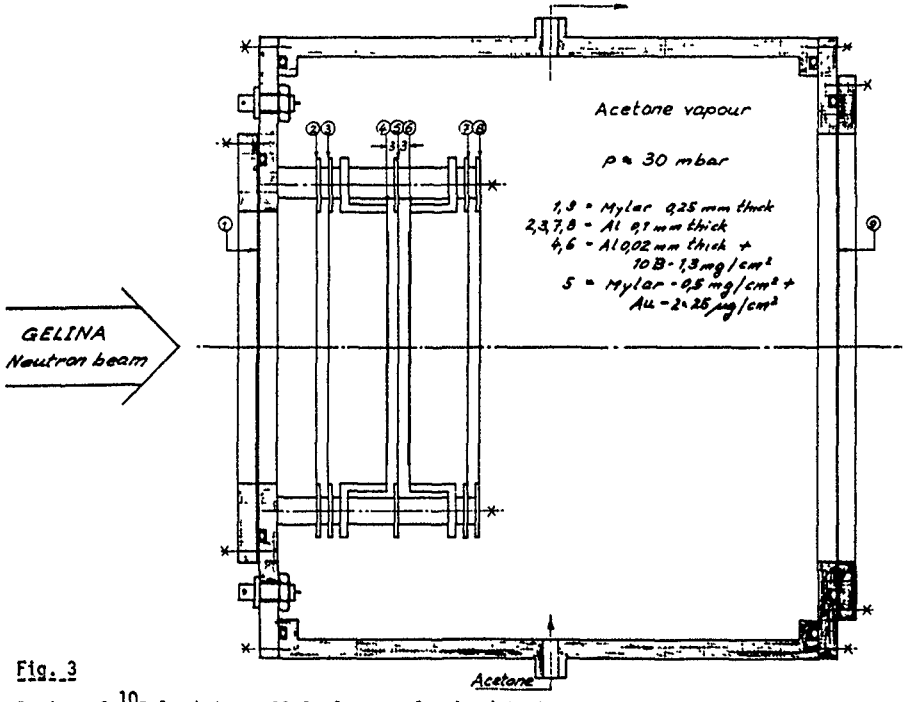

Fig. 3
Design of ^{10}B-loaded parallel plate avalanche detector.

are placed at a distance of 3 mm from the middle electrode. The electrodes are parallel within 0.015 mm.

The middle electrode is a 500 $\mu g/cm^2$ mylar foil, covered on both sides with 20 $\mu g/cm^2$ gold to make it conducting. Since the alphas from the $^{10}B + n \rightarrow \alpha + {}^7Li$ reaction will pass the middle electrode, the 2 counters thus formed may be operated in coincidence or as single detectors.

The gas is 30 mbar aceton vapour, which flows at a rate of 10 to 20 g/h. At the stated pressure and distances the counter is operated with 1775 V. The neutron beam is entering and leaving the housing of the detector through 26 mg/cm^2 mylar windows.

The detector has a timing resolution of 8 ns, but due to the geometry and the thick ^{10}B-layers it can be used only as a neutron spectrum shape detector, as long as the response is proportional to the $^{10}B(n,\alpha_0\alpha_1)^7Li^7Li^*$ cross section.

4) Electronic circuit

The block diagram of the electronics is shown in Fig. 4.

The 2 signals from the avalanche detector are fed via 2 preamplifiers, 2 timing filter amplifiers and 2 discriminators to a coincidence-gate to generate a stop pulse. The time resolution of this gate is 10 ns. In parallel, the outputs from the preamplifiers are fed via 2 spectroscopy-amplifiers and a summer to a discriminator, which serves as a lower level discriminator for the avalanche detector stop pulse.

The outputs from the 3 ion chambers are fed via 3 preamplifiers, 3 main amplifiers and 3 timing discriminators to generate the stop pulses.

An anticoincidence removes the stop pulses generated by the γ-flashes. This precaution is not necessary for the ^{235}U-detector where the γ-flash is too low to pass the discriminator.

To be sure that the stop pulses from the 4 detectors "see" the same dead time in the analyzer the 4 stop pulses are fed through 4 anticoincidence gates which are all closed during 3.5 μs after any stop pulse has arrived in the time-coder.

The time-coder has 21 bits output, which are identical for Tn1 and Tn2. Tn2 sets an additional routing bit (bit 22). There is a separate routing input which acts on bit 23.

3 OR-gates and an one-shot (1 μs) transmit the stop pulses to these 3 inputs, accumulating 4 independent T.O.F.-spectra in the analyzer.

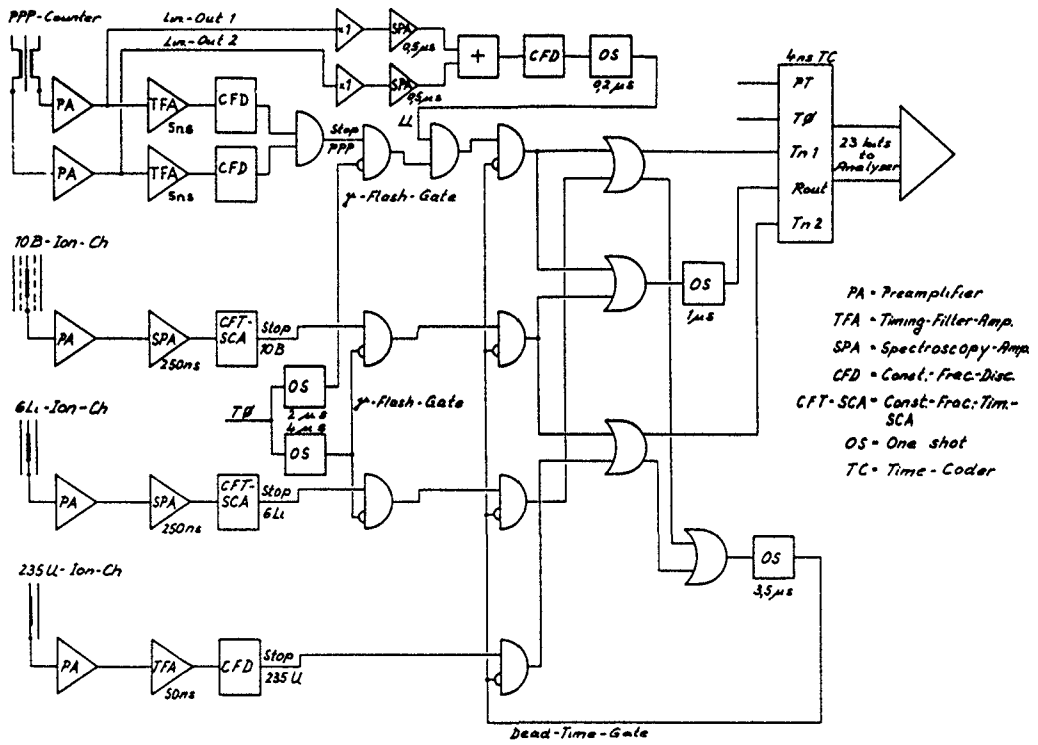

Fig. 4

Block diagramme of the electronics.

III MEASUREMENTS AT ~ 8 M FLIGHT PATH LENGTH

The detectors were installed at flight path 2 as near as possible to the bunker wall as shown in fig. 5. The neutron beam was collimated to a diameter of 4.5 cm by one copper and two lead collimators, each of 100 mm length. Sulfur, sodium and gold black resonance filters were positioned between the lead and copper collimators in order to measure the background level at each of the black resonance energies. A Cd-sheet was used as overlap neutron cut-off filter. Moreover, a 1 cm thick lead disk was put in the neutron beam to reduce the pulse amplitude induced by the γ-flash in the detectors.

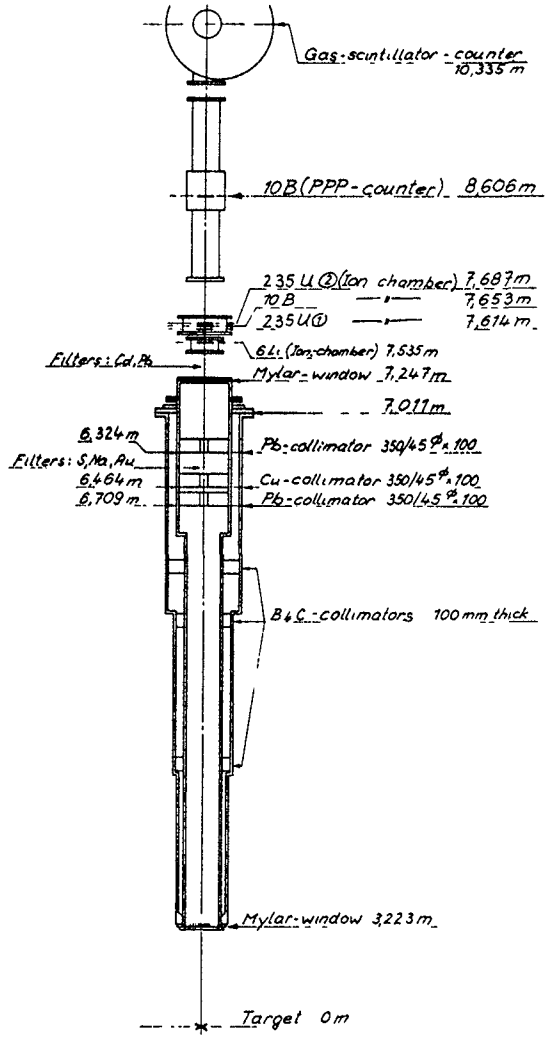

Fig. 5

Setup of the detectors at flight path Nr. 2 at about 8 m distance from the neutron source.

In such a simultaneous measurement of neutron time-of-flight spectra the flight path lengths to the different detectors must be obviously different. In order to obtain immediately comparable spectra, the data were on-line processed to give time-of-flight spectra as if all detectors were positioned at the place of the ^{6}LiF-ionization chamber and also such

that the time zero was moved to channel zero. This on-line processor defined also 5 zones of time compressions always changing the time per channel by a factor of four. Since the timing resolution for the ^{6}LiF- and ^{10}B-loaded ionization chamber was 46 and 32 ns respectively, the first high energy zone from channel 1 to 128 channels was chosen with a channel width of 32 ns. The fifth group then, from channel 513 to 640 had a channel width of 8192 ns. In fig. 6, 7 and 8 the raw time-of-flight spectra of the avalanche-, the ^{10}B- and the ^{6}LiF-ionization chamber detector are shown respectively. The background seen by these detectors and in the geometry of the setup as shown in fig. 5 was about 15 %, 9 % and 8 % at the lowest energy black resonance for the avalanche, ^{10}B and ^{6}Li-detector respectively. This relative high background could not substantially be reduced by wrapping the detectors with Cd sheets.

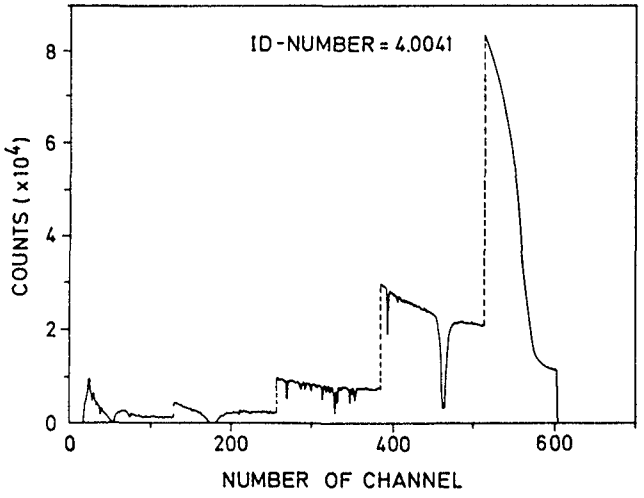

Fig. 6

Neutron time-of-flight spectrum of avalanche detector measured at 8.606 m and normalized to 7.535 m.

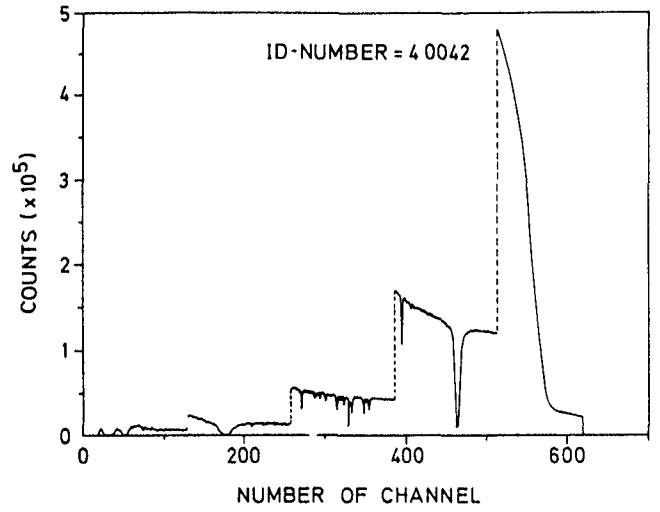

Fig. 7

Neutron time-of-flight spectrum of ^{10}B-ionization chamber measured at 7.653 m and normalized to 7.535 m.

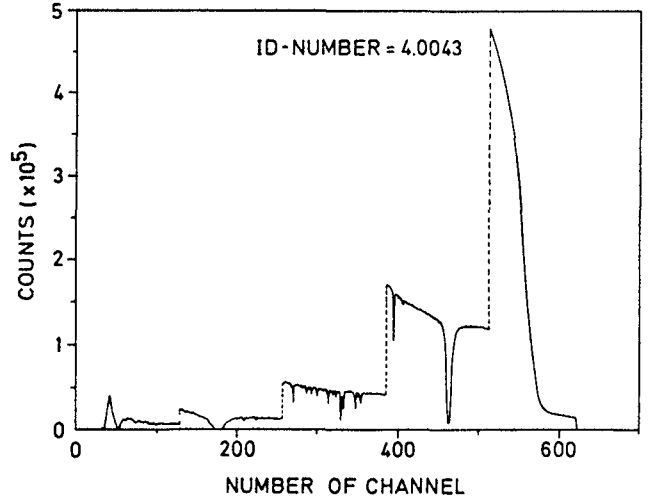

Fig. 8

Neutron time-of-flight spectrum of ^{6}LiF-ionization chamber measured at 7.535 m.

The spectrum measured with the ^{6}Li-chamber was multiplied by 1000 and divided by the avalanche detector spectrum and also by the ^{10}B ionization chamber spectrum, without any further treatment. Both spectra are shown in fig. 9 and 10 and they give a rough idea of their compatability. In a more quantitative analysis the background levels at the three black resonances were fitted with an expression

$$B = a_o + a_1/t$$

where B is the background and t is the neutron flight time. This background was subtracted from the time-of-flight spectra. Then the time-of-flight spectra were converted to energy spectra and were divided by the standard cross sections of the $^{6}Li(n,t)^{4}He$ or the $^{10}B(n,\alpha_o\alpha_1)^{7}Li^{7}Li^{*}$ reactions, depending with which detector the spectrum was measured. The standard cross sections were taken from ref. 1. Fig. 11 shows the ratio of the neutron spectrum measured with the ^{6}Li- and the ^{10}B-ionization chambers in an energy range from 0.7 eV to 100 keV. In an energy range from 0.7 eV to 1 keV this ratio stays constant within a band of about 2 %. Up to 10 keV the deviation from a constant stays within $\pm$ 5 %, whereas at higher neutron energies the deviation from a constant increases steadily. This deviation at neutron energies above 10 keV is probably due to improper subtraction of the backgrounds, but also due to the influence of the γ-flash on the detector thresholds.

Fig. 12 shows the ratio of the neutron fluxes measured with the ^{6}Li-ionization chamber and with the ^{10}B-avalanche detector evaluated in the same way as the previous ratio. In the energy range from 0.7 eV to 0.7 keV this ratio stays within a band of $\pm$ 3 %; however there seems to be a small systematic step below the ^{197}Au black resonance at 4.9 eV. Up to about 10 keV also this ratio stays within a margin of $\pm$ 5 %, whereas at higher neutron energies the deviation from a constant value increases. This deviation has probably the same reasons as in the previous ratio of fig. 11.

As critics to these measurements one must say that the Cd overlap neutron cut-off filter deteriorates the spectrum very much from a few eV up to the keV-range by all the resonance structure. A neutron beam with such a structured energy spectrum would not be wanted for many experiments. The background at this flight path and these detector positions was high. The influence of the γ-flash on the detectors can be seen up to a few μs after its appearance.

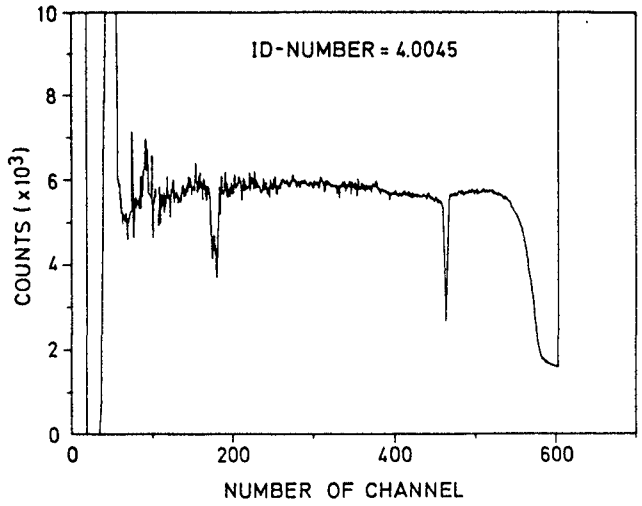

Fig. 9

Ratio of raw neutron time-of-flight spectra measured with ^{6}LiF-ionization chamber and ^{10}B-avalanche detector multiplied by 1000.

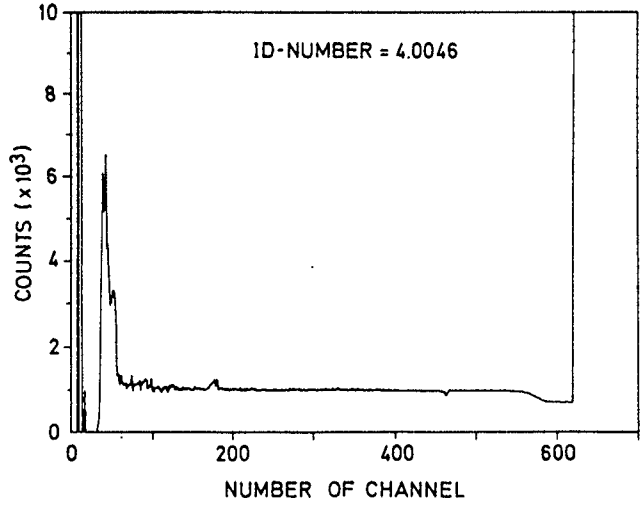

Fig. 10

Ratio of raw neutron time-of-flight spectra measured with ^{6}LiF-ionization chamber and ^{10}B-ionization chamber multiplied by 1000.

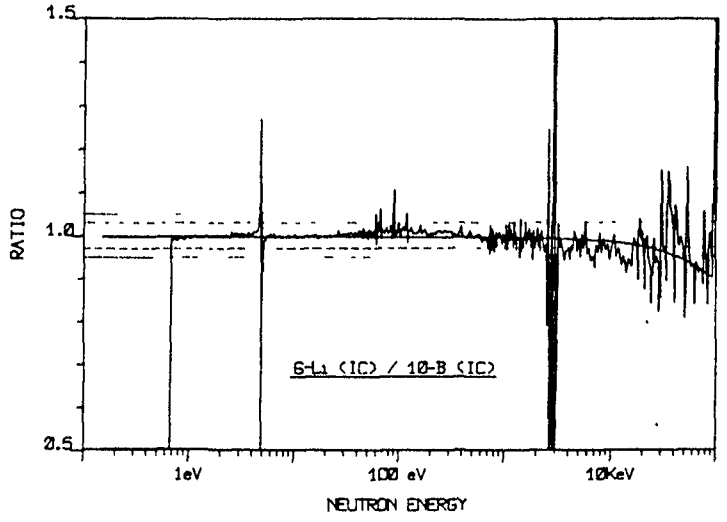

Fig. 11

Neutron fluence ratio measured with ^{6}LiF- and ^{10}B-ionization chambers at about 8 m distance from the neutron source.

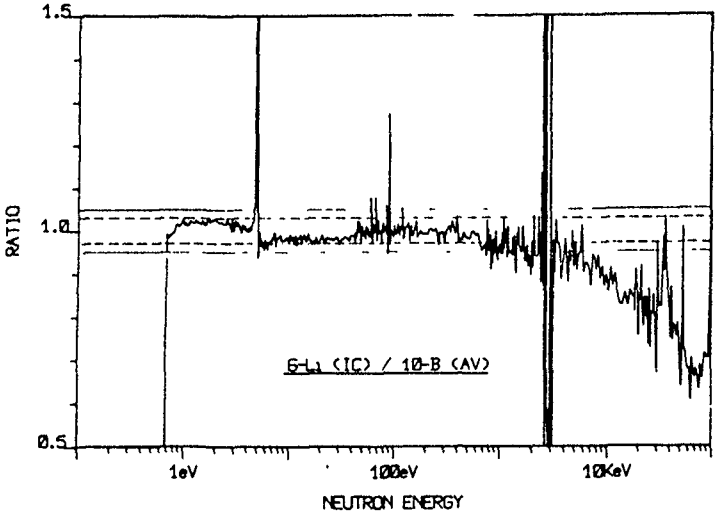

Fig. 12

Neutron fluence ratio measured with ^{6}LiF ionization chamber and ^{10}B-avalanche detector at about 8 m distance from the neutron source.

IV MEASUREMENTS AT ~ 32 M FLIGHT PATH LENGTH

The detectors of the previous measurements at about 8 m flight path length were now installed at flight path 6 of GELINA at a distance of about 32 m from the target. The most relevant dimensions of the setup are shown in fig. 13. The overlap neutron cut-off filter is now a $^{10}B_4C$-filter of 0.419 g.cm^{2} thickness. The electronic setup as well as the on-line processing was the same as at the 8 m measurements. One measuring run without any black resonance filter was carried out for a period of 1 week. A second measurement with a sulfur, sodium and a gold resonance filter was made over a period of three days. The relative backgrounds at the lowest (Au) and at the highest (S) black resonance neutron energies are 14 % and 3.7 % for the ^{6}LiF-ionization chamber, 15 % and 3.3 % for the ^{10}B-ionization chamber and 36 % and 4.6 % for the ^{10}B-avalanche detector. If one, however, subtracts a constant background as obtained from the region where the cut-off filter is black, then one can show that the background which is then left under the black resonances is very small and proportional to the number of counts one would have in the spectrum at these positions, if the filters were not in the beam. Therefore in the present analysis only a constant background was subtracted, since the response ratio of the detectors is not affected by a countrate proportional background. The constant background was obtained by fitting the neutron energy spectrum only at the energies below 40 eV and leaving the background, the parameter in the exponential absorption term for the cut-off filter effect and a normalization factor as free parameters for the spectrum description in this low energy end of the neutron spectrum. The general spectrum shape which is given by $E^{(-\,0.85\,+\,0.0003.\sqrt{E})}$, where E has to be in eV, was kept fixed in these fits over the limited energy range. This is justified since in this spectrum region the spectrum shape is essentially only dependent on the cut-off filter effect $e^{-a\sqrt{E}}$ and on the background B. The following values were obtained :

for the ^{6}LiF-chamber : $B = \frac{1396 \pm 4}{8192}$ ns^{-1} $\quad a = 10.72 \pm 0.04$ eV$^{1/2}$

for the ^{10}B-chamber : $B = \frac{1937 \pm 6}{8192}$ ns^{-1} $\quad a = 10.75 \pm 0.05$ eV$^{1/2}$

for the ^{10}B-avalanche : $B = \frac{1146 \pm 4}{8192}$ ns^{-1} $\quad a = 9.72 \pm 0.09$ eV$^{1/2}$

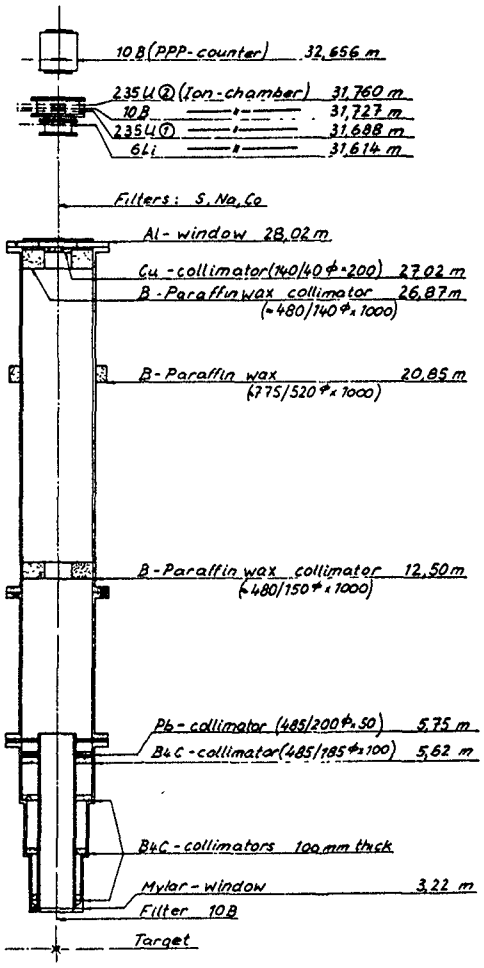

Fig. 13

Experimental setup at 32 m.

There seems to be a small inconsistency in the $^{10}B_4C$ filter constant between the two first detectors and the last one. From the metrological data which are written on the $^{10}B_4C$ filter one calculates a nominal value of the filter constant of a = 11.78 $eV^{1/2}$.

Since also the masses and the areas of the ^{6}LiF- and of the ^{10}B-layers in the ionization chambers are known, the number $\Phi(E)$ of neutrons which have passed the detector per MeV and cm^2 during the measuring time is calculated as function of the neutron energy, according to :

$$\Phi(E) = \frac{(N(t) - B)\cdot A\cdot dt}{2\cdot m\cdot F\cdot L\cdot \sigma(E)\cdot dE}$$

Here N(t) stands for the number of counts measured per ns at times t, B is the according background, A is the molecular or atomic mass of the according layer material in the detector, m is the mass per cm^2, F the area of the layers, L the Avogadro number and $\sigma(E)$ are the $^6Li(n,t)^4He$ or the $^{10}B(n,\alpha_0\alpha_1)^7Li^7Li^*$ standard cross sections which were taken from ref. 1. Figs. 14 and 15 show the neutron energy spectra on an absolute scale as measured with the ^{6}LiF- and ^{10}B-ionization chamber respectively. No correction was made for losses in the layers and for losses below the detection thresholds. These corrections are estimated to be of the order of a few percent. Fig. 16 shows the same spectrum measured with the avalanche detector, however on an arbitrary scale.

The least squares fits were made through each spectrum covering a neutron energy range from 8 eV to 30 keV and from 8 eV to 200 keV. The function used to fit the data was :

$$\Phi(E) = P(1)\cdot E^{(-P(2)+P(3)\sqrt{E})}\cdot e^{-P(4)/\sqrt{E}}$$

The parameters of these fits, their errors and the x^2-value are given in table 1 and the fits are plotted as full lines in Fig. 14 - 16. In the fits from 8 eV to 30 keV the most important parameters P(2) and P(4) of the spectra measured with the ^{6}LiF-and ^{10}B-ionization chambers are in agreement with each other within their statistical errors. A small deviation of these two results with the fit to the spectrum with the ^{10}B-avalanche detector is observed. These differences are three times and six times their errors for the P(2) and P(4) parameter respectively. For the fits in the region between 8 eV and 200 keV the x^2 has somewhat increased and the fits are less perfect at the low energy end of the spectra. This indicates that one should add a further term for the spectrum representation.

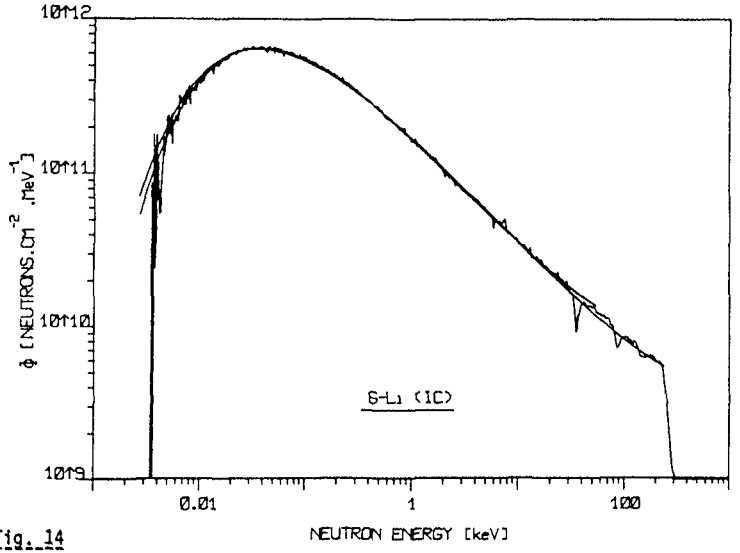

Fig. 14

The neutron fluence per MeV and cm^2 as measured with the ^{6}LiF-ionization chamber at about 32 m is plotted versus the incident neutron energy. The full lines represent two fits to the data for energy ranges of 8 eV to 30 keV and 8 eV to 200 keV.

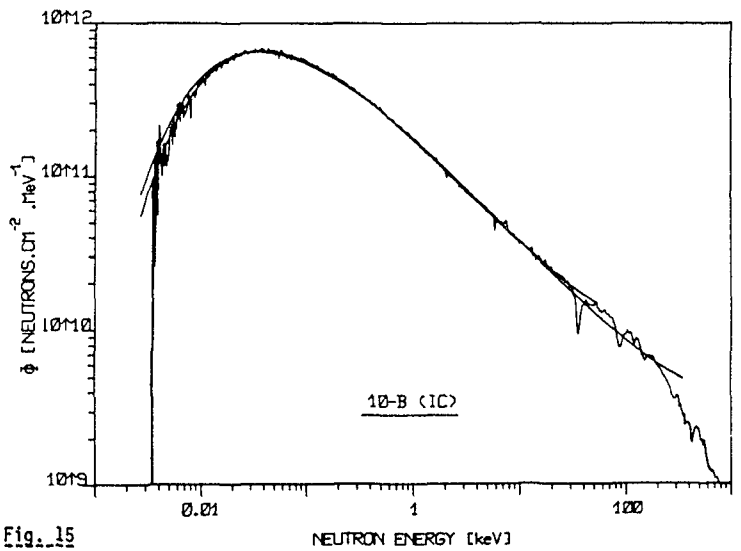

Fig. 15

The neutron fluence per MeV and cm^2 as measured with the ^{10}B-ionization chamber at about 32 m is plotted versus the incident neutron energy. The full lines represent two fits to the data for energy ranges of 8 eV to 30 keV and 8 eV to 200 keV.

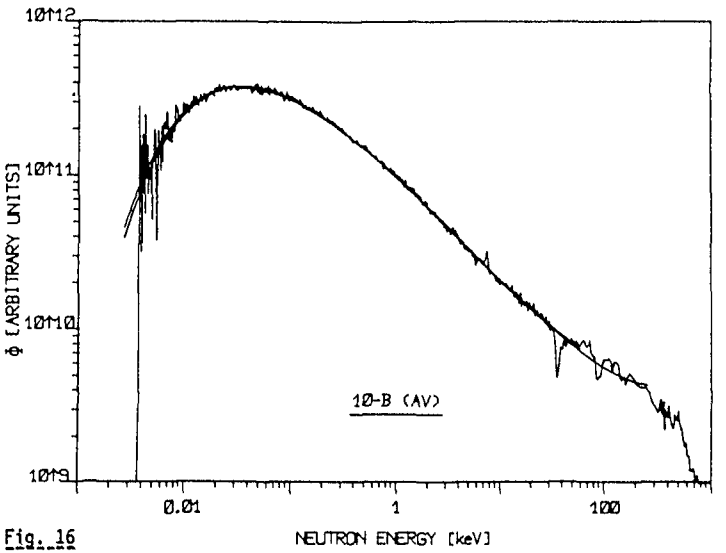

Fig. 16

The neutron fluence per unit energy interval and per unit area in arbitrary units as measured with the ^{10}B-avalanche detector at about 32 m is plotted versus the incident neutron energy. The full lines represent two fits to the data for energy ranges of 8 eV to 30 keV and 8 eV to 200 keV.

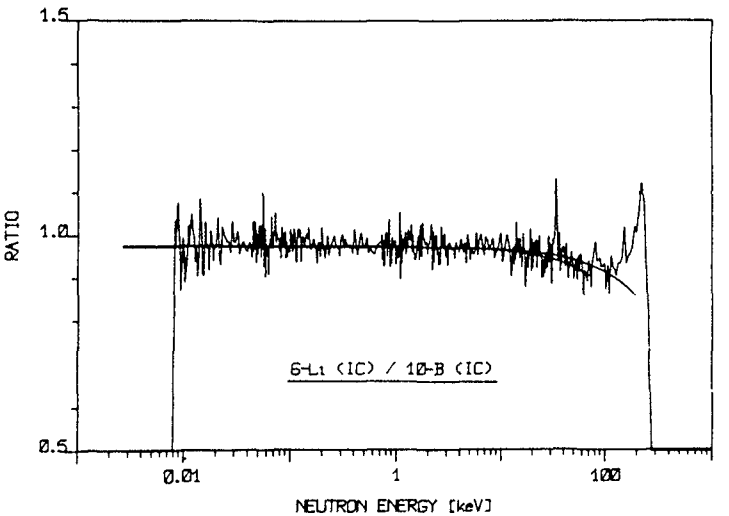

Fig. 17

The ratio of the neutron fluences per MeV and cm^2 as measured with the ^{6}LiF- and ^{10}B-ionization chamber is plotted versus the incident neutron energy. The two full monotonic lines represent fits to the data.

Fig. 17 shows the experimental ratio of the neutron energy spectra as measured with the ^{6}LiF and ^{10}B-ionization chambers. The two lines through the experimental data are obtained from fits with a function

$$R(E) = P(1) + P(2)\cdot E$$

with E in MeV, covering two different neutron energy ranges. The parameters and their errors are P(1) = 0.9823 ± 0.0023, P(2) = - 1.067 ± 0.078 and P(1) = 0.9800 ± 0.0013, P(2) = - 0.634 ± 0.039 for the fit from 8 eV to 70 keV and from 8 eV to 150 keV respectively. In the fit up to 70 keV the deviation from the ratio at 8 eV is 0.1 %, 1.1 % and 3.4 % at 1 keV, 10 keV and 30 keV respectively. The ratio with respect to the ^{10}B-avalanche detector as shown in fig. 18 is somewhat worse, especially at the ends of the spectrum. For the low energy end this is already reflected in the P(4)-parameter as given in table 1.

At this distance of about 32 m also the time-of-flight spectrum with one of the ^{235}U-ionization chambers was measured. The threshold for the timing signals was put just above the pulses from the spontaneous alpha decay. However the count rate of this ^{235}U-detector was about a factor 12 smaller than in the ^{6}LiF- and ^{10}B-ionization chamber and a factor 4.4 smaller than in the ^{10}B-avalanche detector. Therefore the statistical accuracy obtained in this one week run is rather poor. It was however possible to calculate from the experimental data the average cross sections for certain energy intervals. For this purpose the detection efficiencies for the reaction products from the $^{10}B(n,\alpha_0\alpha_1)^{7}Li^{7}Li^{*}$ and the $^{235}U(n,f)$ reactions were estimated to be 0.915 ± 0.010 and 0.980 ± 0.005 respectively. The masses of the ^{10}B and $^{235}UF_4$-layers which enter in the cross section determination are known with an accuracy of only 5 % and 1.5 % respectively. No correction was applied, other than a rather rough background subtraction. The same neutron energy intervals were chosen as in the measurement of Wagemans and Deruytter [2] in order to be able to make a direct comparison with these measurements. This comparison is shown as ratio between the present and their measured average cross sections in fig. 19 in the neutron energy interval from 50 eV to 30 keV. Below 50 eV the present measurements have a too small number of counts in the ^{235}U-spectrum to make a comparison senseful. In the neutron energy range from 30 keV to 200 keV this comparison is continued

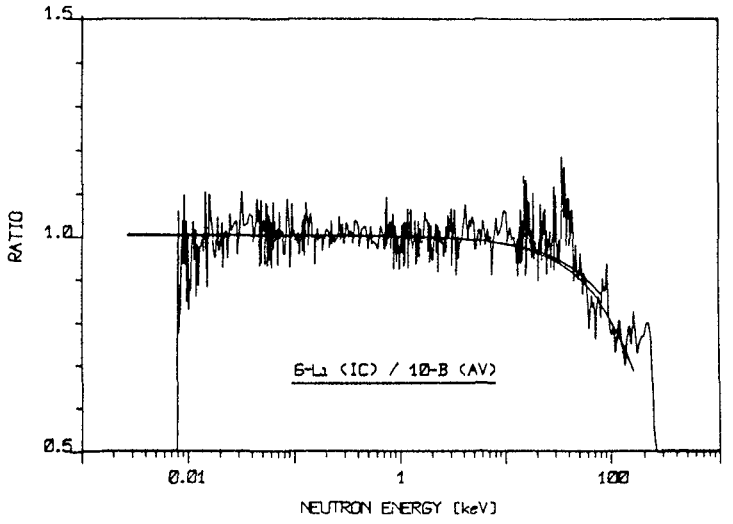

Fig. 18

The ratio of the fluences as measured with the ^{6}LiF-ionization chamber and the ^{10}B-avalanche detector is plotted versus the incident neutron energy. The full monotonic lines represent fits to the data.

TABLE 1

Results of least squares fits to measured neutron energy spectra

	P(1)	ΔP(1)	P(2)	ΔP(2)	P(3)	ΔP(3)	P(4)	ΔP(4)	x^2
6-Li (IC)									
30 keV - 8 eV	$7.885\ 10^{13}$	$1.4\ 10^{12}$	- 0.8523	0.0025	$2.69\ 10^{-4}$	$7\ 10^{-6}$	10.550	0.053	0.6846
200 keV - 8 eV	$5.635\ 10^{13}$	$0.9\ 10^{12}$	- 0.8009	0.0021	$1.18\ 10^{-4}$	$2\ 10^{-6}$	9.651	0.061	1.9517
10-B (IC)									
30 keV - 8 eV	$8.025\ 10^{13}$	$1.4\ 10^{12}$	- 0.8522	0.0025	$2.87\ 10^{-4}$	$7\ 10^{-6}$	10.550	0.053	0.8680
200 keV - 8 eV	$5.360\ 10^{13}$	$1.1\ 10^{12}$	- 0.7891	0.0025	$1.06\ 10^{-4}$	$3\ 10^{-6}$	9.435	0.071	3.1508
10-B (AV)									
30 keV - 8 eV	$4.034\ 10^{13}$	$1.2\ 10^{12}$	- 0.8361	0.0042	$2.40\ 10^{-4}$	$12\ 10^{-6}$	10.002	0.092	0.5931
200 keV - 8 eV	$3.402\ 10^{13}$	$7.4\ 10^{11}$	- 0.8112	0.0028	$1.84\ 10^{-4}$	$3\ 10^{-6}$	9.511	0.082	0.9875

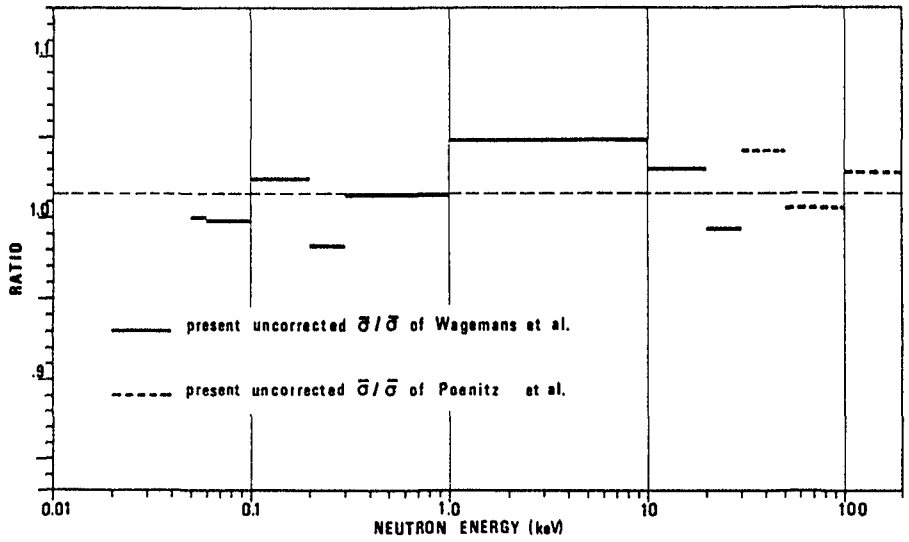

Fig. 19

The ratios of average ^{235}U fission cross sections of the present experiment to those of other authors are plotted versus the incident neutron energy.

with evaluated data of Poenitz and Guenther[3]. The ratios center around a value of 1.015 with a scatter of maximum ± 3.5 %. This result is very well within the error limits of the present experiment.

V. CONCLUSIONS

The presented data show that the ^{6}LiF and ^{10}B-ionization chambers give a spectral ratio which is constant within 1.1 % and 3.4 % in an incident neutron energy range from 8 eV to 10 keV and from 8 eV to 30 keV respectively. The measurement of $^{235}U(n,f)$ with respect to $^{10}B(n,\alpha_0\alpha_1)^{7}Li^{7}Li^{*}$ delivered average fission cross sections of ^{235}U for certain energy intervals in the neutron energy range from 50 eV to 200 keV which compare well within a few percent with data of others, although the ratios were not measured in a strict back to back geometry. These results encourage to try in an improved setup and with less background to measure the $^{6}Li/^{10}B$ and $^{10}B/^{235}U$ cross section ratios in a back to back arrangement, recording also the energy signals for energy dependent detector efficiency corrections.

REFERENCES

1) INDC/NEANDC Nuclear Standard File, 1980 Version. INDC - 36/LN

2) C. Wagemans and A.J. Deruytter,
Proc. of IAEA Consultants' Meeting on the U-235 fast neutron fission cross section and the Cf-252 fission neutron spectrum.
INDC (NDS) - 146, page 79 (1983).

3) A.P. Poenitz and P.T. Guenther
Proc. of the NEANDC/NEACRP specialists'meeting on fast neutron fission cross sections of U-233, U-235, U-238 and Pu-239.
Argonne, Ill., U.S.A. (1976) page 21.

FLUX DETECTOR INTERCOMPARISONS: HIGH EFFICIENCY DETECTORS – PART II

F. CORVI, H. RIEMENSCHNEIDER, T. VAN DER VEEN
Central Bureau for Nuclear Measurements,
Joint Research Centre,
Commission of the European Communities,
Geel

Abstract

An intercomparison of highly efficient neutron flux detectors is under way. The neutron spectrum investigated is that emitted from the moderator surrounding the neutron producing target of the Geel electron Linac and the energy of interest ranges from thermal to about 1 MeV. The results of two intercomparisons are reported here: one deals with a thin ^{6}Li-glass scintillator and a ^{10}B ionization chamber. The second is concerned with the same ^{6}Li-glass and a multiplate ^{235}U fission chamber. Good agreement is obtained in the first case for the range 4 eV to 2 KeV and in the second case from 8 eV to 100 keV.

1. Introduction

In order to check the accuracy with which the relative neutron flux at the Linac is known, an intercomparison of neutron flux detectors is under way. The detectors considered are typically two orders of magnitude more efficient than those considered in the low efficiency intercomparison : if placed at flight distances between 30 and 60 m, they can deliver a spectrum with good statistics is a few hours.

The types of flux detectors, sample size, thickness in at/b of the isotope concerned, the reaction involved and the energy region in which it is considered as a standard are listed in Table 1. Detectors 1 to 5 are the high efficiency detectors under study while nb.6 should be considered rather as a transfer instrument, to ensure a connection with the low efficiency intercomparison.

In the following we report the results of an intercomparison between detectors nb. 5 and nb. 6 and between detectors nb. 5 and nb. 1.

Table 1 : Main parameters of the high efficiency neutron flux detectors under study

Detector type	Size (cm)	Thickness N(at/b)	Reaction	Standard range (MeV)
1. Multi-plate fission chamber	$\emptyset$ = 9.0	0.10×10^{-3}	^{235}U(n,f)	0.1 - 20
2. Au t = 0.6 mm + two C_6D_6 scint.	$\emptyset$ = 9.0	3.58×10^{-3}	Au(n,γ)	0.2 - 3.5
3. ^{10}B slab t = 0.6 mm + two C_6D_6 scint.	$\emptyset$ = 8.0	6×10^{-3}	^{10}B(n,$\alpha\gamma$)	THERM.- 0.2
4. ^{10}B slab t = 3 mm + two C_6D_6 scint.	9.0 x 9.0	0.03	^{10}B(n,$\alpha\gamma$)	THERM.- 0.2
5. ^{6}Li glass t = 0.5 mm	$\emptyset$ = 9.0	0.84×10^{-3}	^{6}Li(n,T)	THERM.- 0.1
6. ^{10}B ionization chamber	$\emptyset$ = 8.4	4.11×10^{-6}	^{10}B(n,α)	THERM.- 0.2

2. Intercomparison between a ^{6}Li-glass and a ^{10}B ionization chamber

Detector nb. 6 is a double gridded ionization chamber having a cathode with back-to-back deposits of ^{10}B of thickness 40 μg/cm^2 each. The design of the chamber is shown in Fig. 1: cathode, anodes and windows are made of Al foils 30 μ thick, while the grids consist of a mesh of stainless steel wires of 0.1 mm diameter. This light construction was chosen in order to minimize any perturbation of the neutron flux so that the chamber can be used in transmission. The chamber is of the continuous gas flow type and uses a mixture of 95% argon and 5% CO_2 at atmospheric pressure. The amplitude spectrum of the anode pulses is shown in Fig. 2. The bias is set below the ^{7}Li pulses: this choice together with the back-to-back configuration rules out any possibility of efficiency variation with neutron energy due to changes in the backward-to-forward emission ratio.

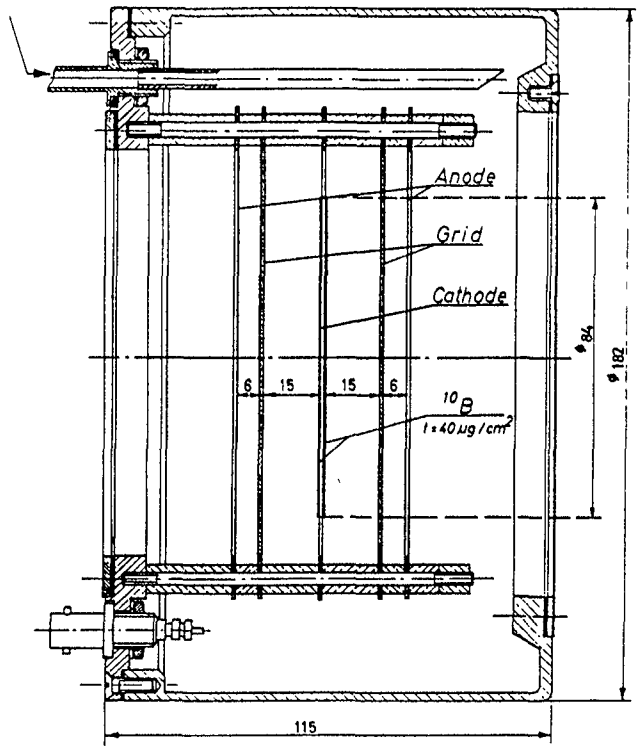

Cross section through the ^{10}B double grid ionization chamber.

Fig. 1

Detector nb. 5 consists of a Li-glass scintillator 0.5 mm thick, enriched to 95% ^{6}Li. The glass lies in air and is viewed by two XP 2040 photomultipliers which are outside the neutron beam: light reflection and light tightness is ensured by a 0.05 mm thick Al foil wrapped around the two PM containers. The experimental set up is shown in Fig. 3: both detectors wereplaced at a 28 m flight path in a neutron beam collimated down to a diameter of about 8 cm. A Cd filter 0.5 mm thick absorbed slow neutrons from previous cycles. The two detectors were operated simultaneously and the background was separately measured with "black resonance" filters of Na, Co, W and Ag.Data were taken in the range from 2.6 eV to 50 keV: for ^{6}Li-glass, the background-to-signal ratio doesn't exceed 1% over the whole energy range. For the ^{10}B-chamber it goes from

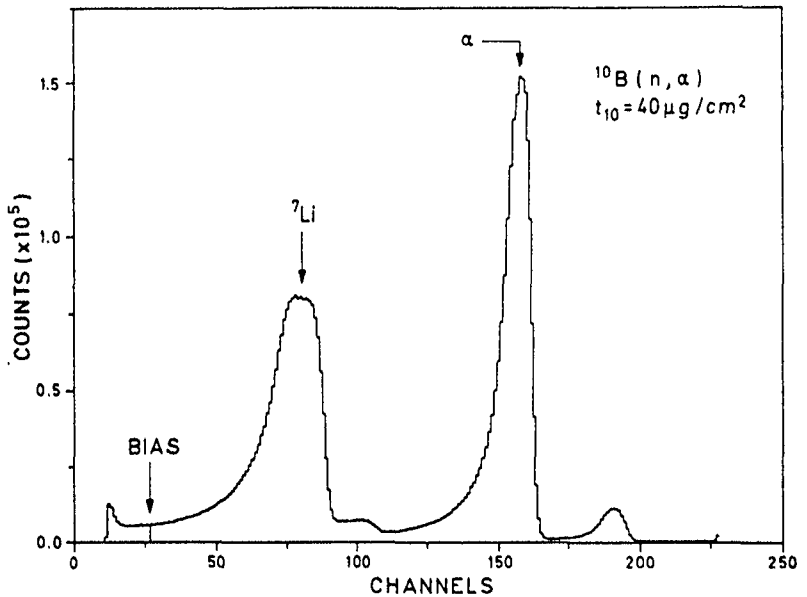

Fig. 2 Amplitude spectrum of the pulses from the anodes of the ^{10}B chamber.

Table 2 : Description of the fission chamber

Number of aluminium plates	21
Thickness of aluminium plates	30 µ
Thickness of end windows	50 µ
Filling gas	methane
Diameter of back-to-back U_3O_8 coatings	9.0 cm
Average thickness of coatings	1.18 mg/cm^2
^{235}U enrichment	99.508 %
Impurities: ^{234}U	0.169 %
^{236}U	0.026 %
^{238}U	0.301 %
Total mass of ^{235}U	2.549 g
Average plate spacing	0.2 cm
Efficiency	0.739

Table 3 : Average ^{235}U cross sections

$E_1 - E_2$ keV	$\bar{\sigma}_f$ barn	$E_1 - E_2$ keV	$\bar{\sigma}_f$ barn	$E_1 - E_2$ keV	$\bar{\sigma}_f$ barn
0.1 - 0.2	20.37	1 - 2	7.178	10 - 20	2.460
0.2 - 0.3	20.16	2 - 3	5.231	20 - 30	2.104
0.3 - 0.4	12.80	3 - 4	4.684	30 - 40	1.975
0.4 - 0.5	13.18	4 - 5	4.157	40 - 50	1.835
0.5 - 0.6	14.88	5 - 6	3.813	50 - 60	1.781
0.6 - 0.7	11.24	6 - 7	3.235	60 - 70	1.727
0.7 - 0.8	10.83	7 - 8	3.148	70 - 80	1.652
0.8 - 0.9	8.051	8 - 9	2.937	80 - 90	1.580
0.9 - 1.0	7.322	9 - 10	3.080	90 - 100	1.532

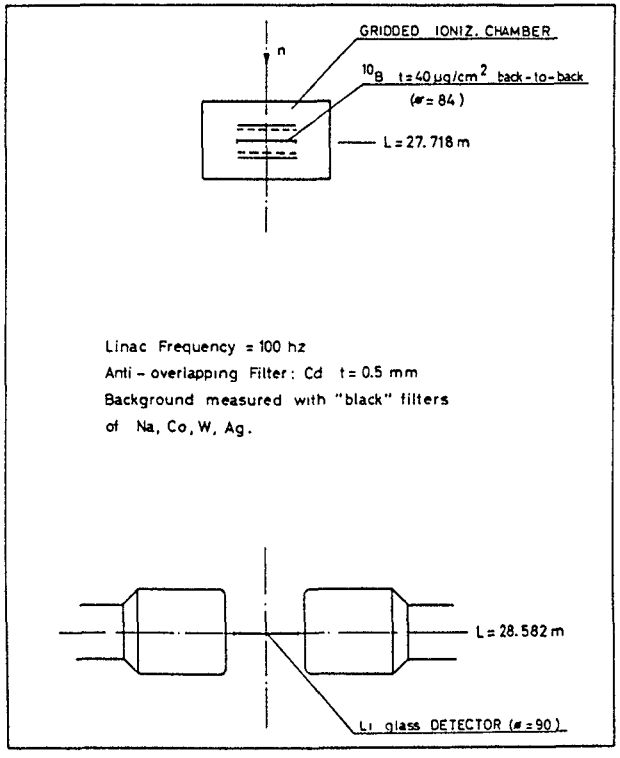

Fig. 3 Experimental set up of the first intercomparison.

0.7% at 1 keV to 2.7% at 5 eV. In order to derive the neutron flux, the counting rates, after background subtraction, were divided by the relative detecting efficiencies taken equal to $\epsilon(E) = N_i \sigma_i(E)$ where N_i are the thicknesses in at/b given in Table 1 and σ_i are the relevant ENDF/B-V cross sections. In the case of the ^6Li-glass, a small multiple scattering effect of the order of 2% and self-shielding corrections at low energy have also been taken into account. The results are given in Figs.4 and 5 in units of neutrons per second and per 4 ns time-of-flight channel. The ratio r of the two spectra is plotted vs energy in Fig. 6.

The following comments can be made:

a) the absolute values of the two fluxes agree very well since the quantity r is centered around unity (at least in its constant part);

b) the fluctuations observed in r below 1000 eV correspond to the Cd resonances and are only due to a slight mismatch of neutron energies and resolution functions;

c) apart from the fluctuations discussed in b), the quantity r is constant within about $\pm$ 1.5% in the range from 4 to 2000 eV;

d) a slight increase of r at low energy is noted, probably due to incorrect background extrapolation below the 5 eV black resonance of silver;

e) as a result of our previuos experience in comparing ^6Li-glass measurements performed in different experimental set ups, we found out that the detector malfunctions at relatively short flight path and time-of-flight values. This effect, which results always in a lack of counts at high neutron energy, is probably due to the influence of the γ-flash. We believe therefore that the strong decrease of the ratio r at high energy visible in Fig. 6, is due to such an effect;

f) in the range from 2 eV to 10000 eV the relative flux of the ^6Li-glass has been fitted by the following function:

$$\phi_T = K \cdot E^{(a_o + a_1 \cdot \sqrt{E})}$$

where

$$a_o = 0.6210 \pm 0.0002$$

$$a_1 = (0.190 \pm 0.002) \cdot 10^{-3}$$

and E is expressed in eV.

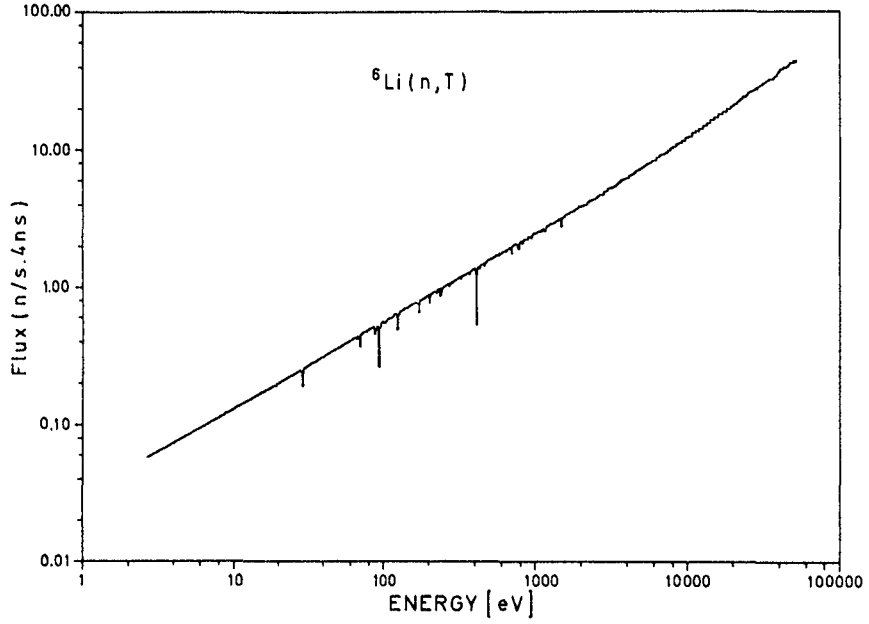

Fig. 4 Neutron spectrum obtained with the ^{6}Li-glass.

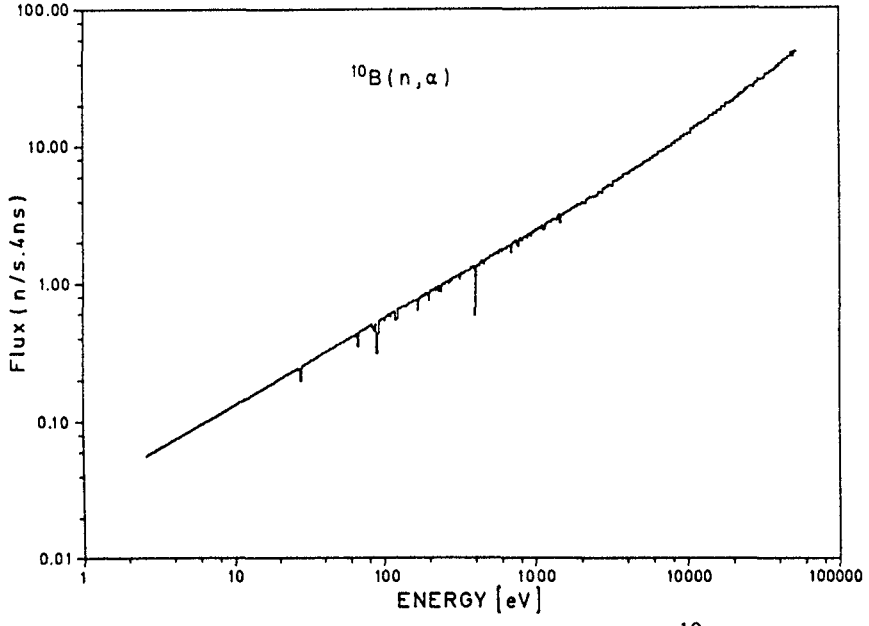

Fig. 5 Neutron spectrum obtained with the ^{10}B chamber.

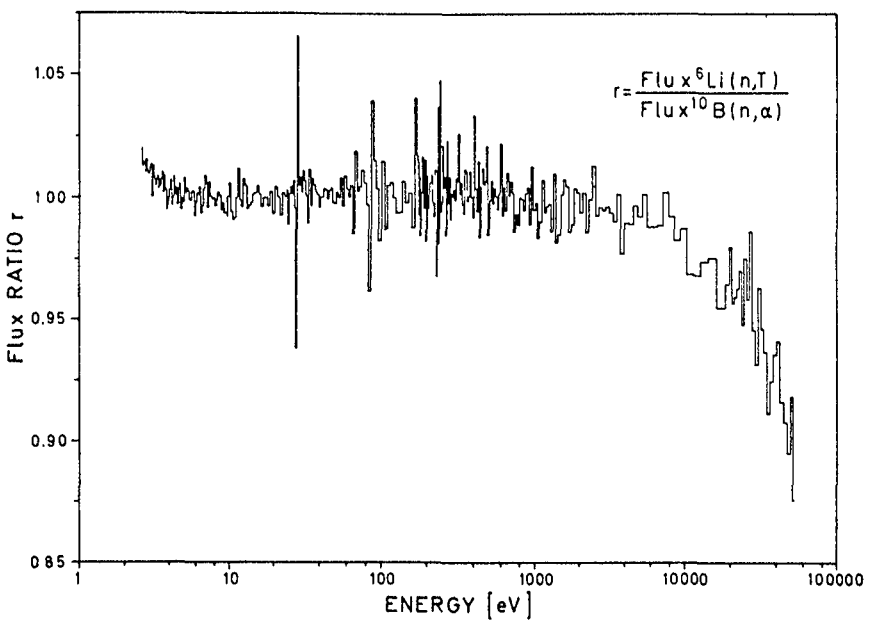

Fig. 6 Ratio of the two spectra of Fig. 4 and 5.

3. Intercomparison of a ^{6}Li-glass and a ^{235}U multiplate fission chamber

The characteristics of the ^{235}U multiplate fission chamber are given in Table 2. The fission chamber was placed at a 28 m flight path and its counting rate as a function of the energy was compared to that of the thin ^{6}Li-glass placed on the same flight path but at a distance of about 58 m. The recording of the two detectors was not performed simultaneously but one after the other and the fission chamber was removed when measuring with the ^{6}Li-glass. The investigated energy range spanned from a few eV up to 100 keV. Knowing the relative efficiency of the ^{6}Li-glass as a function of energy it was possible to convert the yield of the ^{235}U fission chamber into fission cross sections by normalizing at low energy. In fact, the normalization was carried out in two steps: first, a run was performed covering the range from few eV to several keV. Normalizing the data to the ENDF/B-V value of the low energy fission integral $I_{7.8}^{11.0\ eV} = 241.2 \cdot b\text{-}eV$, we obtained for the range 100-1000 eV the value $I_{100}^{1000\ eV} = 1.1890 \cdot 10^{4}$ b-eV (which is in excellent agreement with ENDF/B-V).

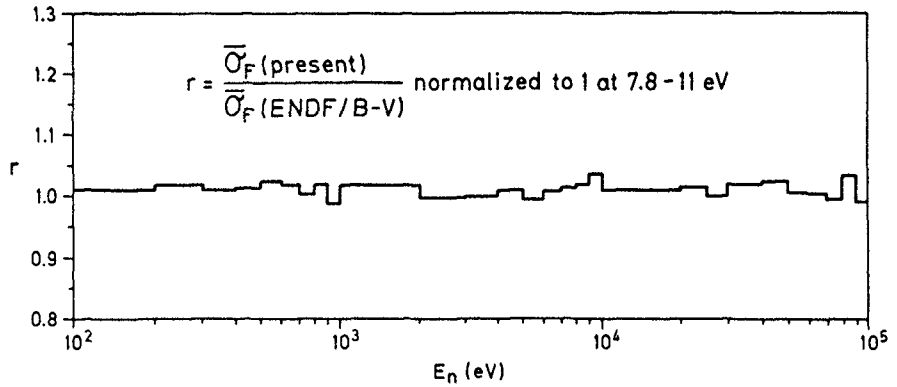

Fig. 7 Average $\bar{\sigma}_f$ values obtained using the neutron flux from the ^{6}Li-glass, compared to ENDF-B/V values. Our data have been normalized to the value $I_{7.8\ eV}^{11\ eV} = 241.2$ b·eV.

This last value was the one actually used to normalize our main run. Values of $\bar{\sigma}_f$ for decimal intervals going from 0.1 to 100 keV are given in Table 3. Statistical errors are negligible while systematic errors mainly associated to uncertainties in the background evaluation of the two runs are estimated to be less or equal to 2.6%. The ratios of the present values to the ENDF-B/V ones are plotted in Fig. 7: the agreement is good over the whole energy range.

SESSION VIII

NEUTRON ENERGY STANDARDS

G.D. JAMES
Atomic Energy Research Establishment,
United Kingdom Atomic Energy Authority,
Harwell, Didcot, Oxfordshire,
United Kingdom

Abstract

Recent publications on the determination of neutron energy are briefly reviewed and the table of neutron energy standards, originally formulated by an INDC sub-group, is revised by changes to three of the standard energies and the addition of an oscillator level at 0 12 eV to the list Work required to improve these standards is indicated

1. Introduction

Neutron energy standards help to ensure that all neutron spectrometers produce data on energy scales that agree to within the estimated errors of measurement This greatly reduces the problems of data intercomparison, evaluation, compilation and analysis Such standards can also be used to establish an energy scale for spectrometers when, for experimental reasons, the basic data required to construct an absolute energy scale cannot be determined In time, improved or additional energy measurements become available and it becomes necessary to consider a revision of the table of recommended energies This paper presents and considers the results and publications concerned with neutron energy determination which have come to my notice since the establishment[1] and revision[2] of a table of recommended neutron energy standards

A table of neutron energies[1], over the energy range 0 6 eV to 12 1 MeV, for forty-one narrow resonances suitable as energy standards was drawn up on the advice of an INDC sub-group on neutron energies in 1977 Some of these energies were later revised[2] The new information which has become available since this revision and its effect on the recommended standards may be summarised as follows Neutron energy measurements above 3 MeV are, at present, dominated by the accurate values measured with ultra-high resolution by Cierjacks et al [3 4] at Karlsruhe These results lead to a revision of the two highest resonance energies given in the table of recommended values At the other energy extreme, it has been suggested[5] that the very sharp first oscillator level in the neutron total cross-section of protons bound in zirconium hydride would provide an excellent low-energy calibration point at 0 12 eV This suggestion is adopted Energy values for five of the listed resonances have become available[6 7] from work on the 387 713 m flight-path of the 150 MeV linear accelerator at CBMN, Geel It will be seen that, except for the level near 2 Mev in the carbon transmission, these values do not agree well with the values in the table The nature of this disagreement is examined and, although the results obtained by combining these resonance energies with the the values in the table are presented, users should be aware of this discrepancy which can be resolved only by further investigation Finally, a detailed study of the determination of experimental neutron energies on the ORELA flight path 1 has been published[8] No resonance energy values are given but the nature of the report is noted

The data to be considered in revising the table of recommended neutron resonance energies are presented and discussed in sect 2, and the revised energies are given in sect 3 The conclusions of this survey and the indications which they give for future work are summarised in sect 4

2. Presentation and discussion of data

The data to be considered in revising the table of recommended neutron energies are presented in table 1 and discussed in the following sub-sections For resonances for which new information is available, table 1 gives the energy listed in the table of standards[2], the new energy value, the weighted mean of these two values, the external error in the weighted mean, derived from the spread of the data, and the internal error, derived from the assigned error values Details on how to derive these quantities are given, for instance, by Topping[9]

Table 1

Isotope	Energy Standard keV	Additional Value keV	Ref	Weighted Mean keV	External Error keV	Internal Error keV
Fe–56	266 766 ± 0 033	267 035 ± 0 035	(7)	266 892	0 134	0 024
S–32	412 330 ± 0 060	412 68 ± 0 07	(6)	412 48	0 17	0 045
S–32	818 720 ± 0 13	819 35 ± 0 17	(6)	818 95	0 30	0 10
O–16	1651 0 ± 2 0	1652 01 ± 0 45	(7)	1651 96	0 22	0 44
C–12	2078 05 ± 0 32	2078 60 ± 0 63	(7)	2078 12	0 23	0 39
C–12	6293 00 ± 5 0	6296 82 ± 0 39	(3)	6296 80	0 32	0 39
C–12	12100 ± 9	12087 ± 9	(4)	12087	1 2	9 0

2.1 Data from Karlsruhe

The work of Cierjacks et al [3] in the determination of neutron resonance energies by transmission measurements employing the neutron time-of-flight spectrometer of the Karlsruhe isochronous cyclotron represents a signal advance in the accurate measurement of neutron energy The measurements presented are on carbon and oxygen in the energy range 3 MeV to 30 MeV and were made with an energy resolution of 5 5 ps m^{-1} They allowed neutron resonance energies of some narrow resonances to be determined to a relative accuracy of $1\,2\times10^{-5}$ and in many cases are more accurate than previously published values by two orders of magnitude These authors present two sets of data suitable as high precision energy standards One is a table of seven resonance energies in the range 3 2 MeV to 6 1 MeV which are suitable for ultra-high resolution measurements and comprise resonances with ratios of resonance width to neutron energy below 10^{-3} The other is a table of thirteen resonances in the energy range 3 7 MeV to 7 8 MeV with a ratio of resonance width to neutron energy in the range 10^{-3} to 10^{-2} These are recommended for the more usual high resolution measurements Only one of these resonances is already in the table of recommended values It is at 6296 82 ± 0 39 keV and is listed in table 1 The error quoted is more than an order of magnitude smaller than the error given in the table of standard energies The two energy values agree to within this larger error

The energy of the resonance at 12087 ± 9 keV has also been measured at Karlsruhe[4] and is included in table 1

2.2 Data from Geel

Table 1 shows the energies for five resonances found by transmission measurements on a 387.713 m flight-path of the 150 MeV electron linear accelerator at CBNM Geel The minimum timing channel width used is 4 ns and the burst width is 4 5 ns The thickness of the neutron source is 10 mm and of the detector, 12 5 mm It is estimated that resonance peak positions are known to ± 2 ns and that the initial delay can also be measured to this accuracy[7] The energy for the resonance at 2078 60 ± 0 63 keV in the transmission of carbon agrees with the value given in the table of standards to within its own error of measurement The incorporation of this value into the recommended standard is discussed in the next sub-section

The other four energy values from Geel do not agree well with the recommended energy values and show a discrepancy which increases with decreasing energy from about one standard deviation at 1651 keV to eight standard deviations at 267 keV The energy behaviour of this discrepancy is illustrated in fig 1 Such behaviour could be interpreted as errors in flight-path length and initial time delay either for the spectrometer at Geel, or for the three flight paths involved in the the determination of the four energies given in the table of recommended energies Equally it may be due to unsuspected errors at all four laboratories This discrepancy can only be resolved by further investigation or when further measurements become available Although table 1 gives the results of combining the Geel data with the recommended energy values, it is suggested that the recommended

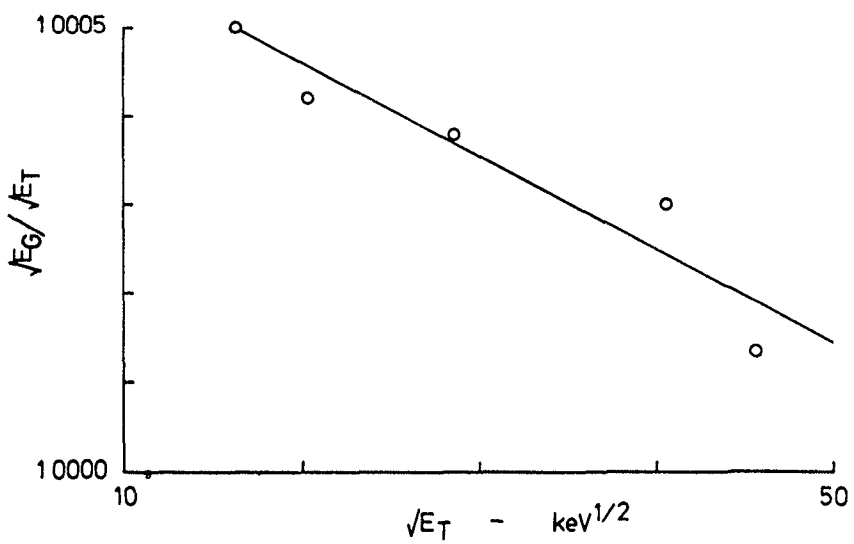

Fig 1 An illustration of the energy dependence of the ratio of the square root of the resonance energy measured at Geel, E_G, to that in the table of recommended energies[2], E_T

energy values should remain unchanged until the discrepancy illustrated in fig. 2 is resolved.

Since the data from Geel were measured, the spectrometer has been improved by a reduction minimum burst width to 0.7 ns and by the availability of 1 ns timing channels.

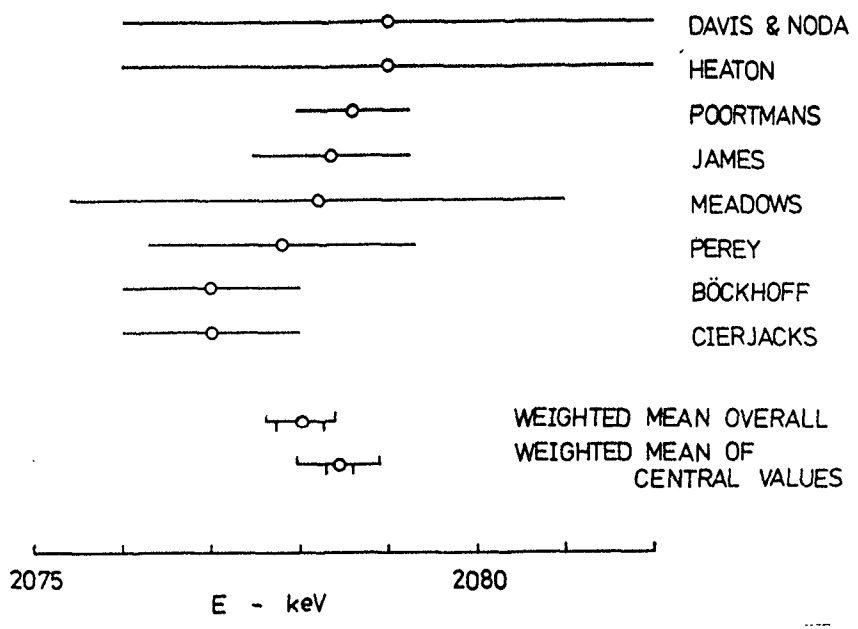

Fig. 2. The energy of the carbon resonance at 2078.43 ± 0.14 keV as measured in eight laboratories. The weighted mean value overall and the weighted mean value of the four more accurately specified central values are shown. For these mean values both the internal and external errors are indicated. They are set by limits shown above and below the error bar respectively.

2.3 The resonance in carbon at 2078.43 ± 0.14 keV

From mesurements on the 387 m flight-path at Geel, Poortmans[7] has provided the value 2078.60 ± 0.63 keV for the the energy of a resonance in the transmission of carbon. This value is illustrated in fig. 2 together with the seven energy values considered previously[1]. The weighted mean overall values is 2078.01 ± 0.24 keV. Here the error derived from the spread of the data is given. The error derived from the quoted errors is 0.41 keV. The four central values and their errors are quoted more precisely than the others. Taken alone these values have a weighted mean of 2078.43 ± 0.14 keV. Again the error given is derived from the spread of the data. The error derived from the quoted errors is 0.48 keV. It is suggested that this energy value which embodies the results with more precisely quoted values each with a precisely quoted, although not always lower, error should now be the recommended energy.

2.4 The oscillator level at 0.12 eV

It has been suggested by Priesmeyer[5] that the very sharp first oscillator level in the neutron total cross-section of protons bound in zirconium hydride would provide an excellent energy calibration point at about 0.12 eV. This cross-section is shown in fig. 3 which is taken from the work of Podewils and Priesmeyer[10]. The figure also shows a theoretical expression for the cross-section based on the work of Fermi. Experiments show that the cross-section minimum near 0.12 eV remains at the same energy independent of sample temperature over the range 25 °C to 890 °C. Further investigations are required to formulate a method of defining the position of this minimum and thus establish accurately the energy at which it occurs. This method may be based on the Fermi theory or may rely on some other mathematical expression taken to represent the data adequately in a narrow energy range close to the cross-section minumum.

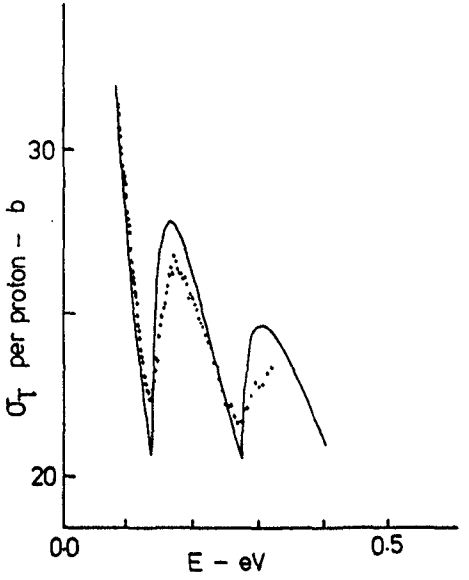

Fig. 3.

The total cross-section per proton of $ZrH_{1.92}$ at 77.4 K compared with the Fermi theory. This figure is derived from fig. 3 of Podewils and Priesmeyer[10].

2.5 ORELA flight path 1

Flight path 1 at ORELA is nominally 200 m in length and has been used extensively for transmission and scattering measurements. The effective flight path length varies with neutron energy, due to moderation effects in the neutron producing target and to the finite thickness of the neutron detector, and Larson et al.[8] have made a detailed study of this variation. Their analysis enables them to develop a distribution function for the time-of-flight energy. The mean time-of-flight energy is the first moment of this

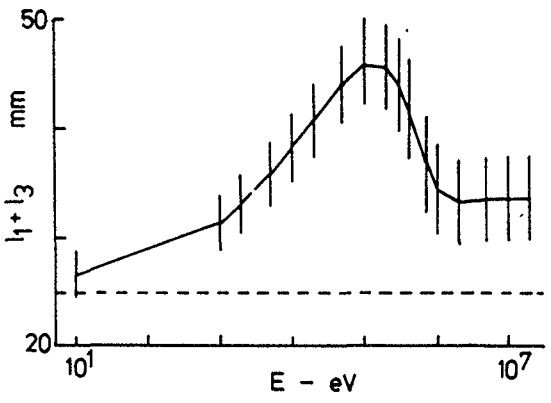

Fig. 4. An illustration of the energy dependence of the mean flight path length of ORELA flight path 1 as given in fig. 5 of Larson et al.[8]. Only the sum $l_1 \pm l_3$ of two end corrections is shown. The dashed line illustrates the energy independent value which would be obtained in the absence of the analysis undertaken by Larson et al.

Table 2

Revised Standard Energies

Isotope	Energy eV	Error eV
H ($ZrH_{1.92}$)	1.2 E-01	
C-12	2.07843E 06	4.8E 02
C-12	6.29680E 06	3.9E 02
C-12	1.2087 E 07	9. E 03

distribution and the width of the energy resolution function is identified with the second moment. It is found that there is approximately a 20 mm difference in the mean effective flight path length as a function of neutron energy. This difference, illustrated in fig. 4, is much larger than the uncertainty in the flight path length at any energy.

3. Revision of recommended standard energies

As a result of the above discussion, it is recommended that three of the energies in the table of recommended energies should be revised and that the oscillator level at about 0.12 eV should be added to the list. These revised values are listed in table 2.

4. Conclusion

From a consideration of data and information on neutron resonance energies and their determination, it is recommended that three of the standard energies should be revised and that the oscillator level near 0.12 eV should be added to the list. There is a need to establish the energy of this oscillator level more accurately from a careful analysis of the cross section data from which it is determined. The discrepancies noted in the four resonances between 266 keV and 1652 keV listed in table 1 will need to be resolved and work on spectrometers capable of helping to resolve this problem should be encouraged. It is suggested, not for the first time[1], that whenever changes are made to a spectrometer which could lead to a change of energy scale the energy of at least one resonance from the list of recommended energies should be confirmed and published. Indeed the confirmation of two widely spaced resonance energies would allow an even better assessment of the quality of the energy scale of a spectrometer.

Acknowledgements

I should like to thank the following for information which has been used in the preparation of this review; S. Cierjacks, H.G. Priesmeyer, F. Poortmans and A.B. Smith.

References

1) G.D. James, Neutron Standards and Applications, NBS Special Publication 493 (National Bureau of Standards, Washington DC, 1977) p. 319
2) G.D. James, Technical Report Series No.227 'Nuclear Data Standards for Nuclear Measurements' (IAEA, Vienna, 1983) p. 65
3) S. Cierjacks, F. Hinterberger, G. Schmalz, D. Erbe, P.v. Rossen and B. Leugers, Nucl. Inst. Methods **169**(1980)185
4) S. Cierjacks, unpublished
5) H.G. Priesmeyer, private communication
6) C.R. Jungmann, H. Weigmann, L. Mewissen, F. Poortmans, E. Cornelis and J.P. Theobald, Nucl. Phys. **A386**(1982)287
7) F. Poortmans, unpublished
8) D.C. Larson, N.M. Larson and J.A. Harvey, Report ORNL/TM-8880 (Oak Ridge National Laboratory, Oak Ridge, 1984)
9) J. Topping, Errors of observation and their treatment (Chapman and Hall, London, 1966) p. 87
10) P. Podewils and H.G. Priesmeyer, Neutron Inelastic Scattering 1977, Vol 2 (IAEA, Vienna, 1978) p. 367

THE ENERGY CALIBRATION PROCEDURE OF TIME-OF-FLIGHT SPECTROMETERS FOR FISSION NEUTRON SPECTRUM MEASUREMENTS

T. WIEDLING
Studsvik Science Research Laboratory,
Studsvik, Sweden

Abstract

This paper aims at a discussion of the technique for time (energy) calibrating a neutron time-of-flight spectrometer that is used to measure continuous fission neutron spectra. Such a calibration requires a number of neutron lines of well-known energies in the whole energy interval of the fission spectrum, i.e. up to 15 to 20 MeV. The $T(p,n)^3He$, $T(d,n)^4He$, and $^9Be(d,n)^{10}B$ reactions are suitable as such neutron line generators. Sources influencing the accuracy of the energy determination of these lines are discussed. By using a large number of well defined reference points in the whole energy interval covered by a fission neutron spectrum, a calibration function can be deduced which expresses the neutron flight time per metre (equivalent to energy) for each channel number of the spectrometer. Such a calibration function is very versatile for the calculation of the energy of any point of a recorded fission neutron spectrum.

1. Introduction

The neutron energy scale problem was discussed a few years ago by James [1], who briefly reviewed the basic methods of determining neutron energies, i.e. that based on direct measurement by time-of-flight and that based on the production of mono-energetic neutron beams generated by mono-energetic charged particles. James also discussed data for neutron resonances and gave a list of a number of narrow resonances which would be useful as standards from 0.6 eV to 12.1 MeV. As James pointed out, discrepancies sometimes seem to exist between the neutron energy scales of neutron spectrometers of different laboratories. This necessarily requires check-ups and refinements of existing techniques and apparatus.

The present paper concerns the specific problem of making the energy calibration for an accelerator based time-of-flight spectrometer used to measure neutron spectra. Neutron spectra from nuclear reactions consist of either discrete lines, resolvable or not by the spectrometer, or continuous distributions as for instance from fission processes. In either case there is a need to measure the energies of the neutron components and their intensities. The determination of the energies of a line spectrum can often rely on a few discrete calibration lines with well known energies. However, this paper will be aimed at the discussion of the energy calibration problems associated with the study and measurement of continuous fission neutron spectra, the study of which has been on the Studsvik program for a number of years [2]. The accurate analysis of a continuous distribution such as that of a fission neutron spectrum would require a detailed knowledge of the energy response of the spectrometer in the whole energy interval of the fission spectrum which extends from the eV range up to 15 to 20 MeV. It would be advantageous to be able to measure the whole spectrum in a single run, but the experimentally observable low energy limit is usually as high as about 100 keV, which is an effect mainly attributable to the scintillator detector properties of the time-of-flight spectrometer. The calibration is evidently a problem of generating a spectrum of neutron lines of well-known energies in the required interval.

The energy calibration procedure for the neutron time-of-flight spectrometer will be discussed in some detail and some viewpoints will be outlined. Results of a calibration of the energy interval 0.4 to 16 MeV will be shown.

2. The Complexity of Energy Determination for Calibration Neutron Lines

The precision with which the energy determination of a charged particle produced neutron beam can be determined will be influenced by a number of effects:

1. The accuracy with which the energy of the accelerator beam is determined
   a. The energy calibration of the accelerator analyzing magnet
   b. The precision of the standard reaction data, if used, for calibration of the analyzing magnet

2. The uncertainties of the nuclear masses used to calculate the energy of a neutron emitted in a reaction.

3. The estimation of the mean target thickness.

4. The estimation of the ion energy loss in the target window (if used to separate gas targets from the vacuum system).

5. The estimation of the ion beam energy loss in target surface deposits.

6. The beam energy modulation introduced by external klystron bunching.

7. The determination of the emission angle of a neutron from the target.

The energy determination is heavily dependent on a careful calibration of the analyzing magnet, which in turn is usually done starting from a number of accurately known reaction energy standards such as the $^{7}Li(p,n)^{7}Be$ threshold.

If the magnetic field is measured by a nuclear magnetic resonance device one arrives at the energy-frequency relation

$$E = k(f) \cdot f^2 \cdot \frac{Z^2}{M} \left[1 - \frac{E}{2Mc^2}\right]$$

(E = energy, M = mass, Z = charge, f = frequency, k(f) = a frequency dependent function).

The factor k(f) can sometimes be considered a constant. However, if the analyzing magnet of the 6 MeV Studsvik Van de Graaff accelerator is taken as an example there will be a 20 keV error in the energy determination at a deuteron energy of 3 MeV if the magnet is calibrated by observing only one calibration point, i.e. the $^{7}Li(p,n)$ threshold at 1.8806 MeV.

The energy standards which are used to calibrate accelerators may be considered well enough known that their uncertainty does not contribute significantly to the uncertainty in the calibration.

Nuclear mass uncertainties are so small that errors in kinematically calculated neutron energies are negligible at the present status of neutron physics measurements.

Neutron time-of-flight measurements with long flight paths often require relatively thick neutron producing targets because of intensity reasons. The energy loss of the incoming ion beam will not be negligible and has thus to be estimated in one way or another. There are also some other effects contributing to a slowing down of the energy of the ions, and these require precautions to be taken. These are related to the preparation and use of the targets. A neutron beam with well specified data cannot be obtained without a careful control of the manufacture of the target with regard to thickness and purity of target material, backing, window (if for a gas target), deposit build up on target surface during preparation, deposit build up on target surface when stored in the reaction chamber connected

to the accelerator vacuum system, deposit on target surface during ion bombardment, etc. The total target thickness is thus defined not only by the specified target material but also by uncontrollable deposits on the target surface and chemical changes (for instance oxidation) of the target material which contribute to the energy reduction of the incoming charged particle beam and to an increased energy spread that effects the energy characteristics of the neutrons produced. Both the beam energy and the spread are easy to calculate with satisfactory accuracy for an ideal target of specified surface density but are difficult or even impossible to estimate in practice, at least if the experimental conditions influencing the target material and causing surface deposits are out of control. The most straightforward way to overcome these difficulties is to have as clean conditions as possible when preparing and storing the target and during the ion irradiations in the experiment. The deposit thickness can in unfavourable conditions be several keV or tens of keV depending on the energy range and the estimate of the thickness could probably only be considered as a crude guess.

Klystron bunchers are frequently used to produce short intense ion pulses. More than one unit can be put in tandem in order to improve the pulse time characteristics. One technique chosen is to have a pre-buncher on the ion source side of the accelerator, for instance a Van de Graaff, and a post-buncher operating on the accelerated and momentum analyzed beam [3]. This beam thus gets a time modulation, the effect of which has to be taken into account since it may not be negligible.

The determination of the emission angle of the neutrons from the target is a problem associated with the definition of the direction of the ion beam and the definition of the neutron detector angle. It is recommended that the energy of the neutron beam should be observed at emission angles to the "left" and to the "right" relative to the direction of the charged particle beam, in order to get an accurate definition of the zero degree angle and to cancel built-in asymmetry effects in the neutron detector arrangement [4].

Kinematically calculated energies of neutrons emitted by a typical accelerator target are suitably checked by a time-of-flight spectrometer tailored for precision measurements of neutron energies. A spectrometer of sufficient resolution should give information about the total target thickness, including the effects of contamination. Estimates or guesses of effects of ion beam energy degradation due to target surface contamination are thus eliminated. However, the design and use of such an instrument is a separate topic.

3 Energy resolution of time-of-flight spectrometer

The energy resolution of a neutron time-of-flight spectrometer is expressed by the relation

$$\frac{\Delta E_n}{E_n} = \text{Constant} \cdot \frac{\Delta t}{L} \cdot E_n^{1/2}$$

where Δt is the total time spread and L is the flight path.

The total time spread can be split up into a number of contributing components:

1. Energy spread in the accelerator beam.

2. Target thickness resulting in charged particle energy loss and straggling.

3. Time spread in a non-zero length target because of finite flight times of accelerator beam charged particles and of neutrons within target space.

4. Time duration of accelerator beam pulse

5. Neutron detection time uncertainty because of a detector of non-zero length (which contributes to the flight path length determination uncertainty).

6. Neutron time spread due to a detector with a non-zero solid angle (which contributes to the flight path length determination uncertainty).

7. Energy spread due to target emission of neutrons in a non-zero solid angle subtended by the target-detector system.

The time duration of the neutron pulse is evidently the result of the processes of items 1 to 4 but the total time uncertainty is also influenced by those of items 5 to 7.

The energy spread in the accelerator beam can reasonably well be neglected at least when it has been cleaned up by an analyzing magnet with data characteristics as for the one usually used in connection with a Van de Graaff.

Neglecting impurity problems of different kinds, which have already been considered in a previous paragraph, the choice of target thickness is made so as to get a satisfactory yield of the lines of the neutron spectrum, enabling observation with good statistics with the proper flight path.

The target length is a parameter which has only to be considered in the case of gas target cells and can be neglected for short solid targets.

The time duration of the accelerator beam pulse is of course of vital importance in time-of-flight measurements. A pulse length of the order of 1 ns contributes significantly to the spectrometer resolution for instance at the high energies of a fission neutron spectrum, but is of little importance at the lower end. This is the trivial dilemma with all neutron time-of-flight measurements which cover a wide energy range that the resolution is strongly degraded with increasing energy.

The detection time uncertainty cannot be made negligibly small over the whole time range of a detector which has to cover the energy interval of a fission neutron spectrum. The detection time uncertainty depends on the neutron energy as well as on the detector size (length), which is one factor influencing the efficiency. The need for efficiency is coupled to the neutron source strength at one's disposal. The problem is to find optimum values of all parameters.

The angular dependence of the energy of the neutrons emitted in a reaction contributes to the energy spread within an angle defined by the detector opening. The choice of solid angle is evidently associated with the neutron flux, detector efficiency, and the neutron energy spread problems. Ideally the detector opening should be so small that its energy spread contribution will be negligible.

It can be difficult to give a proper definition for the flight path length in the case of a detector whose size is not small. These problems have been discussed in some detail by James [1].

4. Time-shifts in neutron time-of-flight spectra

The electronic start or stop pulse of a time-of-flight spectrometer is often obtained from a pick-off device placed somewhere in the path of the accelerator beam and generating a signal each time an ion pulse passes. Since more than one type of ion specimen and also different energies are used in an energy calibration measurement there will be different flight times for the ions from the pick-off to the target. This results in time-shifts in the recordings of the individual spectra and has to be corrected for. The spectrum shift can be calculated when the ion energy and the pick-off-to-target distance are known. This shift can also be calculated by reference to spectrum lines associated with the gamma

production in the target. These corrections may contribute to the introduction of some uncertainty in the time-scale.

5. Neutron calibration line sources

The energy calibration of a neutron detector requires sources emitting neutrons that are well defined with respect to energy and energy spread. A spectrum of neutron energies covering the energy range of a fission neutron spectrum is suitably obtained for example from the $T(p,n)^3He$, $T(d,n)^4He$, and $^9Be(d,n)^{10}B$ reactions which have the advantage of requiring only a modest accelerator energy. The $^9Be(d,n)^{10}B$ reaction has the advantage of emitting several neutron groups at the same bombarding energy. Appropriate neutron energies are selected either by varying the bombarding energy or by observing the neutrons at selected emission angles.

The $^7Li(p,n)^7Be$ and $D(d,n)^3He$ reactions are also convenient sources of monoenergetic neutrons or groups of neutrons. However, the laboratory having an accelerator capable to produce up to 12 MeV deuterons in pulses of short duration (< 1 ns) and a time-of-flight spectrometer capable to resolve most of the neutron groups associated with excited states in ^{10}B would preferably use the $^9Be(d,n)^{10}B$ reaction to calibrate its neutron spectrometer in the whole energy interval making use of the advantage of a target of high quality made in situ at the ordinary target position.

Table 1 gives examples of the choice of angular intervals for the T-p, T-d, and Be-d reactions at an energy of 3 MeV in order to get a large number of calibration lines between 0.43 and 15.9 MeV, i.e. in the energy range of the fission neutron spectrum. The energy spread per degree (i.e. for a linear detector opening of $\pm$ 1°) is given at a few neutron energies and emission angles in Table 2. The data of the table show a relative energy spread of the order of 0.5 per cent per degree or less.

Table 1

Neutron energy ranges covered with the $T(p,n)^3He$, $^9Be(d,n)^{10}B$, and $T(d,n)^4He$ reactions in specified neutron emission angular intervals at a reaction energy of 3 MeV.

Reaction	Angular interval MeV	Neutron energy range MeV
$T(p,n)^3He$	0°-150°	2.216- 0.430
$^9Be(d,n)^{10}B$	0°	7.35 - 1.26*
$T(d,n)^4He$	80°-150°	15.90 -12.23

*Excited states in ^{10}B: 0.718, 1.740, 2.154, 3.587, 4.774, 5.110, 5.920, 6.127 MeV.

Table 2

Neutron energy spread per degree for the $T(p,n)^3He$, $T(d,n)^4He$, and $^4Be(d,n)^{10}B$ reactions at a charged particle energy of 3 MeV and at the neutron emission angles (θ) of 20°, 85°, and 20°, respectively.

Reaction	θ degrees	E_n MeV	$\Delta E_n/\Delta\theta$ MeV/degree	$\Delta E_n/E_n/\Delta\theta$ Percent/degree
$T(p,n)^3He$	20	2.11	0.01	0.5
$T(d,n)^4He$	85	15.55	0.07	0.5
$^9Be(d,n)^{10}B$	20	7.27	0.01	0.2

6. Energy calibration of a specific time-of-flight spectrometer.

The results of an energy calibration of a time-of-flight spectrometer will be briefly reported as an illustration of the previous discussions.

The spectrometer was the one at the Studsvik 6 MeV Van de Graaff machine with a klystron buncher in the high voltage terminal [5] The ion pulse width was typically 1.5 ns The energies of the ions were measured by a magnet with a magnetic resonance spectrometer. The threshold energy of the $^{7}Li(p,n)^{7}Be$ reaction was used as one reference point for the magnet calibration. The neutron detector was a plastic scintillator 10 cm in diameter by 5 cm thick. The flight path was 3 m

The neutron calibration lines were obtained by the T-p, T-d (at 3.0 MeV), and ^{9}Be-d reactions (at 3.0, 4.0, and 5.0 MeV. Targets of T-Ti and of beryllium evaporated on tantalum were used. The thicknesses of the individual targets were 14, 28, and 16 keV, respectively, at 3.0 MeV charged particle energy. A neutron spectrum representative of the $^{9}Be(d,n)^{10}B$ reaction at 3.0 MeV is shown in Fig. 1 The target is evidently somewhat contaminated since neutron lines attributable to the $^{12}C(d,n)^{13}N$ and $^{16}O(d,n)^{17}F$ reactions are also present.

The main contributions to the time spread in the calibration lines come in this measurement from the ion pulse width and the energy dependent neutron time detection uncertainty in the scintillation detector. The target thickness has only a marginal effect, if any, on the total time spread, i.e about 0.8 ns as a maximum (at 430 keV neutron energy) at the pertinent flight path

The uncertainties in the accelerator ion beam energies are negligible. Since all the targets were relatively thin the charged particle energy loss is so small that the contributions to neutron energy uncertainties can be considered small relative to the main error sources. A time uncertainty introduced by a 0 1^{o} degree error in the positioning of the detector should be small or negligible.

Fig. 2 shows typical results of a calibration measurement giving the spectrometer channel number versus neutron flight time in nanoseconds per metre Polynomials of first and second order have been fitted to the experimental data and the coefficients have been calculated by the least squares procedure giving the following results·

$$\tau = 166.38 - 0.16741C$$

and

$$\tau = 162.35 - 0.15441C - 9.833\cdot10^{-6}C^{2}$$

(τ:ns/m, C.channel number, C<1000)

The solid line represents the fitting to the points. On the scale of the figure it is not possible to distinguish the two polynomials. The calibrated time region is equivalent to the energy interval 0.4 to 16 MeV

The second order polynomial fits the experimental data somewhat better than the first order one, as indicated by the minimum values of the expression $x^{2} = W(x_{exp} - x_{calc})^{2}$ (W represents the weight; x_{exp} and x_{calc} are the experimental and calculated data values, respectively). This is also illustrated by the data of Table 3 which compares the energies of some of the experimental calibration lines with those calculated with the polynomials. The data of the table show clearly that the parabolic function gives the best fit. The relative differences are positive up to 8.255 MeV but negative above this value for the linear case contrary to the fitting of the second order polynomial which gives a more random distribution of positive and negative values.

The calibration procedure of the Studsvik spectrometer will be described in detail in a forthcoming paper [6]

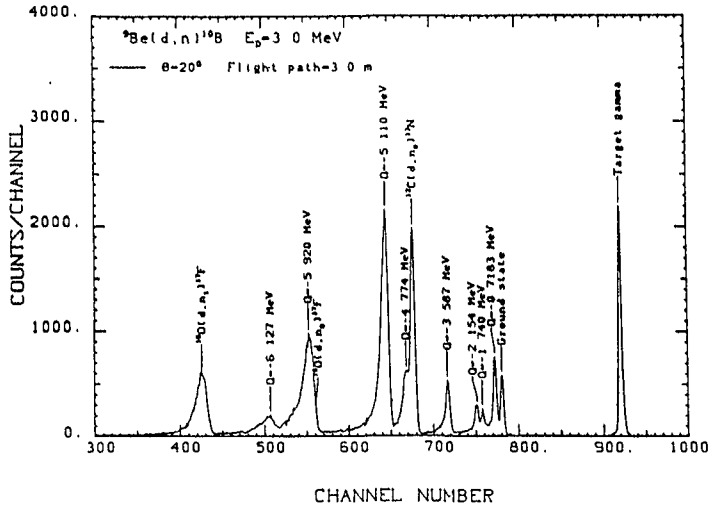

Fig. 1 A typical calibration spectrum of neutrons obtained from the ^{9}Be(d,n)^{10}B reaction at E_d=3.0 MeV.

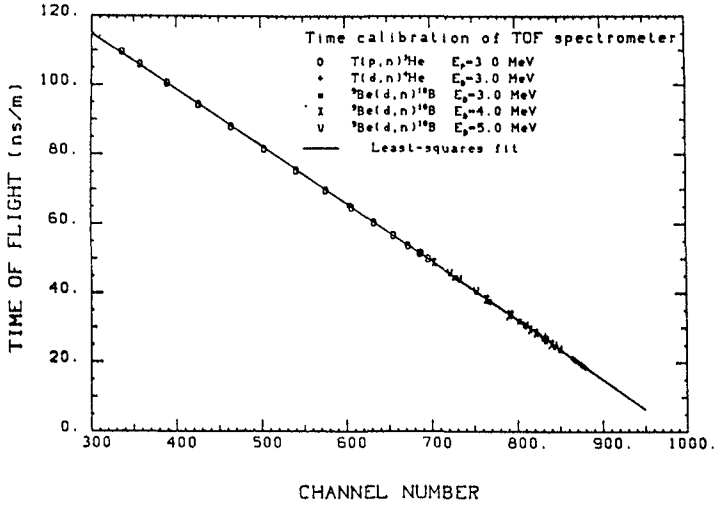

Fig. 2 Energy calibration function of the time-of-flight spectrometer showing neutron flight-time per metre versus spectrometer channel number. The solid line represents the least squares fittings to the experimental points. It is not possible to distinguish first and second order polynomial fittings on the scale of the figure.

Table 3

Comparison of some experimental calibration neutron energies and energies calculated from polynomials fitted to the experimental ones. Also given are the relative differences (in percentages).

E_n(exp)	Linear function		Parabolic function	
MeV	E_n(calc.) MeV	Relative difference	E_n(calc.) MeV	Relative difference
0.435	0.433	0.5	0.439	0.9
0.518	0.514	0.8	0.519	0.2
0.920	0.918	0.2	0.915	-0.5
1.632	1.641	0.6	1.646	-0.4
2.199	2.239	1.8	2.216	0.8
3.593	3.649	1.6	3.618	0.7
4.650	4.673	0.5	4.645	-0.1
7.542	7.491	0.7	7.506	-0.5
8.255	8.219	0.4	8.252	-0.04
12.545	12.164	-3.0	12.345	1.6
13.411	13.064	-2.6	13.291	-0.9
15.209	14.950	-1.7	15.281	0.5
15.548	15.336	-1.4	15.692	0.9

8. Concluding Remarks

The energy calibration procedure for an accelerator based neutron time-of-flight spectrometer has been discussed primarily with regard to its use for measuring continuous neutron spectra, i.e. fission neutron spectra in the energy interval 0.4 to 16 MeV. This interval can be covered by a spectrum of calibration lines which are generated by the reactions T(p,n)^{3}He, T(d,n)^{4}He, and ^{4}Be(d,n)^{10}B. Numerous energy reference points make possible the deduction of a

function that describes well the neutron flight time per metre (equivalent to energy) to each spectrometer channel number, i.e. the neutron energy can be calculated for any channel number desired for the analyses of a fission neutron spectrum.

In conclusion: Some of the experimental criteria necessary for optimum energy calibration accuracy of a time-of-flight spectrometer are: targets with well defined data, accurate charged particle energy determination, clean vacuum target chamber conditions, extreme time resolution obtained by short neutron pulses and small detector time spread, and accurate angular positioning of the neutron detector.

References

1. G.D. James, Neutron Standards and Applications. Proceedings of the Internatonal Specialists Symposium on Neutron Standards and Applications, National Bureau of Standards, Gaithersburg, Maryland (1977)

2. T. Wiedling, EANDC Symposium on Neutron Standards and Flux Normalization, Argonne National Laboratory (1970)
E. Almén, B. Holmqvist, and T. Wiedling, Nuclear Data for Reactors, Conference Proceedings, Helsinki, IAEA (1970).
P-I. Johansson, B. Holmqvist, T. Wiedling, and L. Jéki, Nuclear Cross Sections and Technology, Proceedings of a Conference, Washington, D.C. (1975)
P-I. Johansson and B. Holmqvist, Nucl. Sci. Eng. 62 (1977) 695

3. T. Wiedling, Contribution to the Neutron Interlaboratory Seminar, Oxford 1 - 3 July 1981. The Studsvik Science Research Laboratory Research Report NFL-29 (1981)

4. T. Wiedling, NIM 173 (1980) 335.

5. P. Tykesson and T. Wiedling, NIM 77 (1970) 277

6. P-I. Johansson, B. Holmqvist, and T. Wiedling, NIM. Accepted for publication.

NEUTRON ENERGIES SELECTED BY ISO FOR THE CALIBRATION OF RADIATION PROTECTION INSTRUMENTS

M. COSACK
Physikalisch-Technische Bundesanstalt,
Braunschweig, Federal Republic of Germany

Abstract

ISO/TC 85/SC 2/WG 2 has chosen a number of radionuclide neutron sources with broad spectral neutron distributions for routine calibrations of radiation protection instruments. For the determination of the response as a function of neutron energy several energies were fixed at which nearly monoenergetic neutrons can be produced.

1. Radionuclide Sources

The working group ISO/TC 85/SC 2/WG 2 (Technical Committee: Nuclear Energy; Subcommittee: Radiation Protection; Working Group: Reference Radiation) recently selected a few radionuclide neutron sources with broad spectral distributions as reference fields[1]. The following sources were taken: ^{252}Cf, moderated ^{252}Cf (a spherical heavy-water moderator of diameter 30 cm), $^{241}AmBe(\alpha,n)$ and $^{241}AmB(\alpha,n)$. The criteria for this choice were the availability of reasonable source data and the covering of a range of different spectral distributions and source strengths. The aim was to make calibrations carried out at different laboratories and facilities comparable. The recommendation of a set of sources may, in addition, initiate further investigations which will lead to an improved knowledge of these fields.

2. Monoenergetic Neutrons

Besides radionuclide neutron sources, monoenergetic neutrons are needed in radiation protection for determining the response of instruments as a function of neutron energy[2]. In the past,

Table 1

Neutron Energy MeV	Method of Production	Remarks[1]
2.5×10^{-8} (thermal)	moderated reactor neutron beam or accelerator produced moderated neutrons	
0.001	Sb-Be(γ,n) radionuclide source water moderated	
0.002	Scandium filtered reactor neutron beam or reaction $^{45}Sc(p,n)^{45}Ti$ with accelerator	
0.021	Sb-Be(γ,n) radionuclide source or reaction $^{45}Sc(p,n)^{45}Ti$ with accelerator	
0.024	Iron-aluminium filtered reactor neutron beam or reaction $^{45}Sc(p,n)^{45}Ti$ with accelerator	
0.144	Silicon-filtered reactor beam, accelerator-produced neutrons from reactions $T(p,n)^3He$; $^7Li(p,n)^7Be$	I
0.25	$T(p,n)^3He$; $^7Li(p,n)^7Be$	I
0.565	$T(p,n)^3He$; $^7Li(p,n)^7Be$	I,P
1.2	$T(p,n)^3He$	
2.5	$T(p,n)^3He$	I
3.2	$D(d,n)^3He$	L
5.0	$D(d,n)^3He$	I
14.8	$T(d,n)^4He$	I,P,L
19.0	$T(d,n)^4He$	

[1] The symbols designate the following:

I: One or more international intercomparisons of fluence determinations for monoenergetic neutrons were performed[3)-5)] (see also other contributions to this meeting).

P: There is a maximum of the reaction cross section for the neutron production.

L: These energies can be produced in particular with accelerators with a voltage of a few hundred kV.

energies were chosen rather arbitrarily, and different measurements could only be compared applying interpolations introducing additional uncertainties. This is why the ISO working group decided to compile a list of neutron energies which should preferably be used in neutron detector calibrations (see table 1).

The following points were considered when the energies for this table were selected:

- availability of reactor filters
- cross sections of neutron producing reactions
- neutron cross sections of air (absorption and scattering) and materials frequently used
- possibility of using low-energy particle accelerators
- international intercomparison of fluence measurements for monoenergetic neutrons.

3. Discussion

Of course, the international intercomparisons had already allowed for the above criteria. Taking the energies already used in an international intercomparison offers the advantage of experimental evidence for the accuracy of the fluence measurements in the participating standard laboratories. In consequence, problems in fluence determinations or calibrations which occurred in the evaluation of the intercomparisons were generally solved at the particular laboratory.

With the experience gained in connection with the properties of the neutron fields at specific energies, calibrations of instruments became more reliable. On the other hand large systematic uncertainties may be introduced if the neutron energy is changed to values other than those given in the table. The reason is, of course, the rapidly changing cross sections of the neutron producing reactions or the neutron-induced reactions for relevant materials.

The reasons why ISO compiled a table of energies may also be valid in other fields of research with monoenergetic neutrons. The possibility of a direct intercomparison of measurements and an interchange of data without interpolation or extrapolation is an advantage and may lead to smaller uncertainties and improved reliability.

With regard to the question of what energies should be recommended, there are already a number of energies which have been used quite frequently, as for instance 14.8 MeV or 3.2 MeV, for reasons which are well known. However, to satisfy the needs encountered in different experiments other energies should be added. One proposal is to take the table compiled by ISO covering the energy range from thermal to 19 MeV, but this should perhaps be discussed by this advisory group.

References

1.) P. Champlong, J.L. Chartier, M. Cosack et al.: Proc. of Fourth Symp. on Neutron Dosimetry, München-Neuherberg, CEC, EUR 7448 EN, Vol. I (1981) 387- 394
J.L. Chartier, P. Champlong, M. Cosack, S. Wagner, H. Schraube, H.J. Delafield, J.B. Hunt, I.M.G. Thompson, L. Lembo, R.B. Schwartz, C.O. Widell: Neutron Reference Radiations for Calibrating Neutron Measuring Devices Used for Radiation Protection Purposes and for Determining their Response as a Function of Neutron Energy. ISO/TC 85 Document DP 8529

2.) M. Cosack, H. Lesiecki: Dose Equivalent Survey Meters. Rad. Prot. Dos. (1984)

3.) D. Huynh: International Comparison of Flux Density Measurements for Monoenergetic Fast Neutrons. Metrologia 16 (1980) 31

4.) V.E. Lewis: International Intercomparison of d + T Neutron Fluence and Energy Using Niobium and Zirconium Activation. Metrologia 20 (1984) 49 - 53

5.) H. Liskien: International Fluence Rate Intercomparison for 2.5 MeV and 5.0 MeV Neutrons. Metrologia 20 (1984) 55 - 59

SESSION IX

ACTINIDE HALF-LIVES AS STANDARDS FOR NUCLEAR DATA MEASUREMENTS: CURRENT STATUS

C.W. REICH
Idaho National Engineering Laboratory,
EG&G Idaho Inc.,
Idaho Falls, Idaho,
United States of America

Abstract

The present status of the half-life data is summarized for a number of long-lived actinide nuclides useful as standards for nuclear data measurements and reactor research and technology. The half-life information given draws heavily from the file of recommended decay data generated over a number of years through the activities of an IAEA Coordinated Research Program on the measurement and evaluation of transactinium-isotope nuclear decay data, whose work has recently been completed.

1. INTRODUCTION

One of the more important properties of any radioactive nuclide is its half-life. In addition to its relevance to basic nuclear physics, knowledge of the half-life is required for any application in which quantitative assay of material for radionuclide content is desired. In fission-reactor research and technology, for example, accurate half-life data are required for many areas related to the safeguarding of special nuclear materials. In the precise measurement of neutron-induced reaction cross sections important for studies of fast-reactor fuel cycles, such data are necessary for the accurate mass assay of, and the correction for nuclide decay in, the samples utilized. Half-lives thus represent an important subset of that large body of knowledge commonly referred to as "Nuclear Data". As such, the development of highly accurate values of actinide-nuclide half-lives for use as standards in nuclear research and technology is an important task.

Unfortunately, until roughly the past decade, the status of the half-life data on the longer-lived actinide nuclides was rather poor, especially for those of importance in fast-reactor research. Although many half-life measurements were reported in the literature for a number of these nuclides, the results often differed by many times the quoted (and frequently quite small) errors. The user of such information was confronted with the frustrating and difficult task of trying to choose from among these a reliable value to use for his particular need.

Fortunately, this situation has changed considerably in the past several years. This improvement has resulted in part from the availability and use of improved experimental techniques and a better understanding of all aspects of the measurement process, especially the elucidation of systematic errors in the results. This has led to the production of an impressive body of more accurate half-life information for the longer-lived actinides. In some instances, several measurement groups have joined together in a cooperative effort to arrive at a "recommended" half-life value for selected nuclides through an extensive measurement program employing a variety of different experimental approaches, coupled with a careful evaluation of the resulting data. A good example of this collaborative approach is provided by the U. S. Half-Life Evaluation Committee, consisting of groups from six laboratories, which for several years carried out an extensive measurement program on the longer-lived Pu isotopes important for safeguards-related applications. (For a description of this effort, see, for example, Refs. [1,2].) In addition to the measurement activities, careful evaluations of the available half-life data for several of the important actinides have been published and "best" values recommended, with an emphasis on consideration of systematic sources of error. (See, for example, Refs. [3-5] and additional papers submitted to this conference by N. E. Holden).

Of particular current relevance for the half-lives of actinide nuclides is the IAEA Coordinated Research Program (CRP) on the Measurement and Evaluation of Transactinium Isotope Nuclear Data. Established in 1977, this CRP has as its primary objective the production of a consistent set of transactinium-nuclide decay data (specifically, half-lives, branching fractions and α- and γ-ray emission probabilities) which satisfy the rather stringent accuracy requirements identified at the first two IAEA Advisory Group Meetings on Transactinium Isotope Nuclear Data, held at Karlsruhe in 1975 [6] and at Cadarache in 1979 [7]. The participants in this CRP, representing five measurement groups around the world, have pursued this objective through an active, coordinated program of precise data measurements, supplemented by the critical evaluation of selected data from within the CRP and from other laboratories. Several reports describing the history, objectives and accomplishments of this CRP have been published [8-10]. The final research coordination meeting of the CRP participants has just concluded, and the preparation of a report summarizing the results of this endeavor is presently underway. This report will include, among other things, recommended values for the half-lives (both total and partial) for all the important actinide nuclides and the members of their decay chains. Since one important aspect of the work of this CRP has been to keep abreast of measurement and evaluation activities around the world, it is believed that the information contained in this report will be reasonably complete and up to date. In drawing up the lists of the data to be included in this report, considerable use has been made of the following files of evaluated decay data:

ENSDF, the Evaluated Nuclear Structure Data File, resulting from the evaluation effort of the International Nuclear Structure and Decay Data Evaluation Network. This file represents the base of evaluated nuclear information associated with the preparation of the Nuclear Data Sheets;

the file of evaluated actinide decay data at the Idaho National Engineering Laboratory, which forms the source of decay data for the

Actinide File of ENDF/B, the Evaluated Nuclear Data File/B, used within the U.S. reactor research and technology program; and

the U.K. Chemical Nuclear Data Committee Heavy Element Decay Data File, prepared at the AEE Winfrith Laboratory.

Where no new measurements or evaluations have appeared which would supersede the information in these files, these data are those which have been incorporated into the listings in the CRP summary report.

In the present paper, the current status of actinide-nuclide half-lives, useful as standards in nuclear-data measurements, is summarized. The coverage of nuclides and the categories of half-life data considered (namely, total and partial) follows that given by Vaninbroukx and Lorenz [11]. In Section 2, the total and partial half-life values are given together with their uncertainties. These data are those to be recommended by the IAEA decay-data CRP in its final report. In some instances, they are the same as those included in the most recent version of the list of proposed recommended heavy-element decay data [12], which has been updated and issued on a continuing basis by the CRP participants. In Section 3, comments regarding specific values are given, which provide additional information regarding the listed values and point out outstanding problems which require further study for their resolution.

2. SUMMARY OF HALF-LIFE DATA

In Table 1, the recommended half-life values for those actinide nuclides suitable for nuclear-data standards are given. These data have been carefully considered by the participants in the IAEA CRP for inclusion in the final report summarizing their conclusions and recommendations regarding the current status of actinide-nuclide decay data. A detailed discussion of all the bases for the choice of these particular values is beyond the scope of the present paper. Additional information regarding these is to be given in the summary report.

Values in Table 1 for which no footnotes are given are ones that appear in existing data files and for which no changes are recommended by the CRP participants.

3. COMMENTS REGARDING CERTAIN OF THE HALF-LIFE VALUES

^{233}U: The total half-life value is that recommended by Holden [4] from a critical evaluation of the available data up through 1980. Two recent analyses [16, 17], which had as their objective the production of a

TABLE 1

RECOMMENDED HALF-LIFE DATA FOR SELECTED ACTINIDES

Nuclide	Decay Mode	Half-Life	Notes
^{233}U	α	$(1.592 \pm 0.002) \times 10^5$ y	a
	S.F.	$>2.7 \times 10^{17}$ y	a
^{234}U	α	$(2.457 \pm 0.005) \times 10^5$ y	a
	S.F.	$(1.42 \pm 0.08) \times 10^{16}$ y	b
^{235}U	α	$(7.037 \pm 0.007) \times 10^8$ y	c
	S.F.	$(9.8 \pm 2.8) \times 10^{18}$ y	b
^{238}U	α	$(4.468 \pm 0.005) \times 10^9$ y	-
	S.F.	$(8.2 \pm 0.1) \times 10^{15}$ y	a
^{237}Np	α	$(2.14 \pm 0.01) \times 10^6$ y	a
	S.F.	$>1. \times 10^{18}$ y	-
^{239}Pu	α	$(2.411 \pm 0.003) \times 10^4$ y	a
	S.F.	5.5×10^{15} y	-
^{240}Pu	α	$(6{,}563. \pm 7.)$ y	a
	S.F.	$(1.16 \pm 0.04) \times 10^{11}$ y	d
^{241}Pu	β^-	(14.4 ± 0.1) y	a
	α	$(6.00 \pm 0.05) \times 10^5$ y	e
^{242}Pu	α	$(3.735 \pm 0.022) \times 10^5$ y	d
	S.F.	$(6.8 \pm 0.1) \times 10^{10}$ y	d
^{244}Pu	α	$(8.00 \pm 0.09) \times 10^7$ y	d
	S.F.	$(6.7 \pm 0.3) \times 10^{10}$ y	d
^{252}Cf	Total	(2.645 ± 0.008) y	a
	α	(2.73 ± 0.01) y	a
	S.F.	(85.5 ± 0.3) y	a

a) See the discussion in Section 3 for additional comments.

b) Measured value reported in Ref. [13].

c) Value recommended from the evaluation in Ref. [4].

d) Value recommended from the evaluation in Ref. [14].

e) Value recommended from the evaluation in Ref. [15].

consistent set of thermal neutron constants (e.g., 2200 m/s cross sections, Westcott g-factors and fission neutron yields) from an overall least squares fit to the available experimental data on several actinide nuclides, yield values for the ^{233}U half-life. Divadeenam and Stehn [16] derive the value $(1.59124 \pm 0.00163) \times 10^5$ y for this quantity, while Axton [17] obtains the value $(1.5906 \pm 0.0019) \times 10^5$ y from his analysis. Both of these values are in good agreement with the recommended value given in Table 1.

The spontaneous-fission half-life value is that reported by von Gunten *et al.* [13]. It differs significantly from the value $(1.2 \pm 0.3) \times 10^{17}$ y [18], which is the one presently given in most files of decay data.

^{234}U: This nuclide is an important contaminant in samples of ^{235}U, and an accurate knowledge of its half-life is required in order to achieve reliable mass assays of ^{235}U content in such samples when alpha-particle detection techniques are employed. The total half-life value given in Table 1 was derived from the same base of data as that used by Holden [4], except that the value reported by Meadows was excluded since it has been withdrawn by its author [W. P. Poenitz, private communication (1984)]. In addition, the uncertainties associated with the remaining values were those given by their respective authors. This recommended value is in excellent agreement with the results from two recent analyses [16, 17] of the available neutron nuclear data which had as their objective the production of a consistent set of thermal neutron constants for several actinide nuclides. From their analysis, Divadeenam and Stehn [16] derive the value $(2.45749 \pm 0.00504) \times 10^5$ y for the ^{234}U half-life, and Axton [17] obtains $(2.4580 \pm 0.0051) \times 10^5$ y for this quantity.

From an extensive determination and intercomparison of masses of a number of ^{235}U samples obtained from several laboratories, Poenitz and Meadows [19] have been able to deduce a value of $(2.457 \pm 0.005) \times 10^5$ y for the ^{234}U half-life, also in excellent agreement with the value given in Table 1.

^{238}U: A large body of published information exists on the spontaneous-fission half-life of ^{238}U. This has been prompted, at least in part, by the importance of the ^{238}U spontaneous-fission decay mode in the geochronology of mineral samples. In addition to geological dating utilizing fission-track detection, the uranium-ruthenium technique is a sensitive indicator of fission in uranium deposits. This is due to the relative geochemical stability of ruthenium, its low natural abundance in the earth's crust and the fact that the Ru isotopic yields from ^{238}U spontaneous fission are quite different from those in naturally occurring Ru. (For a more detailed discussion, see, e.g., Refs. [20, 21].) Although at one time measurements of the spontaneous-fission half-life of ^{238}U differed widely (a factor of ~20), in recent years the measured values have tended to be concentrated in two general regions, viz. $\sim 10. \times 10^{15}$ y and $\sim 8. \times 10^{15}$ y. The "true" value is now believed to lie in the latter region, and Holden and Zucker [5] have recently recommended the value of $(8.2 \pm 0.1) \times 10^{15}$ y. With an additional 5 new measurements included in the data base, this latest recommendation is only slightly different from the value $(8.08 \pm 0.26) \times 10^{15}$ y, proposed by Holden in an earlier evaluation [4].

^{237}Np: The difficulty with the presently accepted value of the ^{237}Np half-life is that it is based on the result of only one measurement with a good quoted precision (~0.5 %). Confirmation of this value is highly desirable. Some indication that this value may be significantly in error has recently been given by Meadows [22] from a measurement of the ^{237}Np fission cross section (in the MeV region) relative to that of ^{235}U.

Meadows found that his results exhibited a systematic difference of ~4% from those of other experimenters over a considerable range of neutron energy. One potential source of this discrepancy arises from the mass assay of the ^{237}Np samples, which depends ultimately on the ^{237}Np half-life. A satisfactory resolution of this discrepancy would help support the use of ^{237}Np as a neutron flux standard in the MeV region.

^{239}Pu: The many reported values of the half-life of this nuclide have exhibited a variation much larger than the quoted errors of the different measurements, the range being from $\sim 2.40 \times 10^4$ y to $\sim 2.44 \times 10^4$ y. However, over the past 5 to 6 years the reported values have exhibited a much higher degree of agreement and now tend to cluster around $\sim 2.41 \times 10^4$ y.

The value given in Table 1 is the one recommended by the participants in the CRP and is based on an evaluation at CBNM [23], which takes into account the measurements of the participating laboratories in the U. S. Half-Life Evaluation Committee [1] (who recommend the value (24,119 ± 26) y) and the value (24,100 ± 30) y, measured at CBNM [24].

The recommended value also agrees well with the values 24,101.1 ± 11.7 y and 24,129 ± 29 y quite recently obtained by Divadeenam and Stehn [16] and by Axton [17], respectively, in their derivations of a consistent set of thermal neutron constants from an overall least-squares fit to the available experimental data.

^{240}Pu: The value given for the ^{240}Pu half-life in Table 1 represents the result of an evaluation by R. Vaninbroukx [25] which is based on the measurements carried out by the participating laboratories of the U. S. Half-Life Evaluation Committee [2] (who recommend the value 6,564 ± 11 y) and all the older measurements.

^{241}Pu: Perhaps one of the most exhaustively measured quantities in the field of actinide-nuclide decay data is the half-life of ^{241}Pu. Yet, the results obtained using a wide variety of experimental techniques vary over quite a large range (from ~14.1 to ~15.2 y), many times larger than the typically quoted measurement errors. Considerable effort has been devoted to this problem by the participants in the CRP (and by many other individuals, as well). However, the "true" value of the ^{241}Pu half-life is still uncertain. Most recent measurements seem to definitely exclude those values near the upper end of the range. The three most recent half-life determinations utilizing mass spectrometry [26-28] are consistent with the value (14.36 ± 0.02) y [29]. This value differs appreciably from the results obtained from ^{241}Am in-growth measurements at Harwell [30] and at CBNM [31], which yield values of (14.56 ± 0.15) y and 14.60 ± 0.10 y, respectively. However, sources of systematic error in these latter two measurements have subsequently been identified by their measurers [25] and the results thus called into question. In view of the many problems surrounding the ^{241}Pu half-life, the rather conservative estimate given in Table 1 is recommended at this time.

In his evaluation of the thermal neutron constants of several actinide nuclides, Axton [17] has derived a value for the ^{241}Pu half-life. His result, 14.35 ± 0.19 y, agrees well with the value obtained from the recent mass spectrometry results and with the recommended value in Table 1.

^{252}Cf: The present situation regarding our knowledge of the ^{252}Cf half-life is highly confused. The available information on this important datum has recently been summarized by Smith [32], who has also provided an informative analysis of potential problems associated with many of the individual measurements. The available data appear to cluster around two distinct values for the ^{252}Cf half-life, viz. ~2.638 y and ~2.651 y. Since evidence exists which provides support for the correctness of each of these values, it is not clear which of them represents the "true" ^{252}Cf half-life. Consequently, pending resolution of this discrepancy and following the suggestion of Smith [32], the CRP participants have adopted as an interim value only, the value 2.645 ± 0.008 y. This represents an average of these two values and has an uncertainty large enough to include both of them.

The values given in Table 1 for the partial half-lives of ^{252}Cf have been calculated using this interim value for the total half-life and the value 31.34 ± 0.08 for the alpha/spontaneous fission branching ratio for ^{252}Cf, measured by Aleksandrov et al. [33] and incorporated into the Evaluated Nuclear Structure Data File (ENSDF).

4. CONCLUSIONS

Actinide nuclide half-life data play an important role in many areas of nuclear data measurement and reactor research and technology. As the result of the availability of new experimental data, many of them produced through the collaborative efforts of several measurement groups, the knowledge of those half-lives useful as standards has improved considerably over the past half dozen years or so . However, at the present time, a number of important questions remain unresolved for several nuclides, providing a need for continuing experimental efforts to provide accurate and precise half-life data for the actinide nuclides.

ACKNOWLEDGEMENTS

Useful discussions with R. Vaninbroukx and N. E. Holden during the preparation of this paper are gratefully acknowledged. Helpful comments from A. L. Nichols concerning the manuscript are also greatly appreciated. This work was supported by the U. S. Department of Energy under DOE Contract No. DE-AC07-76ID01570.

REFERENCES

1. Strohm, W. W. , Int. J. Appl. Radiat. Isot. 29, 481 (1978).

2. Strohm, W. W., Int. J. Appl. Radiat. Isot. 35, 155 (1984).

3. Vaninbroukx, R., "Half-Lives of Some Long-Lived Actinides: a Compilation", Euratom Report EUR-5194e (1974).

4. Holden, N. E., "The Uranium Half-Lives: a Critical Review", U. S. DOE Report BNL-NCS-51320 (January, 1981).

5. Holden, N. E. and Zucker, M. S., "^{252}Cf and ^{238}U Nuclear Parameters of Safeguards Interest", U. S. DOE Report BNL-33965 (1983).

6. Proceedings of the IAEA Advisory Group Meeting on Transactinium Isotope Nuclear Data, Karlsruhe, F. R. G., Nov. 3-7, 1975, IAEA-186, Vols. I-III, IAEA, Vienna (1976).

7. Transactinium Isotope Nuclear Data - 1979, IAEA-TECDOC-232, IAEA, Vienna (1980).

8. Vaninbroukx, R., Int. J. Appl. Radiat. Isot. 34, 1259 (1983).

9. Reich, C. W., in K. H. Böckhoff (Ed.) "Nuclear Data for Science and Technology" (D. Riedel, Dordrecht, 1983), pp. 277-280.

10. Reich, C. W. and Vaninbroukx, R., "Current Status of Nuclear Decay Data and Report on the IAEA Coordinated Research Programme on the Measurement and Evaluation of Transactinium Isotope Nuclear Data", invited paper presented at the Third IAEA Advisory Group Meeting on Transactinium Isotope Nuclear Data, Uppsala, Sweden, May 21-25, 1984 (to be published in the proceedings of this conference).

11. Vaninbroukx, R. and Lorenz, A., in Nuclear Data Standards for Nuclear Measurements, Technical Reports Series No. 227 (IAEA, Vienna, 1983), pp. 69-70.

12. Lorenz, A., (Ed.), "Proposed Recommended List of Heavy Element Radionuclide Decay Data - December, 1983 Edition" IAEA Report INDC(NDS) - 149/NE (December, 1983).

13. von Gunten, H. R., Grütter, A., Reist, H. W. and Baggenstos, M., Phys. Rev. C 23, 1110 (1981).

14. Holden, N. E., "Total and Spontaneous Fission Half-Lives of the Uranium and Plutonium Nuclides", contributed paper to this Advisory Group Meeting; also in BNL-NCS-35514-R (November, 1984).

15. Vaninbroukx, R., "Review of the Partial Alpha Half-Life of ^{241}Pu", in Summary Report of the Sixth Research Coordination Meeting on the Measurement and Evaluation of Transactinium Isotope Nuclear Data, Idaho Falls, USA, 21-24 June, 1983, IAEA Report INDC(NDS)-147/GE (November, 1983), pp. 19-23.

16. Divadeenam, M. and Stehn, J. R., "A Least-Squares Fit of Thermal Data for Fissile Nuclei", U. S. DOE Report BNL-NCS-34211 (1984); Ann. Nucl. Energy 11, 375 (1984).

17. Axton, E. J., "Evaluation of the Thermal Neutron Constants of ^{233}U, ^{235}U, ^{239}Pu and ^{241}Pu", invited paper presented at this Advisory Group Meeting. See also, Axton, E. J., European Applied Research Reports 5, 609 (1984).

18. Aleksandrov, B. M., Krivokhatskii, L. S., Malkin, L. Z. and Petrzhak, K. A., At. Energ. 20, 315 (1966), [Sov. J. At. En. 20, 352 (1966)].

19. Poenitz, W. P. and Meadows, J. W., "^{235}U and ^{239}U Sample-Mass Determinations and Intercomparisons", U. S. DOE Report ANL/NDM-84 (November, 1983).

20. Maeck, W. J., Delmore, J. E., Eggleston, R. L. and Spraktes, F. W., "The Measurement of Ruthenium in Uranium Ores and ^{238}U Spontaneous Fission Yields", in Natural Fission Reactors, Proceedings of a Technical Committee Meeting, Paris, 19-21 December, 1977 (IAEA, Vienna, 1978), pp. 521-533.

21. Maeck, W. J., Apt, K. E. and Cowan, G. A., "A Possible Uranium Ruthenium Method for the Measurement of Ore Age", ibid, pp. 535-541.

22. Meadows, J. W., Nucl. Sci. Engr. 85, 271 (1983).

23. Vaninbroukx, R., "Half-Life of ^{239}Pu: Present Status", in Summary Report: Second Coordinated Research Meeting on the Measurement and Evaluation of Transactinium Isotope Nuclear Data, Aix-en-Provence, 30 April-1 May, 1979, IAEA Report INDC(NDS) - 105/N (November, 1979).

24. Vaninbroukx, R., Denecke, B., Gallet, M., Grosse, G., Hendrickx, F. and Zehner, W., Euratom Progress Report NEANDC (E) - 202 3, 26 (1978).

25. Vaninbroukx, R., private communication (August, 1984).

26. Garner, E. L. and Machlan, L. A., Trans. Am. Nucl. Soc. 33, Suppl. 1,3. (1979).

27. Marsh, S. F., Abernathy, R.M., Beckman, R. J. and Rein, J. E., Int. J. Appl. Radiat. Isot. 31, 629 (1980).

28. de Bièvre, P., Gallet, M. and Werz, R., Int. J. Mass Spect. and Ion Phys. 51, 111 (1983).

29. Vaninbroukx, R., "Remarks on the Total Half-Lives of ^{241}Pu and ^{241}Am", in Sixth Research Coordination Meeting on the Measurement and Evaluation of Transactinium Isotope Nuclear Data, Idaho Falls, USA, 21-24 June 1983, IAEA Report INDC(NDS) - 147/GE (November, 1983), pp. 17-18.

30. Whitehead, C., in U.K. Nuclear Data Progress Report for the Period April 1976 to December 1976, UKNDC (76) P86, NEANDC (E) 182U, Vol. 8, INDC (UK) - 29/U (August 1977), p. 41.

31. Vaninbroukx, R., "New Determinations of the Half-Life of ^{241}Pu", in Proceedings of an International Conference on Neutron Physics and Nuclear Data for Reactors and Other Applied Purposes, Harwell, U.K., OECD Nucl. Energy Agency, Paris, 1978, p. 235.

32. Smith, J. R., "Now It's the ^{252}Cf Half-Life Discrepancy", U. S. DOE Report EGG-PBS-6406 (September, 1983).

33. Aleksandrov, B. M., Bak, M. A., Bogdanov, V. G., Bugorkov, S. S., Drapchinskii, L. V., Soloveva, Z. I. and Sorokina, A. V., At. Energ. 28, 361 (1970), [Sov. At. Energy 28, 462 (1970)].

TOTAL AND SPONTANEOUS FISSION HALF-LIVES OF THE URANIUM AND PLUTONIUM NUCLIDES

N.E. HOLDEN
Brookhaven National Laboratory,
Upton, New York,
United States of America

Abstract

The total half-life and the half-life for spontaneous fission are evaluated for the various long-lived nuclides of interest. Recommended values are presented for ^{232}U, ^{233}U, ^{234}U, ^{235}U, ^{236}U, ^{238}U, ^{236}Pu, ^{238}Pu, ^{239}Pu, ^{240}Pu, ^{241}Pu, ^{242}Pu, and ^{244}Pu. The uncertainties are provided at the 95% confidence limit for each of the recommended values.

I. Introduction

The long-lived nuclides of the uranium and plutonium elements are of interest for their use in nuclear reactors, as well as in certain safeguard applications. The total half-lives for the uranium nuclides were reviewed some time ago[1]. At that time, the only spontaneous fission value which was evaluated was ^{238}U. Recently, the plutonium nuclides were reviewed[2] for both total and fission half-lives.

The general procedure followed in this paper has been to review each of the experiments and revise the published values for the latest estimates of the various parameters used by the original authors. For the case of the total half-lives of uranium, only differences from the original work have been discussed.

II. Uranium Isotopes

The only change in the total half-life of the uranium nuclides compared to reference 1 is in the ^{234}U value where Poenitz and Meadows[3] have intercompared 15 samples of ^{235}U from 7 labs and obtained an estimated ^{234}U half-life value. They also left out Meadows earlier value[4] as too uncertain.

For the spontaneous fission measurements, only ^{238}U had been investigated in reference 1 and there are a number of additional values in the literature now[5,6,7,8,9,10].

III. Plutonium Isotopes

It can be noted in the various tables in section VI that the uncertainties quoted by some authors are such that they exclude many other recent measurements from consideration. Undoubtedly, systematic errors have not been carefully considered in these publications.

IV. Discussion of Results

Although the uranium nuclide total half-lives are in reasonable agreement among the various experiments, except perhaps for ^{232}U, more work in evaluation is required for the plutonium nuclides before we have a similar situation. As a result, the recommended values indicate a larger uncertainty than one might obtain by a simple weighted average of data. This procedure (weighted average) is not considered justified at this point. Work will continue in this area.

V References

1 N E Holden, Brookhaven National Lab Report, BNL-NCS-51320 (1981)
2 M S Zucker and N E Holden, Proc 6th ESARDA Symp on Safeguards and Nucl Materials Management Venice, Italy, May 14-18 1984 p 341
3 W P Poenitz and J W Meadows, Argonne National Lab Report, ANL/NDM-84 (Nov 1983)
4 J W Meadows, Argonne National Lab Report, ANL-7610, 44 (1970)
5 M Kase, J Kikuchi and T Doke, Nucl Inst Meth 154, 335 (1978)
6 A G Popeko and G M Ter-Akopian, Nucl Inst Meth 178, 183 (1980)
7 J C Hadler et al, Nucl Tracks 5, 46 (1981)
8 H G de Carvalho et al, Nucl Inst Methods 197, 417 (1982)
9 S N Belenky, M D Skorokhvatov and A V Etenko, Sov Atom Energy 55, 528 (1983)
10 R Vartanian, Helv Phys Acta 57, 416 (1984)
11 A H Jaffey and A Hirsch, unpublished data, 1951 cited in E K Hyde, The Nuclear Properties of the Heavy Elements (Prentice-Hall, Englewood Cliffs, 1964), Vol III, p 75
12 E Segre, Phys Rev 86, 21 (1952)
13. P A Sellars, C M Stevens, M H Studier, Phys Rev 94, 952 (1954)
14 J M Chilton, R A Gilbert, R E Leuze and W S Lyon, J Inorg Nucl Chem 26, 395 (1964)
15 S K Aggarwal et al, Phys Rev C20 1533 (1979)
16 B M Aleksandrov, L.S Krivokhatskii, L Z Malkin and K A Petrzhak, Sov Atom Energy 20, 352 (1966)
17 H R von Gunten, A Greutter, H W Reist and M Baggenstos, Phys Rev C23, 1110 (1981)
18 A H Jaffey K F Flynn, W C Bentley and J O Karttunen, Phys Rev C9, 1991 (1974)
19 R.Vaninbroukx et al, Phys Rev C13, 315 (1976)
20 A M Geidel man et al Izv Akad Nauk SSSR, Ser Fiz 43, 928 (1979)
21 C K Aggarwal, S N Acharya and H C Jain, Radiochem Radioanal Letters 42, 45 (1980)
22 A Ghiorso et al, Phys Rev 87, 163 (1952)
23 E H Fleming Jr, A Ghiorso and B B Cunningham, Phys Rev 88, 642 (1952)
24 P H White G J Wall and F R Pontet, J Nucl Energy A/B19, 33 (1965)
25 P DeBievre et al, Proc Int Conf Chem Nucl Data Meas Appl Canterbury, U K Sept 20-22, 1971 Inst Civil Eng, London p 221 (1972)
26 M Lounsbury and R Durham, Proc Int Conf Chem Nucl Data Meas Appl Canterbury, U K Sept 20-22, 1971 Inst Civil Eng London p 215 (1972)
27 A M Geidel man et al, Izv Akad Nauk SSSR, Ser Fiz 44, 927 (1980)
28 A Greutter et al, Proc Conf Phys Chem of Fission, Rochester, 1973, Vol I, 305 (1974)
29 A O Nier, Phys Rev 55, 150 (1939)
30 G Sayag Compt Rend 232, 2091 (1951)
31 G B Knight, Oak Ridge Nat Lab Report K-663 (Aug 1950)
32 B Wurger, K P Meyer and P Huber, Helv Phys Acta 30 157 (1957)
33 P O Banks and L T Silver, J Geophys Res 71, 4037 (1966)
34 A J Deruytter I G Schroeder and J A More, Nucl Sci Eng 21, 325 (1965)
35 A H Jaffey et al, Phys Rev C4, 1889 (1971)
36 A H Jaffey and A Hirsch, unpublished data, 1949 cited in E K Hyde The Nuclear Properties of the Heavy Elements (Prentice-Hall, Englewood Cliffs, 1964), Vol III, p 75
37 H Conde and M Holmberg, J Nucl Energy 25, 331 (1971)
38 A H Jaffey, H Diamond, A Hirsch and J Mech, Phys Rev 84, 785 (1951)
39 K F Flynn, A H Jaffey W C Bentley and A M Essling, J Inorg Nucl Chem 34 1121 (1972)
40 W J Whitehouse and W Galbraith, Phil Mag 41, 429 (1950)
41 R L Fleischer and P B Price, Phys Rev B133, 2975 (1964)
42 J H Roberts, R Gold and R J Armani, Phys Rev 174, 1482 (1968)
43 A Spadavecchia and B Hahn, Helv Phys Acta 40, 1063 (1967)
44 H R von Gunten, Actinides Rev 1, 275 (1969)
45 D Galliker et al, Helv Phys Acta 43, 593 (1970)
46 D Storzer, Thesis Universitat Heidelberg (1970)
47 J D Kleeman and J F Lovering, Geochim Cosmochim Acta 35, 637 (1971)
48 W M Thury, Acta Phys Aus 33, 375 (1971)
49 M P T Leme, C Renner and M Cattani, Nucl Inst Meth 91, 577 (1971)
50 H A Khan and S A Durrani, Rad Effects 17, 133 (1973)
51 K N Ivanov and K A Petrzhak, Sov Atom Energy 36, 514 (1975)
52 V Emma and S LoNigro, Nucl Inst Meth 128, 355 (1975)
53 G A Wagner et al, Geochim Cosmochim Acta 39, 1279 (1975)
54 K Thiel and W Herr, Earth Planet Sci Letters 30, 50 (1976)
55 D C Hoffman, G P Ford and F O Lawrence, J Inorg Nucl Chem 4, 143 (1957)
56 R A James, A E Florin, H H Hopkins,Jr and A Ghiorso, "The Transuranium Elements, McGraw-Hill, N Y (1959), Paper 22 8, Nat'l Nucl Energy Series, Plutonium Project Record, Div IV Vol 14B Part II, p 160
57 T Nakanishi et al, Nucl Inst Meth in Phys Res 223, 239 (1984)
58 A H Jaffey and J Lerner, Argonne Nat Lab Report ANL-4411, 9 (1950)
59 J F Mech et al, Phys Rev 103, 340 (1956)
60 D C Hoffman, G P Ford and F O Lawrence, J Inorg Nucl Chem 5 6 (1957)
61 W W Strohm and K C Jordan, Trans Amer Nucl Soc 18, 185 (1974)
62 V C Polyukhov et al, Atom Energia 40, 61 (1976)
63 H Diamond, W C Bentley, A H Jaffey and K F Flynn, Phys Rev C15, 1034 (1977)
64 V D Sevostijanov and V P Yartina, Nucl Constants 5 (44), 21 (1981)
65 S K Aggarwal et al, Radiochem Radioanal Letters 46, 69 (1981)
66 A H Jaffey and A Hirsch, Argonne Nat Lab Report ANL-4286 (1949)
67 V A Druin, V P Perelygin and G I Khlebnikov, Sov Phys JETP 13, 913 (1961)
68 J D Hastings and W W Strohm, J Inorg Nucl Chem 34, 25 (1972)
69 R R Gay and R Sher, Bull Amer Phys Soc 20, 160 (1975)
70 B M Aleksandrov et al, Izv Akad Nauk SSSR Ser Fiz 39, 482 (1975)
71. K M Glover, R A P Wiltshire, P J G Rogers and M King, U K Progr Rep NEANDC(E)-162-8 55 (1975)
72 A H Jaffey et al, Phys Rev C16, 354 (1977)
73 L L Lucas, J R Noyce and B M Coursey, Int J Appl Radiat Isotopes 29 501 (1978)
74 S R Gunn, Int J Appl Radiat Isotopes 29, 497 (1978)
75 S F Marsh et al, Int J Appl Radiat Isotopes 29, 509 (1978)
76 P W Seabaugh and K C Jordan, Int J Appl Radiat Isotopes 29 489 (1978)
77 A Prindle et al, Int J Appl Radiat Isotopes 29, 517 (1978)
78 R Vaninbroukx et al, Euratom Progr Rep NEANDC(E)-202-3 26 (1978)
79 D Brown et al, J Radioanal Chem 64, 181 (1981)
80 M G Inghram, D C Hess, P R Fields and G L Pyle, Phys Rev 83 1250 (1951)
81 J P Butler et al, Phys Rev 103, 634 (1956)
82 Ya P Dokuchaev, Atom Energia 6, 74 (1959)
83 F L Oetting, Proc Conf Thermodynamics Nucl Materials, Vienna, Austria Sept 1967 p 55 (1968)
84 A H Jaffey et al, Phys Rev C18, 969 (1978)
85 C R Rudy and K C Jordan, Int J Appl Radiat Isotopes 35 177 (1984)
86 L L Lucas and J R Noyce, Int J Appl Radiat Isotopes 35, 173 (1984)
87 F J Steinkruger, G M Matlack and R J Beckman, Int J Appl Radiat Isotopes 35 171 (1984)
88 R J Beckman, S F Marsh, R M Abernathey and J E Rein Int J Appl Radiat Isotopes 35 163 (1984)
89 E M Kindermann, Hanford Lab Report HW-27660 (1953)
90 F R Barclay et al, Proc Phys Soc (London) A67, 646 (1954)
91 O Chamberlain, G W Farwell and E Segre Phys Rev 94, 156 (1954)
92 V L Mikheev, N K Skobelev, V A Druin and G N Flerov, Sov Phys JETP 10 612 (1959)
93 D E Watt, F J Bannister, J B Laidler and F Brown, Phys Rev 126 264 (1962)
94 L Z Malkin, I D Alkhazov, A S Krivokhatsky and K A Petrzhak Atom Energia 15 158 (1963)
95 P H White, priv comm cited in J Nucl Energy 21, 749 (1967)
96 P Fieldhouse D S Mather and E R Culliford, J Nucl Energy 21 749 (1967)
97 C Budtz-Jorgensen, H H Knitter, M Mailly and R Vogt Euratom Progr Rep NEANDC(E)-212-3 5 (1980
98 C Whitehead, U K Progr Rep NEANDC(E)-182-8, 41 (1977)
99 E L Garner and L A Machlan, Trans Amer Nucl Soc 33, suppl 1, 3 (1979)
100 R Vaninbroukx, Int Conf Neut Phys Nucl Data for Reactors and Other Appl Purposes, Harwell, U K OCED Nucl Energy Agency, Paris, France 1978 p 235
101 S K Aggarwal and H C Jain, Phys Rev C21, 2033 (1980)
102 S F Marsh, R M Abernathey, R J Beckman and J E Rein Int J Appl Radiat Isotopes 31 629 (1980
103 S K Aggarwal, S N Acharya, A R Parab and H C Jain, Radiochem Acta 29 65 (1981)
104 S K Aggarwal, S N Acharya, A R Parab and H C Jain, Phys Rev C23, 1748 (1981)
105 S K Aggarwal, S A Chitambar, A R Parab and H C Jain, Radiochem Radioanal Letters 54 83 (1982
106 P J DeBievre, M Gallet and R Werz, Int J Mass Spectrom Ion Phys 51 111 (1983)
107 J P Butler, M Lounsbury and J S Merritt, Can J Chem 34 253 (1956)
108 C E Bemis,Jr, J Halperin and R Eby, J Inorg Nucl Chem 31 599 (1969)
109 R W Durham and F Molson, Can J Phys 48, 716 (1970)
110 D W Osborne and H E Flotow, Phys Rev C14, 1174 (1976)
111 L S Bulyanitsa et al, Izv Akad Nauk SSSR, Ser Fiz 40, 2075 (1976)
112 J W Meadows, Argonne Nat Lab Report ANL/NDM-38 (1977)
113 S K Aggarwal, S N Acharya, A R Parab and H C Jain, Phys Rev C20 1135 (1979)

114. H.Diamond and R.F Barnes, Phys. Rev. 101, 1064 (1956).
115. P.R.Fields et al., Nat. 212, 131 (1966).
116. P.R.Fields et al., Phys. Rev. 100, 172 (1955).
117. B.M.Gokhberg, S.M.Dubrovina and V.A.Shigih, Sov. J. Nucl. Phys. 25, 11 (1977).

VI. Tabulated Results

Table I Spontaneous Fission Half-life of ^{232}U

Author(Year)	Ref.	$T_{1/2}$ (10^{13} Years)
Jaffey(51)	11	8. (5.5)
Segre(52)	12	> 0.8

Table II Total Half-life of ^{232}U

Author(Year)	Ref.	$T_{1/2}$ (Years)	Comment
Sellars(54)	13	73.6 (3.0)	
Chilton(64)	14	71.7 (0.9)	99.2% enriched sample
Aggarwal(79)	15	68.90 (0.56)	

Table III Spontaneous Fission Half-life of ^{233}U

Author(Year)	Ref.	$T_{1/2}$ (10^{17} Years)	Comment
Segre(52)	12	> 2.7	
Aleksandrov(66)	16	1.2 (0.3)	No mention of correction for ^{232}U. If present to 0.03%, this contribution of ^{232}U would account for discrepancy.
von Gunten(81)	17	> 2.7	97.11% enriched sample

Table IV Total Half-life of ^{233}U

Author(Year)	Ref.	$T_{1/2}$ (10^{5} Years)
Jaffey(74)	18	1.591 (0.001)
Vaninbroukx(76)	19	1.5925 (0.0027)
Geidel'man(79)	20	1.5937 (0.0033)
Aggarwal(80)	21	1.5885 (0.0065)

Table V Spontaneous Fission Half-life of ^{234}U

Author(Year)	Ref.	$T_{1/2}$ (10^{16} Years)
Segre(52)	12	> 0.6
Ghiorso(52)	22	1.6 (0.7)
von Gunten(81)	17	1.42 (0.08)

Table VI Total Half-life of ^{234}U

Author(Year)	Ref.	$T_{1/2}$ (10^{5} Years)	Comment
Fleming(52)	23	2.475 (0.048)	
White(65)	24	2.47 (0.06)	
Meadows(70)	4	2.439 (0.072)	Author withdrew data
DeBievre(72)	25	2.450 (0.008)	
Lounsbury(72)	26	2.458 (0.012)	
Geidel'man(80)	27	2.459 (0.008)	
Poenitz(83)	3	2.457 (0.005)	Mass intercomparison used

Table VII Spontaneous Fission Half-life of ^{235}U

Author(Year)	Ref.	$T_{1/2}$ (10^{18} Years)
Segre(52)	12	0.18
Aleksandrov(66)	16	0.35 (0.09)
Greutter(73)	28	> 1.8
von Gunten(81)	17	9.8 (2.8)

Table VIII Total Half-life of ^{235}U

Author(Year)	Ref.	$T_{1/2}$ (10^{8} Years)
Nier(39)	29	7.04 (0.31)
Sayag(51)	30	6.94 (0.40)
Fleming(52)	23	7.12 (0.31)
Knight(50)	31	7.10 (0.32)
Wurger(57)	32	6.93 (0.27)
White(65)	24	7.12 (0.18)
Banks(66)	33	7.02 (+ 0.14 - 0.06)
Deruytter(65)	34	6.97 (0.19)
Jaffey(71)	35	7.037 (0.011)

Table IX Spontaneous Fission Half-life of ^{238}U

Author(Year)	Ref.	$T_{1/2}$ (10^{16} Years)	Comment
Jaffey(49)	36	2. (1.6)	
Conde(71)	37	2.7 (0.3)	238U/236U = 0.30+-0.03
von Gunten(81)	17	2.43 (0.13)	
Belenky(83)	9	2.7 (0.4)	

Table X Total Half-life of ^{236}U

Author(Year)	Ref.	$T_{1/2}$ (10^{7} Years)
Jaffey(51)	38	2.46 (0.14)
Fleming(52)	23	2.391 (0.057)
Flynn(72)	39	2.3422 (0.0031)

Table XII Partial Half-lives of ^{236}Pu

Author(Year)	Ref.	$T_{1/2}$ (Years)	Decay Mode
Hoffman(57)	55	2.85 (0.10)	alpha
James(59)	56	2.7 (0.3)	alpha
Nakanishi(84)	57	2.87 (0.01)	alpha
Ghiorso(52)	22	3.4 (1.2)x 10^{9}	Spont.Fiss.

Table XIII Alpha Half-life of ^{238}Pu

Author(Year)	Ref.	$T_{1/2}$ (Years)
Jaffey(50)	58	89.59 (0.41)
Mech(58)	59	86 (3.5)
Hoffman(57)	60	86.41 (0.58)
Stoha(74)	61	87.77 (0.023)
Polyukov(76)	62	86.98 (0.39)
Diamond(77)	63	87.71 (0.03)
Sevostijanov(81)	64	86.54 no uncert.
Aggarwal(81)	65	87.98 (0.51)

Table XI Spontaneous Fission Half-life of ^{238}U

Author(Year)	Ref	Spec Act (10^{-17} Years^{-1})
Whitehouse(50)	40	8 38 (0 52)
Segre(52)	12	8 60 (0 29)
Fleischer(64)	41	6 85 (0 20)
Roberts(68)	42	7 03 (0 11)
Spadavecchia(67)	43	8 42 (0 10)
von Gunten(69)	44	8 66 (0 22)
Calliker(70)	45	8 46 (0 06)
Storzer(70)	46	8 49 (0 78)
Kleeman(71)	47	6 8 (0 6)
Thury(71)	48	8 66 (0 43)
Leme(71)	49	7 30 (0 16)
Khan(73)	50	6 82 (0 55)
Ivanov(75)	51	7 12 (0 32)
Emma(75)	52	7 2 (0 2)
Wagner(75)	53	8 7 (0 6)
Thiel(76)	54	8 57 (0 42)
Kase(78)	5	8 22 (0 20)
Popeko(80)	6	7 9 (0 4)
Hadler(81)	7	8 6 (0 4)
de Carvalho(82)	8	11 8 (0 7)
Belenky(83)	9	8 35 (0 40)
Vartanian(84)	10	8 23 (0 43)

Table XIV Spontaneous Fission Half-life of ^{238}Pu

Author(Year)	Ref	$T_{1/2}$ (10^{10} Years)
Segre(52)	12	3 8
Jaffey(49)	66	4 7 (0 4)
Druin(61)	67	5 1 (0 6)
Hastings(72)	68	4 77 (0 14)
Gay(75)	69	4 64 (0 11)

Table XV Half-life of ^{239}Pu

Author(Year)	Ref	$T_{1/2}$ (10^4 Years)	Decay Mode
Aleksandrov(75)	70	2 4060 (0 0038)	Alpha
Glover(75)	71	2 4115 (0 0080)	"
Jaffey(77)	72	2 4131 (0 0016)	"
Lucas(78)	73	2 4112 (0 0016)	"
Gunn(78)	74	2 4102 (0 0020)	"
Marsh(78)	75	2 4164 (0 0014)	"
Seabough(78)	76	2 4101 (0 0020)	"
Prindle(78)	77	2 4051 (0 0016)	"
Vaninbroukx(78)	78	2 4100 (0 0030)	"
Brown(81)	79	2 4088 (0 0051)	"
Segre(52)	12	5 5 x 10^{15} Years	Spont Fiss

Table XVI Alpha Half-life of ^{240}Pu

Author(Year)	Ref	$T_{1/2}$ (Years)
Inghram(51)	80	6505 (45)
Butler(56)	81	6600 (100)
Dokuchaev(59)	82	6610 (55)
Oetting(67)	83	6533 (10)
Jaffey(78)	84	6569 (6)
Rudy(84)	85	6552 4 (1 7)
Lucas(84)	86	6552 2 (5 2)
Steinkryger(84)	87	6571 (7)
Beckman(84)	88	6574 (6 2)

Table XVII Spontaneous Fission Half-life of ^{240}Pu

Author(Year)	Ref	$T_{1/2}$ (10^{11} Years)
Kindermann(53)	89	1 314 (0 028)
Barclay(54)	90	1 225 (0 030)
Chamberlain(54)	91	1 20
Mikheev(59)	92	1 20
Watt(62)	93	1 34 (0 015)
Malkin(63)	94	1 45 (0 02)
White(67)	95	1 27 (0 05)
Fieldhouse(67)	96	1 170 (0 025)
Budtz-Jorgensen(80)	97	1 15 (0 03)

Table XVIII Half-life of ^{241}Pu

Author(Year)	Ref	$T_{1/2}$ (Years)
Stroha(74)	61	14 355 (0 007)
Whitehead(77)	98	14 56 (0 15)
Garner(79)	99	14 38 (0 07)
Vaninbroukx(78)	100	14 60 (0 10)
Aggarwal(80)	101	14 42 (0 09)
Marsh(80)	102	14 38 (0 06)
Aggarwal(81)	103	14 52 (0 08)
Aggarwal(81)	104	14 44 (0 06)
Aggarwal(81)	105	14 32 (0 06)
DeBievre(83)	106	14 33 (0 02)

Table XIX Alpha Half-life of ^{242}Pu

Author(Year)	Ref	$T_{1/2}$ (10^5 Years)
Butler(56)	107	3 649 (0 05)
Butler(56)	81	3 790 (0 05)
Mech(56)	59	3 855 (0 100
Bemis(69)	108	3 823 (0 016)
Durham(70)	109	3 674 (0 07)
Osborne(76)	110	3 763 (0 009)
Bulyanitsa(76)	111	3 702 (0 014)
Meadows(77)	112	3 708 (0 024)
Aggarwal(79)	113	3 754 (0 25)

Table XX Spontaneous Fission Half-life of ^{242}Pu

Author(Year)	Ref.	$T_{1/2}$ (10^{10} Years)
Butler(56)	107	6.65 (0.10)
Mech(56)	59	7.01 (0.19)
Druin(61)	67	6.6 (0.7)
Malkin(63)	94	7.45 (0.17)
Meadows(77)	112	6.74 (0.05)

Table XXI Alpha Half-life of ^{244}Pu

Author(Year)	Ref.	$T_{1/2}$ (10^7 Years)
Diamond(56)	114	7.6 (2)
Butler(56)	81	7.6 (2)
Fields(66)	115	8.12 (0.26)
Beers(69)	108	7.99 (0.10)

Table XXII Spontaneous Fission Half-life of ^{244}Pu

Author(Year)	Ref.	$T_{1/2}$ (10^{10} Years)
Fields(55)	116	2.5 (0.8)
Fields(66)	115	6.67 (0.32)
Goldberg(77)	117	6.8 (0.8)

Table XXIII Recommended Half-lives and Uncertainties

Reference Nuclide	$T_{1/2}$ (total) Years	$T_{1/2}$ (spont.fiss.) Years
^{232}U	69.8 (1.0)	8. (6.) x 10^{13}
^{233}U	1.592 (0.002) x 10^5	> 2.7 x 10^{17}
^{234}U	2.456 (0.005) x 10^5	1.42 (0.08) x 10^{16}
^{235}U	7.037 (0.011) x 10^8	9.8 (2.8) x 10^{18}
^{236}U	2.342 (0.0034) x 10^7	2.43 (0.13) x 10^{16}
^{238}U	4.468 (0.005) x 10^9	8.2 (0.2) x 10^{15}
^{236}Pu	2.9 (0.2)	3.4 (1.2) x 10^9
^{238}Pu	87.7 (0.3)	4.7 (0.2) x 10^{10}
^{239}Pu	2.410 (0.005) x 10^4	5.5 (no uncert.) x 10^{15}
^{240}Pu	6.563 (0.010) x 10^3	1.16 (0.04) x 10^{11}
^{241}Pu	14 4 (0.1)	———
^{242}Pu	3.735 (0.022) x 10^5	6.8 (0.1) x 10^{10}
^{244}Pu	8.00 (0.09) x 10^7	6.7 (0.3) x 10^{10}

TOTAL AND SPONTANEOUS FISSION HALF-LIVES OF THE AMERICIUM AND CURIUM NUCLIDES

N.E. HOLDEN
Brookhaven National Laboratory,
Upton, New York,
United States of America

Abstract

The total half-life and the half-life for spontaneous fission are evaluated for the various long-lived nuclides of interest. Recommended values are presented for ^{241}Am, ^{242m}Am, ^{243}Am, ^{242}Cm, ^{243}Cm, ^{244}Cm, ^{245}Cm, ^{246}Cm, ^{247}Cm, ^{248}Cm, and ^{250}Cm. The uncertainties are provided at the 95% confidence limit for each of the recommended values.

I. Introduction

The long-lived nuclides of the americium and curium elements are of interest for their use in certain safeguard applications.

The general procedure followed in this paper has been to review each of the experiments and list the published values in the enclosed tables. A first estimate of the recommended values is included. Efforts will continue to reevaluate the various experiments to better gauge the systematic errors involved and reassess the total error.

II. References

1. E.Segre, Phys. Rev. 86, 21 (1952).
2. V.L.Mikheev, N.K.Skobelev, V.A.Druin and G.N.Flerov, Sov. Phys. JETP 10, 612 (1960).
3. V.A.Druin, V.L.Mikheev and N.K.Skobelev, Sov. Phys. JETP 13, 216 (1961).
4. D.Galliker, E.Hugentobler and B.Hahn, Helv. Phys. Acta 43, 593 (1970).
5. R.Gold, R.J.Armani and J.H.Roberts, Phys. Rev. C1, 738 (1970).
6. G.R.Hall and T.L.Markin, J. Inorg. Nucl. Chem. 4, 137 (1957).
7. J.C.Wallman, P.Graf and L.Goda, J. Inorg. Nucl. Chem. 7, 199 (1958).
8. F.L.Oetting and S.R.Gunn, J. Inorg. Nucl. Chem. 29, 2659 (1967).
9. R.E.Stone and E.K.Hulet, J. Inorg. Nucl. Chem. 30, 2003 (1968).
10. L.C.Brown and R.C.Propst, J. Inorg. Nucl. Chem. 30, 2591 (1968).
11. J.Jove and R.Robert, Radiochem. Radioanal. Letters 10, 139 (1972).
12. H.Ramthun and W.Muller, Int. J. Appl. Radiat. Isotopes 26, 589 (1975).
13. V.G.Polyukhov, G.A.Timofeev, P.A.Privalova and P.F.Baklanova, Sov. Atom. Energy 36, 402 (1974).
14. J.T.Caldwell, S.C.Fultz, C.D.Bowman and R.W.Hoff, Phys. Rev. 155, 1309 (1967).
15. K.Street, A.Ghiorso and G.T.Seaborg, Phys. Rev. 79, 530 (1950).
16. R.W.Hoff et al., Phys. Rev. 100, 1403 (1955).
17. R.F.Barnes, D.J.Henderson, A.L.Harkness and H.Diamond, J. Inorg. Nucl. Chem. 9, 105 (1959).
18. A.G.Zelenkov et al., Sov. Atom. Energy 47, 1024 (1980).
19. B.M.Aleksandrov, L.S.Krivokhatskii, L.Z.Malkin and K.A.Petrzhak, Sov. Atom. Energy 20, 352 (1966).
20. B.A.Grozdev et al., Sov. Radiochem. 8, 459 (1966).
21. H.Diamond et al., Phys. Rev. 92, 1490 (1953).
22. A.B.Beadle, D.F.Dance, K.M.Glover and J.Milsted, J. Inorg. Nucl. Chem. 12, 359 (1960).
23. V.G.Polyukhov et al., Sov. Atom. Energy 37, 1103 (1974).
24. S.K.Aggarwal, A.R.Parab and H.C.Jain, Phys. Rev. C22, 767 (1980).
25. G.C.Hanna, B.G.Harvey, N.Moss and P.R.Tunnicliffe, Phys. Rev. 81, 466 (1951).
26. R.J.Armani and R.Gold, Proc. Symp. on Standardization of Radionuclides, IAEA-Vienna, Austria,p621 (1967).

27. H Q Zhang, J.C.Xu and T Q.Wan, Chin. J. Nucl. Phys. 1, 21 (1979).
28. K.Raghuraman et al., Radiochem. Radioanal. Letters 55, 1 (1982).
29 H Umezawa, Fifth Research Coordination Meeting on Measurement and Evaluation of Transuranium Isotope Nuclear Data Geel, Belgium. IAEA Rep No. INDC(NDS)-138 p.32 (1982).
30 G C.Hanna, B G Harvey and N.Moss, Phys. Rev. 78, 617 (1950)
31. K.M.Glover and J.Milsted, Nat. 173, 1238 (1954).
32. W.P.Hutchinson and A.G.White, Nat. 173, 1238 (1954)
33 K F Flynn, L E Glendenin and E.P Steinberg, Nucl. Sci Eng 22, 416 (1965).
34. W J Kerrigan and C J Banick, J Inorg Nucl. Chem. 37, 641 (1975)
35. H.Diamond, W.C.Bentley, A.H.Jaffey and K.F.Flynn, Phys. Rev. C15, 1034 (1977).
36. A.V.Jadhav, K.A.Mathew, K Raghuraman and C.K.Sllvaramakrishnan, Proc. Nucl. Chem. and Radiochem. Symp., Waltair, India. Feb. 25-28, 1980 p.184 (1980).
37. S.Usuda and H.Umezawa, J. Inorg. Nucl. Chem. 43, 3081 (1981).
38. S.K.Aggarwal et al., Radiochem. Radioanal. Letters 54, 99 (1982).
39. R.A.P.Wiltshire, Nucl. Inst. Methods in Phys. Res. 223, 535 (1984).
40. A.Ghiorso et al., Phys. Rev. 87, 163 (1952).
41. L.Z.Malkin et al., Sov. At. Energy 15, 955 (1963).
42. D.Metta et al., J. Inorg. Nucl. Chem. 27, 33 (1965).
43. D.M.Barton and P.G.Koontz, J. Inorg. Nucl. Chem. 32, 769 (1970).
44. J.D.Hastings and W.W.Strohm, J. Inorg. Nucl. Chem. 34, 3597 (1972).
45. C.M.Stevens et al., Phys. Rev. 94, 974 (1954).
46. A.M.Friedman et al., Phys. Rev. 95, 1501 (1954).
47. W.T.Carnall, S.Fried and A.L.Harkness, J. Inorg. Nucl. Chem. 17, 12 (1961).
48. W.C.Bentley, J. Inorg. Nucl. Chem. 30, 2007 (1968).
49. W.J.Kerrigan and R.S.Dorsett, J. Inorg. Nucl. Chem. 34, 3803 (1972).
50. E.K.Hulet, S.Thompson and A.Ghiorso, Phys. Rev. 95, 1703 (1954).
51. C.I.Browne et al., J. Inorg. Nucl. Chem. 1, 254 (1955).
52. J.R.Huizenga and H.Diamond, Phys. Rev. 107, 1087 (1957).
53. D.H.Metta, H.Diamond and F.R.Kelly, J. Inorg. Nucl. Chem. 31, 1245 (1969).
54. K.W.MacMurdo, R.M.Harbour and R.W.Benjamin, J. Inorg. Nucl. Chem. 33, 1241 (1971).
55. V.G.Polyukhov, G.A.Timofeev, V.V.Kalygin and P.A.Privalova, Sov. Radiochem. 24, 408 (1982).
56. P.R.Fields et al., Phys. Rev. 102, 180 (1956).
57. S.M.Fried, G.L.Pyle, C.M.Stevens and J.R.Huizenga, J. Inorg. Nucl. Chem. 2, 415 (1956).
58. J.P.Butler, T.A Eastwood, H.G.Jackson and R.P.Schuman, Phys. Rev. 103, 965 (1956).
59. J.E.McCracken et al., J. Inorg. Nucl. Chem. 33, 3251 (1971).
60. V.G.Polyukhov et al., Sov. Radiochem. 19, 414 (1977).
61. H.Diamond, A.M.Friedman, J.E.Gindler and P.R.Fields, Phys. Rev. 105, 679 (1957).
62. P.R.Fields et al., Phys. Rev. 131, 1249 (1963).
63. P.R.Fields et al., Nucl. Phys. A160, 460 (1971).
64. R.P.Schuman, USAEC Rep. No. IN-1218 p.139 (1968).
65. D.N.Metta and P.E.Moreland, J. Inorg. Nucl. Chem. 29, 2822 (1967).

Tabulated Results

Table I Spontaneous Fission Half-life of ^{241}Am

Author(Year)	Ref.	$T_{1/2}$ (10^{14} Years)
Segre(52)	1	> 0.14
Mikheev(60)	2	> 2.
Druin(61)	3	2.3 (0.8)
Galliker(70)	4	0.90 (0.04)
Gold(70)	5	1.147 (0.024)

Table II Total Half-life of ^{241}Am

Author(Year)	Ref.	$T_{1/2}$ (Years)
Hall(57)	6	458.1 (0.5)
Wallman(58)	7	457.7 (1.8)
Oetting(67)	8	432.7 (0.7)
Stone(68)	9	436.6 (3.0)
Brown(68)	10	433. (7.)
Jove(72)	11	426.3 (2.1)
Raathum(75)	12	432 0 (0.2)
Polyukhov(74)	13	432.8 (3.1)

Table III Spontaneous Fission Half-life of ^{242m}Am

Author(Year)	Ref	$T_{1/2}$ (10^{11} Years)
Caldwell(67)	14	9.5 (3.5)

Table IV Partial Half-lives of ^{242m}Am

Author(Year)	Ref.	$T_{1/2}$ (Years)	Decay Mode
Street(50)	15	10000. (no uncert.)	alpha
Hoff(55)	16	850. (no uncert.)	electron capt.
Barnes(67)	17	32000. (1600.)	alpha
Barnes(67)	17	980. (50.)	electron capt.
Barnes(67)	17	152. (7.)	total $T_{1/2}$
Zelenkov(80)	18	141. (2.)	total $T_{1/2}$

Table V Spontaneous Fission Half-life of ^{243}Am

Author(Year)	Ref.	$T_{1/2}$ (10^{14} Years)
Aleksandrov(66)	19	> 0.33 (0.03)
Grozdev(66)	20	2. (0.5)

Table VI Total Half-life of ^{243}Am

Author(Year)	Ref.	$T_{1/2}$ (Years)
Street(50)	15	10000. (no uncert.)
Diamond(53)	21	8100. (600.)
Wallman(58)	7	7951. (48.)
Barnes(67)	17	7289. (160.)
Beadle(60)	22	7224. (50.)
Brown(68)	10	7370. (40.)
Polyukhov(74)	23	7380. (34.)
Aggarwal(80)	24	7358. (42.)

Table VII Spontaneous Fission Half-life of ^{242}Cm

Author(Year)	Ref.	$T_{1/2}$ (10^{6} Years)
Hanna(51)	25	7.2 (0.2)
Amami(67)	26	6.09 (0.18)
Zhang(79)	27	7.46 (0.6)
Raghuraman(82)	28	7.15 (0.15)
Umezawa(82)	29	6.89 (0.17)

Table VIII Total Half-life of ^{242}Cm

Author(Year)	Ref.	$T_{1/2}$ (Days)
Hanna(50)	30	162.5 (2.)
Glover(54)	31	162.46 (0.32)
Hutchinson(54)	32	163.0 (1.8)
Flynn(65)	33	164.4 (0.4)
Kerrigan(75)	34	163.2 (0.2)
Diamond(77)	35	162.76 (0.08)
Zhang(79)	27	163.02 (0.18)
Jadhav(80)	36	162.13 (2.25)
Usuda(81)	37	161.35 (0.30)
Aggarwal(82)	38	163.00 (0.11)
Wiltshire(84)	39	163.0 (0.2)

Table IX Spontaneous Fission Half-life of ^{244}Cm

Author(Year)	Ref.	$T_{1/2}$ (10^7 Years)
Chiorso(52)	40	1.4 (0.2)
Malkin(63)	41	1.46 (0.05)
Metta(65)	42	1.346 (0.006)
Armani(67)	26	1.33 (0.03)
Barton(70)	43	1.250 (0.007)
Hastings(72)	44	1.343 (0.006)

Table X Total Half-life of ^{244}Cm

Author(Year)	Ref.	$T_{1/2}$ (Years)
Stevens(54)	45	19.2 (0.6)
Friedman(54)	46	18.4 (0.5)
Carnall(81)	47	17.59 (0.06)
Bentley(68)	48	18.099 (0.015)
Kerrigan(72)	49	18.12 (0.06)

Table XI Total Half-life of ^{245}Cm

Author(Year)	Ref.	$T_{1/2}$ (Years)
Hulet(54)	50	20000. (no uncert.)
Friedman(54)	46	11500. (5000.)
Browne(55)	51	14300. (2900.)
Huizenga(57)	52	8000. (no uncert.)
Carnall(81)	47	9320. (280.)
Metta(69)	53	8265. (180.)
MacMurdo(71)	54	8532. (53.)
Polyukhov(76)	55	8445. (200.)

Table XII Spontaneous Fission Half-life of ^{246}Cm

Author(Year)	Ref.	$T_{1/2}$ (10^7 Years)
Fields(56)	56	> 1.24
Fried(56)	57	2.0 (0.8)
Metta(69)	53	1.80 (0.01)
MacMurdo(71)	54	1.85 (0.02)

Table XIII Total Half-life of ^{246}Cm

Author(Year)	Ref.	$T_{1/2}$ (Years)
Friedman(54)	46	4000. (600.)
Browne(55)	51	2300. (460)
Butler(56)	58	6620. (320.)
Carnall(81)	47	5480. (170.)
Metta(69)	53	4711. (22.)
MacMurdo(71)	54	4820. (20.)
McCracken(71)	59	4855. (40.)
Polyukhov(76)	60	4852. (76.)

Table XIV Total Half-life of ^{247}Cm

Author(Year)	Ref.	$T_{1/2}$ (10^7 Years)
Diamond(57)	61	> 4.
Fields(63)	62	1.64 (0.24)
Fields(71)	63	1.56 (0.05)

Table XV Spontaneous Fission Half-life of ^{248}Cm

Author(Year)	Ref.	$T_{1/2}$ (10^6 Years)
Butler(56)	58	4.6 (0.5)
Metta(69)	53	4.22 (0.12)
MacMurdo(71)	54	4.20 (0.05)
McCracken(71)	59	4.115 (0.034)

Table XVI Total Half-life of ^{248}Cm

Author(Year)	Ref.	$T_{1/2}$ (10^5 Years)
Schuman(68)	64	4.0 (0.3)
Metta(69)	53	3.84 (0.04)
MacMurdo(71)	54	3.94 (0.04)
McCracken(71)	59	3.703 (0.032)

Table XVII Spontaneous Fission Half-life of ^{250}Cm

Author(Year)	Ref.	$T_{1/2}$ (10^4 Years)
Huizenga(57)	52	2. (no uncert.)
Metta(67)	65	1.13 (0.05)

Table XVIII Recommended Half-lives and Uncertainties

Reference Nuclide	$T_{1/2}$ (total) Years	$T_{1/2}$ (spont.fiss.) Years
^{241}Am	432. (4.)	1.0 (0.1) x 10^{14}
^{242m}Am	141. (6.)	9.5 (3.5) x 10^{11}
^{243}Am	7370. (40.)	2. (0.5) x 10^{14}
^{242}Cm	163.0 (1.0) Days	7.2 (0.2) x 10^6
^{243}Cm	28.5 (0.2)	———
^{244}Cm	18.1 (0.1)	1.3 (0.1) x 10^7
^{245}Cm	8500. (200.)	———
^{246}Cm	4700. (150.)	1.8 (0.1) x 10^7
^{247}Cm	1.6 (0.1) x 10^7	———
^{248}Cm	3.8 (0.1) x 10^5	4.2 (0.1) x 10^6
^{250}Cm	———	1.1 (0.1) x 10^4

EMISSION PROBABILITIES OF SELECTED GAMMA RAYS FOR RADIONUCLIDES USED AS DETECTOR-CALIBRATION STANDARDS

R. VANINBROUKX
Central Bureau for Nuclear Measurements,
Joint Research Centre,
Commission of the European Communities,
Geel

Abstract

A set of values, estimated to consist of the current "best" data is proposed. The recommended values are deduced from the weighted means of all data available at the middle of 1984. The nuclides for which data are given are, according to some adopted criteria, subdivided into two categories:

1. **Primary calibration gamma rays (33 rays)**
2. **Secondary calibration gamma rays (81 rays).**

I. INTRODUCTION

For the reliability of the results of gamma-ray measurements with efficiency calibrated detectors and for the intercomparison of these results, it is essential that the available most accurate and preferably the same decay data for the calibration radionuclides are used by all investigators.

The present evaluation proposes a set of values which is estimated to consist of the current "best" available data. For the detector calibration, the gamma-ray energies are considered to be known to the required accuracy. They have been adopted from the Nuclear Data Sheets. In the present work only the emission probabilities are evaluated.

II. LIST OF RECOMMENDED DATA

The recommended values are evaluated from all known data published up to about the middle of 1984. Generally, the values from the most recent two evaluations for each of the considered nuclides are given. All experimental values not included in at least two of the evaluations taken into account are added. For some particular gamma rays, accurate emission-probability values obtained by combining the well known transition probabilities with the total-internal-conversion-coefficient data evaluated recently by Hansen, 1984, are added too.

From all the considered data, recommended values are deduced by calculating the weighted means according to Topping, 1963. Several experimental data were obtained from measurements with calibrated gamma-ray detectors. For the calibration of these detectors, often the same nuclides and same decay data were used and the results obtained with these calibrated detectors can not be considered as fully independent. Therefore, in the calculation of the uncertainties on the mean values, only the estimated random uncertainties are divided by $\sqrt{n-1}$, where n is the number of available experimental values. Furthermore, it is assumed that for these measurements the systematic uncertainties, due to the efficiency calibration, are at least 0.5 to 2%, according to the photon energy, for gamma rays with energies below 100 keV, and 0.3% above 100 keV.

Generally, only available absolute emission-probability data are considered in the present evaluation. For some restricted cases, where very few absolute data ara available, normalized relative values are considered too.

The nuclides for which emission-probability data are given are subdivided into two categories :

1. Primary calibration gamma rays : Table 1.
2. Secondary calibration gamma rays. Table 2.

Some other nuclides which may be used very occasionally for detector calibration purposes are not considered here. Emission-probability values for them can be taken from the data listed by Hoppes and Schima, 1982 and Lorenz, 1983.

For the first category only nuclides are considered which :

- can be accurately standardized
- have an appropriate half life
- are available with high radionuclidic purity
- have a simple and well known decay scheme, so that corrections for summation effects between coincident photons are small or can be calculated accurately.

Table 1. PRIMARY CALIBRATION GAMMA RAYS

Nuclide	E_γ (keV)	Emission probabilities (P_γ)			
		Reported values	Obtained by	Reference	Recommended value
^{22}Na	1274.5	0.99940 ± 0.00020 0.9994 ± 0.0002 0.9993 ± 0.0002	evaluation idem idem	Martin (1978) Yoshizawa (1980a) Coursol (1982)	0.99935 ± 0.00020
^{24}Na	1368.6	0.99994 ± 0.00003 0.99994 ± 0.00002	evaluation idem	Yoshizawa (1980a) Coursol (1982)	0.99994 ± 0.00002
	2754.0	0.99881 ± 0.00008 0.99876 ± 0.00008	evaluation idem	Yoshizawa (1980a) Coursol (1982)	0.99878 ± 0.00008
^{46}Sc	889.28	0.999840 ± 0.000010 0.999836 ± 0.000016	evaluation idem	Martin (1978) Yoshizawa (1980a)	0.99984 ± 0.00001
	1120.5	0.999870 ± 0.000010 0.999871 ± 0.000012	evaluation idem	Martin (1978) Yoshizawa (1980a)	0.99987 ± 0.00001
^{51}Cr	320.08	0.0983 ± 0.0014 0.0985 ± 0.0009 0.0985 ± 0.0009	evaluation experiment evaluation	Martin (1978) Schötzig (1980) Coursol (982)	0.0985 ± 0.0009

Table 1. Primary calibration gamma rays (cont. 1)

Nuclide	E_γ (keV)	Emission probabilities (P_γ)			
		Reported values	Obtained by	Reference	Recommended value
^{54}Mn	834.84	0.999760 ± 0.000020 0.999746 ± 0.000025 0.99976 ± 0.00002 0.999749 ± 0.000011	evaluation idem idem calculation with P_{tr} = 1.0000 and $\alpha = (2.51 \pm 0.11)10^{-4}$	Martin (1978) Yoshizawa (1980a) Lagoutine (1982) P_{tr} : Verheul 1978) α : Hansen (1984)	0.99975 ± 0.00001
^{57}Co	14.41	0.0954 ± 0.0013 0.0914 ± 0.0024 0.0955 ± 0.0013	evaluation idem calculation with P_{tr} = 0.8779 ±0.0030 and α = 8.18 ± 0.11	Martin (1978) Coursol (1982) P_{tr} : Auble (1977a), Coursol (1982) α : Hansen (1984)	0.093 ± 0.002
	122.06	0.8559 ± 0.0019 0.8568 ± 0.0013 0.8559 ± 0.0015	evaluation idem calculation with P_{tr} = 0.8764 ± 0.0030 and $\alpha = (2.40 \pm 0.14)10^{-2}$	Martin (1978) Coursol (1982) P_{tr} : Auble (1977a), Coursol (1982) α : Hansen (1984)	0.8563 ± 0.0015
	136.47	0.1061 ± 0.0018 0.1058 ± 0.0008 0.1067 ± 0.0013 0.1073 ± 0.0018	evaluation experiment evaluation calculation with P_{tr} = 0.1220 ± 0.0030 and α = 0.137 ± 0.015	Martin (1978) Schötzig (1980) Coursol (1982) P_{tr} : Auble (1977a), Coursol(1982) α : Hansen (1984)	0.1062 ± 0.0010

Table 1. Primary calibration gamma rays (cont. 2)

Nuclide	E_γ (keV)	Emission probabilities (P_γ)			
		Reported values	Obtained by	Reference	Recommended value
^{58}Co	810.78	0.994 ± 0.003 0.99445 ± 0.00010	evaluation idem	Martin (1978) Lagoutine (1982)	0.9944 ± 0.0002
^{60}Co	1173.24	0.9990 ± 0.0002 0.9989 ± 0.0002 0.9989 ± 0.0002	evaluation idem idem	Auble (1979) Yoshizawa (1980a) Coursol (1982)	0.9989 ± 0.0002
	1332.50	0.999824 ± 0.000005 0.999816 ± 0.000015 0.999830 ± 0.00006	evaluation idem idem	Auble (1979) Yoshizawa (1980a) Coursol (1982)	0.99983 ± 0.00001
^{65}Zn	1115.55	0.5075 ± 0.0010 0.5039 ± 0.0026 0.5075 ± 0.0010	evaluation experiment evaluation	Martin (1978) Debertin (1977) Coursol (1984a)	0.5065 ± 0.0020
^{85}Sr	514.00	0.983 ± 0.010 0.984 ± 0.004 0.9929 ± 0.0004 0.988 ± 0.005	evaluation idem idem calculation with P_{tr} = 0.995 ± 0.005 and α = 0.0072 ± 0.0002	Tepel (1980) Yoshizawa (1980a) Coursol (1982) P_{tr} : Tepel (1980), Meyer (1980), Coursol (1982) α : Rösel (1978)	0.988 ± 0.005

Table 1. Primary calibration gamma rays (cont. 3)

Nuclide	E_γ (keV)	Emission probabilities (P_γ)			
		Reported values	Obtained by	Reference	Recommended value
^{88}Y	898.02	0.946 ± 0.005 0.934 ± 0.007 0.937 ± 0.004 0.943 ± 0.004	experiment evaluation experiment experiment	Debertin (1977) Martin (1978) Yoshizawa (1980b) Hoppes (1983)	0.942 ± 0.004
	1836.0	0.9935 ± 0.0003 0.9924 ± 0.0007	evaluation idem	Martin (1978) Yoshizawa (1980a)	0.9930 ± 0.0005
^{94}Nb	702.63	0.9982 ± 0.0001	calculation with P_{tr} = 1.000 and α = 0.00185 ± 0.00005	P_{tr} : Martin (1978) α : Rösel (1978)	0.9982 ± 0.0001
	871.10	0.9989 ± 0.0001	calculation with P_{tr} = 1.000 and α = 0.00108 ± 0.00003	P_{tr} : Martin (1978) α : Rösel (1978)	0.9989 ± 0.0001
^{95}Nb	765.80	0.9980 ± 0.0002 0.9979 ± 0.0002 0.9980 ± 0.0002	evaluation idem idem	Yoshizawa (1980a) Luksch (1983) Coursol (1984a)	0.9980 ± 0.0002

Table 1. Primary calibration gamma rays (cont. 4)

Nuclide	E_γ (keV)	Emission probabilities (P_γ)			
		Reported values	Obtained by	Reference	Recommended value
^{109}Cd	88.03	0.0373 ± 0.0006 0.0361 ± 0.0010 0.0365 ± 0.0006 0.0370 ± 0.0004	evaluation idem idem calculation with P_{tr} = 1.000 and α = 26.0 ± 0.3	Martin (1978) Bertrand (1978) Coursol (1982) P_{tr} : Bertrand (1978) α : Hansen (1984)	0.0368 ± 0.0005
$^{113}In^m$	391.69	0.6490 ± 0.0020 0.6489 ± 0.0017 0.6494 ± 0.0017	evaluation idem calculation with P_{tr} = 1.000 and α = 0.540 ± 0.004	Martin (1978) Coursol (1984b) P_{tr}: Lyttkens (1981) α : Hansen (1984)	0.649± 0.002
$^{115}In^m$	336.23	0.459 ± 0.001 0.458 ± 0.003	evaluation calculation with P_{tr} = 0.950 ± 0.002 and α = 1.072 ± 0.014	Harmatz (1980) P_{tr} : Lederer (1978), Harmatz (1980) α : Hansen (1984)	0.459 ± 0.002
^{125}I	35.49	0.0667 ± 0.0013 0.0666 ± 0.0010 0.0651 ± 0.0013	evaluation idem experiment	Coursol (1982) Tamura (1981) Debertin (1983)	0.0660 ± 0.0010

Table 1. Primary calibration gamma rays (cont. 5)

Nuclide	E_γ (keV)	Emission probabilities (P_γ)			
		Reported values	Obtained by	Reference	Recommended value
^{134}Cs	604.70	0.9764 ± 0.0006 0.9756 ± 0.0032 0.9763 ± 0.0003	evaluation idem idem	Yoshizawa (1980a) Sergeenkov (1981) Coursol (1982)	0.9763 ± 0.0004
	795.84	0.8552 ± 0.0005 0.8544 ± 0.0030 0.8552 ± 0.0003	evaluation idem idem	Yoshizawa (1980a) Sergeenkov (1981) Coursol (1982)	0.8552 ± 0.0004
^{137}Cs	661.66	0.8521 ± 0.0007 0.852 ± 0.002 0.8516 ± 0.0020	evaluation idem experiment	Peker (1983) Coursol (1984b) Ballaux (1983)	0.852 ± 0.001
^{139}Ce	165.85	0.7999 ± 0.0016 0.799 ± 0.003 0.799 ± 0.003 0.7990 ± 0.0005	evaluation idem idem calculation with P_{tr} = 1.000 and α = 0.2516 ± 0.0007	Yoshizawa (1980a) Peker (1981) Coursol (1982) P_{tr} : Peker (1981) α : Hansen (1984)	0.799 ± 0.001
^{141}Ce	145.44	0.4844 ± 0.0041 0.489 ± 0.004 0.485 ± 0.002 0.487 ± 0.006	evaluation experiment evaluation calculation with P_{tr} = 0.699 ± 0.007 and α = 0.435 ± 0.009	Tuli (1978) Schötzig (1980) Coursol (1984b) P_{tr} : Tuli (1978), Coursol (1984b) α : Hansen (1984)	0.486 ± 0.004

Table 1. Primary calibration gamma rays (cont. 6)

Nuclide	E_γ (keV)	Emission probabilities (P_γ)			
		Reported values	Obtained by	Reference	Recommended value
^{198}Au	411.80	0.9556 ± 0.0008 0.9556 ± 0.0007 0.9559 ± 0.0020	evaluation idem calculation with P_{tr} = 0.998 ± 0.001 and α = 0.044 ± 0.002	Yoshizawa (1980a) Lagoutine (1984) P_{tr} : Harmatz (1977), Lagoutine (1984) α : Hansen (1984)	0.9556 ± 0.0007
^{203}Hg	279.20	0.815 ± 0.008 0.8148 ± 0.0008 0.8156 ± 0.0008 0.8149 ± 0.0008	evaluation idem idem calculation with P_{tr} = 1.000 and α = 0.2271 ± 0.0012	Schmorak (1978) Yoshizawa (1980a) Coursol (1982) P_{tr} : Schmorak (1978) α : Hansen (1984)	0.8150 ± 0.0008
^{241}Am	26.35	0.024 ± 0.001 0.0241 ± 0.0005	evaluation experiment	Ellis (1978) Debertin (1983)	0.0241 ± 0.0005
	59.54	0.359 ± 0.006 0.3582 ± 0.0012 0.359 ± 0.003	evaluation experiment evaluation	Ellis (1978) Hutchinson (1983) Bambynek (1984)	0.359 ± 0.003

Table 2. SECONDARY CALIBRATION GAMMA RAYS

Nuclide	E_γ (keV)	Emission probabilities (P_γ)			
		Evaluated values		Weighted mean [a] of recent experimental values	Recommended value
		Evaluation 1	Evaluation 2		
		Lederer (1975)	Coursol (1983)	Balamuth (1983), Norman (1983), Donoghue (1983), Mathews (1983), Davids (1983)	
^{7}Be	477.60	0.1035 ± 0.0008	0.1043 ± 0.0005	0.1060 ± 0.0014	0.1045 ± 0.0010
		Auble (1977b)			
	846.75	0.9887 ± 0.0003			0.9887 ± 0.0003
^{56}Mn	1810.72	0.272 ± 0.008			0.272 ± 0.008
	2113.05	0.143 ± 0.004			0.143 ± 0.004
		Auble (1977b)	Coursol (1984a)	Gehrke (1977), Hautula (1978), Stewart (1980), Yoshizawa (1980b), Grütter (1982)	
	846.76	0.99930 ± 0.00007	0.99926 ± 0.00006	0.99920 ± 0.00007	0.99925 ± 0.00006
	1037.84	0.141 ± 0.002	0.1412 ± 0.0004	0.1407 ± 0.0008	0.1411 ± 0.0005
	1238.29	0.670 ± 0.007	0.668 ± 0.007	0.659 ± 0.004	0.663 ± 0.005
^{56}Co	1360.21	0.0429 ± 0.0004	0.0426 ± 0.0001	0.0426 ± 0.0002	0.0426 ± 0.0002
	1771.35	0.1551 ± 0.0014	0.1548 ± 0.0004	0.1546 ± 0.0007	0.1548 ± 0.0004
	2034.76	0.0778 ± 0.0012	0.0776 ± 0.0003	0.0774 ± 0.0005	0.0776 ± 0.0004
	2598.46	0.1674 ± 0.0022	0.1695 ± 0.0004	0.1704 ± 0.0008	0.1696 ± 0.0004
	3253.42	0.074 ± 0.005	0.0760 ± 0.0015	0.0779 ± 0.0012	0.0770 ± 0.0012

Table 2. Secondary calibration gamma rays (cont. 1)

Nuclide	E_γ (keV)	Emission probabilities (P_γ)			
		Evaluated values		Weighted mean [a] of recent experimental values	Recommended value
		Evaluation 1	Evaluation 2		
		Luksch (1983)	Coursol (1984		
^{95}Zr	724.20	0.4415 ± 0.0023	0.4415 ± 0.0015		0.4415 ± 0.0020
	756.73	0.545 ± 0.002	0.5450 ± 0.0025		0.5450 ± 0.0025
		Martin (1978)	Coursol (1982)		
$^{99}Tc^m$	140.51	0.8897 ± 0.0024	0.890 ± 0.002		0.890 ± 0.002
		Lagoutine (1982)	De Gelder (1983)		
	446.81	0.0368 ± 0.0003	0.0375 ± 0.0003		0.0372 ± 0.0003
	657.76	0.9437 ± 0.0010	0.9464 ± 0.0038		0.9440 ± 0.0010
	677.62	0.1048 ± 0.0010	0.1035 ± 0.0008		0.1040 ± 0.0008
	687.02	0.0644 ± 0.0003	0.0644 ± 0.0006		0.0644 ± 0.0003
	706.68	0.1668 ± 0.0005	0.1644 ± 0.0010		0.1660 ± 0.0010
	744.28	0.0465 ± 0.0006	0.0473 ± 0.0003		0.0470 ± 0.0004
$^{110}Ag^m$	763.94	0.2245 ± 0.0007	0.2229 ± 0.0009		0.2239 ± 0.0008
	818.03	0.0730 ± 0.0004	0.0734 ± 0.0004		0.0732 ± 0.0004
	884.68	0.727 ± 0.003	0.727 ± 0.003		0.727 ± 0.003
	937.49	0.3426 ± 0.0012	0.3436 ± 0.0012		0.3431 ± 0.0012
	1384.30	0.242 ± 0.001	0.2428 ± 0.0008		0.2425 ± 0.0008
	1475.79	0.0398 ± 0.0003	0.0400 ± 0.0002		0.0399 ± 0.0002
	1505.04	0.1305 ± 0.0006	0.1304 ± 0.0005		0.1304 ± 0.0004

Table 2. Secondary calibration gamma rays (cont. 2)

Nuclide	E_γ (keV)	Emission probabilities (P_γ)			
		Evaluated values		Weighted mean [a] of recent experimental values	Recommended value
		Evaluation 1	Evaluation 2		
		Harmatz (1979)	Coursol (1982)		
^{111}In	171.28	0.903 ± 0.003 [b]	0.902 ± 0.003		0.902 ± 0.003
	245.35	0.940 ± 0.002 [b]	0.940 ± 0.002		0.940 ± 0.002
		Meixner (1971)	Martin (1978)	Johnson (1974)	
	602.73	0.982 ± 0.001	0.9792 ± 0.0005	0.983 ± 0.001 [b]	0.9800 ± 0.0010
	645.86	0.0730 ± 0.0010	0.0721 ± 0.0022	0.0740 ± 0.0016	0.0730 ± 0.0010
^{124}Sb	722.79	0.1180 ± 0.0020	0.1126 ± 0.0016	0.1097 ± 0.0020	0.1130 ± 0.0020
	1690.98	0.483 ± 0.001	0.488 ± 0.005	0.504 ± 0.010	0.485 ± 0.003
	2090.94	0.0570 ± 0.009	0.0558 ± 0.0010	0.0576 ± 0.0014	0.0566 ± 0.0009
		Yoshizawa (1980a)	Coursol (1984a)	Chauvenet (1983), Debertin (1983), Yoshizawa (1983)	
	53.16		0.0220 ± 0.0004	0.0219 ± 0.0003	0.0219 ± 0.0003
	79.62		0.0263 ± 0.0008	0.0262 ± 0.0007	0.0262 ± 0.0007
	81.00		0.341 ± 0.005	0.341 ± 0.005	0.341 ± 0.005
^{133}Ba	276.40	0.0715 ± 0.0003	0.0717 ± 0.0004	0.0716 ± 0.0004	0.0716 ± 0.0004
	302.85	0.1828 ± 0.0008	0.1832 ± 0.0007	0.1832 ± 0.0008	0.1831 ± 0.0007
	356.02	0.6200 ± 0.0014	0.620 ± 0.003	0.6200 ± 0.0015	0.6200 ± 0.0014
	383.85	0.0892 ± 0.0004	0.0893 ± 0.0006	0.0892 ± 0.0005	0.0892 ± 0.0005

Table 2. Secondary calibration gamma rays (cont. 3)

Nuclide	E_γ (keV)	Emission probabilities (P_γ)			
		Evaluated values		Weighted mean [a] of recent experimental values	Recommended value
		Evaluation 1	Evaluation 2		
^{152}Eu		Lederer (1978) [c]	Martin (1978)	Gehrke (1977) [c], Debertin (1979), Yoshizawa (1980c) [c], Debertin (1983)	
	121.78	0.2840 ± 0.0036	0.2838 ± 0.0023	0.2843 ± 0.0023	0.2840 ± 0.0023
	244.70	0.0746 ± 0.0013	0.0751 ± 0.0007	0.0751 ± 0.0007	0.0751 ± 0.0007
	344.28	0.2658 ± 0.0041	0.2658 ± 0.0019	0.2660 ± 0.0019	0.2658 ± 0.0019
	411.12	0.0223 ± 0.0002	0.0223 ± 0.0001	0.0223 ± 0.0002	0.0223 ± 0.0002
	443.98	0.0309 ± 0.0004	0.0312 ± 0.0003	0.0313 ± 0.0003	0.0312 ± 0.0003
	778.90	0.1290 ± 0.0018	0.1296 ± 0.0007	0.1296 ± 0.0007	0.1296 ± 0.0007
	964.1	0.1443 ± 0.0020	0.1462 ± 0.0006	0.1463 ± 0.0006	0.1462 ± 0.0006
	1085.9	0.0970 ± 0.0015	0.1016 ± 0.0005	0.1014 ± 0.0006	0.1014 ± 0.0006
	1112.1	0.1353 ± 0.0020	0.1356 ± 0.0006	0.1353 ± 0.0006	0.1354 ± 0.0006
	1408.0	0.2085 ± 0.0009	0.2085 ± 0.0009	0.2085 ± 0.0008	0.2085 ± 0.0008
^{182}Ta		Schmorak (1975) [d]	Martin (1978)	Schötzig (1980), Jin (1983)	
	100.11	0.142 ± 0.003	0.140 ± 0.005	0.1424 ± 0.0025	0.1423 ± 0.0025
	152.43	0.072 ± 0.003	0.0715 ± 0.0019	0.0700 ± 0.0008	0.0702 ± 0.0008
	222.10	0.076 ± 0.003	0.0754 ± 0.0025	0.0757 ± 0.0008	0.0757 ± 0.0008
	1121.3	0.353 ± 0.008	0.349 ± 0.006	0.3532 ± 0.0020	0.3530 ± 0.0020
	1189.0	0.166 ± 0.004	0.164 ± 0.004	0.1641 ± 0.0010	0.1642 ± 0.0010
	1221.4	0.276 ± 0.006	0.273 ± 0.006	0.2715 ± 0.0022	0.2720 ± 0.0022
	1231.0	0.117 ± 0.003	0.1155 ± 0.0025	0.1157 ± 0.0008	0.1157 ± 0.0008

Table 2. Secondary calibration gamma rays (cont. 4)

Nuclide	E_γ (keV)	Emission probabilities (P_γ)			
		Evaluated values		Weighted mean [a] of recent experimental values	Recommended value
		Evaluation 1	Evaluation 2		
^{192}Ir		Shirley (1983)	Coursol (1984c)	Schötzig (1983a)	
	295.96	0.287 ± 0.002	0.287 ± 0.001	0.286 ± 0.003	0.287 ± 0.001
	308.46	0.297 ± 0.002	0.298 ± 0.001	0.298 ± 0.003	0.298 ± 0.001
	316.51	0.830 ± 0.004	0.830 ± 0.003	0.828 ± 0.007	0.830 ± 0.003
	468.07	0.477 ± 0.003	0.478 ± 0.001	0.477 ± 0.004	0.477 ± 0.002
	588.59	0.0448 ± 0.0003	0.0448 ± 0.0002	0.0451 ± 0.0004	0.0449 ± 0.0002
	604.41	0.0809 ± 0.0005	0.0809 ± 0.0003	0.0819 ± 0.0006	0.0811 ± 0.0004
	612.47	0.0526 ± 0.0003	0.0528 ± 0.0003	0.0531 ± 0.0004	0.0528 ± 0.0003
^{207}Bi		Martin (1978)	Yoshizawa (1980)	Yoshizawa (1980b)	
	569.70	0.978 ± 0.005	0.9794 ± 0.0003	0.9794 ± 0.0003	0.979 ± 0.001
	1063.66	0.749 ± 0.011	0.740 ± 0.003	0.740 ± 0.003	0.741 ± 0.003
	1770.2	0.0685 ± 0.0020	0.0687 ± 0.0004	0.0687 ± 0.0004	0.0687 ± 0.0004

Table 2. Secondary calibration gamma rays (cont. 5)

Nuclide	E_γ (keV)	Emission probabilities (P_γ)			
		Evaluated values			
		Evaluation 1	Evaluation 2	Weighted mean [a] of recent experimental values	Recommended value
^{232}U and ^{228}Th decay chains at equilibrium	238.63	Lederer (1978), Several Volumes of Nucl. Data Sheets [e]	Vaninbroukx (1984a)	Sadasivan (1982), Schötzig (1983b), Vaninbroukx (1983), Banham(1984), Gehrke (1984)	
	241.00	0.436 ± 0.013	0.435 ± 0.002	0.435 ± 0.002	0.435 ± 0.002
	510.80	0.039 ± 0.001	0.0404 ± 0.0005	0.0404 ± 0.0005	0.0404 ± 0.0005
	583.14	0.081 ± 0.003	0.0825 ± 0.0014	0.0826 ± 0.0014	0.0825 ± 0.0014
	727.18	0.3084 ± 0.0030	0.3060 ± 0.0017	0.3053 ± 0.0017	0.3060 ± 0.0017
	860.37	0.0665 ± 0.0015	0.0662 ± 0.0006	0.0661 ± 0.0006	0.0662 ± 0.0006
	2614.6	0.0434 ± 0.0010	0.0450 ± 0.0005	0.0450 ± 0.0005	0.0450 ± 0.0005
		0.3586 ± 0.0006	0.3586 ± 0.0006	0.3586 ± 0.0006	0.3586 ± 0.0006
^{243}Am and ^{239}Np at equilibrium	43.5	Martin (1978), Ellis (1981)	Vaninbroukx (1984b,c)	Starozhukov (1977), Popov (1979), Mozhaev (1979), Ahmad (1982), Vaninbroukx (1984d)	
	74.7	0.055 ± 0.005	0.0605 ± 0.0013	0.0605 ± 0.0013	0.0605 ± 0.0013
	106.13	0.60 ± 0.06	0.686 ± 0.015	0.686 ± 0.015	0.686 ± 0.015
	228.19	0.227 ± 0.013	0.272 ± 0.002	0.272 ± 0.002	0.272 ± 0.002
	277.60	0.107 ± 0.006	0.1127 ± 0.0018	0.1127 ± 0.0018	0.1127 ± 0.0018
		0.141 ± 0.004	0.1438 ± 0.0021	0.1440 ± 0.0021	0.1438 ± 0.0021

In the second category nuclides which may be helpful for detector calibrations, but which do not fulfil all the mentioned criteria, are considered. The long-lived *multi-gamma-line nuclides* as e.g. ^{133}Ba, ^{152}Eu and ^{243}Am-^{239}Np are especially well suited for the determination of the long-term efficiency stability of detectors.

Depending on the importance in calibration work of the various nuclides and especially their individual gamma rays, both lists are restricted to rays with emission probabilities higher than 2 to 10%.

Comments on Table 2

(a) The weighted mean values and their uncertainties have been calculated according to Topping, 1963. However, the systematic contributions to the quoted individual uncertainties have not been divided by $\sqrt{n-1}$.

(b) No uncertainties were quoted by the evaluator or author; the uncertainties adopted here were deduced from the estimated uncertainties on the assumed internal conversion coefficients and transition probabilities.

(c) The reported relative emission probabilities (Table 3 of Appendix II) have been normalized to $P_\gamma = 0.2085 \pm 0.0009$ for the 1408 keV ray.

(d) The reported relative emission probabilities have been normalized to $P_\gamma = 0.142 \pm 0.003$ for the 100.1 keV ray.

(e) Detailed references are given by Vaninbroukx, 1984a.

References

Ahmad, I. (1982), Nucl. Instr. and Meth. 193, 9

Auble, R.L. (1977a), Nucl. Data Sheets 20, 327

Auble, R.L. (1977b), Nucl. Data Sheets 20, 253

Auble, R.L. (1979), Nucl. Data Sheets 28, 103

Balamuth, D.P., L. Brown, T.E. Chapuran, J. Klein, R. Middleton and R.W. Zurmühle (1983), Phys. Rev. C27, 1724

Ballaux, C. (1983), Int. J. Appl. Radiat. Isot. 34, 1159

Bambynek, W. (1984), "Selected Gamma-Ray Emission Probabilities in the Decay of ^{241}Am", to be published by IAEA

Banham, M.F. and R. McCrohon (1984), AERE-R11353, in press

Bertrand, F.E. (1978), Nucl, Data Sheets 23, 229

Chauvenet, B., J. Morel and J. Legrand (1983), Int. J. Appl. Radiat. Isot. 34, 479

Coursol, N. (1982), in "Table de Radionucléides", LMRI-CEA, Saclay

Coursol, N. (1983), in "Table de Radionucléides", LMRI-CEA, Saclay

Coursol, N. and F. Lagoutine (1984a), in "Table de Radionucléides", LMRI-CEA, Saclay

Coursol, N. (1984b), in "Table de Radionucléides", LMRI-CEA, Saclay

Davids, C.N., A.J. Elwyn, B.W. Filippone, S.B. Kaufman, K.E. Rehm and J.P. Schiffer (1983), Phys. Rev. C 28, 885

Debertin, K., U. Schötzig, K.F. Walz and H.M. Weiss (1977), PTB-Mitteilungen 87, 22

Debertin, K. (1979), Nucl. Instr. and Meth. 158, 479

Debertin, K. and W. Pessara (1983), Int. J. Appl. Radiat. Isot. 34, 515

De Gelder, P., E. Jacobs and D. De Frenne (1983), Nucl. Data Sheets 38, 545

Donoghue, T.R., E. Sugarbaker, M. Wiescher, T.C. Rinckel and K.E. Sale (1983), Phys. Rev. C 28, 875

Ellis, Y.A. (1978), Nucl. Data Sheets 23, 123 (1978)

Ellis-Akovali, Y.A. (1981), Nucl. Data Sheets 33, 79

Gehrke, R.J., R.G. Helmer and R.C. Greenwood (1977), Nucl. Instr. and Meth. 147, 405

Gehrke, R.J., V.J. Novick and J.D. Baker (1984), Int. J. Appl. Radiat. Isot. 35, 581

Grütter, A. (1982), Int. J. Appl. Radiat. Isot. 33, 533

Hansen, H.H. (1984), "Evaluation of K-Shell and Total Internal Conversion Coefficients for Some Selected Nuclear Transitions", European Appl. Res. Report, in press

Harmatz, B. (1977), Nucl. Data Sheets 21, 377

Harmatz, B. (1979), Nucl. Data Sheets 27, 453

Harmatz, B. (1980), Nucl. Data Sheets 30, 413

Hautula, M., A. Antilla and J. Keinonen (1978), Nucl. Instr. and Methods 150, 599

Hoppes, D.D. and F.F. Schima (1983), Int. J. Appl. Radiat. Isot. 34, 491

Hutchinson, J.M.R. and P.A. Mullen (1983), Int. J. Appl. Radiat. Isot. 34, 543

Jin, J., J. Takada, Y. Iwata and Y. Yoshizawa (1983), Nucl. Instr. and Meth. 212, 259

Johnson, J.R. and K.C. Mann (1974), Can. J. Phys. 52, 406

Lagoutine, F. (1982), in "Table de Radionucléides", LMRI-CEA, Saclay

Lagoutine, F. (1984), in "Table de Radionucléides", LMRI-CEA, Saclay

Lederer, C.M. and V.S. Shirley, Eds. (1978), Table of Isotopes, 7th Edition, John Wiley and Sons, New York

Lorenz, A. (1983), in "Nuclear Data Standards for Nuclear Measurements", Technical Report Series No. 227, IAEA, Vienna, pp. 89-97

Luksch, P. (1983), Nucl. Data Sheets 38, 1

Lyttkens, J., K. Nilson and L.P. Ekström (1981), Nucl. Data Sheets 33, 1

Martin, M.J. (1978), in "A Handbook of Radioactive Measurement Procedures", p. 306, NCRP Report No. 58, NCRP Washington, D.C.

Mathews, G.J., R.C. Haight, R.G. Lanier and R.M. White (1983), Phys. Rev. C 28, 879

Meixner, C. (1971), "Gamma-Energie, Teil I", Jül-811-RX

Meyer, R.A., J.E. Fontanilla, N.L. Smith, C.F. Smith and R.C. Ragaini (1980), Phys. Rev. C 21, 2590

Mozhaev, V.K., V.A. Dulin and Yu. K. Kazanskii (1979), Sov. At. Energy 47, 566

Norman, E.B., T.E. Chupp, K.T. Lesko and J.L. Osborne (1983), Phys. Rev. C 27, 1728

Peker, L.K. (1981), Nucl. Data Sheets 32, 1

Peker, L.K. (1983), Nucl. Data Sheets 38, 87

Popov, Yu.S., D.I. Starozhukov, V.B. Mishenev, P.A. Privalova and A.I. Mishenko (1979), Sov. At. Energy 46, 123

Rösel, F., H.M. Fries, K. Alder and H.C. Pauli (1978), Atomic Data and Nucl. Data Tables 21, 91

Sadasivan, S. and V.M. Raghunat (1982), Nucl. Instr. and Meth. 196, 561

Schmorak, M.R. (1975), Nucl. Data Sheets 14, 559

Schmorak, M.R. (1978), Nucl. Data Sheets 24, 117

Schötzig, U., K. Debertin and K.F. Walz (1980), Nucl. Instr. and Meth. 169, 43

Schötzig, U. (1983a), Nucl. Instr. and Meth. 206, 441

Schötzig, U. and K. Debertin (1983b), Int. J. Appl. Radiat. Isot. 34, 533

Sergeenkov, Yu.V. and V.M. Sigalov (1981), Nucl. Data Sheets 34, 475

Shirley, V.S. and J.M. Dairiki (1983), Nucl. Data Sheets 40, 425

Starozhukov, D.I., Yu.S. Popov and P.A. Privalova (1977), Sov. At. Energy 42, 355

Stewart, N.M. and A.M. Shaban (1980), Z. Phys. A 296, 165

Tamura, T., Z. Matumoto and M. Ohshima (1981), Nucl. Data Sheets 32, 497

Tepel, J.W. (1980), Nucl. Data Sheets 30, 501

Topping, J. (1963), "Errors of Observation and their Treatment", 3rd Ed., Chapman and Hall, London, pp. 87-93

Tuli, J.K. (1978), Nucl. Data Sheets 23, 529

Vaninbroukx, R. and H.H. Hansen (1983), Int. J. Appl. Radiat. Isot. 34, 1395

Vaninbroukx, R. (1984a), "Selected Gamma-Ray-Emission Probabilities at Equilibrium for the ^{232}U-^{208}Pb Decay Chain", to be published by IAEA, Vienna

Vaninbroukx, R. (1984b), "Selected Gamma-Ray-Emission Probabilities in the Decay of ^{239}Np", to be published by IAEA, Vienna

Vaninbroukx, R. (1984c), "Selected Gamma-Ray-Emission Probabilities in the Decay of ^{243}Am", to be published by IAEA, Vienna

Vaninbroukx, R., G. Bortels and B. Denecke, (1984d), Int. J. Appl. Radiat. Isot., in press

Verheul, H. and R.L. Auble (1978), Nucl. Data Sheets 23, 455

Yoshizawa, Y., H. Inoue, M. Hoshi, K. Shizuma and Y. Iwata (1980a), "Evaluation of Gamma-Ray Intensities", JAERI-M8811, NEANDC(J)-63/AL

Yoshizawa, Y., Y. Iwata, T. Kaku, T. Katoh, J.Z. Ruan, T. Kojima and Y. Kawada (1980b), Nucl. Instr. and Meth. 174, 109

Yoshizawa, Y., Y. Iwata and Y. Iinuma (1980c), Nucl. Instr. and Meth. 174, 133

Yoshizawa, Y., Y. Iwata, T. Katoh, J.Z. Ruan and Y. Kawada (1983), Nucl. Instr. and Meth. 212, 249

EMISSION PROBABILITIES OF SELECTED X-RAYS FOR RADIONUCLIDES USED AS DETECTOR-CALIBRATION STANDARDS

W. BAMBYNEK
Central Bureau for Nuclear Measurements,
Joint Research Centre,
Commission of the European Communities,
Geel

Abstract

The current status of the X-ray emission probabilities of radionuclides which are useful for detector calibration is reviewed. As well experimental as compiled and/or evaluated results are considered. A list of recommended data is given including information on the availability of the radionuclides.

1. Introduction

The availability of high-resolution solid-state detectors has extended the field of X-ray spectrometry towards lower energies. Usually, Si(Li) detectors are used for energies between 5 and 25 keV and planar high-purity germanium detectors (HPGe) for 25 to about 100 or 150 keV. Accurate efficiency calibration of these detectors requires reliable standard data.

Various compilations and evaluations of radionuclide data including X-ray emission probabilities have been published in the past. S.K. Sethi and B.S. Negi (1977) and B.S. Negi and S. Sadasivan (1980) estimated KX-ray and LX-ray emission probabilities for analytical applications. Tables of decay data have been published by D.C. Kocher (1981). They were generated by processing the decay data sets from the Evaluated Nuclear Structure Data File (ENSDF) with the computer code MEDLIST.

The tables in Appendix A3 of the Handbook of Radioactivity Measurements Procedures (NRP Report No. 58, 1978), which are widely used, were produced from an earlier data set of ENSDF. These data are superseded by those of D.C. Kocher (1981).

In the present paper we review the current status of X-ray emission probabilities of radionuclides which are useful for detector calibrations. As well experimental as compiled and/or evaluated data are considered. The literature between 1965 and 1984 has been scanned. In the present work transition energies are considered to be known with sufficient accuracy. They are not evaluated. Half lives are given only as indicative values. Data for both quantities are taken from C.M. Lederer (1978) and D.C. Kocher (1981). A list of recommended emission probabilities is given in Tables 1 and 2 including information on the availability of the radionuclides.

Table 1. Primary calibration nuclides and their recommended KX-ray emission probabilities

Nuclide	$T_{1/2}$ (a)	KX rays Z	Element	$E_{K\alpha}$ (b) (keV)	$P_{K\alpha}$ (c) (%)	$E_{K\beta}$ (b) (keV)	$P_{K\beta}$ (c) (%)	P_{KX} (c) (%)	Availability (d)
^{49}V	330 d	22	Ti	4.51	17.9 (11)	4.93	2.4 (2)	20.3 (10)	1
^{51}Cr	27.7 d	23	V	4.95	20.1 (6)	5.43	2.7 (1)	22.8 (3)	13
^{54}Mn	312.7 d	24	Cr	5.41	22.6 (4)	5.95	3.0 (1)	25.6 (8)	14
^{55}Fe	2.7 a	25	Mn	5.89	24.9 (5)	6.49	3.4 (2)	28.3 (10)	12
^{57}Co	207 d	26	Fe	6.40	51.0 (2)	7.06	6.9 (3)	57.9 (34)	12
^{58}Co	70.8 d	26	Fe	6.40	23.5 (4)	7.06	3.2 (1)	26.7 (10)	11
^{65}Zn	244.4 d	29	Cu	8.04	34.1 (6)	8.91	4.6 (1)	38.7 (9)	12
^{85}Sr	64.8 d	37	Rb	13.38	50.0 (8)	14.98	8.7 (8)	58.7 (8)	10
^{88}Y	160.6 d	38	Sr	14.14	51.3 (8)	15.86	9.2 (2)	60.5 (8)	11
^{109}Cd	464 d	47	Ag	22.10	82.1 (18)	25.01	17.3 (7)	99.4 (20)	12
^{111}In	2.8 d	48	Cd	23.11	68.4 (20)	26.18	14.5 (6)	83.0 (2)	5
^{113}Sn	115.1 d	49	In	24.14	79.6 (18)	27.36	17.2 (6)	96.8 (6)	7
^{125}I	60.1 d	52	Te	27.38	113.4 (30)	31.12	25.0 (8)	139.0 (30)	14
^{131}Cs	9.9 d	54	Xe	27.75	60.1 (15)	36.20	14.0 (5)	74.1 (10)	2
^{139}Ce	137.7 d	57	La	33.30	63.9 (17)	37.98	15.3 (5)	79.2 (22	11

(a) Half lives are taken from D.C. Kocher (1981)

(b) Energies are taken from C.M. Lederer (1978)

(c) Uncertainties in units of the last digit(s) are given in parentheses

(d) The figures indicate the number of producers offering reference solutions with certified activity concentration, G. Grosse (1983)

Table 2a. Secondary calibration nuclides and their recommended KX-ray emission probabilities

Nuclide	$T_{1/2}$	KX rays Z	Element	$E_{K\alpha}$ (keV)	$P_{K\alpha}$ (%)	$E_{K\beta}$ (keV)	$P_{K\beta}$ (%)	P_{KX} (%)	Availability
^{67}Ga	3.3 d	30	Zn	8.63	49.5 (12)	9.57	6.9 (6)	56.4 (13)	8
^{75}Se	119.8 d	33	As	10.53	48.9 (30)	11.72	7.6 (6)	56.5 (40)	10
$^{93}Nb^{m}$	16.1 a	41	Nb	16.58	9.27 (20)	18.66	1.79 (10)	11.06 (14)	
^{99}Mo	66.0 h	43	Tc	18.33	9.3 (4)	20.66	1.9 (2)	11.2 (5)	10
^{103}Ru	35.4 d	45	Rh	20.17	7.29 (28)	22.78	1.51 (6)	8.80 (30)	6
^{123}I	13.1 h	52	Te	27.38	70.5 (20)	31.12	15.9 (6)	86.4 (20)	3
^{133}Ba	10.5 a	55	Cs	30.85	98.0 (16)	34.9 - 35.9	23.0 (5)	121.0 (16)	13
^{137}Cs	30.2 a	56	Ba	32.06	5.66 (18)	36.3 - 37.4	1.34 (4)	7.0 (2)	14
^{141}Ce	32.5 d	59	Pr	35.85	13.2 (4)	40.6 - 42.0	3.2 (2)	16.4 (5)	8
^{152}Eu	13.6 a	62	Sm	39.91	59.1 (12)	45.3 - 46.6	14.9 (3)	} 74.8 (12)	10
		64	Gd	42.75	0.648 (22)	48.5 - 50.0	0.176 (18)	}	
				$E_{K\alpha 2}$ (keV)	$P_{K\alpha 2}$ (%)	$E_{K\alpha 1}$ (keV)	$P_{K\alpha 1}$ (%)	$E_{K\beta '1}$ (keV)	$P_{K\beta '1}$ (%)	$E_{K\beta '2}$ (keV)	$P_{K\beta '2}$ (%)		
^{201}Tl	73.1 h	80	Hg	68.90	27.6(10)	70.12	46.9(18)	80.2	16.2(40)	82.5	4.5 (2)	95.2 (10)	2
^{203}Hg	46.6 d	81	Tl	70.83	3.8(2)	72.87	6.4(2)	82.5	2.2(1)	84.9	0.63 (3)	13.0 (4)	12
^{207}Bi	33.4 a	82	Pb	72.80	22.6(12)	74.97	38.2(20)	84.9	13.0(10)	87.3	3.9 (3)	77.7 (40)	3

Table 2b. Secondary calibration nuclides and their recommended LX-ray emission probabilities

Nuclide	$T_{1/2}$	LX rays Z	Element	E_{L1} (keV)	P_{L1} (%)	$E_{L\alpha}$ (keV)	$P_{L\alpha}$ (%)	$E_{L\eta\beta}$ (keV)	$P_{L\eta\beta}$ (%)	$E_{L\gamma}$ (%)	$P_{L\gamma}$ (%)	P_{LX} (%)	Availability
^{207}Bi	33.4 a	82	Pb	9.18	0.51 (6)	10.45	9.58(15)	11.3-15.4	19.6 (22)	11.6-15.8	4.5(6)	34.2(10)	3
^{238}Pu	38.8 a	92	U	11.62	0.26 (3)	13.60	4.1 (2)	17.0	6.24(30)	20.4	1.2(1)	11.8(4)	3
^{241}Am	432.2 a	93	Np	11.9	0.86 (3)	13.9	13.3 (4)	17.8	19.4 (6)	20.8	4.9(2)	38.5(8)	12

2. Definitions and Notations

Emission of X rays originates from the reorganization of the atomic shells after creation of an inner-shell vacancy. From the various production modes for these vacancies, here, only orbital electron capture by the nucleus and internal conversion of γ rays are of interest because they occur during radioactive decay.

For a given radionuclide the emission probability of KX rays, taking into account all possible transitions, is given by

$$P_{KX} = \left(\sum_i P_{EC}(E_i)\, P_K(E_i) + \sum_j b_j \left(\frac{\alpha_K}{1+\alpha}\right)_j \right) \omega_K$$

where $P_{EC}(E_i)$ and $P_K(E_i)$ are the relative transition probabilities to the level of energy E_i by total electron capture and by K-electron capture, respectively. The quantities α_K and α are the K-shell and the total internal conversion coefficients and b_j are the respective relative transition probabilities of the γ transition j; ω_K is the K-shell fluorescence yield.

A similar equation is valid for the LX-ray emission probabilities. However, they depend on the mode of vacancy production in the three L subshells, which is different for internal conversion and for electron capture by the nucleus. In addition, interpretation of LX-ray data is complicated by the transfer of the primary vacancies between the L subshells due to Coster-Kronig transitions (W. Bambynek et al., 1972). Figure 1 shows the most important KX- and LX-ray transitions and their notation.

3. Compilation and Evaluation

From the radionuclides emitting X rays we have selected those which are suited for detector calibration and are readily available, which have sufficient long half lives and total X-ray emission probabilities of greater than 5 %. They are subdivided in primary and secondary calibration nuclides. Their published X-ray emission data are compiled in Tables 3 and 4.

The term primary refers to nuclides the emission probability of which was measured directly without using an efficiency calibrated detector or can be calculated from reliable data. All other nuclides are regarded as secondary calibration nuclides.

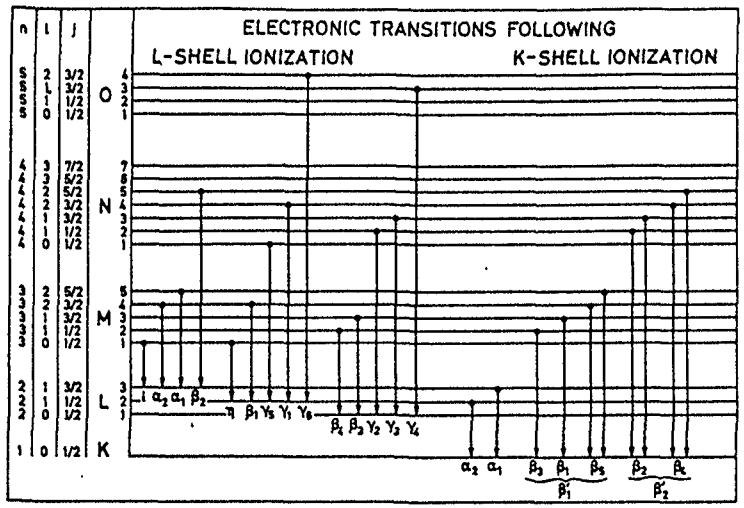

Fig. 1 Most important KX and LX transitions

In the tables the K_α-, K_β- and the total KX-ray emission probabilities are listed. There are a few nuclides with $Z > 65$ for which subdivision into $K_{\alpha 1}$, $K_{\alpha 2}$, $K_{\beta' 1}$ and $K_{\beta' 2}$ seems to be useful. Only very few LX-ray emission probabilities are considered, generally for elements with $Z \geq 82$. They cover the energy range between 9 and 20 keV for which sufficiently accurate K_α or K_β lines from other nuclides are available. The use of LX rays for efficiency calibration of detectors seems to be very limited, that of MX rays is of no importance.

In Fig. 2 the energy vs. Z dependence of these quantities is shown.

Displayed spectra measured with semiconductor detectors can be found in the evaluations of F. Lagoutine and N. Coursol (1982,1984) and in the spectrum catalogues of R.L. Heath (1974) and Ts. Vylov et al. (1980).

The data compiled in Tables 3 and 4 were critically evaluated. All values have been checked and, if necessary, normalized with the to-date best known γ- or X-ray emission probabilities. In addition, the emission probabilities of all nuclides considered have been recalculated with the equation given above and using the following data sources.

- Electron capture probabilities were calculated with electron wave functions of Mann and Waber and exchange and overlap corrections of Bahcall and Vatai,

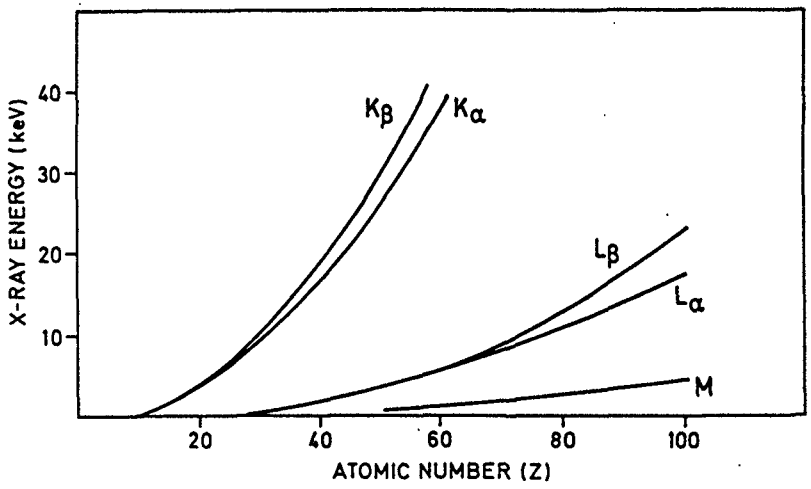

Fig.2 Energies of the characteristic K, L and M lines as function of the atomic number Z

as recalculated by Chen, for $Z \leq 54$ and of Suslov and of Martin and Bichert-Toft for $Z > 54$. The method of calculation and the input data were given by W. Bambynek et al. (1977).

- Fluorescence yields were deduced from the recent evaluation of W. Bambynek (1984).
- Internal conversion data were taken from the compilations of all experimental and evaluation of some selected nuclear transitions of H.H. Hansen (1981, 1984 a, 1984 b). In some cases the evaluated data of F. Lagoutine and N. Coursol (1982, 1984) were used.
- Relative X-ray emission rates K_β/K_α, $K_{\alpha 2}/K_{\alpha 1}$, $K_\beta{}'_1/K_{\alpha 1}$, $K_\beta{}'_2/K_{\alpha 1}$ were taken from S.I. Salem et al. (1984).
- Information on the availability of the radionuclides considered can be found in the compilation of G. Grosse and W. Bambynek (1983).

The uncertainties quoted by the various authors are, as usual, not strictly comparable because they were determined on the basis of different principles. We tried to reestimate the uncertainties corresponding to a 1σ level and used their reciprocals as weights in the calculation of mean values. In general, the maximum of the internal and external error (J. Topping, 1963) was used as uncertainty of the mean. The recommended values of the X-ray emission probabilities are listed in Tables 1 and 2.

Finally it should be noted that the peak shapes of X-ray lines are different from those of γ-ray lines in spectra which are measured with semiconductor detectors. This is due to different natural line width for the two types of radiation. When using the same procedure in the analysis of X- and γ-ray data this can result in calibration errors of several percent as K. Debertin and W. Peßara (1981) have pointed out. The same problem but emphasizing other aspects has been also treated by D.H. Wilkinson (1971) and by C.W. Schulte et al. (1980).

Table 3. Primary calibration nuclides and their X-ray emission probabilities in %

Nuclide	$P_{K\alpha}$ (%)	$P_{K\beta}$ (%)	P_{KX} (%)	Method	First author, year
^{49}V	EC, 100 %, $T_{1/2}$ = 330 (15) d, A 1 [a], P [b]				
	Ti - K_α 4.51 (keV)	Ti - K_β 4.93 (keV)	Ti - KX total		
	17.3 (11)	2.29 (20)	19.6 (11)	MEDLIST	D.C. Kocher (1981)
	22.1 (7)	2.9 (1)	25.0 (10)	Evaluated	Yu.V. Kholnov (1982)
	17.9 (11)	2.4 (2)	20.3 (10)	Recommended values	

(a) A 1 indicates that there is at least one producer offering reference solutions with certified activity concentration, see G. Grosse (1983)

(b) Primary calibration nuclide

^{51}Cr	EC, 100 %, $T_{1/2}$ = 27.704 (4) d, A 13, P				
	V - K_α 4.95 (keV)	V - K_β 5.43 (keV)	V - KX total		
			22.7 (3)	KX, N_0	J.G.V. Taylor (1963)
			19.6 (16)	KX-γ coinc.	A. Mukerji (1967)
	19.7 (40)	2.62 (7)	22.33 (42)	Evaluated	Yu.V. Kholnov (1980)
	19.69 (45)	2.62 (9)	22.31 (46)	MEDLIST	D.C. Kocher (1981)
	20.2 (6)	2.4 (1)	22.6 (7)	Evaluated	N. Coursol (1982)
	20.1 (6)	2.7 (1)	22.8 (3)	Recommended values	

Table 3. Continued

Nuclide	$P_{K\alpha}$ (%)	$P_{K\beta}$ (%)	P_{KX} (%)	Method	First author, year
^{54}Mn	EC, 100 %, $T_{1/2}$ = 312.7 (3) d, A 14, P				
	Cr - K_α 5.41 (keV)	Cr - K_β 5.95 (keV)	Cr - KX total		
			25.7 (4)	KX, N_o	J.G.V. Taylor (1963)
			24.3 (12)	KX, N_o	M. Leistner (1965)
			25.14 (17)	KX, N_o	W. Bambynek (1967a)
			24.90 (53)	KX, N_o	M. Petel (1967)
			24.92 (17)	KX-γ coinc.	W. Hammer (1968)
			24.4 (3)	KX-γ coinc.	A.A. Konstantinov (1973a)
			24.7 (9)	KX-γ coinc.	A. Mukerji (1973)
			25.93 (14)	KX, N_o	P. Magnier (1978)
	22.14 (8)	2.99 (6)	25.13 (6)	Evaluated	Yu.V. Kholnov (1980)
	23.13 (45)	2.94 (10)	25.07 (46)	MEDLIST	D.C. Kocher (1981)
	22.8 (9)	2.7 (1)	25.5 (9)	Evaluated	F. Lagoutine (1982)
	22.6 (4)	3.0 (1)	25.6 (8)	Recommended values	

Nuclide	$P_{K\alpha}$ (%)	$P_{K\beta}$ (%)	P_{KX} (%)	Method	First author, year
^{55}Fe	EC, 100 %, $T_{1/2}$ = 2.7 (1) d, A 12, P				
	Mn - K_α 5.89 (keV)	Mn - K_β 6.49 (keV)	Mn - KX total		
			28.3 (2)	KX, N_o	P. Smith (1982)
	24.4 (13)	3.3 (2)	27.7 (20)	Evaluated	Yu.V. Kholnov (1980)
	24.5 (7)	3.29 (25)	27.8 (14)	MEDLIST	D.C. Kocher (1981)
	24.4 (6)	3.3 (2)	27.7 (20)	Evaluated	F. Lagoutine (1984)
	24.9 (5)	3.4 (2)	28.3 (10)	Recommended values	

^{57}Co	EC, 100 %, $T_{1/2}$ = 270 (9) d, A 12, P				
	Fe - K_α 6.40 (keV)	Fe - K_β 7.06 (keV)	Fe - KX total		
			56.9 (8)	KX-γ coinc.	W. Rubinson (1968) [a]
			58.4 (17)	KX-γ coinc.	A. Mukerji (1973a) [a]
	49.6 (24)	6.7 (3)	56.3 (23)	Evaluated	Yu.V. Kholnov (1980)
	49.4 (9)	6.62 (21)	56.0 (10)	MEDLIST	D.C. Kocher (1981)
	49.8 (16)	6.7 (4)	56.5 (20)	Evaluated	N. Coursol (1982)
	51.0 (2)	6.9 (3)	57.9 (34)	Recommended values	

(a) Internal conversion accounted for with α_K and α values from H.H. Hansen (1984b)

Table 3. Continued

Nuclide	$P_{K\alpha}$ (%)	$P_{K\beta}$ (%)	P_{KX} (%)	Method	First author, year
^{58}Co	EC, 85 %, β^+ 15 %, $T_{1/2}$ = 70.80 (7) d, A 11, P				
	Fe - K_α 6.40 (keV)	Fe - K_β 7.06 (keV)	Fe - KX total		
			25.96 (10)	KX, N_o	W. Bambynek (1968b)
	23.1 (6)	3.1 (1)	26.2 (7)	Evaluated	Yu.V. Kholnov (1980)
	23.2 (4)	3.1 (1)	26.3 (5)	MEDLIST	D.C. Kocher (1981)
	23.0 (8)	3.1 (1)	26.1 (10)	Evaluated	F. Lagoutine (1982)
	23.5 (4)	3.2 (1)	26.7 (10)	Recommended values	

^{65}Zn	EC, 98.54 %, β^+ 1.46 %, $T_{1/2}$ = 244.4 (2) d, A 12, P				
	Cu - K_α 8.04 (keV)	Cu - K_β 8.91 (keV)	Cu - KX total		
			39.4 (6)	KX, N_o	J.G.V. Taylor (1963) [a]
			38.70 (26)	KX-γ coinc.	J.W. Hammer (1968) [a]
			38.4 (2)	KX, N_o	W. Bambynek (1968a) [a]
			38.0 (2)	KX-γ coinc.	A. Mukerji (1973a) [a]
	33.47 (49)	4.62 (5)	38.09 (49)	Evaluated	Yu.V. Kholnov (1980)
	34.1 (6)	4.0 (1)	38.7 (6)	MEDLIST	D.C. Kocher (1982)
	34.1 (6)	4.65 (11)	38.7 (9)	Evaluated	N. Coursol (1984)
	34.1 (6)	4.6 (1)	38.7 (9)	Recommended values	

(a) P_{EC} = 0.9854 (2) used

Table 3. Continued

Nuclide	$P_{K\alpha}$ (%)	$P_{K\beta}$ (%)	P_{KX} (%)	Method	First author, year
^{85}Sr	EC, 100 %, $T_{1/2}$ = 64.84 (3) d, A 10, P				
	Rb - K_α 13.38 (keV)	Rb - K_β 14.98 (keV)	Rb - KX total		
			59.59 (35)	KX-γ coinc.	H.H. Grother (1969)
			58.6 (4)	KX, N_0	W. Bambynek (1970)
			58.66 (47)	KX, N_0	D.L. Thomas (1978)
	50.4 (9)	8.7 (2)	51.1 (7)	Evaluated	Yu.V. Kholnov (1980)
	50.1 (8)	8.7 (2)	58.8 (8)	MEDLIST	D.C. Kocher (1981)
	48.3 (8)	8.8 (2)	57.1 (8)	Evaluated	N. Coursol (1982)
	50.0 (8)	8.7 (2)	58.7 (8)	Recommended values	
^{88}Y	EC, 99.786 %, β^+ 0.214 %, $T_{1/2}$ = 160.60 (4) d, A 11, P				
	Sr - K_α 14.14 (keV)	Sr - K_β 15.86 (keV)	Sr - KX total		
			62.77 (32)	KX-γ coinc.	H.H. Grotheer (1969)
			61.2 (4)	KX, N_0	W. Bambynek (1973)
	51.6 (8)	9.3 (1)	60.9 (8)	Evaluated	Yu.V. Kholnov (1980)
	51.1 (15)	9.0 (4)	60.1 (15)	MEDLIST	D.C. Kocher (1981)
	51.3 (8)	9.2 (2)	60.5 (8)	Recommended values	

Nuclide	$P_{K\alpha}$ (%)	$P_{K\beta}$ (%)	P_{KX} (%)	Method	First author, year
^{109}Cd	EC, 100 %, $T_{1/2}$ = 464 (1) d, A 12, P				
	Ag - K_α 22.10 (keV)	Ag - K_β 25.01 (keV)	Ag - KX total		
			92.4 (4)	I_{KX}/I_γ(88)	J.L. Campbell (1972a) [a]
			94.6 (32)		J.L. Campbell (1972b) [a]
			97.5 (30)		O. Dragoun (1976) [a]
			98.7 (28)		D.D. Hoppes (1982) [a]
			100.0 (15)	Calculated	J. Plch (1979)
	81.4 (14)	17.2 (5)	98.6 (15)	Evaluated	Yu.V. Kholnov (1980)
	82.5 (16)	17.43 (56)	99.9 (17)	MEDLIST	D.C. Kocher (1981)
	82.6 (29)	17.4 (7)	100.0 (40)	Evaluated	N. Coursol (1982)
	82.1 (18)	17.3 (3)	99.4 (20)	Recommended values	

(a) Normalized with P_γ(88) = 3.61 (10) % from F.E. Bertrand (1978)

Table 3. Continued

Nuclide	$P_{K\alpha}$ (%)	$P_{K\beta}$ (%)	P_{KX} (%)	Method	First author, year
^{111}In	EC, 100 %, $T_{1/2}$ = 2.83 (1) d, A 5, P				
	Cd - K_α 23.11 (keV)	Cd - K_β 26.18 (keV)	Cd - KX total		
	68.2 (18)	14.6 (6)	82.8 (19)	MEDLIST	D.C. Kocher (1981)
	68.5 (23)	14.7 (4)	83.3 (3)	Evaluated	N. Coursol (1982)
	68.4 (20)	14.5 (6)	83.0 (20)	Recommended values	
^{113}Sn	EC, 100 %, $T_{1/2}$ = 115.1 (3) d, A 7, P				
	In - K_α 24.14 (keV)	In - K_β 27.36 (keV)	In - KX total		
	79.1 (14)	17.3 (4)	96.4 (15)	Evaluated	Yu.V. Kholnov (1980)
	79.4 (18)	17.2 (5)	96.6 (18)	MEDLIST	D.C. Kocher (1981)
	79.6 (8)	17.2 (2)	96.8 (13)	Evaluated	N. Coursol (1984)
	79.6 (8)	17.2 (2)	96.8 (6)	Recommended values	

Nuclide	P_{LX} (%)	$P_{K\alpha}$ (%)	$P_{K\beta}$ (%)	P_{KX} (%)	Method	First author, year
^{125}I	EC, 100 %, $T_{1/2}$ = 60.14 (11) d, A 14, P					
	Te - LX 3.33 - 4.93 (keV)	Te - K_α 27.38 (keV)	Te - K_β 31.12 (keV)	Te - KX total		
				137.9 (27)	KX-γ coinc., Ge(Li)	E. Karttunen (1969) [a]
				139.3 (25)	KX-γ coinc., Ge(Li)	F. Tolea (1974) [a]
				137.9 (23)	KX-γ coinc., Si(Li)	J. Plch (1974a) [a]
	12.3 (12)	115.2 (18)	26.0 (5)	141.2 (18)	Evaluated	Yu.V. Kholnov (1980)
	15 (6)	112.2 (34)	25.4 (11)	137.6 (36)	MEDLIST	D.C. Kocher (1981)
	12.8 (13)	113.4 (31)	25.6 (8)	139.0 (40)	Evaluated	N. Coursol (1982)
	13 (4)	113.4 (30)	25.6 (8)	139.0 (30)	Recommended values	

(a) Internal conversion accounted for with α_K and α values from N. Coursol (1982)

Table 3. (Continued

Nuclide	P_{LX} (%)	$P_{K\alpha}$ (%)	$P_{K\beta}$ (%)	P_{KX} (%)	Method	First author, year
^{131}Cs	EC, 100 %, $T_{1/2}$ = 9.688 (4) d, A 2, P					
	Xe - LX 3.6 - 5.4 (keV)	Xe - K_α 27.75 (keV)	Xe - K_β 36.20 (keV)	Xe - KX total		
				73.4 (6)	KX, N_o	J. Plch (1974b)
	8.8 (8)	59.6 (4)	13.8 (1)	73.4 (6)	Evaluated	Yu.V. Kholnov (1980)
	9 (3)	60.2 (12)	13.9 (4)	74.1 (12)	MEDLIST	D.C. Kocher (1981)
	9.1 (13)	60.3 (16)	14.0 (5)	74.3 (20)	Evaluated	F. Lagoutine (1982)
	9 (2)	60.1 (15)	14.0 (5)	74.1 (10)	Recommended values	

Table 4. Secondary calibration nuclides and their X-ray emission probabilities in %

Nuclide	$P_{K\alpha}$ (%)	$P_{K\beta}$ (%)	P_{KX} (%)	Method	First author, year
^{67}Ga	EC, 100 %, $T_{1/2}$ = 3.26 (1) d, A 8 [a], S [b]				
	Zn - K_α 8.63 (keV)	Zn - K_β 9.57 (keV)	Zn - KX total		
	49.5 (11)	6.92 (15)	56.42 (11)	Calibrated HP Ge	K. Debertin (1979b)
	48.5 (33)	6.6 (3)	55.1 (33)	MEDLIST	D.C. Kocher (1981)
	48.7 (34)	6.8 (7)	56 (6)	Evaluated	Yu.V. Kholnov (1982)
	50.1 (29)	6.9 (6)	57.0 (30)	Evaluated	F. Lagoutine (1984)
	49.5 (12)	6.9 (6)	56.4 (13)	Recommended values	

(a) A 8 indicates that there are at least eight producers offering reference solutions with certified activity concentration, see G. Grosse (1983)

(b) Secondary calibration nuclide

Nuclide	P_{LX} (%)	$P_{K\alpha}$ (%)	$P_{K\beta}$ (%)	P_{KX} (%)	Method	First author, year
^{139}Ce	EC, 100 %, $T_{1/2}$ = 137.66 (13) d, A 11, P					
	La - LX 4.12 - 6.27 (keV)	La - K_α 33.30 (keV)	La - K_β 37.7 - 38.9 (keV)	La - KX total		
				79.4 (6)	KX-γ coinc., Si(Li)	J. Plch (1975) [a]
				80.7 (20)	I_{KX}/I_γ(165)	J.L. Campbell (1972a) [b]
			15.9(5)		Calibrated HPGe	K. Debertin (1983)
	9.9 (10)	64.1 (7)	15.3(2)	79.4 (9)	Evaluated	Yu.V. Kholnov (1980)
	13 (4)	63.9 (17)	15.2(6)	79.1 (18)	MEDLIST	D.C. Kocher (1981)
	12.2 (23)	64.4 (19)	$K_{\beta'1}$:12.4(5) $K_{\beta'2}$: 3.0(1)	79.9 (3)	Evaluated	N. Coursol (1982)
	11.7 (16)	63.9 (17)	15.3(5)	79.2 (22)	Recommended values	

(a) Internal conversion accounted for with α_K and α from H.H. Hansen (1984)

(b) Normalized with P_γ(165) = 79.9 (1) % from R. Vaninbroukx (1984a)

Nuclide	$P_{K\alpha}$ (%)	$P_{K\beta}$ (%)	P_{KX} (%)	Method	First author, year
^{75}Se	EC, 100 %, $T_{1/2}$ = 119.78 (7) d, A 10, S				
	As - K_α 10.53 (keV)	As - K_β 11.72 (keV)	As - KX total		
			51.4 (21)	Calibrated Ge(Li)	T. Paradellis (1969,1970)
			58.0 (20)	KX-γ coinc.	W.M. Chew (1973) [a]
			55.6 (16)	I_{KX}/I_γ(264)	P. Venugopala Rao (1966) [b]
	46.7 (24)	7.1 (5)	53.8 (36)	Evaluated	Yu.V. Kholnov (1980)
	47.5 (23)	7.3 (5)	54.8 (23)	MEDLIST	D.C. Kocher (1981)
	48.6 (27)	7.4 (6)	56.0 (40)	Evaluated	F. Lagoutine (1982)
	49.5 (15)	8.3 (3)	57.8 (15)	I_{KX}/I_γ(264)	K. Singh (1983) [b]
	48.9 (30)	7.6 (6)	56.5 (40)	Recommended values	

(a) Internal conversion accounted for with data from F. Lagoutine (1982)

(b) Normalized with P_γ(264) = 59.1 (8) % from L.P. Ekström (1981)

Table 4. Continued

Nuclide	$P_{K\alpha}$ (%)	$P_{K\beta}$ (%)	P_{KX} (%)	Method	First author, year
$^{93}Nb^{m}$	IT, 100 %, $T_{1/2}$ = 16.13 (10) a, S				
	Nb - K_α 16.58 (keV)	Nb - K_β 18.66 (keV)	Nb - KX total		
			11.6 (4)	Calibrated Si(Li)	W. Bambynek (1978) / R. Vaninbroukx (1980)
			10.7 (3)	Calibrated Si(Li)	W.G. Alberts (1982)
			11.5 (3)	Calibrated Si(Li)	R. Vaninbroukx (1983)
			11.29 (21)	Calibrated Si(Li)	B.M. Coursey (1984) (a,b)
			11.07 (20)	Calibrated Si(Li)	B.M. Coursey (1984) (a,c)
			11.04 (28)	Calibrated Si(Li)	R.J. Gehrke (1984) (a)
			10.99 (18)	def.Ω, NaI(Tl)	B.M. Coursey (1984) (a,d)
	8.9 (4)	1.7 (1)	10.6 (8)	Evaluated	Yu.V. Kholnov (1980)
	9.45 (43)	1.78 (10)	11.23 (44)	MEDLIST	D.C. Kocher (1981)
	9.27 (20)	1.79 (10)	11.06 (14)	Recommended values	

(a) All the 4 values are based on solutions standardized at CBNM by liquid scintillation counting
(b) Value measured at CBNM
(c) Value measured at PTB
(d) Value measured at NBS using a defined-solid-angle NaI(Tl) counter

Nuclide	$P_{K\alpha}$ (%)	$P_{K\beta}$ (%)	P_{KX} (%)	Method	First author, year
^{99}Mo	β^-, 100 %, $T_{1/2}$ = 66.02 (1) h, A 10, S				
	Tc - K_α 18.33 (keV)	Tc - K_β 20.66 (keV)	Tc - KX total		
	9.55 (49)	1.74 (9)	11.29 (50)	Calibrated Si(Li)	J.K. Dickens (1980)
	8.75 (32)	1.73 (9)	10.48 (32)	MEDLIST	D.C. Kocher (1980)
	9.3 (4)	1.86 (10)	11.16 (46)	Evaluated	N. Coursol (1982)
	9.8 (12)	2.0 (4)	11.8 (22)	Evaluated	Yu.V. Kholnov (1982)
	9.3 (4)	1.9 (2)	11.2 (5)	Recommended values	

Table 4. Continued

Nuclide	$P_{K\alpha}$ (%)	$P_{K\beta}$ (%)	P_{KX} (%)	Method	First author, year
^{103}Ru	β^-, 100 %, $T_{1/2}$ = 35.35 (5) h, A 6, S				
	Rh - K_α 20.17 (keV)	Rh - K_β 22.78 (keV)	Rh - KX total		
	7.2 (2)	1.4 (1)	8.6 (4)	Evaluated	Yu.V. Kholnov (1980)
	7.11 (23)	1.45 (17)	8.56 (24)	MEDLIST	D.C. Kocher (1981)
	7.29 (28)	1.51 (6)	8.80 (29)	Evaluated	N. Coursol (1982)
	7.29 (28)	1.51 (6)	8.80 (30)	Recommended values	

Nuclide	$P_{K\alpha}$ (%)	$P_{K\beta}$ (%)	P_{KX} (%)	Method	First author, year
^{123}I	EC, 100 %, $T_{1/2}$ = 13.13 (10) h, A 3, S				
	Te - K_α 27.38 (keV)	Te - K_β 31.12 (keV)	Te - KX total		
	70.6 (18)	16.0 (6)	86.6 (19)	MEDLIST	D.C. Kocher (1981)
	70.5 (18)	15.9 (6)	86.4 (30)	Evaluated	Yu.V. Kholnov (1982)
	70.6 (23)	15.9 (6)	86.5 (33)	Evaluated	F. Lagoutine (1984)
	70.5 (20)	15.9 (6)	86.4 (20)	Recommended values	

Nuclide	P_{LX} (%)	$P_{K\alpha}$ (%)	$P_{K\beta}$ (%)	P_{KX} (%)	Method	First author, year
^{133}Ba	EC, 100 %, $T_{1/2}$ = 10.5 (1) a, A 13, S					
	Cs - LX 3.80 - 5.70 (keV)	Cs - K_α 30.85 (keV)	Cs - K_β 34.9 - 35.9 (keV)	Cs - KX total		
		66.7 (87)	17.5 (23)		Calibrated Ge(Li)	Y. Gurfinkel (1967) (a)
		107.8 (38)	26.0 (8)	133.8 (39)	I_{KX}/I_γ(81)	S. Faermann (1971) (b)
		99.9 (17)	23.2 (3)	123.1 (7)	I_{KX}/I_γ(365)	W.D. Schmidt-Ott (1972a) (b)
		95.1 (22)	22.9 (6)	118.0 (23)	Calibrated HPGe	U. Schötzig (1976,1977)
		97.1 (16)	23.2 (5)	120.3 (17)	Calibrated HPGe	K. Debertin (1983)
		98.82 (67)	23.16 (15)	122.0 (69)	from ICRM	B. Chauvenet (1983) (c)
		99.46 (15)	23.16 (15)	122.6 (66)	comparison	B. Chauvenet (1983) (d)
		98.6 (43)	23.3 (9)	121.9 (44)	Evaluated	Yu.V. Kholnov (1980)
	17 (5)	97.6 (24)	22.8 (9)	120.4 (26)	MEDLIST	D.C. Kocher (1981)
	15 (6)	98.8 (22)	23.2 (8)	122 (3)	Evaluated	N. Coursol (1984)
	16 (6)	98.0 (16)	23.0 (5)	121.0 (16)	Recommended values	

(a) $K_{\alpha 1}$ and $K_{\beta 1}$ only
(b) Normalized with $P_\gamma(88)$ = 34.1 (5) % and $P_\gamma(365)$ = 62.06 (14) %, respectively from R. Vaninbroukx (1984a)
(c) Arithmetic mean
(d) Weighted mean

Table 4. Continued

Nuclide	P_{LX} (%)	$P_{K\alpha}$ (%)	$P_{K\beta}$ (%)	P_{KX} (%)	Method	First author, year
^{137}Cs	β^-, 100 %, $T_{1/2}$ = 30.17 (3) a, A 14, S					
	Ba - LX 3.95 - 5.97 (keV)	Ba - K_α 32.1 (keV)	Ba - K_β 36.3 - 37.4 (keV)	Ba - KX total		
				7.00 (9)	P_{KX}/P_γ	H.H. Hansen (1969) [a]
		5.60 (12)	1.35 (4)	6.95 (13)	Calibrated HP Ge	K. Debertin (1983)
	0.77 (5)	5.67 (18)	1.34 (5)	7.0 (2)	Evaluated	Yu.V. Kholnov (1980)
	1.0 (3)	5.89 (14)	1.39 (6)	7.28 (19)	MEDLIST	D.C. Kocher (1981)
	0.8 (1)	5.48 (12)	1.30 (3)	6.8 (2)	Evaluated	N. Coursol (1984)
	0.8 (2)	5.66 (18)	1.34 (4)	7.0 (2)	*Recommended values*	

(a) Corrected with ω_K = 0.899

Table 4. Continued

Nuclide	$P_{K\alpha}$ (%)		$P_{K\beta}$ (%)		P_{KX} (%)	Method	First author, year
^{152}Eu	EC, 73 %, β^- 27 % (β^+ 0.019 %), $T_{1/2}$ = 13.6 (2) a, A 10, S						
	Sm - K_α 39.91 (keV)	Gd - K_α 42.75 (keV)	Sm - K_β 45.29-46.58 (keV)	Gd - K_β 48.56-49.96 (keV)	Sm+Gd KX total		
	49.2 (35)		12.2 (9)		61.4(36)	I_{KX}/I_γ(344)	A. Notea (1970) [a,b]
	59.1(16)		15.4 (5)		74.5(17)	$I_{KX}/I_{K\alpha 1}$	S. Faermann (1971) [c]
	48.9(16)	0.66 (2)	12.4 (3)	0.166 (50)	74.5(17)	Calibrated Ge(Li)	B. Dasmahapatra (1972)
	59.1(12)	0.648(22)	14.9 (3)	0.176 (18)	74.8(12)	Calibrated HP Ge	K. Debertin (1979a,1983)
	56.9(23)	0.77 (4)	14.2 (10)	0.18 (2)	72.0(35)	Evaluated	Yu.V. Kholnov (1980)
	58.5(14)	0.614(10)	14.6 (5)	0.156 (7)	73.9(15)	MEDLIST	D.G. Kocher (1981)
	59.1(12)	0.648(22)	14.9 (3)	0.176 (18)	74.8(12)	Recommended values	

(a) Includes both Sm and Gd KX rays
(b) Normalized with P_γ(344) = 26.58 (15) from R. Vaninbroukx (1984a)
(c) Normalized with $P_{K\alpha 1}$ = 37.7 (12) % from D.C. Kocher (1981)

Nuclide	P_{LX} (%)	$P_{K\alpha}$ (%)	$P_{K\beta}$ (%)	P_{KX} (%)	Method	First author, year
^{141}Ce	β^-, 100 %, $T_{1/2}$ = 32.50 (4) d, A 8, S					
	Pr - LX 4.45 - 6.81 (keV)	Pr - K_α 35.85 (keV)	Pr - K_β 40.65 - 41.97 (keV)	Pr - KX total		
				16.2 (14)	I_{KX}/I_γ(145)	J.L. Campbell (1972a) [a]
				16.85 (20)	Calibrated Si(Li)	H.H. Hansen (1979)
	2.2 (1)	12.9 (4)	3.1 (1)	16.0 (5)	Evaluated	Yu.V. Kholnov (1980)
	2.7 (4)	13.78 (45)	3.36 (15)	17.14 (48)	MEDLIST	D.C. Kocher (1981)
	2.9 (5)	13.3 (4)	3.26 (9)	16.6 (6)	Evaluated	N. Coursol (1984)
	2.6 (5)	13.2 (4)	3.2 (2)	16.4 (5)	Recommended values	

(a) Normalized with P_γ(145) = 48.6 (4) % from R. Vaninbroukx (1984a)

Nuclide	P_{LX} (%)	$P_{K\alpha 2}$ (%)	$P_{K\alpha 1}$ (%)	$P_{K\beta'1}$ (%)	$P_{K\beta'2}$ (%)	P_{KX} (%)	Method	First author, year
^{201}Tl	EC, 100 %, $T_{1/2}$ = 73.06 (22) h, A 2, S							
	Hg - LX 8.72-14.85 (keV)	Hg - $K_{\alpha 2}$ 68.90 (keV)	Hg - $K_{\alpha 1}$ 70.12 (keV)	Hg - $K_{\beta'1}$ 80.2 (keV)	Hg - $K_{\beta'2}$ 82.5 (keV)	Hg - KX total		
		27.7(81)	47.3(13)	16.2(41)	4.87(16)	96.1(16)	Calibrated HP Ge	K. Debertin (1979b)
		74.0 (13)		21.0 (4)		95.1(14)	Calibrated HP Ge	E. Funck (1983)
	44 (5)	27.4(12)	46.5(19)	20.5 (9)		94.4(24)	MEDLIST	D.C. Kocher (1981)
		27.4(8)	46.6(12)	16.4(5)	4.6 (2)	95.0(14)	Evaluated	F. Lagoutine (1984)
	44 (5)	27.6(10)	46.9(18)	16.2(40)	4.5 (2)	95.2(10)	Recommended values	

Table 4. Continued

Nuclide	P_{LX} (%)	$P_{K\alpha 2}$ (%)	$P_{K\alpha 1}$ (%)	$P_{K\beta'1}$ (%)	$P_{K\beta'2}$ (%)	P_{KX} (%)	Method	First author, year
^{203}Hg	β^-, 100 %, $T_{1/2}$ = 46.585 (8) d, A 12, S							
	Tl - LX 8.95-15.27 (keV)	Tl - $K_{\alpha 2}$ 70.83 (keV)	Tl - $K_{\alpha 1}$ 72.87 (keV)	Tl - $K_{\beta'1}$ 82.5 (keV)	Tl - $K_{\beta'2}$ 84.9 (keV)	Tl - KX total		
		3.7 (2)	6.4(2)	2.3 (1)	0.6 (4)	13.0(5)	$I_{KX}/I_{K\alpha 1}$, Ge(Li)	J.S. Hansen (1970,1972)[a]
		3.77(12)	6.4(2)	2.20 (8)	0.65(3)	13.0(2)	$I_{KX}/I_{K\alpha 1}$, HP Ge	W.D. Schmidt-Ott (1972b)[a]
	6.0 (6)	3.77(12)	6.4(2)	2.83 (9)		13.0(3)	Evaluated	Yu.V. Kholnov (1980)
	7.2 (8)	4.75(25)	8.0(4)	3.55 (19)		16.3(5)	MEDLIST	D.C. Kocher (1981)
	5.4 (2)	3.8 (2)	6.4(2)	2.2 (1)	0.63(3)	13.0(4)	Evaluated	N. Coursol (1982)
	6.0 (12)	3.8 (2)	6.4(2)	2.2 (1)	0.63(3)	13.0(4)	Recommended values	

(a) Normalized with $P_{K\alpha 1}$ = 6.4 (2)

Nuclide	P_{LX} (%)	$P_{K\alpha 2}$ (%)	$P_{K\alpha 1}$ (%)	$P_{K\beta'1}$ (%)	$P_{K\beta'2}$ (%)	P_{KX} (%)	Method	First author, year
^{207}Bi	EC, 100 %, (β^+ 0.012 %), $T_{1/2}$ = 33.4 (8) a, A 3, S							
	Pb - LX 9.18-15.84 (keV)	Pb - $K_{\alpha 2}$ 72.80 (keV)	Pb - $K_{\alpha 1}$ 74.97 (keV)	Pb - $K_{\beta'1}$ 84.9 (keV)	Pb - $K_{\beta'2}$ 87.3 (keV)	Pb - KX total		
	34.2 (20)					77.7(40)	I_{KX}/I_{γ}(569), Si(Li)	P. Venugopala Rao (1969)[a]
	36.4 (36)						Calibrated Si(Li)	P. Venugopala Rao (1971)
		22.0(24)	38.2(20)	12.3 (7)	3.3(4)	75.8(26)	$I_{KX}/I_{K\alpha 1}$, Ge(Li)	S. Faermann (1971)[b]
		22.4(16)	38.2(20)	13.9 (10)	3.9(3)	78.4(28)	$I_{KX}/I_{K\alpha 1}$, Ge(Li)	J.S. Hansen (1970,1972)[b]
	36 (4)	21.8(6)	36.8(9)	16.3 (5)		74.9(12)	MEDLIST	D.C. Kocher (1981)
		22.6(12)	38.2(20)	16.9 (9)		77.7(40)	Evaluated	Yu.V. Kholnov (1980)
		22.6(12)	38.2(20)	13.0 (10)	3.9(3)	77.7(40)	Recommended KX-ray values	
		Pb - L_l 9.18 (keV)	Pb - L_{α} 10.45 (keV)	Pb - L_{η} 11.35 (keV)	Pb - L_{β} 12.14-15.43 (keV)	Pb - L_{γ} 11.65-15.84 (keV)		
	34.2 (20)	0.51(6)	9.58(15)	0.31 (4)	19.3(22)	4.5(6)	Evaluated	Yu.V. Kholnov (1980)
	34.2 (20)	0.51 (6)	9.58(15)	0.31 (4)	19.3(22	4.5(6)	Recommended LX-ray values	

(a) Normalized with P_{γ}(569) = 97.7 (1) % from D.C. Kocher (1981)

(b) Normalized with $P_{K\alpha 1}$ = 38.2 (20) from Yu.V. Kholnov (1980)

Table 4. Continued

^{238}Pu	α, 100 %, $T_{1/2}$ = 87.75 (3) a, A 3, S							
	U - L_l 11.62 (keV)	U - L_α 13.60 (keV)	U - L_η 15.40 (keV)	U - L_β 17.08 (keV)	U - L_γ 20.46 (keV)	U - LX total	Method	First author, year
	P_{Ll} (%)	$P_{L\alpha}$ (%)	$P_{L\eta}$ (%)	$P_{L\beta}$ (%)	$P_{L\gamma}$ (%)	P_{LX} (%)		
		5.05(6)		7.41(9)	1.48(2)	13.9 (11)	Calibrated Si(Li)	D.G. Vasilik (1976)
	0.26 (1)	4.15(7)		5.61(7)	1.36(2)	11.38(10)	Calibrated Ge(Li)	C.E. Bemis (1977)
	0.26 (3)	4.1 (2)	0.14 (2)	6.1 (3)	1.2 (1)	11.8 (4)	Evaluated	Yu.V. Kholnov (1980)
						11.6 (14)	MEDLIST	D.C. Kocher (1981)
	0.25 (1)	3.9 (4)	0.127(5)	4.87(14)	1.15(32)	10.29(32)	Calibrated Si(Li)	P. Driyák (1984)
	0.26 (3)	4.1 (2)	0.14 (2)	6.1 (3)	1.2 (1)	11.8 (4)	Recommended LX-ray values	

^{241*}Am	α, 100 %, $T_{1/2}$ = 432.2 (5) a, A 12, S							
	N_p - L_l 11.9 (keV)	N_p - L_α 13.9 (keV)	N_p - $L_{\eta\beta}$ 17.8 (keV)	N_p - L_γ 20.8 (keV)	N_p - LX total	Method		First author, year
	P_{Ll} (%)	$P_{L\alpha}$ (%)	$P_{L\eta\beta}$ (%)	$P_{L\gamma}$ (%)	P_{LX} (%)			
		15.1 (14)	23.7 (15)	6.4 (8)	45.2 (21)	I_{LX}/I_γ(60), NaI		J.K. Beling (1952) [b]
	0.47 (7)	9.8	17.8	4.6	32.7	I_{LX}/I_γ(60), bc [a]		P.P. Day (1955) [b]
	0.8	13.5	18.4	5.0	37.7	Calibrated NaI		B.L. Magnusson (1957)
	0.81 (7)	12.6 (9)	19.1 (14)	4.8 (4)	37.3 (17)	I_{LX}/I_γ(60), Si(Li)		R.J. Gehrke (1971) [b]
	0.87 (4)	13.6 (8)	19.3 (12)	5.2 (5)	39.0 (15)	$I_{LX}/I_{L\beta 1}$, Si(Li)		R.L. Watson (1971) [c]
			19.46(46)			Calibrated Si(Li)		W.J. Gallaghor (1974)
	0.83 (2)	13.2 (2)	19.25(30)	4.85(10)	38.2 (4)	Calibrated Si(Li)		J.L. Campbell (1974)
	0.806	12.2	20.4	4.94	39.3	Calibrated Ge(Li)		R. Gunnink (1976)
	0.86 (3)	13.20(3)	19.25(60)	4.85(20)	38.2 (7)	Calibrated Si(Li)		C.E. Bemis (1977)
	0.76 (7)	13.1 (7)	13.3 (9)	4.8 (2)	38.0 (12)	$I_{LX}/I_{\beta 1}$, HPGe		H. Maria (1982) [c]
	0.86 (3)	13.3 (4)	19.4 (6)	4.9 (2)	38.5 (8)	Evaluated		Yu.V. Kholnov (1980)
					43 (5)	MEDLIST		D.C. Kocher (1981)
	0.86 (3)	13.3 (4)	19.4 (6)	4.9 (2)	38.5 (8)	Recommended LX-ray values		

(a) bc = bent crystal spectrometer
(b) Normalized with P_γ(60) = 35.9 (3) %
(c) Normalized with P_γ(26) = 2.4 (1) %

References

W.G. Alberts, R. Hollnagel, K. Knauf, W. Peßara (1982), in: Proc. 4th ASTM-EURATOM Symp. on Reactor Dosimetry, Gaithersburg, 1982, NUREG/CP-0029, Vol.I, p. 433.

W. Bambynek (1967a), Z. Phys. 206, 66.

W. Bambynek (1968a), Z. Phys. 214, 374.

W. Bambynek, E. De Roost, E. Funck (1968b), in: D. Berényi (ed.) Proceedings of the Conference on Electron Capture and Higher Order Processes in Nuclear Decays, Debrecen, Hungary, July 15-18, 1968 (Eötvös Lóránd Physical Society, Budapest, 1968) p. 253.

W. Bambynek, D. Reher (1970), Z. Phys. 238, 49.

W. Bambynek, B. Crasemann, R.W. Fink, H.U. Freund, Hans Mark, C.D. Swift, R.E. Price, P. Venugopala Rao (1972), Rev. Mod. Phys. 44, 716.

W. Bambynek, D. Reher (1973), Z. Phys. 264, 253.

W. Bambynek, H. Behrens, M.H. Chen, B. Crasemann, M.L. Fitzpatrick, K.W.D. Ledingham, H. Genz, M. Mutterer, R.L. Intemann (1977), Rev. Mod. Phys. 49, 77, 961.

W. Bambynek, D. Reher, R. Vaninbroukx (1978), Proceedings of an International Conference on Neutron Physics and Nuclear Data for Reactors and other Applied Purposes, Harwell, September 1978, (OECD Nuclear Energy Agency, Paris 1978) p. 778.

W. Bambynek (1984), International Conference on X-Ray and Inner Shell Processes in Atoms, Molecules and Solids, Leipzig, GDR, August 20-24, 1984, Paper P1.

J.K. Beling, J.O. Newton, B. Rose (1952), Phys. Rev. 86, 797.

C.E. Bemis, Jr., L. Tubbs (1977), US-ERDA Report ORNL-2597, p. 93.

F.E. Bertrand (1978), Nucl. Data Sheets 23, 229.

J.L. Campbell, L.A. McNelles (1972a), Nucl. Instr. and Meth. 98, 433.

J.L. Campbell, L.A. McNelles (1972b), Nucl. Instr. and Meth. 101, 153.

J.L. Campbell, L.A. McNelles (1974), Nucl. Instr. and Meth. 117, 519.

B. Chauvenet, J. Morel, J. Legrand (1983), Int. J. Appl. Radiat. Isot. 34, 479.

W.M. Chew, J.C. McGeorge, R.W. Fink (1973), in: R.W. Fink (1973), p. 197.

B.M. Coursey, R. Vaninbroukx, D. Reher, W. Zehner (1984), CBNM Int. Rep. GE/R/RN/11/84.

N. Coursol (1982), in: F. Lagoutine et al. (1984a), (Evaluation of the nuclides ^{51}Cr, ^{57}Co, ^{85}Sr, ^{99}Mo, ^{103}Ru, ^{109}Cd, ^{111}In, ^{125}I, ^{134}Ce, ^{203}Hg).

N. Coursol (1984), in: F. Lagoutine et al. (1984a), (Evaluation of the nuclides ^{113}Sn, ^{137}Cs, ^{141}Ce).

N. Coursol, F. Lagoutine (1984), in: F. Lagoutine et al. (1984a), (Evaluation of the nuclides ^{65}Zn, ^{133}Ba).

B.K. Dasmahapatra (1972), Radiochem. Radioanal. Letters, 12, 185.

P.P. Day (1955), Phys. Rev. 97, 689.

K. Debertin (1979a), Nucl. Instr. and Meth. 165, 279.

K. Debertin, W. Peßara, U. Schötzig, K.F. Walz (1979b), Int. J. Appl. Radiat. Isot. 30, 551.

K. Debertin, W. Peßara (1981), Nucl. Instr. and Meth. 184, 497.

K. Debertin, W. Peßara (1983), Int. J. Appl. Radiat. Isot. 34, 515.

J.K. Dickens, T.A. Love (1980), Nucl. Instr. and Meth. 175, 535.

O. Dragoun, V. Brabec, M. Ryšavý, J. Plch, J. Zderadička (1976), Z. Phys. A 279, 107.

P. Driyák, Yu.S. Yegorov, V.G. Nedovesov, J. Plch, G.Ye. Shukin (1984), Abstracts of the Lectures of the 34th. Conference on Nuclear Spectroscopy and Nuclear Structure, Alma-Ata 17-20 April 1984 (publishing House, Nauka, Leningrad, 1984) p. 540.

L.P. Ekström (1981), Nucl. Data Sheets 32, 211.

S. Faermann, A. Notea, Y. Segal (1971), Trans. Am. Nucl. Soc. 14, 500.

R.W. Fink, S.T. Manson, J.M. Palms, P. Venugopala Rao (eds.) (1973), Proceedings of the International Conference on Inner-Shell Ionization Phenomena and Future Applications, April 17-22, 1972 (USAEC-Technical Information Center, Oak Ridge, Tenn. 1973), CONF-720404.

E. Funck, K. Debertin, K.F. Walz (1983), Int. J. Nucl. Med. Biol. 10, 137.

W.J. Gallagher, S.J. Cipolla (1974), Nucl. Instr. and Meth. 122, 405.

R.J. Gehrke, R.A. Lokken (1971), Nucl. Instr. and Meth. 97, 219.

R.J. Gehrke, J.W. Rogers, J.D. Baker (1984), Proceedings of the 5th ASTM-EURATOM Symposium on Reactor Dosimetry, Geesthacht, FRG, 24 to 28 September 1984.

H.H. Grotheer, J.W. Hammer, K.W. Hoffmann (1969), Z. Phys. 225, 293.

G. Grosse, W. Bambynek (1983), Physics Data 27-1.

R. Gunnink, J.E. Evans, A.L. Prindle (1976), US-ERDA Report UCRL-52139.

Y. Gurfinkel, A. Notea (1967), Nucl. Instr. and Meth. 57, 173.

J.W. Hammer (1968), Z. Phys. 216, 355.

H.H. Hansen, G. Lowenthal, A. Spernol, W. van der Eijk, R. Vaninbroukx (1969), Z. Phys. 218, 25.

H.H. Hansen, E. Celen, G. Grosse, D. Mouchel, A. Nylandsted Larsen, R. Vaninbroukx (1979), Z. Phys. A 290, 113.

H.H. Hansen (1981), Physics Data 17-1.

H.H. Hansen (1984a), Physics Data 17-2, in press.

H.H. Hansen (1984b), CBNM Internal Report GE/R/RN/01/84, European Appl. Res. Rept. - Nucl. Sci. Technol., in press.

J.S. Hansen, H.U. Freund, R.W. Fink (1970), Nucl. Phys. A 142, 604.

J.S. Hansen, H.U. Freund, R.W. Fink (1972), in: J.H. Hamilton, J.C. Manthuruthil, Radioactivity in Nuclear Spectroscopy (Gordon and Breach, New York, 1972) p. 1329.

R.L. Heath (1974), Gamma-Ray Spectrum Catalogue, Third Edition, USAED Report Physics TID-4500 and ANCR-1000-2 (National Technical Information Service, Springfield, Virginia, 1974).

D.D. Hoppes, F.J. Schima (eds.) (1982), NBS Spec. Publ. 626.

E. Karttunen, H.U. Freund, R.W. Fink (1969), Nucl. Phys. A 131, 343.

Yu.V. Kholnov, V.P. Chechev, S.V. Kamynov, N.K. Kuznenko, V.G. Nedovesov (1980), Characteristics of Radiation from Radioactive Nuclides used in the National Economy: Evaluated Data (Atomizdat, Moscow, 1980).

Yu.V. Kholnov, V.P. Chechev, S.V. Kamynov, N.V. Kuznenko, V.G. Nedovesov (1982), Evaluated Reference Nuclear Data for Radioactive Nuclides used in Industry (Energoizdat, Moscow, 1982).

D.C. Kocher (1981), Radioactive Decay Data Tables (Technical Information Center, US-Department of Energy, 1981), DOE/TIC-11026.

A.A. Konstantinov, T.E. Sazonova, A. Konstantinov (1973), in: R.W. Fink (1973) p. 144.

F. Lagoutine (1982), in: F. Lagoutine et al. (1984a), (Evaluation of the nuclides ^{54}Mn, ^{58}Co, ^{131}Cs, ^{75}Se).

F. Lagoutine (1984), in: F. Lagoutine et al. (1984a), (Evaluation of the nuclides ^{55}Fe, ^{67}Ga, ^{123}I, ^{201}Tl).

F. Lagoutine, N. Coursol, J. Legrand (1984a), Table de Radionucléides (Laboratoire de Métrologie des Rayonnements Ionisants, Gif-sur-Yvette, 1984).

C.M. Lederer, V.S. Shirley (eds.) (1978), Table of Isotopes, 7th Edition (J. Wiley & Sons, New York, 1978).

M. Leistner, K. Friedrich (1965), Atomkernenergie 10, 311.

P. Magnier, J. Bouchard, M. Blondel, J. Legrand, J.P. Perolat, R. Vatin (1978), Z. Phys. A 284, 389.

L.B. Magnusson (1957), Phys. Rev. 107, 161.

H. Maria, J. Dalmasso, G. Ardisson, A. Hachem (1982), X-Ray Spectrometry 11, 79.

A. Mukerji, J.B. McGough, Jr., G.D. Cole (1967), Nucl. Phys. A 100, 81.

A. Mukerji, Lee Chin (1973a), in: R.W. Fink (1973) p. 164.

NCRR Report No. 58 (1978), A Handbook of Radioactivity Measurements Procedures (National Council on Radiation Protection and Measurements, 1978) Appendix A3.

B.S. Negi, S. Sadasivan (1980), X-Ray Spectrometry 9, 159.

A. Notea, E. Elias (1970), Nucl. Instr. and Meth. 86, 269.

T. Paradellis, S. Hontzeas (1969), Nucl. Phys. A 131, 378.

T. Paradellis, S. Hontzeas (1970), Can. J. Phys. 48, 2254.

M. Petel, H. Houtermans (1967), in: Standardization of Radionuclides (IAEA, Vienna, 1967) p. 301.

J. Pchl, J. Zderadička (1974a), Czech. J. Phys. B 24, 131.

J. Pchl, J. Zderadička, L. Kokta (1974b), Int. J. Appl. Radiat. Isot. 25, 433.

J. Pchl, J. Zderadička, O. Dragoun (1975), Int. J. Appl. Radiat. Isot. 26, 579.

J. Pchl, P. Dryák, J. Zderadička, E. Schönfeld, A. Szörényi (1979), Czech. J. Phys. B 29, 1071.

P. Venugapala Rao, R.E. Wood, J.M. Palms (1969), Phys. Rev. 178, 1997.

P. Venugopala Rao, J.M. Palms, R.E. Wood (1971), Phys. Rev. A 3, 1568.

W. Rubinson, K.P. Gopinathan (1968), Phys. Rev. 170, 969

S.I. Salem, S.L. Panossian, R.A. Krause (1974), Atomic Data Nuclear Data Tables 14, 91.

W.-D. Schmidt-Ott, R.W. Fink (1972a), Z. Phys. 249, 286.

W.-D. Schmidt- Ott, J.S. Hansen, R.W. Fink (1972b), Z. Phys. 250, 191.

D. Smith (1982), Nucl. Instr. and Meth. 200, 383.

U. Schötzig, K. Debertin, K.F. Walz (1976), Physikalisch Technische Bundesanstalt, Jahresbericht 1975 (PTB, Februar 1976).

U. Schötzig, K. Debertin, K.F. Walz (1977), Int. J. Appl. Radiat. Isot. 28, 503.

C.W. Schulte, H.H. Jorch, J.L. Campbell (1980), Nucl. Instr. and Meth. 174, 549.

S.K. Sethi, B.S. Negi (1977), X-Ray Spectrometry 6, 192.

K. Singh, Raj Mittal, M.L. Hasiza, H.S. Sahota (1983), Indian J. Phys. 57A, 127.

J.G.V. Taylor, J.S. Merritt (1963), in: Role of Atomic Electrons in Nuclear Transformations (Nuclear Energy Information Center, Warsaw, Poland, 1963) p. 465.

D.J. Thomas (1978), Z. Phys. A 289, 51.

F. Tolea, K.R. Backer, W.D. Schmidt-Ott, R.W. Fink (1974), Z. Phys. 268, 289.

J. Topping (1963), Errors of Observation and their Treatment (Chapman and Hall Ltd., London, 1963).

R. Vaninbroukx (1980), in: C.T. Peng, D.L. Horrockx, E.L. Alpen (eds.), Liquid Scintillation Counting, Vol.I (Academic Press, New York, 1980), p. 43.

R. Vaninbroukx (1983), Int. J. Appl. Radiat. Isot. 34, 1211.

R. Vaninbroukx (1984a), this conference.

R. Vaninbroukx, G. Bortels, B. Denecke (1984b), Int. J. Appl. Radiat. Isot. in press.

D.G. Vasilik, R.W. Martin (1976), Nucl. Instr. and Meth. 135, 405.

Ts. Vylov, G.J. Beyer, V.M. Gorozhankin, Zh. Zhelev, A.I. Ivanov, R.B. Ivanov, V.G. Kalinnikov, M.Ya. Kuznetsova, N.A. Lebedev, M.A. Mikhailova, A.I. Miminov, A.F. Novgorodov, Yu.V. Norseev, Sh. Omanov, B.P. Osipenko, E.K. Stepanov, K. Thieme, V.G. Chumin, A.F. Shchus, Yu.V. Yushkevich (1980), Spektren der Strahlung radioaktiver Nuklide, gemessen mit Halbleiterdetektoren, Report ZfK-399 und INDC(GDR)-151 G.

R.L. Watson, T.K. Li (1971), Nucl. Phys. A 178, 201.

D.H. Wilkinson (1971), Nucl. Instr. and Meth. 95, 259.

WORKING GROUP SESSION I

THE SIMULTANEOUS EVALUATION OF INTERRELATED CROSS-SECTIONS BY GENERALIZED LEAST-SQUARES AND RELATED DATA FILE REQUIREMENTS

W.P. POENITZ
Argonne-West,
Argonne National Laboratory,
Idaho Falls, Idaho,
United States of America

Abstract

Though several cross sections have been designated as standards, they are not basic units and are interrelated by ratio measurements. Moreover, as such interactions as $^{6}Li + n$ and $^{10}B + n$ involve only two and three cross sections respectively, total cross section data become useful for the evaluation process. The problem can be resolved by a simultaneous evaluation of the available absolute and shape data for cross sections, ratios, sums, and average cross sections by generalized least-squares. A data file is required for such evaluation which contains the originally measured quantities and their uncertainty components. Establishing such a file is a substantial task because data were frequently reported as absolute cross sections where ratios were measured without sufficient information on which reference cross section and which normalization were utilized. Reporting of uncertainties is often missing or incomplete. The requirements for data reporting will be discussed.

I. INTRODUCTION

It should be realized that the designation of some cross sections as "standards" is for convenience only. They are not basic units and not standards as they change with every new measurement. This situation can be compared with the problem faced a long time ago, when the meter was defined as 1/40000th of the circumference of the earth. Whereas the problem for the meter could be resolved because it is a basic unit, that for the cross section "standards" is a permanent feature of a derived quantity. It might be preferable to refer to them as reference cross sections instead of as standards. Any absolute cross section measured for a certain reaction, let us assume with an uncertainty of 1%, is completely equivalent to an absolutely measured cross section of a designated "standard", assumed again measured with 1% uncertainty. The moment a ratio between these two cross sections has been measured, the absolute value of the non-standard will, in part, redefine the value of the "standard". This is the consequence of an overdetermination: there are only two unknowns in this example, but three measured values are available.

The aforementioned basic problem with the definition of cross section "standards" becomes obvious with the fact that there is not one "standard" for the same type of quantity (a cross section which is a measure of an interaction

probability in units of cm^2), but several. We may also note that we wish to evaluate these "standards" whereas a standard is defined. The desire for evaluating data is the result of overdetermination. The simplest degree of overdetermination is given by the multiple measurements of the same quantity. A "higher" degree of overdetermination is given by above example, e.g. if two different quantities are measured and a ratio or sum of these two quantities has also been obtained.

The question of how to combine multiple experimental observations is not a problem. It has been resolved ~200 years ago by Gauss and independently by Legendre. With improvements and additions we have today two approaches for the evaluation of data:

1. The generalized least-squares fit (GLSF), and

2. The Bayesian estimation.

If the same data base is used, then both techniques should give nearly identical results. We will consider here only the generalized least-squares fit which is being used for the ENDF/B-VI evaluation.

An a priori is required for the GLSF. However, in contrast to the Bayesian estimation, the a priori has only a secondary effect. It is used for the linearization of the non-linear problem, specifically for the application of the Taylor-series expansion. Adjustments to the a priori are obtained from

$$\delta = (A^T C^{-1} A)^{-1} A^T C^{-1} M$$

where C is the variance-covariance matrix of the measured data, A is the coefficient matrix determined by the Taylor series expansion, A^T its transpose, and M is the measurement vector. C becomes the correlation matrix after appropriate transformation. This has been discussed in more detail previously.[1]

Because several cross sections are involved we refer to this kind of evaluation as an simultaneous evaluation. In Section II we will consider the objects of the evaluation, types of experimental quantities to be used, and the need to reconstruct the originally measured quantities. The requirements for measurements and data reporting will be discussed in Section III. Some remarks on the evaluation of the standards and other principal cross sections will be made in Section IV.

II. THE PARAMETERS AND THE EXPERIMENTAL DATA

Realization of the interrelation of many cross sections has led to the approach of the simultaneous evaluation of the "standards and other principal cross sections" for ENDF/B-VI. The cross sections involved are called the "parameters" or "objects" of the evaluation.

^{6}Li (n,α)	thermal - 3.0 MeV
^{6}Li (n,n)	thermal - 3.0 MeV
^{10}B (n,α_o)	thermal - 1.4 MeV
^{10}B (n,α_1)	thermal - 1.4 MeV
^{10}B (n,n)	thermal - 1.4 MeV
^{197}Au (n,γ)	thermal - 2.8 MeV
^{238}U (n,γ)	thermal - 2.2 MeV
^{235}U (n,f)	thermal - 20.0 MeV
^{239}Pu (n,f)	thermal - 20.0 MeV
^{238}U (n,f)	0.1 - 20.0 MeV

The parameters under consideration are the cross sections at "grid point" energies, however, the process does not put any restriction on the definition of these values other than that the definition must be consistent. For example, the "cross sections" for the light elements at all energies and for the heavy elements at higher neutron energies are indeed the cross sections at the given energies. At lower energies the "cross section" for the heavy elements are the decimal energy interval integrals.

The experimental quantities which are presently implemented in the generalized least-squares nuclear data evaluation code GMA[1] are:

1. Absolute measurements of cross sections.

2. Measurements of the shapes of cross sections.

3. Absolute measurements of the ratios of two cross sections.

4. Measurements of the shapes of the ratios of two cross sections.

5. Absolute measurements of the sums of cross sections (e.g. total cross sections).

6. Measurements of the shapes of the sums of cross sections (e.g. the shape of $\sigma(^{10}B\ (n,\alpha_o+\alpha_1))$).

7. Absolute measurements of the ratios of a cross section vs. the sum of cross sections (e.g. $^{235}U\ (n,f)/^{10}B\ (n,\alpha_o + \alpha_1)$).

8. The measurements of the shapes of the ratio of a cross section vs. the sum of cross sections.

9. The integral of a cross section over a (fission) neutron spectrum.

These quantities have been included in order to handle all data of importance for the evaluation of the standards and other principal cross sections for ENDF/B-VI. Other quantities could be accommodated as easily as it is only a matter of providing for the corresponding Taylor series expansions. The integral of a cross section over a neutron spectrum has been included, however, only values of the $^{235}U(n,f)$ and $^{239}Pu(n,f)$ reactions will be used in the evaluation because the averages of these cross sections over a fission neutron spectrum prove to be insensitive to the knowledge of the neutron spectrum.

It appears obvious that only original experimental information should be used in an evaluation. However, this requirement poses a large problem for the evaluation of a cross section data base. In most cases experimenters have presented their data in a "pre-evaluated" form. For example, if in an experiment the shape of the $^{235}U(n,f)$ cross section has been measured from thermal to 1 KeV and from 100 eV to 100 KeV, using the $^{10}B(n,\alpha)$ reaction for the measurement of the neutron flux, then the experimenter will convert the measured ratios

using some values for the $^{10}B(n,\alpha)$ cross section. He will then normalize the high energy part of his data to the low energy part and he will finally normalize the data to some thermal cross section. There is no reason that the experimentor should not do so if he is interested in the outcome for the $^{235}U(n,f)$ cross section. However he should provide for the data files the unnormalized measurements of the ratio of $^{235}U(n,f)/^{10}B(n,\alpha)$ for the two energy intervals in which they have been obtained. Only the latter should be used in an evaluation. It is the need to reconstruct the originally measured quantities which poses a substantial problem for the evaluator. All too often the reference cross sections are not specified and the separate pieces cannot be obtained.

There is also an unfortunately large amount of confusion about the currently valid data. Data from the same measurement may have been reported repeatedly and may have entered a data file prematurely. Also, errors in a measurement may have been recognized at a later time, but the data may not have been withdrawn from the data files.

III. THE REQUIREMENTS FOR MEASUREMENTS AND DATA REPORTING

Some of the cross sections involved in the simultaneous evaluation for ENDF/B-VI are now quite well known. An example is the $^{235}U(n,f)$ cross section. The uncertainties of the result are ~1% or lower at nearly all energies between thermal and 20 MeV neutron energy. It follows that any new measurement with an uncertainty of ~2% or larger will have only a minor impact. Still, it may be desirable to have some measurements at selected energies in order to check the accuracy with which the past measurements seem to establish this cross section. Such measurements might ease our discomfort with the evaluation result in areas where data discrepancies exist or where individual data sets with the low uncertainties suggested by the evaluation are not in the data base. It appears trivial to request that such new measurements should be of high quality. However, there are many newer measurements for which systematic effects were not recognized, or, if recognized, were not corrected but added to the uncertainties.

There are other cross sections involved in the simultaneous evaluation for which the available data base is unfortunately poor. Examples are the $^{10}B(n,\alpha_1)$ and $^{10}B(n,\alpha)$ cross sections for which very few absolute measurements are available. It is clear that measurements of these quantities are needed. However, any new measurement should be of a "standard type quality", that is:

1. All systematic effects should be considered.
2. All required corrections should be applied and not merely added to the uncertainties.
3. The reproducibility should be proven.
4. The experimental result should be compared with an additional measurement in which as many components are independent (e.g. uncorrelated, see Youden[2]) as possible from the first experiment.
5. Resolution unfolding should be applied.

There are requirements for the reporting of data from any new measurement:

1. The originally measured quantities should be reported.
2. All constants used to derive the reported quantities should be reported. If a constant is not involved as a straightforward factor, then the sensitivity of the result to this constant should also be given (e.g. the half-life in an activation experiment).
3. All corrections applied to the measured data should be given. This permits the later updating with improved secondary data.
4. The statistical uncertainties and estimates of the systematic uncertainties should be given. The latter should be given for each contributing component. The separation of the statistical uncertainties of the reaction rate measurement and the flux measurement is required if two cross sections are measured at the same time.
5. Some estimate on how the systematic uncertainty components are correlated as a function of energy should be given.
6. Correlations with prior experiments should be stated and an estimate of the degree to which such correlations exist should be given.
7. The energy uncertainty and the resolution should be given.

Table I gives as an example the listing of a data set used for the ENDF/B-VI evaluation.

IV. SOME COMMENTS ON THE ENDF/B-VI EVALUATION OF THE STANDARDS AND OTHER PRINCIPAL CROSS SECTIONS

The number of cross section parameters of this evaluation is at present 861. Each data set of a shape measurement adds one parameter. There are currently ~100 shape measurements among the ~300 data sets. The measured quantities reduce to ~4800 values at the grid-point energies. It is clear that the correlation matrix of the experimental data, C, could not be constructed as it would require $\sim 2.10^7$ bytes of memory. However, it has been demonstrated[1] that the grouping of the data sets into "data blocks", which contain the correlated data sets, permits the immediate construction of the matrix $_AT\ C^{-1}{}_A$ which is of size N x N where N is the number of parameters. C is in this case the correlation matrix of the data block. With $N \sim 10^3$ this matrix requires $\sim 4.10^6$ bytes of prompt memory which is available. (The total required memory approximately doubles due to the storage requirements for A, C, M, etc.)

The correlation matrix is constructed in GMA based on the given uncertainty components and correlation factors which are calculated based on the parameters given in the data file. The cross correlations with prior data sets are calculated based on the correlated uncertainty component pairs which are given in the file and a simple factor, also given in the file. The correlations within one data set are calculated based on the totally correlated normalization uncertainties and the systematic uncertainty components which are assumed to be

TABLE I. Example of a Data Set Used for the ENDF/B-VI Evaluation

```
SET NR     YEAR   QUANTITY                AUTHORS                    REFERENCE
  305      1976   AU(N,G)/B10(N,G)        R.GWIN ET AL.              NSE59,79(1975)  ***
TYPE OF QUANTITY   7
ID OF OBJECTS      6  3  4  0  0
DATA SET TAG         2
DATA POINTS          5
NO OF COMMENTS       9

NO OF CORR. MATR. ELEM.      0
NO OF CROSS CORR.            1
*

COMMENTS
C      1     UNCERTAINTIES
C      2     1 NORMALIZATION
C      3     3 STATISTICS
C      4     4 BACKGROUND
C      5     5 GAMMA DET EFF.
C      6     6 N DET EFF.
C      7     7 SELFSHIELDING AND ATTEN.
C      8
C      9     SET 304 IS THE COINC. DATA, 305 IS SUM MODE
*

NORMALIZATION UNCERTAINTIES
     3.0      .0      .0      .0      .0      .0      .0      .0      .0      .0
       2        0       0       0       0       0       0       0       0       0
*

ENERGY DEPENDENT UNCERTAINTY PARAMETERS
  3    9          .00          .00          .00
  4    2          .50          .50          .50
  5    2          .50          .50          .50
  6    2          .50          .50          .50
  7    2          .50          .50          .50
*

DATA
NO   ENERGY /MEV     QUANTITY     DE   RES      UNCERTAINTIES, PC
                                                13   14   15   16   17   18   19   20   21
   1   .1500E-01    .1967E 00    .0  33.3   2.0  3.0   .3   .2  2.9   .0   .0   .0   .0  5.5
   2   .2500E-01    .1922E 00    .0  20.0   2.0  3.0   .8   .4  2.6   .0   .0   .0   .0  5.4
   3   .3000E-01    .1895E 00    .0   3.0   2.0  3.0  1.0   .6  2.5   .0   .0   .0   .0  5.4
   4   .3500E-01    .1852E 00    .0  14.3   2.0  3.0  1.3   .7  2.4   .0   .0   .0   .0  5.5
   5   .4500E-01    .1762E 00    .0  11.1   2.0  3.0  1.8   .9  2.1   .0   .0   .0   .0  5.5
*

CROSS CORELATIONS WITH PRIOR DATA SETS
DATA SET  PRESENT UNC. COMP./ PRIOR UNC. COMP. PAIRS
  304      14  14  16  16  17  17   0   0   0   0   0   0   0   0   0   0   0   0   0   0
             1.0     1.0     1.0      .0      .0      .0      .0      .0      .0      .0
*

THIS IS THE END OF A DATA BLOCK

*****************************************************************************
```

correlated between the energies E_1, E_2 by a function which consists of a constant, a, and a triangle of height b and width c with $a + b \leq 1$.

Though all the correlation matrices of the presently involved ~300 data sets were found to be positive-definite (a requirement to obtain the inverse matrix), a few data blocks were not. It is known that if C is a symmetric matrix a constant p exists such that $C^{\sim} = C + pI$ is positve definite. If C is the variance-covariance matrix of an experimental data block, than this operation implies the addition of a constant statistical uncertainty of $\sqrt{p}$. This reduces the overall weight of the data of the specific data block which might not be acceptable. However, in the present evaluation a transformation has been made such that C is the correlation matrix and $C^{\sim}$ is transformed again to become a correlation matrix. Thus the addition of pI results in a reduction of the correlation coefficients which appears more acceptable because the latter have much larger uncertinties than the uncertainties of the data have.

The resolution of the linear equation system required that at least one data value is available for each parameter. The energy grid has been selected to represent the gross structure of the cross sections. In an energy region were one cross section requires a dense energy grid (e.g. the ^{6}Li + n cross sections over the 240 keV resonance) data may not be available for all other cross section parameters. This problem has been resolved by introducing artificial data sets for each cross section with very large uncertainties.

V. DISCUSSION

It has been demonstrated that a simultaneous evaluation of many interrelated cross sections can be carried out with present computer technology. The major problem is the creation of the corresponding data file. It is nearly impossible to reanalyze ~300-400 data sets, specifically because much information about the measurements is missing. It is felt that it should be the responsibility of the experimenter to assure that his data, including their uncertainties and correlations, are properly included in the data files.

One of the major advantages of a simultaneous evaluation of many cross sections is that it "randomizes" the systematic errors. This can be expected because a much larger variety of measurement techniques is involved than there would be for a single cross section. The simultaneous evaluation also provides consistency of the results as well as cross-materials covariances.

The goal of the present simultaneous evaluation is to obtain "best" values for the involved cross sections based on the available data. Subjective selection of data sets is avoided. This approach should result in an objective evaluation result which is expected to be independent of the evaluator. Still, the evaluator has to estimate (systematic) or guess (statistical) uncertainty components where such information was not given by the experimentor. The possible effect of these estimates by the evaluator on the result will be investigated. For this purpose the uncertainty components have been tagged in the file to indicate their origin.

It is believed that the present simultaneous evaluation, combined with R-matrix fits for the light elements and nuclear model fits for the heavy elements will provide improved evaluated cross sections for ENDF/B-VI.

ACKNOWLEDGMENT

This work was performed under the auspices of the U.S. Department of Energy.

REFERENCES

1. W.P. Poenitz, "Data Interpretation, Objective Evaluation Procedures and Mathematical Techniques for the Evaluation of Energy-dependent Ratio, Shape and Cross Section Data", Proc. Conf. on Nuclear Data Evaluation Methods and Procedures, Brookhaven National Laboratory, Sept. 1980, BNL-NCS-51363, Vol. 1, 249 (1980).

2. W.J. Youden, Technometrics 14, 1 (1972).

A SIMULTANEOUS EVALUATION OF SOME IMPORTANT CROSS-SECTIONS AT 14.70 MeV

T.B. RYVES
National Physical Laboratory,
Teddington, Middlesex,
United Kingdom

Abstract

A simultaneous evaluation of the $^{27}Al(n,\alpha)^{24}Na$, $^{56}Fe(n,p)^{56}Mn$, $^{63}Cu(n,2n)^{62}Cu$, $^{65}Cu(n,2n)^{64}Cu$, $^{197}Au(n,2n)^{196}Au$, $^{93}Nb(n,2n)^{92m}Nb$, $^{32}S(n,p)^{32}P$, and $^{1}H(n,n)^{1}H$ cross sections at an energy 14.70 MeV has yielded a consistent set with uncertainties of 0.6-2.0 %. The data base consisted of 95 activation cross section ratio measurements taken from the published literature, and a generalised weighted least-squares method was employed, the normalisation being to the many measurements where the neutron fluence was determined by the associated particle technique. The published experimental results were corrected where necessary for recent half-life changes, the new ^{64}Cu decay scheme, and recent n-p scattering data which affects the early proton recoil telescope measurements.

The simultaneous evaluation agrees within the errors with several recent evaluations of individual cross sections, but differs from some of the evaluated data files, such as ENDF/BIV, ENDF/BV, JENDL1G and UKNDL1G, by several percent at 14.70 MeV.

It is suggested that all the reactions considered in this evaluation should be included in the list of standard reference data, at least at 14.70 MeV. This particular energy is especially significant because it is close to the mean energy of neutrons produced by low energy deuterons interacting with a tritium target at 0° to the direction of the beam, where an enormous amount of cross section data exists. At present, apart from the U fission cross sections, only the $^{27}Al(n,\alpha)^{24}Na$ reaction is included at this energy, but in fact there is considerable correlation with many other measured cross sections, which should be taken into account. In particular the $^{56}Fe(n,p)^{56}Mn$ reaction has been widely used as a reference by many laboratories, and should certainly be included in the standard reference data from 14 to 20 MeV.

1 INTRODUCTION

Accurate 14 MeV neutron cross sections are required for several physical applications, especially in designing fusion reactors, in neutron dosimetry and for developing refined nuclear theory. An enormous number of measurements of 14 MeV cross sections have now been made, and many recent results claim accuracies approaching 1-3%, although the spread in values is much greater.

This paper describes a simultaneous evaluation of eight important cross sections at 14.70 MeV, where the correlations between the measurements are taken into account. The energy of 14.70 MeV is significant because it is close to the average energy of neutrons produced by low-energy deuterons interacting with a tritium target at 0° to the direction of the beam, the condition where hundreds of measurements have been made. Seven of the evaluated cross sections (listed in Table 1) were measured by the activation technique and, in addition, the n-p cross section was included for the numerous measurements which employed proton recoil telescopes for the determination of the neutron fluence.

2 THEORY OF THE EVALUATION

A full account of the method has been given previously[1]. It is considered that all activation cross sections are in fact measured as ratios relative to some standard cross section, so that the absolute measurement of neutron fluence rate is avoided. Clearly for the majority of measurements wherein a monitor foil or mixed-powder technique is employed, often using the $^{27}Al(n,\alpha)$ or $^{56}Fe(n,p)$ reaction as the reference, the measured quantity is a ratio of cross sections. However, sometimes the neutron fluence rate is determined with a proton recoil telescope, or by the associated particle technique (for the D-T reaction). Other methods have been omitted from this evaluation (e.g. employing fission chambers).

In the case of telescope measurements, the neutron flux depends directly on the H(n,n) differential cross section at 180°, which thus becomes the reference cross section. The associated particle measurement of the neutron fluence is absolute in the sense that it depends only on the solid angle subtended by the α-particle detector (assuming that the D-T kinematical equations are exact), so that here the cross sections are treated as ratio measurements to a 'fictitious' unit cross section (related to the known geometrical area of the α-detector).

Table 1. Results of the evaluation at 14.70 MeV

Reaction	Cross section (mbarn)	Uncertainty (%) Least squares	Systematic	Total
$^{27}Al(n,\alpha)^{24}Na$	113.7	0.6		0.6
$^{56}Fe(n,p)^{56}Mn$	107.8	0.6		0.6
$^{63}Cu(n,2n)^{62}Cu$	537	1.2	0.2 [a]	1.2
$^{65}Cu(n,2n)^{64}Cu$	962	0.9	0.7 [b]	1.2
$^{197}Au(n,2n)^{196}Au$	2160	1.6	0.1 [c]	1.6
$^{93}Nb(n,2n)^{92m}Nb$	451	1.6		1.6
$^{32}S(n,p)^{32}P$	215	1.5		1.5
$^{1}H(n,n)^{1}H$	650	0.8	1.1 [d]	1.4

The least squares uncertainties were computed from eq.(6) of ref.(1) The relevant value of s^2, given by eq.(8), is 2.43 with 87 (=p-8) degrees of freedom.

[a] ^{62}Cu half-life; [b] ^{64}Cu decay scheme; [c] 355 keV γ-ray intensity; [d] cross section anisotropy, affects proton-recoil telescope measurements.

Table 2. Variance-covariance matrix for the results in Table 1

$^{27}Al(n,\alpha)^{24}Na$	0.32	0.20	0.20	0.25	0.30	0.22	0.22	0.20
$^{56}Fe(n,p)^{56}Mn$		0.36	0.22	0.24	0.23	0.21	0.27	0.30
$^{63}Cu(n,2n)^{62}Cu$			1.50	0.49	0.21	0.19	0.29	0.26
$^{65}Cu(n,2n)^{64}Cu$				0.84	0.28	0.24	0.29	0.25
$^{197}Au(n,2n)^{196}Au$					2.54	0.57	0.24	0.22
$^{93}Nb(n,2n)^{92m}Nb$						2.67	0.25	0.21
$^{32}S(n,p)^{32}P$							2.15	0.23
$^{1}H(n,n)^{1}H$								0.64

Variances given in $\%^2$.

The mathematical treatment[1] followed that of Hayes and Axton[2], but was extended to take account of the correlations. Best estimates of the cross sections were obtained according to the generalised least-squares criterion. Because all the input data were ratios of cross sections, it was necessary to fix one cross section in order to obtain a unique solution for the others. In this problem it was decided to set the associated particle 'fictitious' cross section equal to unity, but a value could equally well have been assigned to the n-p scattering cross section, or to some weighted mean of the two, which would have produced a slightly different set of results for the other evaluated cross sections.

3 DATA EVALUATION AND RESULTS

The most recent evaluation of Winkler and Ryves[3] has been up-dated by the inclusion of further experimental results, making a total data base of 95 cross section ratios. The additional data were supplied by Lu Hanlin[4] for Al, ^{56}Fe, Au and Nb relative to the associated particle method, and Csikai[5] for ^{65}Cu, Au and Nb relative to Al. Results are given in Table 1 and covariances in Table 2, and do not differ markedly from previous results[1,3] based on fewer data. As stated previously, a number of early measurements were rejected for various reasons[1], such as inconsistent ratios, large uncertainties, uncertain neutron energy, lack of information, incorrect nuclear data such as half-lives etc. The early proton recoil telescope results were again adjusted for more recent n-p cross section data[6] or relativistic kinematics[7,8]. Finally, as noted before [3], the latest ^{64}Cu decay scheme branching ratios[9] were applied to all ratio measurements involving the $^{65}Cu(n,2n)$ reaction.

4 DISCUSSION

The uncertainties (at the 1 σ level) of the evaluated cross sections at 14.70 MeV lie between 0.6 and 1.6%, and it will be of interest to compare them with other recent evaluations, especially ENDF/BV1. The excellent agreement of the $^{27}Al(n,\alpha)$ cross section with that of Tagesen and Vonach[9] and of $^{63}Cu(n,2n)$ with Tagesen et al[10] is especially gratifying. The evaluated n-p cross section of (650 ± 9) mb is 2% lower than the value of 663 mb calculated by Hopkins and Breit[6], but much of the early proton recoil telescope data is not very well documented, so that the evaluated result may not be entirely reliable.

In view of the importance of the many cross section measurements made at about 14.70 MeV, using low energy deuterons on tritium targets as a source of neutrons, it is proposed that this energy should be treated as a special reference energy at which an evaluation of a number of selected cross sections could be produced, taking into account the correlations between the measurements. Such an evaluation would be quite simple to perform and up-date, especially if no significant correlations exist between different sets of data, and could be used to normalise large energy-dependent data files.

6 REFERENCES

1. Hayes J G and Ryves T B (1981) Ann. nucl. Energy 8 469.
2. Hayes J G and Axton E J (1969) Metrologia 6 21.
3. Winkler G and Ryves T B (1983) Ann. nucl. Energy 10 601.
4. Lu Hanlin (1984) Private communication.
5. Csikai J (1983) Proc. of Int. Conf. on Nucl. Data for Sci. and Technology, Sept. 1982, Antwerp. p.414.
6. Hopkins J C and Breit G (1971) Nucl. Data Tabl. A9 137.
7. Ryves T B, Kolkowski P and Zieba K J (1978) Metrologia 14 127.
8. Thomas D J and Axton E J (1980) Nucl. Instrum. Methods 174 321.
9. Christmas P, Judge S, Ryves T B, Smith D and Winkler G (1983) Nucl. Instrum. Methods 215 397.
10. Tagesen S and Vonach H (1981) Phys. Data 13-3.
11. Tagesen S, Vonach H and Strohmaier B (1979) Phys. Data 13-1.

PROPERTIES OF Cf FISSION FRAGMENT DETECTION SYSTEMS USED FOR NEUTRON TIME-OF-FLIGHT MEASUREMENTS

H. KLEIN, R. BÖTTGER
Physikalisch-Technische Bundesanstalt,
Braunschweig, Federal Republic of Germany

A. CHALUPKA, B. STROHMAIER
Institut für Radiumforschung und Kernphysik,
Vienna, Austria

Abstract

Fission fragment (FF) detectors containing a Cf source are frequently used to measure the spectral fluence distribution of prompt neutrons from the spontaneous fission of Cf by means of time-of-flight (TOF) spectroscopy. The method is applied either to determine the spectral shape using a well defined spectrometer or to calibrate the neutron detection efficiency on the basis of the evaluated Cf neutron spectrum.

In both cases, various properties of the FF detector system influencing both the measured TOF spectrum and the absolute scaling of the analysed spectral distribution, must be carefully investigated. Various methods are discussed to determine the nonisotropic FF detection losses and to investigate the timing properties of the FF detector, including the subsequent fast electronics.

(1) Fission Fragment Detection Efficiency

The advantages of parallel-plate ionization chambers for the detection of fission fragments from the spontaneous fission of Cf-252 are discussed in detail by A. Chalupka[1,2]. Small systems can be realized showing excellent α-particle suppression, sub-nanosecond timing and high FF detection efficiency. Only small corrections have to be considered for the distortion of the prompt fission

neutron spectrum due to the construction materials if this type of detector is used as a start timer in a neutron TOF spectrometer[3,4)]

In this paper the influence of the FF detection losses on the spectral energy distribution and the methods for determining the relevant parameters are discussed.

Detailed investigations[2,3,4)] have proved the assumption that the fraction of undetected fission fragments increases proportionally to the roughness of the source backing. As it is chiefly the fission fragments emitted almost parallel to the backing which are lost, this results in a strongly nonisotropic deficiency. Obviously, the deviation of the measured energy spectrum from the undistorted distribution depends on the position of the neutron TOF detector with respect to the backing plane, if the neutrons are isotropically emitted from fully accelerated fission fragments. The correction may therefore be derived from the ratio of the neutron energy distributions observed at different positions, i.e. perpendicular to or in the plane of the Cf source deposit[5,6)]. On the other hand, additional isotropic losses cannot be determined in this way, and as the mean efficiency $\langle\varepsilon_{FF}\rangle$ is required for an absolute scaling of the spectral fluence distribution, it must be determined in another way.

The scintillation spectrum of the neutron detector is taken independently or in coincidence with an FF detector signal. The ratio depends on the threshold and the position of the neutron detector. The crossing point at about 60 degrees (angle measured to the normal on the plane of the backing) gives the mean efficiency $\langle\varepsilon_{FF}\rangle$ in the limit of a vanishing threshold. On the other hand, the ratio tends to 100 % for increasing threshold and negligible isotropic detection losses. This interpretation is supported by MC simulations performed by A. Chalupka. The energy loss spectrum in the fission chamber and the angular dependent ratio can be simultaneously reproduced for a certain roughness parameter and the associated correction of the analysed energy distribution is calculated[2,4)].

This experimental method allows the mean detection efficiency to be determined with an uncertainty of less than 0.2 % if the corrections for random background and TAC range losses (see section 3) are accounted for correctly. For the nonisotropic detection losses of 5 - 7 % recently reported[3,5,6)] and TOF measurements at 0 degrees, the corrections of the energy spectrum are less than 2 % for energies $E_n > 2$ MeV but reach 12 % for lower energies. It should be emphasized that these corrections can be drastically diminished if the neutron detector is positioned at about 60 degrees[2,4,6)] and an improved source deposited on thin, highly polished Pt-backing[4)] as available from Harwell* is used.

In addition to this, corrections must be taken into account for the absorption and the secondary neutron production in the construction materials, and the inscattering from these materials. This may partially enhance the corrections described above, as the inscattering and neutron production can exceed the absorption of low energy neutrons[4)], in particular.

(2) Time-of-Flight Spectroscopy

Neutron TOF measurements are usually performed with an inverse time scale. In order to avoid dead time losses the high counting rate of the FF detector defining the start of prompt fission neutrons is suitably delayed and used as the stop input for a time to amplitude converter (TAC), which is started by neutron events from the TOF detector. No problems arise with this method if a regularly pulsed neutron source is investigated, but in the case of a continuous source following Poisson statistics, a more sophisticated description is required, in particular if the time interval distribution is modified by a nonextended dead time of the detector system and/or electronics. Recently, Poenitz[5)] pointed out that the TOF spectrum corrected for uncorrelated stop events must be

*delivered by Amersham, Ltd.

properly renormalized. A more generalized description for any nonextended dead time τ in the FF channel has also been reported[7] while the results of an earlier attempt of a general solution[8] can not be applied.

From the formulas given in ref. 7 it can be concluded that besides the dead time τ the time zero intercept of the TAC must be known for a correct analysis. In the case of very small dead times, as assumed in ref. 5, the renormalization factor for the TOF spectrum already corrected for uncorrelated stop events increases with the measured time difference and therefore with increasing energy. On the other hand, for large dead times exceeding the TAC range which may originate from the use of an electronic delay module instead of coaxial delay lines, no time dependent renormalization has to be considered but uncorrelated stop events appear above the highest neutron energies and may be misinterpreted as random events. These spectra must be analysed iteratively.

Different methods are used to determine the nonextended dead time (oscilloscope, multiple source method) but a simple module to measure the time interval distribution is the most powerful instrument for investigating the timing properties of the system as well as for fixing the dead time parameter. Timing problems such as those typically introduced by the ringing of fast amplifier systems or by afterpulses of high gain phototubes can easily be recognized and may cause an extension of the nonextended dead time [4,7]. Unfortunately, no commercially available TAC offers this mode of operation.

As an example of the necessity for a correct analysis we come back to the determination of the FF detection efficiency. The ratio of neutrons measured in coincidence with the FF detector compared with the unconditioned response of the scintillator presupposes that within the TAC window used all correlated neutrons have been taken into account. For this reason, all uncorrelated stop events beyond the TAC range have to be avoided by starting with correlated neutron TOF events at time differences $\Delta t > \tau$ or be estimated for the region between the threshold and the time zero. In this way the efficiency can be determined with uncertainties of less than 0.2 % [4].

Near the threshold of the neutron detector and for energies below the maximum of the energy distribution at about 0.7 MeV, the statistical uncertainty due to these corrections limits the accuracy of neutron spectroscopy. However, the contributions due to uncorrelated stop events can be avoided if fast timing modules with an extended dead time generator and pile up rejection are applied[9]. Unfortunately, suitable electronic modules are still not commercially available.

(3) Conclusions and Recommendations

A Cf source within an FF detector can be a powerful instrument for calibrating the neutron detection efficiency of a TOF detector.

Very high FF detection efficiencies are achieved if Cf deposites on thin, highly-polished Pt backings are used ($\langle\varepsilon_{FF}\rangle \approx 99$ .... 99.5 %)[4]. In any case, the corrections due to a nonisotropic inefficiency are almost negligible if the neutron detector is positioned at about 60° to the normal on the source deposit. The efficiency measurement should be regularly repeated because self-creeping of the Cf changes this property of the FF detector. The construction materials of the low mass detectors should be selected to minimize the distortion of the energy distribution. If theoretical estimates cannot be performed additional experiments are necessary.

The TOF spectra must be analysed iteratively, taking into account the dead time τ of the FF channel and the time zero intercept of the TAC. The timing properties and parameters should be investigated by taking the time interval distribution of the FF timing system and the neutron detector. The proper correction for uncorrelated stop events and the probably energy dependent

renormalization factor can significantly influence the spectral energy distribution evaluated.

Finally, it should be emphasized that the properties of the FF detector and the neutron TOF detector as well as the methods applied for analysing and correcting the measured TOF spectra should be reported, so that all these experiments can be taken into account in the next evaluation of the spectral energy distribution of prompt neutrons from the spontaneous fission of Cf-252.

(4) References

1.) A. Chalupka, NIM 164 (1979) 105 - 112

2.) A. Chalupka, B. Strohmaier, H. Klein, R. Böttger, INDC (NDS) - 146 (1983) 187 - 189

3.) R. Böttger, H. Klein, A. Chalupka, B. Strohmaier, Proc. of the Intern. Conf. on Nuclear Data for Science and Technology, ed. K.H. Böckhoff, D. Reidel Publ. Comp., Eindhoven (1983) p. 484 - 487

4.) R. Böttger, H. Klein, A. Chalupka, B. Strohmaier, to be published

5.) W.P. Pönitz, T. Tamura, sama as ref. 3, p. 465 - 472

6.) H. Märten, D. Neumann, D. Seeliger, INDC (NDS) - 146 (1983) 199 - 212

7.) H. Klein, R. Böttger, A. Chalupka, B. Strohmaier, INDC (NDS) - 146 (1983) 191 - 194

8.) A. Chalupka, NIM 165 (1979) 103 - 107
ERRATUM NIM 250 (1982) 610

9.) O.I. Batenko, M.V. Blinov, G.S. Boykov, V.A. Vitenko, V.A. Rubchenya, INDC (NDS) - 146 (1983) 161 - 173

WORKING GROUP SESSION II

STANDARDS FOR THE FISSION YIELDS MEASUREMENTS

J. BLACHOT
Laboratoire de physique nucléaire,
Département de recherche fondamentale,
CEA, Centre d'études nucléaires de Grenoble,
Grenoble, France

Abstract

Two main methods are now used for the determination of fission yields : The gamma spectrometry, without or with radiochemical separations and the mass spectrometry using isotopic dilution.

Fission yields are needed in burn up determination, dosimetry, safeguards and also in basic science (study of the fission mechanism).

The ^{235}U thermal neutron induced fission yields have been extensively studied. Complete and up to date evaluations for this system are available.

The development of the most important of these fission yields, as standards, could be a good solution. They are easily measured and they allow the fulfilment of all the applications. A short review of all data available will be given.

Only the gamma spectrometry method will be described. Some recommended decay data will be discussed.

The experimental method will be also shortly described.

INTRODUCTION

Fission yields for the most fissioning nuclides are needed to a high accuracy for many purposes. Basic science, reactor physics calculations, shielding calculations, safeguards, decay heat calculations, etc .. are requiring the most available fission yields data. Are the available data sufficient ? To answer this question, we'll first review the status of the fission yields, and we'll describe the main compilations. Referring to the conclusions of Fudge (1) in a recent meeting, we can say that further measurements of the fission yields for ^{237}Np and ^{232}Th are required. To determine these fission yields, should standards be developped ?

Should relative measurements be considered as standards ? Should some important fission products (F.P.) be developped as standarts ? For a contribution to this discussion we'll describe methods to measure the fission yields, and we'll try to suggest a solution.

I - STATUS OF THE FISSION YIELDS -

a)- Status of Experimental Results -

The availability of experimental results for a number of technically important fission reactions is given in Table 1 taken from [2].

The completeness of the experimental information available at this time (1978) is indicated by the number of chains measured and by the fraction of the total yield (%) that these chains represent. $^{235}U(nth,f)$ has the most important number of chain measured, and more than 98% has been measured. We have not tried to update this table, but very few new measurements have been published these last years. The best way to do that would be to use [3], but unfortunately some projected experiences are never published.

b)- Compilations -

Most of the yields can be found in the 2 compilations : Meek-Rider [4,5] and Crouch [6]. Now these authors are retired. Dr. Crouch in 1982, Dr. Rider in 1983.

England at Los Alamos has taken in charge the US evaluation [7]. Crouch's data and programs have been implemented at Winfrith UK [8].

It is not the goal of this paper to discuss in detail the two original evaluations. However the Tables 2 and 3 presented by Cuninghame in Petten [9] illustrate well the difference between these 2 evaluations. In Table 2 Cuninghame has split up the yield curves into their five main parts and averaged the errors, and in Table 3 picked out certain important yields.

One major difference between the two evaluators immediately becomes evident. Crouch has in most cases increased his errors since 1973 while M.R. have reduced theirs. However M.R. shows errors 2-3 times smaller than Crouch. This same disagreement is shown in the individual yield errors given in Table 3 except at mass 141 ?

We have added in the Table 4 for ^{235}U (nTh) the σ given in the version VI of ENDF (7). The σ have yet a little changed. The tendancy is always the same, even if the yields remain the same.

c)- Conservation Rules -

The yields in the evaluation have to satisfy some conservation rules [8]. We have to assume that all fissions are binary. For the most important fissioning nuclides, ternary fissions represent less than 0.25%

$$\Sigma y\ (Z,A) = \Sigma Y\ (A) = 2 \qquad (1)$$

y represents the independent yield and Y the chain yield.

Nucleon conservation gives

$$\sum_{Z,A} Ay\ (Z,A) = \sum_{A} AY\ (A) = AF - Vp \qquad (2)$$

where Vp is the mean number of prompt neutrons per fission.

Table I: Survey on the availability of experimental chain yield values [2]

Reaction	Number of chains measured	Fraction of total measured (%)
227-Ac (nf,f)	13	21
227-Th (nth,f)	29	41
229-Th (nth,f)	50	88
232-Th (nf,f)	50	86
232-Th (n3,f)	26	40.3
232-Th (n11,f)	11	22.5
232-Th (n14,f)	50	59.8
231-Pa (nf,f)	30	43.9
231-Pa (n3,f)	10	14.3
231-Pa (n14,f)	14	29.2
233-U (nth,f)	66	96.5
233-U (nf,f)	58	91.3
233-U (n14,f)	47	56.8
235-U (nth,f)	75	98.1
235-U (nf,f)	59	97.1
235-U (n6,f)	29	41.6
235-U (n7.1,f)	29	43.2
235-U (n8.1,f)	29	40.5
235-U (n9.1,f)	29	39.5
235-U (n14,f)	44	52.2
236-U (nf,f)	32	59.4
238-U (nf,f)	61	86
238-U (n1.5,f)	43	66.4
238-U (n2.0,f)	54	85.1
238-U (n3.9,f)	59	91.5
238-U (n5.5,f)	46	71
238-U (6.0,f)	29	42.5
238-U (n6.9,f)	43	63.4
238-U (n7.1,f)	19	42.2
238-U (n7.7,f)	45	70.5
238-U (n8.1,f)	29	41.8
238-U (n9.1,f)	29	41.1
238-U (n14,f)	70	85.3
237-Np (nf,f)	49	87.1
237-Np (n14,f)	18	26.3
239-Pu (nth,f)	65	91.7
239-Pu (nf,f)	60	94.9
239-Pu (n14,f)	16	21.4
240-Pu (nf,f)	46	60.5
241-Pu (nth,f)	58	83.2
241-Pu (nf,f)	43	77.5
242-Pu (nf,f)	18	31.8
241-Am (nth,f)	46	64.5
242-Am (nth,f)	35	51.3
245-Cm (nth,f)	40	56.9
249-Cm (nth,f)	38	52.4
249-Cf (nth,f)	41	45.6
251-Cf (nth,f)	23	30.4
254-Es (nth,f)	29	43.4
255-Fm (nth,f)	21	28.1

Table 2 [9]

Means of Percentage Errors in Fission Yields (1σ) Shown in Some of the Evaluations Considered for the 1973 and 1977 FPND Panels

Fissile Nuclide	Fission Energy	Section of Mass Yield Curve	Mass Range	Mean of Percentage Errors Reported (1σ)				Suggested 1977 1σ Errors
				Crouch 1973	Meek and Rider 1973	Crouch 1977	Meek and Rider 1977	
^{235}U	Thermal	Light wing	72–84	10.9	15.1	20.5	17.6	19.0
		Light peak	85–104	3.4	1.0	2.7	0.9	1.8
		Valley	105–129	3.7	10.8	16.9	9.6	13.2
		Heavy peak	130–150	1.8	1.1	2.8	1.2	2.0
		Heavy wing	151–161	5.6	8.7	8.2	7.9	8.1
^{239}Pu	Thermal	Light wing	72–87	8.3	15.2	16.2	15.6	15.9
		Light peak	88–109	5.4	3.9	8.2	3.6	5.9
		Valley	110–129	11.7	13.8	17.4	15.1	16.2
		Heavy peak	130–150	5.1	1.7	6.2	1.2	3.7
		Heavy wing	151–161	11.3	9.1	13.5	8.8	11.1
^{235}U	Fast (pile)	Light wing	72–83	–	20.6	18.4	21.2	19.8
		Light peak	84–105	3.8	1.9	5.2	1.4	3.3
		Valley	106–129	10.1	9.3	17.0	10.1	13.5
		Heavy peak	130–150	3.4	1.8	3.8	1.4	2.6
		Heavy wing	151–161	11.3	12.6	15.3	12.2	13.7
^{238}U	Fast (pile)	Light wing	72–85	–	19.6	18.5	18.3	18.4
		Light peak	86–106	8.3	8.4	7.4	3.2	5.3
		Valley	107–129	16.9	13.0	20.5	11.4	16.0
		Heavy peak	130–150	8.6	3.9	6.0	1.8	3.9
		Heavy wing	151–161	13.0	10.7	15.5	9.0	12.2
^{239}Pu	Fast (pile)	Light wing	72–86	9.3	16.4	21.5	11.5	15.5
		Light peak	87–109	5.9	4.1	7.3	2.4	4.9
		Valley	110–129	24.1	10.1	22.1	9.6	15.8
		Heavy peak	130–150	4.7	3.1	4.9	1.6	3.3
		Heavy wing	151–161	8.2	9.8	12.6	8.2	10.4
^{235}U	14 MeV	Light wing	72–83	12.5	21.4	17.0	10.2	13.6
		Light peak	84–110	10.8	9.0	15.5	6.5	11.0
		Valley	111–129	13.6	9.6	16.1	7.8	12.0
		Heavy peak	130–150	8.0	8.4	12.3	5.7	9.0
		Heavy wing	151–161	9.2	14.9	16.0	9.0	12.5

Table 3 [9]

Percentage Errors in Fission Yields (1σ) of Certain Important Nuclides Given in Some of the Evaluations Considered for the 1973 and 1977 FPND Panels

Fissile Nuclide	Fission Energy	Evaluation	Percentage Errors Reported (1σ) for mass:-							
			95	103	108	133	137	140	141	Mean for:- 143, 144, 145 146, 148, 150
^{235}U	Thermal	Crouch 1973	2.0	6.0	12.0	0.5	1.0	0.5	3.0	1.4
		M & R 1973	0.7	2.0	1.4	0.5	0.5	0.5	1.4	0.5
		Crouch 1977	1.6	6.4	6.6	2.8	1.3	1.2	1.9	1.2
		M & R 1977	0.7	1.4	1.4	0.5	0.35	0.5	1.0	0.4
Suggested 1977 1σ error			1.1	3.9	4.0	1.6	0.8	0.9	1.5	0.8
^{239}Pu	Thermal	Crouch 1973	5.0	7.0	4.0	5.0	6.0	5.0	4.0	5.5
		M & R 1973	2.0	2.8	2.8	1.4	1.0	1.0	2.8	0.7
		Crouch 1977	2.9	4.3	3.0	2.5	2.9	5.9	3.3	7.0
		M & R 1977	2.0	2.0	2.8	0.7	0.5	1.0	2.8	0.5
Suggested 1977 1σ error			2.5	3.2	3.3	5.1	1.7	3.5	3.0	3.8
^{235}U	Fast (pile)	Crouch 1973	2.5	5.5	27.0	3.0	5.5	2.0	3.0	3.2
		M & R 1973	1.0	2.0	6.0	1.4	1.0	1.4	2.0	1.1
		Crouch 1977	1.8	2.6	27.4	2.3	4.6	1.5	2.7	2.5
		M & R 1977	1.0	1.4	6.0	1.4	0.7	0.7	2.0	0.8
Suggested 1977 1σ error			1.4	2.0	15.7	1.8	2.7	1.1	2.4	1.6
^{238}U	Fast (pile)	Crouch 1973	6.0	15.0	9.0	-	7.0	2.5	-	9.7
		M & R 1973	2.3	2.8	8.0	2.8	4.0	2.0	8.0	2.3
		Crouch 1977	4.3	6.4	7.7	6.3	5.6	2.1	20.0	4.6
		M & R 1977	1.4	2.0	4.0	1.4	1.0	1.4	2.8	1.1
Suggested 1977 1σ error			2.5	4.2	5.8	3.8	3.3	1.7	11.4	2.9
^{239}Pu	Fast (pile)	Crouch 1973	3.0	4.5	10.0	5.0	10.0	1.5	4.0	3.8
		M & R 1973	2.0	2.0	6.0	2.0	2.0	1.4	4.0	1.6
		Crouch 1977	3.1	6.4	10.3	3.3	8.6	1.9	3.6	3.5
		M & R 1977	1.1	2.0	2.9	1.4	0.7	1.0	2.8	0.8
Suggested 1977 1σ error			2.4	4.2	6.6	2.3	4.7	1.4	3.2	2.2
^{235}U	14 MeV	Crouch 1973	9.0	7.0	20.0	10.0	10.0	5.0	10.0	-
		M & R 1973	6.0	4.0	6.0	6.0	2.0	4.0	8.0	11.0
		Crouch 1977	7.6	5.7	17.6	11.7	10.0	2.6	10.0	15.0
		M & R 1977	6.0	4.0	4.0	6.0	2.8	2.8	6.0	7.8
Suggested 1977 1σ error			6.8	4.9	10.8	8.8	6.4	2.7	8.0	11.4

The yields of complementary elements must be equal ie

$$\sum_{A} y\,(Z,A) = \Sigma Y\,(Z_F - Z,_A) \quad \text{all } Z \tag{3}$$

Averaged over all elements and using (1) this gives :

$$\sum_{A,Z} ZY\,(Z,A) = Z_F \tag{4}$$

This last rule is the weakest, as we can see from the Table 5

The largest deviation (0,06) occurs for $^{235}U(T)$ the nuclide having the largest number of measured yields.

d)- Status of the available compilations -

The version C31 in ENDF/B4 of the Crouch compilation is available through the Data Centres. The yields have been constrained (by least squares) to fit conservation rules (1-3).

The Table 6 taken in the paper of England [7] show that 34 nuclides have fission yields data in ENDF/B.

The chain yields for the 10 main nuclides [7] are given in Annexe 1. Constrains have also be applied to the US evaluations, and most of the final results can be found in the England paper [7]. The mean value of uncertainty are given in Table 7.

Table 4

Percentage errors in fission yields (1σ

^{235}U (n,th)	95	103	106	133	137	140	141
CR 77	1.6	6.4	6.6	2.8	1.3	1.2	1.9
Meek 77	0.7	1.4	1.4	0.5	0.35	0.5	1.0
ENSDF VI	1.0	1.0	1.4	0.35	0.5	0.7	1.0

Fission yields

	95	103	106	133	137	140	141
CR 77	6.51	3.15	0.394	6.75	6.22	6.31	5.81
MR 77	6.50	3.03	0.392	6.70	6.23	6.31	5.84
R 81	6.52	3.03	0.40	6.7	6.19	6.20	5.82
ENS VI 83	6.51	3.03	0.40	6.65	6.14	6.14	5.71

TABLE 5 [7]

Average Charge (Independent Yields, Version E)

NUCLIDE	Zf	Z-AVE	% DEV
^{235}U (T)	92	91 94	-0 06
^{235}U (F)	92	91 99	-0 01
^{235}U (H)	92	91 97	-0 03
^{236}U (F)	92	91 99	-0 01
^{238}U (H)	92	91 98	-0 02
^{239}Pu (T)	94	94 01	0 01
^{239}Pu (F)	94	93 99	-0 01
^{241}Pu (T)	94	94 01	0 01
^{233}U (T)	92	91 98	-0 02
^{232}Th (F)	90	89 97	-0 03
^{233}U (F)	92	92 00	0 00
^{233}U (H)	92	91 99	-0 01
^{236}U (F)	92	91 99	-0 01
^{239}Pu (H)	94	94 00	0 00
^{240}Pu (F)	94	93 99	-0 01
^{241}Pu (F)	94	93 99	-0 01
^{242}Pu (F)	94	94 00	0 00
^{232}Th (H)	90	89 98	-0 02
^{237}Np (F)	93	92 98	-0 02
^{252}Cf (S)	98	97 99	-0 01
^{234}U (F)	92	92 00	0 00
^{237}U (F)	92	92 00	0 00
^{240}Pu (H)	94	94 00	0 00
^{234}U (H)	92	92 00	0 00
^{236}U (H)	92	92 00	0 00
^{238}Pu (F)	94	94 00	0 00
^{241}Am (F)	95	95 00	0 00
^{243}Am (F)	95	95 00	0 00
^{238}Np (F)	93	93 00	0 00
^{242}Cm (F)	96	96 00	-0 01
^{227}Th (T)	90	90 00	0 00
^{229}Th (T)	90	90 02	0 02
^{231}Pa (F)	91	91 00	0 00
^{241}Am (T)	95	95 00	0 00
^{241}Am (H)	95	94 99	-0 01
^{242M}Am (T)	95	95 00	0 00
^{245}Cm (T)	96	95 99	-0 01
^{249}Cf (T)	98	98 01	0 01
^{251}Cf (T)	98	97 99	-0 01
^{254}Es (T)	99	98 99	-0 01
^{250}Cf (S)	98	97 99	-0 01
^{244}Cm (S)	96	95 98	-0 02
^{248}Cm (S)	96	95 99	-0 01
^{253}Es (S)	99	98 99	-0 01
^{254}Fm (S)	100	99 99	-0 01
^{255}Fm (T)	100	99 99	-0 01
^{256}Fm (S)	100	99 99	-0 01
^{237}Np (H)	93	93 00	0 00
^{232}U (T)	92	91 99	-0 01
^{238}U (S)	92	92 00	0 00

Table 6 [7]

ENDF/B FISSION-PRODUCT YIELD SETS [a]

Nuclide	Neutron Energy: Thermal	Fast	14 MeV	Spon
^{227}Th	6			
^{229}Th	6			
^{232}Th		456	56	
^{231}Pa		6		
^{232}U		6		
^{233}U	456	56	56	
^{234}U		6	6	
^{235}U	456	456	456	
^{236}U		56	6	
^{237}U		6		
^{238}U		456	456	6
^{237}Np		56	6	
^{238}Np		6		
^{238}Pu		6		
^{239}Pu	456	456	56	
^{240}Pu		56	6	
^{241}Pu	456	56		

Nuclide	Neutron Energy: Thermal	Fast	14 MeV	Spon
^{242}Pu		56		
^{241}Am	6	6	6	
^{242M}Am	6			
^{243}Am		6		
^{242}Cm		6		
^{244}Cm				6
^{245}Cm	6			
^{248}Cm				6
^{249}Cf	6			
^{250}Cf				6
^{251}Cf	6			
^{252}Cf				56
^{253}Es				6
^{254}Es	6			
^{254}Fm				6
^{255}Fm	6			
^{256}Fm				6

TABLE 7 [7]

Mean Value of Uncertainty in Cumulative Yields

		YC > 10% MEAN	σ	# NUC	YC < 10% MEAN	σ	# NUC
^{235}U	(T)	5	21	190	44	22	818
^{235}U	(F)	8	00	196	49	81	820
^{235}U	(H)	12	92	242	51	64	816
^{238}U	(F)	7	73	220	48	26	775
^{238}U	(H)	10	09	252	49	21	776
^{239}Pu	(T)	7	96	193	49	27	854
^{239}Pu	(F)	9	10	198	52	21	856
^{241}Pu	(T)	9	66	208	49	84	824
^{233}U	(T)	11	99	172	50	90	854
^{232}Th	(F)	11	38	186	47	98	807
^{233}U	(F)	10	48	180	53	41	858
^{233}U	(H)	16	15	231	55	10	841
^{236}U	(F)	13	56	205	53	80	815
^{239}Pu	(H)	14	67	231	54	83	845
^{230}Pu	(F)	13	87	201	52	65	845
^{241}Pu	(F)	12	08	212	52	18	825
^{242}Pu	(F)	17	07	224	54	30	802
^{232}Th	(H)	13	39	275	49	19	756
^{237}Np	(f)	11	20	203	51	33	832
^{252}Cf	(S)	11	21	209	51	10	839
^{234}U	(F)	17	68	193	55	44	851
^{237}U	(F)	19	12	219	53	69	789
^{240}Pu	(H)	15	23	240	54	32	832
^{234}U	(H)	20	93	244	56	13	825
^{236}U	(H)	20	37	255	54	25	798
^{238}Pu	(F)	20	34	198	55	87	852
^{241}Am	(F)	16	62	195	55	02	863
^{243}Am	(F)	20	63	197	55	72	849
^{238}Np	(F)	19	98	214	54	24	814
^{242}Cm	(F)	20	57	172	57	18	901
^{227}Th	(T)	18	09	164	54	41	830
^{229}Th	(T)	12	41	150	49	52	835
^{231}Pa	(F)	15	55	170	54	19	879
^{241}Am	(T)	13	48	188	53	60	856
^{241}Am	(H)	15	89	235	55	75	850
^{242}Am	(T)	15	97	200	53	77	849
^{245}Cm	(T)	12	79	217	53	67	833
^{249}Cf	(T)	14	96	208	54	42	855
^{251}Cf	(T)	17	08	215	54	25	841
^{254}Es	(T)	18	18	244	54	55	789
^{250}Cf	(S)	14	84	193	55	23	884
^{244}Cm	(S)	16	14	181	54	30	885
^{248}Cm	(S)	15	67	213	54	12	822
^{253}Es	(S)	17	68	197	55	66	885
^{254}Fm	(S)	17	16	180	56	34	898
^{255}Fm	(T)	19	44	224	56	01	847
^{256}Fm	(S)	19	29	204	56	38	873
^{237}Np	(H)	20	43	245	56	63	820
^{232}U	(T)	17	18	163	56	37	918
^{238}U	(S)	14	72	195	51	43	759

II - METHODS FOR THE DETERMINATION OF THE FISSION YIELDS -

a)- Description of the methods -

The methods are based on the simultaneous measurement of the activities of several fission products in a single shortly, irradiated and undissolved fissioning sample, by recording the γ-ray spectrum with a Ge(Li) detector. Activity A(t) and cumulative fission yield are related by the equation :

$$A(t) = Y \cdot N_F \cdot F(T,t)$$

with T irradiation time

t time after the end of T (cooling time)

N_F total number of fissions in the sample

F(T,t) includes the Bateman equation for the build-up and decay of the fission product under study. The decay constants λ, of all the members of the A chain, the isomeric branching and in some cases independent yields enter into F(T,t).

The activity results from

$$A = \frac{\dot{N} \times f}{\varepsilon \times \gamma}$$

with $\dot{N}$ counting rate in the full energy peak

ε full energy peak efficiency

γ gamma ray emission probability per decay

f correction factor for random and coincidence summing effects and self-absorption in the sample.

N_F can be determined by an other method in using a fission chamber.

But often N_F is not measured. So we get only relative yields. Generally measurer uses the ^{140}Ba yield as the reference yield (index r) We obtain :

$$Y = \frac{A \times C_R}{A_R \times C} Y_R \qquad \text{Method A}$$

The method B, also called R-value method relates the measured yields to ^{235}U thermal yields.

$$Y = \frac{Y^{*} \times Y_R}{Y_R^{*}}$$

with

$$R = \frac{A \times C_R}{A_R \times C} / \frac{A^{*} \times C_R^{*}}{A_R^{*} \times C^{*}}$$

The asterisk denoting quantities valid for thermal fission of ^{235}U. This method necessitates additional measurements of ^{235}U samples irradiated in a thermal neutron spectrum.

b)- Method for "Standards" -

Method A and method B previously described certainly could be used.

However standard fission yields have to be limited. We suggest that only the following F.P. could be developped as standards. ^{95}Zr, ^{97}Zr, ^{103}Ru, ^{131}I, ^{132}Te, ^{137}Cs, ^{140}Ba, ^{143}Ce, ^{147}Nd.

Method A seems more convenient for a standard method. The measurement of only one fission yield : ie, ^{140}Ba could be made relatively to the ^{235}U(nth).

The decay data for these F.P. are shown in Table 8 taken from the CEA Data bank [10]. It's possible that some dosimetry files have for these F.P. very minor differences.

c)- Experimental Problems -

The precision of the results mainly depend of the gamma ray spectrometry. Corrections for self absorption, dead time, pile up counting losses have to be done correctly. Paper from Debertin [11] are describing very well the technic to solve these problems.

A lot of computer codes now are available on the market to do the analysis of the γ spectra. Many benchmarks have been done in all countries to compare the different codes

Table 8

40 ZR 95 (5/2+)

PERIODE T1/2= 63 980 +/- 0 060 J

	ENERGIE	+/-	KEV	BRANCHEMENT	+/-	%
QBF-	1121 900		3 700	100 000		0 0
QBM-	887 200		3 840	0 0		0 0

** GAMMAS NG = 3 RELATIF A/R= 5486 (55%)

ENERGIE	+/-	KEV	INTENSITE	+/-		ALFA T	+/-	POLAR
234 700	0	140	0 0	0 0	*	2 830	0 0	M4
724 230	0	040	81 000	1 000	*			
756 740	0	040	100 000	0 0	*			

COMMENTAIRES EDITION DU 10/ 4/80
ENSDF 95ZR B- DECAY 72NDS ESD-DCK
** SPIN ET PARITE , VOIE QBF- (9/2+)
VOIE QBM- (1/2-)

40 ZR 97 1/2+

PERIODE T1/2= 16 900 +/- 0 050 H

	ENERGIE	+/-	KEV	BRANCHEMENT	+/-	%
QBF-	2665 000		16 000	5 320		0 0
QBM-	1921 690		16 080	94 680		0 0

** GAMMAS NG = 28 RELATIF A/R= 9275 (33%)

ENERGIE	+/-	KEV	INTENSITE	+/-		ALFA T	+/-	POLAR
111 600	0	400	0 060	0 010				
185 000	2	000	0 040	0 010				
218 870	0	200	0 190	0 020				
254 150	0	200	1 350	0 150		0 041	0 002	
272 270	0	200	0 270	0 040				
294 900	0	500	0 090	0 040	?			
297 400	0	500	0 040	0 020	?			
330 430	0	200	0 120	0 030				
355 390	0	100	2 450	0 250		0 013	0 001	
400 390	0	200	0 350	0 050				
507 630	0	100	5 450	0 550	**			
513 380	0	200	0 600	0 100				
602 410	0	200	1 500	0 150				
690 630	0	200	0 270	0 040	**			
699 200	0	300	0 130	0 020				
703 800	0	100	1 000	0 100				
743 360	0	100	0 0	0 0	*	0 021	0 001	M4
804 530	0	100	0 700	0 070	**			
829 800	0	100	0 240	0 020				
854 900	0	100	0 360	0 040				
971 390	0	100	0 310	0 030				
1021 300	0	300	1 450	0 150	**			
1110 450	0	200	0 120	0 020	?			
1147 950	0	100	2 850	0 300	*			
1276 090	0	100	1 050	0 100	*			
1362 660	0	100	1 450	0 150	**			
1750 460	0	100	1 450	0 150	*			
1851 550	0	100	0 380	0 040	*			

COMMENTAIRES EDITION DU 28/12/81
*ENSDF 78MAXX

44 RU103 (3/2+)

PERIODE T1/2= 39 350 +/- 0 050 J

	ENERGIE	+/-	KEV	BRANCHEMENT	+/-	%
QBF-	762 900		3 600	0 260		0 0
QBM-	723 150		3 600	99 740		0 0

** GAMMAS NG = 19 RELATIF A/R= 8950E-01 (1 1%)

ENERGIE	+/-	KEV	INTENSITE	+/-		ALFA T	+/-	POLAR
42 630	0	040	0 012	0 002		4 000	0 0	M1
53 275	0	010	4 200	0 200	**	2 100	0 0	M1
62 410	0	030	4 7E-03	0	?S	1 320	0 0	M1
113 250	0	070	0 040	0 008				
114 970	0	020	0 089	0 008		0 240	0 0	E2M1
241 880	0	050	0 165	0 017		0 012	0 0	E1
292 700	0	200	0 030	0 030				
294 980	0	020	2 800	0 090	*	0 019	0 000	E2M1
317 720	0	050	6 8E-05	0	**			
317 770	0	220	0 060	0 010	?			
357 390	0	140	0 100	0 030	*	0 016	0 0	E2
443 800	0	020	3 600	0 100		0 008	0 0	E2
497 080	0	013	1000 000	30 000	**	0 005	0 000	E2M1
514 600	0	150	0 054	0 015				
557 040	0	020	9 300	0 0		0 004	0 0	E2
567 870	0	130	0 018	0 008	**			
610 330	0	020	63 000	2 000	**	0 003	0 0	E2M1
612 020	0	030	0 890	0 100	**	0 003	0 0	E2
651 800	0	360	1 9E 03	8 E-04	*			

COMMENTAIRES EDITION DU 17/ 2/83
* 10/12/79 * ENSDF 103RU B- DECAY (39 35 D) 70PE04 73BA52 76MA37
** SPIN ET PARITE , VOIE QBF- 1/2-
VOIE QBM- 7/2+

41 NB 95F (9/2+)

PERIODE T1/2= 35 150 +/- 0 030 J

	ENERGIE	+/-	KEV	BRANCHEMENT	+/-	%
QBF-	925 500		0 500	100 000		0 0

** GAMMAS NG = 1 RELATIF A/R=1 000

ENERGIE	+/-	KEV	INTENSITE	+/-		ALFA T	+/-	POLAR
765 830	0	040	100 000	0 0	*			

COMMENTAIRES EDITION DU 10/ 4/80
ENSDF 95NB B- DECAY (35 15 D) 72NDS, ESD-DCK
** SPIN ET PARITE , VOIE QBF- 5/2+

41 NB 97F (9/2+)

PERIODE T1/2= 72 100 +/- 0 700 M

	ENERGIE	+/-	KEV	BRANCHEMENT	+/-	%
QBF-	1934 000		16 000	100 000		0 0

** GAMMAS NG = 14 RELATIF A/R= 9834 (1

ENERGIE	+/-	KEV	INTENSITE	+/-		ALFA T	+/-	POLAR
177 970	0	300	0 050	0 010				
238 370	0	300	0 050	0 010				
480 900	0	0	0 150	0 020	*			
549 250	0	200	0 050	0 010				
657 920	0	100	100 000	0 0	*	0 002	0 000	
719 470	0	200	0 090	0 010	*			
857 500	0	200	0 050	0 010				
909 570	0	100	0 040	0 010				
1024 500	0	300	0 0	0 0	*			
1117 010	0	200	0 090	0 010	*			
1148 600	0	300	0 050	0 010				
1268 630	0	100	0 160	0 020	*			
1515 640	0	200	0 120	0 020	*			
1629 130	0	200	0 030	0 010	*			

COMMENTAIRES EDITION DU 28/12/81
*ENSDF 78MAXX

Table 8 (suite)

53 I131 7/2+

PERIODE T1/2= 8 040 +/- 0 010 J

	ENERGIE	+/- KEV		BRANCHEMENT	+/- %	
QBF-	970 800	0 600		99 000	0 010	
QBM-	806 870	0 613		1 000	0 010	

** GAMMAS NG = 19 RELATIF A/R=1 008 (99%)

ENERGIE	+/- KEV	INTENSITE	+/-		ALFA T	+/-	POLAR
80 180	0 010	2 600	0 040	*	1 570	0 0	E2M1
85 920	0 150	9 0E-05	5 E-05		1 300	0 0	
163 930	0 010	0 0	0 0	*	0 0	0 0	M4
177 210	0 010	0 263	0 003	**	0 230	0 0	E2M1
232 170	0 150	1 4E-03	8 E-04				
272 490	0 020	0 056	0 001				
284 300	0 010	6 010	0 060		0 050	0 0	E2
295 830	0 150	7 0E-04	4 E-04				
302 410	0 150	4 5E-03	9 E-04				
318 080	0 020	0 079	0 003		0 035	0 0	
324 640	0 030	0 022	0 004				
325 780	0 010	0 249	0 005		0 033	0 0	E2M1
358 380	0 150	9 1E-03	2 E-04				
364 480	0 010	80 600	0 800	*	0 023	0 0	E2M1
404 800	0 010	0 056	0 002	*			
502 990	0 010	0 358	0 005	**	0 009	0 0	E2
636 970	0 010	7 210	0 080	*	0 005	0 0	E2
642 700	0 010	0 218	0 003				
722 890	0 010	1 790	0 020	*	0 005	0 0	E2M1

COMMENTAIRES EDITION DU 11/ 4/80
ENSDF 131I B- DECAY NBS-MJM 76NDS
** SPIN ET PARITE . VOIE QBF- 3/2+
VOIE QBM- 11/2-

52 TE132 0+

PERIODE T1/2= 78 200 +/- 0 800 H

	ENERGIE	+/- KEV	BRANCHEMENT	+/- %
QBF-	493 000	4 000	100 000	0 0

** GAMMAS NG = 4 RELATIF A/R= 8820 (45%)

ENERGIE	+/- KEV	INTENSITE	+/-		ALFA T	+/-	POLAR
49 720	0 010	16 300	1 100	*	5 720	0 060	E2M1
111 760	0 080	2 100	0 200		0 670	0 080	E2M1
116 300	0 080	2 200	0 200		0 590	0 080	E2M1
228 160	0 060	100 000	0 0		0 099	0 0	E2

COMMENTAIRES EDITION DU 28/12/81
*ENSDF 78MAXX

55 CS137

PERIODE T1/2= 30 170 +/- 0 034 A 75BUN

	ENERGIE	+/- KEV		BRANCHEMENT	+/- %	
QBF-	1173 200	0 900	75BUN	5 300	0 0	75BUN
QBM-	512 400	0 0	75BUN	94 700	0 0	75BUN

COMMENTAIRES EDITION DU 28/ 6/78

56 BA140 0+

PERIODE T1/2= 12 746 +/- 0 010 J

	ENERGIE	+/- KEV	BRANCHEMENT	+/- %
QBF-	1035 000	10 000	100 000	0 0

** GAMMAS NG = 12 RELATIF A/R= 2439 (90%)

ENERGIE	+/- KEV	INTENSITE	+/-		ALFA T	+/-	POLAR
13 850	0 050	4 900	0 500		54 900	0 0	M1
29 970	0 050	44 000	4 000	*	5 700	0 200	E2M1
44 270	0 100	0 060	0 0	*	37 000	0 0	E2
113 560	0 030	0 074	0 008	?	0 680	0 0	M1
118 840	0 120	0 210	0 020		0 670	0 0	M1
132 840	0 120	0 830	0 070		0 490	0 0	M1
162 640	0 050	25 460	0 330	*	0 279	0 0	E2M1
304 840	0 020	17 630	0 210		0 051	0 0	E2M1
423 695	0 030	12 800	0 600		0 022	0 0	M1
437 550	0 030	7 910	0 160		0 020	0 0	M1
467 570	0 050	0 600	0 050	*	0 012	0 0	E2
537 320	0 080	100 000	0 0		0 012	0 0	M1

COMMENTAIRES EDITION DU 4/ 9/80 79NDS
* 10/12/79 * ENSDF 140BA B- DECAY
** SPIN ET PARITE . VOIE QBF- 3-

56 BA137M 11/2-

PERIODE T1/2= 2 552 +/- 0 002 M

	ENERGIE	+/- KEV	BRANCHEMENT	+/- %
QIT	661 647	0 009	100 000	0 0

** GAMMAS NG = 1 RELATIF A/R=1 000

ENERGIE	+/- KEV	INTENSITE	+/-		ALFA T	+/-	POLAR
661 640	0 010	89 900	0 400	*	0 112	0 000	M4

COMMENTAIRES EDITION DU 28/12/81
*ENSDF 78MAXX

58 CE144 0+

PERIODE T1/2= 284 900 +/- 0 200 J

	ENERGIE	+/- KEV	BRANCHEMENT	+/- %
QBF-	318 200	2 000	100 000	0 0
QBM-	259 170	2 030	0 0	0 0

** GAMMAS NG = 7 RELATIF A/R= 1109 (1 4%)

ENERGIE	+/- KEV	INTENSITE	+/-		ALFA T	+/-	POLAR
33 620	0 010	2 600	0 200		4 790	0 0	M1
40 890	0 050	3 600	0 400	**	2 790	0 110	E2M1
53 430	0 010	0 860	0 050		8 090	0 0	M1
59 030	0 030	1 0E-02	0	*	1 26E+03	0	M3
80 106	0 005	10 200	1 000	*	2 490	0 0	M1
99 960	0 020	0 350	0 030	*	2 140	0 0	E2
133 544	0 005	100 000	4 000	*	0 579	0 0	M1

COMMENTAIRES EDITION DU 4/ 9/80
* 11/08/79 * ENSDF 144CE B- DECAY 79NDS
** SPIN ET PARITE . VOIE QBF- 0-
VOIE QBM- 3-

60 ND147 5/2-

PERIODE T1/2= 10 980 +/- 0 010 J

	ENERGIE	+/- KEV	BRANCHEMENT	+/- %
QBF-	895 800	0 900	100 000	0 0

** GAMMAS NG = 15 RELATIF A/R= 2790 (3 9%)

ENERGIE	+/- KEV	INTENSITE	+/-		ALFA T	+/-	POLAR
91 106	0 020	100 000	0 0	*	2 060	0 002	E2M1
120 480	0 050	1 420	0 150		0 930	0 010	E2M1
154 000	1 000	0 200	0 0				
196 640	0 040	0 730	0 060		0 235	0 001	E2M1
275 374	0 015	2 870	0 180		0 094	0 001	E2M1
319 411	0 018	7 000	0 400		0 062	0 001	E2M1
398 155	0 020	3 120	0 200		0 035	0 001	E2M1
410 480	0 030	0 500	0 030	*	0 021	0 0	E2
439 895	0 022	4 300	0 300		0 025	0 001	E2M1
489 240	0 028	0 550	0 030	*	0 021	0 0	E2M1
531 016	0 022	46 900	2 600	*	0 016	0 000	E2M1
589 350	0 040	0 164	0 016				
594 803	0 030	0 950	0 060		0 008	0 0	E2M1
680 520	0 150	0 070	0 015	*			
685 902	0 035	2 910	0 180	*	0 007	0 000	E2M1

COMMENTAIRES EDITION DU 12/ 7/79
ENSDF 147ND B- DECAY (10 98 D) 74HEYW 77AL34 78NDS

58 CE143 3/2-

PERIODE T1/2= 33 000 +/- 0 200 H

	ENERGIE	+/- KEV	BRANCHEMENT	+/- %
QBF-	1455 000	3 600	100 000	0 0

** GAMMAS NG = 41 RELATIF A/R= 4200 (9 5%)

ENERGIE	+/- KEV	INTENSITE	+/-		ALFA T	+/-	POLAR
57 365	0 001	28 000	3 000	*	6 580	0 0	E2M1
122 100	0 500	0 025	0 006		1 090	0 0	E2
139 670	0 050	0 230	0 070		0 657	0 0	E2
169 000	1 000	0 700	0 800				
216 000	1 000	0 490	0 050		0 0	0 0	E2M1
231 560	0 030	4 800	0 500		0 127	0 0	E2M1
293 262	0 021	100 000	0 0		0 063	0 0	E2M1
338 000	1 000	0 680	0 070				
350 590	0 050	8 000	0 800	*	0 031	0 0	E2
371 100	0 400	0 050	0 010		0 037	0 0	E2M1
377 000	1 000	0 150	0 020				
389 490	0 180	0 070	0 020		0 007	0 0	E1
400 000	1 000	0 230	0 020				
413 000	1 000	0 072	0 007				
433 020	0 070	0 320	0 070		0 025	0 0	E2M1
439 000	1 000	0 280	0 030				
447 210	0 140	0 160	0 030		0 0	0 0	E2M1
490 360	0 070	4 700	0 500	*	0 018	0 0	M1
497 910	0 190	0 080	0 020				
550 000	1 000	0 170	0 020				
556 860	0 210	0 060	0 020	?	0 0	0 0	E2
587 280	0 150	0 580	0 100		0 0	0 0	E2M1
658 000	1 000	0 030	0 003				
664 550	0 100	12 500	1 300		0 0	0 0	E2M1
709 200	0 400	0 020	0 005				
721 960	0 110	12 200	1 200	*	0 0	0 0	M1
791 100	0 300	0 040	0 010				
802 000	1 000	0 089	0 009				
806 460	0 230	0 060	0 020	?			
809 930	0 230	0 060	0 020		0 005	0 0	M1
880 390	0 130	2 200	0 200		0 004	0 0	M1
891 100	0 400	0 030	0 010				
937 800	0 300	0 080	0 020	*	0 002	0 0	E2
1002 970	0 210	0 160	0 030		0 003	0 0	M1
1031 500	0 300	0 040	0 010				
1047 000	0 300	0 020	0 010				
1060 500	0 300	0 080	0 020	*	0 0	0 0	E2M1
1102 980	0 180	0 870	0 120		0 0	0 0	E2M1
1314 000	1 000	0 080	0 008	*			
1324 600	0 400	0 030	0 010				
1339 900	0 800	9 0E-03	3 E-03				

COMMENTAIRES EDITION DU 12/ 7/79
ENSDF: 143CE B- DECAY 75DA20,71LU05,68GR19 78NDS

Evidently gamma spectra have to be taken at different time after the irradiation. So it is possible to minimize the interference in energies of the main peaks. With the help of γ Tables [13], it's also easy to check the possible interfering gammas.

The availabily of good gamma standard will help to solve the efficiency corrections. The well known ^{152}Eu is sufficient for the most of the cases [12].

d)- Benchmark -

The best way to improve the fission yields standards would be to organize benchmarks between laboratories. One benchmark has been arranged in US for ^{238}U and ^{237}Np. The results are given in Table 9 taken from the paper of Fudge [1].

Table 9 Uranium-238 Chain Yield Ratios [1]

Fission Product Nuclide	Source				
	Rider A	Crouch B B/A	I.L.R.R. C C/A	I.N.E.L. D D/A	ENDF/B5 E/A
^{95}Zr	1.00	1.039	1.016	0.977	1.000
^{97}Zr	1.00	1.002	1.023	1.094	0.996
^{103}Ru	1.00	1.016	1.005	-	0.987
^{106}Ru	1.00	0.867	-	-	1.012
^{131}I	1.00	0.981	1.006	1.005	0.997
^{132}Te	1.00	0.983	-	1.013	0.994
^{137}Cs	1.00	0.987	0.998	1.007	0.998
^{140}Ba	1.00	1.038	1.029	0.974	1.021
^{141}Ce	1.00	-	-	0.940	1.004
^{143}Ce	1.00	1.011	0.917	1.005	0.993
^{144}Ce	1.00	1.004	1.088	0.996	0.998

Neptunium-237 Chain Yield Ratios

Fission Product Nuclide	Source				
	Rider A	Crouch B B/A	I.L.R.R. C C/A	I.N.E.L. D D/A	ENDF/B5 E/A
^{95}Zr	1.00	1.023	1.042	0.994	1.002
^{97}Zr	1.00	0.966	1.120	1.001	-
^{103}Ru	1.00	1.005	1.059	0.900	1.004
^{106}Ru	1.00	0.830	-	1.133	-
^{131}I	1.00	0.774	-	1.036	-
^{132}Te	1.00	0.780	-	1.049	-
^{137}Cs	1.00	-	1.053	1.037	1.016
^{140}Ba	1.00	1.055	1.049	1.003	1.004
^{141}Ce	1.00	0.778	-	0.978	-
^{143}Ce	1.00	1.127	-	1.016	-
^{144}Ce	1.00	0.685	-	1.011	1.017

REFERENCES

1 - FUDGE A.J. NEANDC SPECIALISTS MEETING ON YIELDS AND DECAY DATA OF FISSION PRODUCTS NUCLIDES. BROOKHAVEN OCT 24 1983 EDITED BY R.E. CHRIEN, T.W. BURROWS, P. 121

2 - DENSCHLAG H.O. NEUTRON PHYSICS AND NUCLEAR DATA HARWELL SEPT 1978 P. 569

3 - LAMMER M. PROGRESS IN FISSION PRODUCT NUCLEAR DATA INDC (NDS)-130/G+P

4 - MEEK M.E. AND RIDER B.F. NEDO-12154-1 (1974) AND REFERENCES THEREIN

5 - *RIDER B.F. NEDO-12154-3(B) (1980) AND REFERENCES THEREIN AND* NEDO-12154-3(C) (1981)

6 - CROUCH E. A. C. ATOMIC DATA AND NUCLEAR DATA TABLES 19, 417 1977 *REFERENCES THEREIN*

7 - ENGLAND T.R., RIDER B.F. REF(1), P. 33

8 - JAMES M.F. PRIVATE COMMUNICATION

9 - CUNINGHAME J.G. IN FISSION PRODUCTS NUCLEAR DATA - 1977, VOL 1, P. 351 (IAEA-213) AND DISCUSSION IN IAEA-213, VOL II P775 ET SEQ.

10 - BLACHOT J. FICHE C. REF(2), P. 215

11 - DEBERTIN K. SCHOTZIG U. NUCL. INST. METH. 158, 471 (1979), 140, P. 337 (1977)

12 - DEBERTIN K. NUCL. INST. METH. 158, 479

13 - BLACHOT J., FICHE C. NUCL. DAT. TABLES 20, 241 (1977)

Chain Yields per 100 Fissions and Uncertainties, Version E [7]

MASS	U235T	U235F	U235H	U238F	U238H
66	6 608E-08 +/- 32 00	6 569E-07 +/- 23 00	2 930E-04 +/- 8 00	3 726E-06 +/- 32 00	8 449E-05 +/- 11 00
67	3 428E-07 +/- 32 00	2 110E-06 +/- 23 00	6 696E-04 +/- 8 00	2 155E-05 +/- 32 00	1 386E-04 +/- 16 00
68	5 658E-07 +/- 32 00	3 661E-06 +/- 23 00	9 088E-04 +/- 11 00	9 954E-06 +/- 16 00	2 985E-04 +/- 16 00
69	1 227E-06 +/- 32 00	7 901E-06 +/- 23 00	1 414E-03 +/- 32 00	1 290E-05 +/- 16 00	5 008E-04 +/- 16 00
70	2 841E-06 +/- 32 00	1 732E-05 +/- 23 00	2 418E-03 +/- 11 00	1 604E-05 +/- 16 00	9 002E-04 +/- 16 00
71	6 598E-06 +/- 32 00	4 220E-05 +/- 23 00	4 042E-03 +/- 11 00	2 009E-05 +/- 16 00	1 591E-03 +/- 16 00
72	2 524E-05 +/- 11 00	1 506E-04 +/- 23 00	6 066E-03 +/- 8 00	6 076E-05 +/- 32 00	2 994E-03 +/- 11 00
73	9 604E-05 +/- 32 00	4 910E-04 +/- 16 00	1 161E-02 +/- 11 00	2 080E-04 +/- 23 00	5 220E-03 +/- 11 00
74	3 209E-04 +/- 23 00	1 081E-03 +/- 23 00	1 743E-02 +/- 11 00	2 787E-04 +/- 32 00	8 001E-03 +/- 16 00
75	1 054E-03 +/- 23 00	6 936E-03 +/- 16 00	2 764E-02 +/- 11 00	4 845E-04 +/- 32 00	1 386E-02 +/- 16 00
76	3 300E-03 +/- 32 00	1 127E-02 +/- 23 00	4 097E-02 +/- 11 00	8 025E-04 +/- 23 00	2 197E-02 +/- 16 00
77	7 553E-03 +/- 8 00	2 925E-02 +/- 11 00	6 815E-02 +/- 11 00	3 310E-03 +/- 11 00	3 127E-02 +/- 8 00
78	2 070E-02 +/- 8 00	5 429E-02 +/- 11 00	1 022E-01 +/- 11 00	1 126E-02 +/- 23 00	4 084E-02 +/- 11 00
79	4 329E-02 +/- 6 00	8 505E-02 +/- 11 00	1 716E-01 +/- 8 00	3 278E-02 +/- 23 00	1 690E-01 +/- 11 00
80	1 270E-01 +/- 6 00	1 146E-01 +/- 23 00	2 598E-01 +/- 11 00	4 721E-02 +/- 32 00	2 127E-01 +/ 16 00
81	1 906E-01 +/- 4 00	2 091E-01 +/- 11 00	2 980E-01 +/- 11 00	1 083E-01 +/- 16 00	3 324E-01 +/- 11 00
82	3 224E-01 +/- 2 80	3 262E-01 +/- 11 00	6 077E-01 +/- 11 00	2 133E-01 +/- 16 00	4 526E-01 +/- 16 00
83	5 394E-01 +/- 0 50	5 734E-01 +/- 1 00	1 111E+00 +/- 6 00	3 952E-01 +/- 1 40	6 690E-01 +/ 2 80
84	1 003E+00 +/- 0 70	1 024E+00 +/- 1 40	1 544E+00 +/- 11 00	8 194E 01 +/- 1 40	1 124E+00 +/- 2 80
85	1 317E+00 +/- 0 35	1 350E+00 +/- 0 70	1 658E+00 +/- 2 80	7 398E 01 +/- 1 00	1 003E+00 +/- 1 40
86	1 968E+00 +/- 0 50	1 939E+00 +/- 1 00	2 626E+00 +/- 11 00	1 286E+00 +/- 1 00	1 571E+00 +/- 2 80
87	2 558E+00 +/- 0 50	2 482E+00 +/- 1 00	2 440E+00 +/- 4 00	1 604E+00 +/- 1 00	1 685E+00 +/- 2 00
88	3 565E+00 +/- 0 70	3 483E+00 +/- 0 70	3 374E+00 +/- 4 00	2 054E+00 +/- 1 40	2 215E+00 +/- 2 00
89	4 771E+00 +/- 1 00	4 412E+00 +/- 1 40	4 139E+00 +/- 2 80	2 784E+00 +/- 2 00	2 914E+00 +/- 2 00
90	5 755E+00 +/- 1 00	5 444E+00 +/- 0 70	4 594E+00 +/- 2 80	3 239E+00 +/- 1 40	3 166E+00 +/- 2 80
91	5 910E+00 +/- 1 00	5 721E+00 +/- 0 70	4 871E+00 +/- 4 00	3 979E+00 +/- 2 00	3 764E+00 +/- 2 80
92	5 977E+00 +/- 1 00	5 830E+00 +/- 1 00	5 164E+00 +/- 8 00	4 288E+00 +/- 2 80	3 926E+00 +/- 2 80
93	6 349E+00 +/- 0 70	6 244E+00 +/- 0 70	5 250E+00 +/- 6 00	4 892E+00 +/- 2 00	4 475E+00 +/- 2 80
94	6 417E+00 +/- 1 00	6 288E+00 +/- 0 70	5 221E+00 +/- 11 00	4 765E+00 +/- 4 00	4 894E+00 +/- 8 00
95	6 507E+00 +/- 1 00	6 414E+00 +/- 0 50	5 180E+00 +/- 4 00	5 106E+00 +/- 1 00	4 963E+00 +/- 2 00
96	6 274E+00 +/- 1 00	6 190E+00 +/- 0 70	5 299E+00 +/- 8 00	5 996E+00 +/- 4 00	5 578E+00 +/- 11 00
97	5 937E+00 +/- 0 70	5 984E+00 +/- 0 50	5 564E+00 +/- 6 00	5 546E+00 +/- 0 70	5 305E+00 +/- 2 00
98	5 747E+00 +/- 1 00	5 911E+00 +/- 0 50	4 215E+00 +/- 8 00	5 862E+00 +/- 1 00	5 457E+00 +/- 11 00
99	6 091E+00 +/- 1 00	5 765E+00 +/- 1 40	5 088E+00 +/- 2 80	6 163E+00 +/- 1 40	5 685E+00 +/- 1 40
100	6 232E+00 +/- 1 00	6 274E+00 +/- 1 00	4 042E+00 +/- 8 00	6 672E+00 +/- 1 00	4 996E+00 +/- 11 00
101	5 170E+00 +/- 1 00	5 199E+00 +/- 1 40	3 532E+00 +/- 8 00	6 202E+00 +/- 1 40	5 611E+00 +/- 2 80
102	4 308E+00 +/- 1 00	4 355E+00 +/- 1 00	3 333E+00 +/- 11 00	6 440E+00 +/- 1 00	4 609E+00 +/- 8 00
103	3 030E+00 +/- 1 00	3 241E+00 +/- 1 00	3 198E+00 +/- 2 80	6 299E+00 +/- 1 00	4 651E+00 +/- 2 00
104	1 909E+00 +/- 1 40	2 067E+00 +/- 2 00	2 187E+00 +/- 8 00	5 033E+00 +/- 1 00	3 587E+00 +/- 5 00
105	9 603E-01 +/- 1 40	1 169E+00 +/- 2 80	1 875E+00 +/- 4 00	4 075E+00 +/- 2 00	3 233E+00 +/- 2 00
106	3 999E-01 +/- 1 40	5 309E-01 +/- 1 00	1 577E+00 +/- 4 00	2 473E+00 +/- 1 40	2 434E+00 +/- 4 00
107	1 449E-01 +/- 2 80	2 763E-01 +/- 11 00	1 320E+00 +/- 11 00	1 234E+00 +/- 8 00	1 728E+00 +/- 6 00
108	5 091E-02 +/- 4 00	1 144E-01 +/- 16 00	1 210E+00 +/- 11 00	6 010E 01 +/- 16 00	1 222E+00 +/- 16 00
109	2 993E-02 +/- 8 00	8 254E-02 +/- 11 00	1 263E+00 +/- 4 00	2 423E 01 +/- 11 00	1 217E+00 +/- 8 00
110	2 514E-02 +/- 4 00	6 055E-02 +/- 16 00	1 113E+00 +/- 11 00	1 347E-01 +/- 16 00	1 025E+00 +/- 11 00
111	1 849E-02 +/- 4 00	4 266E-02 +/- 2 00	1 127E+00 +/- 2 80	7 478E-02 +/- 2 00	1 040E+00 +/- 2 80
112	1 279E-02 +/- 4 00	3 705E-02 +/- 2 00	1 104E+00 +/- 8 00	5 527E-02 +/- 4 00	1 006E+00 +/- 6 00
113	1 444E-02 +/- 6 00	3 21 E-02 +/- 2 80	1 111E+00 +/- 8 00	5 146E-02 +/ 8 00	9 289E-01 +/- 6 00
114	1 251E-02 +/- 6 00	3 193E-02 +/- 2 80	1 086E+00 +/- 11 00	3 828E 02 +/- 16 00	7 184E-01 +/- 11 00
115	1 044E-02 +/- 8 00	2 831E-02 +/- 6 00	9 867E-01 +/- 4 00	3 294E-02 +/- 6 00	8 392E-01 +/- 4 00
116	1 521E-02 +/- 6 00	3 369E-02 +/- 2 00	1 085E+00 +/- 11 00	3 940E 02 +/- 11 00	6 753E-01 +/- 11 00
117	9 834E-03 +/- 8 00	2 946E-02 +/- 11 00	1 082E+00 +/- 8 00	3 658E-02 +/- 11 00	7 090E-01 +/- 8 00
118	7 034E-03 +/- 16 00	2 875E-02 +/- 11 00	1 104E+00 +/- 11 00	3 984E 02 +/- 11 00	8 344E-01 +/- 11 00
119	7 283E-03 +/- 11 00	2 804E-02 +/- 8 00	1 108E+00 +/- 11 00	3 439E 02 +/- 16 00	7 353E 01 +/- 11 00

MASS	U235T	U235F	U235H	U238F	U238H
120	7 514E-03 +/- 11 00	2 857E-02 +/- 8 00	1 113E+00 +/- 8 00	3 443E-02 +/- 16 00	7 898E-01 +/- 11 00
121	1 152E-02 +/- 6 00	3 299E-02 +/- 8 00	9 804E 01 +/- 6 00	3 773E-02 +/- 11 00	7 651E-01 +/- 4 00
122	8 785E-03 +/- 11 00	2 726E-02 +/- 11 00	1 170E+00 +/- 11 00	3 619E-02 +/- 16 00	8 627E-01 +/- 11 00
123	1 443E-02 +/- 4 00	3 890E-02 +/- 11 00	1 217E+00 +/- 11 00	3 891E-02 +/- 16 00	9 357E-01 +/- 11 00
124	1 737E-02 +/- 11 00	4 684E-02 +/- 11 00	1 316E+00 +/- 11 00	4 269E-02 +/- 16 00	1 050E+00 +/- 11 00
125	2 683E-02 +/- 4 00	5 411E-02 +/- 8 00	1 488E+00 +/- 8 00	4 565E-02 +/- 8 00	1 193E+00 +/- 6 00
126	4 454E-02 +/- 8 00	8 572E-02 +/- 11 00	1 503E+00 +/- 4 00	5 109E 02 +/- 8 00	1 365E+00 +/- 16 00
127	1 161E-01 +/- 4 00	3 024E-01 +/- 4 00	2 040E+00 +/- 4 00	1 331E-01 +/- 4 00	1 505E+00 +/- 6 00
128	3 315E-01 +/- 2 80	3 953E-01 +/- 11 00	2 490E+00 +/- 11 00	4 179E-01 +/- 6 00	1 675E+00 +/- 8 00
129	6 607E-01 +/- 6 00	8 443E-01 +/- 4 00	3 567E+00 +/- 8 00	9 441E-01 +/- 4 00	2 076E+00 +/- 8 00
130	1 733E+00 +/- 2 00	1 713E+00 +/- 6 00	3 648E+00 +/- 8 00	1 839E+00 +/- 6 00	3 202E+00 +/- 11 00
131	2 875E+00 +/- 0 50	3 209E+00 +/- 0 70	4 098E+00 +/- 2 80	3 232E+00 +/- 1 40	4 050E+00 +/- 2 00
132	4 282E+00 +/- 0 35	4 651E+00 +/- 0 70	4 883E+00 +/- 2 80	5 137E+00 +/ 1 40	4 846E+00 +/- 1 40
133	6 654E+00 +/- 0 35	6 716E+00 +/- 0 50	5 587E+00 +/- 6 00	6 748E+00 +/- 0 50	6 125E+00 +/- 2 00
134	7 780E+00 +/- 0 50	7 641E+00 +/- 0 50	5 729E+00 +/- 2 80	7 845E+00 +/- 2 00	6 547E+00 +/- 2 00
135	6 492E+00 +/- 0 35	6 565E+00 +/- 0 70	4 556E+00 +/- 4 00	6 950E+00 +/- 0 70	5 890E+00 +/- 2 00
136	6 267E+00 +/- 0 35	6 216E+00 +/- 0 50	3 334E+00 +/- 4 00	6 897E+00 +/- 2 80	5 744E+00 +/- 2 00
137	6 136E+00 +/- 0 50	6 210E+00 +/- 0 35	2 924E+00 +/- 2 80	5 999E+00 +/- 0 70	4 986E+00 +/- 2 00
138	6 627E+00 +/- 0 70	6 666E+00 +/- 0 70	4 584E+00 +/- 6 00	5 694E+00 +/- 1 40	4 859E+00 +/- 2 80
139	6 235E+00 +/- 1 00	6 327E+00 +/- 0 50	4 749E+00 +/- 4 00	5 630E+00 +/- 1 00	5 046E+00 +/- 2 80
140	6 134E+00 +/- 0 70	5 949E+00 +/- 0 70	4 493E+00 +/- 2 80	5 813E+00 +/- 0 70	4 619E+00 +/- 1 40
141	5 711E+00 +/- 1 00	5 891E+00 +/- 1 40	4 490E+00 +/- 4 00	5 404E+00 +/- 2 00	4 357E+00 +/- 2 80
142	5 733E+00 +/- 0 70	5 510E+00 +/- 1 00	4 248E+00 +/- 6 00	4 564E+00 +/- 1 00	4 100E+00 +/- 4 00
143	5 945E+00 +/- 0 35	5 715E+00 +/- 0 50	3 827E+00 +/- 2 80	4 584E+00 +/- 0 70	3 933E+00 +/- 2 80
144	5 443E+00 +/- 0 35	5 265E+00 +/- 0 70	3 147E+00 +/- 2 80	4 539E+00 +/- 0 70	3 655E+00 +/- 2 80
145	3 910E+00 +/- 0 35	3 765E+00 +/- 0 50	2 732E+00 +/- 6 00	3 776E+00 +/- 0 70	3 014E+00 +/- 4 00
146	2 977E+00 +/- 0 35	2 915E+00 +/- 0 50	2 235E+00 +/- 11 00	3 415E+00 +/- 0 70	2 094E+00 +/- 11 00
147	2 218E+00 +/- 0 50	1 120E+00 +/- 0 70	1 626E+00 +/- 4 00	2 542E+00 +/- 1 00	2 094E+00 +/- 2 00
148	1 657E+00 +/- 0 35	1 679E+00 +/- 0 35	1 218E+00 +/- 11 00	2 090E+00 +/- 0 70	1 759E+00 +/- 16 00
149	1 054E+00 +/- 1 00	1 031E+00 +/- 0 70	6 602E-01 +/- 8 00	1 613E+00 +/- 1 00	1 427E+00 +/- 6 00
150	6 434E-01 +/- 0 50	6 839E-01 +/- 0 50	5 183E-01 +/- 11 00	1 263E+00 +/- 1 00	1 099E+00 +/- 16 00
151	4 052E-01 +/- 0 70	4 110E-01 +/- 0 70	3 623E-01 +/- 8 00	8 017E-01 +/- 1 40	8 144E-01 +/- 6 00
152	2 587E-01 +/- 1 00	2 758E-01 +/- 2 00	2 621E-01 +/- 11 00	5 235E-01 +/- 1 00	5 888E-01 +/- 16 00
153	1 480E-01 +/- 2 80	1 602E-01 +/- 2 80	2 070E-01 +/- 11 00	3 818E-01 +/- 2 00	3 938E-01 +/- 6 00
154	7 225E-02 +/- 1 00	7 438E-02 +/- 4 00	1 137E-02 +/- 11 00	2 143E-01 +/- 1 00	2 564E-01 +/- 16 00
155	2 939E-02 +/- 4 00	4 043E-02 +/- 11 00	6 480E-02 +/- 11 00	1 278E-01 +/- 16 00	1 579E-01 +/- 16 00
156	1 341E-02 +/- 2 80	2 027E-02 +/- 2 80	5 378E-02 +/- 2 80	6 728E-02 +/- 2 00	1 093E-01 +/- 2 80
157	5 162E-03 +/- 8 00	6 766E-03 +/- 16 00	3 837E-02 +/- 11 00	3 714E-02 +/- 16 00	8 379E-02 +/- 16 00
158	1 989E-03 +/- 16 00	2 208E-03 +/- 16 00	2 389E-02 +/- 11 00	1 660E-02 +/- 16 00	4 334E-02 +/- 16 00
159	8 893E-04 +/- 6 00	2 756E-03 +/- 11 00	1 225E 02 +/- 8 00	7 158E 03 +/- 16 00	2 635E-02 +/- 11 00
160	1 146E-04 +/- 32 00	1 083E-03 +/- 16 00	7 301E-03 +/- 11 00	3 047E 03 +/- 23 00	1 594E-02 +/- 16 00
161	7 845E-05 +/- 4 00	3 241E-04 +/- 8 00	5 167E-03 +/- 8 00	1 154E-03 +/- 8 00	8 340E-03 +/- 4 00
162	6 909E-06 +/- 32 00	5 392E-05 +/- 23 00	2 832E-03 +/- 11 00	2 751E-04 +/- 32 00	6 040E-03 +/- 16 00
163	2 778E-06 +/- 32 00	8 991E-06 +/- 23 00	1 613E-03 +/- 11 00	1 649E 04 +/- 32 00	3 453E-03 +/- 16 00
164	8 708E-07 +/- 32 00	5 401E-06 +/- 23 00	9 931E-04 +/- 11 00	1 007E-04 +/- 32 00	2 027E-03 +/- 16 00
165	6 578E-07 +/- 23 00	2 158E-06 +/- 23 00	5 471E-04 +/- 11 00	6 574E-05 +/- 23 00	1 116E-03 +/- 16 00
166	2 920E-07 +/- 23 00	8 957E-07 +/- 23 00	2 780E-04 +/- 8 00	4 579E-05 +/- 32 00	6 349E-04 +/- 8 00
167	1 675E-07 +/- 23 00	3 590E-07 +/- 23 00	1 885E-04 +/- 11 00	3 904E 05 +/- 16 00	3 753E-04 +/- 16 00
168	3 825E-08 +/- 23 00	8 991E-08 +/- 23 00	1 084E-04 +/- 11 00	2 292E-05 +/- 32 00	2 035E-04 +/- 16 00
169	1 565E-08 +/- 23 00	5 394E-08 +/- 23 00	7 901E-05 +/- 8 00	1 375E-05 +/- 32 00	1 305E-04 +/- 8 00
170	3 281E-09 +/- 23 00	1 805E-08 +/- 23 00	3 299E-05 +/- 11 00	8 235E-06 +/- 32 00	6 058E-05 +/- 16 00
171	1 565E-09 +/- 23 00	6 269E-09 +/- 23 00	1 794E-05 +/- 11 00	4 611E 06 +/- 32 00	3 358E-05 +/- 16 00
172	5 397E-10 +/- 23 00	1 792E-09 +/- 23 00	1 662E-05 +/- 8 00	8 606E 06 +/- 32 00	2 161E-05 +/- 16 00

Annexe I (Cont.)

MASS	PU239T	PU239F	PU241T	U233T	TH232F
66 1	877E-07 +/- 23 00 8	183E-07 +/- 16 00 1	370E-07 +/- 23 00 2	602E-07 +/- 23 00 1	184E-06 +/- 32 00
67 3	754E-07 +/- 23 00 2	699E-06 +/- 16 00 2	545E-07 +/- 23 00 1	179E-06 +/- 23 00 4	077E-06 +/- 32 00
68 1	313E-06 +/- 23 00 7	929E-06 +/- 16 00 5	874E-07 +/- 23 00 3	629E-06 +/- 23 00 1	494E-05 +/- 32 00
69 4	690E-06 +/- 23 00 2	941E-05 +/- 16 00 1	273E-06 +/- 23 00 9	980E-06 +/- 23 00 3	450E-05 +/- 32 00
70 1	591E-05 +/- 23 00 8	133E-05 +/- 16 00 4	604E-06 +/- 23 00 3	913E-05 +/- 23 00 6	752E-05 +/- 23 00
71 2	899E-05 +/- 23 00 1	770E-04 +/- 32 00 6	853E-06 +/- 23 00 1	724E-04 +/- 23 00 1	715E-04 +/- 23 00
72 9	726E-05 +/- 45 00 4	529E-04 +/- 32 00 2	545E-05 +/- 23 00 4	986E-04 +/- 23 00 4	247E-04 +/- 16 00
73 2	365E-04 +/- 23 00 7	006E-04 +/- 23 00 5	909E-05 +/- 16 00 1	086E-03 +/- 23 00 6	519E-04 +/- 16 00
74 5	477E-04 +/- 32 00 1	633E-03 +/- 16 00 9	790E-05 +/- 23 00 2	722E-03 +/- 23 00 1	179E-03 +/- 16 00
75 1	277E-03 +/- 32 00 2	332E-03 +/- 23 00 2	937E-04 +/- 23 00 8	159E-03 +/- 23 00 2	898E-03 +/- 16 00
76 2	828E-03 +/- 32 00 5	453E-03 +/- 16 00 9	791E-04 +/- 23 00 1	452E-02 +/- 23 00 6	890E-03 +/- 16 00
77 6	686E-03 +/- 11 00 1	207E-02 +/- 8 00 1	958E-03 +/- 23 00 2	601E-02 +/- 23 00 1	159E-02 +/- 8 00
78 2	752E-02 +/- 11 00 2	808E-02 +/- 16 00 8	973E-03 +/- 8 00 5	444E-02 +/- 23 00 4	559E-02 +/- 8 00
79 4	667E-02 +/- 23 00 5	929E-02 +/- 8 00 1	536E-02 +/- 16 00 1	502E-01 +/- 11 00 7	818E-02 +/- 11 00
80 1	147E-01 +/- 16 00 9	745E-02 +/- 16 00 2	991E-02 +/- 16 00 2	359E-01 +/- 23 00 1	985E-01 +/- 16 00
81 1	713E-01 +/- 16 00 1	346E-01 +/- 11 00 6	355E-02 +/- 16 00 3	670E-01 +/- 4 00 4	773E-01 +/- 11 00
82 2	061E-01 +/- 23 00 2	103E-01 +/- 8 00 1	380E-01 +/- 8 00 5	855E-01 +/- 2 80 1	100E+00 +/- 16 00
83 2	967E-01 +/- 0 70 3	108E-01 +/- 2 00 2	016E-01 +/- 2 00 1	014E+00 +/- 1 00 2	175E+00 +/- 2 00
84 4	724E-01 +/- 2 00 4	923E-01 +/- 1 40 3	526E-01 +/- 2 00 1	688E+00 +/- 1 00 3	992E+00 +/- 2 00
85 5	753E-01 +/- 0 50 6	016E-01 +/- 1 00 4	068E-01 +/- 1 40 2	227E+00 +/- 1 00 4	158E+00 +/- 1 40
86 7	647E-01 +/- 0 70 7	805E-01 +/- 1 40 5	960E-01 +/- 2 00 2	848E+00 +/- 1 40 6	553E+00 +/- 2 00
87 9	990E-01 +/- 0 70 1	023E+00 +/- 1 40 7	575E-01 +/- 2 00 4	034E+00 +/- 1 40 6	934E+00 +/- 2 80
88 1	342E+00 +/- 1 40 1	323E+00 +/- 1 40 9	788E-01 +/- 2 00 5	459E+00 +/- 1 40 7	291E+00 +/- 2 00
89 1	691E+00 +/- 2 80 1	727E+00 +/- 2 00 1	221E+00 +/- 4 00 6	335E+00 +/- 2 00 7	559E+00 +/- 4 00
90 2	082E+00 +/- 2 00 2	032E+00 +/- 1 00 1	539E+00 +/- 2 00 6	838E+00 +/- 1 40 7	968E+00 +/- 4 00
91 2	488E+00 +/- 1 00 2	499E+00 +/- 1 40 1	871E+00 +/- 2 00 6	551E+00 +/- 1 00 7	385E+00 +/- 2 00
92 3	003E+00 +/- 1 40 3	014E+00 +/- 1 00 2	333E+00 +/- 2 00 6	542E+00 +/- 1 40 6	852E+00 +/- 2 80
93 3	840E+00 +/- 1 40 3	811E+00 +/- 1 00 2	986E+00 +/- 2 00 6	953E+00 +/- 1 40 6	786E+00 +/- 4 00
94 4	340E+00 +/- 2 00 4	199E+00 +/- 1 00 3	430E+00 +/- 2 00 6	797E+00 +/- 1 40 5	713E+00 +/- 6 00
95 4	878E+00 +/- 2 00 4	670E+00 +/- 1 00 3	963E+00 +/- 2 00 6	347E+00 +/- 1 40 5	665E+00 +/- 2 80
96 4	956E+00 +/- 2 80 4	811E+00 +/- 1 00 4	431E+00 +/- 2 00 5	635E+00 +/- 1 00 4	444E+00 +/- 6 00
97 5	340E+00 +/- 2 00 5	318E+00 +/- 0 70 4	698E+00 +/- 2 00 5	498E+00 +/- 1 40 4	465E+00 +/- 1 40
98 5	894E+00 +/- 2 00 5	653E+00 +/- 1 00 4	977E+00 +/- 2 00 5	175E+00 +/- 1 40 3	709E+00 +/- 6 00
99 6	169E+00 +/- 2 00 5	956E+00 +/- 2 00 6	077E+00 +/- 2 00 4	877E+00 +/- 2 00 2	961E+00 +/- 2 00
100 6	819E+00 +/- 4 00 6	556E+00 +/- 0 70 6	272E+00 +/- 2 00 4	379E+00 +/- 1 40 1	382E+00 +/- 6 00
101 5	997E+00 +/- 1 40 6	653E+00 +/- 1 00 6	286E+00 +/- 2 00 3	168E+00 +/- 1 40 7	249E+01 +/- 11 00
102 6	075E+00 +/- 2 00 6	706E+00 +/- 1 00 6	658E+00 +/- 2 00 2	404E+00 +/- 1 40 3	737E-01 +/- 11 00
103 6	947E+00 +/- 2 00 6	846E+00 +/- 1 00 6	739E+00 +/- 4 00 1	593E+00 +/- 2 00 1	565E-01 +/- 4 00
104 6	017E+00 +/- 2 00 6	535E+00 +/- 1 00 7	099E+00 +/- 2 00 9	755E-01 +/- 2 80 9	175E-02 +/- 11 00
105 5	586E+00 +/- 2 00 5	344E+00 +/- 2 80 6	254E+00 +/- 2 80 4	939E-01 +/- 2 80 5	180E-02 +/- 2 80
106 4	328E+00 +/- 2 80 4	362E+00 +/- 1 40 6	127E+00 +/- 2 00 2	453E 01 +/- 2 00 5	320E-02 +/- 8 00
107 3	265E+00 +/- 6 00 2	957E+00 +/- 8 00 5	145E+00 +/- 11 00 1	131E-01 +/- 4 00 5	189E-02 +/- 11 00
108 2	115E+00 +/- 6 00 1	927E+00 +/- 8 00 3	599E+00 +/- 11 00 7	287E-02 +/- 6 00 6	272E-02 +/- 16 00
109 1	699E+00 +/- 8 00 1	590E+00 +/- 6 00 2	259E+00 +/- 6 00 4	326E-02 +/- 8 00 5	252E-02 +/- 6 00
110 6	279E-01 +/- 6 00 6	213E-01 +/- 8 00 1	340E+00 +/- 8 00 3	713E-02 +/- 4 00 7	259E-02 +/- 16 00
111 2	935E-01 +/- 2 80 3	547E-01 +/- 2 00 5	704E-01 +/- 4 00 1	944E-02 +/- 8 00 7	451E-02 +/- 6 00
112 1	229E-01 +/- 2 80 1	903E-01 + - 2 80 2	366E-01 +/- 4 00 1	381E-02 +/- 8 00 8	004E-02 +/- 6 00
113 7	979E-02 +/- 4 00 1	268E-01 +/- 2 00 1	545E-01 +/- 6 00 1	312E-02 +/- 8 00 8	034E-02 +/- 4 00
114 5	877E-02 +/- 4 00 9	366E-02 +/- 2 00 7	342E-02 +/- 23 00 1	251E-02 +/- 8 00 7	507E-02 +/- 16 00
115 3	687E-02 +/- 4 00 7	017E-02 +/- 6 00 4	481E-02 +/- 16 00 1	258E-02 +/- 6 00 5	781E-02 +/- 4 00
116 4	840E-02 +/- 8 00 5	896E-02 +/- 6 00 2	913E-02 +/- 32 00 1	313E-02 +/- 11 00 7	362E-02 +/- 16 00
117 4	825E-02 +/- 8 00 6	859E-02 +/- 11 00 2	547E-02 +/- 23 00 1	204E-02 +/- 8 00 5	916E-02 +/- 2 80
118 3	933E-02 +/- 11 00 6	159E-02 +/- 11 00 2	428E-02 +/- 32 00 1	261E-02 +/- 8 00 6	298E-02 +/- 11 00
119 4	028E-02 +/- 11 00 5	966E-02 +/- 11 00 2	428E-02 +/- 32 00 1	293E-02 +/- 8 00 5	703E-02 +/- 16 00

Annexe I (Cont.)

MASS	PU239T	PU239F	PU241T	U233T	TH232F
120 3	613E-02 +/- 11 00 5	657E-02 +/- 11 00 2	618E-02 +/- 23 00 1	425E-02 +/- 8 00 5	416E-02 +/- 16 00
121 3	730E-02 +/- 8 00 6	161E-02 +/- 11 00 2	667E-02 +/- 32 00 1	554E-02 +/- 11 00 4	728E-02 +/- 6 00
122 5	472E-02 +/- 11 00 7	256E-02 +/- 11 00 2	668E-02 +/- 32 00 1	528E-02 +/- 11 00 3	642E-02 +/- 16 00
123 4	011E-02 +/- 23 00 7	310E-02 +/- 16 00 2	773E-02 +/- 32 00 1	905E-02 +/- 32 00 2	926E-02 +/- 16 00
124 1	003E-01 +/- 11 00 1	235E-01 +/- 11 00 3	308E-02 +/- 32 00 2	520E-02 +/- 11 00 2	639E-02 +/- 16 00
125 1	131E-01 +/- 8 00 1	345E-01 +/- 8 00 4	905E-02 +/- 8 00 1	103E-01 +/- 11 00 3	360E-02 +/- 11 00
126 2	549E-01 +/- 8 00 2	863E-01 +/- 8 00 8	294E-02 +/- 16 00 2	518E-01 +/- 16 00 4	795E-02 +/- 16 00
127 4	981E-01 +/- 6 00 5	107E-01 +/- 8 00 2	333E-01 +/- 4 00 5	585E-01 +/- 11 00 7	551E-02 +/- 6 00
128 6	939E-01 +/- 11 00 8	923E-01 +/- 6 00 3	876E-01 +/- 23 00 8	098E-01 +/- 11 00 1	821E-01 +/- 16 00
129 1	387E+00 +/- 4 00 1	495E+00 +/- 6 00 8	381E-01 +/- 23 00 1	616E+00 +/- 16 00 2	824E-01 +/- 4 00
130 2	049E+00 +/- 16 00 2	372E+00 +/- 8 00 1	839E+00 +/- 11 00 2	165E+00 +/- 23 00 8	084E-01 +/- 16 00
131 3	874E+00 +/- 0 50 3	885E+00 +/- 0 70 3	091E+00 +/- 1 40 3	495E+00 +/- 1 00 1	615E+00 +/- 2 00
132 5	420E+00 +/- 0 70 5	323E+00 +/- 1 00 4	563E+00 +/- 1 40 4	799E+00 +/- 1 40 2	898E+00 +/- 1 40
133 7	019E+00 +/- 0 70 6	951E+00 +/- 0 70 6	736E+00 +/- 1 00 6	043E+00 +/- 1 00 3	944E+00 +/- 2 00
134 7	666E+00 +/- 0 70 7	389E+00 +/- 0 70 7	921E+00 +/- 1 40 6	133E+00 +/- 1 00 5	351E+00 +/- 2 00
135 7	610E+00 +/- 0 70 7	561E+00 +/- 0 70 7	243E+00 +/- 1 40 6	163E+00 +/- 2 00 5	491E+00 +/- 2 00
136 7	182E+00 +/- 1 00 7	040E+00 +/- 1 40 7	117E+00 +/- 1 40 6	865E+00 +/- 4 00 5	623E+00 +/- 2 00
137 6	685E+00 +/- 0 50 6	581E+00 +/- 0 70 6	720E+00 +/- 1 40 6	818E+00 +/- 0 70 5	800E+00 +/- 4 00
138 6	102E+00 +/- 1 40 6	129E+00 +/- 1 00 6	599E+00 +/- 2 00 5	906E+00 +/- 2 00 7	021E+00 +/- 11 00
139 5	534E+00 +/- 4 00 5	602E+00 +/- 1 40 6	231E+00 +/- 2 00 6	292E+00 +/- 4 00 7	146E+00 +/- 2 00
140 5	378E+00 +/- 1 00 5	293E+00 +/- 0 70 5	732E+00 +/- 2 00 6	515E+00 +/- 1 40 7	815E+00 +/- 2 00
141 5	299E+00 +/- 2 00 5	091E+00 +/- 2 80 4	892E+00 +/- 1 40 6	525E+00 +/- 2 80 7	320E+00 +/- 2 80
142 4	894E+00 +/- 1 00 4	803E+00 +/- 0 70 4	784E+00 +/- 1 40 6	694E+00 +/- 1 40 6	495E+00 +/- 4 00
143 4	442E+00 +/- 0 50 4	349E+00 +/- 0 50 4	590E+00 +/- 1 40 5	942E+00 +/- 1 00 6	588E+00 +/- 2 00
144 3	744E+00 +/- 0 50 3	692E+00 +/- 1 00 4	209E+00 +/- 1 00 4	671E+00 +/- 1 00 7	893E+00 +/- 2 80
145 2	997E+00 +/- 0 50 3	007E+00 +/- 0 50 3	269E+00 +/- 1 40 3	428E+00 +/- 1 00 5	287E+00 +/- 2 80
146 2	466E+00 +/- 0 50 2	457E+00 +/- 0 70 2	789E+00 +/- 1 40 2	569E+00 +/- 0 70 4	539E+00 +/- 2 80
147 2	027E+00 +/- 1 40 1	986E+00 +/- 1 00 2	285E+00 +/- 1 40 1	746E+00 +/- 2 80 2	926E+00 +/- 4 00
148 1	639E+00 +/- 0 50 1	654E+00 +/- 0 35 1	938E+00 +/- 1 00 1	289E+00 +/- 1 00 1	992E+00 +/- 2 80
149 1	226E+00 +/- 1 00 1	240E+00 +/- 0 70 1	476E+00 +/- 1 40 7	731E 01 +/- 2 80 1	059E+00 +/- 6 00
150 9	677E-01 +/- 0 50 9	922E-01 +/- 0 70 1	216E+00 +/- 1 40 5	066E-01 +/- 1 40 3	471E-01 +/- 16 00
151 7	545E-01 +/- 2 00 7	644E 01 +/- 1 40 9	134E-01 +/- 1 40 3	138E-01 +/- 2 00 3	551E-01 +/- 6 00
152 5	795E-01 +/- 1 40 5	977E-01 +/- 2 80 7	192E 01 +/- 1 40 2	124E 01 +/ 2 80 7	527E-02 +/- 16 00
153 3	502E-01 +/- 6 00 4	191E-01 +/- 4 00 5	411E-01 +/- 4 00 9	735E-02 +/- 6 00 6	443E 02 +/- 8 00
154 2	657E-01 +/- 1 40 2	619E-01 +/- 2 00 3	802E-01 +/- 2 00 4	641E 02 +/- 2 80 6	842E 03 +/- 23 00
155 1	593E-01 +/- 11 00 2	023E-01 +/- 11 00 2	422E-01 +/- 8 00 2	41E-02 +/- 23 00 3	598E-03 +/- 23 00
156 1	188E-01 +/- 2 80 1	434E 01 +/- 4 00 1	719E-01 +/- 2 80 1	153E-02 +/- 6 00 2	541E-03 +/- 11 00
157 7	258E-02 +/- 6 00 1	039E-01 +/- 8 00 1	353E-01 +/- 4 00 5	313E 03 +/- 8 00 9	271E-04 +/- 23 00
158 3	737E-02 +/- 23 00 6	232E-02 +/- 16 00 9	426E-02 +/- 23 00 2	260E-03 +/- 32 00 4	611E-04 +/- 32 00
159 1	974E-02 +/- 6 00 3	691E-02 +/- 11 00 4	800E-02 +/- 4 00 7	773E 04 +/- 6 00 9	699E-05 +/- 32 00
160 8	549E-03 +/- 32 00 2	228E-02 +/- 16 00 2	095E-02 +/- 23 00 3	175E-04 +/- 32 00 6	868E-05 +/- 32 00
161 4	681E-03 +/- 6 00 7	984E-03 +/- 4 00 8	464E-03 +/- 4 00 1	113E-04 +/- 6 00 1	440E-05 +/- 23 00
162 2	126E-03 +/- 32 00 5	602E-03 +/- 23 00 2	723E-03 +/- 23 00 1	527E-05 +/- 32 00 7	929E-06 +/- 32 00
163 8	594E-04 +/- 32 00 2	539E-03 +/- 45 00 9	824E-04 +/- 23 00 7	142E-06 +/- 32 00 4	611E-06 +/- 32 00
164 3	243E-04 +/- 32 00 1	566E-03 +/- 45 00 3	152E-04 +/- 23 00 2	351E-06 +/- 32 00 2	021E-06 +/- 32 00
165 1	284E-04 +/- 23 00 8	150E-04 +/- 32 00 9	845E-05 +/- 23 00	450E-07 +/- 23 00 3	512E-07 +/- 23 00
166 6	387E-05 +/- 16 00 5	899E-04 +/- 32 00 6	598E-05 +/- 23 00 4	524E-07 +/- 32 00 1	372E-07 +/- 32 00
167 1	758E-05 +/- 32 00 2	574E-04 +/- 32 00 2	985E-05 +/- 23 00 6	323E-08 +/- 32 00 9	701E-08 +/- 32 00
168 4	915E-06 +/- 32 00 7	365E-05 +/- 32 00 1	361E-05 +/- 23 00 1	627E-08 +/- 32 00 5	262E-08 +/- 32 00
169 1	666E-06 +/- 32 00 2	481E-05 +/- 32 00 5	760E-06 +/- 23 00 5	515E-09 +/- 32 00 2	672E-08 +/- 32 00
170 3	499E-07 +/- 64 00 7	271E-06 +/- 32 00 1	676E-06 +/- 23 00 1	638E-09 +/- 32 00 1	061E-08 +/- 32 00
171 1	672E-07 +/- 32 00 2	478E-06 +/- 32 00 3	142E-07 +/- 23 00 5	429E-10 +/- 32 00 4	611E-09 +/- 32 00
172 4	934E-08 +/- 32 00 7	367E-07 +/- 32 00 1	047E-07 +/- 23 00 1	808E-10 +/- 32 00 2	371E-09 +/- 32 00

CROSS-SECTION MEASUREMENTS OF $^{56}Fe(n,p)^{56}Mn$ AND $^{27}Al(n,\alpha)^{24}Na$ BETWEEN 14.0 AND 19.9 MeV

K. KUDO, T. MICHIKAWA, T. KINOSHITA,
Y. HINO, Y. KAWADA
Electrotechnical Laboratory,
Sakura-mura, Niihari-gun, Ibaraki,
Japan

Abstract

The standard cross section of $^{27}Al(n,\alpha)^{24}Na$ reaction and the $^{56}Fe(n,p)^{56}Mn$ cross section so often used to measure fast neutron fluence rate were measured in the neutron energy range from 14.0 to 19.9 MeV by the activation method, using a proton recoil telescope to determine the neutron fluence rate of the irradiation field. The results show difference of up to 10% in the $^{27}Al(n,\alpha)^{24}Na$ cross section at 19.9 MeV, and systematic higher values in the $^{56}Fe(n,p)^{56}Mn$ cross section except at 19.9 MeV compared with those of ENDF/B-V.

The cross sections for the reactions $^{56}Fe(n,p)^{56}Mn$ and $^{27}Al(n,\alpha)^{24}Na$ were measured by the activation method in the neutron energy range from 14.0 to 19.9 MeV.

Monoenergetic neutrons were produced through the D-T reaction by bombarding a Ti-T target with deuterons, which were accelerated up to 3.3 MeV by a Van de Graaff (Pelletron 4UH-HC) or up to 270 keV by a Cockcroft type accelerator. The activation samples as shown in Table 1 were set at distances of 55 to 120 mm from the target and arranged in the order Al, Fe and Al for one irradiation. The neutron fluence rates for all energies were measured by a proton recoil telescope[1] positioned between 20 and 50 cm from the target, and an associated α counting technique was also used at 14.0, 14.6 and 14.8 MeV to get the more precise values.

Table 1. Physical constants used in our measurements

1. Properties of target foils and their constants

reaction	$^{27}Al(n,\alpha)^{24}Na$	$^{56}Fe(n,p)^{56}Mn$
purity	99.99%	99.9%
size	25.4mm$^{\phi}$, 56mg/cm^2	25.4mm$^{\phi}$, 78mg/cm^2
isotopic abundance	100%	91.68%(^{56}Fe)
		2.17% (^{57}Fe)
half life	14.959 h[11]	2.5785 h[12]
β efficiency	0.796	0.727
K value	0.003	0.0177

2. n-p elastic cross section for hydrogen

ENDF/B-V[2]

3. hydrogen content in polyethylene radiators

(14.39± 0.07) wt.%

4. cross section of ^{56}Mn production from $^{57}Fe(n,np)$ and $^{57}Fe(n,d)$

by T. Asami[5] and S.M. Qaim[6].

3 ~ 6.5 MeV neutrons produced by D(d,n) reaction, which increase with deuteron bombardment, contribute to the additional activities of the ^{24}Na and ^{56}Mn. The neutron yields from D(d,n) reaction were measured by a calibrated ^{3}He detector (400 kPa of ^{3}He and 200 kPa of Kr gases) for each deuteron energy. One of the pulse height spectrum at 1.84 MeV deuteron energy was shown in Fig.1. The peak induced by D(d,n) reaction corresponding to the neutron energy 5.07 MeV is shown on the figure with recoil edges due to the recoil He induced by 5.07 and 18.04 MeV neutrons, and a thermal neutron peak at the lowest energy region. The extra activity by the d+D neutrons were finally calculated by the help of the published ^{27}Al(n,α)^{24}Na and ^{56}Fe(n,p)^{56}Mn cross section.[2]

In order to estimate secondary neutrons from the target backing and the target assembly, the neutron spectrum at the foil position was calculated numerically at each neutron energy, taking account of the angular distribution of T(d,n) reaction[3] and the differential elastic and inelastic cross sections[4] etc. The each induced activity was estimated by multipling the cross section to the calculated neutron spectrum, and the secondary neutron fluence rate above 10 MeV was taken into account.

As the activation samples used in the ^{56}Fe(n,p) cross sectin measurements were the natural iron as shown in Table 1, the extra ^{56}Mn activity from the ^{57}Fe(n,np) reaction etc. should be subtracted from the total ^{56}Mn activity. The calculated response curve of the ^{57}Fe(n,np) corss section[5] was normalized at 14.7 MeV by the Qaim's evaluation.[6]

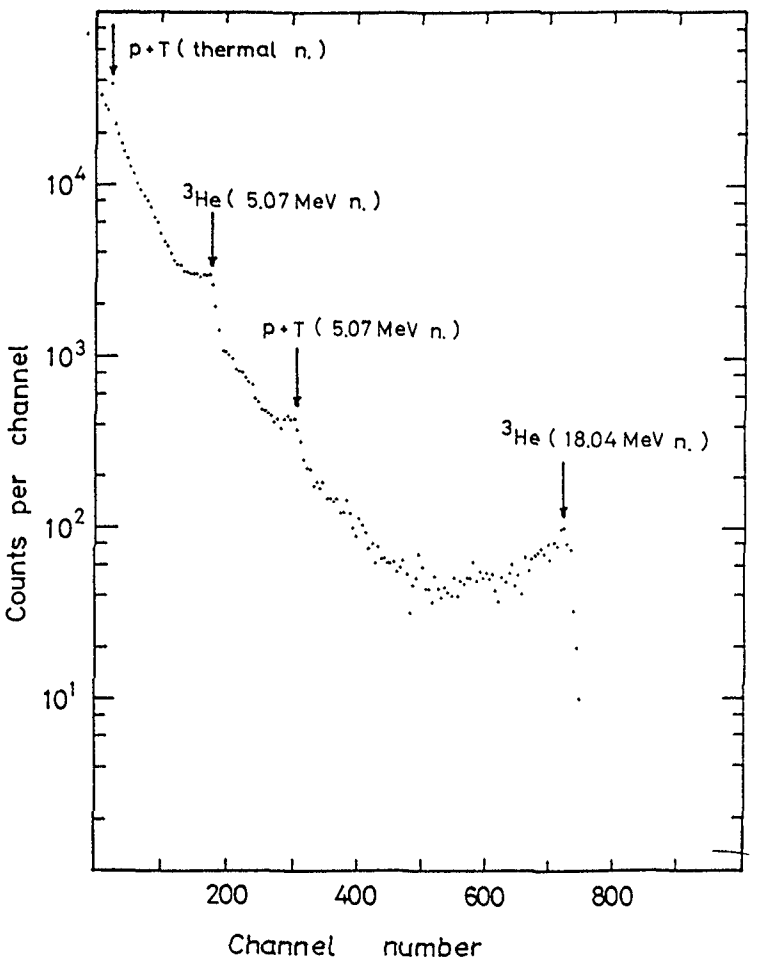

Figure 1. Pulse height spectrum of neutrons from ^{3}He detector at 1.84 MeV deuteron bombardment on Ti-T target.

The activities of ^{24}Na and ^{56}Mn, normally 0.03 ~ 4 dps/mg produced by 14 ~ 20 MeV monoenergetic neutron irradiations, were measured by using a 4πβ CH_4 gas flow proportional counter. The absolute β efficiencies for Al and Fe foils were

Table 2. Uncertainties for cross section measurements

Origin	Uncertainty (%)	
(1) flux measurement		
n-p cross section of hydrogen	1.0	
anisotropy of n-p scattering	1.0	
radiator composition of hydrogen	0.7	
internal telescope geometry	0.9	
target-to-telescope distance	0.3	
background subtraction	0.5 ~ 1.0	
neutron energy	0.2	
neutron attenuation in Al window of telescope	0.2	
(2) activity measurement	^{56}Mn	^{24}Na
β counting efficiency	0.3	0.3
K value	0.5	0.2
contribution of ^{56}Mn from other reactions	0.1 ~ 0.5	0.0
(3) foil irradiation and others		
contribution of d+D neutrons	0.2 ~ 5.0	0.1 ~ 3.0
contribution of secondary neutrons	0.2	0.2
target-to-foil distance	0.4 ~ 0.7	0.4 ~ 0.7
(4) statistics		
flux measurement	0.3	0.3
activity measurement	0.1 ~ 0.2	0.1 ~ 0.2

Table 3. Cross sections for $^{27}Al(n,\alpha)^{24}Na$ and $^{56}Fe(n,p)^{56}Mn$ reaction

neutron energy En(MeV)	$^{27}Al(n,\alpha)^{24}Na$ σ (mb)	$^{56}Fe(n,p)^{56}Mn$ σ (mb)
14.0 ± 0.05	122.9±2.1	116.4±2.0
14.6 ± 0.1	113.4±1.5	110.0±1.5
14.8 ± 0.1	111.6±1.7	106.2±1.6
15.21±0.28	105.2±2.4	100.0±2.2
15.88±0.14	99.0±2.3	91.4±2.2
16.98±0.10	80.4±2.0	75.6±1.9
18.04±0.11	66.0±1.8	64.4±1.7
19.87±0.15	44.9±1.8	47.9±2.7

determined by the $4\pi\beta$-γ coincidence technique[7] after the irradiation of intense neutrons.

Small corrections which are related to the effects due to the efficiency of the $4\pi\beta$ counter to γ rays, and specially to the complex decay scheme of the ^{56}Mn, were made by adopting the results of our previous measurements[8],[9] as described in Table 1.

The uncertainties of the measurements and the cross sections of the $^{27}Al(n,\alpha)^{24}Na$ and the $^{56}Fe(n,p)^{56}Mn$ reactions are given in Table 2 ~ 3 and Figures 2 ~ 3, and the ratio of the $^{27}Al(n,\alpha)^{24}Na$ cross section to the $^{56}Fe(n,p)^{56}Mn$ cross section is also shown in Fig.4. The results agree closely with the recent measurements of Ryves[10] between 14 and 16 MeV, but lie 5 ~ 15% above his results in the higher energy region.

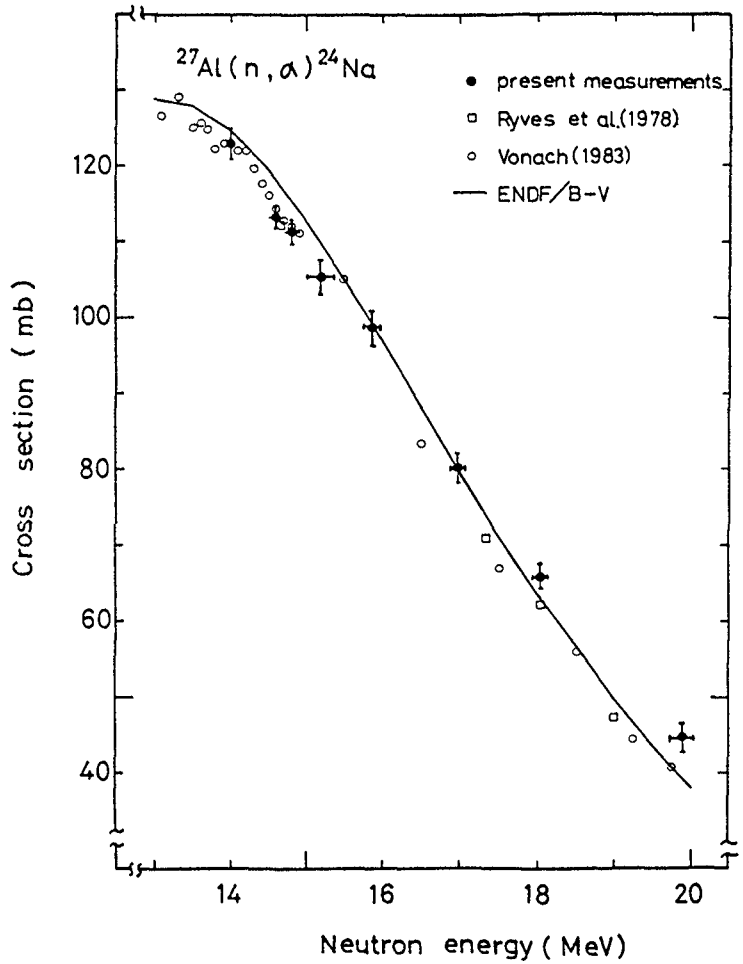

Figure 2. $^{27}Al(n,\alpha)^{24}Na$ cross section.

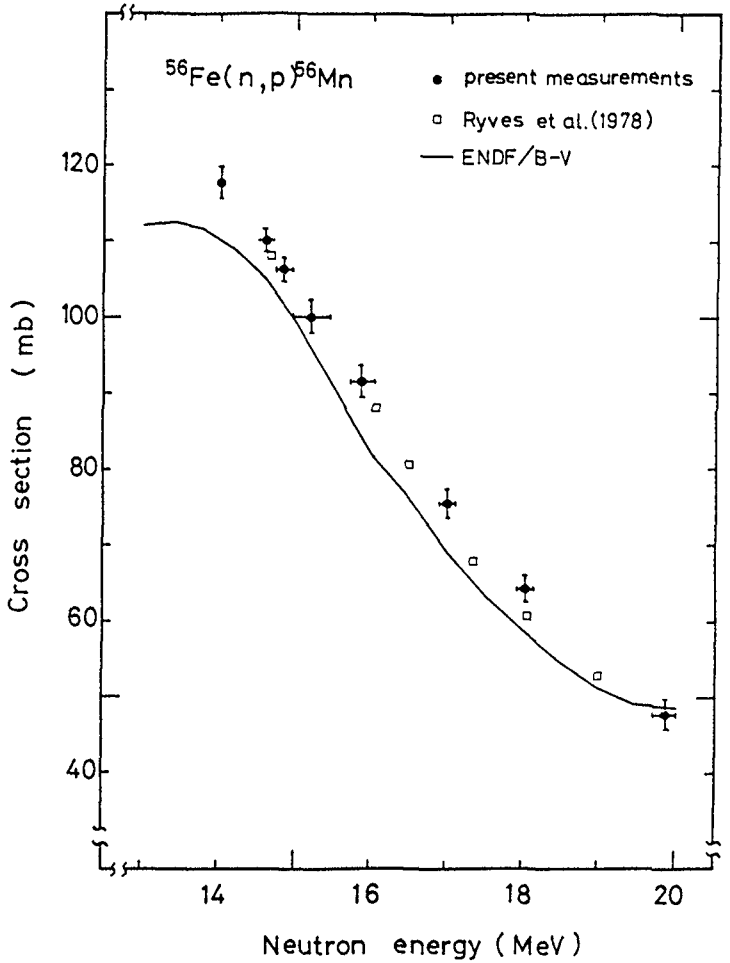

Figure 3. $^{56}Fe(n,p)^{56}Mn$ cross section.

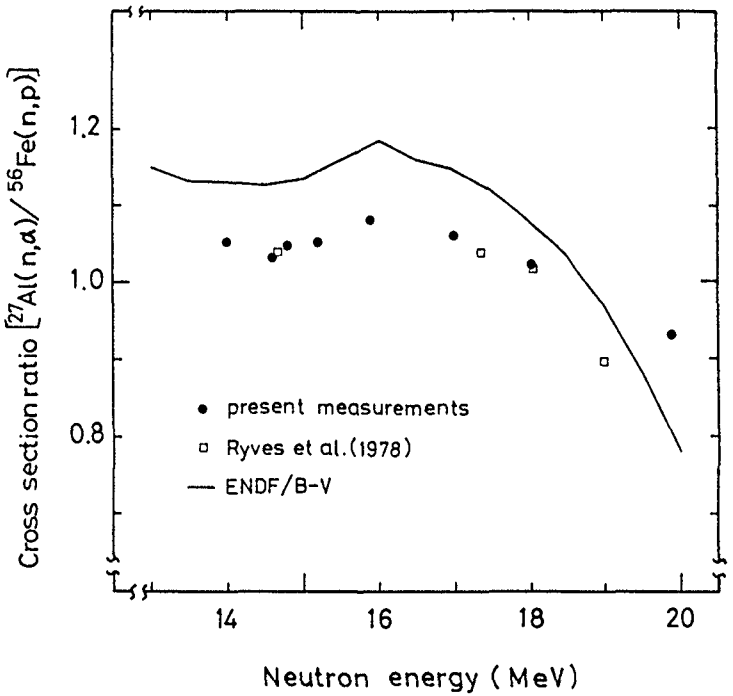

Figure 4. Ratio of $^{27}Al(n,\alpha)^{24}Na$ to $^{56}Fe(n,p)^{56}Mn$ cross sections.

REFERENCES

1. N. Kobayashi, T. Kinoshita and T. Michikawa: Bulltin of the Electrotechnical Laboratory 47, 140 (1983).
2. Evaluated Neutron Data File, ENDF/B-V (1979).
3. H. Liskien and A. Paulsen: Nucl. Data Table 11, 569 (1973).
4. Evaluated Neutron Data File, ENDF/B-IV (1974).
5. T. Asami (JAERI): private communication.
6. S.M. Qaim: Nucl.Phys. A325, 255 (1979).
7. Y. Kawada: Researches of the Electrotechnical Laboratory, No.730 (1972).
8. K. Kudo: Nucl.Instr.Meth. 141, 325 (1977).
9. Y. Kawada: Int.J.Appl.Radiat.Isotopes 20, 413 (1969).
10. T.B. Ryves, P. Kolkowski and K.J. Zieba: J.Phys.G 4, 1783 (1978).
11. D.D. Hoppes and F.J. Schima: NBS Special Pub. 626 (1982).
12. Table of Isotopes 7th. Edition (1978).

454 NEUTRON PRODUCTION USING GAS TARGETS

H. KLEIN
Physikalisch-Technische Bundesanstalt,
Braunschweig, Federal Republic of Germany

Abstract

Gas targets are often used to produce neutrons via the reactions $T(p,n)^3He$, $D(d,n)^3He$ and $T(d,n)^4He$, because the neutron background caused by the construction materials can be easily determined. For practical reasons the reaction $D(d,n)^3He$ is chiefly applied in the energy range 6 MeV $\leq E_n \leq$ 14 MeV, but a gas target causes problems due to the finite geometry, the kinematics and the structure of the differential cross section, in particular for experiments performed in close geometry. Monte Carlo simulations allow the most important parameters or distributions required for the correction and interpretation of fluence measurements or activation and scattering experiments to be calculated. The application of this method is particularly recommended if the evaluated angular distribution of this reaction is used to calibrate fast neutron detectors. The resulting uncertainties cannot be reliably estimated, when no complete covariance analysis of the differential cross section is available.

(1) Neutron Production in the Energy Range of 6 MeV $\leq E_n \leq$ 14 MeV

The reaction $D(d,n)^3He$ is chiefly applied if "monoenergetic" neutron fields are required in the energy range from 6 MeV to 14 MeV. Deuterium gas targets are easily handled and a high flux density of unpolarized neutrons can be achieved at a reasonable energy resolution. While the neutron background due to construction materials can be determined experimentally the distortions due to low energy background from the break-up reaction D(d,np)D have to be corrected for.

Since the unified evaluation of various reactions producing neutrons in this energy range is available[1] it seems to be justified to also apply the angular distribution of this reaction for calibration purposes, in particular for neutron energies below 14 MeV. Nevertheless, problems arise due to the pronounced structure of the differential cross section, the kinematics and the finite size of a gas target. A sensitivity study shows that the mean deuteron energy within the gas and the mean neutron emission angle must be determined very carefully.

The distortion of the neutron field due to the construction material of the gas cell and the beam stop may be different for experiments performed in close geometry or for detector systems to be calibrated at a large distance, and must therefore be calculated or at least estimated. It will be demonstrated that a realistic Monte Carlo simulation is required to calculate the corrections and the most relevant parameters or distributions necessary for the analysis of the experiment.

(2) Experimental Results

The properties of the neutron energy distribution produced by means of the reaction $D(d,n)^3He$ using a gas target have been intensively studied[2]. Clean net spectra are obtained even for large emission angles. For neutron emission at 0 degrees the width of the rectangular energy distribution is usually determined by the energy loss of the projectiles within the gas but limited by the straggling of the energy loss in the entrance foil. On the other hand, the angle straggling of the deuteron beam due to multiple small angle scattering in the foil determined the energy resolution for emission angles $\vartheta_n \geq 30$ degrees.

The extreme gradients $dE_n/d\vartheta_n$ and $d\sigma/d\vartheta_n$ at forward angles create special problems, in particular due to be finite length of the neutron source and the angle straggling of the projectiles.

Experiments performed close to the target can be interpreted best by complete simulation. Besides the complex geometry the field distortion due to the construction material can be taken into account.

A versatile Monte Carlo code has been developed at the PTB by B.R.L. Siebert[3]. First, parts of the code were tested by investigating the neutron energy resolution[2]. Then the neutron detection efficiency of a proton recoil telescope was calculated[4], where significant corrections for neutron inscattering from construction materials were obtained. The same corrections arise if neutron detectors are calibrated at large distances but they strongly depend on the neutron emission angle and the experimental method applied.

With a combination of precise TOF measurements and the realistic simulation, the mean deuteron energy could be determined with uncertainties of less than 30 keV for energies up to 11 MeV, while the emission angle could be fixed with uncertainties of typically 0.1 to 0.2 degrees. Thus, uncertainties of less than 2 % were estimated for the expected neutron fluence at emission angles up to 120° if calculated on the basis of the evaluated cross section. In fact, a comparison of the fluence measurements near the target (proton recoil telescope) and at a larger distance (calibrated liquid scintillator) agreed within ± 2 % for the energy range of 6 MeV ≤ E_n ≤ 14 MeV[5]. On the other hand, the measured neutron fluence was lower than expected. As this deviation increased with the pressure of the target, this points to a problem in determining the effective length and pressure of the gas heated by the energy loss of the projectiles.

However, an absolute scaling is not required if the angular distribution is investigated. Reasonable agreement is obtained with the experimental data reported by M. Drosg[2] for deuteron energies around 7 MeV, but significant deviations are obtained for higher projectile energies. The final analysis for the entire energy range of 3 MeV ≤ E_d ≤ 11 MeV is in progress.
Finally it should be mentioned that this MC description of the neutron source is also part of the simulation of scattering experiments necessary to calculate sample size corrections[6]

(3) Conclusion and Recommendations

Reliably evaluated differential cross sections for the reaction $D(d,n)^3He$ are required if the angular distribution is applied for calibration purposes. Deuterium gas targets can be handled experimentally without any problems. An almost realistic Monte Carlo simulation is recommended to take into account the finite size and the various influences of the construction materials. Care must be taken in determining the mean projectile energy within the gas target and the effective angle of the neutron emission. From the preliminary results obtained for the angular distribution we conclude that the evaluation should be repeated and include a covariance analysis. In this way the energy-dependent neutron detection efficiency may be calibrated with uncertainties of less than 3 % applying this reaction. Similar results are to be expected for tritium gas targets used for the reactions $T(p,n)^3He$ and $T(d,n)^4He$. Fortunately, the differential cross section does not show such a pronounced structure, but on the other hand the distortions due to the construction material increase. Here too, a realistic Monte Carlo simulation is therefore to be recommended.

(4) References

1. M. Drosg, NSE 67 (1978) 190 - 220

2. H. Klein, H.J. Brede, B.R.L. Siebert, NIM 193 (1982) 635 - 644

3. B.R.L. Siebert, H.J. Brede, H. Lesiecki,
PTB report ND-23, Braunschweig 1982

4. B.R.L. Siebert, H.J. Brede, H. Lesiecki,
submitted for publication in NIM

5. H. Klein, R. Böttger, G. Dietze, to be published

6. H. Klein, B.R.L. Siebert, R. Böttger, H.J. Brede,
H. Schölermann, Proc. of the Int. Conf. on Nuclear Data for
Science and Technology, ed. K.H. Böckhoff, D. Reidel Publ. Comp.
Eindhofen (1983) p. 891 - 894

CANDIDATES FOR FAST NEUTRON STANDARDS AMONG NEUTRON PRODUCING REACTIONS

M. DROSG
Institut für Experimentalphysik,
University of Vienna,
Vienna, Austria

Abstract

Neutron fields from charged particle reactions are examined for their suitableness as standards. Very accurate differential neutron production cross sections are available from measurements of the associated charged particles, e.g. for the reaction $^{3}H(p,^{3}He)n$, $^{2}H(d,^{3}He)n$ and $^{2}H(t,\alpha)n$. However, these cross sections are usually not available at those energies and angles needed in fast neutron work. Therefore, measured neutron data over the ranges of interest must be used. By applying the ratio (or quasi-absolute) method reference cross sections of reactions involving the same target were combined and by exchanging projectile and target nuclei the two target types were combined, too. Thus unified differential cross sections for the monoenergetic neutron production by the hydrogen isotopes are available which use simultaneously all associated charged particle data of the three reactions as cross section reference. An energy dependent evaluation of all available data yielded cross sections with *a minimum* total absolute error of less than 2 %. This small uncertainty justifies the attempt to choose some of these cross sections as fast neutron flux standard. The procedure selecting these standards is fully discussed. In addition it is shown how these proposed standards can be connected through time reversal with the $n-^{6}Li$ and $n-^{10}B$ standard.

Aside from absolute standards there is a need of relative ones which can be used for easy calibration of the energy response of neutron detectors. In energy discriminating systems (e.g. time-of-flight systems) the measurement of a single continuous standard spectrum would be sufficient. Such a standard would be difficult to transfer because of site dependent background conditions. The dependence on the environment of the source can strongly be reduced by using either resolvable multiple line neutron spectra, allowing simple background subtraction or by the employment of sources which deliver neutrons in a narrow forward cone only, e.g. inverse (p,n) reactions. The latter procedure depends on heavy ion acceleration which is already availabe at several installations. Presently, data on the candidates for such

standards are so sparse that one can only consider them for future use.

At the moment a point-by-point measurement of the energy response using differential cross sections of the monoenergetic neutron production by the hydrogen isotopes is state-of-the-art. By selecting optimum excitation functions and angular distributions this procedure can be improved and standardized. Proposals toward this end are presented which take into account the accuracy of the reference cross sections as well as the practicability of their application.

I. INTRODUCTION:

Nearly all absolute differential cross section measurements with neutrons depend directly or indirectly on a standard. Generally, these standards comprise reactions used for neutron detection. However, there appears to be a need for transferable standard neutron fields. The main problem lies in the transferability which is limited by the background originating from the source (accelerator and target structure) and the environment. Controlling the environment is in many cases impractical if not impossible. Therefore, a negligible background or the possibility to discriminate against it is a necessity if the same neutron standard fields should be employed at different installations.

From the experimenter's point of view several types of neutron reference fields would be useful, e.g.

a) absolute "monoenergetic" neutron fields at several energies to allow e.g. a straight-forward calculation of the flux at the location of the sample

b) a field with a well defined wide energy distribution at the location of the sample (like the ^{252}Cf spectrum, used as a relative flux standard in instrument calibration)

c) (relative) "monoenergetic" standard neutron angular distributions or excitation functions for use as a step-by-step relative flux standard

d) other neutron reference spectra for special applications.

The last group will not be discussed here further. Just one example will be given: For difficult experiments, like the measurement of double differential neutron emission cross sections, it would be very beneficial to have a reference spectrum available to check the experimental procedure and the data reduction (multiple scattering etc.) for systematic errors.

The discussion here will be restricted to neutron fields generated by charged particles from an accelerator.

II. BASIC REQUIREMENTS FOR ACCELERATOR BASED STANDARD NEUTRON PRODUCING REACTIONS.

Desirable properties of a standard neutron field generated by accelerators are summarized in Table 1.

Table 1. Requirements for the Generation of Standard Neutron Fields by Accelerators.

1. Data of standard: adequate accuracy, moderate dependence on energy and angle
2. Practicability:
   a) Availability: easy access to target material, projectile type and projectile energy
   b) Reproducibility: stable machine operation, well defined and reproducible target construction, controlled background situation
   c) Simplicity: simple preparation and handling of target: standard equipment for measuring neutron yield, solid angle, target thickness (evenness, isotopic and chemical purity), (effective) beam energy, (effective) angle, intensity of incoming beam.
3. Directness: small and straight-forward corrections, reliable input data for corrections.
4. Purity: no other disturbing radiations

Among these requirements the availability and reproducibility are most important. The others will loose their importance in the course of time by refinements and improvements in the measuring technique.

III. MONOENERGETIC NEUTRON PRODUCTION

The properties of a neutron field from monoenergetic neutron sources are summarized in Table 2. Amid the generally used reactions $^{7}Li(p,n)^{7}Be$ and $^{3}H(p,n)^{3}He$ would be especially attractive, because their cross sections can be connected to the n-^{6}Li and n-^{10}B standard by time reversal of the standard and by applying the quasi-absolute measuring method (1). In addition, the cross section scale of $^{2}H(d,n)^{3}He$ and $^{3}H(d,n)^{4}He$ has been tied to that of $^{3}H(p,n)^{3}He$ (2). So it seems feasible to tie monoenergetic neutron production cross sections to the n-^{6}Li and n-^{10}B cross sections with uncertainties of less than 2 % using present day techniques. However, the

Table 2. Properties of the Neutron Field from Mono-energetic Neutron Sources at the Location of the Sample (or Detector):

1. Primary neutrons:
1.1. Neutron energy
1.1.1.Energy distribution (resolution)
1. Variation of acceleration voltage
2. Energy straggling of charged particles in the target (e.g.entrance foil and gas)
3. Energy loss in the active volume of the target
4. Inhomogeneities in the active (and in the upstream portion of the nonactive) volume of the target
5. Energy spread from angular spread
a) divergence of charged particles (intrinsic beam divergence, angular straggling)
b) divergence of neutron beam (finite aperture)
c) beam diameter
1.1.2.Energy definition
1. Calibration of mean beam energy
2. Mean energy loss in target (dependent on the specific energy loss and the areal density)
3. Shift of mean neutron energy due to the kinematics of the reaction
a) Offset of assumed 0° from the charged particle beam direction
b) Difference between effective and geometric reaction angle due to the angular spread of the charged particle beam (intrinsic divergence, angular straggling in target) and of the emitted neutron beam (finite aperture)
4. Mean emission angle with respect to assumed 0° direction
1.2. Neutron intensity *)
1.2.1.Intensity distribution
1. Dependence of cross section on charged particle energy
2. Dependence of cross section on angle
1.2.2.Mean Intensity
1. Areal density of active isotope
2. Absolute value of effective cross section
3. Solid angle
2. Secondary neutrons: **)
2.1. Intrinsic background (from target isotope)
2.1.1.Direct intrinsic background
1. Intensity distribution
2. Energy distribution
2.1.2.Inscattered intrinsic background (air, beam stop, room)
1. Dependence on energy anisotropy
2. Dependence on cross section anisotropy
2.2. Structural background
2.2.1.Direct structural background (dependent on set-up)
1. From admixtures to the target isotope
2. From construction (entrance foil, backing, beam-stop)
3. From the beam line upstream of the target
2.2.2.Inscattered structural background
3. Induced gamma rays: **)

*) Kinematics considerations similar to those in 1.1 have been omitted
**) Most considerations of part 1 are also applicable

---

situation becomes less favorable, when the practical realisation of an absolute standard neutron field by these reactions is considered.

A) Absolute Standards:

Because triton beams are generally not available, the $^{2}H(t,n)^{4}He$ and $^{1}H(t,n)^{3}He$ reaction are not suited. For an absolute standard, also $^{3}H(d,n)^{4}He$ and $^{3}H(p,n)^{3}He$ do not qualify, because the accuracy in determining the areal density of tritium in the target is insufficient. Finally, lithium targets are usually so uneven that the areal density at the location of the beam spot cannot be determined reliably.

So, practicability rules out all but two reactions, namely $^{2}H(d,n)^{3}He$ and $^{1}H(^{7}Li,n)^{7}Be$. Although heavy ion beams are no handicap in neutron production any more, at present time the $^{7}Li-^{1}H$ reaction must be ruled out because the $p-^{7}Li$ data (3) are not accurate enough (see Fig. 1) so that only the $^{2}H(d,n)^{3}He$ reaction remains as candidate for an absolute standard.

The following discussion will be restricted to gas targets, because only these give the well defined areal density required. However, when determining the actual length of such a target, the flexure of the entrance foil must be taken into account. In additon, the beam heating must be corrected for. The corrections for the interactions of the charged particle beam in the entrance foil (energy loss, energy and angular straggling) decrease with energy and so the input data for these corrections become more reliable. For this reason the projectile energy should not be too low.

Turning now to our candidate d-D we can see from Fig. 1 to Fig. 5 a strong increase with energy of

a) the (maximum) shape uncertainty in the differential cross sections (3-6)

b) the relative energy spread from the kinematics

c) the change in cross section at 0 ° because of the finite opening angle

d) the (maximum) change in the differential cross sections in case of a 0 ° offset, and

e) the intrinsic background relative to primary neutron intensity (3,7).

Contrary to that the energy dependence of the zero degree cross section is quite small. It even drops with energy (see Fig. 6).

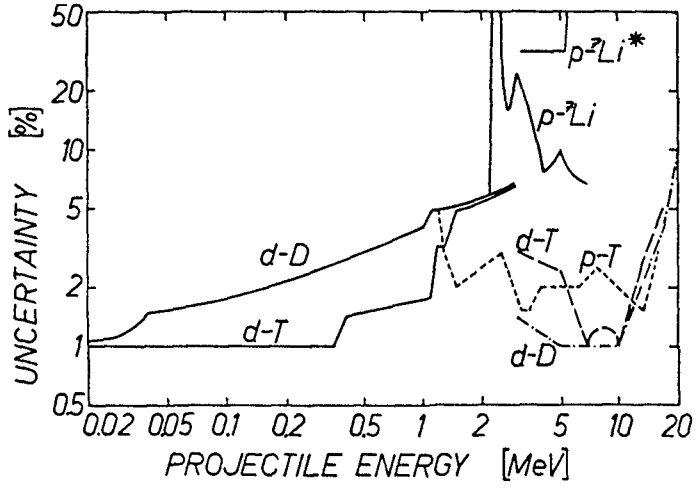

Fig.1 Shape uncertainties of the differential cross sections for monoenergetic neutron production. The full lines are worst case figures derived from Refs.3 and 4, the other are estimates based on Ref.6.

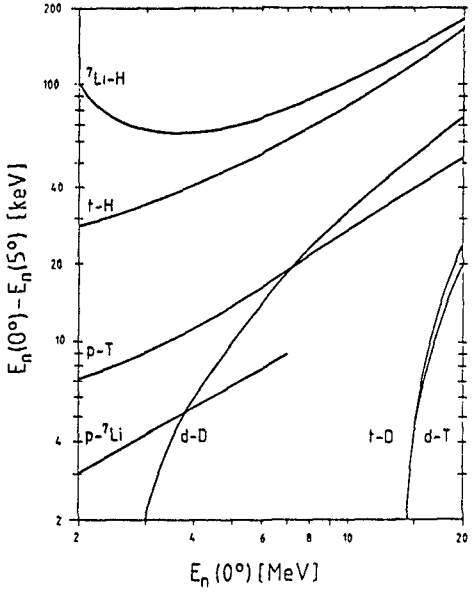

Fig.2 Energy dependence of the maximum geometric neutron energy spread at 0° due to a 5° opening angle of the sample for projectiles without energy spread.

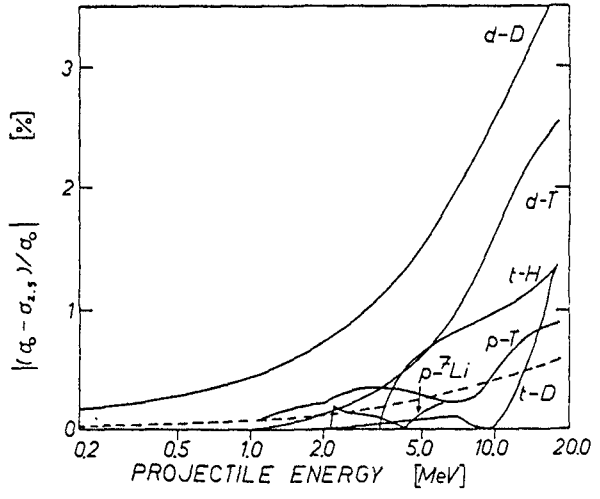

Fig.3 Energy dependence of the percentage change of the differential cross section for an angle change from 0° to 2.5°. The dashed curve is for the d-D reaction with an angle change from 0° to 1°.

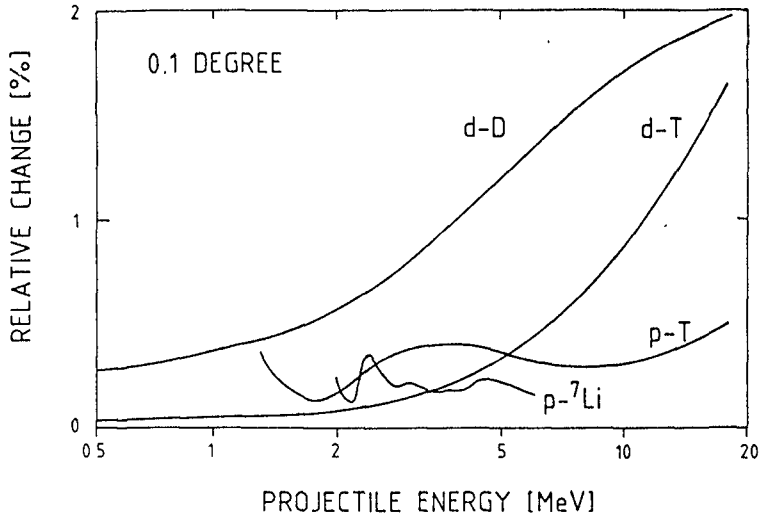

Fig.4 Maximum percentage change in the differential cross sections at the given projectile energy when the 0° position is offset by 0.1 degree.

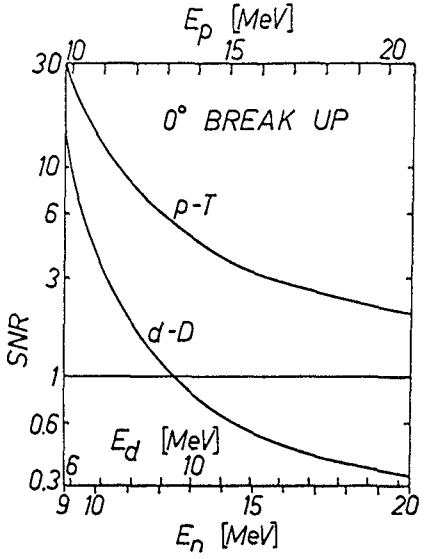

Fig.5 Signal-to-noise-ratio SNR from the intrinsic background of the p-T and d-D reaction at 0° in dependence of the primary neutron energy.

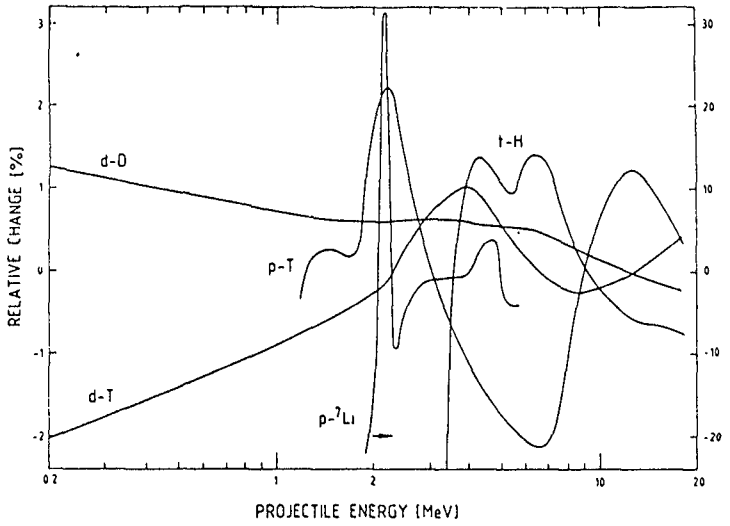

Fig.6 Percentage change of the 0° cross section for a 1% change of the projectile energy. Use the right hand scale for the p-^{7}Li reaction.

From all this it is evident that the deuteron energy for a standard neutron field by the d-D reaction should be less than 10 MeV. On the other hand, low energies must be avoided, because otherwise the (energy and angular) dispersion of the charged particle beam in the entrance foil is difficult to correct for.

Therefore energies near 5 MeV seem the best. From Table 3 it can be seen that total absolute uncertainties of less than 2 % can be expected for the differential cross sections at 5 MeV.

In additon the 0 ° excitation function between 5 and 14 MeV can be considered as a standard. The shape error in this energy range is about ± 1 % and the total absolute error of each point close to ± 1.5 % .

Table 3. Uncertainties and Corrections of the Differential Cross Sections of the d-D Reaction

Energy	4 MeV	5 MeV	6 MeV
Uncertainties:			
Shape Uncertainty of Diff. Cross Section	1.2 %	1.0 %	1.0 %
(Max.) Uncertainty From a 0.1° Angular Shift	1.0 %	1.2 %	1.3 %
Scale Uncertainty Resulting From the Energy Uncertainty *)	0.6 %	0.5 %	0.4 %
Basic Scale Uncertainty	>1.0 %	1.0 %	1.0 %
Total Cross Section Uncertainty	>2.0 %	1.9 %	2.0 %
Corrections:			
Relative Energy Spread From a 5° Opening Angle	0.15 %	0.20 %	0.26 %
Relative Intensity Drop From 0° to 2.5°	1.25 %	1.5 %	1.75 %

*) 0.2 % of accelerating voltage + 10 % of energy loss in 5.3 mg/cm² molybdenum foil.

B) Relative Standards:

The main application of relative standards is the calibration of the energy response of detectors. Monoenergetic sources can be used for this purpose in a step by step fashion, either by using angular distributions or excitation functions. The latter requires that the target thickness at the location of the beam remains constant. So solid targets cannot be used easily, and the excitation function of p-^{7}Li is of little use. Besides the strong energy dependence (Fig. 6) makes a use below 2.5 MeV very questionable.

From the same figure it can be seen that also the p-T excitation function requires a quite accurate energy determination over most of the energy range.(See (8) for a recent discussion of energy calibrations.) So it is not well suited for general use. However, the d-T reaction is another candidate: between 6 and 11 MeV the shape uncertainty is ±1 %, increasing to ±3 % at 2.5 MeV and at 16 MeV (2.6).

Reference angular distributions should be chosen at those energies where the energy dependence (Fig. 6) and the angular dependence (Fig. 4) are not serious. Presently, for accuracy reasons, p-^{7}Li must be excluded (see Figs. 1 and 7). Angular distributions of the p-T reaction between 2.8 and 4.2 MeV and between 10 and 14.5 MeV have small shape uncertainties (± 2 %) and a reasonable small energy dependence. However, presently the zero degree offset at 3.1 MeV may be as big as 0.6 ° resulting in an additional maximum shape uncertainty of 2.4 % (see Fig. 8).
For the d-T reaction the shape uncertainty is less than 2% for energies below 1.1 MeV and between 5.4 and 12.4 MeV, with minima at 7 and 10 MeV. Therefore relative standards should be chosen in these energy ranges.

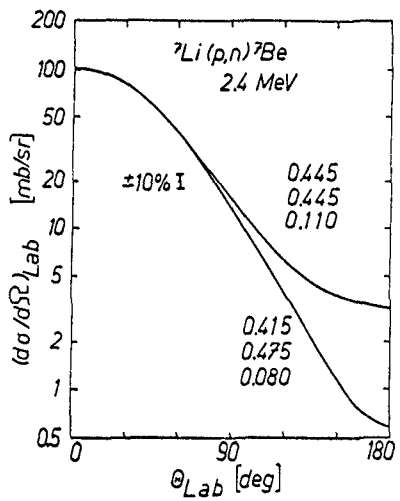

Fig.7 Differential cross sections of ^{7}Li(p,n)^{7}Be at 2.4 MeV using the recommended Legendre coefficients of Ref.3. The worst case alternative solution (± 0.030 uncertainty of the coefficients) is shown, too.

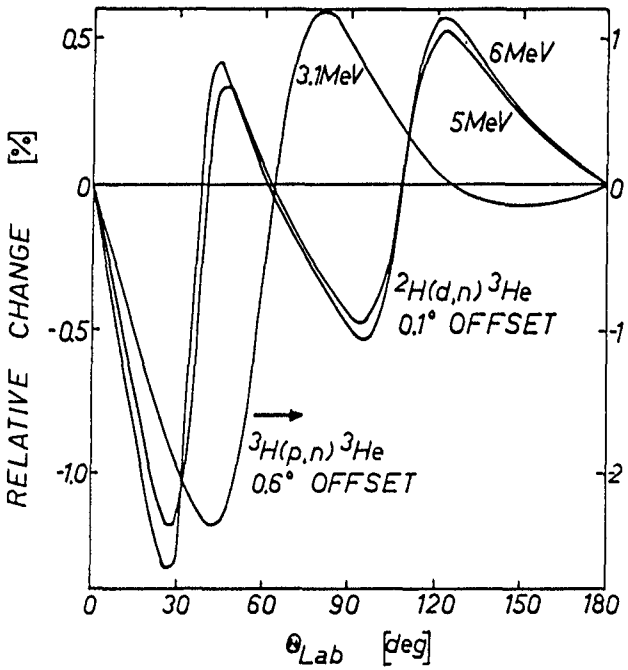

Fig.8 Angular dependence of the percentage change in the differential cross sections for $^{2}H(d,n)^{3}He$ at 5 and 6 MeV and for $^{3}H(p,n)^{3}He$ at 3.1 MeV when the 0^{o} position is offset by 0.1^{o} and 0.6^{o}, resp. .

IV. NEUTRON ENERGY DISTRIBUTIONS

Standard neutron energy spectra would be very useful for detector calibrations. Obviously, it is very advantageous to calibrate the detector in the actual measuring geometry, i.e. to use an accelerator source rather than a radioactive source (e.g. ^{252}Cf.) As was discussed before, the transferability of such a standard depends on the insensitivity to background. Therefore two approaches should be considered:

sources with a continuous neutron spectrum with neutron confinement in a forward cone

sources with several (resp. many) lines which allow background subtraction.

A) Continuous Spectra:

From a practical view point a reference spectrum to be used with "14 MeV" neutron generators would be especially useful. This would require exothermic reactions e.g. (d,n). However, the background emitted in a solid angle of 4 π would prevent the transfer of such a field. Besides, (d,n) reactions with the elements carbon and oxygen (which are frequent impurities in samples), will contribute unreproducible background. A further complication is the self target build-up contributing background by the d-D reaction.

Endothermic two body reactions emit neutrons only into a forward cone for projectile energies E_o between the threshold energy E_{th} and that energy at which the center-of-mass velocity of the neutron becomes as big as the energy of the center of mass. The half angle θ of this cone at the projectile energy E_o can be derived from the (nonrelativistic) equation

$$\sin^2\theta = \frac{M2 \cdot M4}{M1 \cdot M3} \left(1 - \frac{E_{th}}{E_p} \right) \qquad /1/$$

The masses Mi are those of the projectile, the target, the neutron and of the residual nucleus, resp.. Expressed in neutron energy E_n at 0 ° this formula becomes (nonrelativistically)

$$(1+\sin\theta)^2 = \frac{E_n}{E_p} \cdot \left(1+\frac{M2}{M1}\right) \cdot \frac{M3+M4}{M3} \qquad /2/$$

At a given zero-degree neutron energy E_n the collimation will become the narrower

a) the smaller M2 is with respect to M1
b) the smaller the total mass is
c) the bigger the absolute value of Q is.

As long as the projectile energy E_o stays below the threshold for 3-body neutron production, all the intrinsic neutrons are contained in this cone with a maximum opening angle according to formula /2/. Then, by completely stopping projectiles with an energy E_o in a target, a reproducible continuous neutron spectrum at 0° with a maximum energy E_n is obtained.

Table 4 summarizes relevant reaction data in the low Z range. Unfortunately, condition a) restricts candidates more or less to inverse (p,n) reactions if a maximum neutron energy of at least 10 MeV is aimed at. So gas targets of considerable length must be used for stopping the beam completely . In addition, the entrance foil will contribute background, the seriousness of which is difficult to predict.

Presently, only few installations would be able to accelerate the heavy ions to energies required for 14 MeV neutron production. Fig. 9 shows that the machine energy must be the higher the narrower the cone is (in accordance with condition c) from above). Observe also that the minimum energy in the distribution increases with decreasing opening angle (see Table 4).

Table 4. Reaction Data for Contained Emission of Continous Neutron Spectra at 0^o

Reaction	Threshold		E_n=10 MeV			E_n= 14 MeV			Upper Limit[a]		
	E_p(MeV)	E_n(MeV)	E_p(MeV)	θ_m(deg)	$E_{n\pi}$ (MeV)[b]	E_p(MeV)	θ_m(deg)	$E_{n\pi}$(MeV)[b]	E_p(MeV)	E_n(MeV)	θ_m(deg)
$^1H(t,n)^3He$	3.051	0.573	14.875	63.1	0.033	20.180	67.1	0.024	25.011	17.640	69.6
$^1H(^7Li,n)^7Be$	13.095	1.439	-	-	-	-	-	-	25.732	8.184	44.5
$^1H(^{10}Be,n)^{10}B$	2.478	0.206	31.299	73.7	0.004	43.297	76.2	0.003	51.267	16.659	77.2
$^1H(^{10}B,n)^{10}C$	48.492	4.031	59.190	25.2	1.625	69.797	33.5	1.161	92.284	21.924	43.5
$^1H(^{11}B,n)^{11}C$	32.967	2.534	51.068	36.5	0.643	63.449	43.9	0.459	122.986	32.659	58.8
$^1H(^{14}C,n)^{14}N$	9.323	0.584	44.653	62.8	0.034	60.532	66.9	0.025	121.821	29.449	73.9
$^1H(^{14}N,n)^{14}O$	98.302	5.533	96.245	16.7	3.061	108.677	25.7	2.187	157.248	27.298	41.5
$^1H(^{15}N,n)^{15}O$	56.177	3.316	75.067	30.1	1.100	90.636	38.1	0.786	172.138	33.806	55.1
$^1H(^{18}O,n)^{18}F$	45.980	2.310	75.360	38.6	0.534	94.454	45.8	0.382	129.284	21.156	53.4
$^1H(^{19}F,n)^{19}Ne$	79.824	3.821	99.728	26.5	1.460	118.389	34.8	1.043	149.908	20.386	43.1
$^4He(^{16}O,n)^{19}Ne$	60.646	2.487	71.842	59.0	0.059	-	-	-	76.988[c]	12.435	90.0

a) Limit for 3-body break-up with neutron emission

b) Energy of second neutron group at 0^o_{Lab} from $180^o_{c.m.}$

c) Maximum energy for containment of the neutrons

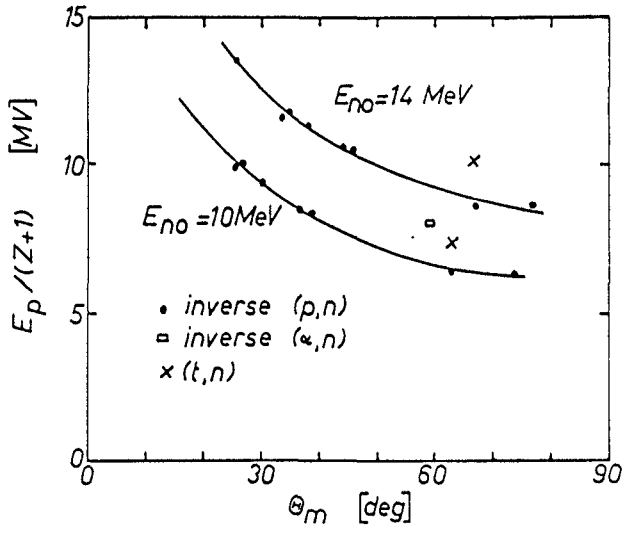

Fig. 9 Maximum opening angle θ_m of the contained neutron beam versus minimum terminal energy of a Tandem accelerator when producing 14 and 16 MeV neutrons by the reactions of Table 4. The curves are only meant to guide the eye.

B) Multiline Spectra:

If the structure in the background is wider than the energy resolution, usually, a reliable background subtraction under isolated peaks is possible. Therefore, a detector calibration at a number of discrete energies could be performed using a calibrated multiline spectrum. A reaction with many lines, well resolvable, and with small energy dependence of the cross section near the energy of interest must be found. The spectrum should extend to rather high energies, e.g. 14 MeV. The latter demand suggests positive Q-value reactions (e.g. (d,n) reactions).

To provide intrinsically clean conditions, the projectile energy must not be much above the threshold for 3-body neutron production. Therefore, the low disintegration energy of deuterons limits the maximum attainable neutron energies in (d,n) reactions. Besides, as mentioned above, oxygen and carbon impurities contribute background in (d,n) reactions. A way out seems the inverse (d,n) reaction. Higher neutron energies at the same center-of-mass energy are obtained and the neutron energies from excited states are farther apart. The necessary projectile energies are moderate so that they can be provided by many accelerators. The main problem will be the target, both in the case of gas targets (entrance foil and beam stop) and in the case of solid targets as well. However, in the case of gas targets a background run with the empty cell might give an adequate correction.

If a smaller energy range is acceptable (p,n) ractions can be chosen. By using structural materials (e.g. for beam stops) with high (p,n) threshold (like ^{28}Si(9), ^{58}Ni, etc.) clean background conditions can be obtained. As shown above, inverse (p,n) reactions require too high machine energies to be considered for general use, although they produce an optimum neutron field: neutrons of discrete energies, contained in a forward cone. According to formula /1/ the neutrons from the excited states are even stronger collimated than those from the ground state. For lower neutron energies the reaction $^1H(^7Li,n)^7Be$ (10) can be useful. At 25 MeV (below the break-up threshold) 4 neutron lines occur at

energies of 7.85, 6.89, 0.48 and 0.27 MeV which might be sufficient in some cases. The relation between the projectile energy and the 4 neutron energies is shown in Fig.10.

Table 5. Kinematics Data for Selected Multiline Neutron (All energies in MeV)

Reaction Type	2-Body Reaction Q	$E_n(0°)$*)	3-Body Neutron Threshold	Reaction Q
$^{14}C(p,n)^{14}N$	-0.626	8.138	8.765	-8.177
$^{11}B(p,n)^{11}C$	-2.764	8.558	11.341	-10.310
$^{2}H(^{13}C,n)^{14}N$	5.326	13.236	16.587	-2.225
$^{2}H(^{27}Al,n)^{28}Si$	9.361	13.288	8.987	-0.624
$^{2}H(^{30}Si,n)^{31}P$	5.072	13.561	35.331	-2.225
$^{2}H(^{31}P,n)^{32}S$	6.640	8.836	5.057	-0.309
$^{2}H(^{10}B,n)^{11}C$	6.466	10.895	6.442	-1.079
$^{2}H(^{9}Be,n)^{10}B$	4.361	4.908	0.547	-0.100

*) Maximum zero-degree neutron energy at the 3-body threshold energy

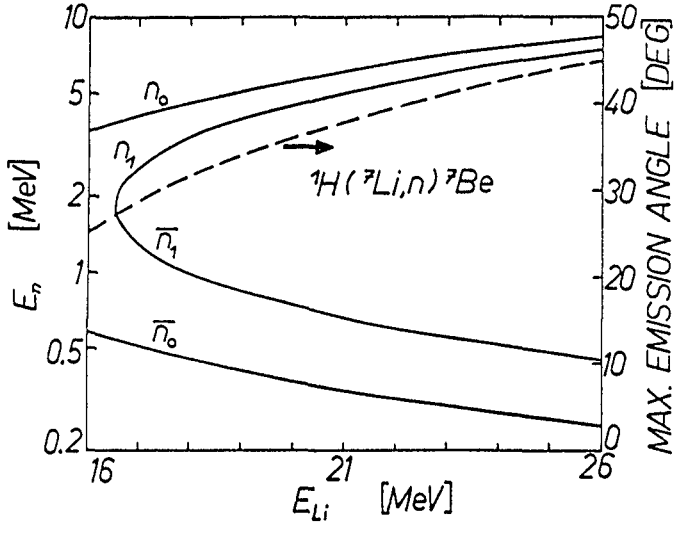

Fig.10 Energy relations and maximum opening angle (right hand scale) for the 4 neutron lines of the $^1H(^7Li,n)^7Be$ reaction.

Table 5 summarizes data for selected multiline neutron spectra. At lower energies $^{14}C(p,n)^{14}N$ (11) and $^{11}B(p,n)^{11}C$ (12) give reasonable spectra, among the inverse (d,n) reactions the following reactions were conspicuous: $^{2}H(^{13}C,n)^{14}N$ (13,14), $^{2}H(^{27}Al,n)^{28}Si$ (15,16), $^{2}H(^{30}Si,n)^{31}P$ (17), $^{2}H(^{31}P,n)^{32}S$ (17), $^{2}H(^{10}B,n)^{11}C$ (18,19) and $^{2}H(^{9}Be,n)^{10}B$ (20,21). Other candidates that seemed suitable but were dropped later on because of too low yield, dense levels or because of exothermic break up with neutron production are $^{29}Si(\tau,n)^{31}S$ (22), $^{38}Ar(d,n)^{39}K$ (23), $^{17}O(d,n)^{18}F$ (24), $^{18}O(p,n)^{18}F$ (25), $^{19}F(d,n)^{20}Ne$ (26) and $^{23}Na(d,n)^{24}Mg$ (26-28).

V. CONCLUSION

At present time only cross sections of the $^{2}H(d,n)^{3}He$ reaction can be recommended for an absolute standard. For relative standards cross sections of both $^{3}H(d,n)^{4}He$ and $^{3}H(p,n)^{3}He$ can be considered. The accuracy of the $^{7}Li(p,n)^{7}Be$ cross sections is not at all satisfactory yet.

There are no neutron energy spectra available which fullfill all the requirements of a standard. Potential candidates for standards of continuous and multiline spectra are presented. Their practical realisation with an adequate accuracy is still open. If a standard multiline energy spectrum is chosen, it can at the same time serve as a neutron energy standard.

REFERENCES :

(1) M.DROSG, Contributed Paper, this Conference
(2) M.DROSG, Nucl.Sci.Eng.67, 190 (1978)
(3) H.LISKIEN, A.PAULSEN, Atomic Data and Nucl.Data Tables 15, 57 (1975)
(4) H.LISKIEN, A.PAULSEN, Nucl.Data Tables 11,569(1973)
(5) M.DROSG, Z.Phys.A300, 315(1981) and Report LA-8532, Los Alamos Scient.Lab. (1980)
(6) M.DROSG, O.SCHWERER, to be published
(7) M.DROSG, pp.201 Proc.IAEA Consultants Meeting on Neutron Source Properties, Report INDC(NDS)-114/GT (1980)
(8) N.OLSSON, B.TROSTELL, Nucl.Instr.Meth.224,142 (1984)
(9) M.DROSG, G.F.AUCHAMPAUGH, Nucl.Instr.Meth.140, 515(1977), see also Report LA-6459-MS, Los Alamos Scient.Lab. (1976)
(10) J.H.DAVE, C.R.GOULD, S.A.WENDER, S.M.SHAFROTH, Nucl. Instr.Meth.Phys.Res.200, 285 (1982)
(11) C.WONG, J.D.ANDERSON, J.McCLURE, B.POHL, Phys.Rev.160, 769 (1967)
(12) J.C.OVERLEY, R.R.BORCHERS, Nucl.Phys.65,156 (1965)
(13) J.R.BOBBITT, M.P.ETTEN, G.H.LENZ, Nucl.Phys.A203, 353 (1973)

(14) J.BOMMER, M.EKPO, H.FUCHS, K.GRABISCH, H.KLUGE, Nucl.Phys.A251,257 (1975)
(15) B.LAWERGREN, G.C.MORRISON, A.T.G.FERGUSON, Nucl.Phys.A106, 455 (1968)
(16) W.BOHNE et al., Nucl.Phys.A131,273 (1969)
(17) J.UZUREAU, A.ADAM, O.BERSILLON, S.JOLY, Nucl.Phys.A267, 217 (1976)
(18) J.C.OVERLEY, Nucl.Phys.49,537 (1963)
(19) W.BOHNE et al., Nucl.Phys.A157,593 (1970)
(20) D.W.GLASGOW, D.G.FOSTER, Jr., Nucl.Phys.A99,170 (1967)
(21) Y.S.PARK, A.NIILER, R.A.LINDGREN, Phys.Rev.C8, 1557 (1973)
(22) J.M.DAVISON et al., Nucl.Phys.A240,253 (1975)
(23) M.HAGEN, U.JANETZKI, K.-H.MAIER, H.FUCHS, Nucl.Phys. A152, 404 (1970)
(24) D.ARDOUIN, J.UZUREAU, R.TAMISTER, L.-H.ROSIER, P.AVIGNON, C.R.Acad.Sc.Paris, 273,B561 (1971)
(25) J.D.ANDERSON, S.D.BLOOM, C.WONG, W.F.HORNYAK, V.A.MADSEN, Phys.Rev.177,1416 (1969)
(26) B.T.LAWERGREN, A.T.G.FERGUSON, G.C.MORRISON, Nucl.Phys.A108, 325 (1968)
(27) S.M.TANG, B.D.SOWERBY, D.M.SHEPPARD, Nucl.Phys.A125, 289 (1969)
(28) H.FUCHS, K.GRABISCH, P.KRAAZ, G.RÖSCHERT, Nucl.Phys. A122,59 (1968)

ABOUT ^{237}Np FISSION CROSS-SECTION STANDARDIZATION

A.A. GOVERDOVSKIJ
Institute of Physics and Power Engineering,
Obninsk,
Union of Soviet Socialist Republics

Fast neutron-induced fission cross-section of ^{237}Np is twice as much ^{238}U fission cross-section, therefore it may be more convenient for neutron flux monitoring in the threshold cross-section measurements ($E_n > 5$ MeV). However, there are any complications:
a) energy dependance of σ_f^7 is more complicated, than σ_f^8 ;
b) ^{237}Np samples are more α and β, γ -active ;
c) illustrative comparisons of the evaluated result[1] of σ_f(Np-237)/ σ_f(U-235)$=R_5^7$ with some measured values[2-11] are given in Figure. From Fig. it can be seen that all results[2,3,4,5,8,10] are in good agreement with the shape of the Np-237:U-235 ratio, but there are a great systematic absolute scatter of point groups. There is a 5-10% tendency for the values[4,5,6] to be systematically higher than the results[2,3,8,10]. Absolute value[7] is in good agreement with the second group. The measurement[6] include high methodical uncertainties. Thus, the total uncertainties of the nuclear data about σ_f^7 are higher than σ_f^8;
d) ^{238}Np fission probability is relatively high near observational threshold ($E_n \leq 0{,}5$ MeV)[2,12], that may be very important for using of the high backgraund neutron source.

RECOMENDATION

1. The fission cross-section of ^{238}U is more reliable standard cross-section, than ^{237}Np (a,c,d).
2. It is very reasonably to use of the the ^{236}U fission cross-section for more effective neutron flux

monitoring with the 1-1.5% accuracy. The shape of thise cross-section is simple and subthreshold fission probability is very low.

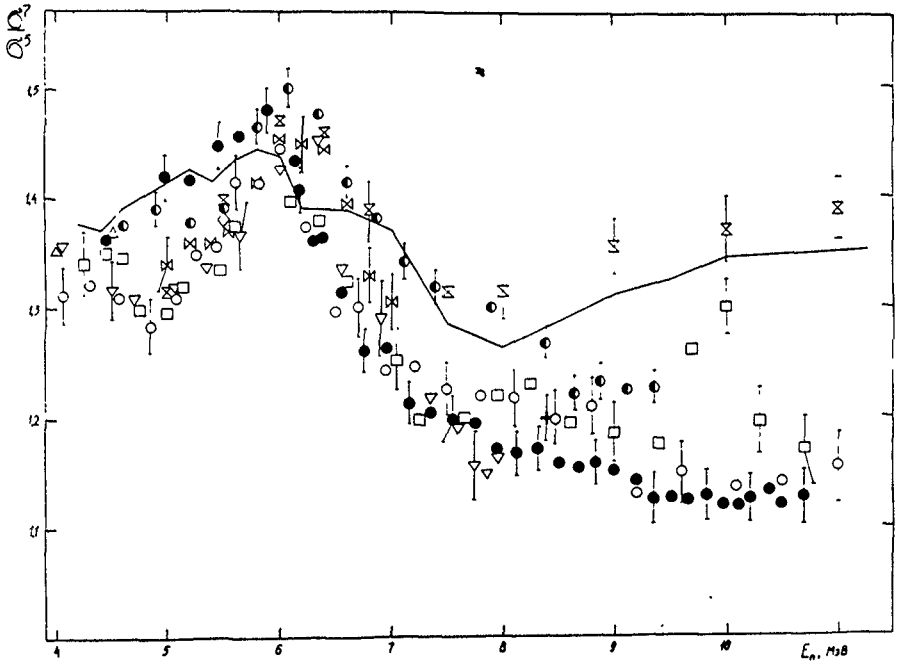

$^{237}Np:^{235}U$ fission cross-section ratio:

○ - 2 ,□ - 3 ,◐ - 4 ,⋈ - 5 ,⧖ - 6 ,+ - 7 ,
▽ - 8 ,◇ - 9 ,● - 10, △ - 11, —— - ENDF-B/V

REFERENCES

1. ENDF-B/5 3rd ed.,BNL,1979, Np-237(mat 1337),U-235(mat 1395).
2. Behrens J.W.,et.al.-Nucl.Sci.Engng.,1982,v.80,p.393.
3. Carlson A.D.,et.al.-In: Proc.Int.Conf.,Knoxville,1979,p.971.
4. Meadows J.W.- Nucl.Sci.Engng.,1983,v.85,p.271.
5. Fursov B.I.,et.al.-At.Energy,1978,v.45,p.440.
6. Pankratov V.M.-At.Energy,v.14,p.177.
7. Arlt R.,et.al.-Jahresbericht,ZfK-488,1982,s.20.
8. Schmitt H.W.,Murray R.B.-Phys.Rev.,1959,v.116,p.1575.
9. White P.H.,Warner G.P.-J.Nucl.Energy,1967,v.21,p.671.
10. Goverdovsky A.A.,et.al.-Preprint FEI-1552,Obninsk,1984.
11. Stein W.E.,et.al.-In:Proc.Int.Conf.NeutronCross-Section Technology,Washington,1966,v.2,p.623.
12. Davey W.G.-Nucl.Sci.Engng,1966,v.26,p.146.

WORKING GROUP SESSION III

APPLICATION OF THE DUAL THIN SCINTILLATOR NEUTRON FLUX MONITOR IN A $^{235}U(n,f)$ CROSS-SECTION MEASUREMENT

M.S. DIAS, A.D. CARLSON, R.G. JOHNSON, O.A. WASSON
National Bureau of Standards,
Gaithersburg, Maryland,
United States of America

Abstract

The fission cross section for ^{235}U was measured over the 1 to 6 MeV energy range using the National Bureau of Standards neutron time-of-flight facility at the NBS 100-MeV electron linac. The recently developed dual thin scintillator (DTS) neutron detector was used as the neutron flux monitor. The DTS flux monitor was placed ~ 200 m from the source. At ~ 69 m on the same flight path a well-characterized fission chamber containing ~ 100 $\mu g/cm^2$ of ^{235}U was located. The background for both detectors was reduced to negligible levels. Two parameter data (pulse height and time-of-flight) were taken for both detectors with a computer based system. Since the experiment was devised primarily to verify the accuracy of the DTS detector as an absolute neutron flux monitor, only moderate energy resolution was planned ($\Delta E/E \approx 10\%$). The cross section uncertainty obtained was ~ 2%.

INTRODUCTION

Recently a new concept in neutron flux monitors employing proton recoil scintillators has been developed at NBS. The detector, which is called the dual thin scintillator (DTS) neutron detector[1] uses a thin plastic scintillator to keep multiple scattering corrections small. A second thin plastic scintillator is used to experimentally eliminate the pulse height distortion due to proton escape.

The DTS detector has been calibrated using the time-correlated associated-particle technique and Monte Carlo simulations. To further test the DTS detector as a neutron flux monitor, it has been used for this purpose in a measurement of the ^{235}U neutron-induced fission cross section over the 1-6 MeV range. The measurement is closely related to the 0.3 to 3.0 MeV

measurement using the NBS Black Detector as the neutron flux monitor.[2] For the present measurement the DTS detector was placed at the same position as the Black Detector.

Since this measurement was devised primarily to verify the accuracy of the DTS detector as an absolute flux monitor, only moderate energy resolution was planned ($\Delta E/E \approx 15\%$).

This report presents preliminary results of the measurement. These results may be subject to minor revision and should not be used until final corrections are made.

EXPERIMENTAL METHOD

A general description of the NBS Neutron Time-of-Flight Facility has been described previously.[3] The present measurements were made at the 200-m flight path of this facility as shown in Fig. 1. The large parallel-plate ionization fission chamber[4] with 170.9 ± 2.0 mg of ^{235}U was located at 69.466 m from the neutron producing target. The absolute neutron fluence was monitored by the DTS detector located at 200.765 m. The NBS linac operated with a 30-ns pulse width, 720-Hz repetition rate, and with 1.7 kW on target.

Details on the design and calibration of the DTS detector, which is shown in Fig. 2, have been described in a recent paper.[1] A brief summary follows. The detector consists of two thin NE110 plastic scintillators optically separated from each other and independently coupled to photomultiplier tubes. The two scintillators are 0.2565 cm in thickness and 4.70 and 4.90 cm in diameter. Each scintillator is coupled to a pair of photomultipliers by a rectangular (5.3 cm by 12.0 cm) plastic light guide. The primary advantage of this detector concept is that all calculated corrections to the efficiency are kept small. For a thin scintillator multiple scattering corrections are small. Although distortion of the proton recoil spectrum due to escape of protons is large for a single thin sciintillator, the use of a second scintillator experimentally eliminates this correction.

The absolute efficiency of the DTS detector has been calculated for the 1 to 15 MeV range using Monte Carlo techniques. The efficiency was also measured at 2.44 MeV and 14.0 MeV using the time-correlated associated-particle technique at the NBS 3-MV Positive-Ion Van de Graaff. The agreement between the calculated and measured efficiencies is $\lesssim 1.7\%$.

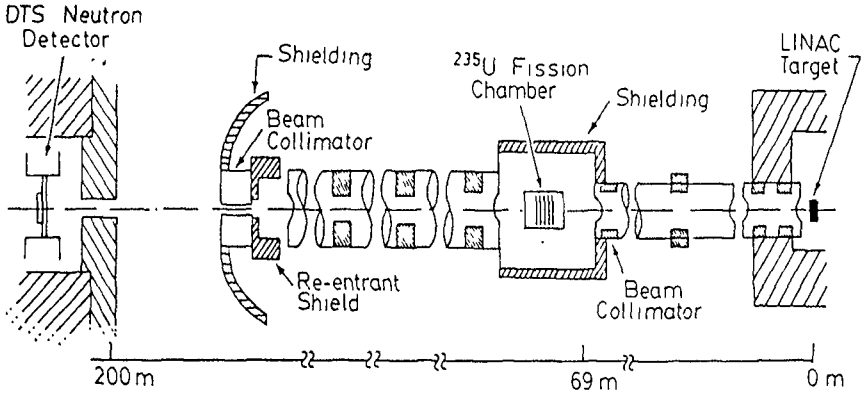

1. Experimental geometry for the ^{235}U neutron-induced cross-section measurement.

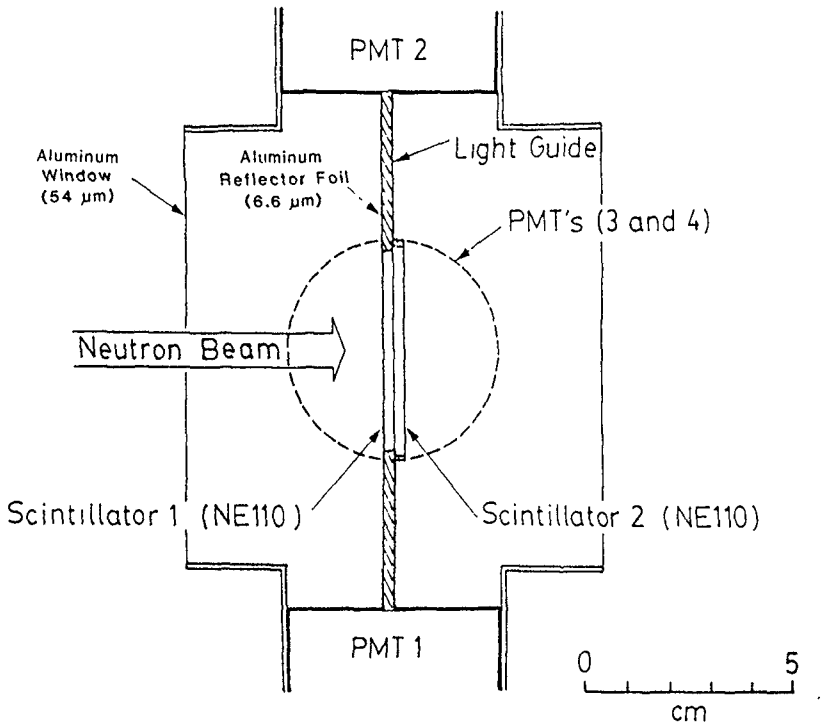

2. Geometry of the dual thin scintillator (DTS) detector.

Shielding for the DTS detector at the 200-m flight path consisted of 20 cm of Pb and 20 cm of borated-polyethylene. The neutron beam was collimated to an area of 1.1459 cm^2 incident on the center of the scintillators. Time-independent background was measured by opening a time gate just before the next beam pulse. The largest potential source of time-dependent background was due to high-energy neutrons scattered by the detector then scattered back later in time by the shielding. This source was eliminated by opening the time gate for these high energy neutrons and operating in a one stop per start mode.

DATA ANALYSIS

Data from both the fission chamber and the DTS detector were taken in two-parameter mode (pulse-height and time-of-flight). The data were analyzed by a comprehensive computer program that calculated the fission chamber and DTS detector yields (corrected for dead time and background). The neutron detector yields were then normalized to match the time width and flight path at the fission chamber. The neutron fluence was determined for each time-of-flight channel by correcting for detection efficiency and neutron attenuation in materials between the fission chamber and the neutron detector. The latter correction was made using cross sections from ENDF/B-V.[5] Also, the neutron yields were smeared by a Gaussian function to match the broader time resolution of the fission chamber. Ratios of the corrected fission chamber and neutron detector yields were multiplied by the appropriate scale factor to give the $^{235}U(n,f)$ cross section per time-of-flight channel together with its statistical uncertainty. The data was then grouped into the desired energy intervals.

The efficiency of the DTS neutron detector was calculated using the following interpolation formula:

$$\varepsilon_B = \sigma_H \, (A_1 + A_2\sigma_C + A_3\sigma_H) \qquad (1)$$

where ε_B is the biased efficiency, σ_H is the hydrogen elastic cross section, σ_C is the carbon elastic plus inelastic cross section, and A_i are fitting constants. The parameters of Eq. (1) were determined by fitting the Monte Carlo calculations of the efficiency for a 30% energy bias. The calculations were in turn normalized to the associated-particle technique calibrations.

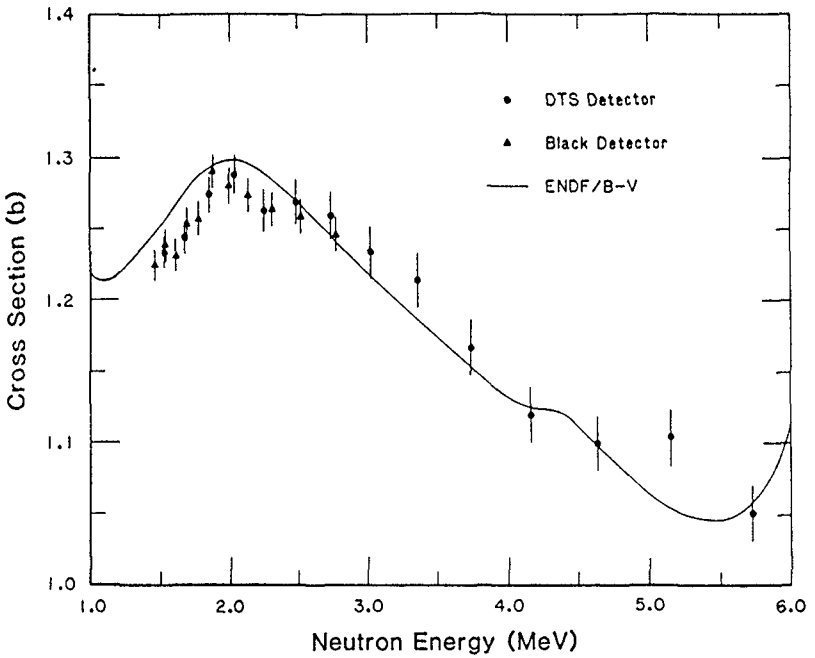

3. $^{235}U(n,f)$ cross section in the 1-6 MeV range.
   Circles - DTS detector as the neutron flux monitor.
   Triangles - Black Detector as the neutron flux monitor.
   Solid line - ENDF/B-V evaluation.
   The error bars represent statistical uncertainties only.

RESULTS AND CONCLUSIONS

The data were grouped so that the energy resolution $\Delta E/E$ was approximately 10% throughout the energy range (1.45 to 6.00 MeV). The statistical error which is obtained with this grouping is ~ 1.0% at the lowes energy and increases to ~ 1.9% at the highest energies. At this time the systematic errors have not been fully evaluated, nevertheless, they will be dominated by the DTS detector efficiency uncertainty (approximately 1.7% at low energies decreasing to 1.1%) and by uncertainty in the ^{235}U mass (approximately 1.2%).

In Fig. 3 the preliminary results of the present experiment are presented. The error bars are statistical uncertainties only. Also shown ar

partial results from the NBS measurement using the Black Detector as the flux monitor and the ENDF/B-V evaluation. In the region of overlap there is good agreement between the two measurements but both results are somewhat lower than ENDF/B-V. Above ~ 2.5 MeV the present results are in reasonable agreement with ENDF/B-V.

It must be emphasized that this is a preliminary report. Systematic corrections and their uncertainties have not been finalized. Careful evaluation of these corrections can cause changes in these results by ~ 1.0 %.

REFERENCES

*Present address: Instituto de Pesquisas Energéticas e Nucleares - São Paulo-Brazil.

1. M.S. Dias, R.G. Johnson, and O.A. Wasson, Design and Calibration of an Absolute Flux Detector for 1-15 MeV Neutrons, Nucl. Instr. and Meth. 224 (1984) 532.

2. A.D. Carlson, J.W. Behrens, R.G. Johnson, and G.E. Cooper, Absolute Measurements of the $^{235}U(n,f)$ Cross Section from 0.3 to 3 MeV, contribution to this conference.

3. O.A. Wasson, R.A. Schrack, and G.P. Lamaze, Neutron Flux Monitoring and Data Analysis for Neutron Standard Reaction Cross Sections, Nucl. Sci. Eng. 68 (1978) 170.

4. J.B. Czirr and G.S. Sidhu, Fission Cross Section of Uranium-235 from 0.8 to 4 MeV, Nucl. Sci. Eng. 58 (1975) 371.

5. ENDF/B-V, Report BNL-NCS-1754 (ENDF-201), ed. R. Kinsey, available from the National Nuclear Data Center, Brookhaven National Laboratory, Upton, NY (July 1979).

INVESTIGATION FOR A PRECISE AND EFFICIENT NEUTRON FLUENCE DETECTOR BASED ON THE n-p SCATTERING PROCESS

H.-H. KNITTER, C. BUDTZ-JØRGENSEN, H. BAX
Central Bureau for Nuclear Measurements,
Joint Research Centre,
Commission of the European Communities,
Geel

Abstract

An ionization chamber with Frisch grid is used to detect the recoil protons induced by fast neutrons in an advantageous 2π-geometry. The working principles of the detector are explained. Recoil proton spectrum measurements are made at several incident neutron energies below 2 MeV using four radiator foils of different thicknesses. These measurements permit a proton energy calibration of the detector and the determination of proton stopping powers for the radiator foil material. Proton recoil spectra are interpreted by Monte Carlo calculations with the aim of understanding closely the spectrum shape and to obtain the total number of proton recoils.

INTRODUCTION

A feasibility study for a neutron fluence detector working on the basis of the neutron,proton or perhaps on the n-carbon scattering process is in progress. An ionization chamber with Frisch grid is used to measure the recoil particles emitted from a radiator foil positioned coplanar with and in the centre of the circular chamber cathode. This detector is intended to be used as an absolute neutron fluence detector in measurements of neutron standard cross sections. The detector study should of course reveal with what accuracy the neutron fluence can be measured and which neutron energy range can be covered. At present these questions cannot be answered, but the investigations done so far and the difficulties encountered will be reported.

EXPERIMENTAL SET-UP

The experimental set-up as it was used in test measurements is shown in Fig. 1. The cathode of the chamber which supports on one side a radiator foil and on the other side an uranium-tetrafluoride layer was positioned at a distance of 10 cm from the neutron producing target of the 7 MV Van de Graaff under the zero degree direction with respect to the incident proton beam. In beam direction there is the Frisch grid at a distance of 2.5 cm from the cathode and the grid is followed in 0.6 cm distance by the recoil chamber anode. In backward direction there is at present a parallel plate ionization chamber to detect the fission fragments from the UF_4-layers. From the recoil ionization chamber two signals per recoil are registered. The first, the anode signal q_a is proportional to the recoil energy

$$q_a \cong E \qquad (1)$$

The second signal obtained from the cathode q_c is a function of the recoil energy E, the cos ϑ of the emission angle with respect to the normal of the cathode and of the quantity $\bar{X}(E,A,Z)$.

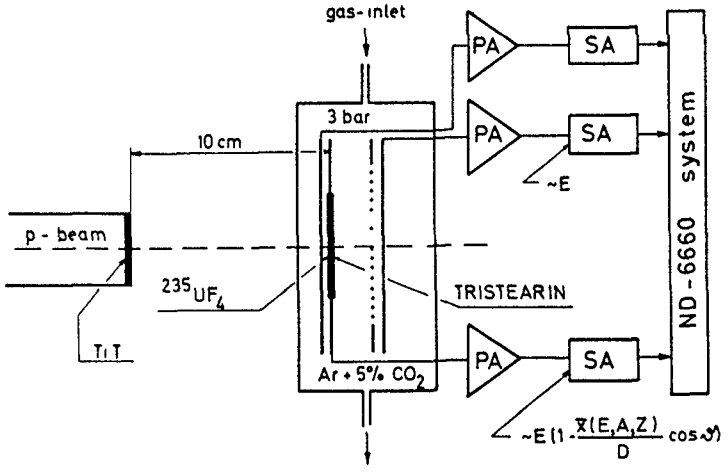

FIG. 1

Experimental set-up to study proton recoil ionization chamber.

$$q_c \cong E\left(1 - \frac{\bar{X}(E,A,Z)}{D} \cdot \cos\vartheta\right) \qquad (2)$$

A is the atomic weight and Z the electric charge of the recoil, D the distance between cathode and grid, $\bar{X}(E,A,Z)$ the distance from the origin of the recoil track at the cathode to the centre of charge of this track. The quantity $\bar{X}(E,A,Z)$ depends on the particle type and energy and on the position of the origin of the ion trace if the trace does not start at the cathode. The registration of these two signals for one event permits therefore a rather effective background discrimination by selecting an area of interest for the recoils in a two dimensional representation on the plane formed by the anode signal q_a and by the ratio of cathode to anode signals

$$q_c/q_a \cong \left(1 - \frac{\bar{X}(E,A,Z)}{D} \cdot \cos\vartheta\right) \qquad (3)$$

Fig. 2 shows such a bi-parametric spectrum for recoil protons measured at 1.895 MeV incident neutron energy which shows a clear ridge for the recoil protons. The largest sensitivity with respect to particle type and

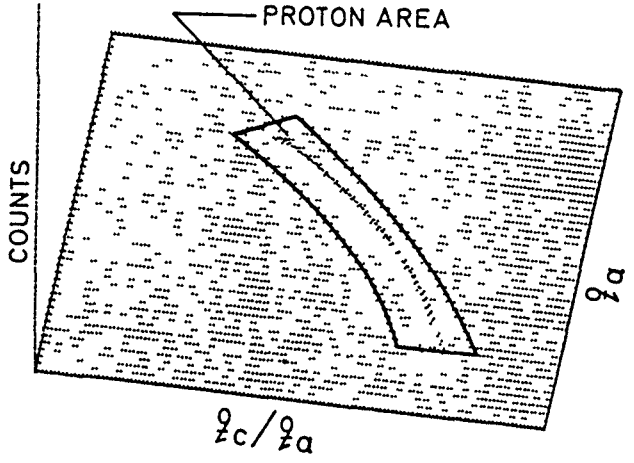

FIG. 2

Background subtracted bi-parametric proton recoil spectrum. The events are plotted versus the anode signal q_a and versus the ratio of cathode to anode signals q_c/q_a.

cos ϑ for this detector one obtains for the condition

$$\bar{X}(E,A,Z) \approx \frac{1}{2} D \approx \frac{1}{2} R_o \qquad (4)$$

where R_o is the range of the recoils at zero degree.
Therefore the range of the zero degree recoils should be just as long as the distance D between cathode and grid.

This condition between range and cathode grid distance leads us to look for the dependence of the range of the recoils in the counter gas as function of energy. Fig. 3 shows in a radial plot for the forward emission angles the proton and carbon recoil ranges for different incident neutron energies.

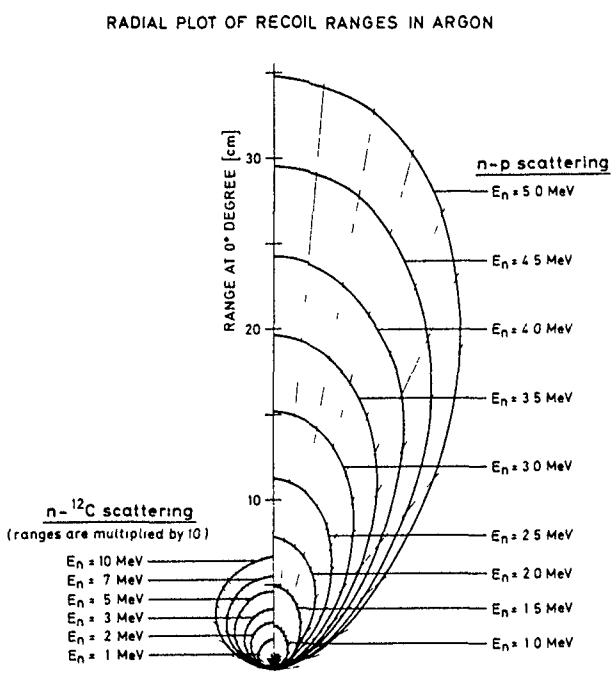

FIG. 3

Radial plot of proton and carbon recoil ranges in argon at NTP for incident neutron energies as marked.

The range for protons between 0.1 MeV and 5 MeV in argon at NTP changes between about 0.3 cm and 35 cm. For a fixed distance of D = 3 cm this requires a pressure range between 0.1 and 12 bars. For comparison the carbon ranges are also plotted. They are much shorter than the proton ranges, e.g. only 0.45 cm at 5 MeV. The better knowledge of the angle integrated neutron scattering cross section of carbon compared to the n-p cross section, 0.5 % and 0.9 % respectively, and the simple composition of a carbon layer compared to tristearin or any other hydrogen containing sample would be advantages of a carbon recoil detector. However, there are also some important facts which are very much in favour for the n-p detector, like higher countrate in the same neutron flux for the same relative energy losses of protons and carbons in their respective radiator foils as well as the much simpler angular distributions for the n-p process. Therefore at present we are looking only for the n-p process.

TEST MEASUREMENTS

In order to check energy linearity of the response and to understand the operation of the detector more clearly, measurements with tristearin radiator foils were performed at the incident neutron energies of 0.297 MeV, 0.597 MeV, 1.096 MeV, 1.495 MeV and 1.895 MeV. The tristearin radiator foils which were used in these measurements had thicknesses of 0.148 mg.cm^{-2}, 0.323 mg.cm^{-2}, 0.370 mg.cm^{-2} and 0.625 mg.cm^{-2}. A set of recoil spectra taken at 1.895 MeV with an argon + 5 % CO_2 gas pressure of 3 bar are shown in Fig. 4. One sees the long plateaus of the proton recoils and, at lower energies, the recoils of the carbon and oxygen ions which are also present in the tristearin and in the counter gas. Fig. 5 shows the according background subtracted proton recoil spectra. Here the sample thickness effects can be clearly seen. In the thickest radiator foil for example a recoil proton at zero degree with respect to the normal of the cathode can loose about 10 % of its energy at a 1.895 MeV incident neutron energy.

An interpretation of the shape of the recoil spectrum is needed in order to be able to obtain from the measured spectrum the total number of proton recoil events which took place in the radiator foil. For this purpose it is

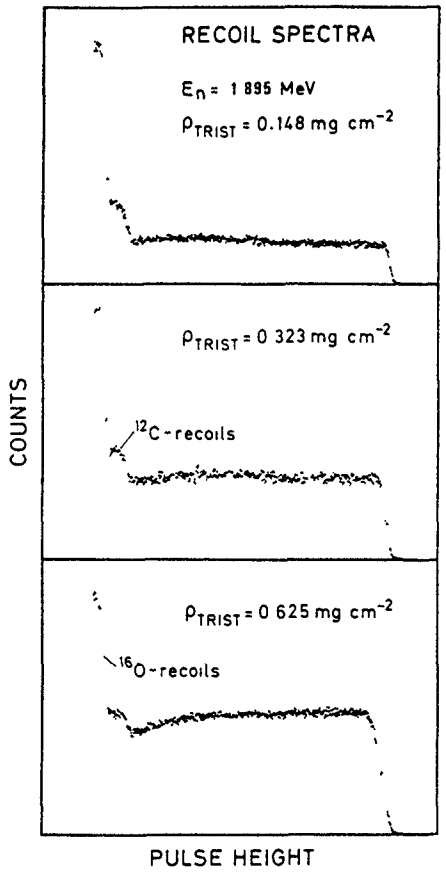

FIG. 4

Recoil spectra measured with three tristearin radiator foils of different thicknesses at 1.895 MeV incident neutron energy.

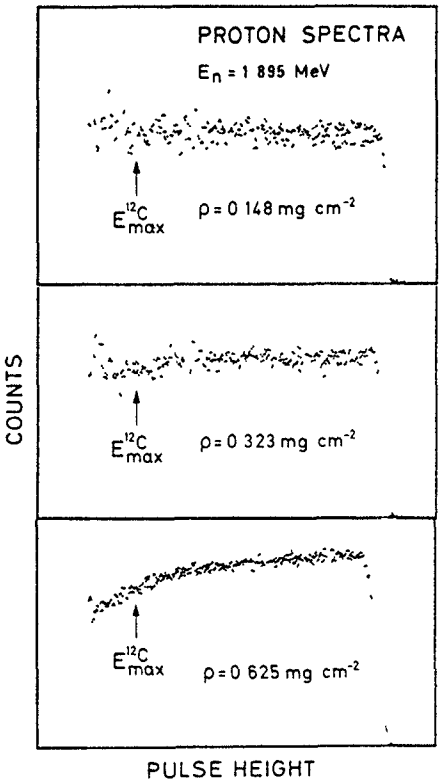

FIG. 5

Proton recoil spectra, background subtracted.

needed to have a calibration between proton energy and channel number and to check the linearity of the detector response with the proton energy. Therefore, from all the measurements, which were made with the same gas pressure of 3 bar, the channel numbers at half the fall at the high energy end of each spectrum were evaluated as indicated in Fig. 6. The results of these evaluations are shown together in Fig. 7. For each incident neutron energy the radiator thickness of a measurement is plotted versus the above mentioned channel value. The measurements at each neutron energy, done with different radiator foil thicknesses, were extrapolated to zero foil thickness to obtain the channel value which corresponds to the average incident neutron energy or to the corresponding proton energy. The above four calibration points at 0.597 MeV, 1.096 MeV, 1.495 MeV and 1.895 MeV together with the zero point show linearity within the experimental errors. The accuracy of the proton energy calibration above 0.5 MeV is better than 0.5 %. This is shown by a least squares fit through the experimental results.

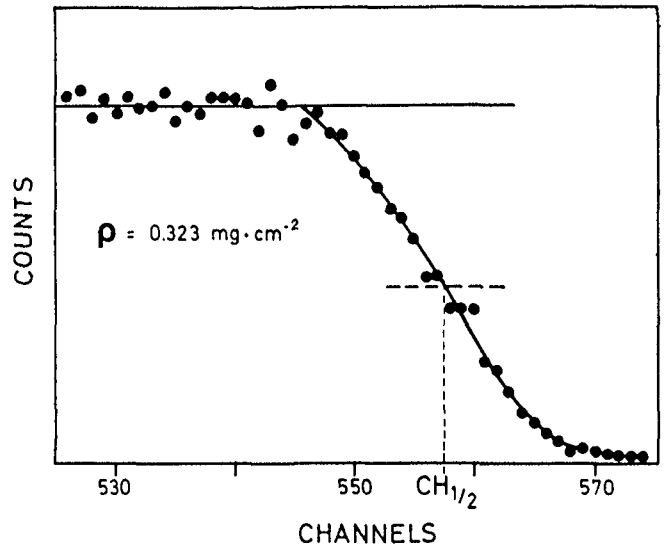

FIG. 6

Upper end of proton recoil spectrum is shown. $CH_{1/2}$ is the channel for which the number of protons has dropped to half the height of the plateau.

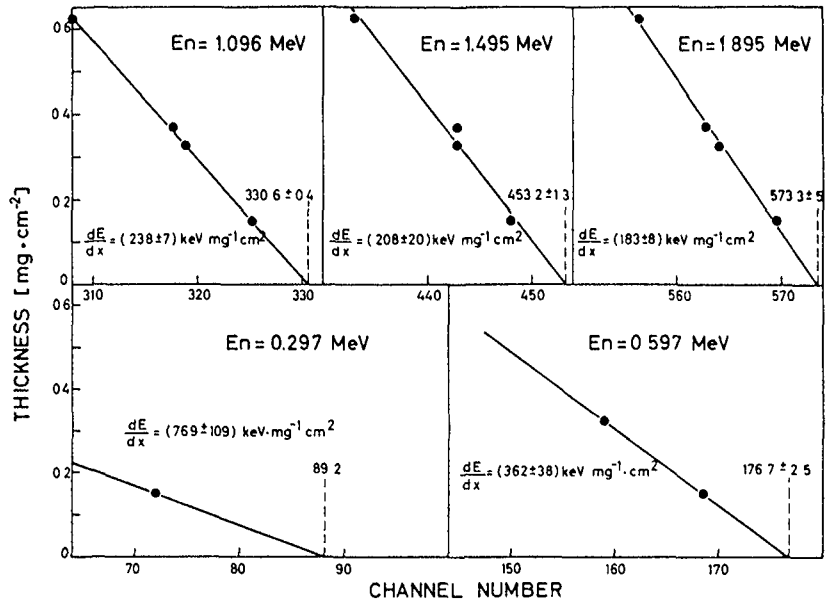

FIG. 7

The full points are the channels of the recoil spectra where the proton number dropped to half that at the plateau for different radiator foil thicknesses and neutron energies. The measurements at each neutron energy are plotted in a subsection. The full lines represent least squares fits through the experimental points when the number of measurements is larger than 2. At 0.297 MEV the full line is determined by the one measured point and the proton energy calibration as obtained from the other four energies.

The rises of the straight lines in Fig. 7 give the stopping powers of protons in tristearin at the energies corresponding to the incident neutron energies. Fig. 8 shows a comparison of the experimental stopping powers with values of refs. 1 and 2. Below about 1 MeV there is a real discrepancy between the stopping power of ref. 2 and the two other data sets.

INTERPRETATION OF PROTON RECOIL SPECTA

For understanding more closely the spectrum shape and to obtain the total number of proton recoil events which took place in the foil, the experiment was simulated by Monte Carlo calculations. The calculations considered the TiT target thickness, the neutron emission angle and the according kinematics, the nominal thickness of the radiator, the n-p scattering law, the energy loss of the protons in the radiator as well as the electronic resolution of the detector. For the stopping power of tristearin data were used which follow below 2 MeV the own measurements and which, below 200 keV, approach and then follow the data of ref. 1. This curve is shown in Fig. 8 as a dashed line. Fig. 9 now compares the Monte Carlo spectrum for 1.895 MeV incident neutron energy with the experimental spectrum measured with the thickest sample of 0.625 $mg \cdot cm^{-2}$ tristearin at the same neutron energies.

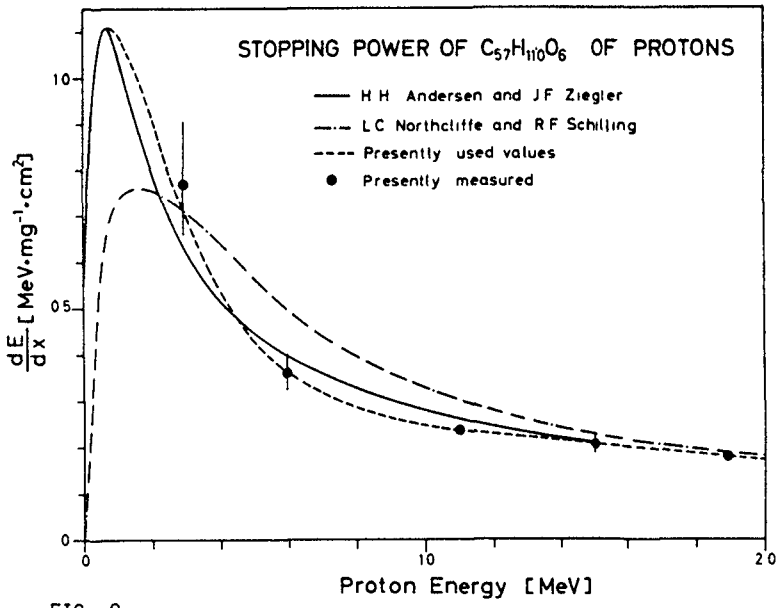

FIG. 8

Stopping power of tristearin is plotted versus proton energy.

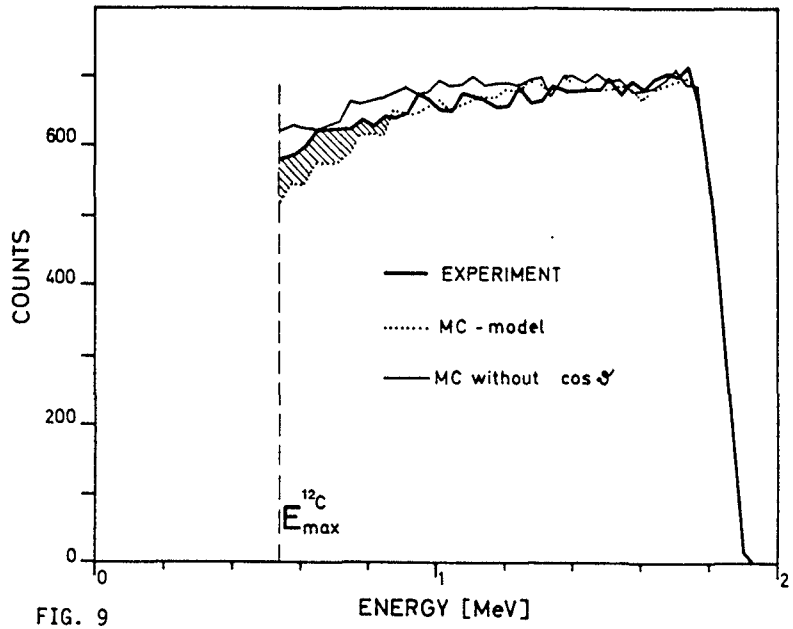

FIG. 9

Comparison between experimental and Monte Carlo spectra.

In both spectra always 10 neighbouring channels were added in order to have less statistical fluctuations. It is seen, that the shapes of the spectra, full line experiment, dotted line Monte Carlo spectrum, agree nicely down to about 0.9 MeV. Below that energy the spectra deviate up to 7 % or in area by about 1.5 % as indicated in Fig. 9. This discrepancy cannot be explained by the uncertainties in the stopping power of tristearin. It is possible that inhomogeneities of the tristearin layer, which are up to 250 %, as observed with a microscope, are one important reason for the mismatch between Monte Carlo model and experiment. The inhomogeneities are formed by cristallization during the evaporation process. For layers with such extreme inhomogeneities the 1/cos ϑ-law for the path length to be passed by the protons on their way in the radiator is then not valid and can cause the observed difference in spectrum shape. In the investigation of alpha active actinide layers it is seen (3), that a strict 1/cos ϑ dependence for the average path length,which is to be passed by alphas emitted under an angle ϑ with respect to the normal of the layer, is only valid for homogeneous layers. For inhomogeneous layers with corns and crystals the dependence on cos ϑ is much weaker. Therefore, Monte Carlo calculations were performed with the extreme assumption of no dependence of the path length on the emission angle. The result of this calculation for the 0.625 mg·cm^{-2} thick tristearin radiator at E_n = 1.895 MeV is shown in Fig. 9 with a full but thin line. This line lies now above the experimental spectrum as one would expect from the extreme assumption made.

Some reservations should be made also with respect to the isotopic composition of the radiator material which might not correspond to the stechiometric composition of tristearin ($C_{57}H_{110}O_6$).

CONCLUSIONS

The measurements have to be repeated with homogeneous radiator foils. Also other chemical compounds should be tried as radiator material. The 0.9 % accuracy of the n-p angle integrated standard cross section is not sufficient if one aims accuracies below 1 %. Other possibilities to circumvent the use of the values of the n-p cross section should perhaps be investigated.

REFERENCES

1. H.H. Andersen and J.F. Ziegler,
Hydrogen-Stopping Powers and Ranges in all Elements, Vol. 3,
Pergamon Press (1977).

2. L.C. Northcliffe and R.F. Schilling,
Nuclear Data Tables 17, 233 (1970).

3. C. Budtz-Jørgensen, H.-H. Knitter and G. Bortels,
Proc. 12th World Conference of the International Nuclear Target Development Society, Antwerp, Belgium, 25 - 28 Sept. 1984.
To be published in N.I.M.

ASSAYING OF ^{235}U FISSION LAYERS FOR NUCLEAR MEASUREMENTS WITH A GRIDDED IONIZATION CHAMBER

C. BUDTZ-JØRGENSEN, H.-H. KNITTER
Central Bureau for Nuclear Measurements,
Joint Research Centre,
Commission of the European Communities,
Geel

Abstract

An ionization chamber with a Frisch grid is used to determine both the energy (E) of the charged particles emitted from the sample positioned coplanar with the cathode, and the cosine of the emission angle (ϑ) with respect to the normal of the cathode. Using the combined information on cos ϑ and E, problems in particle counting due to sample absorption and scattering effects can be circumvented and sample source strengths are readily determined to an accuracy of 0.3 %. However, it is emphasized that the source strength can be determined from the particles emitted in a large solid angle close to 2π steradian, which means a considerable higher efficiency than for the conventional low geometry counting techniques. Moreover the present method, within reasonable limits is insensitive to source shape and thickness homogeneity.

The technique will be illustrated by measurements of alpha particles and fission fragments emitted from a set of four vacuum evaporated UF_4, three electrodeposited and one suspension-sprayed $^{235}U_3O_8$ layers.

INTRODUCTION

Assaying of samples to be used in nuclear measurements rarely involves only a determination of the mass and the isotopic composition of the sample material. A useful sample must also be characterized by its thickness homogeneity and effective thickness so that the energy losses which the studied nuclear particles suffer in the layer can be estimated. For nuclear

cross section measurements where a 2π measuring geometry is used, e.g. fission cross section measurements, the above sample qualities are very important for a correct determination of the number of induced events lost by absorption in the foil. In two recent papers[1,2] we presented a method for charged particle counting employing energy and angle information from gridded ion chambers. It was demonstrated that the simultaneous measurement of cosine of the emission angle ϑ with respect to the normal of the layer and the charged particle energy circumvented problems in particle counting due to sample absorption and scattering effects. Using this technique sample source strengths are readily determined to an accuracy of 0.3 %. Moreover the source strengths can be obtained from the particles emitted in large solid angles close to 2π retaining the high counting efficiency of the ion chamber. The purpose of the present paper is to further illustrate the capabilities of the technique and especially to show how the technique can be used to investigate the quality of ^{235}U sample layers.

EXPERIMENTAL DETAILS

The present investigations were based on a gridded ion chamber where signals from the anode and the cathode wre used to derive both the energy (E) of the ionizing particle and the cosine of its emission angle (ϑ) with respect to the normal to the electrodes. The working principle and the data processing procedures used in connection with these chambers are described in Refs.1 to 6. Three sets of ^{235}U layers, four UF_4 samples vacuum evaporated onto highly polished stainless steel disks, one sample prepared by electrospraying of a U_3O_8 suspension and three samples prepared by electrolysis using an uranyl-nitrate solution[7]) were compared. All samples were fabricated at CBNM and their metrological data are given in Table I.

SOURCE STRENGTH AND BIPARAMETRIC ALPHA SPECTRA

The upper part of Fig. 1 shows the pulse height distribution of the anode signals obtained from the 75 $\mu g \cdot cm^{-2}$ thick UF_4 sample. The two main alpha lines from the decay of ^{234}U and ^{235}U are only partly separated and a low-

Table I : Metrological data of the investigated samples

Sample	Prep. Method	Nominal thickn. [$\mu g \cdot cm^{-2}$]	Diameter [cm]	Isotopic Composition [at %]
25A-27 25A-36 25A-93 25A-96	Vacuum-evaporated UF_4	15 75 300 500	1.27	^{234}U : 0.176 ^{235}U : 99.361 ^{236}U : 0.029 ^{238}U : 0.433
Sp3024-1	Suspension-sprayed U_3O_8	100	2.8	as above
ROLF-32B ROLF-33 ROLF-34	Electrolysis U_3O_8	25 75 400	3.0	^{234}U : 1.658 ^{235}U : 97.663 ^{236}U : 0.150 ^{238}U : 0.530

energy tail due to self-absorption and scattering is visible. The lower part of Fig. 1 shows the pulse height distribution of the cathode signals, which is broadened due to the cos ϑ dependence. The upper part of Fig. 2 is a plot of the biparametric distribution of the number of alpha events versus the anode signal and versus the ratio of cathode to anode signal. This ratio is for a single alpha line distributed between $[1 - \bar{X}(E)/d]$ and 1 [see Eqs. (1) and (2)] .

The lower part of Fig. 2 gives the biparametric distribution of cos ϑ and E for the 75 $\mu g \cdot cm^{-2}$ sample. The cos ϑ distributions are, even for the rather thin samples, strongly influenced by the sample thickness. However, the low energy tail is mainly distributed close to cos ϑ = 0. For larger cos ϑ values the energy spectra have below the peaks a nearly energy independent tail with vanishing content. This is illustrated in Fig. 3, where three different alpha apectra belonging to the angular cone $0.9 \leq \cos \vartheta \leq 1.0$ are displayed. For an angular cone such that cos $\vartheta > 0.3$ the tail content below 3 MeV was for most of the samples less than 0.1 %. This is important since it means that only the lowest cos ϑ intervals are influenced by backscattering and losses due to self-absorption.

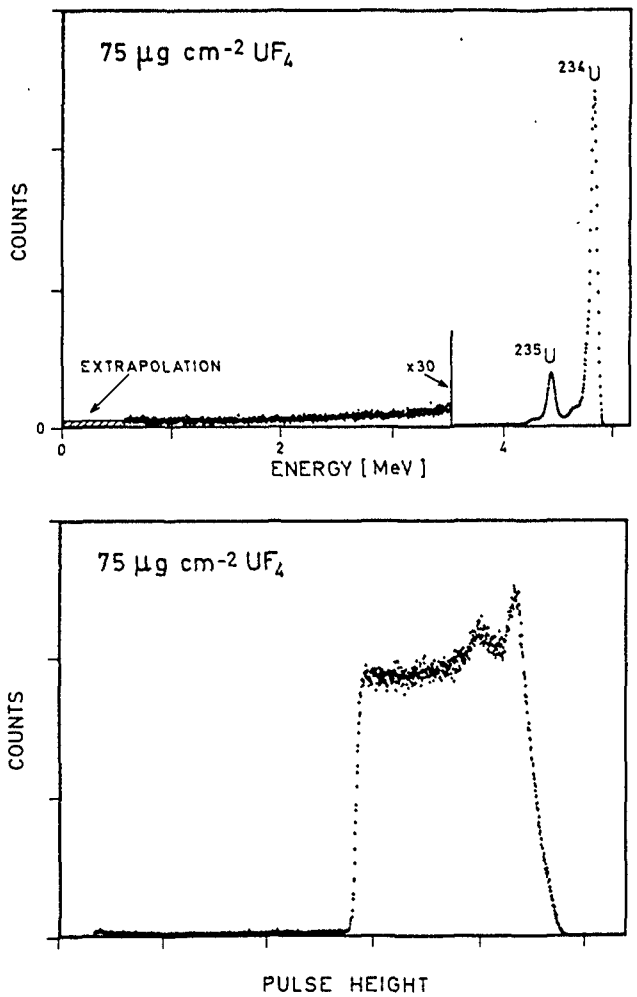

Fig. 1
The pulse height distributions for the anode and cathode signals are plotted in the upper and lower part of the figure respectively.

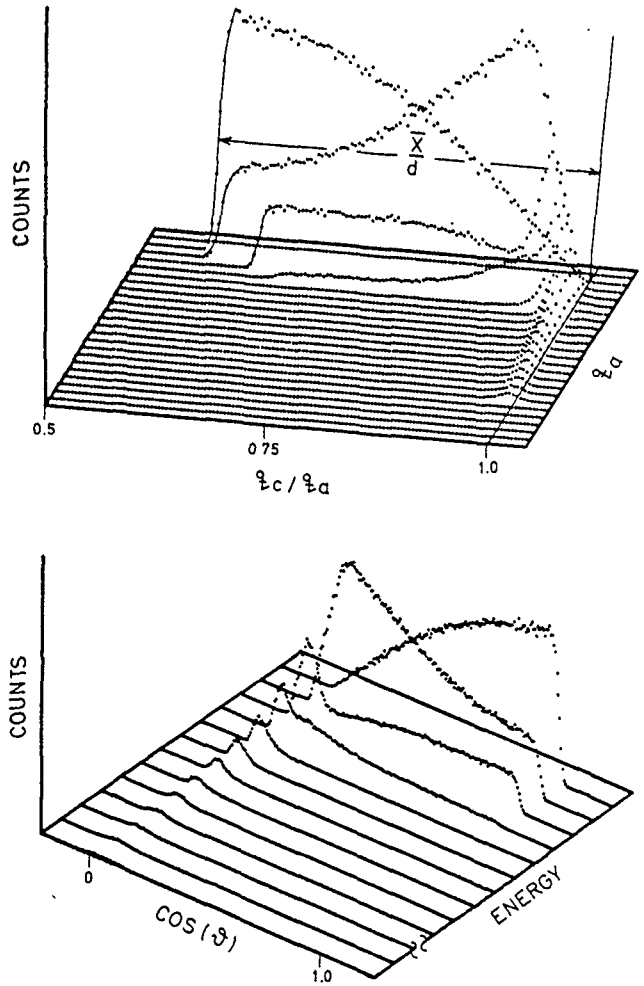

Fig. 2
The upper part shows a biparametric distribution of the number of alpha events versus the anode signal and versus the ratio of the cathode-to anode signal. The lower part shows the number of alpha events versus the alpha energy and versus the cos ϑ with high resolution in the cos ϑ-parameter. Both spectra are measured with the 75 $\mu g/cm^2$ sample.

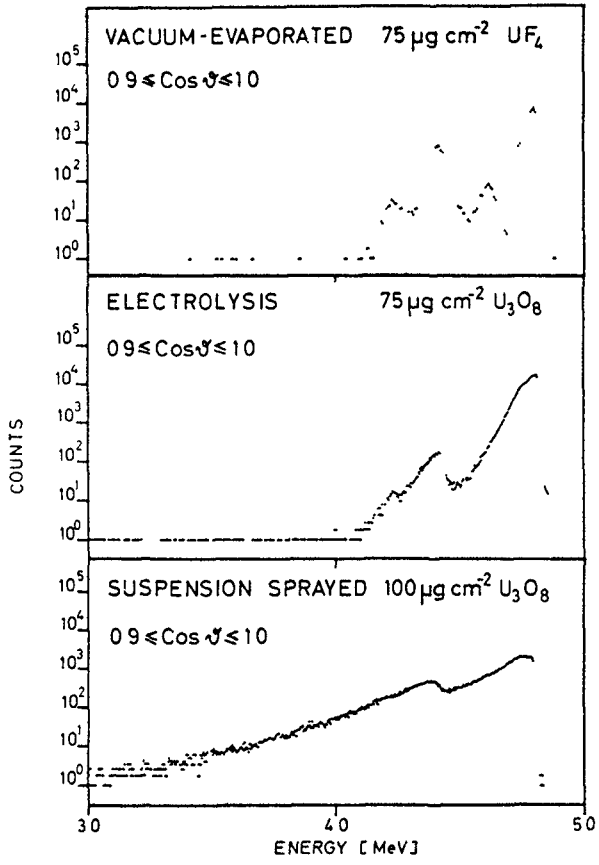

Fig. 3
Alpha particle energy spectra.

It is believed that the low-energy signals originate from alpha particles that have lost an appreciable amount of energy in the sample ($\vartheta \sim 90$ deg) or in the backing ($\vartheta > 90$ deg) and then made a large Rutherford scattering out into the active volume of the detector. Therefore these events do not initially belong to the selected angular cone.

The determination of the source strength is based on the cos ϑ distribution integrated over all alpha lines in the energy spectrum. Figure 4 displays this distribution for the 75 $\mu g \cdot cm^{-2}$ UF_4 sample. The distribution has a

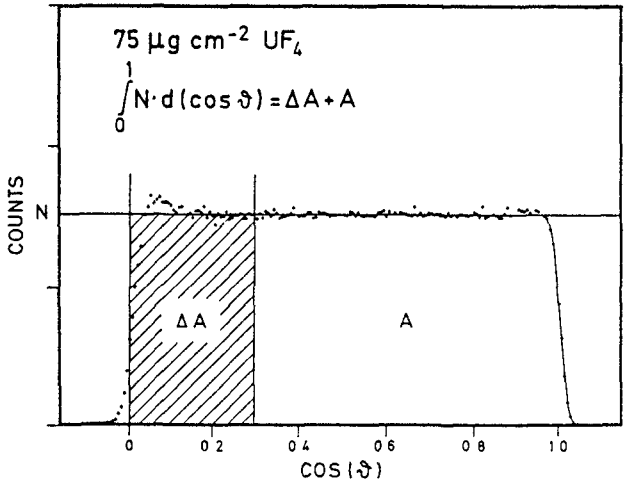

Fig. 4
The cos ϑ -distribution measured for the 75 $\mu g/cm^2$ sample and integrated over all alpha lines is shown.

rectangular shape as expected from an isotropic distribution. However, a small top is visible close to cos ϑ = 0. This is very likely due to back-scattered alpha particles, which, because of the strongly forward-peaked Rutherford scattering law, will leave the sample with angles close to ϑ = 90 deg. According to the discussion above, a lower limit $(\cos \vartheta)_{min}$ can be found such that the effects of backscattering and self-absorption are negligible for cos $\vartheta > (\cos \vartheta)_{min}$. Therefore, the height, N, of the plateau in the cos ϑ distribution above $(\cos \vartheta)_{min} = 0.3$ has the same value as it would have in the ideal case where no scattering or self-absorption was present. The true source strength Φ can be determined from

$$\Phi = 2 \cdot \int_0^1 N \cdot d(\cos \vartheta) = 2 \cdot (A + \Delta A), \qquad (4)$$

where A is the number of counts summed above $(\cos \vartheta)_{min}$ and $\Delta A = N \cdot (\cos \vartheta)_{min}$ is the extrapolation from $(\cos \vartheta)_{min}$ down to cos ϑ = 0.

Compared to conventional low-geometry counting techniques, the error sources of the present method originate from the detector-associated electronics instead of geometrical uncertainties. The systematic errors of this counting technique are discussed in detail in ref. 1,2 and amount to 0.2 - 0.3 %.

Table II : Strengths of the four UF_4 alpha sources as determined by the present method "cos ϑ"and the low geometry counting.

Sample	"cos ϑ" [s^{-1}]	Low geometry [s^{-1}]
25A - 27	8.89 ± 0.03	
25A - 36	44.03 ± 0.11	44.16 ± 0.13[a]
25A - 93	165.24 ± 0.51	165.35 ± 0.26[a]
25A - 96	273.26 ± 0.98	272.60 ± 0.41[a]

a) values obtained from ref. (8)

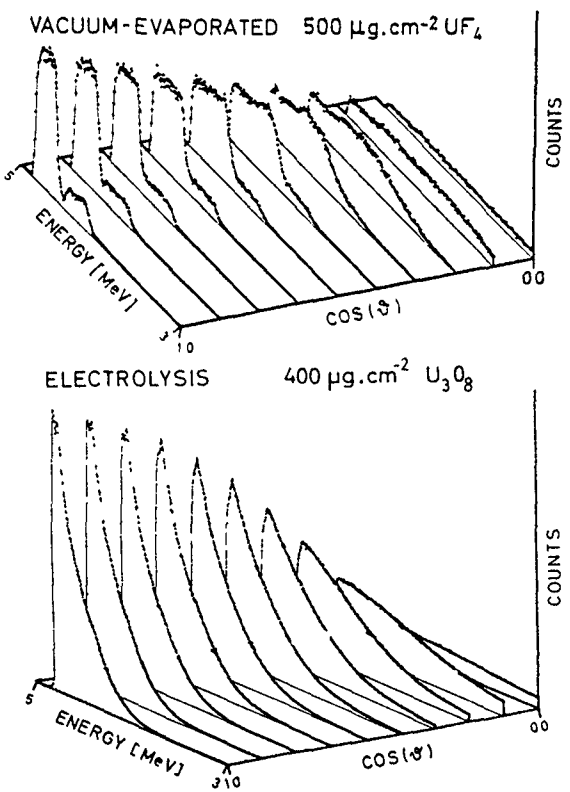

Fig. 5
Biparametric distributions versus cos ϑ and the alpha particle energy for two different samples with high resolution in the particle energy.

The second column of Table II gives the activities of the four UF_4 samples as determined from the cos ϑ distributions. The third column gives the activities for the three most active samples as independently measured by conventional low-geometry counting[8]. The results of the two methods agree within the stated uncertainties of ~ 0.3 %.

It should be emphasized that the present technique has an angular-detection efficiency close to 2π which in many cases is several orders of magnitude larger than used in conventional low-geometry counting. The method also has the advantage that it is independent of sample shapes and thickness inhomogeneities as long as these quantities stay within reasonable limits.

As mentioned earlier the sample quantities such as microscopic homogeneity and effective thickness strongly affect the biparametric (cos ϑ,E) alpha spectra as shown in Fig. 5. Here the energy distributions for the 500 $\mu g \cdot cm^{-2}$ evaporated UF_4 and the electroplated 400 $\mu g \cdot cm^{-2} U_3O_8$ samples are displayed with high resolution and cos ϑ intervals are given in steps of 0.1. The thicker UF_4 samples gave flat topped energy distributions for which it was found[1,2] that the widths, FWHM, increased inversely proportional to cos ϑ being proportional to the path lengths of the alpha particles in the layers. However, the samples prepared by the two other techniques did not produce similar spectra. These spectra have all a sharp edge at 4.774 MeV but with a broad exponential low energy tailing, at most pronounced for the sprayed sample, as can be seen from Fig. 3 where the three preparation techniques are compared. Note that the three samples have about the same areal density. Also the average sample energy loss :

$$< \Delta E > = E_0 - < E > \qquad (5)$$

was larger for the latter two techniques. Here E_0 is the unperturbed alpha line energy and $< E >$ is the centroid of the measured energy distribution. The average energy losses $< \Delta E >$ were determined from the shape of the ^{234}U 4.774 MeV line and are for the electroplated and sprayed samples shown in Fig. 6 as function of cos ϑ. Correction was made for the contribution of other (^{235}U) lines under the 4.774 MeV tail assuming that all lines have identical shapes. From Fig. 6 it can be seen that the average energy losses for the electroplated samples are nearly inversely proportional to cos ϑ whereas the sprayed sample shows a much weaker cos ϑ dependence. It is likely that the electroplated samples are continuous layers, although having large thickness variations, whereas

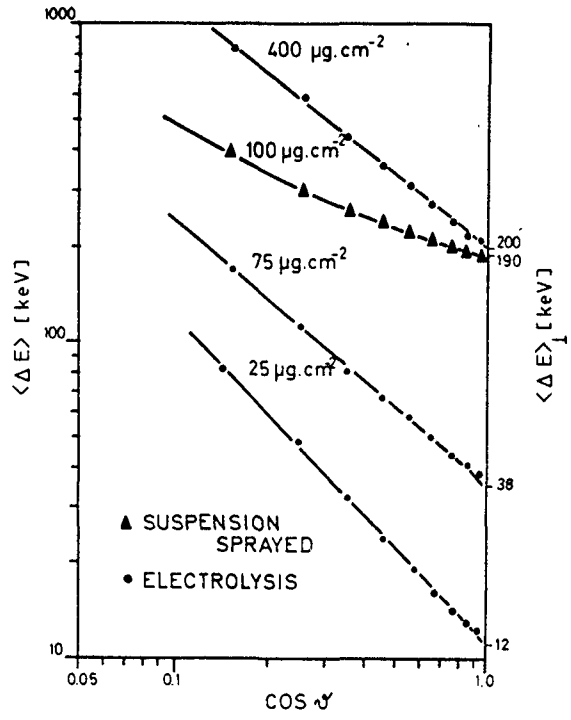

Fig. 6
The average energy loss of the alpha particles emitted from different samples is plotted versus cos ϑ in double logarithmic scale. On the right hand side the vertical energy losses are indicated for each sample.

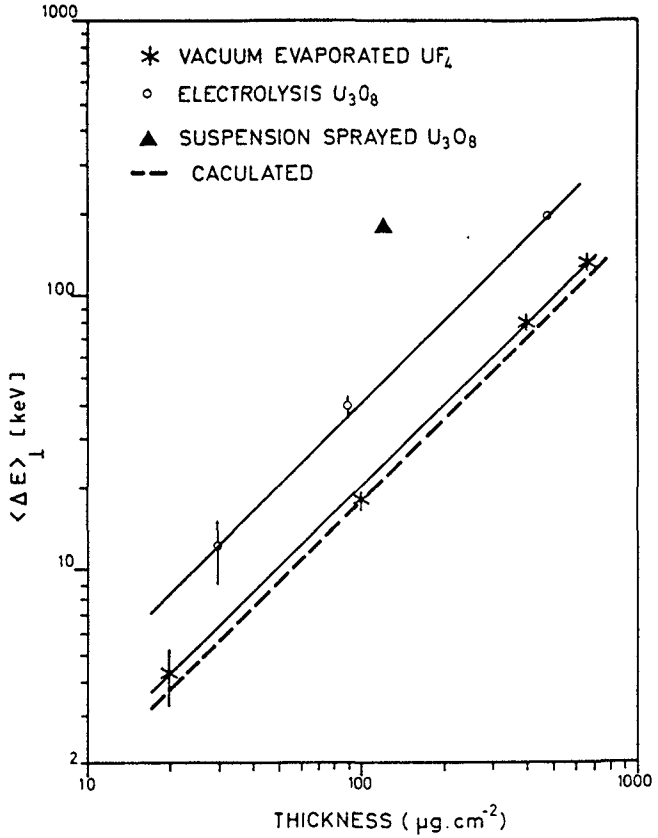

Fig. 7
The vertical alpha particle energy losses measured for the different samples are plotted versus their respective average sample thicknesses.

the sprayed sample consists of corns lying more or less isolated on the backing. However, it is more important that the average energy losses are much larger, especially for the sprayed sample, than expected from their areal density. This can be seen from Fig. 7 where the vertical energy losses $< \Delta E >_{\perp}$ for all the samples are compared. For the UF_4 layers this energy loss is proportional to the areal layer density and is only 15 % larger than the calculated values based on the alpha stopping power data of Ref. 9. The energy losses for the electroplated samples display the same thickness linearity, however, the average energy losses are about a factor 2.5 larger than expected for layers having uniform thicknesses. For the sprayed sample the increase of the energy loss due to nonuniformity is close to a factor 10. However, the sample contains grains with thicknesses of more than a factor 50 of the areal density giving rise to energy losses of more than 1 MeV, see Fig.3 . Such characteristics make it very doubtful whether the sample is useful in a nuclear physics experiment, since energy losses and absorption losses of the studied nuclear particles can totally obscure the experimental results.

Actinide samples like the ones discussed are very often used in nuclear experiments where the fission process is studied. The sample qualities enter critically in such measurements, since they determine the energy resolution by which the fission fragment energy can be measured. An important correction to fission cross section determinations is due to the losses of fission events by absorption in the sample. The following section discusses the proposed method for absolute charged particle counting with respect to fission fragments. The measurements were made with the vacuum evaporated UF_4 and the suspension sprayed U_3O_8 sample.
The ion chamber was mounted in front of a CBNM Van de Graaff beam line and neutrons were produced using the $^7Li(p,n)$ reaction. The neutrons were "thermalized" in blocks of paraffin to ensure that the neutron-induced fission events gave an isotropic angular distribution of the fission fragments. The distance between the cathode and the grid was 2.5 cm and the chamber was operated at 1-bar pressure, which was sufficient to stop the fragments in the active volume between the cathode and the grid. The cos ϑ value belonging to each fission fragment was calculated using Eq.(3). Fig. 8 displays the biparametric distribution of cos ϑ and the fragment energy. Again, it is seen that energy degradation of the fragment occurs for cos ϑ approaching zero. However, in this case there is also a high-energy tail, barely visible in the figure, distributed close to cos ϑ = 0. This tail stems from fission events where the fragment initially emitted downward into the backing is scattered out in the detector volume where its ionization charge is added to the ionization of the unscattered fragment. Due to the strongly forward-peaked scattering cross section, this only happens, as observed, close to cos ϑ = 0. As in the case for alpha particles, a cos ϑ value $(\cos\vartheta)_{min}$ can be found such that the fission spectra have no tailing for cos $\vartheta > (\cos\vartheta)_{min}$. This is illustrated in the upper part of Fig. 9, which is a plot of the integrated fission fragment energy spectrum for cos $\vartheta \geq 0.5$ measured with the 75 $\mu g \cdot cm^{-2}$ UF_4 sample. However, a similar spectrum with no low energy tailing was not found for the 100 $\mu g \cdot cm^{-2}$ suspension-sprayed U_3O_8 sample for which the energy spectrum in the same cos ϑ interval is given in the lower half of Fig. 9. The valley between the light and heavy fragment peaks is filled and an appreciable low-energy tail is observed. The difference between the two types

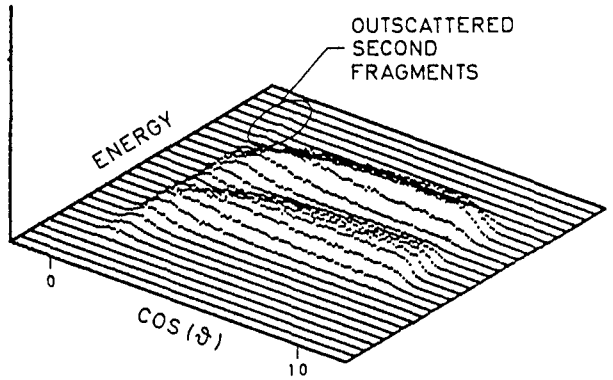

Fig. 8
The biparametric distribution of fission fragments is plotted versus the fragment energy and versus cos ϑ with high resolution in the cos ϑ parameter. The spectrum was measured with the 75 $\mu g/cm^2$ vacuum evaporated UF_4 sample.

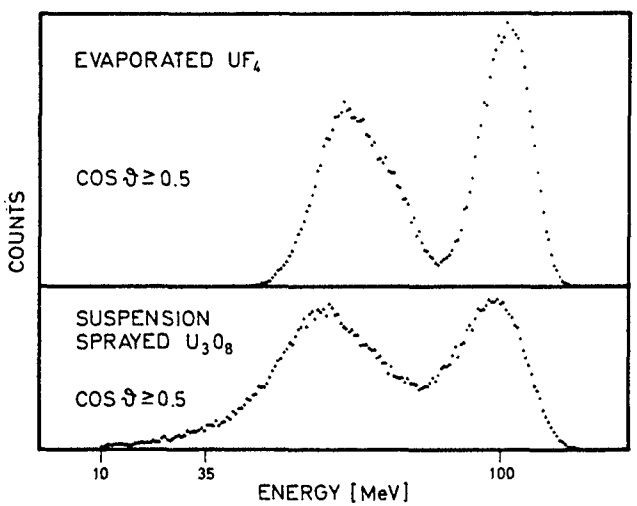

Fig. 9.
Fission fragment energy spectra for cos $\vartheta > 0.5$ are shown for the 75 $\mu g/cm^2$ vacuum evaporated UF_4 sample and for the 100 $\mu g/cm^2$ U_3O_8 suspension sprayed sample in the upper and lower part of the figure respectively.

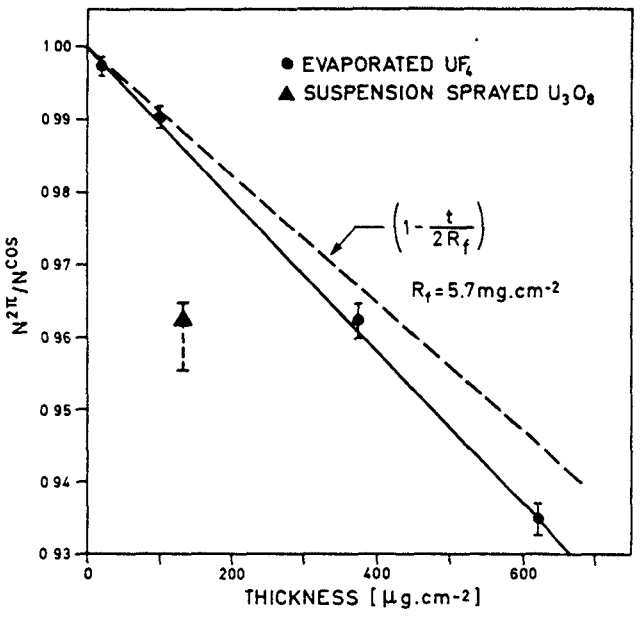

Fig. 10.
The ratio of the 2π-countrate and the total number of fission events determined from the cos ϑ distribution is plotted versus the sample thickness.

of samples is also demonstrated by a comparison of the fraction of events falling in the low-energy tail between 10 and 35 MeV as function of cos ϑ. The tail content for the evaporated UF_4 sample decreases rapidly with cos ϑ becoming negligible, $< 10^{-2}$%, for cos $\vartheta > 0.3$. The tail content for the sprayed sample changes weakly with cos ϑ and amounts still to 0.4 % in the cos ϑ interval from 0.9 to 1. This means that even fission fragments emitted with a direction perpendicular to the sample can encounter appreciable energy losses and it is certainly a possibility that some of these fragments can be stopped completely in the sample. Although the nominal sample thickness ~ 100 $\mu g \cdot cm^{-2}$ is small compared to the fission fragment ranges, the sample must contain grains, which individually can have sizes larger than the fission fragment ranges confirming the conclusions drawn from the alpha particle spectra. This makes it extremely difficult to

correct for self-absorption in the sample, since usual correction formulas are no longer valid. This is more serious, since suspension-sprayed or -painted samples often have been used in fission cross-section measurements, especially with more exotic samples where the material losses in connection with vacuum evaporation cannot be tolerated. For fast-neutron-induced fission cross-section measurements, lacking or incorrect absorption corrections can lead to a wrong determination of the cross-section shape due to the energy dependence of the fission fragment angular distributions.
The true number, N^{cos}, of neutron-induced fission events was determined in the same way as described in the section on alpha-particle counting. However, due to the shorter range of the fission fragments, it was necessary to increase $(\cos \vartheta)_{min}$ up to cos $\vartheta = 0.6$ for the thickest of the samples to assure that there were no fission events with energies lower than the bias level. The ratios $N^{2\pi}/N^{cos}$ between the 2π counting and the intensities found from the cos ϑ distributions are plotted in Fig. 10. For the four UF_4 samples, this ratio has a linear dependence with sample thickness, which extrapolated to zero thickness yields a value $N^{2\pi}/N^{cos} = 1.000 \pm 0.002$. The inefficiency, $1 - N^{2\pi}/N^{cos}$, of the 2π counting is for the UF_4 samples given by

$$\Delta_{UF_4} = (10.5 \pm 0.7) \cdot t \ \% \ , \qquad (6)$$

where the thickness t is given in $mg \cdot cm^{-2}$ of UF_4. It should be remembered that the 2π counting is affected both by self-absorption and by the extrapolation of the fragment spectrum down to zero pulse height. The layer absorption loss was calculated using the range tables of Ref. 10. The calculated absorption is shown in Fig. 10 as a dashed line and has a somewhat weaker thickness dependence than experimentally observed. It should, however, be noted that the ranges of heavy ions in matter probably are not known to better than 20 % (Ref. 10).

Also given in Fig. 10 is the $N^{2\pi}/N^{cos}$ ratio obtained from the sprayed U_3O_8 sample. As discussed previously, the biparametric distribution of cos ϑ and E measured on this sample showed that there did not exist a cos ϑ value above which there was no self-absorption. Therefore the cos ϑ distribution for this sample can only be used to determine a lower limit for the loss of

fission fragments in the sample. However, this limit, $\Delta_{U_3O_8}$ = 3.7 ± 0.3 %, is a factor of ~ 3 more than expected for an evaporated UF_4 sample of similar thickness which, again, confirms that this type of sample, due to its self-absorption problems, should not be used in fission cross-section measurements.

CONCLUSIONS

The biparametric method of measuring both the energies of the charged particles and their emission angles with respect to the normal of a plane source gives a clear and vivid picture of the processes that these particles experience on their different ways out from the source layer into the directly facing counter gas. In the two-parametric spectra, it is clearly seen in which parameter range they are undisturbed. This information permits in the case of the alpha particles and in that of the fission fragments, a determination of the absolute number of decay events with an accuracy of better than 0.3 and 0.5 % respectively. The error sources of earlier methods like backscattering, absorption processes, source shapes, and source inhomogeneities are circumvented by the present method. An important strength of the present method is also the large solid angle for the particle detection.

ACKNOWLEDGMENTS

The authors are very indebted to J. Van Audenhove, J. Pauwels and R. Obernhuber for their skillful preparation of the uranium layers. We greatly appreciate the contribution of B. Denecke who performed the low-geometry measurements. The authors are also grateful to H. Bax, R. Vogt and the Van de Graaff crew for their technical assistance during the execution of the investigations.

REFERENCES

1. C. Budtz-Jørgensen and H.-H. Knitter,
Nucl. Sci. Eng. 86, 10 (1984).

2. C. Budtz-Jørgensen and H.-H. Knitter,
Nucl. Instr. Meth. 223, 295 (1984).

3. H.-H. Knitter and C. Budtz-Jørgensen,
Proc. of the International Conference on Nuclear Cross Sections for Technology, Knoxville, U.S.A., Oct. 1979,
NBS Spec. Publ. 594, p. 947 (1980).

4. H.-H. Knitter, C. Budtz-Jørgensen, D.L. Smith, and D. Marletta,
Nucl. Sci. Eng. 83, 229 (1983).

5. J.W. Meadows and C. Budtz-Jørgensen,
Proc. Int. Conf. on Nuclear Data for Science and Technology,
Antwerp, Sept. 1982, page 740, D.Reidel Publ. Company, Dordrecht, NL.

6. C. Budtz-Jørgensen and J.W. Meadows,
Lecture Notes in Physics, Vol. 158, 111 (1982).

7. R. Obernhuber,
Private Communication (1984) CBNM, 2440 Geel, Belgium and Danmarks Ingeniør Academi, 2800 Lyngby.

8. B. Denecke,
Private Communication (1983), CBNM, 2440 Geel, Belgium.

9. J.F. Ziegler,
Handbook of Stopping Powers and Ranges in all Elemental Matter,
Vol. 4, Pergamon Press, New York (1977).

10. U. Littmark and J.F. Ziegler,
Handbook of Stopping Powers and Ranges of Ions in Matter, Vol. 6,
Pergamon Press, New York (1980).

FINAL RESULTS OF THE INTERNATIONAL ^{235}U SAMPLE INTERCOMPARISON AND THE HALF-LIFE OF ^{234}U

W.P. POENITZ, J.W. MEADOWS
Argonne-West,
Argonne National Laboratory,
Idaho Falls, Idaho,
United States of America

Abstract

Finalized values were recieved from all laboratories which contributed samples to the ^{235}U mass intercomparison carried out at Argonne National Laboratory. A least-squares fit was made which included the quoted masses and the absolute low-geometry and relative 2π-geometry alpha data as well as the relative fission ratios measured at ANL. Correlations between the measured values were taken into account. The values quoted by the contributing laboratories were found to be within ±0.35% of the values obtained from the LS fit.

Very precise values for the isotopic composition were known for two of the sample materials which permitted a determination of the half-life of ^{234}U. The value obtained is $T_{1/2} = (2.457 \pm 0.005) \times 10^5$ years. Including this value in the present data base results in a current best value of $T_{1/2} = (2.4566 \pm 0.0044) \times 10^5$ years.

I. INTRODUCTION

An intercomparison of ^{235}U samples from several U.S. laboratories was carried out in 1979.[1] This intercomparison was extended in 1982/3 in order to include samples from several European laboratories. A list of the contributing laboratories is given in Table I. The results from the 1982/3 measurements at Argonne National Laboratory were reported at the IAEA Consultants Meeting on the U-235 Fast-neutron Fission Cross Section held in Smolenice in 1983.[2] Finalized values have been received from all contributing laboratories and the present paper summarizes and discusses this intercomparison. A more detailed description has been given elsewhere.[3]

Fifteen ^{235}U samples (see Table II) made from six different enriched materials (see Table III) were involved in the intercomparison. Absolute and relative alpha decay rates and relative fission ratios were measured.

TABLE I. Contributing Laboratories

Laboratory		Samples Provided by
AERE	Atomic Energy Research Establishment, Harwell, UK	R. Wiltshire
ANL	Argonne National Laboratory Argonne, Illinois, USA	R. Armani J. Meadows
BRC	Centre d'Etudes de Bruyeres-le-Chatel, Montrouge Cedex, France	G. Grenier
CBNM	Central Bureau of Nuclear Measurements, Geel, Belgium, EURATOM	J. Pauwels
KRI	Kloplin Radium Institute, Leningrad, USSR	V. Shpakov
LANL	Los Alamos National Laboratory New Mexico, USA	D. Barton
NBS	National Bureau of Standards, Washington, D.C., USA	D. Gilliam

II. ALPHA COUNTING

The alpha-counting rates of all samples were determined with a low-geometry counter. The geometry factor was ~0.0045 but some samples were also counted with a geometry factor of ~0.0010. Systematic uncertainties due to the geometry factors were estimated to be 0.1-0.2%. The accuracy of the absolute alpha counting was checked against other counters to that precision. Additional systematic uncertainties are due to less well defined errors caused by sample backing warping, impurities, and nonuniform area densities. These were estimated to be 0.1-0.3%. Statistical uncertainties were 0.1-0.2%. The results from the absolute alpha counting and the derived masses (based on the specific activities of Table III) are given in Table IV. The present alpha decay rates agree well with the quoted decay rates.

Samples of the same material and deposited on the same backing were also counted with a 2π counter in order to obtain ratios with negligible statistical uncertainty.

TABLE II. ^{235}U Sample Specifications

Fissile Sample Deposit					Backing			
Sample	Material	Compound	Dep. Techn.	Diam. cm	Approx. Thickness $\mu g/cm^2$ [a]	Material	Thickness cm	Diameter cm
ANL-R5	U5-S-U4	U_3O_8	EP	2.22	20.6	SS	0.0127	4.445
ANL-N3	U5-S-U4	U_3O_8	EP	1.27	41.1	SS	0.0254	1.905
ANL-5-1	U5-S-U4	$UO_2 \cdot H_2O$	EP	2.49	210.4	SS	0.0254	6.985
ANL-5-2	U5-S-U4		EP	2.50	164.2	SS	0.0254	6.985
ANL-SST5	U5-Th	UF_4	EV	2.54	81.2	SS	0.0254	6.985
LANL-S1	INS-1	U_3O_8	EV	2.00	95.1	Pt	0.0127	4.763
LANL-S3	INS-1	U_3O_8	EV	2.00	537.9	Pt	0.0127	4.763
NBS25-S-52	INS-1	UO_2	EV	1.27	182.0	Pt	0.0127	1.905
KRI VI	U5-P	U_3O_8	HFS	2.1	220.7	Cr-Ni	0.010+	2.100+
KRI XV	U5-P	U_3O_8	HFS	2.1	260.2	Cr-Ni	0.010+	2.100+
BRC	U5-NBS	U_3O_8	?	1.2945	85.8	Ta	0.03 (0.05)	2.771
AERE-A	U5-UK	U_3O_8	EV	2.0	110.4	SS	0.0394	2.699
AERE-B	U5-UK	U_3O_8	EV	2.0	110.6	SS	0.0394	2.699
CBMN-33	U5-NBS	UF_4	EV	1.27	96.0	SS	0.015	1.905
CBMN-36	U5-NBS	UF_4	EV	1.27	197.0	SS	0.015	1.905

EV = Evaporation, EP = Electroplating, HFS = High Frequency Sputtering, SS = Stainless Steel, and + = Additional Material due to the Brass Mounting Ring.

[a] These are only approximate values used for the calculation of the total fission-fragment absorption.

TABLE III. Isotopic Compositions and Specific Activities of the ^{235}U Samples

	Isotopic Compositions, Wt.%				Specific Activities, γ/min μg				
Material	^{234}U	^{235}U	^{236}U	^{238}U	Isotopic Dilution	Isot. Comp. Half-L.[b]	Colorim.	Others	Average[c]
LANL[a] INS-1	0.0607	99.7457	0.0655	0.1277	13.338 ±0.024	13.26 ±0.13		13.30 ±0.08	13.33 ±0.02
NBS INS-1					13.412 ±0.067	13.26 ±0.13		13.38 ±0.16	13.38 ±0.07
ANL U5-S-U4	1.027	98.397	0.450	0.125	146.24 ±0.25	147.2 ±0.7	146.1 ±0.9		146.3 >0.3
ANL M-Th	0.852	93.244	0.334	5.570		122.6[e] ±0.7	124.1[e] ±0.7		
KRI U5-P	0.00111 0.00111[d]	99.9972	0.0017			4.954 ±0.015			
AERE U5-UK	1.1104	92.409	0.315	6.165		158.3 ±0.5			
CBNM/ BRC U5-NBS	1.6582	97.663	0.1497	0.5296	234.5 ±0.2	233.9 ±0.7			234.0 ±0.7

[a] Isotopic composition is an average of CBNM, NBS and LANL determinations.

[b] Present values.

[c] Uncertainty limited to lowest uncertainty of individual values.

[d] From present alpha spectroscopy.

[e] Values not used. Mass defined relative to ANL U5-SU4.

TABLE IV. Results from the Present Alpha Counting of the ^{235}U Samples

Sample	Alpha-decay rate, α_{ps} Quoted	Present	Uncertainties, % Stat.	Syst. 1	Syst. 2	Present Determination of Mass, μg U
ANL R5		194.1 ± 0.6	0.1	0.2	0.2	79.60 ± 0.29
ANL N3		127.2 ± 0.4	0.2	0.2	0.1	52.17 ± 0.19
ANL 5-1		2602 ± 6	0.1	0.1	0.2	1067 ± 4
ANL 5-2		2035 ± 5	0.1	0.1	0.2	834.6 ± 2.7
ANL SST5		847.8 ± 1.7	0.1	0.1	0.1	418.1 ± 1.6
LANL S1		66.52 ± 0.2	0.2	0.2	0.2	299.4 ± 1.2
LANL S3		375.1 ± 1.1	0.1	0.2	0.2	1688.6 ± 5.7
NBS	50.82 ± 0.25	50.97 ± 0.13	0.1	0.2	0.1	228.6 ± 1.3
KRI VI	62.6 ± 2.0	62.94 ± 0.2	0.2	0.2	0.1	762.7 ± 3.3
KRI XV	74.4 ± 2.2	73.97 ± 0.2	0.2	0.2	0.1	896.2 ± 3.9
BRC		454.9 ± 1.4	0.2	0.2	0.1	116.7 ± 0.5
AERE A	912.7 ± 5.0[a]	914.1 ± 3.2[a]	0.1	0.2	0.3	346.5 ± 1.6
AERE B	917.3 ± 4.6[a]	914.9 ± 3.2[a]	0.1	0.2	0.3	346.8 ± 1.6
CBNM 33	476.3 ± 4.1	476.7 ± 1.2	0.1	0.2	0.1	122.3 ± 0.5
CBNM 36	976.9 ± 8.3	977.3 ± 2.5	0.1	0.2	0.1	250.7 ± 1.0

[a]Excluding impurities.

TABLE V. Results of the ^{235}U Mass Ratio Measurements

U-Mass Ratio		Uncertainties,%[a] Statistics	Transm., Scatt.	FFA, Extr.	Source Ang.	Total
5-2/SST-5	1.9983	0.2	0.1	0.2	0.0	0.32
R5 /SST-5	0.1902	0.2	0.2	0.2	0.1	0.37
S1 /SST-5	0.7170	0.2	0.2	0.2	0.1	0.37
NBS/SST-5	0.5480	0.2	0.2	0.2	0.3	0.47
N3 /SST-5	0.1242	0.2	0.2	0.2	0.3	0.47
S3 /SST-5	4.0378	0.2	0.2	0.2	0.2	0.41
S1 /5-2	0.3587	0.2	0.2	0.2	0.2	0.41
S1 /R5	3.7766	0.2	0.2	0.2	0.1	0.37
S1 /NBS	1.2984	0.2	0.2	0.2	0.1	0.37
NBS/5-2	0.2726	0.2	0.2	0.2	0.3	0.47
5-1/5-2	1.2805	0.1	0.1	0.1	0.0	0.20
5-2/V1	1.1033	0.2	0.3	0.2	0.1	0.44
NBS/UKA	0.6640	0.2	0.3	0.2	0.2	0.47
NBS/V1	0.3006	0.2	0.1	0.2	0.2	0.37
V1 /UKA	2.1821	0.2	0.1	0.3	0.0	0.39
V1 /BRC	6.5084	0.2	0.1	0.3	0.2	0.44
UKB/SST-5	0.8340	0.2	0.1	0.2	0.2	0.37
XV /SST-5	2.1531	0.2	0.3	0.3	0.1	0.49
R5 /UKA	0.2292	0.2	0.1	0.2	0.1	0.33
BRC/SST-5	0.2794	0.2	0.1	0.2	0.3	0.44
UKA/BRC	2.9681	0.3	0.1	0.2	0.2	0.44
UKA/36	1.3754	0.2	0.1	0.4	0.2	0.51
5-2/33	6.8354	0.2	0.1	0.3	0.3	0.49
5-2/36	3.3326	0.2	0.1	0.2	0.3	0.44
UKB/UKA	0.9990	0.3	0.1	0.1	0.0	0.35
36 V1	0.3357	0.2	0.2	0.3	0.2	0.48
XV /V1	1.1771	0.2	0.1	0.2	0.0	0.32
NBS/BRC	1.9590	0.2	0.2	0.3	0.0	0.42

[a]The uncertainties for counting statistics, the corrections for neutron transmission and scattering effects, for FF absorption and fission spectra extrapolation, and for the $^{7}Li(p,n)$ neutron source anisotropy are given. The total uncertainty contains a 0.1% contribution for the uncertainty of the isotopic composition and fission events in isotopes other than ^{235}U.

III. FISSION-RATIO MEASUREMENTS

The present fission-ratio measurements were carried out in a back-to-back ionization chamber. Measurements were made at 600 ± 100 KeV neutron energy utilizing the $^{7}Li(p,n)$ reaction with a pulsed and bunched proton beam. The samples were located at a distance of ~5 cm from the neutron source and measurements were made with two different orientations of the fission chambers such that once one sample faced the target, then the other. Corrections were applied for:

1. The differences of the distances for the two samples from the neutron source,
2. The transmission losses and scattering gains,
3. The losses of fission fragments below the electronic threshold,
4. The fission events from isotopes other than ^{235}U,
5. The angular distribution of the source neutrons, and
6. The total fission fragment absorption.

The uncertainties caused by some of these corrections become negligible due to the measurements with the two orientations of the fission chamber.

An interesting "by-product" of the present investigation is the finding that the fission-fragment range used for the calculation of the total fission fragment absorption can be checked by comparing the product of the alpha energy width and the assumed range with other samples. A linear relationship

$$\Delta E_{\alpha} \cdot R_f \sim \delta$$

appears to be valid. Here ΔE_{α} is the width of a specific alpha particle observed in a low-geometry alpha spectrum, R_f is the fission fragment range, and δ is the thickness of the fissile deposit. This is demonstrated in Fig. 1.

Fifteen ^{235}U samples were involved in the present intercomparison, thus measurements of 14 ratios would have been sufficient to derive the ratio between any two sample masses. A sensible 105 ratio could have been measured between these samples, however, one ratio measurement required an average exposure time of six hours. As a compromise, a total number of 28 ratios were measured. The results from these fission ratio measurements are given in Table V.

IV. DISCUSSION OF THE RESULTS

Best values for the masses of the 15 uranium samples involved in the present intercomparison have been determined based upon the masses quoted by the contributing laboratories, the masses derived from the present absolute alpha counting, and the relative 2π alpha and fission ratio measurements. The over-determination of the available data has been removed by least-squares adjustments

$$\delta = (A^{T}C^{-1}A)^{-1}A^{T}C^{-1}M,$$

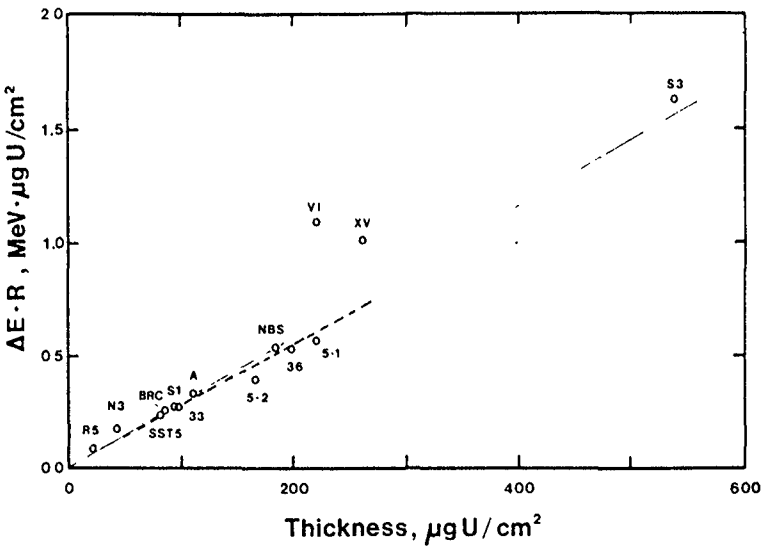

Alpha Energy Loss Multiplied with the FF Range as a Function of the Sample Thickness. The Values of the KRI Samples is shown Assuming UO_2.

Fig. 1.

where A is the coefficient matrix, and C is the variance-covariance matrix of the measurement vector M. Correlations arising from the use of the average specific-activity values of Table III for the present absolute mass determinations and from the application of various factors and corrections in the present alpha and fission measurements have been taken into account. The result of the LS analysis and its correlation matrix are given in Table VI. The masses quoted for the samples by the contributing laboratories are also given in Table VI. The average differences between the quoted masses and the results of the LS analysis are shown in Fig. 2 in percent. The agreement within $\lesssim$ ± 0.3% is very encouraging for future $^{235}U(n,f)$-cross section or reaction rate measurements. The differences are covered in all cases by the quoted uncertainties, which, more often than not, appear to be quite conservative. It is therefore concluded, that ^{235}U masses and fission rate measurements are sufficiently accurate to permit reaction rate measurements in reactor test facilities or in cross section experiments with the required accuracy.

TABLE VI. Comparison of the Quoted ^{235}U Masses with the LS-Fit Results

Samples	U-Mass, µg Quoted	LS-Fit	Correlation Matrix R5	N3	5-1	5-2	SST5	S1	S3	NBS	VI	XV	BRC	A	B	33	36
ANL -R5	79.60±0.19	79.32±0.15	1.00														
-N3	52.17±0.19	52.03±0.13	0.39	1.00													
-5-1	1067 ± 4	1066.4 ±2.1	0.45	0.41	1.00												
-5-2	834.6 ±2.7	833.7 ±1.3	0.51	0.43	0.74	1.00											
-SST5	418.1 ±1.6	417.3 ±0.7	0.57	0.41	0.47	0.68	1.00										
LANL-S1	298.7 ±0.3	298.7 ±0.3	0.26	0.15	0.20	0.25	0.21	1.00									
-S3	1688.3 ±3.0	1687.5 ±2.1	0.19	0.12	0.16	0.20	0.18	0.64	1.00								
NBS	228.5 ±1.2	228.6 ±0.4	0.29	0.19	0.25	0.31	0.28	0.46	0.31	1.00							
KRI -VI	757.9 ±7.6[a]	760.2 ±1.4	0.35	0.25	0.33	0.44	0.44	0.20	0.15	0.36	1.00						
-XV	901.0 ±9.0[a]	893.0 ±1.8	0.31	0.22	0.30	0.40	0.41	0.17	0.13	0.30	0.75	1.00					
BRC	116.1 ± [b]	116.5 ±0.3	0.33	0.22	0.26	0.35	0.41	0.18	0.14	0.31	0.43	0.33	1.00				
AERE-A	345.9 ±2.2	346.4 ±0.6	0.47	0.27	0.31	0.42	0.50	0.20	0.16	0.32	0.48	0.36	0.53	1.00			
-B	347.7 ±2.2	347.2 ±0.7	0.43	0.26	0.30	0.41	0.49	0.19	0.15	0.30	0.45	0.35	0.53	0.88	1.00		
CBNM-33	121.9 ±0.4	122.2 ±0.2	0.21	0.16	0.23	0.31	0.28	0.10	0.08	0.16	0.28	0.24	0.18	0.25	0.23	1.00	
-36	250.0 ±0.9	250.7 ±0.4	0.24	0.18	0.25	0.34	0.31	0.11	0.09	0.19	0.33	0.28	0.22	0.29	0.27	0.76	1.00

[a]Based on given areal density and total area.
[b]Restated for $T_{1/2}$ (^{234}U) = $2.456 \cdot 10^5$ yrs.

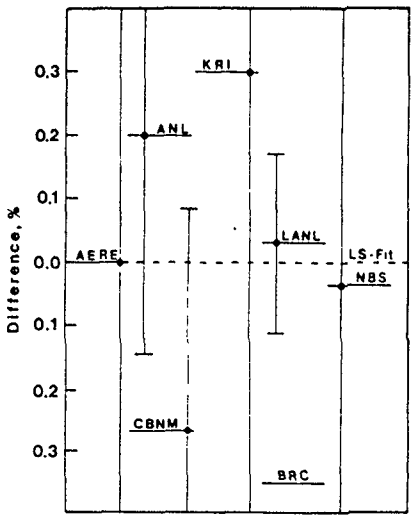

The Comparison of the Quoted ^{235}U Masses with the Least Squares Fit "Best" Values.

Fig. 2.

V. THE ^{234}U HALF-LIFE

The ^{234}U half-life is important for the mass assay of ^{235}U samples. Available experimental values are not consistent and a conflict exists with values obtained from fitting thermal parameters. Very accurate values are given for the isotopic compositions of two of the fissile materials involved in the present intercomparison (AERE and CBNM). The absolute alpha-decay rates and absolute masses of the corresponding samples can be used to determine the half-life of ^{234}U. For this purpose, all input data based upon the ^{234}U half-life was removed and the LS fit was repeated. The average value obtained for the half-life of ^{234}U from the four samples (AERE-A,-B;CBNM-33,36) is

$$T_{1/2}(^{234}U) = (2.457 \pm 0.005) \cdot 10^5 \text{ yrs.}$$

This is in good agreement with the latest measurement of $2.459 \cdot 10^5$ yrs by Geidelman et al.[4] as well as with the evaluated value of $2.455 \cdot 10^5$ yrs by Holden[5], and its modification to $2.456 \cdot 10^5$ yrs. as used in the present work. Inclusion of the present value for the half-life of ^{234}U in the set of values revised by Holden[5], and the elimination of the value by Meadows[6], results in a current value of

$$T_{1/2}\ (^{234}U) = (2.4566 + 0.0044) \cdot 10^5 \text{ yrs}$$

which is recommended as the best value to be used.

ACKNOWLEDGEMENT

This work was performed under the auspices of the U.S. Department of Energy. Dr. R.J. Armani provided some alpha count rates.

REFERENCES

1. W.P. Poenitz, J.W. Meadows, and R.J. Armani, "U^{235} Fission Mass and Counting Comparison and Standardization," Argonne National Laboratory Report ANL/NDM-48 (1979).

2. W.P. Poenitz and J.W. Meadows, Proc. Spec. Meeting on the ^{235}U Fission Cross Section, Intern. Atomic Energy Agency, Smolenice (1983), p. 27.

3. W.P. Poenitz and J.W. Meadows, Argonne National Laboratory Report ANL/NDM-84 (1983).

4. A.M. Geidelman et al., Izv. Acad. Nauk. SSSR, Ser. Fiz. 44, 927 (1980).

5. N.E. Holden, "The Uranium Half-lives: A Critical Review," Brookhaven National Laboratory Report BNL-NC5-51320 (1981).

6. J.W. Meadows, "The Alpha Half-life of ^{234}U", Argonne National Laboratory Report ANL-7610, 44 (1970).

LIST OF PARTICIPANTS

AUSTRALIA	J.W. Boldeman AAEC Research Establishment Private Mail Bag Sutherland, N.S.W. 2232
AUSTRIA	M. Drosg Institut für Experimentalphysik der Universität Wien Strudlhofgasse 4 A-1090 Vienna
BELGIUM	C. Wagemans Centre d'Etude de l'Energie Nucléaire C.E.N./S.C.K. Boeretang 200 B-2400 Mol
CHINA, PEOPLE'S REPUBLIC OF	Yuan Han-Rong Chinese Nuclear Data Center Beijing Atomic Energy Institute Ministry of Nuclear Industry Beijing
FRANCE	J. Blachot DRF/LCPN Centre d'Etudes Nucléaires de Grenoble Ave. des Martyrs 53 B.P. N° 85, Centre de Tri F-38041 Grenoble Cédex
	Nelcy Coursol CEA/ORIS/Saclay F-91191 Gif-sur-Yvette
GERMAN DEMOCRATIC REPUBLIC	D. Seeliger Sektion Physik Technische Universität Dresden Mommsenstrasse 13 DDR-8027 Dresden
GERMANY, FEDERAL REPUBLIC OF	M. Cosack Physikalisch Technische Bundesanstalt Abteilung 7 Bundesallee 100 D-3300 Braunschweig
	H. Klein Physikalisch Technische Bundesanstalt Abteilung 7 Bundesallee 100 D-3300 Braunschweig
GERMANY, FEDERAL REPUBLIC OF cont.	W. Mannhart Physikalisch Technische Bundesanstalt Abteilung 6 Bundesallee 100 D-3300 Braunschweig
	H.-W. Müller Fachinformationszentrum Energie, Physik, Mathematik GmbH (Fiz4) Kernforschungszentrum D-7514 Eggenstein-Leopoldshafen
HUNGARY	A. Lajtai Central Research Institute for Physics The Hungarian Academy of Sciences P.O. Box 49 H-1525 Budapest
ITALY	G. Reffo C.R.E.E. Clementel E.N.E.A. Via Mazzini 2 I-40138 Bologna
JAPAN	Y. Kanda Department of Energy Conversion Engineering Kyushu University 33 Sakamoto, Kasuga Kasuga-shi 816
	K. Kudo Electrotechnical Laboratory Agency of Industrial Science and Technology 1-1-4 Umezono, Sakura-mura Ibaraki-ken 305
	T. Michikawa Electrotechnical Laboratory Agency of Industrial Science and Technology 1-1-4 Umezono, Sakura-mura Ibaraki-ken 305
SUDAN	Farouk Habbani Department of Physics Faculty of Science University of Khartoum P.O. Box 321 Khartoum
SWEDEN	H. Condé Gustaf Werner Institute Uppsala University P.O. Box 531 S-751 21 Uppsala

SWEDEN cont.	T. Wiedling The Studsvik Science Research Laboratory S-611 82 Nykoeping
UNION OF SOVIET SOCIALIST REPUBLICS	M.V. Blinov Radievyj Institut V.G. Khlopina Ul. Rentgena 1 Leningrad P-22
	N.V. Kornilov Institute of Physics and Power Engineering Obninsk, Kaluga Region
UNITED KINGDOM	D.B. Gayther B.418, U.K. Atomic Energy Authority Atomic Energy Research Establishment Harwell, Didcot, Oxon OX11 ORA
	T.B. Ryves National Physics Laboratory Teddington, Middlesex TW11 OLW
	M.G. Sowerby Nuclear Physics Division, B.418 U.K. Atomic Energy Authority Atomic Energy Research Establishment Harwell, Didcot, Oxon OX11 ORA
UNITED STATES OF AMERICA	Allan D. Carlson National Bureau of Standards Gaithersburg, Maryland 20899
	Gerlad M. Hale T-2 Nuclear Data MS-243 Los Alamos National Laboratory Los Alamos, New Mexico 87545
	David G. Madland Theoretical Division Los Alamos National Laboratory Los Alamos, New Mexico 87545
	Wolfgang P. Poenitz Applied Physics Division, B.774, ZPPR ANL, Argonne-West, P.O. Box 2528 Idaho Falls, Idaho 83403
	Charles W. Reich Idaho National Engineering Laboratory EG & G Idaho Inc. P.O. Box 1625 Idaho Falls, Idaho 83415

BUREAU INTERNATIONAL DES POIDS ET MESURES	V.D. Huynh Pavillon de Breteuil F-92310 Sèvres
CENTRAL BUREAU FOR NUCLEAR MEASUREMENTS Steenweg naar Retie B-2440, Belgium	E.J. Axton W. Bambynek C. Bastian A. Brusegan C. Budtz-Jörgensen F. Corvi A.J. Deruytter H.-H. Knitter H. Liskien J. Pauwels (part-WG) R. Vaninbroukx J.A. Wartena E. Wattecamps C. Straede
INTERNATIONAL ATOMIC ENERGY AGENCY	K. Okamoto (Scientific Secretary) IAEA Nuclear Data Section P.O. Box 100 A-1400 Vienna, Austria
OECD Nuclear Energy Agency	Bernd Neumann NEA Data Bank P.B. N° 9 (Bât. 45) F-91190 Gif-sur-Yvette France